

ION AND WATER TRANSPORT IN CELL DEATH

EDITED BY: Markus Ritter, Yasunobu Okada, Alexander A. Mongin and
Giovanna Valenti

PUBLISHED IN: Frontiers in Cell and Developmental Biology



frontiers

Frontiers eBook Copyright Statement

The copyright in the text of individual articles in this eBook is the property of their respective authors or their respective institutions or funders. The copyright in graphics and images within each article may be subject to copyright of other parties. In both cases this is subject to a license granted to Frontiers.

The compilation of articles constituting this eBook is the property of Frontiers.

Each article within this eBook, and the eBook itself, are published under the most recent version of the Creative Commons CC-BY licence.

The version current at the date of publication of this eBook is CC-BY 4.0. If the CC-BY licence is updated, the licence granted by Frontiers is automatically updated to the new version.

When exercising any right under the CC-BY licence, Frontiers must be attributed as the original publisher of the article or eBook, as applicable.

Authors have the responsibility of ensuring that any graphics or other materials which are the property of others may be included in the CC-BY licence, but this should be checked before relying on the CC-BY licence to reproduce those materials. Any copyright notices relating to those materials must be complied with.

Copyright and source acknowledgement notices may not be removed and must be displayed in any copy, derivative work or partial copy which includes the elements in question.

All copyright, and all rights therein, are protected by national and international copyright laws. The above represents a summary only. For further information please read Frontiers' Conditions for Website Use and Copyright Statement, and the applicable CC-BY licence.

ISSN 1664-8714

ISBN 978-2-88971-558-9

DOI 10.3389/978-2-88971-558-9

About Frontiers

Frontiers is more than just an open-access publisher of scholarly articles: it is a pioneering approach to the world of academia, radically improving the way scholarly research is managed. The grand vision of Frontiers is a world where all people have an equal opportunity to seek, share and generate knowledge. Frontiers provides immediate and permanent online open access to all its publications, but this alone is not enough to realize our grand goals.

Frontiers Journal Series

The Frontiers Journal Series is a multi-tier and interdisciplinary set of open-access, online journals, promising a paradigm shift from the current review, selection and dissemination processes in academic publishing. All Frontiers journals are driven by researchers for researchers; therefore, they constitute a service to the scholarly community. At the same time, the Frontiers Journal Series operates on a revolutionary invention, the tiered publishing system, initially addressing specific communities of scholars, and gradually climbing up to broader public understanding, thus serving the interests of the lay society, too.

Dedication to Quality

Each Frontiers article is a landmark of the highest quality, thanks to genuinely collaborative interactions between authors and review editors, who include some of the world's best academicians. Research must be certified by peers before entering a stream of knowledge that may eventually reach the public - and shape society; therefore, Frontiers only applies the most rigorous and unbiased reviews.

Frontiers revolutionizes research publishing by freely delivering the most outstanding research, evaluated with no bias from both the academic and social point of view. By applying the most advanced information technologies, Frontiers is catapulting scholarly publishing into a new generation.

What are Frontiers Research Topics?

Frontiers Research Topics are very popular trademarks of the Frontiers Journals Series: they are collections of at least ten articles, all centered on a particular subject. With their unique mix of varied contributions from Original Research to Review Articles, Frontiers Research Topics unify the most influential researchers, the latest key findings and historical advances in a hot research area! Find out more on how to host your own Frontiers Research Topic or contribute to one as an author by contacting the Frontiers Editorial Office: frontiersin.org/about/contact

ION AND WATER TRANSPORT IN CELL DEATH

Topic Editors:

Markus Ritter, Paracelsus Medical University, Austria

Yasunobu Okada, National Institute for Physiological Sciences (NIPS), Japan

Alexander A. Mongin, Albany Medical College, United States

Giovanna Valenti, University of Bari Aldo Moro, Italy

Citation: Ritter, M., Okada, Y., Mongin, A. A., Valenti, G., eds. (2021). Ion and Water Transport in Cell Death. Lausanne: Frontiers Media SA.
doi: 10.3389/978-2-88971-558-9

Table of Contents

- 05 Editorial: Ion and Water Transport in Cell Death**
Markus Ritter, Alexander A. Mongin, Giovanna Valenti and Yasunobu Okada
- 08 Ion Transport in Eryptosis, the Suicidal Death of Erythrocytes**
Michael Föller and Florian Lang
- 17 Ferroptosis in Acute Central Nervous System Injuries: The Future Direction?**
Lesang Shen, Danfeng Lin, Xiaoyi Li, Haijian Wu, Cameron Lenahan, Yuanbo Pan, Weilin Xu, Yiding Chen, Anwen Shao and Jianmin Zhang
- 33 Plasma Membrane Pores Drive Inflammatory Cell Death**
Benedikt Kolbrink, Theresa Riebeling, Ulrich Kunzendorf and Stefan Krautwald
- 42 Iron Metabolism in Ferroptosis**
Xin Chen, Chunhua Yu, Rui Kang and Daolin Tang
- 56 Comparison of Anti-oncotic Effect of TRPM4 Blocking Antibody in Neuron, Astrocyte and Vascular Endothelial Cell Under Hypoxia**
Shunhui Wei, See Wee Low, Charlene Priscilla Poore, Bo Chen, Yahui Gao, Bernd Nilius and Ping Liao
- 68 Ion Transport in Plant Cell Shrinkage During Death**
François Bouteau, David Reboutier, Daniel Tran and Patrick Laurenti
- 71 A Reverse-Osmosis Model of Apoptotic Shrinkage**
Priyanka S. Rana and Michael A. Model
- 79 The Relationship Between Actin Cytoskeleton and Membrane Transporters in Cisplatin Resistance of Cancer Cells**
Takahiro Shimizu, Takuto Fujii and Hideki Sakai
- 90 Balance of Na^+ , K^+ , and Cl^- Unidirectional Fluxes in Normal and Apoptotic U937 Cells Computed With All Main Types of Cotransporters**
Valentina E. Yurinskaya, Igor A. Vereninov and Alexey A. Vereninov
- 101 Acid- and Volume-Sensitive Chloride Currents in Human Chondrocytes**
Michael Kittl, Martina Winklmayr, Katharina Helm, Johannes Lettner, Martin Gaisberger, Markus Ritter and Martin Jakab
- 121 Ions, the Movement of Water and the Apoptotic Volume Decrease**
Carl D. Bortner and John A. Cidlowski
- 137 Ca^{2+} Dependence of Volume-Regulated VRAC/LRRC8 and TMEM16A Cl^- Channels**
Raquel Centeio, Jiraporn Ousingsawat, Rainer Schreiber and Karl Kunzelmann
- 151 The Role of Eryptosis in the Pathogenesis of Renal Anemia: Insights From Basic Research and Mathematical Modeling**
Gabriela Ferreira Dias, Nadja Grobe, Sabrina Rogg, David J. Jörg, Roberto Pecoits-Filho, Andréa Novais Moreno-Amaral and Peter Kotanko
- 165 Voltage-Gated Potassium Channels as Regulators of Cell Death**
Magdalena Bachmann, Weiwei Li, Michael J. Edwards, Syed A. Ahmad, Sameer Patel, Ildiko Szabo and Erich Gulbins

- 182 Mitochondrial Ion Channels of the Inner Membrane and Their Regulation in Cell Death Signaling**
Andrea Urbani, Elena Prosdocimi, Andrea Carrer, Vanessa Checchetto and Ildikò Szabò
- 192 Cell Death Induction and Protection by Activation of Ubiquitously Expressed Anion/Cation Channels. Part 1: Roles of VSOR/VRAC in Cell Volume Regulation, Release of Double-Edged Signals and Apoptotic/Necrotic Cell Death**
Yasunobu Okada, Ravshan Z. Sabirov, Kaori Sato-Numata and Tomohiro Numata
- 212 Intracellular Ca^{2+} Imbalance Critically Contributes to Paraptosis**
Eunhee Kim, Dong Min Lee, Min Ji Seo, Hong Jae Lee and Kyeong Sook Choi
- 227 Positive Inotropic Effects of ATP Released via the Maxi-Anion Channel in Langendorff-Perfused Mouse Hearts Subjected to Ischemia-Reperfusion**
Hiroshi Matsuura, Akiko Kojima, Yutaka Fukushima, Yu Xie, Xinya Mi, Ravshan Z. Sabirov and Yasunobu Okada
- 235 The Role of pH_i in Intestinal Epithelial Proliferation—Transport Mechanisms, Regulatory Pathways, and Consequences**
Mahdi Amiri, Ursula E. Seidler and Katerina Nikolovska
- 242 Neurodegeneration Upon Dysfunction of Endosomal/Lysosomal CLC Chloride Transporters**
Shroddha Bose, Hailan He and Tobias Stauber
- 258 Roles of Ion and Water Channels in the Cell Death and Survival of Upper Gastrointestinal Tract Cancers**
Atsushi Shiozaki, Yoshinori Marunaka and Eigo Otsuji
- 267 From Pinocytosis to Methuosis—Fluid Consumption as a Risk Factor for Cell Death**
Markus Ritter, Nikolaus Bresgen and Hubert H. Kerschbaum
- 304 Transient Receptor Potential (TRP) Ion Channels Involved in Malignant Glioma Cell Death and Therapeutic Perspectives**
Florence Lefranc



Editorial: Ion and Water Transport in Cell Death

Markus Ritter^{1,2,3,4*}, Alexander A. Mongin⁵, Giovanna Valenti⁶ and Yasunobu Okada^{7,8,9}

¹ Center for Physiology, Pathophysiology and Biophysics, Institute for Physiology and Pathophysiology, Paracelsus Medical University, Salzburg, Austria, ² Kathmandu University, Dhulikhel, Nepal, ³ Ludwig Boltzmann Institute for Arthritis and Rehabilitation, Salzburg, Austria, ⁴ Gastein Research Institute, Paracelsus Medical University, Salzburg, Austria, ⁵ Department of Neuroscience and Experimental Therapeutics, Albany Medical College, Albany, NY, United States, ⁶ Department of Biosciences, Biotechnologies and Biopharmaceutics, University of Bari Aldo Moro, Bari, Italy, ⁷ Division of Cell Signaling, National Institute for Physiological Sciences (NIPS), Okazaki, Japan, ⁸ Department of Physiology, School of Medicine, Aichi Medical University, Nagakute, Japan, ⁹ Department of Physiology, Kyoto Prefectural University of Medicine, Kyoto, Japan

Keywords: cell death, ion transport, water transport, apoptosis, necrosis, cell volume regulation, cell hydration

Editorial on the Research Topic

Ion and Water Transport in Cell Death

The flow of water across cellular membranes determines the dynamics of cellular hydration and volume, both of which govern a plentitude of fundamental functions, including cell death (CD) (Lang et al., 1993, 1998, 2007; Haussinger, 1996; Hoffmann et al., 2009; Okada et al., 2021; Okada et al.). The aforementioned reviews suggest that changes in the directionality of water transport involve a variety of mechanisms; they can be osmotically obligated in their nature and coupled to the movement of ions and organic osmolytes, driven by hydrostatic pressure, or determined by “ingestion” and “excretion” during endo/exocytotic processes.

The significance of water transport and cell volume in CD has been recognized for a long time. Injurious cell swelling, which was initially described as oncosis (from Greek *ὄγκος*, i.e. tumor/swelling), represents a hallmark of the unregulated form of CD—necrosis (von Recklinghausen, 1910; Majno and Joris, 1995; Weerasinghe and Buja, 2012). Similar increases in cell volume are prominent in several other related modes of CD, such as secondary necrosis (aponecrosis), pyroptosis, and ferroptosis (Formigli et al., 2000; Zong and Thompson, 2006; Silva, 2010; D’Arcy, 2019; Okada et al., 2019; Nirmala and Lopus, 2020; Riegman et al., 2020). While necrosis was initially considered to be a result of uncontrolled water accumulation, recent studies suggest that this form of CD starts with tightly controlled normotonic cell swelling, termed necrotic volume increase (NVI) (Barros et al., 2001; Okada et al., 2001, 2021; Orlov and Hamet, 2004; Lang and Hoffmann, 2013a,b; Orlov et al., 2013a,b; Bortner and Cidlowski, 2014; Model, 2014; Bortner and Cidlowski). In contrast, the highly regulated mode of CD, apoptosis, is generally associated with cell volume decrease (Majno and Joris, 1995; Lang et al., 1998; Maeno et al., 2000; Hoffmann et al., 2009). Apoptosis is initiated by the early and precisely regulated normotonic cell shrinkage, termed apoptotic volume decrease (AVD), which is driven by activation of distinct ion channels and transporters (Maeno et al., 2000; Okada et al., 2001). Additionally, the emerging research indicates that the precise regulation of ion and water transport across organellar membranes is also indispensable for normal cell function, and its disturbances may cause CD and disease (Maltese and Overmeyer, 2014; Li et al., 2020; Saric and Freeman, 2020; Chadwick et al., 2021; Bouteau et al.; Ritter et al.; Urbani et al.). Apart from the two major types of CD, apoptosis and necrosis, numerous additional (sub)forms of CD have been identified. These include aponecrosis, oncosis, necroptosis, parthanatos, anoikis, entotic CD, NETotic CD, immunogenic CD, lysosome-dependent CD, ferroptosis, oxoapoptosis, sarmoptosis, autosis, autolysis, paraptosis, pyroptosis, alkaliptosis, phagoptosis, eryptosis, chondroptosis, autophagic CD, mitoptosis, methuosis, and the mitotic

OPEN ACCESS

Edited and reviewed by:

You-Wen He,
Duke University, United States

*Correspondence:

Markus Ritter
markus.ritter@pmu.ac.at

Specialty section:

This article was submitted to
Cell Death and Survival,
a section of the journal
Frontiers in Cell and Developmental
Biology

Received: 11 August 2021

Accepted: 13 August 2021

Published: 09 September 2021

Citation:

Ritter M, Mongin AA, Valenti G and
Okada Y (2021) Editorial: Ion and
Water Transport in Cell Death.
Front. Cell Dev. Biol. 9:757033.
doi: 10.3389/fcell.2021.757033

catastrophe-driven CD (Galluzzi et al., 2018). Although all these forms of CD involve very diverse and distinct mechanisms (Green and Llambi, 2015; Galluzzi et al., 2018; Nirmala and Lopus, 2020), their successful execution relies on tightly regulated transport of ions, organic solutes and water across the plasma membrane and/or organelle membranes (Lang et al., 1998; Okada and Maeno, 2001; Chen et al., 2008; Hoffmann et al., 2009; Orlov et al., 2013c; Maltese and Overmeyer, 2014; Mongin, 2016; Okada et al., 2019, 2021; Okada et al.). Understanding these mechanisms is crucial for our comprehension of the basic principles of normal and abnormal biological processes.

The objective of this Research Topic was to collect state-of-the-art Reviews and cutting-edge original research articles exploring ions and water transport in cell death. This timely subject has attracted significant enthusiasm of the scientific community. The initial Call for Contributions resulted in 23 accepted manuscripts covering various aspects of the pivotal roles of ion and water transport in cell death. The collection encompasses four Original Research papers (Centeio et al.; Kittl et al.; Wei et al.; Yurinskaya et al.), two Brief Research Reports (Rana and Model; Matsuura et al.), 11 Reviews (Bachmann et al.; Bortner and Cidlowski; Bose et al.; Chen et al.; Dias et al.; Foller and Lang; Kim et al.; Lefranc; Ritter et al.; Okada et al.; Shimizu et al.), four Mini Reviews (Kolbrink et al.; Urbani et al.; Amiri et al.; Shiozaki et al.), one Hypotheses article (Shen et al.), and one Opinion article (Bouteau et al.). These publications are contributed by 98 authors. While in the production, the Research Topic was met with high interest within the scientific community; it accumulates the steadily increasing number of views and downloads from all parts of the world (<https://www.frontiersin.org/research-topics/13260/ion-and-water-transport-in-cell-death#impact>).

The articles in this Research Topic cover a large variety of types of CD, including apoptosis (Bachmann et al.; Bortner and Cidlowski; Okada et al.; Rana and Model; Shimizu et al.; Urbani et al.; Yurinskaya et al.; Shiozaki et al.; Lefranc), necrosis (Bouteau et al.; Kittl et al.; Okada et al.; Lefranc), aponecrosis (Wei et al.), necroptosis and pyroptosis (Kolbrink et al.; Okada et al.), ferroptosis (Chen et al.; Okada et al.; Shen et al.; Lefranc), paraptosis (Kim et al.), eryptosis (Dias et al.; Foller and Lang), methuosis (Ritter et al.) as well as plant vacuolar CD (Bouteau et al.). From the standpoint of the mechanisms of CD-inducing processes, the Topic contributors discuss the functional significance of numerous specific anion channels, cation channels, and ion transporters (Bachmann et al.; Bortner and Cidlowski; Bouteau et al.; Kim et al.; Kittl et al.; Kolbrink et al.; Okada et al.; Rana and Model; Shen et al.; Shimizu et al.; Urbani et al.; Wei et al.; Yurinskaya et al.; Amiri et al.; Lefranc; Ritter et al.; Shiozaki et al.). To facilitate reading of this collection, we provide cross-references to the related ion transport mechanisms in **Supplementary Tables 1–3** (referring to anion channels, cation channels, and transporters, respectively). Additionally, this collection discusses the important roles in CD for the water channels, aquaporins (AQPs) (Bortner and Cidlowski; Shiozaki et al.), and mechanistic contributions for some organic signaling

molecules (such as ATP, glutamate and glutathione) which are released *via* anion channels (Okada et al.; Matsuura et al.).

It is also important to place each CD type in the context of the pathogenesis of different human diseases. The contributors discuss the role of apoptosis in ischemia/reperfusion (I/R) injury, including excitotoxicity (Okada et al.), chronic neurodegenerative disorders, including Alzheimer's disease (Bachmann et al.), cancer (Shiozaki et al.), and chemoresistance of cancer (Bachmann et al.; Okada et al.; Shimizu et al.); necrosis in I/R injury including lactacidotoxicity (Okada et al.), osteoarthritis (Kittl et al.), and cancer (Lefranc); aponecrosis in I/R injury (Wei et al.); necroptosis and pyroptosis in I/R injury, neurodegeneration, cancer, skin inflammation, and crystallopathies (Kolbrink et al.); ferroptosis in I/R injury (Chen et al.; Shen et al.), neurodegeneration (Chen et al.; Rana and Model), cancer (Chen et al.), and acute CNS injury (Shen et al.); paraptosis in I/R injury and chemoresistance of cancer (Kim et al.); as well as eryptosis in anemia and chronic kidney disease (CKD) (Dias et al.; Foller and Lang). There is a hope in the field that further elucidation of molecular mechanisms of ion and water transport underlining these CD processes is likely to provide accurate targets for therapy of CD-associated diseases and for the treatment of chemo-resistant cancer.

Collectively, the contributions from the Research Topic emphasize the progress in the field of physiological/pathophysiological mechanisms of cell death and their roles in the pathogenesis of various diseases.

AUTHOR CONTRIBUTIONS

All authors contributed equally to the editorial work of this Research Topic and to this Editorial and approved it for publication.

FUNDING

This work in the laboratories of the Research Topic editors was supported by National Institutes of Health (grants R01 NS061953, R01 NS11943 to AAM), the Japan Society for the Promotion of Science (Grant-in-Aid for Scientific Research #17K19517 to YO), POR Puglia Innonetwork (regional project H6GG787 to GV), and Agenzia Spaziale Italiana (GV).

ACKNOWLEDGMENTS

We would like to express our gratitude to all the authors who contributed to this Research Topic as well as all reviewers/editors of the submitted manuscripts. We also thank the Frontiers Editorial Office for assistance and support.

SUPPLEMENTARY MATERIAL

The Supplementary Material for this article can be found online at: <https://www.frontiersin.org/articles/10.3389/fcell.2021.757033/full#supplementary-material>

REFERENCES

- Barros, L. F., Hermosilla, T., and Castro, J. (2001). Necrotic volume increase and the early physiology of necrosis. *Comp. Biochem. Physiol. A Mol. Integr. Physiol.* 130, 401–409. doi: 10.1016/S1095-6433(01)00438-X
- Bortner, C. D., and Cidlowski, J. A. (2014). Ion channels and apoptosis in cancer. *Philos. Trans. R Soc. Lond. B Biol. Sci.* 369:20130104. doi: 10.1098/rstb.2013.0104
- Chadwick, S. R., Wu, J. Z., and Freeman, S. A. (2021). Solute transport controls membrane tension and organellar volume. *Cell Physiol. Biochem.* 55, 1–24. doi: 10.33594/000000318
- Chen, J. M., Sepramaniam, S., Armugam, A., Choy, M. S., Manikandan, J., Melendez, A. J. (2008). Water and ion channels: crucial in the initiation and progression of apoptosis in central nervous system? *Curr. Neuropharmacol.* 6, 102–116. doi: 10.2174/157015908784533879
- D'Arcy, M. S. (2019). Cell death: a review of the major forms of apoptosis, necrosis and autophagy. *Cell Biol. Int.* 43, 582–592. doi: 10.1002/cbin.11137
- Formigli, L., Papucci, L., Tani, A., Schiavone, N., Tempestini, A., Orlandini, G. E., (2000). Aponecrosis: morphological and biochemical exploration of a syncratic process of cell death sharing apoptosis and necrosis. *J. Cell. Physiol.* 182, 41–49. doi: 10.1002/(SICI)1097-4652(200001)182:1<41::AID-JCP5>3.0.CO;2-7
- Galluzzi, L., Vitale, I., Aaronson, S. A., Abrams, J. M., Adam, D., Agostinis, P., (2018). Molecular mechanisms of cell death: recommendations of the Nomenclature Committee on Cell Death 2018. *Cell. Death Differ.* 25, 486–541. doi: 10.1038/s41418-017-0012-4
- Green, D. R., and Llambi, F. (2015). Cell Death Signaling. *Cold Spring Harb. Perspect. Biol.* 7:a006080. doi: 10.1101/cshperspect.a006080
- Haussinger, D. (1996). The role of cellular hydration in the regulation of cell function. *Biochem. J.* 313 (Pt 3), 697–710. doi: 10.1042/bj3130697
- Hoffmann, E. K., Lambert, I. H., and Pedersen, S. F. (2009). Physiology of cell volume regulation in vertebrates. *Physiol. Rev.* 89, 193–277. doi: 10.1152/physrev.00037.2007
- Lang, F., Busch, G. L., Ritter, M., Volk, H., Waldegger, S., Gulbins, E., (1998). Functional significance of cell volume regulatory mechanisms. *Physiol. Rev.* 78, 247–306. doi: 10.1152/physrev.1998.78.1.247
- Lang, F., Foller, M., Lang, K., Lang, P., Ritter, M., Vereninov, A., (2007). Cell volume regulatory ion channels in cell proliferation and cell death. *Methods Enzymol.* 428, 209–225. doi: 10.1016/S0076-6879(07)28011-5
- Lang, F., and Hoffmann, E. K. (2013a). CrossTalk proposal: cell volume changes are an essential step in the cell death machinery. *J. Physiol.* 591, 6119–6121. doi: 10.1113/jphysiol.2013.258632
- Lang, F., and Hoffmann, E. K. (2013b). Rebuttal from Florian Lang and Else K. Hoffmann. *J. Physiol.* 591:6127. doi: 10.1113/jphysiol.2013.265231
- Lang, F., Ritter, M., Volk, H., and Haussinger, D. (1993). The biological significance of cell volume. *Ren. Physiol. Biochem.* 16, 48–65. doi: 10.1159/000173751
- Li, P., Hu, M., Wang, C., Feng, X., Zhao, Z., Yang, Y., (2020). LRRC8 family proteins within lysosomes regulate cellular osmoregulation and enhance cell survival to multiple physiological stresses. *Proc. Natl. Acad. Sci. U.S.A.* 117, 29155–29165. doi: 10.1073/pnas.2016539117
- Maeno, E., Ishizaki, Y., Kanaseki, T., Hazama, A., and Okada, Y. (2000). Normotonic cell shrinkage because of disordered volume regulation is an early prerequisite to apoptosis. *Proc. Natl. Acad. Sci. U.S.A.* 97, 9487–9492. doi: 10.1073/pnas.140216197
- Majno, G., and Joris, I. (1995). Apoptosis, oncosis, and necrosis. An overview of cell death. *Am. J. Pathol.* 146, 3–15.
- Maltese, W. A., and Overmeyer, J. H. (2014). Methuosis: nonapoptotic cell death associated with vacuolization of macropinosome and endosome compartments. *Am. J. Pathol.* 184, 1630–1642. doi: 10.1016/j.ajpath.2014.02.028
- Model, M. A. (2014). Possible causes of apoptotic volume decrease: an attempt at quantitative review. *Am. J. Physiol. Cell Physiol.* 306, C417–C424. doi: 10.1152/ajpcell.00328.2013
- Mongin, A. A. (2016). Volume-regulated anion channel—a frenemy within the brain. *Pflugers Arch.* 468, 421–441. doi: 10.1007/s00424-015-1765-6
- Nirmala, J. G., and Lopus, M. (2020). Cell death mechanisms in eukaryotes. *Cell Biol. Toxicol.* 36, 145–164. doi: 10.1007/s10565-019-09496-2
- Okada, Y., and Maeno, E. (2001). Apoptosis, cell volume regulation and volume-regulatory chloride channels. *Comp. Biochem. Physiol. A Mol. Integr. Physiol.* 130, 377–383. doi: 10.1016/S1095-6433(01)00424-X
- Okada, Y., Maeno, E., Shimizu, T., Dezaki, K., Wang, J., and Morishima, S. (2001). Receptor-mediated control of regulatory volume decrease (RVD) and apoptotic volume decrease (AVD). *J. Physiol.* 532, 3–16. doi: 10.1111/j.1469-7793.2001.0003g.x
- Okada, Y., Numata, T., Sato-Numata, K., Sabirov, R. Z., Liu, H., Mori, S. I., (2019). Roles of volume-regulatory anion channels, VSOR and Maxi-Cl, in apoptosis, cisplatin resistance, necrosis, ischemic cell death, stroke and myocardial infarction. *Curr. Top. Membr.* 83, 205–283. doi: 10.1016/bs.ctm.2019.03.001
- Okada, Y., Sato-Numata, K., Sabirov, R. Z., and Numata, T. (2021). Cell death induction and protection by activation of ubiquitously expressed anion/cation channels. Part 2: functional and molecular properties of ASOR/PAC channels and their roles in cell volume dysregulation and acidotoxic cell death. *Front. Cell Dev. Biol.* 9:702317. doi: 10.3389/fcell.2021.702317
- Orlov, S. N., and Hamet, P. (2004). Apoptosis vs. oncosis: role of cell volume and intracellular monovalent cations. *Adv. Exp. Med. Biol.* 559, 219–233. doi: 10.1007/0-387-23752-6_21
- Orlov, S. N., Model, M. A., and Grygorczyk, R. (2013a). CrossTalk opposing view: the triggering and progression of the cell death machinery can occur without cell volume perturbations. *J. Physiol.* 591, 6123–6125. doi: 10.1113/jphysiol.2013.258624
- Orlov, S. N., Model, M. A., and Grygorczyk, R. (2013b). Rebuttal from Sergei N. Orlov, Michael M. Model and Ryszard Grygorczyk. *J. Physiol.* 591, 6129. doi: 10.1113/jphysiol.2013.265264
- Orlov, S. N., Platonova, A. A., Hamet, P., and Grygorczyk, R. (2013c). Cell volume and monovalent ion transporters: their role in cell death machinery triggering and progression. *Am. J. Physiol. Cell Physiol.* 305, C361–C372. doi: 10.1152/ajpcell.00040.2013
- Riegman, M., Sagie, L., Galed, C., Levin, T., Steinberg, N., Dixon, S. J., (2020). Ferroptosis occurs through an osmotic mechanism and propagates independently of cell rupture. *Nat. Cell. Biol.* 22, 1042–1048. doi: 10.1038/s41556-020-0565-1
- Saric, A., and Freeman, S. A. (2020). Endomembrane tension and trafficking. *Front. Cell Dev. Biol.* 8:611326. doi: 10.3389/fcell.2020.611326
- Silva, M. T. (2010). Secondary necrosis: the natural outcome of the complete apoptotic program. *FEBS Lett.* 584, 4491–4499. doi: 10.1016/j.febslet.2010.10.046
- von Recklinghausen, F. (1910). *Untersuchungen Über Rachitis und Osteomalacie*. Jena: G. Fischer.
- Weerasinghe, P., and Buja, L. M. (2012). Oncosis: an important non-apoptotic mode of cell death. *Exp. Mol. Pathol.* 93, 302–308. doi: 10.1016/j.yexmp.2012.09.018
- Zong, W. X., and Thompson, C. B. (2006). Necrotic death as a cell fate. *Genes Dev.* 20, 1–15. doi: 10.1101/gad.1376506

Conflict of Interest: The authors declare that the research was conducted in the absence of any commercial or financial relationships that could be construed as a potential conflict of interest.

Publisher's Note: All claims expressed in this article are solely those of the authors and do not necessarily represent those of their affiliated organizations, or those of the publisher, the editors and the reviewers. Any product that may be evaluated in this article, or claim that may be made by its manufacturer, is not guaranteed or endorsed by the publisher.

Copyright © 2021 Ritter, Mongin, Valenti and Okada. This is an open-access article distributed under the terms of the Creative Commons Attribution License (CC BY). The use, distribution or reproduction in other forums is permitted, provided the original author(s) and the copyright owner(s) are credited and that the original publication in this journal is cited, in accordance with accepted academic practice. No use, distribution or reproduction is permitted which does not comply with these terms.



Ion Transport in Eryptosis, the Suicidal Death of Erythrocytes

Michael Föller^{1*} and Florian Lang²

¹ Department of Physiology, University of Hohenheim, Stuttgart, Germany, ² Department of Physiology Institute of Physiology, University of Tübingen, Tübingen, Germany

OPEN ACCESS

Edited by:

Markus Ritter,
Paracelsus Medical University, Austria

Reviewed by:

Carlo Brugnara,
Boston Children's Museum,
United States
Carl David Bortner,
National Institute of Environmental
Health Sciences (NIEHS),
United States
Ethereia Pretorius,
Stellenbosch University, South Africa

*Correspondence:

Michael Föller
michael.foeller@uni-hohenheim.de

Specialty section:

This article was submitted to
Cell Death and Survival,
a section of the journal
Frontiers in Cell and Developmental
Biology

Received: 30 April 2020

Accepted: 18 June 2020

Published: 08 July 2020

Citation:

Föller M and Lang F (2020) Ion
Transport in Eryptosis, the Suicidal
Death of Erythrocytes.
Front. Cell Dev. Biol. 8:597.
doi: 10.3389/fcell.2020.00597

Erythrocytes are among the most abundant cells in mammals and are perfectly adapted to their main functions, i.e., the transport of O₂ to peripheral tissues and the contribution to CO₂ transport to the lungs. In contrast to other cells, they are fully devoid of organelles. Similar to apoptosis of nucleated cells erythrocytes may enter suicidal death, eryptosis, which is characterized by the presentation of membrane phosphatidylserine on the cell surface and cell shrinkage, hallmarks that are also typical of apoptosis. Eryptosis may be triggered by an increase in the cytosolic Ca²⁺ concentration, which may be due to Ca²⁺ influx via non-selective cation channels of the TRPC family. Eryptosis is further induced by ceramide, which sensitizes erythrocytes to the eryptotic effect of Ca²⁺. Signaling regulating eryptosis further involves a variety of kinases including AMPK, PAK2, cGKI, JAK3, CK1 α , CDK4, MSK1/2 and casein kinase. Eryptosis-dependent shrinkage is induced by K⁺ efflux through Ca²⁺-activated K⁺ channel K_{Ca}3.1, the Gardos channel. Eryptotic cells are phagocytosed and may adhere to endothelial cells. Eryptosis may help prevent hemolysis since defective erythrocytes usually undergo eryptosis followed by rapid clearance from circulating blood. Excessive eryptosis stimulated by various diseases and xenobiotics may result in anemia and/or impaired microcirculation. This review focuses on the significance and mechanisms of eryptosis as well as on the ion fluxes involved. Moreover, a short summary of further ion transport mechanisms of the erythrocyte membrane is provided.

Keywords: phosphatidylserine, Ca²⁺, shrinkage, gardos channel, apoptosis

INTRODUCTION

The number of erythrocytes or red blood cells (RBCs) exceeds the numbers of most other cells in the human body and amounts to 4–6 $\times 10^6$ per μ l of blood (Nemkov et al., 2018). With a total of approx. 5 l of blood, every human being has about 25 $\times 10^{12}$ circulating erythrocytes. The main function of erythrocytes is the transport of O₂ from the lung to organs, tissues, and cells which they need for oxidative phosphorylation. Erythrocytes are perfectly adapted to this task in that they are full of hemoglobin, the O₂-carrying molecule, without having any cell organelles such as mitochondria, ribosomes, or a nucleus. Therefore, the metabolism of erythrocytes is restricted to degradation of glucose without O₂. They cannot utilize energy-rich fatty acids at all. Moreover, mature erythrocytes do not have RNA or DNA and cannot synthesize proteins. Owing

to these limitations, they have simply been described as “bags of hemoglobin” rather than real cells (D’Alessandro and Zolla, 2017).

Normal cells can undergo apoptosis, a form of programmed cell death (D’Arcy, 2019). It allows cells to die in a controlled sequence of events that affect the cytosol and different organelles. For example, it comprises the breakdown of the mitochondrial potential, karyopyknosis (shrinkage of the nucleus and chromatin condensation) with subsequent DNA degradation, Ca^{2+} influx and Ca^{2+} -dependent enzymatic digestion of intracellular proteins as well as breakdown of the phosphatidylserine asymmetry of the cell membrane (Guo et al., 2009; D’Arcy, 2019). The latter results in the appearance of phosphatidylserine in the outer membrane leaflet whereas it can only be found in the inner leaflet in non-apoptotic cells (Segawa and Nagata, 2015). Apparently, apoptosis as such is not possible in erythrocytes due to the lack of organelles. However, it has become clear that also erythrocytes, the lifespan of which has a median of 120 days in human beings, can actively undergo a controlled suicidal death program which is in many aspects comparable to apoptosis of nucleated cells (Föller et al., 2008b; Lang et al., 2008). Hence, it has been called eryptosis and is mainly characterized by two hallmarks that are also typical of apoptosis (Repsold and Joubert, 2018): The externalization of membrane phosphatidylserine at the cell surface and the loss of cell volume, i.e., cell shrinkage (Föller et al., 2008b; Lang et al., 2008). The Nomenclature Committee on Cell Death 2018 did not recommend use of the term “eryptosis” despite its “unquestionable relevance” for the reason that it is “extremely complex [...] to define the death of entities that—in physiological conditions—exist in a debatable state between life and death (such as erythrocytes and viruses)” (Galluzzi et al., 2018). Nevertheless, we use the term “eryptosis” in this review because we believe that it well reflects the similarities to apoptosis of nucleated cells and at the same time points to the obvious limitations associated with erythrocytes being cells without organelles.

SIGNIFICANCE OF ERYPTOSIS

Erythrocytes may become damaged during their lifetime such that they are lysed and release hemoglobin (hemolysis) (Föller et al., 2008b). Although plasma protein haptoglobin binds free hemoglobin with high affinity, the lysis of a great number of erythrocytes can exceed its binding capacity (Shih et al., 2014). If so, plasma hemoglobin can freely be filtered in the kidney and may precipitate in kidney tubules resulting in kidney damage and ultimately in acute kidney injury (AKI), a condition with high mortality often requiring intensive care treatment (Qian et al., 2010). Eryptosis may be a mechanism to prevent this potentially life-threatening complication of hemolysis by initiating a suicidal death program in damaged red blood cells that provides for the controlled removal of the affected cell before the damage may cause uncontrolled hemolysis (Föller et al., 2008b). Along these lines, eryptosis is triggered

by a broad spectrum of endogenous and exogenous noxious insults including (bacterial) toxins, pharmaceutical drugs, several clinical conditions and acute and chronic diseases, as well as further biotic and abiotic stressors including oxidative stress or hyperthermia (Lang and Lang, 2015).

Cells of the mononuclear phagocyte system (MPS) such as macrophages recognize phosphatidylserine on the surface of eryptotic cells by means of specific receptors (Bonomini et al., 2001; Mandal et al., 2002; Segawa and Nagata, 2015). This interaction prompts the phagocytosis of the dying erythrocytes, resulting in its engulfment and intracellular degradation. Hence, phosphatidylserine exposure in eryptosis serves as an “eat-me” signal (Bonomini et al., 2001; Mandal et al., 2002; Segawa and Nagata, 2015).

PATHOPHYSIOLOGY OF ERYPTOSIS

The presentation of phosphatidylserine on the surface of eryptotic cells can have two major pathophysiological implications: On the one hand, it initiates phagocytosis of erythrocytes (Mandal et al., 2002), on the other hand it mediates the adherence of erythrocytes to vascular endothelium cells which also express phosphatidylserine receptors (Setty and Betal, 2008; Wautier et al., 2011).

Excessive eryptosis initiating the phagocytosis of many red blood cells may therefore result in an acute loss of erythrocytes, i.e., anemia (Lang F. et al., 2017). In line with this, many of the aforementioned stimulators of eryptosis are associated with anemia, i.e., the pharmaceutical drugs triggering eryptosis are known to cause anemia as an adverse effect and the eryptosis-associated diseases are paralleled or even characterized by anemia (Lang and Lang, 2015).

The adherence of eryptotic erythrocytes to vascular endothelium cells also mediated by the phosphatidylserine receptor may impair microcirculation. Hence, stimulators of eryptosis may not only cause anemia, but also cardiovascular complications due to impeded microcirculation (Pretorius, 2018).

The induction of eryptosis may, however, have beneficial consequences, too: Malaria, a tropical disease threatening hundreds of million people world-wide and responsible for several hundred thousand deaths every year, is caused by protozoan *Plasmodium falciparum*, an unicellular eukaryote (Föller et al., 2009a; Boulet et al., 2018). During the infection, the pathogen invades erythrocytes and matures in the red cell, finally causing its lysis thereby releasing new parasites that can infect further erythrocytes. The lysis causes cyclical periods of fever, the hallmark of malaria (Föller et al., 2009a; Boulet et al., 2018). Given the dependence of the parasite on intraerythrocytic maturation, the early induction of eryptosis appears to be a promising therapeutic strategy as it could result in the phagocytosis of the affected erythrocyte and the inside parasite, thus in the clearance of the pathogen (Föller et al., 2008; Boulet et al., 2018). A big flaw of most common therapeutic approaches in malaria that target the parasite is the development of resistance. Therefore, the stimulation of eryptosis, a therapeutic strategy aiming at the

host, could be helpful to prevent resistance (Foller et al., 2008; Boulet et al., 2018).

PHOSPHATIDYL SERINE EXTERNALIZATION IN ERYPTOSIS

In erythrocytes, the activities of the enzymes scramblase and flippase (aminophospholipid translocase) determine the distribution of phosphatidylserine among the inner and outer membrane leaflet (Pretorius et al., 2016): Flippase translocates phosphatidylserine from the outer leaflet to the inner leaflet, thereby maintaining phosphatidylserine asymmetry in non-eryptotic cells (Pretorius et al., 2016). Conversely, scramblase shifts phosphatidylserine from inside to outside (Pretorius et al., 2016). Both enzymes are Ca^{2+} -regulated with Ca^{2+} inhibiting flippase and activating scramblase (Weiss et al., 2012). Upon induction of eryptosis, an increase in the cytosolic Ca^{2+} concentration inhibits flippase and activates scramblase resulting in the appearance of phosphatidylserine on the surface of the dying erythrocyte.

In patients with sickle cell disease, phosphatidylserine externalization is found in subsets of reticulocytes, young cells, and partly also in mature erythrocytes (Jong et al., 2001). Interestingly, phosphatidylserine exposure can be reversed in sickle cell disease, particularly in young erythrocytes (Yasin et al., 2003).

CELL SHRINKAGE IN ERYPTOSIS

Apart from externalization of phosphatidylserine, cell shrinkage is another hallmark of eryptosis (Föller et al., 2008b). The loss of cell volume is due to the efflux of K^+ ions which is paralleled by efflux of Cl^- and osmotically obliged water (Föller et al., 2008b). Human erythrocytes express Ca^{2+} -regulated inwardly rectifying K^+ channels which are also known as Gardos channels ($\text{K}_{\text{Ca}3.1}$) encoded by *KCNN4* (Hoffman et al., 2003). The increase in the cytosolic Ca^{2+} concentration as an initial event in eryptosis leads to the formation of Ca^{2+} /calmodulin that is associated with the Gardos channel thereby activating it (Oliván-Viguera et al., 2013). At 2 μM Ca^{2+} , Gardos channel activity is maximal (Thomas et al., 2011). Gardos channel-mediated K^+ efflux hyperpolarizes the cell membrane. As a consequence, hyperpolarization drives anion exit through Cl^- channels (Dyrda et al., 2010). The cell volume loss upon Gardos channel activation is in large part rate-limited by efflux of Cl^- following K^+ efflux (Thomas et al., 2011). In unstimulated erythrocytes, the Gardos channel as well as most other cation channels are closed resulting in a low cation leakage. A certain mutation of the *KCNN4* gene enhances the Ca^{2+} sensitivity of the Gardos channel and accounts for hereditary xerocytosis, an autosomal-dominant disease (Rapetti-Mauss et al., 2015). It is characterized by dehydrated erythrocytes and hemolytic anemia (Rapetti-Mauss et al., 2015).

The activation of Gardos K^+ channels with subsequent cell shrinkage is not only a hallmark of eryptosis but also enhances erythrocyte phosphatidylserine exposure stimulated by energy

depletion or Ca^{2+} ionophore ionomycin (Lang P. A. et al., 2003). Hence, Gardos channel-mediated K^+ loss is itself a trigger of eryptosis (Lang K. S. et al., 2003).

Patients with sickle cell disease have a subfraction of erythrocytes (app. 4%) that exhibit a relatively high intracellular Na^+ and low intracellular K^+ concentration (Bookchin et al., 2000). Such erythrocytes are also found in healthy humans (<0.03%) and do not dehydrate ("valinomycin-resistant") when exposed to K^+ ionophore valinomycin or a Ca^{2+} ionophore (Bookchin et al., 2000).

Ca^{2+} ENTRY INTO ERYTHROCYTES

An increase in the cytosolic Ca^{2+} concentration is an early event in the orchestration of eryptosis and initiates hallmarks of eryptosis, phosphatidylserine externalization and cell shrinkage (Föller et al., 2009b). Under resting conditions in non-stimulated erythrocytes the cytosolic free Ca^{2+} concentration is in the range of 50 nM (Bogdanova et al., 2013), a value several orders lower than the free plasma Ca^{2+} concentration (around 1.5 mM) and comparable to the free cytosolic Ca^{2+} concentration in nucleated cells. Total cytosolic Ca^{2+} also includes Ca^{2+} ions bound by Ca^{2+} -binding proteins such as calmodulin and amounts to 5–6 μM (Bookchin and Lew, 1980; Bogdanova et al., 2013).

Ca^{2+} entry into erythrocytes is incompletely understood. Clearly, the low basal Ca^{2+} conductance of unstimulated erythrocytes can be increased, suggesting the presence of Ca^{2+} channels in the membrane. These Ca^{2+} -permeable channels exhibit a low conductance in non-stimulated erythrocytes (Duranton et al., 2002). They are regulated by the Cl^- concentration, as replacement of extracellular Cl^- by gluconate or other anions such as Br^- , SCN^- , or I^- strongly up-regulates their conductance (Duranton et al., 2002). Moreover, these Ca^{2+} -permeable channels are activated by oxidative stress (Duranton et al., 2002) and hyperosmotic shock (extracellular osmolality of 850 mOsm) and can be inhibited by ethylisopropylamiloride (Lang K. S. et al., 2003) and erythropoietin (Myssina et al., 2003). They have a permselectivity of $\text{Cs}^+ > \text{K}^+ > \text{Na}^+ = \text{Li}^+ \gg \text{NMDG}^+$ (Duranton et al., 2002).

Activators of the cation channels include prostaglandin E_2 (PGE_2) (Lang et al., 2005). Phospholipase A_2 cleaves phospholipids in the cell membrane, releasing arachidonic acid. Cyclooxygenase is the key enzyme for the generation of prostaglandins from arachidonic acid. Prostaglandin E_2 (PGE_2) is an important eicosanoid, contributing to pain by sensitizing peripheral nociceptors, to fever and local inflammation (Ricciotti and FitzGerald, 2011). The isosmotic replacement of extracellular Cl^- and hyperosmotic shock induce PGE_2 synthesis in erythrocytes which in turn activates Ca^{2+} influx through the Ca^{2+} -permeable cation channel (Lang et al., 2005). Hence, PGE_2 is a major regulator of eryptosis by inducing Ca^{2+} influx (Lang et al., 2005).

Interestingly, ionotropic glutamate NMDA receptors permeable to Ca^{2+} contribute to Ca^{2+} homeostasis in erythrocytes (Makhro et al., 2013; Kaestner et al., 2020). Furthermore, human erythrocytes express GluA1, a subunit

of ionotropic glutamate AMPA receptors that are also Ca^{2+} permeable if devoid of subunit GluA2 (Föller et al., 2009b). AMPA receptor antagonists attenuate the increase in cytosolic Ca^{2+} following removal of extracellular Cl^- or glucose, maneuvers inducing eryptosis by stimulating Ca^{2+} entry (Föller et al., 2009b).

TRP channels are a large family of cation channels permeable to different cations, expressed in many different cell types, and having a broad spectrum of physiological functions (Ramsey et al., 2006). TRPC2, TRPC3 and TRPC6 are Ca^{2+} -permeable members of the TRPC family of channels expressed in erythrocyte precursor cells (Hirschler-Laszkiewicz et al., 2011, 2012). Erythropoietin induces Ca^{2+} entry into these cells through TRPC3 (Hirschler-Laszkiewicz et al., 2011). In mature human erythrocytes, TRPC6 may contribute to Ca^{2+} entry in eryptosis (Föller et al., 2008) whereas TRPC4/5 may be more relevant in mature murine erythrocytes (Danielczok et al., 2017).

Ca^{2+} entry into erythrocytes is also induced by shear stress (Larsen et al., 1981; Johnson and Gannon, 1990; Thomas et al., 2011). Erythrocytes express the mechanosensitive cation channel PIEZO1 (see below) permeable to Ca^{2+} (Cahalan et al., 2015). Indeed, mechanical stress induces PIEZO1-dependent Ca^{2+} influx into erythrocytes that, in turn, stimulates Gardos channel-mediated K^+ efflux and shrinkage (Cahalan et al., 2015).

Human erythrocytes also express voltage-dependent $\text{Ca}_v2.1$ Ca^{2+} channels as confirmed by Western Blotting (Andrews et al., 2002). Pharmacological inhibition of $\text{Ca}_v2.1$ with ω -agatoxin-TK suppresses Ca^{2+} influx into erythrocytes induced by phorbol 12-myristate 13-acetate (PMA) (Andrews et al., 2002). According to this study, PKC regulates $\text{Ca}_v2.1$ -mediated Ca^{2+} entry into erythrocytes (Andrews et al., 2002). This view is challenged by another study postulating that at least two different Ca^{2+} influx pathways exist in erythrocytes with one being independent of $\text{Ca}_v2.1$ and another indirectly activated by $\text{PKC}\alpha$ (Wagner-Britz et al., 2013). $\text{PKC}\alpha$ also regulates eryptosis induced by energy depletion (Klarl et al., 2006).

Ca^{2+} ATPASE

The plasma membrane P-type Ca^{2+} ATPase (PMCA) is expressed in human erythrocytes (Bogdanova et al., 2013). It is equipped with a Ca^{2+} /calmodulin binding site interacting with Ca^{2+} /calmodulin and enabling it to sense an elevation of the cytosolic Ca^{2+} concentration (Bogdanova et al., 2013). In this case, it pumps Ca^{2+} out of the cell at the expense of ATP which is degraded by the enzyme (Bogdanova et al., 2013). Ceramide or arachidonic acid induce the activity of the Ca^{2+} ATPase (Bogdanova et al., 2013).

ROLE OF CERAMIDE AND KINASES IN ERYPTOSIS

Apart from intracellular Ca^{2+} , ceramide is a major cellular initiator of eryptosis (Lang et al., 2004). Ceramide is generated by sphingomyelinase, a phosphodiesterase that cleaves membrane

sphingolipid sphingomyelin (Zeidan and Hannun, 2010). Ceramide is involved in apoptosis of nucleated cells mediated by the death receptor CD95 (Gulbins et al., 1995). It triggers eryptosis by sensitizing the cell to Ca^{2+} , but it does not induce Ca^{2+} influx (Lang et al., 2004). Moreover, hyperosmotic shock induces eryptosis also by stimulating sphingomyelinase-dependent ceramide formation in erythrocytes, an effect explaining why hyperosmotic shock-stimulated eryptosis is also observed in the absence of extracellular Ca^{2+} (Lang et al., 2004).

Regulators of eryptosis further include diverse kinases including AMP-activated protein kinase AMPK (Föller et al., 2009c; Zelenak et al., 2011), p21-activated kinase PAK2 (Zelenak et al., 2011), cGMP-dependent protein kinase type I cGKI (Föller et al., 2008a), Janus kinase JAK3 (Bhavsar et al., 2011), casein kinase CK1 α (Kucherenko et al., 2012; Zelenak et al., 2012), cyclin-dependent kinase CDK4 (Lang et al., 2015b), and mitogen- and stress-activated kinase MSK1/2 (Lang et al., 2015a) as suggested by pharmacological approaches and/or experiments with knockout mice.

ROLE OF OXIDATIVE STRESS IN ERYPTOSIS

Erythrocytes are permanently challenged by oxidative stress (Cimen, 2008). Despite having powerful reactive oxygen species (ROS) scavengers including glutathione, superoxide dismutase, or catalase, ROS is an important trigger of eryptosis *in vivo*, especially in certain clinical conditions (Lang et al., 2014). In mice deficient for the modifier subunit of glutamate-cysteine ligase (*gclm*^{-/-} mice), the erythrocyte glutathione level is only 10% of the normal value (Föller et al., 2013). Nevertheless, no enhanced eryptosis is observed in unchallenged mice. Upregulated catalase may contribute to this effect (Föller et al., 2013). If the mice are, however, exposed to additional oxidative stress in the form of phenylhydrazine, eventually fatal hemolysis is the consequence (Föller et al., 2013).

Ca^{2+} -permeable cation channels initiating eryptosis are activated by ROS (Duranton et al., 2002), and higher *in vitro* susceptibility of erythrocytes from *gclm*^{-/-} mice to eryptosis can be blocked by antioxidant Trolox (Föller et al., 2013). In addition, erythrocyte Cl^- channels contributing to shrinkage in eryptosis are also sensitive to ROS (Huber et al., 2002).

Oxidative stress may contribute to enhanced eryptosis in several clinical conditions including diabetes, chronic kidney disease, Wilson's disease, malaria, and iron deficiency (Lang et al., 2014). In erythrocytes from patients with sickle cell anemia, antioxidants inhibit K^+ , Cl^- cotransport, and Gardos channel-mediated K^+ efflux as well as phosphatidylserine exposure (Al Balushi et al., 2019). Hence, also the erythrocyte K^+ permeability is dependent on ROS, at least in erythrocytes from patients with sickle cell disease (Al Balushi et al., 2019).

A recent study uncovered that lysates of erythrocytes contain a vast number of pro-inflammatory and anti-inflammatory cytokines, chemokines, and mediators including C-C chemokines (CTACK, Eotaxin, MCP-1, MCP-3, MIP-1 α , MIP-1 β , RANTES), members of the CSF family (G-CSF, GM-CSF, M-CSF), C-X-C

chemokines (GRO- α , IL-8, IP-10, MIG, SDF-1 α), FGF growth factors (bFGF), IL-3, IL-5, IFN α 2, IFN γ , members of the IL-1 family, LIF, IL-12(p40), IL-12(p70), IL-17, MIF, PDGF-bb, VEGF, TNF α , TNF β , and TRAIL (Karsten et al., 2018). Whether or not these mediators are involved in the regulation of eryptosis should be addressed in future investigations.

A selection of important mechanisms of eryptosis is summarized in **Figure 1**.

FURTHER Ca^{2+} -DEPENDENT PROCESSES IN ERYTHROCYTES

An elevation of the cytosolic Ca^{2+} concentration results in lower O_2 affinity of hemoglobin (Bogdanova et al., 2013; Makhro et al., 2013).

Endothelial NO synthase (eNOS)-dependent NO production is stimulated by an increase in the cytosolic Ca^{2+} concentration (Ulker et al., 2011; Bogdanova et al., 2013). By the same token, NO inhibits eryptosis (Nicolay et al., 2008).

Calpain 1 (μ -calpain) is a cysteine protease that is activated by an elevation of the intracellular Ca^{2+} concentration (Bogdanova et al., 2013). It is expressed in human erythrocytes (Hatanaka et al., 1984) and degrades membrane-associated proteins

(Bogdanova et al., 2013). Calpain is likely to contribute to the breakdown of proteins in eryptosis (Lang et al., 2006).

FURTHER ION TRANSPORT MECHANISMS IN ERYTHROCYTES

Erythrocytes express the mechanosensitive non-selective cation channel PIEZO1 which is stretch-activated (Zarychanski et al., 2012; Bae et al., 2013) and opens upon mechanical stress also allowing cell volume loss (Badens and Guizouarn, 2016). Mutations of the FAM38A gene encoding PIEZO1 are responsible for hereditary xerocytosis (Zarychanski et al., 2012; Bae et al., 2013).

The anion exchanger 1 (AE1 or SLC4A1) is encoded by the SLC4A1 gene and is also known under the name Band 3 (Abbas et al., 2018). The two different names hint at distinct functions: It is the most abundant protein of the erythrocyte membrane and part of its cytoskeleton by interacting with ankyrin or band 4.2, other cytoskeleton proteins (Kümpornsin et al., 2011). As an anion exchanger, it mediates the electroneutral exchange of Cl^- ions for HCO_3^- ions which is part of the mechanism of CO_2 transport from peripheral tissues and organs to the lung (Abbas et al., 2018). In this respect, it is also known as Hamburger

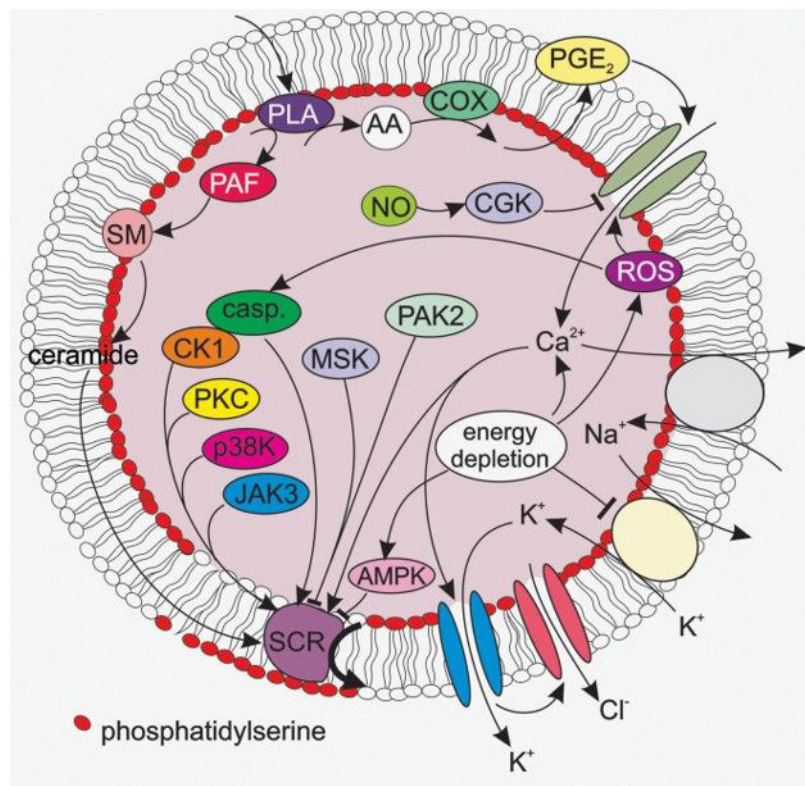


FIGURE 1 | A selection of signaling pathways relevant for eryptosis. AA, arachidonic acid; AMPK, AMP-activated kinase; casp, caspases; cGK, cGMP-dependent protein kinase 1; CK1, casein kinase 1; COX, cyclooxygenase; JAK3, janus kinase 3; MSK, mitogen- and stress- activated kinase; PAK2, p21-activated kinase 2; p38 MAPK, p38 mitogen-activated protein kinase; PAF, platelet activating factor; PGE₂, prostaglandin E₂; PKC, protein kinase C; PLA, phospholipase A; SCR, scramblase; SM, sphingomyelinase. The figure was taken from the review by Lang E. et al. (2017).

phenomenon or chloride shift (Colombo et al., 2020). Several mutations of the SLC4A1 gene are described which result in Na⁺ and/or K⁺ leakage (Guizouarn et al., 2007; Ellory et al., 2009; Barneaud-Rocca et al., 2013; Reithmeier et al., 2016). This phenomenon is not fully explained and may be due to the mutation changing AE1 into a cation channel or activating other cation channels in the erythrocyte membrane (Guizouarn et al., 2007; Ellory et al., 2009; Barneaud-Rocca et al., 2013).

In erythrocytes infected with *P. falciparum* endogenous inwardly and outwardly rectifying Cl[−] channels are activated (Huber et al., 2002). Moreover, similar anion conductances can be induced by oxidative stress (Huber et al., 2002). Hyperpolarization-activated CLCN2 chloride channels in the erythrocyte membrane contribute to this anion conductance of *Plasmodium berghei*-infected mouse erythrocytes and participate in cell volume regulation (Huber et al., 2004). These channels exhibit a 5 pS conductance and are inhibited by Zn²⁺ (Thomas et al., 2011). They are small conductance chloride channels (SCC) characterized by alternating long-lasting phases of opening and closing (Thomas et al., 2011).

Maxi-anion channels with a conductance of several hundred pS up to the nS range have been suggested to be involved in anion transport across the erythrocyte membrane (Glogowska et al., 2010). According to this study, they are not active *per se*, but can be induced by serum components and exhibit multifaceted gating mechanisms and kinetics (Glogowska et al., 2010).

An erythrocyte anion channel with particular relevance in malaria infection is part of the family of voltage-dependent anion channels (VDAC), presumably VDAC3 (Thomas et al., 2011). In the erythrocyte membrane, VDAC is part of a peripheral-type benzodiazepine receptor complex which is in addition made up by adenine nucleotide transporter (ANT) and a translocator protein (TSPO) (Thomas et al., 2011). This peripheral-type benzodiazepine receptor complex may be the molecular correlate for the maxi-anion channel suggested by a previous study (Glogowska et al., 2010). However, whether or not maxi anion channels are identical to VDACs is controversially discussed (Pinto et al., 2010). In *Plasmodium*-infected erythrocytes, the peripheral-type benzodiazepine receptor complexes involving VDAC are up-regulated and may contribute to the “new permeability pathways” that are induced in erythrocytes by the malaria pathogen and required for their intraerythrocytic survival (Bouyer et al., 2011). In line with this, pharmacological inhibition of the peripheral-type benzodiazepine receptor compromises the growth of the pathogen (Bouyer et al., 2011).

Also the gene encoding glucose carrier GLUT1 which accomplishes glucose uptake by erythrocytes can be affected by

a mutation that renders the carrier into a cation channel with Na⁺, K⁺ as well as Ca²⁺ conductance. Simultaneously, glucose transport is impaired (Weber et al., 2008).

The Rhesus-associated glycoprotein (RHAG) is an ammonia (NH₃) carrier (Ripoche et al., 2004). Importantly, it is part of the Rhesus blood group system and can transport NH₃, NH₄⁺, as well as CO₂. Mutations of the gene encoding RHAG account for overhydrated stomatocytosis characterized by hemolytic anemia and red blood cells with an enhanced cation leakage which is higher for Na⁺ than for K⁺ (Stewart et al., 2011). As a consequence, the erythrocytes are swollen (overhydrated) due to an elevated intracellular Na⁺ concentration that, in turn, enhances Na⁺/K⁺ ATPase activity. The latter results in higher need for ATP which is generated in glycolysis (Darghouth et al., 2011).

From electrophysiological recordings (patch clamping), the expression of a low conductance cation channel in erythrocytes was concluded in early studies (Kaestner, 2011). It is supposed to have a conductance of 8–17 pS (Kaestner, 2011).

It is yet unknown whether and to which extent the further ion transport mechanisms presented in this section are required for the cellular machinery initiating and executing eryptosis. Clearly, future studies are needed to address this issue.

PERSPECTIVES

Ion transport in eryptosis is still incompletely understood. Future research should address the molecular identity of the channels and transporters involved. The specific pharmacological targeting of ion transport mechanisms required for the execution of eryptosis may turn out to be favorable in different clinical conditions including anemia, impaired microcirculation, or malaria.

AUTHOR CONTRIBUTIONS

MF and FL wrote the review. Both authors contributed to the article and approved the submitted version.

FUNDING

MF work on eryptosis is supported by a grant from the Deutsche Stiftung für Herzforschung e.V. (F/04/18).

REFERENCES

- Abbas, Y. M., Toye, A. M., Rubinstein, J. L., and Reithmeier, R. A. F. (2018). Band 3 function and dysfunction in a structural context. *Curr. Opin. Hematol.* 25, 163–170. doi: 10.1097/MOH.0000000000000418
- Al Balushi, H., Hannemann, A., Rees, D., Brewin, J., and Gibson, J. S. (2019). The effect of antioxidants on the properties of red blood cells from patients with sickle cell anemia. *Front. Physiol.* 10:976. doi: 10.3389/fphys.2019.00976
- Andrews, D. A., Yang, L., and Low, P. S. (2002). Phorbol ester stimulates a protein kinase C-mediated agatoxin-TK-sensitive calcium permeability pathway in human red blood cells. *Blood* 100, 3392–3399. doi: 10.1182/blood.V100.9.3392
- Badens, C., and Guizouarn, H. (2016). Advances in understanding the pathogenesis of the red cell volume disorders. *Br. J. Haematol.* 174, 674–685. doi: 10.1111/bjh.14197
- Bae, C., Gnanasambandam, R., Nicolai, C., Sachs, F., and Gottlieb, P. A. (2013). Xerocytosis is caused by mutations that alter the kinetics of the

- mechanosensitive channel PIEZO1. *Proc. Natl. Acad. Sci. U.S.A.* 110, E1162–E1168. doi: 10.1073/pnas.1219777110
- Barneaud-Rocca, D., Etchebest, C., and Guizouarn, H. (2013). Structural model of the anion exchanger 1 (SLC4A1) and identification of transmembrane segments forming the transport site. *J. Biol. Chem.* 288, 26372–26384. doi: 10.1074/jbc.M113.465989
- Bhavsar, S. K., Gu, S., Bobbala, D., and Lang, F. (2011). Janus kinase 3 is expressed in erythrocytes, phosphorylated upon energy depletion and involved in the regulation of suicidal erythrocyte death. *Cell. Physiol. Biochem.* 27, 547–556. doi: 10.1159/000329956
- Bogdanova, A., Makhro, A., Wang, J., Lipp, P., and Kaestner, L. (2013). Calcium in red blood cells—a perilous balance. *Intern. J. Mol. Sci.* 14, 9848–9872. doi: 10.3390/ijms14059848
- Bonomini, M., Sirilli, V., Reale, M., and Arduini, A. (2001). Involvement of phosphatidylserine exposure in the recognition and phagocytosis of uremic erythrocytes. *Am. J. Kidney Dis.* 37, 807–814. doi: 10.1016/S0272-6386(01)80130-X
- Bookchin, R. M., Etzion, Z., Sorette, M., Mohandas, N., Skepper, J. N., and Lew, V. L. (2000). Identification and characterization of a newly recognized population of high-Na⁺, low-K⁺, low-density sickle and normal red cells. *Proc. Natl. Acad. Sci. U.S.A.* 97, 8045–8050. doi: 10.1073/pnas.130198797
- Bookchin, R. M., and Lew, V. L. (1980). Progressive inhibition of the Ca pump and Ca:Ca exchange in sickle red cells. *Nature* 284, 561–563. doi: 10.1038/284561a0
- Boulet, C., Doerig, C. D., and Carvalho, T. G. (2018). Manipulating eryptosis of human red blood cells: a novel antimalarial strategy? *Front. Cell. Infect. Microbiol.* 8:419. doi: 10.3389/fcimb.2018.00419
- Bouyer, G., Cuff, A., Egée, S., Kmiecik, J., Maksimova, Y., Glogowska, E., et al. (2011). Erythrocyte peripheral type benzodiazepine receptor/voltage-dependent anion channels are upregulated by *Plasmodium falciparum*. *Blood* 118, 2305–2312. doi: 10.1182/blood-2011-01-329300
- Cahalan, S. M., Lukacs, V., Ranade, S. S., Chien, S., Bandell, M., and Patapoutian, A. (2015). Piezo1 links mechanical forces to red blood cell volume. *eLife* 4:e07370. doi: 10.7554/eLife.07370
- Cimen, M. Y. B. (2008). Free radical metabolism in human erythrocytes. *Clin. Chim. Acta* 390, 1–11. doi: 10.1016/j.cca.2007.12.025
- Colombo, R., Wu, M. A., Castelli, A., Fossali, T., Rech, R., Ottolina, D., et al. (2020). The effects of severe hemoconcentration on acid-base equilibrium in critically ill patients: the forgotten role of buffers in whole blood. *J. Crit. Care* 57, 177–184. doi: 10.1016/j.jccr.2020.02.016
- D'Alessandro, A., and Zolla, L. (2017). Proteomic analysis of red blood cells and the potential for the clinic: what have we learned so far? *Expert Rev. Proteom.* 14, 243–252. doi: 10.1080/14789450.2017.1291347
- Danielczok, J., Hertz, L., Ruppenthal, S., Kaiser, E., Petkova-Kirova, P., Bogdanova, A., et al. (2017). Does erythropoietin regulate TRPC channels in red blood cells? *Cell. Physiol. Biochem.* 41, 1219–1228. doi: 10.1159/000464384
- D'Arcy, M. S. (2019). Cell death: a review of the major forms of apoptosis, necrosis and autophagy. *Cell Biol. Intern.* 43, 582–592. doi: 10.1002/cbin.11137
- Darghouth, D., Koehl, B., Heilier, J. F., Madalinski, G., Bovee, P., Bosman, G., et al. (2011). Alterations of red blood cell metabolome in overhydrated hereditary stomatocytosis. *Haematologica* 96, 1861–1865. doi: 10.3324/haematol.2011.045179
- Durant, C., Huber, S. M., and Lang, F. (2002). Oxidation induces a Cl⁻-dependent cation conductance in human red blood cells. *J. Physiol.* 539, 847–855. doi: 10.1113/jphysiol.2001.013040
- Dyrda, A., Cytlak, U., Ciusaszkiewicz, A., Lipinska, A., Cuff, A., Bouyer, G., et al. (2010). Local membrane deformations activate Ca²⁺-dependent K⁺ and anionic currents in intact human red blood cells. *PLoS One* 5:e9447. doi: 10.1371/journal.pone.0009447
- Ellory, J. C., Guizouarn, H., Borgese, F., Bruce, L. J., Wilkins, R. J., and Stewart, G. W. (2009). Review. Leaky Cl⁻-HCO₃⁻ exchangers: cation fluxes via modified AE1. *Philos. Trans. R. Soc. Lond.* 364, 189–194. doi: 10.1098/rstb.2008.0154
- Föller, M., Bobbala, D., Koka, S., Huber, S. M., Gulbins, E., and Lang, F. (2009a). Suicide for survival—death of infected erythrocytes as a host mechanism to survive malaria. *Cell. Physiol. Biochem.* 24, 133–140. doi: 10.1159/000233238
- Föller, M., Mahmud, H., Gu, S., Kucherenko, Y., Gehring, E.-M., Shumilina, E., et al. (2009b). Modulation of suicidal erythrocyte cation channels by an AMPA antagonist. *J. Cell. Mol. Med.* 13, 3680–3686. doi: 10.1111/j.1582-4934.2009.00745.x
- Föller, M., Sopjani, M., Koka, S., Gu, S., Mahmud, H., Wang, K., et al. (2009c). Regulation of erythrocyte survival by AMP-activated protein kinase. *FASEB J.* 23, 1072–1080. doi: 10.1096/fj.08-121772
- Föller, M., Feil, S., Ghoreschi, K., Koka, S., Gerling, A., Thunemann, M., et al. (2008a). Anemia and splenomegaly in cGKI-deficient mice. *Proc. Natl. Acad. Sci. U.S.A.* 105, 6771–6776. doi: 10.1073/pnas.0708940105
- Föller, M., Huber, S. M., and Lang, F. (2008b). Erythrocyte programmed cell death. *IUBMB Life* 60, 661–668. doi: 10.1002/iub.106
- Föller, M., Harris, I. S., Elia, A., John, R., Lang, F., Kavanagh, T. J., et al. (2013). Functional significance of glutamate-cysteine ligase modifier for erythrocyte survival in vitro and in vivo. *Cell Death Differ.* 20, 1350–1358. doi: 10.1038/cdd.2013.70
- Foller, M., Kasinathan, R. S., Koka, S., Lang, C., Shumilina, E., Birnbaumer, L., et al. (2008). TRPC6 contributes to the Ca(2+) leak of human erythrocytes. *Cell. Physiol. Biochem.* 21, 183–192. doi: 10.1159/000113760
- Galluzzi, L., Vitale, I., Aaronson, S. A., Abrams, J. M., Adam, D., Agostinis, P., et al. (2018). Molecular mechanisms of cell death: recommendations of the nomenclature committee on cell death 2018. *Cell Death Differ.* 25, 486–541. doi: 10.1038/s41418-017-0012-4
- Glogowska, E., Dyrda, A., Cuff, A., Bouyer, G., Egée, S., Bennekou, P., et al. (2010). Anion conductance of the human red cell is carried by a maxi-anion channel. *Blood Cells Mol. Dis.* 44, 243–251. doi: 10.1016/j.bcmd.2010.02.014
- Guizouarn, H., Martial, S., Gabillat, N., and Borgese, F. (2007). Point mutations involved in red cell stomatocytosis convert the electroneutral anion exchanger 1 to a nonselective cation conductance. *Blood* 110, 2158–2165. doi: 10.1182/blood-2006-12-063420
- Gulbins, E., Bissonnette, R., Mahboubi, A., Martin, S., Nishloka, W., Brunner, T., et al. (1995). FAS-induced apoptosis is mediated via a ceramide-initiated RAS signaling pathway. *Immunity* 2, 341–351. doi: 10.1016/1074-7613(95)90142-6
- Guo, J., Lao, Y., and Chang, D. C. (2009). “Calcium and apoptosis,” in *Handbook of Neurochemistry and Molecular Neurobiology: Neural Signaling Mechanisms*, eds A. Lajtha, and K. Mikoshiba (Boston, MA: Springer), 597–622.
- Hatanaka, M., Yoshimura, N., Murakami, T., Kannagi, R., and Murachi, T. (1984). Evidence for membrane-associated calpain I in human erythrocytes. Detection by an immunoelectrophoretic blotting method using monospecific antibody. *Biochemistry* 23, 3272–3276. doi: 10.1021/bi00309a023
- Hirschler-Laszkiewicz, I., Tong, Q., Waybill, K., Conrad, K., Keefer, K., Zhang, W., et al. (2011). The transient receptor potential (TRP) channel TRPC3 TRP domain and AMP-activated protein kinase binding site are required for TRPC3 activation by erythropoietin. *J. Biol. Chem.* 286, 30636–30646. doi: 10.1074/jbc.M111.238360
- Hirschler-Laszkiewicz, I., Zhang, W., Keefer, K., Conrad, K., Tong, Q., Chen, S.-J., et al. (2012). Trpc2 depletion protects red blood cells from oxidative stress-induced hemolysis. *Exper. Hematol.* 40, 71–83. doi: 10.1016/j.exphem.2011.09.006
- Hoffman, J. F., Joiner, W., Nehrke, K., Potapova, O., Foye, K., and Wickrema, A. (2003). The hSK4 (KCNN4) isoform is the Ca²⁺-activated K⁺ channel (Gardos channel) in human red blood cells. *Proc. Natl. Acad. Sci. U.S.A.* 100, 7366–7371. doi: 10.1073/pnas.1232342100
- Huber, S. M., Durant, C., Henke, G., van de Sand, C., Heussler, V., Shumilina, E., et al. (2004). Plasmodium induces swelling-activated ClC-2 anion channels in the host erythrocyte. *J. Biol. Chem.* 279, 41444–41452. doi: 10.1074/jbc.M407618200
- Huber, S. M., Uhlemann, A.-C., Gamper, N. L., Durant, C., Kremsner, P. G., and Lang, F. (2002). *Plasmodium falciparum* activates endogenous Cl⁻ channels of human erythrocytes by membrane oxidation. *EMBO J.* 21, 22–30. doi: 10.1093/emboj/21.1.22
- Johnson, R. M., and Gannon, S. A. (1990). Erythrocyte cation permeability induced by mechanical stress: a model for sickle cell cation loss. *Am. J. Physiol.* 259, C746–C751. doi: 10.1152/ajpcell.1990.259.5.C746
- Jong, K., de Larkin, S. K., Styles, L. A., Bookchin, R. M., and Kuypers, F. A. (2001). Characterization of the phosphatidylserine-exposing subpopulation of sickle cells. *Blood* 98, 860–867. doi: 10.1182/blood.v98.3.860
- Kaestner, L. (2011). Cation channels in erythrocytes - historical and future perspective. *TOBIOJ* 4, 27–34. doi: 10.2174/1874196701104010027
- Kaestner, L., Bogdanova, A., and Egee, S. (2020). Calcium channels and calcium-regulated channels in human red blood cells. *Adv. Exper. Med. Biol.* 1131, 625–648. doi: 10.1007/978-3-030-12457-1_25

- Karsten, E., Breen, E., and Herbert, B. R. (2018). Red blood cells are dynamic reservoirs of cytokines. *Sci. Rep.* 8:3101. doi: 10.1038/s41598-018-21387-w
- Klarl, B. A., Lang, P. A., Kempe, D. S., Niemoeller, O. M., Akel, A., Sobiesiak, M., et al. (2006). Protein kinase C mediates erythrocyte "programmed cell death" following glucose depletion. *Am. J. Physiol. Cell Physiol.* 290, C244–C253. doi: 10.1152/ajpcell.00283.2005
- Kucherenko, Y., Zelenak, C., Eberhard, M., Qadri, S. M., and Lang, F. (2012). Effect of casein kinase 1 α activator pyruvium pamoate on erythrocyte ion channels. *Cell. Physiol. Biochem.* 30, 407–417. doi: 10.1159/000339034
- Kümpornsin, K., Jiemsup, S., Yongkiettrakul, S., and Chookajorn, T. (2011). Characterization of band 3-ankyrin-Protein 4.2 complex by biochemical and mass spectrometry approaches. *Biochem. Biophys. Res. Commun.* 406, 332–335. doi: 10.1016/j.bbrc.2011.02.026
- Lang, E., Bissinger, R., Fajol, A., Salker, M. S., Singh, Y., Zelenak, C., et al. (2015a). Accelerated apoptotic death and in vivo turnover of erythrocytes in mice lacking functional mitogen- and stress-activated kinase MSK1/2. *Sci. Rep.* 5:17316. doi: 10.1038/srep17316
- Lang, E., Zelenak, C., Eberhard, M., Bissinger, R., Rotte, A., Ghashghaieina, M., et al. (2015b). Impact of cyclin-dependent kinase CDK4 inhibition on eryptosis. *Cell. Physiol. Biochem.* 37, 1178–1186. doi: 10.1159/000430241
- Lang, E., Bissinger, R., Qadri, S. M., and Lang, F. (2017). Suicidal death of erythrocytes in cancer and its chemotherapy: a potential target in the treatment of tumor-associated anemia. *Intern. J. Cancer* 141, 1522–1528. doi: 10.1002/ijc.30800
- Lang, F., Bissinger, R., Abed, M., and Artunc, F. (2017). Eryptosis - the neglected cause of anemia in end stage renal disease. *Kidney Blood Press. Res.* 42, 749–760. doi: 10.1159/000484215
- Lang, E., and Lang, F. (2015). Triggers, inhibitors, mechanisms, and significance of eryptosis: the suicidal erythrocyte death. *Biomed. Res. Intern.* 2015:513518. doi: 10.1155/2015/513518
- Lang, F., Abed, M., Lang, E., and Föller, M. (2014). Oxidative stress and suicidal erythrocyte death. *Antioxid. Redox Sign.* 21, 138–153. doi: 10.1089/ars.2013.5747
- Lang, F., Gulbins, E., Lerche, H., Huber, S. M., Kempe, D. S., and Föller, M. (2008). Eryptosis, a window to systemic disease. *Cell. Physiol. Biochem.* 22, 373–380. doi: 10.1159/000185448
- Lang, F., Lang, K. S., Lang, P. A., Huber, S. M., and Wieder, T. (2006). Mechanisms and significance of eryptosis. *Antioxid. Redox Signal.* 8, 1183–1192. doi: 10.1089/ars.2006.8.1183
- Lang, K. S., Myssina, S., Brand, V., Sandu, C., Lang, P. A., Berchtold, S., et al. (2004). Involvement of ceramide in hyperosmotic shock-induced death of erythrocytes. *Cell Death Differ.* 11, 231–243. doi: 10.1038/sj.cdd.4401311
- Lang, K. S., Myssina, S., Tanneur, V., Wieder, T., Huber, S. M., Lang, F., et al. (2003). Inhibition of erythrocyte cation channels and apoptosis by ethylisopropylamiloride. *Naunyn Schmiedeb. Arch. Pharmacol.* 367, 391–396. doi: 10.1007/s00210-003-0701-z
- Lang, P. A., Kaiser, S., Myssina, S., Wieder, T., Lang, F., and Huber, S. M. (2003). Role of Ca²⁺-activated K⁺ channels in human erythrocyte apoptosis. *Am. J. Physiol.* 285, C1553–C1560. doi: 10.1152/ajpcell.00186.2003
- Lang, P. A., Kempe, D. S., Myssina, S., Tanneur, V., Birka, C., Laufer, S., et al. (2005). PGE(2) in the regulation of programmed erythrocyte death. *Cell Death Differ.* 12, 415–428. doi: 10.1038/sj.cdd.4401561
- Larsen, F. L., Katz, S., Roufogalis, B. D., and Brooks, D. E. (1981). Physiological shear stresses enhance the Ca²⁺ permeability of human erythrocytes. *Nature* 294, 667–668. doi: 10.1038/294667a0
- Makhro, A., Hänggi, P., Goede, J. S., Wang, J., Brüggemann, A., Gassmann, M., et al. (2013). N-methyl-D-aspartate receptors in human erythroid precursor cells and in circulating red blood cells contribute to the intracellular calcium regulation. *Am. J. Physiol.* 305, C1123–C1138. doi: 10.1152/ajpcell.00031.2013
- Mandal, D., Moitra, P. K., Saha, S., and Basu, J. (2002). Caspase 3 regulates phosphatidylserine externalization and phagocytosis of oxidatively stressed erythrocytes. *FEBS Lett.* 513, 184–188. doi: 10.1016/S0014-5793(02)02294-9
- Myssina, S., Huber, S. M., Birka, C., Lang, P. A., Lang, K. S., Friedrich, B., et al. (2003). Inhibition of erythrocyte cation channels by erythropoietin. *J. Am. Soc. Nephrol.* 14, 2750–2757. doi: 10.1097/01.asn.0000093253.42641.c1
- Nemkov, T., Reisz, J. A., Xia, Y., Zimmering, J. C., and D'Alessandro, A. (2018). Red blood cells as an organ? How deep omics characterization of the most abundant cell in the human body highlights other systemic metabolic functions beyond oxygen transport. *Expert Rev. Proteom.* 15, 855–864. doi: 10.1080/14789450.2018.1531710
- Nicolay, J. P., Liebig, G., Niemoeller, O. M., Koka, S., Ghashghaieina, M., Wieder, T., et al. (2008). Inhibition of suicidal erythrocyte death by nitric oxide. *Pflugers Archiv.* 456, 293–305. doi: 10.1007/s00424-007-0393-1
- Oliván-Viguera, A., Valero, M. S., Murillo, M. D., Wulff, H., García-Otín, A.-L., Arbonés-Mainar, J.-M., et al. (2013). Novel phenolic inhibitors of small/intermediate-conductance Ca²⁺-activated K⁺ channels, KCa3.1 and KCa2.3. *PLoS One* 8:e58614. doi: 10.1371/journal.pone.0058614
- Pinto, V., de, Messina, A., Lane, D. J. R., and Lawen, A. (2010). Voltage-dependent anion-selective channel (VDAC) in the plasma membrane. *FEBS Lett.* 584, 1793–1799. doi: 10.1016/j.febslet.2010.02.049
- Pretorius, E. (2018). Erythrocyte deformability and eryptosis during inflammation, and impaired blood rheology. *Clin. Hemorheol. Microcirc.* 69, 545–550. doi: 10.3233/CH-189205
- Pretorius, E., Du Plooy, J. N., and Bester, J. (2016). A comprehensive review on eryptosis. *Cell. Physiol. Biochem.* 39, 1977–2000. doi: 10.1159/000447895
- Qian, Q., Nath, K. A., Wu, Y., Daoud, T. M., and Sethi, S. (2010). Hemolysis and acute kidney failure. *Am. J. Kidney Dis.* 56, 780–784. doi: 10.1053/j.ajkd.2010.03.025
- Ramsey, I. S., Delling, M., and Clapham, D. E. (2006). An introduction to TRP channels. *Annu. Rev. Physiol.* 68, 619–647. doi: 10.1146/annurev.physiol.68.040204.100431
- Rapetti-Mauss, R., Lacoste, C., Picard, V., Guitton, C., Lombard, E., Loosveld, M., et al. (2015). A mutation in the gardos channel is associated with hereditary xerocytosis. *Blood* 126, 1273–1280. doi: 10.1182/blood-2015-04-642496
- Reithmeier, R. A. F., Casey, J. R., Kalli, A. C., Sansom, M. S. P., Alguet, Y., and Iwata, S. (2016). Band 3, the human red cell chloride/bicarbonate anion exchanger (AE1, SLC4A1), in a structural context. *Biochim. Biophys. Acta* 1858, 1507–1532. doi: 10.1016/j.bbame.2016.03.030
- Repsold, L., and Joubert, A. M. (2018). Eryptosis: an erythrocyte's suicidal type of cell death. *Biomed. Res. Intern.* 2018:9405617. doi: 10.1155/2018/9405617
- Ricciotti, E., and FitzGerald, G. A. (2011). Prostaglandins and inflammation. *Arterioscler. Thromb. Vasc. Biol.* 31, 986–1000. doi: 10.1161/ATVBAHA.110.207449
- Ripoche, P., Bertrand, O., Gane, P., Birkenmeier, C., Colin, Y., and Cartron, J.-P. (2004). Human rhesus-associated glycoprotein mediates facilitated transport of NH(3) into red blood cells. *Proc. Natl. Acad. Sci. U.S.A.* 101, 17222–17227. doi: 10.1073/pnas.0403704101
- Segawa, K., and Nagata, S. (2015). An apoptotic 'eat me' signal: phosphatidylserine exposure. *Trends Cell Biol.* 25, 639–650. doi: 10.1016/j.tcb.2015.08.003
- Setty, B. N. Y., and Betal, S. G. (2008). Microvascular endothelial cells express a phosphatidylserine receptor: a functionally active receptor for phosphatidylserine-positive erythrocytes. *Blood* 111, 905–914. doi: 10.1182/blood-2007-07-099465
- Shih, A. W. Y., McFarlane, A., and Verhovsek, M. (2014). Haptoglobin testing in hemolysis: measurement and interpretation. *Am. J. Hematol.* 89, 443–447. doi: 10.1002/ajh.23623
- Stewart, A. K., Shmukler, B. E., Vandorpe, D. H., Rivera, A., Heneghan, J. F., Li, X., et al. (2011). Loss-of-function and gain-of-function phenotypes of stomatocytosis mutant RhAG F65S. *Am. J. Physiol. Cell Physiol.* 301, C1325–C1343. doi: 10.1152/ajpcell.00054.2011
- Thomas, S. L. Y., Bouyer, G., Cuff, A., Egée, S., Glogowska, E., and Ollivaux, C. (2011). Ion channels in human red blood cell membrane: actors or relics? *Blood Cells Mol. Dis.* 46, 261–265. doi: 10.1016/j.bcmd.2011.02.007
- Ulker, P., Yaras, N., Yalcin, O., Celik-Ozenci, C., Johnson, P. C., Meiselman, H. J., et al. (2011). Shear stress activation of nitric oxide synthase and increased nitric oxide levels in human red blood cells. *Nitr. Oxide* 24, 184–191. doi: 10.1016/j.niox.2011.03.003
- Wagner-Britz, L., Wang, J., Kaestner, L., and Bernhardt, I. (2013). Protein kinase C α and P-type Ca channel CaV2.1 in red blood cell calcium signalling. *Cell. Physiol. Biochem.* 31, 883–891. doi: 10.1159/000350106
- Wautier, M.-P., Héron, E., Picot, J., Colin, Y., Hermine, O., and Wautier, J.-L. (2011). Red blood cell phosphatidylserine exposure is responsible for increased erythrocyte adhesion to endothelium in central retinal vein occlusion. *J. Thromb. Haemost.* 9, 1049–1055. doi: 10.1111/j.1538-7836.2011.04251.x

- Weber, Y. G., Storch, A., Wuttke, T. V., Brockmann, K., Kempfle, J., Maljevic, S., et al. (2008). GLUT1 mutations are a cause of paroxysmal exertion-induced dyskinesias and induce hemolytic anemia by a cation leak. *J. Clin. Invest.* 118, 2157–2168. doi: 10.1172/JCI34438
- Weiss, E., Cytlak, U. M., Rees, D. C., Osei, A., and Gibson, J. S. (2012). Deoxygenation-induced and Ca(2+) dependent phosphatidylserine externalisation in red blood cells from normal individuals and sickle cell patients. *Cell Calc.* 51, 51–56. doi: 10.1016/j.ceca.2011.10.005
- Yasin, Z., Witting, S., Palascak, M. B., Joiner, C. H., Rucknagel, D. L., and Franco, R. S. (2003). Phosphatidylserine externalization in sickle red blood cells: associations with cell age, density, and hemoglobin F. *Blood* 102, 365–370. doi: 10.1182/blood-2002-11-3416
- Zarychanski, R., Schulz, V. P., Houston, B. L., Maksimova, Y., Houston, D. S., Smith, B., et al. (2012). Mutations in the mechanotransduction protein PIEZO1 are associated with hereditary xerocytosis. *Blood* 120, 1908–1915. doi: 10.1182/blood-2012-04-422253
- Zeidan, Y. H., and Hannun, Y. A. (2010). The acid sphingomyelinase/ceramide pathway: biomedical significance and mechanisms of regulation. *Curr. Mol. Med.* 10, 454–466. doi: 10.2174/156652410791608225
- Zelenak, C., Eberhard, M., Jilani, K., Qadri, S. M., Macek, B., and Lang, F. (2012). Protein kinase CK1 α regulates erythrocyte survival. *Cell. Physiol. Biochem.* 29, 171–180. doi: 10.1159/000337598
- Zelenak, C., Föller, M., Velic, A., Krug, K., Qadri, S. M., Viollet, B., et al. (2011). Proteome analysis of erythrocytes lacking AMP-activated protein kinase reveals a role of PAK2 kinase in eryptosis. *J. Proteom. Res.* 10, 1690–1697. doi: 10.1021/pr101004j

Conflict of Interest: The authors declare that the research was conducted in the absence of any commercial or financial relationships that could be construed as a potential conflict of interest.

Copyright © 2020 Föller and Lang. This is an open-access article distributed under the terms of the Creative Commons Attribution License (CC BY). The use, distribution or reproduction in other forums is permitted, provided the original author(s) and the copyright owner(s) are credited and that the original publication in this journal is cited, in accordance with accepted academic practice. No use, distribution or reproduction is permitted which does not comply with these terms.



Ferroptosis in Acute Central Nervous System Injuries: The Future Direction?

Lesang Shen^{1†}, Danfeng Lin^{2†}, Xiaoyi Li³, Haijian Wu⁴, Cameron Lenahan^{5,6}, Yuanbo Pan^{5,6}, Weilin Xu^{5,6}, Yiding Chen^{1*}, Anwen Shao^{4*} and Jianmin Zhang⁴

¹ Department of Breast Surgery, The Second Affiliated Hospital, Zhejiang University School of Medicine, Hangzhou, China,

² Department of Surgical Oncology, The Second Affiliated Hospital, Zhejiang University School of Medicine, Hangzhou, China, ³ Department of Nuclear Medicine and PET-CT Center, The Second Hospital, Zhejiang University School of Medicine, Hangzhou, China, ⁴ Department of Neurosurgery, The Second Affiliated Hospital, Zhejiang University School of Medicine, Hangzhou, China, ⁵ Burrell College of Osteopathic Medicine, Las Cruces, NM, United States, ⁶ Center for Neuroscience Research, School of Medicine, Loma Linda University, Loma Linda, CA, United States

OPEN ACCESS

Edited by:

Alexander A. Mongin,
Albany Medical College, United States

Reviewed by:

Sandra Hewett,
Syracuse University, United States
Chunying Li,
Georgia State University,
United States

*Correspondence:

Anwen Shao
21118116@zju.edu.cn;
anwenshao@sina.com
Yiding Chen
ydchen@zju.edu.cn

[†] These authors have contributed
equally to this work

Specialty section:

This article was submitted to
Cell Death and Survival,
a section of the journal
Frontiers in Cell and Developmental
Biology

Received: 11 March 2020

Accepted: 18 June 2020

Published: 15 July 2020

Citation:

Shen L, Lin D, Li X, Wu H,
Lenahan C, Pan Y, Xu W, Chen Y,
Shao A and Zhang J (2020)
Ferroptosis in Acute Central Nervous
System Injuries: The Future Direction?
Front. Cell Dev. Biol. 8:594.
doi: 10.3389/fcell.2020.00594

Acute central nervous system (CNS) injuries, such as stroke, traumatic brain injury (TBI), and spinal cord injury (SCI) present a grave health care challenge worldwide due to high morbidity and mortality, as well as limited clinical therapeutic strategies. Established literature has shown that oxidative stress (OS), inflammation, excitotoxicity, and apoptosis play important roles in the pathophysiological processes of acute CNS injuries. Recently, there have been many studies on the topic of ferroptosis, a form of regulated cell death characterized by the accumulation of iron-dependent lipid peroxidation. Some studies have revealed an emerging connection between acute CNS injuries and ferroptosis. Ferroptosis, induced by the abnormal metabolism of lipids, glutathione (GSH), and iron, can accelerate acute CNS injuries. However, pharmaceutical agents, such as iron chelators, ferrostatin-1 (Fer-1), and liproxstatin-1 (Lip-1), can inhibit ferroptosis and may have neuroprotective effects after acute CNS injuries. However, the specific mechanisms underlying this connection has not yet been clearly elucidated. In this paper, we discuss the general mechanisms of ferroptosis and its role in stroke, TBI, and SCI. We also summarize ferroptosis-related drugs and highlight the potential therapeutic strategies in treating various acute CNS injuries. Additionally, this paper suggests a testable hypothesis that ferroptosis may be a novel direction for further research of acute CNS injuries by providing corresponding evidence.

Keywords: ferroptosis, iron metabolism, lipid metabolism, stroke, traumatic brain injury, spinal cord injury, therapy

INTRODUCTION

Acute CNS injuries, including stroke, TBI, and SCI, are a major burden of morbidity and mortality worldwide (GBD, 2016, 2019). Each year, approximately 80 million individuals in the United States suffer a stroke. Moreover, deaths caused by stroke contribute to nearly 5% of all deaths in the United States. Ischemic stroke accounts for 87% of all strokes, with ICH comprising the remaining 10% (Benjamin et al., 2019). Another neurological disease worth mentioning is TBI, which has a global incidence of more than 50 million cases annually (Maas et al., 2017; Jiang et al., 2019). Regarding the mechanisms associated with acute CNS injuries, previous literature has shown that

various mechanisms, including OS, inflammation, excitotoxicity, and apoptosis, play important roles in the pathophysiological processes of acute CNS, and targeting these mechanisms may provide neuroprotection (Roth et al., 2014; Chamorro et al., 2016; Duan et al., 2019; Nazemi et al., 2020). However, there is a lack of effective therapeutic strategies in treating long-term CNS injuries. Patients who survive CNS injuries often have long-term disabilities due to substantial neurological deficits and impaired tissue function, therefore requiring subsequent lifelong care. New therapeutic approaches are urgently required to improve outcomes of patients with acute CNS injuries. In recent years, there has been increasing interest in ferroptosis, suggesting a potential role of ferroptosis in acute CNS injuries and offering opportunities for novel pharmacological interventions, as ferroptosis can be modulated by small molecules (Friedmann Angeli et al., 2014; Lewerenz et al., 2018; Alim et al., 2019).

Ferroptosis, first observed in response to treatment of tumor cells via small-molecule chemical probes, is a newly identified form of regulated cell death characterized by the accumulation of iron-mediated lipid peroxides (Dixon et al., 2012). It differs from other programmed cell deaths (e.g., apoptosis, necrosis, and autophagy) at the morphological, biological, and genetic levels (Dixon et al., 2012). Regarding the function of ferroptosis within the tumor, it is associated with malignant transformation, cancer progression, and drug resistance [for review see Su et al. (2020)]. Moreover, ferroptosis regulation may be useful for anti-cancer therapy (Guo et al., 2019; Su et al., 2020). Although ferroptosis was first defined in cancer cells and has potential in cancer treatment, the latest experimental results have identified its role in the pathophysiology of acute organ injuries, such as acute kidney, lung, and brain injuries (Dixon et al., 2012; Friedmann Angeli et al., 2014; Kenny et al., 2019; Hu et al., 2020; Li Y.C. et al., 2020). More importantly, ferroptosis can cause neuronal cell death and neurological deficits in CNS injuries and human neurodegenerative diseases (Dixon et al., 2012; Morris et al., 2018). Therefore, targeting ferroptosis through effective anti-ferroptotic agents may provide direction for treating acute CNS injuries (Tuo et al., 2017; Zille et al., 2017; Kenny et al., 2019).

Abbreviations: 4-HNE, 4-hydroxy-2-nonenal; AA, arachidonic acid; ACSL4, acyl-CoA synthetase long-chain family member 4; AdA, adrenic acid; ALOX5, arachidonate 5-lipoxygenase; BBB, blood–brain barrier; BMSC, bone marrow mesenchymal stem cells; BPS, bathophenanthrolinedisulfonic acid; BSO, buthionine sulfoximine; CCI, cortical impact injury; CNS, central nervous system; CoQ10, coenzyme Q10; COX-2, cyclooxygenase-2; DFO, deferoxamine; DFP, deferiprone; DMT1, divalent metal transporter 1; EC, (-)-epicatechin; Fe^{2+} , ferrous iron; Fe^{3+} , ferric iron; Fer-1, ferrostatin-1; FPN, ferroportin; FSP1, ferroptosis suppressor protein 1; FTH1, ferritin heavy chain 1; FTL, ferritin light chain; GPX4, glutathione peroxidases 4; GSH, glutathione; Hb, hemoglobin; HIF-1 α , hypoxia-inducible factor 1 α ; HIF-1 β , hypoxia-inducible factor prolyl hydroxylase; I/R, ischemia/reperfusion; ICH, intracerebral hemorrhage; IREB2, iron metabolism essential factor iron response element binding protein 2; Lip-1, liprostatin-1; LOX, lipoxygenases; LPCAT3, lysophosphatidylcholine acyltransferase 3; MCAO, middle cerebral artery occlusion; MDA, malondialdehyde; NAC, N-acetylcysteine; NACA, N-acetylcysteine amide; Nrf2, nuclear factor erythroid 2-related factor; OS, oxidative stress; PEBP1, phosphatidylethanolamine-binding protein 1; PTGS2, prostaglandin-endoperoxide synthase 2; PUFA, polyunsaturated fatty acid; ROS, reactive oxygen species; RSL3, RAS synthetic lethal 3; SBI, secondary brain injury; SCI, spinal cord injury; Se, selenium; STEAP3, six-transmembrane epithelial antigen of the prostate 3; TBI, traumatic brain injury; TEM, transmission electron microscopy; Tf, transferrin; TFR, transferrin receptor.

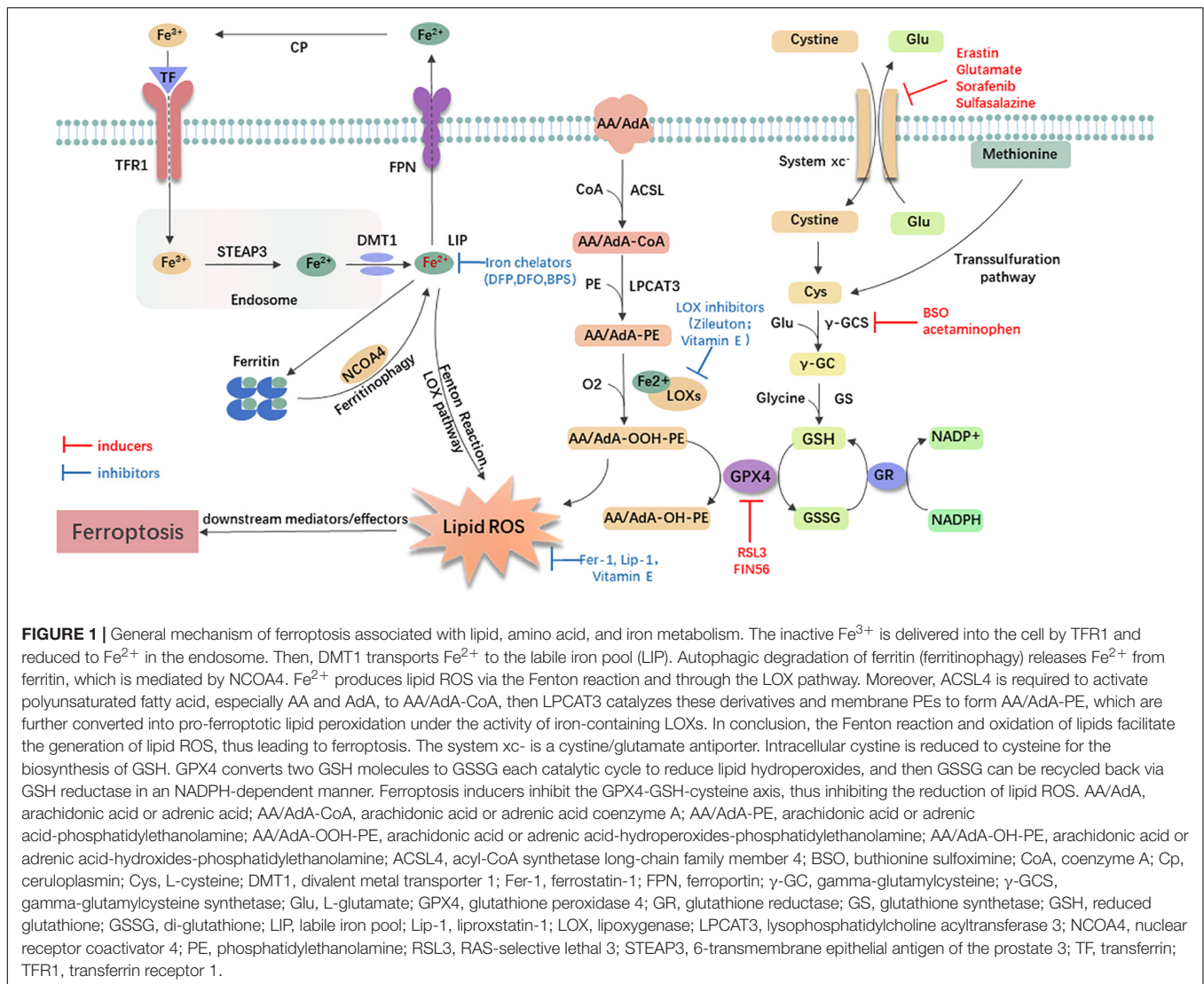
So, what is the underlying mechanism of ferroptosis, and how does it affect acute CNS injuries?

DISCOVERY AND MECHANISMS OF FERROPTOSIS

Small-molecule probes are valuable tools for studying different types of regulated cell death (Gangadhar and Stockwell, 2007). During the identification of ferroptosis, there were two important chemical probes. Ferroptosis inducers, erastin, and RSL3, were discovered in a phenotypic small molecule-screening study (Dolma et al., 2003; Yang and Stockwell, 2008). Erastin, a synthetic compound, was capable of inducing non-apoptotic cell death to selectively kill HRAS-mutant engineered cancer cells, and in this process, there was no evidence of caspase activation or apoptotic hallmarks (Dolma et al., 2003; Yagoda et al., 2007). Another compound was RSL3, found in 2008, and capable of triggering a similar form of non-apoptotic and iron-dependent oxidative cell death (Yang and Stockwell, 2008). This erastin- and RSL3-induced cell death did not exhibit the morphological or biochemical features of apoptosis, and inhibition of necroptosis or autophagy had no effect on this mode of cell death (Wolpaw et al., 2011; Dixon et al., 2012; Yang et al., 2014). However, this manner of cell death could be prevented by the iron chelator, DFO, and antioxidants (e.g., Vitamin E) (Dolma et al., 2003; Yagoda et al., 2007; Yang and Stockwell, 2008). Therefore, the term “ferroptosis” was first proposed in 2012 to describe this novel iron-dependent non-apoptotic cell death (Dixon et al., 2012). Hallmark contributions of ferroptosis were well-displayed by Hirschhorn and Stockwell (2019) and Li J. et al. (2020) [for review see Hirschhorn and Stockwell (2019); Li J. et al. (2020)]. Hadian and Stockwell (2020) drew a Snapshot to provide an overview of ferroptosis-related pathways. Although the exact mechanisms of ferroptosis are still being explored, the initiation and execution of ferroptosis involve several biological processes, including lipid, GSH, and iron metabolism, as well as other regulatory processes (Dixon et al., 2012; **Figure 1**).

Lipid Metabolism Related to Ferroptosis

Lipid metabolism is closely linked to the regulation of ferroptosis. The accumulation of lipid peroxidation seems to be a key process in the execution phase, in which PUFAs play an important role (Stockwell et al., 2017; Wenzel et al., 2017; Yamada et al., 2020). Usually, free PUFAs, especially AA and AdA are esterified to membrane phospholipids [mainly PUFA-containing phosphatidylethanolamines (PEs)]. With the presence of two lipid-metabolic enzymes, ACSL4 and LPCAT3, these membrane phospholipids undergo oxidation to drive ferroptosis (Doll et al., 2017; Kagan et al., 2017). The knockout of ACSL4 or loss of LPCAT3 resulted in significant resistance of certain non-neuronal cells to ferroptosis (Dixon et al., 2015; Yuan et al., 2016; Doll et al., 2017; Kagan et al., 2017). Following the generation of AA/AdA-PE, activated LOXs catalyze AA/AdA-PE into pro-ferroptotic lipid peroxidation AA/AdA-OOH-PE (Yang et al., 2016; Lei et al., 2019). The role of the LOXs in ferroptosis is also supported by a study indicating that genetic depletion



or inhibition of LOXs by inhibitors [e.g., zileuton (Liu et al., 2015) and Vitamin E hydroquinone (Hinman et al., 2018)] could protect against ferroptosis in some cell types (Seiler et al., 2008; Yang et al., 2016). Recently, PEBP1 was shown to bind 15-LOX and alter the substrate specificity, changing it from free fatty acid to AA-PE, thereby promoting lipid oxidation (Wenzel et al., 2017). Furthermore, lipid peroxidation is thought to play a role in the final phase of ferroptosis, although the downstream mechanisms remain unclear (Lei et al., 2019). In one hypothesis, lipid peroxides may decompose into reactive toxic aldehydes, such as MDA or 4-HNEs. These decomposed substances react with proteins, nucleic acids, and membrane lipids to initiate ferroptosis (Domingues et al., 2013; Zhong and Yin, 2015). Dixon et al. also favored the hypothesis that showed that increased expression of AKRF1C genes could suppress ferroptosis by encoding aldoketoreductases to detoxify the end-products of lipid peroxidation (Dixon and Stockwell, 2014; Stockwell et al., 2017). As for inhibitors of lipid peroxidation, ferrostatins are the novel synthetic antioxidants that specifically trap lipid radicals

and exert anti-ferroptotic function. Fer-1, the first-generation ferrostatin, prevents ferroptosis induced by erastin and RSL3 in HT1080 cells (Dixon et al., 2012). Lip-1 is another recently discovered ferroptosis inhibitor. It can prevent the accumulation of lipid ROS and inhibit erastin- or RSL3- induced ferroptosis *in vitro* (Friedmann Angeli et al., 2014). In conclusion, AA/AdA-related lipid metabolism can induce ferroptosis, and inhibiting LOXs or lipid peroxidation may have protective effects.

Glutathione Metabolism Related to Ferroptosis

Previous studies have identified that two major mechanisms, the Se-dependent GPX4-GSH-cysteine axis (Friedmann Angeli et al., 2014; Yang et al., 2014; Friedmann Angeli and Conrad, 2018; Ingold et al., 2018) and the FSP1-ubiquinone (CoQ10)-NAD(P)H pathway (Bersuker et al., 2019; Doll et al., 2019), were associated with lipid peroxidation and ferroptotic cell death. Additionally, the FSP1-CoQ10-NAD(P)H pathway is a complementary system

to the GPX4-GSH-cysteine axis for controlling ferroptosis. In this axis, key steps include cystine uptake via system xc⁻, reduction of cystine to cysteine, GSH biosynthesis, and GPX4-mediated reduction of phospholipid hydroperoxides to lipid alcohols. During the process, the cystine/glutamate antiporter (system xc⁻) which consists of the light-chain subunit xCT (SLC7A11) and the heavy-chain subunit CD98 (SLC3A2) exchanges intracellular glutamate for extracellular cystine at a ratio of 1:1. Cystine is then reduced to cysteine for GSH synthesis [for review see Xie et al. (2016)]. In this regard, several agents [e.g., glutamate and erastin (Dixon et al., 2012), sulfasalazine (Gout et al., 2001), and sorafenib (Dixon et al., 2014)] can inhibit the system xc⁻ to cause the decreased acquisition of precursors and GSH depletion, ultimately leading to ferroptosis. Other agents, including BSO (Sun et al., 2018) and acetaminophen (Lorincz et al., 2015), were observed directly blocking GSH synthesis. Conversely, ferroptosis induced by cystine deprivation can be reversed by reagents that increase the level of intracellular cysteine/cystine. For example, an *in vitro* study showed that when in the presence of β -mercaptoethanol, the cells were able to constantly utilize cystine through a mixed disulfide of β -mercaptoethanol and cysteine (Ishii et al., 1981). In addition, the loss of cysteinyl-tRNA synthetase, as Hayano et al. (2016) indicated, could trigger the transsulfuration pathway and lead to inhibition of ferroptosis induced by cystine deprivation.

Glutathione peroxidases 4 is a type of selenoprotein that contains one selenocysteine at the active site and seven cysteines. It plays an important role in regulating ferroptosis, and its inhibition promotes ferroptosis (Yang et al., 2016). Regarded as the only GPX that can eliminate biomembrane lipid peroxidation, GPX4 has a unique ability in ferroptosis. It is capable of reducing the toxic, membranous lipid hydroperoxides into non-toxic lipid alcohols (Brigelius-Flohé and Maiorino, 2013; Yang et al., 2014). Increasing GPX4 has been shown to be beneficial in many models of disease by inhibiting ferroptosis (Lan et al., 2020; Shen et al., 2020). However, knockdown or inactivation of GPX4 contributes to the accumulation of lipid peroxidation and initiation of ferroptosis (Park et al., 2019; Ye et al., 2020). For example, RSL3 directly inactivated GPX4 by covalently binding to selenocysteine to trigger ferroptosis (Yang et al., 2014, 2016), and FIN56 promoted degradation of GPX4 (Shimada et al., 2016).

Iron Metabolism Related to Ferroptosis

Besides lipid and GSH metabolism, the essential trace element for life, iron, is indispensable for the execution of ferroptosis (Dixon and Stockwell, 2014). The circulating Fe³⁺ and TF complex are endocytosed into cells by the membrane protein transferrin receptor 1 (TFR1). In the endosome, Fe³⁺ is reduced to Fe²⁺ by STEAP3, and Fe²⁺ is then released into unstable iron pools mediated by DMT1, or stored in ferritin, which is composed of FTL and FTH1 (Yang and Stockwell, 2008; Dixon et al., 2012). Excessive Fe²⁺ is exported through the membrane protein FPN and oxidized by ferroxidases, such as ceruloplasmin (Bogdan et al., 2016; Shang et al., 2020). In this process, iron accumulation (Shang et al., 2020) and administration of iron-bound, rather than iron-free TF, promote erastin-induced

ferroptosis (Gao et al., 2015). On the contrary, using some iron chelators [e.g., DFP (Wu et al., 2020), DFO (Wu et al., 2018; Chen et al., 2020), and BPS (Codonotti et al., 2018)] may suppress ferroptosis and provide a potential therapeutic approach for diseases. In fact, there are some iron-chelating agents under clinical development for the treatment of cancers [for review see Brown et al. (2020)]. Moreover, inhibition of the IREB2 increases the expression of FTL and FTH1, thus decreasing sensitivity to ferroptosis (Gammella et al., 2015).

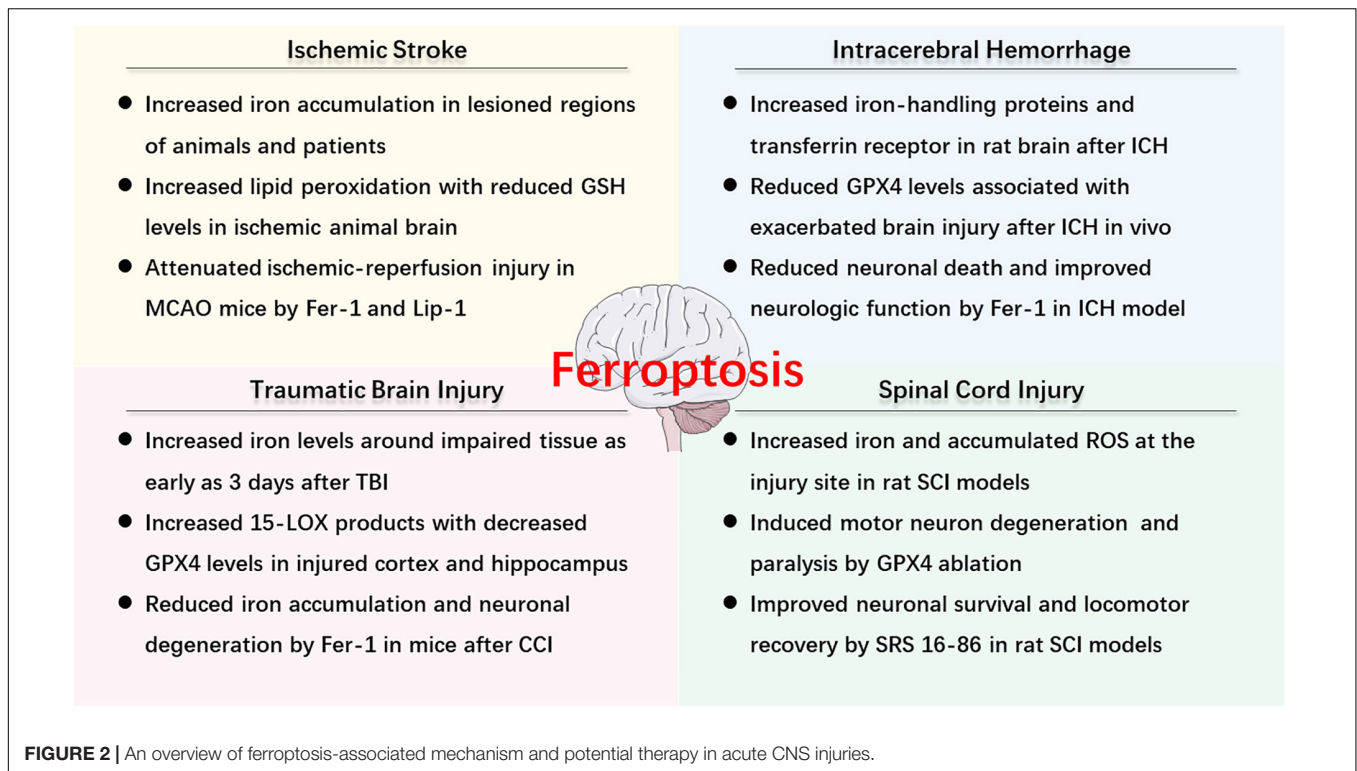
Although the importance of intracellular free iron in ferroptosis is confirmed, the regulatory mechanism of iron remains unknown. To date, the evidence has shown that the non-enzymatic free radical chain reaction involving Fenton Chemistry, in which Fe²⁺ is converted to Fe³⁺ with increased ROS (Winterbourn, 1995; He et al., 2020), and enzymatic processes (most notably the lipoxygenase pathway, LOXs), contributed to the formation of lipid peroxides in ferroptosis. Moreover, iron may promote ferroptosis through other iron-dependent enzymes, such as HIF-PHDs (Siddiq et al., 2009). Therefore, iron metabolism is one of the mechanisms of ferroptosis, and utilizing iron chelators to decrease iron may be useful for treating diseases.

THE ROLE AND MECHANISM OF FERROPTOSIS IN ACUTE CNS INJURIES

As described above, ferroptosis is an iron-dependent cell death that involves abnormal metabolism of lipids, GSH, and iron. The methods of measurement in evaluating ferroptosis in diverse diseases mainly depend on monitoring the levels of iron and lipid peroxidation, the activity of GPX4, as well as the ability of ferroptosis inhibitors (e.g., iron chelators, LOX inhibitors, and ferrostatins) to reduce cell death [for review see Xie et al. (2016)]. Observations of typical morphological features under a TEM also contribute to the distinguishing characteristics of ferroptosis compared to other cell deaths, both *in vitro* and *in vivo* (Friedmann Angeli et al., 2014; Alim et al., 2019; Li et al., 2019d). Recently, numerous studies have confirmed the hypothesis of ferroptosis in the pathophysiology of acute CNS injuries, including stroke (Alim et al., 2019; Guan et al., 2019), TBI (Kenny et al., 2019; Xiao et al., 2019; Xie et al., 2019), and SCI (Dinc et al., 2013; Hu et al., 2017). More studies are included in the following text and Figure 2 is a brief summary of ferroptosis in acute CNS injuries.

The Role and Mechanism of Ferroptosis in Ischemic Stroke

Ischemic stroke occurs when the blood flow to a certain portion of the brain is obstructed secondary to occlusion of cerebral arteries. The following deprivation of oxygen and energy triggers an ischemic cascade, such as OS and inflammation, resulting in neuronal excitotoxicity and cell death (Khoshnam et al., 2017; Li et al., 2019a; Zhang K. et al., 2019). Before ferroptosis was defined, iron accumulation [for review see Selim and Ratan (2004)] had been found in lesioned regions, such as the basal ganglia and the hippocampal area of the brain, and iron overload exaggerated neuronal damage during reperfusion (Dietrich and Bradley, 1988;



Kondo et al., 1995; Lipscomb et al., 1998; Park et al., 2011). In MCAO animals, the iron intake was positively associated with the infarct volume (Castellanos et al., 2002; García-Yébenes et al., 2012). Consistently, one *in vitro* study demonstrated that holo-transferrin increased ROS production, and caused neuronal cell death induced by deprivation of oxygen and glucose (DeGregorio-Rocasolano et al., 2018). The experimental results also illustrated that administration of exogenous apotransferrin reduced brain damage and improved neurological outcomes with decreased lipid peroxidation, supporting the involvement of ferroptosis in ischemia (DeGregorio-Rocasolano et al., 2018). What's more, the iron levels in the brain increased as humans age (Ward et al., 2014), which may exacerbate ischemic stroke. Recently, the tau-iron interaction has been proposed as an effective modulator of ferroptosis in ischemic stroke. The tau knockout mice were found to have increased protection from ferroptotic cell death following I/R injury, and the benefit of tau knockout was reinstated in older mice using iron-targeting interventions (Tuo et al., 2017). In this regard, iron chelation therapy reduced ischemic damage and improved outcome in mammals after ischemic stroke (Freret et al., 2006; Hanson et al., 2009). Consistently, Speer et al. (2013) found that the iron-dependent HIF-PHDs served as a target of metal chelators in ferroptosis, and the administration of iron chelators could inhibit HIF-PHDs, rather than suppress Fenton's Reaction or ROS production, providing beneficial effects on subjects.

Additionally, other ferroptosis-associated mechanisms, such as LOXs-mediated pathology (Yang et al., 2016) and the GPX4-GSH-cysteine axis (Cho et al., 2007; Guan et al., 2019), were found to be involved in brain ischemia. MDA, a marker

of oxidized lipids, was noticeably elevated, and this change correlated with increased activity of LOXs in an ischemic animal brain (Yigitkanli et al., 2013; Guan et al., 2019). Treatment with 12/15-LOX inhibitor (ML351) was shown to reduce infarct sizes and reperfusion damage in a mouse model (Rai et al., 2014). Moreover, Tuo et al. (2017) observed that brain damage was significantly attenuated by ferroptosis inhibitors, Lip-1, and Fer-1, in an MCAO model. As for the GPX4-GSH-cysteine axis, various groups provide direct evidence supporting that inhibition of system xc- induces ferroptosis and aggravates ischemia. Lan et al. (2020) found that acute cerebral ischemia-induced neuronal ferroptosis and treatment with Naotaifang increased the expression levels of xCT, GPX4 and GSH, and the number of Nissl bodies in MCAO rats. These data suggested that Naotaifang may rescue ischemic stroke by inhibiting ferroptosis through the xCT/GPX4 pathways (Lan et al., 2020). Huang et al. (2019) also observed that inhibition of system xc- with erastin aggravated ferroptosis and augment of liver regeneration protected the kidney from ischemia-reperfusion injury in ferroptosis through GSH/GPX system. Guan et al. (2019) and Cho et al. (2007) identified reduced levels of GSH and decreased activities of GPX4 in ischemia. However, many researchers hold opposing views and state that activated system xc- can exacerbate ischemic cerebral injury due to increased glutamate. In their studies, xCT was expressed in significant concentrations in astrocytes in the mouse brain (Jackman et al., 2012; Thorn et al., 2015; Ottestad-Hansen et al., 2018). Increased activity of system xc- (Soria et al., 2014) promoted the release of glutamate which may contribute to excitotoxicity in pathological situations (e.g., oxygen and glucose deprivation), leading to neuronal death

(Thorn et al., 2015; Ottestad-Hansen et al., 2018). Hsieh et al. (2017) used both *in vitro* and *in vivo* models to reveal that HIF-1 α triggered long-lasting glutamate excitotoxicity via activation of system xc- dependent glutamate outflow. HIF-1 α conditional knockout mouse had reduced extracellular glutamate in cerebral ischemia-reperfusion, suggesting that system xc- was a promising therapeutic target (Hsieh et al., 2017). Therefore, inhibition of system xc- can induce ferroptosis to promote neuronal death due to GSH depletion and activation of system xc- can also increase neuronal death because of glutamate-associated excitotoxicity. Whether induction of system xc- activity is beneficial or detrimental might depend on the pathway of induction and whether inhibition of system xc- or induction of xCT is the more promising neuroprotective strategy remains to be explored.

Other studies have confirmed the benefits of the necroptosis inhibitor, necrostatin-1, indicating that alternative forms of regulated cell death were involved in ischemic brain injury (Degterev et al., 2005). However, necrostatin-1 was later found to protect against ferroptosis through an unknown target (Friedmann Angeli et al., 2014). These results suggest that there is the direct involvement of ferroptosis in the pathogenesis of ischemic stroke. What about ferroptosis in hemorrhagic stroke?

The Role and Mechanism of Ferroptosis in ICH

After ICH, there is a consequent physical disruption of the neurovascular architecture due to the mass effects and elevated pressure surrounding hemorrhagic sites, inducing primary brain injury. Subsequently, iron accumulates as a result of the degradation of Hb and its metabolite, heme, which contributes to SBI (Hu et al., 2016). Previous data have identified multiple forms of cell death after ICH, including necrosis, apoptosis, and autophagy (Qureshi et al., 2001, 2003; Wang et al., 2015; Li et al., 2018). To date, multiple laboratories have provided converging lines of evidence that support the role of ferroptosis in ICH with the presence of observed molecular markers and morphological features (Li et al., 2017; Zille et al., 2017; Zhang et al., 2018; Alim et al., 2019), and the underlying mechanisms of ferroptosis in ICH are analogous to those of ischemic stroke. It was identified that iron overload stimulated neuronal ferroptosis, which aggravated brain damage (Wu et al., 2003, 2011). Besides, as one of the major upstream regulators of ferroptosis, GPX4 inactivation also contributes to ICH (Forcina and Dixon, 2019). It was found that levels of GPX4 were reduced and brain injury was exacerbated in a rat model of ICH induced by autologous blood injection, whereas overexpression of GPX4 was able to alleviate SBI and improve neurological outcomes (Zhang et al., 2018). Li et al. (2017) also indicated that administration of Fer-1 reduced Hb-induced cell death and iron deposition, prevented impairment of GPX4 activity *in vitro*, and improved neurologic function in collagenase-induced ICH models.

Many recent studies have suggested potential approaches to reduce brain damage. Zille et al. (2017) revealed that several ferroptosis inhibitors, including Fer-1, DFO, Trolox (a lipid peroxidation inhibitor), and NAC (a cell-permeable cysteine analog), were able to alleviate Hb- and heme-induced cell death

in vitro. Alim et al. (2019) also supported the role of Fer-1 by showing that inhibition of ferroptosis by Fer-1 exerted a long-term cerebroprotective effect in *in vitro* and *in vivo* ICH models. Dharmalingam et al. (2020) synthesized a multifunctional nanoparticle that protected cells from both senescence and ferroptosis, leading to a reduction of heme/iron-induced toxicity in experimental ICH. In addition, Karuppagounder et al. (2018) found that ALOX5 inhibition could protect against ICH- or heme-induced ferroptosis *in vivo* following ICH.

Furthermore, the role of ferroptosis in ICH is supported by altered levels of other ferroptosis-related molecules. For example, phospho-ERK1/2, regarded as a molecular feature of ferroptosis (Yagoda et al., 2007), was significantly increased in mice with ICH, but the MEK inhibitor, U0126, inhibited this type of cell death (Zille et al., 2017). In addition, the expression levels of PTGS2 were also significantly increased in *in vitro* and *in vivo* ICH models (Li et al., 2017; Alim et al., 2019). Moreover, PTGS2 has been revealed as part of the downstream signaling pathway of ferroptosis in cancer cells (Yang et al., 2014). Notably, a gene product of PTGS2, known as COX-2, was substantially increased in neurons after ICH, and treatment with Fer-1 could reduce its expression and ICH-induced SBI, implying that COX-2 might be used as a biomarker of ferroptosis (Zhao et al., 2007; Li et al., 2017; Alim et al., 2019). Thus far, there is little evidence that shows the relationship between ferroptosis and subarachnoid hemorrhage. More studies are warranted to investigate this promising topic.

The Role and Mechanism of Ferroptosis in TBI

The previous literature has shown that TBI shares many mechanisms (e.g., OS, inflammation, mitochondrial dysfunction, and neuronal cell death) with stroke (Blennow et al., 2016). In addition to these mechanisms, multiple studies have demonstrated that ferroptosis may contribute to the neuronal cell death and functional outcome in TBI (Ayton et al., 2014; Stockwell et al., 2017). The altered levels of various ferroptosis biomarkers provide evidence of ferroptosis in TBI. Studies have detected elevated iron concentrations around the impaired tissue as early as 3 days after injury, occurring in adult and aged mice models of controlled CCI (Portbury et al., 2016, 2017; Xie et al., 2019). The evidence also suggested that increased iron accumulation was negatively associated with cognitive outcomes in chronic TBI patients (Lu et al., 2015), while iron chelators exhibited neuroprotective effects by diminishing iron-mediated brain damage (Zhang et al., 2013; Khalaf et al., 2018). According to recent studies, ferroptosis was identified in TBI through the detection of ferroptosis-associated molecules, such as 15-LOX and GPX4. For instance, there were enhanced levels of 15-HpETE-PE and 15-LOX2 in the injured cortex and ipsilateral hippocampus, and decreased levels of GPX4 in a pediatric rat CCI model, suggesting that ferroptosis might occur within the first hour after TBI (Wenzel et al., 2017). Researchers also showed a preponderance of 15-LOX products in CCI-injured adult mice, and increased ACSL4 and 15-LOX2 expression in TBI, when compared with naive groups (Kenny et al., 2019).

Moreover, numerous experimental and clinical studies observed the increased levels of MDA and 4-HNE in either the injured brain or serum following TBI (Hall et al., 2004; Readnower et al., 2010; Lorente et al., 2015; Xiao et al., 2019; Xie et al., 2019). As for the morphological features, Xie et al. (2019) first verifiably identified the ferroptotic features around brain injury lesions of TBI models at 3 days after CCI. As ferroptosis was shown to participate in TBI by the above work, inhibiting ferroptosis may be useful in treating TBI. For example, treatment with Fer-1 significantly diminished iron accumulation, reduced neuronal cell death, and attenuated neuronal degeneration (Kenny et al., 2019; Xie et al., 2019). More details regarding therapy can be found in the next section.

The Role and Mechanism of Ferroptosis in SCI

In traumatic SCI, the primary injury causes immediate cellular damage and initiates a continuous secondary injury cascade to induce ischemia, inflammation, and cell death [for review see Ahuja et al. (2017)]. Notably, following the rupture of the blood-spinal cord barrier and blood vessels, hemorrhage occurs in the acute phase of SCI and may last for days (Tran et al., 2018). Like other acute CNS diseases, ferroptosis occurs in SCI, and is accompanied by increased iron and accumulated ROS at the site of injury (Liu et al., 2011; Visavadiya et al., 2016; Hao et al., 2017), as well as excessive lipid peroxidation (Dinc et al., 2013; Hu et al., 2017). This phenomenon is more apparent during the first several hours (Liu et al., 2004). In adult mouse models, Chen et al. (2015) observed that conditional ablation of Gpx4 in neurons could induce motor neuron degeneration and cause rapid paralysis, but this result was delayed by supplementation with vitamin E, suggesting that ferroptosis accelerated SCI. Therefore, anti-ferroptotic seems to have potential in SCI, though there are few studies. Feng et al. (2019) established a rat model of DFO and confirmed the positive role of DFO in treating SCI. In the DFO group, there were lower iron concentrations, markedly increased GPX4 expression, and increased neuronal survival (Feng et al., 2019). In the study conducted by Zhang Y. et al. (2019) treatment with the third-generation ferrostatin, SRS 16-86, increased neuronal survival and promoted locomotor recovery in the SCI model, providing potential therapeutic strategies for SCI. Indeed, it is well-known that the excitotoxicity caused by glutamate accumulation preceded neuronal death and reuptake failure of astrocytes, and also induced ferroptotic cell death to stimulate secondary injury after SCI (Dixon et al., 2014; Ahuja et al., 2017). The relationship between ferroptosis or excitotoxicity in SCI requires further studies.

POTENTIAL AND EMERGING THERAPY TARGETING FERROPTOSIS IN ACUTE CNS INJURIES

As ferroptosis may be a significant pathogenic pathway in acute CNS injuries, its therapeutic potential should be taken into consideration. Ferroptosis inhibitors (including iron chelators,

ferrostatins, liproxstatins, LOX inhibitors, and antioxidants) may prevent iron accumulation or lipid peroxidation, thus offering therapeutic options for treating acute CNS injuries (Table 1).

Targeting Ferroptosis Therapy in Ischemic Stroke

The mainstay of treatment for acute ischemic stroke is rapid recanalization by mechanical thrombectomy or recombinant tissue plasminogen activator, the only approved thrombolytic agent. It is important to salvage the penumbra, which surrounds the region of the infarct and promotes functional recovery. However, the overall efficacy is limited due to the narrow window of opportunity (Sandercock et al., 2012), but even after timely recanalization, infarct volume often continues to increase in I/R injury (Nour et al., 2013). As previous methods have failed in clinical use, such as blocking excitotoxicity, the role of ferroptosis has been highlighted (Khoshnam et al., 2017; Tuo et al., 2017), and new therapeutic approaches targeting ferroptosis or combined therapies are highly desirable.

As mentioned above, Lip-1 and Fer-1 are both compounds with specific anti-ferroptotic activity. Intranasal administration of Lip-1 and Fer-1, either immediately or 6 h after reperfusion, significantly reduced neuronal damage and functional deficits in MCAO mice, indicating the possible translational value of special exogenous ferroptosis inhibitors (Tuo et al., 2017).

In addition, CoQ10 is an endogenous lipid-soluble antioxidant with established efficacy in suppressing the initiation and amplification of lipid peroxidation (Morris et al., 2013; Viswanathan et al., 2017), presenting a promising candidate for ferroptosis inhibition. Intriguingly, *in vivo* studies have reported that oral CoQ10 administration markedly improved neurological outcomes in both rat MCAO models and acute ischemic stroke patients (Ramezani et al., 2018; Nasoohi et al., 2019). This neuroprotective benefit of CoQ10 was associated with its anti-apoptotic effect, as the levels of peroxidation products were not altered (Nasoohi et al., 2019). The authors attributed this to a relatively higher dose and multiple potential mechanisms of CoQ10. Of note, it is worth considering whether inhibition of ferroptosis is involved.

Recently, Guan et al. (2019) found that carvacrol, a plant-derived monoterpenic phenol, inhibited hippocampal neuronal damage and reduced functional deficits in gerbils following I/R injury. Furthermore, treatment with carvacrol (100 mg/kg, intraperitoneally) for two consecutive weeks after reperfusion was associated with decreased ROS, reduced iron overload, and increased levels of GPX4, suggesting a possible neuroprotective role of carvacrol via ferroptosis inhibition (Guan et al., 2019). Carvacrol is thought to easily cross the BBB because of the small molecular weight and the lipophilic profile (Savelev et al., 2004). A previous study has proven the benefits of carvacrol when administered intraperitoneally at 2 h after reperfusion. When administered intracerebroventricularly, the treatment window was prolonged to 6 h (Yu et al., 2012). When administered safely, carvacrol may be regarded as a potential therapeutic agent.

Edaravone is an effective radical scavenger that inhibits lipid oxidation by scavenging chain-initiating water-soluble radicals

TABLE 1 | Ferroptosis-associated drugs in treating the acute CNS injuries.

Disease	Drug	Type	Administration Route	Function and Mechanism
Ischemic stroke	Liproxstatin-1 (Lip-1)	Lipid peroxides inhibitor	Intranasal	Attenuated motor function deficits, cognitive impairment; improved neuroscores; reduced infarct volumes in middle cerebral artery occlusion (MACO) mice.
	Ferrostatin-1 (Fer-1)	Lipid peroxides inhibitor	Intranasal	Attenuated neurological deficits and infarct volumes in MACO mice.
	ML351	Inhibitor of 15-lipoxygenase-1	Intravenous	Reduced neurological impairment and infarct volume in MACO mice.
	Amyloid precursor protein ectodomain	Protein stabilizing ferroportin to export iron	Intravenous	Improved neuroscores and infarct volume; prevented iron accumulation in the lesioned hemisphere in MACO mice.
	Ceruloplasmin	Copper regulating iron-mediated transport	Intraperitoneal	Suppressed ischemia-induced hippocampal iron elevation in the lesioned hemisphere in MACO mice.
	Carvacrol	Monoterpenic phenol	Intraperitoneal	Reduced neuronal cell death, increased GPx4 expression in gerbils I/R hippocampal neurons (<i>in vitro</i>); decreased the level of lipid peroxide and MDA, TFR, increased the Fpn1 expression; alleviated neuronal degeneration and memory deficits in I/R gerbils.
	Deferoxamine	Iron chelator	Intraperitoneal	Suppressed the level of MDA.
	Edaravone	Free radical scavenger; A clinically approved drug for treating acute ischemic stroke	Not applicable	Suppressed the accumulation of lipid peroxidation and ROS production; inhibited ferroptosis induced by cystine deprivation, erastin and RSL3 by scavenging radical species in non-neuronal cells (<i>in vitro</i>).
ICH	Tat-linked Self Peptide	BBB-permeable peptide containing selenocysteine	Intraperitoneal	Reduced infarct volume in rodent MCAO model.
	Ferrostatin-1	Lipid peroxides inhibitor	Intracerebroventricular or intraperitoneal	Prevented lipid ROS, MDA and GPx activity deficit (<i>in vitro</i>); inhibited Hb/ferrous-induced and hemin/hemoglobin-induced neuronal death (<i>in vitro</i>); reduced iron deposition and lipid ROS; diminished injury volume; rescued degenerating neurons, and corrected neurologic deficit in collagenase-induced ICH model; suppressed the level of GPX4; alleviated neuronal dysfunction; moderated brain atrophy and exerted long-term neuroprotective effects in autologous blood infusion model of ICH.
	Liproxstatin-1	Lipid peroxides inhibitor	Intraperitoneal	Inhibited Hb-induced cell death; decreased neurologic deficits and lesion volume; rescued neuronal cells in collagenase-induced ICH model.
	Zileuton/BW B70/BW A4C	Arachidonate 5-lipoxygenase (ALOX5) inhibitors	Not applicable	Inhibited Hb/hemin-induced cell death (<i>in vitro</i>).
	Compound 968	Glutaminase inhibitor	Intraperitoneal	Decreased degenerating neurons.
	Deferoxamine	Iron chelator	Intraperitoneal	Inhibited hemin/hemoglobin-induced neuronal death.
	N-acetylcysteine (NAC)	Glutathione prodrug; Thiol-containing redox modulatory compound		Inhibited hemin/hemoglobin-induced neuronal death (<i>in vitro</i>); increased glutathione, decreased nuclear ALOX5-derived reactive lipid species, reduced neuronal death, improved functional recovery in collagenase-induced mouse model of ICH.
	Trolox	Water soluble lipid peroxidation inhibitor	Not applicable	Inhibited hemin/hemoglobin-induced neuronal death (<i>in vitro</i>).
	U0126	Extracellular-signaling kinase 1/2 (ERK1/2) inhibitor	Not applicable	Inhibited hemin/hemoglobin-induced neuronal death (<i>in vitro</i>).
	(-)-Epicatechin	Brain-permeable flavanol	Orally	Diminished heme oxygenase-1 expression and brain iron deposition via an Nrf2-independent pathway, reduced lesion volume and ameliorated neurologic deficits in collagenase/autologous blood/thrombi-induced ICH model.

(Continued)

TABLE 1 | Continued

Disease	Drug	Type	Administration Route	Function and Mechanism
TBI	Loxothiazolidine-4-carboxylate (OTC)	Cysteine prodrug	Not applicable	Inhibited hemin-induced neuronal death (<i>in vitro</i>).
	Glutathione ethyl ester	Membrane permeable form of glutathione	Not applicable	Inhibited hemin-induced neuronal death (<i>in vitro</i>).
	Tat SelPep	BBB-permeable peptide containing selenocysteine	Intraperitoneal	Increased GPX4 expression; prevented hemin-induced ferroptosis and preserved cell bodies and neurites of neurons (<i>in vitro</i>); unregulated transcriptional expression of GPX4; inhibited cell death and improved function in collagenase-induced ICH model.
	Selenium	Essential micronutrient	Intracerebroventricular	Diminished cell death and improved functional recovery in a mouse model of ICH.
	Ferrostatin-1	Lipid peroxides inhibitor	Intracerebroventricular	Reduced neuronal death in mechanical stretch-elicited TBI model (<i>in vitro</i>); reduced iron accumulation, neuron degeneration and lesion volume; ameliorated cognitive and motor function deficits in the adult controlled cortical impact injury (CCI) mouse model.
	Triacsin C	Acyl-CoA synthetase long-chain family member 4 (ACSL4) inhibitor	Not applicable	Reduced neuronal cell death in mechanical stretch-elicited TBI model (<i>in vitro</i>).
	Liproxstatin-1	Lipid peroxides inhibitor	Not applicable	Reduced neuronal cell death in mechanical stretch-elicited TBI model (<i>in vitro</i>).
SCI	Baicalein	12/15-lipoxygenase inhibitor	Intraperitoneal	Reduced neuronal cell death in mechanical stretch-elicited TBI model (<i>in vitro</i>); attenuated phosphatidylethanolamine oxidation and improved function in CCI mouse model.
	miR-212-5p agomir	MicroRNAs agomir	Intracerebroventricular	Improved memory and learning in CCI mice.
	Deferoxamine	Iron chelator	Intraperitoneal	Increased xCT, GSH, and GPX4 levels; protected neurons and promoted long-term functional recovery in rat contusion SCI model.
	SRS 16-86	Small molecule ferroptosis specific inhibitor	Intraperitoneal	Upregulated GPX4, GSH and xCT levels; down-regulated the expression of 4HNE; increased neuronal survival and promoted functional recovery in rat contusion SCI model.

and chain-carrying lipid peroxyl radicals due to its amphiphilicity (Watanabe et al., 2018). There are several papers describing its alleviatory effects on neurological symptoms in ischemia models, and its effective treatment window of at least 3 h after embolism (Nishi et al., 1989; Kawai et al., 1997; Lapchak and Zivin, 2009). In the clinical setting, the appropriate dosage and course of edaravone use for patients suffering from acute ischemic stroke include intravenous administration of 60 mg daily for up to 14 days (Feng et al., 2011). Homma et al. (2019) recently indicated that edaravone participates in rescuing ferroptotic cell death induced by cystine deprivation, erastin, and RSL3 (Homma et al., 2019). In addition, edaravone was confirmed to suppress the accumulation of Fe^{2+} and lipid peroxidation *in vitro*, which are known as the metabolic characteristics of ferroptosis.

Targeting Ferroptosis Therapy in ICH

Currently, there are no proven medical or surgical treatments that substantially improve the neurological outcomes in patients with ICH because of multiple underlying mechanisms, including inflammation, excitotoxicity, and OS (Keep et al., 2012). As emerging studies suggest that ferroptosis is involved in SBI after

ICH, and contributes to 80% of whole-cell death *in vitro* (Li et al., 2017; Zille et al., 2017), ferroptosis-based treatments could be highly considered.

Li et al. demonstrated the neuroprotective effects of Fer-1 by striatum injection immediately after and by cerebral ventricular injection 2 h after collagenase-induced ICH [for review see Li et al. (2017)]. Intraperitoneal administration of Fer-1 (a 3-h delay and then once daily) in the autologous blood infusion model of ICH was also shown to improve long-term neurological function (Alim et al., 2019). Moreover, when combined with other inhibitors of either apoptosis or necrosis, Fer-1 was found to be more effective at reducing Hb-induced cell death, which should be further investigated in *in vivo* models (Li et al., 2017).

Various evidence has shown that iron chelators reduce Hb- and iron-induced neurotoxicity attenuates brain edema, and improve functional neurologic outcomes after ICH (Nakamura et al., 2004; Wu et al., 2012; Hatakeyama et al., 2013). A meta-analysis of 20 studies involving animal models of ICH revealed that DFO was neuroprotective, particularly when administered 2–4 h after ICH induction (Cui et al., 2015), whereas there

remains a lack of conclusive clinical evidence regarding iron chelators (Zeng et al., 2018).

N-acetylcysteine (Gilbert et al., 1991; Leslie et al., 1992; Varga et al., 1997) is an FDA-approved cysteine prodrug capable of regulating the activity of system xc⁻ and the biosynthesis of GSH [for review see Berk et al. (2013)]. Interestingly, a recent study reported that systemic administration of NAC post-injury reduced neuronal death and improved behavior following ICH in mice (Karuppagounder et al., 2018). They further pointed out that NAC inhibited hemin- and ICH-induced ferroptosis by neutralizing nuclear ALOX5-derived toxic lipid species (Karuppagounder et al., 2018). This process relied on increased GSH and enhanced activity of GSH-dependent antioxidant enzymes. Considering the poor absorption of direct GSH administration and the insufficient capacity of GSH to cross the BBB (Witschi et al., 1992), NAC may be treated as an adjuvant therapy candidate capable of penetrating the BBB to enter the brain (Farr et al., 2003).

In addition, EC, a brain-permeable flavanol, was shown to reduce early brain injury and improve neurologic deficits in multiple experimental ICH models when administered orally at 3 h post-treatment and subsequent daily administration (Chang et al., 2014). The neuroprotective effects of EC were partially associated with decreased iron deposition and modulation of ferroptosis-related gene expression, indicating the possible ability of EC to inhibit ICH-induced ferroptotic cell death (Chang et al., 2014).

Se is indispensable for the ferroptosis-resistant function of GPX4 (Ingold et al., 2018). It was recently uncovered that Se could amplify an adaptive transcriptional program response to neuronal ferroptosis (Alim et al., 2019), making it a potential therapeutic strategy. Further studies discovered that injection of Se directly into the mouse cerebral ventricle following ICH was associated with elevated GPX4 levels, diminished ferroptotic death, as well as improved functional recovery. Moreover, the researchers developed a peptide (Tat SelPep), which contained a Tat transduction domain combined with selenoprotein P. Intraperitoneal injection of Tat SelPep showed similar effects compared to Se, but with reduced toxicity and a wider treatment window, with benefits shown even at 6 h post-injury (Alim et al., 2019).

Targeting Ferroptosis Therapy in TBI

When contemplating feasible treatments for TBI, researchers focus on secondary events, which cause delayed damage, to provide applicable therapeutic windows for interventions [for review see Lozano et al. (2015)]. Given that there are currently no effective treatments approved by clinical trials for TBI patients (Pearn et al., 2017), there exists a pressing need for developing more innovative methods, such as targeting ferroptotic cell death in a highly regulated manner. The ferroptosis signaling molecules can be prevented as a result of reducing PE oxidation by inhibiting the ability of 15LOX/PEBP1 complexes to produce 15-HpETE-PE, administering 15LOX inhibitors, or augmenting the GPX4/GSH system to remove oxidized PE products (Wenzel et al., 2017; Kenny et al., 2019).

Baicalein is a polyphenolic antioxidant 12/15-LOX inhibitor and is well-known to exert neuroprotective effects in cerebral ischemia [for review see Liang et al. (2017)]. Recently, Kenny et al. (2019) demonstrated that baicalein decreased the accumulation of pro-ferroptotic PE oxidation, but not pro-apoptotic cardiolipin oxidation after CCI, indicating that the 15-LOX inhibitory effects of baicalein may have an anti-ferroptotic role in TBI. Several studies have also revealed a reduction of functional and histological damage with the immediate administration of baicalein post-injury (Chen et al., 2008; Kenny et al., 2019). With low levels of toxicity and the ability to cross the BBB (Tsai et al., 2002), baicalein offers great promise in clinical settings if the effect of delayed drug delivery is evaluated.

As mentioned above, NAC is a precursor for GSH, and it has been shown to confer antioxidant and neuroprotective effects after pre-clinical TBI (Eakin et al., 2014; Senol et al., 2014). As for adult patients, a double-blinded and placebo-controlled study indicated that supplementation of oral NAC had significant short-term benefits on neurological symptoms and sequelae resolution after blast-induced mild TBI (Hoffer et al., 2013). Due to the low bioavailability of NAC, the compound, NACA, was developed with increased membrane permeability, and its neuroprotection was associated with the activation of the Nrf2-antioxidant response elements signaling pathway in a mouse model of TBI (Zhou et al., 2018). It is well-established that Nrf2 regulates xCT and GPX4, whose inhibition initiates ferroptosis and promotes target genes that mediate the antioxidant and iron metabolic status of cells (Zhou et al., 2018), suggesting another anti-ferroptotic mechanism of NACA.

In a mouse CCI model of TBI, Fer-1 treatment had been injected directly into the cerebral ventricle 0.5 h after injury, causing a reduction in neuronal death and other associated functional defects (Xie et al., 2019). However, more research should be implemented to uncover feasible drug-delivery methods.

Moreover, a recent study demonstrated the role of miR-212-5p in suppressing ferroptosis after TBI, partially by targeting PTGS2 (Xiao et al., 2019). Further results showed that intracerebroventricular injection of miR-212-5p agomir improved spatial memory and learning in CCI mice, suggesting that miR-212-5p may serve as a potential ferroptosis inhibitor to be used in treating TBI. As previously discussed, the oxidation of AA/AdA-PE is a critical step in ferroptosis execution. Therefore, inhibition of ACSL (such as triacsin C and thiazolidinedione) and formation of AA/AdA-esterified PE may also protect against ferroptosis after TBI (Doll et al., 2017; Kagan et al., 2017; Kenny et al., 2019).

Targeting Ferroptosis Therapy in SCI

There are no neuroprotective or neurodegenerative strategies currently approved for acute traumatic SCI, but several are currently undergoing clinical trials (Badhiwala et al., 2018). The concept of “time is spine” is commonly applied in the management of patients with SCI. Since ferroptosis is likely involved in the acute phases of SCI, therapies targeting ferroptosis are promising (Badhiwala et al., 2018; Zhang Y. et al., 2019).

Targeting iron is one of the treatment strategies. The iron chelator, DFO, reportedly reduced iron accumulation and lipid peroxidation, while modulating the inflammatory response in SCI (Paterniti et al., 2010; Liu et al., 2011; Dinc et al., 2013; Hao et al., 2017). Experimental evidence indicated that DFO improved motor function recovery when injected intraperitoneally post-SCI (Paterniti et al., 2010; Liu et al., 2011; Hao et al., 2017). Moreover, DFO showed neuroprotective effects comparable with methylprednisolone, an effective antioxidant agent that is contentious for the treatment of SCI because of harmful side effects (Dinc et al., 2013; Silva et al., 2014). However, oral treatment of deferiasirox, another FDA-approved iron chelator, failed to remove iron from the injured spinal cord, but markedly depleted the systemic iron (Sauerbeck et al., 2013). Considering the detrimental side effects (e.g., anemia) and the absence of potent neuroprotection, systemic administration may not be the ideal approach of iron chelators (Grossman et al., 2012; Sauerbeck et al., 2013).

Besides, previous studies have demonstrated that NAC administration suppressed OS, attenuated neuroinflammation, and improved neuronal survival and neurological recovery following SCI in rodent models (Karalija et al., 2012, 2014; Guo et al., 2015). When administered immediately after SCI, NACA, an amide derivative of NAC, improved mitochondrial function, antioxidant GSH levels, and functional recovery in SCI mice (Patel et al., 2014). These two GSH precursors facilitate the biosynthesis of intracellular GSH. In addition, the GSH antioxidant system plays a pivotal role in the regulation of ferroptosis (Lv et al., 2019).

Recently, Li et al. (2019b) observed that CoQ10, a promising ferroptosis inhibitor previously mentioned, exerted protective effects by decreasing OS partly through activation of the Nrf-2 signaling pathway after SCI. Moreover, Nrf-2 is regarded as a significant mitigator of lipid peroxidation and ferroptosis [for review see Dodson et al. (2019)]. Furthermore, CoQ10 was shown to protect BMSCs from OS, and improved the therapeutic efficacy in combination with BMSC transplantation, suggesting a promising therapy for SCI (Li et al., 2019c).

Besides, post-injury intraperitoneal injection of SRS 16-86 proved to be more potent and stable than Fer-1. It also attenuated the ferroptotic mitochondrial morphology in damaged areas, and improved neurological deficits in SCI model, suggesting the role of ferroptosis-specific inhibitors in the treatment of SCI (Zhang Y. et al., 2019).

DISCUSSION AND PERSPECTIVE: WILL FERROPTOSIS BE THE FUTURE DIRECTION?

In this article, we primarily focus on the roles and therapeutic potential of ferroptosis in various acute CNS injury processes, including stroke, TBI, and SCI. Pharmacological effects of multiple inducers and inhibitors of ferroptosis lie at the intersection of lipid, amino acid, and iron metabolism. Although some progress has been made in ferroptosis, there are still

controversial questions that have not been fully studied. First, the relationship between ferroptosis and other forms of cell death remains unknown. For example, p53 is an important regulator, both in apoptosis and ferroptosis, while autophagy plays a role in the process of ferroptosis via ferritinophagy. As ferroptosis is involved in acute CNS injuries complicated by necrosis, apoptosis, and autophagy, a head-to-head comparison of individual inhibitors or various combinations of inhibitors is required in further studies. Second, the special molecular markers (e.g., caspase activation for apoptosis or the autophagosome marker, LC3-II, for autophagy) for identifying ferroptosis are still lacking. While the increased mRNA levels of PTGS2 were found in cells undergoing ferroptosis, it did not affect ferroptosis progress (Yang et al., 2014). The specificity of PTGS2 expression or its gene product, COX-2, for ferroptosis needs to be explored in the context of different pathophysiologic processes. Actually, there is copious evidence for the role of COX-2 in several acute neurological disorders (e.g., ischemic and hemorrhagic strokes) (Gong et al., 2001; Tomimoto et al., 2002). The research of additional ferroptosis markers is of great importance for *in vivo* studies in the future. Moreover, the exact role of iron and the final molecular executor in ferroptosis remains unclear. Considering the complexity of the CNS, the biochemical regulation, as well as the sensitivity of ferroptosis in different cell types (neurons, astrocytes, microglia, or oligodendrocytes), also requires explication.

Potential treatment options targeting ferroptosis (e.g., iron chelators, ferrostatins, NAC, and CoQ10) have shown neuroprotective effects in acute CNS injuries. However, these benefits are largely based on animal models and have not yet translated into clinical application. Furthermore, studies are necessary to clarify the appropriate therapeutic window, clinically feasible routes of administration, and BBB penetration ability of anti-ferroptotic agents. Among the above-mentioned agents, edaravone is the only approved drug with proven clinical efficacy and safety, while others should be explored in further clinical studies. More in-depth and comprehensive research on ferroptosis should be conducted to develop therapeutic methods and eventually alleviate the burden of acute CNS injuries in the future.

AUTHOR CONTRIBUTIONS

All the authors participated in analyzing and discussing the literature, commenting on, and read and approved the final manuscript. AS and YC supervised the research, led the discussion, and wrote and revised the manuscript.

FUNDING

This work was funded by the National Natural Science Foundation of China (81701144, 81371433, and 81870916), and Major Science and Technology Project in the medical and health of Zhejiang Province (WKJ-ZJ-1615:2016149634).

REFERENCES

- Ahuja, C. S., Wilson, J. R., Nori, S., Kotter, M. R. N., Druschel, C., Curt, A., et al. (2017). Traumatic spinal cord injury. *Nat. Rev. Dis. Primers* 3:17018.
- Alim, I., Caulfield, J. T., Chen, Y., Swarup, V., Geschwind, D. H., Ivanova, E., et al. (2019). Selenium drives a transcriptional adaptive program to block ferroptosis and treat stroke. *Cell* 177, 1262–1279.e25. doi: 10.1016/j.cell.2019.03.032
- Ayton, S., Zhang, M., Roberts, B. R., Lam, L. Q., Lind, M., McLean, C., et al. (2014). Ceruloplasmin and β -amyloid precursor protein confer neuroprotection in traumatic brain injury and lower neuronal iron. *Free Radic. Biol. Med.* 69, 331–337. doi: 10.1016/j.freeradbiomed.2014.01.041
- Badhiwala, J. H., Ahuja, C. S., and Fehlings, M. G. (2018). Time is spine: a review of translational advances in spinal cord injury. *J. Neurosurg. Spine* 30, 1–18. doi: 10.3171/2018.9.spine18682
- Benjamin, E. J., Muntner, P., Alonso, A., Bittencourt, M. S., Callaway, C. W., Carson, A. P., et al. (2019). Heart disease and stroke statistics-2019 update: a report from the American Heart Association. *Circulation* 139, e56–e528.
- Berk, M., Malhi, G. S., Gray, L. J., and Dean, O. M. (2013). The promise of N-acetylcysteine in neuropsychiatry. *Trends Pharmacol. Sci.* 34, 167–177. doi: 10.1016/j.tips.2013.01.001
- Bersuker, K., Hendricks, J. M., Li, Z., Magtanong, L., Ford, B., Tang, P. H., et al. (2019). The CoQ oxidoreductase FSP1 acts parallel to GPX4 to inhibit ferroptosis. *Nature* 575, 688–692. doi: 10.1038/s41586-019-1705-2
- Blennow, K., Brody, D. L., Kochanek, P. M., Levin, H., McKee, A., Ribbers, G. M., et al. (2016). Traumatic brain injuries. *Nat. Rev. Dis. Primers* 2:16084.
- Bogdan, A. R., Miyazawa, M., Hashimoto, K., and Tsuji, Y. (2016). Regulators of iron homeostasis: new players in metabolism, cell death, and disease. *Trends Biochem. Sci.* 41, 274–286. doi: 10.1016/j.tibs.2015.11.012
- Brigelius-Flohé, R., and Maiorino, M. (2013). Glutathione peroxidases. *Biochim. Biophys. Acta* 1830, 3289–3303.
- Brown, R. A. M., Richardson, K. L., Kabir, T. D., Trinder, D., Ganss, R., and Leedman, P. J. (2020). Altered iron metabolism and impact in cancer biology, metastasis, and immunology. *Front. Oncol.* 10:476. doi: 10.3389/fonc.2020.00476
- Castellanos, M., Puig, N., Carbonell, T., Castillo, J., Martinez, J., Rama, R., et al. (2002). Iron intake increases infarct volume after permanent middle cerebral artery occlusion in rats. *Brain Res.* 952, 1–6. doi: 10.1016/s0006-8993(02)03179-7
- Chamorro, A., Dirnagl, U., Urra, X., and Planas, A. M. (2016). Neuroprotection in acute stroke: targeting excitotoxicity, oxidative and nitrosative stress, and inflammation. *Lancet Neurol.* 15, 869–881. doi: 10.1016/s1474-4422(16)00114-9
- Chang, C. F., Cho, S., and Wang, J. (2014). (-)-Epicatechin protects hemorrhagic brain via synergistic Nrf2 pathways. *Ann. Clin. Transl. Neurol.* 1, 258–271. doi: 10.1002/acn3.54
- Chen, L., Hambright, W. S., Na, R., and Ran, Q. (2015). Ablation of the Ferroptosis inhibitor glutathione peroxidase 4 in neurons results in rapid motor neuron degeneration and paralysis. *J. Biol. Chem.* 290, 28097–28106. doi: 10.1074/jbc.m115.680090
- Chen, S. F., Hsu, C. W., Huang, W. H., and Wang, J. Y. (2008). Post-injury baicalein improves histological and functional outcomes and reduces inflammatory cytokines after experimental traumatic brain injury. *Br. J. Pharmacol.* 155, 1279–1296. doi: 10.1038/bjp.2008.345
- Chen, X., Li, D., Sun, H. Y., Wang, W. W., Wu, H., Kong, W., et al. (2020). Relieving ferroptosis may partially reverse neurodegeneration of the auditory cortex. *FEBS J.* [Epub ahead of print].
- Cho, S., Szteto, H. H., Kim, E., Kim, H., Tolhurst, A. T., and Pinto, J. T. (2007). A novel cell-permeable antioxidant peptide, SS31, attenuates ischemic brain injury by down-regulating CD36. *J. Biol. Chem.* 282, 4634–4642. doi: 10.1074/jbc.m609388200
- Codenotti, S., Poli, M., Asperti, M., Zizioli, D., Marampon, F., and Fanzani, A. (2018). Cell growth potential drives ferroptosis susceptibility in rhabdomyosarcoma and myoblast cell lines. *J. Cancer Res. Clin. Oncol.* 144, 1717–1730. doi: 10.1007/s00432-018-2699-0
- Cui, H.-J., He, H.-Y., Yang, A. L., Zhou, H.-J., Wang, C., Luo, J.-K., et al. (2015). Efficacy of deferoxamine in animal models of intracerebral hemorrhage: a systematic review and stratified meta-analysis. *PLoS One* 10:e0127256. doi: 10.1371/journal.pone.0127256
- DeGregorio-Rocasolano, N., Marti-Sistac, O., Ponce, J., Castello-Ruiz, M., Millan, M., Guirao, V., et al. (2018). Iron-loaded transferrin (Tf) is detrimental whereas iron-free Tf confers protection against brain ischemia by modifying blood Tf saturation and subsequent neuronal damage. *Redox Biol.* 15, 143–158. doi: 10.1016/j.redox.2017.11.026
- Degterev, A., Huang, Z., Boyce, M., Li, Y., Jagtap, P., Mizushima, N., et al. (2005). Chemical inhibitor of nonapoptotic cell death with therapeutic potential for ischemic brain injury. *Nat. Chem. Biol.* 1, 112–119. doi: 10.1038/nchembio711
- Dharmalingam, P., Talakatta, G., Mitra, J., Wang, H., Derry, P. J., Nilewski, L. G., et al. (2020). Pervasive genomic damage in experimental intracerebral hemorrhage: therapeutic potential of a mechanistic-based carbon nanoparticle. *ACS Nano* 14, 2827–2846. doi: 10.1021/acsnano.9b05821
- Dietrich, R. B., and Bradley, W. G. (1988). Iron accumulation in the basal ganglia following severe ischemic-anoxic insults in children. *Radiology* 168, 203–206. doi: 10.1148/radiology.168.1.3380958
- Dinc, C., Iplikcioglu, A. C., Atabey, C., Eroglu, A., Topuz, K., Ipcioglu, O., et al. (2013). Comparison of deferoxamine and methylprednisolone: protective effect of pharmacological agents on lipid peroxidation in spinal cord injury in rats. *Spine* 38, E1649–E1655.
- Dixon, S. J., Lemberg, K. M., Lamprecht, M. R., Skouta, R., Zaitsev, E. M., Gleason, C. E., et al. (2012). Ferroptosis: an iron-dependent form of nonapoptotic cell death. *Cell* 149, 1060–1072. doi: 10.1016/j.cell.2012.03.042
- Dixon, S. J., Patel, D., Welsch, M., Skouta, R., Lee, E., Hayano, M., et al. (2014). Pharmacological inhibition of cystine-glutamate exchange induces endoplasmic reticulum stress and ferroptosis. *Elife* 3:e02523.
- Dixon, S. J., and Stockwell, B. R. (2014). The role of iron and reactive oxygen species in cell death. *Nat. Chem. Biol.* 10, 9–17. doi: 10.1038/nchembio.1416
- Dixon, S. J., Winter, G. E., Musavi, L. S., Lee, E. D., Snijder, B., Rebsamen, M., et al. (2015). Human haploid cell genetics reveals roles for lipid metabolism genes in nonapoptotic cell death. *ACS Chem. Biol.* 10, 1604–1609. doi: 10.1021/acscchembio.5b00245
- Dodson, M., Castro-Portuguez, R., and Zhang, D. D. (2019). NRF2 plays a critical role in mitigating lipid peroxidation and ferroptosis. *Redox Biol.* 23:101107. doi: 10.1016/j.redox.2019.101107
- Doll, S., Freitas, F. P., Shah, R., Aldrovandi, M., da Silva, M. C., Ingold, I., et al. (2019). FSP1 is a glutathione-independent ferroptosis suppressor. *Nature* 575, 693–698. doi: 10.1038/s41586-019-1707-0
- Doll, S., Proneth, B., Tyurina, Y. Y., Panzilius, E., Kobayashi, S., Ingold, I., et al. (2017). ACSL4 dictates ferroptosis sensitivity by shaping cellular lipid composition. *Nat. Chem. Biol.* 13, 91–98. doi: 10.1038/nchembio.2239
- Dolma, S., Lessnick, S. L., Hahn, W. C., and Stockwell, B. R. (2003). Identification of genotype-selective antitumor agents using synthetic lethal chemical screening in engineered human tumor cells. *Cancer Cell* 3, 285–296. doi: 10.1016/s1535-6108(03)00050-3
- Domingues, R. M., Domingues, P., Melo, T., érez-Sala, D. P., Reis, A., and Spickett, C. M. (2013). Spickett, lipoxidation adducts with peptides and proteins: deleterious modifications or signaling mechanisms? *J. Proteom.* 92, 110–131. doi: 10.1016/j.jpro.2013.06.004
- Duan, J. L., Cui, J., Yang, Z. F., Guo, C., Cao, J. Y., Xi, M. M., et al. (2019). Neuroprotective effect of Apelin 13 on ischemic stroke by activating AMPK/GSK-3 β /Nrf2 signaling. *J. Neuroinflamm.* 16:24.
- Eakin, K., Baratz-Goldstein, R., Pick, C. G., Zindel, O., Balaban, C. D., Hoffer, M. E., et al. (2014). Efficacy of N-acetyl cysteine in traumatic brain injury. *PLoS One* 9:e90617. doi: 10.1371/journal.pone.0090617
- Farr, S. A., Poon, H. F., Dogrukol-Ak, D., Drake, J., Banks, W. A., Eyerman, E., et al. (2003). The antioxidants alpha-lipoic acid and N-acetylcysteine reverse memory impairment and brain oxidative stress in aged SAMP8 mice. *J. Neurochem.* 84, 1173–1183. doi: 10.1046/j.1471-4159.2003.01580.x
- Feng, S., Yang, Q., Liu, M., Li, W., Yuan, W., Zhang, S., et al. (2011). Edaravone for acute ischaemic stroke. *Cochrane Database Syst Rev* 12:CD007230.
- Feng, S.-Q., Yao, X., Zhang, Y., Hao, J., Duan, H.-Q., Zhao, C.-X., et al. (2019). Deferoxamine promotes recovery of traumatic spinal cord injury by inhibiting ferroptosis. *Neural Regen. Res.* 14, 532–541.
- Forcina, G. C., and Dixon, S. J. (2019). GPX4 at the crossroads of lipid homeostasis and ferroptosis. *Proteomics* 19:e1800311.
- Freret, T., Valable, S., Chazalviel, L., Saulnier, R., Mackenzie, E. T., Petit, E., et al. (2006). Delayed administration of deferoxamine reduces brain damage and

- promotes functional recovery after transient focal cerebral ischemia in the rat. *Eur. J. Neurosci.* 23, 1757–1765. doi: 10.1111/j.1460-9568.2006.04699.x
- Friedmann Angeli, J. P., and Conrad, M. (2018). Selenium and GPX4, a vital symbiosis. *Free Radic. Biol. Med.* 127, 153–159. doi: 10.1016/j.freeradbiomed.2018.03.001
- Friedmann Angeli, J. P., Schneider, M., Proneth, B., Tyurina, Y. Y., Tyurin, V. A., Hammond, V. J., et al. (2014). Inactivation of the ferroptosis regulator Gpx4 triggers acute renal failure in mice. *Nat. Cell. Biol.* 16, 1180–1191. doi: 10.1038/ncb3064
- Gammella, E., Recalcati, S., Rybinska, I., Buratti, P., and Cairo, G. (2015). Iron-induced damage in cardiomyopathy: oxidative-dependent and independent mechanisms. *Oxid. Med. Cell. Longev.* 2015:230182.
- Gangadhar, N. M., and Stockwell, B. R. (2007). Chemical genetic approaches to probing cell death. *Curr. Opin. Chem. Biol.* 11, 83–87. doi: 10.1016/j.cbpa.2006.11.033
- Gao, M., Monian, P., Quadri, N., Ramasamy, R., and Jiang, X. (2015). Glutaminolysis and transferrin regulate ferroptosis. *Mol. Cell* 59, 298–308. doi: 10.1016/j.molcel.2015.06.011
- García-Yébenes, I., Sobrado, M., Moraga, A., Zarruk, J. G., Romera, V. G., Pradillo, J. M., et al. (2012). Iron overload, measured as serum ferritin, increases brain damage induced by focal ischemia and early reperfusion. *Neurochem. Int.* 61, 1364–1369. doi: 10.1016/j.neuint.2012.09.014
- GBD (2016). Global, regional, and national burden of stroke, 1990–2016: a systematic analysis for the Global Burden of disease study 2016. *Lancet Neurol.* 18, 439–458.
- GBD (2019). Global, regional, and national burden of traumatic brain injury and spinal cord injury, 1990–2016: a systematic analysis for the Global Burden of disease study 2016. *Lancet Neurol.* 18, 56–87.
- Gilbert, K. R., Aizenman, E., and Reynolds, I. J. (1991). Oxidized glutathione modulates N-Methyl-D-aspartate-induced and depolarization-induced increases in intracellular Ca²⁺ in cultured rat forebrain neurons. *Neurosci. Lett.* 133, 11–14. doi: 10.1016/0304-3940(91)90045-u
- Gong, C., Ennis, S. R., Hoff, J. T., and Keep, R. F. (2001). Inducible cyclooxygenase-2 expression after experimental intracerebral hemorrhage. *Brain Res.* 901, 38–46. doi: 10.1016/s0006-8993(01)02186-2
- Gout, P. W., Buckley, A. R., Simms, C. R., and Bruchovsky, N. (2001). Sulfasalazine, a potent suppressor of lymphoma growth by inhibition of the x(c)(-) cystine transporter: a new action for an old drug. *Leukemia* 15, 1633–1640. doi: 10.1038/sj.leu.2402238
- Grossman, R. G., Frankowski, R. F., Burau, K. D., Toups, E. G., Crommett, J. W., Johnson, M. M., et al. (2012). Incidence and severity of acute complications after spinal cord injury. *J. Neurosurg. Spine* 17, 119–128.
- Guan, X., Li, X., Yang, X., Yan, J., Shi, P., Ba, L., et al. (2019). The neuroprotective effects of carvacrol on ischemia/reperfusion-induced hippocampal neuronal impairment by ferroptosis mitigation. *Life Sci.* 235:116795. doi: 10.1016/j.lfs.2019.116795
- Guo, J., Li, Y., Chen, Z., He, Z., Zhang, B., Li, Y., et al. (2015). N-acetylcysteine treatment following spinal cord trauma reduces neural tissue damage and improves locomotor function in mice. *Mol. Med. Rep.* 12, 37–44. doi: 10.3892/mmr.2015.3390
- Guo, Y., Liu, X., Liu, D., Li, K., Wang, C., Liu, Y., et al. (2019). Inhibition of BECN1 suppresses lipid peroxidation by increasing Xc(-) activity in early brain injury after subarachnoid hemorrhage. *J. Mol. Neurosci.* 67, 622–631. doi: 10.1007/s12031-019-01272-5
- Hadian, K., and Stockwell, B. R. (2020). SnapShot: ferroptosis. *Cell* 181, 1188–1188.e1. doi: 10.1016/j.cell.2020.04.039
- Hall, E. D., Detloff, M. R., Johnson, K., and Kupina, N. C. (2004). Peroxynitrite-mediated protein nitration and lipid peroxidation in a mouse model of traumatic brain injury. *J. Neurotrauma* 21, 9–20. doi: 10.1089/089771504772695904
- Hanson, L. R., Roeytenberg, A., Martinez, P. M., Coppes, V. G., Sweet, D. C., Rao, R. J., et al. (2009). Intranasal deferoxamine provides increased brain exposure and significant protection in rat ischemic stroke. *J. Pharmacol. Exp. Ther.* 330, 679–686. doi: 10.1124/jpet.108.149807
- Hao, J., Li, B., Duan, H.-Q., Zhao, C.-X., Zhang, Y., Sun, C., et al. (2017). Mechanisms underlying the promotion of functional recovery by deferoxamine after spinal cord injury in rats. *Neural. Regen. Res.* 12, 959–968.
- Hatakeyama, T., Okauchi, M., Hua, Y., Keep, R. F., and Xi, G. (2013). Deferoxamine reduces neuronal death and hematoma lysis after intracerebral hemorrhage in aged rats. *Transl. Stroke Res.* 4, 546–553. doi: 10.1007/s12975-013-0270-5
- Hayano, M., Yang, W. S., Corn, C. K., Pagano, N. C., and Stockwell, B. R. (2016). Loss of cysteinyl-tRNA synthetase (CARS) induces the transsulfuration pathway and inhibits ferroptosis induced by cystine deprivation. *Cell Death Differ.* 23, 270–278. doi: 10.1038/cdd.2015.93
- He, Y. J., Liu, X. Y., Xing, L., Wan, X., Chang, X., and Jiang, H. L. (2020). Fenton reaction-independent ferroptosis therapy via glutathione and iron redox couple sequentially triggered lipid peroxide generator. *Biomaterials* 241:119911. doi: 10.1016/j.biomaterials.2020.119911
- Hinman, A., Holst, C. R., Latham, J. C., Bruegger, J. J., Ulas, G., McCusker, K. P., et al. (2018). Vitamin E hydroquinone is an endogenous regulator of ferroptosis via redox control of 15-lipoxygenase. *PLoS One* 13:e0201369. doi: 10.1371/journal.pone.0201369
- Hirschhorn, T., and Stockwell, B. R. (2019). The development of the concept of ferroptosis. *Free Radic. Biol. Med.* 133, 130–143. doi: 10.1016/j.freeradbiomed.2018.09.043
- Hoffer, M. E., Balaban, C., Slade, M. D., Tsao, J. W., and Hoffer, B. (2013). Amelioration of acute sequelae of blast induced mild traumatic brain injury by N-acetyl cysteine: a double-blind, placebo controlled study. *PLoS One* 8:e54163. doi: 10.1371/journal.pone.0054163
- Homma, T., Kobayashi, S., Sato, H., and Fujii, J. (2019). Edaravone, a free radical scavenger, protects against ferroptotic cell death in vitro. *Exp. Cell Res.* 384:111592. doi: 10.1016/j.yexcr.2019.111592
- Hsieh, C. H., Lin, Y. J., Chen, W. L., Huang, Y. C., Chang, C. W., Cheng, F. C., et al. (2017). HIF-1 α triggers long-lasting glutamate excitotoxicity via system xc(-) in cerebral ischaemia-reperfusion. *J. Pathol.* 241, 337–349. doi: 10.1002/path.4838
- Hu, W., Wang, H., Liu, Z., Liu, Y., Wang, R., Luo, X., et al. (2017). Neuroprotective effects of lycopene in spinal cord injury in rats via antioxidative and antiapoptotic pathway. *Neurosci. Lett.* 642, 107–112. doi: 10.1016/j.neulet.2017.02.004
- Hu, X., Tao, C., Gan, Q., Zheng, J., Li, H., and You, C. (2016). Oxidative stress in intracerebral hemorrhage: sources, mechanisms, and therapeutic targets. *Oxid. Med. Cell. Longev.* 2016:215391.
- Hu, Z. X., Zhang, H., Yi, B., Yang, S. K., Liu, J., Hu, J., et al. (2020). VDR activation attenuate cisplatin induced AKI by inhibiting ferroptosis. *Cell Death Dis.* 11:73.
- Huang, L. L., Liao, X. H., Sun, H., Jiang, X., Liu, Q., and Zhang, L. (2019). Augmenter of liver regeneration protects the kidney from ischaemia-reperfusion injury in ferroptosis. *J. Cell. Mol. Med.* 23, 4153–4164. doi: 10.1111/jcmm.14302
- Ingold, I., Berndt, C., Schmitt, S., Doll, S., Poschmann, G., Buday, K., et al. (2018). Selenium utilization by GPX4 is required to prevent hydroperoxide-induced ferroptosis. *Cell* 172, 409–422.e21. doi: 10.1016/j.cell.2017.11.048
- Ishii, T., Bannai, S., and Sugita, Y. (1981). Mechanism of growth stimulation of L1210 cells by 2-mercaptoethanol in vitro. Role of the mixed disulfide of 2-mercaptoethanol and cysteine. *J. Biol. Chem.* 256, 12387–12392.
- Jackman, N. A., Melchior, S. E., Hewett, J. A., and Hewett, S. J. (2012). Non-cell autonomous influence of the astrocyte system xc(-) on hypoglycaemic neuronal cell death. *ASN Neuro* 4:e00074.
- Jiang, J. Y., Gao, G. Y., Feng, J. F., Mao, Q., Chen, L. G., Yang, X. F., et al. (2019). Traumatic brain injury in China. *Lancet Neurol.* 18, 286–295.
- Kagan, V. E., Mao, G., Qu, F., Angeli, J. P., Doll, S., Croix, C. S., et al. (2017). Oxidized arachidonic and adrenic PEs navigate cells to ferroptosis. *Nat. Chem. Biol.* 13, 81–90. doi: 10.1038/nchembio.2238
- Karalija, A., Novikova, L. N., Kingham, P. J., Wiberg, M., and Novikov, L. N. (2012). Neuroprotective effects of N-acetyl-cysteine and acetyl-L-carnitine after spinal cord injury in adult rats. *PLoS One* 7:e41086. doi: 10.1371/journal.pone.0041086
- Karalija, A., Novikova, L. N., Kingham, P. J., Wiberg, M., and Novikov, L. N. (2014). The effects of N-acetyl-cysteine and acetyl-L-carnitine on neural survival, neuroinflammation and regeneration following spinal cord injury. *Neuroscience* 269, 143–151. doi: 10.1016/j.neuroscience.2014.03.042
- Karuppagounder, S. S., Alin, L., Chen, Y., Brand, D., Bourassa, M. W., Dietrich, K., et al. (2018). N-acetylcysteine targets 5 lipoxygenase-derived, toxic lipids and can synergize with prostaglandin E2 to inhibit ferroptosis and improve

- outcomes following hemorrhagic stroke in mice. *Ann. Neurol.* 84, 854–872. doi: 10.1002/ana.25356
- Kawai, H., Nakai, H., Suga, M., Yuki, S., Watanabe, T., and Saito, K. I. (1997). Effects of a novel free radical scavenger, MCI-186, on ischemic brain damage in the rat distal middle cerebral artery occlusion model. *J. Pharmacol. Exp. Ther.* 281, 921–927.
- Keep, R. F., Hua, Y., and Xi, G. (2012). Intracerebral haemorrhage: mechanisms of injury and therapeutic targets. *Lancet Neurol.* 11, 720–731. doi: 10.1016/s1474-4422(12)70104-7
- Kenny, E. M., Fidan, E., Yang, Q., Anthonymuthu, T. S., New, L. A., Meyer, E. A., et al. (2019). Ferroptosis contributes to neuronal death and functional outcome after traumatic brain injury. *Crit. Care Med.* 47, 410–418. doi: 10.1097/ccm.0000000000003555
- Khalaf, S., Ahmad, A. S., Chamara, K. V. D. R., and Doré, S. (2018). Unique properties associated with the brain penetrant iron chelator HBED reveal remarkable beneficial effects after brain trauma. *J. Neurotrauma* 36, 43–53. doi: 10.1089/neu.2017.5617
- Khoshnam, S. E., Winlow, W., Farzaneh, M., Farbood, Y., and Moghaddam, H. F. (2017). Pathogenic mechanisms following ischemic stroke. *Neurol. Sci.* 38, 1167–1186. doi: 10.1007/s10072-017-2938-1
- Kondo, Y., Ogawa, N., Asanuma, M., Ota, Z., and Mori, A. (1995). Regional differences in late-onset iron deposition, ferritin, transferrin, astrocyte proliferation, and microglial activation after transient forebrain ischemia in rat brain. *J. Cereb. Blood Flow Metab.* 15, 216–226. doi: 10.1038/jcbfm.1995.27
- Lan, B., Ge, J. W., Cheng, S. W., Zheng, X. L., Liao, J., He, C., et al. (2020). Extract of Naotiaifang, a compound Chinese herbal medicine, protects neuron ferroptosis induced by acute cerebral ischemia in rats. *J. Integr. Med.* [Epub ahead of print].
- Lapchak, P. A., and Zivin, J. A. (2009). The lipophilic multifunctional antioxidant edaravone (radicut) improves behavior following embolic strokes in rabbits: a combination therapy study with tissue plasminogen activator. *Exp. Neurol.* 215, 95–100. doi: 10.1016/j.expneurol.2008.09.004
- Lei, P., Bai, T., and Sun, Y. (2019). Mechanisms of Ferroptosis and relations with regulated cell death: a review. *Front. Physiol.* 10:139. doi: 10.3389/fphys.2019.00139
- Leslie, S. W., Brown, L. M., Trent, R. D., Lee, Y. H., Morris, J. L., Jones, T. W., et al. (1992). Stimulation of N-Methyl-D-aspartate receptor-mediated calcium entry into dissociated neurons by reduced and oxidized glutathione. *Mol. Pharmacol.* 41, 308–314.
- Lewerenz, J., Ates, G., Methner, A., Conrad, M., and Maher, P. (2018). Oxytosis/Ferroptosis-(Re-) Emerging roles for oxidative stress-dependent non-apoptotic cell death in diseases of the central nervous system. *Front. Neurosci.* 12:214. doi: 10.3389/fnins.2018.00214
- Li, J., Cao, F., Yin, H. L., Huang, Z. J., Lin, Z. T., Mao, N., et al. (2020). Ferroptosis: past, present and future. *Cell Death Dis.* 11:88.
- Li, Q., Han, X., Lan, X., Gao, Y., Wan, J., Durham, F., et al. (2017). Inhibition of neuronal ferroptosis protects hemorrhagic brain. *JCI Insight* 2:e90777.
- Li, Q., Weiland, A., Chen, X., Lan, X., Han, X., Durham, F., et al. (2018). Ultrastructural characteristics of neuronal death and white matter injury in mouse brain tissues after intracerebral hemorrhage: coexistence of ferroptosis, autophagy, and necrosis. *Front. Neurol.* 9:581. doi: 10.3389/fneur.2018.00581
- Li, S., Jiang, D., Rosenkrans, Z. T., Barnhart, T. E., Ehlerding, E. B., Ni, D., et al. (2019a). Aptamer-conjugated framework nucleic acids for the repair of cerebral ischemia-reperfusion injury. *Nano Lett.* 19, 7334–7341. doi: 10.1021/acs.nanolett.9b02958
- Li, X., Zhan, J., Hou, Y., Chen, S., Hou, Y., Xiao, Z., et al. (2019b). Coenzyme Q10 suppresses oxidative stress and apoptosis via activating the Nrf-2/NQO-1 and NF-κB signaling pathway after spinal cord injury in rats. *Am. J. Transl. Res.* 11, 6544–6552.
- Li, X., Zhan, J., Hou, Y., Hou, Y., Chen, S., Luo, D., et al. (2019c). Coenzyme Q10 regulation of apoptosis and oxidative stress in H₂O₂ induced BMSC death by modulating the Nrf-2/NQO-1 signaling pathway and its application in a model of spinal cord injury. *Oxid. Med. Cell. Longev.* 2019:6493081.
- Li, X., Zhuang, X., and Qiao, T. (2019d). Role of ferroptosis in the process of acute radiation-induced lung injury in mice. *Biochem. Biophys. Res. Commun.* 519, 240–245. doi: 10.1016/j.bbrc.2019.08.165
- Li, Y. C., Cao, Y. M., Xiao, J., Shang, J. W., Tan, Q., Ping, F., et al. (2020). Inhibitor of apoptosis-stimulating protein of p53 inhibits ferroptosis and alleviates intestinal ischemia/reperfusion-induced acute lung injury. *Cell Death Differ.*
- Liang, W., Huang, X., and Chen, W. (2017). The effects of baicalin and baicalein on cerebral ischemia: a review. *Aging Dis.* 8, 850–867.
- Lipscomb, D. C., Gorman, L. G., Traystman, R. J., and Hurn, P. D. (1998). Low molecular weight iron in cerebral ischemic acidosis in vivo. *Stroke* 29, 487–492.
- Liu, J., Tang, T., and Yang, H. (2011). Protective effect of deferoxamine on experimental spinal cord injury in rat. *Injury* 42, 742–745. doi: 10.1016/j.injury.2010.08.028
- Liu, J.-B., Tang, T.-S., and Xiao, D.-S. (2004). Changes of free iron contents and its correlation with lipid peroxidation after experimental spinal cord injury. *Chin J. Traumatol.* 7, 229–232.
- Liu, Y., Wang, W., Li, Y., Xiao, Y., Cheng, J., and Jia, J. (2015). The 5-Lipoxygenase inhibitor zileuton confers neuroprotection against glutamate oxidative damage by inhibiting ferroptosis. *Biol. Pharm. Bull.* 38, 1234–1239. doi: 10.1248/bpb.b15-00048
- Lorente, L., Martín, M. M., Abreu-González, P., Ramos, L., Argüeso, M., Cáceres, J. J., et al. (2015). Association between serum malondialdehyde levels and mortality in patients with severe brain trauma injury. *J. Neurotrauma* 32, 1–6. doi: 10.1089/neu.2014.3456
- Lorincz, T., Jemnitz, K., Kardon, T., Mandl, J., and Szarka, A. (2015). Ferroptosis is involved in acetaminophen induced cell death. *Pathol. Oncol. Res.* 21, 1115–1121. doi: 10.1007/s12253-015-9946-3
- Lozano, D., Gonzales-Portillo, G. S., Acosta, S., de la Pena, I., Tajiri, N., Kaneko, Y., et al. (2015). Neuroinflammatory responses to traumatic brain injury: etiology, clinical consequences, and therapeutic opportunities. *Neuropsychiatr. Dis. Treat.* 11, 97–106.
- Lu, L., Cao, H., Wei, X., Li, Y., and Li, W. (2015). Iron deposition is positively related to cognitive impairment in patients with chronic mild traumatic brain injury: assessment with susceptibility weighted imaging. *BioMed Res. Int.* 2015:470676.
- Lv, H., Zhen, C., Liu, J., Yang, P., Hu, L., and Shang, P. (2019). Unraveling the potential role of glutathione in multiple forms of cell death in cancer therapy. *Oxid. Med. Cell. Longev.* 2019:3150145.
- Maas, A. I. R., Menon, D. K., Adelson, P. D., Andelic, N., Bell, M. J., Belli, A., et al. (2017). In, and investigators, traumatic brain injury: integrated approaches to improve prevention, clinical care, and research. *Lancet Neurol.* 16, 987–1048.
- Morris, G., Anderson, G., Berk, M., and Maes, M. (2013). Coenzyme Q10 depletion in medical and neuropsychiatric disorders: potential repercussions and therapeutic implications. *Mol. Neurobiol.* 48, 883–903. doi: 10.1007/s12035-013-8477-8
- Morris, G., Berk, M., Carvalho, A. F., Maes, M., Walker, A. J., and Puri, B. K. (2018). Why should neuroscientists worry about iron? The emerging role of ferroptosis in the pathophysiology of neurodegenerative diseases. *Behav. Brain Res.* 341, 154–175. doi: 10.1016/j.bbr.2017.12.036
- Nakamura, T., Keep, R. F., Hua, Y., Schallert, T., Hoff, J. T., and Xi, G. (2004). Deferoxamine-induced attenuation of brain edema and neurological deficits in a rat model of intracerebral hemorrhage. *J. Neurosurg.* 100, 672–678. doi: 10.3171/jns.2004.100.4.0672
- Nasoohi, S., Simani, L., Khodaghali, F., Nikseresht, S., Faizi, M., and Naderi, N. (2019). Coenzyme Q10 supplementation improves acute outcomes of stroke in rats pretreated with atorvastatin. *Nutr. Neurosci.* 22, 264–272. doi: 10.1080/1028415x.2017.1376928
- Nazemi, Z., Nourbakhsh, M. S., Kiani, S., Heydari, Y., Ashtiani, M. K., Daemi, H., et al. (2020). Co-delivery of minocycline and paclitaxel from injectable hydrogel for treatment of spinal cord injury. *J. Control Release* 321, 145–158. doi: 10.1016/j.jconrel.2020.02.009
- Nishi, H., Watanabe, T., Sakurai, H., Yuki, S., and Ishibashi, A. (1989). Effect of MCI-186 on brain edema in rats. *Stroke* 20, 1236–1240. doi: 10.1161/01.str.20.9.1236
- Nour, M., Scalzo, F., and Liebeskind, D. S. (2013). Ischemia-reperfusion injury in stroke. *Interv. Neurol.* 1, 185–199.
- Ottstad-Hansen, S., Hu, Q. X., Follin-Arbelet, V. V., Bentea, E., Sato, H., Massie, A., et al. (2018). The cystine-glutamate exchanger (xCT, Slc7a11) is expressed in significant concentrations in a subpopulation of astrocytes in the mouse brain. *Glia* 66, 951–970. doi: 10.1002/glia.23294
- Park, T. J., Park, J. H., Lee, G. S., Lee, J. Y., Shin, J. H., Kim, M. W., et al. (2019). Quantitative proteomic analyses reveal that GPX4 downregulation during myocardial infarction contributes to ferroptosis in cardiomyocytes. *Cell Death Dis.* 10:835.

- Park, U. J., Lee, Y. A., Won, S. M., Lee, J. H., Kang, S.-H., Springer, J. E., et al. (2011). Blood-derived iron mediates free radical production and neuronal death in the hippocampal CA1 area following transient forebrain ischemia in rat. *Acta Neuropathol.* 121, 459–473. doi: 10.1007/s00401-010-0785-8
- Patel, S. P., Sullivan, P. G., Pandya, J. D., Goldstein, G. A., VanRooyen, J. L., Yonutas, H. M., et al. (2014). N-acetylcysteine amide preserves mitochondrial bioenergetics and improves functional recovery following spinal trauma. *Exp. Neurol.* 257, 95–105. doi: 10.1016/j.expneurol.2014.04.026
- Paterniti, I., Mazzon, E., Emanuela, E., Paola, R. D., Galuppo, M., Bramanti, P., et al. (2010). Modulation of inflammatory response after spinal cord trauma with deferoxamine, an iron chelator. *Free Radic. Res.* 44, 694–709. doi: 10.3109/10715761003742993
- Pearn, M. L. I., Niesman, R., Egawa, J., Sawada, A., Almenar-Queralt, A., Shah, S. B., et al. (2017). Pathophysiology associated with traumatic brain injury: current treatments and potential novel therapeutics. *Cell. Mol. Neurobiol.* 37, 571–585. doi: 10.1007/s10571-016-0400-1
- Portbury, S. D., Hare, D. J., Sgambelloni, C., Finkelstein, D. I., and Adlard, P. A. (2016). A time-course analysis of changes in cerebral metal levels following a controlled cortical impact. *Metallomics* 8, 193–200. doi: 10.1039/c5mt00234f
- Portbury, S. D., Hare, D. J., Sgambelloni, C. J., Bishop, D. P., Finkelstein, D. I., Doble, P. A., et al. (2017). Age modulates the injury-induced metallomic profile in the brain. *Metallomics* 9, 402–410. doi: 10.1039/c6mt00260a
- Qureshi, A. I., Ling, G. S., Khan, J., Suri, M. F., Miskolczi, L., Guterman, L. R., et al. (2001). Quantitative analysis of injured, necrotic, and apoptotic cells in a new experimental model of intracerebral hemorrhage. *Crit. Care Med.* 29, 152–157. doi: 10.1097/00003246-200101000-00030
- Qureshi, A. I., Suri, M. F. K., Ostrow, P. T., Kim, S. H., Ali, Z., Shatla, A. A., et al. (2003). Apoptosis as a form of cell death in intracerebral hemorrhage. *Neurosurgery* 52, 1041–1047.
- Rai, G., Joshi, N., Jung, J. E., Liu, Y., Schultz, L., Yasgar, A., et al. (2014). Potent and selective inhibitors of human reticulocyte 12/15-lipoxygenase as anti-stroke therapies. *J. Med. Chem.* 57, 4035–4048. doi: 10.1021/jm401915r
- Ramezani, M., Sahraei, Z., Simani, L., Heydari, K., and Shahidi, F. (2018). Coenzyme Q10 supplementation in acute ischemic stroke: is it beneficial in short-term administration? *Nutr. Neurosci.* 1–6. doi: 10.1080/1028415x.2018.1541269 [Epub ahead of print].
- Readnower, R. D., Chavko, M., Adeeb, S., Conroy, M. D., Pauly, J. R., McCarron, R. M., et al. (2010). Increase in blood-brain barrier permeability, oxidative stress, and activated microglia in a rat model of blast-induced traumatic brain injury. *J. Neurosci. Res.* 88, 3530–3539. doi: 10.1002/jnr.22510
- Roth, T. L., Nayak, D., Atanasijevic, T., Koretsky, A. P., Latour, L. L., and McGavern, D. B. (2014). Transcranial amelioration of inflammation and cell death after brain injury. *Nature* 505, 223–228. doi: 10.1038/nature12808
- Sandercock, P., Wardlaw, J. M., Lindley, R. I., Dennis, M., Cohen, G., Murray, G., et al. (2012). The benefits and harms of intravenous thrombolysis with recombinant tissue plasminogen activator within 6 h of acute ischaemic stroke (the third international stroke trial [IST-3]): a randomised controlled trial. *Lancet* 379, 2352–2363. doi: 10.1016/s0140-6736(12)60768-5
- Sauerbeck, A., Schonberg, D. L., Laws, J. L., and McTigue, D. M. (2013). Systemic iron chelation results in limited functional and histological recovery after traumatic spinal cord injury in rats. *Exp. Neurol.* 248, 53–61. doi: 10.1016/j.expneurol.2013.05.011
- Savelev, S. U., Okello, E. J., and Perry, E. K. (2004). Butyryl- and acetylcholinesterase inhibitory activities in essential oils of *Salvia* species and their constituents. *Phytother. Res.* 18, 315–324. doi: 10.1002/ptr.1451
- Seiler, A., Schneider, M., Förster, H., Roth, S., Wirth, E. K., Culmsee, C., et al. (2008). Glutathione peroxidase 4 senses and translates oxidative stress into 12/15-lipoxygenase dependent- and AIF-mediated cell death. *Cell Metab.* 8, 237–248. doi: 10.1016/j.cmet.2008.07.005
- Selim, M. H., and Ratan, R. R. (2004). The role of iron neurotoxicity in ischemic stroke. *Ageing Res. Rev.* 3, 345–353. doi: 10.1016/j.arr.2004.04.001
- Senol, N., Naziroglu, M., and Yürüker, V. (2014). N-acetylcysteine and selenium modulate oxidative stress, antioxidant vitamin and cytokine values in traumatic brain injury-induced rats. *Neurochem. Res.* 39, 685–692. doi: 10.1007/s11064-014-1255-9
- Shang, Y., Luo, M., Yao, F., Wang, S., Yuan, Z., and Yang, Y. (2020). Ceruloplasmin suppresses ferroptosis by regulating iron homeostasis in hepatocellular carcinoma cells. *Cell Signal.* 72:109633. doi: 10.1016/j.cellsig.2020.109633
- Shen, L. D., Qi, W. H., Bai, J. J., Zuo, C. Y., Bai, D. L., Gao, W. D., et al. (2020). Resibufogenin inhibited colorectal cancer cell growth and tumorigenesis through triggering ferroptosis and ROS production mediated by GPX4 inactivation. *Anat. Rec.* [Epub ahead of print].
- Shimada, K., Skouta, R., Kaplan, A., Yang, W. S., Hayano, M., Dixon, S. J., et al. (2016). Global survey of cell death mechanisms reveals metabolic regulation of ferroptosis. *Nat. Chem. Biol.* 12, 497–503. doi: 10.1038/nchembio.2079
- Siddiq, A., Aminova, L. R., Troy, C. M., Suh, K., Messer, Z., Semenza, G. L., et al. (2009). Selective inhibition of hypoxia-inducible factor (HIF) prolyl-hydroxylase 1 mediates neuroprotection against normoxic oxidative death via HIF- and CREB-independent pathways. *J. Neurosci.* 29, 8828–8838. doi: 10.1523/jneurosci.1779-09.2009
- Silva, N. A., Sousa, N., Reis, R. L., and Salgado, A. J. (2014). From basics to clinical: a comprehensive review on spinal cord injury. *Prog. Neurobiol.* 114, 25–57. doi: 10.1016/j.pneurobio.2013.11.002
- Soria, F. N., Perez-Samartin, A., Martin, A., Gona, K. B., Llop, J., Szczupak, B., et al. (2014). Extrasynaptic glutamate release through cystine/glutamate antiporter contributes to ischemic damage. *J. Clin. Invest.* 124, 3645–3655. doi: 10.1172/jci71886
- Speer, R. E., Karuppagounder, S. S., Basso, M., Sleiman, S. F., Kumar, A., Brand, D., et al. (2013). Hypoxia-inducible factor prolyl hydroxylases as targets for neuroprotection by "antioxidant" metal chelators: from ferroptosis to stroke. *Free Radic. Biol. Med.* 62, 26–36. doi: 10.1016/j.freeradbiomed.2013.01.026
- Stockwell, B. R., Friedmann Angeli, J. P., Bayir, H., Bush, A. I., Conrad, M., Dixon, S. J., et al. (2017). Ferroptosis: a regulated cell death nexus linking metabolism, redox biology, and disease. *Cell* 171, 273–285. doi: 10.1016/j.cell.2017.09.021
- Su, Y., Zhao, B., Zhou, L., Zhang, Z., Shen, Y., Lv, H., et al. (2020). Ferroptosis, a novel pharmacological mechanism of anti-cancer drugs. *Cancer Lett.* 483, 127–136. doi: 10.1016/j.canlet.2020.02.015
- Sun, Y., Zheng, Y., Wang, C., and Liu, Y. (2018). Glutathione depletion induces ferroptosis, autophagy, and premature cell senescence in retinal pigment epithelial cells. *Cell Death Dis.* 9:753.
- Thorn, T. L., He, Y., Jackman, N. A., Lobner, D., Hewett, J. A., and Hewett, S. J. (2015). A cytotoxic co-operative interaction between energy deprivation and glutamate release from system xc⁻ mediates aglycemic neuronal cell death. *ASN Neuro* 7:759091415614301.
- Tomimoto, H., Shibata, M., Ihara, M., Akiguchi, I., Ohtani, R., and Budka, H. (2002). A comparative study on the expression of cyclooxygenase and 5-lipoxygenase during cerebral ischemia in humans. *Acta Neuropathol.* 104, 601–607. doi: 10.1007/s00401-002-0590-0
- Tran, A. P., Warren, P. M., and Silver, J. (2018). The biology of regeneration failure and success after spinal cord injury. *Physiol. Rev.* 98, 881–917. doi: 10.1152/physrev.00017.2017
- Tsai, T. H., Liu, S. C., Tsai, P. L., Ho, L. K., Shum, A. Y. C., and Chen, C. F. (2002). The effects of the cyclosporin A, a P-glycoprotein inhibitor, on the pharmacokinetics of baicalin in the rat: a microdialysis study. *Br. J. Pharmacol.* 137, 1314–1320. doi: 10.1038/sj.bjp.0704959
- Tuo, Q. Z., Lei, P., Jackman, K. A., Li, X. L., Xiong, H., Li, X. L., et al. (2017). Tau-mediated iron export prevents ferroptotic damage after ischemic stroke. *Mol. Psychiatry* 22, 1520–1530. doi: 10.1038/mp.2017.171
- Varga, V., Jenei, Z., Janaky, R., Saransaari, P., and Oja, S. S. (1997). Glutathione is an endogenous ligand of rat brain N-methyl-D-aspartate (n.d.) and 2-amino-3-hydroxy-5-methyl-4-isoxazolepropionate (AMPA) receptors. *Neurochem. Res.* 22, 1165–1171.
- Visavadiya, N. P., Patel, S. P., VanRooyen, J. L., Sullivan, P. G., and Rabchevsky, A. G. (2016). Cellular and subcellular oxidative stress parameters following severe spinal cord injury. *Redox Biol.* 8, 59–67. doi: 10.1016/j.redox.2015.12.011
- Viswanathan, V. S., Ryan, M. J., Dhruv, H. D., Gill, S., Eichhoff, O. M., Seashore-Ludlow, B., et al. (2017). Dependency of a therapy-resistant state of cancer cells on a lipid peroxidase pathway. *Nature* 547, 453–457.
- Wang, K.-Y., Wu, C.-H., Zhou, L.-Y., Yan, X.-H., Yang, R.-L., Liao, L.-M., et al. (2015). Ultrastructural changes of brain tissues surrounding hematomas after intracerebral hemorrhage. *Eur. Neurol.* 74, 28–35. doi: 10.1159/000434631
- Ward, R. J., Zucca, F. A., Duyn, J. H., Crichton, R. R., and Zecca, L. (2014). The role of iron in brain ageing and neurodegenerative disorders. *Lancet Neurol.* 13, 1045–1060. doi: 10.1016/s1474-4422(14)70117-6

- Watanabe, K., Tanaka, M., Yuki, S., Hirai, M., and Yamamoto, Y. (2018). How is edaravone effective against acute ischemic stroke and amyotrophic lateral sclerosis? *J. Clin. Biochem. Nutr.* 62, 20–38. doi: 10.3164/jcbn.17-62
- Wenzel, S. E., Tyurina, Y. Y., Zhao, J., St Croix, C. M., Dar, H. H., Mao, G., et al. (2017). PEBP1 wards ferroptosis by enabling lipoxygenase generation of lipid death signals. *Cell* 171, 628–641.e26. doi: 10.1016/j.cell.2017.09.044
- Winterbourn, C. C. (1995). Toxicity of iron and hydrogen peroxide: the Fenton reaction. *Toxicol. Lett.* 8, 969–974. doi: 10.1016/0378-4274(95)03532-x
- Witschi, A., Reddy, S., Stofer, B., and Lauterburg, B. H. (1992). The systemic availability of oral glutathione. *Eur. J. Clin. Pharmacol.* 43, 667–669. doi: 10.1007/bf02284971
- Wolpaw, A. J., Shimada, K., Skouta, R., Welsch, M. E., Akavia, U. D., Pe'er, D., et al. (2011). Modulatory profiling identifies mechanisms of small molecule-induced cell death. *Proc. Natl. Acad. Sci. U.S.A.* 108, E771–E780.
- Wu, C., Zhao, W., Yu, J., Li, S., Lin, L., and Chen, X. (2018). Induction of ferroptosis and mitochondrial dysfunction by oxidative stress in PC12 cells. *Sci. Rep.* 8:574.
- Wu, H., Wu, T., Li, M., and Wang, J. (2012). Efficacy of the lipid-soluble iron chelator 2,2'-dipyridyl against hemorrhagic brain injury. *Neurobiol. Dis.* 45, 388–394. doi: 10.1016/j.nbd.2011.08.028
- Wu, H., Wu, T., Xu, X., Wang, J., and Wang, J. (2011). Iron toxicity in mice with collagenase-induced intracerebral hemorrhage. *J. Cereb. Blood Flow Metab.* 31, 1243–1250. doi: 10.1038/jcbfm.2010.209
- Wu, J., Hua, Y., Keep, R. F., Nakamura, T., Hoff, J. T., and Xi, G. (2003). Iron and iron-handling proteins in the brain after intracerebral hemorrhage. *Stroke* 34, 2964–2969. doi: 10.1161/01.str.0000103140.52838.45
- Wu, J., Yang, J. J., Cao, Y., Li, H., Zhao, H., Yang, S., et al. (2020). Iron overload contributes to general anaesthesia-induced neurotoxicity and cognitive deficits. *J. Neuroinflamm.* 17:110.
- Xiao, X., Jiang, Y., Liang, W., Wang, Y., Cao, S., Yan, H., et al. (2019). miR-212-5p attenuates ferroptotic neuronal death after traumatic brain injury by targeting Ptg2. *Mol. Brain* 12:78.
- Xie, B. S., Wang, Y. Q., Lin, Y., Mao, Q., Feng, J. F., Gao, G. Y., et al. (2019). Inhibition of ferroptosis attenuates tissue damage and improves long-term outcomes after traumatic brain injury in mice. *CNS Neurosci. Ther.* 25, 465–475. doi: 10.1111/cns.13069
- Xie, Y., Hou, W., Song, X., Yu, Y., Huang, J., Sun, X., et al. (2016). Ferroptosis: process and function. *Cell Death Differ.* 23, 369–379. doi: 10.1038/cdd.2015.158
- Yagoda, N., von Rechenberg, M., Zaganjor, E., Bauer, A. J., Yang, W. S., Fridman, D. J., et al. (2007). RAS-RAF-MEK-dependent oxidative cell death involving voltage-dependent anion channels. *Nature* 447, 864–868.
- Yamada, N., Karasawa, T., Kimura, H., Watanabe, S., Komada, T., Kamata, R., et al. (2020). Ferroptosis driven by radical oxidation of n-6 polyunsaturated fatty acids mediates acetaminophen-induced acute liver failure. *Cell Death Dis.* 11:144.
- Yang, W. S., Kim, K. J., Gaschler, M. M., Patel, M., Shchepinov, M. S., and Stockwell, B. R. (2016). Peroxidation of polyunsaturated fatty acids by lipoxygenases drives ferroptosis. *Proc. Natl. Acad. Sci. U.S.A.* 113, E4966–E4975.
- Yang, W. S., SriRamaratnam, R., Welsch, M. E., Shimada, K., Skouta, R., Viswanathan, V. S., et al. (2014). Regulation of ferroptotic cancer cell death by GPX4. *Cell* 156, 317–331. doi: 10.1016/j.cell.2013.12.010
- Yang, W. S., and Stockwell, B. R. (2008). Synthetic lethal screening identifies compounds activating iron-dependent, nonapoptotic cell death in oncogenic-RAS-harboring cancer cells. *Chem. Biol.* 15, 234–245. doi: 10.1016/j.chembiol.2008.02.010
- Ye, L. F., Chaudhary, K. R., Zandkarimi, F., Harken, A. D., Kinslow, C. J., Upadhyayula, P. S., et al. (2020). Radiation-induced lipid peroxidation triggers ferroptosis and synergizes with ferroptosis inducers. *ACS Chem. Biol.* 15, 469–484. doi: 10.1021/acscmbio.9b00939
- Yigitkanli, K., Pekcec, A., Karatas, H., Pallast, S., Mandeville, E., Joshi, N., et al. (2013). Inhibition of 12/15-lipoxygenase as therapeutic strategy to treat stroke. *Ann. Neurol.* 73, 129–135. doi: 10.1002/ana.23734
- Yu, H., Zhang, Z. L., Chen, J., Pei, A., Hua, F., Qian, X., et al. (2012). Carvacrol, a food-additive, provides neuroprotection on focal cerebral ischemia/reperfusion injury in mice. *PLoS One* 7:e33584. doi: 10.1371/journal.pone.0033584
- Yuan, H., Li, X., Zhang, X., Kang, R., and Tang, D. (2016). Identification of ACSL4 as a biomarker and contributor of ferroptosis. *Biochem. Biophys. Res. Commun.* 478, 1338–1343. doi: 10.1016/j.bbrc.2016.08.124
- Zeng, L., Tan, L., Li, H., Zhang, Q., Li, Y., and Guo, J. (2018). Deferoxamine therapy for intracerebral hemorrhage: a systematic review. *PLoS One* 13:e0193615. doi: 10.1371/journal.pone.0193615
- Zhang, K., Tu, M., Gao, W., Cai, X., Song, F., Chen, Z., et al. (2019). Hollow prussian blue nanozymes drive neuroprotection against ischemic stroke via attenuating oxidative stress, counteracting inflammation, and suppressing cell apoptosis. *Nano Lett.* 19, 2812–2823. doi: 10.1021/acsnanolett.8b04729
- Zhang, L., Hu, R., Li, M., Li, F., Meng, H., Zhu, G., et al. (2013). Deferoxamine attenuates iron-induced long-term neurotoxicity in rats with traumatic brain injury. *Neurol. Sci.* 34, 639–645. doi: 10.1007/s10072-012-1090-1
- Zhang, Y., Sun, C., Zhao, C., Hao, J., Zhang, Y., Fan, B., et al. (2019). Ferroptosis inhibitor SRS 16-86 attenuates ferroptosis and promotes functional recovery in contusion spinal cord injury. *Brain Res.* 1706, 48–57. doi: 10.1016/j.brainres.2018.10.023
- Zhang, Z., Wu, Y., Yuan, S., Zhang, P., Zhang, J., Li, H., et al. (2018). Glutathione peroxidase 4 participates in secondary brain injury through mediating ferroptosis in a rat model of intracerebral hemorrhage. *Brain Res.* 1701, 112–125. doi: 10.1016/j.brainres.2018.09.012
- Zhao, X., Zhang, Y., Strong, R., Zhang, J., Grotta, J. C., and Aronowski, J. (2007). Distinct patterns of intracerebral hemorrhage-induced alterations in NF-kappaB subunit, iNOS, and COX-2 expression. *J. Neurochem.* 101, 652–663. doi: 10.1111/j.1471-4159.2006.04414.x
- Zhong, H., and Yin, H. (2015). Role of lipid peroxidation derived 4-hydroxynonenal (4-HNE) in cancer: focusing on mitochondria. *Redox Biol.* 4, 193–199. doi: 10.1016/j.redox.2014.12.011
- Zhou, Y., Wang, H.-D., Zhou, X.-M., Fang, J., Zhu, L., and Ding, K. (2018). N-acetylcysteine amide provides neuroprotection via Nrf2-ARE pathway in a mouse model of traumatic brain injury. *Drug Des. Dev. Ther.* 12, 4117–4127. doi: 10.2147/dddt.s179227
- Zille, M., Karuppagounder, S. S., Chen, Y., Gough, P. J., Bertin, J., Finger, J., et al. (2017). Neuronal death after hemorrhagic stroke in vitro and in vivo shares features of ferroptosis and necroptosis. *Stroke* 48, 1033–1043. doi: 10.1161/strokeaha.116.015609

Conflict of Interest: The authors declare that the research was conducted in the absence of any commercial or financial relationships that could be construed as a potential conflict of interest.

Copyright © 2020 Shen, Lin, Li, Wu, Lenahan, Pan, Xu, Chen, Shao and Zhang. This is an open-access article distributed under the terms of the Creative Commons Attribution License (CC BY). The use, distribution or reproduction in other forums is permitted, provided the original author(s) and the copyright owner(s) are credited and that the original publication in this journal is cited, in accordance with accepted academic practice. No use, distribution or reproduction is permitted which does not comply with these terms.



Plasma Membrane Pores Drive Inflammatory Cell Death

Benedikt Kolbrink, Theresa Riebeling, Ulrich Kunzendorf and Stefan Krautwald*

Department of Nephrology and Hypertension, University Hospital Schleswig-Holstein, Kiel, Germany

OPEN ACCESS

Edited by:

Yasunobu Okada,
National Institute for Physiological
Sciences (NIPS), Japan

Reviewed by:

Elodie Lafont,
INSERM U1242 Laboratoire COSS,
France
Carsten Culmsee,
University of Marburg, Germany

*Correspondence:

Stefan Krautwald
krautwald@nephro.uni-kiel.de

Specialty section:

This article was submitted to
Cell Death and Survival,
a section of the journal
Frontiers in Cell and Developmental
Biology

Received: 30 June 2020

Accepted: 03 August 2020

Published: 21 August 2020

Citation:

Kolbrink B, Riebeling T,
Kunzendorf U and Krautwald S (2020)
Plasma Membrane Pores Drive
Inflammatory Cell Death.
Front. Cell Dev. Biol. 8:817.
doi: 10.3389/fcell.2020.00817

Necroptosis and pyroptosis are two forms of regulated cell death. They are executed by the proteins mixed-lineage kinase domain-like (MLKL) and gasdermin D (GSDMD), respectively. Once activated by numerous pathways, these proteins form membrane pores that allow the influx and efflux of various ions, proteins, and water, ultimately resulting in the death of the cell. These modalities of cell death are considered highly inflammatory because of the release of inflammatory cytokines and damage-associated molecular patterns, and are thereby not only deleterious for the dying cell itself, but also its environment or the entire organism. The relevance for these processes has been observed in various physiological and pathophysiological conditions, ranging from viral and bacterial infections over autoimmune and chronic inflammatory diseases to ischemic organ damage. In recent years, initial *in vitro* experiments have shed light on a range of connections between necroptosis and pyroptosis. Initial *in vivo* studies also indicate that, in many disease models, these two forms of cell death cannot be considered individually, as they demonstrate a complex interaction. In this article, we provide an overview of the currently known structure, pathways of activation, and functions of MLKL and GSDMD. With emerging evidence for an interconnection between necroptosis and pyroptosis in not only *in vitro*, but also *in vivo* models of disease, we highlight in particular the clinical relevance of the crosslinks between these two forms of inflammatory cell death and their implications for novel therapeutic strategies in a variety of diseases.

Keywords: necroptosis, pyroptosis, MLKL, GSDMD, regulated cell death, necroinflammation

INTRODUCTION

In recent years, a variety of different forms of regulated cell death (RCD) has been discovered, and many of the underlying molecular mechanisms have been deciphered (Galluzzi et al., 2018; Tang et al., 2019). The permeabilization of the plasma membrane by pore-forming proteins plays a crucial role in only two distinct necrotic forms of RCD, namely necroptosis and pyroptosis. Both are considered inflammatory RCD, as the dying cells release miscellaneous damage-associated molecular patterns (DAMPs) and pro-inflammatory cytokines that induce profound inflammation of the surrounding tissue (Bergsbaken et al., 2009; Pasparakis and Vandenabeele, 2015). Apart from the obvious similarities, however, there are also subtle and less subtle differences, cross-links, and cooperation in the development of diseases between necroptosis and pyroptosis. Herein, we focus on the executing proteins mixed-lineage kinase domain-like (MLKL) and gasdermin D (GSDMD),

and provide an overview of their known mechanisms of activation and membrane permeabilization and the clinical relevance of understanding their interconnections.

NECROPTOSIS AND MLKL

Mixed-lineage kinase domain-like is the most terminal known indispensable effector protein of necroptosis. It is a 54 kDa protein that consists of an N-terminal four-helix bundle (4HB) and the C-terminal pseudokinase domain (PKD), which are connected by a two-helix linker brace (Petrie et al., 2017). In necroptosis, MLKL is activated by receptor-interacting serine/threonine protein kinase 3 (RIPK3) via phosphorylation of the residues T357/S358 in humans or S345 in mice (Sun et al., 2012; Murphy et al., 2013; Rodriguez et al., 2016). To date, three different activation pathways of MLKL in the context of necroptosis have been described: the first and best characterized begins by death receptor signaling via TNFR1, TRAIL or Fas ligand, and is mediated by RIPK1. The second pathway follows the activation of toll-like receptor (TLR) 3 and 4 and is mediated via the adaptor protein TRIF (also known as TICAM1), whereas the third characterized pathway follows activation of the cytosolic RNA sensor ZBP1 (also known as DAI). Common to all these pathways is that, in the absence or impairment of caspase function, the RHIM domain-containing proteins RIPK1, TRIF, or ZBP1 bind RIPK3 via their respective RHIM domains to form the so-called necrosome, which is followed by RIPK3 autophosphorylation and consecutive activation of MLKL (Weinlich et al., 2017; Shan et al., 2018; Malireddi et al., 2019). Whether necroptosis is dependent on the generation of mitochondrial reactive oxygen species (ROS) has also been discussed, but more recent data have challenged this hypothesis. The evidence for and against this idea is described in detail (Marshall and Baines, 2014). Recently, it was shown that, at least for RIPK1-dependent necroptosis, ROS enhance the activation of RIPK1 by autophosphorylation in a positive feedback loop (Zhang et al., 2017). However, the exact mechanism of how MLKL is phosphorylated by RIPK3 and hence activated differs among species and has not been resolved. In human cells, RIPK3 needs to bind MLKL via its PKD to phosphorylate and activate it (Sun et al., 2012; Petrie et al., 2018), whereas in murine cells, MLKL is not recruited to RIPK3, and phosphorylation alone is sufficient for inducing necroptosis (Murphy et al., 2013; Hildebrand et al., 2014; Jacobsen et al., 2016). For different vertebrates, it was shown recently that varying conformations of the PKD in particular play an important role in species-specific activation of MLKL (Davies et al., 2020).

The structure of the membrane pore formed by MLKL has not been resolved to date. It is generally agreed that phosphorylation of the PKD leads to a conformational change that exposes the 4HB, which results in MLKL oligomerization in the cytoplasm, traffic to the cell periphery via Golgi-microtubule-actin-dependent mechanisms and subsequent membrane translocation by binding phosphatidylinositol phosphates (PIPs), but there is disagreement about whether MLKL forms trimers, tetramers, or

hexamers (Cai et al., 2014; Chen et al., 2014; Dondelinger et al., 2014; Wang H. et al., 2014; Samson et al., 2020). Recently, we visualized necroptotic cell death in the presence of polyethylene glycols (PEGs) of different sizes and were able to estimate that the membrane pores executing necroptosis had inner diameters of around 4 nm (Ros et al., 2017). Once inserted into the plasma membrane, MLKL oligomers increase membrane permeability to cations, which leads to calcium and sodium influx and potassium efflux from the cell along the concentration gradients. This is followed by the influx of water into the cell along the osmotic gradient, and results in a unique morphology of the dying necroptotic cell, that is described as explosion-like (Chen et al., 2016; Xia et al., 2016).

The relevance for necroptosis has been shown in the pathophysiology of various diseases, both infectious and non-infectious. From a historical perspective, the concept of necroptosis was originally discovered in that small molecules, the so-called necrostatins, could suppress necrotic cell death in certain settings (Degterev et al., 2005). The next step was the discovery of RIPK1 as the target molecule of necrostatins and the subsequent identification of the other proteins involved in necroptosis, which then enabled investigations in knockout animals and animal models of specific diseases (Degterev et al., 2008; Silke et al., 2015). In an infectious context, necroptosis is a double-edged sword. It is of particular importance in the defense against viral pathogens and intracellular bacteria, although the mechanisms vary and have not been definitively elucidated. For specific infections, necroptosis has positive effects on the removal of pathogens, as shown in murine models of herpes simplex virus, cytomegalovirus, vaccinia virus, and influenza A virus (Cho et al., 2009; Upton et al., 2012; Wang X. et al., 2014; Nogusa et al., 2016). Remarkably, the clearance of *Listeria monocytogenes* also relies on RIPK3 and MLKL, which in this case does not lead to the death of the host cell, but inhibits bacterial growth by direct binding of MLKL to the bacteria (Sai et al., 2019). However, there are adverse effects of necroptosis in infections. In mouse models of infection with *Salmonella enterica* or *Staphylococcus aureus*, triggering of necroptosis by the pathogens is a deleterious process for the host (Robinson et al., 2012; Kitur et al., 2015). Apart from infections, necroptosis also has a function in sterile pathologies. Genetic deletion or pharmacological inhibition of RIPK1/3 and MLKL improve the outcome in models of systemic inflammatory response syndrome (Zelic et al., 2018; Moerke et al., 2019), and ischemia-reperfusion injury of the kidney (Müller et al., 2017), brain (Naito et al., 2020), and heart (Luedde et al., 2014). The RIPK3-MLKL axis is also involved in crystallopathies induced by cytotoxic crystals (Mulay et al., 2016). Cancer metastasis also depends on necroptosis (Strilic et al., 2016). As shown recently, necroptosis also plays a role in inflammatory skin diseases. In a mouse model of psoriasis, it was shown that inhibition of the RIPK1-RIPK3-MLKL axis has a protective effect (Duan et al., 2020), and that, in the absence of RIPK1 in keratinocytes, ZBP1-induced necroptosis leads to massive inflammation of the skin (Devos et al., 2020). The fact that two very different stimuli can trigger necroptosis via different pathways underlines the complexity of this topic, especially with regard to possible therapeutic interventions. A function of the

necroptosis signaling pathway has also been demonstrated in a broad range of other disease models, which is reviewed elsewhere in greater detail (Weinlich et al., 2017). Most recently, certain homozygous mutations in the *Mkl* gene that lead to a lethal inflammatory phenotype in mice were described for the first time. For unknown reasons, this phenotype seems to be caused by hyperinflammation of the mediastinum and salivary glands. In heterozygous human individuals, however, these mutations are associated with increased incidence of the autoimmune disease chronic recurrent multifocal osteomyelitis (Hildebrand et al., 2020). Taken together, there is ever growing evidence for necroptosis as a promising target for therapeutic efforts in a multitude of highly relevant diseases, although the mechanisms require further clarification.

PYROPTOSIS AND GSDMD

Pyroptosis is executed by the proteins of the gasdermin family. This chapter focuses on GSDMD, as it is so far the best characterized of these homologous pore-forming proteins and is conserved in humans and mice. GSDMD is a cytosolic 53 kDa protein expressed in immune cells and epithelia, and consists of a cytotoxic N-terminal domain (GSDMD-N), a linker region, and an inhibitory C-terminal domain (GSDMD-C) (Kuang et al., 2017). Although structurally similar at first glance, GSDMD is, in contrast to MLKL, not activated via phosphorylation but through proteolytic cleavage (Kayagaki et al., 2015; Shi et al., 2015). Two major pathways of GSDMD activation have been described. The so-called canonical pathway is dependent on the formation of multiprotein complexes called inflammasomes. Inflammasomes are formed by cytosolic pattern recognition receptors (PRRs) termed nucleotide-binding oligomerization domain (NOD) and leucine-rich repeat (LRR) receptors (NLRs), absent in melanoma 2 (AIM2)-like receptors, and retinoic acid-inducible gene I (RIG I)-like receptors. One of the best studied of these is the NLR protein 3 (NLRP3) inflammasome (Broz and Dixit, 2016). Canonical activation of the NLRP3 inflammasome requires two steps: in the first priming step, DAMPs or pathogen-associated molecular patterns (PAMPs) activate various PRRs such as TLRs, which leads to upregulation in the synthesis of critical inflammasome components such as NLRP3 itself, apoptosis-associated speck-like protein containing a caspase recruitment domain (ASC), procaspase-1, and the inactive precursor cytokines pro-interleukin (IL)-1 β and pro-IL-18. A second step is needed for inflammasome activation. A critical element of this activation step are changes in intracellular potassium and chloride concentrations, the function of which we have gained better understanding in recent years. To assemble the NLRP3 inflammasome, cytosolic ASC oligomers or specks must first be formed, and this process is dependent on chloride efflux from the cell. This chloride efflux relies on the translocation of chloride intracellular channels (CLICs) to the plasma membrane and is an indispensable upstream event of NLRP3 inflammasome activation (Tang et al., 2017; Green et al., 2018). Besides the CLICs, chloride outflow from the volume-regulated anion channel (VRAC) is also described in this

context, which can be inhibited by certain non-steroidal anti-inflammatory drugs (Daniels et al., 2016). In addition to chloride, potassium efflux is also necessary for inflammasome activation, and can be triggered by various mechanisms. Ionophores and bacterial toxins such as nigericin or streptolysin O can facilitate potassium efflux, making the NLRP3 inflammasome a sensor of deleterious microorganisms (Petrilli et al., 2007; Greaney et al., 2015). In addition, cell damage in the surrounding tissue, through which ATP enters the extracellular space, can be sensed by the ligand-gated purinergic P2X7 ion channel receptor (P2X7R). Thus, the cell membrane is permeabilized for cations, and potassium efflux becomes possible (Alves et al., 2014). The potassium efflux then leads to the association of NIMA-related kinase 7 (NEK7) with NLRP3 and subsequent inflammasome activation, which is followed by the cleavage of procaspase-1 into its active form and the processing and release of IL-1 β and IL-18 (Munoz-Planillo et al., 2013; He et al., 2016). As with the execution of necroptosis, the influence of disturbances in the redox homeostasis of the cell and ROS generation from several sources on NLRP3 inflammasome activation has also been discussed, although the underlying mechanisms are not fully understood (reviewed in Abais et al., 2015). The further details of canonical inflammasome activation exceed the scope of this review, and are described excellently elsewhere (Schroder and Tschopp, 2010; Broz and Dixit, 2016). Besides the canonical pathway, there are other means of initiating pyroptosis. The non-canonical pathway is a “shortcut” for the activating GSDMD. Upon sensing intracellular bacterial lipopolysaccharide (LPS), the inflammatory caspases-4/5 (in humans) and caspase-11 (in mice) can directly cleave GSDMD and initiate pyroptosis (Shi et al., 2014). GSDMD can also be activated directly by caspase-8 when transforming growth factor β -activated kinase 1 (TAK1), a central regulator of cell death and survival in a variety of settings, is inhibited, as described in the case of *Yersinia pseudotuberculosis* infection (Orning et al., 2018; Sarhan et al., 2018). Apart from this, GSDMD activation by the proteases cathepsin G and neutrophil elastase has been reported in myeloid cells (Sollberger et al., 2018; Burgener et al., 2019).

Common to all these pathways initiating pyroptosis is the proteolytic cleavage of GSDMD in the linker region, which releases GSDMD-N from its autoinhibition by GSDMD-C. GSDMD-N forms oligomers that create membrane pores. Therefore, GSDMD-N translocates exclusively to the inner leaflet of cell membranes by binding PIPs, phosphatidic acid, and phosphatidylserine (Ding et al., 2016; Liu et al., 2016). The nanostructure of the gasdermin pore has been described for mouse gasdermin A3 via cryo-electron microscopy. It appears to be a 26–28-fold symmetric, anti-parallel β -barrel pore with an inner diameter of 18 nm (Ruan et al., 2018). The size of the human GSDMD-N pore is estimated to be 10–20 nm (Ding et al., 2016; Sborgi et al., 2016). GSDMD-N also has the ability to bind cardiolipin, and there are reports of gasdermin-mediated permeabilization of mitochondria contributing to pyroptotic cell death (de Vasconcelos et al., 2019; Rogers et al., 2019). The GSDMD-N pore is structurally and functionally different from the MLKL pore. Intracellular osmolality is unchanged during

pyroptosis, as the GSDMD-N pore is unselective and allows free diffusion of ions and water as well as the release of processed cytokines, the first and foremost being IL-1 β and IL-18 (Heilig et al., 2018). This difference also finds its expression in the varying morphology between necroptosis and pyroptosis. In pyroptosis, there is no swelling or explosive rupture of the cells, but a flattening of the cytoplasm, as cytoplasmic fluid leaks through the pores (Chen et al., 2016).

Analogous to necroptosis, most of the understanding of the (patho-)physiological role of pyroptosis has been generated through the utilization of animal models deficient for the inflammatory caspases, inflammasome components, IL-1 and IL-18, or GSDMD. Countering infections is doubtless one of the most crucial roles of pyroptosis. The clearance of viral, bacterial, fungal, and protozoan infections relies on it to differing extents, depending on the underlying microorganism and context (Man et al., 2017). Direct lysis of bacteria through its ability to bind cardiolipin in the bacterial cell wall has been described for GSDMD-N (Liu et al., 2016). Counterintuitively, and all the more surprising, is the fact that *Gsdmd*-deficient mice showed improved survival in a model of infectious peritonitis by *Escherichia coli*, as *Gsdmd* deficiency in this case prolonged neutrophil survival and therefore improved bacterial clearance (Kambara et al., 2018). These findings once again underscore the complexity of RCD in disease. Besides infectious diseases, there is also evidence that pyroptosis has a role in sterile diseases, and these largely overlap those in which necroptosis has also shown relevance, such as in ischemia-reperfusion injury of the heart (Qiu et al., 2017), brain (Yang F. et al., 2014), and kidney (Yang J.R. et al., 2014), crystallopathies (Ludwig-Portugall et al., 2016; Goldberg et al., 2017), Alzheimer's disease (Han et al., 2020), and other neurodegenerative pathologies (McKenzie et al., 2020) and a multitude of other inflammatory diseases (Goldberg et al., 2017). Of particular note in this context is the recent discovery that ticagrelor – a substance usually administered in coronary heart disease due to its inhibitory properties on platelet aggregation – also inhibits the NLRP3 inflammasome and therefore pyroptosis by blocking the CLIC-dependent chloride efflux (Huang et al., 2020). This interesting double effect could explain part of the good efficacy after coronary interventions. However, much of this research has been conducted through genetic ablation or pharmacological inhibition of the NLRP3 inflammasome, and requires future testing of the models in specific *Gsdmd* knockout mice to clearly discriminate the exact contribution of pyroptosis itself from other inflammasome-driven effects.

CROSSLINKS BETWEEN NECROPTOSIS AND PYROPTOSIS

Although it was and still is necessary to consider the different forms of RCD in isolation to decipher their molecular pathways, there is emerging evidence for combined action of specific forms of RCD in particular diseases. We ourselves first demonstrated that ischemia-reperfusion injury of the kidney was not only mediated by necroptosis (Linkermann et al., 2012), but also

by the combination of necroptosis and ferroptosis, an iron-dependent form of regulated cell death driven by phospholipid peroxidation (Müller et al., 2017), and was greatly ameliorated by combined targeting of necroptosis and the RCD cyclophilin D-mediated mitochondrial permeability transition (Linkermann et al., 2013). Other authors have reported the cooperation of apoptosis and necroptosis in the pathology of ischemic stroke (Naito et al., 2020).

Recently, such an interaction has also become apparent between necroptosis and pyroptosis. Initial *in vitro* studies have shown RIPK3-dependent processing of IL-1 in the absence of the inhibitors of apoptosis proteins (IAPs), which play a critical role in several RCD pathways and human disease (Vince et al., 2012). The refined and complex mechanism of this process has been elucidated in further excellent research (Yabal et al., 2014; Lawlor et al., 2017). At the same time, a role for MLKL has been brought into play, and inflammasome activation dependent on the RIPK1-RIPK3-MLKL axis in dendritic cells has been reported (Kang et al., 2013) as well as MLKL-dependent and -independent RIPK3-mediated inflammasome activation (Kang et al., 2015; Lawlor et al., 2015). In 2017, it was shown that the activation of MLKL is sufficient for inflammasome assembly and the release of mature IL-1 β even in absence of GSDMD, a prime example of how different forms of RCD can compensate for each other (Gutierrez et al., 2017). Only weeks later, a second group similarly reported a cell-intrinsic activation of the NLRP3 inflammasome by MLKL during the induction of necroptotic cell death (Conos et al., 2017). These two studies also clearly identified the underlying mechanism: MLKL-mediated potassium efflux from the cell is the indispensable activation step analogous to the canonical pathway of inflammasome activation (Figure 1).

The first strong indications of an *in vivo* connection have been reported in a mouse model of *S. aureus* pneumonia, in which the inhibition of MLKL-dependent necroptosis decreased caspase-1 activation and IL-1 β processing (Kitur et al., 2015). Second, in a mouse model of oral infection with *Salmonella enterica* serovar *Typhimurium*, MLKL-dependent initiation of pyroptosis in the caecum was needed for effective clearance of the pathogen, whereas *Mkl*-deficient mice died significantly faster than their wild-type counterparts (Yu et al., 2018). Especially interesting in this case is the fact that Yu and colleagues showed, via the generation of bone marrow chimeras, that MLKL and therefore pyroptosis in non-hematopoietic cells conferred the protective effect against infection. Up to that point, a connection between MLKL and inflammasome activation had, to our knowledge, only been reported in cells of myeloid heritage. Another noteworthy connection between necroptosis and pyroptosis was found in the effect of the small molecule necrosulfonamide (NSA). NSA was initially described in a groundbreaking work by Xiaodong Wang's group (Sun et al., 2012). It covalently binds to human MLKL via the Cys86 residue, inhibiting its activation by RIPK3 and consequently necroptosis. Surprisingly, NSA is also capable of binding GSDMD via Cys191, inhibiting pyroptotic cell death not only *in vitro* in human and mouse cell lines but also *in vivo* in murine sepsis models (Rathkey et al., 2018). Most recently, a mouse model of combined *Ripk3/Gsdmd*

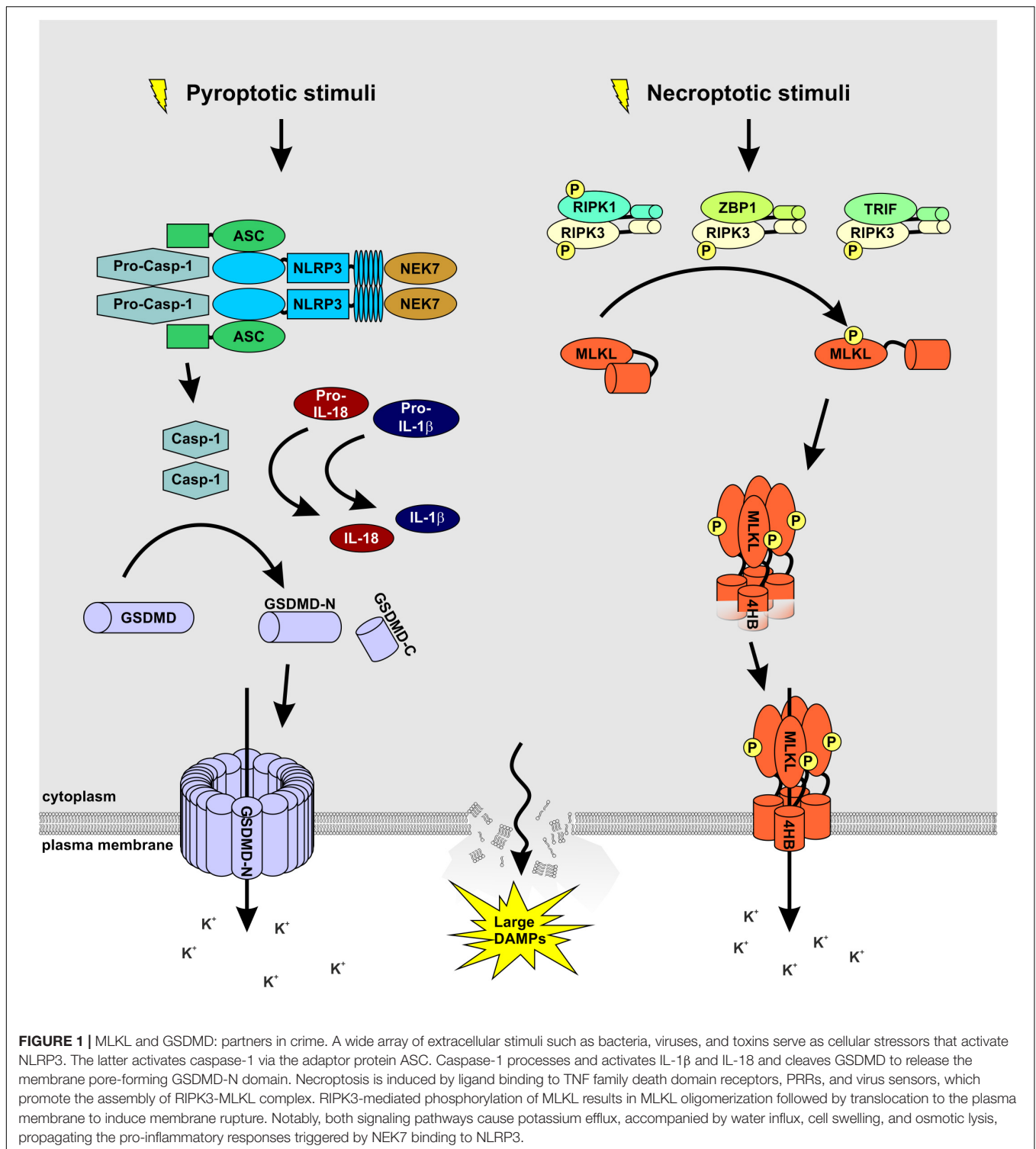


FIGURE 1 | MLKL and GSDMD: partners in crime. A wide array of extracellular stimuli such as bacteria, viruses, and toxins serve as cellular stressors that activate NLRP3. The latter activates caspase-1 via the adaptor protein ASC. Caspase-1 processes and activates IL-1 β and IL-18 and cleaves GSDMD to release the membrane pore-forming GSDMD-N domain. Necroptosis is induced by ligand binding to TNF family death domain receptors, PRRs, and virus sensors, which promote the assembly of RIPK3-MLKL complex. RIPK3-mediated phosphorylation of MLKL results in MLKL oligomerization followed by translocation to the plasma membrane to induce membrane rupture. Notably, both signaling pathways cause potassium efflux, accompanied by water influx, cell swelling, and osmotic lysis, propagating the pro-inflammatory responses triggered by NEK7 binding to NLRP3.

and *Mkl1/Gsdmd* knockout was reported. The double knockout showed significantly better protection in a mouse model of polymicrobial sepsis, and by generating bone marrow chimeras, the relevance of hematopoietic as well as non-hematopoietic cells in the model could be documented (Chen et al., 2020). Latterly, a connection between the three different forms of RCD

pyroptosis, apoptosis, and necroptosis (PAN) has been shown *in vitro*. Evidence that these three forms of cell death may be linked has been found in specific settings. In influenza A virus infection, ZBP1 is a central regulator of PAN (Kuriakose et al., 2016; Kesavardhana et al., 2017). Additionally, the genetic- or pathogen-induced loss of TAK1 can also trigger pyroptosis,

apoptosis, and necroptosis (Malireddi et al., 2018; Orning et al., 2018; Podder et al., 2019). This threefold activation of the cell death pathways was eventually termed PANoptosis (Malireddi et al., 2019). The most recent research in this field shows that this process is under the control of a master protein complex termed the PANoptosome (Christgen et al., 2020). Despite all this excellent work, our mechanistic understanding of these processes *in vivo* remains very vague. Based on the available data, it can be assumed that necroptosis and pyroptosis in particular play a common role not only in sepsis, but in a variety of other diseases, and we eagerly await further research in this area.

CONCLUSION AND CLINICAL RELEVANCE

Over the last few years, it has become clear that the forms of inflammatory RCD have a critical position in the pathophysiology of almost all known diseases. Membrane pores and ion fluxes play a central role in these cell death processes and are already promising targets for therapeutic approaches. However, it is becoming equally clear that different cell death pathways have context-dependent positive or negative impacts in that they can compensate for each other and have synergistic or antagonistic effects. Therefore, their therapeutic applications in humans must be tested with great care, and it must be clarified beyond doubt whether and to what extent the different forms of RCD are advantageous or disadvantageous in the respective disease and how they are interconnected. A further complicating factor is that an attempt at therapeutic

intervention in one pathway may unexpectedly have an impact on others. Besides testing combined gene knockouts in disease models, it would be of special interest to see whether a combined pharmacological approach of inhibiting necroptosis and pyroptosis would generate the same effect. Future efforts will have to focus on these interactions, as intervening in these pathways promises new and better treatment options for many previously poorly treatable diseases, including stroke, myocardial infarction, acute and chronic kidney failure, sepsis, systemic inflammatory response syndrome, and cancer.

AUTHOR CONTRIBUTIONS

UK contributed valuable ideas. TR generated the figure. BK and SK wrote the manuscript with input from all authors.

FUNDING

Work in the Krautwald lab was supported by a grant by the Deutsche Forschungsgemeinschaft [DFG, German Research Foundation, Projektnummer 400339789 (KR 1690/6-1)] and by the Dr. Werner Jackstädt-Stiftung.

ACKNOWLEDGMENTS

We thank Maike Berger and Katja Bruch for their excellent technical assistance. We would like to apologize to the many authors whose work we could not cite due to space restrictions.

REFERENCES

- Abais, J. M., Xia, M., Zhang, Y., Boini, K. M., and Li, P. L. (2015). Redox regulation of NLRP3 inflammasomes: ROS as trigger or effector? *Antioxid. Redox Signal.* 22, 1111–1129. doi: 10.1089/ars.2014.5994
- Alves, L. A., de Melo Reis, R. A., de Souza, C. A., de Freitas, M. S., Teixeira, P. C., Neto Moreira Ferreira, D., et al. (2014). The P2X7 receptor: shifting from a low- to a high-conductance channel - an enigmatic phenomenon? *Biochim. Biophys. Acta* 1838, 2578–2587. doi: 10.1016/j.bbame.2014.05.015
- Bergsbaken, T., Fink, S. L., and Cookson, B. T. (2009). Pyroptosis: host cell death and inflammation. *Nat. Rev. Microbiol.* 7, 99–109. doi: 10.1038/nrmicro2070
- Broz, P., and Dixit, V. M. (2016). Inflammasomes: mechanism of assembly, regulation and signalling. *Nat. Rev. Immunol.* 16, 407–420. doi: 10.1038/nri.2016.58
- Burgener, S. S., Leborgne, N. G. F., Snipas, S. J., Salvesen, G. S., Bird, P. I., and Benarafa, C. (2019). Cathepsin G inhibition by Serpinb1 and Serpinb6 prevents programmed necrosis in neutrophils and monocytes and reduces GSDMD-driven inflammation. *Cell Rep.* 27, 3646–3656.e5. doi: 10.1016/j.celrep.2019.05.065
- Cai, Z., Jitkaew, S., Zhao, J., Chiang, H. C., Choksi, S., Liu, J., et al. (2014). Plasma membrane translocation of trimerized MLKL protein is required for TNF-induced necroptosis. *Nat. Cell Biol.* 16, 55–65. doi: 10.1038/ncb2883
- Chen, H., Li, Y., Wu, J., Li, G., Tao, X., Lai, K., et al. (2020). RIPK3 collaborates with GSDMD to drive tissue injury in lethal polymicrobial sepsis. *Cell Death Differ.* doi: 10.1038/s41418-020-0524-1 [Epub ahead of print].
- Chen, X., He, W. T., Hu, L., Li, J., Fang, Y., Wang, X., et al. (2016). Pyroptosis is driven by non-selective gasdermin-D pore and its morphology is different from MLKL channel-mediated necroptosis. *Cell Res.* 26, 1007–1020. doi: 10.1038/cr.2016.100
- Chen, X., Li, W., Ren, J., Huang, D., He, W. T., Song, Y., et al. (2014). Translocation of mixed lineage kinase domain-like protein to plasma membrane leads to necrotic cell death. *Cell Res.* 24, 105–121. doi: 10.1038/cr.2013.171
- Cho, Y. S., Challa, S., Moquin, D., Genga, R., Ray, T. D., Guildford, M., et al. (2009). Phosphorylation-driven assembly of the RIP1-RIP3 complex regulates programmed necrosis and virus-induced inflammation. *Cell* 137, 1112–1123. doi: 10.1016/j.cell.2009.05.037
- Christgen, S., Zheng, M., Kesavardhana, S., Karki, R., Malireddi, R. K. S., Banoth, B., et al. (2020). Identification of the PANoptosome: a molecular platform triggering pyroptosis, Apoptosis, and necroptosis (PANoptosis). *Front. Cell. Infect. Microbiol.* 10:237. doi: 10.3389/fcimb.2020.00237
- Conos, S. A., Chen, K. W., De Nardo, D., Hara, H., Whitehead, L., Nunez, G., et al. (2017). Active MLKL triggers the NLRP3 inflammasome in a cell-intrinsic manner. *Proc. Natl. Acad. Sci. U.S.A.* 114, E961–E969. doi: 10.1073/pnas.1613305114
- Daniels, M. J., Rivers-Auty, J., Schilling, T., Spencer, N. G., Watremez, W., Fasolino, V., et al. (2016). Fenamate NSAIDs inhibit the NLRP3 inflammasome and protect against Alzheimer's disease in rodent models. *Nat. Commun.* 7:12504. doi: 10.1038/ncomms12504
- Davies, K. A., Fitzgibbon, C., Young, S. N., Garnish, S. E., Yeung, W., Coursier, D., et al. (2020). Distinct pseudokinase domain conformations underlie divergent activation mechanisms among vertebrate MLKL orthologues. *Nat. Commun.* 11:3060. doi: 10.1038/s41467-020-16823-3
- de Vasconcelos, N. M., Van Opdenbosch, N., Van Gorp, H., Parthoens, E., and Lamkanfi, M. (2019). Single-cell analysis of pyroptosis dynamics reveals conserved GSDMD-mediated subcellular events that precede plasma membrane rupture. *Cell Death Differ.* 26, 146–161. doi: 10.1038/s41418-018-0106-7

- Degterev, A., Hitomi, J., Gernsmeider, M., Ch'en, I. L., Korkina, O., Teng, X., et al. (2008). Identification of RIP1 kinase as a specific cellular target of necrostatins. *Nat. Chem. Biol.* 4, 313–321. doi: 10.1038/nchembio.83
- Degterev, A., Huang, Z., Boyce, M., Li, Y., Jagtap, P., Mizushima, N., et al. (2005). Chemical inhibitor of nonapoptotic cell death with therapeutic potential for ischemic brain injury. *Nat. Chem. Biol.* 1, 112–119. doi: 10.1038/nchembio711
- Devos, M., Tanghe, G., Gilbert, B., Dierick, E., Verheirstraeten, M., Nemegeer, J., et al. (2020). Sensing of endogenous nucleic acids by ZBP1 induces keratinocyte necroptosis and skin inflammation. *J. Exp. Med.* 217:e20191913. doi: 10.1084/jem.20191913
- Ding, J., Wang, K., Liu, W., She, Y., Sun, Q., Shi, J., et al. (2016). Pore-forming activity and structural autoinhibition of the gasdermin family. *Nature* 535, 111–116. doi: 10.1038/nature18590
- Dondelinger, Y., Declercq, W., Montessuit, S., Roelandt, R., Goncalves, A., Bruggeman, L., et al. (2014). MLKL compromises plasma membrane integrity by binding to phosphatidylinositol phosphates. *Cell Rep.* 7, 971–981. doi: 10.1016/j.celrep.2014.04.026
- Duan, X., Liu, X., Liu, N., Huang, Y., Jin, Z., Zhang, S., et al. (2020). Inhibition of keratinocyte necroptosis mediated by RIPK1/RIPK3/MLKL provides a protective effect against psoriatic inflammation. *Cell Death Dis.* 11:134. doi: 10.1038/s41419-020-2328-0
- Galluzzi, L., Vitale, I., Aaronson, S. A., Abrams, J. M., Adam, D., Agostinis, P., et al. (2018). Molecular mechanisms of cell death: recommendations of the nomenclature committee on cell death 2018. *Cell Death Differ.* 25, 486–541. doi: 10.1038/s41418-017-0012-4
- Goldberg, E. L., Asher, J. L., Molony, R. D., Shaw, A. C., Zeiss, C. J., Wang, C., et al. (2017). beta-hydroxybutyrate deactivates neutrophil NLRP3 inflammasome to relieve gout flares. *Cell Rep.* 18, 2077–2087. doi: 10.1016/j.celrep.2017.02.004
- Greaney, A. J., Leppla, S. H., and Moayeri, M. (2015). Bacterial exotoxins and the inflammasome. *Front. Immunol.* 6:570. doi: 10.3389/fimmu.2015.00570
- Green, J. P., Yu, S., Martin-Sanchez, F., Pelegrin, P., Lopez-Castejon, G., Lawrence, C. B., et al. (2018). Chloride regulates dynamic NLRP3-dependent ASC oligomerization and inflammasome priming. *Proc. Natl. Acad. Sci. U.S.A.* 115, E9371–E9380. doi: 10.1073/pnas.1812744115
- Gutierrez, K. D., Davis, M. A., Daniels, B. P., Olsen, T. M., Ralli-Jain, P., Tait, S. W., et al. (2017). MLKL activation triggers NLRP3-mediated processing and release of IL-1 β independently of Gasdermin-D. *J. Immunol.* 198, 2156–2164. doi: 10.4049/jimmunol.1601757
- Han, C., Yang, Y., Guan, Q., Zhang, X., Shen, H., Sheng, Y., et al. (2020). New mechanism of nerve injury in Alzheimer's disease: β -amyloid-induced neuronal pyroptosis. *J. Cell. Mol. Med.* 24, 8078–8090. doi: 10.1111/jcmm.15439
- He, Y., Zeng, M. Y., Yang, D., Motro, B., and Nunez, G. (2016). NEK7 is an essential mediator of NLRP3 activation downstream of potassium efflux. *Nature* 530, 354–357. doi: 10.1038/nature16959
- Heilig, R., Dick, M. S., Sborgi, L., Meunier, E., Hiller, S., and Broz, P. (2018). The gasdermin-D pore acts as a conduit for IL-1 β secretion in mice. *Eur. J. Immunol.* 48, 584–592. doi: 10.1002/eji.201747404
- Hildebrand, J. M., Kauppi, M., Majewski, I. J., Liu, Z., Cox, A. J., Miyake, S., et al. (2020). A missense mutation in the MLKL brace region promotes lethal neonatal inflammation and hematopoietic dysfunction. *Nat. Commun.* 11:3150. doi: 10.1038/s41467-020-16819-z
- Hildebrand, J. M., Tanzer, M. C., Lucet, I. S., Young, S. N., Spall, S. K., Sharma, P., et al. (2014). Activation of the pseudokinase MLKL unleashes the four-helix bundle domain to induce membrane localization and necroptotic cell death. *Proc. Natl. Acad. Sci. U.S.A.* 111, 15072–15077. doi: 10.1073/pnas.1408987111
- Huang, B., Qian, Y., Xie, S., Ye, X., Chen, H., Chen, Z., et al. (2020). Ticagrelor inhibits the NLRP3 inflammasome to protect against inflammatory disease independent of the P2Y12 signaling pathway. *Cell. Mol. Immunol.* doi: 10.1038/s41423-020-0444-5 [Epub ahead of print].
- Jacobsen, A. V., Lowes, K. N., Tanzer, M. C., Lucet, I. S., Hildebrand, J. M., Petrie, E. J., et al. (2016). HSP90 activity is required for MLKL oligomerization and membrane translocation and the induction of necroptotic cell death. *Cell Death Dis.* 7:e2051. doi: 10.1038/cddis.2015.386
- Kambara, H., Liu, F., Zhang, X., Liu, P., Bajrami, B., Teng, Y., et al. (2018). Gasdermin D exerts anti-inflammatory effects by promoting neutrophil death. *Cell Rep.* 22, 2924–2936. doi: 10.1016/j.celrep.2018.02.067
- Kang, S., Fernandes-Alnemri, T., Rogers, C., Mayes, L., Wang, Y., Dillon, C., et al. (2015). Caspase-8 scaffolding function and MLKL regulate NLRP3 inflammasome activation downstream of TLR3. *Nat. Commun.* 6:7515. doi: 10.1038/ncomms8515
- Kang, T. B., Yang, S. H., Toth, B., Kovalenko, A., and Wallach, D. (2013). Caspase-8 blocks kinase RIPK3-mediated activation of the NLRP3 inflammasome. *Immunity* 38, 27–40. doi: 10.1016/j.immuni.2012.09.015
- Kayagaki, N., Stowe, I. B., Lee, B. L., O'Rourke, K., Anderson, K., Warming, S., et al. (2015). Caspase-11 cleaves gasdermin D for non-canonical inflammasome signalling. *Nature* 526, 666–671. doi: 10.1038/nature15541
- Kesavardhana, S., Kuriakose, T., Guy, C. S., Samir, P., Malireddi, R. K. S., Mishra, A., et al. (2017). ZBP1/DAI ubiquitination and sensing of influenza vRNPs activate programmed cell death. *J. Exp. Med.* 214, 2217–2229. doi: 10.1084/jem.20170550
- Kitur, K., Parker, D., Nieto, P., Ahn, D. S., Cohen, T. S., Chung, S., et al. (2015). Toxin-induced necroptosis is a major mechanism of *Staphylococcus aureus* lung damage. *PLoS Pathog.* 11:e1004820. doi: 10.1371/journal.ppat.1004820
- Kuang, S., Zheng, J., Yang, H., Li, S., Duan, S., Shen, Y., et al. (2017). Structure insight of GSDMD reveals the basis of GSDMD autoinhibition in cell pyroptosis. *Proc. Natl. Acad. Sci. U.S.A.* 114, 10642–10647. doi: 10.1073/pnas.1708194114
- Kuriakose, T., Man, S. M., Subbarao Malireddi, R. K., Karki, R., Kesavardhana, S., Place, D. E., et al. (2016). ZBP1/DAI is an innate sensor of influenza virus triggering the NLRP3 inflammasome and programmed cell death pathways. *Sci. Immunol.* 1:aag2045. doi: 10.1126/sciimmunol.aag2045
- Lawlor, K. E., Feltham, R., Yabal, M., Conos, S. A., Chen, K. W., Ziehe, S., et al. (2017). XIAP loss triggers RIPK3- and Caspase-8-driven IL-1 β activation and cell death as a consequence of TLR-MyD88-induced cIAP1-TRAF2 degradation. *Cell Rep.* 20, 668–682. doi: 10.1016/j.celrep.2017.06.073
- Lawlor, K. E., Khan, N., Mildenhall, A., Gerlic, M., Croker, B. A., D'Cruz, A. A., et al. (2015). RIPK3 promotes cell death and NLRP3 inflammasome activation in the absence of MLKL. *Nat. Commun.* 6:6282. doi: 10.1038/ncomms7282
- Linkermann, A., Bräsen, J. H., Darding, M., Jin, M. K., Sanz, A. B., Heller, J. O., et al. (2013). Two independent pathways of regulated necrosis mediate ischemia-reperfusion injury. *Proc. Natl. Acad. Sci. U.S.A.* 110, 12024–12029. doi: 10.1073/pnas.1305538110
- Linkermann, A., Bräsen, J. H., Himmerkus, N., Liu, S., Huber, T. B., Kunzendorf, U., et al. (2012). Rip1 (receptor-interacting protein kinase 1) mediates necroptosis and contributes to renal ischemia/reperfusion injury. *Kidney Int.* 81, 751–761. doi: 10.1038/ki.2011.450
- Liu, X., Zhang, Z., Ruan, J., Pan, Y., Magupalli, V. G., Wu, H., et al. (2016). Inflammasome-activated gasdermin D causes pyroptosis by forming membrane pores. *Nature* 535, 153–158. doi: 10.1038/nature18629
- Ludwig-Portugall, I., Bartok, E., Dhana, E., Evers, B. D., Primiano, M. J., Hall, J. P., et al. (2016). An NLRP3-specific inflammasome inhibitor attenuates crystal-induced kidney fibrosis in mice. *Kidney Int.* 90, 525–539. doi: 10.1016/j.kint.2016.03.035
- Luedde, M., Lutz, M., Carter, N., Sosna, J., Jacoby, C., Vucur, M., et al. (2014). RIP3, a kinase promoting necroptotic cell death, mediates adverse remodeling after myocardial infarction. *Cardiovasc. Res.* 103, 206–216. doi: 10.1093/cvr/cvu146
- Malireddi, R. K. S., Gurung, P., Mavuluri, J., Dasari, T. K., Klco, J. M., Chi, H., et al. (2018). TAK1 restricts spontaneous NLRP3 activation and cell death to control myeloid proliferation. *J. Exp. Med.* 215, 1023–1034. doi: 10.1084/jem.20171922
- Malireddi, R. K. S., Kesavardhana, S., and Kanneganti, T.-D. (2019). ZBP1 and TAK1: master regulators of NLRP3 inflammasome/pyroptosis, Apoptosis, and necroptosis (PAN-optosis). *Front. Cell. Infect. Microbiol.* 9:406. doi: 10.3389/fcimb.2019.00406
- Man, S. M., Karki, R., and Kanneganti, T. D. (2017). Molecular mechanisms and functions of pyroptosis, inflammatory caspases and inflammasomes in infectious diseases. *Immunol. Rev.* 277, 61–75. doi: 10.1111/immr.12534
- Marshall, K. D., and Baines, C. P. (2014). Necroptosis: is there a role for mitochondria? *Front. Physiol.* 5:323. doi: 10.3389/fphys.2014.00323
- McKenzie, B. A., Dixit, V. M., and Power, C. (2020). Fiery cell death: pyroptosis in the central nervous system. *Trends Neurosci.* 43, 55–73. doi: 10.1016/j.tins.2019.11.005
- Moerke, C., Bleibaum, F., Kunzendorf, U., and Krautwald, S. (2019). Combined knockout of RIPK3 and MLKL reveals unexpected outcome in tissue injury and inflammation. *Front. Cell. Dev. Biol.* 7:19. doi: 10.3389/fcell.2019.00019
- Mulay, S. R., Desai, J., Kumar, S. V., Eberhard, J. N., Thomasova, D., Romoli, S., et al. (2016). Cytotoxicity of crystals involves RIPK3-MLKL-mediated necroptosis. *Nat. Commun.* 7:10274. doi: 10.1038/ncomms10274

- Müller, T., Dewitz, C., Schmitz, J., Schröder, A. S., Bräsen, J. H., Stockwell, B. R., et al. (2017). Necroptosis and ferroptosis are alternative cell death pathways that operate in acute kidney failure. *Cell. Mol. Life Sci.* 74, 3631–3645. doi: 10.1007/s00018-017-2547-4
- Munoz-Planillo, R., Kuffa, P., Martinez-Colon, G., Smith, B. L., Rajendiran, T. M., and Nunez, G. (2013). K(+) efflux is the common trigger of NLRP3 inflammasome activation by bacterial toxins and particulate matter. *Immunity* 38, 1142–1153. doi: 10.1016/j.immuni.2013.05.016
- Murphy, J. M., Czabotar, P. E., Hildebrand, J. M., Lucet, I. S., Zhang, J. G., Alvarez-Diaz, S., et al. (2013). The pseudokinase MLKL mediates necroptosis via a molecular switch mechanism. *Immunity* 39, 443–453. doi: 10.1016/j.immuni.2013.06.018
- Naito, M. G., Xu, D., Amin, P., Lee, J., Wang, H., Li, W., et al. (2020). Sequential activation of necroptosis and apoptosis cooperates to mediate vascular and neural pathology in stroke. *Proc. Natl. Acad. Sci. U.S.A.* 117, 4959–4970. doi: 10.1073/pnas.1916427117
- Nogusa, S., Thapa, R. J., Dillon, C. P., Liedmann, S., Oguin, T. H. III, Ingram, J. P., et al. (2016). RIPK3 activates parallel pathways of MLKL-driven necroptosis and FADD-mediated Apoptosis to protect against influenza A virus. *Cell Host Microbe* 20, 13–24. doi: 10.1016/j.chom.2016.05.011
- Orning, P., Weng, D., Starheim, K., Ratner, D., Best, Z., Lee, B., et al. (2018). Pathogen blockade of TAK1 triggers caspase-8-dependent cleavage of gasdermin D and cell death. *Science* 362, 1064–1069. doi: 10.1126/science.aau2818
- Pasparakis, M., and Vandenabeele, P. (2015). Necroptosis and its role in inflammation. *Nature* 517, 311–320. doi: 10.1038/nature14191
- Petrie, E. J., Hildebrand, J. M., and Murphy, J. M. (2017). Insane in the membrane: a structural perspective of MLKL function in necroptosis. *Immunol. Cell. Biol.* 95, 152–159. doi: 10.1038/icb.2016.125
- Petrie, E. J., Sandow, J. J., Jacobsen, A. V., Smith, B. J., Griffin, M. D. W., Lucet, I. S., et al. (2018). Conformational switching of the pseudokinase domain promotes human MLKL tetramerization and cell death by necroptosis. *Nat. Commun.* 9, 2422. doi: 10.1038/s41467-018-04714-7
- Petrilli, V., Papin, S., Dostert, C., Mayor, A., Martinon, F., and Tschopp, J. (2007). Activation of the NALP3 inflammasome is triggered by low intracellular potassium concentration. *Cell Death Differ.* 14, 1583–1589. doi: 10.1038/sj.cdd.4402195
- Podder, B., Gutta, C., Rozanc, J., Gerlach, E., Feoktistova, M., Panayotova-Dimitrova, D., et al. (2019). TAK1 suppresses RIPK1-dependent cell death and is associated with disease progression in melanoma. *Cell Death Differ.* 26, 2520–2534. doi: 10.1038/s41418-019-0315-8
- Qiu, S., Lei, S., Zhao, B., Wu, Y., Su, W., Liu, M., et al. (2017). NLRP3 inflammasome activation-mediated pyroptosis aggravates myocardial ischemia/reperfusion injury in diabetic rats. *Oxid. Med. Cell. Longev.* 2017, 9743280. doi: 10.1155/2017/9743280
- Rathkey, J. K., Zhao, J., Liu, Z., Chen, Y., Yang, J., Kondolf, H. C., et al. (2018). Chemical disruption of the pyroptotic pore-forming protein gasdermin D inhibits inflammatory cell death and sepsis. *Sci. Immunol.* 3, eaat2738. doi: 10.1126/sciimmunol.aat2738
- Robinson, N., McComb, S., Mulligan, R., Dudani, R., Krishnan, L., and Sad, S. (2012). Type I interferon induces necroptosis in macrophages during infection with *Salmonella enterica* serovar typhimurium. *Nat. Immunol.* 13, 954–962. doi: 10.1038/ni.2397
- Rodriguez, D. A., Weinlich, R., Brown, S., Guy, C., Fitzgerald, P., Dillon, C. P., et al. (2016). Characterization of RIPK3-mediated phosphorylation of the activation loop of MLKL during necroptosis. *Cell Death Differ.* 23, 76–88. doi: 10.1038/cdd.2015.70
- Rogers, C., Erkes, D. A., Nardone, A., Aplin, A. E., Fernandes-Alnemri, T., and Alnemri, E. S. (2019). Gasdermin pores permeabilize mitochondria to augment caspase-3 activation during apoptosis and inflammasome activation. *Nat. Commun.* 10, 1689. doi: 10.1038/s41467-019-09397-2
- Ros, U., Pena-Blanco, A., Hanggi, K., Kunzendorf, U., Krautwald, S., Wong, W. W., et al. (2017). Necroptosis execution is mediated by plasma membrane nanopores independent of calcium. *Cell Rep.* 19, 175–187. doi: 10.1016/j.celrep.2017.03.024
- Ruan, J., Xia, S., Liu, X., Lieberman, J., and Wu, H. (2018). Cryo-EM structure of the gasdermin A3 membrane pore. *Nature* 557, 62–67. doi: 10.1038/s41586-018-0058-6
- Sai, K., Parsons, C., House, J. S., Kathariou, S., and Ninomiya-Tsuji, J. (2019). Necroptosis mediators RIPK3 and MLKL suppress intracellular *Listeria* replication independently of host cell killing. *J. Cell. Biol.* 218, 1994–2005. doi: 10.1083/jcb.201810014
- Samson, A. L., Zhang, Y., Geoghegan, N. D., Gavin, X. J., Davies, K. A., Mlodzionoski, M. J., et al. (2020). MLKL trafficking and accumulation at the plasma membrane control the kinetics and threshold for necroptosis. *Nat. Commun.* 11, 3151. doi: 10.1038/s41467-020-16887-1
- Sarhan, J., Liu, B. C., Muendlein, H. I., Li, P., Nilson, R., Tang, A. Y., et al. (2018). Caspase-8 induces cleavage of gasdermin D to elicit pyroptosis during *Yersinia* infection. *Proc. Natl. Acad. Sci. U.S.A.* 115, E10888–E10897. doi: 10.1073/pnas.1809548115
- Sborgi, L., Ruhl, S., Mulvihill, E., Pipercevic, J., Heilig, R., Stahlberg, H., et al. (2016). GSDMD membrane pore formation constitutes the mechanism of pyroptotic cell death. *EMBO J.* 35, 1766–1778. doi: 10.15252/embo.201694696
- Schroder, K., and Tschopp, J. (2010). The inflammasomes. *Cell* 140, 821–832. doi: 10.1016/j.cell.2010.01.040
- Shan, B., Pan, H., Najafav, A., and Yuan, J. (2018). Necroptosis in development and diseases. *Genes Dev.* 32, 327–340. doi: 10.1101/gad.312561.118
- Shi, J., Zhao, Y., Wang, K., Shi, X., Wang, Y., Huang, H., et al. (2015). Cleavage of GSDMD by inflammatory caspases determines pyroptotic cell death. *Nature* 526, 660–665. doi: 10.1038/nature15514
- Shi, J., Zhao, Y., Wang, Y., Gao, W., Ding, J., Li, P., et al. (2014). Inflammatory caspases are innate immune receptors for intracellular LPS. *Nature* 514, 187–192. doi: 10.1038/nature13683
- Silke, J., Rickard, J. A., and Gerlic, M. (2015). The diverse role of RIP kinases in necroptosis and inflammation. *Nat. Immunol.* 16, 689–697. doi: 10.1038/ni.3206
- Sollberger, G., Choidas, A., Burn, G. L., Habenberger, P., Di Lucrezia, R., Kordes, S., et al. (2018). Gasdermin D plays a vital role in the generation of neutrophil extracellular traps. *Sci. Immunol.* 3, eaar6689. doi: 10.1126/sciimmunol.aar6689
- Strilic, B., Yang, L., Albarran-Juarez, J., Wachsmuth, L., Han, K., Müller, U. C., et al. (2016). Tumour-cell-induced endothelial cell necroptosis via death receptor 6 promotes metastasis. *Nature* 536, 215–218. doi: 10.1038/nature19076
- Sun, L., Wang, H., Wang, Z., He, S., Chen, S., Liao, D., et al. (2012). Mixed lineage kinase domain-like protein mediates necrosis signaling downstream of RIP3 kinase. *Cell* 148, 213–227. doi: 10.1016/j.cell.2011.11.031
- Tang, D., Kang, R., Berghe, T. V., Vandenabeele, P., and Kroemer, G. (2019). The molecular machinery of regulated cell death. *Cell Res.* 29, 347–364. doi: 10.1038/s41422-019-0164-5
- Tang, T., Lang, X., Xu, C., Wang, X., Gong, T., Yang, Y., et al. (2017). CLICs-dependent chloride efflux is an essential and proximal upstream event for NLRP3 inflammasome activation. *Nat. Commun.* 8, 202. doi: 10.1038/s41467-017-00227-x
- Upton, J. W., Kaiser, W. J., and Mocarski, E. S. (2012). DAI/ZBP1/DLM-1 complexes with RIP3 to mediate virus-induced programmed necrosis that is targeted by murine cytomegalovirus vIRA. *Cell Host Microbe* 11, 290–297. doi: 10.1016/j.chom.2012.01.016
- Vince, J. E., Wong, W. W., Gentle, I., Lawlor, K. E., Allam, R., O'Reilly, L., et al. (2012). Inhibitor of apoptosis proteins limit RIP3 kinase-dependent interleukin-1 activation. *Immunity* 36, 215–227. doi: 10.1016/j.immuni.2012.01.012
- Wang, H., Sun, L., Su, L., Rizo, J., Liu, L., Wang, L. F., et al. (2014). Mixed lineage kinase domain-like protein MLKL causes necrotic membrane disruption upon phosphorylation by RIP3. *Mol. Cell* 54, 133–146. doi: 10.1016/j.molcel.2014.03.003
- Wang, X., Li, Y., Liu, S., Yu, X., Li, L., Shi, C., et al. (2014). Direct activation of RIP3/MLKL-dependent necrosis by herpes simplex virus 1 (HSV-1) protein ICP6 triggers host antiviral defense. *Proc. Natl. Acad. Sci. U.S.A.* 111, 15438–15443. doi: 10.1073/pnas.1412767111
- Weinlich, R., Oberst, A., Beere, H. M., and Green, D. R. (2017). Necroptosis in development, inflammation and disease. *Nat. Rev. Mol. Cell Biol.* 18, 127–136. doi: 10.1038/nrm.2016.149
- Xia, B., Fang, S., Chen, X., Hu, H., Chen, P., Wang, H., et al. (2016). MLKL forms cation channels. *Cell Res.* 26, 517–528. doi: 10.1038/cr.2016.26
- Yabal, M., Müller, N., Adler, H., Knies, N., Gross, C. J., Damgaard, R. B., et al. (2014). XIAP restricts TNF- and RIP3-dependent cell death and

- inflammasome activation. *Cell Rep.* 7, 1796–1808. doi: 10.1016/j.celrep.2014.05.008
- Yang, F., Wang, Z., Wei, X., Han, H., Meng, X., Zhang, Y., et al. (2014). NLRP3 deficiency ameliorates neurovascular damage in experimental ischemic stroke. *J. Cereb. Blood Flow Metab.* 34, 660–667. doi: 10.1038/jcbfm.2013.242
- Yang, J. R., Yao, F. H., Zhang, J. G., Ji, Z. Y., Li, K. L., Zhan, J., et al. (2014). Ischemia-reperfusion induces renal tubule pyroptosis via the CHOP-caspase-11 pathway. *Am. J. Physiol. Renal Physiol.* 306, F75–F84. doi: 10.1152/ajprenal.00117.2013
- Yu, S. X., Chen, W., Liu, Z. Z., Zhou, F. H., Yan, S. Q., Hu, G. Q., et al. (2018). Non-hematopoietic MLKL protects against *salmonella* mucosal infection by enhancing inflammasome activation. *Front. Immunol.* 9:119. doi: 10.3389/fimmu.2018.00119
- Zelic, M., Roderick, J. E., O'Donnell, J. A., Lehman, J., Lim, S. E., Janardhan, H. P., et al. (2018). RIP kinase 1-dependent endothelial necroptosis underlies systemic inflammatory response syndrome. *J. Clin. Invest.* 128, 2064–2075. doi: 10.1172/JCI96147
- Zhang, Y., Su, S. S., Zhao, S., Yang, Z., Zhong, C. Q., Chen, X., et al. (2017). RIP1 autophosphorylation is promoted by mitochondrial ROS and is essential for RIP3 recruitment into necrosome. *Nat. Commun.* 8:14329. doi: 10.1038/ncomms14329

Conflict of Interest: The authors declare that the research was conducted in the absence of any commercial or financial relationships that could be construed as a potential conflict of interest.

Copyright © 2020 Kolbrink, Riebeling, Kunzendorf and Krautwald. This is an open-access article distributed under the terms of the Creative Commons Attribution License (CC BY). The use, distribution or reproduction in other forums is permitted, provided the original author(s) and the copyright owner(s) are credited and that the original publication in this journal is cited, in accordance with accepted academic practice. No use, distribution or reproduction is permitted which does not comply with these terms.



Iron Metabolism in Ferroptosis

Xin Chen^{1,2}, Chunhua Yu², Rui Kang² and Daolin Tang^{1,2*}

¹ Guangzhou Municipal and Guangdong Provincial Key Laboratory of Protein Modification and Degradation, The Third Affiliated Hospital, School of Basic Medical Sciences, Guangzhou Medical University, Guangzhou, China, ² Department of Surgery, UT Southwestern Medical Center, Dallas, TX, United States

Ferroptosis is a form of regulated cell death that is characterized by iron-dependent oxidative damage and subsequent plasma membrane ruptures and the release of damage-associated molecular patterns. Due to the role of iron in mediating the production of reactive oxygen species and enzyme activity in lipid peroxidation, ferroptosis is strictly controlled by regulators involved in many aspects of iron metabolism, such as iron uptake, storage, utilization, and efflux. Translational and transcriptional regulation of iron homeostasis provide an integrated network to determine the sensitivity of ferroptosis. Impaired ferroptosis is implicated in various iron-related pathological conditions or diseases, such as cancer, neurodegenerative diseases, and ischemia-reperfusion injury. Understanding the molecular mechanisms underlying the regulation of iron metabolism during ferroptosis may provide effective strategies for the treatment of ferroptosis-associated diseases. Indeed, iron chelators effectively prevent the occurrence of ferroptosis, which may provide new approaches for the treatment of iron-related disorders. In this review, we summarize recent advances in the theoretical modeling of iron-dependent ferroptosis, and highlight the therapeutic implications of iron chelators in diseases.

Keywords: ferroptosis, cell death, iron, lipid peroxidation, disease

INTRODUCTION

Despite its essential role in life, excessive iron is toxic due to its ability to generate reactive oxygen species (ROS) and to even trigger cell death. There are two main distinct categories of cell death, namely accidental cell death (ACD) and regulated cell death (RCD) (Galluzzi et al., 2018). ACD is usually due to irreparable damage after external or internal physical and chemical stimulation, and it occurs in an uncontrollable way, whereas RCD involves a precise signaling pathway controlled by designated cellular machinery. Compared with ACD, RCD has received extensive attention due to it being closely related to pathologic conditions and human diseases, which can be targeted by small molecule compounds or drugs. A growing number of RCD types have been proposed, such as necroptosis, pyroptosis, ferroptosis, and alkaliptosis. They may share similar necrotic morphology, but their molecular mechanisms are different (Tang et al., 2019).

Ferroptosis is a type of oxidative cell death that is induced by the accumulation of iron-mediated lipid peroxidation (Xie et al., 2016a; Stockwell et al., 2017). Its name was coined in 2012 as the discovery of small molecules (e.g., erastin and RSL3) selectively induced a non-apoptotic form of RCD in cancer cells that can be blocked by iron chelators or lipophilic antioxidants (e.g., vitamin E/ α -tocopherol and ferrostatin-1) (Dixon et al., 2012). The morphological features of ferroptosis are distinct from apoptotic cell death. Apoptotic cells are characterized by membrane blebbing,

OPEN ACCESS

Edited by:

Giovanna Valenti,
University of Bari Aldo Moro, Italy

Reviewed by:

Jianbo Sun,
Sun Yat-sen University, China
Kuanyu Li,
Nanjing University, China

*Correspondence:

Daolin Tang
daolin.tang@utsouthwestern.edu

Specialty section:

This article was submitted to
Cell Death and Survival,
a section of the journal
Frontiers in Cell and Developmental
Biology

Received: 31 July 2020

Accepted: 17 September 2020

Published: 07 October 2020

Citation:

Chen X, Yu C, Kang R and Tang D
(2020) Iron Metabolism in Ferroptosis.
Front. Cell Dev. Biol. 8:590226.
doi: 10.3389/fcell.2020.590226

cellular shrinkage, nuclear fragmentation, and chromatin condensation, whereas ferroptotic cells show typical necrotic morphology, such as an incomplete plasma membrane and the release of intracellular contents, especially damage-associated molecular patterns (DAMPs) (Wen et al., 2019). Ultrastructural analysis further revealed that the mitochondria of ferroptotic cells show a loss of structural integrity and smaller size (Dixon et al., 2012), whereas mitochondria are usually swollen in apoptotic cells (Tang et al., 2019).

Autophagy is a lysosome-dependent degradation system through which cells break down various cargos, such as organelles and proteins. There is a complex interaction between autophagy and lipid metabolism (Xie et al., 2020). Although an early study showed that ferroptosis is unrelated to autophagy, increased autophagy flux is indeed widely observed in the ferroptotic response (Zhou et al., 2019; Liu J. et al., 2020). While autophagy plays an adaptive role in protecting cells from environmental stress, it can promote ferroptosis in many cases (Zhou et al., 2019; Liu J. et al., 2020). Specifically, selective autophagy (e.g., ferritinophagy, lipophagy, and clockophagy) is involved in mediating ferroptotic cell death through the degradation of anti-ferroptosis regulators (Gao et al., 2016; Hou et al., 2016; Bai et al., 2019; Yang et al., 2019). Autophagy regulators, such as beclin 1 (BECN1) (Song et al., 2018), mechanistic target of rapamycin kinase (MTOR) (Liu Y. et al., 2020), and a lysosomal protease cathepsin B (CTSB) (Gao et al., 2018) contribute to ferroptotic cell death through affecting lipid peroxidation. Since there are many different types of selective autophagy, the relationship between autophagy and ferroptosis in regulating cell fate needs further investigation (Kang and Tang, 2017).

In this review, we first introduce the molecular mechanisms of ferroptosis and then focus on a discussion of regulators of iron metabolism in ferroptosis (Table 1). Finally, we describe the therapeutic implications of iron chelators in the damage and diseases associated with ferroptosis.

CORE MOLECULAR MECHANISMS OF FERROPTOSIS

The central role of lipid peroxidation in driving ferroptotic cell death indicates that ferroptosis can be caused by the collapse of the glutathione (GSH)-glutathione peroxidase 4 (GPX4) antioxidant systems (Figure 1). System x_c^- is a heterodimeric transmembrane complex composed of light chain, solute carrier family 7 member 11 (SLC7A11/xCT), and heavy chain, solute carrier family 3 member 2 (SLC3A2). After entering the cells by system x_c^- , cystine is quickly reduced to cysteine, which is mainly utilized for the synthesis of GSH. As a potent low molecular weight antioxidant in cells, GSH is utilized by GPX4, which uses highly nucleophilic selenocysteine to reduce lipid peroxides into lipid alcohols. The pharmacological inhibitors of system x_c^- (e.g., erastin) and GPX4 (e.g., RSL3) are the classical two ferroptosis inducers. In addition, several GPX4-independent anti-ferroptosis pathways have recently been identified, such as the apoptosis-inducing factor mitochondria-associated 2 (AIFM2)-mediated CoQ10 production pathway (Bersuker et al., 2019; Doll et al., 2019),

and the endosomal sorting complex required for transport-III (ESCRT-III)-dependent membrane repair pathway (Dai et al., 2020). These findings indicate that multiple antioxidants and membrane repair pathways limit the oxidative damage caused by ferroptosis, although their selectivity and specificity in ferroptosis are still unclear.

Lipid peroxidation results in the oxidation of polyunsaturated fatty acid (PUFA) of the membrane lipids. An impaired antioxidant system can cause or accelerate lethal lipid peroxidation, which is inhibited by various synthetic antioxidants (e.g., ferrostatin-1 and liproxstatin-1). Acyl-CoA synthetase long-chain family member 4 (ACSL4) is a crucial pro-ferroptotic regulator by catalyzing the synthesis of long-chain polyunsaturated CoAs, especially arachidonic acid, thus enriching cellular membranes with PUFA (Yuan et al., 2016b; Doll et al., 2017; Kagan et al., 2017). Several hypotheses have been proposed to explain the subsequent oxidation of PUFA after ACSL4-mediated PUFA synthesis (Figure 1). First, nicotinamide adenine dinucleotide phosphate (NADPH) oxidases (NOXs), a class of membrane-bound enzyme complexes that catalyzes the production of superoxides, contributes to iron-dependent accumulation of lipid peroxidation during ferroptosis (Dixon et al., 2012; Xie et al., 2017; Yang et al., 2020). Second, lipoxygenases (ALOXs) drive ferroptosis through directly catalyzing the oxygenation of PUFA (Yang et al., 2016; Kagan et al., 2017). Third, cytochrome P450 oxidoreductase (POR) coupled to cytochrome P450 (CYP) monooxygenases represents an alternative source of ROS for the induction of ferroptosis-related lipid peroxidation (Zou et al., 2020). Fourth, ROS generated by the electron leakage of the mitochondrial electron transport chain (ETC) may be another factor leading to lipid peroxidation in the process of ferroptosis in some cases (Gao et al., 2019). However, since NOXs, ALOXs, and CYP are all large family enzymes, it is difficult to determine which member of these enzymes is responsible for the ferroptosis.

REGULATORS OF IRON METABOLISM IN FERROPTOSIS

Although the exact mechanisms related to iron in ferroptosis remain obscure, there is no doubt about the key role of iron metabolism in the process of ferroptosis, because (1) Iron chelators block ferroptotic cell death *in vitro* and *in vivo* (Dixon et al., 2012); (2) Increased cellular labile iron is usually observed during the induction of ferroptosis (Hou et al., 2016); (3) An exogenous supplement of iron increases the sensitivity of cells to ferroptosis inducers (e.g., erastin) (Dixon et al., 2012); (4) Excessive heme and non-heme iron can directly induce ferroptosis (Li et al., 2017); (5) Several heme and non-heme iron-containing enzymes, such as ALOXs, NOXs, and CYP, are responsible for the production of lipid peroxidation (Dixon et al., 2012; Yang et al., 2016; Kagan et al., 2017; Xie et al., 2017; Yang et al., 2020; Zou et al., 2020); and (6) Iron-mediated ROS production by Fenton reaction promotes lipid peroxidation in ferroptosis (Dixon et al., 2012). Thus, multiple regulators of iron metabolism involved in iron uptake, storage, utilization, and

TABLE 1 | Main proteins modulating iron metabolism in ferroptosis.

Gene	Description	Functions	Diseases/models	References
CISD1	CDGSH iron sulfur domain 1	Regulates mitochondrial iron homeostasis	Cancer	Yuan et al., 2016a
CISD2	CDGSH iron sulfur domain 2	Regulates mitochondrial iron homeostasis	Cancer	Kim et al., 2018
CP	Ceruloplasmin	Mediates oxidation of Fe ²⁺ to Fe ³⁺	Cancer, ischemic stroke	Shang et al., 2020; Tuo et al., 2017
FTH1	Ferritin heavy chain 1	Stores iron	<i>Drosophila</i>	Mumbauer et al., 2019
FTL	Ferritin light chain	Stores iron	<i>Drosophila</i>	Mumbauer et al., 2019
FTMT	Ferritin mitochondrial	Stores iron	Neuronal cells	Wang et al., 2016
HMOX1	Heme oxygenase 1	Catabolizes heme	Cancer, ferroptotic damage in heart and renal proximal tubular cells	Kwon et al., 2015; Chang et al., 2018; Fang et al., 2019; Adedoyin et al., 2018; Sun et al., 2016b
HSPB1	Heat shock protein family B small member 1	Inhibits iron uptake	Cancer	Sun et al., 2015
IREB2	Iron-responsive element binding protein 2	Regulates the translation of mRNAs that affect iron homeostasis	Cancer	Dixon et al., 2012
LTF	Lactotransferrin	Transports iron	Cancer	Wang et al., 2020
NCOA4	Nuclear receptor coactivator 4	Mediates ferritinophagy	Cancer, chronic obstructive pulmonary disease, aging, liver fibrosis	Hou et al., 2016; Gao et al., 2016; Yoshida et al., 2019; Masaldan et al., 2018; Kong et al., 2019; Chen G.Q. et al., 2020
NFS1	NFS1 cysteine desulfurase	Mediates biosynthesis of the Fe-S cluster	Cancer	Alvarez et al., 2017
PCBP1	Poly(RC) binding protein 1	Iron chaperones	Hepatic steatosis	Protchenko et al., 2020
PROM2	Prominin-2	Promotes ferritin export	Cancer	Brown et al., 2019
SLC25A28	Solute carrier family 25 member 28	Mediates mitochondrial iron import	Hepatic stellate cells	Zhang et al., 2020
SLC39A14	Solute carrier family 39 member 14	Mediates iron uptake	Liver fibrosis	Yu et al., 2020
SLC40A1	Solute carrier family 40 member 1	Mediates iron export	Cancer, testicular ischemia-reperfusion injury	Geng et al., 2018; Li L. et al., 2018
TF	Transferrin	Transports iron	Cancer	Gao et al., 2015
TFRC	Transferrin receptor	Mediates iron uptake	Cancer	Gao et al., 2015; Ooko et al., 2015; Song et al., 2016; Wu et al., 2019; Yang and Stockwell, 2008

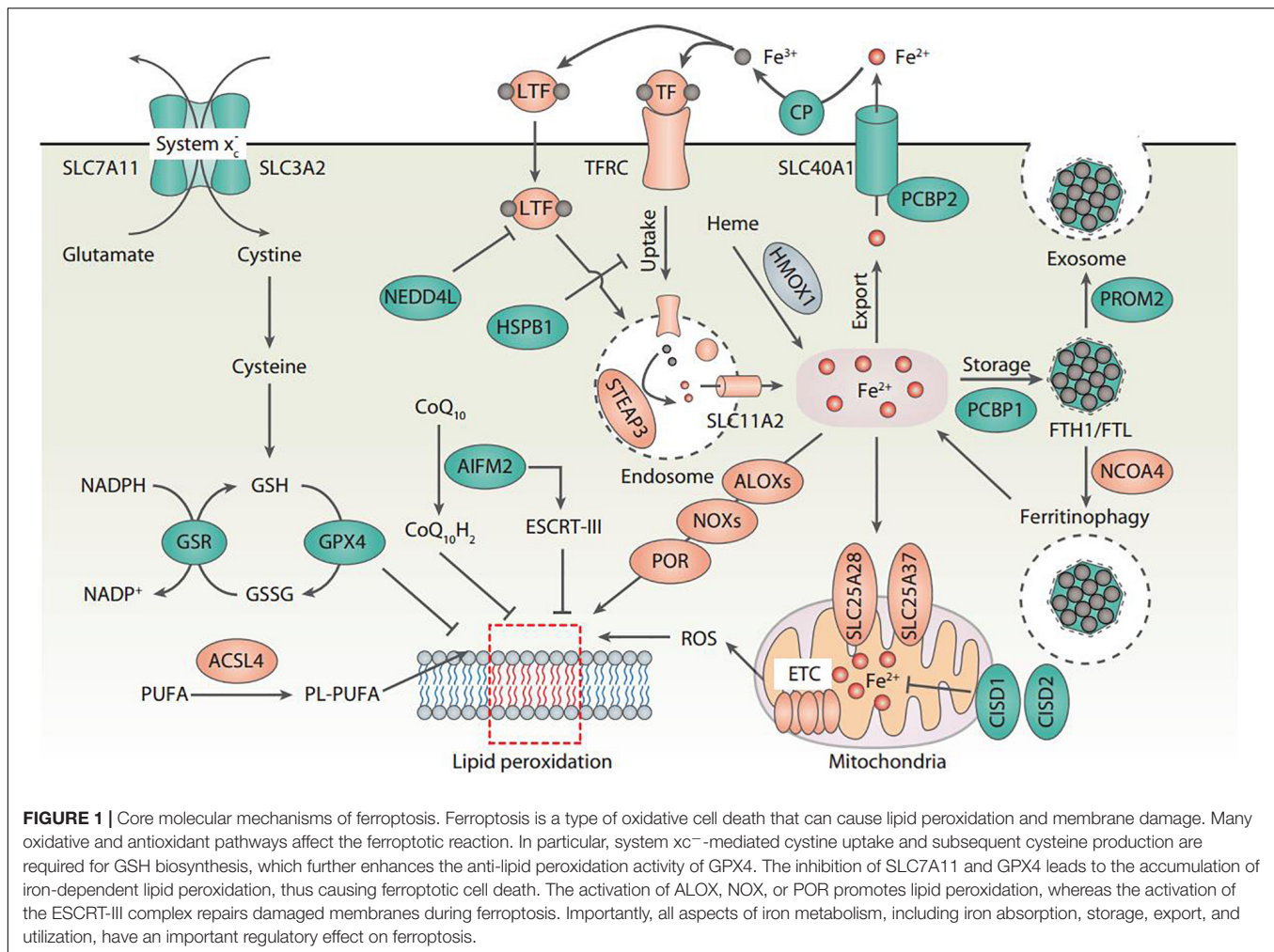
efflux may impact the sensitivity of ferroptosis (**Figure 1**), which are discussed below.

Transferrin and Lactotransferrin

Transferrin (TF) is a 76-kDa glycoprotein that tightly, but reversibly, binds to iron in the blood and transports it to various tissues and organs. TF contains two globular lobes at the N- and C-termini, each of which can bind to one ferric ion (Fe³⁺), as well as other metal ions (e.g., copper, zinc, and manganese) with different affinities. The iron-binding properties of TF are highly dependent on changes in pH. Iron efficiently binds to TF outside the cells at pH ~7.4 and iron releases from TF when delivery to acidic endosomes (pH ~5.5) by receptor-mediated endocytosis. Low serum levels of TF usually occur in patients with chronic inflammatory states or in hospitalized patients with poor clinical outcomes. When there is adequate nutrition, TF levels can be retained at a high level. In humans, due to homozygous or compound heterozygous mutations in TF genes, atransferrinemia is a rare autosomal recessive metabolic

disorder. This disease is associated with microcytic anemia and hemosiderosis in the heart and liver. Hypotransferrinemic (Trf^{hpx/hpx}) mice carry a spontaneous mutation linked to the TF locus (Bernstein, 1987). They are born alive, but die before weaning due to refractory iron-deficient hypochromic anemia. The Trf^{hpx/hpx} mice also survive when treated with serum or TF injections (Trenor et al., 2000).

Transferrin is required for the induction of ferroptotic cell death based on nutrient depletion experiments (Gao et al., 2015). For example, in the presence of serum, cell death induced by the deprivation of amino acids takes the form of ferroptosis, instead of apoptosis or necroptosis (Gao et al., 2015). This amino acid starvation-induced ferroptosis is probably due to cystine starvation and subsequent cellular GSH depletion. TF is essential for this amino acid starvation-induced ferroptosis (Gao et al., 2015). Serum without macromolecules (e.g., TF) fails to mimic the ferroptosis-inducing activity, while the addition of recombinant iron-saturated holo-TF induces cell death in the same condition (Gao et al., 2015). Consistently,



iron-free apotransferrin (apo-TF) fails to produce cell death-inducing activity (Gao et al., 2015). Similarly, co-treatment with holo-TF significantly increases artesunate-induced ferroptosis in pancreatic cancer cells (Eling et al., 2015). These findings suggest that TF is a key positive regulator of ferroptotic cell death. However, hepatocyte-specific TF knockout mice are more susceptible to high-iron diet-induced ferroptotic liver fibrosis (Yu et al., 2020), indicating that hepatic TF plays a protective role in ferroptosis-induced liver fibrosis. Patients with liver cirrhosis have reduced levels of hepatic TF and increased levels of hepatic iron (Yu et al., 2020), supporting the idea of a protective role for hepatic TF in maintaining liver function.

Lactotransferrin (LTF) is a member of the TF family that is responsible for increased intracellular iron during chronic inflammation and tissue injury. Similar to TF, LTF functions as a promoter of ferroptosis in cancer cells (Wang et al., 2020). In contrast, LTF protein degradation that is mediated by neural precursor cell-expressed developmentally downregulated gene 4 (NEDD4)-like E3 ubiquitin protein ligase (NEDD4L) blocks iron-dependent lipid peroxidation during ferroptotic cancer cell death (Wang et al., 2020). These findings indicate that targeting ubiquitin-proteasome system-dependent LTF protein

degradation may enhance the anticancer activity of ferroptosis-based therapy. The direct role of LTF-mediated ferroptosis in non-cancer cells and tissue injury remains to be further studied.

Transferrin Receptor

Transferrin receptor (TFRC/TFR1) is a dimeric glycoprotein receptor for iron-loaded TF at the surface of plasma. The extracellular domains of TFRC have high affinity to bind diferric TF, as compared to monoferric TF or apo-TF. Following binding to TFRC, the TF-TFRC complex is internalized via receptor-mediated endocytosis. In the endosome (an acidic environment), the released iron needs to be reduced from Fe^{3+} to Fe^{2+} by transmembrane ferrireductase STEAP3. Once the iron is released into cytosol through solute carrier family 11 member 2 (SLC11A2/DMT1), TFRC and TF are recycled back to the cell surface and extracellular fluid, respectively. Transferrin receptor 2 (TFR2) is a homolog to TFRC, but is unrelated to iron transport and instead is linked to iron sensing. TFRC knockout mice exhibited early embryonic lethality, which is the result of impaired erythroid and neuronal development (Levy et al., 1999). A homozygous p.Tyr20His mutation in TFRC in human patients causes immunodeficiency combined with impaired development

or function of T and B lymphocytes (Jabara et al., 2016). Both the patients and the TFRC^{Y20H/Y20H} mice had only mild anemia, which may be due to an accessory TfR1 endocytosis signal provided by STEAP3 (Jabara et al., 2016). Interestingly, the selective inactivation of TFRC in murine intestinal epithelial cells induces a severe disruption of the epithelial barrier, which is fully rescued by the enforced expression of a mutant allele of TFRC that is unable to serve as a receptor for TF (Chen et al., 2015). These findings suggest that, in some contexts, TFRC also plays a role independent of the classical function of iron absorption.

The increased expression of TFRC in malignant cells is mainly to meet the high requirement of iron for cell proliferation. Therefore, inducing ferroptosis in TFRC-expressed cancers is a potential cancer treatment strategy. In addition to cancer, reduced TFRC palmitoylation has been demonstrated to contribute to neurodegeneration accompanied by brain iron accumulation, while the antimalarial agent artesunate can reverse the abnormal TFRC palmitoylation in cultured fibroblasts of neurodegeneration subjects (Drecourt et al., 2018). Since artesunate has been shown to induce ferroptosis in cancer cells, whether TFRC palmitoylation also contributes to its antitumor activity of ferroptosis needs further validation (Eling et al., 2015). The expression of TFRC in cancer cells is positively correlated with the ferroptotic response induced by artemisinin derivatives (Ooko et al., 2015) or erastin (Song et al., 2016; Wu et al., 2019). For example, oncogenic RAS renders cells sensitive to erastin-induced ferroptosis through upregulating the expression of TFRC, thus enriching the cellular iron pool (Yang and Stockwell, 2008). The knockdown of TFRC also ameliorates erastin-induced ferroptosis in RAS mutation cells (Yang and Stockwell, 2008). Moreover, the knockdown of TFRC inhibits cystine starvation-triggered ferroptotic cell death (Gao et al., 2015), supporting the requirement of iron import for ferroptosis. The antibody of TFRC (3F3-FMA) was recently identified by screening monoclonal antibodies generated from immunizing mice with membrane fractions from piperazine erastin-treated cells (Feng et al., 2020). The accumulation of TFRC (3F3-FMA) is specific to ferroptosis, but not to apoptosis (Feng et al., 2020). Thus, in addition to ACSL4, TFRC may serve as a biomarker for the sensitivity of ferroptosis.

Solute Carrier Family 39 Member 8, and Member 14

The SLC39/ZIP family is made up of transmembrane proteins that act as broad-scope metal ion transporters, mediating the uptake of a variety of nutritionally important divalent metals, such as zinc, iron, and manganese. Among the SLC39 family members, solute carrier family 39 member 14 (SLC39A14/ZIP14) and solute carrier family 39 member 8 (SLC39A8/ZIP8) are the most closely related transporters. They mediate the iron uptake through directly transporting non-transferrin-bound iron (NTBI) across the cell membrane. The knockout of SLC39A8 in mice causes a combination of stunted growth, severe anemia, and a dysregulation of hematopoiesis and organ development *in utero*, as well as neonatal lethality (Galvez-Peralta et al., 2012). SLC39A8^{-/-} newborns exhibit a decreased level of zinc and iron in several tissues (Galvez-Peralta et al., 2012).

Mice lacking SLC39A14 show growth retardation and impaired gluconeogenesis, which may be due to impaired G-protein-coupled receptor (GPCR) signaling required for systemic growth. The loss of SLC39A14 in mice also markedly reduces the liver's absorption of NTBI and prevents hepatic iron overload in mouse models of hemochromatosis (Jenkitkasemwong et al., 2015). As expected, the conditional knockout of hepatic SLC39A14 reduces iron accumulation in liver and ferroptosis-mediated liver fibrosis, indicating that SLC39A14-mediated iron uptake promotes ferroptotic liver injury and disease (Yu et al., 2020). Whether SLC39A8 plays a role similar to that of SLC39A14 in promoting ferroptosis *in vivo* remains to be further studied.

Ferritin Heavy Chain 1 and Ferritin Light Chain

Ferritin is a cytosolic iron storage protein composed of two subunits, namely ferritin heavy chain 1 (FTH1) and ferritin light chain (FTL). Twenty-four ferritin subunits are assembled into a high molecular weight apoferritin shell, which can chelate up to approximately 4500 iron atoms. FTH1 has ferroxidase activity and can convert Fe²⁺ to Fe³⁺, which is important for subsequent iron entry into the ferritin mineral core, an event that is helped by FTL. The inactivation of FTH1 by homologous recombination in mice is embryonically lethal, whereas the knockout of FTL leads to embryonic lethality in approximately 50% of newborn mice (Li et al., 2015). These findings indicate a different role of FTL and FTH1 in embryonic development. FTL knockout mice exhibit systemic and brain iron dyshomeostasis but no obvious signs of neurodegeneration (Li et al., 2015). Mutations in FTL in humans results in a neurodegenerative disease (namely hereditary ferritinopathy), which is characterized by ferritin-containing intracellular inclusion bodies and increased iron in the brain and other organ systems. Patients who lack FTL (but not FTH1) experience idiopathic generalized seizures and atypical restless leg syndrome, which may be due to increased ROS production and cell damage in fibroblasts (Cozzi et al., 2013).

In addition to cytosolic ferritin, the overexpression of mitochondrial ferritin (FTMT) in neuronal cells inhibits erastin-induced ferroptosis and increases the cellular labile iron pool (Wang et al., 2016). Consistently, wild-type flies (rather than FTMT overexpressing transgenic flies) died within 3 weeks after being fed an erastin-containing diet (Wang et al., 2016). The depletion of FTH1 in *Drosophila* larval wing disks leads to ferroptosis-associated severe growth defects, while the depletion of FTL causes only minor defects (Mumbauer et al., 2019). Although these findings indicate that ferritin has protective effects on ferroptosis in various models, the benefits of FTH1 and FTL on ferroptosis are not the same.

Nuclear Receptor Coactivator 4

The degradation of ferritin can be completed by ferritinophagy, which is a type of selective autophagy mediated by nuclear receptor coactivator 4 (NCOA4). Like the knockdown of autophagy-related 5 (ATG5) or ATG7, the knockdown of NCOA4 also blocks ferritin degradation and suppresses erastin-induced ferroptosis in fibroblasts and pancreatic cancer cells,

whereas the overexpression of NCOA4 promotes ferroptosis by degrading ferritin (Hou et al., 2016). These findings provide the first direct link between autophagy and ferroptosis. Increased ferritinophagy is also required for cystine starvation-induced ferroptotic cell death (Gao et al., 2016). Accordingly, the knockdown of ATG3, ATG13, BECN1, and microtubule-associated protein 1 light chain 3 beta (MAP1LC3B) limits cystine starvation- or erastin-induced ferroptosis by blocking ferritin degradation and iron accumulation in fibroblasts (Gao et al., 2016). In addition to classical ferroptosis activators, non-classical ferroptosis activators can contribute to ferroptotic cell death via ferritinophagy. Such activators include dihydroartemisinin, JQ1, siramesine/lapatinib, or salinomycin in various cancer cells, indicating a wider role of ferritinophagy in promoting ferroptotic cancer cell death (Zhou et al., 2019; Liu J. et al., 2020).

NCOA4-mediated ferritinophagy also plays a role in cigarette smoke-induced ferroptosis in lung epithelial cells (Yoshida et al., 2019), supporting a role of ferroptosis in the pathogenesis of cigarette smoke-induced chronic obstructive pulmonary disease. Ferritinophagy-mediated iron accumulation may regulate the process of aging in cells (Masaldan et al., 2018) and carbon tetrachloride (CCl₄)-induced liver fibrosis in mice (Kong et al., 2019). These results further strengthen a link between ferritinophagy and ferroptosis in various diseases. Autophagy-independent lysosomal degradation of ferritin also promotes dihydroartemisinin-induced ferroptotic cancer cell death (Chen G.Q. et al., 2020), indicating an alternative mechanism leading to ferritin degradation during ferroptosis.

Prominin-2

Prominin-2 (PROM2) is a member of the prominin family of pentaspan membrane glycoproteins, and is selectively associated with plasma membrane protrusions. Ferritin can be released into the extracellular space by PROM2-mediated exosomes, which drives ferroptosis resistance (Brown et al., 2019). RSL3-induced PROM2 upregulation is observed in ferroptosis-resistant cells (e.g., MCF10A and Hs578t), but not in ferroptosis-sensitive cells (e.g., MDA-MB-231) (Brown et al., 2019), indicating that the induction of PROM2 expression may be correlated with resistance to ferroptosis. The knockdown of PROM2 expression increases sensitivity to ferroptosis in ferroptosis-resistant cells, while the overexpression of PROM2 inhibits ferroptosis in ferroptosis-sensitive cells (Brown et al., 2019). Mechanistically, PROM2 localizes to multivesicular bodies (MVBs) and promotes the formation of MVBs during ferroptosis. Upon fusion of MVBs with the plasma membrane, ferritin-containing exosomes are released into the extracellular space, thus resulting in decreased ferroptosis sensitivity (Brown et al., 2019). PROM2 might interact with the ESCRT-III complex, which promotes membrane repair in RCD, including ferroptosis (Dai et al., 2020). The relationship between PROM2 and ESCRT-III during ferroptosis needs to be confirmed in the future.

Solute Carrier Family 40 Member 1

Solute carrier family 40 member 1 (SLC40A1/ferroportin/FPN1) is the only known transmembrane exporter of non-heme iron. Hepcidin antimicrobial peptide (HAMP) is a peptide hormone

secreted by the liver that binds to SLC40A1 and induces internalization of SLC40A1 for degradation. It is generally accepted that Fe²⁺ transported out of the cell by SLC40A1 need to be oxidized by ferroxidase (e.g., ceruloplasmin [CP]) to facilitate Fe³⁺ loading on TF. Mutations in SLC40A1 in humans were first reported in 2001 and were found to cause autosomal dominant hemochromatosis (also known as ferroportin disease) (Njajou et al., 2001). Patients with an N144D mutation in the SLC40A1 gene have experienced parenchymal iron loading and cirrhosis. Asparagine 144 may also be important for the function of SLC40A1, because two other disease-causing mutations, N144H (Njajou et al., 2001) and N144T (Arden et al., 2003), have also been identified in autosomal dominant hemochromatosis. The global knockout of SLC40A1 in mice leads to embryonic lethality, while the selective knockout of SLC40A1 in postnatal intestine results in severe iron deficiency (Donovan et al., 2005). Erastin induces the downregulation of SLC40A1 expression in SH-SY5H neuroblastoma cells, which can be reversed by ferroptosis inhibitors, such as ferrostatin-1, an iron chelator, or N-acetyl cysteine (NAC) (Geng et al., 2018). The knockdown of SLC40A1 by RNAi or HAMP-mediated downregulation of SLC40A1 promotes erastin-induced ferroptosis, while ponasterone (a SLC40A1 inducer) impedes this process (Geng et al., 2018). Similarly, the knockdown of SLC40A1 enhances oxygen-glucose deprivation and reoxygenation (OGd/R)-induced ferroptosis in testicular ischemia-reperfusion (I/R) injury sertoli cells (Li L. et al., 2018). In contrast, the overexpression of SLC40A1 or treatment with ponasterone rescues OGd/R-induced ferroptosis by decreasing iron accumulation in sertoli cells (Li L. et al., 2018).

The ferroptosis suppression function of CP is dependent on SLC40A1 (Shang et al., 2020). The depletion of CP promotes erastin- and RSL3-induced ferroptotic cell death, whereas the overexpression of CP suppresses ferroptosis in hepatocellular carcinoma cells (Shang et al., 2020). Intraperitoneal CP treatment has a protective effect on ferroptotic damage after ischemic stroke in mice (Tuo et al., 2017). Collectively, these findings indicate that SLC40A1/CP acts as a negative regulator of ferroptosis.

Heme Oxygenase 1

Heme, derived primarily from hemoglobin and myoglobin, is a major source of dietary iron in mammals. Heme oxygenase 1 (HMOX1/HO-1) catabolizes heme into three products: carbon monoxide (CO), biliverdin, and free iron. Biliverdin is then reduced to bilirubin by biliverdin reductase (BLVR). HMOX1 can be induced not only by heme but also by a variety of stimuli, such as cytokines, endotoxin, heat shock, and heavy metals, leading to speculation that HMOX1 may play a role in maintaining redox homeostasis. HMOX1 knockout mice have anemia and iron accumulation in liver and kidney, which is associated with oxidative damage and tissue injury. An example of human HMOX1 deficiency was found in a 6-year-old boy suffering from growth retardation, anemia, leukocytosis, thrombocytosis, coagulation abnormalities, and hyperlipidemia (Kawashima et al., 2002), indicating an important role of HMOX1 in human health.

Heme oxygenase 1 plays a dual role in ferroptosis induction. On the one hand, erastin induces the expression of HMOX1, which may promote ferroptosis in HT1080 fibrosarcoma cells.

The HMOX1 inhibitor zinc protoporphyrin IX (ZnPP) prevents erastin-induced ferroptotic cell death, whereas the HMOX1 inducer hemin accelerates erastin-induced ferroptosis in HT1080 cells (Kwon et al., 2015). Furthermore, CO-releasing molecules also promote erastin-induced ferroptotic cell death (Kwon et al., 2015), indicating that CO produced by HMOX1 may be an endogenous pro-ferroptosis molecule of ferroptosis. Consistently, the knockout of HMOX1 suppresses, whereas the overexpression of HMOX1 promotes, ferroptotic cancer cell death induced by erastin (Kwon et al., 2015) or BAY 11-7085 (NFKB inhibitor alpha [NFKBIA/IKBA] inhibitor) (Chang et al., 2018). In addition to its affect in cancer models, the inhibition of HMOX1 by ZnPP protects against doxorubicin-induced ferroptotic damage in heart (Fang et al., 2019). On the other hand, HMOX1 also has the ability to inhibit ferroptosis in some cases. For example, erastin and RSL3 treatment increases the expression of HMOX1 in renal proximal tubular cells (Adedoyin et al., 2018). The knockout of HMOX1 increases erastin- or RSL3-induced cell death in renal proximal tubular cells (Adedoyin et al., 2018) or liver cancer cells (Sun et al., 2016b). Thus, the role of HMOX1 in ferroptosis may depend on the context.

Poly(RC) Binding Proteins

Poly(RC) binding proteins (PCBPs) are iron chaperones that deliver Fe^{2+} to different proteins through a metal-mediated, protein-protein interaction. The targets of PCBP1 and PCBP2 include iron-dependent Egl-9 family hypoxia-inducible factor (EGLN/PHD) and hypoxia-inducible factor 1 subunit alpha inhibitor (HIF1AN/FIH1) that play a role in regulating the transcriptional activity of hypoxia-inducible factor 1 subunit alpha (HIF1A/HIF1 α) (Nandal et al., 2011). The depletion of PCBP1 or PCBP2 in cells leads to the loss of EGLN activity, while the addition of excess Fe^{2+} or purified Fe-PCBP1 restores the activity of EGLN (Nandal et al., 2011). As an iron chaperone in the cytosol, PCBP1 directly binds Fe^{2+} and delivers it to ferritin. Consequently, the depletion of PCBP1 suppresses ferritin iron loading and increases cytosolic iron pools in human cells. Interestingly, PCBP2, but not PCBP1, binds to and receives iron from the iron importer SLC11A2 or transfers iron to the iron exporter SLC40A1 (Yanatori et al., 2014). The silencing of PCBP2 expression suppresses SLC11A2-dependent iron uptake and SLC40A1-dependent iron export, indicating that PCBP2 acts as a regulator of iron transport (Yanatori et al., 2014). Moreover, HMOX1 can bind to PCBP2 in the presence of heme, whereas iron-loaded PCBP2 loses its affinity for HMOX1, supporting the role of PCBP2 in heme catabolism and iron transport metabolism. PCBP1 and PCBP2 are essential for mouse embryonic development, but they may play distinct roles in organism function. *Pcbp1*-null embryos are rendered non-viable in the peri-implantation stage (4.5 to 8.5 days postcoitum). Although the differentiation of red blood cells and megakaryocytes is impaired, *Pcbp2*-null embryos undergo normal development until midgestation (12.5 to 13.5 days postcoitum) (Ghanem et al., 2016). Mice heterozygous for either *Pcbp1* or *Pcbp2* null alleles display a slight reduction in initial postpartum weight (Ghanem et al., 2016).

Poly(RC) binding proteins 1 has been shown to limit ferroptosis in hepatocytes (Protchenko et al., 2020). Mice lacking *Pcbp1* in hepatocytes show defects in iron homeostasis and develop liver disease with hepatic steatosis, inflammation, and degeneration (Protchenko et al., 2020). Transcriptome analysis reveals the activation of lipid biosynthetic and oxidative stress response pathways, including the anti-ferroptotic regulator GPX4. Although PCBP1-deleted hepatocytes are iron-deficient, the supplementation of iron dose doesn't inhibit the hepatic steatosis, indicating that hepatic steatosis may not require iron deficiency. Paradoxically, hepatocytes lacking PCBP1 show increased redox activity and unchaperoned iron, therefore causing lipid peroxidation (Protchenko et al., 2020). Restricting dietary iron and the supplementing of antioxidant vitamin E can prevent hepatic steatosis associated with ferroptosis (Protchenko et al., 2020). Overall, these findings suggest that PCBP1 plays a complex role in the regulation of ferroptosis-related liver disease.

Solute Carrier Family 25 Member 37, and Member 28

Solute carrier family 25 member 37 (SLC25A37/mitoferrin-1) and solute carrier family 25 member 28 (SLC25A28/mitoferrin-2) are the key mitochondrial iron importers for heme and iron-sulfur (Fe-S) cluster biogenesis. Due to the difference in turnover between SLC25A37 and SLC25A28, SLC25A37 is highly expressed in erythroid cells, whereas SLC25A28 is ubiquitously expressed in various cells. The loss of *Slc25a37* in mice leads to embryonic lethality, indicating an important role of SLC25A37 in development (Troade et al., 2011). The selective deletion of SLC25A37 in adult hematopoietic tissues leads to severe anemia, suggesting that the lethality of SLC25A37 depletion might be due to defects in hematopoiesis (Troade et al., 2011). Interestingly, the selective deletion of SLC25A37 in hepatocytes has no phenotype under normal conditions, but it can cause protoporphyria and hepatotoxicity in delta aminolevulinic acid (a precursor of porphyrin biosynthesis)-fed animals (Troade et al., 2011). These findings indicate a tissue- and stress-dependent role of SLC25A37 in diseases.

The activity of SLC25A28 in ferroptosis is regulated by the bromodomain-containing protein 7 (BRD7) tumor protein p53 (TP53) pathway. In hepatic stellate cells, ferroptosis inducers increase the expression of BRD7 by inhibiting its proteasome degradation (Zhang et al., 2020). Upregulated BRD7 further promotes mitochondrial translocation of TP53 by directly binding to its N-terminal transactivation domain. Mutations of serine 392, which are necessary for TP53 mitochondrial translocation, block the binding of BRD7 to TP53 and subsequent ferroptosis induction. Importantly, mitochondrial TP53 interacts with SLC25A28 and enhances the activity of SLC25A28, leading to the mitochondrial accumulation of iron and mitochondria ETC-mediated ROS. The knockdown of SLC25A28 impairs BRD7-TP53 signaling-mediated ferroptotic cell death, whereas the overexpression of SLC25A28 facilitates ferroptosis. The PINK1-PARK2 (critical mediators of mitophagy) pathway mediates the degradation of SLC25A37 and SLC25A28, therefore

increasing mitochondrial iron accumulation (Li C. et al., 2018). However, the function of mitophagy in ferroptosis remains uncertain. Due to the depletion of mitochondria, parkin-overexpressed HT1080 cells are less sensitive to ferroptosis caused by cystine starvation or erastin (Gao et al., 2019). The pharmacological inhibition of ETC also suppresses ROS production and subsequent lipid peroxidation and ferroptosis (Gao et al., 2019). Taken together, these findings indicate that both the ubiquitin-proteasome system (UPS) and autophagy pathways play a role in regulating mitochondrial iron-dependent ferroptosis by affecting the stability of mitochondrial iron importers.

CISD1 and CISD2

NEET proteins (also known as CISD proteins) belong to the Fe-S protein family and are characterized by a unique CDGSH motif in their Fe-S cluster-binding domain. There are three members of CISD, namely CDGSH iron sulfur domain 1 (CISD1/mitoNEET), CDGSH iron sulfur domain 2 (CISD2/NAF1), and CDGSH iron sulfur domain 3 (CISD3). CISD1 and CISD3 are outer mitochondrial membrane proteins, whereas CISD2 is mainly located in the endoplasmic reticulum (ER) and mitochondria-associated ER membranes. CISD1 and CISD2 promote tumor growth and metastasis by regulating mitochondrial iron and ROS metabolism. CISD1 and CISD2 were discovered as unexpected targets for the peroxisome proliferator activated receptor gamma (PPARG) agonist pioglitazone (Colca et al., 2004). Pioglitazone is an anti-diabetic drug used in patients with type II diabetes, which also stabilizes CISD1 and CISD2.

As expected, increased CISD1 expression suppresses erastin-induced ferroptosis in human hepatocellular carcinoma cells by limiting mitochondrial iron uptake (Yuan et al., 2016a). Moreover, the knockdown of CISD1 by RNAi increases, whereas stabilization of CISD1 by pioglitazone inhibits, mitochondrial iron uptake and subsequent ferroptosis in response to erastin (Yuan et al., 2016a). Similar to CISD1 as a repressor of ferroptosis, CISD2 is associated with resistance to sulfasalazine-induced ferroptosis in head and neck cancer (Kim et al., 2018). Gene inhibition of CISD2 increases mitochondrial iron accumulation and restores the sensitivity of ferroptosis-resistant cells to sulfasalazine-induced cell death (Kim et al., 2018). In addition to inhibiting ferroptosis, pioglitazone also has the ability to enhance sulfasalazine- or buthionine sulfoximine (BSO)-induced ferroptosis (Kim et al., 2018; Homma et al., 2020). The opposing effects of pioglitazone on ferroptosis in different situations may be due to the difference in cellular localization or function between CISD1 and CISD2 and unknown targets.

Heat Shock Protein Family B Small Member 1

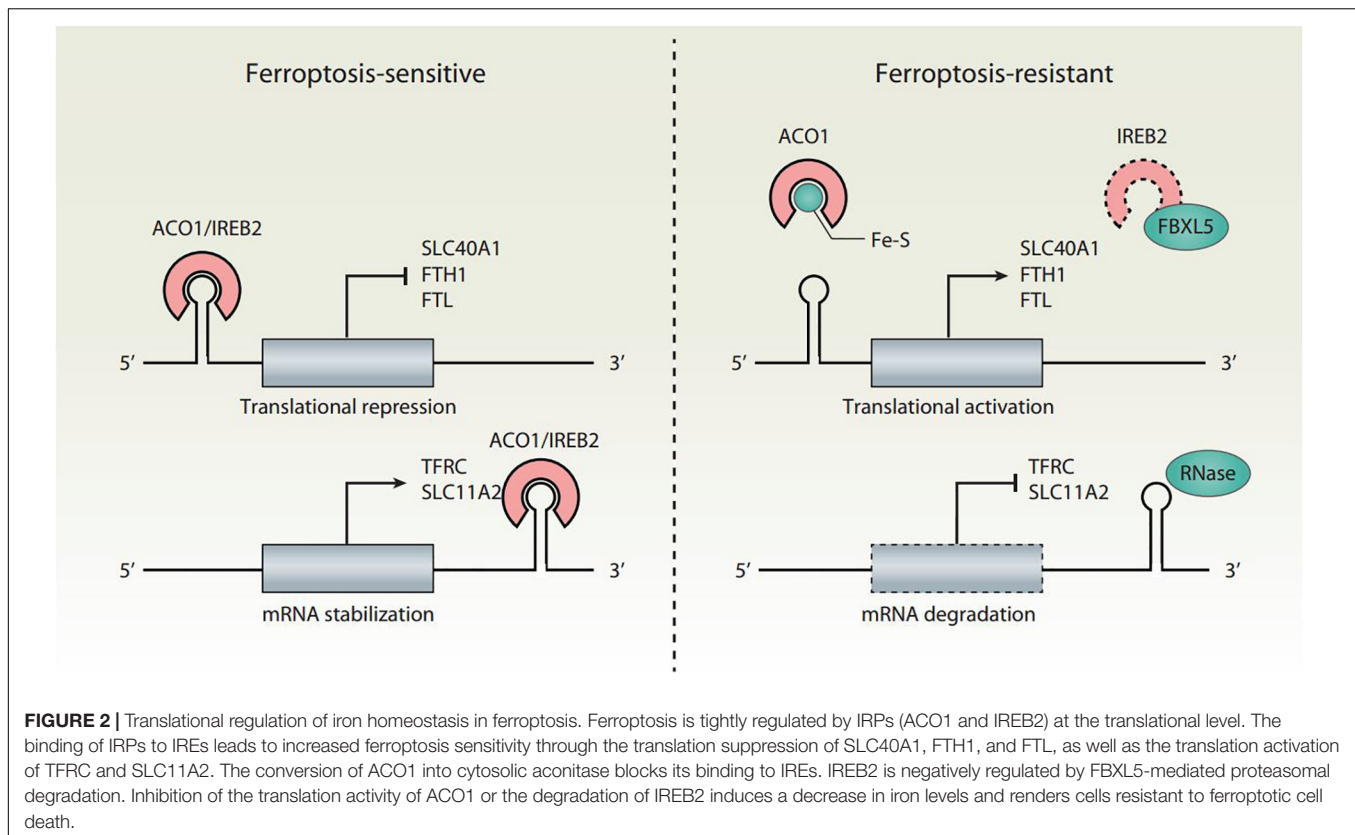
Heat shock proteins (HSPs) are a class of functionally related stress proteins. When cells are subjected to high temperature or other environmental stress, the expression of HSPs is upregulated to prevent cell damage and death. In addition to helping proteins fold normally, several HSPs also have the ability to regulate iron metabolism. In particular, the expression of heat shock protein

family B small member 1 (HSPB1, a member of small HSPs) is increased in erastin-induced ferroptosis (Sun et al., 2015). Protein kinase C (PRKC) further mediates HSPB1 phosphorylation, which stabilizes the actin cytoskeleton (Sun et al., 2015). Finally, a larger actin cytoskeleton inhibits iron uptake and subsequent lipid peroxidation and ferroptosis (Sun et al., 2015). In addition, HSPB1 can inhibit TFRC-mediated iron uptake (Chen et al., 2006), which may also help fight ferroptosis. Collectively, increased HSPB1 expression can promote ferroptosis resistance by blocking iron uptake.

Aconitase 1 and Iron-Responsive Element Binding Protein 2

Cellular iron homeostasis is tightly regulated at the posttranscriptional level by iron regulatory proteins (IRPs), including aconitase 1 (ACO1/IRP1) and iron-responsive element binding protein 2 (IREB2/IRP2), to adapt to a change of iron levels (Figure 2). ACO1 is a Fe-S cluster protein that exists in two forms. When iron is abundant, ACO1 exists in the Fe-S cluster in the form of cytoplasmic aconitase. When iron is lacking, ACO1 presents in the Fe-S cluster as a regulator of translation. Unlike ACO1, IREB2 is mainly regulated by protein degradation. IREB2 is degraded when iron is excessive, and stable when iron is deficient (Iwai et al., 1998). The iron-responsive elements (IREs) located in the untranslated regions (UTRs) of mRNAs are conserved hairpin structures and can be targeted by IRPs. Depending on the iron charge, the main iron metabolism mRNA is regulated by IRPs, including the genes involved in iron import (e.g., TFRC and SLC11A2), storage (e.g., FTH1 and FTL), and export (e.g., SLC40A1). However, the combination of IRP and IRE located in the 5' UTR and 3' UTR has the opposite effect. The binding of IRPs to 5' IRE leads to the inhibition of translation of mRNA, whereas the binding to 3' IRE causes the promotion of translation of mRNA by inhibiting the degradation of mRNA. For example, under the condition of iron deficiency, IRPs bind to the 3' IREs of TFRC and SLC11A2 mRNAs and the 5' IREs of SLC40A1 and FTH1/FTL mRNAs. As a result, IRP decreases the synthesis of TFRC and SLC11A2, and increases the synthesis of SLC40A1 and FTH1/FTL mRNAs. An excess of cytosolic iron results in translational inhibition of TFRC and SLC11A2, and translational induction of SLC40A1 and FTH1/FTL.

Both ACO1 and IREB2 have an impact on ferroptosis sensitivity (Figure 2). The knockdown of NFS1 cysteine desulfurase (the biosynthetic enzyme of the Fe-S cluster) makes cancer cells susceptible to ferroptosis (Alvarez et al., 2017). Mechanistically, NFS1 suppression activates the iron starvation response in an ACO1-dependent manner, therefore upregulating the expression of TFRC and downregulating the expression of FTH1 (Alvarez et al., 2017). Silencing IREB2 confers protection against erastin-induced ferroptosis, but not against other forms of cell death induced by staurosporine, rotenone, rapamycin, MG132, camptothecin, or thapsigargin (Dixon et al., 2012). In contrast, the knockdown of F-box and leucine-rich repeat protein 5 (FBXL5) or the E3 ubiquitin ligase-mediated proteasomal degradation of IREB2 enhances erastin-induced ferroptosis (Dixon et al., 2012). Therefore, the dysregulation of



the IRP system can lead to iron-related effector changes, thereby regulating ferroptosis.

Transcription Factors

Several transcription factors regulate ferroptosis by controlling the expression of genes involved in iron-related metabolism. Among them, nuclear factor erythroid 2-like 2 (NFE2L2/NRF2) is the key transcription factor that regulates cytoprotective responses to ferroptotic damage. One mechanism of its anti-ferroptotic effect is the upregulation of several genes involved in iron metabolism, such as FTH1 (Sun et al., 2016b), SLC40A1, HMOX1 (Shin et al., 2018; Fang et al., 2019), and metallothionein 1G (MT1G) (Sun et al., 2016a). BTB domain and CNC homolog 1 (BACH1) is a heme-binding transcription factor involved in the regulation of the oxidative stress and heme/iron-related metabolic pathways. The activation of BACH1 enhances erastin-induced ferroptosis through transcriptional downregulation of FTH1, FTL, and SLC40A1 (Nishizawa et al., 2020). The transcription factor metal regulatory transcription factor 1 (MTF1) regulates the expression of several iron-related genes, such as FTH1, FTL, and SLC40A1, and is responsible for ATM serine/threonine kinase inhibition-rescued ferroptosis (Chen P.H. et al., 2020). Cell-to-cell contact can protect cancer cells from ferroptosis by inhibiting the expression of TFRC mediated by transcription factor yes-associated protein 1 (YAP1) (Wu et al., 2019). Heat shock transcription factor 1 (HSF1) is required for erastin-induced expression of HSPB1, which inhibits ferroptosis by blocking cytoskeleton-mediated iron uptake as discussed

above (Sun et al., 2015). These findings suggest that multiple stress-related transcription factors play a context-dependent role in ferroptosis.

In addition, hypoxia-inducible factor (HIF) also plays a complex role in ferroptosis, which is regulated by EGLNs (oxygen and iron-dependent enzymes). Under normal oxygen conditions, EGLNs hydroxylate the HIF α subunit, which facilitates its interaction with the von Hippel-Lindau E3 ubiquitin ligase complex and ultimately leads to the proteasome degradation of the HIF α subunit. Under conditions of hypoxia or iron depletion, the activity of EGLNs is inhibited, leading to the stabilization of the HIF subunit, and at the same time the heterodimerization of the α and β subunits of HIF. HIF1 or HIF2 regulates many genes involved in iron homeostasis, such as TFRC, SLC11A2, SLC40A1, CP, HMOX1, and HAMP. Stabilizing HIF1A by hypoxia or cobalt chloride inhibits ferroptosis (Yang et al., 2019), whereas endothelial PAS domain protein 1 (EPAS1/HIF2A) promotes ferroptosis in certain cancer cells (Zou et al., 2019). However, the key downstream genes (not limited to iron metabolism) responsible for HIF-mediated regulation of ferroptosis still need to be further researched.

THERAPEUTIC IMPLICATIONS OF IRON CHELATORS

Impaired ferroptotic pathways are implicated in various pathologic conditions (e.g., I/R injury and infection) and diseases

(e.g., cancer and neurodegenerative diseases) (Xie et al., 2016a; Stockwell et al., 2017). Iron chelators are currently used to treat iron overload diseases. Numerous studies have shown that iron chelators can block ferroptosis *in vitro* and *in vivo*, as described below.

Deferoxamine

Deferoxamine (DFO) is a natural product isolated from the soil bacterium *Streptomyces pilosus*, and used in the treatment of iron overload patients or aluminum poisoning. As an iron chelator, DFO is a polar molecule with low membrane permeability, which can enter cells through endocytosis. It reacts with Fe^{3+} , especially Fe^{3+} in the form of methanesulfonate, and generates a stable octahedral coordination compound, feroxamine, which can be eliminated by the kidneys. DFO has also been shown to stabilize HIF1A by inhibiting the activity of iron-dependent EGLNs, or induce the transcriptional upregulation of HIF1A (Wang and Semenza, 1993). Since DFO was first discovered to have an inhibitory effect on ferroptosis caused by erastin and RSL3, DFO is the drug most widely used to inhibit lipid peroxidation-mediated ferroptosis under various conditions (Dixon et al., 2012). In addition to treating iron overload, DFO also has potential antitumor activity against a variety of cancers *in vivo* and *in vitro* (Buss et al., 2003). However, ferroptosis plays a dual role in cancer biology. Notably, DFO is poorly absorbed and cleared quickly, resulting in ineffective oral administration. Therefore, increasing DFO absorption and metabolic stability is a challenge for its application.

Deferasirox

Deferasirox is a membrane-permeable iron chelator and the first oral medication approved by the Food and Drug Administration (FDA) for chronic iron overload in the body caused by multiple blood transfusions. It can also be used to treat chronic iron overload in patients with certain blood diseases that do not require blood transfusion (non-transfusion-dependent thalassemia). Deferasirox is a tridentate ligand selective for Fe^{3+} that binds Fe^{3+} at a ratio of 2:1 to form a stable complex. The deferasirox-iron complex is excreted through the kidneys. Unlike iron, deferasirox has a low affinity for zinc and copper. Moreover, deferasirox has a property of inhibiting nuclear factor kappa B (NFkB) (Messa et al., 2010), indicating that deferasirox may be used for limiting inflammation responses in immune cells. Indeed, deferasirox and DFO inhibit hemin-induced ferroptotic cell death and ROS generation in human monocytes (Imoto et al., 2018), thereby increasing the possibility that iron-dependent ferroptosis is involved in activating inflammation.

Deferiprone

Deferiprone is an oral iron chelator approved by the FDA. When blood transfusion causes iron overload, it can be used as a second-line drug for thalassemia syndrome. Deferiprone combines with Fe^{3+} in a ratio of 3:1 to form a stable complex, which is then eliminated in the urine. Deferiprone is selective for iron, but has a relatively low affinity for other metals (e.g., zinc, copper, and aluminum). Compared to DFO and deferasirox, deferiprone is most effective in the chelation of cardiac iron and equivalent to

DFO in the chelation of liver iron. In differentiated Lund human mesencephalic cells, deferiprone is able to specifically inhibit erastin- and glutamate-induced ferroptosis (Do Van et al., 2016). However, whether deferiprone can protect against ferroptosis-mediated tissue damage *in vivo* is unclear.

Ciclopirox

Ciclopirox is a synthetic broad-spectrum antifungal drug that has been approved by the FDA for the topical dermatological treatment of epidermal mold. This agent is particularly effective in treating tinea versicolor. In addition, ciclopirox has also been shown to exhibit anti-inflammatory effects in human polymorphonuclear cells. The antibacterial and anti-inflammatory properties of ciclopirox may be due to its high affinity for trivalent cations (e.g., Fe^{3+} and Al^{3+}), and Fe^{3+} and Al^{3+} are essential cofactors in enzymes. For example, ciclopirox exhibits anti-inflammatory activity by inhibiting the activity of iron-containing arachidonate 5-lipoxygenase (ALOX5) and prostaglandin endoperoxide synthase (PTGS/cyclooxygenase) (Hanel et al., 1991). Ciclopirox is capable of inhibiting ferroptotic cell death, but whether this anti-ferroptosis activity of ciclopirox depends on the inhibition of ALOX5 or PTGS activity is unclear (Dixon et al., 2012).

Dextrazoxane

Dextrazoxane is a cyclic derivative of EDTA that easily penetrates cell membranes. It is an orphan drug approved by the FDA and can be used in protecting the heart from the cardiotoxic effects of anthracyclines, such as doxorubicin. The precise cardioprotective mechanism of dextrazoxane is not fully understood, but several mechanisms have been proposed. First, the cardioprotective activity of dextrazoxane appears due to the inhibition of the formation of a toxic iron anthracycline complex. Second, dextrazoxane is a pro-drug converted intracellularly to a ring-opened bidentate iron-chelating agent that interferes with iron-mediated ROS production. Third, the cardioprotective activity of dextrazoxane also involves the inhibition of topoisomerase II-mediated DNA double-strand breaks. Fourth, dextrazoxane or ferostatin-1 inhibits ferroptosis in a doxorubicin-induced cardiac injury model (Fang et al., 2019). Of note, other studies suggest that Mito-FerroGreen (MFG, a fluorescence indicator specifically chelating Fe^{2+} in mitochondria), but not dextrazoxane and DFO, prevents doxorubicin-induced lipid peroxidation and mitochondria-dependent ferroptosis in cardiomyopathy (Tadokoro et al., 2020), indicating that mitochondrial iron may play a major role in mediating ferroptotic heart damage.

Baicalein

Baicalein is a flavonoid extracted from *Scutellaria baicalensis* Georgi and has free 5,6,7- hydroxyl groups that form complexes with iron in a stoichiometry of 1:1. Compared to a natural product library of 143 compounds, baicalein showed the strongest protection against erastin-induced ferroptotic cell death in human pancreatic cancer cell lines (Xie et al., 2016b). Baicalein reverses erastin-induced intracellular iron accumulation, GSH depletion, and GPX4 degradation (Xie et al., 2016b). In addition to cancer cells, baicalein exerts neuroprotective effects on

posttraumatic epileptic seizures by repressing ferroptotic cell death in mouse models (Li et al., 2019). Baicalein is also effective in inhibiting ferric ammonium citrate (FAC)-induced HT22 hippocampal neuron damage (Li et al., 2019). Moreover, baicalein markedly decreases iron-induced lipid peroxidation and inhibits the expression of arachidonate 12-lipoxygenase (ALOX12) or arachidonate 15-lipoxygenase (ALOX15) in HT22 cells (Li et al., 2019). In addition to its iron chelator activity, baicalein also inhibits the activity of several oxidases (e.g., ALOXs), which may also contribute to its anti-ferroptosis effect (Yang et al., 2016).

Other Iron Chelators

Another Fe^{2+} chelator is 2,2'-bipyridine, which is membrane-permeant and known to sequester iron from labile iron pool (LIP) in cells. The 2,2'-bipyridine may enter mitochondria and chelate mitochondrial iron, therefore decreasing the generation of ROS (Chang et al., 2016). As expected, 2,2'-bipyridine is an inhibitor of ferroptosis by decreasing iron-dependent lipid peroxidation (Dixon et al., 2012). Additionally, 1,10-phenanthroline is also an Fe^{2+} chelating agent, with coordination properties similar to 2,2'-bipyridine. The 1,10-phenanthroline blocks zero-valent iron nanoparticle-induced mitochondrial ROS accumulation and subsequent ferroptosis *in vitro* (Huang et al., 2019).

CONCLUSION AND PERSPECTIVES

Excess of free reactive iron can cause various types of cell death, including a recently recognized type, ferroptosis. Although the core molecular effector of ferroptosis is unclear, ferroptosis is induced by the activation of iron-dependent lipid peroxidation (Kuang et al., 2020). Significant progress has been made in dissecting the mechanisms that lead to lipid peroxidation and how antioxidant systems or stress proteins regulate ferroptosis. However, the exact contribution of iron-mediated ROS production and iron-containing enzymes in ferroptosis and its dynamic relationship with other types of RCDs is still poorly understood. In ferroptosis, whether any proteins

act downstream of lipid peroxidation and how they are affected by iron homeostasis remains an enigma. Further studies are needed to determine and develop optimal targeted therapy for the specific ferroptosis-associated disease. In addition, further evidence is needed to show improved prognosis when ferroptotic cell death is selectively blocked. Nevertheless, recent work has begun to clarify the involvement of ferroptosis in different aspects of diseases (e.g., cancer, neurodegenerative diseases, and I/R injury-related diseases). Generally, it can be expected that treatment strategies aimed at suppressing ferroptotic signals and pathways will benefit iron overload diseases. In particular, the use of iron chelating agents as potential therapeutic agents has been widely considered in the treatment of ferroptotic diseases, although these iron chelators have different pharmacokinetic and metabolic properties. Despite the great potential value, further *in vivo* studies must be conducted to clarify the molecular mechanism and mode of action of these iron chelators. There are still challenges to develop a candidate iron chelator with relatively low toxicity and high efficiency. Overall, it is necessary to further study the mechanism of iron-dependent lipid peroxidation in order to establish more accurate targets for ferroptosis-associated diseases (Chen X. et al., 2020). Whether iron overload is enough to cause ferroptosis in various cells or tissues also needs to be investigated.

AUTHOR CONTRIBUTIONS

XC, CY, RK, and DT conceptualized and wrote the manuscript. All authors contributed to the article and approved the submitted version.

ACKNOWLEDGMENTS

We thank Dave Primm (Department of Surgery, University of Texas Southwestern Medical Center) for his critical reading of the manuscript.

REFERENCES

- Adedoyin, O., Boddu, R., Traylor, A., Lever, J. M., Bolisetty, S., George, J. F., et al. (2018). Heme oxygenase-1 mitigates ferroptosis in renal proximal tubule cells. *Am. J. Physiol. Renal Physiol.* 314, F702–F714. doi: 10.1152/ajprenal.00044.2017
- Alvarez, S. W., Sviderskiy, V. O., Terzi, E. M., Papagiannakopoulos, T., Moreira, A. L., Adams, S., et al. (2017). NFS1 undergoes positive selection in lung tumours and protects cells from ferroptosis. *Nature* 551, 639–643. doi: 10.1038/nature24637
- Arden, K. E., Wallace, D. F., Dixon, J. L., Summerville, L., Searle, J. W., Anderson, G. J., et al. (2003). A novel mutation in ferroportin1 is associated with haemochromatosis in a Solomon Islands patient. *Gut* 52, 1215–1217. doi: 10.1136/gut.52.8.1215
- Bai, Y., Meng, L., Han, L., Jia, Y., Zhao, Y., Gao, H., et al. (2019). Lipid storage and lipophagy regulates ferroptosis. *Biochem. Biophys. Res. Commun.* 508, 997–1003. doi: 10.1016/j.bbrc.2018.12.039
- Bernstein, S. E. (1987). Hereditary hypotransferrinemia with hemosiderosis, a murine disorder resembling human atransferrinemia. *J. Lab. Clin. Med.* 110, 690–705.
- Bersuker, K., Hendricks, J. M., Li, Z., Magtanong, L., Ford, B., Tang, P. H., et al. (2019). The CoQ oxidoreductase FSP1 acts parallel to GPX4 to inhibit ferroptosis. *Nature* 575, 688–692. doi: 10.1038/s41586-019-1705-2
- Brown, C. W., Amante, J. J., Chhoy, P., Elaimy, A. L., Liu, H., Zhu, L. J., et al. (2019). Prominin2 drives ferroptosis resistance by stimulating iron export. *Dev. Cell* 51:e4. doi: 10.1016/j.devcel.2019.10.007
- Buss, J. L., Torti, F. M., and Torti, S. V. (2003). The role of iron chelation in cancer therapy. *Curr. Med. Chem.* 10, 1021–1034. doi: 10.2174/0929867033457638
- Chang, H. C., Wu, R., Shang, M., Sato, T., Chen, C., Shapiro, J. S., et al. (2016). Reduction in mitochondrial iron alleviates cardiac damage during injury. *EMBO Mol. Med.* 8, 247–267. doi: 10.15252/emmm.201505748
- Chang, L. C., Chiang, S. K., Chen, S. E., Yu, Y. L., Chou, R. H., and Chang, W. C. (2018). Heme oxygenase-1 mediates BAY 11-7085 induced ferroptosis. *Cancer Lett.* 416, 124–137. doi: 10.1016/j.canlet.2017.12.025
- Chen, A. C., Donovan, A., Ned-Sykes, R., and Andrews, N. C. (2015). Noncanonical role of transferrin receptor 1 is essential for intestinal homeostasis. *Proc. Natl. Acad. Sci. U.S.A.* 112, 11714–11719. doi: 10.1073/pnas.1511701112
- Chen, G. Q., Benthani, F. A., Wu, J., Liang, D., Bian, Z. X., and Jiang, X. (2020). Artemisinin compounds sensitize cancer cells to ferroptosis by regulating iron homeostasis. *Cell Death Diff.* 27, 242–254. doi: 10.1038/s41418-019-0352-3

- Chen, H., Zheng, C., Zhang, Y., Chang, Y. Z., Qian, Z. M., and Shen, X. (2006). Heat shock protein 27 downregulates the transferrin receptor 1-mediated iron uptake. *Int. J. Biochem. Cell Biol.* 38, 1402–1416. doi: 10.1016/j.biocel.2006.02.006
- Chen, P. H., Wu, J., Ding, C. C., Lin, C. C., Pan, S., Bossa, N., et al. (2020). Kinome screen of ferroptosis reveals a novel role of ATM in regulating iron metabolism. *Cell Death Diff.* 27, 1008–1022. doi: 10.1038/s41418-019-0393-7
- Chen, X., Li, J., Kang, R., Klionsky, D. J., and Tang, D. (2020). Ferroptosis: machinery and regulation. *Autophagy* 1–28. doi: 10.1080/15548627.2020.1810918 [Epub ahead of print].
- Colca, J. R., McDonald, W. G., Waldon, D. J., Leone, J. W., Lull, J. M., Bannow, C. A., et al. (2004). Identification of a novel mitochondrial protein ("mitoNEET") cross-linked specifically by a thiazolidinedione photoprobe. *Am. J. Physiol. Endocrinol. Metab.* 286, E252–E260. doi: 10.1152/ajpendo.00424.2003
- Cozzi, A., Santambrogio, P., Privitera, D., Broccoli, V., Rotundo, L. I., Garavaglia, B., et al. (2013). Human L-ferritin deficiency is characterized by idiopathic generalized seizures and atypical restless leg syndrome. *J. Exp. Med.* 210, 1779–1791. doi: 10.1084/jem.20130315
- Dai, E., Meng, L., Kang, R., Wang, X., and Tang, D. (2020). ESCRT-III-dependent membrane repair blocks ferroptosis. *Biochem. Biophys. Res. Commun.* 522, 415–421. doi: 10.1016/j.bbrc.2019.11.110
- Dixon, S. J., Lemberg, K. M., Lamprecht, M. R., Skouta, R., Zaitsev, E. M., Gleason, C. E., et al. (2012). Ferroptosis: an iron-dependent form of nonapoptotic cell death. *Cell* 149, 1060–1072. doi: 10.1016/j.cell.2012.03.042
- Do Van, B., Gouel, F., Jonneaux, A., Timmerman, K., Gele, P., Petrucci, M., et al. (2016). Ferroptosis, a newly characterized form of cell death in Parkinson's disease that is regulated by PKC. *Neurobiol. Dis.* 94, 169–178. doi: 10.1016/j.nbd.2016.05.011
- Doll, S., Freitas, F. P., Shah, R., Aldrovandi, M., da Silva, M. C., Ingold, I., et al. (2019). FSP1 is a glutathione-independent ferroptosis suppressor. *Nature* 575, 693–698. doi: 10.1038/s41586-019-1707-0
- Doll, S., Proneth, B., Tyurina, Y. Y., Panzilius, E., Kobayashi, S., Ingold, I., et al. (2017). ACSL4 dictates ferroptosis sensitivity by shaping cellular lipid composition. *Nat. Chem. Biol.* 13, 91–98. doi: 10.1038/nchembio.2239
- Donovan, A., Lima, C. A., Pinkus, J. L., Pinkus, G. S., Zon, L. I., Robine, S., et al. (2005). The iron exporter ferroportin/Slc40a1 is essential for iron homeostasis. *Cell Metab.* 1, 191–200. doi: 10.1016/j.cmet.2005.01.003
- Drecourt, A., Babdor, J., Dussiot, M., Petit, F., Goudin, N., Garfa-Traore, M., et al. (2018). Impaired transferrin receptor palmitoylation and recycling in neurodegeneration with brain iron accumulation. *Am. J. Hum. Genet.* 102, 266–277. doi: 10.1016/j.ajhg.2018.01.003
- Eling, N., Reuter, L., Hazin, J., Hamacher-Brady, A., and Brady, N. R. (2015). Identification of artesunate as a specific activator of ferroptosis in pancreatic cancer cells. *Oncoscience* 2, 517–532. doi: 10.18632/oncoscience.160
- Fang, X., Wang, H., Han, D., Xie, E., Yang, X., Wei, J., et al. (2019). Ferroptosis as a target for protection against cardiomyopathy. *Proc. Natl. Acad. Sci. U.S.A.* 116, 2672–2680. doi: 10.1073/pnas.1821022116
- Feng, H., Schorpp, K., Jin, J., Yozwiak, C. E., Hoffstrom, B. G., Decker, A. M., et al. (2020). Transferrin receptor is a specific ferroptosis marker. *Cell Rep* 30:e7. doi: 10.1016/j.celrep.2020.02.049
- Galluzzi, L., Vitale, I., Aaronson, S. A., Abrams, J. M., Adam, D., Agostinis, P., et al. (2018). Molecular mechanisms of cell death: recommendations of the nomenclature committee on Cell Death 2018. *Cell Death Diff.* 25, 486–541. doi: 10.1038/s41418-017-0012-4
- Galvez-Peralta, M., He, L., Jorge-Nebert, L. F., Wang, B., Miller, M. L., Eppert, B. L., et al. (2012). ZIP8 zinc transporter: indispensable role for both multiple-organ organogenesis and hematopoiesis in utero. *PLoS One* 7:e36055. doi: 10.1371/journal.pone.0036055
- Gao, H., Bai, Y., Jia, Y., Zhao, Y., Kang, R., Tang, D., et al. (2018). Ferroptosis is a lysosomal cell death process. *Biochem. Biophys. Res. Commun.* 503, 1550–1556. doi: 10.1016/j.bbrc.2018.07.078
- Gao, M., Monian, P., Pan, Q., Zhang, W., Xiang, J., and Jiang, X. (2016). Ferroptosis is an autophagic cell death process. *Cell Res.* 26, 1021–1032. doi: 10.1038/cr.2016.95
- Gao, M., Monian, P., Quadri, N., Ramasamy, R., and Jiang, X. (2015). Glutaminolysis and transferrin regulate ferroptosis. *Mol. Cell* 59, 298–308. doi: 10.1016/j.molcel.2015.06.011
- Gao, M., Yi, J., Zhu, J., Minikes, A. M., Monian, P., Thompson, C. B., et al. (2019). Role of Mitochondria in Ferroptosis. *Mol. Cell* 73, e3. doi: 10.1016/j.molcel.2018.10.042
- Geng, N., Shi, B. J., Li, S. L., Zhong, Z. Y., Li, Y. C., Xua, W. L., et al. (2018). Knockdown of ferroportin accelerates erastin-induced ferroptosis in neuroblastoma cells. *Eur. Rev. Med. Pharmacol. Sci.* 22, 3826–3836. doi: 10.26355/eurrev_201806_15267
- Ghanem, L. R., Kromer, A., Silverman, I. M., Chatterji, P., Traxler, E., Penzo-Mendez, A., et al. (2016). The poly(C) binding protein pcbb2 and its retrotransposed derivative pcbb1 are independently essential to mouse development. *Mol. Cell Biol.* 36, 304–319. doi: 10.1128/MCB.00936-15
- Hanel, H., Smith-Kurtz, E., and Pastowsky, S. (1991). Therapy of seborrheic eczema with an antifungal agent with an antiplogistic effect. *Mycoses* 34(Suppl. 1), 91–93.
- Homma, T., Kobayashi, S., and Fujii, J. (2020). Cysteine preservation confers resistance to glutathione-depleted cells against ferroptosis via CDGSH iron sulphur domain-containing proteins (CISDs). *Free Radic. Res.* 54, 397–407. doi: 10.1080/10715762.2020.1780229
- Hou, W., Xie, Y., Song, X., Sun, X., Lotze, M. T., Zeh, H. J., et al. (2016). Autophagy promotes ferroptosis by degradation of ferritin. *Autophagy* 12, 1425–1428. doi: 10.1080/15548627.2016.1187366
- Huang, K. J., Wei, Y. H., Chiu, Y. C., Wu, S. R., and Shieh, D. B. (2019). Assessment of zero-valent iron-based nanotherapeutics for ferroptosis induction and resensitization strategy in cancer cells. *Biomater. Sci.* 7, 1311–1322. doi: 10.1039/c8bm01525b
- Imoto, S., Kono, M., Suzuki, T., Shibuya, Y., Sawamura, T., Mizokoshi, Y., et al. (2018). Haemin-induced cell death in human monocytic cells is consistent with ferroptosis. *Transfus Apher. Sci.* 57, 524–531. doi: 10.1016/j.transci.2018.05.028
- Iwai, K., Drake, S. K., Wehr, N. B., Weissman, A. M., LaVaute, T., Minato, N., et al. (1998). Iron-dependent oxidation, ubiquitination, and degradation of iron regulatory protein 2: implications for degradation of oxidized proteins. *Proc. Natl. Acad. Sci. U.S.A.* 95, 4924–4928. doi: 10.1073/pnas.95.9.4924
- Jabara, H. H., Boyden, S. E., Chou, J., Ramesh, N., Massaad, M. J., Benson, H., et al. (2016). A missense mutation in TFRC, encoding transferrin receptor 1, causes combined immunodeficiency. *Nat. Genet.* 48, 74–78. doi: 10.1038/ng.3465
- Jenkitkasemwong, S., Wang, C. Y., Coffey, R., Zhang, W., Chan, A., Biel, T., et al. (2015). SLC39A14 is required for the development of hepatocellular iron overload in murine models of hereditary hemochromatosis. *Cell Metab.* 22, 138–150. doi: 10.1016/j.cmet.2015.05.002
- Kagan, V. E., Mao, G., Qu, F., Angeli, J. P., Doll, S., Croix, C. S., et al. (2017). Oxidized arachidonic and adrenic PEs navigate cells to ferroptosis. *Nat. Chem. Biol.* 13, 81–90. doi: 10.1038/nchembio.2238
- Kang, R., and Tang, D. (2017). Autophagy and Ferroptosis - What's the Connection? *Curr. Pathobiol. Rep.* 5, 153–159. doi: 10.1007/s40139-017-0139-5
- Kawashima, A., Oda, Y., Yachie, A., Koizumi, S., and Nakanishi, I. (2002). Heme oxygenase-1 deficiency: the first autopsy case. *Hum. Pathol.* 33, 125–130. doi: 10.1053/hupa.2002.30217
- Kim, E. H., Shin, D., Lee, J., Jung, A. R., and Roh, J. L. (2018). Cisd2 inhibition overcomes resistance to sulfasalazine-induced ferroptotic cell death in head and neck cancer. *Cancer Lett.* 432, 180–190. doi: 10.1016/j.canlet.2018.06.018
- Kong, Z., Liu, R., and Cheng, Y. (2019). Artesunate alleviates liver fibrosis by regulating ferroptosis signaling pathway. *Biomed. Pharmacother.* 109, 2043–2053. doi: 10.1016/j.biopha.2018.11.030
- Kwon, M. Y., Park, E., Lee, S. J., and Chung, S. W. (2015). Heme oxygenase-1 accelerates erastin-induced ferroptotic cell death. *Oncotarget* 6, 24393–24403. doi: 10.18632/oncotarget.5162
- Kuang, F., Liu, J., Tang, D., and Kang, D. (2020). Oxidative damage and antioxidant defense in ferroptosis. *Front. Cell Dev. Biol.* doi: 10.3389/fcell.2020.586578
- Levy, J. E., Jin, O., Fujiwara, Y., Kuo, F., and Andrews, N. C. (1999). Transferrin receptor is necessary for development of erythrocytes and the nervous system. *Nat. Genet.* 21, 396–399. doi: 10.1038/7727
- Li, C., Zhang, Y., Cheng, X., Yuan, H., Zhu, S., Liu, J., et al. (2018). PINK1 and PARK2 suppress pancreatic tumorigenesis through control of mitochondrial iron-mediated immunometabolism. *Dev. Cell* 46:e8. doi: 10.1016/j.devcel.2018.07.012

- Li, L., Hao, Y., Zhao, Y., Wang, H., Zhao, X., Jiang, Y., et al. (2018). Ferroptosis is associated with oxygen-glucose deprivation/reoxygenation-induced Sertoli cell death. *Int. J. Mol. Med.* 41, 3051–3062. doi: 10.3892/ijmm.2018.3469
- Li, Q., Han, X., Lan, X., Gao, Y., Wan, J., Durham, F., et al. (2017). Inhibition of neuronal ferroptosis protects hemorrhagic brain. *JCI Insight* 2:e90777. doi: 10.1172/jci.insight.90777
- Li, Q., Li, Q. Q., Jia, J. N., Sun, Q. Y., Zhou, H. H., Jin, W. L., et al. (2019). Baicalein exerts neuroprotective effects in FeCl₃-induced posttraumatic epileptic seizures via suppressing ferroptosis. *Front. Pharmacol.* 10:638. doi: 10.3389/fphar.2019.00638
- Li, W., Garringer, H. J., Goodwin, C. B., Richine, B., Acton, A., VanDuyn, N., et al. (2015). Systemic and cerebral iron homeostasis in ferritin knock-out mice. *PLoS One* 10:e0117435. doi: 10.1371/journal.pone.0117435
- Liu, J., Kuang, F., Kroemer, G., Klionsky, D. J., Kang, R., and Tang, D. (2020). Autophagy-dependent ferroptosis: machinery and regulation. *Cell Chem. Biol.* 27, 420–435. doi: 10.1016/j.chembiol.2020.02.005
- Liu, Y., Wang, Y., Liu, J., Kang, R., and Tang, D. (2020). Interplay between MTOR and GPX4 signaling modulates autophagy-dependent ferroptotic cancer cell death. *Cancer Gene. Ther.* doi: 10.1038/s41417-020-0182-y [Epub ahead of print].
- Masaldan, S., Clatworthy, S. A. S., Gamell, C., Meggyesy, P. M., Rigopoulos, A. T., Haupt, S., et al. (2018). Iron accumulation in senescent cells is coupled with impaired ferritinophagy, and inhibition of ferroptosis. *Red. Biol.* 14, 100–115. doi: 10.1016/j.redox.2017.08.015
- Messa, E., Carturan, S., Maffe, C., Pautasso, M., Bracco, E., Roetto, A., et al. (2010). Deferasirox is a powerful NF- κ B inhibitor in myelodysplastic cells and in leukemia cell lines acting independently from cell iron deprivation by chelation and reactive oxygen species scavenging. *Haematologica* 95, 1308–1316. doi: 10.3324/haematol.2009.016824
- Mumbauer, S., Pascual, J., Kolotuev, I., and Hamaratoglu, F. (2019). Ferritin heavy chain protects the developing wing from reactive oxygen species and ferroptosis. *PLoS Genet* 15:e1008396. doi: 10.1371/journal.pgen.1008396
- Nandal, A., Ruiz, J. C., Subramanian, P., Ghimire-Rijal, S., Sinnamon, R. A., Stemmler, T. L., et al. (2011). Activation of the HIF prolyl hydroxylase by the iron chaperones PCBP1 and PCBP2. *Cell Metab.* 14, 647–657. doi: 10.1016/j.cmet.2011.08.015
- Nishizawa, H., Matsumoto, M., Shindo, T., Saigusa, D., Kato, H., Suzuki, K., et al. (2020). Ferroptosis is controlled by the coordinated transcriptional regulation of glutathione and labile iron metabolism by the transcription factor BACH1. *J. Biol. Chem.* 295, 69–82. doi: 10.1074/jbc.RA119.009548
- Njajou, O. T., Vaessen, N., Joosse, M., Berghuis, B., van Dongen, J. W., Breuning, M. H., et al. (2001). A mutation in SLC11A3 is associated with autosomal dominant hemochromatosis. *Nat. Genet.* 28, 213–214. doi: 10.1038/90038
- Ooko, E., Saeed, M. E., Kadioglu, O., Sarvi, S., Colak, M., Elmasaoudi, K., et al. (2015). Artemisinin derivatives induce iron-dependent cell death (ferroptosis) in tumor cells. *Phytomedicine* 22, 1045–1054. doi: 10.1016/j.phymed.2015.08.002
- Protchenko, O., Baratz, E., Jadhav, S., Li, F., Shakoury-Elizeh, M., Gavrilova, O., et al. (2020). Iron chaperone PCBP1 protects murine liver from lipid peroxidation and steatosis. *Hepatology* doi: 10.1002/hep.31328 [Epub ahead of print].
- Shang, Y., Luo, M., Yao, F., Wang, S., Yuan, Z., and Yang, Y. (2020). Ceruloplasmin suppresses ferroptosis by regulating iron homeostasis in hepatocellular carcinoma cells. *Cell Signal.* 72:109633. doi: 10.1016/j.cellsig.2020.109633
- Shin, D., Kim, E. H., Lee, J., and Roh, J. L. (2018). Nrf2 inhibition reverses resistance to GPX4 inhibitor-induced ferroptosis in head and neck cancer. *Free Radic. Biol. Med.* 129, 454–462. doi: 10.1016/j.freeradbiomed.2018.10.426
- Song, X., Xie, Y., Kang, R., Hou, W., Sun, X., Epperly, M. W., et al. (2016). FANCD2 protects against bone marrow injury from ferroptosis. *Biochem. Biophys. Res. Commun.* 480, 443–449. doi: 10.1016/j.bbrc.2016.10.068
- Song, X., Zhu, S., Chen, P., Hou, W., Wen, Q., Liu, J., et al. (2018). AMPK-mediated BECN1 phosphorylation promotes ferroptosis by directly blocking system Xc(-) Activity. *Curr. Biol.* 28:e5. doi: 10.1016/j.cub.2018.05.094
- Stockwell, B. R., Friedmann Angeli, J. P., Bayir, H., Bush, A. I., Conrad, M., Dixon, S. J., et al. (2017). Ferroptosis: a regulated cell death nexus linking metabolism. *Red. Biol. Dis. Cell* 171, 273–285. doi: 10.1016/j.cell.2017.09.021
- Sun, X., Niu, X., Chen, R., He, W., Chen, D., Kang, R., et al. (2016a). Metallothionein-1G facilitates sorafenib resistance through inhibition of ferroptosis. *Hepatology* 64, 488–500. doi: 10.1002/hep.28574
- Sun, X., Ou, Z., Chen, R., Niu, X., Chen, D., Kang, R., et al. (2016b). Activation of the p62-Keap1-NRF2 pathway protects against ferroptosis in hepatocellular carcinoma cells. *Hepatology* 63, 173–184. doi: 10.1002/hep.28251
- Sun, X., Ou, Z., Xie, M., Kang, R., Fan, Y., Niu, X., et al. (2015). HSPB1 as a novel regulator of ferroptotic cancer cell death. *Oncogene* 34, 5617–5625. doi: 10.1038/nc.2015.32
- Tadokoro, T., Ikeda, M., Ide, T., Deguchi, H., Ikeda, S., Okabe, K., et al. (2020). Mitochondria-dependent ferroptosis plays a pivotal role in doxorubicin cardiotoxicity. *JCI Insight* 5:e132747. doi: 10.1172/jci.insight.132747
- Tang, D., Kang, R., Berghe, T. V., Vandenabeele, P., and Kroemer, G. (2019). The molecular machinery of regulated cell death. *Cell Res.* 29, 347–364. doi: 10.1038/s41422-019-0164-5
- Trenor, C. C. III, Campagna, D. R., Sellers, V. M., Andrews, N. C., and Fleming, M. D. (2000). The molecular defect in hypotransferrinemic mice. *Blood* 96, 1113–1118. doi: 10.1182/blood.v96.3.1113
- Troadec, M. B., Warner, D., Wallace, J., Thomas, K., Spangrude, G. J., Phillips, J., et al. (2011). Targeted deletion of the mouse Mitoferrin1 gene: from anemia to protoporphyria. *Blood* 117, 5494–5502. doi: 10.1182/blood-2010-11-319483
- Tuo, Q. Z., Lei, P., Jackman, K. A., Li, X. L., Xiong, H., Li, X. L., et al. (2017). Tau-mediated iron export prevents ferroptotic damage after ischemic stroke. *Mol. Psychiatry* 22, 1520–1530. doi: 10.1038/mp.2017.171
- Wang, G. L., and Semenza, G. L. (1993). Desferrioxamine induces erythropoietin gene expression and hypoxia-inducible factor 1 DNA-binding activity: implications for models of hypoxia signal transduction. *Blood* 82, 3610–3615. doi: 10.1182/blood.v82.12.3610.bloodjournal82123610
- Wang, Y., Liua, Y., Liua, J., Kang, R., and Tang, D. (2020). NEDD4L-mediated LTF Protein degradation limits ferroptosis. *Biochem. Biophys. Res. Commun.* 531, 581–587. doi: 10.1021/acschembio.7b01082
- Wang, Y. Q., Chang, S. Y., Wu, Q., Gou, Y. J., Jia, L., Cui, Y. M., et al. (2016). The Protective Role of Mitochondrial Ferritin on Erastin-Induced Ferroptosis. *Front Aging Neurosci* 8:308. doi: 10.3389/fnagi.2016.00308
- Wen, Q., Liu, J., Kang, R., Zhou, B., and Tang, D. (2019). The release and activity of HMGB1 in ferroptosis. *Biochem. Biophys. Res. Commun.* 510, 278–283. doi: 10.1016/j.bbrc.2019.01.090
- Wu, J., Minikes, A. M., Gao, M., Bian, H., Li, Y., Stockwell, B. R., et al. (2019). Intercellular interaction dictates cancer cell ferroptosis via NF2-YAP signalling. *Nature* 572, 402–406. doi: 10.1038/s41586-019-1426-6
- Xie, Y., Hou, W., Song, X., Yu, Y., Huang, J., Sun, X., et al. (2016a). Ferroptosis: process and function. *Cell Death Diff.* 23, 369–379. doi: 10.1038/cdd.2015.158
- Xie, Y., Li, J., Kang, R., and Tang, D. (2020). Interplay between lipid metabolism and autophagy. *Front. Cell Dev. Biol.* 8:431. doi: 10.3389/fcell.2020.00431
- Xie, Y., Song, X., Sun, X., Huang, J., Zhong, M., Lotze, M. T., et al. (2016b). Identification of baicalein as a ferroptosis inhibitor by natural product library screening. *Biochem. Biophys. Res. Commun.* 473, 775–780. doi: 10.1016/j.bbrc.2016.03.052
- Xie, Y., Zhu, S., Song, X., Sun, X., Fan, Y., Liu, J., et al. (2017). The tumor suppressor p53 Limits Ferroptosis by Blocking DPP4 Activity. *Cell Rep.* 20, 1692–1704. doi: 10.1016/j.celrep.2017.07.055
- Yanatori, I., Yasui, Y., Tabuchi, M., and Kishi, F. (2014). Chaperone protein involved in transmembrane transport of iron. *Biochem. J.* 462, 25–37. doi: 10.1042/BJ20140225
- Yang, M., Chen, P., Liu, J., Zhu, S., Kroemer, G., Klionsky, D. J., et al. (2019). Clockophagy is a novel selective autophagy process favoring ferroptosis. *Sci. Adv.* 5:eaaw2238. doi: 10.1126/sciadv.aaw2238
- Yang, W. H., Huang, Z., Wu, J., Ding, C. C., Murphy, S. K., and Chi, J. T. (2020). A TAZ-ANGPTL4-NOX2 axis regulates ferroptotic cell death and chemoresistance in epithelial ovarian cancer. *Mol. Cancer Res.* 18, 79–90. doi: 10.1158/1541-7786.MCR-19-0691
- Yang, W. S., Kim, K. J., Gaschler, M. M., Patel, M., Shchepinov, M. S., and Stockwell, B. R. (2016). Peroxidation of polyunsaturated fatty acids by lipoxygenases drives ferroptosis. *Proc. Natl. Acad. Sci. U.S.A.* 113, E4966–E4975. doi: 10.1073/pnas.1603244113

- Yang, W. S., and Stockwell, B. R. (2008). Synthetic lethal screening identifies compounds activating iron-dependent, nonapoptotic cell death in oncogenic-RAS-harboring cancer cells. *Chem. Biol.* 15, 234–245. doi: 10.1016/j.chembiol.2008.02.010
- Yoshida, M., Minagawa, S., Araya, J., Sakamoto, T., Hara, H., Tsubouchi, K., et al. (2019). Involvement of cigarette smoke-induced epithelial cell ferroptosis in COPD pathogenesis. *Nat. Commun.* 10:3145. doi: 10.1038/s41467-019-10991-7
- Yu, Y., Jiang, L., Wang, H., Shen, Z., Cheng, Q., Zhang, P., et al. (2020). Hepatic Transferrin Plays a Role in Systemic Iron Homeostasis and Liver Ferroptosis. *Blood* 136, 726–739. doi: 10.1182/blood.2019002907
- Yuan, H., Li, X., Zhang, X., Kang, R., and Tang, D. (2016a). Cisd1 inhibits ferroptosis by protection against mitochondrial lipid peroxidation. *Biochem. Biophys. Res. Commun.* 478, 838–844. doi: 10.1016/j.bbrc.2016.08.034
- Yuan, H., Li, X., Zhang, X., Kang, R., and Tang, D. (2016b). Identification of ACSL4 as a biomarker and contributor of ferroptosis. *Biochem. Biophys. Res. Commun.* 478, 1338–1343. doi: 10.1016/j.bbrc.2016.08.124
- Zhang, Z., Guo, M., Shen, M., Kong, D., Zhang, F., Shao, J., et al. (2020). The BRD7-P53-SLC25A28 axis regulates ferroptosis in hepatic stellate cells. *Red. Biol.* 36, 101619. doi: 10.1016/j.redox.2020.101619
- Zhou, B., Liu, J., Kang, R., Klionsky, D. J., Kroemer, G., and Tang, D. (2019). Ferr*optosis is a type of autophagy-dependent cell death. *Semin. Cancer Biol.* doi: 10.1016/j.semcancer.2019.03.002
- Zou, Y., Li, H., Graham, E. T., Deik, A. A., Eaton, J. K., Wang, W., et al. (2020). Cytochrome P450 oxidoreductase contributes to phospholipid peroxidation in ferroptosis. *Nat. Chem. Biol.* 16, 302–309. doi: 10.1038/s41589-020-0472-6
- Zou, Y., Palte, M. J., Deik, A. A., Li, H., Eaton, J. K., Wang, W., et al. (2019). A GPX4-dependent cancer cell state underlies the clear-cell morphology and confers sensitivity to ferroptosis. *Nat. Commun.* 10:1617. doi: 10.1038/s41467-019-09277-9

Conflict of Interest: The authors declare that the research was conducted in the absence of any commercial or financial relationships that could be construed as a potential conflict of interest.

Copyright © 2020 Chen, Yu, Kang and Tang. This is an open-access article distributed under the terms of the Creative Commons Attribution License (CC BY). The use, distribution or reproduction in other forums is permitted, provided the original author(s) and the copyright owner(s) are credited and that the original publication in this journal is cited, in accordance with accepted academic practice. No use, distribution or reproduction is permitted which does not comply with these terms.



Comparison of Anti-oncotic Effect of TRPM4 Blocking Antibody in Neuron, Astrocyte and Vascular Endothelial Cell Under Hypoxia

Shunhui Wei¹, See Wee Low¹, Charlene Priscilla Poore¹, Bo Chen¹, Yahui Gao¹, Bernd Nilius² and Ping Liao^{1,3,4*}

¹ Calcium Signaling Laboratory, Department of Research, National Neuroscience Institute, Singapore, Singapore,

² Department of Cellular and Molecular Medicine, KU Leuven, Leuven, Belgium, ³ Duke-NUS Medical School, Singapore,

Singapore, ⁴ Health and Social Sciences, Singapore Institute of Technology, Singapore, Singapore

OPEN ACCESS

Edited by:

Yasunobu Okada,
National Institute for Physiological
Sciences (NIPS), Japan

Reviewed by:

Geeta Upadhyay,
Uniformed Services University of the
Health Sciences, United States
Tomohiro Numata,
Fukuoka University, Japan

*Correspondence:

Ping Liao
ping_liao@nni.com.sg

Specialty section:

This article was submitted to
Cell Death and Survival,
a section of the journal
Frontiers in Cell and Developmental
Biology

Received: 15 May 2020

Accepted: 30 September 2020

Published: 19 October 2020

Citation:

Wei S, Low SW, Poore CP,
Chen B, Gao Y, Nilius B and Liao P
(2020) Comparison of Anti-oncotic
Effect of TRPM4 Blocking Antibody
in Neuron, Astrocyte and Vascular
Endothelial Cell Under Hypoxia.
Front. Cell Dev. Biol. 8:562584.
doi: 10.3389/fcell.2020.562584

In stroke and other neurological diseases, Transient Receptor Potential Melastatin 4 (TRPM4) has been reported to cause oncotic cell death which is due to an excessive influx of sodium ions. Following stroke, hypoxia condition activates TRPM4 channel, and the sodium influx via TRPM4 is further enhanced by an increased TRPM4 expression. However, the effect of TRPM4 inhibition on oncotic cell death, particularly during the acute stage, remains largely unknown. Recently, we have developed a polyclonal antibody M4P that specifically inhibits TRPM4 channel. M4P blocks the channel via binding to a region close to the channel pore from extracellular space. Using M4P, we evaluated the acute effect of blocking TRPM4 in neurons, astrocytes, and vascular endothelial cells. In a rat stroke model, M4P co-localized with neuronal marker NeuN and endothelial marker vWF, whereas few GFAP positive astrocytes were stained by M4P in the ipsilateral hemisphere. When ATP was acutely depleted in cultured cortical neurons and microvascular endothelial cells, cell swelling was induced. Application of M4P significantly blocked TRPM4 current and attenuated oncosis. TUNEL assay, PI staining and western blot on cleaved Caspase-3 revealed that M4P could ameliorate apoptosis after 24 h hypoxia exposure. In contrast, acute ATP depletion in cultured astrocytes failed to demonstrate an increase of cell volume, and application of M4P or control IgG had no effect on cell volume change. When TRPM4 was overexpressed in astrocytes, acute ATP depletion successfully induced oncosis which could be suppressed by M4P treatment. Our results demonstrate that comparing to astrocytes, neurons, and vascular endothelial cells are more vulnerable to hypoxic injury. During the acute stage of stroke, blocking TRPM4 channel could protect neurons and vascular endothelial cells from oncotic cell death.

Keywords: ischemic stroke, TRPM4, swelling, cell death, therapeutic antibody

INTRODUCTION

Stroke is a leading cause of disability worldwide, and of all strokes, more than 80% are ischemic (Virani et al., 2020). Cerebral edema is common among stroke patients, particularly after reperfusion. There are two types of edema, cytotoxic, and vasogenic, which are caused by cell swelling or increased vascular permeability (Rosenberg, 1999). It has been reported that stroke patients with severe edema have a mortality of up to 60–80% (Hacke et al., 1996; Berrouschot et al., 1998). Harnessing cerebral edema is thus pivotal in improving stroke outcome. However, neuroprotective agents targeting cerebral edema have not been translated into clinical treatments. For example, blockers for NMDA receptor failed to show beneficial effects due to their narrow therapeutic windows and adverse effects (Wu and Tymianski, 2018). One major reason is that the cellular and molecular mechanisms underlying cerebral edema remain largely unclear.

There are two types of cell death in stroke: cell swelling, also known as oncosis or oncotic cell death (Weerasinghe and Buja, 2012), and programmed cell death (Majno and Joris, 1995). Oncosis is caused by increased membrane permeability which leads to cell swelling. Whereas in programmed apoptosis, cell shrinkage and fragmentation into apoptotic bodies are typical features. Following oncosis or apoptosis, cells undergo irreversible necrosis and phagocytosis (Lipton, 1999). In stroke, there have a heterogeneous distribution of oncotic and apoptotic processes across affected brain regions (Charriaut-Marlangue et al., 1996). At the point of insult, the death pathway varies among cell types as well (Martin et al., 1998). Understanding the mechanisms behind such differences could pave the way for novel therapies.

Recently, novel evidence has emerged regarding the pathophysiological role of the transient receptor potential (TRP) channels in stroke (Zhang and Liao, 2015). Among the largest TRP subfamily, transient receptor potential melastatin (TRPM), several members have demonstrated as potential drug targets for stroke. Activation of TRPM2, an oxidative stress-sensitive channel, contributes to neuronal death following hypoxia/ischemia. TRPM2 inhibition has been shown to yield a neuroprotective effect in stroke reperfusion and global cerebral hypoxia (Toda et al., 2019; Hong et al., 2020). Another member TRPM7 has a unique property of both cation permeability and kinase activity (Inoue et al., 2020). TRPM7 plays an important role in cell volume regulation (Numata et al., 2007), excessive influx of the metal ions Ca^{2+} , Mg^{2+} , and Zn^{2+} through TRPM7 is highly toxic (Inoue et al., 2010). In addition to suppress metal ion overloading, blocking TRPM7 could also inhibit ROS production in neurons following hypoxia (Aarts et al., 2003). The most extensively studied TRPM channel in stroke is TRPM4 which has been found to play an important role in oncotic cell death (Gerzanich et al., 2009; Loh et al., 2019). TRPM4 is an ATP-sensitive non-selective cation channel that can be activated by an increased intracellular Ca^{2+} level as well as ATP depletion (Vennekens and Nilius, 2007). Both TRPM4 expression and activity are enhanced after stroke (Loh et al., 2014; Chen et al.,

2019b). Under hypoxic condition, excessive Na^{+} influx via TRPM4 contributes to intracellular ionic imbalance, leading to cell swelling (Gerzanich et al., 2009; Schattling et al., 2012). Therefore, TRPM4 has become a potential target for stroke management (Walcott et al., 2012; Loh et al., 2014; Hu and Song, 2017; Chen et al., 2019b).

Sulfonylurea receptor-1 (SUR1) has been reported to interact with TRPM4, forming a SUR1-TRPM4 channel complex (Simard et al., 2010). SUR1 blocker glibenclamide is believed to block the channel complex and yields a therapeutic effect on stroke (Kurland et al., 2013). However, glibenclamide requires the presence of SUR1 which needs to be expressed at a certain level to yield a pharmacological effect (Woo et al., 2013). Without SUR1, glibenclamide could not inhibit TRPM4 channel activity (Sala-Rabanal et al., 2012). Recently, we have developed a polyclonal antibody M4P that specifically inhibits TRPM4 channel (Chen et al., 2019a). M4P binds to a region close to the channel pore from extracellular space and yields an inhibitory effect via two mechanisms: (1) blocks TRPM4 current directly; (2) down regulates TRPM4 expression on cell membrane. In a rat model of stroke reperfusion, application of M4P ameliorated reperfusion injury by protecting blood–brain barrier (BBB) and improved stroke outcome (Chen et al., 2019a).

In this study, we extended our research on M4P to its anti-oncotic effect on various cell types within the brain including neurons, astrocytes and vascular endothelial cells. Although TRPM4 has been well documented in stroke, the exact role of TRPM4 inhibition on oncotic cell death, particularly during the acute stage, remains largely unclear. Using M4P as a specific blocker for TRPM4, we are able to decipher how TRPM4 engages in disease progression immediately after ischemia which is common in stroke and many other disorders of central nervous system.

MATERIALS AND METHODS

Animal Model of Middle Cerebral Artery Occlusion (MCAO)

This study was approved and conducted in accordance with the guidelines of the Institutional Animal Care and Use Committee of the National Neuroscience Institute, Singapore. The stroke model has been described previously (Loh et al., 2014; Chen et al., 2019a,b). In brief, male Sprague Dawley rats weighing approximately 250–280 g were anesthetized with ketamine (75 mg/kg) and xylazine (10 mg/kg) intraperitoneally. Rectal temperature was monitored using a rectal probe, connecting to the PowerLab 4/35 by a T-type pod (MLT1403&312, RET-2, AD Instruments). The left common carotid artery (CCA), internal carotid artery (ICA) and external carotid artery (ECA) were dissected out. A silicon-coated filament (0.37 mm, Cat #403756PK10, Doccol Corp., Redlands, CA, United States) was introduced into the left ICA through ECA. Cerebral blood flow of the animals was monitored by a Laser-Doppler flowmetry (moorVMS-LDF2TM, Moor Instruments Inc., Wilmington, DE, United States). Animals with $\leq 70\%$ cerebral blood flow reduction were excluded from the study.

Generation of Polyclonal Antibody M4P

The production of rabbit polyclonal antibody M4P has been described in our recent publication (Chen et al., 2019a). M4P was designed to bind to and block rat TRPM4 channel specifically.

Primary Rat Cortical Neurons, Astrocytes and Rat Brain Microvascular Endothelial Cells (RBMVECs) Culture

Primary cortical neurons were prepared from embryonic day 18 (E18) pregnant Sprague Dawley rats. Fetal brain cortex was dissociated and digested for 40 min in Earle's Balanced Salt Solution (EBSS, Thermo Fisher Scientific, Waltham, MA, United States) containing 20 U/mL papain (Worthington, Lakewood, NJ, United States). Dissociated cells were seeded on 12 mm round glass coverslips coated with poly-L-lysine and laminin and placed into 60 mm tissue culture dishes with neuron culture medium containing Neurobasal Medium, 2% B27 supplement, 1% GlutaMAX supplement (Thermo Fisher Scientific, Waltham, MA, United States). Medium was replaced 1 day after plating, and half of the medium was changed every 3 days. The cells were treated with 4 μ M cytosine arabinoside from days *in vitro* (DIV) 3–6 to restrict mitotic cell proliferation and maintained for 10–21 days in neuron culture medium at 37°C.

For primary culture of cortical astrocytes, cells from cerebral cortex were digested, dissociated, and maintained for 10 days in DMEM supplemented with 10% FBS. Cultures were then treated with 10 μ M Ara-C, shaken at 240 rpm for 6 h to remove oligodendrocyte precursor cells and replanted for experiments.

Rat brain microvascular endothelial cells were purchased from Cell Applications Inc (Cell Applications, San Diego, CA, United States). The culture Growth Medium and Basal medium (contains no growth supplement) were also obtained from Cell Applications Inc. Cells at passages 5–10 were used for study as per the manufacturer's recommendation.

Hypoxia Induction

For acute oxygen-glucose deprivation (OGD) during patch clamp recording, the cells (neurons, astrocytes, or vascular endothelial cells) were perfused with an anoxic artificial cerebrospinal fluid (aCSF) containing 5 mM Na₂N₃ and 10 mM 2-deoxyglucose.

For 24-h OGD, the cells were grown in respective hypoxic media and placed in a polycarbonate hypoxia induction chamber (Modular Incubator Chamber, #27310, STEMCELL Technologies Inc., Vancouver, BC, Canada). The chamber was first flushed with a gas mixture containing 1% O₂, 5% CO₂, and 94% N₂ for 5 min to purge the ambient air from the chamber. Following that, the hypoxia chamber was tightly sealed, and placed in a 37°C incubator for 24 h. The hypoxic medium for neurons contains serum-free low glucose EBSS medium, pH7.4 (1.8 mM CaCl₂; 0.8 mM MgSO₄; 5.3 mM KCl; 26.2 mM NaHCO₃; 117.2 mM NaCl; 1 mM NaH₂PO₄; 1.85 mM D-Glucose) with 100 U/ml Penicillin-Streptomycin. For astrocytes, the hypoxic medium is DMEM with free glucose. For RBMVECs, the hypoxic medium is the Basal Medium

purchased from Cell Applications (Cell Applications Inc., San Diego, CA, United States).

Immunofluorescent Staining and Western Blot

Immunofluorescent staining was performed as previously described (Loh et al., 2014). In brief, the rats were sacrificed and perfused 1 day after stroke induction. Then, the brains were harvested and sectioned at 10 μ m in thickness. Following fixation with 4% paraformaldehyde, the brain slice was incubated in 100 μ l blocking serum (10% fetal bovine serum in 0.2% PBST) for 1 h. The samples were then incubated with primary antibodies overnight at 4 °C. Primary antibodies include M4P (rabbit, 10 ng/ μ l), anti-NeuN (MAB377, Millipore, Burlington, MA, United States, 1:250), anti-GFAP (IF03L, Millipore, Burlington, MA, United States, 1:200), and anti-vWF (AB7356, Millipore, Burlington, MA, United States, 1:200). After washing with 0.1% Triton/phosphate-buffered saline, the slides were incubated with secondary antibodies before being visualized using a laser scanning confocal microscope system (FV31S-SW Fluoview, Olympus, Tokyo, Japan). Secondary antibodies include donkey anti-rabbit conjugated with Alexa Fluor 488 and chicken anti-mouse conjugated with Alexa Fluor 594 (Catalog # A-21206, and A-21201, Life Technologies Corporation, Grand Island, NY, United States).

To perform western blot, 30 μ g of total protein was resolved on 10% SDS-PAGE gels at 80V, and electrophoretically transferred to PVDF membranes (1620177, Bio-Rad, Santa Rosa, CA, United States) at 100V for 2 h at 4°C. After blocking with StartingBlock (PBS) blocking buffer (37538, Thermo Fisher Scientific, Waltham, MA, United States) for 1 h at room temperature, membranes were incubated overnight at 4°C with primary polyclonal antibody for cleaved Caspase-3 (# 9661, Cell Signaling Technology Inc., Danvers, MA, United States) and subsequent secondary goat anti-rabbit IgG (A4914, Sigma-Aldrich, St. Louis, MO, United States, 1:5000). After probing with the ECL system, the membrane was incubated with the RestoreTM PLUS Western Blot Stripping Buffer (#46428, Thermo Fisher Scientific, Waltham, MA, United States). Primary anti- β -actin (A1978, Sigma-Aldrich, St. Louis, MO, United States, 1:5000) and secondary goat anti-mouse IgG or (A4416 Sigma-Aldrich, St. Louis, MO, United States, 1:5000) were then used for the detection of β -actin.

TUNEL (Terminal Deoxynucleotidyl Transferase dUTP Nick End Labeling) Assay for Apoptosis

TUNEL labeling was performed using the In Situ Cell Death Detection Kit, Fluorescein (11684795910, Roche Diagnostics, Germany). The cells cultured on glass coverslips were treated and fixed with 4% paraformaldehyde for TUNEL staining according to the manufacturer's instructions. The cells were counterstained with DAPI to visualize the cell nuclei. The glass coverslips then mounted onto glass slides and the images were captured with a laser scanning confocal microscope system (FV31S-SW Fluoview, Olympus, Tokyo, Japan).

PI (Propidium Iodide) Assay

The treated cells on glass coverslips were added with culture media containing 1:100 dilution of 1 mg/mL of the PI stock solution (P1304MP, Thermo Fisher Scientific, Waltham, MA, United States). The cells were incubated for 15 min in a cell culture humidified incubator set at 37°C with 5% CO₂. After which, the cells were washed three times with PBS and fixed with 4% paraformaldehyde. The cells were counterstained with DAPI and mounted onto glass slides. The images were captured with the confocal microscope.

Transfection

Transfection was performed on cell cultures on coated coverslips in 24-well plates using Lipofectamine-2000 (Life Technologies, Carlsbad, CA, United States) according to the manufacturer's instructions. The transfection mix consisted 1 µg plasmid DNA and 1.5 µl LipofectamineTM 2000 reagent for each well. Mouse TRPM4 (pIRES-EGFP-TRPM4) was transiently expressed in astrocytes, TRPM2 or TRPM7 was co-transfected with GFP-containing vector pEGFP-N1 in HEK 293 cells. Mouse TRPM2 (Myc-DDK-tagged) was purchased from OriGene (CAT # MR225380, OriGene, Technologies Inc., Rockville, MD, United States), pcDNA4/TO mTRPM7 was a gift from Andrew Scharenberg (Addgene plasmid # 45482; RRID: Addgene_45482)¹.

Electrophysiology

Whole-cell patch clamp was used to examine the electrophysiological properties of the cultured cells at room temperature. Patch electrodes were pulled using a Flaming/Brown micropipette puller (P-1000, Sutter Instrument, Novato, CA, United States) and polished with a microforge (MF-200, WPI Inc., Sarasota, FL, United States). Whole-cell currents were recorded using a patch clamp amplifier (Multiclamp 700B equipped with Digidata 1440A, Molecular Devices, San Jose, CA, United States). The bath solution contained (in millimole/liter): NaCl 140, CaCl₂ 2, KCl 2, MgCl₂ 1, glucose 20, and HEPES 20 at pH 7.4. The internal solution contained (in millimole/liter): CsCl 156, MgCl₂ 1, EGTA 10, and HEPES 10 at pH 7.2 adjusted with CsOH (Schattling et al., 2012). Rabbit IgG or M4P was added into bath solution at a concentration of 20.8 µg/ml for 30 min before recording. Ischemia/Hypoxia was induced by applying a bath solution containing 5 mM NaN₃ and 10 mM 2-deoxyglucose (2-DG) continuously through a MicroFil (34 Gauge, WPI Inc., United States) around 10 µm away from the recording cells. The flow rate was 200 µl/min. The current-voltage relations were measured by applying voltage ramps for 250 ms from -100 to +100 mV at a holding potential of -70 mV for neurons, or 0 mV for astrocyte and vascular endothelial cells. The sampling rate was 20 kHz and the filter setting was 1 KHz. Data were analyzed using pClamp 10, version 10.2 (Molecular Devices, San Jose, CA, United States). Cell membrane capacitance was recorded by online capacitance measurement in Clampex of pClamp 10 with the update rate at 100 Hz and Membrane Test function was used to set the compensation every 1 min). The images of every

cell were also captured before and after hypoxia induction to compare the changes of cell size.

For TRPM2 current recording in HEK 293 cells, the bath solution contained (in millimole/liter): NaCl 140, CaCl₂ 2, KCl 2, MgCl₂ 1, glucose 20 and HEPES 20 at pH 7.4. The pipette solution contained (in millimole/liter): Cs-methanesulfonate 145, NaCl 8, EGTA 1 and HEPES 10 at pH 7.2 adjusted with CsOH (Du et al., 2009), free internal Ca²⁺ [Ca²⁺]_i was adjusted to 100 µM based on calculations using Maxchelator² (Du et al., 2009). For TRPM7 current recording in HEK 293 cells, 24 h after transfection, TRPM7 expression was induced by adding 1 µg/ml tetracycline to DMEM culture medium. Whole-cell patch clamp was performed 18–26 h after induction, the divalent-free bath solution was used which containing (in millimole/liter : NaCl 145, EGTA 10, glucose 10 and HEPES 20 at pH 7.4 (Jiang et al., 2005), the pipette solution contained (in millimole/liter): Cs-methanesulfonate 145, NaCl 8, EGTA 1 and HEPES 10 at pH 7.2 adjusted with CsOH. For all HEK 293 cells recording, 250-ms voltage ramps from -100 to +100 mV was applied. Holding potential: 0 mV.

Statistical Analysis

Data are expressed as the mean ± S.E.M. Statistical analyses were performed using GraphPad Prism version 6.0. Two-tailed unpaired student's *t*-test was used to compare two means. One-way ANOVA with Bonferroni's multiple comparison test was used to compare ≥3 means.

RESULTS

M4P Detects Upregulated TRPM4 Expression in Ischemic Stroke

To study the expression of TRPM4 in various cell types after stroke, a permanent MCAO model was created in male Sprague Dawley rats. It has been reported that the expression of TRPM4 is low in all cell types in the contralateral hemisphere after stroke (Loh et al., 2014). In this study, TRPM4 expression in the ipsilateral hemisphere was detected by the rat TRPM4 specific antibody M4P. We focus on the area close to the infarct core where the tissue is still viable, but has been affected by hypoxia. M4P was found to co-localize with neuronal marker NeuN and endothelial cell marker vWF. In contrast, few GFAP positive astrocytes were stained by M4P (Figure 1A). In contralateral hemisphere, the expression of TRPM4 was low in all cell types (Figure 1B). This result suggests that comparing to astrocytes, TRPM4 expression is higher in neuron and vascular endothelial cell following stroke induction.

M4P Inhibits TRPM4 Activity in Cortical Neurons and Ameliorate Hypoxia-Induced Cell Swelling

To investigate the role of TRPM4 inhibition on neurons, cortical neurons were pre-incubated with M4P or control rabbit IgG for

¹<https://n2t.net/addgene:45482>

²<https://somapp.ucdmc.ucdavis.edu/pharmacology/bers/maxchelator/webmaxc/webmaxc.htm>

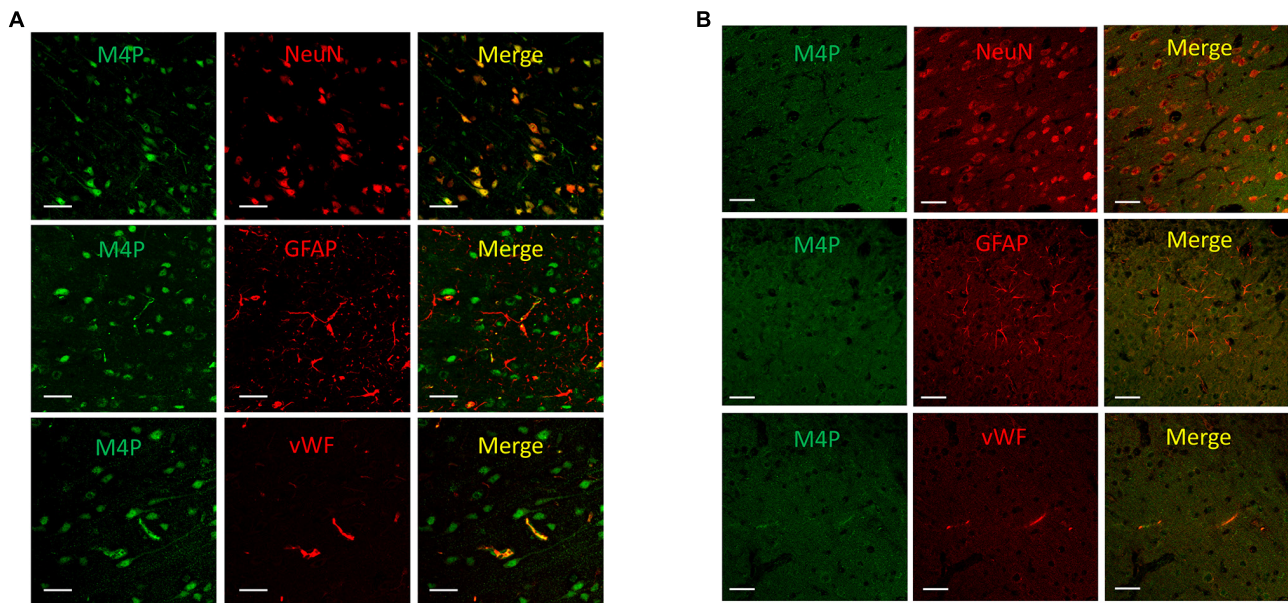


FIGURE 1 | Using M4P to detect TRPM4 expression in a rat model of stroke. **(A)** Brain slices from ipsilateral hemisphere were double stained with M4P and neuronal marker NeuN (upper panel), astrocyte marker GFAP (middle panel), or endothelial cell marker vWF (lower panel). **(B)** Immunofluorescent staining of TRPM4 expression in the contralateral hemisphere. Scale bars 50 μm .

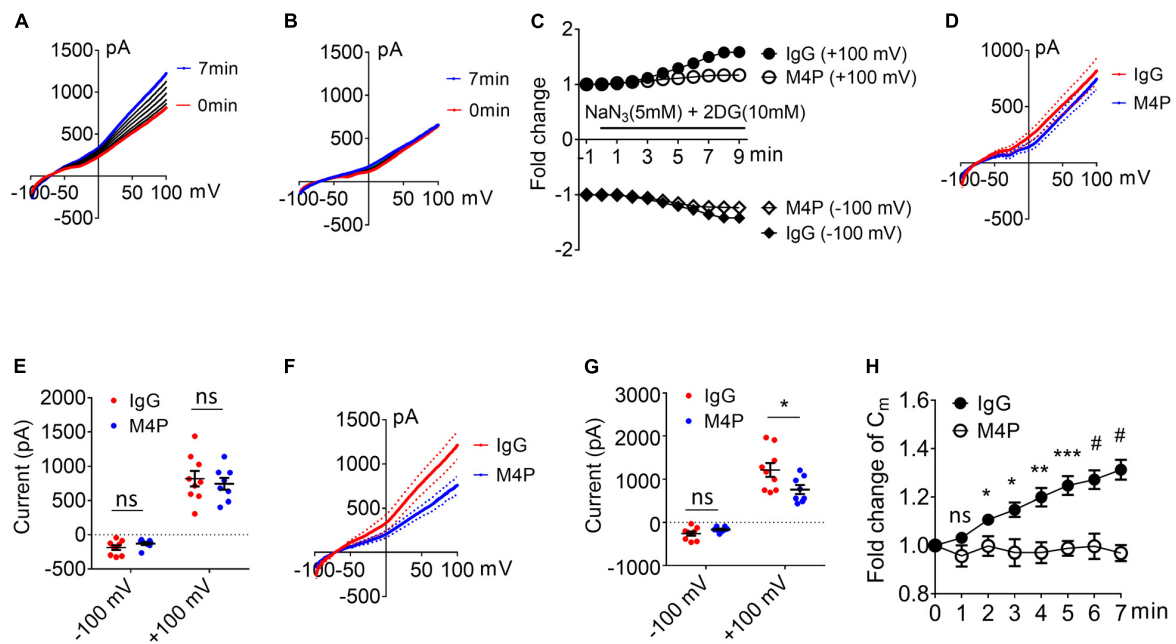


FIGURE 2 | M4P blocks TRPM4 activity in cultured cortical neurons and prevents hypoxia-induced cell swelling. **(A)** Sample traces from a cortical neuron pre-treated with control rabbit IgG (20.8 $\mu\text{g}/\text{ml}$) for 30 min. Acute hypoxia was induced by adding 5 mM NaN_3 and 10 mM 2-DG to the neuron for 7 min. 250-ms voltage ramps from -100 to $+100$ mV was applied at 1 min interval. Holding potential: -70 mV. The pipette solution contained a calculated $7.4 \mu\text{M}$ free Ca^{2+} . **(B)** Sample traces from a cortical neuron pre-treated with M4P at 20.8 $\mu\text{g}/\text{ml}$ for 30 min. The recording protocol is similar to that described in **(A)**. **(C)** Time-dependent current changes at ± 100 mV from **(A,B)**. All currents were normalized to baseline before hypoxic induction. **(D)** Summarized current-voltage relationship at 0 min under hypoxia for control IgG ($n = 9$) and M4P ($n = 8$) treatments. **(E)** Summary of currents at -100 and 100 mV at 0 min under hypoxia. Control IgG: $n = 9$; M4P: $n = 8$. **(F)** Summarized current-voltage relationship at 7 min under hypoxia for control IgG ($n = 9$) and M4P ($n = 8$) treatments. **(G)** Summary of currents at -100 and 100 mV at 7 min under hypoxia. Control IgG: $n = 9$; M4P: $n = 8$. **(H)** Time course of normalized membrane capacitance (C_m) under hypoxic conditions. Control IgG: $n = 9$; M4P: $n = 8$. Statistical analysis was performed by two tailed unpaired student's t -test for **(E,G)**, and two-way ANOVA test with *post hoc* Bonferroni's analysis for **H**. * $p < 0.05$, ** $p < 0.01$, *** $p < 0.001$, and # $p < 0.0001$, ns, non-significant.

30 min before patch clamping. To induce acute hypoxia, 5 mM sodium azide (NaN_3) and 10 mM 2-deoxyglucose (2-DG) was applied to the cells during recording to inhibit mitochondrial respiration and energy metabolism (Chen et al., 2019a). Current-voltage relationship of cortical neurons were obtained by whole-cell patch clamp ramp protocols applied from -100 to +100 mV. The neurons were held at -70 mV to reflect the native resting membrane potential. Under control IgG treatment, the current exhibited a continuous rise during the 7-min hypoxia incubation (Figures 2A,C). Whereas no current increase was observed with M4P treatment (Figures 2B,C). Before hypoxia induction, we did not observe difference between M4P and IgG treated cells (Figures 2D,E). We further compared the currents at 7 min after hypoxia induction, and found that the TRPM4 activity was significantly blocked by M4P application. At +100 mV, the current was reduced by 37.5%, from 1214.3 ± 160.9 pA in control IgG group to 758.3 ± 97.8 pA in M4P group (Figures 2F,G). This result suggests that the current increase by acute hypoxia is mainly contributed by TRPM4 channel. Next, we measured cell volume change after acute hypoxia. As cell membrane capacitance (C_m) has been reported to have a positive linear correlation with cell volume (Sato et al., 1996), we monitored C_m changes as a surrogate of cell volume during the 7-min hypoxia treatment (Figure 2H). In control IgG group, the C_m was found to increase gradually. At 7 min, the C_m has reached 131.3% of baseline level before hypoxia induction. In M4P treated cells, no change was observed during the 7-min hypoxia treatment.

To validate the results from C_m measurement, we further captured the images of the cells before and after hypoxia

treatment, and analyzed cell area using ImageJ software. Sample images taken at 0 min and 7 min of the same cell clearly showed that acute hypoxia treatment could induce cell area increase (Figure 3A). Summary of cell area quantification demonstrated that in IgG treatment group, the cell area at 7 min was increased to $136.8 \pm 2.9\%$ of baseline (Figure 3B), similar to the result from C_m measurement. Again, neurons with M4P treatment showed no significant change in cell area after 7-min hypoxia induction (Figure 3B). This result clearly indicates that acute hypoxia is able to induce cell swelling in cortical neurons, and blocking TRPM4 current with M4P antibody could attenuate cytotoxic edema. To investigate whether M4P application could protect neurons from apoptotic cell death, we cultured the cells in a hypoxic medium and incubated them in a hypoxia/anoxia chamber containing 1% O_2 , 5% CO_2 , and 94% N_2 for 24 h. Cleaved Caspase-3, a marker of apoptosis, was detected with western blot (Figure 3C). Analysis of cleaved Caspase-3 expression revealed that M4P treatment successfully attenuated hypoxia-induced apoptosis (Figure 3D). TUNEL assay (Figures 3E,F), PI staining (Figures 3G,H) also revealed that M4P could ameliorate apoptosis after 24 h hypoxia exposure.

M4P Inhibits TRPM4 Activity in RBMVEC and Ameliorate Hypoxia-Induced Cell Swelling

The integrity of the BBB is compromised in stroke, and cerebral vascular endothelial cells are critical to sense hypoxia and respond by disrupting barrier function (Shah and Abbruscato,

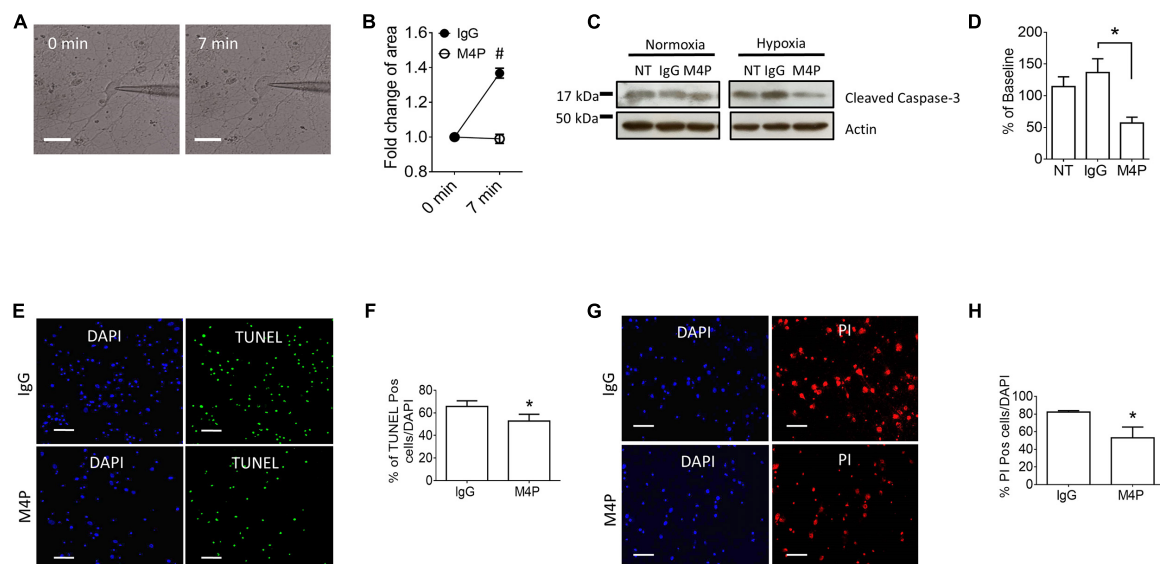


FIGURE 3 | M4P inhibits hypoxia-induced cell swelling and cell death in cortical neurons. **(A)** Representative images of a neuron taken before (0 min) and after hypoxia induction (7 min). Scale bars: 20 μm . **(B)** Summary of normalized cell body areas with IgG ($n = 9$) or M4P ($n = 8$) treatment. **(C)** Western blot of cleaved Caspase-3 in cortical neurons incubated with IgG or M4P at 10.4 $\mu\text{g}/\text{ml}$ for 24 h, NT, non-treatment. **(D)** Summary of Cleaved Caspase-3 expression (normalized to actin) under hypoxia. $n = 4$ for IgG, M4P, and NT. **(E)** TUNEL assay of cortical neurons under hypoxia condition for 24 h treated with IgG (upper panel) or M4P (lower panel). Scale bars: 50 μm . **(F)** Quantification of TUNEL positive cells (TUNEL Pos cells), $n = 4$. **(G)** PI assay of cortical neurons under hypoxia condition for 24 h treated with IgG (upper panel) or M4P (lower panel). Scale bar: 50 μm . **(H)** Quantification of PI positive cells (PI Pos cells), $n = 3$. In **(B,F,H)**, statistical analysis was performed by two tailed unpaired student's t -test; in **(D)**, by one-way ANOVA with Bonferroni's *post hoc* analysis. * $p < 0.05$ and # $p < 0.0001$.

2014). To study the role of TRPM4 in vascular endothelial cells, we cultured rat brain microvascular endothelial cells (RBMVECs). Current-voltage relationship of RBMVECs were first obtained by whole-cell patch clamp using ramp protocols applied from -100 to $+100$ mV. The potential was held at 0 mV which is different to the -70 mV for neurons. Similarly as to neurons, RBMVECs were incubated with $20.8 \mu\text{g/ml}$ IgG or M4P for 30 min before patch clamping. Under control IgG treatment, the current was gradually rising during the 7 -min hypoxia incubation (Figures 4A,C). Whereas no current increase was observed with M4P treatment (Figures 4B,C). Similar as in neurons, we did not observe an effect of M4P on vascular endothelial cells before hypoxia treatment (Figures 4D,E). We further compared the currents at 7 min after hypoxia induction, and found that the TRPM4 activity was significantly blocked by M4P application. At $+100$ mV, the current was reduced by 77% , from 254.2 ± 29.0 pA in control IgG group to 58.4 ± 11.0 pA in M4P group (Figures 4F,G). This 77% reduction is even higher than the 37.5% reduction found in neurons. At -100 mV, the current from RBMVECs was reduced by 81% , from -248.4 ± 74.0 pA in control IgG group to -46.16 ± 9.0 pA in M4P group (Figures 4F,G). This result suggests that comparing to neurons, acute hypoxia is likely to induce relatively higher current increase in vascular endothelial cells which can be inhibited by blocking TRPM4 channel. Next,

we examined whether acute hypoxia could change cell volume in RBMVECs. The membrane capacitance (C_m) was measured at different time points under hypoxic conditions (Figure 4H). In control IgG treated cells, the C_m started to increase significantly as early as 2 min after hypoxia induction. By 7 min, the C_m was increased to 132% of baseline at 0 min. In contrast, M4P treatment successfully inhibited C_m increase induced by hypoxia (Figure 4H).

We further measured cell area changes in RBMVECs before and after hypoxia treatment by image analysis. Sample images taken at 0 and 7 min of the same cell clearly showed that acute hypoxia treatment could induce cell area increase (Figure 5A). At 7 min, the cell area was increased to $134.3 \pm 3.0\%$ of baseline in control IgG group (Figure 5B), similar to the result from C_m measurement in Figure 4H. Again, M4P application significantly reduced the change of cell area under hypoxic conditions (Figure 5B). After 24 -hr incubation under OGD, western blot on cleaved Caspase-3 showed that M4P treatment could reduce hypoxia-induced apoptosis (Figures 5C,D). TUNEL assay (Figures 5E,F), PI staining (Figures 5G,H) also revealed that M4P could ameliorate hypoxia-induced apoptosis after 24 h hypoxia exposure. This result clearly indicates that acute hypoxia is able to induce cell swelling in vascular endothelial cells, and blocking TRPM4 current with M4P antibody could attenuate cytotoxic edema and apoptosis.

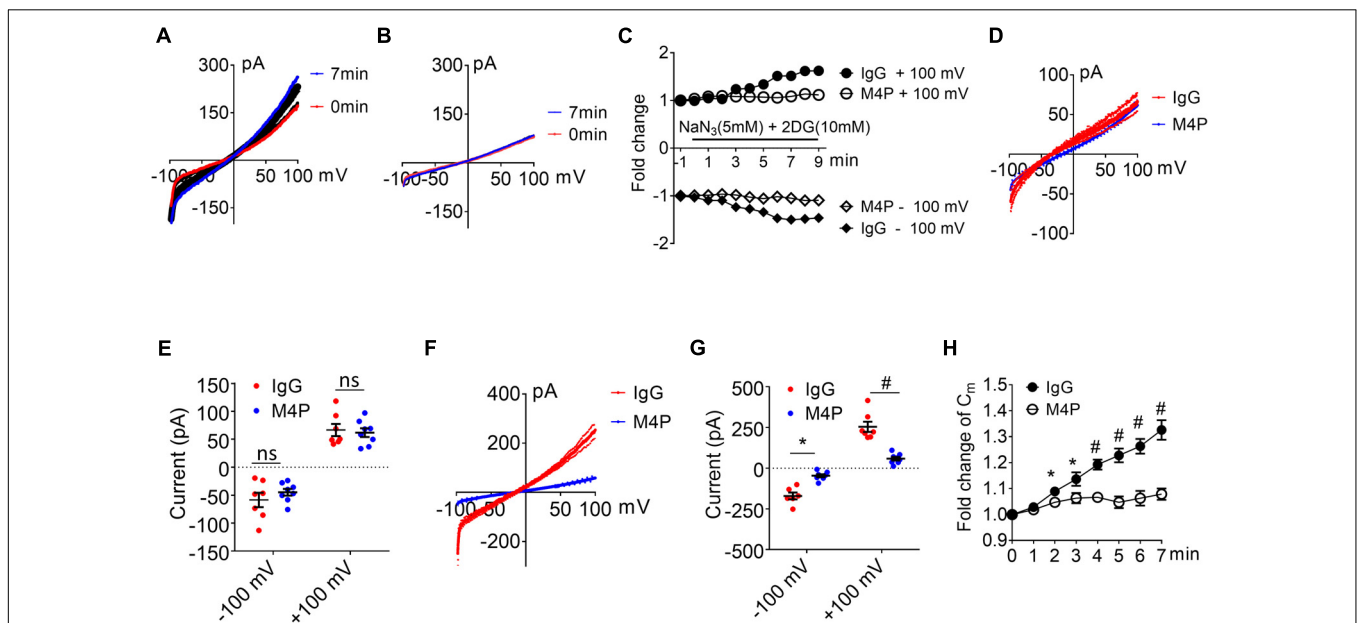
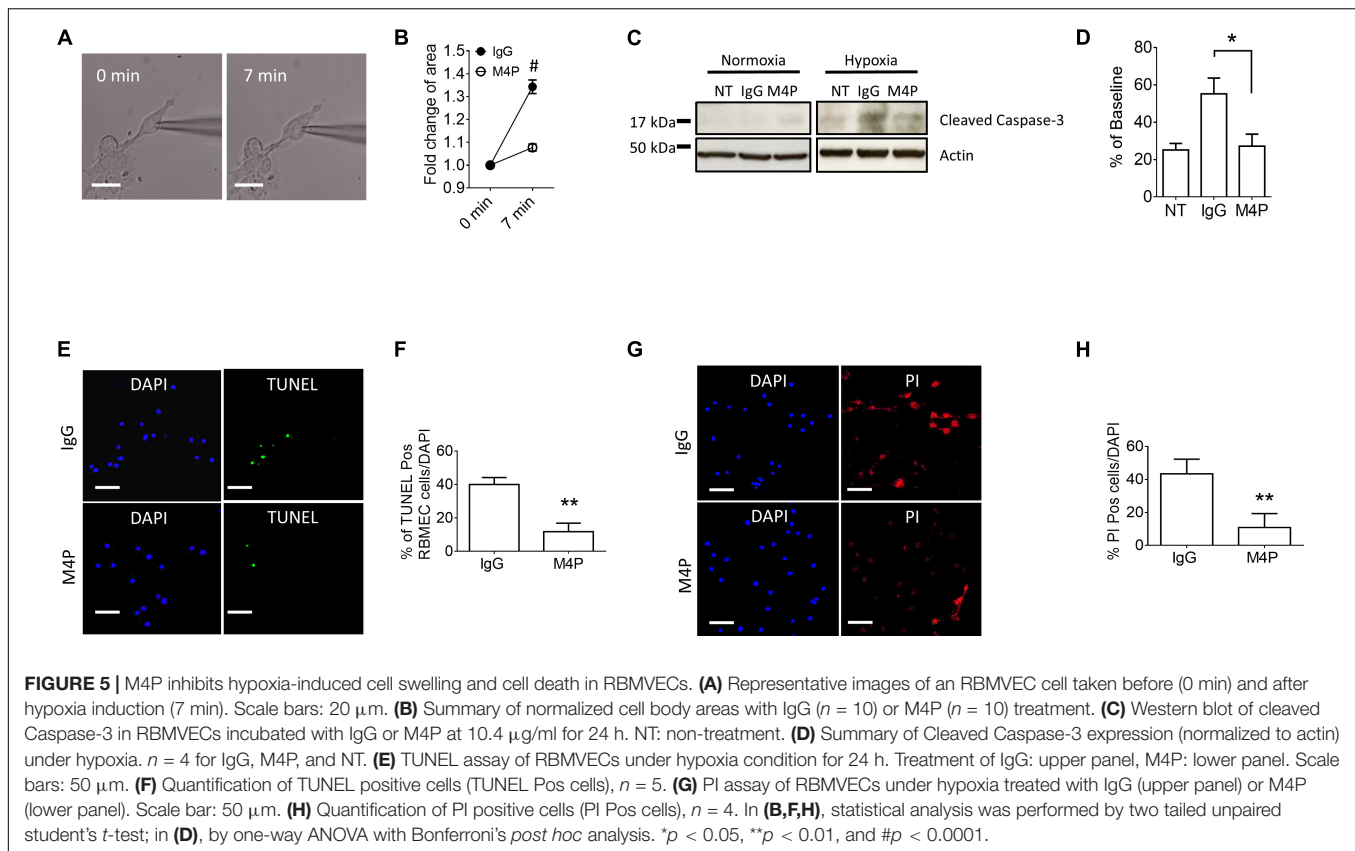


FIGURE 4 | M4P blocks TRPM4 activity in cultured rat brain microvascular endothelial cells (RBMVECs) and prevents hypoxia-induced cell swelling. (A) Sample traces from an RBMVEC cell pre-treated with control rabbit IgG ($20.8 \mu\text{g/ml}$) for 30 min. Acute hypoxia was induced by adding 5 mM NaN_3 and 10 mM 2-DG to the cell for 7 min. 250 -ms voltage ramps from -100 to $+100$ mV was applied at 1 min interval. Holding potential: 0 mV. The pipette solution contained a calculated $7.4 \mu\text{M}$ free Ca^{2+} . (B) Sample traces from an RBMVEC cell pre-treated with M4P at $20.8 \mu\text{g/ml}$ for 30 min. The recording protocol is similar to that described in (A). (C) Time-dependent current changes at ± 100 mV from (A,B). All currents were normalized to baseline before hypoxic induction. (D) Summarized current-voltage relationship at 0 min under hypoxia for control IgG ($n = 7$) and M4P ($n = 8$) treatments. (E) Summary of currents at -100 and 100 mV at 0 min under hypoxia. Control IgG: $n = 7$; M4P: $n = 8$. (F) Summarized current-voltage relationship at 7 min under hypoxia for control IgG ($n = 7$) and M4P ($n = 8$) treatments. (G) Summary of currents at -100 and 100 mV at 7 min under hypoxia. Control IgG: $n = 7$; M4P: $n = 8$. (H) Time course of normalized membrane capacitance (C_m) under hypoxic conditions. Control IgG: $n = 7$; M4P: $n = 8$. Statistical analysis was performed by two tailed unpaired student's t -test for (E,G), and two-way ANOVA test with *post hoc* Bonferroni's analysis for (H). * $p < 0.05$, # $p < 0.0001$, ns, non-significant.



M4P Doesn't Affect Astrocytes During Acute Hypoxia

To examine the effect of blocking TRPM4 in astrocytes, we first measured the current-voltage relationship in primary cultured astrocytes under 7-min hypoxic conditions (**Figures 6A–C**). The cells were pre-incubated with control IgG and M4P for 30 min, and the 250-ms voltage ramps were applied at 1 min interval. Acute hypoxia induction did not elicit current change in both IgG and M4P treated astrocytes. We did not observe an effect of M4P on astrocytes before hypoxia treatment (**Figures 6D,E**). Comparing the currents after 7 min hypoxia incubation, there was no difference between IgG and M4P treated cells (**Figures 6F,G**), $p = 0.07$ and $p = 0.24$ for -100 mV and $+100$ mV, respectively. Time course of normalized membrane capacitance (C_m) did not show difference between IgG ($n = 7$) or M4P ($n = 7$) groups (**Figure 6H**). Likewise, images taken before and after hypoxia induction revealed no changes in terms of cell areas (**Figures 6I,J**).

Next, we examined whether the lack of response to hypoxia is because the expression level of TRPM4 is low in astrocytes. We overexpressed mouse TRPM4 in astrocytes and treated with IgG and M4P under hypoxic condition. The results from TRPM4 overexpressed astrocytes showed that TRPM4 current was increased under hypoxia with IgG treatment (**Figure 7A**). In contrast, M4P treatment successfully inhibited TRPM4 currents (**Figure 7B**). M4P reduced TRPM4 current significantly at -100 mV before hypoxia induction (-405.90 ± 19.37 pA for

IgG treatment, -236.78 ± 21.05 pA for M4P treatment) (**Figures 7C,D**). The effect of TRPM4 inhibition was more remarkable at 7 min after hypoxia treatment (at -100 mV, -787.84 ± 98.32 pA for IgG treatment, and -264.45 ± 33.10 pA for M4P treatment; at 100 mV, 648.46 ± 117.41 pA for IgG treatment, 176.81 ± 32.37 pA for M4P treatment) (**Figures 7E,F**). Importantly, in TRPM4 overexpression astrocytes, acute hypoxia successfully induced cell swelling in IgG group, and M4P treatment again inhibited cell volume increase (**Figure 7G**).

M4P Does Not Affect TRPM2 and TRPM7 Channels

We have shown previously that M4P does not interact with TRPM5, a close member of TRPM4 (Chen et al., 2019a). Here, we further examined the effect of M4P on TRPM2 and TRPM7 which have been reported to play a role in hypoxia (Aarts et al., 2003; Toda et al., 2019; Hong et al., 2020). In TRPM2 overexpressed HEK 293 cells, no difference was identified for TRPM2 currents activated by $100 \mu\text{M}$ $[\text{Ca}^{2+}]_i$ between IgG and M4P treatments (**Figures 8A,B**). This result suggests that M4P doesn't affect TRPM2 channel. In TRPM7 overexpressed HEK 293 cells, to amplified TRPM7 channel current, divalent-free bath solution was used with the removal of both Ca^{2+} and Mg^{2+} . No difference was identified for TRPM7 currents between IgG and M4P treatments (**Figures 8C,D**), suggesting that M4P doesn't interact with TRPM7 channel.

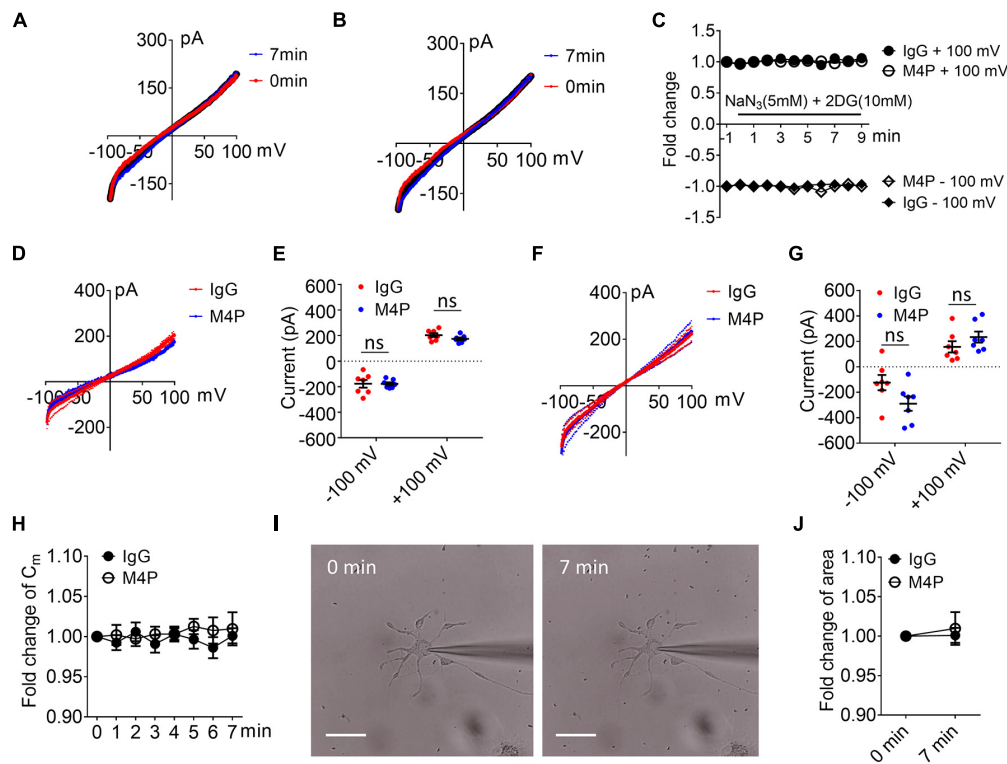


FIGURE 6 | Effect of M4P on cultured rat astrocytes. **(A)** Sample traces from an astrocyte pre-treated with control rabbit IgG (20.8 $\mu\text{g/ml}$) for 30 min. Acute hypoxia was induced by adding 5 mM NaN_3 and 10 mM 2-DG to the cell for 7 min. 250-ms voltage ramps from -100 to +100 mV was applied at 1 min interval. Holding potential: 0 mV. The pipette solution contained a calculated 7.4 μM free Ca^{2+} . **(B)** Sample traces from an astrocyte pre-treated with M4P at 20.8 $\mu\text{g/ml}$ for 30 min. The recording protocol is similar to that described in **(A)**. **(C)** Time-dependent current changes at ± 100 mV from **(A,B)**. All currents were normalized to baseline before hypoxic induction. **(D)** Summarized current-voltage relationship at 0 min under hypoxia for control IgG ($n = 7$) and M4P ($n = 7$) treatments. **(E)** Summary of currents at -100 and 100 mV at 0 min under hypoxia. Control IgG: $n = 7$; M4P: $n = 7$. **(F)** Summarized current-voltage relationship at 7 min under hypoxia for control IgG ($n = 7$) and M4P ($n = 7$) treatments. **(G)** Summary of currents at -100 and 100 mV at 7 min under hypoxia. Control IgG: $n = 7$; M4P: $n = 7$. **(H)** Time course of normalized membrane capacitance (C_m) under hypoxic conditions. Control IgG: $n = 7$; M4P: $n = 7$. **(I)** Representative images of an astrocyte taken before (0 min) and after hypoxia induction 7 min. Scale bars: 20 μm . **(J)** Summary of normalized cell body areas with IgG ($n = 7$) or M4P ($n = 7$) treatment. In **(E,G,J)**, statistical analysis was performed by two tailed unpaired student's *t*-test, in **(H)**, by two-way ANOVA test with *post hoc* Bonferroni's analysis. No significant difference was observed in all tests, ns, non-significant.

DISCUSSION

It is known that cerebral edema evolves in stages, and each stage is characterized by distinct morphological and molecular changes. Cytotoxic edema, or cellular swelling, appears within minutes after acute central nervous system injuries such as stroke (Stokum et al., 2016). Therefore, targeting cellular swelling within the hyperacute stage following disease onset has a great therapeutic potential. In this study, we found that cultured neurons and vascular endothelial cells exhibited cell swelling immediately after hypoxic induction. On the contrary, acute hypoxia failed to induce cell swelling in astrocytes, suggesting that the pathophysiological process varies among different cells in the brain after hypoxia. This finding corroborates earlier reports showing that comparing to neurons, astrocytes are more resistant to OGD (Almeida et al., 2002; Panickar and Norenberg, 2005).

To unravel the underlying mechanism of cell swelling, we first examined the expression of TRPM4 channel in a rat model of stroke. It has been reported that under ischemic/hypoxic

conditions, influx of monovalent cations via TRPM4 causes cell swelling and necrotic cell death (Simard et al., 2006, 2012; Gerzanich et al., 2009). Within the area surrounding the infarct core, TRPM4 expression demonstrated a differential profile depending on cell types. Both neurons and vascular endothelial cells were positively stained by M4P, whereas astrocytes showed negative staining. This result is in line with our earlier reports showing that TRPM4 is upregulated in neurons and vascular endothelial cells following stroke induction (Loh et al., 2014; Chen et al., 2019a,b). It should be noted that in these reports, TRPM4 level is very low in healthy tissues, and its upregulation occurs at least 2–6 h after stroke induction (Loh et al., 2014; Chen et al., 2019b). So, it is critical to understand whether TRPM4, at its baseline level, could affect cell functions immediately after hypoxic induction, particularly on cell volume changes.

In cultured neurons and vascular endothelial cells, acute hypoxia enhances membrane permeability which can be inhibited by TRPM4 blocking antibody M4P, suggesting that TRPM4 activation is a major cause of ionic influx at this stage. The

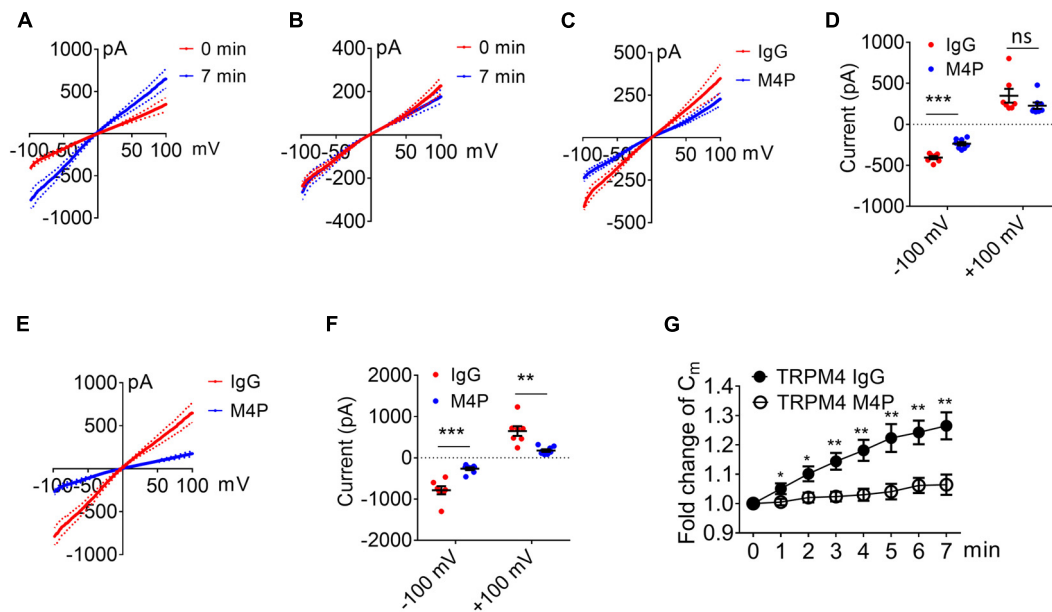


FIGURE 7 | TRPM4 overexpression induces oncotic current under hypoxia in cultured rat astrocytes. **(A)** Summarized current-voltage relationship of TRPM4 overexpressed astrocytes ($n = 7$) at 0 min and 7 min under hypoxia. These cells were pre-treated with control rabbit IgG (20.8 $\mu\text{g/ml}$) for 30 min. Acute hypoxia was induced by adding 5 mM NaN_3 and 10 mM 2-DG to the cell for 7 min. 250-ms voltage ramps from -100 to +100 mV was applied at 1 min interval. Holding potential: 0 mV. The pipette solution contained a calculated 7.4 μM free Ca^{2+} . **(B)** Summarized current-voltage relationship at 0 min and 7 min under hypoxia for TRPM4 overexpressed astrocytes ($n = 7$) pre-treated with M4P (20.8 $\mu\text{g/ml}$) for 30 min. **(C)** Summarized current-voltage relationship at 0 min under hypoxia for control IgG ($n = 7$) and M4P ($n = 7$) treatments. **(D)** Summary of currents at -100 and 100 mV at 0 min under hypoxia. Control IgG: $n = 7$; M4P: $n = 7$. **(E)** Summarized current-voltage relationship at 7 min under hypoxia for control IgG ($n = 7$) and M4P ($n = 7$) treatments. **(F)** Summary of currents at -100 and 100 mV at 7 min under hypoxia. Control IgG: $n = 7$; M4P: $n = 7$. **(G)** Time course of normalized membrane capacitance (C_m) under hypoxic conditions. Control IgG: $n = 7$; M4P: $n = 7$. In **(D,F)**, statistical analysis was performed by two tailed unpaired student's t -test, in **(G)**, by two-way ANOVA test with *post hoc* Bonferroni's analysis. * $p < 0.05$, ** $p < 0.01$, *** $p < 0.001$, ns, non-significant.

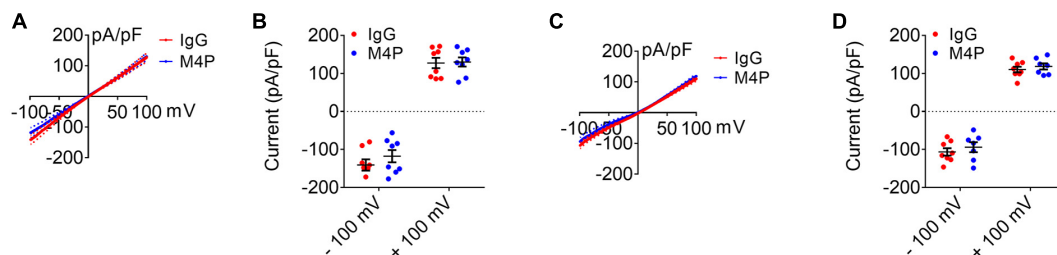


FIGURE 8 | Effect of M4P on TRPM2 and TRPM7 overexpressed HEK 293 cells. **(A)** Summarized current-voltage relationship for TRPM2 overexpressed HEK 293 cells pre-treated with control rabbit IgG (20.8 $\mu\text{g/ml}$) ($n = 8$) or M4P (20.8 $\mu\text{g/ml}$) ($n = 8$) for 30 min. 250-ms voltage ramps from -100 to +100 mV was applied. Holding potential: 0 mV. The pipette solution contained a calculated 100 μM free Ca^{2+} . **(B)** Summary of current density for TRPM2 overexpressed HEK 293 cells at -100 and 100 mV. Control IgG: $n = 8$; M4P: $n = 8$. **(C)** Summarized current-voltage relationship for TRPM7 overexpressed HEK 293 cells pre-treated with control rabbit IgG (20.8 $\mu\text{g/ml}$) ($n = 8$) or M4P (20.8 $\mu\text{g/ml}$) ($n = 7$) for 30 min. 250-ms voltage ramps from -100 to +100 mV was applied. Holding potential: 0 mV. Divalent-free bath solution was used. **(D)** Summary of current density for TRPM7 overexpressed HEK 293 cells at -100 and 100 mV. Control IgG: $n = 8$; M4P: $n = 7$. In **(B,D)**, statistical analysis was performed by two tailed unpaired student's t -test, no significant difference was observed between IgG and M4P treatment in all tests.

corresponding sodium influx via TRPM4 will cause an osmotic imbalance, leading to water entry and subsequent cell swelling or cytotoxic edema (Loh et al., 2019). As expected, we observed a significant increase of cell volume as early as 2 min after hypoxia induction in control IgG treated cells. Given that the cell swelling was almost completely abrogated by M4P treatment, we believe that TRPM4 is a major and important contributor to oncotic current in neurons and vascular endothelial cells immediately after hypoxia

occurs. As the protein level of TRPM4 only increases several hrs after hypoxia (Loh et al., 2014; Chen et al., 2019b), the enhanced channel activity is most likely caused by the intracellular hypoxic changes which are characterized by a decrease of ATP level and an increase of Ca^{2+} (Vennekens and Nilius, 2007). Our results from neurons prove that M4P only suppresses current increase following hypoxia induction, but has no effect on the baseline currents under normoxia condition. A similar result

was observed in vascular endothelial cells. Therefore, blocking TRPM4 can yield a protective role immediately after hypoxia attack, even before the upregulation of TRPM4 protein.

In contrast to neuron and vascular endothelial cell, acute hypoxia induction had no effect on current flow and cell volume in astrocytes, indicating that astrocytes are more resistant to hypoxia. Furthermore, neither M4P nor control IgG treatment could affect currents, suggesting that TRPM4 channel does not play a role in astrocyte during acute hypoxia. Importantly, when TRPM4 was transfected into astrocytes, acute hypoxia successfully induced cell swelling which could be inhibited by M4P treatment. These data suggest that with the absence of TRPM4, astrocytes are more resistance to acute hypoxia-induced oncosis. Our results do not contradict with a previous study showing that TRPM4 contribute to cell swelling in astrocytes (Stokum et al., 2018). In that study, astrocytes were activated overnight with TNF α , IFN γ , and LPS, a strong stimulus to initiate gliosis. TRPM4 expression is thereby upregulated and likely to cause oncosis. Whereas in our study, astrocytes were recorded without pre-stimulation. Thus, one can hypothesize that immediately after hypoxia, the baseline level of TRPM4 in astrocytes is too low to yield any impact on cell volume change, if there is any.

In healthy brain, large molecules such as antibody are unable to cross BBB. However, under pathological conditions such as stroke and head injury, impaired BBB could no longer serve as an effective barrier to therapeutic antibodies (Yu et al., 2013). In head injury, BBB is disrupted immediately, and therapeutic antibodies can easily enter the brain almost immediately. Whereas in stroke, BBB integrity is relatively intact right after occlusion. Hence, M4P application during this stage could mainly act on vascular endothelial cells and prevent acute oncotic cell death. This is of clinical importance as preserved BBB will attenuate vasogenic edema and improve the efficacy of reperfusion therapy by ameliorating associated side effects. Recently, we have observed this protective effect of M4P in a rat stroke model (Chen et al., 2019a). When BBB becomes leaky at later point of time, M4P can easily enter the brain and bind to neurons. Therefore, blocking TRPM4 for a long time could still yield a beneficial effect as manifested by our results showing a reduction of apoptosis in both neurons and vascular endothelial cells.

REFERENCES

- Aarts, M., Iihara, K., Wei, W. L., Xiong, Z. G., Arundine, M., Cerwinski, W., et al. (2003). A key role for TRPM7 channels in anoxic neuronal death. *Cell* 115, 863–877. doi: 10.1016/s0092-8674(03)01017-1
- Almeida, A., Delgado-Esteban, M., Bolanos, J. P., and Medina, J. M. (2002). Oxygen and glucose deprivation induces mitochondrial dysfunction and oxidative stress in neurones but not in astrocytes in primary culture. *J. Neurochem.* 81, 207–217. doi: 10.1046/j.1471-4159.2002.00827.x
- Berrouschot, J., Sterker, M., Bettin, S., Koster, J., and Schneider, D. (1998). Mortality of space-occupying ('malignant') middle cerebral artery infarction under conservative intensive care. *Intensive Care Med.* 24, 620–623. doi: 10.1007/s001340050625
- Charriaut-Marlangue, C., Margail, I., Represa, A., Popovici, T., Plotkine, M., and Ben-Ari, Y. (1996). Apoptosis and necrosis after reversible focal ischemia: an

CONCLUSION

In conclusion, our data have uncovered a previously unknown function of TRPM4 on cell swelling during acute ischemia/hypoxia. During the hyperacute stage of stroke or other acute brain injuries, neurons and vascular endothelial cells, rather than astrocytes, are more likely to develop cell swelling or cytotoxic edema. TRPM4 plays a key role during such process, and blocking TRPM4 is a good therapeutic approach to prevent oncosis.

DATA AVAILABILITY STATEMENT

The raw data supporting the conclusion of this article will be made available by the authors, without undue reservation.

ETHICS STATEMENT

This study was approved and conducted in accordance with the guidelines of the Institutional Animal Care and Use Committee of the National Neuroscience Institute, Singapore.

AUTHOR CONTRIBUTIONS

PL and BN conceived and directed the project. SW and PL conceived, analyzed the data, and wrote the manuscript. SW, BC, YG, SL, and CP performed the experiments and analyzed the data. All authors contributed to the article and approved the submitted version.

FUNDING

This work was supported by grants NMRC/OFIRG/0070/2018 and NMRC/CIRG/1425/2015 from the Singapore Ministry of Health's National Medical Research Council.

in situ DNA fragmentation analysis. *J. Cereb. Blood Flow Metab.* 16, 186–194. doi: 10.1097/00004647-199603000-00002

- Chen, B., Gao, Y., Wei, S., Low, S. W., Ng, G., Yu, D., et al. (2019a). TRPM4-specific blocking antibody attenuates reperfusion injury in a rat model of stroke. *Pflugers Arch.* 471, 1455–1466. doi: 10.1007/s00424-019-02326-8
- Chen, B., Ng, G., Gao, Y., Low, S. W., Sandanaraj, E., Ramasamy, B., et al. (2019b). Non-invasive multimodality imaging directly shows TRPM4 inhibition ameliorates stroke reperfusion injury. *Transl. Stroke Res.* 10, 91–103. doi: 10.1007/s12975-018-0621-3
- Du, J., Xie, J., and Yue, L. (2009). Intracellular calcium activates TRPM2 and its alternative spliced isoforms. *Proc. Natl. Acad. Sci. U.S.A.* 106, 7239–7244. doi: 10.1073/pnas.0811725106
- Gerzanich, V., Woo, S. K., Vennekens, R., Tsybalyuk, O., Ivanova, S., Ivanov, A., et al. (2009). De novo expression of Trpm4 initiates secondary hemorrhage in spinal cord injury. *Nat. Med.* 15, 185–191. doi: 10.1038/nm.1899

- Hacke, W., Schwab, S., Horn, M., Spranger, M., De Georgia, M., and von Kummer, R. (1996). 'Malignant' middle cerebral artery territory infarction: clinical course and prognostic signs. *Arch. Neurol.* 53, 309–315. doi: 10.1001/archneur.1996.00550040037012
- Hong, D. K., Kho, A. R., Lee, S. H., Jeong, J. H., Kang, B. S., Kang, D. H., et al. (2020). Transient receptor potential melastatin 2 (TRPM2) inhibition by antioxidant, N-acetyl-L-cysteine, reduces global cerebral ischemia-induced neuronal death. *Int. J. Mol. Sci.* 21:6026. doi: 10.3390/ijms21176026
- Hu, H. J., and Song, M. (2017). Disrupted ionic homeostasis in ischemic stroke and new therapeutic targets. *J. Stroke Cerebrovasc. Dis.* 26, 2706–2719. doi: 10.1016/j.jstrokecerebrovasdis.2017.09.011
- Inoue, K., Branigan, D., and Xiong, Z. G. (2010). Zinc-induced neurotoxicity mediated by transient receptor potential melastatin 7 channels. *J. Biol. Chem.* 285, 7430–7439. doi: 10.1074/jbc.M109.040485
- Inoue, K., Xiong, Z. G., and Ueki, T. (2020). The TRPM7 channel in the nervous and cardiovascular systems. *Curr. Protein Pept. Sci.* doi: 10.2174/1389203721666200605170938 [Epub ahead of print].
- Jiang, J., Li, M., and Yue, L. (2005). Potentiation of TRPM7 inward currents by protons. *J. Gen. Physiol.* 126, 137–150. doi: 10.1085/jgp.200409185
- Kurland, D. B., Tosun, C., Pampori, A., Karimy, J. K., Caffes, N. M., Gerzanich, V., et al. (2013). Glibenclamide for the treatment of acute CNS injury. *Pharmaceuticals* 6, 1287–1303. doi: 10.3390/ph6101287
- Lipton, P. (1999). Ischemic cell death in brain neurons. *Physiol. Rev.* 79, 1431–1568. doi: 10.1152/physrev.1999.79.4.1431
- Loh, K. P., Ng, G., Yu, C. Y., Fhu, C. K., Yu, D., Vennekens, R., et al. (2014). TRPM4 inhibition promotes angiogenesis after ischemic stroke. *Pflugers Arch.* 466, 563–576. doi: 10.1007/s00424-013-1347-4
- Loh, K. Y., Wang, Z., and Liao, P. (2019). Oncotic cell death in stroke. *Rev. Physiol. Biochem. Pharmacol.* 176, 37–64. doi: 10.1007/112_2018_13
- Majno, G., and Joris, I. (1995). Apoptosis, oncosis, and necrosis. An overview of cell death. *Am. J. Pathol.* 146, 3–15.
- Martin, L. J., Al-Abdulla, N. A., Brambrink, A. M., Kirsch, J. R., Sieber, F. E., and Portera-Cailliau, C. (1998). Neurodegeneration in excitotoxicity, global cerebral ischemia, and target deprivation: a perspective on the contributions of apoptosis and necrosis. *Brain Res. Bull.* 46, 281–309. doi: 10.1016/s0361-9230(98)00024-0
- Numata, T., Shimizu, T., and Okada, Y. (2007). TRPM7 is a stretch- and swelling-activated cation channel involved in volume regulation in human epithelial cells. *Am. J. Physiol. Cell Physiol.* 292, C460–C467. doi: 10.1152/ajpcell.00367.2006
- Panickar, K. S., and Norenberg, M. D. (2005). Astrocytes in cerebral ischemic injury: morphological and general considerations. *Glia* 50, 287–298. doi: 10.1002/glia.20181
- Rosenberg, G. A. (1999). Ischemic brain edema. *Prog. Cardiovasc. Dis.* 42, 209–216.
- Sala-Rabanal, M., Wang, S., and Nichols, C. G. (2012). On potential interactions between non-selective cation channel TRPM4 and sulfonylurea receptor SUR1. *J. Biol. Chem.* 287, 8746–8756. doi: 10.1074/jbc.M111.336131
- Satoh, H., Delbridge, L. M., Blatter, L. A., and Bers, D. M. (1996). Surface:volume relationship in cardiac myocytes studied with confocal microscopy and membrane capacitance measurements: species-dependence and developmental effects. *Biophys. J.* 70, 1494–1504. doi: 10.1016/s0006-3495(96)79711-4
- Schattling, B., Steinbach, K., Thies, E., Kruse, M., Menigoz, A., Ufer, F., et al. (2012). TRPM4 cation channel mediates axonal and neuronal degeneration in experimental autoimmune encephalomyelitis and multiple sclerosis. *Nat. Med.* 18, 1805–1811. doi: 10.1038/nm.3015
- Shah, K., and Abbruscato, T. (2014). The role of blood-brain barrier transporters in pathophysiology and pharmacotherapy of stroke. *Curr. Pharm. Des.* 20, 1510–1522. doi: 10.2174/13816128113199990465
- Simard, J. M., Chen, M., Tarasov, K. V., Bhatta, S., Ivanova, S., Melnitchenko, L., et al. (2006). Newly expressed SUR1-regulated NC(Ca-ATP) channel mediates cerebral edema after ischemic stroke. *Nat. Med.* 12, 433–440. doi: 10.1038/nm1390
- Simard, J. M., Kahle, K. T., and Gerzanich, V. (2010). Molecular mechanisms of microvascular failure in central nervous system injury—synergistic roles of NKCC1 and SUR1/TRPM4. *J. Neurosurg.* 113, 622–629. doi: 10.3171/2009.11.JNS081052
- Simard, J. M., Woo, S. K., and Gerzanich, V. (2012). Transient receptor potential melastatin 4 and cell death. *Pflugers Arch.* 464, 573–582. doi: 10.1007/s00424-012-1166-z
- Stokum, J. A., Gerzanich, V., and Simard, J. M. (2016). Molecular pathophysiology of cerebral edema. *J. Cereb. Blood Flow Metab.* 36, 513–538. doi: 10.1177/0271678X15617172
- Stokum, J. A., Kwon, M. S., Woo, S. K., Tsybalyuk, O., Vennekens, R., Gerzanich, V., et al. (2018). SUR1-TRPM4 and AQP4 form a heteromultimeric complex that amplifies ion/water osmotic coupling and drives astrocyte swelling. *Glia* 66, 108–125. doi: 10.1002/glia.23231
- Toda, T., Yamamoto, S., Umehara, N., Mori, Y., Wakamori, M., and Shimizu, S. (2019). Protective effects of duloxetine against cerebral ischemia-reperfusion injury via transient receptor potential melastatin 2 inhibition. *J. Pharmacol. Exp. Ther.* 368, 246–254. doi: 10.1124/jpet.118.253922
- Vennekens, R., and Nilius, B. (2007). Insights into TRPM4 function, regulation and physiological role. *Handb. Exp. Pharmacol.* 179, 269–285. doi: 10.1007/978-3-540-34891-7_16
- Virani, S. S., Alonso, A., Benjamin, E. J., Bittencourt, M. S., Callaway, C. W., Carson, A. P., et al. (2020). Heart disease and stroke statistics-2020 update: a report from the American heart association. *Circulation* 141, e139–e596. doi: 10.1161/CIR.0000000000000757
- Walcott, B. P., Kahle, K. T., and Simard, J. M. (2012). Novel treatment targets for cerebral edema. *Neurotherapeutics* 9, 65–72. doi: 10.1007/s13311-011-0087-4
- Weerasinghe, P., and Buja, L. M. (2012). Oncosis: an important non-apoptotic mode of cell death. *Exp. Mol. Pathol.* 93, 302–308. doi: 10.1016/j.yexmp.2012.09.018
- Woo, S. K., Kwon, M. S., Ivanov, A., Gerzanich, V., and Simard, J. M. (2013). The sulfonylurea receptor 1 (Sur1)-transient receptor potential melastatin 4 (Trpm4) channel. *J. Biol. Chem.* 288, 3655–3667. doi: 10.1074/jbc.M112.428219
- Wu, Q. J., and Tymianski, M. (2018). Targeting NMDA receptors in stroke: new hope in neuroprotection. *Mol. Brain* 11:15.
- Yu, C. Y., Ng, G., and Liao, P. (2013). Therapeutic antibodies in stroke. *Transl. Stroke Res.* 4, 477–483. doi: 10.1007/s12975-013-0281-2
- Zhang, E., and Liao, P. (2015). Brain transient receptor potential channels and stroke. *J. Neurosci. Res.* 93, 1165–1183. doi: 10.1002/jnr.23529

Conflict of Interest: The authors declare that the research was conducted in the absence of any commercial or financial relationships that could be construed as a potential conflict of interest.

Copyright © 2020 Wei, Low, Poore, Chen, Gao, Nilius and Liao. This is an open-access article distributed under the terms of the Creative Commons Attribution License (CC BY). The use, distribution or reproduction in other forums is permitted, provided the original author(s) and the copyright owner(s) are credited and that the original publication in this journal is cited, in accordance with accepted academic practice. No use, distribution or reproduction is permitted which does not comply with these terms.



Ion Transport in Plant Cell Shrinkage During Death

François Bouteau^{1*}, David Rebutier², Daniel Tran³ and Patrick Laurenti¹

¹ Université de Paris, Laboratoire Interdisciplinaire des Energies de Demain, Paris, France, ² UMR 6290-IGDR Expression Génétique et Développement Faculté de Médecine, Rennes, France, ³ Agroscope, Institute for Plant Production Systems, Conthey, Switzerland

Keywords: plant, cell death, ion channel, shrinkage, stress

INTRODUCTION

Cell death (CD) is a fundamental biological process that is indispensable in all living organisms (Ameisen, 2002). Phloem differentiation, root cap, aerenchyma formation, and leaf senescence are examples of developmental CD in plants. CD also occurs in response to pathogen attacks, and to abiotic stresses such as salinity, drought or pollutants. Studies of past decades characterized CD in plant, as a surprisingly complex phenomenon with various forms and multiple pathways to achieve CD. Number of molecular actors and involved-processes such as reactive oxygen species (ROS), caspases, autophagic activities, mitochondrial dysfunction with release of cytochrome c and other apoptogenic proteins, DNA laddering, etc., have been highlighted (Reape et al., 2008; van Doorn et al., 2011). van Doorn et al. (2011) proposed a classification of plant cell deaths based on morphological characteristics. They distinguished two main classes of CD: vacuolar cell death and necrosis. During vacuolar cell death, the cell contents are removed by autophagy-like process and release of hydrolases from collapsed lytic vacuoles. Necrosis is characterized by early rupture of the plasma membrane, shrinkage of the protoplast and absence of vacuolar cell death features. They recommended abandoning terms “apoptotic-like,” because the features often cited are also found in other types of CD, whereas cytological characteristics such as formation of apoptotic bodies and phagocytosis are absent in plants. One can notice however that the absence of these morphological characteristics is obviously due to the presence of a rigid cell wall in plants. On the contrary, the team of McCabe defends the idea of an apoptotic-like CD in plants. Based on features shared with animal apoptosis, this CD shows protoplast shrinkage with a central regulatory role for the mitochondria and cell degradation mediated by proteases (Reape and McCabe, 2010). This proposition has recently been reinforced with data showing that the vacuole may carry out functions that are analogous to animal phagocytosis to remove unwanted plant cells (Dickman et al., 2017). In plant CD, the presence of the cell wall prevents cell swelling. Cell shrinkage is an event recorded in most cases, being thus one of the main hallmarks of plant CD (Reape and McCabe, 2010; van Doorn et al., 2011). Accordingly, one of the most frequent technics used to quantify plant CD is the recording of electrolyte leakage. These leakages are supposed to be due to the rupture of the plasma membrane during necrotic cell death (van Doorn et al., 2011) or by the insertion in plasma membrane of toxins with pore forming properties (Klusener and Weiler, 1999). While in animal cells the successful execution of various forms of CD relies on early activation of distinct ion channels (Okada and Maeno, 2001; Bortner and Cidlowski, 2007), the role of ion channels during plant CD remains poorly documented although there is mounting evidence that electrolyte leakages from plant cells could be mediated by plasma membrane ion channels in responses to various CD-inducing stresses.

OPEN ACCESS

Edited by:

Markus Ritter,
Paracelsus Medical University, Austria

Reviewed by:

Hubert Hannes Kerschbaum,
University of Salzburg, Austria
Igor Pottosin,
University of Colima, Mexico

*Correspondence:

François Bouteau
francois.bouteau@u-paris.fr

Specialty section:

This article was submitted to
Cell Death and Survival,
a section of the journal
Frontiers in Cell and Developmental
Biology

Received: 28 May 2020

Accepted: 08 September 2020

Published: 19 October 2020

Citation:

Bouteau F, Rebutier D, Tran D and
Laurenti P (2020) Ion Transport in
Plant Cell Shrinkage During Death.
Front. Cell Dev. Biol. 8:566606.
doi: 10.3389/fcell.2020.566606

ION CHANNEL REGULATIONS IN PLANT CD

An increase in K^+ outward rectifying conductances (KORC) was recorded in response to various CD-inducing microbe-derived molecules, such as harpins (El-Maarouf et al., 2001; Haapalainen et al., 2012), deoxinivalenol (DON) (Yekkour et al., 2015) or CD-inducing ROS stress (Demidchik et al., 2010, 2014), like ozone (Tran et al., 2013a). Conductances with different activation kinetics and selectivity (Demidchik et al., 2014) are likely triggered by GORK or SKOR channels (Tran et al., 2013a; Demidchik et al., 2014), but could also be provoked by annexins, cyclic nucleotide-gated channels and ionotropic glutamate receptors. Nonetheless, the use of K^+ channel blockers decreases KORC, CD-extent (Haapalainen et al., 2012), cell shrinkage (Yekkour et al., 2015) or even activation of metacaspases (Tran et al., 2013a), proteases and endonucleases (Demidchik et al., 2014, 2018). Recently, gork1-1 mutants lacking K^+ efflux channel were also shown to have fewer autophagosomes compared to the wild-type plant upon ROS-induced CD (Demidchik, 2018). Activation of K^+ efflux through KORC is supposed to result in dramatic K^+ loss from plant cells and promotes CD (Demidchik et al., 2018) and K^+ loss was effectively shown to be involved in tobacco cell death induced by palmitoleic acid and ceramide (Peters and Chin, 2007). Interestingly, *Nicotiana benthamiana* plants undergoing oxidative stress and transiently expressing CED-9, an anti-apoptotic gene from the bcl-2 family (Craig, 1995), are capable of preventing K^+ efflux and maintaining intracellular K^+ homeostasis (Shabala et al., 2007).

In response to ozone or DON, plant cells rapidly activate anion currents, followed by a delayed activation of KORC (Tran et al., 2013a; Yekkour et al., 2015), the whole ion efflux being thus transiently not electroneutral. Such increases in anion currents were also recorded with other CD-inducing microbe-derived molecules, such as harpins (Reboutier et al., 2007), fusaric acid (Bouizgarne et al., 2006), oxalic acid (Errakhi et al., 2008), cryptogein (Gauthier et al., 2007), or with ozone (Kadono et al., 2010), drought (Dauphin et al., 2001) or hydroxyl radicals (Pottosin et al., 2018). The anion currents recorded present the features of slow anion channels encoded by the slac family (Hedrich, 2012), although the instantaneous current could be carried out, to some extent, by fast activating anion channels from ALMT family (Hedrich, 2012). Either way, inhibition of anion currents with anion channel blockers reduced CD-extent (Errakhi et al., 2008; Kadono et al., 2010; Yekkour et al., 2015), vacuolar collapse and cell shrinkage (Gauthier et al., 2007; Yekkour et al., 2015). It also prevented mitochondrial dysfunction (Errakhi et al., 2008; Kadono et al., 2010), caspase-like activities (Tran et al., 2013b) and the accumulation of transcripts encoding vacuolar processing enzymes (Gauthier et al., 2007; Kadono et al., 2010), that belongs to a family of proteases displaying a caspase 1-like activity.

In plant the vacuolar collapse seems a key step in cell shrinkage but to our knowledge the role of vacuolar conductances is poorly documented. Therefore, further studies are needed to decipher the role of vacuolar channels in this process.

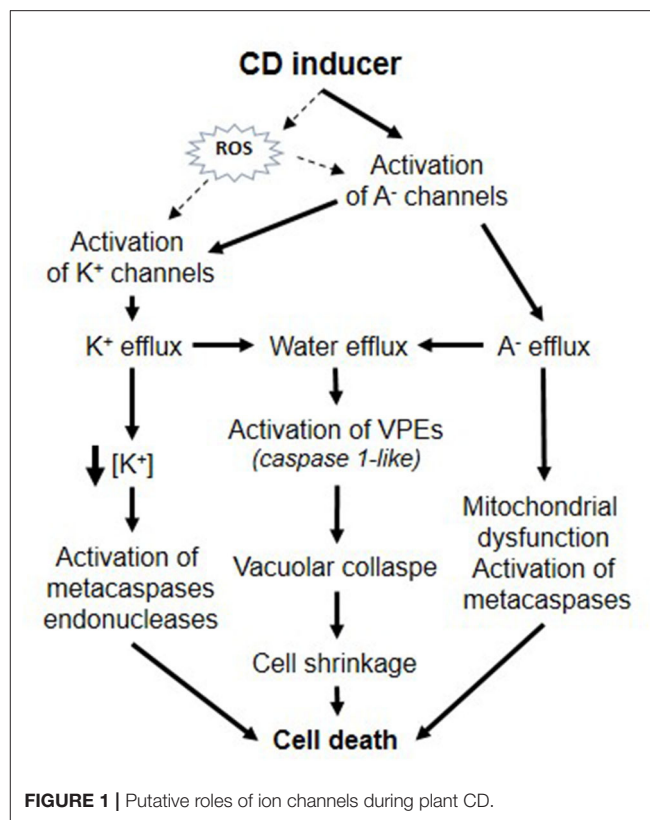


FIGURE 1 | Putative roles of ion channels during plant CD.

CONCLUSION

As a whole, these data are reminiscent of those described in numerous studies in animal cells and show that plant CD could involve specific modifications of ion transporter activities that could be significant and crucial in the successful propagation of CD (Figure 1). Activation of plasma membrane anion channels and KORC lead to solute loss leading to water release and thus, cell shrinkage could be a major hallmark in plant CD similarly to animal apoptosis. In animal cells, the induction of apoptosis volume decrease is attained by a tightly coupled operation between anion and K^+ channels and is prevented by application of blockers of Cl^- or K^+ channels (Okada and Maeno, 2001). Furthermore, as in animal models, activation of ion channels was found to precede various CD-inducing process like metacaspase activation. Some CD mechanisms in plant and animals appear mechanistically very similar. According to the sin hypothesis (Ameisen, 2002), the origin of the capacity for self-destruction may be very ancient and due to an intrinsic capacity of the cell in inducing self-destruction. The regulation of ionic channels are involved in numerous vital processes, the control of cell metabolism, volume, and permeability in all organisms and could be a conserved target due to their intrinsic potential to lead cell death. Ion channel mediated CD could thus have a deeply rooted origin and have independently evolved in eukaryotic lineages and multicellular plants and animals.

AUTHOR CONTRIBUTIONS

FB, DR, DT, and PL conceived and wrote the manuscript. All authors contributed to the article and approved the submitted version.

REFERENCES

- Ameisen, J. C. (2002). On the origin, evolution, and nature of programmed cell death: a timeline of four billion years. *Cell Death Differ.* 9, 367–393. doi: 10.1038/sj.cdd.4400950
- Bortner, C. D., and Cidlowski, J. A. (2007). Cell shrinkage and monovalent cation fluxes: role in apoptosis. *Arch. Biochem. Biophys.* 462, 176–188. doi: 10.1016/j.abb.2007.01.020
- Bouizgarne, B., El-Maarouf-Bouteau, H., Frankart, C., Reboutier, D., Madiona, K., Pennarun, A. M., et al. (2006). Early physiological responses of *Arabidopsis thaliana* cells to fusaric acid: toxic and signalling effects. *New Phytol.* 169, 209–218. doi: 10.1111/j.1469-8137.2005.01561.x
- Craig, R. W. (1995). The bcl-2 gene family. *Semin. Cancer Biol.* 6, 35–43. doi: 10.1006/scbi.1995.0005
- Dauphin, A., El-Maarouf, H., Vienney, N., Rona, J. P., and Bouteau, F. (2001). Effect of desiccation on potassium and anion currents from young root hairs: implication on tip growth. *Physiol. Plant.* 113, 79–84. doi: 10.1034/j.1399-3054.2001.1130111.x
- Demidchik, V. (2018). ROS-activated ion channels in plants: biophysical characteristics, physiological functions and molecular nature. *Int J Mol Sci.* 19, 1263. doi: 10.3390/ijms19041263
- Demidchik, V., Cuin, T. A., Svistunenko, D., Smith, S. J., Miller, A. J., Shabala, S., et al. (2010). Arabidopsis root K⁺-efflux conductance activated by hydroxyl radicals: single-channel properties, genetic basis and involvement in stress-induced cell death. *J. Cell Sci.* 123, 1468–1479. doi: 10.1242/jcs.064352
- Demidchik, V., Straltsova, D., Medvedev, S. S., Pozhvanov, G. A., Sokolik, A., and Yurin, V. (2014). Stress-induced electrolyte leakage: the role of K⁺-permeable channels and involvement in programmed cell death and metabolic adjustment. *J. Exp. Bot.* 65, 1259–1270. doi: 10.1093/jxb/eru004
- Demidchik, V., Tyutereva, E. V., and Voitsekhovskaja, O. V. (2018). The role of ion disequilibrium in induction of root cell death and autophagy by environmental stresses. *Funct Plant Biol.* 45, 28–46. doi: 10.1071/FP16380
- Dickman, M., Williams, B., Li, Y., de Figueiredo, P., and Wolpert, T. (2017). Reassessing apoptosis in plants. *Nat. Plants* 3, 773–779. doi: 10.1038/s41477-017-0020-x
- El-Maarouf, H., Barny, M. A., Rona, J. P., and Bouteau, F. (2001). Harpin, a hypersensitive response elicitor from *Erwinia amylovora*, regulates ion channel activities in *Arabidopsis thaliana* suspension cells. *FEBS Lett.* 497, 82–84. doi: 10.1016/S0014-5793(01)02441-3
- Errakhi, R., Meimoun, P., Lehner, A., Briand, J., Corbineau, F., Rona, J. P., et al. (2008). Anion channel activity is necessary to induce ethylene synthesis and programmed cell death in response to oxalic acid. *J. Exp. Bot.* 59, 3121–3129. doi: 10.1093/jxb/ern166
- Gauthier, A., Lamotte, O., Reboutier, D., Bouteau, F., Pugin, A., and Wendehenne, D. (2007). Cryptogein-induced anion effluxes: electrophysiological properties and analysis of the mechanisms through which they contribute to the elicitor-triggered cell death. *Plant Signal. Behav.* 2, 89–98. doi: 10.4161/psb.2.2.4015
- Haapalainen, M., Dauphin, A., Li, C. M., Bailly, G., Tran, D., Briand, J., et al. (2012). HrpZ harpins from different *Pseudomonas syringae* pathovars differ in molecular interactions and in induction of anion channel responses in *Arabidopsis thaliana* suspension cells. *Plant Physiol Biochem.* 51, 168–174. doi: 10.1016/j.plaphy.2011.10.022
- Hedrich, R. (2012). Ion channels in plants. *Physiol. Rev.* 92, 1777–1811. doi: 10.1152/physrev.00038.2011
- Kadono, T., Tran, D., Errakhi, R., Hiramatsu, T., Meimoun, P., Briand, J., et al. (2010). Increased anion channel activity is an unavoidable event in ozone-induced programmed cell death. *Plos ONE* 5:e13373. doi: 10.1371/journal.pone.0013373
- Klusener, B., and Weiler, E. W. (1999). Pore-forming properties of elicitors of plant defense reactions and cellulytic enzymes. *FEBS Lett.* 459, 263–266. doi: 10.1016/S0014-5793(99)01261-2
- Okada, Y., and Maeno, E. (2001). Apoptosis, cell volume regulation and volume-regulatory chloride channels. *Comp. Biochem. Physiol. A Mol. Integr. Physiol.* 130, 377–383. doi: 10.1016/S1095-6433(01)00424-X
- Peters, J., and Chin, C. K. (2007). Potassium loss is involved in tobacco cell death induced by palmitoleic acid and ceramide. *Arch. Biochem. Biophys.* 465, 180–186. doi: 10.1016/j.abb.2007.05.025
- Pottosin, I., Zepeda-Jazi, I., Bose, J., and Shabala, S. (2018). An anion conductance, the essential component of the hydroxyl-radical-induced ion current in plant roots. *Int. J. Mol. Sci.* 19:897. doi: 10.3390/ijms19030897
- Reape, T. J., and McCabe, P. F. (2010). Apoptotic-like regulation of programmed cell death in plants. *Apoptosis* 15, 249–256. doi: 10.1007/s10495-009-0447-2
- Reape, T. J., Molony, E. M., and McCabe, P. F. (2008). Programmed cell death in plants: distinguishing between different modes. *J. Exp. Bot.* 59, 435–444. doi: 10.1093/jxb/erm258
- Reboutier, D., Frankart, C., Briand, J., Biligui, B., Rona, J. P., Haapalainen, M., et al. (2007). Antagonistic action of harpin proteins: HrpWea from *Erwinia amylovora* suppresses HrpNea-induced cell death in *Arabidopsis thaliana*. *J. Cell. Sci.* 120, 3271–3278. doi: 10.1242/jcs.011098
- Shabala, S., Cuin, T. A., Prisma, L., and Nemchinov, L. G. (2007). Expression of animal CED-9 anti-apoptotic gene in tobacco modifies plasma membrane ion fluxes in response to salinity and oxidative stress. *Planta* 227, 189–197. doi: 10.1007/s00425-007-0606-z
- Tran, D., El-Maarouf-Bouteau, H., Rossi, M., Biligui, B., Briand, J., Kawano, T., et al. (2013a). Post-transcriptional regulation of GORK channels by superoxide anion contributes towards increases in outward rectifying K⁺ currents. *New Phytol.* 198, 1039–1048. doi: 10.1111/nph.12226
- Tran, D., Rossi, M., Biligui, B., Kawano, T., Mancuso, S., and Bouteau, F. (2013b). Ozone-induced caspase-like activities are dependent on early ion channel regulations and ROS generation in *Arabidopsis thaliana* cells. *Plant Signal. Behav.* 8:e25170. doi: 10.4161/psb.25170
- van Doorn, W. G., Beers, E. P., Dangel, J. L., Franklin-Tong, V. E., Gallois, P., Hara-Nishimura, I., et al. (2011). Morphological classification of plant cell deaths. *Cell Death Differ.* 18, 1241–1246. doi: 10.1038/cdd.2011.36
- Yekkour, A., Tran, D., Arbelet-Bonnin, D., Briand, J., Mathieu, F., Lebrhi, A., et al. (2015). Effect of Fusarium mycotoxin deoxynivalenol on *Nicotiana tabacum* cells: early events lead to programmed cell death. *Plant Sci.* 238, 148–157. doi: 10.1016/j.plantsci.2015.06.004

ACKNOWLEDGMENTS

This study contributes to IdEx University of Paris ANR-18-IDEX-0001.

Conflict of Interest: The authors declare that the research was conducted in the absence of any commercial or financial relationships that could be construed as a potential conflict of interest.

Copyright © 2020 Bouteau, Reboutier, Tran and Laurenti. This is an open-access article distributed under the terms of the Creative Commons Attribution License (CC BY). The use, distribution or reproduction in other forums is permitted, provided the original author(s) and the copyright owner(s) are credited and that the original publication in this journal is cited, in accordance with accepted academic practice. No use, distribution or reproduction is permitted which does not comply with these terms.



A Reverse-Osmosis Model of Apoptotic Shrinkage

Priyanka S. Rana and Michael A. Model*

Department of Biological Sciences, Kent State University, Kent, OH, United States

OPEN ACCESS

Edited by:

Markus Ritter,
Paracelsus Medical University, Austria

Reviewed by:

Irena Levitan,
University of Illinois at Chicago,
United States
Boris Musset,
Paracelsus Medical Private University,
Nuremberg, Germany

*Correspondence:

Michael A. Model
mmodel@kent.edu

Specialty section:

This article was submitted to
Cell Death and Survival,
a section of the journal
Frontiers in Cell and Developmental
Biology

Received: 29 July 2020

Accepted: 05 October 2020

Published: 23 October 2020

Citation:

Rana PS and Model MA (2020)
A Reverse-Osmosis Model
of Apoptotic Shrinkage.
Front. Cell Dev. Biol. 8:588721.
doi: 10.3389/fcell.2020.588721

The standard theory of apoptotic volume decrease (AVD) posits activation of potassium and/or chloride channels, causing an efflux of ions and osmotic loss of water. However, in view of the multitude of possible channels that are known to support apoptosis, a model based on specific signaling to a channel presents certain problems. We propose another mechanism of apoptotic dehydration based on cytoskeletal compression. As is well known, cytoskeleton is not strong enough to expel a substantial amount of water against an osmotic gradient. It is possible, however, that an increase in intracellular pressure may cause an initial small efflux of water, and that will create a small concentration gradient of ions, favoring their exit. If the channels are open, some ions will exit the cell, relieving the osmotic gradient; in this way, the process will be able to continue. Calculations confirm the possibility of such a mechanism. An increase in membrane permeability for water or ions may also result in dehydration if accompanied even by a constant cytoskeletal pressure. We review the molecular processes that may lead to apoptotic dehydration in the context of this model.

Keywords: cytoskeleton, cytoskeletal contraction, apoptotic volume decrease, intracellular pressure, osmolytes, potassium channels

INTRODUCTION

The remarkable and often the most noticeable feature of apoptosis is a decrease in cell size. While many other characteristics of apoptosis are often cell- and stimulus-dependent, shrinkage occurs very reliably. Numerous publications investigating various aspects of apoptotic volume decrease (AVD) have appeared in the 1990–2000s and resulted in a significant progress in our understanding of this phenomenon.

When apoptosis was first recognized as a distinct type of cell death, it was dubbed “shrinkage necrosis” (Kerr, 1971) because cells undergoing this type of death become smaller. This observation was surprising because, when exposed to an unfavorable environment, cells are expected to accumulate water, increase their volume and eventually lose membrane integrity. Water accumulation is a natural response to cessation of the Na^+ - K^+ pump activity (Armstrong, 2003) and is a hallmark of unregulated necrotic death (Zong and Thompson, 2006). If the opposite occurs during apoptosis, one is tempted to conclude that cell shrinkage is a purposeful response.

AVD occurs early in apoptosis, often before caspase activation (Maeno et al., 2000). It can continue for several hours (Maeno et al., 2000; l’Hoste et al., 2010; Poulsen et al., 2010;

Kasim et al., 2013), and cells often reduce their volume by 10–20% (Model, 2014). Sometimes, application of potassium or chloride channel inhibitors simultaneously with an apoptotic stimulus prevents caspase activation as well as all other signs of apoptosis (Maeno et al., 2000; Wei et al., 2004). These facts have been interpreted in the sense that either the loss of water or the loss of potassium is a necessary step in apoptosis development.

It is worth noting that a decrease in apoptotic cell size can be brought about by two mechanisms, dehydration and fragmentation. Because of the sensitivity of shrinkage to potassium and chloride, dehydration has received much more attention in the literature and in effect has become synonymous with AVD. But these two paths are not always easy to distinguish from one another, and not every instance of cell volume decrease should automatically be attributed to dehydration (Model, 2014; Model et al., 2018). Dehydration can often be surmized (though not definitively established) by prominent cell borders in bright-field transmission images (Figure 1). It can be more rigorously demonstrated by buoyant density centrifugation (Wyllie and Morris, 1982; Yamada and Ohyama, 1988; Cohen et al., 1992; Patterson et al., 1995; Yurinskaya et al., 2005) or by combined phase/volume measurements (Model and Schonbrun, 2013; Model et al., 2018). A loss of osmotically active ions in UV-irradiated U937 cells with preservation of the amount of phosphorus (Fernández-Segura et al., 1999) can be taken as another evidence of dehydration. Apoptotically-induced activation of outward Cl^- currents (Porcelli et al., 2004; Okada et al., 2006; Ernest et al.,

2008) also indirectly supports the notion of water loss since chloride is, theoretically, the main correlate of intracellular water (Armstrong, 2003; Fraser and Huang, 2007).

But chloride cannot leave the cell alone, without being accompanied by a cation (potassium), and the outward electrochemical drive for potassium is usually stronger than that for chloride. Thus, the standard model of AVD presumes an early activation of potassium channels, which stimulate an efflux of chloride; the resulting loss of osmolytes leads to osmotic dehydration (Yu, 2003; Lang et al., 2005; Bortner and Cidlowski, 2007; Lang and Hoffmann, 2012; Kondratskyi et al., 2015). One general difficulty with this theory has already been pointed out by other authors. “Very different types of K^+ channels have been implicated in activation of apoptosis, like voltage-gated K_v channels, ATP-regulated K_{ATP} channels, two-pore K^+ channels, several types of Ca^{2+} -dependent K^+ channels and others. The variety of K^+ channels that have been implicated in apoptosis suggests that in principle any type of K^+ channel can support apoptosis, but it is not entirely clear how this can operate as a specific switch driving cells into regulated cell death” (Kunzelmann, 2016). Indeed, one would expect that such a universal phenomenon as apoptotic dehydration should have a more universal reason than relying on activation of specific channels present in each particular cell type.

Cytoskeleton-Driven, Ion-Dependent Dehydration

Here we wish to propose an alternative, or rather a complementary, mechanism of dehydration. It is not only ions that can drive water, but water can also drive ions through whatever channels happen to be available. One possible scenario would involve cytoskeleton-mediated intracellular pressure (IP).

IP in animal cells is conceptually similar to turgor in plant cells, although much smaller in magnitude—from tens to thousands Pa (Chengappa et al., 2018). The existence of intracellular pressure is evident from membrane blebs—the areas where membrane-cytoskeleton linkages mediated by numerous lipid-protein and protein-protein interactions (Doherty and McMahon, 2008) are weakened, and membrane forms protruding bubbles (Dai and Sheetz, 1999). Such blebs are frequently observed in apoptotic cells.

IP is believed to result from contraction of the actomyosin cytoskeleton. Since cell membranes are permeable to water, the existence of hydrostatic pressure implies that cells with stable water content must maintain a slight excess of intracellular osmolarity to keep water in balance. This is analogous to the balance of the Starling forces in blood capillaries.

We hypothesize that the balance of hydrostatic and osmotic forces becomes disrupted in apoptotic cells due to an increased cytoskeletal tension. Cytoskeleton has been long dismissed as a possible dehydration factor because the osmotic pressure that needs to be overcome to push water out of the cell is much stronger than any forces that can develop within the cytoskeleton; thus, researchers have come to believe that it is impossible for the cytoskeleton to produce any substantial

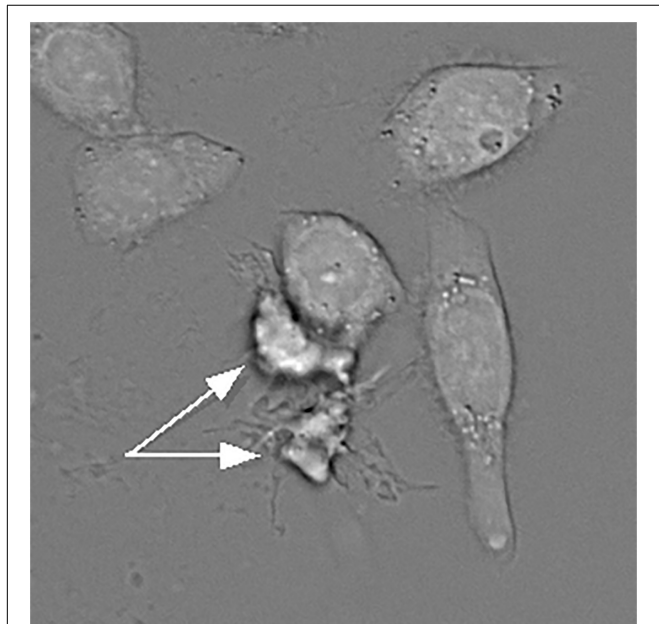


FIGURE 1 | A bright-field transmission image of HeLa cells treated with actinomycin D. Two apoptotic and apparently dehydrated HeLa cells indicated by the arrows have much darker borders. However, this feature alone can only serve as a suggestion, but not as a definitive proof of dehydration. Water content can be accurately quantified under a transmission microscope as described by Mudrak et al. (2018).

water loss (Janmey, 1998). However, the situation would change radically if ion transport is taken into consideration. Suppose that a cell, initially at equilibrium, has developed a higher IP. This excess of pressure would result in a small water efflux, as in reverse osmosis, which, in turn, would create a slight increase in intracellular concentration of ions. If ion channels were blocked, water efflux would stop at this point because cytoskeleton would not be able to push against the ever-increasing concentration difference. But if ion channels were open, some ions would exit the cell down the concentration gradient (also aided by an excess of hydrostatic pressure inside). That would relieve the osmotic resistance and enable the cytoskeleton to push a little further, so that shrinkage would be able to continue.

As the following calculations show, the balance can be disrupted not only by an increase in hydrostatic pressure, but also by an increase in membrane permeability for ions (which makes the model equivalent to the standard one) or for water.

We will first describe the model in quantitative terms and then will discuss the experimental evidence for the cytoskeletal mechanism.

THEORY

Shrinkage rate due to cytoskeletal compression can be estimated as follows.

Consider a cell with volume V immersed in a solution with osmolarity C_0 ; the internal concentration of osmolytes is $C_i = C_0 + \Delta C$, where ΔC is a small positive number. Additional cytoskeletal pressure S (which can be expressed in equivalent concentration units by dividing physical pressure by RT , which equals to $2.5 \cdot 10^6 \text{ Pa} \cdot \text{L} \cdot \text{mol}^{-1}$ at 300K) causes an efflux of water and cell volume decrease, according to:

$$\frac{1}{\rho} \frac{dV}{dt} = -[S - (C_i - C_0)] A P_w = - (S - \Delta C) A P_w \quad (1)$$

where ρ is the molar volume of water ($18 \text{ cm}^3/\text{mol}$), A is the surface area of the cell (cm^2), and P_w is membrane permeability for water (cm/s). We can assume for simplicity that S , A , and P_w remain constant and only ΔC changes with time. Time-dependent changes in ΔC result from two factors: a decrease in the cell volume V (cm^3) and an efflux of the osmolyte. If the total molar amount of the osmolyte present in the cell is N (mol), then:

$$\begin{aligned} \frac{dC_i}{dt} &= \frac{d}{dt} \left(\frac{N}{V} \right) = \frac{d}{dt} \frac{V dN - N dV}{V^2} = \frac{dN/dt}{V} - N \frac{dV/dt}{V^2} \\ &= \frac{dN/dt}{V} - C_i \frac{dV/dt}{V} \end{aligned} \quad (2)$$

Time derivative of the volume dV/dt is expressed by Eq. 1, and the change in the amount of osmolyte dN/dt is expressed through membrane permeability for the osmolyte:

$$\frac{dN}{dt} = - (S + \Delta C) A P_i \quad (3)$$

Since

$$\frac{dC_i}{dt} = \frac{d\Delta C}{dt}$$

we obtain:

$$\frac{d\Delta C}{dt} = - \frac{S + \Delta C}{V} A P_i + \frac{C_0 + \Delta C}{V} (S - \Delta C) \rho A P_w \quad (4)$$

We can further assume that the process has reached a quasi-steady state, when ΔC remains nearly constant; this allows us to estimate the rate of shrinkage by equating $\frac{d\Delta C}{dt}$ to zero. By neglecting quadratic terms and taking into account that $C_0 \gg S$, we find that, in a steady state:

$$\Delta C \approx S \frac{C_0 \rho P_w - P_i}{C_0 \rho P_w + P_i} \quad (5)$$

For an impermeant membrane ($P_i = 0$), the concentration difference becomes equal to S .

To find the rate of volume change, we substitute Eq. 5 into Eq. 1 and obtain:

$$\frac{dV}{dt} = \frac{2 \rho A P_i P_w}{C_0 \rho P_w + P_i} S \quad (6)$$

As expected, shrinkage depends both on water and osmolyte permeabilities. For a spherical cell with radius r (cm), the relative rate of shrinkage will be:

$$\frac{dV/V_0}{dt} = \frac{6 \rho P_i P_w}{r (C_0 \rho P_w + P_i)} S \quad (7)$$

To evaluate this expression, we assume $r = 5 \cdot 10^{-4} \text{ cm}$ and $C_0 = 10^{-4} \text{ mol/cm}^3$ and use some literature values for the other parameters: $P_i = 10^{-5} \text{ cm/s}$ (Strickholm, 1981), $P_w = 2 \cdot 10^{-3} \text{ cm/s}$ (Farinas et al., 1997), and $S = 1,000 \text{ Pa}$ (Chengappa et al., 2018), which correspond to $10^3 \text{ Pa} / (2.5 \cdot 10^6 \text{ Pa} \cdot \text{L} \cdot \text{mol}^{-1}) = 4 \cdot 10^{-7} \text{ mol/cm}^3$. That gives us the shrinkage rate of more than 40% per hour. Even though the parameters have been chosen rather arbitrarily, this estimate demonstrates that cytoskeleton-driven shrinkage is possible.

DISCUSSION

The standard theory of the AVD postulates that some yet unidentified early apoptotic reactions alter membrane permeability in such a way that intracellular osmolytes begin to come out of the cell. Because potassium is the only major ion with electrochemical gradient strongly favoring its exit, it is best suited for the role. However, leakage of potassium alone would immediately cause hyperpolarization that would terminate the process. To keep electroneutrality, potassium can be replaced with sodium, but that would fail to produce any osmotic imbalance. The only way inorganic ions can cause shrinkage is when the exit of potassium exceeds the entry of sodium, and the charge difference is balanced by the loss of chloride.

The results with ionophores agree with this reasoning. Specific potassium ionophore valinomycin causes cell volume loss only when anion exchange is allowed (Dise and Goodman, 1985), but

since cells are normally permeable for chloride to some extent, application of valinomycin to intact cells results in a volume decrease (Rana et al., unpublished). A detailed analysis of ion and water balance in the presence of various membrane channels and transporters (Vereninov et al., 2004, 2007) confirms that an increase in potassium permeability may cause AVD, especially if accompanied by a reduced activity of the $\text{Na}^+\text{-K}^+$ pump. To our knowledge, IP has not been included in any of the previous models.

At the same time, the idea that hydrostatic pressure may affect cell volume is not entirely new. Bereiter-Hahn and Strohmeier (1987) suggested that calcium-dependent intracellular pressure is strong enough to prevent osmotic fluxes. However, that effect was only observed in hypotonic media, and therefore the intracellular pressure in their case was rather a passive resistance to stretch, which is different from active compression that we are hypothesizing. Another model of cell volume regulation assumes that changes in cell volume affect membrane tension and mechanosensitive channels, providing a negative feedback for volume maintenance (Jiang and Sun, 2013).

We approached the problem from a different angle. Equation (6) does not aim to describe a specific molecular process; we omit the membrane potential from the picture, and the nature of the membrane-permeant osmolyte is not even specified. Thus, our model is different from the detailed descriptions of osmotic balance found in the works of other authors (Armstrong, 2003; Fraser and Huang, 2004; Vereninov et al., 2004, 2007). Nevertheless, our result proves that cytoskeletal compression is in principle capable of slowly expelling water if accompanied by an efflux of osmolytes. Equation (6) predicts that the rate of shrinkage should be proportional to IP; it should also be an increasing function of ion and water permeabilities and a decreasing function of external osmolarity. All these trends can be subject to experimental test.

Intracellular Pressure

The dependence of the AVD rate on IP is the critical feature of our model; moreover, we suggest that IP increases during apoptosis. The frequent occurrence of apoptotic blebs indicates that this indeed may be the case, with one qualification that blebs may result either from an increase in IP or from loosening of membrane attachment to the cytoskeleton. Most likely, both factors are in operation, but only the first one is relevant to our model.

The only known mechanism of IP generation is actomyosin contraction (Mills et al., 1998; Hagmann et al., 1999; Miñambres et al., 2006; Tinevez et al., 2009). The force is created by non-muscle myosin II, whose activity is regulated by phosphorylation by various kinases (Vicente-Manzanares et al., 2009), most importantly by myosin light chain kinase (MLCK) and by Rho-associated protein kinase (ROCK; Amano et al., 2010). MLCK is controlled by calcium and, indeed, persistent calcium elevation is a typical feature of apoptosis (Hajnóczky et al., 2003; Orrenius et al., 2003). Furthermore, MLCK activation during apoptosis has been demonstrated directly (Mills et al., 1998; Petrache et al., 2003; Nusbaum et al., 2004). On the other hand, buffering of intracellular calcium did not prevent a decrease in forward light scatter from apoptotic Jurkat cells (Scoltock et al., 2000), nor

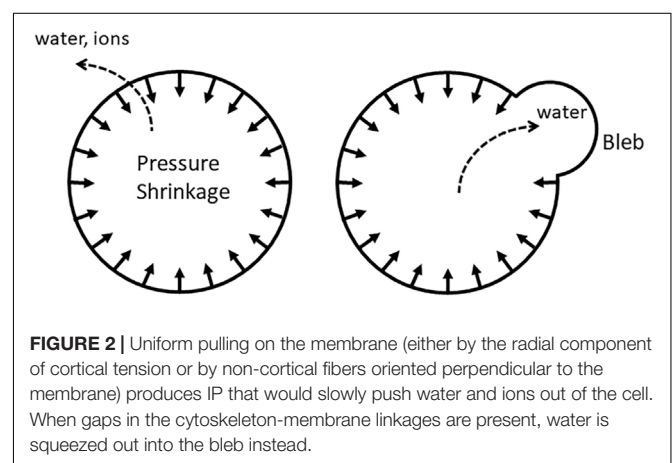
did it affect the loss of potassium and chloride in staurosporine-treated HeLa cells (Dezaki et al., 2012). The significance of these negative results is unclear because cell volume has not been measured in these works directly. Other authors did associate calcium with AVD, but only through its stimulatory effect on calcium-dependent chloride channels (Hoffmann et al., 2015).

The role of ROCK in apoptosis has also been a subject of investigation, mostly in connection to bleb formation. Under normal conditions, ROCK is activated by Rho GTPase but, during apoptosis, ROCK is cleaved by caspases 2 and 3 with release of a constitutively active fragment (Ndozangue-Touriguine et al., 2008; Street and Bryan, 2011). ROCK activation is responsible for apoptotic blebbing and detachment of apoptotic bodies (Street and Bryan, 2011).

Conceivably, not every type of cytoskeletal tension would translate into an increased IP; the cytoskeleton must form a continuous shell and be firmly attached to the membrane, so that it would be effectively pulling the membrane inside; such actin-myosin rings are in fact observed during apoptosis (Coleman and Olson, 2002; Miñambres et al., 2006; Ndozangue-Touriguine et al., 2008; Povea-Cabello et al., 2017). The shape of the membrane may also play a role: the membrane must be sufficiently convex, so that cortical tension would have a radial component (Figure 2). Alternatively, inward pulling may be mediated by non-cortical filaments.

A more direct evidence in favor of the cytoskeletal hypothesis comes from two observations. Firstly, a myosin II inhibitor, blebbistatin, causes a slight but measurable increase in the volume of normal mitotic cells (Stewart et al., 2011). Our preliminary experiments on the effect of blebbistatin on apoptotic cells did show inhibition of water loss, but much more extensive studies would be needed for definitive conclusions. The problem with blebbistatin is that it inhibits apoptosis in general (Xiao et al., 2009; Street et al., 2010; Li et al., 2018; Chai et al., 2019). While such inhibition is compatible with the view that (1) cytoskeletal compression causes dehydration and that (2) dehydration is needed for apoptosis, one cannot claim that blebbistatin inhibits AVD if apoptosis is no longer present.

The second observation is that apoptotic water loss requires intact actin cytoskeleton. We subjected Madin-Darby Canine Kidney cells to a treatment with 2 mM staurosporine and



measured intracellular water content, as described in Mudrak et al. (2018). After 3 h, cells lost 4.2% of their water (SEM 0.15 based on 45 cells analyzed in 3 separate experiments). However, the presence of 0.4 mM of the actin-depolymerizing drug cytochalasin D completely abrogated water loss (0.00 ± 0.03 , 31 cells in 3 experiments; $P < 0.0001$). A related finding has been reported by Bortner et al. (2008), who noticed that cytochalasin prevents potassium loss during apoptosis.

The other fact that agrees with the cytoskeletal model is that shrinkage does not occur in actively blebbing cells (Kasim et al., 2013; Gibbons et al., 2016), presumably because blebs provide an internal reservoir for water (Tinevez et al., 2009; Gibbons et al., 2016; **Figure 2**). Incidentally, blebbing in healthy cells also occurs with volume preservation (Langridge and Kay, 2006; Young and Mitran, 2010). On the other hand, application of blebbistatin or inhibition of ROCK by Y-27632 not prevent the development of cells with shrunken appearance (Kasim et al., 2013). However, neither water content nor IP have been determined in that study.

Unlike intracellular water, which can be quantified non-invasively under a regular transmission microscope (Mudrak et al., 2018), measuring IP in animal cells is a more challenging undertaking. The servo-null method that uses a microelectrode inserted into the cytoplasm (Kelly and Macklem, 1991; Petrie and Koo, 2014) may be the most direct and the least affected by the stiffness of the cytoskeleton because the needle penetrates past the cortical layer. A pressure-sensitive microinterferometer internalized by cells (Gómez-Martínez et al., 2013) is another interesting and apparently gentle technique for IP measurements.

Ion Permeability

Permeability for ions should be an integral part of any dehydration scheme and does not represent a unique feature of our hypothesis. The value of 1.3×10^{-5} cm/s used in our calculations has been reported for K^+ in the resting axon (Strickholm, 1981). Even though some other published numbers are smaller (Costa et al., 1989; Fraser and Huang, 2004), an increase in potassium permeability and the loss of potassium from apoptotic cells have been convincingly demonstrated (Yu et al., 1997; Dallaporta et al., 1998), and this observation is the main buttress for the ionic theory of the AVD. Clearly, if ion permeability during apoptosis is sufficient to allow potassium out by electrochemical gradient alone, it should be all the more sufficient when electrochemical gradient is assisted by pressure. Volume-regulated anion channels (VRAC) that pass chloride and organic osmolytes also become activated during apoptosis (Osei-Owusu et al., 2018). Multiple ion fluxes are always interconnected (Vereninov et al., 2007), and the single P_i and C_0 in Eq. 6 should be interpreted as cumulative parameters.

Water Permeability

If dehydration is the essence of the AVD, it is only natural that water permeability should be a factor. The assumed value for water permeability, $P_w = 2 \cdot 10^{-3}$ cm/s, seems to be typical, although the numbers vary from 3 to 6×10^{-4} cm/s in MDCK cells (Farinas and Verkman, 1996; Zelenina and Brismar, 2000) to 0.1 cm/s in the rat proximal tubule (Preisig and Berry, 1985).

When water permeability is high, Eq. 7 turns into:

$$\frac{dV/V_0}{dt} = \frac{6\rho P_i P_w}{r(C_0 \rho P_w + P_i)} S \approx \frac{6P_i}{rC_0} S \quad (8)$$

and ion permeability becomes the only limiting factor.

The dependence of apoptosis on water permeability has been demonstrated by several authors using either chemical inhibition of aquaporins or by comparing similar cell types with different aquaporin expression (Jablonski et al., 2004; Flamenco et al., 2009; Younts and Hughes, 2009; Lakner et al., 2011; Zhang et al., 2011). To explain the relationship between apoptosis and aquaporins, Jablonski et al. (2004) suggested that, when aquaporins are blocked, the loss of potassium exceeds the loss of water, and a drop in potassium concentration causes apoptosis. Whether this is so or not, our main focus here is on the loss of water rather than on caspase activation and other degradative processes. The published results do not provide enough information to test Eq. 6, and more pointed and quantitative experiments would be desirable.

Osmolarity

Cells adapt to a large range of osmolarities, and even the osmolarity of commercial DMEM media from different sources may vary from 230 to 360 mOsm. Although it is technically straightforward to manipulate osmolarity to test its effect on the AVD rate, varying levels of osmolarity may affect too many processes (Burg et al., 2007), and it would be difficult to guarantee that any changes in shrinkage rate are due to the described mechanism.

CONCLUSION

The main claim of our hypothesis is that cytoskeletal pressure plays an active role in apoptotic water loss. The attractiveness of this proposition is that cytoskeletal rearrangements appear to be a general feature of apoptosis and therefore, this mechanism would not have to rely on specific properties of ion channels. The effect of blebbistatin on cell volume (Stewart et al., 2011) and the dependence of AVD on actin show that the model is not in conflict with observations. Its more direct testing may proceed in two main directions.

- (1) Demonstration of an increased IP during AVD. It is unclear whether the existing technology would be adequate for the task. For example, puncturing apoptotic cells with a needle may be difficult to perform, and the use of intracellular microinterferometer may not have been sufficiently developed.
- (2) Manipulation of myosin activity by drugs. The previously mentioned difficulty with blebbistatin (namely, its interference with apoptosis) could possibly be circumvented by applying it at later stages, when apoptosis has become irreversible.

It is less clear if quantification of the dependence of the AVD rate on ion and water permeability to test Eq. 6 can be

accurate enough to distinguish between this model and the model based on ion channel activation (Vereninov et al., 2004, 2007). Moreover, these mechanisms are not mutually exclusive, and both are likely to operate in parallel.

DATA AVAILABILITY STATEMENT

The raw data supporting the conclusions of this article will be made available by the authors, without undue reservation, to any qualified researcher.

AUTHOR CONTRIBUTIONS

PR performed the experiments and participated in writing the manuscript. MM conceived the model and wrote the

manuscript. All authors contributed to the article and approved the submitted version.

FUNDING

The work was supported by the Research Council of the Kent State University.

ACKNOWLEDGMENTS

We gratefully acknowledge the feedback and comments from Drs. M. Kurokawa, A. Vereninov, J. Bereiter-Hahn, and R. Petrie.

REFERENCES

- Amano, M., Nakayama, M., and Kaibuchi, K. (2010). Rho-kinase/ROCK: a key regulator of the cytoskeleton and cell polarity. *Cytoskeleton* 67, 545–554. doi: 10.1002/cm.20472
- Armstrong, C. M. (2003). The Na/K pump, Cl ion, and osmotic stabilization of cells. *Proc. Natl. Acad. Sci. U.S.A.* 100, 6257–6262. doi: 10.1073/pnas.0931278100
- Bereiter-Hahn, J., and Strohmeier, R. (1987). “Hydrostatic pressure in metazoan cells in culture: its involvement in locomotion and shape generation,” in *Cytomechanics*, eds W.-E. Reif, J. Bereiter-Hahn, O. Roger Anderson (Berlin: Springer), 261–272. doi: 10.1007/978-3-642-72863-1_18
- Bortner, C. D., and Cidlowski, J. A. (2007). Cell shrinkage and monovalent cation fluxes: role in apoptosis. *Arch. Biochem. Biophys.* 462, 176–188. doi: 10.1016/j.abb.2007.01.020
- Bortner, C. D., Sifre, M. I., and Cidlowski, J. A. (2008). Cationic gradient reversal and cytoskeleton-independent volume regulatory pathways define an early stage of apoptosis. *J. Biol. Chem.* 283, 7219–7229. doi: 10.1074/jbc.M70780.9200
- Burg, M. B., Ferraris, J. D., and Dmitrieva, N. I. (2007). Cellular response to hyperosmotic stresses. *Physiology* 87, 1441–1474. doi: 10.1152/physrev.00056
- Chai, R., Gao, S., Cheng, C., Wang, M., Jiang, P., Wang, Y., et al. (2019). Blebbistatin inhibits neomycin-induced apoptosis in hair cell-like HEI-OC-1 cells and in cochlear hair cells. *Front. Cell. Neurosci.* 13:590. doi: 10.3389/fncel.2019.00590
- Chengappa, P., Sao, K., Jones, T. M., and Petrie, R. J. (2018). Intracellular pressure: a driver of cell morphology and movement. *Int. Rev. Cell. Mol. Biol.* 337, 185–211. doi: 10.1016/bs.ircmb.2017.12.005
- Cohen, G. M., Sun, X. M., Snowden, R. T., Dinsdale, D., and Skilleter, D. N. (1992). Key morphological features of apoptosis may occur in the absence of internucleosomal DNA fragmentation. *Biochem. J.* 286, 331–334. doi: 10.1042/bj2860331
- Coleman, M. L., and Olson, M. F. (2002). Rho GTPase signalling pathways in the morphological changes associated with apoptosis. *Cell Death Differ.* 9, 493–504. doi: 10.1038/sj.cdd.4400987
- Costa, P. F., Emilio, M. G., Fernandes, P. L., Gil Ferreira, H., and Gil Ferreira, K. (1989). Determination of ionic permeability coefficients of the plasma membrane of *Xenopus laevis* oocytes under voltage clamp. *J. Physiol.* 413, 199–211. doi: 10.1113/jphysiol.1989.sp017649
- Dai, J., and Sheetz, M. P. (1999). Membrane tether formation from blebbing cells. *Biophys. J.* 77, 3363–3370. doi: 10.1016/S0006-3495(99)77168-7
- Dallaporta, B., Hirsch, T., Susin, S. A., Zamzami, N., Larochette, N., Brenner, C., et al. (1998). Potassium leakage during the apoptotic degradation phase. *J. Immunol.* 160, 5605–5615.
- Dezaki, K., Maeno, E., Sato, K., Akita, T., and Okada, Y. (2012). Early-phase occurrence of K⁺ and Cl[−] efflux in addition to Ca²⁺ mobilization is a prerequisite to apoptosis in HeLa cells. *Apoptosis* 17, 821–831. doi: 10.1007/s10495-012-0716-3
- Dise, C. A., and Goodman, D. B. (1985). The relationship between valinomycin-induced alterations in membrane phospholipid fatty acid turnover, membrane potential, and cell volume in the human erythrocyte. *J. Biol. Chem.* 260, 2869–2874.
- Doherty, G. J., and McMahon, H. T. (2008). Mediation, modulation, and consequences of membrane-cytoskeleton interactions. *Annu. Rev. Biophys.* 37, 65–95. doi: 10.1146/annurev.biophys.37.032807.125912
- Ernest, N. J., Habela, C. W., and Sontheimer, H. (2008). Cytoplasmic condensation is both necessary and sufficient to induce apoptotic cell death. *J. Cell Sci.* 121, 290–297. doi: 10.1242/jcs.017343
- Farinas, J., Kneen, M., Moore, M., and Verkman, A. S. (1997). Plasma membrane water permeability of cultured cells and epithelia measured by light microscopy with spatial filtering. *J. Gen. Physiol.* 110, 283–296. doi: 10.1085/jgp.110.3.283
- Farinas, J., and Verkman, A. S. (1996). Cell volume and plasma membrane osmotic water permeability in epithelial cell layers measured by interferometry. *Biophys. J.* 71, 3511–3522. doi: 10.1016/s0006-3495(96)79546-2
- Fernández-Segura, E., Cañizares, F. J., Cubero, M. A., Warley, A., and Campos, A. (1999). Changes in elemental content during apoptotic cell death studied by electron probe X-ray microanalysis. *Exp. Cell Res.* 253, 454–462. doi: 10.1006/excr.1999.4657
- Flamenco, P., Galizia, L., Rivarola, V., Fernandez, J., Ford, P., and Capurro, C. (2009). Role of AQP2 during apoptosis in cortical collecting duct cells. *Biol. Cell.* 101, 237–250. doi: 10.1042/BC20080050
- Fraser, J. A., and Huang, C. L. (2007). Quantitative techniques for steady-state calculation and dynamic integrated modelling of membrane potential and intracellular ion concentrations. *Prog. Biophys. Mol. Biol.* 94, 336–372. doi: 10.1016/j.pbiomolbio.2006.10.001
- Fraser, J. A., and Huang, C. L. H. (2004). A quantitative analysis of cell volume and resting potential determination and regulation in excitable cells. *J. Physiol.* 559, 459–478. doi: 10.1113/jphysiol.2004.065706
- Gibbons, B. A., Kharel, P., Robinson, L. C., Synowicki, R. A., and Model, M. A. (2016). Volume measurements and fluorescent staining indicate an increase in permeability for organic cation transporter substrates during apoptosis. *Exp. Cell Res.* 344, 112–119. doi: 10.1016/j.yexcr.2016.03.018
- Gómez-Martínez, R., Hernández-Pinto, A. M., Duch, M., Vázquez, P., Zinoviev, K., de la Rosa, E. J., et al. (2013). Silicon chips detect intracellular pressure changes in living cells. *Nat. Nanotechnol.* 8, 517–521. doi: 10.1038/nnano.2013.118
- Hagmann, J., Burger, M. M., and Dagan, D. (1999). Regulation of plasma membrane blebbing by the cytoskeleton. *J. Cell. Biochem.* 73, 488–499. doi: 10.1002/(SICI)1097-4644(19990615)73:4<488::AID-JCB7>3.0.CO;2-P
- Hajnóczky, G., Davies, E., and Madesh, M. (2003). Calcium signaling and apoptosis. *Biochem. Biophys. Res. Commun.* 304, 445–454. doi: 10.1016/S0006-291X(03)00616-8
- Hoffmann, E. K., Sørensen, B. H., Sauter, D. P., and Lambert, I. H. (2015). Role of volume-regulated and calcium-activated anion channels in cell volume

- homeostasis, cancer and drug resistance. *Channels* 9, 380–396. doi: 10.1080/19336950.2015.1089007
- Jablonski, E. M., Webb, A. N., McConnell, N. A., Riley, M. C., and Hughes, F. M. Jr. (2004). Plasma membrane aquaporin activity can affect the rate of apoptosis but is inhibited after apoptotic volume decrease. *Am. J. Physiol. Cell Physiol.* 286, C975–C985. doi: 10.1152/ajpcell.00180.2003
- Janmey, P. A. (1998). The cytoskeleton and cell signaling: component localization and mechanical coupling. *Physiol. Rev.* 78, 763–781. doi: 10.1152/physrev.1998.78.3.763
- Jiang, H., and Sun, S. X. (2013). Cellular pressure and volume regulation and implications for cell mechanics. *Biophys. J.* 105, 609–619. doi: 10.1016/j.bpj.2013.06.021
- Kasim, N. R., Kuželová, K., Holoubek, A., and Model, M. A. (2013). Live fluorescence and transmission-through-dye microscopic study of actinomycin D-induced apoptosis and apoptotic volume decrease. *Apoptosis* 18, 521–532. doi: 10.1007/s10495-013-0804-z
- Kelly, S. M., and Macklem, P. T. (1991). Direct measurement of intracellular pressure. *Am. J. Physiol.* 260, C652–C657. doi: 10.1152/ajpcell.1991.260.3.C652
- Kerr, J. F. (1971). Shrinkage necrosis: a distinct mode of cellular death. *J. Pathol.* 105, 13–20. doi: 10.1002/path.1711050103
- Kondratsky, A., Kondratska, K., Skryma, R., and Prevarskaya, N. (2015). Ion channels in the regulation of apoptosis. *Biochim. Biophys. Acta* 1848, 2532–2546. doi: 10.1016/j.bbame.2014.10.030
- Kunzelmann, K. (2016). Ion channels in regulated cell death. *Cell. Mol. Life Sci.* 73, 2387–2403. doi: 10.1007/s00018-016-2208-z
- Lakner, A. M., Walling, T. L., McKillop, I. H., and Schrum, L. W. (2011). Altered aquaporin expression and role in apoptosis during hepatic stellate cell activation. *Liver Int.* 31, 42–51. doi: 10.1111/j.1478-3231.2010.02356.x
- Lang, F., Föller, M., Lang, K. S., Lang, P. A., Ritter, M., Gulbins, E., et al. (2005). Ion channels in cell proliferation and apoptotic cell death. *J. Membr. Biol.* 205, 147–157. doi: 10.1007/s00232-005-0780-5
- Lang, F., and Hoffmann, E. K. (2012). Role of ion transport in control of apoptotic cell death. *Comprehensive Physiol.* 2, 2037–2061. doi: 10.1002/cphy.c110046
- Langridge, P. D., and Kay, R. R. (2006). Blebbing of Dictyostelium cells in response to chemoattractant. *Exp. Cell Res.* 312, 2009–2017. doi: 10.1016/j.yexcr.2006.03.007
- l'Hoste, S., Chargui, A., Belfodil, R., Corcelle, E., Duranton, C., Rubera, I., et al. (2010). CFTR mediates apoptotic volume decrease and cell death by controlling glutathione efflux and ROS production in cultured mice proximal tubules. *Am. J. Physiol. Renal Physiol.* 298, F435–F453. doi: 10.1152/ajprenal.00286.2009
- Li, F., Fan, X., Zhang, Y., Zhang, Y., Ma, X., Kou, J., et al. (2018). Inhibition of myosin IIA-actin interaction prevents ischemia/reperfusion induced cardiomyocytes apoptosis through modulating PINK1/Parkin pathway and mitochondrial fission. *Int. J. Cardiol.* 271, 211–218. doi: 10.1016/j.ijcard.2018.04.079
- Maeno, E., Ishizaki, Y., Kanaseki, T., Hazama, A., and Okada, Y. (2000). Normotonic cell shrinkage because of disordered volume regulation is an early prerequisite to apoptosis. *Proc. Natl. Acad. Sci. U.S.A.* 97, 9487–9492. doi: 10.1073/pnas.140216197
- Mills, J. C., Stone, N. L., Erhardt, J., and Pittman, R. N. (1998). Apoptotic membrane blebbing is regulated by myosin light chain phosphorylation. *J. Cell Biol.* 140, 627–636. doi: 10.1083/jcb.140.3.627
- Miñambres, R., Guasch, R. M., Perez-Aragó, A., and Guerri, C. (2006). The RhoA/ROCK-1/MLC pathway is involved in the ethanol-induced apoptosis by anoikis in astrocytes. *J. Cell Sci.* 119, 271–282. doi: 10.1242/jcs.02723
- Model, M. A. (2014). Possible causes of apoptotic volume decrease: an attempt at quantitative review. *Am. J. Physiol.* 306, C417–C424. doi: 10.1152/ajpcell.00328.2013
- Model, M. A., Mudrak, N. J., Rana, P. S., and Clements, R. J. (2018). Staurosporine-induced apoptotic water loss is cell- and attachment-specific. *Apoptosis* 23, 449–455. doi: 10.1007/s10495-018-1471-x
- Model, M. A., and Schonbrun, E. (2013). Optical determination of intracellular water in apoptotic cells. *J. Physiol.* 591, 5843–5849. doi: 10.1113/jphysiol.2013.263228
- Mudrak, N. J., Rana, P. S., and Model, M. A. (2018). Calibrated brightfield-based imaging for measuring intracellular protein concentration. *Cytometry Part A* 93, 297–304. doi: 10.1002/cyto.a.23145
- Ndozangue-Tourigine, O., Hamelin, J., and Bréard, J. (2008). Cytoskeleton and apoptosis. *Biochem. Pharmacol.* 76, 11–18. doi: 10.1016/j.bcp.2008.03.016
- Nusbaum, P., Laine, C., Seveau, S., Lesavre, P., and Halbwachs-Mecarelli, L. (2004). Early membrane events in polymorphonuclear cell (PMN) apoptosis: membrane blebbing and vesicle release, CD43 and CD16 down-regulation and phosphatidylserine externalization. *Biochem. Soc. Trans.* 32, 477–479. doi: 10.1042/bst0320477
- Okada, Y., Shimizu, T., Maeno, E., Tanabe, S., Wang, X., and Takahashi, N. (2006). Volume-sensitive chloride channels involved in apoptotic volume decrease and cell death. *J. Membr. Biol.* 209, 21–29. doi: 10.1007/s00232-005-0836-6
- Orrenius, S., Zhivotovsky, B., and Nicotera, P. (2003). Regulation of cell death: the calcium-apoptosis link. *Nat. Rev. Mol. Cell. Biol.* 4, 552–565. doi: 10.1038/nrm1150
- Osei-Owusu, J., Yang, J., del Carmen Vitery, M., and Qiu, Z. (2018). Molecular biology and physiology of volume-regulated anion channel (VRAC). *Curr. Top. Membr.* 81, 177–203. doi: 10.1016/bs.ctm.2018.07.005
- Patterson, S. D., Grossman, J. S., D'Andrea, P., and Latter, G. I. (1995). Reduced numatrin/B23/nucleophosmin labeling in apoptotic Jurkat T-lymphoblasts. *J. Biol. Chem.* 270, 9429–9436. doi: 10.1074/jbc.270.16.9429
- Petrache, I., Birukov, K., Zaiman, A. L., Crow, M. T., Deng, H., Wadgaonkar, R., et al. (2003). Caspase-dependent cleavage of myosin light chain kinase (MLCK) is involved in TNF- α -mediated bovine pulmonary endothelial cell apoptosis. *FASEB J.* 17, 407–416. doi: 10.1096/fj.02-0672com
- Petrie, R. J., and Koo, H. (2014). Direct measurement of intracellular pressure. *Curr. Protoc. Cell Biol.* 63, 12–19. doi: 10.1002/0471143030.cb1209s63
- Porcelli, A. M., Ghelli, A., Zanna, C., Valente, P., Ferroni, S., and Rugolo, M. (2004). Apoptosis induced by staurosporine in ECV304 cells requires cell shrinkage and upregulation of Cl⁻ conductance. *Cell Death Differ.* 11, 655–662. doi: 10.1038/sj.cdd.4401396
- Poulsen, K. A., Andersen, E. C., Hansen, C. F., Klausen, T. K., Hougaard, C., Lambert, I. H., et al. (2010). Deregulation of apoptotic volume decrease and ionic movements in multidrug-resistant tumor cells: role of chloride channels. *Am. J. Physiol. Cell Physiol.* 298, C14–C25. doi: 10.1152/ajpcell.00654.2008
- Povea-Cabello, S., Oropesa-Ávila, M., de la Cruz-Ojeda, P., Villanueva-Paz, M., de la Mata, M., Suárez-Rivero, J. M., et al. (2017). Dynamic reorganization of the cytoskeleton during apoptosis: the two coffins hypothesis. *Int. J. Mol. Sci.* 18:2393. doi: 10.3390/ijms18112393
- Preisig, P. A., and Berry, C. A. (1985). Evidence for transcellular osmotic water flow in rat proximal tubules. *Am. J. Physiol. Renal Physiol.* 249, F124–F131. doi: 10.1152/ajprenal.1985.249.1.F124
- Scoltock, A. B., Bortner, C. D., St, J., Bird, G., Putney, J. W. Jr., and Cidlowski, J. A. (2000). A selective requirement for elevated calcium in DNA degradation, but not early events in anti-Fas-induced apoptosis. *J. Biol. Chem.* 275, 30586–30596. doi: 10.1074/jbc.M004058200
- Stewart, M. P., Helenius, J., Toyoda, Y., Ramanathan, S. P., Muller, D. J., and Hyman, A. A. (2011). Hydrostatic pressure and the actomyosin cortex drive mitotic cell rounding. *Nature* 469, 226–230. doi: 10.1038/nature09642
- Street, C. A., and Bryan, B. A. (2011). Rho kinase proteins—pleiotropic modulators of cell survival and apoptosis. *Anticancer. Res.* 31, 3645–3657.
- Street, C. A., Routhier, A. A., Spencer, C., Perkins, A. L., Masterjohn, K., Hackathorn, A., et al. (2010). Pharmacological inhibition of Rho-kinase (ROCK) signaling enhances cisplatin resistance in neuroblastoma cells. *Int. J. Oncol.* 37, 1297–1305. doi: 10.3892/ijo_00000781
- Strickholm, A. (1981). Ionic permeability of K, Na, and Cl in potassium-depolarized nerve. Dependency on pH, cooperative effects, and action of tetrodotoxin. *Biophys. J.* 35, 677–697. doi: 10.1016/S0006-3495(81)84820-5
- Tinevez, J. Y., Schulte, U., Salbreux, G., Roensch, J., Joanny, J. F., and Paluch, E. (2009). Role of cortical tension in bleb growth. *Proc. Natl. Acad. Sci. U.S.A.* 106, 18581–18586. doi: 10.1073/pnas.0903353106
- Vereninov, A. A., Goryachaya, T. S., Moshkov, A. V., Vassilieva, I. O., Yurinskaya, V. E., Lang, F., et al. (2007). Analysis of the monovalent ion fluxes in U937 cells under the balanced ion distribution: recognition of ion transporters responsible for changes in cell ion and water balance during apoptosis. *Cell Biol. Int.* 31, 382–393. doi: 10.1016/j.cellbi.2007.01.023
- Vereninov, A. A., Yurinskaya, V. E., and Rubashkin, A. A. (2004). The role of potassium, potassium channels, and symporters in the apoptotic cell volume

- decrease: experiment and theory. *Doklady Biol. Sci.* 398, 417–420. doi: 10.1023/B:DOBS.0000046672.99148.fb
- Vicente-Manzanares, M., Ma, X., Adelstein, R. S., and Horwitz, A. R. (2009). Non-muscle myosin II takes centre stage in cell adhesion and migration. *Nat. Rev. Mol. Cell Biol.* 10, 778–790. doi: 10.1038/nrm2786
- Wei, L., Xiao, A. Y., Jin, C., Yang, A., Lu, Z. Y., and Yu, S. P. (2004). Effects of chloride and potassium channel blockers on apoptotic cell shrinkage and apoptosis in cortical neurons. *Pflügers Arch.* 448, 325–334. doi: 10.1007/s00424-004-1277-2
- Wyllie, A. H., and Morris, R. G. (1982). Hormone-induced cell death. Purification and properties of thymocytes undergoing apoptosis after glucocorticoid treatment. *Am. J. Pathol.* 109, 78–87.
- Xiao, L., Eto, M., and Kazanietz, M. G. (2009). ROCK mediates phorbol ester-induced apoptosis in prostate cancer cells via p21Cip1 up-regulation and JNK. *J. Biol. Chem.* 284, 29365–29375. doi: 10.1074/jbc.M109.007971
- Yamada, T., and Ohyama, H. (1988). Radiation-induced interphase death of rat thymocytes is internally programmed (apoptosis). *Int. J. Radiat. Biol. Relat. Stud. Phys. Chem. Med.* 53, 65–75. doi: 10.1080/09553008814550431
- Young, J., and Mitran, S. (2010). A numerical model of cellular blebbing: a volume-conserving, fluid-structure interaction model of the entire cell. *J. Biomech.* 43, 210–220. doi: 10.1016/j.jbiomech.2009.09.025
- Younts, T. J., and Hughes, J. (2009). “Emerging role of water channels in regulating cellular volume during oxygen deprivation and cell death,” in *Brain Hypoxia and Ischemia with Special Emphasis on Development*, eds G. G. Haddad, and S. P. Yu (New York: Humana Press), 79–96. doi: 10.1007/978-1-60327-579-8_5
- Yu, S. P. (2003). Regulation and critical role of potassium homeostasis in apoptosis. *Prog. Neurobiol.* 70, 363–386. doi: 10.1016/S0301-0082(03)00090-X
- Yu, S. P., Yeh, C. H., Sensi, S. L., Gwag, B. J., Canzoniero, L. M., Farhangrazi, Z. S., et al. (1997). Mediation of neuronal apoptosis by enhancement of outward potassium current. *Science* 278, 114–117. doi: 10.1126/science.278.5335.114
- Yurinskaya, V., Goryachaya, T., Guzova, I., Moshkov, A., Rozanov, Y., Sakuta, G., et al. (2005). Potassium and sodium balance in U937 cells during apoptosis with and without cell shrinkage. *Cell Physiol. Biochem.* 16, 155–162. doi: 10.1159/000089841
- Zelenina, M., and Brismar, H. (2000). Osmotic water permeability measurements using confocal laser scanning microscopy. *Eur. Biophys. J.* 29, 165–171. doi: 10.1007/PL00006645
- Zhang, L., Li, J., Jiang, Z., Sun, L., Mei, X., Yong, B., et al. (2011). Inhibition of aquaporin-1 expression by RNAi protects against aristolochic acid I-induced apoptosis in human proximal tubular epithelial (HK-2) cells. *Biochem. Biophys. Res. Commun.* 405, 68–73. doi: 10.1016/j.bbrc.2010.12.128
- Zong, W. X., and Thompson, C. B. (2006). Necrotic death as a cell fate. *Genes Dev.* 20, 1–15. doi: 10.1101/gad.1376506

Conflict of Interest: The authors declare that the research was conducted in the absence of any commercial or financial relationships that could be construed as a potential conflict of interest.

Copyright © 2020 Rana and Model. This is an open-access article distributed under the terms of the Creative Commons Attribution License (CC BY). The use, distribution or reproduction in other forums is permitted, provided the original author(s) and the copyright owner(s) are credited and that the original publication in this journal is cited, in accordance with accepted academic practice. No use, distribution or reproduction is permitted which does not comply with these terms.



The Relationship Between Actin Cytoskeleton and Membrane Transporters in Cisplatin Resistance of Cancer Cells

Takahiro Shimizu*, Takuto Fujii and Hideki Sakai

Department of Pharmaceutical Physiology, Faculty of Pharmaceutical Sciences, University of Toyama, Toyama, Japan

OPEN ACCESS

Edited by:

Markus Ritter,
Paracelsus Medical University, Austria

Reviewed by:

Christian Mayr,
Paracelsus Medical University, Austria
Kengo Watanabe,
Institute for Systems Biology (ISB),
United States

*Correspondence:

Takahiro Shimizu
takshimi@pha.u-toyama.ac.jp

Specialty section:

This article was submitted to
Cell Death and Survival,
a section of the journal
Frontiers in Cell and Developmental
Biology

Received: 22 August 2020

Accepted: 05 October 2020

Published: 27 October 2020

Citation:

Shimizu T, Fujii T and Sakai H
(2020) The Relationship Between
Actin Cytoskeleton and Membrane
Transporters in Cisplatin Resistance
of Cancer Cells.
Front. Cell Dev. Biol. 8:597835.
doi: 10.3389/fcell.2020.597835

Cisplatin [*cis*-diamminedichloroplatinum (II)] is a platinum-based anticancer drug widely used for the treatment of various cancers. It forms interstrand and intrastrand cross-linking with DNA and block DNA replication, resulting in apoptosis. On the other hand, intrinsic and acquired cisplatin resistance restricts its therapeutic effects. Although some studies suggest that dramatic epigenetic alternations are involved in the resistance triggered by cisplatin, the mechanism is complicated and remains poorly understood. Recent studies reported that cytoskeletal structures regulate cisplatin sensitivity and that activities of membrane transporters contribute to the development of resistance to cisplatin. Therefore, we focus on the roles of actin filaments and membrane transporters in cisplatin-induced apoptosis. In this review, we summarize the relationship between actin cytoskeleton and membrane transporters in the cisplatin resistance of cancer cells.

Keywords: cisplatin resistance, actin filament, membrane transporter, anion channel, apoptosis

INTRODUCTION

Cisplatin [*cis*-diamminedichloroplatinum (II)], a platinum-based anticancer drug, is a widely used chemotherapeutic drug in the treatment of various cancers including testicular, bladder, prostate, ovarian, head and neck, small cell lung, non-small cell lung, esophageal, cervical, and stomach cancers (Lebwohl and Canetta, 1998; Boulikas and Vougiouka, 2004). Cisplatin enters inside cancer cells in a balance between influx and efflux through membrane transporters. The accumulated cisplatin forms intrastrand and interstrand adducts with DNA, which interferes with DNA replication and transcription. The cisplatin-triggered DNA damage activates a variety of signaling pathways such as a tumor suppressor p53 and mitogen-activated protein kinases (MAPKs), leading to apoptotic cell death (Siddik, 2003). However, the cisplatin treatment is limited in cancer therapy because cancer cells develop acquired resistance to cisplatin. The molecular mechanisms involved in the cisplatin resistance are complicated. Generally, the following three events, (1) reduced intracellular cisplatin accumulation, (2) increased DNA damage repair, and (3) inactivation of the apoptotic signaling pathways, are associated with the cisplatin resistance

(Siddik, 2003; Tanida et al., 2012; Zhu et al., 2016; Lambert and Sørensen, 2018). We, therefore, begin the review by providing an overview of the cisplatin-resistant mechanism.

REDUCED INTRACELLULAR CISPLATIN ACCUMULATION IN CISPLATIN RESISTANCE

The independent influx and efflux pathways regulate the amount of cellular cisplatin in cancer cells (**Figure 1**). Although the mechanism of cisplatin uptake remains poorly understood, cisplatin passes through the plasma membrane via facilitated diffusion. The copper transporter 1 (CTR1), the first member of the solute carrier transporter 31 family (SLC31A1), is demonstrated to play a pivotal role in the cisplatin influx (Howell et al., 2010; Liu et al., 2012). The deletion of CTR1 not only reduced intracellular cisplatin accumulation but also increased the cisplatin resistance (Ishida et al., 2002; Lin et al., 2002). Besides, some cisplatin-resistant cancer cells exhibited low expression of CTR1 (Song et al., 2004; Kalayda et al., 2012). These results suggest that the downregulation of CTR1 contributes to the cisplatin resistance. The organic cation transporters (OCT), which belong to the SLC22 family, are known to transport organic cations containing medicines down an electrochemical gradient. Several reports showed that the overexpression of OCT1-3 (SLC22A1-3) enhanced cisplatin uptake and cisplatin-triggered cytotoxicity (Ciarimboli et al., 2005; Yonezawa et al., 2006; Li et al., 2012). Recently, the expression of OCT6 [SLC22A16, also called carnitine transporter 2 (CT2)] is demonstrated to contribute to the cisplatin uptake and its cytotoxicity (Kunii et al., 2015). These results suggest that these OCT proteins might function as influx transporters of cisplatin. Further studies are awaited to clarify the importance of OCT proteins in the cisplatin resistance.

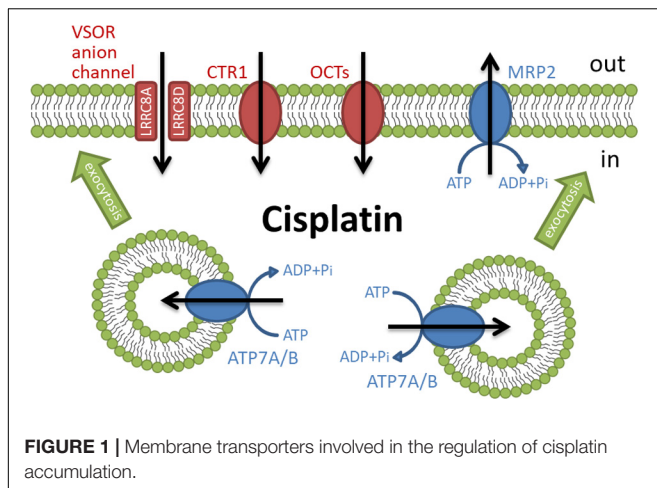
Volume-sensitive outwardly rectifying (VSOR) anion channels (called volume-regulated anion channels: VRAC) are also considered to mediate cisplatin influx (Planells-Cases et al., 2015; Jentsch et al., 2016) and contribute to the cisplatin resistance (Lee et al., 2007; Shimizu et al., 2008). The VSOR anion channels generally play principal roles in cell volume recovering after cell swelling and initial cell shrinkage on apoptotic cell death (Okada et al., 2001; Shimizu et al., 2004; Pedersen et al., 2016; Okada et al., 2019). Recent studies demonstrated that the VSOR anion channels are composed of hetero-hexameric leucine-rich repeat-containing 8 (LRRC8) proteins with four membrane-spanning domains and intracellular C-terminal leucine-rich repeat domains (Qiu et al., 2014; Voss et al., 2014; Deneka et al., 2018; Kasuya et al., 2018; Kefauver et al., 2018). The LRRC8 family consists of five members LRRC8A to LRRC8E. LRRC8A is an essential component to form VSOR anion channels. Interestingly, the stoichiometry of LRRC8 proteins modifies the electrophysiological properties of VSOR anion channels. The combination of LRRC8A with LRRC8C or LRRC8E exhibits slower or faster inactivation of VSOR anion channel currents at positive potentials, respectively (Voss et al., 2014; Ullrich et al., 2016). LRRC8D regulates the permeability

of VSOR anion channels (Lee et al., 2014; Planells-Cases et al., 2015). The transport of organic compounds such as osmolyte taurine, antibiotic blasticidin S, and chemotherapeutic cisplatin is dependent on the incorporation of LRRC8D into VSOR anion channels. Thus, cisplatin would pass through LRRC8D-containing VSOR anion channels. Consistently, the structural study using the cryo-electron microscopy revealed that LRRC8D homo-hexamers have a wider pore compared with LRRC8A (Nakamura et al., 2020). Intriguingly, ovarian cancer patients with low LRRC8D expression significantly exhibited poor prognosis in cisplatin therapies (Planells-Cases et al., 2015).

Some ATP-dependent active transporters are involved in the cisplatin efflux. ATP7A and ATP7B are known to be P-type ATPases to export an excess of copper (Li et al., 2018). These transporters located at the *trans*-Golgi network sequester copper from the cytosol and the accumulated copper in the *trans*-Golgi network might be released from the cell via a secretory vesicle pathway (Suzuki and Gitlin, 1999). ATP7A and ATP7B similarly transport cisplatin and regulate cisplatin sensitivity (Samimi et al., 2004). Interestingly, these transporters mainly existed at the *trans*-Golgi network in the cisplatin-sensitive cancer cells but distributed in more peripherally located vesicles in its cisplatin-resistant cells (Kalayda et al., 2008). These results suggest that cisplatin regulates the rapid trafficking of these transporters between the *trans*-Golgi network and the secretory vesicles. Moreover, several cisplatin-resistant cancer cells exhibited an increased expression of ATP7A and ATP7B (Katano et al., 2002). Multidrug resistance-associated protein 2 (MRP2), a member of the ATP-binding cassette (ABC) transporter family, also exports cisplatin as a conjugate with glutathione (Koike et al., 1997; Kawabe et al., 1999) and contributes to the cisplatin resistance (Taniguchi et al., 1996; Cui et al., 1999; Hinoshita et al., 2000). MRP2 localizes in the apical membrane of various cells and the ability of MRP2 to transport cisplatin confers the cisplatin resistance (Borst et al., 1999). Besides, cancer patients with a high level of MRP2 expression showed less sensitivity to cisplatin therapies (Korita et al., 2010; Yamasaki et al., 2011; Halon et al., 2013). Thus, the active transporters such as ATP7A/B and MRP2 regulate cisplatin efflux, although the ways to transport cisplatin are different. These results suggest that the expression of these ATP-dependent cisplatin exporters decreases intracellular cisplatin accumulation, resulting in the cisplatin resistance of cancer cells.

INCREASED DNA DAMAGE REPAIR IN CISPLATIN RESISTANCE

Accumulated cisplatin forms interstrand and intrastrand cross-link with DNA, resulting in DNA damage. Two different pathways generally contribute to DNA repair: nucleotide excision repair (NER) and mismatch repair (MMR). The NER removes the bulky DNA adducts induced by cisplatin. On the other hand, the MMR corrects single-strand DNA errors during DNA replication. The protein expression involved in the NER and MMR processes positively and negatively correlates with the cisplatin resistance, respectively. The following reviews describe



the detailed mechanism of the NER and MMR process in the cisplatin resistance (Martin et al., 2008; Rocha et al., 2018; Damia and Brogini, 2019).

INACTIVATED APOPTOTIC SIGNALING PATHWAY IN CISPLATIN RESISTANCE

Apoptosis, a programmed cell death observed in old and unwanted cells, is characterized by morphological and biochemical features such as initial cell shrinkage (called apoptotic volume decrease: AVD), cell membrane blebbing, cytochrome c release, chromatin condensation, caspase activation, DNA fragmentation, and apoptotic body formation (Maeno et al., 2000; Saraste and Pulkki, 2000; Okada et al., 2001; Barros et al., 2003). Cisplatin activates multiple signaling pathways such as reactive oxygen species (ROS), a tumor suppressor gene p53, and mitogen-activated protein kinases (MAPKs) to induce these phenomena.

As mentioned above, the VSOR anion channels mediate the cisplatin influx. On the other hand, the VSOR anion channels also contribute to the induction of AVD, a hallmark of an early stage of apoptosis. The AVD is accompanied by a coupled activation of K^+ channels and the VSOR anion channels (Maeno et al., 2000; Okada et al., 2001; Shimizu et al., 2004). Importantly, the AVD precedes other apoptotic events because blockers of K^+ channels and the VSOR anion channels inhibited cytochrome c release, caspase activation, and DNA fragmentation triggered by mitochondria- and death receptor-mediated apoptotic inducers in various types of cells (Maeno et al., 2000). The VSOR anion channel activities are also essential for cisplatin-induced apoptosis in human epidermoid carcinoma KB cells (Ise et al., 2005). A VSOR anion channel blocker not only suppressed caspase activation and cell death after exposure to cisplatin but also lowered the concentration dependence of cisplatin on cell viability. Intriguingly, the cisplatin-resistant cells including KCP-4 cells derived from KB cells (Lee et al., 2007), mouse Ehrlich ascites tumor cells (MDR-EATC: Poulsen et al., 2010), and human lung adenocarcinoma A549/CDDP cells (Min et al., 2011) exhibited downregulation of VSOR anion channel activities.

Notably, the expression of LRRC8 members, components of the VSOR anion channel, is comparable between the parent KB cells and its cisplatin-resistant KCP-4 cells (Okada et al., 2017; Shimizu et al., 2020). These results suggest that the activation signals but not the expression of the VSOR anion channels are associated with the cisplatin resistance of KCP-4 cells. Histone deacetylases (HDACs) are essential enzymes for the regulation of gene expression. Their inhibition enhances gene transcription and reverses aberrant epigenetic changes associated with cancers (Bolden et al., 2006). Interestingly, HDAC inhibitors such as trichostatin A and apicidin recovered the function of the VSOR anion channels in KCP-4 cells, resulting in the enhanced cisplatin potency (Lee et al., 2007; Shimizu et al., 2008). This result strengthens that the AVD triggered by cisplatin-induced activation of the VSOR anion channels is pivotal for the induction of apoptosis.

We previously demonstrated that staurosporine, a mitochondria-mediated apoptotic inducer, generated ROS, resulting in the activation of the VSOR anion channels (Shimizu et al., 2004). Thus, ROS production is one of the factors inducing AVD. The mitochondrial electron transport chain in the mitochondrial inner membrane and the NADPH oxidase complex (NOX) at the plasma membrane are the major ROS generators (Liu et al., 2002; Meitzler et al., 2014; Kim et al., 2019). The mitochondrial electron transport chain generates superoxide converted to hydrogen peroxide in the intermembrane space or the matrix of mitochondria. The transmembrane enzyme NOX produces superoxide from oxygen. Cisplatin exposure induced the ROS production via the electron transport chain impairment triggered by direct damage of mitochondrial DNA (Marullo et al., 2013) and the activation of NOX isoforms at the plasma membrane (Kim et al., 2010). Some cisplatin-resistant cancer cells highly expressed superoxide dismutase 1, a superoxide scavenger, compared with the parent cells (Brown et al., 2009; Hour et al., 2010). Liu et al. (2020) recently found an increased expression of mitochondrial apurinic/aprimidinic endonuclease 1 (mtAPE1) in cisplatin-resistant cancer cells. The mtAPE1 expression negatively correlated with intracellular ROS levels. These results suggest that the redox homeostasis contributes to the cisplatin resistance.

The activation of a tumor suppressor gene p53 is known to be essential for cisplatin-mediated apoptosis. As a transcriptional factor, p53 controls the gene transcription to promote apoptosis (Fridman and Lowe, 2003). The members of the Bcl-2 family are one of the transcriptional targets for p53. During apoptosis, p53 promotes the transcription of pro-apoptotic proteins including Bax, Puma, Noxa, and Bid (Miyashita et al., 1994; Oda et al., 2000; Nakano and Voutsden, 2001; Sax et al., 2002) and suppress that of anti-apoptotic proteins Bcl-2 (Wu et al., 2001). Interestingly, cancer patients who respond to cisplatin had a higher frequency of p53-positive cells than non-responders (Garzetti et al., 1996). These suggest that the cisplatin efficacy positively correlates with the function of p53 among cancers. Importantly, half of the cancer patients carry mutations of p53 (Toledo and Wahl, 2006).

Mitogen-activated protein kinases (MAPKs), serine/threonine kinases, play pivotal roles in physiological functions such as cell survival, proliferation, migration, and apoptosis (Dhillon et al., 2007). In mammals, members of the MAPK family include

extracellular signal-regulated kinase (ERK), c-Jun N-terminal kinase (JNK), and p38 kinase. The activation of these MAPKs is essential for cisplatin-induced apoptosis. Not only cisplatin activates all ERK, JNK, and p38 kinase during apoptosis, but also reduced activation of these MAPKs correlates with the cisplatin resistance (Brozovic and Osmak, 2007). In cisplatin-induced apoptosis, the p53 transcriptional activity preceded the activation of p38 (Bragado et al., 2007). Since all MAPKs target and phosphorylate p53 at its different positions (Yue and López, 2020), on the other hand, MAPKs are an upstream signal of p53-mediated regulation. These results suggest that there might be the crosstalk between p53 and MAPKs in cisplatin-triggered signaling pathways, resulting in positive feedback loops (see Figure 2).

THE ROLE OF THE ACTIN CYTOSKELETON IN CISPLATIN-INDUCED APOPTOSIS

The actin cytoskeleton is a principal structure that is essential for various cellular functions such as intracellular trafficking, contraction, motility, and apoptosis (Desouza et al., 2012). The monomer actin, a globular protein (G-actin), forms actin

filaments (F-actin) by twisting two strands of G-actin. The F-actin structure is highly dynamic. The F-actin reversibly polymerizes and depolymerizes during cellular functions. The Rho family of small GTPase is an indispensable regulator of the actin cytoskeleton organization (Mokady and Meiri, 2015). The Rho GTPases function as molecular switch shifting between two conformations: a GDP-bound inactive state and a GTP-bound active state. The increased activities of Rho GTPases regulate the rearrangement of the actin cytoskeleton organization by interacting with various effector proteins.

The actin cytoskeleton dramatically changes in the apoptotic process (Desouza et al., 2012). However, the actin cytoskeleton organization during apoptosis seems to be complicated. Some cells showed actin polymerization after apoptotic stimuli (Ishimoto et al., 2011), whereas the other cells exhibited actin depolymerization during apoptosis (Udi et al., 2011; Ohno et al., 2013). Consistently, a stabilizer of F-actin, jasplakinolide, induced apoptosis (Posey and Bierer, 1999; Odaka et al., 2000). On the other hand, an inhibitor of actin polymerization, cytochalasin D, also resulted in apoptotic responses (Suria et al., 1999; Paul et al., 2002). Surprisingly, both jasplakinolide and cytochalasin D initiate apoptosis in the same human airway epithelial 1HAEO⁻ cells (White et al., 2001). These results suggest that the F-actin dynamics rather than the states of actin cytoskeleton would be associated with apoptotic induction.

In the case of cisplatin-triggered apoptosis, the actin cytoskeleton is markedly modified. Table 1 summarizes the effects of cisplatin on F-actin in various types of cells. Cisplatin increased cell stiffness via the stabilization of F-actin in several human prostate cells (Raudenska et al., 2019) and also depolymerized F-actin in human mammary carcinoma MCF-7 cells (Zeidan et al., 2008) and porcine oocytes (Zhou et al., 2019). We observed that cisplatin enhanced the F-actin staining in KB cells (Figure 3A). Interestingly, cisplatin-induced F-actin rearrangement is reported to be an initial phase of apoptosis (Kruidering et al., 1998; Rebillard et al., 2010). Besides, cisplatin changes membrane organization and fluidity during early apoptosis (Martinho et al., 2019). Thus, the regulation of actin cytoskeleton dynamics would be a membrane-associated signaling pathway in cisplatin-induced apoptosis.

How do actin cytoskeleton dynamics modulate cisplatin-induced apoptosis? One of the answers is that F-actin regulates the expression and function of membrane transporters involved in cisplatin transport. The previous reports demonstrated that the rearrangement of F-actin increased the expression of cisplatin importer CTR1 (Abdellatef et al., 2015) and that the translocation of cisplatin exporters, ABC7A and ABC7B, from the *trans*-Golgi network to the plasma membrane is regulated by the formation of F-actin (Cobbold et al., 2002; Gupta et al., 2016). It is well known that the actin cytoskeleton regulates the VSOR anion channels, which contributes to cisplatin influx and sustained cell shrinkage during early apoptosis. The regulation patterns are dependent on cell types: the actin polymerization involves the activation of VSOR anion channels in some cells (Fatherazi et al., 1994; Zhang et al., 1997; Wei et al., 2003; Catacuzzano et al., 2014; Burow et al., 2015), whereas the VSOR anion channel activation requires the F-actin disruption in the other cells (Levitan et al.,

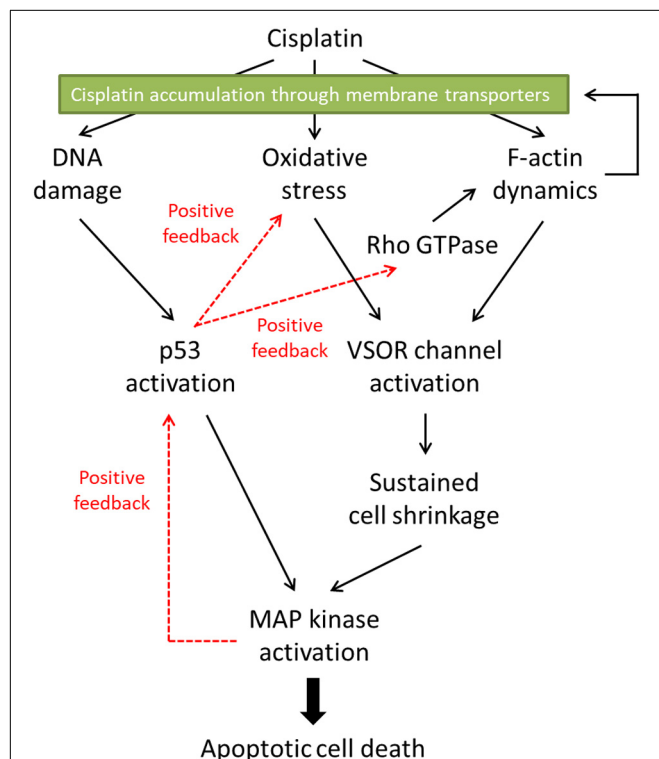
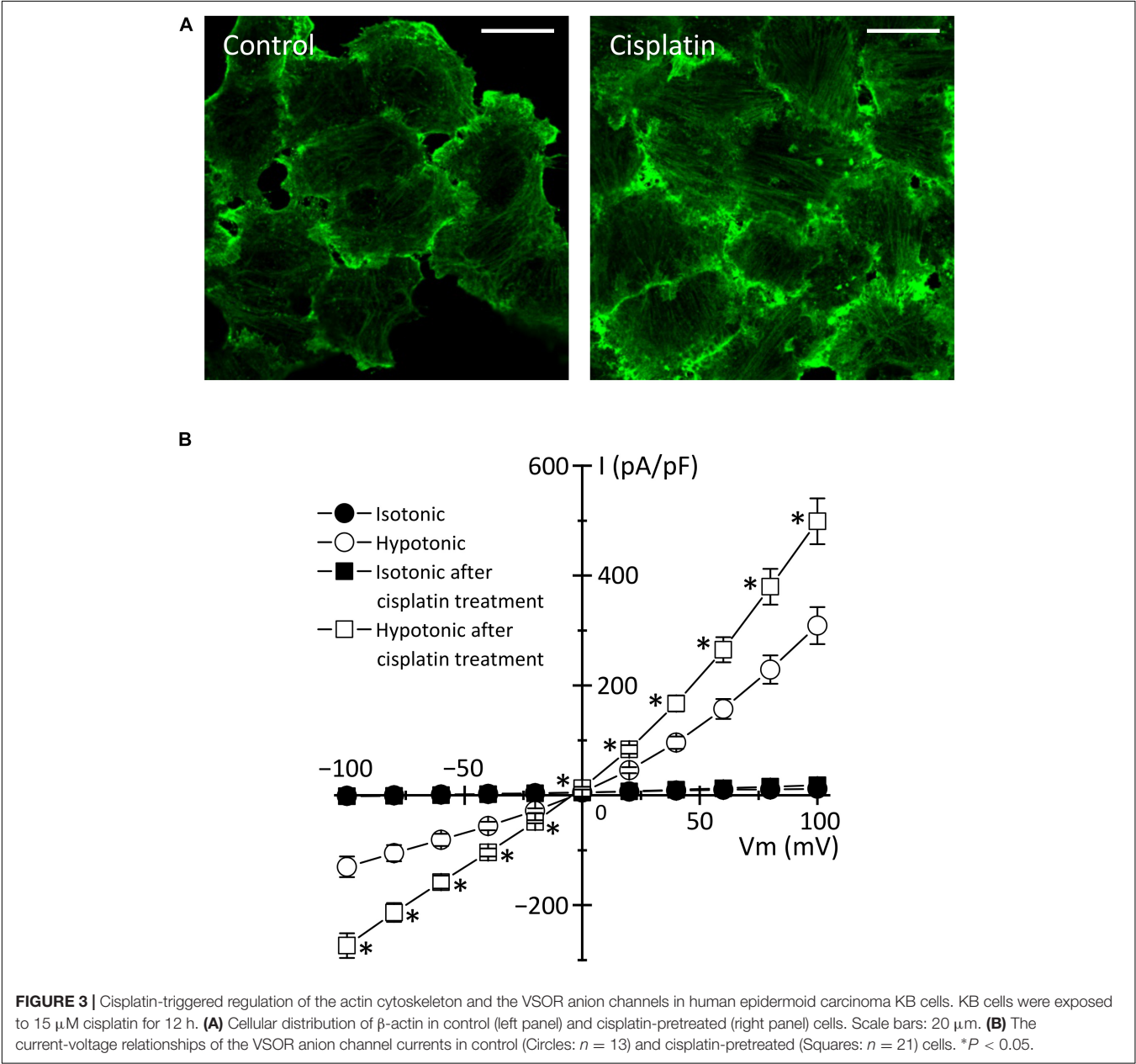


FIGURE 2 | The proposed signaling pathways in cisplatin-induced apoptosis. Cisplatin-resistant cancer cells may interfere with the F-actin dynamics, resulting in the inhibition of the subsequent apoptotic signals. Furthermore, the disturbed F-actin dynamics could reduce the functional expression of cisplatin transporters on the plasma membrane, decreasing the cisplatin accumulation in the cells.

TABLE 1 | F-actin regulation triggered by cisplatin in various types of cells.

Cells	A state of the actin cytoskeleton	Reference
Human prostatic epithelial PNT1A cells. Human prostate carcinoma 22Rv1 and PC-3 cells.	Increased number and length of F-actin.	Raudenska et al., 2019
Human colon carcinoma HT-29 cells	Transient actin polymerization at cell edges.	Rebillard et al., 2010
Human epidermoid carcinoma KB cells	Enhanced staining for F-actin.	Figure 3
Human mammary carcinoma MCF-7 cells	Disruption of membrane-bound F-actin.	Zeidan et al., 2008
Porcine oocytes	Impaired assembly of F-actin.	Zhou et al., 2019
Primary porcine proximal tubular cells. Porcine renal proximal tubular LLC-PK1 cells.	Depolymerization of F-actin.	Kruidering et al., 1998
Cisplatin-resistant human ovarian cancer CP70, OVCAR5-CisR, PE06, and SKOV3-CisR cells.	High density of F-actin networks.	Sharma et al., 2012, 2014
Cisplatin-resistant human epidermoid carcinoma KB-CP20 cells. Cisplatin-resistant human liver carcinoma 7404-CP20 cells.	Cluster type of actin cytoskeleton.	Shen et al., 2004
Cisplatin-resistant human epidermoid carcinoma KCP-4 cells.	Disrupted F-actin networks.	Shimizu et al., 2020



1995; Shen et al., 1999; Morishima et al., 2000). Intriguingly, the cisplatin-induced formation of the F-actin structure enhanced the activities of the VSOR anion channel currents in KB cells (**Figure 3B**). These regulations of membrane transporters by the actin cytoskeleton organization would change the cisplatin accumulation, modulating the following apoptotic processes.

THE CISPLATIN-RESISTANT CELLS EXHIBIT ABNORMAL ACTIN CYTOSKELETON DYNAMICS

Although the mechanism of the cisplatin resistance is quite complicated, the dynamic changes in the actin cytoskeleton organization are recently known to be involved in the cisplatin resistance. Some cisplatin-resistant cancer cells have higher stiffness than their parent cells sensitive to cisplatin (Sharma et al., 2012, 2014). In contrast, the other cancer cells with the cisplatin resistance exhibit the disrupted actin cytoskeleton compared with their cisplatin-sensitive cells (**Figure 4**; Shen et al., 2004; Shimizu et al., 2020). Although little is known about how the difference of F-actin occurs in the cisplatin-resistant cells, the different expression of Rho GTPases may contribute. The Rho subfamily of Rho GTPases composed of RhoA, RhoB, and RhoC is one of the key regulators of actin cytoskeletal organization (Aspenström et al., 2004). Cancer cells exhibit distinct expression

levels of these proteins: RhoA and RhoC are highly expressed, whereas RhoB is downregulated in various human tumors (Mokady and Meiri, 2015). Interestingly, the decrease in RhoB expression was associated with the cisplatin resistance in human laryngeal carcinoma cells (Čimborá-Zovko et al., 2010). Therefore, the expression balance of these Rho GTPases might modulate the F-actin dynamics and the subsequent sensitivity to cisplatin in cancer cells. Notably, the cisplatin-induced p53 transcriptional activity is linked with the Rho GTPase pathways (Xia and Land, 2007). The epigenetic regulation of Rho GTPases by p53 may alter the F-actin organization. This pathway would cause positive feedback loops (see **Figure 2**), which might contribute to the chronic changes in the actin cytoskeleton of cisplatin-resistant cells. In the cisplatin resistance, the barrier function of the actin cytoskeleton might not be essential, because the cells with disturbed F-actin exhibit the cisplatin resistance. The membrane-associated signaling pathways regulated by the F-actin dynamics may modulate the cisplatin resistance.

THE REGULATION OF VSOR ANION CHANNELS BY ACTIN CYTOSKELETON IN CISPLATIN-RESISTANT CELLS

We and others previously demonstrated that some cisplatin-resistant cancer cells exhibited decreased activities of the VSOR

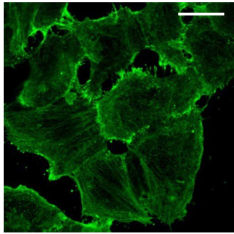
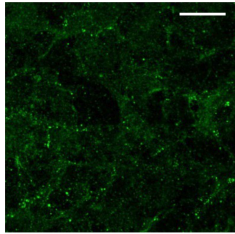
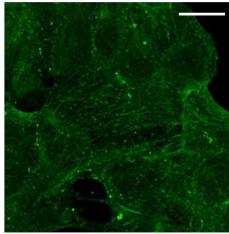
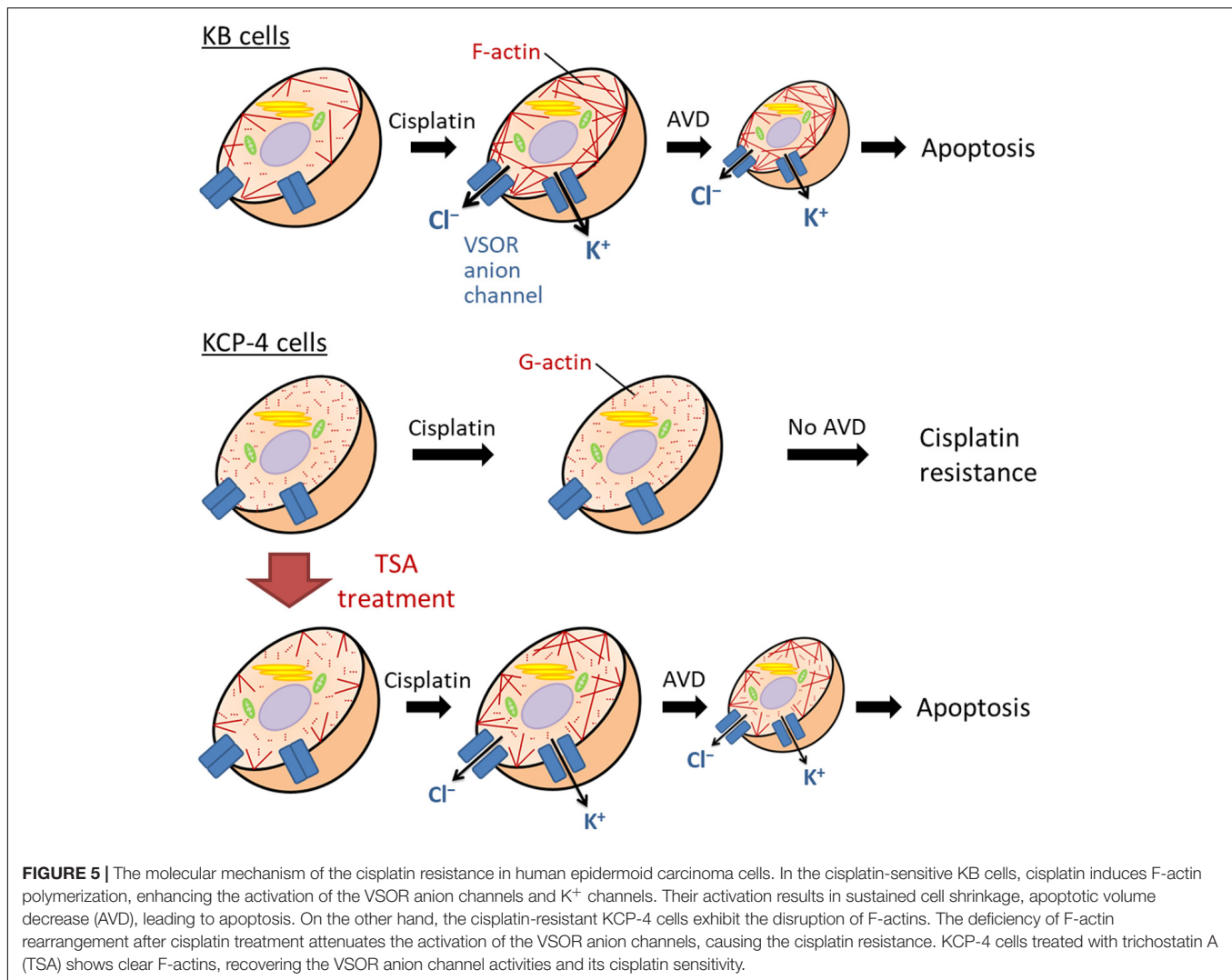
	KB cells	KCP-4 cells	KCP-4 cells treated with TSA
β -actin image			
F-actin network	++	–	+
VSOR activity	++	–	+
Cisplatin-induced apoptosis	++	–	+

FIGURE 4 | The relationship between actin network, VSOR activity, and cisplatin-induced apoptosis. Cellular distribution of β -actin in human epidermoid carcinoma KB cells (**left**), its cisplatin-resistant KCP-4 cells (**middle**), and KCP-4 cells treated with 400 nM trichostatin A (TSA) for 30 h (**right**) are shown in the upper lane. Scale bars: 20 μ m. The degrees of F-actin network, VSOR activity, and cisplatin-induced apoptosis in each cell group are indicated as ++: strongly positive, +: positive, and –: negative. There is a close relationship between them.



anion channels compared with their parent cells sensitive to cisplatin (Lee et al., 2007; Poulsen et al., 2010; Min et al., 2011). In the cisplatin-resistant KCP-4 cells, interestingly, the downregulation of the VSOR anion channels was associated with the disruption of F-actin but not the expression of LRRC8 members (Shimizu et al., 2020). Additionally, the inhibition of actin cytoskeleton dynamics by β -actin knockdown or cytochalasin D treatment in the parent KB cells decreased the VSOR anion channel currents and suppressed cisplatin-induced apoptosis. Intriguingly, treatment of KCP-4 cells with an HDAC inhibitor trichostatin A, which promotes gene transcription, induced a marked increase of β -actin. The KCP-4 cells exposed to trichostatin A exhibited clear F-actin and recovered the VSOR anion channel activities, resulting in the restoration of cisplatin sensitivity (Figure 4: Lee et al., 2007; Shimizu et al., 2020). These results suggest that the defect of the VSOR anion channel activities by impaired F-actin dynamics contributes to the cisplatin resistance. Figure 5 illustrates how the VSOR anion channel modulates the sensitivity to cisplatin in KB and KCP-4 cells. As described above, the VSOR anion channels play

essential roles in apoptotic induction. The dysfunction of the VSOR anion channels would decrease the cisplatin influx and suppress initial cell shrinkage during apoptosis, leading to the cisplatin resistance.

DISCUSSION/CONCLUSION

The cisplatin resistance of cancer cells is one of the therapeutic problems. In this review, we summarized the roles of the actin cytoskeleton and membrane transporters in cisplatin-induced apoptosis and the cisplatin resistance. Figure 2 indicates the proposed signaling pathways in cisplatin-induced apoptosis. Cisplatin generates oxidative stress and modulates F-actin dynamics, resulting in the activation of the VSOR anion channels. The following sustained cell shrinkage is reported to activate the stress-responsive MAPK cascade for the apoptotic induction (Hasegawa et al., 2012). Cisplatin also induces DNA damage by cross-linking or in response to generated oxidative stress (Salehi et al., 2018). The DNA damage activates a transcriptional factor

p53, which causes the subsequent MAPK phosphorylation to induce apoptosis. This p53-mediated MAPK activation would be mediated by the accumulation of ROS (Shi et al., 2014). Besides, the increased activity of MAPK triggers further activation of p53 (Yue and López, 2020). On the other hand, the p53 activation would regulate the F-actin dynamics via the Rho GTPase activities (Xia and Land, 2007; Rebillard et al., 2010). These signals create positive feedback loops. Thus, the signal cascade induced by cisplatin would be complex.

Many mechanisms involved in reduced intracellular cisplatin accumulation, increased DNA damage repair, and inactivation of the apoptotic signaling pathway contribute to the cisplatin resistance. We here propose that the regulation of membrane transporters by the actin cytoskeleton dynamics has a significant role in the cisplatin resistance. The state of F-actin may not be critical, because some cisplatin-resistant cancer cells have different states of the actin cytoskeleton. The impaired F-actin dynamics may modulate the expression and function of membrane transporters carrying cisplatin. Several cisplatin-resistant cancer cells showed decreased activities of the VSOR anion channels. The actin cytoskeleton organization would contribute to the functional defect of the VSOR anion channels. However, we do not know

how impaired actin dynamics modulate the VSOR anion channel activities in the cisplatin-resistant cancer cells. Further understandings of the relationship between F-actin dynamics and the VSOR anion channel function would be attractive. The VSOR anion channel is responsible for the early events of apoptosis, such as the cisplatin influx and the sustained cell shrinkage AVD. Given that reduced activities of the VSOR anion channels closely correlate with the cisplatin resistance of cancer cells, the VSOR anion channels may be one of the potential therapeutic targets to overcome the cisplatin resistance.

AUTHOR CONTRIBUTIONS

TS, TF, and HS wrote and edited the manuscript. All authors contributed to the article and approved the submitted version.

FUNDING

This work was in part supported by JSPS KAKENHI Grant Numbers JP15K15029, JP16K08490, and JP17K08531.

REFERENCES

- Abdellatef, S. A., Tange, R., Sato, T., Ohi, A., Nabatame, T., and Taniguchi, A. (2015). Nanostructures control the hepatocellular responses to a cytotoxic agent “cisplatin.” *Biomed. Res. Int.* 2015:925319. doi: 10.1155/2015/925319
- Aspenström, P., Fransson, Å., and Saras, J. (2004). Rho GTPases have diverse effects on the organization of the actin filament system. *Biochem. J.* 377, 327–337. doi: 10.1042/BJ20031041
- Barros, L. F., Kanaseki, T., Sabirov, R., Morishima, S., Castro, J., Bittner, C. X., et al. (2003). Apoptotic and necrotic blebs in epithelial cells display similar neck diameters but different kinase dependency. *Cell Death Differ.* 10, 687–697. doi: 10.1038/sj.cdd.4401236
- Bolden, J. E., Peart, M. J., and Johnstone, R. W. (2006). Anticancer activities of histone deacetylase inhibitors. *Nat. Rev. Drug Discov.* 5, 769–784. doi: 10.1038/nrd2133
- Borst, P., Evers, R., Kool, M., and Wijnholds, J. (1999). The multidrug resistance protein family. *Biochim. Biophys. Acta Biomembr.* 1461, 347–357. doi: 10.1016/S0005-2736(99)00167-4
- Boulikas, T., and Vougiouka, M. (2004). Recent clinical trials using cisplatin, carboplatin and their combination chemotherapy drugs. *Oncol. Rep.* 11, 559–595. doi: 10.3892/or.11.3.559
- Bragado, P., Armesilla, A., Silva, A., and Porras, A. (2007). Apoptosis by cisplatin requires p53 mediated p38 α MAPK activation through ROS generation. *Apoptosis* 12, 1733–1742. doi: 10.1007/s10495-007-0082-8
- Brown, D. P. G., Chin-Sinex, H., Nie, B., Mendonca, M. S., and Wang, M. (2009). Targeting superoxide dismutase 1 to overcome cisplatin resistance in human ovarian cancer. *Cancer Chemother. Pharmacol.* 63, 723–730. doi: 10.1007/s00280-008-0791-x
- Brozovic, A., and Osmak, M. (2007). Activation of mitogen-activated protein kinases by cisplatin and their role in cisplatin-resistance. *Cancer Lett.* 251, 1–16. doi: 10.1016/j.canlet.2006.10.007
- Burrow, P., Klapperstück, M., and Markwardt, F. (2015). Activation of ATP secretion via volume-regulated anion channels by sphingosine-1-phosphate in RAW macrophages. *Pflügers Arch. Eur. J. Physiol.* 467, 1215–1226. doi: 10.1007/s00424-014-1561-8
- Catacuzzeno, L., Michelucci, A., Sforza, L., Aiello, F., Sciacaluga, M., Fioretti, B., et al. (2014). Identification of key signaling molecules involved in the activation of the swelling-activated chloride current in human glioblastoma cells. *J. Membr. Biol.* 247, 45–55. doi: 10.1007/s00232-013-9609-9
- Ciarimboli, G., Ludwig, T., Lang, D., Pavenstädt, H., Koepsell, H., Piechota, H. J., et al. (2005). Cisplatin nephrotoxicity is critically mediated via the human organic cation transporter 2. *Am. J. Pathol.* 167, 1477–1484. doi: 10.1016/S0002-9440(10)61234-5
- Čimbora-Zovko, T., Fritz, G., Mikac, N., and Osmak, M. (2010). Downregulation of RhoB GTPase confers resistance to cisplatin in human laryngeal carcinoma cells. *Cancer Lett.* 295, 182–190. doi: 10.1016/j.canlet.2010.02.025
- Cobbold, C., Monaco, A. P., Ponnambalam, S., and Francis, M. J. (2002). Novel membrane traffic steps regulate the exocytosis of the Menkes disease ATPase. *Hum. Mol. Genet.* 11, 2855–2866. doi: 10.1093/hmg/11.23.2855
- Cui, Y., König, J., Buchholz, U., Spring, H., Leier, I., and Keppler, D. (1999). Drug resistance and ATP-dependent conjugate transport mediated by the apical multidrug resistance protein, MRP2, permanently expressed in human and canine cells. *Mol. Pharmacol.* 55, 929–937.
- Damia, G., and Broggini, M. (2019). Platinum resistance in ovarian cancer: role of DNA repair. *Cancers* 11:119. doi: 10.3390/cancers11010119
- Deneka, D., Sawicka, M., Lam, A. K. M., Paulino, C., and Dutzler, R. (2018). Structure of a volume-regulated anion channel of the LRRC8 family. *Nature* 558, 254–259. doi: 10.1038/s41586-018-0134-y
- Desouza, M., Gunning, P. W., and Stehn, J. R. (2012). The actin cytoskeleton as a sensor and mediator of apoptosis. *Bioarchitecture* 2, 75–87. doi: 10.4161/bioa.20975
- Dhillon, A. S., Hagan, S., Rath, O., and Kolch, W. (2007). MAP kinase signalling pathways in cancer. *Oncogene* 26, 3279–3290. doi: 10.1038/sj.onc.1210421
- Fatherazi, S., Izutsu, K. T., Wellner, R. B., and Belton, C. M. (1994). Hypotonically activated chloride current in HSG cells. *J. Membr. Biol.* 142, 181–193.
- Fridman, J. S., and Lowe, S. W. (2003). Control of apoptosis by p53. *Oncogene* 22, 9030–9040. doi: 10.1038/sj.onc.1207116
- Garzetti, G. G., Ciavattini, A., Provinciali, M., Di Stefano, G., Lucarini, G., Goteri, G., et al. (1996). Expression of p53 and apoptosis of tumor cells in locally advanced cervical carcinoma after cisplatin based neoadjuvant chemotherapy. *Anticancer Res.* 16, 3229–3234.
- Gupta, A., Schell, M. J., Bhattacharjee, A., Lutsenko, S., and Hubbard, A. L. (2016). Myosin Vb mediates Cu⁺ export in polarized hepatocytes. *J. Cell Sci.* 129, 1179–1189. doi: 10.1242/jcs.175307

- Halon, A., Materna, V., Donizy, P., Matkowski, R., Rabczynski, J., Lage, H., et al. (2013). MRP2 (ABCC2, cMOAT) expression in nuclear envelope of primary fallopian tube cancer cells is a new unfavorable prognostic factor. *Arch. Gynecol. Obstet.* 287, 563–570. doi: 10.1007/s00404-012-2589-7
- Hasegawa, Y., Shimizu, T., Takahashi, N., and Okada, Y. (2012). The apoptotic volume decrease is an upstream event of MAP kinase activation during staurosporine-induced apoptosis in HeLa cells. *Int. J. Mol. Sci.* 13, 9363–9379. doi: 10.3390/ijms13079363
- Hinoshita, E., Uchiumi, T., Taguchi, K. I., Kinukawa, N., Tsuneyoshi, M., Maehara, Y., et al. (2000). Increased expression of an ATP-binding cassette superfamily transporter, multidrug resistance protein 2, in human colorectal carcinomas. *Clin. Cancer Res.* 6, 2401–2407. doi: 10.1158/1078-0432.CCR-00-0133
- Hour, T.-C., Lai, Y.-L., Kuan, C.-I., Chou, C.-K., Wang, J.-M., Tu, H.-Y., et al. (2010). Transcriptional up-regulation of SOD1 by CEBPD: a potential target for cisplatin resistant human urothelial carcinoma cells. *Biochem. Pharmacol.* 80, 325–334. doi: 10.1016/j.bcp.2010.04.007
- Howell, S. B., Safaei, R., Larson, C. A., and Sailor, M. J. (2010). Copper transporters and the cellular pharmacology of the platinum-containing cancer drugs. *Mol. Pharmacol.* 77, 887–894. doi: 10.1124/mol.109.063172
- Ise, T., Shimizu, T., Lee, E. L., Inoue, H., Kohno, K., and Okada, Y. (2005). Roles of volume-sensitive Cl⁻ channel in cisplatin-induced apoptosis in human epidermoid cancer cells. *J. Membr. Biol.* 205, 139–145. doi: 10.1007/s00232-005-0779-y
- Ishida, S., Lee, J., Thiele, D. J., and Herskowitz, I. (2002). Uptake of the anticancer drug cisplatin mediated by the copper transporter Ctr1 in yeast and mammals. *Proc. Natl. Acad. Sci. U.S.A.* 99, 14298–14302. doi: 10.1073/pnas.162491399
- Ishimoto, T., Ozawa, T., and Mori, H. (2011). Real-time monitoring of actin polymerization in living cells using split luciferase. *Bioconjug. Chem.* 22, 1136–1144. doi: 10.1021/bc100595z
- Jentsch, T. J., Lutter, D., Planells-Cases, R., Ullrich, F., and Voss, F. K. (2016). VRAC: molecular identification as LRRC8 heteromers with differential functions. *Pflügers Arch. Eur. J. Physiol.* 468, 385–393. doi: 10.1007/s00424-015-1766-5
- Kalayda, G. V., Wagner, C. H., Buß, I., Reedijk, J., and Jaehde, U. (2008). Altered localisation of the copper efflux transporters ATP7A and ATP7B associated with cisplatin resistance in human ovarian carcinoma cells. *BMC Cancer* 8:175. doi: 10.1186/1471-2407-8-175
- Kalayda, G. V., Wagner, C. H., and Jaehde, U. (2012). Relevance of copper transporter 1 for cisplatin resistance in human ovarian carcinoma cells. *J. Inorg. Biochem.* 116, 1–10. doi: 10.1016/j.jinorgbio.2012.07.010
- Kasuya, G., Nakane, T., Yokoyama, T., Jia, Y., Inoue, M., Watanabe, K., et al. (2018). Cryo-EM structures of the human volume-regulated anion channel LRRC8. *Nat. Struct. Mol. Biol.* 25, 797–804. doi: 10.1038/s41594-018-0109-6
- Katano, K., Kondo, A., Safaei, R., Holzer, A., Samimi, G., Mishima, M., et al. (2002). Acquisition of resistance to cisplatin is accompanied by changes in the cellular pharmacology of copper. *Cancer Res.* 62, 6559–6565.
- Kawabe, T., Chen, Z. S., Wada, M., Uchiumi, T., Ono, M., Akiyama, S. I., et al. (1999). Enhanced transport of anticancer agents and leukotriene C4 by the human canalicular multispecific organic anion transporter (cMOAT/MRP2). *FEBS Lett.* 456, 327–331. doi: 10.1016/S0014-5793(99)00979-5
- Kefauver, J. M., Saotome, K., Dubin, A. E., Pallesen, J., Cottrell, C. A., Cahalan, S. M., et al. (2018). Structure of the human volume regulated anion channel. *eLife* 7:E38461. doi: 10.7554/eLife.38461
- Kim, H.-J., Lee, J.-H., Kim, S.-J., Oh, G. S., Moon, H.-D., Kwon, K.-B., et al. (2010). Roles of NADPH oxidases in cisplatin-induced reactive oxygen species generation and ototoxicity. *J. Neurosci.* 30, 3933–3946. doi: 10.1523/JNEUROSCI.6054-09.2010
- Kim, S. J., Kim, H. S., and Seo, Y. R. (2019). Understanding of ROS-inducing strategy in anticancer therapy. *Oxid. Med. Cell. Longev.* 2019:5381692. doi: 10.1155/2019/5381692
- Koike, K., Kawabe, T., Tanaka, T., Toh, S., Uchiumi, T., Wada, M., et al. (1997). A canalicular multispecific organic anion transporter (cMOAT) antisense cDNA enhances drug sensitivity in human hepatic cancer cells. *Cancer Res.* 57, 5475–5479.
- Korita, P. V., Wakai, T., Shirai, Y., Matsuda, Y., Sakata, J., Takamura, M., et al. (2010). Multidrug resistance-associated protein 2 determines the efficacy of cisplatin in patients with hepatocellular carcinoma. *Oncol. Rep.* 23, 965–972. doi: 10.3892/or_00000721
- Kruidering, M., Van De Water, B., Zhan, Y., Baelde, J. J., De Heer, E., Mulder, G. J., et al. (1998). Cisplatin effects on F-actin and matrix proteins precede renal tubular cell detachment and apoptosis in vitro. *Cell Death Differ.* 5, 601–614. doi: 10.1038/sj.cdd.4400392
- Kunii, E., Oguri, T., Kasai, D., Ozasa, H., Uemura, T., Takakuwa, O., et al. (2015). Organic cation transporter OCT6 mediates cisplatin uptake and resistance to cisplatin in lung cancer. *Cancer Chemother. Pharmacol.* 75, 985–991. doi: 10.1007/s00280-015-2723-x
- Lambert, I. H., and Sørensen, B. H. (2018). Facilitating the cellular accumulation of Pt-based chemotherapeutic drugs. *Int. J. Mol. Sci.* 19:2249. doi: 10.3390/ijms19082249
- Lebwohl, D., and Canetta, R. (1998). Clinical development of platinum complexes in cancer therapy: an historical perspective and an update. *Eur. J. Cancer* 34, 1522–1534. doi: 10.1016/S0959-8049(98)00224-X
- Lee, C. C., Freinkman, E., Sabatini, D. M., and Ploegh, H. L. (2014). The protein synthesis inhibitor blasticidin S enters mammalian cells via Leucine-rich repeat-containing protein 8D. *J. Biol. Chem.* 289, 17124–17131. doi: 10.1074/jbc.M114.571257
- Lee, E. L., Shimizu, T., Ise, T., Numata, T., Kohno, K., and Okada, Y. (2007). Impaired activity of volume-sensitive Cl⁻ channel is involved in cisplatin resistance of cancer cells. *J. Cell. Physiol.* 211, 513–521. doi: 10.1002/jcp.20961
- Levitan, I., Almonte, C., Mollard, P., and Garber, S. S. (1995). Modulation of a volume-regulated chloride current by F-actin. *J. Membr. Biol.* 147, 283–294.
- Li, Q., Peng, X., Yang, H., Rodriguez, J. A., and Shu, Y. (2012). Contribution of organic cation transporter 3 to cisplatin cytotoxicity in human cervical cancer cells. *J. Pharm. Sci.* 101, 394–404. doi: 10.1002/jps.22752
- Li, Y.-Q., Yin, J.-Y., Liu, Z.-Q., and Li, X.-P. (2018). Copper efflux transporters ATP7A and ATP7B: novel biomarkers for platinum drug resistance and targets for therapy. *IUBMB Life* 70, 183–191. doi: 10.1002/iub.1722
- Lin, X., Okuda, T., Holzer, A., and Howell, S. B. (2002). The copper transporter CTR1 regulates cisplatin uptake in *Saccharomyces cerevisiae*. *Mol. Pharmacol.* 62, 1154–1159. doi: 10.1124/mol.62.5.1154
- Liu, J. J., Lu, J., and McKeage, M. J. (2012). Membrane transporters as determinants of the pharmacology of platinum anticancer drugs. *Curr. Cancer Drug Targets* 12, 962–986. doi: 10.2174/156800912803251199
- Liu, Y., Fiskum, G., and Schubert, D. (2002). Generation of reactive oxygen species by the mitochondrial electron transport chain. *J. Neurochem.* 80, 780–787. doi: 10.1046/j.0022-3042.2002.00744.x
- Liu, Y., Zhang, Z., Li, Q., Zhang, L., Cheng, Y., and Zhong, Z. (2020). Mitochondrial APE1 promotes cisplatin resistance by downregulating ROS in osteosarcoma. *Oncol. Rep.* 44, 499–508. doi: 10.3892/or.2020.7633
- Maeno, E., Ishizaki, Y., Kanaseki, T., Hazama, A., and Okada, Y. (2000). Normotonic cell shrinkage because of disordered volume regulation is an early prerequisite to apoptosis. *Proc. Natl. Acad. Sci. U.S.A.* 97, 9487–9492. doi: 10.1073/pnas.140216197
- Martin, L. P., Hamilton, T. C., and Schilder, R. J. (2008). Platinum resistance: the role of DNA repair pathways. *Clin. Cancer Res.* 14, 1291–1295. doi: 10.1158/1078-0432.CCR-07-2238
- Martinho, N., Santos, T. C. B., Florindo, H. F., and Silva, L. C. (2019). Cisplatin-membrane interactions and their influence on platinum complexes activity and toxicity. *Front. Physiol.* 10:1898. doi: 10.3389/fphys.2018.01898
- Marullo, R., Werner, E., Degtyareva, N., Moore, B., Altavilla, G., Ramalingam, S. S., et al. (2013). Cisplatin induces a mitochondrial-ROS response that contributes to cytotoxicity depending on mitochondrial redox status and bioenergetic functions. *PLoS One* 8:e81162. doi: 10.1371/journal.pone.0081162
- Meitzler, J. L., Antony, S., Wu, Y., Juhasz, A., Liu, H., Jiang, G., et al. (2014). NADPH oxidases: a perspective on reactive oxygen species production in tumor biology. *Antioxid. Redox Signal.* 20, 2873–2889. doi: 10.1089/ars.2013.5603
- Min, X., Li, H., Hou, S., He, W., Liu, J., Hu, B., et al. (2011). Dysfunction of volume-sensitive chloride channels contributes to cisplatin resistance in human lung adenocarcinoma cells. *Exp. Biol. Med.* 236, 483–491. doi: 10.1258/ebm.2011.010297
- Miyashita, T., Krajewski, S., Krajewska, M., Wang, H. G., Lin, H. K., Liebermann, D. A., et al. (1994). Tumor suppressor p53 is a regulator of bcl-2 and bax gene expression in vitro and in vivo. *Oncogene* 9, 1799–1805.

- Mokady, D., and Meiri, D. (2015). RhoGTPases – A novel link between cytoskeleton organization and cisplatin resistance. *Drug Resist. Updat.* 19, 22–32. doi: 10.1016/j.drup.2015.01.001
- Morishima, S., Shimizu, T., Kida, H., and Okada, Y. (2000). Volume expansion sensitivity of swelling-activated Cl⁻ channel in human epithelial cells. *Jpn. J. Physiol.* 50, 277–280. doi: 10.2170/jphysiol.50.277
- Nakamura, R., Numata, T., Kasuya, G., Yokoyama, T., Nishizawa, T., Kusakizako, T., et al. (2020). Cryo-EM structure of the volume-regulated anion channel LRRC8D isoform identifies features important for substrate permeation. *Commun. Biol.* 3:240. doi: 10.1038/s42003-020-0951-z
- Nakano, K., and Vousden, K. H. (2001). PUMA, a novel proapoptotic gene, is induced by p53. *Mol. Cell* 7, 683–694. doi: 10.1016/S1097-2765(01)00214-3
- Oda, E., Ohki, R., Murasawa, H., Nemoto, J., Shibue, T., Yamashita, T., et al. (2000). Noxa, a BH3-only member of the Bcl-2 family and candidate mediator of p53-induced apoptosis. *Science* 288, 1053–1058. doi: 10.1126/science.288.5468.1053
- Odaka, C., Sanders, M. L., and Crews, P. (2000). Jasplakinolide induces apoptosis in various transformed cell lines by a caspase-3-like protease-dependent pathway. *Clin. Diagn. Lab. Immunol.* 7, 947–952. doi: 10.1128/CDLI.7.6.947-952.2000
- Ohno, O., Morita, M., Kitamura, K., Teruya, T., Yoneda, K., Kita, M., et al. (2013). Apoptosis-inducing activity of the actin-depolymerizing agent aphyronine A and its side-chain derivatives. *Bioorgan. Med. Chem. Lett.* 23, 1467–1471. doi: 10.1016/j.bmcl.2012.12.052
- Okada, T., Islam, M. R., Tsiiforova, N. A., Okada, Y., and Sabirov, R. Z. (2017). Specific and essential but not sufficient roles of LRRC8A in the activity of volume-sensitive outwardly rectifying anion channel (VSOR). *Channels* 11, 109–120. doi: 10.1080/19336950.2016.1247133
- Okada, Y., Maeno, E., Shimizu, T., Dezaki, K., Wang, J., and Morishima, S. (2001). Receptor-mediated control of regulatory volume decrease (RVD) and apoptotic volume decrease (AVD). *J. Physiol.* 532, 3–16. doi: 10.1111/j.1469-7793.2001.0003g.x
- Okada, Y., Okada, T., Sato-Numata, K., Islam, M. R., Ando-Akatsuka, Y., Numata, T., et al. (2019). Cell volume-activated and volume-correlated anion channels in mammalian cells: their biophysical, molecular, and pharmacological properties. *Pharmacol. Rev.* 71, 49–88. doi: 10.1124/pr.118.015917
- Paul, C., Manero, F., Gonin, S., Kretz-Remy, C., Viot, S., and Arrigo, A.-P. (2002). Hsp27 as a negative regulator of cytochrome C release. *Mol. Cell. Biol.* 22, 816–834. doi: 10.1128/mcb.22.3.816-834.2002
- Pedersen, S. F., Okada, Y., and Nilius, B. (2016). Biophysics and physiology of the volume-regulated anion channel (VRAC)/volume-sensitive outwardly rectifying anion channel (VSOR). *Pflugers Arch. Eur. J. Physiol.* 468, 371–383. doi: 10.1007/s00424-015-1781-6
- Planells-Cases, R., Lutter, D., Guyader, C., Gerhards, N. M., Ullrich, F., Elger, D. A., et al. (2015). Subunit composition of VRAC channels determines substrate specificity and cellular resistance to P t-based anti-cancer drugs. *Embo J.* 34, 2993–3008. doi: 10.15252/embj.201592409
- Posey, S. C., and Bierer, B. E. (1999). Actin stabilization by jasplakinolide enhances apoptosis induced by cytokine deprivation. *J. Biol. Chem.* 274, 4259–4265. doi: 10.1074/jbc.274.7.4259
- Poulsen, K. A., Andersen, E. C., Hansen, C. F., Klausen, T. K., Hougaard, C., Lambert, I. H., et al. (2010). Deregulation of apoptotic volume decrease and ionic movements in multidrug-resistant tumor cells: role of chloride channels. *Am. J. Physiol. Cell Physiol.* 298, C14–C25. doi: 10.1152/ajpcell.00654.2008
- Qiu, Z., Dubin, A. E., Mathur, J., Tu, B., Reddy, K., Miraglia, L. J., et al. (2014). SWELL1, a plasma membrane protein, is an essential component of volume-regulated anion channel. *Cell* 157, 447–458. doi: 10.1016/j.cell.2014.03.024
- Raudenska, M., Kratochvilova, M., Vicar, T., Gumulec, J., Balvan, J., Polanska, H., et al. (2019). Cisplatin enhances cell stiffness and decreases invasiveness rate in prostate cancer cells by actin accumulation. *Sci. Rep.* 9:1660. doi: 10.1038/s41598-018-38199-7
- Rebillard, A., Jouan-Lanhouet, S., Jouan, E., Legembre, P., Pizon, M., Sergeant, O., et al. (2010). Cisplatin-induced apoptosis involves a Fas-ROCK-ezrin-dependent actin remodelling in human colon cancer cells. *Eur. J. Cancer* 46, 1445–1455. doi: 10.1016/j.ejca.2010.01.034
- Rocha, C. R. R., Silva, M. M., Quinet, A., Cabral-Neto, J. B., and Menck, C. F. M. (2018). DNA repair pathways and cisplatin resistance: an intimate relationship. *Clinics* 73:e478s. doi: 10.6061/clinics/2018/e478s
- Salehi, F., Behboudi, H., Kavooosi, G., and Ardestani, S. K. (2018). Oxidative DNA damage induced by ROS-modulating agents with the ability to target DNA: a comparison of the biological characteristics of citrus pectin and apple pectin. *Sci. Rep.* 8:13902. doi: 10.1038/s41598-018-32308-2
- Samimi, G., Katano, K., Holzer, A. K., Safaei, R., and Howell, S. B. (2004). Modulation of the cellular pharmacology of cisplatin and its analogs by the copper exporters ATP7A and ATP7B. *Mol. Pharmacol.* 66, 25–32. doi: 10.1124/mol.66.1.25
- Saraste, A., and Pulkki, K. (2000). Morphologic and biochemical hallmarks of apoptosis. *Cardiovasc. Res.* 45, 528–537. doi: 10.1016/S0008-6363(99)00384-3
- Sax, J. K., Fei, P., Murphy, M. E., Bernhard, E., Korsmeyer, S. J., and El-Deiry, W. S. (2002). BID regulation by p53 contributes to chemosensitivity. *Nat. Cell Biol.* 4, 842–849. doi: 10.1038/ncb866
- Sharma, S., Santiskulvong, C., Bentolila, L. A., Rao, J. Y., Dorigo, O., and Gimzewski, J. K. (2012). Correlative nanomechanical profiling with super-resolution F-actin imaging reveals novel insights into mechanisms of cisplatin resistance in ovarian cancer cells. *Nanomed. Nanotechnol. Biol. Med.* 8, 757–766. doi: 10.1016/j.nano.2011.09.015
- Sharma, S., Santiskulvong, C., Rao, J., Gimzewski, J. K., and Dorigo, O. (2014). The role of Rho GTPase in cell stiffness and cisplatin resistance in ovarian cancer cells. *Integr. Biol.* 6, 611–617. doi: 10.1039/c3ib40246k
- Shen, D.-W., Liang, X.-J., Gawinowicz, M. A., and Gottesman, M. M. (2004). Identification of cytoskeletal [14C]carboplatin-Binding proteins reveals reduced expression and disorganization of actin and filamin in cisplatin-resistant cell lines. *Mol. Pharmacol.* 66, 789–793. doi: 10.1124/mol.66.4.789
- Shen, M. R., Chou, C. Y., Hsu, K. F., Hsu, K. S., and Wu, M. L. (1999). Modulation of volume-sensitive Cl⁻ channels and cell volume by actin filaments and microtubules in human cervical cancer HT-3 cells. *Acta Physiol. Scand.* 167, 215–225. doi: 10.1046/j.1365-201x.1999.00611.x
- Shi, Y., Nikulenkov, F., Zawacka-Pankau, J., Li, H., Gabdoulline, R., Xu, J., et al. (2014). ROS-dependent activation of JNK converts p53 into an efficient inhibitor of oncogenes leading to robust apoptosis. *Cell Death Differ.* 21, 612–623. doi: 10.1038/cdd.2013.186
- Shimizu, T., Fujii, T., Ohtake, H., Tomii, T., Takahashi, R., Kawashima, K., et al. (2020). Impaired actin filaments decrease cisplatin sensitivity via dysfunction of volume-sensitive Cl⁻ channels in human epidermoid carcinoma cells. *J. Cell. Physiol.* 235, 9589–9600. doi: 10.1002/jcp.29767
- Shimizu, T., Lee, E. L., Ise, T., and Okada, Y. (2008). Volume-sensitive Cl⁻ channel as a regulator of acquired cisplatin resistance. *Anticancer Res.* 28, 75–84.
- Shimizu, T., Numata, T., and Okada, Y. (2004). A role of reactive oxygen species in apoptotic activation of volume-sensitive Cl⁻ channel. *Proc. Natl. Acad. Sci. U.S.A.* 101, 6770–6773. doi: 10.1073/pnas.0401604101
- Siddik, Z. H. (2003). Cisplatin: mode of cytotoxic action and molecular basis of resistance. *Oncogene* 22, 7265–7279. doi: 10.1038/sj.onc.12.06933
- Song, I. S., Savaraj, N., Siddik, Z. H., Liu, P., Wei, Y., Wu, C. J., et al. (2004). Role of human copper transporter Ctr1 in the transport of platinum-based antitumor agents in cisplatin-sensitive and cisplatin-resistant cells. *Mol. Cancer Ther.* 3, 1543–1549.
- Suria, H., Chau, L. A., Negrou, E., Kelvin, D. J., and Madrenas, J. (1999). Cytoskeletal disruption induces T cell apoptosis by a caspase-3 mediated mechanism. *Life Sci.* 65, 2697–2707. doi: 10.1016/S0024-3205(99)00538-X
- Suzuki, M., and Gitlin, J. D. (1999). Intracellular localization of the Menkes and Wilson's disease proteins and their role in intracellular copper transport. *Pediatr. Int.* 41, 436–442. doi: 10.1046/j.1442-200x.1999.01090.x
- Tanida, S., Mizoshita, T., Ozeki, K., Tsukamoto, H., Kamiya, T., Kataoka, H., et al. (2012). Mechanisms of cisplatin-induced apoptosis and of cisplatin sensitivity: potential of BIN1 to act as a potent predictor of cisplatin sensitivity in gastric cancer treatment. *Int. J. Surg. Oncol.* 2012:862879. doi: 10.1155/2012/862879

- Taniguchi, K., Wada, M., Kohno, K., Nakamura, T., Kawabe, T., Kawakami, M., et al. (1996). A human canalicular multispecific organic anion transporter (cMOAT) gene is overexpressed in cisplatin-resistant human cancer cell lines with decreased drug accumulation. *Cancer Res.* 56, 4124–4129.
- Toledo, F., and Wahl, G. M. (2006). Regulating the p53 pathway: in vitro hypotheses, in vivo veritas. *Nat. Rev. Cancer* 6, 909–923. doi: 10.1038/nrc2012
- Udi, J., Wider, D., Catusse, J., Schnerch, D., Follo, M., Ihorst, G., et al. (2011). Multikinase inhibitor sorafenib induces apoptosis, CD138-downregulation, actin depolymerization and inhibition of M210B4-triggered chemotaxis in multiple myeloma cell lines and synergizes with proteasome inhibitor bortezomib. *Blood* 118:2380. doi: 10.1182/blood.v118.21.2380.2380
- Ullrich, F., Reincke, S. M., Voss, F. K., Stauber, T., and Jentsch, T. J. (2016). Inactivation and anion selectivity of volume-regulated anion channels (VRACs) depend on c-terminal residues of the first extracellular loop. *J. Biol. Chem.* 291, 17040–17048. doi: 10.1074/jbc.M116.739342
- Voss, F. K., Ullrich, F., Münch, J., Lazarow, K., Lutte, D., Mah, N., et al. (2014). Identification of LRRC8 heteromers as an essential component of the volume-regulated anion channel VRAC. *Science* 344, 634–638. doi: 10.1126/science.1252826
- Wei, H., Mei, Y. A., Sun, J. T., Zhou, H. Q., and Zhang, Z. H. (2003). Regulation of swelling-activated chloride channels in embryonic chick heart cells. *Cell Res.* 13, 21–28. doi: 10.1038/sj.cr.7290147
- White, S. R., Williams, P., Wojcik, K. R., Sun, S., Hiemstra, P. S., Rabe, K. F., et al. (2001). Initiation of apoptosis by actin cytoskeletal derangement in human airway epithelial cells. *Am. J. Respir. Cell Mol. Biol.* 24, 282–294. doi: 10.1165/ajrcmb.24.3.3995
- Wu, Y., Mehew, J. W., Heckman, C. A., Arcinas, M., and Boxer, L. M. (2001). Negative regulation of bcl-2 expression by p53 in hematopoietic cells. *Oncogene* 20, 240–251. doi: 10.1038/sj.onc.1204067
- Xia, M., and Land, H. (2007). Tumor suppressor p53 restricts Ras stimulation of RhoA and cancer cell motility. *Nat. Struct. Mol. Biol.* 14, 215–223. doi: 10.1038/nsmb1208
- Yamasaki, M., Makino, T., Masuzawa, T., Kurokawa, Y., Miyata, H., Takiguchi, S., et al. (2011). Role of multidrug resistance protein 2 (MRP2) in chemoresistance and clinical outcome in oesophageal squamous cell carcinoma. *Br. J. Cancer* 104, 707–713. doi: 10.1038/sj.bjc.6606071
- Yonezawa, A., Masuda, S., Yokoo, S., Katsura, T., and Inui, K. I. (2006). Cisplatin and oxaliplatin, but not carboplatin and nedaplatin, are substrates for human organic cation transporters (SLC22A1-3 and multidrug and toxin extrusion family). *J. Pharmacol. Exp. Ther.* 319, 879–886. doi: 10.1124/jpet.106.110346
- Yue, J., and López, J. M. (2020). Understanding MAPK signaling pathways in apoptosis. *Int. J. Mol. Sci.* 21:2346. doi: 10.3390/ijms21072346
- Zeidan, Y. H., Jenkins, R. W., and Hannun, Y. A. (2008). Remodeling of cellular cytoskeleton by the acid sphingomyelinase/ceramide pathway. *J. Cell Biol.* 181, 335–350. doi: 10.1083/jcb.200705060
- Zhang, J., Larsen, T. H., and Lieberman, M. (1997). F-actin modulates swelling-activated chloride current in cultured chick cardiac myocytes. *Am. J. Physiol. Physiol.* 273, C1215–C1224. doi: 10.1152/ajpcell.1997.273.4.C1215
- Zhou, C., Zhang, X., ShiYang, X., Wang, H., and Xiong, B. (2019). Tea polyphenol protects against cisplatin-induced meiotic defects in porcine oocytes. *Aging* 11, 4706–4719. doi: 10.18632/aging.102084
- Zhu, H., Luo, H., Zhang, W., Shen, Z., Hu, X., and Zhu, X. (2016). Molecular mechanisms of cisplatin resistance in cervical cancer. *Drug Des. Dev. Ther.* 10, 1885–1895. doi: 10.2147/DDDT.S106412

Conflict of Interest: The authors declare that the research was conducted in the absence of any commercial or financial relationships that could be construed as a potential conflict of interest.

Copyright © 2020 Shimizu, Fujii and Sakai. This is an open-access article distributed under the terms of the Creative Commons Attribution License (CC BY). The use, distribution or reproduction in other forums is permitted, provided the original author(s) and the copyright owner(s) are credited and that the original publication in this journal is cited, in accordance with accepted academic practice. No use, distribution or reproduction is permitted which does not comply with these terms.



Balance of Na^+ , K^+ , and Cl^- Unidirectional Fluxes in Normal and Apoptotic U937 Cells Computed With All Main Types of Cotransporters

Valentina E. Yurinskaya¹, Igor A. Vereninov² and Alexey A. Vereninov^{1*}

¹ Laboratory of Cell Physiology, Institute of Cytology, Russian Academy of Sciences, St-Petersburg, Russia, ² Peter the Great St-Petersburg Polytechnic University, St-Petersburg, Russia

OPEN ACCESS

Edited by:

Markus Ritter,
Paracelsus Medical University, Austria

Reviewed by:

Silvia Dossena,
Paracelsus Medical University, Austria
Dandan Sun,
University of Pittsburgh, United States

*Correspondence:

Alexey A. Vereninov
vereninov@gmail.com

Specialty section:

This article was submitted to
Cell Death and Survival,
a section of the journal
Frontiers in Cell and Developmental
Biology

Received: 05 August 2020

Accepted: 30 September 2020

Published: 06 November 2020

Citation:

Yurinskaya VE, Vereninov IA and
Vereninov AA (2020) Balance of Na^+ ,
 K^+ , and Cl^- Unidirectional Fluxes
in Normal and Apoptotic U937 Cells
Computed With All Main Types
of Cotransporters.
Front. Cell Dev. Biol. 8:591872.
doi: 10.3389/fcell.2020.591872

Fluxes of monovalent ions through the multiple pathways of the plasma membrane are highly interdependent, and their assessment by direct measurement is difficult or even impossible. Computation of the entire flux balance helps to identify partial flows and study the functional expression of individual transporters. Our previous computation of unidirectional fluxes in real cells ignored the ubiquitous cotransporters NKCC and KCC. Here, we present an analysis of the entire balance of unidirectional Na^+ , K^+ , and Cl^- fluxes through the plasma membrane in human lymphoid U937 cells, taking into account not only the Na/K pump and electroconductive channels but all major types of cotransporters NC, NKCC, and KCC. Our calculations use flux equations based on the fundamental principles of macroscopic electroneutrality of the system, water balance, and the generally accepted thermodynamic dependence of ion fluxes on the driving force, and they do not depend on hypotheses about the molecular structure of the channel and transporters. A complete list of the major inward and outward Na^+ , K^+ , and Cl^- fluxes is obtained for human lymphoid U937 cells at rest and during changes in the ion and water balance for the first 4 h of staurosporine-induced apoptosis. It is shown how the problem of the inevitable multiplicity of solutions to the flux equations, which arises with an increase in the number of ion pathways, can be solved in real cases by analyzing the ratio of ouabain-sensitive and ouabain-resistant parts of K^+ (Rb^+) influx (OSOR) and using additional experimental data on the effects of specific inhibitors. It is found that dynamics of changes in the membrane channels and transporters underlying apoptotic changes in the content of ions and water in cells, calculated without taking into account the KCC and NKCC cotransporters, differs only in details from that calculated for cells with KCC and NKCC. The developed approach to the assessment of unidirectional fluxes may be useful for understanding functional expression of ion channels and transporters in other cells under various conditions. Attached software allows reproduction of all calculated data under presented conditions and to study the effects of the condition variation.

Keywords: cell ion homeostasis, membrane transport, ion channels, sodium pump, cotransporters, ion fluxes calculation, apoptosis

INTRODUCTION

Apoptosis is one of the three main types of cell death, along with autophagy and necrosis itself (Galluzzi et al., 2018). A hallmark of apoptosis is a specific cell shrinkage or, at least, the absence of swelling and rupture of the plasma membrane (Yurinskaya et al., 2005). This is due to specific apoptotic changes in monovalent ion homeostasis, which is closely related to cell water balance regulation (Maeno et al., 2000, 2012; Okada et al., 2001; Lang et al., 2005; Lang and Hoffmann, 2012, 2013). Until now, the quantitative study of changes in channels and transporters responsible for specific apoptotic changes in the balance of Na⁺, K⁺, and Cl⁻ has been based on the use of staurosporine-treated U937 cells and computer modeling without considering KCC and NKCC cotransporters (Yurinskaya et al., 2019). However, these cation-coupled Cl⁻ cotransporters of the gene family SLC12 attract much attention in the recent decade (Gagnon and Delpire, 2013; Jentsch, 2016; Delpire and Gagnon, 2018). They can transport Cl⁻ against an electrochemical gradient and create a non-equilibrium distribution of Cl⁻ across the membrane. This is what makes Cl⁻ an active player in various physiological processes (Jentsch, 2016) since the permeability of the Cl⁻ channels can affect the entire homeostasis of monovalent ions only when Cl⁻ is in a non-equilibrium state. The interplay of various Cl⁻ coupled cotransporters and Cl⁻ channels has been particularly intensively studied in connection with signal transmission in neurons (Kaila et al., 2014; Doyon et al., 2016; Currin et al., 2020; Wilke et al., 2020). Progress in the molecular biology of the cation-coupled Cl⁻ cotransporters is exciting; however, their functional expression and role in maintaining Cl⁻ homeostasis in non-polarized cells is investigated much worse because electrophysiological methods cannot be applied here, and possible tools are rather limited. It was said: “Electrical activity in neurons requires a seamless functional coupling between plasmalemmal ion channels and ion transporters. Although ion channels have been studied intensively for several decades, research on ion transporters is in its infancy” (Kaila et al., 2014).

In our previous study, the cells with the sodium pump, electroconductive Na⁺, K⁺, and Cl⁻ channels and only one cotransporter NC were considered (Yurinskaya et al., 2019). It was found that the permeability of Cl⁻ channels significantly changes at the early stage of apoptosis. How the presence of KCC and NKCC will affect the behavior of cells and how the parameters of the main ion pathways obtained by calculations will change were unknown. An increase in the number of considered ionic paths significantly increases the difficulties of finding the parameters, and these problems are also the subject of the current study. We believe that the developed approach is a useful tool for studying the fluxes of monovalent ions across the plasma membrane with all major ion pathways.

MATERIALS AND METHODS

Cell Cultures

U937 human histiocytic lymphoma cells were obtained from the Russian Cell Culture Collection (Institute of Cytology, Russian

Academy of Sciences, cat. number 160B2). The cells were cultured in RPMI 1640 medium supplemented with 10% fetal bovine serum (FBS) at 37°C and 5% CO₂. For the induction of apoptosis, the cells, at a density of 1×10^6 cells/ml, were exposed to 1 μM staurosporine (STS) for 0.5–4 h. All the incubations were done at 37°C.

Reagents

RPMI 1640 medium and FBS (HyClone Standard) were purchased from Biolot (Russia). STS and ouabain were from Sigma-Aldrich (Germany), and Percoll was purchased from Pharmacia (Sweden). The isotope ³⁶Cl⁻ was from “Isotope” (Russia). Salts were of analytical grade and were from Reagent (Russia).

Experimental Procedures

Details of the experimental methods used were described in our previous study (Yurinskaya et al., 2019). Intracellular K⁺, Na⁺, and Rb⁺ contents were determined by flame emission on a Perkin-Elmer AA 306 spectrophotometer, and the intracellular Cl⁻ was measured using a radiotracer ³⁶Cl⁻. Cell water content was estimated by the buoyant density of the cells in continuous Percoll gradient, and it was calculated as $v_{prot.} = (1 - \rho/\rho_{dry})/[0.72(\rho - 1)]$, where ρ is the measured buoyant density of the cells and ρ_{dry} is the cell dry mass density, which was given as 1.38 g ml⁻¹. The share of protein in dry mass was given as 72%. The cell ion and water content were calculated in micromoles per gram of protein.

Statistical Analysis

Statistical analysis of experimental data was carried out using Student's *t*-test and is presented in our original publications (Vereninov et al., 2008; Yurinskaya et al., 2011).

Computation

Computation of the monovalent ion flux balance, membrane potential, and ion electrochemical gradients was performed using the computational program and appropriate executable file BEZ01B as earlier (Vereninov et al., 2014; Yurinskaya et al., 2019). Basic symbols and definitions used are shown in **Table 1**. The input data (file DataB.txt, in supplement) are the following: extracellular and intracellular concentrations (na_0 , k_0 , cl_0 , and B_0 ; na , k , and cl); kv ; the pump rate coefficient (β); the pump Na/K stoichiometric coefficient (γ); parameter kb ; channel permeability coefficients (pna , pk , and pcl); and the rate coefficients for the NC, KC, and NKCC cotransporters (inc , ikc , and $inkcc$). The terms NC, NKCC, and KC, cotransport, or cotransporter, depending on the context, reflect the way these carriers work, but not their genetic identity, which is irrelevant in our study. Therefore, the abbreviations NC and KC are used, but not NCC and KCC. It is known that unidirectional Na⁺–Cl⁻ coupled cotransport with 1:1 stoichiometry may be performed both by a single transport protein, like thiazide-sensitive Na⁺–Cl⁻ cotransporter (Gamba, 2005), and by two functionally coupled exchangers, NHE and Cl⁻/HCO₃⁻ (Garcia-Soto and Grinstein, 1990; Hoffmann et al., 2009). The genetically identified

cotransporters NKCC1 (SLC12A2) and KCC1 (SLC12A4) are expressed in U937 cells^{1,2}.

The rate coefficient of the sodium pump (*beta*) was calculated as the ratio of the Na⁺ pump efflux to the cell Na⁺ content where the Na⁺ pump efflux was estimated by ouabain-sensitive (OS) K⁺(Rb⁺) influx assuming proportions of [Rb]_o and [K]_o, respectively, and Na/K pump flux stoichiometry of 3:2. *kb* is a parameter of a linear decrease of *beta* over time. Coefficients of ion channel permeability were selected by trial and error, and rate coefficients of cotransporters, *inc*, *ikc*, and *inkcc*, were selected in view of the effects of inhibitors (see text below). Electrochemical gradients for Na⁺, K⁺, or Cl⁻, *mun*, *muk*, or *mucl*, respectively, were calculated by the following equations: $mun = 26.7 \cdot \ln([Na]_i/[Na]_o) + U$, $muk = 26.7 \cdot \ln([K]_i/[K]_o) + U$, and $mucl = 26.7 \cdot \ln([Cl]_i/[Cl]_o) - U$ and given in mV. The results of computations appear in the file RESB.txt (its example is given in the supplement). Equivalent exchange fluxes 1:1 are

¹<https://www.proteinatlas.org/ENSG00000064651-SLC12A2/blood>

²<https://www.proteinatlas.org/ENSG00000124067-SLC12A4/blood>

TABLE 1 | Basic symbols and definitions.

Symbol	Definitions and units
NC, NKCC, KC	Types of cotransporters
[Na] _i , [K] _i , [Cl] _i , <i>na</i> , <i>k</i> , <i>cl</i>	Concentration of ions in cell water, mM
[Na] _o , [K] _o , [Cl] _o , <i>nao</i> , <i>kO</i> , <i>clO</i>	Concentration of ions in external medium, mM
<i>BO</i>	External concentrations of membrane-impermeant non-electrolytes, mM
<i>A</i>	Intracellular content of membrane-impermeant osmolytes, mmol, may be related to g cell protein or cell number
<i>V</i>	Cell water volume, mL, may be related to g cell protein or cell number
<i>V/A</i>	Cell water content per unit of <i>A</i>
<i>z</i>	Mean valence of membrane-impermeant osmolytes, <i>A</i>
OSOR	Ratio of ouabain-sensitive to ouabain-resistant Rb ⁺ (K ⁺) influx
<i>pNa</i> , <i>pK</i> , <i>pCl</i> , <i>pna</i> , <i>pk</i> , <i>pcl</i>	Permeability coefficients, min ⁻¹
<i>Beta</i> , <i>β</i>	Pump rate coefficient, min ⁻¹
<i>Gamma</i> , <i>γ</i>	Na/K pump flux stoichiometry, dimensionless
<i>kv</i>	Ratio of “new” to “old” media osmolarity when the external osmolarity is changed
<i>U</i>	Membrane potential, MP, mV
PUMP	K ⁺ influx or Na ⁺ efflux via the pump, μmol·min ⁻¹ ·(ml cell water) ⁻¹
IChannel, INC, IKC, INKCC	Unidirectional influxes of Na, K, or Cl via channels or cotransport, μmol·min ⁻¹ ·(ml cell water) ⁻¹
EChannel, ENC, EKC, ENKCC	Unidirectional effluxes of Na, K, or Cl via channels or cotransport, μmol·min ⁻¹ ·(ml cell water) ⁻¹
<i>inc</i> , <i>ikc</i> , <i>inkcc</i>	Cotransport rate coefficients, ml·μmol ⁻¹ ·min ⁻¹ for <i>inc</i> and <i>ikc</i> , and ml ³ ·μmol ⁻³ ·min ⁻¹ for <i>inkcc</i>
<i>mun</i> , <i>muk</i> , <i>mucl</i>	Transmembrane electrochemical potential difference for Na ⁺ , K ⁺ , or Cl ⁻ , mV
<i>kb</i>	Parameter of linear decrease of <i>beta</i> over time

not considered when calculating the ionic homeostasis of the cell, since they do not change the concentration of Na⁺ and Cl⁻ in the cell. Their calculation is considered in our previous study (Vereninov et al., 2016).

RESULTS

Normal U937 Cells

Measured and Computed Characteristics of the Ion Homeostasis in Cell With NKCC and KC Cotransporters

The measured and computed data obtained for the cell with the NC cotransport only and for the cell with the NKCC and KC cotransports are presented in **Table 2**. The experimental data are taken from our previous studies (Vereninov et al., 2008; Yurinskaya et al., 2011, and yet unpublished materials). Two variants of normal U937 cells with different measured characteristics, Cells *A* and *B*, are considered to show how computed characteristics depend on the inevitable variability of the real cells. The intracellular concentration of ions; the ratio of ouabain-sensitive to ouabain-resistant influx of Rb⁺(K⁺), OSOR, and their derivatives; the concentration and charge of “impermeable” intracellular anions, *A^z*, and the pump rate coefficient *beta* belong to the group of “measured” characteristics. The coefficient *beta* is easily and reliably calculated from the measured ouabain-sensitive influx of Rb⁺, the known relationship between the external concentrations of Rb⁺ and K⁺, and the known stoichiometry of the pump, i.e., ratio of the pump K⁺ influx to the pump Na⁺ efflux. Intracellular Na⁺ and Rb⁺ are analyzed in the same sample, and this reduces possible errors. Determination of kinetic parameters characterizing channels and transporters, unidirectional and total fluxes, and membrane potential *U* requires solving differential equations. For this, the original computer program is used (Vereninov et al., 2016; Yurinskaya et al., 2019). The data obtained in this way form a group of “computed” characteristics.

The “computed” characteristics depend not only on the experimental data used but also on the chosen list of ion pathways and on the relationship between the parameters characterizing the properties of the pathways. Shown are two different sets of parameters, *X* and *Y*, for two different cell variants, *A* and *B*. Both sets of *X* and *Y* give cells with almost the same characteristics, like those measured in real cells. Thus, it can be assumed that real cells can also achieve the same monovalent ion homeostasis in different ways. The number of solutions to the flux balance equations in a cell with only NC cotransport was discussed earlier (Yurinskaya et al., 2019). The introduction of the NKCC and KC cotransporters into consideration increases the number of possible solutions to the system of equations describing cell ion homeostasis. Parameters *X* and *Y* are chosen as examples of possible differences that result in unidirectional NKCC and NC fluxes in the range possible for real U937 cells, as follows from the data on the effects of NKCC and KC inhibitors. We are currently unable to determine which of the *X* or *Y* options is more appropriate for real cells. However, the computation can show what additional measured characteristics can help to

TABLE 2 | Basic characteristics of ion distribution, measured in two variants of normal resting U937 cells (cells A and B) and computed for schemes with and without NKCC and KC cotransporters at two chosen sets of NKCC and KC parameters (X and Y).

Characteristics		Cells A		Cells B		
Measured						
[K] _i , [Na] _i , [Cl] _i , mM	117, 32, 40			147, 38, 45		
Cell density, g/ml	1.054			1.053		
A ^z , mM	121			80		
z	−0.90			−1.75		
beta	0.029			0.039		
OSOR	5.61			3.89		
Chosen	NC only	+ (NKCC and KC)		NC only	+ (NKCC and KC)	
		X	Y		X	Y
inc	3E-5	1E-5	2.8E-5	3E-5	2.5E-5	7E-5
ikc	–	2.4E-5	8.8E-5	–	1E-5	8E-5
inkcc	–	4E-10	8E-10	–	11.4E-9	8E-9
Computed						
U, mV	−29.9	−30.8	−34.7	−44.7	−29.4	−45.0
mucl	+ 1.5	+2.3	+ 6.3	+19.4	+ 4.1	+19.8
mun	−69.3	−70.2	−74.1	−79.5	−64.2	−79.9
muk	+ 50.3	+49.4	+ 45.5	+41.6	+ 56.9	+41.3
pna	0.0041	0.00355	0.00215	0.00382	0.00535	0.0017
pk	0.0115	0.01	0.0058	0.022	0.013	0.0115
pcl	0.0125	0.0102	0.005	0.0091	0.028	0.011
Partial influxes,% of total influx						
INa Channels	95.1	83.4	53.7	69.3	69.9	28.7
INa NC	4.9	16.2	45.4	30.7	23.0	66.2
INa NKCC	–	0.4	0.9	–	7.1	5.1
IK pump	84.8	84.0	82.8	79.0	79.0	78.0
IK Channels	15.2	13.3	8.0	21.0	9.9	10.9
IK KC	–	2.2	7.9	–	0.5	4.2
IK NKCC	–	0.6	1.2	–	10.5	6.9

The concentration of ions, impermeant intracellular anions A, their charge z, pump rate coefficient beta, and OSOR—ratio of ouabain-sensitive to ouabain-resistant components of K⁺(Rb⁺) influx—are determined as described in section “Materials and Methods.” Symbols, definitions, and units are given in **Table 1**. Partial fluxes are given in% to the sum of fluxes, excluding a 1:1 exchange flux. Cell variants A and B differ due to the use of different subline U937 cells studied in different years. The experimental data are taken from our previous study (Vereninov et al., 2008; Yurinskaya et al., 2011, and yet unpublished materials).

select the best option. For example, variants B–X and B–Y differ significantly in the resting membrane potential, in the K⁺(Rb⁺) influx sensitive to inhibitors, in the electrochemical Cl[−] gradient, and, consequently, in the effect of changes in the Cl[−] channel permeability on the entire ionic homeostasis. Variants A–X and A–Y differ significantly in K⁺(Rb⁺) influx sensitive to the specific NKCC and KC inhibitors, bumetanide, and DIOA, respectively. The difficulty here lies in the low values of the partial fluxes NKCC and KC in U937 cells (see below). The parameters of the main ion pathways computed at different variants of the NKCC and KC rate coefficients are different. However, the range of their variation can be estimated by computing the desired options.

Ion Fluxes

Figure 1 shows the relationship between all quantitatively significant components of the unidirectional fluxes of Na⁺, K⁺, and Cl[−] in U937 cells (B–Y) calculated on the assumption that seven types of ionic pathways exist in their plasma membrane

in a balanced cell state: the Na/K ATPase pump; the Na⁺, K⁺, and Cl[−] electroconductive channels; the NC, NKCC, and KC cotransporters; and the coupled ion exchange with a 1:1 stoichiometry, which is especially important in consideration of Na⁺ and Cl[−] unidirectional fluxes. The equivalent exchange Na/Na and Cl/Cl constitutes the dominant part of the entire unidirectional flux of these ions through the cell membrane. These exchange fluxes are not associated with changes in intracellular ion concentrations and differences in electrical potentials in the cell membrane or with its conductivity and cannot be measured by electrophysiological methods. However, they are extremely significant when the transport of ions across the membrane is studied by measuring fluxes using radioisotopes. These measurements show that the fluxes underlying the 1:1 exchange of ions across the membrane can be significantly higher in real cells than those considered in a simple pump-leak model. The presented data on the overall exchange fluxes of Na⁺ and Cl[−] in the normal U937 cells have been obtained using radiotracers

K ⁺	Na ⁺	Cl ⁻	A ^z
In cytoplasm, mM			
147	38	45	80
In the medium, mM			
5.8	140	116	–
Electrochemical potential gradients across the cell membrane, mV			
+41.3	-79.9	+19.8	
Resting potential U -45.0 mV			

A^z - impermeant intracellular anions with the charge z -1.75
 OSOR 3.89 Vol/A 12.5 mL/mmol
 OSOR - ratio of ouabain-sensitive to ouabain-resistant components of K⁺(Rb⁺) influx, an important cell characteristic.

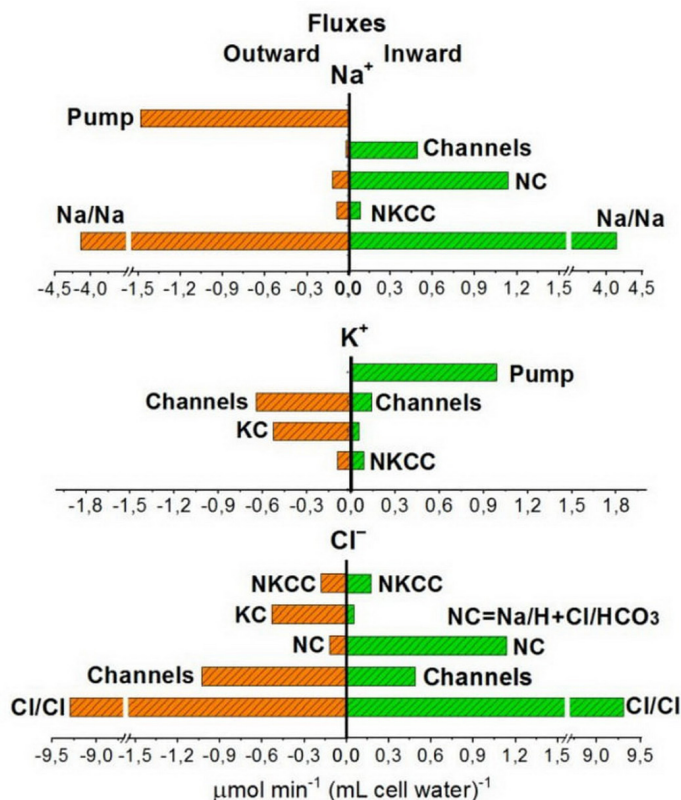


FIGURE 1 | Ion distribution and unidirectional K⁺, Na⁺, and Cl⁻ fluxes in normal U937 cells under the balanced state. Cells B–Y from **Table 2** are given as an example. Other details are on the plot.

²²Na⁺ and ³⁶Cl⁻ or low concentrations of Li⁺ as an analog of Na⁺ for most of the Na⁺ pathways except the pump (Vereninov et al., 2007, 2016; Yurinskaya et al., 2011). The dominance of the 1:1 exchange flux in the entire Cl⁻ flux across the plasma membrane is known for other cells (Hoffmann et al., 1979; Hoffmann, 1982, 2001). Fluxes related to the Na/Na and Cl/Cl equivalent exchange are not considered further in the calculation of the flux balance.

Computation shows that the effect of the NKCC cotransport on the asymmetry in the balanced distribution of K⁺, Na⁺, and Cl⁻ in U937 cells is small, because the influx and efflux of ions mediated by NKCC differ insignificantly and the net NKCC flux is small in comparison with other net fluxes (**Table 3**). Importantly, the unidirectional NKCC influx accounts for 0.4 and 0.9% of the total Na⁺ influx in cells A but 7.1 and 5.1% in cells B in variants X and Y, respectively (**Table 2**). Detection of such a small bumetanide-inhibitable NKCC influx in the presence of a large background Na/Na equivalent exchange is impossible. The Na⁺ net flux via NKCC is small as the driving force for NKCC is small. The driving force for NKCC cotransport is $\mu_{\text{Na}} + \mu_{\text{K}} + 2\mu_{\text{Cl}} = -16.2 \div -16$ mV in cells A and $+0.9 \div +1$ mV in cells B (**Table 2**).

The balanced unequilibrium distribution of Na⁺ (μ_{Na} is $-64 \div -80$ mV depending on variants) is determined mostly by the relationship between the Na⁺ pump flux uphill and

Na⁺ flux downhill through not only the channels but also via the NC pathway. This means that the Na⁺ flux through the NC route significantly “loads” the pump in the studied U937 cells. Computation shows that NC cotransport is a strong regulator of intracellular Na⁺ concentration with all the ensuing consequences.

A small share of KC influx in the entire K⁺ influx in the considered cells (0.5–7.9% depending on the options) (**Table 2**) makes it difficult to study KC fluxes with inhibitors. At the same time, the net K⁺ flux via KC can be comparable with the net K⁺ flux through the channels (see examples A–Y and B–Y, **Table 3**). Therefore, the effect of KC cotransporter on the entire cell ion homeostasis can be significant.

Computation makes it possible to quantify the effect of the NC, NKCC, and KC cotransporters on generation of the Cl⁻ electrochemical gradient across the cell membrane. The NC cotransport is the most important here, at least in U937 cells. KC and NC cotransports are antagonists as the net Cl⁻ flux due to the KC cotransport is directed out of the cell whereas that due to the NC cotransport, in contrast, is directed into the cell (**Table 3**). The movement of Cl⁻ into the cell due to NC or from the cell due to KC leads to a non-equilibrium distribution of Cl⁻ across the membrane in a balanced state and changes the apparent content of “impermeant” anions in the cell. According to the theory of the double Donnan system, the amount of “impermeant” anions in a

TABLE 3 | Net and unidirectional K⁺, Na⁺, and Cl⁻ fluxes in normal resting U937 cells calculated for two variants of cells and for two different sets of cotransport parameters, X and Y.

Ion		Net fluxes				Influx				Efflux			
Cells A-X: <i>pna</i> 0.00355, <i>pk</i> 0.01, <i>pcl</i> 0.0102, <i>inc</i> 1E-5, <i>ikc</i> 2.4E-5, and <i>inkcc</i> 4E-10													
K ⁺	Channel	PUMP	NKCC	KC	IChannel	PUMP	INKCC	IKC	EChannel	PUMP	ENKCC	EKC	
		-0.5248	0.6189	0.002	-0.0961	0.0977	0.6189	0.0044	0.0161	-0.6225	-	-0.0024	-0.1123
Na ⁺	Channel	NC	NKCC	PUMP	IChannel	INC	INKCC	PUMP	EChannel	ENC	ENKCC	PUMP	
		0.7767	0.1496	0.002	-0.9283	0.8372	0.1624	0.0044	-	-0.0605	-0.0128	-0.0024	-0.9283
Cl ⁻	Channel	NC	NKCC	KC	IChannel	INC	INKCC	IKC	EChannel	ENC	ENKCC	EKC	
		-0.0575	0.1496	0.004	-0.0961	0.6296	0.1624	0.0087	0.0161	-0.6870	-0.0128	-0.0048	-0.1123
Cells A-Y: <i>pna</i> 0.00215, <i>pk</i> 0.0058, <i>pcl</i> 0.005, <i>inc</i> 2.8E-5, <i>ikc</i> 8.8E-5, and <i>inkcc</i> 8E-10													
K ⁺	Channel	PUMP	NKCC	KC	IChannel	PUMP	INKCC	IKC	EChannel	PUMP	ENKCC	EKC	
		-0.2702	0.6184	0.0041	-0.3523	0.0601	0.6184	0.009	0.0592	-0.3304	-	-0.0049	-0.4115
Na ⁺	Channel	NC	NKCC	PUMP	IChannel	INC	INKCC	PUMP	EChannel	ENC	ENKCC	PUMP	
		0.5046	0.4189	0.0041	-0.9276	0.5381	0.4547	0.009	-	-0.0335	-0.0358	-0.0049	-0.9276
Cl ⁻	Channel	NC	NKCC	KC	IChannel	INC	INKCC	IKC	EChannel	ENC	ENKCC	EKC	
		-0.0748	0.4189	0.0081	-0.3523	0.2823	0.4547	0.0179	0.0592	-0.3572	-0.0358	-0.0098	-0.4115
Cells B-X: <i>pna</i> 0.00535, <i>pk</i> 0.013, <i>pcl</i> 0.028, <i>inc</i> 2.5E-5, <i>ikc</i> 1E-5, and <i>inkcc</i> 11.4E-9													
K ⁺	Channel	PUMP	NKCC	KC	IChannel	PUMP	INKCC	IKC	EChannel	PUMP	ENKCC	EKC	
		-0.9244	0.9882	-0.0044	-0.0594	0.1243	0.9882	0.1246	0.0067	-1.0487	-	-0.1290	-0.0661
Na ⁺	Channel	NC	NKCC	PUMP	IChannel	INC	INKCC	PUMP	EChannel	ENC	ENKCC	PUMP	
		1.1235	0.3632	-0.0044	-1.4823	1.2351	0.406	0.1246	-	-0.1116	-0.0428	-0.1290	-1.4823
Cl ⁻	Channel	NC	NKCC	KC	IChannel	INC	INKCC	IKC	EChannel	ENC	ENKCC	EKC	
		-0.2950	0.3632	-0.0088	-0.0594	1.7825	0.406	0.2491	0.0067	-2.0776	-0.0428	-0.2579	-0.0661
Cells B-Y: <i>pna</i> 0.0017, <i>pk</i> 0.0115, <i>pcl</i> 0.011, <i>inc</i> 7E-5, <i>ikc</i> 8E-5, and <i>inkcc</i> 8E-9													
K ⁺	Channel	PUMP	NKCC	KC	IChannel	PUMP	INKCC	IKC	EChannel	PUMP	ENKCC	EKC	
		-0.5096	0.988	-0.0031	-0.4753	0.1381	0.988	0.0874	0.0538	-0.6477	-	-0.0905	-0.5291
Na ⁺	Channel	NC	NKCC	PUMP	IChannel	INC	INKCC	PUMP	EChannel	ENC	ENKCC	PUMP	
		0.4679	1.017	-0.0031	-1.4820	0.4927	1.1368	0.0874	-	-0.0248	-0.1197	-0.0905	-1.4820
Cl ⁻	Channel	NC	NKCC	KC	IChannel	INC	INKCC	IKC	EChannel	ENC	ENKCC	EKC	
		-0.5357	1.017	-0.0061	-0.4753	0.4889	1.1368	0.1748	0.0538	-1.0246	-0.1197	-0.1809	-0.5291

Basic ionic characteristics of cells A and B and parameters X and Y are given in Table 2. Parameters in computation: Cells A, *na* 32, *k* 117, *cl* 40, and *beta* 0.029; Cells B, *na* 38, *k* 147, *cl* 45, and *beta* 0.039. The following parameters are the same for both variants: *na0* 140, *k0* 5.8, *cl0* 116, *B0* 48.2, *gamma* 1.5, *kv* 1.0, *hp* 240, and *kb* = 0. Specific sets of channel permeability coefficients and cotransporter parameters are shown in the table. Fluxes are given in $\mu\text{mol}\cdot\text{min}^{-1}\cdot(\text{ml cell water})^{-1}$. Calculation performed as described in section "Materials and Methods." Cells under the balanced state and Cl⁻ and Na⁺ fluxes via exchangers 1:1 are omitted.

cell is a basic factor creating the asymmetry in distribution of ions across the cell membrane and the electrical potential difference at the membrane. Thus, NC and KC cotransporters turn out to be important regulators of the ionic, electrical, and water balance of the cell as a whole due to their influence on the unequilibrium distribution of Cl⁻. The Cl⁻ unequilibrium distribution also makes the Cl⁻ channel permeability an important regulator of the entire ionic homeostasis of the cell. The interaction of the NC, NKCC, and KC cotransporters and Cl⁻ channels is well tested using our computational program.

Apoptotic Changes in the Net and Unidirectional Fluxes of Na⁺, K⁺, and Cl⁻, Underlying the Change in Ionic and Water Balance in U937 Cells Treated With STS

The dynamics of apoptotic changes in the measured characteristics of ionic balance in U937 cells treated with STS, and changes in the rate coefficients for the main transporters

and channels, calculated for the cell with the NKCC and KC cotransporters are shown in Figure 2. The measured linear decrease in the rate coefficient of the Na/K pump remains an important factor in the apoptotic alteration of cell ionic balance in the cell with NKCC and KC like in the cell with NC only. It should be noted that the pump K⁺ and Na⁺ fluxes in apoptotic cells decrease with time more slowly than the pump rate coefficient *beta* due to an increase in intracellular Na⁺ during apoptosis (Table 4). This is a good example that the pump coefficient *beta* is a more adequate characteristic of the intrinsic properties of the pump. The data in Figure 2A show that a decrease in pump activity gives good agreement between calculated and experimental results for K⁺ and Na⁺, but not for Cl⁻, cell water, and OSOR (Figures 2C,D). Changes in the permeability coefficients of ion channels are required.

Changes in pCl, pK, and pNa, which give good agreement between the calculated and observed dynamics of the ion and water content during apoptosis, turn out to be practically the same (qualitatively) as in the cell without NKCC and KC in A-X cells, but with more significant changes in pCl

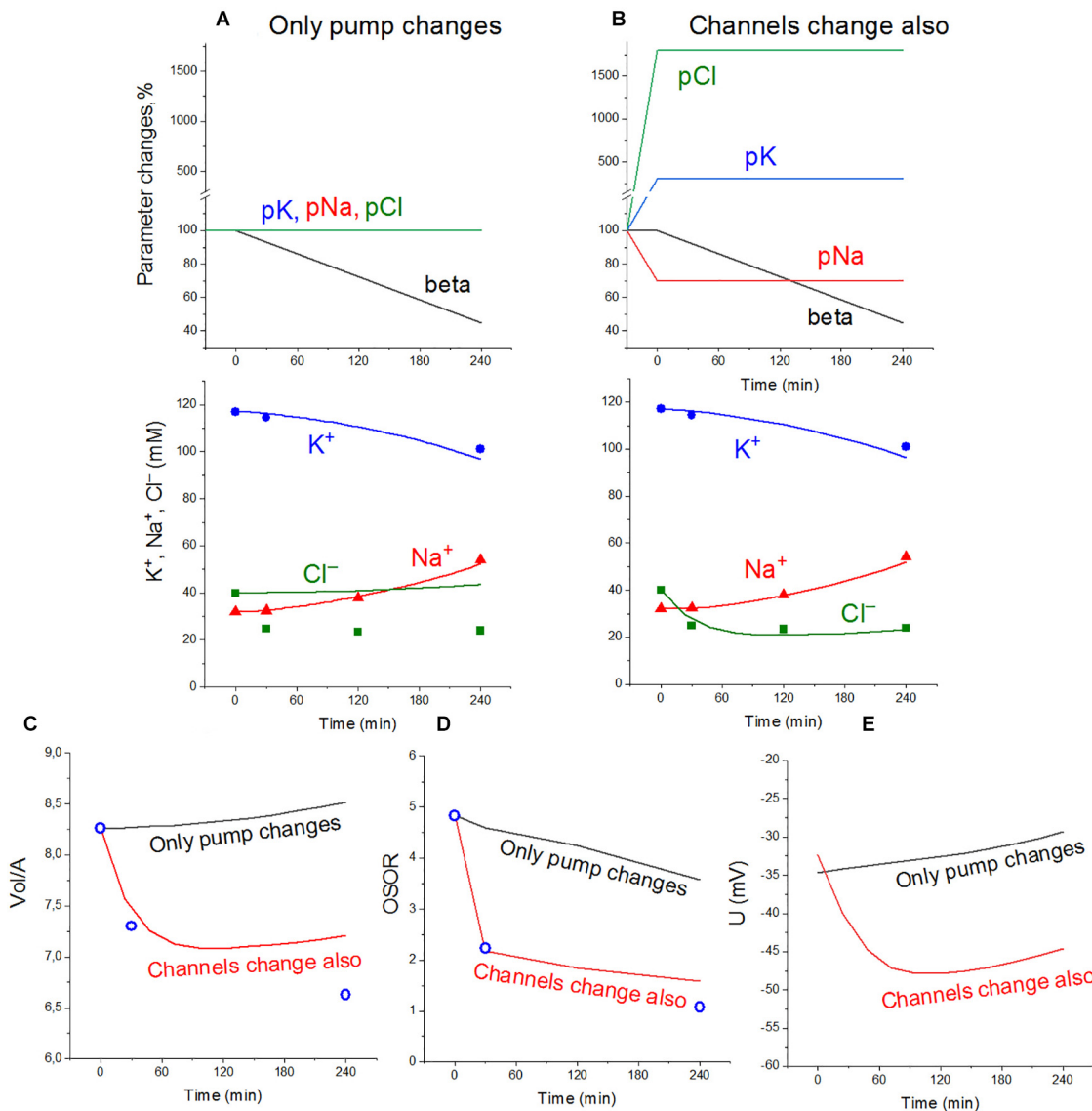


FIGURE 2 | Apoptotic changes in measured and calculated intracellular concentrations of Na⁺, K⁺, and Cl⁻ (A,B), cell water Vol/A (C), OSOR (D), and calculated membrane potential U (E) in U937 cells. Cells A–Y from Table 2 are given as an example of apoptotic cells treated with STS. Experimental data are shown by symbols; calculated, by lines. (A) Only a linear decrease of the pump rate coefficient β from an initial 0.029–0.013 at 4 h (coefficient $k_b = 0.000068 t > 0$). (B) Additional changes in channel permeability shown on the top graphs: $p_{Na} 0.00215_{t=0} \rightarrow 0.0015_{t>0}$; $p_{Cl} 0.005_{t=0} \rightarrow 0.09_{t>0}$; $p_K 0.0058_{t=0} \rightarrow 0.0174_{t>0}$; inc , ikc , and $inkcc$ rate coefficients remain constant throughout. Initial parameters: $na0$ 140; $k0$ 5.8; $cl0$ 116; $B0$ 48.2; k_v 1.0; na 32; k 117; cl 40; β 0.029; γ 1.50; p_{Na} 0.00215; p_K 0.0058; p_{Cl} 0.005; inc 2.8E-5; ikc 8.8E-5; and $inkcc$ 8E-10.

in A–Y cells (Table 5). The experimental data obtained for the studied U937 cells do not allow one to accurately determine the changes in parameter values but are sufficient to determine the extent of possible parameter changes. Our conclusion is that apoptotic changes in unidirectional and net fluxes of Na⁺, K⁺, and Cl⁻ in the studied U937 cells are caused by a gradual decrease in the pumping coefficient by about a factor of 2 in 4 h, steep increase in the integral permeability of the Cl⁻ channel by 6–18 times (depending on the selected cell), increase in the permeability of the integral K⁺ channel by about 3 times, and decrease in the permeability

of the integral Na⁺ channel by 30%. The introduction of the KC and NKCC cotransporters into the calculations did not change the general mechanism of apoptotic changes in ionic homeostasis.

DISCUSSION

The importance of cotransporters in maintaining cellular ion homeostasis and active Cl⁻ transport against an electrochemical gradient is generally known (Russell, 2000; Hoffmann et al., 2009;

TABLE 4 | Dynamics of the net and unidirectional K⁺, Na⁺, and Cl⁻ fluxes during apoptosis of U937 cells.

Ion	Time, min	Net flux total	Pump beta	Influx				Efflux			
K ⁺				PUMP	IChannel	IKC	INKCC	EChannel	PUMP	EKC	ENKCC
	0	0.0000	0.029	0.6184	0.0601	0.0592	0.0090	-0.3304	-	-0.4115	-0.0049
	30	-0.2829	0.027	0.5801	0.1985	0.0592	0.0087	-0.8442	-	-0.2829	-0.0023
	60	-0.0732	0.025	0.5562	0.2121	0.0592	0.0087	-0.7443	-	-0.2284	-0.0016
	240	-0.1330	0.013	0.4386	0.2077	0.0592	0.0087	-0.6484	-	-0.1967	-0.0022
Na ⁺				IChannel	INC	PUMP	INKCC	PUMP	ENC	EChannel	ENKCC
	0	0.0000	0.029	0.5381	0.4547	-	0.0090	-0.9276	-0.0358	-0.0335	-0.0049
	30	-0.0412	0.027	0.4130	0.4547	-	0.0087	-0.8701	-0.0250	-0.0202	-0.0023
	60	+ 0.0290	0.025	0.4413	0.4547	-	0.0087	-0.8343	-0.0212	-0.0187	-0.0016
	240	+ 0.1717	0.013	0.4321	0.4547	-	0.0087	-0.6579	-0.0337	-0.0301	-0.0022
Cl ⁻				IChannel	INC	IKC	INKCC	EChannel	ENC	EKC	ENKCC
	0	0.0000	0.029	0.2823	0.4547	0.0592	0.0179	-0.3572	-0.0358	-0.4115	-0.0098
	30	-0.3194	0.027	4.3633	0.4547	0.0592	0.0175	-4.9016	-0.0250	-0.2829	-0.0046
	60	-0.1075	0.025	3.8964	0.4547	0.0592	0.0175	-4.2824	-0.0212	-0.2284	-0.0031
	240	-0.0379	0.013	4.0421	0.4547	0.0592	0.0175	-4.3010	-0.0337	-0.1967	-0.0043

Cells A and set of parameters Y are shown as an example. STS is introduced in the media at $t = 0$. Fluxes are given in $\mu\text{mol}\cdot\text{min}^{-1}\cdot(\text{ml cell water})^{-1}$. Calculation is performed as described in section "Materials and Methods." Basic characteristics of cells and parameters are given in Table 2. Parameters change at $t > 0$: pna 0.00215 to 0.0015; pk 0.0058 to 0.0174; pcl 0.005 to 0.09; kb $0_{t=0}$ to 0.000068 $_{t>0}$; inc, ikc, and inkcc remain unchanged; see Figure 2. Cl⁻ and Na⁺ fluxes through 1:1 exchangers are not included in the calculation.

TABLE 5 | Changes in the permeability coefficients of Na⁺, K⁺, and Cl⁻ channels obtained for apoptotic U937 cells by computation at a different set of parameters of NC, KC, and NKCC cotransporters (cells A in Table 2).

Cotransporters		Channel permeability	Resting	In apoptosis	Apoptotic to resting
NC only		pCl	0.0125	0.068	5.4
		pNa	0.0041	0.003	0.73
		pK	0.0115	0.030	2.6
NC, KC, and NKCC	X	pCl	0.0102	0.065	6.4
		pNa	0.00355	0.0025	0.70
		pK	0.010	0.033	3.3
	Y	pCl	0.005	0.09	18
		pNa	0.00215	0.0015	0.70
		pK	0.0058	0.0174	3.0

Lang and Hoffmann, 2012, 2013; Jentsch, 2016; Delpire and Gagnon, 2018; Dmitriev et al., 2019). However, only a few studies have considered the cotransporters in the quantitative description of the entire balance of ion fluxes across the cell membrane. Lew was the first to find that the balance in human reticulocytes with a non-equilibrium balanced distribution of Cl⁻ cannot be explained without NC (Lew et al., 1991). NC and KC cotransporters were included in cellular ionic homeostasis model by Hernández and Cristina (1998). The NKCC cotransport was considered when modeling the ionic balance in cardiomyocytes (Terashima et al., 2006). The balance of Cl⁻ fluxes through cotransporters and channels was not considered in the early fundamental studies of cotransporters in erythrocytes because the distribution of Cl⁻ is determined in these cells by a powerful Cl⁻/HCO₃⁻ exchanger, but not by Cl⁻ channels.

Later, the interplay between various cation-coupled Cl⁻ cotransporters (SLC12 gene family) and Cl⁻ channels has been intensively studied in relation to signal transduction in neurons (Kaila et al., 2014; Doyon et al., 2016; Currin et al., 2020;

Wilke et al., 2020), in astroglia physiology (Wilson and Mongin, 2018) and in phagocytosis (Wang, 2016; Perry et al., 2019). Unfortunately, in all these cases, it was extremely difficult to obtain a complete set of accurate and reliable experimental data necessary for quantitative description of the entire flux balance across the cell membrane. Computer calculations show that small variations in the input data may produce substantially different results.

The use of ion-sensitive dyes and calcein to determine the cell water, Cl⁻, and Na⁺ allows us to measure mainly the relative changes in their values, but absolute value measurements may not be reliable enough due to calibration difficulties. Recently, we have found that measurements of Na⁺ concentration in U937 cells by the direct flame emission method and by the ANG-2 dye method give substantially different results (Yurinskaya et al., 2020b).

It is important that U937 cells cultured in suspension allow the determination of the cell water content by measuring the buoyant density without known problems in estimation of extracellular

water in the sample. These cells also allow determining cell ions both by direct flame emission and by ion-sensitive dyes using flow cytometry. It is also important that cells cultured in suspension remain intact during transfer to a flow cytometer or to a density gradient. The detachment of cells from the substrate, enzymatically or mechanically, when working with adherent cell cultures, always affects their ionic composition. We use computer calculations and cell experimental data to analyze the role of the NKCC and KC cotransporters in the ionic balance of cells at rest and in early apoptosis. Our program allows one to quickly test various sets of parameters characterizing the kinetics of ion transport through multiple pathways of the cell membrane. By combining measured and computed data, we were able to compare pathway behavior in normal and apoptotic cells.

One of the most important and difficult problems in this area is the determination of the real values of the parameters based on real experimental data, rather than searching additional parameters characterizing all variety of channels or transporters. To quantitatively analyze the relationships between fluxes through multiple ionic pathways in the cell membrane, it is sufficient to use the driving forces for each type of pathway that are known and linear coefficients for each pathway and each type of ion. The number of even simplified parameters turns out to be rather large. In our case, it is impossible to predict theoretically how many sets of parameters will give the same result and how to obtain a unique set of parameters that provide agreement between experimental and calculated data (Yurinskaya et al., 2019). However, a unique set of parameters can be obtained if auxiliary information from the experiment is used in addition to mathematical solutions. In the present study, the ratio of ouabain-sensitive to ouabain-resistant components of rubidium influx (OSOR) helped to select the right set of parameters. OSOR is easily and reliably obtained from experimental data. Its value is included in the output table calculated by our computing program. The use of bumetanide and DIOA, specific blockers of NKCC and KC fluxes, gave an upper limit for Rb⁺ (K⁺) influxes mediated by these transporters in our study. Calculations predict different membrane potential for a different set of NKCC and KC parameters. Hence, the measurement of membrane potential can determine which of the X or Y parameter sets in **Table 2** is correct for the cells in question. We suggest that reliable membrane potential data can be obtained using voltage-sensitive dyes such as DiBaC4 rather than microelectrodes. An interesting comparison of the two methods has been made recently (Bonzanni et al., 2020). Measuring multiple cell characteristics can solve the problem of multiple parameters.

U937 cells are an established model in the experimental study of apoptosis. The calculation of apoptotic changes in cell ionic homeostasis in our previous study concerned the interaction between pump, channels, and NC cotransport without NKCC and KC. The effects of the cotransporters NKCC and KC on changes in the flux balance during apoptosis remained unexplored. Calculation of the net and unidirectional Na⁺, K⁺, and Cl⁻ fluxes via KC and NKCC pathways in the studied cells showed that the difference in the effects of the specific inhibitors of KC and NKCC on the uptake Rb⁺ (K⁺) as in conventional

methods of testing KC and NKCC cotransport does not reflect their impact upon the entire ionic homeostasis. The effect of the net KC flux on the entire ionic balance is higher than the net NKCC flux because the driving force in the KC pathway is higher than in the NKCC pathway. Whereas NC plays a critical role in generating *mucl*, the driving force for the Cl⁻ net flux through channels with all its consequences, the NKCC cotransport is practically ineffective in creating *mucl*, while KC can only reduce it.

An increase in the permeability of Cl⁻ channels at the early stage of apoptosis, found by calculations, is in good agreement with numerous electrophysiological data indicating an increase in the integral conductance of chloride channels VRAC during apoptosis (Hoffmann et al., 2015; Kondratskyi et al., 2015; Jentsch, 2016; Pedersen et al., 2016; Wanitchakool et al., 2016). We studied the expression of these channels in U937 cells under our experimental conditions using an antibody against the outer loop of the LRRC8A VRAC subunit (Yurinskaya et al., 2020a). It was found that the number of channels expressed in the membrane does not change to the extent comparable with the changes in the integral permeability of Cl⁻ channels. This indicates a change in the internal properties of the channels, but not their number in the membrane.

Calculation shows that the net fluxes out of cells of all three ions, K⁺, Na⁺, and Cl⁻, arise at the early stage of apoptosis (**Table 4**). The K⁺ net flux out of cells is the one of the most significant causes of the known apoptotic decrease of K⁺ content in cells and their concomitant apoptotic shrinkage (Yurinskaya et al., 2005). The significant K⁺ net flux out of cells arises at the early stage of apoptosis mostly due to an increase of the channel K⁺ efflux caused by an increase in channel permeability and also due to a decrease of the pump K⁺ influx. It should be noted that the K⁺ and Cl⁻ channel fluxes increase in both directions, but the increase in efflux exceeds the increase in influxes. The net Cl⁻ flux out of cells underlies the initial drop in Cl⁻ content and concentration observed in apoptotic cells. It is caused not only by an increase of pCl from 0.005 to 0.09 but also by a shift in the membrane potential toward hyperpolarization due to an increase in pK. The shift in the membrane potential causes an increase in Cl⁻ electrochemical potential difference. The initially outward net Na⁺ flux reverses later to the inward net flux and Na⁺ content, and concentration in apoptotic cells begins to increase. This is because the apoptotic decrease in the pump efflux outweighs the decrease in channel Na⁺ influx (**Table 4**). It has been shown earlier that pNa decrease and pK increase alone without a pCl increase could also be sufficient to get agreement between real and calculated chloride concentrations for the first 30 min. However, this variant should be rejected as the OSOR value becomes unrealistically low (Yurinskaya et al., 2019).

Non-zero net fluxes of all three K⁺, Na⁺, and Cl⁻ ions in U937 cells during STS-induced apoptosis indicate that a balanced ion distribution is not achieved within the first 4 h. In our earlier study (Yurinskaya et al., 2011), it was hypothesized that a balanced state takes place in apoptotic U937 cells under the discussed conditions. At that time, data on the distribution

of Cl⁻ were scarce, and the computational tool was not yet sufficiently developed. Based on that hypothetical assumption it was concluded that “A decrease in the channel permeability of the plasma membrane for Na⁺ is proved to be crucial for preventing cell swelling due to the decrease in the Na⁺/K⁺ pump activity in cells undergoing apoptosis whereas opening of the K⁺ and Cl⁻ channels is not required”. This conclusion should be considered at present as incorrect.

It would be very interesting to learn about the role of monovalent ions not only at the early 4 h stage of STS-induced apoptosis in U937 cells, despite the fact that this model is popular and that the developed approach to studying apoptosis in other cells may have a more general significance. The role of monovalent ions in the subsequent development of apoptosis is no less interesting, since understanding apoptosis in its entirety is necessary for solving many practical problems, for example, searching for targets of anticancer drugs. Unfortunately, there are still no necessary data on changes in the ion content, water balance, and sodium pump fluxes at the late stages of apoptosis. A quantitative description of ionic processes during late apoptosis is a matter of the future.

CONCLUSION

A developed approach enables us to obtain a complete list of the inward and outward Na⁺, K⁺, and Cl⁻ fluxes via all major pathways across the plasma membrane including NKCC and KC cotransporters in U937 cells at rest and during the first 4 h of apoptosis induced by staurosporine.

The problem of the inevitable multiplicity of solutions to the flux equations arising with an increase in the number of paths for ions can be solved in real cases if we take into account the ratio of the ouabain-sensitive and ouabain-resistant parts of the influx K⁺(Rb⁺) and use additional experimental data on the effects of specific inhibitors or some other data.

The dynamics of changes in plasma membrane channels and transporters, which underlie apoptotic changes in the content of ions and water in cells, calculated earlier without taking into account the KC and NKCC cotransporters, differs from that calculated for cells with the KC and NKCC cotransporters only in details.

REFERENCES

- Bonzanni, M., Payne, S. L., Adelfio, M., Kaplan, D. L., Levin, M., and Oudin, M. J. (2020). Defined extracellular ionic solutions to study and manipulate the cellular resting membrane potential. *Biol. Open.* 9:bio048553. doi: 10.1242/bio.048553
- Curran, C. B., Trevelyan, A. J., Akerman, C. J., and Raimondo, J. V. (2020). Chloride dynamics alter the input-output properties of neurons. *PLoS Comput. Biol.* 16:e1007932. doi: 10.1371/journal.pcbi.1007932
- Delpire, E., and Gagnon, K. B. (2018). Water homeostasis and cell volume maintenance and regulation. *Curr. Top. Membr.* 81, 3–52. doi: 10.1016/bs.ctm.2018.08.001
- Dmitriev, A. V., Dmitriev, A. A., and Linsenmeier, R. A. (2019). The logic of ionic homeostasis: cations are for voltage, but not for

The developed approach to determining unidirectional fluxes can be useful for studying the functional expression of ion channels and transporters in other cells.

DATA AVAILABILITY STATEMENT

The original contributions presented in the study are included in the article/**Supplementary Material**, further inquiries can be directed to the corresponding author.

AUTHOR CONTRIBUTIONS

AV wrote the manuscript with input from all authors. All authors contributed to the design of the experiments, performed the experiments, analyzed the data, and approved the final version of the manuscript and agreed to be accountable for all aspects of the work. All persons designated as authors qualify for authorship, and all those who qualify for authorship are listed.

FUNDING

The research was supported (VY and AV) by the State assignment of Russian Federation No. 0124-2019-0003 and by a grant from the Director of the Institute of Cytology of RAS.

ACKNOWLEDGMENTS

We thank Dr. Tatyana Goryachaya for excellent assistance in the experiments with cells. We are grateful to Drs. AV and AA Dmitriev (Department of Biomedical Engineering, Northwestern University, Evanston, Illinois, United States) for correcting the manuscript and suggestions for improvement.

SUPPLEMENTARY MATERIAL

The Supplementary Material for this article can be found online at: <https://www.frontiersin.org/articles/10.3389/fcell.2020.591872/full#supplementary-material>

- volume. *PLoS Comput. Biol.* 15:e1006894. doi: 10.1371/journal.pcbi.1006894
- Doyon, N., Vinay, L., Prescott, S. A., and De Koninck, Y. (2016). Chloride regulation: a dynamic equilibrium crucial for synaptic inhibition. *Neuron* 89, 1157–1172.
- Gagnon, K. B., and Delpire, E. (2013). Physiology of SLC12 transporters: lessons from inherited human genetic mutations and genetically engineered mouse knockouts. *Am. J. Physiol. Cell Physiol.* 304, C693–C714. doi: 10.1152/ajpcell.00350.2012
- Galluzzi, L., Vitale, I., Aaronson, S. A., Abrams, J. M., Adam, D., Agostinis, P., et al. (2018). Molecular mechanisms of cell death: recommendations of the Nomenclature Committee on Cell Death 2018. *Cell Death Differ.* 25, 486–541. doi: 10.1038/s41418-017-0012-4
- Gamba, G. (2005). Molecular physiology and pathophysiology of electroneutral cation-chloride cotransporters. *Physiol. Rev.* 85, 423–493.

- Garcia-Soto, J. J., and Grinstein, S. (1990). Determination of the transmembrane distribution of chloride in rat lymphocytes: role of Cl⁻-HCO₃⁻-exchange. *Am. J. Physiol. Cell. Physiol.* 258, C1108–C1116.
- Hernández, J. A., and Cristina, E. (1998). Modeling cell volume regulation in nonexcitable cells: the roles of the Na⁺ pump and of cotransport systems. *Am. J. Physiol.* 275, C1067–C1080.
- Hoffmann, E. K. (1982). Anion exchange and anion-cation co-transport systems in mammalian cells. *Philos. Trans. R. Soc. Lond. B Biol. Sci.* 299, 519–535.
- Hoffmann, E. K. (2001). The pump and leak steady-state concept with a variety of regulated leak pathways. *J. Membr. Biol.* 184, 321–330.
- Hoffmann, E. K., Lambert, I. H., and Pedersen, S. F. (2009). Physiology of cell volume regulation in vertebrates. *Physiol. Rev.* 89, 193–277.
- Hoffmann, E. K., Simonsen, L. O., and Sjøholm, C. (1979). Membrane potential, chloride exchange, and chloride conductance in Ehrlich mouse ascites tumour cells. *J. Physiol.* 296, 61–84. doi: 10.1113/jphysiol.1979.sp012991
- Hoffmann, E. K., Sørensen, B. H., Sauter, D. P. R., and Lambert, I. H. (2015). Role of volume-regulated and calcium-activated anion channels in cell volume homeostasis, cancer and drug resistance. *Channels* 9, 380–396. doi: 10.1080/19336950.2015.1089007
- Jentsch, T. J. (2016). VRACs and other ion channels and transporters in the regulation of cell volume and beyond. *Nat. Rev. Mol. Cell. Biol.* 17, 293–307. doi: 10.1038/nrm.2016.29
- Kaila, K., Price, T. J., Payne, J. A., Puskarjov, M., and Voipio, J. (2014). Cation-chloride cotransporters in neuronal development, plasticity and disease. *Nat. Rev. Neurosci.* 15, 637–654. doi: 10.1038/nrn3819
- Kondratskiy, A., Kondratska, K., Skryma, R., and Prevarskaya, N. (2015). Ion channels in the regulation of apoptosis. Special issue: membrane channels and transporters in cancers. *Biochim. Biophys. Acta* 1848, 2532–2546.
- Lang, F., Föller, M., Lang, K. S., Lang, P. A., Ritter, M., Gulbins, E., et al. (2005). Ion channels in cell proliferation and apoptotic cell death. *J. Membr. Biol.* 205, 147–157. doi: 10.1007/s00232-005-0780-5
- Lang, F., and Hoffmann, E. K. (2012). Role of ion transport in control of apoptotic cell death. *Compr. Physiol.* 2, 2037–2061.
- Lang, F., and Hoffmann, E. K. (2013). CrossTalk proposal: cell volume changes are an essential step in the cell death machinery. *J. Physiol.* 591, 6119–6121. doi: 10.1113/jphysiol.2013.258632
- Lew, V. L., Freeman, C. J., Ortiz, O. E., and Bookchin, R. M. (1991). A mathematical model of the volume, pH, and ion content regulation in reticulocytes. Application to the pathophysiology of sickle cell dehydration. *J. Clin. Invest.* 87, 100–112.
- Maeno, E., Ishizaki, Y., Kanaseki, T., Hazama, A., and Okada, Y. (2000). Normotonic cell shrinkage because of disordered volume regulation is an early prerequisite to apoptosis. *Proc. Natl. Acad. Sci. U.S.A.* 97, 9487–9492.
- Maeno, E., Tsubata, T., and Okada, Y. (2012). Apoptotic volume decrease (AVD) is independent of mitochondrial dysfunction and initiator caspase activation. *Cells* 1, 1156–1167. doi: 10.3390/cells1041156
- Okada, Y., Maeno, E., Shimizu, T., Dezaki, K., Wang, J., and Morishima, S. (2001). Receptor-mediated control of regulatory volume decrease (RVD) and apoptotic volume decrease (AVD). *J. Physiol.* 532, 3–16.
- Pedersen, S. F., Okada, Y., and Nilius, B. (2016). Biophysics and physiology of the volume-regulated anion channel (VRAC)/Volume-sensitive outwardly rectifying anion channel (VSOR). *Pflugers Arch. Eur. J. Physiol.* 468, 371–383. doi: 10.1007/s00424-015-1781-6
- Perry, J. S. A., Morioka, S., Medina, C. B., Etchegaray, J. I., Barron, B., Raymond, M. H., et al. (2019). Interpreting an apoptotic corpse as anti-inflammatory involves a chloride sensing pathway. *Nat. Cell. Biol.* 21, 1532–1543. doi: 10.1038/s41556-019-0431-1
- Russell, J. M. (2000). Sodium-potassium-chloride cotransport. *Physiol. Rev.* 80, 211–276.
- Terashima, K., Takeuchi, A., Sarai, N., Matsuoka, S., Shim, E. B., Leem, C. H., et al. (2006). Modelling Cl⁻ homeostasis and volume regulation of the cardiac cell. *Philos. Trans. A Math. Phys. Eng. Sci.* 364, 1245–1265.
- Vereninov, A. A., Goryachaya, T. S., Moshkov, A. V., Vassilieva, I. O., Yurinskaya, V. E., Lang, F., et al. (2007). Analysis of the monovalent ion fluxes in U937 cells under the balanced ion distribution: recognition of ion transporters responsible for changes in cell ion and water balance during apoptosis. *Cell Biol. Int.* 31, 382–393.
- Vereninov, A. A., Rubashkin, A. A., Goryachaya, T. S., Moshkov, A. V., Rozanov, Y. M., Shirokova, A. V., et al. (2008). Pump and channel K⁺(Rb⁺) fluxes in apoptosis of human lymphoid cell line U937. *Cell. Physiol. Biochem.* 22, 187–194.
- Vereninov, I. A., Yurinskaya, V. E., Model, M. A., Lang, F., and Vereninov, A. A. (2014). Computation of pump-leak flux balance in animal cells. *Cell. Physiol. Biochem.* 34, 1812–1823. doi: 10.1159/000366382
- Vereninov, I. A., Yurinskaya, V. E., Model, M. A., and Vereninov, A. A. (2016). Unidirectional flux balance of monovalent ions in cells with Na⁺/Na⁺ and Li⁺/Na⁺ exchange: experimental and computational studies on lymphoid U937 cells. *PLoS One* 11:e0153284. doi: 10.1371/journal.pone.0153284
- Wang, G. (2016). Chloride flux in phagocytes. *Immunol. Rev.* 273, 219–231.
- Wanitchakool, P., Ousingsawat, J., Sirianant, L., MacAulay, N., Schreiber, R., and Kunzelmann, K. (2016). Cl⁻ channels in apoptosis. *Eur. Biophys. J.* 45, 599–610. doi: 10.1007/s00249-016-1140-3
- Wilke, B. U., Kummer, K. K., Leitner, M. G., and Kress, M. (2020). Chloride - the underrated ion in nociceptors. *Front. Neurosci.* 14:287. doi: 10.3389/fnins.2020.00287
- Wilson, C. S., and Mongin, A. A. (2018). Cell volume control in healthy brain and neuropathologies. *Curr. Top. Membr.* 81, 385–455. doi: 10.1016/bs.ctm.2018.07.006
- Yurinskaya, V., Aksenov, N., Moshkov, A., Goryachaya, T., Shemery, A., and Vereninov, A. (2020a). Flow fluorometry quantification of anion channel VRAC subunit LRRC8A at the membrane of living U937 cells. *Channels* 14, 45–52. doi: 10.1080/19336950.2020.1730535
- Yurinskaya, V., Aksenov, N., Moshkov, A., Goryachaya, T., and Vereninov, A. (2020b). Fluorometric Na⁺ evaluation in single cells using flow cytometry: comparison with flame emission assay. *Cell. Physiol. Biochem.* 54, 556–566. doi: 10.33594/000000239
- Yurinskaya, V., Goryachaya, T., Guzova, I., Moshkov, A., Rozanov, Y., Sakuta, G., et al. (2005). Potassium and sodium balance in U937 cells during apoptosis with and without cell shrinkage. *Cell. Physiol. Biochem.* 16, 155–162.
- Yurinskaya, V. E., Rubashkin, A. A., and Vereninov, A. A. (2011). Balance of unidirectional monovalent ion fluxes in cells undergoing apoptosis: why does Na⁺/K⁺ pump suppression not cause cell swelling? *J. Physiol.* 589, 2197–2211.
- Yurinskaya, V. E., Vereninov, I. A., and Vereninov, A. A. (2019). A tool for computation of changes in Na⁺, K⁺, Cl⁻ channels and transporters due to apoptosis by data on cell ion and water content alteration. *Front. Cell Dev. Biol.* 7:58. doi: 10.3389/fcell.2019.00058

Conflict of Interest: The authors declare that the research was conducted in the absence of any commercial or financial relationships that could be construed as a potential conflict of interest.

Copyright © 2020 Yurinskaya, Vereninov and Vereninov. This is an open-access article distributed under the terms of the Creative Commons Attribution License (CC BY). The use, distribution or reproduction in other forums is permitted, provided the original author(s) and the copyright owner(s) are credited and that the original publication in this journal is cited, in accordance with accepted academic practice. No use, distribution or reproduction is permitted which does not comply with these terms.



Acid- and Volume-Sensitive Chloride Currents in Human Chondrocytes

Michael Kittl¹, Martina Winklmayr², Katharina Helm¹, Johannes Lettner¹,
Martin Gaisberger^{1,2,3}, Markus Ritter^{1,2,3} and Martin Jakab^{1*}

¹ Institute of Physiology and Pathophysiology, Paracelsus Medical University, Salzburg, Austria, ² Ludwig Boltzmann Institute for Arthritis and Rehabilitation, Paracelsus Medical University, Salzburg, Austria, ³ Gastein Research Institute, Paracelsus Medical University, Salzburg, Austria

OPEN ACCESS

Edited by:

Tobias Stauber,
Medical School Hamburg, Germany

Reviewed by:

Richard Barrett-Jolley,
University of Liverpool,
United Kingdom
Florian Ullrich,
Helmholtz Association of German
Research Centers (HZ), Germany

*Correspondence:

Martin Jakab
martin.jakab@pmu.ac.at

Specialty section:

This article was submitted to
Cell Death and Survival,
a section of the journal
Frontiers in Cell and Developmental
Biology

Received: 14 July 2020

Accepted: 13 October 2020

Published: 13 November 2020

Citation:

Kittl M, Winklmayr M, Helm K,
Lettner J, Gaisberger M, Ritter M and
Jakab M (2020) Acid-
and Volume-Sensitive Chloride
Currents in Human Chondrocytes.
Front. Cell Dev. Biol. 8:583131.
doi: 10.3389/fcell.2020.583131

Chondrocytes face extreme alterations of extracellular osmolarity and pH, which force them to appropriately regulate their cell volume (CV) and cellular pH. Perturbations of these mechanisms lead to chondrocyte death and ultimately to osteoarthritis (OA), the most common chronic joint diseases worldwide. OA hallmarks are altered cartilage hydration and severe fluid acidification. Impaired CV regulation and acidotoxicity contribute to disease progression and volume-sensitive anion channels are upregulated in OA. This study assessed the effect of hypotonicity and extracellular acidification on chondrocyte Cl⁻ conductances and CV regulation. Cl⁻ currents and membrane potentials were measured in human C28/I2 cells and primary human chondrocytes using the patch clamp technique. Intracellular pH was assessed by BCECF fluorescence, CV measurements were performed using the Coulter method, and cell viability/cell death by a resazurin assay. Hypotonic cell swelling caused activation of a volume-sensitive outwardly rectifying (VSOR) Cl⁻ current followed by a regulatory volume decrease (RVD), which was attenuated by the Cl⁻ channel blocker DCPIB. Extracellular, but not intracellular acidification to pH ≤ 5.0 elicited an acid-sensitive outwardly rectifying (ASOR) Cl⁻ conductance. Activation of either current depolarized the cell membrane potential. Under simultaneous hypotonic and acidic stimulation, VSOR and ASOR currents transiently coactivated, giving rise to a mixed current phenotype. Over time the VSOR current gradually vanished and the residual conductance showed a pure ASOR current phenotype. Extracellular acidification caused an isotonic CV gain and a complete suppression of RVD under hypotonic conditions. The results suggest that deactivation of the VSOR current under acidic conditions impairs CV regulation in chondrocytes, which is likely to compromise chondrocyte viability.

Keywords: acidic, chloride, current, chondrocytes, osteoarthritis, pH, volume, RVD

INTRODUCTION

Osteoarthritis (OA) is one of the most common chronic joint diseases worldwide. Its prevalence is increasing constantly due to aging of the population (Vos et al., 2012; Palazzo et al., 2016). As yet there are no disease-modifying drugs available and medical care is mainly limited to pain reduction. In severe cases of OA, joint replacement is the last therapeutic possibility. OA is characterized by (1) elevated catabolic responses, (2) inflammation of the synovial compartments, (3) subchondral

bone alterations, and (4) osteophyte formation, which affect the whole joint and cause disability by progressive cartilage destruction (Man and Mologhianu, 2014). In view of the disease burden and the lack of remedies, studies on the onset and progression of OA as well as potential new targets for therapy are required.

Articular cartilage consists of extracellular matrix (ECM) and embedded chondrocytes, which are the sole cellular residents of the tissue. The ECM is highly hydrated with a water content of approximately 70% and hypertonic. Upon mechanical loadings, cartilage deformation, cell membrane stretch, and water extrusion lead to changes in both fluid volume and osmotic pressure (Maroudas et al., 1991; Sophia Fox et al., 2009). Under load, the osmotic concentration of the ECM can rise up to approximately 480 mosm/kg, which decreases again during relaxation (Lewis et al., 2011a). In this specific environment, chondrocytes need to actively adapt their cell volume (CV) based on the prevalent osmotic pressure. In general, a hypertonic challenge causes cell shrinkage, which is opposed by a gain of solutes and water through a process termed regulatory volume increase (RVI). Cells exposed to a hypotonic environment gain volume through passive water uptake and compensate cell swelling by extruding solutes, which osmotically drives the efflux of water [regulatory volume decrease (RVD)] (reviewed, e.g., in Lang et al., 1998; Hoffmann et al., 2009). By mediating the efflux of Cl^- and organic osmolytes, volume-sensitive outwardly rectifying (VSOR) anion channels/currents [also known as swelling-activated Cl^- currents, $\text{I}_{\text{Cl,swell}}$, or volume-regulated anion currents (VRAC)] are critically involved in RVD in virtually any cell type. They contribute to the regulation of ion homeostasis, transepithelial transport, and electrical excitability, and are tightly linked to cell migration, phagocytosis, proliferation, and apoptosis (Jentsch et al., 2002; Jakab and Ritter, 2006; Okada et al., 2006; Hoffmann, 2011; Harl et al., 2013; Pedersen et al., 2016; Kittl et al., 2018). The function of the VSOR current in CV and membrane potential regulation has also been shown in chondrocytes (Wilkins et al., 2000; Isoya et al., 2009; Funabashi et al., 2010; Lewis et al., 2011a,b; Ponce et al., 2012; Kumagai et al., 2016), where the Cl^- current might indirectly affect matrix protein synthesis by modulating intracellular Ca^{2+} levels (Alford et al., 2003).

Importantly, the onset of OA is characterized by tissue swelling and enhanced hydration, leading to a decrease in osmolality and altered ionic composition (Bush and Hall, 2005). In OA patients, the osmolality of the synovial fluid is hypoosmotic (249–277 mosm/kg) compared to healthy subjects (295–340 mosm/kg) (Bertram and Krawetz, 2012). OA is also accompanied by an acidification of the extracellular space, which significantly affects cartilage metabolism and inhibits matrix synthesis (Wu et al., 2007; Sun et al., 2018). Under physiological conditions, the pH of cartilage is weakly acidic (pH 7.2–6.9), but under pathological conditions, the environment is further acidified by the production of pro-inflammatory factors and enhanced anaerobic glycolysis (Hall et al., 1996; Wilkins et al., 2000). Intraoperative *in situ* pH measurements revealed massive acidification in primary OA patients, ranging from pH 7.1 at stage 0 to pH 5.5 at stage 3 (Konttinen et al., 2002).

In different cell types, extracellular acidification elicits an acid-sensitive outwardly rectifying (ASOR) Cl^- current (Auzanneau et al., 2003; Nobles et al., 2004; Lambert and Oberwinkler, 2005; Yamamoto and Ehara, 2006; Wang et al., 2007; Kajiya et al., 2009; Kucherenko et al., 2009; Sato-Numata et al., 2013, 2014, 2016, 2017; Capurro et al., 2015; Kurita et al., 2015; Valinsky et al., 2017; Kittl et al., 2019). The ASOR current shows similarities to VSOR currents like its pharmacological profile, ion permeability sequence, and outward rectification. It was therefore debated if the two conductances are manifestations of the same channel protein(s) activated either by cell swelling or acidification, or if different entities constitute the VSOR and ASOR channel pore (Nobles et al., 2004; Lambert and Oberwinkler, 2005; Capurro et al., 2015). Most studies focused on whole-cell Cl^- currents either under hypotonic or acidic conditions, so that currently little is known about the functional interrelation and possible coexistence of the two currents under simultaneous hypotonic and acidic conditions. In a previous paper, we could show in microglial cells that VSOR and ASOR currents can be simultaneously active for a short period until the ASOR current eventually becomes dominating and we found that RVD was abrogated under acidic conditions in these cells (Kittl et al., 2019).

Cell swelling has been suggested to be one of the first changes in OA (Bush and Hall, 2003, 2005). Impaired CV regulation under hypoosmotic and acidic conditions prevailing in OA could therefore have a detrimental effect on chondrocyte viability and function and disease progression. The aim of our study was to investigate Cl^- conductances and CV regulation in chondrocytes under these conditions. We report on the functional expression of ASOR channels in human chondrocytes and possible effects of the interrelation of ASOR and VSOR Cl^- currents on CV homeostasis.

MATERIALS AND METHODS

Salts, Chemicals, Drugs

All salts and chemicals were *p.a.* grade. Nigericin and tamoxifen were purchased from Sigma-Aldrich-Merck (Darmstadt, Germany), DCPIB (4-[(2-butyl-6,7-dichloro-2-cyclopentyl-2,3-dihydro-1-oxo-1H-inden-5 yl)oxy]butanoic acid) from Tocris (Abingdon, United Kingdom), and BCECF-AM [2',7'-bis-(2-carboxyethyl)-5-(and-6)-carboxyfluorescein, acetoxymethyl ester] from Merck-Calbiochem (Darmstadt, Germany). Stock solutions of nigericin (5 mg/ml) and DCPIB (100 mM) were prepared in ethanol. Tamoxifen and BCECF-AM were dissolved in dimethyl sulfoxide (DMSO) to give stock solutions of 40 and 100 mM, respectively. Stocks were stored in aliquots at 20°C until use.

Cell Culture

Human immortalized C28/I2 cells (Goldring et al., 1994; Finger et al., 2003) were cultured in 25 cm² flasks with DMEM/HAM's F-12 medium (Biochrom, Berlin, Germany) supplemented with 5% fetal bovine serum (FBS Superior, Biochrom) and antibiotic-antimycotic solution (100 U/ml penicillin, 0.1 mg/ml

streptomycin, 0.25 $\mu\text{g}/\text{ml}$ amphotericin-B; Sigma-Aldrich). C28/I2 cells were kept at 37°C in a humidified atmosphere of 5% CO_2 (standard culture conditions). Subcultures were established once a week until passage 25. Primary chondrocytes were isolated from total human knee arthroplasty samples with informed consent and ethical approval by the Ethics Committee of Salzburg (415-E/1965/4-2015) as described in Winklmayr et al. (2019). In brief, cartilage samples were removed from subchondral bone and crashed into small pieces. After washing with phosphate-buffered saline (PBS), they were put on a shaker and digested overnight in DMEM/HAM's F-12 supplemented with FBS and 2 mg/ml collagenase (Thermo Fisher) at 37°C . After 24 h, cells were (1) centrifuged, (2) washed twice with PBS, (3) resuspended in medium, and (4) seeded as required for the following experiments. Primary chondrocytes were used up to passage 2.

Patch Clamp

Cells were seeded on 0.01% poly-D-lysine (PDL)-coated coverslips (\varnothing 12 mm) and cultured for at least 24 h in DMEM/HAM's F-12 medium. Coverslips were transferred to a RC-25 recording chamber (Warner Instruments, Hamden, CT, United States) and mounted on a Nikon Eclipse TE2000-U inverted microscope. Experiments were performed at room temperature in the whole-cell perforated patch clamp mode using 130 μM amphotericin to the pipette solution unless otherwise stated. Recordings were started as soon as the serial resistance was below 30 $\text{M}\Omega$ for the perforated configuration and below 10 $\text{M}\Omega$ if the ruptured configuration was applied. Patch electrode resistances were 4–9 $\text{M}\Omega$. After establishing the whole-cell configuration, cells were superfused with an extracellular solution and data were recorded using an EPC-10 amplifier controlled by PatchMaster software (HEKA, Lambrecht/Pfalz, Germany). Cell membrane potential (V_{mem}) recordings were performed in the zero-current clamp mode. The intracellular (pipette) solution contained (in mM): K_2SO_4 70, NaCl 10, KCl 10, MgCl_2 4, CaCl_2 2, 4-(2-hydroxyethyl)-1-piperazineethanesulfonic acid (HEPES) free acid (FA) 5, ethylene glycol-bis(β -aminoethyl ether)-N,N,N',N'-tetraacetic acid (EGTA) 10 (249 mosm/kg, pH 7.2 adjusted with KOH). The extracellular solution contained (in mM): NaCl 140, KCl 5.6, CaCl_2 2.5, MgCl_2 1.5, HEPES FA 10, glucose 4.5, and mannitol 5 (300 mosm/kg, pH 4.5 adjusted with HCl, pH 7.4 adjusted with NaOH). Voltage clamp recordings of Cl^- currents under neutral and acidic conditions were performed under symmetrical intra- and extracellular Cl^- conditions. The extracellular solution consisted of (in mM): NaCl 100, CaCl_2 2.5, MgCl_2 2.5, HEPES FA 10, and mannitol 80 (300 mosm/kg, pH 7.2 adjusted with NaOH). Mannitol was omitted to obtain a hypotonic (220 mosm/kg) solution for VSOR activation. To assess pH dependencies, the extracellular solution was titrated with HCl to a pH ranging from 4.5 to 5.0. We used HEPES FA buffer also for solutions with a pH < 5.0 since we did not find any difference to results obtained in control experiments using 2-(N-morpholino)ethanesulfonic acid (MES) hydrate. The pipette solution contained (in mM): CsCl 100, MgCl_2 5, HEPES FA 10, EGTA 11, raffinose 60, Mg-ATP 2

(303 mosm/kg, pH 7.2 adjusted with CsOH). The pipette solution was titrated to pH 4.5 (HCl) to assess the effect of an intracellular acidification. The currents were monitored in response to voltage ramps (500 ms duration, 10-s interval) and voltage steps (500 ms duration, increments of 20 mV) from -100 to $+100$ mV. The holding potential between the ramps/steps was 0 mV to desensitize voltage-activated currents. Bath solution exchange was performed with a valve-controlled gravity-driven perfusion system (ALA Scientific Instruments, Farmingdale, NY, United States) at a flow rate of 3–5 ml/min. Osmolalities of intra- and extracellular solutions were measured using a vapor pressure osmometer (Wescor, Logan, UT, United States).

Cell Volume Measurements

C28/I2 cells were harvested by Trypsin/EDTA after growing under standard conditions. The cell suspension was split into aliquots, which were centrifuged for 4 min at $200 \times g$. The supernatants were discarded. Immediately before the first measurement (timepoint 0), the cell pellet was re-suspended in 20 ml of an extracellular solution containing (in mM): NaCl 100, KCl 5.6, CaCl_2 2.5, MgCl_2 1.5, HEPES FA 10, glucose 4.5, and mannitol 80 (300 mosm/kg). A hypotonic extracellular solution (220 mosm/kg) was obtained by the omission of mannitol. To measure the effect of acidification, the extracellular solution was adjusted to pH 7.4 and 4.5 titrated with NaOH or HCl, respectively. For the pH 4.5 solutions, MES hydrate was used instead of HEPES FA. DCPIB (10 μM) was added to the samples as indicated. The mean CVs (MCV in fl) in the different samples were alternately measured every 5 min over 60 min on a Beckman Coulter Z2 particle counter (Beckman Coulter, Krefeld, Germany) based on measuring changes in electrical resistance produced by non-conductive particles suspended in an electrolyte solution (Coulter method). Calibration for particle size was done using 10- μm Flow-Check fluorospheres (Beckman-Coulter). Data were analyzed with the Multisizer Software (Beckman-Coulter) using a 600-fl cutoff to exclude apoptotic cells and cell debris.

Intracellular pH (pH_i) Measurements

Cells were seeded in 96-well black microplates with clear bottom at a density of 1.5×10^5 cells/ml and kept under standard conditions for 24–48 h. Cells were loaded with 5 μM of the membrane permeable pH-sensitive dye BCECF-AM for 30 min at 37°C in serum-free medium. After removal of the loading medium 100 μl of extracellular solution containing (in mM): NaCl 140, KCl 5.6, CaCl_2 2.5, MgCl_2 1.5, HEPES FA 10, glucose 4.5, and mannitol 5 (300 mosm/kg) with the pH adjusted to 7.4, 6.0, 5.0, or 4.5 were added into the wells in quadruplicates. Fluorescence measurements (bottom readings) were performed at 37°C in a humidity cassette on a Spark 20M multimode plate reader (Tecan, Austria). BCECF was alternately excited at 440 and 490 nm using the built-in monochromator and emission was measured at 535 nm (20-nm bandwidth, 40 μs integration time) every 5 min over 75 min. Readings from wells containing non-BCECF-loaded cells were used for background subtraction. 490/440 nm ratios calculated from the corrected

fluorescence intensity values were converted to absolute pH using the high K^+ /nigericin calibration method (cells on the same microplate were exposed to solutions titrated to pH 8.0, 7.0, 6.0, or 5.0 in the presence of 140 mM KCl and 10 $\mu\text{g}/\text{ml}$ nigericin; for pH interpolation, the 490/440 nm fluorescence ratios obtained from these samples were fitted with a second-order polynomial function).

Cell Viability Assay

Viability measurements were performed as previously described by Helm et al. (2017). Briefly, after incubation for 2 or 4 h in an extracellular solution containing (in mM): NaCl 140, KCl 5.6, CaCl_2 2.5, MgCl_2 1.5, HEPES FA 10, glucose 4.5, and mannitol 5 (300 mosm/kg) with the pH adjusted to 7.4 or 7.0–3.0 in 0.5-pH-steps, cell viability was measured in each half of the 96-well microplate using the resazurin assay (7-hydroxy-3H-phenoxazin-3-one-10-oxide sodium salt; Sigma–Aldrich). The culture supernatant was replaced by 100 μl DMEM containing 0.5 mM resazurin (stock solution 2.5 mM in PBS). After 1 h of incubation at 37°C, 90 μl of the supernatant was transferred to a new 96-well microplate and stored at –20°C until measurement. The fluorescence of the product (resorufin) was detected at $\lambda_{\text{ex}} = 535$ nm and $\lambda_{\text{em}} = 595$ nm using a Zenyth microplate reader (Intensity-top-measurement; Anthos, Salzburg, Austria). Mean viability values were corrected for blank values (without cells) and related to untreated controls (UTC, without apoptosis inducer). All treatments were measured in quadruplicate wells.

Statistics

Data are expressed as means \pm standard error of the means (SEM) of at least three independent biological replicates ($n \geq 3$). In all experimental series, solvent control samples were included. Statistical tests applied are specified in the figure legends. Means were considered significantly different at p -values < 0.05 ($*p < 0.05$). Data were analyzed and plotted using GraphPad Prism 8 (GraphPad Software, La Jolla, CA, United States) or Igor Pro 8 (WaveMetrics, Portland, OR, United States).

RESULTS

Extracellular Acidification Induces an Acid-Sensitive Outwardly Rectifying (ASOR) Cl^- Current

Under control conditions (isotonic, pH 7.2), whole-cell currents in C28/I2 cells were small. Lowering the extracellular pH to ≤ 5.0 led to an increase in the whole-cell Cl^- conductance, which was fully reversible by reapplying control conditions. The current–voltage (I – V) relationship shifted from linear at pH 7.2 and 5.5 (baseline currents) to strongly outwardly rectifying at pH 5.0 and 4.5 (ASOR current). **Figure 1A** shows the mean current amplitudes recorded at pH 7.2, 5.5, 5.0, and 4.5. Using a voltage step protocol, currents were analyzed at the beginning and at the end of 500-ms voltage pulses (I_1 and I_2 , respectively). In C28/I2 cells, the ASOR current amplitudes recorded at

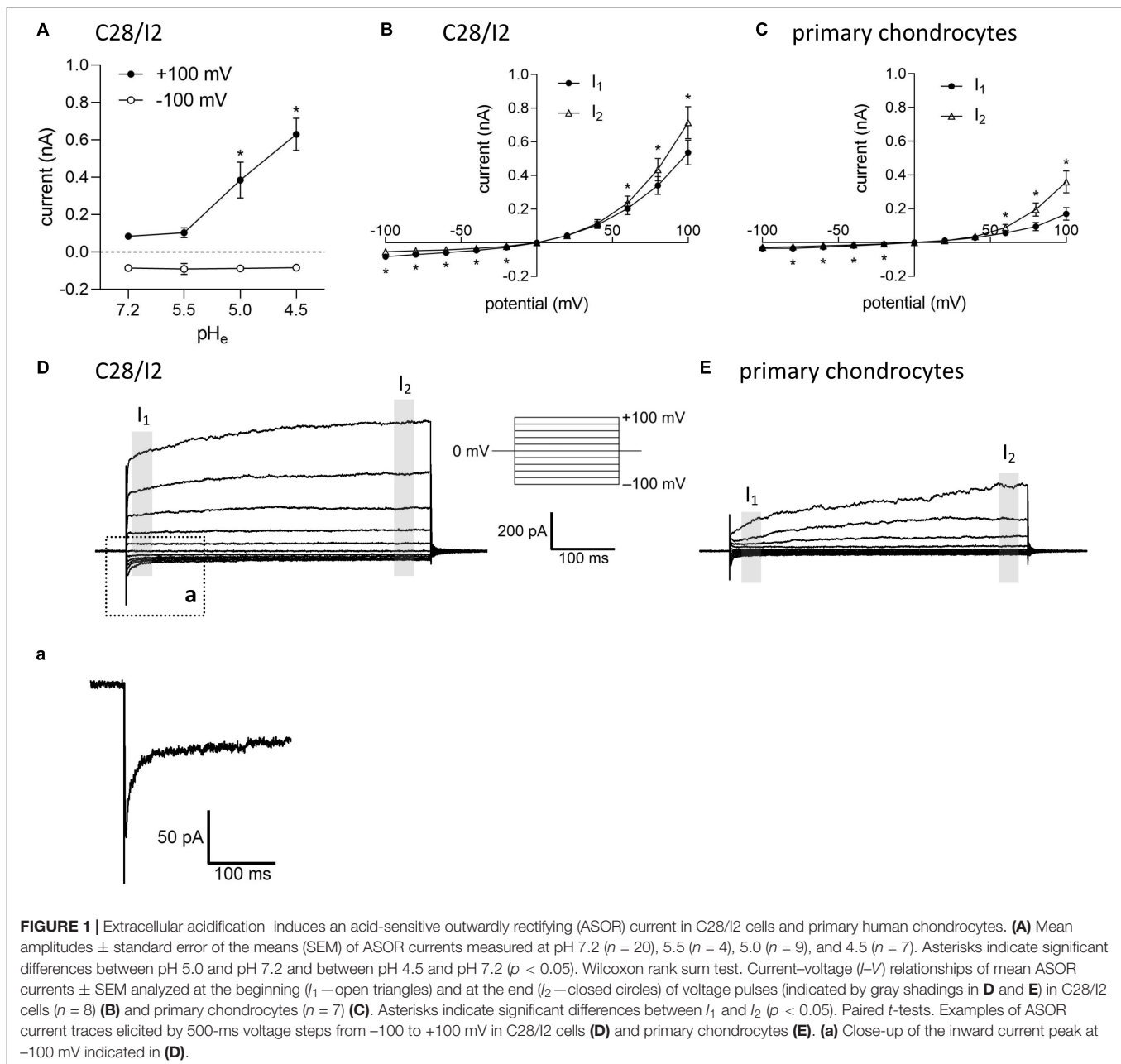
pH 4.5 showed time-dependent activation at constant positive holding potentials (+100 mV) and an initial negative current peak at –100 mV [**Figures 1B,D** and trace expansion (a)]. In primary chondrocytes, currents at pH 4.5 displayed the same characteristics; however, mean maximum current amplitudes were smaller as in C28/I2 cells (**Figures 1C,E**). Time-dependent changes in current amplitudes at constant holding potentials of +100 and –100 mV were quantified by calculating I_2/I_1 ratios with values > 1 indicating time-dependent activation and values < 1.0 indicating time-dependent inactivation as shown in **Figures 3G, 4G** for C28/I2 cells and primary chondrocytes, respectively. The time span for the ASOR current to reach peak values varied between the experiments, ranging from 5 up to 10 min (6.74 ± 0.65 min; $n = 7$).

ASOR Current Activation Requires Extracellular but Not Intracellular Acidification

In their native environment, chondrocytes are confronted with a substantial acidic load. In addition to intracellular acid loading due to lactate production under hypoxic conditions, there is constant leakage of H^+ ions into the cells from the acidic extracellular space (Wilkins et al., 2000). To test, in how far exposure to a low extracellular pH (pH_e) leads to an intracellular acidification in our experimental system, we monitored the intracellular pH (pH_i) in C28/I2 cells by using the pH-sensitive dye BCECF. Immediately after reducing pH_e to 6.5, 6.0, 5.5, 5.0, or 4.5, the pH_i significantly decreased to pH 6.5–5.8, depending on the degree of extracellular acidification, but did not reach values as low as the prevailing pH_e . After 5–10 min, the pH_i started to slowly but not fully recover within 80 min to values of 6.5–6.9 (**Figure 2A**). The decline in the pH_i might be sensed by ASOR channels and cause their activation. Therefore, we next investigated in C28/I2 cells, if intracellular acidification elicits the ASOR current. For this purpose, we performed patch clamp experiments in the ruptured configuration and used an acidic pipette solution (pH 4.5) to acidify the intracellular milieu. As shown in **Figure 2B**, decreasing the pH_i via the pipette solution neither affected basal whole-cell currents nor elicited an ASOR current unless an acidic extracellular solution was applied, which shows that only extracellular acidification can trigger ASOR current activation. Furthermore, cell viability measurements revealed that C28/I2 cells tolerate extracellular acidification to pH values as low as 4.5 for an extended period (4 h). Below a pH_e of 4.5 cell viability steeply declined and virtually all cells died (**Figure 2C**). We therefore did not expose cells to a pH_e lower than 4.5.

Extracellular Hypotonicity Induces a Volume-Sensitive Outwardly Rectifying (VSOR) Cl^- Current, Which Is Affected by Low pH_e

In virtually all cells, swelling leads to the activation of volume-regulated anion channels (VRAC) also known as VSOR anion channels, which give rise to swelling-dependent Cl^- currents



(termed $\text{ICl}_{\text{swell}}$ or ICl_{vol}) with amply described, characteristic features (reviewed, e.g., in Pedersen et al., 2016). As shown in **Figures 3, 4**, exposure of C28/I2 cells and primary chondrocytes, respectively, to a hypotonic extracellular solution (25% reduction in extracellular osmolality under pH 7.2) caused a reversible VSOR current activation. Compared to the ASOR current, the VSOR current was only weakly outwardly rectifying with an almost linear I - V relation at full current activation and showed a slower activation time course. While the ASOR current rapidly reached peak amplitudes, the VSOR current developed more slowly over time, reaching an activation plateau after approximately 10 min (10.17 ± 3.11 min; $n = 9$). During this slow activation, the VSOR current showed two

different time-dependent manifestations at constant positive potentials ($+100$ mV). At half-maximal current amplitudes ($I_{\frac{1}{2}\text{max}}$), the current in both C28/I2 cells (**Figures 3A,B,G**) and primary chondrocytes (**Figures 4A,B,G**) displayed time-dependent inactivation, whereas at maximal current amplitudes (I_{max}) time-dependent inactivation was no longer evident (**Figures 3C,D,G, 4C,D,G**). At half-maximal activation, VSOR currents at -100 mV were equal at I_1 and I_2 , while at I_{max} the current slightly inactivated over time. We next investigated the response of maximal VSOR currents (VSOR I_{max}) to strong acidification (VSOR I_{max} —pH 4.5). Immediately after reducing pH_e , time-dependent inactivation at positive potentials was accentuated in C28/I2 cells (**Figures 3E,F**) as well as in primary

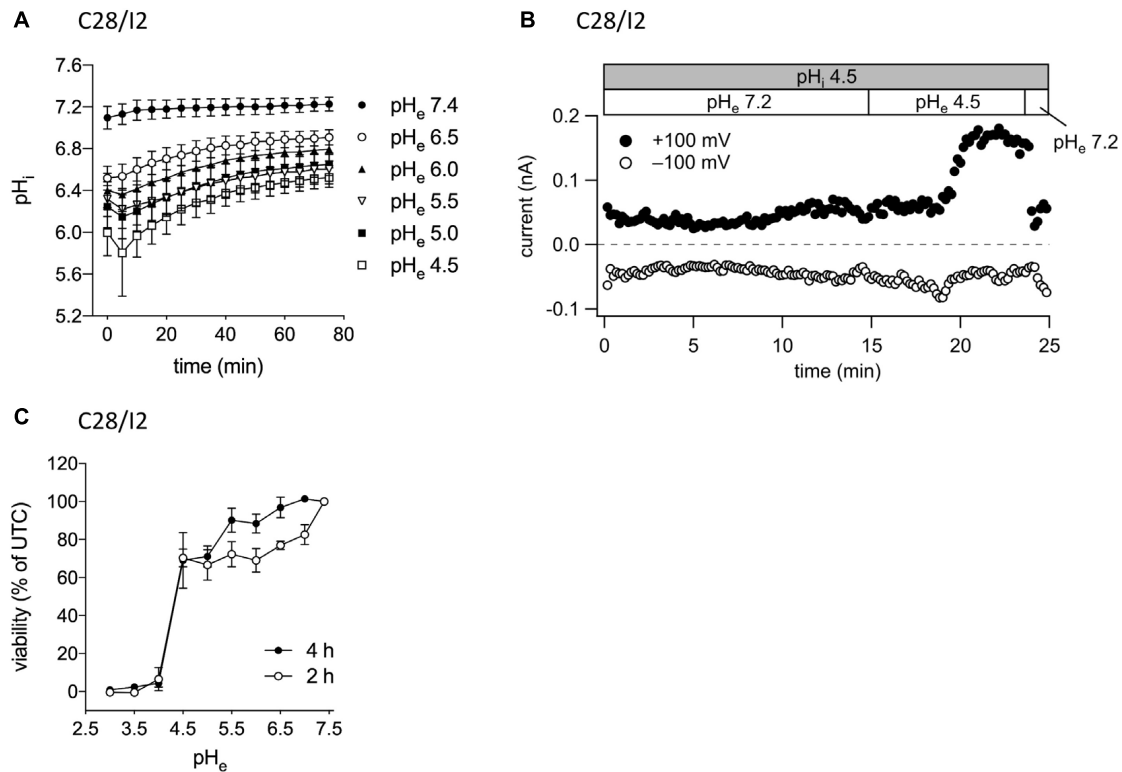


FIGURE 2 | ASOR current activation requires extracellular but not intracellular acidification. **(A)** Intracellular pH measurements in C28/I2 cells at different timepoints after extracellular acidification (pH 6.5, 6.0, 5.5, 5.0, and 4.5) versus control conditions (pH 7.4); means \pm SEM ($n = 6$). **(B)** ASOR current time course in C28/I2 cells (single experiment) using an acidic intracellular (pipette) solution (pH_i 4.5). Each circle represents the current at +100 mV (upper trace) and -100 mV (lower trace) measured in response to 500-ms voltage ramps applied every 10 s. The recording was performed in the ruptured patch clamp configuration. **(C)** Viability of C28/I2 cells after 2 and 4 h of exposure to pH 3.0, 3.5, 4.0, 4.5, 5.0, 5.5, 6.0, 6.5, 7.0, and 7.4; means \pm SEM ($n = 3-4$).

chondrocyte (Figures 4E,F). This is also reflected in Figures 3H, 4H showing lower mean amplitudes at I_2 than at I_1 . At negative potentials (-100 mV) acidification did not significantly change the current phenotype. Mean ASOR currents in C28/I2 cells and primary chondrocytes were smaller than VSOR currents and the I_2/I_1 ratios were >1 at +100 mV and <1 at -100 mV, indicating time-dependent activation and inactivation at constant positive and negative potentials, respectively (Figures 3G,H, 4G,H).

ASOR and VSOR Current Sensitivities to the Cl^- Channel Blockers DCPIB and Tamoxifen

Next, we tested the Cl^- channel blocker DCPIB on the ASOR and VSOR current in C28/I2 cells and primary human chondrocytes. Data are shown in Figures 5A-F. While VSOR currents in wide range of cell types are efficiently blocked by DCPIB (for review see Pedersen et al., 2015), ASOR currents have been shown in two studies to be largely DCPIB-insensitive (Sato-Numata et al., 2016; Kittl et al., 2019). In the present study, ASOR and VSOR outward currents showed approximately the same sensitivities to 10 μM DCPIB at +100 mV, i.e., an inhibition of $\sim 65\%$ in C28/I2 cells and $\sim 67\%$ in primary chondrocytes. At

-100 mV, the VSOR current was blocked by $\sim 68\%$ in C28/I2 cells and $\sim 66\%$ in primary chondrocytes, whereas the ASOR inward current was less sensitive with an inhibition of $\sim 18\%$ in C28/I2 cells and no effect in primary chondrocytes. The block was reversible upon applying acidic or a hypotonic solution without DCPIB (not shown for primary chondrocytes). In accordance with previous work (Nobles et al., 2004; Yamamoto and Ehara, 2006; Sato-Numata et al., 2016), the VSOR channel blocker tamoxifen (10 μM) was ineffective on ASOR currents in C28/I2 cells, but reversibly suppressed both outward and inward VSOR currents by $\sim 90\%$ (Figure 5G). Time courses of ASOR and VSOR current inhibition by DCPIB and tamoxifen are shown in Supplementary Figure S1.

ASOR as Well as VSOR Current Activation Depolarizes the Cell Membrane Potential (V_{mem})

We next tested if ASOR and VSOR current activation in C28/I2 cells affected the membrane potential (V_{mem}). Figures 6A,C show examples of V_{mem} recordings before, during, and after the application of an acidic, or hypotonic solution, respectively. Mean V_{mem} values \pm SEM under the respective conditions are shown in Figures 6B,D. The average resting V_{mem}

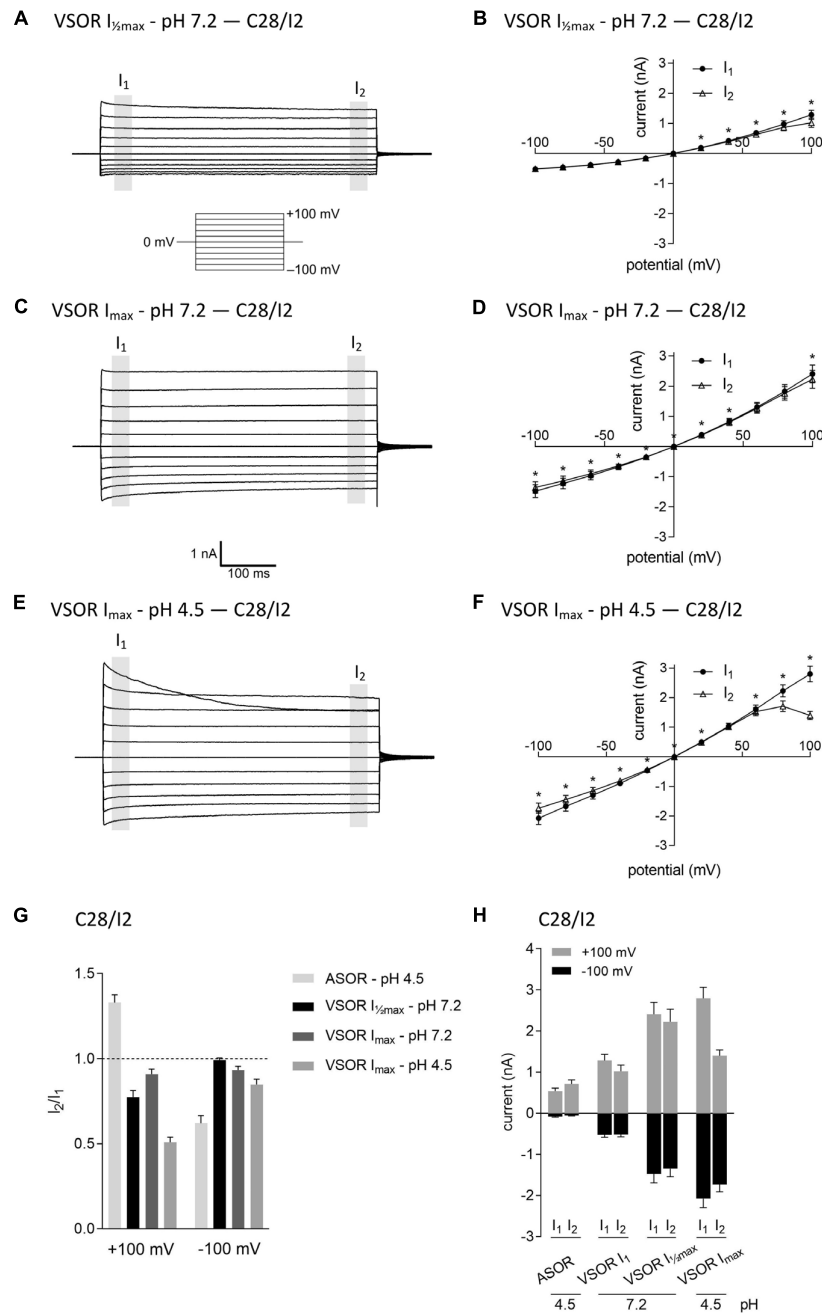


FIGURE 3 | The volume-sensitive outwardly rectifying (VSOR) current in C28/I2 cells is affected by low pH. Examples of VSOR current traces elicited by 500-ms voltage steps from -100 to $+100$ mV obtained at half-maximal VSOR current amplitudes (VSOR $I_{1/2\text{max}}$ - pH 7.2) (**A**), at maximal VSOR current amplitudes (VSOR I_{max} - pH 7.2) (**C**), and at maximal VSOR current amplitudes immediately after reducing pH_e to 4.5 (VSOR I_{max} - pH 4.5) (**E**). (**B, D, F**) I - V relationships of mean VSOR currents analyzed at the beginning (I_1 —closed circles) and at the end (I_2 —open triangles) of voltage pulses (indicated by gray shadings in **A**, **C**, and **E**). (**B**) VSOR $I_{1/2\text{max}}$ - pH 7.2 ($n = 10$). (**D**) VSOR I_{max} - pH 7.2 ($n = 11$). (**F**) VSOR I_{max} - pH 4.5 ($n = 9$). Asterisks indicate significant differences between I_1 and I_2 ($p < 0.05$). Paired t -tests. (**G, H**) I_2/I_1 ratios and mean current amplitudes, respectively, of ASOR currents and VSOR $I_{1/2\text{max}}$ - pH 7.2, VSOR I_{max} - pH 7.2, and VSOR I_{max} - pH 4.5 currents at $+100$ and -100 mV. Means \pm SEM ($n = 9$ – 11). I_2/I_1 ratio > 1 , time-dependent activation; I_2/I_1 ratio < 1 , time-dependent inactivation.

under isotonic conditions and pH 7.4 was approximately -60 mV. Upon application of acidic (pH 4.5), or hypotonic (230 mosm/kg) extracellular solution, cells depolarized to ~ -34 mV ($n = 3$) and ~ -43 mV ($n = 5$), respectively. By

switching from current- to voltage clamp during the acidity-induced depolarization, we verified ASOR current activation (insets in **Figure 6A**). The re-application of control solutions caused a rapid repolarization of V_{mem} .

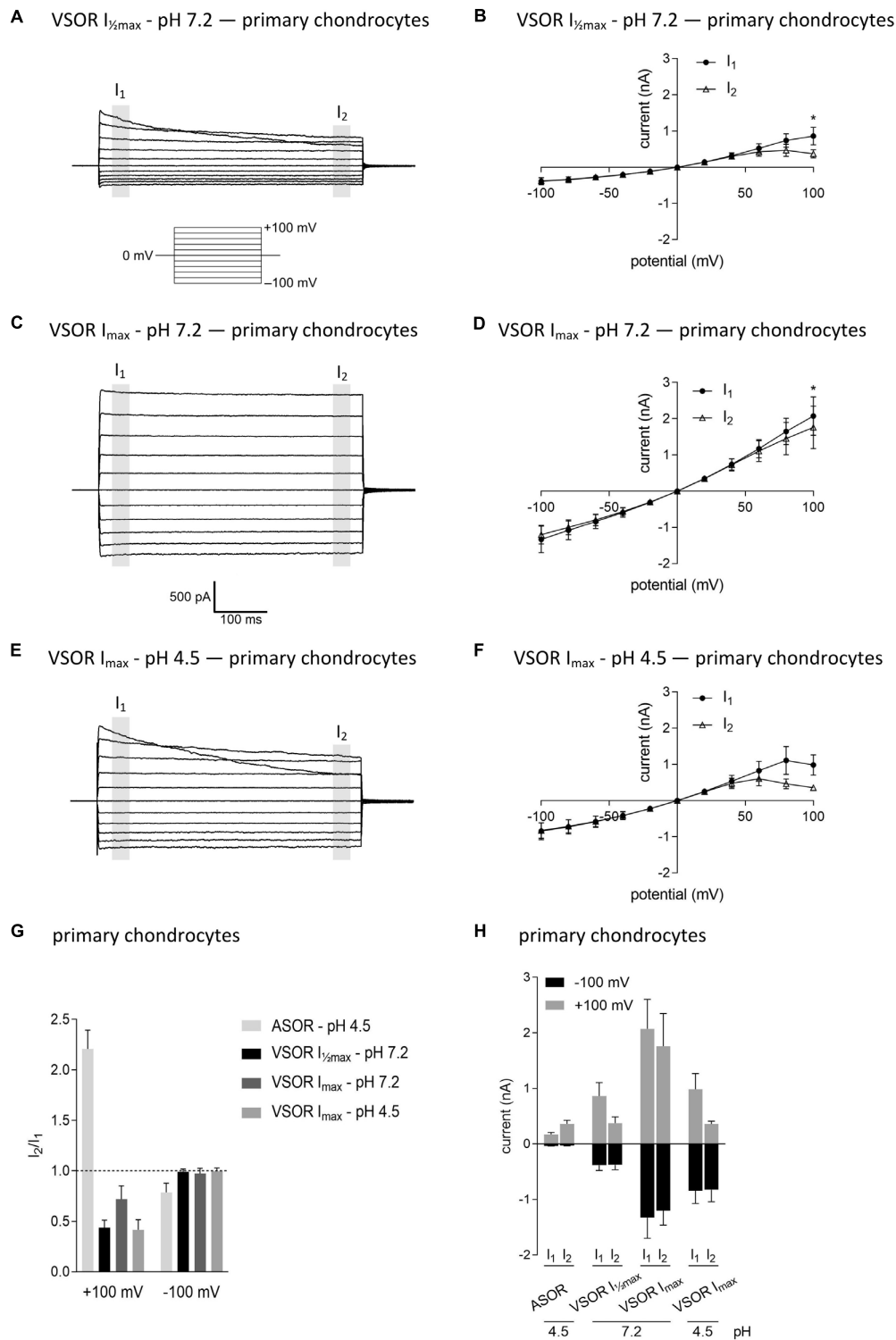


FIGURE 4 | The volume-sensitive outwardly rectifying (VSOR) current in primary chondrocytes is affected by low pH. VSOR current traces elicited by 500-ms voltage steps from -100 mV to $+100$ mV obtained at half-maximal VSOR current amplitudes (VSOR $I_{1/2\max}$ —pH 7.2) (**A**), at maximal VSOR current amplitudes (VSOR I_{\max} —pH 7.2) (**C**), and at maximal VSOR current amplitudes immediately after reducing pH_e to 4.5 (VSOR I_{\max} —pH 4.5) (**E**). (**B,D,F**) I - V relationships of mean VSOR currents analyzed at the beginning (I_1 —closed circles) and at the end (I_2 —open triangles) of voltage pulses (indicated by gray shadings in **A**, **C**, and **E**). (**B**) VSOR $I_{1/2\max}$ —pH 7.2 ($n = 5$). (**D**) VSOR I_{\max} —pH 7.2 ($n = 6$). (**F**) VSOR I_{\max} —pH 4.5 ($n = 3$). Asterisks indicate significant differences between I_1 and I_2 ($p < 0.05$). Paired t -tests. (**G,H**) I_2/I_1 ratios and mean current amplitudes, respectively, of ASOR currents and VSOR $I_{1/2\max}$ —pH 7.2, VSOR I_{\max} —pH 7.2, and VSOR I_{\max} —pH 4.5 currents at $+100$ and -100 mV. Means \pm SEM. (**G**) $n = 3$ –7 (I_2/I_1 ratio > 1 , time-dependent activation; I_2/I_1 ratio < 1 , time-dependent inactivation). (**H**) $n = 2$ –3.

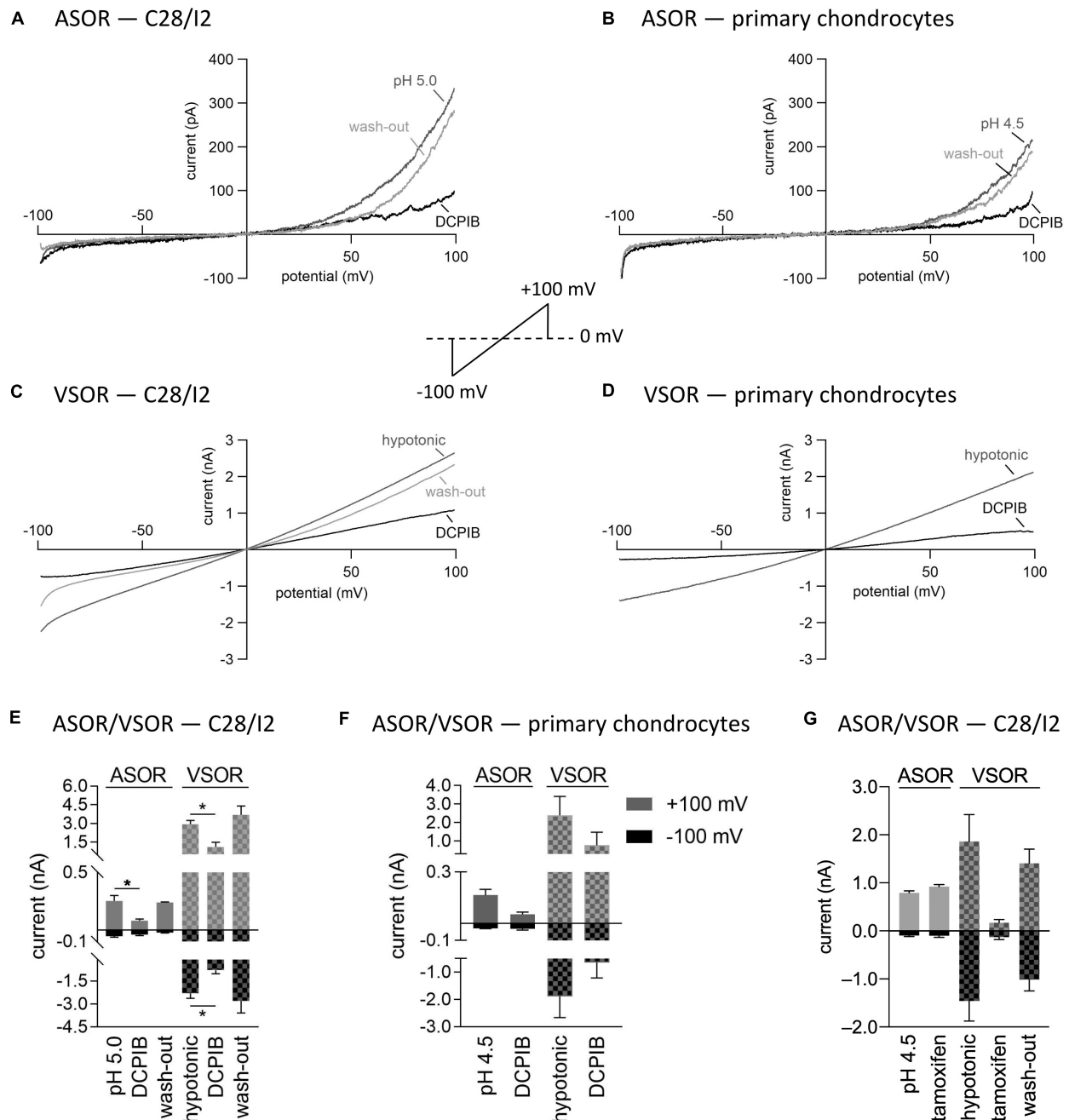


FIGURE 5 | Volume- and acid-sensitive outwardly rectifying (VSOR and ASOR) current sensitivities to the Cl^- channel blockers DCPIB and tamoxifen. **(A,B)** and **(C,D)** Representative current-voltage relationship obtained by 500-ms voltage ramps under acidic and hypotonic conditions in the absence and presence of DCPIB (10 μM) in C28/I2 cells and primary human chondrocytes, respectively. **(E,F)** Mean peak currents \pm SEM under acidic and hypotonic conditions in the absence and presence of 10 μM DCPIB in C28/I2 ($n = 2-4$) and primary chondrocytes ($n = 2-3$), respectively. **(G)** Mean peak currents \pm SEM under acidic and hypotonic conditions in the absence and presence of 10 μM tamoxifen in C28/I2 ($n = 3$). Asterisks in **(E)** indicate significant differences between pH 5.0 and DCPIB and between hypotonic and DCPIB ($p < 0.05$). Paired t -tests.

Interplay Between ASOR and VSOR Currents—Effect of External Acidification on VSOR Currents

As shown in **Figures 3, 4**, in both C28/I2 cells and primary chondrocytes, the acute effect of extracellular acidification

to pH 4.5 on maximally activated VSOR currents was an acceleration of current inactivation at +100 mV. In a next set of experiments, we investigated the response of VSOR currents to prolonged extracellular acidification. Therefore, we first elicited the VSOR current by applying a hypotonic solution and then

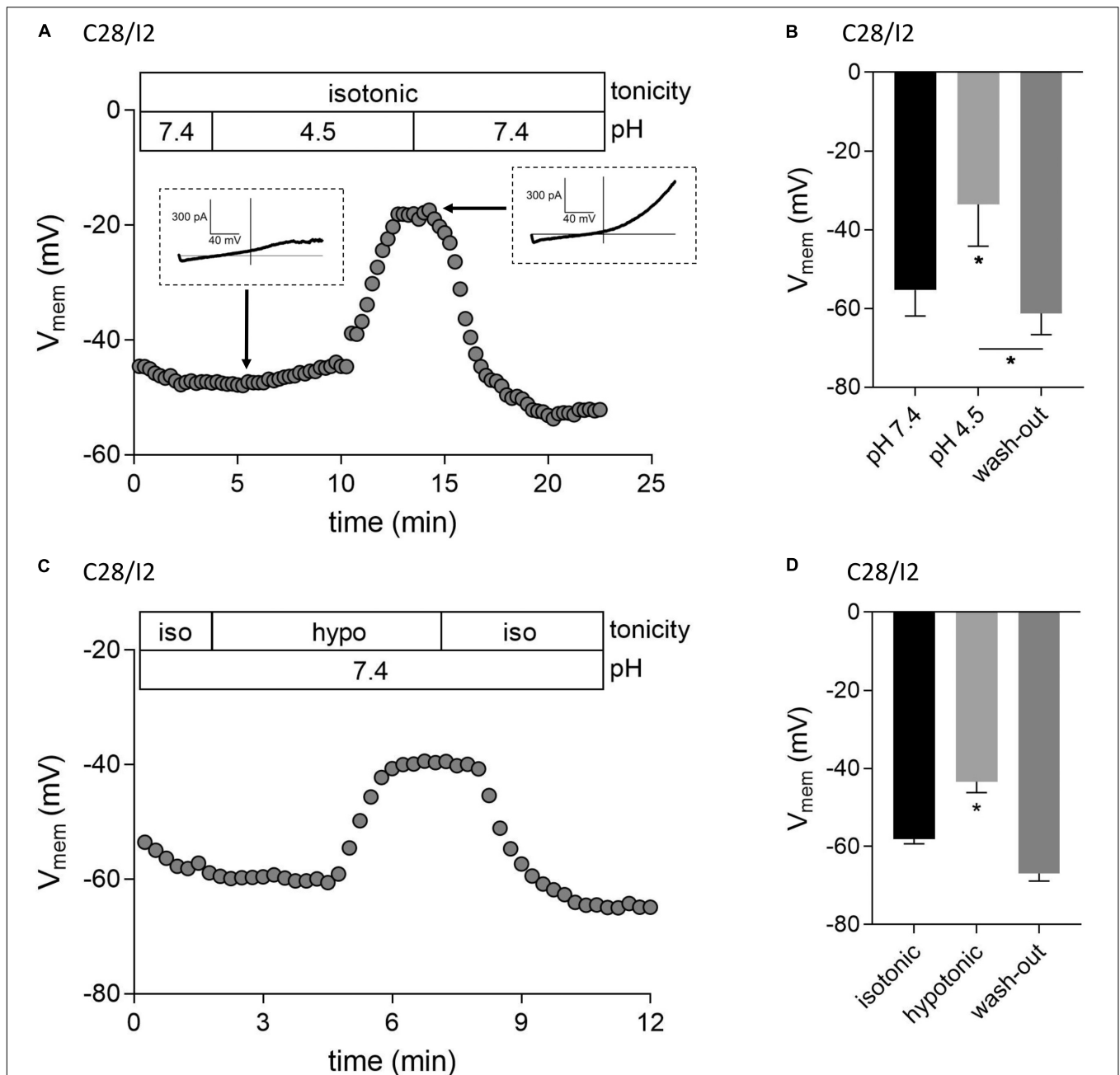


FIGURE 6 | Acidic and hypotonic conditions lead to depolarization of the cell membrane potential (V_{mem}). V_{mem} recordings of single C28/I2 chondrocytes at pH 7.4, pH 4.5, and pH 7.4 again (wash-out) (**A**), and under isotonic (iso), hypotonic (hypo), and isotonic (wash-out) (**C**). Each circle represents the mean V_{mem} obtained over 15 s. Insets in (**A**) show whole-cell Cl^- currents at the indicated timepoints in response to 500-ms voltage ramps from -100 to $+100$ mV from membrane potentials prevailing at the respective timepoints. (**B,D**) Mean $V_{\text{mem}} \pm \text{SEM}$ under the conditions given in (**A**) and (**C**) ($n = 3$ and $n = 3-6$, respectively). Asterisks in (**B**) indicate significant differences between pH 7.4 and pH 4.5 and between pH 4.5 and wash-out ($p < 0.05$). In (**D**), the asterisk indicates a significant difference between isotonic and hypotonic conditions ($p < 0.05$). Paired t -tests.

additionally lowered the external pH to 4.5 to test for a possible simultaneous, overlapping activation of both VSOR and ASOR currents. Results from C28/I2 cells and primary chondrocytes are shown in **Figures 7, 8**, respectively. Currents were measured every 10 s in response to voltage ramps and currents at $+100$ and -100 mV were plotted over time as shown in panels A. To

analyze the prevailing current phenotypes, 500-ms current-steps from -100 to $+100$ mV were applied at 10 different timepoints (1)–(10) in C28/I2 cells and at eight different timepoints (1)–(8) in primary chondrocytes. Mean whole-cell Cl^- currents, original current tracings, and I_2/I_1 ratios at these timepoints are shown in panels B, C–F, and G–H, respectively.

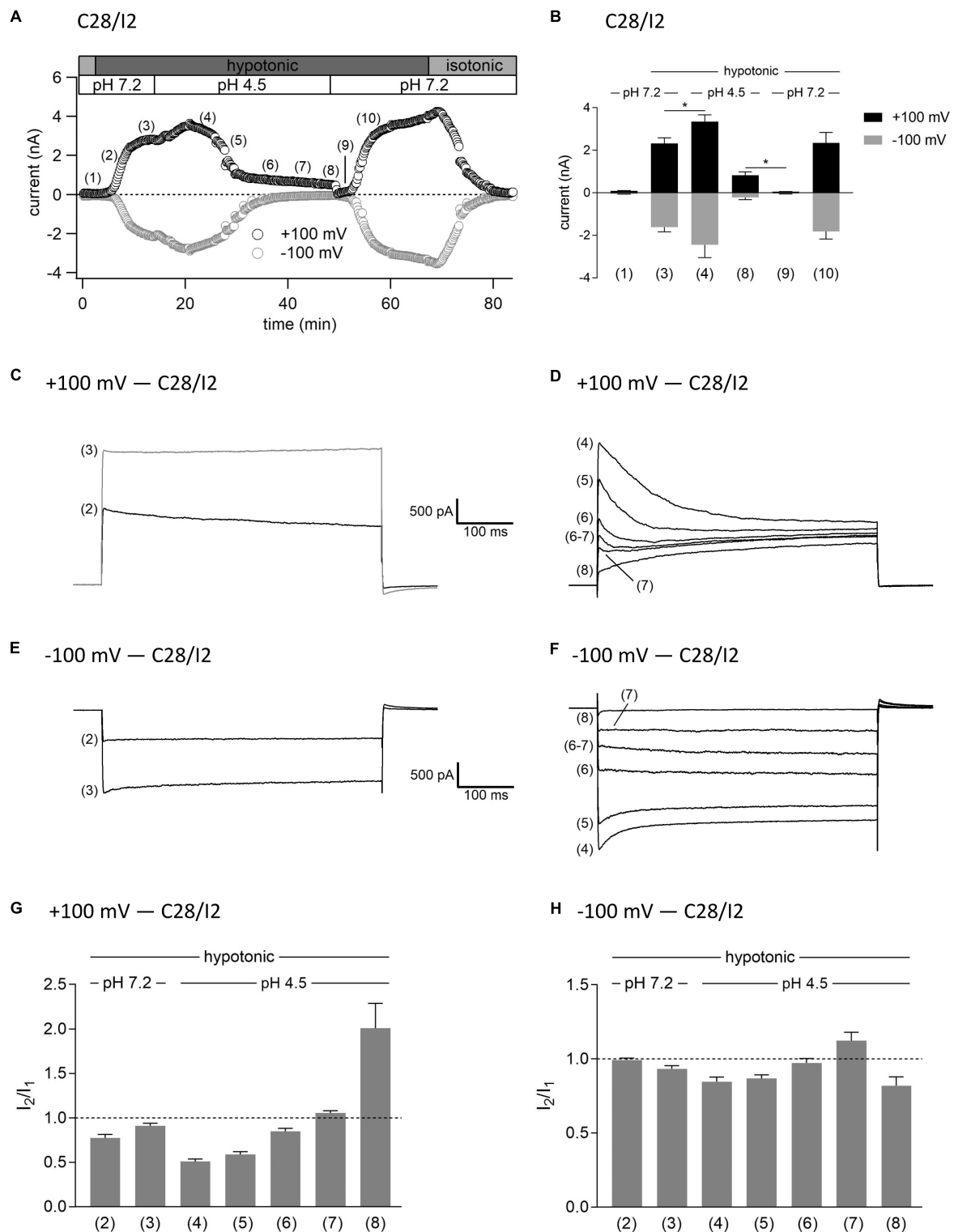


FIGURE 7 | Interplay between ASOR and VSOR currents in C28/I2 cells—effect of external acidification on VSOR currents. **(A)** Time course of a single experiment under isotonic (300 mosm/kg) and hypotonic (220 mosm/kg) conditions at pH 7.2 or 4.5 as indicated. Each circle represents the current at +100 mV (upper trace) and -100 mV (lower trace) measured in response to 500-ms voltage ramps applied every 10 s. **(B)** Mean current amplitudes \pm SEM measured at the timepoints (1)–(10) as indicated in **(A)** ($n = 5$ –11). $*p < 0.05$ as indicated. Paired t -tests. Representative current traces in response to 500-ms voltage steps to +100 and -100 mV recorded at the timepoints marked in **(A)** at +100 mV **(C,D)** and -100 mV **(E,F)**. I_2/I_1 ratios \pm SEM obtained at the timepoints indicated in **(A)** at +100 mV ($n = 5$ –11) **(G)** and at -100 mV ($n = 4$ –11) **(H)**; I_2/I_1 ratio > 1 , time-dependent activation; I_2/I_1 ratio < 1 , time-dependent inactivation.

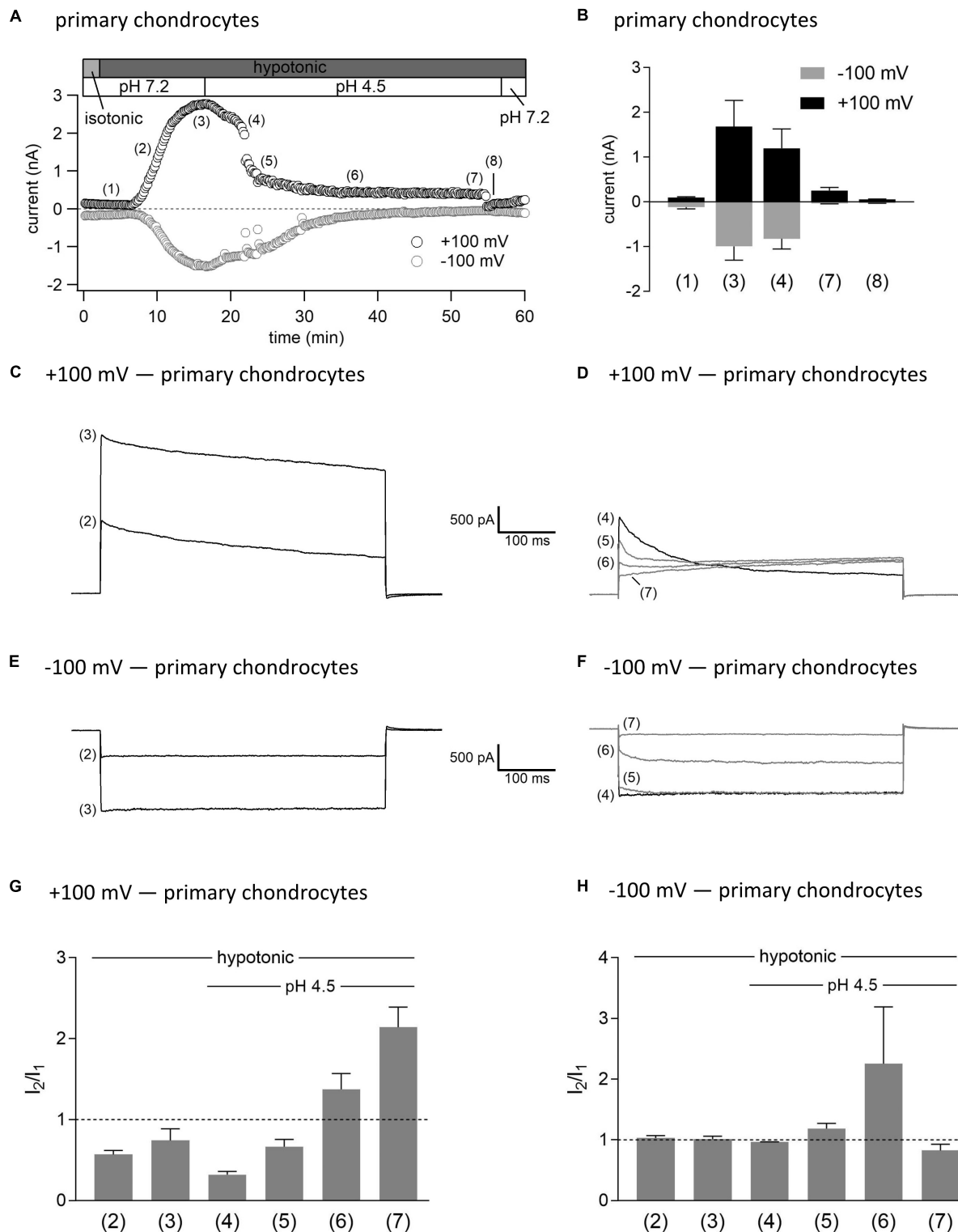


FIGURE 8 | Interplay between ASOR and VSOR currents in primary human chondrocytes—effect of external acidification on VSOR currents. **(A)** Time course of a single experiment under isotonic (300 mosm/kg) and hypotonic (220 mosm/kg) conditions at pH 7.2 or 4.5 as indicated. Each circle represents the current at +100 mV (upper trace) and -100 mV (lower trace) measured in response to 500-ms voltage ramps applied every 10 s. **(B)** Mean current amplitudes ± SEM measured at the timepoints (1)–(8) as indicated in **(A)** ($n = 3$). Representative current traces in response to 500-ms voltage steps to +100 and -100 mV recorded at the timepoints marked in **(A)** at +100 mV **(C,D)** and -100 mV **(E,F)**. I_2/I_1 ratios ± SEM obtained at the timepoints indicated in **(A)** at +100 mV ($n = 2$ –3) **(G)** and at -100 mV ($n = 2$ –3) **(H)**; I_2/I_1 ratio > 1, time-dependent activation; I_2/I_1 ratio < 1, time-dependent inactivation.

Switching from isotonic [timepoint (1)] to hypotonic conditions at pH 7.2 was followed by a gradual VSOR current activation. At timepoint (2), when the VSOR current was half-maximally activated, a typical time-dependent inactivation at +100 mV was observed, which was absent at full current activation [timepoint (3)], similar as shown in **Figures 3, 4** (I_2/I_1 ratio ~ 1). At -100 mV, the VSOR current phenotype shifted during its activation from linear at half-maximal VSOR current amplitudes to a slight time-dependent inactivation over time at maximal VSOR current amplitudes. Additional acidification to pH 4.5 led to different responses in C28/I2 cells and primary chondrocytes. In C28/I2 cells, the whole cell Cl^- current increased, whereas in primary chondrocytes, a decrease was observed immediately after acidification [timepoint (4)]. The current phenotype at this timepoint, however, was similar in both cell types, displaying a steep inactivation at +100 mV and a moderate inactivation at -100 mV, similar as in **Figures 3, 4** (panels E, F). Under continued acidity and hypotonicity, in both cell types, the whole-cell currents slowly decreased until a pure ASOR current appeared [C28/I2 cells: timepoint (8); primary chondrocytes: timepoint (7)], exhibiting typical time-dependent current facilitation at +100 mV and an initial inward current peak at -100 mV. Current traces at timepoints (5), (6), and (7) in C28/I2 cells and timepoints (5) and (6) in primary chondrocytes showed mixed characteristics of ASOR and VSOR phenotypes with an initial inactivation followed by current activation over time at +100 mV and a slight time-dependent activation at -100 mV consistent with a progressive transition from an exclusive VSOR to a pure ASOR current. The I_2/I_1 ratio at +100 mV displayed a nadir at timepoint (4), followed by an increase during current superimposition [C28/I2 cells: timepoints (5), (6), and (7); primary chondrocytes: timepoints (5) and (6)] and a maximum, when the ASOR current became the dominating conductance (timepoints 8 and 7 in C28/I2 cells and primary chondrocytes, respectively). At -100 mV, the I_2/I_1 ratios show a U-shaped transition with two maxima at timepoint (2) and (7) and a minimum at timepoints (4) and (5) in C28/I2 cells, which was less pronounced in primary chondrocytes. In primary chondrocytes as well as in C28/I2 cells, the mean amplitude of the dominating ASOR current was significantly smaller than during the phase of current superimposition, indicating that the VSOR current was fully deactivated by strong acidification. This became evident after stepping back from pH 4.5 to pH 7.2 under continued hypotonic conditions, which caused a rapid ASOR current deactivation followed by a short timeframe at baseline current levels [C28/I2 cells: timepoint (9); primary chondrocytes: timepoint (8)]. Thereafter, the VSOR current slowly recovered from acidic inhibition to become fully reactivated [C28/I2 cells: timepoint (10); not shown for primary chondrocytes].

Interplay Between ASOR and VSOR Currents—Effect of Hypotonicity on ASOR Currents

In this set of experiments on C28/I2 cells, we have chosen the opposite approach to test the effect of hypotonicity on the fully

activated ASOR current. **Figure 9A** shows the time course of currents at +100 and -100 mV of a single experiment. Mean whole-cell Cl^- currents, original current tracings elicited by 500-ms voltage steps to +100 and -100 mV and I_2/I_1 ratios at timepoints (1)–(6) marked in panel A are shown in panels B, C–F, and G–H, respectively. By acidification we first activated the ASOR current to a stable plateau showing typical time-dependent activation over time at +100 mV [timepoint (2)] with an I_2/I_1 ratio > 1 , and then simultaneously exposed the cells to hypotonicity. In a first phase, the whole-cell Cl^- current significantly increased further [timepoint (3)]. However, continued exposure to hypotonicity and acidity [timepoints (3)–(5)] caused a gradual decrease of the peak current to values measured under acidity alone [timepoint (6) compared to timepoint (2)]. Currents at maximum activation [timepoint (3)] showed steep inactivation over time at +100 mV, equal to the current phenotype of VSOR I_{max} —pH 4.5 in **Figure 3** and maximum currents in **Figure 7**. During the following declining phase, the whole-cell Cl^- current changed to a pure ASOR current phenotype with typical time-dependent facilitation at +100 mV [timepoint (6)]. Two transition states with characteristics of both the ASOR and VSOR current are shown at timepoints (4) and (5). This transformation is also evident from current tracings at -100 mV. The I_2/I_1 ratio at +100 mV gave values < 1 during superimposition of ASOR and VSOR current [timepoints (3) and (4)] and increased with progressive dominance of the ASOR current [values > 1 at timepoints (5) and (6)]. At -100 mV the I_2/I_1 ratio showed an inverted U-shaped transition with lowest values at timepoints (2) and (6) and a maximum at timepoint (5).

Interplay Between ASOR and VSOR Currents—Effect of Simultaneous Exposure to Hypotonicity and Acidity

In a last series of patch clamp experiments on C28/I2 cells, we investigated the activation kinetics of whole-cell Cl^- currents under simultaneous acidic and hypotonic conditions. **Figure 10A** shows the time course of currents at +100 and -100 mV of a single experiment. Mean whole-cell Cl^- currents, original current tracings at +100 and -100 mV and I_2/I_1 ratios at timepoints marked in panel A are shown in **Figures 10B, C–F, and G–H**, respectively. Current activation under hypotonic and acidic (pH 4.5) conditions resembled the activation time course of the VSOR current observed under hypotonic stimulation alone (**Figure 7**). However, time-dependent inactivation at +100 mV at maximum current activation [timepoint (3)] was more pronounced compared to hypotonic exposure alone (I_2/I_1 ratio < 1). This is most likely due to a superimposition of two processes—hypotonic VSOR current activation on the one hand and accelerated time-dependent current inactivation at positive potentials at low pH on the other hand as shown in **Figure 3** (VSOR I_{max} —pH 4.5) and at timepoint (4) in **Figure 7D**. Continued exposure to pH 4.5 and hypotonicity again led to a progressive decline in current amplitudes and a transformation to an exclusive ASOR current phenotype

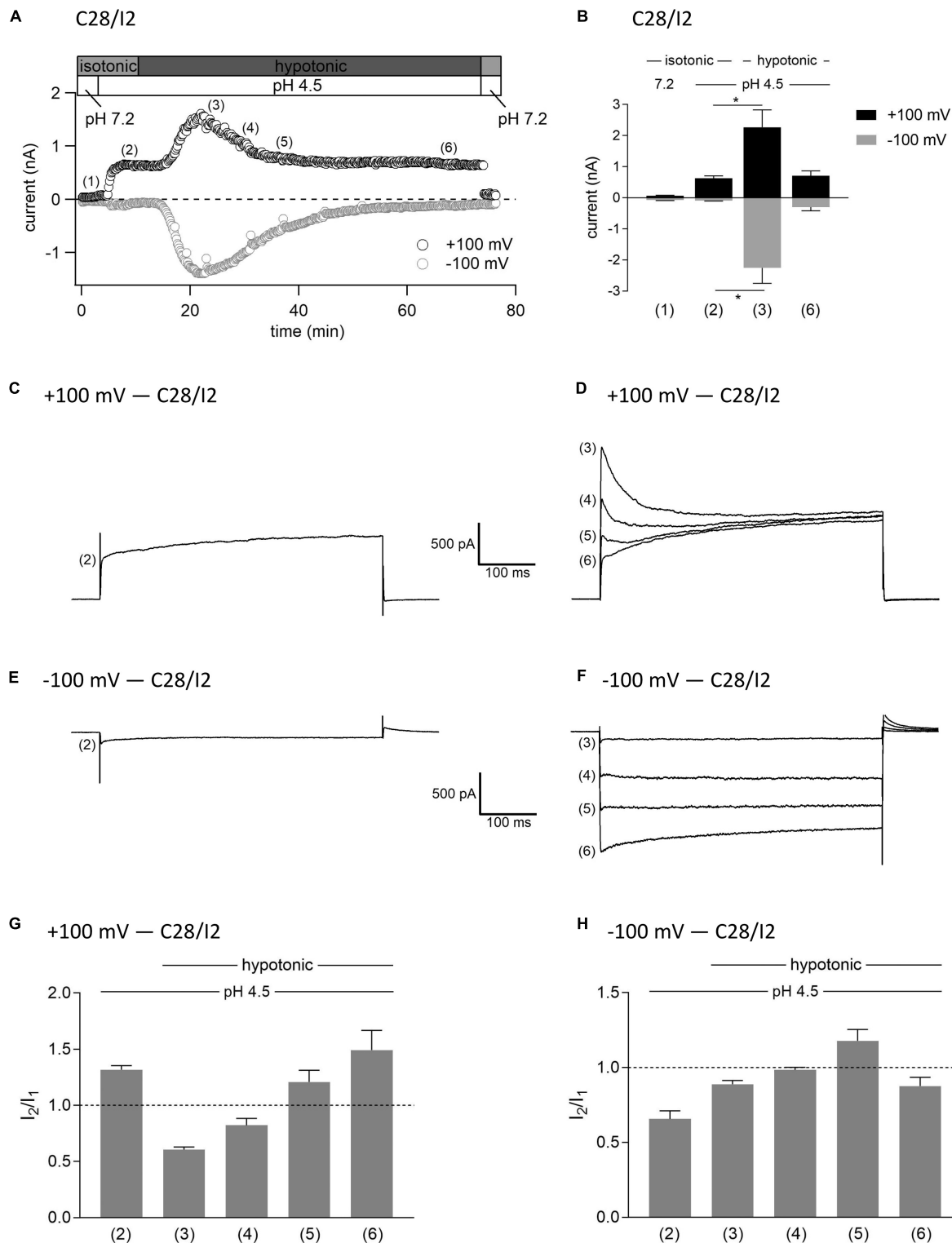


FIGURE 9 | Interplay between ASOR and VSOR currents—effect of hypotonicity on ASOR currents in C28/I2 cells. **(A)** Time course of a single experiment under isotonic (300 mosm/kg) and hypotonic (220 mosm/kg) conditions at pH 7.2 or 4.5 as indicated. Each circle represents the current at +100 mV (upper trace) and -100 mV (lower trace) measured in response to 500-ms voltage ramps applied every 10 s. **(B)** Mean current amplitudes \pm SEM measured at the timepoints (1)–(6) as indicated in **(A)** ($n = 3$ –8). * $p < 0.05$ as indicated. Paired t -test. Representative current traces in response to 500-ms voltage steps to +100 and -100 mV recorded at the timepoints marked in **(A)** at +100 mV **(C,D)** and at -100 mV **(E,F)**. I_2/I_1 ratios \pm SEM obtained at the timepoints as indicated in **(A)** at +100 mV ($n = 5$ –11) **(G)** and at -100 mV ($n = 4$ –11) **(H)**; I_2/I_1 ratio > 1 , time-dependent activation; I_2/I_1 ratio < 1 , time-dependent inactivation.

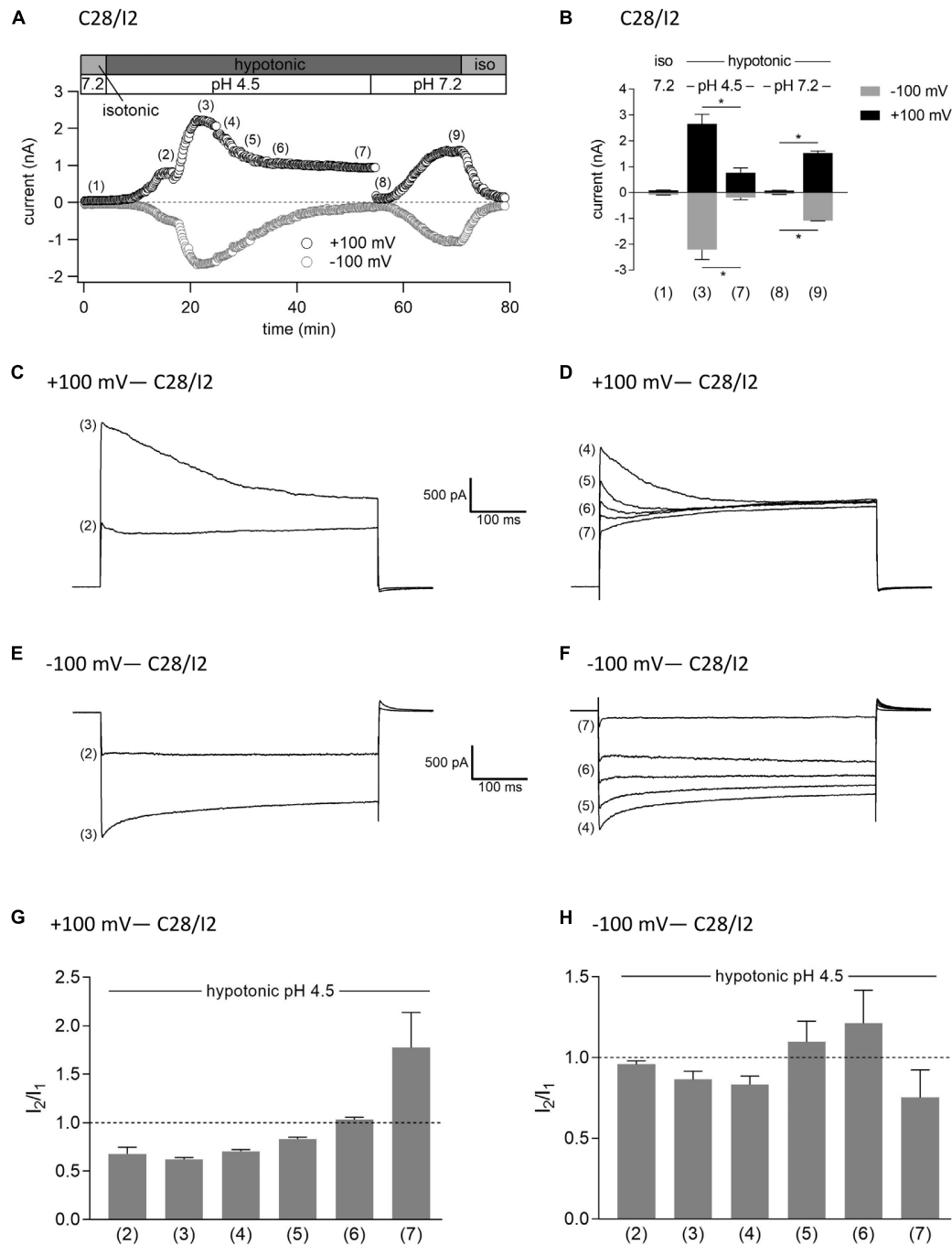


FIGURE 10 | Interrelation between ASOR and VSOR currents—effect of simultaneous application of acidic and hypotonic conditions in C28/I2 cells. **(A)** Time course of a single experiment under isotonic (300 mosm/kg) and hypotonic (220 mosm/kg) conditions at pH 7.2 or 4.5 as indicated. Each circle represents the current at +100 mV (upper trace) and -100 mV (lower trace) measured in response to 500-ms voltage ramps applied every 10 s. **(B)** Mean current amplitudes ± SEM measured at the timepoints (1)–(9) as indicated in **(A)** ($n = 3$ –6). * $p < 0.05$ as indicated. Paired t -tests. Representative current–voltage relationship obtained by 500-ms voltage ramps recorded at the timepoints marked in **(A)** at +100 mV **(C,D)** and at -100 mV **(E,F)**. I_2/I_1 ratios ± SEM obtained at the timepoints as indicated in **(A)** at +100 mV ($n = 3$ –6) **(G)** and at -100 mV ($n = 3$ –6) **(H)**; I_2/I_1 ratio > 1 , time-dependent activation; I_2/I_1 ratio < 1 , time-dependent inactivation.

as observed in the previous experimental series shown in **Figures 7–9**, which is reflected in the current tracings and I_2/I_1 ratios at timepoints (4)–(7). After switching to normal extracellular pH (7.2), the ASOR current rapidly deactivated, and

even though cells were still exposed to hypotonicity, whole-cell Cl^- currents transiently dropped to baseline levels [timepoint (8)] until the onset of VSOR current reactivation to a new maximum at timepoint (9).

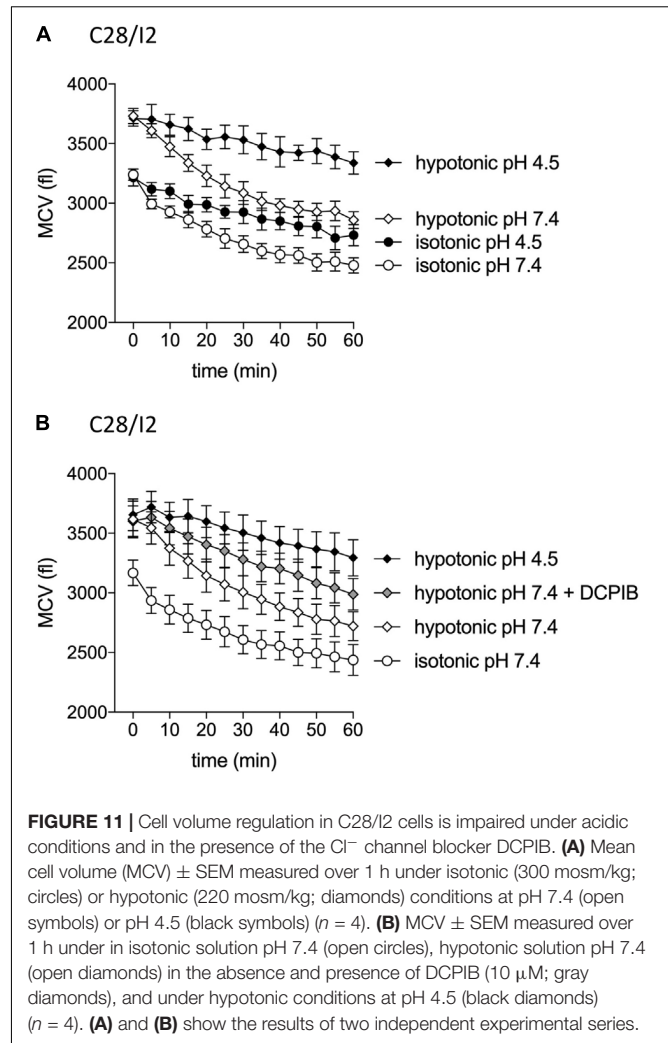
Effect of Acidification on Cell Volume Regulation

The VSOR current is essential for the RVD response by extruding Cl^- ions to counteract osmotic cell swelling. Given that the VSOR current gets deactivated by strong acidification while the ASOR current gets activated, we hypothesized that the cells' volume regulatory ability might be affected at low pH. To test this, we performed CV measurements in C28/I2 cells under isotonic (300 mosm/kg) or hypotonic (220 mosm/kg) conditions at pH 7.4 or 4.5 and in the absence or presence of the Cl^- channel blocker DCPIB. Under isotonic pH 7.4 (control) conditions, we observed a 20–25% cell shrinkage from ~ 3200 to ~ 2450 fl ($n = 4$) (Figures 11A,B), which was attenuated under acidic (pH 4.5) conditions (shrinkage from ~ 3200 to ~ 2700 fl, i.e., a 15% volume loss; $n = 4$; Figure 11A). On average, at the first timepoint (0 min), the MCV of cells exposed to a hypotonic extracellular solution was ~ 490 fl (Figure 11A) and ~ 450 fl (Figure 11B) higher as under isotonic control conditions. After 60 min under hypotonic conditions and pH 7.4, the MCV was ~ 380 and ~ 280 fl higher compared to cells kept under isotonic conditions, respectively, indicating a moderate RVD response. Under hypotonic and acidic conditions (hypotonic pH 4.5), the difference in MCV after 1 h increased to ~ 860 fl in both series of experiments. Similarly, RVD was impaired by DCPIB (10 μM); after 60 min the difference to the MCV measured under control conditions increased to ~ 550 fl (Figure 11B).

DISCUSSION

In the present study we characterized an acid-sensitive and a volume-sensitive outwardly rectifying (ASOR and VSOR, respectively) Cl^- current in human C28/I2 chondrocytes and primary human chondrocytes. In detail, we investigated the mutual interdependence of the two currents and possible functional consequences of their interplay on chondrocyte CV regulation. Given their important role in CV homeostasis in chondrocytes on the one hand, and the relationship between deranged CV regulation, chondrocyte apoptosis, and OA on the other hand, Cl^- channels have come into focus of OA research (Roach et al., 2004; Isoya et al., 2009; Lewis et al., 2011a,b; Perez-Hernandez et al., 2012; Ponce et al., 2012; Kumagai et al., 2016; Yamamura et al., 2018; Hall, 2019).

Acid-sensitive outwardly rectifying currents with remarkably similar pH sensitivities, phenotypes, activation kinetics, and pharmacological profiles have been described in various cell types like microglia, myocytes, HeLa cells, neurons, Sertoli cells, distal tubular cells, erythrocytes, or osteoclasts (Auzanneau et al., 2003; Nobles et al., 2004; Lambert and Oberwinkler, 2005; Wang et al., 2007; Kajiya et al., 2009; Sato-Numata et al., 2013, 2014, 2016, 2017; Capurro et al., 2015; Valinsky et al., 2017; Kittl et al., 2019), but the knowledge on acid-sensitive Cl^- currents in chondrocytes is sparse. There is only one report on an ASOR-type Cl^- current in human OUMS-27 chondrocytes (Kurita et al., 2015). In line with these studies, we found the ASOR current in human C28/I2 and primary chondrocytes activated at an extracellular pH of ≤ 5.0 , showed pronounced outward rectification and



current facilitation (activation over time) at constant positive holding potentials. Intracellular acidification by dialysis of the cell with a pH 4.5-pipette solution did not activate the current, which is in accordance with previous studies on osteoclasts (Kajiya et al., 2009) and microglial cells (Kittl et al., 2019), and suggests an extracellular location of the proton binding site(s). Independence on intracellular pH is also supported by the finding that intracellular buffering of protons with 100 mM HEPES did not affect ASOR current activation in HEK293 cells (Lambert and Oberwinkler, 2005).

Volume-sensitive outwardly rectifying currents are activated by osmotic cell swelling and are ubiquitously existent in mammalian cells. Over the past decades, their biophysical characteristics, pharmacological profiles, and functions in CV regulation have been described in detail, as reviewed, e.g., in Jentsch et al. (2002), Jakab and Ritter (2006), Okada et al. (2006), Hoffmann (2011), and Pedersen et al. (2016). In the present study, we found that exposure to hypotonicity (230 mosm/kg) led to the activation of a typical VSOR Cl^- current in human articular chondrocytes, similar as previously described in rabbit and rat chondrocytes (Isoya et al., 2009; Ponce et al., 2012;

Kumagai et al., 2016). Its inhibition by DCPIB impeded RVD during hypoosmotic challenge, which underlines the significance of the VSOR current for CV homeostasis in chondrocytes. Similar to the ASOR current, the VSOR current exhibited outward rectification, although less pronounced. The VSOR current showed typical time-dependent activation at constant positive holding potentials, which allowed a clear phenotypical discrimination from the ASOR current with its time-dependent activation at positive potentials. Inactivation of the maximally activated VSOR current (VSOR I_{max}) over time at positive potentials became more pronounced immediately after lowering the extracellular pH, similar as previously observed in microglial cells (Kittl et al., 2019), which is also in line with earlier observations in *Xenopus* oocytes (Ackerman et al., 1994), C6 glioma cells (Jackson and Strange, 1995), BC3H1 mouse myoblasts (Voets et al., 1997), mouse neuroblastoma cells (Voets et al., 1997), or bovine pulmonary artery cells (Nilius et al., 1998). Increasing the extracellular concentration of Ca^{2+} and Mg^{2+} had a comparable effect on the inactivation kinetics (Voets et al., 1997), suggesting that Ca^{2+} -, Mg^{2+} -, and H^+ ions might bind to the extracellular side of the channel to enhance time-dependent inactivation.

From numerous studies in many cell types, the ethacrynic acid derivative DCPIB is known as a potent VSOR current blocker (Pedersen et al., 2016). In our previous study on microglial cells (Kittl et al., 2019) and a study on HeLa cells by Sato-Numata et al. (2016), the VSOR current was virtually fully suppressed by 10 μM DCPIB, while at this concentration, the ASOR current was only inhibited by $\sim 20\%$ in microglial cells and unaffected in HeLa cells. In the present study, however, we did not observe a difference in the DCPIB sensitivity between the VSOR and ASOR current. Both conductances were inhibited by 65–68% by 10 μM DCPIB in C28/I2 cells as well as in primary chondrocytes. In contrast to DCPIB, the sensitivities of ASOR and VSOR currents to tamoxifen were markedly different. In line with previous work on HeLa cells (Sato-Numata et al., 2016), HEK293 cells (Nobles et al., 2004), cardiac myocytes (Yamamoto and Ehara, 2006), and BV-2 microglial cells (Kittl et al., 2019), tamoxifen at 10 μM did not affect ASOR currents, but almost fully blocked VSOR currents by $\sim 90\%$.

Importantly, we found temporary ASOR and VSOR currents co-activation, when cells were simultaneously exposed to hypotonicity and acidic pH with superimposed currents and a mixed current phenotype. We observed this superimposition in three different experimental settings, and it was independent if (1) cells were first exposed to low pH to activate the ASOR current and then additionally to hypotonic conditions to activate the VSOR current, (2) cells were first exposed to hypotonic and then additionally to acidic conditions, or (3) cells were simultaneously exposed to hypotonic and acidic conditions. In each setting, after a period of current superimposition and under continued hypotonic conditions, we observed a transition to a pure ASOR current phenotype, indicating that the VSOR current was fully deactivated under low pH. The accelerated time-dependent inactivation of VSOR I_{max} at positive potentials observed immediately after exposure to pH 4.5 might be interpreted as the onset phase of VSOR current inactivation by

low pH, which eventually leads to full current deactivation upon prolonged exposure to strongly acidic conditions.

Regarding the biophysical properties, activation kinetics, and DCPIB sensitivities of ASOR and VSOR currents, as well as the pH-sensitivity of the VSOR current and its complete deactivation under pH 4.5 we got identical results in the C28/I2 cell line—a well-established cell model that has been shown to phenotypically resemble articular chondrocytes (Goldring et al., 1994; Finger et al., 2003)—and in primary human chondrocytes. This suggests that our findings might show applicability also *in vivo*.

Including our previous work on microglial cells (Kittl et al., 2019), only few studies investigated the interrelation between ASOR and VSOR currents by combining hypoosmotic and acidic challenges. In line with our results in chondrocytes shown here, and our previous report on microglial cells (Kittl et al., 2019), Lambert and Oberwinkler (2005) provided evidence that ASOR and VSOR currents can be simultaneously active in HEK293T cells and reasoned that ASOR and VSOR channels are distinct populations of ion channels. In contrast, Nobles et al. (2004) postulated that ASOR and VSOR currents are manifestations of the same channel complex. Indeed, some biophysical similarities between ASOR and VSOR currents like outward rectification and ion permeability sequences might suggest a common molecular basis. However, there are distinct differences between ASOR and VSOR currents, such as more pronounced outward rectification of ASOR currents, current activation *versus* inactivation at constant positive membrane potentials, time courses of current activation, and differences in their pharmacological profiles. Studies in recent years, which identified members of the leucine-rich repeat containing 8 protein family (LRRC8 isoforms A-E; LRRC8A is also known as SWELL1) (Qiu et al., 2014; Voss et al., 2014; Sato-Numata et al., 2016, 2017; Syeda et al., 2016; Schober et al., 2017; Deneka et al., 2018) (reviewed in Pedersen et al., 2015; Stauber, 2015; Jentsch et al., 2016) and TMEM206 (Ullrich et al., 2019; Yang et al., 2019) as essential pore-forming components of VSOR and ASOR channels, respectively, provide compelling evidence that different molecular entities are underlying the two currents. Importantly, Sato-Numata et al. (2016, 2017) could show that LRRC8 family members are not involved in ASOR current activity. The reason for the acidity-induced deactivation and the functional and molecular interrelation of other proteins which might be associated with VSOR currents (Suzuki and Mizuno, 2004; Benedetto et al., 2016; Bae et al., 2019; Okada, 2019) needs further investigation.

Severe local acidosis is a hallmark of many diseases or disease-associated conditions including ischemia, cancer, and inflammation. In high-resolution measurements on tumor cell surfaces, Puppulin et al. (2018) could resolve highly localized variations of the proton concentration with an average pH of 6.7 and most acidic values of 5.1. OA is associated with chronic joint inflammation and acidification. Intraoperative *in situ* pH measurements in patients could show an OA stage-dependent cartilage acidification ranging from pH 7.1 at stage 0 to a value as low as pH 5.5 at stage 3 (Kontinen et al., 2002). Moreover, OA is associated with increased matrix hydration, reduced osmolality of the synovial fluid of 249–277 mosm/kg

compared to 295–340 mosm/kg in healthy subjects (Bertram and Krawetz, 2012), and more pronounced hypoxia compared to physiological conditions (Milner et al., 2012). Chondrocytes reside in a bradytrophic, hypoxic, and acidic environment already under normal conditions, in which they constantly need to adapt their CV based on the prevalent osmotic pressures and mechanical loads (Hall et al., 1996; Wilkins et al., 2000). In OA, the developing hypoosmotic and acidic environment poses additional challenges to the chondrocytes' CV and pH regulatory mechanisms. Therefore, we were interested in how far CV homeostasis in chondrocytes was affected under hypoosmotic or acidic conditions alone, and specifically in combination of both. Under isotonic conditions and normal pH, we observed a gradual cell shrinkage, which was attenuated under acidic conditions, similar as described in microglial cells (Kittl et al., 2019), HeLa cells (Wang et al., 2007), and cortical neurons (Sato-Numata et al., 2014). We assume that this was due to acid-induced counter-swelling caused by the activity of the Na^+/H^+ exchanger (NHE) (Behmanesh and Kempinski, 2000) and probably by the activation of acid-sensing ion channels (ASICs) (Staunton et al., 2013) or other acid-sensitive cation channels expressed in chondrocytes, such as TRPM7 (Qian et al., 2019). Along with the ASOR current, their activation might also contribute to the depolarization of the membrane potential, which we could measure upon acidification.

In rabbit knee chondrocytes after anterior cruciate ligament transection (ACLT) as an OA model, Kumagai et al. (2016) found significantly higher VSOR current amplitudes, increased hypoosmotic cell swelling, and increased caspase 3/7 activity compared to sham surgery controls. These changes were evident prior to the onset of histologically apparent cartilage loss. In OA, the cartilage becomes hypocellular due to apoptosis and there is a clear correlation between the degree of cartilage damage and chondrocyte apoptosis (Hwang and Kim, 2015). Importantly, along with an increased number of primary lysosomes, autophagic vacuoles, and endoplasmic reticulum membranes, apoptosis in chondrocytes, termed chondroptosis, is associated with cell swelling rather than cell shrinkage [apoptotic volume decrease (AVD)] as a hallmark of classical apoptosis (Bush and Hall, 2003; Roach et al., 2004; Okada et al., 2006; Hwang and Kim, 2015; Hall, 2019).

In any case, chondrocyte swelling arising from reduced tissue osmolarity in OA is likely to augment the risk of cell damage or cell death during mechanical loading, since chondrocytes in swollen cartilage are highly sensitive to impact load (Hall, 2019). Tissue acidification during OA could adversely add to the deleterious effect of hypotonic stress, might lead to a breakdown of chondrocyte CV homeostasis, and push chondrocytes toward cell death. We found in two experimental series higher mean CVs when cells were concomitantly exposed to acidic and hypotonic conditions compared to sole hypoosmotic exposition. We assume that this resulted from acidotoxic cell swelling as observed under isotonic conditions plus an impaired RVD due to acidity-induced deactivation of VSOR channels. Therefore, we conclude that (1) VSOR current deactivation by acidity has similar functional consequences as the pharmacological inhibition of the current by DCPIB and (2) ASOR channels activated under acidic

conditions cannot functionally replace VSOR channels in driving an RVD response.

Summarizing our findings, this study shows that CV homeostasis of chondrocytes is massively impaired under acidic and hypotonic conditions, which are characteristic for the osteoarthritic cartilage. Cell swelling under these conditions is likely to compromise cell viability and promote apoptosis. Since the maintenance of the ECM exclusively depends on chondrocytes, compromised CV homeostasis and viability are crucial factors promoting articular cartilage degeneration and the progression of OA.

DATA AVAILABILITY STATEMENT

The original contributions presented in the study are included in the article/**Supplementary Material**. Further inquiries can be directed to the corresponding author.

ETHICS STATEMENT

Primary chondrocytes were isolated from total human knee arthroplasty samples with informed consent and ethical approval by the Ethics Committee of Salzburg (415-E/1965/4-2015).

AUTHOR CONTRIBUTIONS

MK, MR, and MJ contributed to conceptualization. MK, MW, and MJ contributed to formal analysis. MJ contributed to funding acquisition. MK, MW, KH, JL, MG, and MJ contributed to investigation. MR and MJ contributed to supervision. MK, MW, MG, and MJ contributed to validation. MK contributed to visualization. MK and MJ contributed to writing—original draft. MK, MW, MG, MR, and MJ contributed to writing—review and editing. All authors contributed to the article and approved the submitted version.

FUNDING

This project was supported by the research support funds of the Paracelsus Medical University, E-19/29/153-KIT to MK.

ACKNOWLEDGMENTS

We thank Julia Fuchs and Leman Emin for the skilled technical and administrative assistance and Hubert Kerschbaum (Department of Biosciences, University of Salzburg, Austria) for helpful comments and discussions.

SUPPLEMENTARY MATERIAL

The Supplementary Material for this article can be found online at: <https://www.frontiersin.org/articles/10.3389/fcell.2020.583131/full#supplementary-material>

REFERENCES

- Ackerman, M. J., Wickman, K. D., and Clapham, D. E. (1994). Hypotonicity Activates a Native Chloride Current in *Xenopus*-Oocytes. *J. Gen. Physiol.* 103, 153–179. doi: 10.1085/jgp.103.2.153
- Alford, A. I., Yellowley, C. E., Jacobs, C. R., and Donahue, H. J. (2003). Increases in cytosolic calcium, but not fluid flow, affect aggrecan mRNA levels in articular chondrocytes. *J. Cell. Biochem.* 90, 938–944. doi: 10.1002/jcb.10715
- Auzanneau, C., Thoreau, V., Kitzis, A., and Becq, F. A. (2003). novel voltage-dependent chloride current activated by extracellular acidic pH in cultured rat Sertoli cells. *J. Biol. Chem.* 278, 19230–19236. doi: 10.1074/jbc.M301096200
- Bae, Y., Kim, A., Cho, C. H., Kim, D., Jung, H. G., Kim, S. S., et al. (2019). TTYH1 and TTYH2 Serve as LRRC8A-Independent Volume-Regulated Anion Channels in Cancer Cells. *Cells* 8:562. doi: 10.3390/cells8060562
- Behmanesh, S., and Kempinski, O. (2000). Mechanisms of endothelial cell swelling from lactacidosis studied in vitro. *Am. J. Physiol. Heart Circ. Physiol.* 279, H1512–H1517. doi: 10.1152/ajpheart.2000.279.4.H1512
- Benedetto, R., Sirianant, L., Pankonien, I., Wanitchakool, P., Ousingsawat, J., Cabrita, I., et al. (2016). Relationship between TMEM16A/anoctamin 1 and LRRC8A. *Pflug. Arch.* 468, 1751–1763. doi: 10.1007/s00424-016-1862-1
- Bertram, K. L., and Krawetz, R. J. (2012). Osmolarity regulates chondrogenic differentiation potential of synovial fluid derived mesenchymal progenitor cells. *Biochem. Biophys. Res. Comm.* 422, 455–461. doi: 10.1016/j.bbrc.2012.05.015
- Bush, P. G., and Hall, A. C. (2003). The volume and morphology of chondrocytes within non-degenerate and degenerate human articular cartilage. *Osteoarthritis Cartilage* 11, 242–251. doi: 10.1053/S1063-4584-(02)00369-2
- Bush, P. G., and Hall, A. C. (2005). Passive osmotic properties of in situ human articular chondrocytes within non-degenerate and degenerate cartilage. *J. Cell. Physiol.* 204, 309–319. doi: 10.1002/jcp.20294
- Capurro, V., Gianotti, A., Caci, E., Ravazzolo, R., Galletta, L. J. V., and Zegarra-Moran, O. (2015). Functional analysis of acid-activated Cl⁻ channels: Properties and mechanisms of regulation. *Bba Biomembranes* 1848, 105–114. doi: 10.1016/j.bbamem.2014.10.008
- Deneka, D., Sawicka, M., Lam, A. K. M., Paulino, C., and Dutzler, R. (2018). Structure of a volume-regulated anion channel of the LRRC8 family. *Nature* 558, 254–259. doi: 10.1038/s41586-018-0134-y
- Finger, F., Schörle, C., Zien, A., Gebhard, P., Goldring, M. B., and Aigner, T. (2003). Molecular Phenotyping of Human Chondrocyte Cell Lines T/C-28a2, T/C-28a4, and C-28/12. *Arthritis Rheum.* 48, 3395–3403. doi: 10.1002/art.11341
- Funabashi, K., Fujii, M., Yamamura, H., Ohya, S., and Imaizumi, Y. (2010). Contribution of Chloride Channel Conductance to the Regulation of Resting Membrane Potential in Chondrocytes. *J. Pharmacol. Sci.* 113, 94–99. doi: 10.1254/jphs.10026sc
- Goldring, M. B., Birkhead, J. R., Suen, L. F., Yamin, R., Mizuno, S., Glowacki, J., et al. (1994). Interleukin-1 β -modulated Gene Expression in Immortalized Human Chondrocytes. *J. Clin. Invest.* 94, 2307–2316. doi: 10.1172/jci117595
- Hall, A. C. (2019). The Role of Chondrocyte Morphology and Volume in Controlling Phenotype-Implications for Osteoarthritis, Cartilage Repair, and Cartilage Engineering. *Curr. Rheumatol. Rep.* 21:38. doi: 10.1007/s11926-019-0837-6
- Hall, A. C., Horwitz, E. R., and Wilkins, R. J. (1996). The cellular physiology of articular cartilage. *Exp. Physiol.* 81, 535–545. doi: 10.1113/expphysiol.1996.sp003956
- Harl, B., Schmolzer, J., Jakab, M., Ritter, M., and Kerschbaum, H. H. (2013). Chloride channel blockers suppress formation of engulfment pseudopodia in microglial cells. *Cell Physiol. Biochem.* 31, 319–337. doi: 10.1159/000343370
- Helm, K., Beyreis, M., Mayr, C., Ritter, M., Jakab, M., Kiesslich, T., et al. (2017). In Vitro Cell Death Discrimination and Screening Method by Simple and Cost-Effective Viability Analysis. *Acta Physiol.* 221, 176–176. doi: 10.1159/000460910
- Hoffmann, E. K. (2011). Ion channels involved in cell volume regulation: effects on migration, proliferation, and programmed cell death in non adherent EAT cells and adherent ELA cells. *Cell Physiol. Biochem.* 28, 1061–1078. doi: 10.1159/000335843
- Hoffmann, E. K., Lambert, I. H., and Pedersen, S. F. (2009). Physiology of cell volume regulation in vertebrates. *Physiol. Rev.* 89, 193–277. doi: 10.1152/physrev.00037.2007
- Hwang, H. S., and Kim, H. A. (2015). Chondrocyte Apoptosis in the Pathogenesis of Osteoarthritis. *Int. J. Mol. Sci.* 16, 26035–26054. doi: 10.3390/ijms161125943
- Isoya, E., Toyoda, F., Imai, S., Okumura, N., Kumagai, K., Omatsu-Kanbe, M., et al. (2009). Swelling-Activated Cl⁻ Current in Isolated Rabbit Articular Chondrocytes: Inhibition by Arachidonic Acid. *J. Pharmacol. Sci.* 109, 293–304. doi: 10.1254/jphs.08278fp
- Jackson, P. S., and Strange, K. (1995). Characterization of the Voltage-Dependent Properties of a Volume-Sensitive Anion Conductance. *J. Gen. Physiol.* 105, 661–676. doi: 10.1085/jgp.105.5.661
- Jakab, M., and Ritter, M. (2006). Cell Volume Regulatory Ion Transport in the Regulation of Cell Migration. *Contrib. Nephrol.* 152, 161–180. doi: 10.1159/000096322
- Jentsch, T. J., Lutter, D., Planells-Cases, R., Ullrich, F., and Voss, F. K. V. R. A. C. (2016). molecular identification as LRRC8 heteromers with differential functions. *Pflug. Arch.* 468, 385–393. doi: 10.1007/s00424-015-1766-5
- Jentsch, T. J., Stein, V., Weinreich, F., and Zdebik, A. A. (2002). Molecular structure and physiological function of chloride channels. *Physiol. Rev.* 82, 503–568. doi: 10.1152/physrev.00029.2001
- Kajiya, H., Okamoto, F., Ohgi, K., Nakao, A., Fukushima, H., and Okabe, K. (2009). Characteristics of ClC7 Cl⁻ channels and their inhibition in mutant (G215R) associated with autosomal dominant osteopetrosis type II in native osteoclasts and hClcn7 gene-expressing cells. *Pflug. Arch. Eur. J. Phy.* 458, 1049–1059. doi: 10.1007/s00424-009-0689-4
- Kittl, M., Dobias, H., Beyreis, M., Kiesslich, T., Mayr, C., Gaisberger, M., et al. (2018). Glycine Induces Migration of Microglial BV-2 Cells via SNAT-Mediated Cell Swelling. *Cell Physiol. Biochem.* 50, 1460–1473. doi: 10.1159/000494646
- Kittl, M., Helm, K., Beyreis, M., Mayr, C., Gaisberger, M., Winklmayr, M., et al. (2019). Acid- and Volume-Sensitive Chloride Currents in Microglial Cells. *Int. J. Mol. Sci.* 20:3475. doi: 10.3390/ijms20143475
- Kontinen, Y. T., Mandelin, J., Li, T. F., Salo, J., Lassus, J., Liljestrom, M., et al. (2002). Acidic Cysteine Endoprotease Cathepsin K in the Degeneration of the Superficial Articular Hyaline Cartilage in Osteoarthritis. *Arthritis Rheum.* 46, 953–960. doi: 10.1002/art.10185
- Kucherenko, Y. V., Morsdorf, D., and Lang, F. (2009). Acid-Sensitive Outwardly Rectifying Anion Channels in Human Erythrocytes. *J. Membr. Biol.* 230, 1–10. doi: 10.1007/s00232-009-9179-z
- Kumagai, K., Toyoda, F., Staunton, C. A., Maeda, T., Okumura, N., Matsuura, H., et al. (2016). Activation of a chondrocyte volume-sensitive Cl⁻ conductance prior to macroscopic cartilage lesion formation in the rabbit knee anterior cruciate ligament transection osteoarthritis model. *Osteoarthritis Cartilage* 24, 1786–1794. doi: 10.1016/j.joca.2016.05.019
- Kurita, T., Yamamura, H., Suzuki, Y., Giles, W. R., and Imaizumi, Y. (2015). The ClC-7 Chloride Channel Is Downregulated by Hypoosmotic Stress in Human Chondrocytes. *Mol. Pharmacol.* 88, 113–120. doi: 10.1124/mol.115.098160
- Lambert, S., and Oberwinkler, J. (2005). Characterization of a proton-activated, outwardly rectifying anion channel. *J. Physiol.* 567, 191–213. doi: 10.1113/jphysiol.2005.089888
- Lang, F., Busch, G. L., Ritter, M., Volkl, H., Waldegger, S., Gulbins, E., et al. (1998). Functional Significance of Cell Volume Regulatory Mechanisms. *Physiol. Rev.* 78, 247–306. doi: 10.1152/physrev.1998.78.1.247
- Lewis, R., Asplin, K. E., Bruce, G., Dart, C., Mobasheri, A., and Barrett-Jolley, R. (2011a). The Role of the Membrane Potential in Chondrocyte Volume Regulation. *J. Cell Physiol.* 226, 2979–2986. doi: 10.1002/jcp.22646
- Lewis, R., Feetham, C. H., and Barrett-Jolley, R. (2011b). Cell Volume Regulation in Chondrocytes. *Cell Physiol. Biochem.* 28, 1111–1122. doi: 10.1159/000335847
- Man, G. S., and Mologhianu, G. (2014). Osteoarthritis pathogenesis – a complex process that involves the entire joint. *J. Med. Life* 7, 37–41.
- Maroudas, A., Wachtel, E., Grushko, G., Katz, E. P., and Weinberg, P. (1991). The Effect of Osmotic and Mechanical Pressures on Water Partitioning in Articular Cartilage. *Biochim. Biophys. Acta* 1073, 285–294. doi: 10.1016/0304-4165(91)90133-2
- Milner, P. I., Wilkins, R. J., and Gibson, J. S. (2012). “Cellular Physiology of Articular Cartilage in Health and Disease,” in *Principles of Osteoarthritis – Its Definition, Character, Derivation and Modality-Related Recognition*, ed. B. M. Rothschild (London: IntechOpen), 567–590. doi: 10.5772/1487pp
- Nilius, B., Prenen, J., and Droogmans, G. (1998). Modulation of volume-regulated anion channels by extra- and intracellular pH. *Pflug. Arch. Eur. J. Phy.* 436, 742–748. doi: 10.1007/s004240050697

- Nobles, M., Higgins, C. F., and Sardini, A. (2004). Extracellular acidification elicits a chloride current that shares characteristics with $\text{I}_{\text{Cl(swell)}}$. *Am. J. Physiol. Cell Physiol.* 287, C1426–C1435. doi: 10.1152/ajpcell.00549.2002
- Okada, Y. (2019). Tweety Homologs (TTYH) Freshly Join the Journey of Molecular Identification of the VRAC/VSOR Channel Pore. *Exp. Neurobiol.* 28, 131–133. doi: 10.5607/en.2019.28.2.131
- Okada, Y., Shimizu, T., Maeno, E., Tanabe, S., Wang, X., and Takahashi, N. (2006). Volume-sensitive chloride channels involved in apoptotic volume decrease and cell death. *J. Membr. Biol.* 209, 21–29. doi: 10.1007/s00232-005-0836-6
- Palazzo, C., Nguyen, C., Lefevre-Colau, M. M., Rannou, F., and Poiraudau, S. (2016). Risk factors and burden of osteoarthritis. *Ann. Phys. Rehabil. Med.* 59, 134–138. doi: 10.1016/j.rehab.2016.01.006
- Pedersen, S. F., Klausen, T. K., and Nilius, B. (2015). The identification of a volume-regulated anion channel: an amazing Odyssey. *Acta Physiol.* 213, 868–881. doi: 10.1111/apha.12450
- Pedersen, S. F., Okada, Y., and Nilius, B. (2016). Biophysics and Physiology of the Volume-Regulated Anion Channel (VRAC)/Volume-Sensitive Outwardly Rectifying Anion Channel (VSOR). *Pflug. Arch. Eur. J. Phys.* 468, 371–383. doi: 10.1007/s00424-015-1781-6
- Perez-Hernandez, E., Perez-Hernandez, N., Hernandez-Hernandez, F.d.I.C., and Kouri-Flores, J. B. (2012). *Principles of Osteoarthritis- Its Definition, Character, Derivation and Modality-Related Recognition*. London: Intech. doi: 10.5772/1487
- Ponce, A., Jimenez-Pena, L., and Tejeda-Guzman, C. (2012). The Role of Swelling-Activated Chloride Currents ($\text{I}_{\text{CL,swell}}$) in the Regulatory Volume Decrease Response of Freshly Dissociated Rat Articular Chondrocytes. *Cell Physiol. Biochem.* 30, 1254–1270. doi: 10.1159/000343316
- Puppulin, L., Hosogi, S., Sun, H., Matsuo, K., Inui, T., Kumamoto, Y., et al. (2018). Bioconjugation strategy for cell surface labelling with gold nanostructures designed for highly localized pH measurement. *Nat. Commun.* 9:5278. doi: 10.1038/s41467-018-07726-5
- Qian, N., Ichimura, A., Takei, D., Sakaguchi, R., Kitani, A., Nagaoka, R., et al. (2019). TRPM7 channels mediate spontaneous Ca^{2+} fluctuations in growth plate chondrocytes that promote bone development. *Sci. Signal* 12:eaaw4847. doi: 10.1126/scisignal.aaw4847
- Qiu, Z. Z., Dubin, A. E., Mathur, J., Tu, B., Reddy, K., Miraglia, L. J., et al. (2014). SWELL1, a Plasma Membrane Protein. Is an Essential Component of Volume-Regulated Anion Channel. *Cell* 157, 447–458. doi: 10.1016/j.cell.2014.03.024
- Roach, H. I., Aigner, T., and Kouri, J. B. (2004). Chondroptosis: a Variant of Apoptotic Cell Death in Chondrocytes? *Apoptosis* 9, 265–277. doi: 10.1023/b:appt.0000025803.17498.26
- Sato-Numata, K., Numata, T., and Okada, Y. (2014). Temperature sensitivity of acid-sensitive outwardly rectifying (ASOR) anion channels in cortical neurons is involved in hypothermic neuroprotection against acidotoxic necrosis. *Channels* 8, 278–283. doi: 10.4161/chan.27748
- Sato-Numata, K., Numata, T., Inoue, R., and Okada, Y. (2016). Distinct pharmacological and molecular properties of the acid-sensitive outwardly rectifying (ASOR) anion channel from those of the volume-sensitive outwardly rectifying (VSOR) anion channel. *Pflug. Arch. Eur. J. Phys.* 468, 795–803. doi: 10.1007/s00424-015-1786-1
- Sato-Numata, K., Numata, T., Inoue, R., Sabirov, R. Z., and Okada, Y. (2017). Distinct contributions of LRRC8A and its paralogs to the VSOR anion channel from those of the ASOR anion channel. *Channels* 11, 167–172. doi: 10.1080/19336950.2016.1230574
- Sato-Numata, K., Numata, T., Okada, T., and Okada, Y. (2013). Acid-sensitive outwardly rectifying (ASOR) anion channels in human epithelial cells are highly sensitive to temperature and independent of ClC-3 . *Pflug. Arch. Eur. J. Phys.* 465, 1535–1543. doi: 10.1007/s00424-013-1296-y
- Schober, A. L., Wilson, C. S., and Mongin, A. A. (2017). Molecular composition and heterogeneity of the LRRC8-containing swelling-activated osmolyte channels in primary rat astrocytes. *J. Physiol.* 595, 6939–6951. doi: 10.1113/JP275053
- Sophia Fox, A. J., Bedi, A., and Rodeo, S. A. (2009). The basic science of articular cartilage: structure, composition, and function. *Sports Health* 1, 461–468. doi: 10.1177/1941738109350438
- Stauber, T. (2015). The volume-regulated anion channel is formed by LRRC8 heteromers - molecular identification and roles in membrane transport and physiology. *Biol. Chem.* 396, 975–990. doi: 10.1515/hsz-2015-0127
- Staunton, C. A., Lewis, R., and Barrett-Jolley, R. (2013). Ion Channels and Osteoarthritic Pain: Potential for Novel Analgesics. *Curr. Pain Headache. Rep.* 17:378. doi: 10.1007/s11916-013-0378-z
- Sun, C., Wang, S. M., and Hu, W. (2018). Acid-sensing ion channel 1a mediates acid-induced inhibition of matrix metabolism of rat articular chondrocytes via the MAPK signaling pathway. *Mol. Cell. Biochem.* 443, 81–91. doi: 10.1007/s11010-017-3212-9
- Suzuki, M., and Mizuno, A. A. (2004). Novel Human Cl^- Channel Family Related to *Drosophila flightless* Locus. *J. Biol. Chem.* 279, 22461–22468. doi: 10.1074/jbc.M313813200
- Syeda, R., Qiu, Z., Dubin, A. E., Murthy, S. E., Florendo, M. N., Mason, D. E., et al. (2016). LRRC8 Proteins Form Volume-Regulated Anion Channels that Sense Ionic Strength. *Cell* 164, 499–511. doi: 10.1016/j.cell.2015.12.031
- Ullrich, F., Blin, S., Lazarow, K., Daubitz, T., von Kries, J. P., and Jentsch, T. J. (2019). Identification of TMEM206 proteins as pore of PAORAC/ASOR acid-sensitive chloride channels. *Elife* 8:e49187. doi: 10.7554/eLife.49187.001
- Valinsky, W. C., Touyz, R. M., and Shrier, A. (2017). Characterization of constitutive and acid-induced outwardly rectifying chloride currents in immortalized mouse distal tubular cells. *Bba. Gen. Subjects* 1861, 2007–2019. doi: 10.1016/j.bbagen.2017.05.004
- Voets, T., Droogmans, G., and Nilius, B. (1997). Modulation of voltage-dependent properties of a swelling-activated Cl^- current. *J. Gen. Physiol.* 110, 313–325. doi: 10.1085/jgp.110.3.313
- Vos, T., Flaxman, A. D., Naghavi, M., Lozano, R., Michaud, C., Ezzati, M., et al. (2012). Years lived with disability (YLDs) for 1160 sequelae of 289 diseases and injuries 1990–2010: a systematic analysis for the Global Burden of Disease Study 2010. *Lancet* 380, 2163–2196. doi: 10.1016/S0140-6736(12)61729-2
- Voss, F. K., Ullrich, F., Munch, J., Lazarow, K., Lutter, D., Mah, N., et al. (2014). Identification of LRRC8 Heteromers as an Essential Component of the Volume-Regulated Anion Channel VRAC. *Science* 344, 634–638. doi: 10.1126/science.1252826
- Wang, H. Y., Shimizu, T., Numata, T., and Okada, Y. (2007). Role of acid-sensitive outwardly rectifying anion channels in acidosis-induced cell death in human epithelial cells. *Pflug. Arch. Eur. J. Phys.* 454, 223–233. doi: 10.1007/s00424-006-0193-z
- Wilkins, R. J., Browning, J. A., and Ellory, J. C. (2000). Surviving in a Matrix: Membrane Transport in Articular Chondrocytes. *J. Membr. Biol.* 177, 95–108. doi: 10.1007/s002320001103
- Winklmayr, M., Gaisberger, M., Kittl, M., Fuchs, J., Ritter, M., and Jakab, M. (2019). Dose-Dependent Cannabidiol-Induced Elevation of Intracellular Calcium and Apoptosis in Human Articular Chondrocytes. *J. Orthop. Res.* 37, 2540–2549. doi: 10.1002/jor.24430
- Wu, M. H., Urban, J. P. G., Cui, Z. F., Cui, Z., and Xu, X. (2007). Effect of extracellular pH on matrix synthesis by chondrocytes in 3D agarose gel. *Biotechnol. Prog.* 23, 430–434. doi: 10.1021/bp060024v
- Yamamoto, S., and Ehara, T. (2006). Acidic extracellular pH-activated outwardly rectifying chloride current in mammalian cardiac myocytes. *Am. J. Physiol. Heart C* 290, H1905–H1914. doi: 10.1152/ajpheart.00965.2005
- Yamamura, H., Suzuki, Y., and Imaizumi, Y. (2018). Physiological and Pathological Functions of Cl^- Channels in Chondrocytes. *Biol. Pharm. Bull.* 41, 1145–1151. doi: 10.1248/bpb.b18-00152
- Yang, J. H., Chen, J. N., Vitery, M. D., Osei-Owusu, J., Chu, J. C., Yu, H. Y., et al. (2019). PAC, an evolutionarily conserved membrane protein, is a proton-activated chloride channel. *Science* 364:395. doi: 10.1126/science.aav9739

Conflict of Interest: The authors declare that the research was conducted in the absence of any commercial or financial relationships that could be construed as a potential conflict of interest.

Copyright © 2020 Kittl, Winklmayr, Helm, Lettner, Gaisberger, Ritter and Jakab. This is an open-access article distributed under the terms of the Creative Commons Attribution License (CC BY). The use, distribution or reproduction in other forums is permitted, provided the original author(s) and the copyright owner(s) are credited and that the original publication in this journal is cited, in accordance with accepted academic practice. No use, distribution or reproduction is permitted which does not comply with these terms.



Ions, the Movement of Water and the Apoptotic Volume Decrease

Carl D. Bortner* and John A. Cidlowski*

Signal Transduction Laboratory, Department of Health and Human Services, National Institute of Environmental Health Sciences, National Institutes of Health, Research Triangle Park, NC, United States

OPEN ACCESS

Edited by:

Markus Ritter,
Paracelsus Medical University, Austria

Reviewed by:

Alexey Vereninov,
Russian Academy of Sciences (RAS),
Russia
Karl Kunzelmann,
University of Regensburg, Germany

*Correspondence:

Carl D. Bortner
bortner@niehs.nih.gov
John A. Cidlowski
cidlowski@niehs.nih.gov

Specialty section:

This article was submitted to
Cell Death and Survival,
a section of the journal
Frontiers in Cell and Developmental
Biology

Received: 28 September 2020

Accepted: 04 November 2020

Published: 25 November 2020

Citation:

Bortner CD and Cidlowski JA
(2020) Ions, the Movement of Water
and the Apoptotic Volume Decrease.
Front. Cell Dev. Biol. 8:611211.
doi: 10.3389/fcell.2020.611211

The movement of water across the cell membrane is a natural biological process that occurs during growth, cell division, and cell death. Many cells are known to regulate changes in their cell volume through inherent compensatory regulatory mechanisms. Cells can sense an increase or decrease in their cell volume, and compensate through mechanisms known as a regulatory volume increase (RVI) or decrease (RVD) response, respectively. The transport of sodium, potassium along with other ions and osmolytes allows the movement of water in and out of the cell. These compensatory volume regulatory mechanisms maintain a cell at near constant volume. A hallmark of the physiological cell death process known as apoptosis is the loss of cell volume or cell shrinkage. This loss of cell volume is in stark contrast to what occurs during the accidental cell death process known as necrosis. During necrosis, cells swell or gain water, eventually resulting in cell lysis. Thus, whether a cell gains or loses water after injury is a defining feature of the specific mode of cell death. Cell shrinkage or the loss of cell volume during apoptosis has been termed apoptotic volume decrease or AVD. Over the years, this distinguishing feature of apoptosis has been largely ignored and thought to be a passive occurrence or simply a consequence of the cell death process. However, studies on AVD have defined an underlying movement of ions that result in not only the loss of cell volume, but also the activation and execution of the apoptotic process. This review explores the role ions play in controlling not only the movement of water, but the regulation of apoptosis. We will focus on what is known about specific ion channels and transporters identified to be involved in AVD, and how the movement of ions and water change the intracellular environment leading to stages of cell shrinkage and associated apoptotic characteristics. Finally, we will discuss these concepts as they apply to different cell types such as neurons, cardiomyocytes, and corneal epithelial cells.

Keywords: apoptosis, AVD, RVI, RVD, ion channels, water channels, aquaporins

INTRODUCTION

Cell survival depends on maintaining cellular stability from altered environmental conditions that occur from both inside and outside the cell. Cellular stability is accomplished through numerous homeostatic processes which allows cells to self-regulate and/or adjust various biological systems providing an unvarying environment to thrive and flourish. Examples of biological systems that

cells maintain include glucose levels, acid-base balance, calcium levels, and fluid volume. Cellular stress results in the activation of a variety of Intracellular mechanisms including the DNA damage response, the unfolded protein response, cell senescence, and regulated cell death (Galluzzi et al., 2018). What drives the homeostatic balance of many biological systems is the movement of monovalent ions that results in a change in water content to alter the concentration of glucose, acids/bases, and calcium. Therefore, ionic fluidity and the movement of water via this mechanism or through specific water channels have a dramatic impact on cell viability. Failure of these homeostatic processes can signal the cell to die. Interestingly, even in death, cells attempt to maintain some sense of biological homeostasis by undergoing a programmed cell death process known as apoptosis. As such, activation of apoptosis is the body's attempt to remove unwanted or dying cells without affecting neighboring healthy cells.

NECROSIS VS. APOPTOSIS

Over centuries of scientific discovery, the analysis of dying cells has not been a field of rigorous study. Cells die due to injury, accident damage, or “old age” after fulfilling their purpose to a point where they are no longer needed. Up until the early 1970s, necrosis was the term used to describe dying cells defined as an accidental cell death process characterized by cell swelling followed by eventual cell lysis. The release of intracellular products of the dying cell into the extracellular space results in an inflammatory response leading to further damage in the surrounding tissue. As the corpse of a dead cell does not lend one a great deal of substance to explore, attention focused on understanding the inflammatory response, the attraction of leukocytes, and the removal of the dead cell material. However, observations by Kerr (1965, 1970) led to the understanding of a distinctive type of necrosis termed “shrinkage necrosis” (Kerr, 1971). From these early studies, it was evident that the loss of cell volume or cell shrinkage was a distinguishing feature of this controlled cell deletion process. Further study defined this event as a vital, active, and inherently programmed biological process known as apoptosis (Kerr et al., 1972).

There are many discriminating features when comparing necrosis to apoptosis (Nikoletopoulou et al., 2013; D'Arcy, 2019). Necrosis is initiated from external factors that results in detrimental effects on the cell including ATP depletion, cell swelling, membrane disruption, and eventual lysis culminating in an inflammatory response. In contrast, apoptosis is considered a physiological mode of cell death initiated by inherent mechanisms that results in chromatin condensation, cell shrinkage, membrane blebbing leading to the formation of apoptotic bodies that are engulfed by neighboring cells or macrophages. Therefore, apoptosis culminates in a silent process with no noticeable symptoms. Given the distinct cellular events surrounding death by necrosis vs. death by apoptosis, the change in cellular morphology is the most visible characteristic that can easily discriminate between these two diverse modes of cell death.

While necrosis and apoptosis exemplify the extreme modes of cell death, many other cell death processes have been

identified and defined. Necroptosis is an inflammatory form of regulated (programmed) necrotic cell death considered a viral defense mechanism that lacks caspase activation resulting in leakage of the cellular contents into the extracellular space. Similarly, pyroptosis is a highly inflammatory form of programmed cell death that occurs frequently upon infection with intracellular pathogens and is characterized by the formation of the inflammasome (pyroosome). While caspase-dependent, pyroptosis uses a distinct set of proteolytic enzymes (caspases 1, 4, and 5) then apoptosis and the activation of pore-forming proteins known as gasdermins results in water influx and cell membrane rupture. Thus, similar to necroptosis, pyroptosis is not considered immunologically silent. Additionally, ferroptosis is an iron-dependent programmed cell death characterized by the accumulation of lipid peroxides triggered by the failure of the glutathione-dependent antioxidant defense mechanism. Cells undergoing ferroptosis typically contract, then swell, releasing their intracellular contents. The most similar mode of cell death that mimics apoptosis is the death of red blood cells known as eryptosis. Insults such as hyperosmolarity, oxidative stress, and heavy metal exposure can result in erythrocytes undergoing cell death characterized by cell shrinkage, membrane blebbing, activation of proteases, and externalization of phosphatidylserine. A comparison of the characteristics that define these modes of cell death is shown in **Table 1**.

In total, there have been 34 different modes of cell death described in the literature (Liu et al., 2018b). This includes the orderly degradation and recycling of cellular components known as autophagy; an ischemic cell death resulting from ATP depletion known as oncosis; death of anchorage-dependent cells that detach from the surrounding extracellular matrix known as anoikis; and a programmed mode of necrotic cell death in fibroblasts known as nemosis. While many of these modes of cell death are similar in nature, they can provide a unique characterization of the physiology in a clinical or pathological setting. For example, mitotic catastrophe that occurs due to premature or inappropriate entry of cells into mitosis is the most common mode of cell death in cancer cells exposed to various chemotherapeutic treatments. Thus, the use of mitotic catastrophe has a very relevant connotation in this clinical setting. In this review, we will focus on the classical physiological mode of cell death, apoptosis; and examine cell death in several cell type model systems in regards to ion and water movement that results in the loss of cell volume.

MAINTAINING FLUID VOLUME HOMEOSTASIS

Alterations in cell morphology are key in distinguishing necrosis and apoptosis, thus variations in cellular water content must occur suggesting that maintaining water balance is critical for cell survival. Thus, inherent cellular mechanisms have developed to combat changes in the extracellular environment that impacts a cell's hydration state. In general, a sudden change in solute concentration surrounding a cell results in an osmotic stress, also described as an osmotic shock. When the extracellular

TABLE 1 | Characteristics of various regulated modes of cell death.

Characteristic	Apoptosis	Necrosis	Necroptosis	Pyroptosis	Ferroptosis	Eryptosis
Cell shrinkage	Yes	No	No	No	No	Yes
Cell swelling	No	Yes	Yes	Yes	No	No
Nucleus fragmentation	No	No	No	Yes	No	No
Membrane blebbing	Yes	No	Yes	Yes	No	Yes
Caspase activation	Yes	No	No	Yes	No	Yes
DNA fragmentation	Yes	No	No	Yes	No	No
Cell lysis	No	Yes	Yes	Yes	no	No
Inflammation	No	Yes	Yes	Yes	Yes	Yes
Regulated	Yes	No	Yes	Yes	Yes	Yes

solute concentration is low (hypo-osmotic stress), cells can rapidly gain water. In contrast, when the extracellular solute concentration is high (hyper-osmotic stress), a rapid loss of water occurs from cells. Simply noted, water will flow in the direction of higher solute concentration, signifying solute flux as a central determinant of water movement. As cells have a defined perimeter and limited capacity to either contract or expand, most cells respond to changes in these environmental conditions with rapid ionic fluxes that alter their intracellular environment to adjust to the change in the extracellular environment (Lang et al., 1998; Hoffmann and Pedersen, 2011; Pasantes-Morales, 2016; Delpire and Gagnon, 2018).

The gain in water that occurs when cells encounter a hypo-osmotic environment (a decrease in external osmolarity) is immediately countered with an active recovery process known as regulatory volume decrease (RVD). This inherent adaptation process involves the flux of ions, mainly potassium and chloride, along with various organic osmolytes from the cell (Hoffmann, 2000; Yang et al., 2012). Potassium is the most abundant monovalent ion in the cell and permeates from the cell through various channels including voltage-gated, Ca^{2+} -activated, inwardly rectifying, and two-pore-domain potassium channels (Pasantes-Morales, 2016). The precise potassium channels activated during RVD appears to be both cell-type and stimulus-specific. Along with potassium channels, voltage-sensitive chloride channels also have a key role in RVD in maintaining an overall electrically neutral ionic state. The voltage-regulated anion channel (VRAC) has been a channel of intense interest as VRAC is also permeate to large molecules such as gluconate and glutamate that can further facilitate a restoration in cell volume (Pedersen et al., 2016).

Cells encountering a hyper-osmotic environment (an increase in external osmolarity) immediately shrink and activate a regulatory volume increase (RVI). During this process, various mechanisms are activated to increase the concentration of intracellular osmolytes. Sodium is the most abundant ion outside the cell, and sodium enters the cell through various electroneutral cotransporters and exchangers including the Na^+-Cl^- cotransporter (NCC), the $\text{Na}^+/\text{K}^+/\text{2Cl}^-$ cotransporter (NKCC), and the Na^+-H^+ exchanger coupled to the $\text{Cl}^-/\text{HCO}_3^-$ exchanger (Pasantes-Morales, 2016). Additionally, the initial increase in intracellular sodium that

occurs during RVI is alleviated through the activation of the $\text{Na}^+-\text{K}^+-\text{ATPase}$, that resets the initial intracellular ionic environment. Similar to the activation of RVD, the precise transporters and exchangers activated during RVI is not completely understood and occurs in both a cell-type and stimulus-specific manner.

The importance of inherent volume regulatory mechanisms in protecting cells from adverse changes in the extracellular environment was illustrated when T-cells, that lack a normal RVI, were subject to hypertonic stress (Bortner and Cidlowski, 1996). In the absence of an inherent RVI, these T-cells shrank and underwent a rapid and systematic cell death that was shown to be apoptosis, while cells such as COS-7, L-cells, and PC12 cells, that can regulate their volume via RIV, were resistant to hypertonic-induced stress and survived. Increased tonicity augmented serum-deprived induced apoptosis in vascular smooth muscle cells (Orlov et al., 1996). In support of the concept of volume regulatory mechanisms protecting cells from death, inhibition of hypertonicity-induced cation channels was shown to sensitize HeLa cells to undergo apoptosis when the extracellular osmolality was increased (Shimizu et al., 2006). Interestingly, while hyperosmolality did not initially induce apoptosis in rat hepatocytes that respond with an RVI, Reinehr et al. (2002) showed this condition did target the CD95 receptor to the plasma membrane sensitizing the cells to Fas ligand-induced apoptosis. While in the clinical setting, mannitol therapy has been widely used for acute and subacute reduction in brain edemas resulting from closed-head trauma, and ischemic brain swelling to improve cerebral blood flow, Malek et al. (1998) pointed out potential deleterious effect of hyperosmotic treatment on the vascular endothelium due to mannitol's ability to induce apoptosis. This suggests caution should be exercised for the clinical use of osmotic diuretics such as mannitol to avoid detrimental and often lethal effects to surrounding cells and tissue.

THE ADVENT OF AVD

A defining characteristic of cell death as outlined earlier is a change in cell volume. This simple and straightforward visual cue allows one to immediately categorize the two most common

modes of cell death that has or is occurring. The loss of cell volume that occurs during apoptosis and gain in cell volume as observed during necrosis both occur in the absence of osmotic changes in the extracellular environment. Consequently, the term necrotic volume increase (NVI) was proposed to describe the influx of sodium, lactate, and other osmolytes into cells leading to cell swelling during this accidental or necrotic cell death process (Barros et al., 2001). NVI is thought to be due in part to a dysregulation of the inherent RVD, specifically an impairment of volume-sensitive Cl^- channels (Okada et al., 2004, 2019) and subsequently, an acid-sensitive outwardly rectifying (ASOR) anion channel (Wang et al., 2007).

In contrast, the term apoptotic volume decrease (AVD) has been applied to describe the loss of cell volume or cell shrinkage during the physiological or apoptotic cell death process (Maeno et al., 2000; Okada et al., 2004). What became apparent from early studies investigating the loss of cell volume during apoptosis was that AVD most likely was not a novel volume mechanism, but occurred via sharing or commandeering inherent RVD channels/transporters for a new purpose during the programmed process (Okada et al., 2001, 2004; Okada and Maeno, 2001). Of particular note is VRAC; the volume-activated anion channel that is essential to the apoptotic death machinery. VRAC is activated by a change in intracellular ionic strength, increased intracellular calcium, ROS, and phosphorylation (Kunzelmann, 2016), however a complete understanding these signaling cascades is not known. The exact nature of this channel remained unknown until the recent identification of LRRC8 proteins as a key component of VRAC (Qiu et al., 2014; Voss et al., 2014). While LRRC8 isoforms have been shown to contribute to RVD and sense changes in ionic strength (Syeda et al., 2016), it has been suggested that this volume-regulated anion channel may not be essential for AVD (Planells-Cases et al., 2015; Jentsch, 2016; Sirianant et al., 2016). Moreover, it is important to note that the reprogramming of RVD to AVD during apoptosis must likely involves the inactivation of RVI that would normally compensate for a loss of cell volume.

As ion flux was known to underlie cell volume regulatory processes, ion channels became a central focus for AVD. Two-pore domain K^+ ($\text{K}2\text{P}$) channels were suggested to underlie potassium efflux during AVD in mouse embryos (Trimarchi et al., 2002). AVD was shown to be accelerated upon staurosporine-induced apoptosis of COS-7 and pulmonary artery smooth muscle cells (PASMC) overexpressing a delayed-rectifier voltage-gated K^+ channel (Brevnova et al., 2004). Studies using a calcium-induced apoptosis lymphocyte/thymocyte model showed that AVD could be blocked with inhibitors of IKCa1 , preventing the externalization of phosphatidylserine and cell death (Elliott and Higgins, 2003). In endothelial cells challenged with staurosporine, AVD was inhibited with the chloride channel blocker phloretin, again preserving cell viability (Porcelli et al., 2004).

Early X-ray microanalysis showed an increase in intracellular sodium coupled with a decrease in intracellular potassium within 3 h of oxidized low-density lipoprotein exposure in monocyte-macrophages (Skepper et al., 1999). Subsequent X-ray microanalysis studies confirmed a two-phase change in

intracellular using staurosporine-treated U937 cells (Arrebola et al., 2005a,b, 2006). These authors showed during late stage apoptosis the potassium concentration continued to decrease, while chloride increased along with an increase in sodium. In a follow-up study, this group also showed that the initial stage of apoptosis in UV-induced U937 cells were characterized by a decrease in potassium and chloride, with the largest decrease occurring from the mitochondria (Arrebola et al., 2006). An earlier study by Bortner and Cidlowski (2003) had showed an increase in intracellular sodium in anti-Fas treated Jurket cells, that was in part to be due to the inhibition of the Na^+/K^+ -ATPase, as direct inhibition of this ionic pump with ouabain enhanced apoptosis. This study also that cell shrinkage could be uncoupled from apoptosis, which was later confirmed in a study comparing staurosporine- and etoposide-induced apoptosis in U937 cells (Yurinskaya et al., 2005a).

Additionally, several other studies also eluded to an increase in intracellular sodium that accompanied the initial loss of intracellular potassium during AVD (Jonas et al., 1994; Offen et al., 1995; Fernandez-Segura et al., 1999; Yurinskaya et al., 2005b). What was clear from these early studies on AVD was while no single ionic channel or pathway could account for the loss of cell volume during apoptosis, the movement of ions was a critical part of the cell death process. More recent studies have solidified this relationship between AVD and ion flux, as a computational study on the redistribution of ions and water underlying AVD in staurosporine treated human lymphoma cells (U937) concluded that along with a significant increase in chloride and potassium permeability coupled with a decreased permeability of sodium, there was also the progressive decrease in the Na^+/K^+ activity (Yurinskaya et al., 2019).

In some model systems, it has been suggested that apoptosis can occur in the absence of a loss of cell volume. A modest decrease in cell volume in serum-deprived vascular smooth muscle cells does not trigger the apoptotic machinery (Orlov et al., 2004). Interestingly, Nolin et al. (2016) reported swelling of the whole cell prior to its entry into apoptosis; a phenomenon also noted in an earlier study using time-lapse, dual-image surface reconstruction of staurosporine treated vascular smooth muscle cells (Platonova et al., 2012). These studies illustrate that more refined changes can occur during AVD, that typically may go unnoticed in many apoptotic model systems.

STAGES OF AVD

Following initial studies describing various ion flux pathways and transporters that were involved in and defined AVD, the overall nature of this process was examined which focused on both water and ion movement. Radiation-induced changes in cell size of rat thymocytes was shown to occur in two distinct stages (Klassen et al., 1993). An early reversal of intracellular ions was observed which defined an initial or primary stage of apoptosis in lymphocytes (Bortner et al., 2008). Of interest was this primary stage of AVD occurred during both intrinsic and extrinsic apoptosis. During the primary stage of AVD, an increase in intracellular sodium, coupled to a decrease in intracellular

potassium occurred that resulted in a 20–40% decrease in cell volume. It was hypothesized that this reversal of intracellular ions was the cell's attempt to compensate for the loss of one ion (potassium) for another (sodium), however, in total, an overall decrease in cell volume occurred. During the secondary stage of AVD, both intracellular sodium and potassium were lost resulting in an 80–85% decrease in cell volume. Additionally, this secondary stage was shown to be prevented upon disruption of the actin cytoskeleton (Bortner et al., 2008). Poulsen et al. (2010) described three distinct stages of AVD in cisplatin-induced Ehrlich ascites tumor cells; an early, transitional, and secondary stage. The early and secondary stages were defined with a loss of ions, specifically potassium, sodium, and chloride, that resulted in a 30% loss of water (early stage), and a further reduction in water in the secondary stage. The transitional stage was defined solely with an increase in sodium and chloride. Interestingly in both aforementioned studies, the increase in intracellular sodium suggests a counter or protective response even as a cell is dying. Interestingly, a protective response was illustrated by Yurinskaya et al. (2012) where U937 cells under hypertonic stress initially responded with an RVI prior to AVD. Whether RVI and AVD are independently activated and AVD is observed only apparent at a later time; or RVI becomes inhibited or fails signaling AVD is unclear.

The use of live fluorescence and transmission-through-dye microscopy showed two morphologically distinct stages of volume changes (Kasim et al., 2013). Using actinomycin-D treated HeLa cells, the first stage was defined by extensive blebbing with a temporary volume increase, while the second stage showed a 40% decrease in cell volume and was considered to represent AVD. Interestingly in this model system, both stages had an increase in intracellular sodium, which again suggests a protective cellular response even in the act of dying. In a latter study, correlative light and cryo-scanning transmission electron microscopy (cryo-STEM) was employed to study stage-specific changes in water and ion movement in actinomycin D treated HeLa cells (Nolin et al., 2016). This technology allowed the authors to observe changes of water and ions not only in the cell as a whole, but also in various cellular compartments. Overall, the authors observed a loss of potassium throughout the entire cell death process. Since previous studies suggested an early increase in sodium and loss of chloride, followed by a decrease in sodium coupled to a further decrease in chloride, the latter appeared to be restricted to the mitochondria. Finally, during the late stage of cell death, an increase in sodium and chloride was noted that may ensue due to a loss of membrane integrity. Overall, these studies illustrate a complex and multifaceted nature of volume dynamics during cell death.

Many studies, including the one outlined above, have shown that the concept of AVD or cell shrinkage during apoptosis is not a simple and straight-forward process. Of particular note is the idea that AVD is distinct and independent from the loss of cell volume that occurs upon separation of apoptotic bodies. Overall, the volume dynamics that reflect AVD is a direct consequence of ion flux. The observation of whether a cell shrinks or not during the cell death process appears to be both cell-type and stimulus specific (Yurinskaya et al., 2005a; Orlov et al., 2013). Therefore,

water content of non-apoptotic and apoptotic cells may not be of much consequence, as it is not the change in cell volume that is critical, but the flux of ions that has a greater impact on the cell death program.

THE RELEVANCE OF AVD TO OTHER APOPTOTIC EVENTS

Prior to AVD becoming an acknowledged scientific concept, intracellular ions were known to play a critical role in water loss during apoptosis (McCarthy and Cotter, 1997; Yu et al., 1997, 1999a). Furthermore, and as mentioned above, many studies support the idea of ion flux having a critical role in the apoptotic program, with the change in cell volume a by-product of this ion movement. However, the question remained as to what consequence these ion fluxes have on apoptosis? Early it was shown that DNA degradation during apoptosis in anti-Fas treated Jurkat cells correlated with the shrunken population of cells, and inhibition of cell shrinkage via high extracellular potassium prevented this characteristic (Bortner et al., 1997). Interestingly, anti-Fas treatment of Jurkat cells initially placed in hypotonic medium to swell and activate an RVD, thus lowering the intracellular potassium and chloride concentration, resulted in enhanced cell death, suggesting that a change in ions was having a greater effect on the cell death program than the actual change in cell size. In a follow-up study, normal intracellular levels of potassium were shown to inhibit both apoptotic DNA fragmentation and caspase-3 activation, however, once the caspase was activated, the level of intracellular potassium had no consequence (Hughes et al., 1997). An early study examining calcium signaling during apoptosis showed that anti-Fas treated Jurkat cells under complete calcium-free conditions resulted in only the inhibition of DNA fragmentation, suggesting nuclear activity was the only component of the apoptotic machinery that was sensitive to changes in intracellular calcium (Scoltock et al., 2000). Additionally, it was shown that elevated extracellular potassium prevented phosphatidylserine externalization, mitochondrial depolarization, and cytochrome c release, along with caspase activation upon both chemical and death receptor induced apoptosis (Thompson et al., 2001). This same group also showed that physiological concentrations of potassium inhibited cytochrome c-dependent apoptosome formation, thus preventing the activation of caspase-9 (Cain et al., 2001). In a more recent study, Tanaka et al. (2015) examined the relationship between AVD and translocation of phosphatidylserine on the cell surface and membrane blebbing using time-lapsed imaging coupled with scanning ion conductance microscopy. Here, the authors using staurosporine-treated neurons reported that the loss of cell volume occurred prior to the externalization of phosphatidylserine and membrane blebbing, suggesting that these morphological events may be independent of AVD and the concurrent ion flux during apoptosis.

Since our initial understanding of the important role ion fluxes play in regulating the apoptotic machinery, considerable attention has focused on the specific channels and transports

involved in this process, that may or may not contribute to AVD. In an early study using human leukemia cells (HL-60), apoptotic change in intracellular ions was prevented upon inhibition of the Na^+ , K^+ -ATPase pump or the Ca^{2+} -dependent K^+ channel (McCarthy and Cotter, 1997). Caspase-dependent stimulation of voltage-gated potassium (Kv1.3) channels was shown in Fas-ligand treated Jurkat cells to result in potassium efflux, cell shrinkage, and apoptosis (Storey et al., 2003). While potassium is a major intracellular ion whose loss would result in a reduction of cell volume, it is not the only ion to consider in understanding the relevance of AVD. The early and rapid increase in intracellular sodium shown to occur during anti-Fas induced apoptosis resulted in a depolarization of the plasma membrane (Bortner et al., 2001). The depolarization of the plasma membrane had previously been shown to occur in part via the inhibition of the Na^+/K^+ -ATPase (Bortner et al., 2001; Mann et al., 2001). Thus, over the past 2 plus decades, many studies have solidified the critical role for ion flux in regulating the apoptosis process (reviewed in Lang and Hoffmann, 2012; Kondratskyi et al., 2015).

Conversely, Börjesson et al. (2011) suggested that a decrease in intracellular potassium concentration is not obligatory for apoptosis. In an oocyte model treated with staurosporine, a loss of intracellular potassium was observed along with the activation of caspase-3. Interestingly, when oocytes densely expressed Shaker voltage-gated potassium channels, a loss of potassium was not observed, implying that the dense Kv channel expression makes oocytes resistant to apoptosis. However, caspase-3 activity was still observed. While the authors concluded that a decrease in intracellular potassium concentration is not required for apoptosis, other ions known to have a role in decreasing the overall ionic strength was not explored. Largely, these afore-mentioned studies illustrated the importance of ions in the programmed cell death process and suggested that an overall decrease in intracellular ionic strength permits the activation of the apoptotic machinery.

LINKING APOPTOSIS AND WATER MOVEMENT: AQUAPORINS

Water channels, or selective water pores known as aquaporins (AQPs) play a critical role in mediating cellular water flow, and are crucial for the regulation of water homeostasis. Aquaporins provide a mechanism for the rapid movement of water across diverse membranes having a major regulatory effect in regard to changes in cell volume (Day et al., 2014). In the early 2000's, Krane et al. (2001) reported that salivary acinar cells deficient in aquaporin 5 (AQP5) had a decrease in water permeability in response to hypertonicity-induced cell shrinkage and hypotonicity-induced cell swelling. While it is unclear exactly how aquaporins regulate this movement of water, it has been proposed that a critical factor is the number of channels expressed on the cell membrane. AQP5 was shown to have a dose-responsive decrease in response to a hypotonic stimulus (Sidhaye et al., 2006). This study

also showed that inhibition of the cation channel transient receptor potential vanilloid (TRPV) 4 prevented the reduction of AQP5. In a latter study, a rapid translocation of AQP1 was shown to occur under hypotonic conditions coupled with an increase in intracellular calcium (Conner et al., 2012). As these studies involved different aquaporins, both studies indicated that alterations in calcium were required for the change or translocation of the channels while illustrating their response in the regulatory volume response. Additionally, these studies indicate that ions, particularly calcium, may have an important regulatory role in water channel function, as opposed to regulation at the level of the channel itself. Furthermore, while initially thought to facilitate only the movement of water, it is now understood that aquaporins can also permeate other small solutes such as anions, urea, and glycerol, that would also have a role in the volume regulatory response.

Aquaporins have been shown to play a vital role during cell death as inhibition of aquaporin 1 (AQP1) was shown to prevent AVD and the subsequent downstream apoptotic events such as cell shrinkage, mitochondrial membrane permeability, caspase 3 activation, and DNA degradation (Jablonski et al., 2004). Additionally, decreased expression of APQ8 and APQ9 correlated with the lack of water movement in apoptotic-resistant tumor cells (Jablonski et al., 2006). Overexpression of AQP3 and AQP9 in human melanoma cells significantly increase the chemoresistance of these cells to arsenite via down-regulation of p53 and up-regulation of Bcl-2 and XIAP (Gao et al., 2012). Thus, like the overall mechanism of apoptosis, the role aquaporins play during cell death process appears to be cell-type and stimulus specific.

Since the mid 1990's, an increasing number of studies have focused on aquaporins and the movement of water, with many focusing on specific physiological systems or pathological conditions (Tait et al., 2008; Zeleina, 2010; Ma et al., 2011; Schey et al., 2014; Tie et al., 2017). For example, in the central nervous system, aquaporin 4 (AQP4) is noted as the main water channel. Lactacystin (proteasomal-inhibition) induced apoptosis in cortical neurons showed AQP4 was highly downregulated suggesting other AQPs may be involved during programmed cell death (Chen et al., 2008). Interestingly, this study showed that APQ8 and APQ9 were highly upregulated upon lactacystin treatment. However, when staurosporine was used to induce apoptosis, both APQ8 and APQ9 were down regulated, suggesting aquaporins expression and function during apoptosis is stimulus specific. In a myocardial infarction model, cardiomyocytes deficient in AQP1 showed a reduced level of apoptosis, suggesting AQP1 has a positive role in the execution of the cell death process (Li et al., 2015). And as early as 2004, aquaporins, specifically AQP1 was shown to be decreased in human cornea endothelial disease, and in mouse corneas subjected to corneal endothelial injury (Macnamara et al., 2004). Thus, as is the case for ion channels and transporters, aquaporins are expressed in a range of cells and show a variety of roles in regards to apoptosis.

ION MOVEMENT AND AVD IN UNIQUE MODEL SYSTEMS

Lymphoid cells have been a favorite model system to study AVD and apoptosis. However, over the past decade, other cell type such as neuronal cells, cardiomyocytes, and corneal epithelial cells have been increasingly studied due to their unique characteristics and prevalence in various human diseases. While the brain as a whole shows an RVI upon hypertonic perturbations, cultured and acutely isolated neurons do not. Similarly, reports of RVI in cardiomyocytes are limited to murine atrial cardiac myocyte cultured cell lines such as HL-1 (Cacace et al., 2014). As both neurons and cardiomyocytes have an RVD, it is of interest to determine their relationship to AVD upon apoptosis. While corneal epithelial cells can regulate their cell volume under both hypertonic or hypotonic conditions, the cornea is shielded by a protective tear film that makes this a model of interest in understanding ion flux and fluid movement upon cell death.

NEURONAL CELLS AND CELL DEATH

Neuronal cells offer an attractive model to study the movement of water, ions and apoptosis. Early on it was shown that mouse neocortical neurons treated with staurosporine or serum deprivation resulted in an early enhancement of delayed rectifier (IK) currents and a loss of intracellular potassium resulting in apoptosis (Yu et al., 1997). Apoptosis was reduced upon addition of the potassium channel blocker TEA or elevated extracellular potassium. In turn, exposure of neuronal cells to the K⁺ ionophore valinomycin or the K⁺-channel opener cromakalin induced apoptosis, suggesting that neuronal cell death may follow a similar series of ion flux as observed in more classical model systems. Shortly after this, NMDA receptor-mediated potassium flux was shown to contribute to neuronal apoptosis during brain ischemia (Yu et al., 1999a), signifying an expansion of ion flux beyond classical voltage-gated ion channels. In a second study from this group, inhibition of potassium channels with clofilium attenuated C2-ceramide induced neuronal apoptosis (Yu et al., 1999b), as well as hypoxia- and ischemia-induced neuronal death, both *in vitro* and *in vivo* (Wei et al., 2003). These early studies illustrating the critical role for potassium during neuronal cell death set the stage for further scientific investigation of neuronal cell death.

Neurons, like every other cell in the body, can also be subjected to changes in their extracellular environment. Upon encountering a condition of decreased osmolality, neurons will undergo RVD to achieve a homeostatic balance of water and ions. This RVD occurs via classical ionic channels and transport mechanisms similar to other cell types, and is observed in many neuronal cells including peripheral sympathetic neurons, cerebellar granular cells, along with numerous neuronal cultured cell lines (Wilson and Mongin, 2018). It was suggested that AVD in neurons appears to occur by similar ionic mechanisms to those activated during hypoosmotic-induced RVD (Pasantes-Morales and Tuz, 2006). Cation-chloride cotransporters (CCC) such as the chloride-importing Na–K–2Cl cotransporter (NKCC1)

and the chloride-exporting potassium–chloride cotransporter (KCC2) have a significant role in the regulation of neuronal cell volume, along with their role in neurotransmission in the nervous system. These transporters are oppositely regulated via serine–threonine phosphorylation that inhibits NKCC1, but activates KCC2, upon dephosphorylation possibly through the WNK2 kinase (Gamba, 2005; Rinehart et al., 2011; **Figure 1**). The dephosphorylation of these transporters promotes the efflux of ions, specifically potassium and chloride from the cell resulting in loss of water. Interestingly, numerous studies involving neurons (both primary and cultured) failed to demonstrate a classical RVI response upon hyperosmotic exposure. Additionally, a lack of RVI was also observed in most studies involving cultured astrocytes (reviewed in Wilson and Mongin, 2018). A sound hypothesis for the absence of RVI in various neuronal cells has yet to be proposed, although it has been suggested that cultured neuronal cells may not have the required transmembrane ionic gradients that favor RVI.

During development, proper formation of synapses between neurons in the brain is known to occur via apoptosis. Furthermore, apoptosis is also the most common mode of cell death in various neurodegenerative diseases with increased apoptosis associated with Alzheimer's and Parkinson's disease (Yuan and Yankner, 2000), suggesting that apoptosis plays a variety of roles within the central nervous system. As mentioned earlier, and similar to other apoptotic model systems, the loss of intracellular potassium is known to have a critical impact in coordinating the cell death program. Early studies showing the enhancement of delayed rectifier (IK) potassium currents during apoptosis in neocortical neurons, were followed by studies on cultured cortical neurons treated with a variety of apoptotic inducers that showed the involvement of ion flux. Inhibition of chloride channels prevented cell shrinkage, but had no significant effect on caspase activation or DNA fragmentation (Wei et al., 2004; **Figure 1**). In contrast to chloride channel inhibition, inhibition of potassium channels prevented cell shrinkage, caspase activation, and DNA fragmentation (**Figure 1**). This study suggests that potassium and chloride have distinct roles during apoptosis, with inhibition of potassium flux exhibiting a greater neuroprotective effect. Furthermore, studies such as these highlight the critical role potassium plays in regulating the apoptotic machinery, again in line with more classical apoptotic model systems.

Over the years, numerous potassium channels have been identified in neuronal cells that have a function during apoptosis including voltage-gated K⁺ channels, inwardly rectifying K⁺ channels, and background channels such as tandem pore domain TWIK and TASK (Chen et al., 2008). Many of these studies have relied on channel inhibition to show their contribution in the cell death process. Of the various potassium channels identified, the delayed rectifier current mediated by Kv2.1 channel has a critical role in apoptogenic potassium efflux in several types of neuronal cells including cortical, nigral, and hippocampal neurons. Pal et al. (2003, 2006) showed that potassium efflux during neuronal cell death involved newly inserted Kv2.1 channels into the cell membrane. As Kv2.1 channels are known to form clusters in the soma and proximal dendrites, Justice et al. (2017) discovered

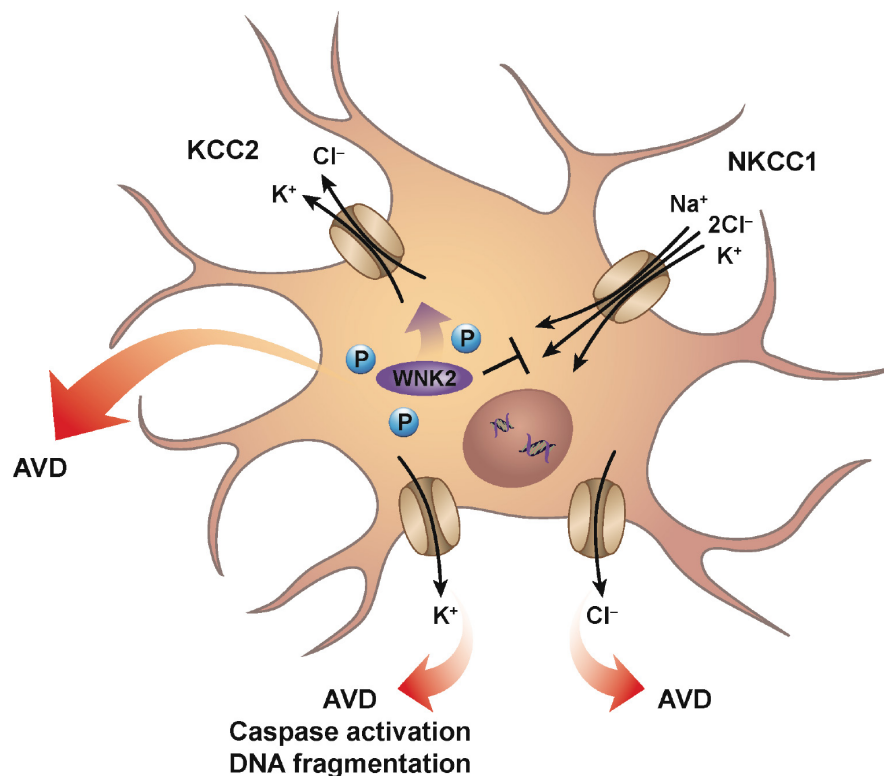


FIGURE 1 | Neuronal AVD. Mechanisms similar for classical RVD are engaged during neuronal AVD. Ionic cotransporters and cotransporters, mainly involving the flux of chloride are activated to counter the imbalance of intracellular water due to hypotonic conditions. For example, conventional ionic transport mechanisms such as NKCC1 and KCC2 are oppositely-regulated via serine–threonine phosphorylation such that dephosphorylation results in the inhibition of NKCC1, while simultaneously activating KCC2. The net result is the loss of both intracellular potassium and chloride with the parallel decrease in water. Additionally, individual potassium and chloride channels have also been shown to have a role during neuronal AVD. Interestingly, potassium channel activation was shown to result in AVD, caspase activation, and DNA fragmentation, while chloride channel activation resulted in only AVD.

that disruption of these clusters prevented the apoptogenic increase in potassium currents, thus increasing neuronal viability upon exposure to oxidative stress. Recently in primary neurons, Kv2.1 was shown to be substrate for the aspartyl protease BACE2, and upon channel cleavage prevented the outward potassium efflux resulting in reduced apoptosis (Liu et al., 2018a). Furthermore, methamphetamine results in pro-apoptotic effects in primary hippocampal neurons that are abrogated upon inhibition or knockdown of Kv2.1 (Zhu et al., 2018b), suggesting potassium channel inactivation without the use of drugs that specifically block the channel can regulate the apoptotic program. Additionally, this study showed that p38 mitogen-activated protein kinase (MAPK) was also involved as inhibition of this kinase attenuated methamphetamine-induced pro-apoptotic effects and the upregulation of Kv2.1. Moreover, phosphorylation of what are considered pro-apoptotic residues on the N- and C-terminus of Kv2.1 via Src and p38 enhanced the insertion of this potassium channel in the plasma membrane, thus increasing the loss of intracellular potassium during apoptosis (He et al., 2015).

Like many other apoptotic model systems, potassium has been the cationic ion of emphasis, however, as mentioned earlier sodium also has a critical role in the cell death program,

and has been an ion of focus of numerous studies involving neuronal apoptosis. Sun et al. (2020) showed flufenamic acid and mefenamic acid were neuroprotective by inhibiting voltage-gated sodium channels in a glutamate-induced apoptotic model using neuroblast-like SH-SY5Y cells. In a model resembling epilepsy, hippocampal neurons from rats injected with kainic acid (an NMDA type glutamate receptor agonist) underwent apoptosis that was attenuated upon inclusion of various voltage-gated sodium channel blockers (Das et al., 2010). An increase in intracellular sodium following abnormal hyperexcitation can result in death of neurons, and a recent study probing the mechanism of this model suggested this death occurs via sodium accumulation and/or concomitant potassium loss that impairs mitochondrial function (Kawasaki et al., 2019). Genistein, a primary isoflavone found in soybeans, was shown to inhibit cell death in an *in vitro* model of primary neurons under hypoxic-ischemia (oxygen–glucose deprivation) conditions in part by reversing the classic increase in potassium efflux and decreasing the sodium influx (Ma et al., 2016). Additionally, this group in a latter study employing a different hypoxic-ischemia model (sodium dithionite and glucose deprivation) in cultured rat primary neurons showed that a specific zinc-chelator, TPEN, suppressed apoptosis in primary neurons (Zhang et al., 2017),

however whether this was a direct inhibition of ion channels or a change in channel function due to reduced levels of zinc was not determined.

Potassium channel activation is not always congruent with triggering of apoptosis, especially in neurons. Interestingly, potassium channels are common targets for neuroprotective molecules. Activation of mitochondrial ATP-sensitive potassium channels (mKATP) prevented neuronal cell death after ischemia in neonatal rats (Rajapakse et al., 2002), essentially mimicking the protective effects mediated by the preconditioning phenomenon. In an oxygen–glucose deprivation model of cell death in primary rat cortical neurons, diazoxide, a potassium channel activator attenuated neuronal cell death (Kis et al., 2003). Of interest in this study was that a mitochondrial ATP-sensitive potassium blocker (5-hydroxydecanoate) abolished this protective effect, while a non-selective KATP channel blocker (glibenclamide) did not, suggesting the reliance of mKATP for this resistance. Since this early deduction of neuroprotection via opening of mKATP, numerous studies have expanded on this discovery. Neuroprotection via mitochondrial ATP-sensitive potassium channels enhance cell survival against oxidative stress (Yang et al., 2016). In a chronic morphine (CM) preconditioning study of ischemia/reperfusion hippocampal CA1 neurons, inhibition of mKATP channels with 5-hydroxydecanoate (5-HD) significantly increased apoptosis, suggesting that CM preconditioning obstructs apoptosis via activation of mKATP channels (Arabian et al., 2018). Various studies have suggested that the protection afforded by the activation of potassium channels may be due to membrane potential hyperpolarization, and/or increased repolarization speed effectively reducing the level of calcium entry and ATP consumption; both considered pro-apoptotic events. Thus, pharmacological modulation of mKATP has become a promising new therapeutic approach for the treatment of neurodegenerative diseases such as Alzheimer's (Virgili et al., 2013), along with the treatment of cardiovascular and various oncological diseases (Citi et al., 2018).

CARDIOMYOCYTES AND AVD

While cardiomyocytes are known to respond to hypoosmotic stress with an RVD, the presence of an RVI under hyperosmotic stress has not been well documented in these cells. It has been shown that HL-1 cardiac myocytes can regulate their volume to hypertonic stress with a classical RVI (Cacace et al., 2014), however, at present, no study has documented the presence of an RVI in primary cardiomyocytes. In the absence of this inherent RVI response, cardiac myocytes respond with a rapid and robust apoptotic response upon hyperosmotic stress (Morales et al., 2000; Galvez et al., 2001). Maldonado et al. (2005) showed that this rapid and pronounced apoptosis in response to hyperosmotic stress in cardiomyocytes could be attenuated by treatment with insulin-like growth factor (IGF-1), setting in motion a series of calcium-related phosphorylation events. More recently, hyperosmotic stress was shown to induce cell death in adult rat cardiomyocytes via mechanism promoting endoplasmic reticulum stress (ERS; Burgos et al., 2019). In this

study, cardiomyocytes placed in a hyperosmotic environment resulted in increased expression of various ERS markers, along with an increase in caspase-3 expression and the loss of cell viability. Furthermore, 4-BPA (an inhibitor of ERS), chelating calcium using EGTA, and inhibition of CaMKII prevented hyperosmotic-induced cell death. Interestingly, Zhu et al. (2018a) suggest that in the absence of the protective nature of an RVI response, cardiomyocytes invoke an autophagic pathway to provide a cardioprotective strategy in response to hyperosmotic stress. The complex nature of volume regulatory process in cardiomyocytes was illustrated by Rojas-Rivera et al. (2009). These authors showed that hypo-osmotic stress-induced increase in intracellular calcium, thus activating RVD, however, this also resulted in an increase ROS (**Figure 2**). This masking of RVD via the increased ROS resulted in necrotic blebs and cell death. Interestingly, the overexpression of catalase, lowered ROS content, and restored RVD (**Figure 2**).

In the mid 1990s, studies investigating ischemia reperfusion injury showed that cell death of cardiomyocytes occurred predominantly through the programmed cell death process or apoptosis (Cheng et al., 1996; Kajstura et al., 1996). Furthermore, myocardial ischemia can result in osmotic stress on cardiomyocytes that affects the overall functioning of the heart (Wright and Ress, 1998). Subsequent studies examining cardiomyocyte apoptosis and the loss of cell volume showed that volume-sensitive ion channels played a role in AVD (D'Anglemont de Tassigny et al., 2004; Wang et al., 2005b; Okada et al., 2006). Specifically, volume-sensitive chloride channels ($I_{Cl,vol}$) known to play a role in the regulation of cell volume (RVD), were also shown to be active during AVD (D'Anglemont de Tassigny et al., 2004; **Figure 2**). In adult rabbit ventricular cardiomyocyte treated with doxorubicin and C(2)-ceramide to initiate cell death, AVD and apoptosis were abolished upon exposure to the $I_{Cl,vol}$ inhibitors 5-nitro-2-(3-phenylpropylamino) benzoic acid (NPPB) or indanyloxyacetic acid 94 (IAA-94; D'Anglemont de Tassigny et al., 2004; **Figure 2**). Additionally, volume-sensitive outwardly rectifying (VSOR) chloride channels were shown to be involved in staurosporine treated primary mouse ventricular myocytes (Okada et al., 2006) and neonatal rat cardiomyocytes (Liu et al., 2013) undergoing apoptosis. Recently, inhibition of (VOSR) chloride channels were shown to improve cardiac contractility and survivability in a turnicamycin-induced cardiomyocyte ER stress model (Shen et al., 2014). In a follow-up study, Wang et al. (2017) showed during high glucose-induced apoptosis, chloride channel blockers DIDS and DCPIB prevented activation of (VSOR) chloride channels and improved the viability of cardiomyocytes.

What is noteworthy about the volume-sensitive channels during AVD is their activation in the absence of cell swelling. While the precise nature of the isotonic activation of volume-sensitive channels is unknown, Okada et al. (2006) hypothesized several mechanisms that may permit channel activity including a lower threshold for the channel volume set point in apoptotic cells, the presence of reactive oxygen species, kinase activation and/or changes in the level of ATP as plausible mechanisms for channel activation. Subsequently, Liu et al. (2013) showed that PI3K/Akt played a major role in the activation of (VSOR)

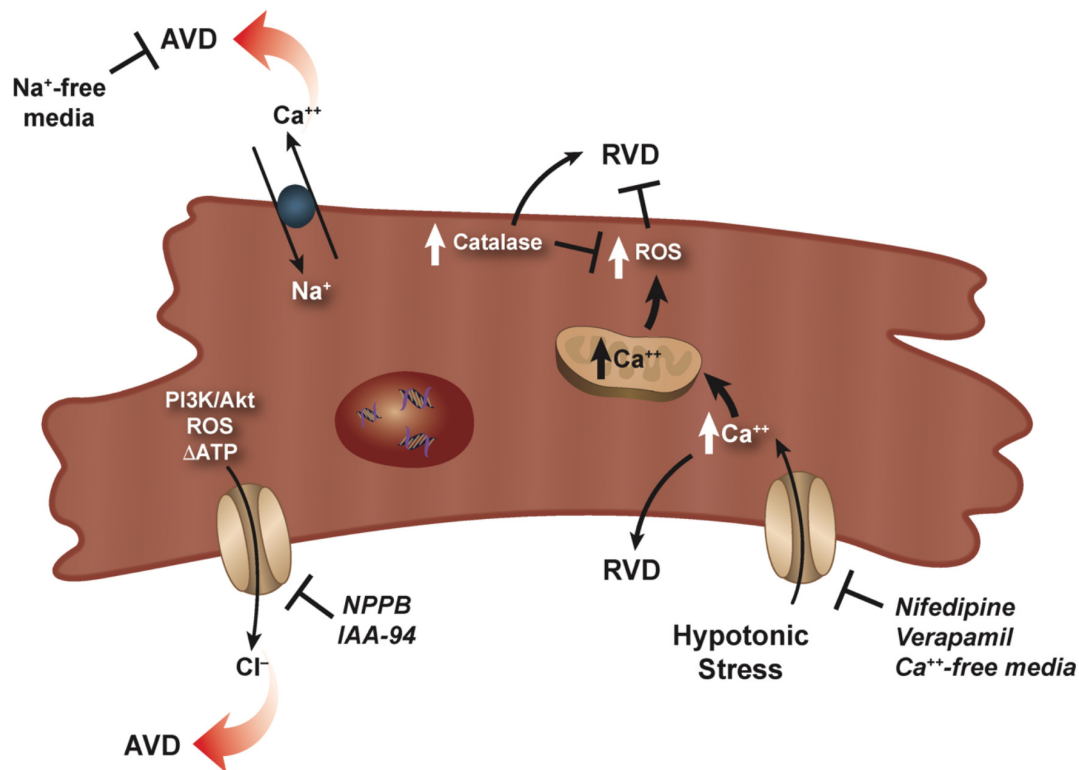


FIGURE 2 | RVD and AVD in cardiomyocytes. Dual role of calcium for RVD in cardiomyocytes is illustrated as a hypotonic-induced increase in intracellular calcium activates RVD. However, a simultaneous increase in ROS masks and/or prevents RVD. RVD can be restored via overexpression of catalase which lowers the ROS concentration. Activation of volume-sensitive chloride channels via kinases, ROS, and/or changes in the level of ATP were shown to have a major effect on cardiomyocyte AVD, which can be prevented upon addition of specific chloride channel blockers. Additionally, reverse mode of the Na–Ca exchanger can also result in AVD as sodium-free conditions prevents this loss of cell volume.

chloride channels during staurosporine-induced cardiomyocyte death (**Figure 2**). Additionally, Shen et al. (2014) suggested the involvement of the C/EBP homologous protein CHOP and Wnt inactivation upon ER stress in cardiomyocytes. Regardless of the precise mechanism, it is well-established that volume-sensitive ion channels become activated during cardiomyocyte apoptosis and result in the concomitant egress of water from the cells and persistent cell shrinkage defined as AVD.

Interestingly, beside studies examining the role of chloride channels during cardiomyocyte AVD, little information exists on other ionic flux that may be involved during apoptosis. In an oxidative stress model, cardiomyocytes treated with H₂O₂ showed a marked increase in intracellular sodium and calcium via reverse mode of the Na–Ca exchanger resulting in apoptosis (Yang et al., 2004; **Figure 2**). Interestingly, apoptosis was completely prevented under sodium-free conditions, but not calcium-free. Additionally, apoptosis occurred when a sodium ionophore cocktail in calcium-free medium was used instead of H₂O₂, suggesting the increase in intracellular sodium alone can signal the programmed cell death process in cardiomyocytes.

Glucocorticoids have been a classical apoptotic agent from the very first reports defining this physiological programmed cell death process. Intriguingly, treatment of cardiomyocytes with the synthetic glucocorticoid dexamethasone resulted

in cardiac hypertrophy, and protected these cells from both serum deprivation and TNF α -induced apoptosis (Ren et al., 2012). Earlier studies showed that dexamethasone inhibited serum deprivation- and UV-C-induced apoptosis in rat hepatoma cells (Evans-Storms and Cidlowski, 2000; Scoltock et al., 2006). Interestingly in the latter study (Scoltock et al., 2006), dexamethasone did not prevent anti-Fas-induced apoptosis in hepatoma cells, suggesting the protective nature of glucocorticoids may be specific to agents that activate the intrinsic, and not the extrinsic apoptotic process.

CORNEAL EPITHELIAL CELLS AND AVD

The corneal epithelium, the outermost layer of the cornea composed of several layers of non-keratinized, stratified squamous epithelia cells that covers the front of the cornea, is shielded by a protective tear film consisting of an electrolyte- and protein-rich aqueous-mucus layer. The cornea functions to protect the intraocular contents of the eye along with serving as the principal optical element allowing formation of an image on the retina. Precise maintenance of electrolytes forming the osmotic gradient between the tear film and the ocular surface epithelia is important for cellular function and homeostasis. The

ionic composition of tear film has been established *in situ* along with showing a critical role for aquaporins (water channels) in maintaining osmotically driven water transport across the cornea and tear film layer (Levin and Verkman, 2004; Ruiz-Ederra et al., 2009; Woodward et al., 2012). An imbalance of electrolytes in the tear film layer is a hallmark of many ocular diseases, most notably dry eye. Thus, the corneal epithelium is the main cellular barrier between the external environment and the operative components of the visual system.

As the osmotic gradient between the tear film and the ocular surface cell epithelia is vital, corneal epithelial cells are known to have various inherent volume regulatory mechanisms (Al-Nakkashj et al., 2004; Capó-Aponte et al., 2005, 2007). Similar to other cells in the body, volume regulatory mechanisms in corneal epithelial cells are comprised of analogous channels and transporters namely volume-regulated anion channels, potassium channels, the K-Cl and Na-K-Cl cotransporters, and the Na-K-ATPase. Additionally, channels such as the non-selective cation channel (Transient Receptor Potential Vanilloid 4; TRPV4) have been shown to have a role in RVD, as a decrease in TRPV4 expression and activity in corneal epithelial cells suppresses RVD (Pan et al., 2008).

Along with various channels and transporters involved in volume regulatory responses, kinase signaling pathways have also been shown to have a critical role. In a swelling-induced model of rabbit corneal epithelial cells, activation of extracellular signal-regulated kinase (ERK) and stress-activated protein kinase/c-Jun N-terminal kinase (SAPK/JNK) preceded both chloride and potassium channel activity in the RVD response (Pan et al., 2007). During hyperosmotic stress-induced corneal epithelial cell death (an *in vitro* dry eye model), activation of Polo-like kinase 3 (Plk3) and c-Jun were observed to promote the cell death program (Wang et al., 2011). In a recent study, KIOM-2015EW (a hot water extract of maple leaves) was shown it could protect the ocular surface from hyperosmolar stress in part by inhibiting MAPK kinase signaling (Kim et al., 2018).

While corneal epithelial cells have inherent cell volume regulatory mechanisms, they are still at risk of environmental insults. From exposure to fresh water while swimming, use of hypotonic eye drops, or pathological conditions such as dry eye disease, corneal epithelial cells can experience periods of persistent hypotonic or hypertonic stress that can lead to cell death. Additionally, other events can also have a negative impact on the eyes ranging from not eating a well-balanced diet to too much time in front of a computer and/or cellphone screen. Furthermore, while most people are aware of the harmful effects of UV light on the skin, few consider the equaling damaging effects excessive UV light has on the eyes. The corneal epithelium is continually exposed to ambient outdoor UVB and UVA. Therefore, it is not surprising that many diseases of the eye can be traced back to excessive UV light including cataracts, macular degeneration, and cancer of the eye.

It has been known for over 20 years that UV exposure results in corneal epithelial cell apoptosis (Podslochy et al., 2000; Lu et al., 2003). What also became apparent very early was the

role potassium channels played in corneal epithelial cell death (Wang et al., 2003, 2005a). UV irradiation resulted in corneal epithelial cell apoptosis through the hyperactivation of potassium channels in the cell membrane (Lu, 2006), and inhibition of potassium channels with specific potassium channel blockers resulted in a reduction of numerous apoptotic characteristics including caspase activity, and DNA degradation (Ubels et al., 2010, 2011; Glupker et al., 2016). The opening of potassium channels leads to a rapid loss of intracellular potassium, fast cell shrinkage, and consequentially the activation of stress-related signaling pathways including the c-Jun N-terminal kinase cascade and p53 activation. Not surprisingly, elevated extracellular potassium was shown to prevent apoptosis in UV-B exposed corneal epithelial cells (Singleton et al., 2009), including reducing caspase activity (Leerar et al., 2016). Additionally, in this study the authors showed that caspase-9 had little activation, while caspase-8 was activated upon UV-B exposure, suggesting a major route of apoptotic induction was through the extrinsic pathway. However, a latter study by Ubels et al. (2016) suggested that the intrinsic apoptotic pathway is the major contributor to UVB-induced apoptosis in human corneal limbal epithelial cells, but TNF-R1 and FADD pathway still played an integral part in the UVB-induced potassium efflux (Boersma et al., 2017). What was clear from these and other studies where high extracellular potassium was shown to prevent the deleterious effects of UV exposure on corneal epithelial cells (Schotanus et al., 2011; Ubels et al., 2011) is that the relatively high concentration of potassium in tears works to suppress the loss of potassium from corneal epithelial cells in response to UV exposure. Therefore, tears function as a defensive measure in protecting the ocular surface not only from changes in extracellular osmolality, but also from ambient UV radiation.

Finally, elevated tear osmolarity exposes corneal epithelial cells to extracellular osmotic stress; a key pathological factor in dry eye disease. To combat the loss of cell volume or cell shrinkage as a result of this hypertonic stress on corneal epithelial cells, organic osmolytes such as betaine that can act as an osmo-protectant have been studied (Garrett et al., 2013). The presence of betaine in hypertonic-stressed human corneal limbal epithelial cells reduced the loss of cell volume from 27 to 11%, reduced caspase-8, -9, and -3/7 activity, and increased cell viability, suggesting agents such as betaine stabilized corneal epithelial cell volume under hyperosmotic stress, thus limiting the extent of apoptosis.

PERSPECTIVES

The morphological loss of cell volume or AVD is a defining characteristic of apoptosis and suggests it plays a critical role during cell death. Whether it's simply to decrease the size of cells to be easily phagocytized by resident macrophage and/or neighboring cells, or as an essential component of the apoptotic machinery, AVD is unique to this mode of programmed cell death. While many questions remain as to the role AVD plays during apoptosis, what has become apparently clear from

studies on AVD and water movement in less common model systems is the existence of cell-type specific mechanisms for apoptosis. The extension of apoptotic studies in models such as neuronal cells, cardiomyocytes, and corneal epithelial cells has illustrated how individual cells employ their endogenous channels, transporters, and/or exchangers to carry out the AVD process and aids our understanding of how ionic and water flux relate to the execution of apoptosis. Finally, additional information gained from studying AVD in diverse model systems extends our knowledge of cell death and the role it plays in human disease.

REFERENCES

- Al-Nakkash, L., Iserovich, P., Coca-Prados, M., Yang, H., and Reinach, P. S. (2004). Functional and molecular characterization of a volume-activated chloride channel in rabbit corneal epithelial cells. *J. Membr. Biol.* 201, 41–49. doi: 10.1007/s00232-004-0706-5
- Arabian, M., Aboutaleb, N., Soleimani, M., Ajami, M., Habibe, R., and Pazoki-Toroudi, H. (2018). Activation of mitochondrial KATP channels mediates neuroprotection induced by chronic morphine preconditioning in hippocampal CA-1 neurons following cerebral ischemia. *Adv. Med. Sci.* 63, 213–219. doi: 10.1016/j.advms.2017.11.003
- Arrebola, F., Canizares, F. J., Cubero, M. A., Crespo, P. V., Warley, A., and Fernandez-Segura, E. (2005a). Biphasic behavior of changes in elemental composition during staurosporine-induced apoptosis. *Apoptosis* 10, 1317–1331. doi: 10.1007/s10495-005-2718-x
- Arrebola, F., Fernandez-Segura, E., Campos, A., Crespo, P. V., Skepper, J. N., and Warley, A. (2006). Changes in intracellular electrolyte concentrations during apoptosis induced by UV irradiation of human myeloblastic cells. *Am. J. Physiol. Cell Physiol.* 290, C638–C649.
- Arrebola, F., Zabiti, S., Canizares, F. J., Cubero, M. A., Crespo, P. V., and Fernandez-Segura, E. (2005b). Changes in intracellular sodium, chloride, and potassium concentrations in staurosporine-induced apoptosis. *J. Cell. Physiol.* 204, 500–507. doi: 10.1002/jcp.20306
- Barros, L. F., Hermosilla, T., and Castro, J. (2001). Necrotic volume increase and the early physiology of necrosis. *Comp. Biochem. Physiol. A Mol. Integr. Physiol.* 130, 401–409.
- Boersma, P. M., Haarsma, L. D., Schotanus, M. P., and Ubels, J. L. (2017). TNF-R1 and FADD mediate UVB-induced activation of K⁺ channels in corneal epithelial cells. *Exp. Eye Res.* 154, 1–9. doi: 10.1016/j.exer.2016.11.003
- Börjesson, S. I., Englund, U. H., Asif, M. H., Willander, M., and Elinder, F. (2011). Intracellular K⁺ concentration decrease is not obligatory for apoptosis. *J. Biol. Chem.* 286, 39823–39828. doi: 10.1074/jbc.m111.262725
- Bortner, C. D., and Cidlowski, J. A. (1996). Absence of volume regulatory mechanisms contributes to the rapid activation of apoptosis in thymocytes. *Am. J. Physiol. Cell Physiol.* 271, C950–C961.
- Bortner, C. D., and Cidlowski, J. A. (2003). Uncoupling cell shrinkage from apoptosis reveals that Na⁺ influx is required for volume loss during programmed cell death. *J. Biol. Chem.* 278, 39176–39184. doi: 10.1074/jbc.m303516200
- Bortner, C. D., Gomez-Angelats, M., and Cidlowski, J. A. (2001). Plasma membrane depolarization with repolarization in an early molecular event in anti-Fas induced apoptosis. *J. Biol. Chem.* 276, 4304–4314. doi: 10.1074/jbc.m005171200
- Bortner, C. D., Hughes, F. M. Jr., and Cidlowski, J. A. (1997). A primary role for K⁺ and Na⁺ efflux in the activation of apoptosis. *J. Biol. Chem.* 272, 32436–32442. doi: 10.1074/jbc.272.51.32436
- Bortner, C. D., Sifre, M. I., and Cidlowski, J. A. (2008). Cationic gradient reversal and cytoskeleton-independent volume regulatory pathways define an early stage of apoptosis. *J. Biol. Chem.* 283, 7219–7229. doi: 10.1074/jbc.m707809200
- Brevnova, E. E., Playoshyn, O., Zhang, S., and Yuan, J. X. (2004). Overexpression of human KCNA5 increases IK V and enhances apoptosis. *Am. J. Physiol. Cell Physiol.* 287, C715–C722.
- Burgos, J. I., Morell, M., Mariángelo, J. I., and Petroff, M. V. (2019). Hyperosmotic stress promotes endoplasmic reticulum stress-dependent apoptosis in adult rat cardiac myocytes. *Apoptosis* 24, 785–797. doi: 10.1007/s10495-019-01558-4
- Cacace, V. I., Finkelstejn, A. G., Tasso, L. M., Kusnier, C. F., Gomez, K. A., and Fischbarg, J. (2014). Regulatory volume increase and regulatory volume decrease in HL-1 atrial myocytes. *Cell. Physiol. Biochem.* 33, 1745–1757. doi: 10.1159/000362955
- Cain, K., Langlais, C., Sun, X. M., Bronw, D. G., and Cohen, G. M. (2001). Physiological concentrations of K⁺ inhibit cytochrome c-dependent formation of the apoptosome. *J. Biol. Chem.* 276, 42985–41990.
- Capó-Aponte, J. E., Iserovich, P., and Reinach, P. S. (2005). Characterization of regulatory volume behavior by fluorescence quenching in human corneal epithelial cells. *J. Membr. Biol.* 207, 11–22. doi: 10.1007/s00232-005-0800-5
- Capó-Aponte, J. E., Wang, Z., Bildin, V. N., Iserovich, P., Pan, Z., Zhang, F., et al. (2007). Functional and molecular characterization of multiple K-Cl cotransporter isoforms in corneal epithelial cells. *Exp. Eye Res.* 84, 1090–1103. doi: 10.1016/j.exer.2007.02.007
- Chen, M. J., Sepramaniam, S., Armugam, A., Choy, M. S., Manikandan, J., Melendez, A. J., et al. (2008). Water and ion channels: crucial in the initiation and progression of apoptosis in central nervous system? *Curr. Neuropharmacol.* 6, 102–116. doi: 10.2174/157015908784533879
- Cheng, W., Kajstura, J., Nitahara, J. A., Li, B., Reiss, K., Liu, Y., et al. (1996). Programmed myocyte cell death affects the viable myocardium after infarction in rats. *Exp. Cell Res.* 226, 316–327. doi: 10.1006/excr.1996.0232
- Citi, V., Calderone, V., Martelli, A., Breschi, M. C., and Testai, L. (2018). Pathophysiological role of mitochondrial potassium channels and their modulation by drugs. *Curr. Med. Chem.* 25, 2661–2674. doi: 10.2174/0929867324666171012115300
- Conner, M. T., Conner, A. C., Bland, C. E., Taylor, L. H. J., Brown, J. E. P., Parri, H. R., et al. (2012). Rapid aquaporin translocation regulates cellular water flow: mechanism of hypotonicity-induced subcellular localization of aquaporin 1 water channel. *J. Biol. Chem.* 287, 11516–11525. doi: 10.1074/jbc.m111.329219
- D'Anglemont de Tassigny, A., Souktani, R., Henry, P., Ghaleh, B., and Berdeaux, A. (2004). Volume-sensitive chloride channels (Cl_vVol) mediate doxorubicin-induced apoptosis through apoptotic volume decrease in cardiomyocytes. *Fundam. Clin. Pharmacol.* 18, 531–538. doi: 10.1111/j.1472-8206.2004.00273.x
- D'Arcy, M. S. (2019). Cell death: a review of the major forms of apoptosis, necrosis and autophagy. *Cell Biol. Int.* 43, 582–592. doi: 10.1002/cbin.11137
- Das, A., McDowell, M., O'Dell, C. M., Busch, M. E., Simth, J. A., Ray, S. K., et al. (2010). Post-treatment with voltage-gated Na⁺ channel blocker attenuates kainic acid-induced apoptosis in rat primary hippocampal neurons. *Neurochem. Res.* 35, 2175–2183. doi: 10.1007/s11064-010-0321-1
- Day, R. E., Kitchen, P., Owen, D. S., Bland, C., Marshall, L., Conner, A. C., et al. (2014). Human aquaporins: regulators of transcellular water flow. *Biochim. Biophys. Acta* 1849, 1492–1506. doi: 10.1016/j.bbagen.2013.09.033
- Delpire, E., and Gagnon, K. B. (2018). Water homeostasis and cell volume maintenance and regulation. *Curr. Top. Membr.* 81, 3–52. doi: 10.1016/bs.ctm.2018.08.001

AUTHOR CONTRIBUTIONS

CB and JC wrote the review. Both authors contributed to the article and approved the submitted version.

FUNDING

This research was supported by the Intramural Research Program of the NIH, National Institute of Environmental Health Sciences IZ1AE3090079.

- Elliott, J. I., and Higgins, C. F. (2003). IKCa1 activity is required for cell shrinkage, phosphatidylserine translocation and death in T lymphocyte apoptosis. *EMBO Rep.* 4, 189–194. doi: 10.1038/sj.embor.embor722
- Evans-Storms, R. B., and Cidlowski, J. A. (2000). Delineation of an antiapoptotic action of glucocorticoids in hepatoma cells: the role of nuclear factor- κ B. *Endocrinology* 141, 1854–1862. doi: 10.1210/endo.141.5.7466
- Fernandez-Segura, E., Canizares, F. J., Cubero, M. A., Warley, A., and Campos, A. (1999). changes in elemental content during apoptotic cell death by electron probe X-ray microanalysis. *Exp. Cell Res.* 253, 454–462. doi: 10.1006/excr.1999.4657
- Galluzzi, L., Yamazaki, T., and Groemer, G. (2018). Linking cellular stress to systemic homeostasis. *Nat. Rev. Mol. Cell Biol.* 19, 731–745. doi: 10.1038/s41580-018-0068-0
- Galvez, A., Morales, M. P., Eltit, J. M., Ocaranza, P., Campos, X., Sapag-Hagar, M., et al. (2001). A rapid and strong apoptotic process is triggered by hyperosmotic stress in cultured rat cardiac myocytes. *Cell Tissue Res.* 304, 279–285. doi: 10.1007/s004410100358
- Gamba, G. (2005). Molecular physiology and pathophysiology of electroneutral cation-chloride cotransporters. *Physiol. Rev.* 85, 423–493. doi: 10.1152/physrev.00011.2004
- Gao, L., Gao, Y., Li, X., Howell, P., Kumar, R., Su, X., et al. (2012). Aquaporins mediate the chemoresistance of human melanoma cells to arsenite. *Mol. Oncol.* 6, 81–87. doi: 10.1016/j.molonc.2011.11.001
- Garrett, Q., Khandekar, N., Shih, S., Flanagan, J. L., Simmons, P., Vehige, J., et al. (2013). Betaine stabilizes cell volume and protects against apoptosis in human corneal epithelial cells under hyperosmotic stress. *Exp. Eye Res.* 108, 33–41. doi: 10.1016/j.exer.2012.12.001
- Glupker, C. D., Boersma, P. M., Schotanus, M. P., Haarsma, L. D., and Ubels, J. L. (2016). Apoptosis of corneal epithelial cells caused by ultraviolet B-induced loss of K(+) is inhibited by Ba(2). *Ocul. Surf.* 14, 401–409. doi: 10.1016/j.jtos.2016.05.001
- He, K., McCord, M. C., Hartnett, K. A., and Aizenman, E. (2015). Regulation of pro-apoptotic phosphorylation of Kv2.1 K⁺ channels. *PLoS One* 10:e0129498. doi: 10.1371/journal.pone.0129498
- Hoffmann, E. K. (2000). Intracellular signaling involved in volume regulatory decrease. *Cell Physiol. Biochem.* 10, 273–288. doi: 10.1159/000016356
- Hoffmann, E. K., and Pedersen, S. F. (2011). Cell volume homeostatic mechanisms: effector and signaling pathways. *Acta Physiol.* 202, 465–485. doi: 10.1111/j.1748-1716.2010.02190.x
- Hughes, F. M. Jr., Bortner, C. D., Purdy, G. D., and Cidlowski, J. A. (1997). Intracellular K⁺ suppresses the activation of apoptosis in lymphocytes. *J. Biol. Chem.* 272, 30567–30576. doi: 10.1074/jbc.272.48.30567
- Jablonski, E. M., Webb, A. N., Mattocks, M. A., Sokolov, E., Koniaris, L. G., Hughes, F. M. Jr., et al. (2006). Decreased aquaporin expression leads to increased carcinoma resistance to apoptosis in hepatocellular carcinoma. *Cancer Lett.* 250, 36–46. doi: 10.1016/j.canlet.2006.09.013
- Jablonski, E. M., Webb, A. N., McConnell, N. A., Riley, M. C., and Hughes, F. M. Jr. (2004). Plasma membrane aquaporin activity can affect the rate of apoptosis but is inhibited after apoptotic volume decrease. *Am. J. Physiol. Cell Physiol.* 286, C975–C985.
- Jentsch, T. J. (2016). VRACs and other ion channels and transporters in the regulation of cell volume and beyond. *Nat. Rev. Mol. Cell Biol.* 17, 293–307. doi: 10.1038/nrm.2016.29
- Jonas, D., Walev, I., Berger, T., Leibtrau, M., Palmer, M., and Bhakdi, S. (1994). Novel path to apoptosis: small transmembrane pores created by staphylococcal alpha-toxin in T lymphocytes evokes internucleosomal DNA degradation. *Infect. Immunol.* 62, 1304–1312. doi: 10.1128/iai.62.4.1304-1312.1994
- Justice, J. A., Schulien, A. J., He, K., Hartnett, K. A., Aizenman, E., and Shah, N. H. (2017). Disruption of Kv2.1 somato-dendritic clusters prevents the apoptogenic increase in potassium currents. *Neuroscience* 354, 158–167. doi: 10.1016/j.neuroscience.2017.04.034
- Kajstura, J., Cheng, W., Reiss, K., Clark, W. A., Sonnenblick, E. H., Krajewski, S., et al. (1996). Apoptotic and necrotic myocyte deaths are independent contributing variables of infarct size in rats. *Lab. Invest.* 74, 86–107.
- Kasim, N. R., Kuželová, K., Holoubek, A., and Model, M. A. (2013). Live fluorescence and transmission-through-dye microscopic study of actinomycin D-induced apoptosis and apoptotic volume decrease. *Apoptosis* 18, 521–532. doi: 10.1007/s10495-013-0804-z
- Kawasaki, K., Suzuki, Y., Yamamura, H., and Imaizumi, Y. (2019). Rapid Na⁺ accumulation by a sustained action potential impairs mitochondria function and induces apoptosis in HEK293 cells expressing non-inactivating Na⁺ channels. *Biochem. Biophys. Res. Commun.* 513, 269–274. doi: 10.1016/j.bbrc.2019.03.129
- Kerr, J. F. R. (1965). A histochemical study of the hypertrophy and ischemic injury of rat liver with special reference to changes in lysosomes. *J. Pathol. Bact.* 90, 419–435. doi: 10.1002/path.1700900210
- Kerr, J. F. R. (1970). Liver cell defaecation: an electron-microscope study of the discharge of lysosomal residual bodies into the intercellular space. *J. Pathol.* 100, 99–103. doi: 10.1002/path.1711000204
- Kerr, J. F. R. (1971). Shrinkage necrosis: a distinct mode of cell death. *J. Pathol.* 105, 13–20. doi: 10.1002/path.1711050103
- Kerr, J. F. R., Wyllie, A. H., and Currie, A. R. (1972). Apoptosis: a basic biological phenomenon with wide-ranging implications in tissue kinetics. *Br. J. Cancer* 26, 239–257. doi: 10.1038/bjc.1972.33
- Kim, Y. H., Oh, T. W., Park, E., Yim, N. H., Park, K. I., Cho, W. K., et al. (2018). Anti-inflammatory and anti-apoptotic effects of Acer Palmatum Thumb. Extract, KIOM-2015EW, in a hyperosmolar-stress-induced in vitro dry eye model. *Nutrients* 10:282. doi: 10.3390/nu10030282
- Kis, B., Nagy, K., Snipes, J. A., Rajapakse, N. C., Horiguchi, T., Grover, G. J., et al. (2003). Diazoxide induces delayed pre-conditioning in cultured rat cortical neurons. *J. Neurochem.* 87, 969–980. doi: 10.1046/j.1471-4159.2003.02072.x
- Klassen, N. V., Walker, P. R., Ross, C. K., Cygler, J., and Lach, B. (1993). Two-stage cell shrinkage and the OER for radiation-induced apoptosis of rat thymocytes. *Int. J. Radiat. Biol.* 64, 571–581. doi: 10.1080/09553009314551791
- Kondratskyi, A., Kondratska, K., Shryma, R., and Prevarskaia, N. (2015). Ion channels in the regulation of apoptosis. *Biochim. Biophys. Acta* 1848, 2532–2546.
- Krane, C. M., Melvin, J. E., Nguyen, H. V., Richardson, L., Towne, J. E., Doetschman, T., et al. (2001). Salivary acinar cells from aquaporin 5-deficient mice have decreased membrane water permeability and altered cell volume regulation. *J. Biol. Chem.* 276, 23412–23420.
- Kunzelmann, K. (2016). Ion channels in regulated cell death. *Cell Mol. Life Sci.* 73, 2387–2403. doi: 10.1007/s00018-016-2208-z
- Lang, F., Busch, G. L., and Völkl, H. (1998). The diversity of volume regulatory mechanisms. *Cell Physiol. Biochem.* 8, 1–45. doi: 10.1159/000096284
- Lang, F., and Hoffmann, E. K. (2012). Role of ion transport in control of apoptotic cell death. *Compr. Physiol.* 2, 2037–2061.
- Leerar, J. R., Glupker, C. D., Schotanus, M. P., and Ubels, J. L. (2016). The effect of K(+) on caspase activity of corneal epithelial cells exposed to UVB. *Exp. Eye Res.* 151, 23–25. doi: 10.1016/j.exer.2016.07.014
- Levin, M. H., and Verkman, A. S. (2004). Aquaporin-dependent water permeation at mouse ocular surface: in vivo microfluorimetric measurements in cornea and conjunctiva. *Invest. Ophthalmol. Vis. Sci.* 45, 4423–4432. doi: 10.1167/iovs.04-0816
- Li, L., Weng, Z., Yao, C., Song, Y., and Ma, T. (2015). Aquaporin-1 deficiency protects against myocardial infarction by reducing both edema and apoptosis in mice. *Sci. Rep.* 5:13807. doi: 10.1038/srep13807
- Liu, F., Zhang, Y., Liang, Z., Sun, Q., Liu, H., Zhao, J., et al. (2018a). Cleavage of potassium channel Kv2.1 by BACE2 reduces neuronal apoptosis. *Mol. Psychiatry* 23, 1542–12554. doi: 10.1038/s41380-018-0060-2
- Liu, X., Yang, W., Guan, Z., Yu, W., Fan, B., Xu, N., et al. (2018b). There are only four basic modes of cell death, although there are many ad-hoc variants adapted to different situations. *Cell Biosci.* 8:6.
- Liu, Y., Wang, B., Zhang, W. W., Liu, J. N., Shen, M. Z., Ding, M. G., et al. (2013). Modulation of staurosporine-activated volume-sensitive outwardly rectifying Cl⁻ channel by PI3K/Akt in cardiomyocytes. *Curr. Pharm. Des.* 19, 4859–4864. doi: 10.2174/1381612811319270008

- Lu, L. (2006). Stress-induced corneal epithelial apoptosis mediated by K⁺ channel activation. *Prog. Retin. Eye Res.* 25, 515–538. doi: 10.1016/j.preteyeres.2006.07.004
- Lu, L., Wang, L., and Shell, B. (2003). UV-induced signaling pathways associated with corneal epithelial cell apoptosis. *Invest. Ophthalmol. Vis. Sci.* 44, 5102–5109. doi: 10.1167/iovs.03-0591
- Ma, T. H., Gao, H. W., Fang, X. D., and Yang, H. (2011). Expression and function of aquaporins in peripheral nervous system. *Acta Pharmacol. Sin.* 32, 711–715. doi: 10.1038/aps.2011.63
- Ma, X. L., Zhang, F., Wang, Y. X., He, C. C., Tian, K., Wang, H. G., et al. (2016). Genistein inhibition of OGD-induced brain neuron death correlates with its modulation of apoptosis, voltage-gated potassium and sodium currents and glutamate signal pathway. *Chem. Biol. Interact.* 254, 73–82. doi: 10.1016/j.cbi.2016.05.033
- Macnamara, E., Sams, G. W., Smith, K., Ambati, J., Singh, N., and Ambati, B. K. (2004). Aquaporin-1 expression is decreased in human and mouse corneal endothelial dysfunction. *Mol. Vis.* 10, 51–56.
- Maeno, E., Ishizaki, Y., Kanaseki, T., Hazama, A., and Okada, Y. (2000). Normotonic cell shrinkage because of disordered volume regulation is an early prerequisite to apoptosis. *Proc. Natl. Acad. Sci. U.S.A.* 97, 9487–9492. doi: 10.1073/pnas.140216197
- Maldonado, C., Cea, P., Adasme, T., Collao, A., Diaz-Araya, G., Chiong, M., et al. (2005). IGF-1 protects cardiac myocytes from hyperosmotic stress-induced apoptosis via CREB. *Biochem. Biophys. Res. Commun.* 336, 1112–1118. doi: 10.1016/j.bbrc.2005.08.245
- Malek, A. M., Goss, G. G., Jiang, L., Izumo, S., and Alper, S. L. (1998). Mannitol at clinical concentrations activates multiple signaling pathways and induces apoptosis in endothelial cells. *Stroke* 29, 2631–2640. doi: 10.1161/01.str.29.12.2631
- Mann, C. L., Bortner, C. D., Jewell, C. M., and Cidlowski, J. A. (2001). Glucocorticoids-induced plasma membrane depolarization during thymocyte apoptosis: association with cell shrinkage and degradation of the Na⁺/K⁺-adenosine triphosphatase. *Endocrinology* 142, 5059–5068. doi: 10.1210/endo.142.12.8516
- McCarthy, J. V., and Cotter, T. G. (1997). Cell shrinkage and apoptosis: a role for potassium and sodium ion efflux. *Cell Death Differ.* 4, 756–770. doi: 10.1038/sj.cdd.4400296
- Morales, M. P., Galvez, A., Eltit, J. M., Ocaranza, P., Diaz-Araya, G., and Lavandero, S. (2000). IGF-1 regulates apoptosis of cardiac myocytes induced by osmotic stress. *Biochem. Biophys. Res. Commun.* 270, 1029–1035. doi: 10.1006/bbrc.2000.2550
- Nikolotopoulou, V., Markaki, M., Palikaras, K., and Tavernarakis, N. (2013). Crosstalk between apoptosis, necrosis, and autophagy. *Biochim. Biophys. Acta* 1833, 3448–3459. doi: 10.1016/j.bbamcr.2013.06.001
- Nolin, F., Michel, J., Wortham, L., Tcheliidze, P., Banchet, V., Lalun, N., et al. (2016). Stage-specific changes in the water, Na⁺, Cl[−] and K⁺ contents of organelles during apoptosis demonstrated by a targeted cryo correlative analytical approach. *PLoS One* 11:e0148727. doi: 10.1371/journal.pone.0148727
- Offen, D., Zic, I., Gorogin, S., Garzilai, A., Malik, Z., and Melamed, E. (1995). Dopamine-induced programmed cell death in mouse thymocytes. *Biochem. Biophys. Acta* 1268, 171–177. doi: 10.1016/0167-4889(95)00075-4
- Okada, Y., and Maeno, E. (2001). Apoptosis, cell volume regulation and volume-regulatory chloride channels. *Comp. Biochem. Physiol. A Mol. Integr. Physiol.* 130, 377–383. doi: 10.1016/s1095-6433(01)00424-x
- Okada, Y., Maeno, E., Shimizu, T., Dezaki, K., Wang, J., and Morishima, S. (2001). Receptor-mediated control of regulatory volume decrease (RVD) and apoptotic volume decrease (AVD). *J. Physiol.* 532, 3–16. doi: 10.1111/j.1469-7793.2001.0003g.x
- Okada, Y., Maeno, E., Shimizu, T., Manabe, K., Mori, S., and Nabekura, T. (2004). Dual roles of plasmalemmal chloride channels in induction of cell death. *Pflügers Arch.* 448, 287–295. doi: 10.1007/s00424-004-1276-3
- Okada, Y., Numata, T., Sato-Numata, K., Sabirov, R. Z., Liu, H., Mori, S. I., et al. (2019). Roles of volume-regulatory anion channels, VSOR and Maxi-Cl in apoptosis, cisplatin resistance, necrosis, ischemic cell death, stroke and myocardial infarction. *Curr. Top. Membr.* 83, 205–283. doi: 10.1016/bs.ctm.2019.03.001
- Okada, Y., Shimizu, T., Maeno, E., Tanabe, S., Wang, X., and Takahashi, N. (2006). Volume-sensitive chloride channels involved in apoptotic volume decrease and cell death. *J. Membr. Biol.* 209, 21–29. doi: 10.1007/s00232-005-0836-6
- Orlov, S. N., Dam, T. V., Tremblay, J., and Hamet, P. (1996). Apoptosis in vascular smooth muscle cells: role of cell shrinkage. *Biochem. Biophys. Res. Commun.* 221, 708–715. doi: 10.1006/bbrc.1996.0661
- Orlov, S. N., Pchejetski, D., Taurin, S., Thorin-Trascases, N., Maximov, G. V., Pshezhetsky, A. V., et al. (2004). Apoptosis in serum-deprived vascular smooth muscle cells: evidence for cell-volume-independent mechanism. *Apoptosis* 9, 55–66. doi: 10.1023/b:appt.0000012122.47197.03
- Orlov, S. N., Platonova, A. A., Hamet, P., and Grygorczyk, R. (2013). Cell volume and monovalent ion transporters: their role in cell death machinery triggering and progression. *Am. J. Physiol. Cell Physiol.* 305, C361–C372.
- Pal, S., Hartnett, K. A., Nerbonne, J. M., Levitan, E. S., and Aizenman, E. (2003). Mediation of neuronal apoptosis by Kv2.1-encoded potassium channels. *J. Neurosci.* 23, 4798–4802. doi: 10.1523/jneurosci.23-12-04798.2003
- Pal, S. K., Takimoto, K., Aizenman, E., and Levitan, E. S. (2006). Apoptotic surface delivery of K⁺ channels. *Cell Death Differ.* 13, 661–667. doi: 10.1038/sj.cdd.4401792
- Pan, Z., Capó-Aponte, J. E., Zhang, F., Wang, Z., Pokorny, K. S., and Reinach, P. S. (2007). Differential dependence of regulatory volume decrease behavior in rabbit corneal epithelial cells on MAPK superfamily activation. *Exp. Eye Res.* 84, 978–990. doi: 10.1016/j.exer.2007.02.004
- Pan, Z., Yang, H., Mergler, S., Liu, H., Tachado, S. D., Zhang, F., et al. (2008). Dependence of regulatory volume decrease on transient receptor potential Vanilloid 4 (TRPV4) expression in human corneal epithelial cells. *Cell Calcium* 44, 374–385. doi: 10.1016/j.ceca.2008.01.008
- Pasantes-Morales, H. (2016). Channels and volume changes in the life and death of the cell. *Mol. Pharmacol.* 90, 358–370. doi: 10.1124/mol.116.104158
- Pasantes-Morales, H., and Tuz, K. (2006). Volume changes in neurons: hyperexcitability and neuronal death. *Contrib. Nephrol.* 152, 221–240. doi: 10.1159/000096326
- Pedersen, S. F., Okada, Y., and Niliius, B. (2016). Biophysics and physiology of the volume-regulated anion channel (VRAC/Volume-sensitive outwardly rectifying anion channel VSOR). *Pflügers Arch.* 468, 371–383. doi: 10.1007/s00424-015-1781-6
- Planells-Cases, R., Lutter, D., Guyader, C., Gerhards, N. M., Ullrich, F., Elger, D. A., et al. (2015). Subunit composition of VRAC channels determines substrate specificity and cellular resistance to Pt-based anti-cancer drugs. *EMBO J.* 34, 2993–3008. doi: 10.15252/embj.201592409
- Platonova, A., Koltsova, S. V., Hamet, P., Grygorczyk, R., and Orlov, S. N. (2012). Swelling rather than shrinkage precedes apoptosis in serum-deprived vascular smooth muscle cells. *Apoptosis* 17, 429–438. doi: 10.1007/s10495-011-0694-x
- Podsieloch, A., Gan, L., and Fagerholm, P. (2000). Apoptosis in UV-exposed rabbit corneas. *Cornea* 19, 99–103. doi: 10.1097/00003226-200001000-00019
- Porcelli, A. M., Ghelli, A., Zanna, C., Valente, P., Ferroni, S., and Rugolo, M. (2004). Apoptosis induced by staurosporine in ECV304 cells requires cell shrinkage and upregulation of Cl[−] conductance. *Cell Death Differ.* 11, 655–662. doi: 10.1038/sj.cdd.4401396
- Poulsen, K. A., Andersen, E. C., Hansen, C. F., Klausen, T. K., Hougaard, C., Lambert, I. H., et al. (2010). Deregulation of apoptotic volume decrease and ionic movements in multidrug-resistant tumor cells: role of chloride channels. *Am. J. Physiol. Cell Physiol.* 298, C14–C25.
- Qiu, Z., Dubin, A. E., Mathur, J., Tu, B., Reddy, K., Miraglia, L. J., et al. (2014). SWELL1, a plasma membrane protein is an essential component of volume-regulated anion channel. *Cell* 157, 447–458. doi: 10.1016/j.cell.2014.03.024
- Rajapakse, N., Shimizu, K., Kris, B., Snipes, J., Lacza, Z., and Busija, D. (2002). Activation of mitochondrial ATP-sensitive potassium channels prevents neuronal cell death after ischemia in neonatal

- rats. *Neurosci. Lett.* 327, 208–212. doi: 10.1016/s0304-3940(02)00413-5
- Reinehr, R., Graf, D., Fischer, R., Schliess, F., and Häussinger, D. (2002). Hyperosmolarity triggers CD95 membrane trafficking and sensitizes rat hepatocytes toward CD95L-induced apoptosis. *Hepatology* 36, 602–614. doi: 10.1053/jhep.2002.35447
- Ren, R., Oakley, R. H., Cruz-Topete, D., and Cidlowski, J. A. (2012). Dual role of glucocorticoids in cardiomyocyte hypertrophy and apoptosis. *Endocrinology* 153, 5346–5360. doi: 10.1210/en.2012-1563
- Rinehart, J., Vázquez, N., Kahle, K. T., Hodson, C. A., Ring, A. M., Glucicek, E. E., et al. (2011). WNK2 kinase is a novel regulator of essential neuronal cation-chloride cotransporters. *J. Biol. Chem.* 286, 30171–30180. doi: 10.1074/jbc.m111.222893
- Rojas-Rivera, D., Diaz-Elizondo, J., Parra, V., Salas, D., Contreras, A., Toro, B., et al. (2009). Regulatory volume decrease in cardiomyocytes is modulated by calcium influx and reactive oxygen species. *FEBS Lett.* 583, 3485–3492. doi: 10.1016/j.febslet.2009.10.003
- Ruiz-Ederra, J., Levin, M. H., and Verkman, A. S. (2009). In situ fluorescence measurement of tear film [Na⁺], [K⁺], [Cl⁻], and pH in mice shown marked hypertonicity in aquaporin-5 deficiency. *Invest. Ophthalmol. Vis. Sci.* 50, 2132–2138. doi: 10.1167/iov.08-3033
- Schey, K. L., Wang, Z., Wenke, J. L., and Qi, Y. (2014). Aquaporins in the eye: expression, function, and roles in ocular disease. *Biochim. Biophys. Acta* 1840, 1513–1523. doi: 10.1016/j.bbagen.2013.10.037
- Schotanus, M. P., Koetje, L. R., Van Dyken, R. E., and Ubels, J. L. (2011). Stratified corneal limbal epithelial cells are protected from UVB-induced apoptosis by elevated extracellular K⁺. *Exp. Eye Res.* 93, 735–740. doi: 10.1016/j.exer.2011.09.005
- Scotstock, A. B., Bortner, C. D., St Bird, G. J., Putney, J. W. Jr., and Cidlowski, J. A. (2000). A selective requirement for elevated calcium in DNA degradation, but not early events in anti-Fas-induced apoptosis. *J. Biol. Chem.* 275, 30586–30696. doi: 10.1074/jbc.m004058200
- Scotstock, A. B., Heimlich, G., and Cidlowski, J. A. (2006). Glucocorticoids inhibit the apoptotic actions of UV-C but not Fas ligand in hepatoma cells: direct evidence for a critical role of Bcl-xL. *Cell Death Differ.* 14, 840–850. doi: 10.1038/sj.cdd.4402071
- Shen, M., Wang, L., Wang, B., Wang, T., Yang, G., Shen, L., et al. (2014). Activation of volume-sensitive outwardly rectifying chloride channel by ROS contributes to ER stress and cardiac contractile dysfunction: involvement of CHOP through Wnt. *Cell Death Dis.* 5, e1528. doi: 10.1038/cddis.2014.479
- Shimizu, T., Wehner, F., and Okada, Y. (2006). Inhibition of hypertonicity-induced cation channels sensitizes HeLa cells to shrinkage-induced apoptosis. *Cell Physiol. Biochem.* 18, 295–302. doi: 10.1159/000097607
- Sidhay, V. K., Guler, A. D., Schweitzer, K. S., D'Alessio, F., Caterina, M. J., and King, L. S. (2006). Transient receptor potential vanilloid 4 regulates aquaporin-5 abundance under hypotonic conditions. *Proc. Natl. Acad. Sci. U.S.A.* 103, 4747–4752. doi: 10.1073/pnas.0511211103
- Singleton, K. R., Will, D. S., Schotanus, M. P., Haarsma, L. D., Koetje, L. R., Bardolph, S. L., et al. (2009). Elevated extracellular K⁺ inhibits apoptosis of corneal epithelial cells exposed to UV-B radiation. *Exp. Eye Res.* 89, 140–151. doi: 10.1016/j.exer.2009.02.023
- Siriant, L., Wanichakool, P., Ousingsawat, J., Benedetto, R., Zormpa, A., Cabrita, I., et al. (2016). Non-essential contribution of LRRC8A to volume regulation. *Pflugers Arch.* 468, 805–816. doi: 10.1007/s00424-016-1789-6
- Skepper, J. N., Karydis, I., Garnett, M. R., Hegyi, L., Hardwick, S. J., Warley, A., et al. (1999). Changes in elemental concentrations are associated with early stages of apoptosis in human monocyte-macrophages exposed to oxidized low-density lipoprotein: An X-ray microanalytical study. *J. Pathol.* 188, 100–106. doi: 10.1002/(sici)1096-9896(199905)188:1<100::aid-path306>3.0.co;2-o
- Storey, N. M., Gomez-Angelats, M., Bortner, C. D., Armstrong, D. L., and Cidlowski, J. A. (2003). Stimulation of Kv1.3 potassium channels by death receptors during apoptosis in Jurkat T lymphocytes. *J. Biol. Chem.* 278, 33319–33326. doi: 10.1074/jbc.m300443200
- Sun, J. F., Zhao, M. Y., Xu, Y. J., Su, Y., Kong, X. H., and Wang, Z. Y. (2020). Fenamates inhibit human sodium channel Nav1.2 and protect glutamate-induced injury in SH-S5SY cells. *Cell Mol. Neurobiol.* 40, 1405–1416. doi: 10.1007/s10571-020-00826-1
- Syeda, R., Qiu, Z., Dubin, A. E., Murthy, S. E., Florendo, M. N., Mason, D. E., et al. (2016). LRRC8 proteins form volume-regulated anion channels that sense ionic strength. *Cell* 164, 499–511. doi: 10.1016/j.cell.2015.12.031
- Tait, M. J., Saadoun, S., Bell, B. A., and Papadopoulos, M. C. (2008). Water movements in the brain: role of aquaporins. *Trends Neurosci.* 31, 37–43. doi: 10.1016/j.tins.2007.11.003
- Tanaka, A., Tanaka, R., Kasai, N., Tsukada, S., Okajima, T., and Sumitomo, K. (2015). Time-lapse imaging of morphological changes in a single neuron during the early stages of apoptosis using scanning ion conductance microscopy. *J. Struct. Biol.* 191, 32–38. doi: 10.1016/j.jsb.2015.06.002
- Thompson, G. J., Langlais, C., Cain, K., Conley, E. C., and Cohen, G. M. (2001). Elevated extracellular [K⁺] inhibits death-receptor- and chemical-mediated apoptosis prior to caspase activation and cytochrome c release. *Biochem. J.* 357, 137–145. doi: 10.1042/0264-6021:3570137
- Tie, L., Wnag, D., Shi, Y., and Li, X. (2017). Aquaporins in cardiovascular system. *Adv. Exp. Med. Biol.* 969, 105–113. doi: 10.1007/978-94-024-1057-0_6
- Trimarchi, J. R., Liu, L., Smith, P. J., and Keefe, D. L. (2002). Apoptosis recruits two-pore domain potassium channels used for homeostatic volume regulation. *Am. J. Physiol. Cell Physiol.* 282, C588–C594.
- Ubels, J. L., Glupker, C. D., Schotanus, M. P., and Haarsma, L. D. (2016). Involvement of the extrinsic and intrinsic pathways in ultraviolet B-induced apoptosis in corneal epithelial cells. *Exp. Eye Res.* 145, 36–35.
- Ubels, J. L., Schotanus, M. P., Bardolph, S. L., Haarsma, L. D., Koetje, L. R., and Louters, J. R. (2010). Inhibition of UV-B induced apoptosis in corneal epithelial cells by potassium channel modulators. *Exp. Eye Res.* 90, 216–222. doi: 10.1016/j.exer.2009.10.005
- Ubels, J. L., Van Dyken, R. E., Louters, J. R., Schotanus, M. P., and Haarsma, L. D. (2011). Potassium ion fluxes in corneal epithelial cells exposed to UVB. *Exp. Eye Res.* 92, 425–431. doi: 10.1016/j.exer.2011.02.019
- Virgili, N., Mancera, P., Wappenhans, B., Sorrosal, G., Biber, K., Pugliese, M., et al. (2013). K(ATP) channel opener diaoxide prevents neurodegeneration: a new mechanism of active via antioxidative pathway activation. *PLoS One* 8:e75189. doi: 10.1371/journal.pone.0075189
- Voss, F. K., Ullrich, F., Munch, J., Lazarow, K., Lutter, D., Mah, N., et al. (2014). Identification of LRRC8 heteromers as an essential component of the volume-regulated anion channel VRAC. *Science* 344, 634–638. doi: 10.1126/science.1252826
- Wang, H. Y., Shimizu, T., Numata, T., and Okada, Y. (2007). Role of acid-sensitive outwardly rectifying anion channels in acidosis-induced cell death in human epithelial cells. *Pflugers Arch.* 454, 223–233. doi: 10.1007/s00424-006-0193-z
- Wang, L., Dai, W., and Lu, L. (2005a). Ultraviolet irradiation-induced K(+) channel activity involving p53 activation in corneal epithelial cells. *Oncogene* 24, 3020–3027. doi: 10.1038/sj.onc.1208547
- Wang, L., Dai, W., and Lu, L. (2011). Hyperosmotic stress-induced corneal epithelial cell death through activation of Polo-like Kinase 3 and c-Jun. *Invest. Ophthalmol. Vis. Sci.* 52, 3200–3206. doi: 10.1167/iov.10-6485
- Wang, L., Li, T., and Lu, L. (2003). UV-induced corneal epithelial cell death by activation of potassium channels. *Invest. Ophthalmol. Vis. Sci.* 44, 5095–5101. doi: 10.1167/iov.03-0590
- Wang, L., Shen, M., Guo, X., Wang, B., Xia, Y., Wang, N., et al. (2017). Volume-sensitive outwardly rectifying chloride channel blockers protect against high glucose-induced apoptosis of cardiomyocytes via autophagy activation. *Sci. Rep.* 7:44265. doi: 10.1038/srep44265
- Wang, X., Takahashi, N., Uramoto, H., and Okada, Y. (2005b). Chloride channel inhibition prevents ROS-dependent apoptosis induced by ischemia-reperfusion in mouse cardiomyocytes. *Cell. Physiol. Biochem.* 16, 147–154. doi: 10.1159/000089840
- Wei, L., Xiao, A. Y., Jin, C., Yang, A., Lu, Z. Y., and Yu, S. P. (2004). Effects of chloride and potassium channel blockers on apoptotic cell shrinkage and

- apoptosis in cortical neurons. *Pflugers Arch.* 448, 325–334. doi: 10.1007/s00424-004-1277-2
- Wei, L., Yu, S. P., Gottron, F., Snider, B. J., Zipfel, G. J., and Choi, D. W. (2003). Potassium channel blockers attenuate hypoxia- and ischemia-induced neuronal death in vitro and in vivo. *Stroke* 34, 1281–1286. doi: 10.1161/01.str.0000065828.18661.1e
- Wilson, C. S., and Mongin, A. A. (2018). Cell volume control in healthy brain and neuropathologies. *Curr. Top. Membr.* 81, 385–455. doi: 10.1016/bs.ctm.2018.07.006
- Woodward, A. M., Senchyna, M., and Argüeso, P. (2012). Differential contribution of hypertonic electrolytes to corneal epithelial dysfunction. *Exp. Eye Res.* 100, 98–100. doi: 10.1016/j.exer.2012.04.014
- Wright, A. R., and Ress, S. A. (1998). Cardiac cell volume: crystal clear or murky waters: a comparison with other cell types. *Pharmacol. Ther.* 80, 89–121.
- Yang, H. Q., Foster, M. N., Jana, K., Ho, J., Rindler, M. J., and Coetzee, W. A. (2016). Plasticity of sarcolemmal KATP channel surface expression: relevance during ischemia and ischemic preconditioning. *Am. J. Physiol. Heart Circ. Physiol.* 310, H1558–H1566.
- Yang, K. T., Pan, S. F., Chien, C. L., Hsu, S. M., Tseng, Y. Z., Wang, S. M., et al. (2004). Mitochondrial Na⁺ overload is caused by oxidative stress and leads to activation of the caspase 3-dependent apoptotic machinery. *FASEB J.* 18, 1442–1444. doi: 10.1096/fj.03-1038fje
- Yang, L., Zhu, L., Xu, Y., Zhang, H., Ye, W., Mao, J., et al. (2012). Uncoupling of K⁺ and Cl[−] transport across the cell membrane in the process of regulatory volume decrease. *Biochem. Pharmacol.* 84, 292–302. doi: 10.1016/j.bcp.2012.05.006
- Yu, S. P., Yeh, C., Strasser, U., Tian, M., and Choi, D. W. (1999a). NMDA receptor-mediated K⁺ efflux and neuronal apoptosis. *Science* 284, 336–339. doi: 10.1126/science.284.5412.336
- Yu, S. P., Yeh, C. H., Gottron, F., Wang, X., Grabb, M. C., and Choi, D. W. (1999b). Role of the outward delayed rectifier K⁺ current in ceramide-induced caspase activation and apoptosis in cultured cortical neurons. *J. Neurochem.* 73, 933–941. doi: 10.1046/j.1471-4159.1999.0730933.x
- Yu, S. P., Yeh, C. H., Sensi, S. L., Gwag, B. J., Canzoniero, L. M., Farhangrazi, Z. S., et al. (1997). Mediation of neuronal apoptosis by enhancement of outward potassium current. *Science* 278, 114–117. doi: 10.1126/science.278.5335.114
- Yuan, J., and Yankner, B. A. (2000). Apoptosis in nervous system. *Nature* 407, 802–809.
- Yurinskaya, V., Goryachaya, T., Guzhova, I., Moshkov, A., Rozanov, Y., Sakuta, G., et al. (2005a). Potassium and sodium balance in U937 cells during apoptosis with and without cell shrinkage. *Cell. Physiol. Biochem.* 16, 155–162. doi: 10.1159/000089841
- Yurinskaya, V., Moshkov, A., Rozanov, Y., Shirokova, A., Vassilieva, I., Shumilina, E., et al. (2005b). Thymocyte K⁺, Na⁺ and water balance during dexamethasone- and etoposide-induced apoptosis. *Cell. Physiol. Biochem.* 16, 15–22. doi: 10.1159/000087727
- Yurinskaya, V., Moshkov, A., Wibberley, A. V., Lang, F., Model, M. A., and Vereninov, A. (2012). Dual response of human leukemia U937 cells to hypertonic shrinkage: initial regulatory volume increase (RVI) and delayed apoptotic volume decrease (AVD). *Cell. Physiol. Biochem.* 30, 964–973. doi: 10.1159/000341473
- Yurinskaya, V. E., Vereninov, I. A., and Vereninov, A. A. (2019). A tool for computation of changes in Na⁺, K⁺, Cl[−] channels and transporters due to apoptosis by data on cell ion and water content alteration. *Front. Cell. Dev. Biol.* 7:58. doi: 10.3389/fcell.2019.00058
- Zeileina, M. (2010). Regulation of brain aquaporins. *Neurochem. Int.* 57, 468–488. doi: 10.1016/j.neuint.2010.03.022
- Zhang, F., Ma, X. L., Wang, Y. X., He, C. C., Tian, K., Wang, H. G., et al. (2017). TPEN, a specific Zn²⁺ chelator, inhibits sodium dithionite and glucose deprivation (SDGD)-induced neuronal death by modulating apoptosis, glutamate signaling, and voltage-gated K⁺ and Na⁺ channels. *Cell. Mol. Neuro.* 37, 235–250. doi: 10.1007/s10571-016-0364-1
- Zhu, H., Cao, W., Zhao, P., Wang, J., Qian, Y., and Li, Y. (2018a). Hyperosmotic stress stimulates autophagy via the NFAT/mTOR pathway in cardiomyocytes. *Int. J. Mol. Med.* 42, 3459–3466.
- Zhu, J., Zang, S., Chen, X., Jiang, L., Gu, A., Cheng, J., et al. (2018b). Involvement of the delayed rectifier outward potassium channel Kv2.1 in methamphetamine-induced neuronal apoptosis via the p38 mitogen-activated protein kinase signaling pathway. *J. Appl. Toxicol.* 38, 696–704. doi: 10.1002/jat.3576

Conflict of Interest: The authors declare that the research was conducted in the absence of any commercial or financial relationships that could be construed as a potential conflict of interest.

Copyright © 2020 Bortner and Cidlowski. This is an open-access article distributed under the terms of the Creative Commons Attribution License (CC BY). The use, distribution or reproduction in other forums is permitted, provided the original author(s) and the copyright owner(s) are credited and that the original publication in this journal is cited, in accordance with accepted academic practice. No use, distribution or reproduction is permitted which does not comply with these terms.



Ca²⁺ Dependence of Volume-Regulated VRAC/LRRC8 and TMEM16A Cl⁻ Channels

Raquel Centeio, Jiraporn Ousingsawat, Rainer Schreiber and Karl Kunzelmann*

Physiological Institute, University of Regensburg, Regensburg, Germany

OPEN ACCESS

Edited by:

Markus Ritter,
Paracelsus Medical University, Austria

Reviewed by:

Carles Solsona,
University of Barcelona, Spain
Christophe Duranton,
UMR 7370 Laboratoire de Physio
Médecine Moléculaire (LP2M), France

*Correspondence:

Karl Kunzelmann
karl.kunzelmann@ur.de

Specialty section:

This article was submitted to
Cell Death and Survival,
a section of the journal
Frontiers in Cell and Developmental
Biology

Received: 20 August 2020

Accepted: 04 November 2020

Published: 01 December 2020

Citation:

Centeio R, Ousingsawat J,
Schreiber R and Kunzelmann K
(2020) Ca²⁺ Dependence
of Volume-Regulated VRAC/LRRC8
and TMEM16A Cl⁻ Channels.
Front. Cell Dev. Biol. 8:596879.
doi: 10.3389/fcell.2020.596879

All vertebrate cells activate Cl⁻ currents ($I_{Cl,swell}$) when swollen by hypotonic bath solution. The volume-regulated anion channel VRAC has now been identified as LRRC8/SWELL1. However, apart from VRAC, the Ca²⁺-activated Cl⁻ channel (CaCC) TMEM16A and the phospholipid scramblase and ion channel TMEM16F were suggested to contribute to cell swelling-activated whole-cell currents. Cell swelling was shown to induce Ca²⁺ release from the endoplasmic reticulum and to cause subsequent Ca²⁺ influx. It is suggested that TMEM16A/F support intracellular Ca²⁺ signaling and thus Ca²⁺-dependent activation of VRAC. In the present study, we tried to clarify the contribution of TMEM16A to $I_{Cl,swell}$. In HEK293 cells coexpressing LRRC8A and LRRC8C, we found that activation of $I_{Cl,swell}$ by hypotonic bath solution (Hypo; 200 mosm/l) was Ca²⁺ dependent. TMEM16A augmented the activation of LRRC8A/C by enhancing swelling-induced local intracellular Ca²⁺ concentrations. In HT₂₉ cells, knockdown of endogenous TMEM16A attenuated $I_{Cl,swell}$ and changed time-independent swelling-activated currents to VRAC-typical time-dependent currents. Activation of $I_{Cl,swell}$ by Hypo was attenuated by blocking receptors for inositol trisphosphate and ryanodine (IP₃R; RyR), as well as by inhibiting Ca²⁺ influx. The data suggest that TMEM16A contributes directly to $I_{Cl,swell}$ as it is activated through swelling-induced Ca²⁺ increase. As activation of VRAC is shown to be Ca²⁺-dependent, TMEM16A augments VRAC currents by facilitating Hypo-induced Ca²⁺ increase in submembraneous signaling compartments by means of ER tethering.

Keywords: VRAC, CaCC, TMEM16 proteins, anoctamin, ANO1

INTRODUCTION

Cell swelling activates Cl⁻ currents ($I_{Cl,swell}$) that are known as volume-regulated anion channels (VRAC) (Jentsch, 2016; Pedersen et al., 2016; Strange et al., 2019). VRAC is now identified as LRRC8/SWELL1 (Qiu et al., 2014; Voss et al., 2014). Its hexameric structure has been reported in four independent cryo-EM studies (Deneka et al., 2018; Kasuya et al., 2018; Kefauver et al., 2018; Kern et al., 2019). The essential subunit LRRC8A along with a variable combination

of additional four paralogous proteins LRRC8B-E forms heteromers with different kinetic properties. Numerous studies show a contribution of these channels to cellular resistance toward cisplatin and other anticancer drugs (Ise et al., 2005; Mahmud et al., 2008; Planells-Cases et al., 2015) and possibly growth of cancer (Lemonnier et al., 2004; Kunzelmann et al., 2019; Liu and Stauber, 2019; Lu et al., 2019). Others reported a role of VRAC in apoptotic cell death (Gulbins et al., 2000; Okada et al., 2006; Wanitchakool et al., 2016). Despite structural information, the mechanism for activation of VRAC/LRRC8 channels remains incompletely understood. While lowering intracellular ionic strength is an essential prerequisite (Cannon et al., 1998; Sabirov et al., 2000; Syeda et al., 2016), intracellular Ca^{2+} was shown to be important for activation of $\text{I}_{\text{Cl,swell}}$ and for cellular volume regulation (Mccarty and O'neil, 1992; Lemonnier et al., 2002; Akita et al., 2011; Benedetto et al., 2016; Liu et al., 2019).

Cell swelling activates not only VRAC/LRRC8 but also Ca^{2+} -dependent TMEM16A (Almaca et al., 2009; Benedetto et al., 2016; Liu et al., 2019) and TMEM16F channels/scramblases (Juul et al., 2014; Sirianant et al., 2016a). Our earlier results show that both TMEM16A and LRRC8 contribute to $\text{I}_{\text{Cl,swell}}$ (Benedetto et al., 2016) in a Ca^{2+} -dependent manner. This has been shown also for serum-induced current activation (Zhang et al., 2020). In fact, we demonstrated that LRRC8 is not essential for $\text{I}_{\text{Cl,swell}}$ or cellular volume regulation (Milenkovic et al., 2015; Sirianant et al., 2016b). Particularly in differentiated naïve cells in tissues, and in epithelial cells with large transport capacity, the physiological relevance of LRRC8 may be limited (Almaca et al., 2009; Milenkovic et al., 2015; Sirianant et al., 2016b).

Previous studies did not answer the question whether LRRC8 and TMEM16A/F are activated in parallel to give rise to $\text{I}_{\text{Cl,swell}}$, or whether TMEM16 proteins, particularly TMEM16A, support activation of LRRC8 by facilitating Ca^{2+} signals near the plasma membrane (Benedetto et al., 2016; Cabrita et al., 2017). For comparison, such a Ca^{2+} -modulating effect of TMEM16A is fundamental for activation of CFTR as demonstrated *in vitro* and *in vivo* in mouse and human (Von Kleist et al., 1975; Benedetto et al., 2017, 2019b; Park et al., 2020), which express both proteins endogenously. The data provide evidence that TMEM16A supports Ca^{2+} release from endoplasmic reticulum (ER) and cause Ca^{2+} influx that activates TMEM16A and supports activation of LRRC8.

MATERIALS AND METHODS

Cells Culture

All cells were grown at 37°C in a humidified atmosphere with 5% (v/v) CO_2 . Human embryonic kidney HEK293T cells (Simmons, 1990) stably expressing iodide-sensitive enhanced yellow fluorescent protein (eYFP-I152L; HEK-YFP; Amgen, Thousand Oaks, California, United States) were grown in DMEM low-glucose medium supplemented with 10% (v/v) fetal bovine serum (FBS), 1% (v/v) L-glutamine 200 mM, and 10 mM HEPES (all from Capricorn Scientific, Ebsdorfergrund, Germany), in the presence of selection antibiotic puromycin

0.5 $\mu\text{g/mL}$ (Sigma-Aldrich, Missouri, United States). Cells stably coexpressing TMEM16A (HEK-YFP-TMEM16A) were cultured under additional hygromycin B (150 $\mu\text{g/mL}$; Capricorn Scientific, Ebsdorfergrund, Germany). HT29 human colonic carcinoma epithelial cells stably expressing eYFP-I152L (HT29-YFP, kindly provided by Prof. Luis Galletta, TIGEM, Pozzuoli, and Prof. Nicoletta Pedemonte, Istituto Giannina Gaslini, Genua, Italy.) were cultured in McCoy's 5A medium supplemented with 10% (v/v) FBS and 1 mg/mL G418 selection antibiotic (all from Capricorn Scientific, Ebsdorfergrund, Germany).

RT-PCR, siRNA, and cDNAs

Human LRRC8A (NM_00127244.1) and LRRC8C (NM_032270.5) were sub-cloned into the bicistronic vector pIRES2 (Clontech Laboratories/Takara Bio United States, Mountain View, California, United States) using standard methods. The construct was verified by sequencing (Microsynth SeqLab, Göttingen, Germany). Transfection of cDNAs into HEK293T cells was performed using standard protocols for Lipofectamine 3000 (Invitrogen, Carlsbad, California, United States). CD8 cDNA was co-transfected to allow for detection of overexpressing cells by binding of anti-CD8 labeled beads (Dynabeads[®]M-450 Epoxy; Invitrogen, Carlsbad, California, United States). Knockdown of TMEM16A and LRRC8A in HT29 cells was performed through transfection by electroporation of the siRNAs siTMEM16A (5-GGUUCCAGCCUACCUCACUAACUU-3, Invitrogen, Carlsbad, California, United States) and/or siLRRC8A (5-CCAAGCUCAUCGUCCUCAA-3, Ambion, Austin, Texas, United States), using a Neon Transfection System (Invitrogen, Carlsbad, California, United States) with a program of three pulses, 1,650 V, and 10 ms. Scrambled siRNA (Silencer[®]Select Negative Control siRNA #1, Ambion, Austin, Texas, United States) was transfected as negative control. All experiments were performed 48–72 h after transfection.

Western Blotting

Protein was isolated from cells using a lysing buffer containing 25 mM Tris-HCl pH 7.4, 150 mM NaCl, 1 mM EDTA, 5% glycerol, 0.43% Nonidet P-40, 100 mM dithiothreitol (both from PanReac AppliChem, Barcelona, Spain), and 1× protease inhibitor mixture (Roche, Basel, Switzerland). Proteins were then separated by an 8.5% SDS-PAGE and transferred to a PVDF membrane (GE Healthcare, Munich, Germany). Membranes were incubated with primary rabbit monoclonal anti-TMEM16A/DOG1 antibody (#NBP1-49799; Novus Biologicals, Littleton, Colorado, United States; 1:500 in 1% (w/v) NFM/TBS-T) or rabbit polyclonal anti-LRRC8A antibody (#HPA016811; Sigma-Aldrich, St. Louis, Missouri, United States; 1:1,000 in 1% (w/v) BSA/TBS-T) for 2.5 h at room temperature. A rabbit polyclonal anti- β -actin antibody (A2066; Sigma-Aldrich, St. Louis, Missouri, United States; 1:10,000 in 5% (w/v) NFM/TBS-T) was used for loading control. Membranes were then incubated with horseradish peroxidase (HRP)-conjugated goat polyclonal anti-rabbit secondary antibody (#31460; Invitrogen, Carlsbad, California, United States) at RT for 2 h,

and immunoreactive signals were visualized using a SuperSignal Chemiluminescent Substrate detection kit (#34577; Thermo Fisher Scientific, Waltham, Massachusetts, United States).

Patch Clamping

Cells were patch clamped on glass cover slips. If not indicated otherwise, patch pipettes were filled with a cytosolic-like solution containing (mM) KCl 30, K-gluconate 95, NaH₂PO₄ 1.2, Na₂HPO₄ 4.8, EGTA 1, Ca-gluconate 0.758, MgCl₂ 1.03, D-glucose 5, ATP 3; 290 mosm/l; pH 7.2. The free Ca²⁺ concentration (Ca²⁺ activity) was 0.1 μ M. To adjust pipette Ca²⁺ concentrations to 0.01 μ M, the pipette-filling solution contained (mM) KCl 30, K-gluconate 95, NaH₂PO₄ 1.2, Na₂HPO₄ 4.8, EGTA 1, Ca-gluconate 0.209, MgCl₂ 1.03, D-glucose 5, and ATP 3; 290 mosm/l; pH 7.2. Free Ca²⁺ concentrations were calculated according to a program developed at the Max Planck institute for biophysics (Frankfurt, Germany). Ca²⁺ activities (free Ca²⁺ concentrations) were originally validated by potentiometric determination using Ca²⁺-sensitive electrodes. In some experiments, patch pipettes were filled with CsCl buffer containing (mM) CsCl 125, NaH₂PO₄ 1.2, Na₂HPO₄ 4.8, EGTA 1, Ca-gluconate 0.209, MgCl₂ 1.03, D-glucose 5, and ATP 3; pH 7.2. In these experiments, a CsCl buffer was used as bath solution, containing 145 CsCl, 0.4 KH₂PO₄, 1.6 K₂HPO₄, 4.6 D-glucose, 1 MgCl₂, and 1.3 Ca²⁺ gluconate, 290 mosm/l; pH 7.4.

Coverslips were mounted in a perfused bath chamber on the stage of an inverted microscope (IM35, Zeiss) and kept at 37°C. The bath was perfused continuously with Ringer solution at a rate of 8 ml/min. For activation of volume-dependent Cl⁻ currents, isotonic Ringer bath solution (300 mosm/l; mM: 145 NaCl, 0.4 KH₂PO₄, 1.6 K₂HPO₄, 4.6 D-glucose, 1 MgCl₂, 1.3 Ca²⁺ gluconate, pH 7.4) was changed to hypotonic bath solution (Hypo; 200 mosm/l) by removing 50 mM NaCl from Ringer solution. Patch-clamp experiments were performed in the fast whole-cell configuration. Patch pipettes had an input resistance of 4–6 M Ω when filled with the cytosolic-like (physiological) solution. Currents were corrected for serial resistance. The access conductance was measured continuously and was 60–140 nS. Currents (voltage clamp) and voltages (current clamp) were recorded using a patch-clamp amplifier (EPC 7, List Medical Electronics, Darmstadt, Germany), the LIH1600 interface, and PULSE software (HEKA, Lambrecht, Germany) as well as Chart software (AD Instruments, Spechbach, Germany). Data were stored continuously on a computer hard disc and analyzed using PULSE software. In regular intervals, membrane voltage (V_c) was clamped in steps of 20 mV from –100 to +100 mV from a holding voltage of –100 mV. Current density was calculated by dividing whole-cell currents by cell capacitance.

YFP Quenching

Quenching of the intracellular fluorescence generated by stable transfection of the iodide (I⁻)-sensitive enhanced yellow fluorescent protein (eYFP-I152L) was used to measure anion conductance. YFP fluorescence was excited at 490 nm using a high-speed polychromatic illumination system for microscopic fluorescence measurements (Visitron Systems, Puchheim, Germany), and the emitted light at 535 \pm 25 nm was

detected with a CoolSnap HQ CCD camera (Roper Scientific, Planegg, Germany/Visitron Systems, Puchheim, Germany). Cells were grown on coverslips and mounted in a thermostatically controlled imaging chamber adapted to an inverted microscope (Axiovert S100, Zeiss, Oberkochen, Germany), maintained at 37°C, and perfused at a rate of 5 mL/min. After a brief period under standard Ringer solution (in mM: NaCl 145, KH₂PO₄ 0.4, K₂HPO₄ · 3 H₂O 1.6, glucose 5, MgCl₂ · 6 H₂O 1, Ca-gluconate · 1 H₂O 1.3), cells were stimulated with hypotonic (200 mosm/l) solution with the following composition (in mM): NaCl 45, KH₂PO₄ 0.4, K₂HPO₄ · 3 H₂O 1.6, glucose 5, MgCl₂ · 6 H₂O 1, Ca-gluconate · 1 H₂O 1.3, Na-gluconate 50) or isotonic solution as control (in mM: NaCl 45, KH₂PO₄ 0.4, K₂HPO₄ · 3 H₂O 1.6, glucose 5, MgCl₂ · 6 H₂O 1, Ca-gluconate · 1 H₂O 1.3, Na-gluconate 50, mannitol 100). Quenching of YFP-fluorescence by I⁻ influx was induced by replacing 50 mM extracellular gluconate by I⁻. Control of experiment, imaging acquisition, and data analysis were done with the software package MetaFluor (Universal Imaging, Bedford Hills, New York, United States). Autofluorescence was negligible. For quantitative analysis, cells with low or excessively high fluorescence were discarded. Changes in fluorescence induced by I⁻ uptake are expressed as initial rates of maximal fluorescence decrease (au/s).

Alternatively, YFP-quenching measurements were performed on a fluorescence microplate reader (NOVOstar, BMG Labtech, Ortenberg, Germany) kept at 37°C, using an excitation wavelength of 485 nm and emission detection at 520 nm. Cells were plated in transparent 96-well plates (Sarstedt, Nümbrecht, Germany), cultured 48–72 h to 80–90% confluence, and incubated with or without test compounds in standard Ringer solution (300 mosm/l). After a short basal fluorescence reading, cells were stimulated with a hypotonic (200 mosm/l) solution (in mM: NaCl 21.67, NaI 26.67, KH₂PO₄ 0.4, K₂HPO₄ · 3 H₂O 1.6, glucose 5, MgCl₂ · 6 H₂O 1, Ca-gluconate · 1 H₂O 1.3, Mannitol 58) added by automated injection through a syringe pump, or isotonic solution (in mM: NaCl 21.67, NaI 26.67, KH₂PO₄ 0.4, K₂HPO₄ · 3 H₂O 1.6, glucose 5, MgCl₂ · 6 H₂O 1, Ca-gluconate · 1 H₂O 1.3, mannitol 193.3) as control. For ATP stimulation, cells were incubated with or without test compounds in a gluconate-substituted Ringer solution (in mM: NaCl 100, Na-gluconate 40, KCl 5, MgCl₂ · 6 H₂O 1, CaCl₂ · 2 H₂O 2, glucose 10, HEPES 10) and ATP was added in a symmetrical I⁻-substituted Ringer solution (in mM: NaCl 100, NaI 40, KCl 5, MgCl₂ · 6 H₂O 1, CaCl₂ · 2 H₂O 2, D-glucose 10, HEPES 10). The final I⁻ concentration on each well was 20 mM for every experiment. Total intracellular YFP-fluorescence intensity in each well was measured continuously. Background fluorescence was subtracted, and data was normalized to the initial fluorescence. The initial rate of maximal fluorescence decay caused by I⁻ influx was then calculated as a measure of anion conductance.

Ca²⁺ Measurements

Cells were seeded on glass coverslips and loaded with 2 μ M Fura-2, AM Ester (Biotium, Hayward, California, United States), and 0.02% Pluronic F-127 (Invitrogen, Carlsbad, California, United States) in standard Ringer solution (in mM: NaCl 145,

KH₂PO₄ 0.4, K₂HPO₄ · 3 H₂O 1.6, glucose 5, MgCl₂ · 6 H₂O 1, Ca-gluconate · 1 H₂O 1.3) for 1 h at room temperature. Cells were then mounted in a thermostatically controlled imaging chamber adapted to an inverted microscope (Axiovert S100, Zeiss, Oberkochen, Germany), maintained at 37°C and perfused at a rate of 5 mL. Fura-2 was excited at 340/380 nm using a high-speed polychromatic illumination system for microscopic fluorescence measurements (Visitron Systems, Puchheim, Germany), and emission was recorded between 470 and 550 nm using a CoolSnap HQ CCD camera (Roper Scientific, Planegg, Germany/Visitron Systems, Puchheim, Germany). Cells were stimulated with ATP or hypotonic (200 mosm/l) solution (in mM: NaCl 95, KH₂PO₄ 0.4, K₂HPO₄ · 3 H₂O 1.6, glucose 5, MgCl₂ · 6 H₂O 1, Ca-gluconate · 1 H₂O 1.3). Intracellular calcium ([Ca²⁺]_i) was calculated from the 340/380-nm fluorescence ratio after background subtraction using the formula $[Ca^{2+}]_i = Kd \times (R - R_{min}) / (R_{max} - R) \times (S_{f2}/S_{b2})$, where R is the observed fluorescence ratio. The values R_{max} and R_{min} (maximum and minimum ratios) and the constant S_{f2}/S_{b2} (fluorescence of free and Ca²⁺-bound Fura-2 at 380 nm) were calculated using 2 μM ionomycin (Calbiochem, San Diego, California, United States), 5 μM nigericin (Sigma-Aldrich, St. Louis, Missouri, United States), 10 μM monensin (Sigma-Aldrich, St. Louis, Missouri, United States), and 5 mM EGTA (Carl Roth, Karlsruhe, Germany) to equilibrate intracellular and extracellular Ca²⁺ in intact Fura-2-loaded cells. The dissociation constant (Kd) for the Fura-2-Ca²⁺ complex was taken as 224 nM. Control of experiment, imaging acquisition, and data analysis were done with the software package MetaFluor (Universal Imaging, Bedford Hills, New York, United States).

Materials and Statistical Analysis

Suramin, U73122, 2-APB, dantrolene, and NS3728 were from Sigma-Aldrich, St. Louis, Missouri, United States. Niclosamide, Ani9, and DCPIB were from Tocris, Bristol, United Kingdom. Xestospongine C and niclosamide ethanolamine were from Cayman Chemical, Ann Arbor, Michigan, United States. Probenecid was from MP Biomedicals, Irvine, California, United States. Data are shown as individual traces or as summaries with mean values ± SEM and number of experiments given in each figure's legend. For statistical analysis, paired or unpaired Student's *t*-test was used as appropriate. A *p*-value of < 0.05 was accepted as a statistically significant difference (indicated by # for unpaired data and by * for paired data).

RESULTS

Activation of Endogenous and Overexpressed VRAC Is Ca²⁺ Dependent

Earlier studies suggested a requirement of Ca²⁺ for activation of I_{Cl,swell} and stimulation of endogenous LRRC8/Swell1 (Akita and Okada, 2011; Benedetto et al., 2016). Here we directly validated the Ca²⁺ dependence of LRRC8 currents by coexpressing both LRRC8A and LRRC8C in HEK293 cells, using a bicistronic expression plasmid. **Figure 1A** shows

strong increase of LRRC8A expression when compared with endogenous LRRC8A expression (overexpression of LRRC8C not shown). Overexpression of LRRC8A/C largely augmented the whole-cell currents activated by hypotonic (200 mosm/l) bath solution (Hypo) in the presence of an intracellular (pipette, 290 mosm/l) Ca²⁺ concentration of 100 nM. Overexpressed LRRC8A/C was very rapidly activated by Hypo-induced cell swelling (**Figure 1B**). Gradual decrease of intracellular (i.e., patch pipette) Ca²⁺ concentrations to 10 and to 0 nM gradually inhibited hypo-activation of the endogenous I_{Cl,swell}, as well as the overexpressed LRRC8A/C currents (**Figures 1C,D**). The experiments indicate a requirement of Ca²⁺ for activation of VRAC/LRRC8.

TMEM16A Supports Activation of I_{Cl,swell} in HEK293 Cells Overexpressing LRRC8A/C

It has been reported that TMEM16A (and TMEM16F) take part in whole-cell current activated through hypotonic cell swelling (I_{Cl,swell}), although these proteins are not known to be directly activated by cell swelling (Almacá et al., 2009; Benedetto et al., 2016; Sirianant et al., 2016a; Liu et al., 2019). Here we examined the impact of TMEM16A on activation of VRAC at different intracellular Ca²⁺ concentrations. At an intracellular resting Ca²⁺ concentration of 100 nM, endogenous VRAC (mock) and overexpressed LRRC8A/C were readily activated by osmotic cell swelling (200 mosm/l; Hypo). However, activation was compromised at 10 nM intracellular Ca²⁺ ([Ca²⁺]_i) (**Figure 2A**). Even at low (10 nM) [Ca²⁺]_i, overexpression of TMEM16A increased hypotonic activation of endogenous VRAC and overexpressed LRRC8A/C (**Figures 2A,B**). This could suggest that Ca²⁺ influx is also relevant for activation of VRAC, as suggested earlier (Sirianant et al., 2016a).

We intended to perform similar experiments with overexpressed TMEM16A at 100 nM pipette Ca²⁺, to examine how the presence of TMEM16A would affect volume activation of VRAC. However, we found overexpressed TMEM16A to be active even at this basal intracellular Ca²⁺ concentration and without any additional Ca²⁺ increase by hormonal stimulation or by Ca²⁺ ionophores (**Figure 3**). In these experiments, we used CsCl buffer as patch pipette filling solution (100 nM Ca²⁺; 290 mosm/l) and an extracellular CsCl buffer (1.3 mM Ca²⁺; 300 mosm/l), to exclude any possible contribution of K⁺ currents. In contrast to mock-transfected cells, TMEM16A-overexpressing cells demonstrated a large basal Cl[−] inward current that was inhibited by removal of extracellular Cl[−], causing a right shift of the reversal potential (**Figures 3A,B**). Only overexpressed, but not endogenous TMEM16A, was found to be active at basal intracellular [Ca²⁺]_i levels, which has been examined in detail earlier (Sirianant et al., 2016a; Schreiber et al., 2018). Thus, it was difficult to assess the contribution of overexpressed TMEM16A to swelling activation of VRAC in HEK293 cells at [Ca²⁺]_i of 100 nM.

Overexpressed TMEM16A was not active under basal conditions with 10 nM intracellular Ca²⁺ (**Figure 2**). Overexpression of TMEM16A together with LRRC8A/C further

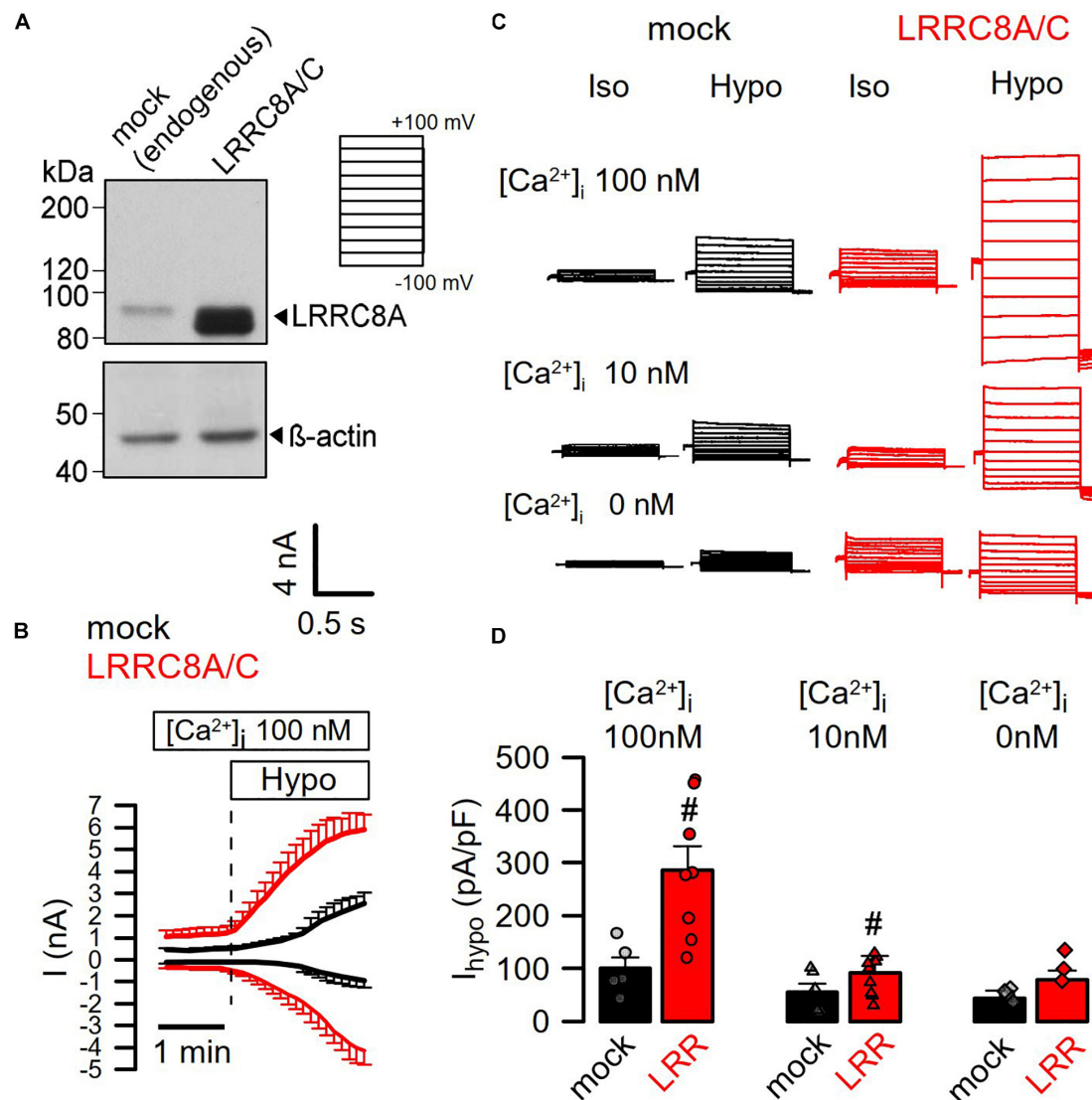


FIGURE 1 | Activation of LRRC8A/C is Ca²⁺ dependent. **(A)** Coexpression of LRRC8A and LRRC8C by a bicistronic vector. Detection of LRRC8A by Western blotting. **(B)** Continuous recording of whole-cell currents activated by hypotonic cell swelling (Hypo, 200 mosm/l). Patch pipette [Ca²⁺]_i was 100 nM; extracellular Ringer [Ca²⁺]_o was 1.3 mM. **(C)** Whole-cell current overlays obtained with 100, 10, or 0 nM Ca²⁺ in the patch pipette filling solution. Clamp voltages ranged from −100 to +100 mV in steps of 20 mV. **(D)** Summary of Hypo-induced whole-cell current densities (V_c = +100 mV) obtained in mock-transfected and LRRC8A/C-expressing HEK293 cells ($p < 0.001$ and < 0.01 , respectively). Mean ± SEM; $n = 5$ –9 for each series). [#]Significant increase when compared to mock (unpaired t -tests). Blots were done as replicates.

augmented $I_{Cl,swell}$, but it remained unclear whether TMEM16A itself is activated during cell swelling (by Ca²⁺ store release or Ca²⁺ influx) or whether TMEM16A supports activation of LRRC8A/C. We therefore performed additional experiments in HT₂₉ cells, which express both ion channels endogenously.

TMEM16A Supports Activation of $I_{Cl,swell}$ in HT₂₉ Cells Expressing Endogenous LRRC8 and TMEM16A

We reexamined the role of TMEM16A for activation of LRRC8/VRAC in HT₂₉ cells, which produce large endogenous

Ca²⁺-activated Cl[−] currents and swelling-activated VRAC currents (Centeio et al., 2020; **Figure 4**). As shown in **Figures 1, 2**, these experiments were performed with cytosolic-like pipette-filling solution (290 mosm/l, Ca²⁺ 100 nM, pH 7.2; c.f. Methods). The bath was perfused with Ringer solution (300 mosm/l; Ca²⁺ 1.3 mM, pH 7.4). siRNA knockdown of endogenous TMEM16A attenuated hypo-induced whole-cell currents and changed time-independent $I_{Cl,swell}$ to VRAC-typical time-dependent currents (**Figures 4A–D**). Notably, the blocker of TMEM16A, niclosamide (1 μM), inhibited $I_{Cl,swell}$ significantly from 182 ± 22 to 78 ± 9.2 pA/pF ($n = 5$). Knockdown of endogenous LRRC8A strongly attenuated

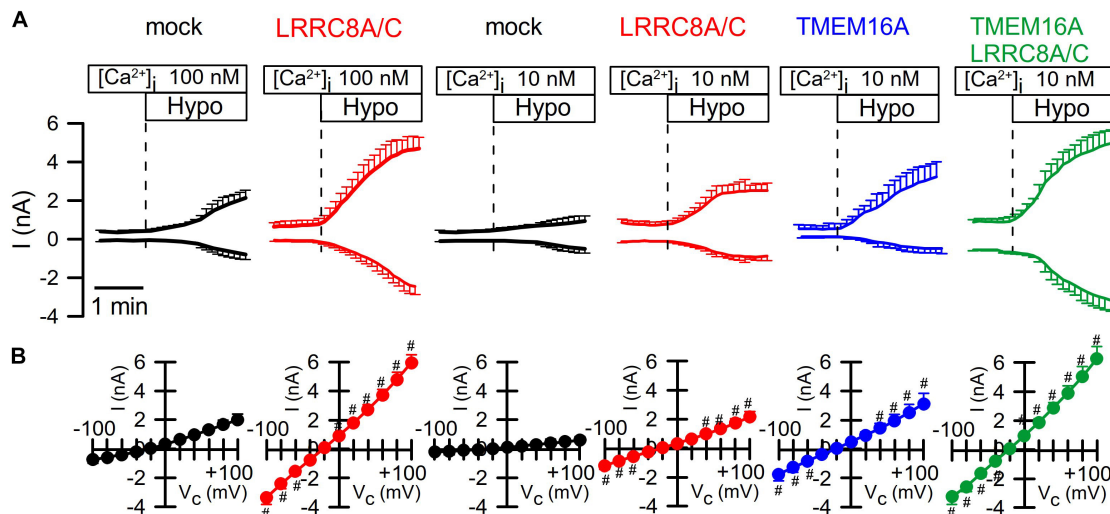


FIGURE 2 | TMEM16A is activated by Hypo and augments $I_{Cl,swell}$. **(A)** Continuous recording of whole cell currents activated in HEK293 cells by hypotonic cell swelling (Hypo, 200 mosm/l). **(B)** Current/voltage relationships of Hypo-activated whole-cell currents. TMEM16A is activated by Hypo and further augments $I_{Cl,swell}$ in cells coexpressing TMEM16A and LRRC8A/C. Mean \pm SEM; $n = 8-11$ for each series). #Significant increase when compared to mock ($p < 0.05-0.0001$; unpaired t -tests).

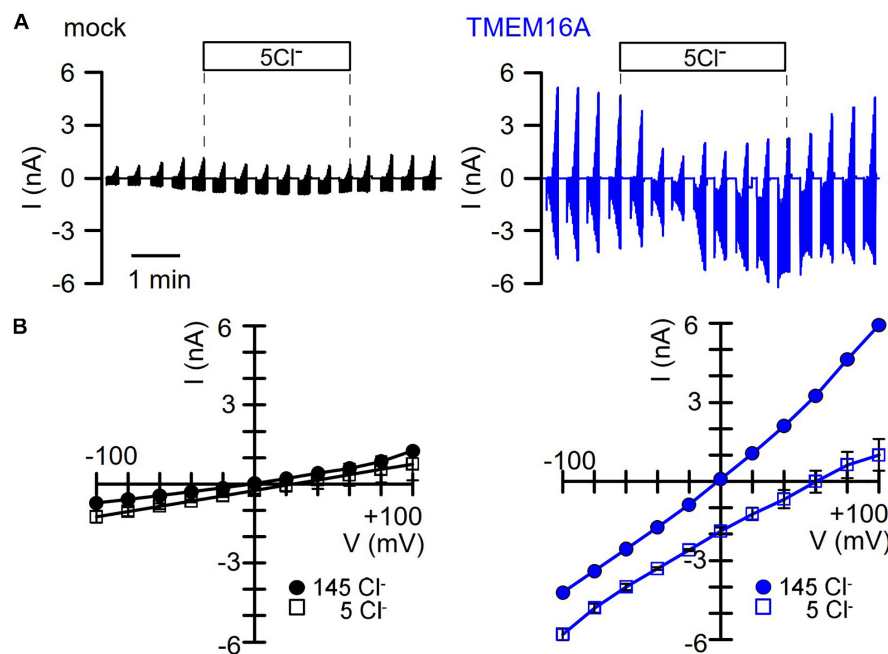
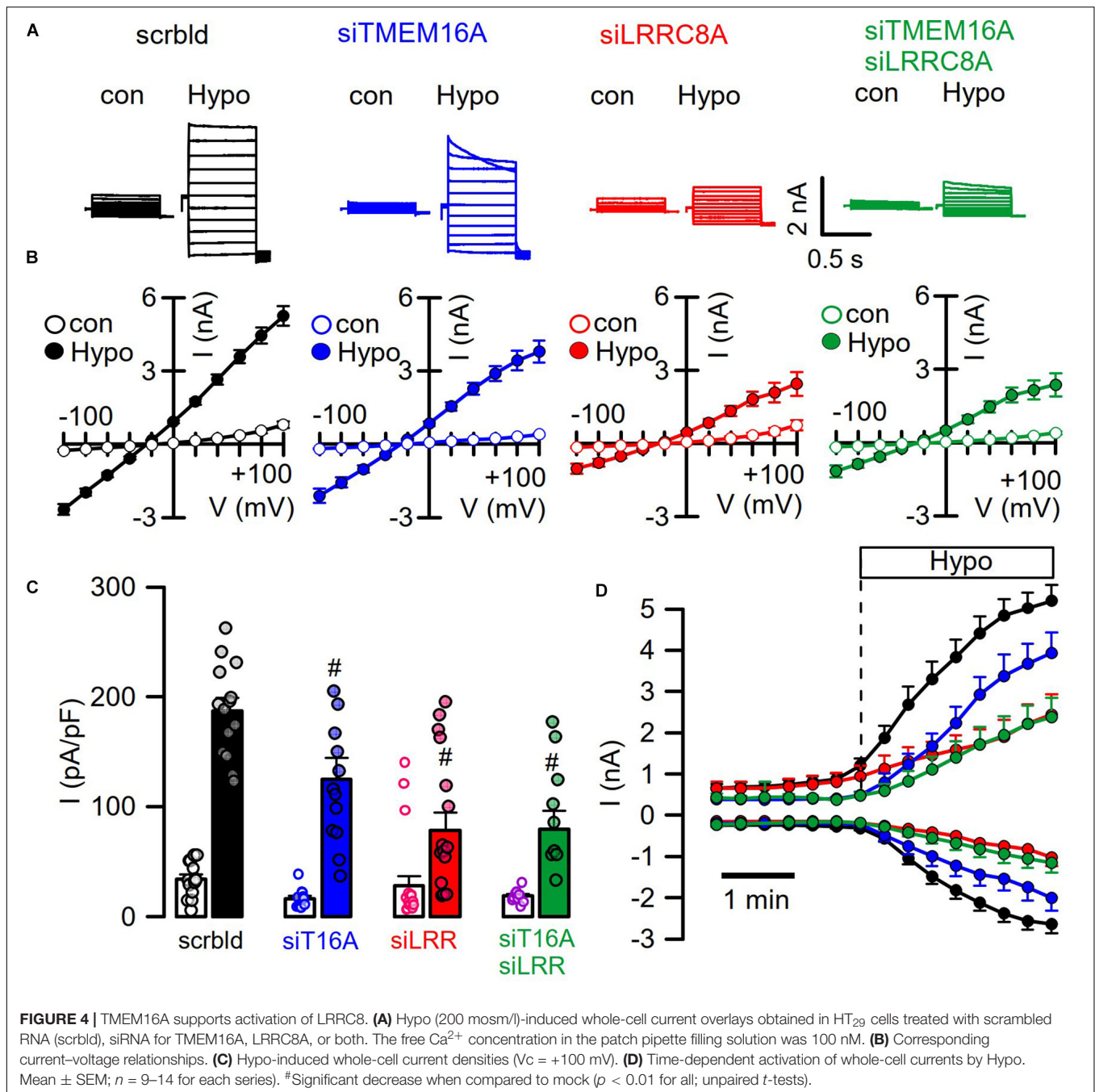


FIGURE 3 | TMEM16A overexpressed in HEK293 cells is spontaneously active. **(A)** Continuous current recordings of a mock-transfected and a TMEM16A-expressing HEK293 cell. In these experiments, the pipette filling solution and the bath solution contained CsCl (c.f. Methods). Cl⁻ removal from the extracellular bath solution except of 5 mM (5Cl⁻) had very little effect on the mock-transfected cell but strongly depolarized the TMEM16A-expressing cell. **(B)** Corresponding I/V curves indicate small currents and little effect of 5Cl⁻ in mock-transfected cells, while currents were large and strongly inhibited with a shift of the reversal potential in TMEM16A-overexpressing cells.

$I_{Cl,swell}$, while additional knockout of TMEM16A did not further attenuate $I_{Cl,swell}$. These data suggest that TMEM16A expressed in HT₂₉ cells supports activation of LRRC8/VRAC, probably by facilitating hypo-induced Ca²⁺ release from ER Ca²⁺ stores.

The contribution of TMEM16A to swelling activation of endogenous VRAC was examined in mock-transfected HEK293 cells (-T16A) or HEK293 cells overexpressing TMEM16A (+T16A) at different extracellular hypotonicities. VRAC was activated by extracellular bath solution of different hypotonicities



(275, 240, 200, and 150 mosm/l). The data demonstrate an increase in hypotonic activation of VRAC by coexpression of TMEM16A, which was more significant at less severe hypotonicity (**Supplementary Figure S1**). These experiments were performed at 10 nM intracellular Ca²⁺ concentration.

Contribution of TMEM16A to I_{Cl,swell} Under Non-voltage Clamp Conditions

As cell swelling and volume regulation take place under non-voltage clamp conditions, we examined the role of

TMEM16A for activation of I_{Cl,swell} in iodide quenching experiments using halide-sensitive yellow fluorescent protein (YFP). When applying hypotonic bath solution (200 mosm/l), immediate increase in YFP-fluorescence is expected due to rapid uptake of water through aquaporins, dilutions of anions, and de-quenching of YFP fluorescence, which occurs within seconds (Benedetto et al., 2016). This is followed by iodide-induced quenching, as VRAC channels are swelling activated, thus allowing entry of iodide (**Figure 6B**). Analysis of the maximal rate of quenching showed a clear activation of halide conductance by Hypo (**Figure 6C**). siRNA knockdown

of TMEM16A or LRRC8A (**Figures 6A,D**) showed similar results as in patch-clamp experiments: Knockdown of TMEM16A attenuated the Hypo-induced quenching, while it did not further reduce quenching inhibited by siLRRC8A (**Figures 6E,F**). It should be noted that in previous studies we observed an inverse correlation between expression of TMEM16A and LRRC8A. For example, TMEM16A was found to be strongly upregulated in cells that lacked expression of LRRC8A (Benedetto et al., 2016). Thus, it may not be surprising to find that LRRC8A was less efficiently downregulated with parallel knockdown of TMEM16A (Western blot in **Figure 6A**).

Hypotonicity Activates TMEM16A-Dependent Ca^{2+} Increase

When analyzing instantaneous peak current densities, the VRAC blocker DCPIB inhibited $I_{\text{Cl,swell}}$ independent of siRNA-TMEM16A, while siRNA-LRRC8A strongly inhibited instantaneous peak currents (**Figure 5A**). However, knockdown of TMEM16A induced pronounced time-dependent inactivation of $I_{\text{Cl,swell}}$, and the same was observed for knockdown of TMEM16F (Sirianant et al., 2016a; **Figure 5B**). Notably, TMEM16F has also been reported to conduct Ca^{2+} ions, apart from its ability to scramble phospholipids (Yang et al., 2012). Thus, TMEM16 proteins maintain $I_{\text{Cl,swell}}$ activity, possibly by supporting ER Ca^{2+} release and through activation of Ca^{2+} influx (Benedetto et al., 2016; Cabrita et al., 2017). To further elucidate the contribution of Ca^{2+} store release to activation of $I_{\text{Cl,swell}}$, cells were swollen in the presence of IP3R-inhibitor 2-ABP or the RyR inhibitor dantrolene, which both inhibited $I_{\text{Cl,swell}}$ (**Figure 5C**). Activation of CaCC in HT₂₉ cells by the purinergic ligand ATP was entirely dependent on TMEM16A, as shown by siRNA-TMEM16A, and knockdown of LRRC8A did not compromise activation of CaCC (**Figures 5D,E**). This indicates that Ca^{2+} increase alone is not sufficient to activate VRAC/LRRC8A. Unlike stimulation of $I_{\text{Cl,swell}}$, activation of CaCC was only inhibited by 2-ABP, but not by dantrolene (**Figure 5F**). Using the Ca^{2+} sensor Fura-2, we examined how TMEM16A affects Ca^{2+} increase induced by ATP and Hypo (200 mosm/l). ATP induced a typical peak (ER- Ca^{2+} store release) and plateau (Ca^{2+} influx; SOCE) response, which were both inhibited in the absence of TMEM16A (Cabrita et al., 2017; **Figure 5G**). The Hypo-induced Ca^{2+} increase was much smaller but was also inhibited by siRNA-TMEM16A (**Figure 5H**). Taken together, the data demonstrate the role of TMEM16A for swelling-induced Ca^{2+} increase, which is important for full activation of $I_{\text{Cl,swell}}$.

In additional experiments, we varied the iodide concentration in the hypotonic bath solution between 0 and 50 mM (**Figures 6G,H**). It is shown that at 0 mM iodide, no quenching takes place but only cell swelling, as indicated by an increase in fluorescence. With increasing iodide concentrations in the extracellular buffer, the maximum of YFP dequenching is no longer reached and the rate of YFP quenching increases. The data suggest a very fast activation of VRAC, which probably parallels the decrease in intracellular ionic strength

(Syeda et al., 2016). In contrast, the regulatory volume decrease (RVD) takes considerably longer as indicated by the delayed YFP—re-quenching in the presence of 0 mM iodide.

We examined concentration-dependent quenching by ATP and found pronounced inhibition of quenching by siRNA-TMEM16A (**Figures 7A,B**). Notably, at pronounced stimulation with saturating concentrations of ATP (50, 100 μM), ATP-induced quenching was slightly but significantly inhibited by siLRRC8A. This suggests a contribution of VRAC to ATP-induced halide permeability. We examined the effects of a number of different inhibitors on activation of $I_{\text{Cl,swell}}$ by testing them individually in HT₂₉ cells. We decided to analyze the effects of the various inhibitors in YFP-quenching experiments with non-dialyzed cells and under non-voltage clamp conditions (instead of whole-cell patch clamping), to leave intracellular Ca^{2+} signaling untouched and to avoid artifacts due to voltage clamping.

Three different inhibitors of IP3R-mediated ER Ca^{2+} -store release, xestospongin C, suramin, and probenecid, blocked ATP-induced activation of halide permeability (**Figure 7C**). Hypo (200 mosm/l)-induced quenching was blocked by the VRAC blocker DCPIB, but not by the TMEM16A blocker Ani9 (Seo et al., 2016), suggesting that the presence of TMEM16A, but not its Cl^- conductance, supports activation of $I_{\text{Cl,swell}}$ (**Figure 7D**). Surprisingly, the inhibitory effect of DCPIB on Hypo-induced quenching, i.e., activation of VRAC, was rather weak. However, this is probably explained by the strong voltage dependence of VRAC inhibition by DCPIB. During YFP measurements, DCPIB was applied under non-voltage clamp conditions, i.e., at the intrinsic negative membrane voltage of the HT₂₉ cells, which is around -40 mV. In additional patch-clamp experiments, we found indeed weak inhibition of VRAC by DCPIB at negative clamp voltages but a much more pronounced inhibition at depolarized clamp voltages (**Supplementary Figure S2**). The cystic fibrosis transmembrane conductance regulator (CFTR), another Cl^- channel expressed in HT₂₉ cells, is unlikely to contribute to $I_{\text{Cl,swell}}$, as the CFTR inhibitor CFTRinh172 (30 μM) did not inhibit activation of VRAC (data not shown).

A number of compounds inhibiting IP3R- and RyR-mediated ER Ca^{2+} -store release, such as suramin, U73122, probenecid, and dantrolene, as well as NS3728 (Helix et al., 2003), inhibited activation of $I_{\text{Cl,swell}}$. HT₂₉ cells were found to express all three paralogs of the IP3 receptor as well as the ryanodine receptor RyR2, along with the TRPV4 channel, which is the Ca^{2+} influx channel most frequently found to have a role in volume regulation (Pasantes-Morales, 2016; **Supplementary Figure S3**). The contribution of Ca^{2+} influx for activation of VRAC was demonstrated by exposing the cells to hypotonic solution in the presence of low (1 μM) extracellular Ca^{2+} , which attenuated the activation of VRAC (**Figures 7E,F**). Taken together, Ca^{2+} may not be a prerequisite for activation of VRAC. However, Ca^{2+} store release and Ca^{2+} influx facilitate its activation, which is in line with earlier observations (Akita et al., 2011; Sirianant et al., 2016a; Liu et al., 2019). TMEM16A facilitates intracellular compartmentalized Ca^{2+} increase and thus supports activation of VRAC. Along with swelling activation of VRAC, TMEM16A

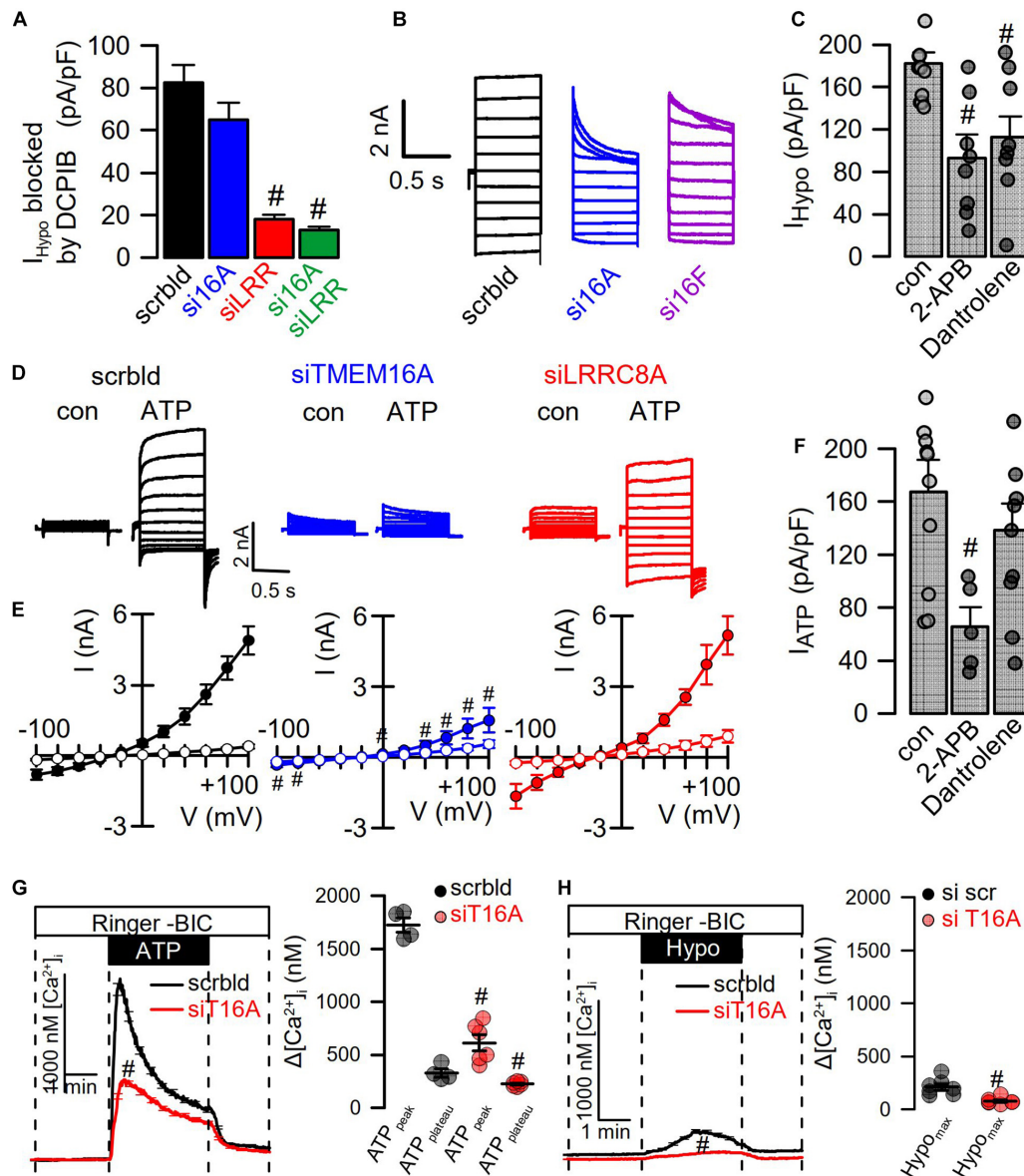


FIGURE 5 | Hypotonicity activates TMEM16A-dependent Ca^{2+} increase. **(A)** Summary of Hypo (200 mosm/l)-induced current densities inhibited by DCPIB in HT₂₉ cells ($n = 9-15$). The free Ca^{2+} concentration in the patch pipette filling solution was 100 nM. **(B)** Hypo-induced whole-cell current overlays in HT₂₉ cells treated with scrambled RNA (scrbld), siRNA for TMEM16A, or both TMEM16F. **(C)** Effect of 2-APB (50 μM ; $p < 0.001$) and dantrolene (50 μM ; $p < 0.001$) on Hypo-induced currents densities ($V_c = +100$ mV) ($n = 9-11$). **(D)** ATP (100 μM)-induced whole-cell current overlays in the absence or presence of siRNAs. **(E)** Corresponding current-voltage relationships ($n = 9-11$). **(F)** Effect of 2-APB (50 μM ; $p < 0.001$) and dantrolene (50 μM) on ATP-induced current densities ($V_c = +100$ mV) ($n = 7-9$). **(G)** Effect of TMEM16A-siRNA on ATP-induced Ca^{2+} -increase ($n = 21-45$; $p < 0.000004$ and $p < 0.01$, respectively). **(H)** Effect of TMEM16A-siRNA on Hypo-induced Ca^{2+} -increase ($n = 21-55$; $p < 0.003$). Plateau Ca^{2+} was determined at the end of the plateau. Mean \pm SEM; # significant decrease (unpaired t -test).

is activated through swelling-induced rise in intracellular Ca^{2+} . The extent of this coregulation of $I_{\text{Cl,swell}}$ is cell dependent and depends on expression of TMEM16 proteins.

DISCUSSION

The present study examines activation of $I_{\text{Cl,swell}}$ in two different cell lines. HEK293 cells were used because these cells do

not express TMEM16A and express only very low levels of LRRC8A. Thus, the cell line was ideal to examine the effects of overexpressed TMEM16A and LRRC8A/C. In contrast, HT₂₉ cells express both TMEM16A and LRRC8A and show large ATP-stimulated, i.e., Ca^{2+} activated TMEM16A Cl^- currents and pronounced swelling-activated LRRC8A/VRAC Cl^- currents. LRRC8A (VRAC) and TMEM16A (CaCC) are independent molecular entities and Cl^- channels activated by cell swelling or intracellular Ca^{2+} . Although TMEM16 proteins are not VRACs

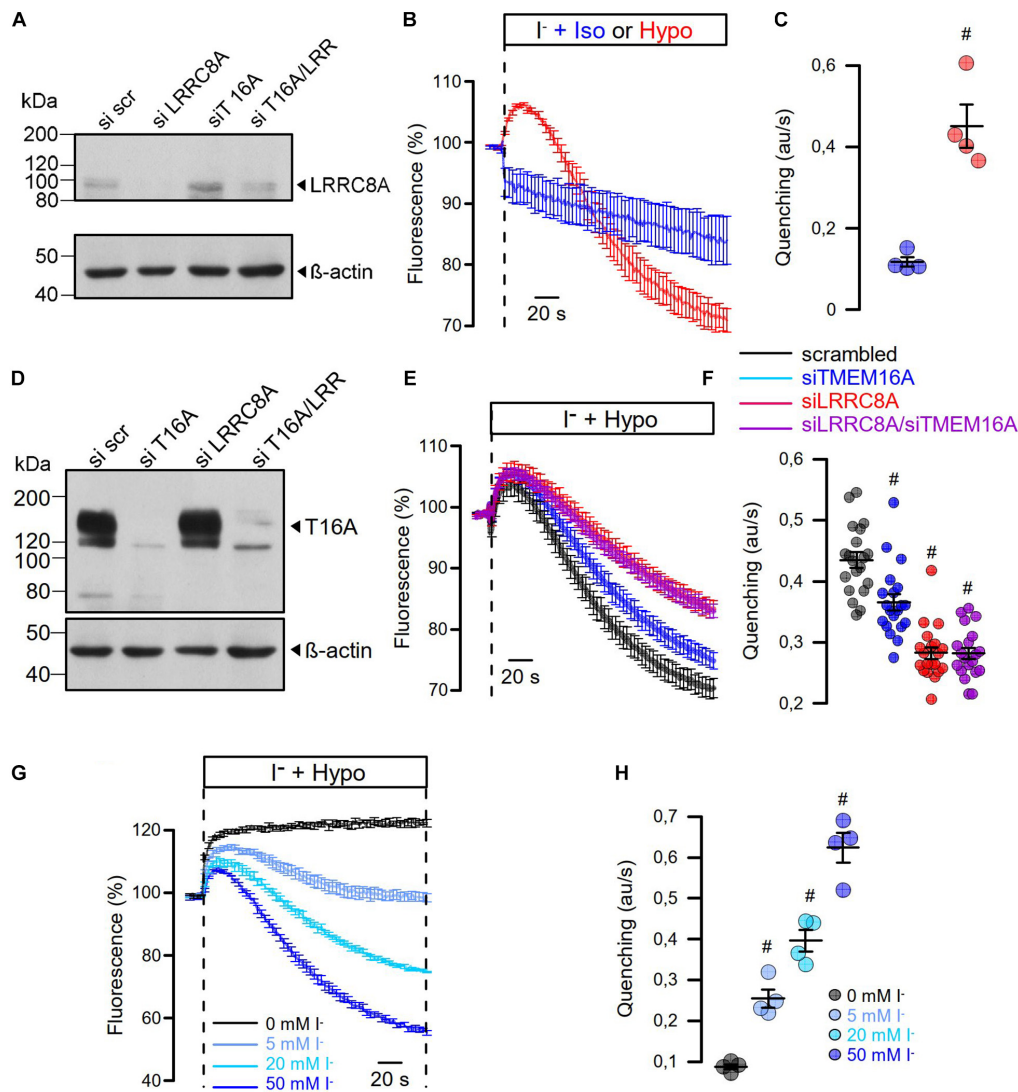


FIGURE 6 | Hypo-induced anion permeability measured under non-voltage clamp conditions. **(A)** siRNA knockdown of LRRRC8A detected by Western blotting. The knockdown efficiency was 72%. Knockdown of TMEM16A enhanced the expression of LRRRC8A, corresponding to Benedetto et al. (2016). **(B)** Summary of time dependence for YFP quenching induced by 20 mM iodide in the presence of isotonic Ringer (Iso; 300 mosmol/l) or Hypo (200 mosmol/l). **(C)** Summary of initial rate of quenching (arbitrary units/s) ($n = 4$; $p < 0.006$). **(D)** siRNA knockdown of TMEM16A detected by Western blotting. **(E)** Summary of time dependence for Hypo-induced YFP quenching in the absence or presence of siRNA. **(F)** Summary of initial rates of quenching (arbitrary units/s) ($n = 19$). $p < 0.0005$ (siTMEM16A), $p < 2 \times 10^{-11}$ (siLRRRC8A), $p < 2 \times 10^{-11}$ (siLRRRC8A/siTMEM16A). **(G,H)** Hypo-induced YFP quenching was absent in the presence of 0 mM extracellular iodide but was gradually increased with 5 mM ($n = 4$; $p < 0.003$), 20 mM ($n = 4$; $p < 0.0009$), and 50 mM ($n = 4$; $p < 0.0005$). Mean \pm SEM; # significant increase or decrease, respectively (unpaired t -test). Blots were done as replicates.

per se, previous data suggest a role in $I_{Cl,swell}$ (Almaca et al., 2009; Juul et al., 2014; Benedetto et al., 2016; Sirianant et al., 2016a; Liu et al., 2019; Zhang et al., 2020). Analysis of $I_{Cl,swell}$ in tissues from mice lacking expression of TMEM16A (Almaca et al., 2009), TMEM16F (Ousingsawat et al., 2015; Sirianant et al., 2016a), and TMEM16K (Hammer et al., 2015; Wanitchakool et al., 2017) shows reduced $I_{Cl,swell}$ and regulatory volume decrease (RVD). The contribution of TMEM16A and other TMEM16-proteins to $I_{Cl,swell}$ and volume regulation is cell dependent and may be particularly relevant in highly differentiated native (non-cultured) cells. Equally important appear the patch-clamp

conditions under which $I_{Cl,swell}$ are measured, which may explain some of the earlier controversial findings regarding the role of TMEM16F (Almaca et al., 2009; Shimizu et al., 2013; Juul et al., 2014; Sirianant et al., 2016a).

Patch-clamp experiments showed more impressive effects of TMEM16A (and TMEM16F) on activation of VRAC at depolarized clamp voltages. TMEM16A and TMEM16F mainly abolish time-dependent inactivation of VRAC. This has also been described in detail in a previous study (Sirianant et al., 2016a). Thus, the impact of TMEM16A is less remarkable at negative clamp voltages and under

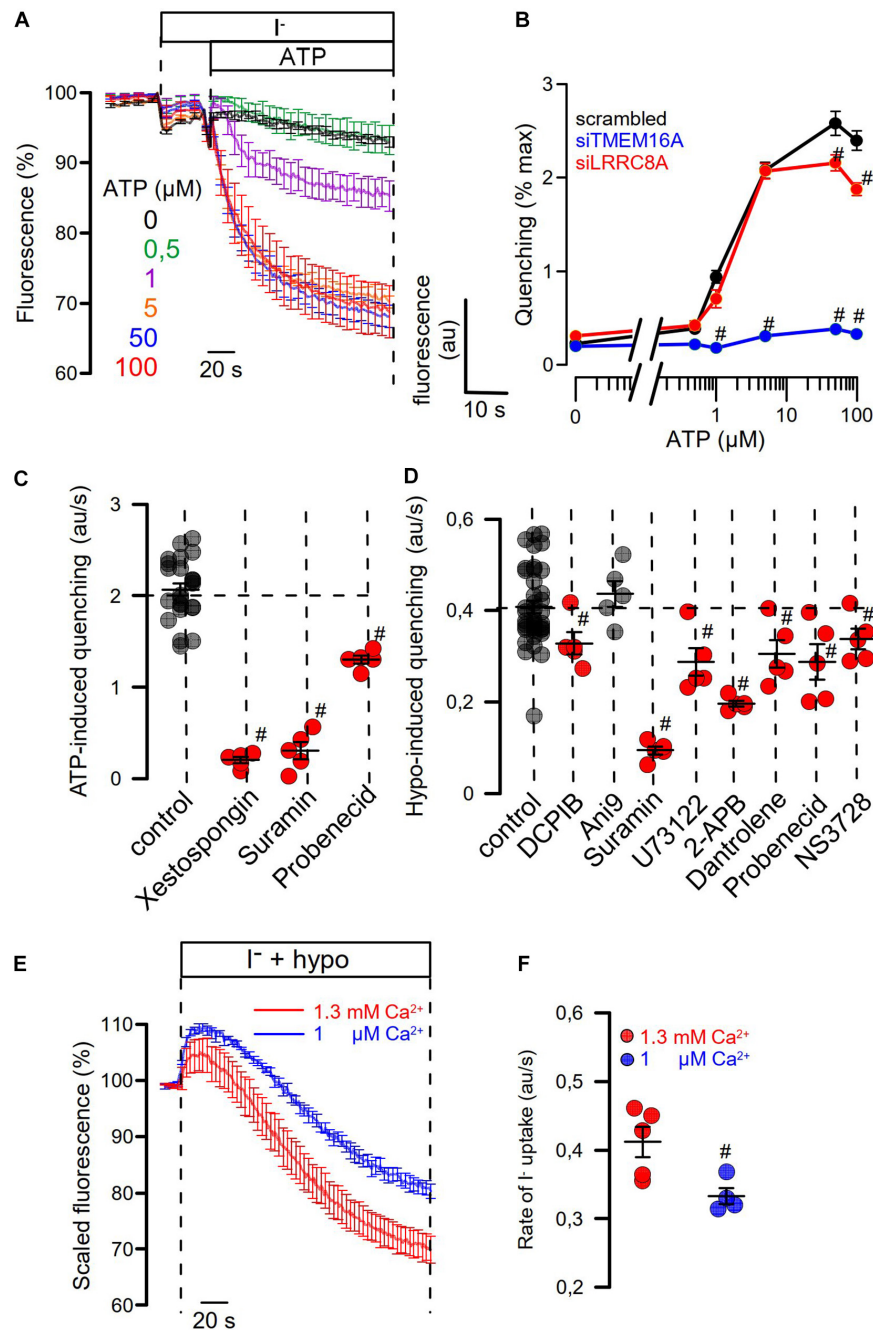


FIGURE 7 | Role of Ca^{2+} signaling for Hypo- and ATP-induced anion permeability. **(A)** Time-dependent YFP quenching induced by different concentrations of ATP ($n = 3-5$). **(B)** Concentration dependence of ATP-induced quenching (arbitrary units/s) and effects of knockdown of TMEM16A or LRRC8A ($n = 4$). **(C)** Summary of ATP-induced quenching in the absence (control) or presence of IP3R blockers xestospongine C (10 μM ; $p < 10^{-19}$), suramin (500 μM ; $p < 10^{-7}$), and probenecid (1 mM; $p < 2 \times 10^{-9}$) ($n = 4-5$). **(D)** Summary of Hypo (200 mosm/l)-induced quenching in the absence (control) or presence of DCPIB (30 μM ; $p < 0.02$), Anil9 (10 μM), suramin (500 μM ; $p < 2 \times 10^{-7}$), U73122 (10 μM ; $p < 0.01$), 2-APB (50 μM ; $p < 10^{-17}$), dantrolene (50 μM ; $p < 0.02$), probenecid (1 mM; $p < 0.03$), and NS3728 (10 μM ; $p < 0.03$) ($n = 4-5$). **(E,F)** The contribution of Ca^{2+} influx on Hypo-induced quenching was examined by exposing the cells to a hypotonic solution in the presence of physiological (1.3 mM; $n = 5$) or low (1 μM ; $n = 4$; $p < 0.02$) extracellular Ca^{2+} concentration. Mean \pm SEM; # significant inhibition (unpaired t -test).

non-voltage clamp conditions. Nevertheless, even at negative membrane voltages the impact of TMEM16A was found to be significant (Figure 6 and Supplementary Figure S4). While a number of transport properties were ascribed to LRRC8/VRAC

(Planells-Cases et al., 2015; Lutter et al., 2017; Kang et al., 2018; Stuhlmann et al., 2018; Zhou et al., 2020), its physiological relevance in terms of volume regulation is still a matter of debate. We found that cells are able to perform RVD also in the absence of

LRRC8A (Milenkovic et al., 2015; Benedetto et al., 2016; Sirianant et al., 2016b), while other different members of the TMEM16A family, CFTR, and the KCl cotransporter KCC clearly contribute to volume regulation (Sirianant et al., 2016b; Wanitchakool et al., 2016). We found that activation of $I_{Cl,swell}$ was fast (within 1 min), which, however, was still somewhat delayed when compared to immediate cell swelling (within seconds) (Benedetto et al., 2016). This suggested additional regulatory steps, apart from direct opening of VRAC by low ionic strength (Syeda et al., 2016). Others and we proposed Ca^{2+} -dependent unfolding of caveolae-like membrane reserves upon cell swelling and activation of $I_{Cl,swell}$ (Groulx et al., 2006; Kozera et al., 2009; Benedetto et al., 2016).

This additional mechanism may require Ca^{2+} increase in an intracellular compartment close to the plasma membrane (Akita et al., 2011; Benedetto et al., 2016; Liu et al., 2019). Liu et al. showed that intracellular Ca^{2+} was necessary but not sufficient to activate LRRC8A-mediated currents (Liu et al., 2019). Lemonnier and coworkers provided evidence for a colocalization of VRAC with store-operated Ca^{2+} channels and showed that activation of VRAC was strongly dependent on Ca^{2+} release through IP3R (Lemonnier et al., 2002). They concluded that VRAC is regulated within Ca^{2+} microdomains. Similarly, Akita and collaborators suggested that VRAC/VSOR channels can be activated by PLC-coupled GPCRs, which depends on Ca^{2+} store release in close vicinity of the channel (Akita and Okada, 2011) and proposed a Ca^{2+} nanodomain-mediated component of VRAC (Akita et al., 2011).

Our present data may help to clarify the role of TMEM16 proteins for Ca^{2+} -dependent activation of VRAC. The role of TMEM16A and other members of the TMEM16-family for ER Ca^{2+} release was found meanwhile in numerous tissues (Jin et al., 2016; Cabrita et al., 2017; Wanitchakool et al., 2017; Benedetto et al., 2019a; Centeio et al., 2020; Park et al., 2020). TMEM16A-controlled Ca^{2+} release is also essential for activation of CFTR (Benedetto et al., 2017, 2019b; Park et al., 2020). Thus, cell swelling-induced Ca^{2+} release from the ER and activation of VRAC is facilitated in the presence of TMEM16 proteins. Because knockdown of TMEM16A but not inhibition of TMEM16A by Ani9 attenuated activation of

VRAC, it suggests that ER-tethering by TMEM16A rather than Cl^- transport supports activation of VRAC (Jin et al., 2013; Cabrita et al., 2017).

Along this line, TMC8, a member of the closely related family of transmembrane channel-like TMC proteins, also controlled activation of VRAC and volume regulation (Sirianant et al., 2014). Depending on the cell type, swelling-induced Ca^{2+} release will activate TMEM16 proteins and CFTR (Thiele et al., 1998; Wanitchakool et al., 2016), which parallels activation of VRAC. This circumstance may explain many earlier findings, such as the overlapping Cl^- channel pharmacology (Koslosky et al., 1994; Rottgen et al., 2018; Centeio et al., 2020).

DATA AVAILABILITY STATEMENT

The raw data supporting the conclusions of this article will be made available by the authors, without undue reservation, to any qualified researcher.

AUTHOR CONTRIBUTIONS

RC, JO, and RS performed the experiments and analyzed the data. RC, RS, and KK wrote the manuscript. All authors contributed to the article and approved the submitted version.

FUNDING

This work was supported by the Deutsche Forschungsgemeinschaft (DFG, German Research Foundation) project number 387509280, SFB 1350 (project A3), DFG KU756/14-1, and UK CF Trust SRC013.

SUPPLEMENTARY MATERIAL

The Supplementary Material for this article can be found online at: <https://www.frontiersin.org/articles/10.3389/fcell.2020.596879/full#supplementary-material>

REFERENCES

- Akita, T., Fedorovich, S. V., and Okada, Y. (2011). Ca^{2+} nanodomain-mediated component of swelling-induced volume-sensitive outwardly rectifying anion current triggered by autocrine action of ATP in mouse astrocytes. *Cell Physiol. Biochem.* 28, 1181–1190. doi: 10.1159/000335867
- Akita, T., and Okada, Y. (2011). Regulation of bradykinin-induced activation of volume-sensitive outwardly rectifying anion channels by Ca^{2+} nanodomains in mouse astrocytes. *J. Physiol.* 589, 3909–3927. doi: 10.1113/jphysiol.2011.208173
- Almaca, J., Tian, Y., Aldehni, F., Ousingsawat, J., Kongsuphol, P., Rock, J. R., et al. (2009). TMEM16 proteins produce volume regulated chloride currents that are reduced in mice lacking TMEM16A. *J. Biol. Chem.* 284, 28571–28578. doi: 10.1074/jbc.M109.010074
- Benedetto, R., Cabrita, I., Schreiber, R., and Kunzelmann, K. (2019a). TMEM16A is indispensable for basal mucus secretion in airways and intestine. *FASEB J.* 33, 4502–4512. doi: 10.1096/fj.201801333rrr
- Benedetto, R., Ousingsawat, J., Cabrita, I., Pinto, M., Lérias, J., Wanitchakool, P., et al. (2019b). Plasma membrane localized TMEM16 Proteins are Indispensable for expression of CFTR. *J. Mol. Med.* 97, 711–722. doi: 10.1007/s00109-019-01770-4
- Benedetto, R., Ousingsawat, J., Wanitchakool, P., Zhang, Y., Holtzman, M. J., Amaral, M., et al. (2017). Epithelial chloride transport by CFTR requires TMEM16A. *Sci. Rep.* 7:12397. doi: 10.1038/s41598-017-10910-0
- Benedetto, R., Sirianant, L., Pankonien, I., Wanitchakool, P., Ousingsawat, J., Cabrita, I., et al. (2016). Relationship between TMEM16A/anoctamin 1 and LRRC8A. *Pflugers Arch.* 468, 1751–1763. doi: 10.1007/s00424-016-1862-1
- Cabrita, I., Benedetto, R., Fonseca, A., Wanitchakool, P., Sirianant, L., Skryabin, B. V., et al. (2017). Differential effects of anoctamins on intracellular calcium signals. *Faseb J.* 31, 2123–2134. doi: 10.1096/fj.201600797rr
- Cannon, C. L., Basavappa, S., and Strange, K. (1998). Intracellular ionic strength regulates the volume sensitivity of a swelling-activated anion channel. *Am. J. Physiol.* 275, C416–C422. doi: 10.1152/ajpcell.1998.275.2.C416

- Centeio, R., Cabrita, I., Benedetto, R., Talbi, K., Ousingsawat, J., Schreiber, R., et al. (2020). Pharmacological inhibition and activation of the Ca(2+) activated Cl(−) channel TMEM16A. *Int. J. Mol. Sci.* 21:2557. doi: 10.3390/ijms21072557
- Deneka, D., Sawicka, M., Lam, A. K. M., Paulino, C., and Dutzler, R. (2018). Structure of a volume-regulated anion channel of the LRRC8 family. *Nature* 558, 254–259. doi: 10.1038/s41586-018-0134-y
- Groulx, N., Boudreault, F., Orlov, S. N., and Grygorczyk, R. (2006). Membrane reserves and hypotonic cell swelling. *J. Membr. Biol.* 214, 43–56. doi: 10.1007/s00232-006-0080-8
- Gulbins, E., Jekle, A., Ferlinz, K., Grassme, H., and Lang, F. (2000). Physiology of apoptosis. *Am. J. Physiol. Renal. Physiol.* 279, F605–F615. doi: 10.1152/ajprenal.2000.279.4.F605
- Hammer, C., Wanitchakool, P., Sirianant, L., Papiol, S., Monnheimer, M., Faria, D., et al. (2015). A coding variant of ANO10, affecting volume regulation of macrophages, is associated with Borrelia seropositivity. *Mol. Med.* 21, 26–37. doi: 10.2119/molmed.2014.00219
- Helix, N., Strobaek, D., Dahl, B. H., and Christophersen, P. (2003). Inhibition of the endogenous volume-regulated anion channel (VRAC) in HEK293 cells by acidic di-aryl-ureas. *J. Membr. Biol.* 196, 83–94. doi: 10.1007/s00232-003-0627-x
- Ise, T., Shimizu, T., Lee, E. L., Inoue, H., Kohno, K., and Okada, Y. (2005). Roles of volume-sensitive Cl[−] channel in cisplatin-induced apoptosis in human epidermoid cancer cells. *J. Membr. Biol.* 205, 139–145. doi: 10.1007/s00232-005-0779-y
- Jentsch, T. J. (2016). VRACs and other ion channels and transporters in the regulation of cell volume and beyond. *Nat. Rev. Mol. Cell Biol.* 10, 293–307. doi: 10.1038/nrm.2016.29
- Jin, X., Shah, S., Du, X., Zhang, H., and Gamper, N. (2016). Activation of Ca²⁺-activated Cl[−] channel ANO1 by localized Ca²⁺ signals. *J. Physiol.* 594, 19–30. doi: 10.1113/jphysiol.2014.275107
- Jin, X., Shah, S., Liu, Y., Zhang, H., Lees, M., Fu, Z., et al. (2013). Activation of the Cl[−] Channel ANO1 by Localized Calcium Signals in Nociceptive Sensory Neurons Requires Coupling with the IP3 Receptor. *Sci. Signal.* 6:ra73. doi: 10.1126/scisignal.2004184
- Juul, C. A., Grubb, S., Poulsen, K. A., Kyed, T., Hashem, N., Lambert, I. H., et al. (2014). Anoctamin 6 differs from VRAC and VSOAC but is involved in apoptosis and supports volume regulation in the presence of Ca. *Pflugers Arch.* 466, 1899–1910. doi: 10.1007/s00424-013-1428-4
- Kang, C., Xie, L., Gunasekar, S. K., Mishra, A., Zhang, Y., Pai, S., et al. (2018). SWELL1 is a glucose sensor regulating beta-cell excitability and systemic glycaemia. *Nat. Commun.* 9:367. doi: 10.1038/s41467-017-02664-0
- Kasuya, G., Nakane, T., Yokoyama, T., Jia, Y., Inoue, M., Watanabe, K., et al. (2018). Cryo-EM structures of the human volume-regulated anion channel LRRC8. *Nat. Struct. Mol. Biol.* 25, 797–804. doi: 10.1038/s41594-018-0109-6
- Kefauver, J. M., Saotome, K., Dubin, A. E., Pallesen, J., Cottrell, C. A., Cahalan, S. M., et al. (2018). Structure of the human volume regulated anion channel. *eLife* 7:e38461. doi: 10.7554/eLife.38461.026
- Kern, D. M., Oh, S., Hite, R. K., and Brohawn, S. G. (2019). Cryo-EM structures of the DCPIB-inhibited volume-regulated anion channel LRRC8A in lipid nanodiscs. *eLife* 8:e42636.
- Koslowsky, T., Hug, T., Ecke, D., Klein, P., Greger, R., Gruenert, D. C., et al. (1994). Ca²⁺ and swelling induced activation of ion conductances in bronchial epithelial cells. *Pflugers Arch.* 428, 597–603. doi: 10.1007/bf00374583
- Kozera, L., White, E., and Calaghan, S. (2009). Caveolae act as membrane reserves which limit mechanosensitive I(Cl,swell) channel activation during swelling in the rat ventricular myocyte. *PLoS One* 4:e8312. doi: 10.1371/journal.pone.0008312
- Kunzelmann, K., Ousingsawat, J., Benedetto, R., Cabrita, I., and Schreiber, R. (2019). Contribution of anoctamins to cell survival and cell death. *Cancers* 19, E382.
- Lemonnier, L., Prevarskaya, N., Shuba, Y., Vanden Abeele, F., Nilius, B., Mazurier, J., et al. (2002). Ca²⁺ modulation of volume-regulated anion channels: evidence for colocalization with store-operated channels. *FASEB J.* 16, 222–224.
- Lemonnier, L., Shuba, Y., Crepin, A., Roudbaraki, M., Slomianny, C., Mauroy, B., et al. (2004). Bcl-2-dependent modulation of swelling-activated Cl[−] current and ClC-3 expression in human prostate cancer epithelial cells. *Cancer Res.* 64, 4841–4848. doi: 10.1158/0008-5472.can-03-3223
- Liu, T., and Stauber, T. (2019). The volume-regulated anion channel LRRC8/VRAC is dispensable for cell proliferation and migration. *Int. J. Mol. Sci.* 20:2663. doi: 10.3390/ijms20112663
- Liu, Y., Zhang, H., Men, H., Du, Y., Xiao, Z., Zhang, F., et al. (2019). Volume-regulated Cl(−) current: contributions of distinct Cl(−) channel and localized Ca(2+) signals. *Am. J. Physiol. Cell Physiol.* 317, C466–C480.
- Lu, P., Ding, Q., Li, X., Ji, X., Li, L., Fan, Y., et al. (2019). SWELL1 promotes cell growth and metastasis of hepatocellular carcinoma in vitro and in vivo. *EBioMedicine* 48, 100–116. doi: 10.1016/j.ebiom.2019.09.007
- Lutter, D., Ullrich, F., Lueck, J. C., Kempa, S., and Jentsch, T. J. (2017). Selective transport of neurotransmitters and modulators by distinct volume-regulated LRRC8 anion channels. *J. Cell Sci.* 130, 1122–1133.
- Mahmud, H., Foller, M., and Lang, F. (2008). Suicidal erythrocyte death triggered by cisplatin. *Toxicology* 249, 40–44. doi: 10.1016/j.tox.2008.04.003
- Mccarty, N. A., and O'neil, R. G. (1992). Calcium signalling in volume regulation. *Physiol. Rev.* 72, 1037–1061.
- Milenkovic, A., Brandl, C., Milenkovic, V. M., Jendrike, T., Sirianant, L., Wanitchakool, P., et al. (2015). Bestrophin1 is the volume-regulated anion channel in mouse sperm and human retinal pigment epithelium. *Proc. Natl. Acad. Sci. U.S.A.* 112, E2630–E2639.
- Okada, Y., Shimizu, T., Maeno, E., Tanabe, S., Wang, X., and Takahashi, N. (2006). Volume-sensitive chloride channels involved in apoptotic volume decrease and cell death. *J. Membr. Biol.* 209, 21–29. doi: 10.1007/s00232-005-0836-6
- Ousingsawat, J., Wanitchakool, P., Kmit, A., Romao, A. M., Jantarajit, W., Schreiber, S., et al. (2015). Anoctamin 6 mediates effects essential for innate immunity downstream of P2X7-receptors in macrophages. *Nat. Commun.* 6:6245.
- Park, J. H., Ousingsawat, J., Cabrita, I., Bettels, R. E., Große-Onnebrink, J., Schmalstieg, C., et al. (2020). TMEM16A deficiency: a potentially fatal neonatal disease resulting from impaired chloride currents. *J. Med. Genet.* jmedgenet-2020-106978. [Epub ahead of print].
- Pasantes-Morales, H. (2016). Channels and volume changes in the life and death of the cell. *Mol. Pharmacol.* 90, 358–370. doi: 10.1124/mol.116.104158
- Pedersen, S. F., Okada, Y., and Nilius, B. (2016). Biophysics and physiology of the volume-regulated anion channel (VRAC)/volume-sensitive outwardly rectifying anion channel (VSOR). *Pflugers Arch.* 468, 371–383. doi: 10.1007/s00424-015-1781-6
- Planells-Cases, R., Lutter, D., Guyader, C., Gerhards, N. M., Ullrich, F., Elger, D. A., et al. (2015). Subunit composition of VRAC channels determines substrate specificity and cellular resistance to Pt-based anti-cancer drugs. *EMBO J.* 34, 2993–3008. doi: 10.15252/embj.201592409
- Qiu, Z., Dubin, A. E., Mathur, J., Tu, B., Reddy, K., Miraglia, L. J., et al. (2014). SWELL1, a plasma membrane protein, is an essential component of volume-regulated anion channel. *Cell* 157, 447–458. doi: 10.1016/j.cell.2014.03.024
- Rottgen, T. S., Nickerson, A. J., and Rajendran, V. M. (2018). Calcium-activated Cl(−) Channel: insights on the molecular identity in epithelial tissues. *Int. J. Mol. Sci.* 19:1432. doi: 10.3390/ijms19051432
- Sabirov, R. Z., Prenen, J., Tomita, T., Droogmans, G., and Nilius, B. (2000). Reduction of ionic strength activates single volume-regulated anion channels (VRAC) in endothelial cells. *Pflugers Arch.* 439, 315–320. doi: 10.1007/s004240050945
- Schreiber, R., Ousingsawat, J., Wanitchakool, P., Sirianant, L., Benedetto, R., Reiss, K., et al. (2018). Regulation of TMEM16A/ANO1 and TMEM16F/ANO6 ion currents and phospholipid scrambling by Ca²⁺ and plasma membrane lipid. *J. Physiol.* 596, 217–229. doi: 10.1113/jp275175
- Seo, Y., Lee, H. K., Park, J., Jeon, D. K., Jo, S., Jo, M., et al. (2016). Ani9, a novel potent small-molecule ANO1 inhibitor with negligible effect on ANO2. *PLoS One* 11:e0155771. doi: 10.1371/journal.pone.0155771
- Shimizu, T., Iehara, T., Sato, K., Fujii, T., Sakai, H., and Okada, Y. (2013). TMEM16F is a component of a Ca²⁺-activated Cl[−] channel but not a volume-sensitive outwardly rectifying Cl[−] channel. *Am. J. Physiol. Cell Physiol.* 304, C748–C759.
- Simmons, N. L. (1990). A cultured human renal epithelioid cell line responsive to vasoactive intestinal peptide. *Exp. Physiol.* 75, 309–319. doi: 10.1113/expphysiol.1990.sp003406
- Sirianant, L., Ousingsawat, J., Tian, Y., Schreiber, R., and Kunzelmann, K. (2014). TMC8 (EVER2) attenuates intracellular signaling by Zn²⁺ and Ca²⁺ and

- suppresses activation of Cl⁻ currents. *Cell Signal.* 26, 2826–2833. doi: 10.1016/j.cellsig.2014.09.001
- Sirianant, L., Ousingsawat, J., Wanitchakool, P., Schreiber, R., and Kunzelmann, K. (2016a). Cellular Volume regulation by Anoctamin 6:Ca²⁺, phospholipase A₂, osmosensing. *Pflügers Arch.* 468, 335–349. doi: 10.1007/s00424-015-1739-8
- Sirianant, L., Wanitchakool, P., Ousingsawat, J., Benedetto, R., Zormpa, A., Cabrita, I., et al. (2016b). Non-essential contribution of LRRC8A to volume regulation. *Pflügers Arch.* 468, 1789–1796.
- Strange, K., Yamada, T., and Denton, J. S. (2019). A 30-year journey from volume-regulated anion currents to molecular structure of the LRRC8 channel. *J. Gen. Physiol.* 151, 100–117. doi: 10.1085/jgp.201812138
- Stuhlmann, T., Planells-Cases, R., and Jentsch, T. J. (2018). LRRC8/VRAC anion channels enhance beta-cell glucose sensing and insulin secretion. *Nat. Commun.* 9:1974.
- Syeda, R., Qiu, Z., Dubin, A. E., Murthy, S. E., Florendo, M. N., Mason, D. E., et al. (2016). LRRC8 proteins form volume-regulated anion channels that sense ionic strength. *Cell* 164, 499–511. doi: 10.1016/j.cell.2015.12.031
- Thiele, I. E., Hug, M. J., Hübner, M., and Greger, R. (1998). Expression of cystic fibrosis transmembrane conductance regulator alters the response to hypotonic cell swelling and ATP of chinese hamster ovary cells. *Cell Physiol. Biochem.* 8, 61–74. doi: 10.1159/000016271
- Von Kleist, S., Chany, E., Burtin, P., King, M., and Fogh, J. (1975). Immunohistology of the antigenic pattern of a continuous cell line from a human colon tumor. *J. Natl. Cancer Inst.* 55, 555–560. doi: 10.1093/jnci/55.3.555
- Voss, F. K., Ullrich, F., Munch, J., Lazarow, K., Lutter, D., Mah, N., et al. (2014). Identification of LRRC8 heteromers as an essential component of the volume-regulated anion channel VRAC. *Science* 344, 634–638. doi: 10.1126/science.1252826
- Wanitchakool, P., Ousingsawat, J., Sirianant, L., Cabrita, I., Faria, D., Schreiber, R., et al. (2017). Cellular defects by deletion of ANO10 are due to deregulated local calcium signaling. *Cell Signal.* 30, 41–49. doi: 10.1016/j.cellsig.2016.11.006
- Wanitchakool, P., Ousingsawat, J., Sirianant, L., Macaulay, N., Schreiber, R., and Kunzelmann, K. (2016). Cl⁻ channels in apoptosis. *Eur. Biophys. J.* 45, 599–610. doi: 10.1007/s00249-016-1140-3
- Yang, H., Kim, A., David, T., Palmer, D., Jin, T., Tien, J., et al. (2012). TMEM16F Forms a Ca²⁺-Activated Cation Channel Required for Lipid Scrambling in Platelets during Blood Coagulation. *Cell* 151, 111–122. doi: 10.1016/j.cell.2012.07.036
- Zhang, H., Liu, Y., Men, H., Zhang, F., and Zhang, H. (2020). LRRC8A and ANO1 contribute to serum-induced VRAC in a Ca²⁺-dependent manners. *J. Pharmacol. Sci.* 143, 176–181. doi: 10.1016/j.jphs.2020.04.003
- Zhou, C., Chen, X., Planells-Cases, R., Chu, J., Wang, L., Cao, L., et al. (2020). Transfer of cGAMP into bystander cells via LRRC8 volume-regulated anion channels augments sting-mediated interferon responses and anti-viral immunity. *Immunity* 52, 767.e6–781.e6.

Conflict of Interest: The authors declare that the research was conducted in the absence of any commercial or financial relationships that could be construed as a potential conflict of interest.

Copyright © 2020 Centeio, Ousingsawat, Schreiber and Kunzelmann. This is an open-access article distributed under the terms of the Creative Commons Attribution License (CC BY). The use, distribution or reproduction in other forums is permitted, provided the original author(s) and the copyright owner(s) are credited and that the original publication in this journal is cited, in accordance with accepted academic practice. No use, distribution or reproduction is permitted which does not comply with these terms.



The Role of Eryptosis in the Pathogenesis of Renal Anemia: Insights From Basic Research and Mathematical Modeling

Gabriela Ferreira Dias^{1,2}, Nadja Grobe², Sabrina Rogg³, David J. Jörg³, Roberto Pecoits-Filho^{1,4}, Andréa Novais Moreno-Amaral¹ and Peter Kotanko^{2,5*}

¹ Graduate Program in Health Sciences, Pontifícia Universidade Católica do Paraná, Curitiba, Brazil, ² Renal Research Institute, New York, NY, United States, ³ Fresenius Medical Care Deutschland GmbH, Bad Homburg, Germany, ⁴ Arbor Research Collaborative for Health, Ann Arbor, MI, United States, ⁵ Icahn School of Medicine at Mount Sinai, New York, NY, United States

OPEN ACCESS

Edited by:

Markus Ritter,
Paracelsus Medical University, Austria

Reviewed by:

Etheresia Pretorius,
Stellenbosch University, South Africa
Marianna H. Antonelou,
National and Kapodistrian University
of Athens, Greece

*Correspondence:

Peter Kotanko
Peter.Kotanko@rrny.com

Specialty section:

This article was submitted to
Cell Death and Survival,
a section of the journal
Frontiers in Cell and Developmental
Biology

Received: 23 August 2020

Accepted: 16 October 2020

Published: 09 December 2020

Citation:

Dias GF, Grobe N, Rogg S,
Jörg DJ, Pecoits-Filho R,
Moreno-Amaral AN and Kotanko P
(2020) The Role of Eryptosis in
the Pathogenesis of Renal Anemia:
Insights From Basic Research
and Mathematical Modeling.
Front. Cell Dev. Biol. 8:598148.
doi: 10.3389/fcell.2020.598148

Red blood cells (RBC) are the most abundant cells in the blood. Despite powerful defense systems against chemical and mechanical stressors, their life span is limited to about 120 days in healthy humans and further shortened in patients with kidney failure. Changes in the cell membrane potential and cation permeability trigger a cascade of events that lead to exposure of phosphatidylserine on the outer leaflet of the RBC membrane. The translocation of phosphatidylserine is an important step in a process that eventually results in eryptosis, the programmed death of an RBC. The regulation of eryptosis is complex and involves several cellular pathways, such as the regulation of non-selective cation channels. Increased cytosolic calcium concentration results in scramblase and floppase activation, exposing phosphatidylserine on the cell surface, leading to early clearance of RBCs from the circulation by phagocytic cells. While eryptosis is physiologically meaningful to recycle iron and other RBC constituents in healthy subjects, it is augmented under pathological conditions, such as kidney failure. In chronic kidney disease (CKD) patients, the number of eryptotic RBC is significantly increased, resulting in a shortened RBC life span that further compounds renal anemia. In CKD patients, uremic toxins, oxidative stress, hypoxemia, and inflammation contribute to the increased eryptosis rate. Eryptosis may have an impact on renal anemia, and depending on the degree of shortened RBC life span, the administration of erythropoiesis-stimulating agents is often insufficient to attain desired hemoglobin target levels. The goal of this review is to indicate the importance of eryptosis as a process closely related to life span reduction, aggravating renal anemia.

Keywords: kidney failure, anemia, eryptosis, erythropoietin, phosphatidylserine, calcium, hypoxia, oxidative stress

INTRODUCTION

Red blood cells (RBCs) are vital to life, and their oxygen carrying role is indispensable to the function of tissues and organs. In healthy humans, RBCs undergo senescence and cell death after around 120 days. RBCs can also undergo a distinct mechanism of death, a process of programmed RBC death similar to apoptosis, called eryptosis (Qadri et al., 2017). This may occur throughout the

RBC lifetime, even before senescence under various stress conditions, and it is increased in kidney failure patients for reasons only partially understood (Abed et al., 2014; Bissinger et al., 2016; Dias et al., 2018). The RBC plasma membrane acts as a selective barrier that ensures a constant internal composition, by controlling the active and passive transfer of ions and molecules. Composed of more than 50 transmembrane proteins, the membrane regulates RBC shape, as well as mobility, deformability, and ion and macromolecules transport (Mohandas and Gallagher, 2008). Membrane proteins play an important role in regulating RBC volume by controlling the movement of ions and thus assure cell deformability while traversing capillaries and spleen sinusoids (Gallagher, 2013; Glogowska and Gallagher, 2015). Fluidity of the cytoplasm and cell volume regulation are necessary for capillary transit and transport of O₂ and CO₂ (Narla and Mohandas, 2017). Beyond their primary O₂-carrying function, RBCs are essential for systemic metabolic processes, such as pH regulation, nitric oxide production, and immune responses (Nemkov et al., 2018; Rifkind et al., 2018).

The capability to perform these functions decreases as RBCs approach senescence. In healthy subjects, a delicate balance between RBC death and production rates is maintained, resulting in stable RBC counts in the peripheral blood.

In kidney failure, the erythropoiesis rate is reduced, leading to fewer circulating RBCs. It is well established that the main cause of renal anemia is an inadequately low renal erythropoietin (Epo) synthesis combined with functional iron deficiency. Additionally, kidney patients show a dysregulation of oxygen sensing via the hypoxia-inducible factor pathway (Guedes et al., 2020). Erythropoiesis-stimulating agents (ESAs) are routinely used to compensate for the shortfall in endogenous Epo production. However, hypo-responsiveness to ESA is seen in 5–10% of anemic CKD patients. These patients do not achieve prescribed hemoglobin targets despite high ESA doses. This can be partially explained by accentuated inflammation and iron deficiency (Ogawa and Nitta, 2015). A less recognized potential cause of ESA hypo-responsiveness is decreased RBC life span. Eryptosis may reduce RBC survival and contribute to renal anemia since in some patients the erythropoiesis rate cannot compensate for this increased loss (Lang et al., 2017). In this review, we describe the role of eryptosis in the pathogenesis of renal anemia, an aspect frequently neglected in the clinical practice.

THE PATHOGENESIS OF RENAL ANEMIA: THE EPO-CENTRIC VIEW

Most chronic kidney disease (CKD) patients suffer from anemia at some point in the course of their illness. Epo levels in CKD patients are well below those seen in anemic non-kidney failure patients at the same level of hematocrit. The first cases of patients with renal anemia treated with ESA showed a dramatic effect: A few days after initiation of ESA therapy, their hematocrit approached normal levels, necessitating a reduction in ESA dose. The marked increase in RBC mass following treatment with ESA was accompanied by enhanced utilization of iron

stores, as reflected in a decline in serum iron and serum ferritin (Eschbach et al., 1987; Bunn, 2013). To many of those who witnessed these first results, the challenges of treating renal anemia may have become a matter of the past. However, decades later, many open questions have remained.

ERYPTOSIS PATHWAYS: OVERVIEW

Anemia is considered as a non-conventional risk factor in patients with CKD, especially in those on dialysis (Iseki and Kohagura, 2007). As discussed above, renal anemia is mainly attributed to decreased production of Epo by diseased kidneys, compromising erythropoiesis. In addition, several studies indicate that eryptosis is increased in CKD patients leading to early and accelerated elimination of circulating RBCs (Abed et al., 2014; Bissinger et al., 2016; Bonan et al., 2016; Dias et al., 2018).

Eryptosis is characterized by RBCs undergoing morphologic changes such as cell shrinkage, membrane scrambling, and the exposure of phosphatidylserine (PS) (Lang and Qadri, 2012). These changes are stimulated by Ca²⁺ influx into the RBCs through non-selective Ca²⁺ channels, which in turn can be activated by prostaglandin E₂ (PGE₂) formation, oxidative and osmotic stress, as well as Cl[−] efflux (Lang et al., 2007). Activation of Ca²⁺ channels results in an increase of cytosolic Ca²⁺, which can further induce floppase to expose PS on the cell surface and subsequent recognition, engulfment, and degradation of RBCs by macrophages (Lang et al., 2012) and pro-inflammatory monocytes (Bonan et al., 2016). Ca²⁺ may also stimulate sphingomyelinase to form ceramide, which in turn activates scramblase and culminates in loss of asymmetry of the RBC cell membrane and PS exposure (Lang et al., 2010).

Although eryptosis and senescence result in RBC death and clearance from circulation, the mechanisms driven by each pathway differ considerably. While eryptosis is orchestrated by the mechanisms mentioned above, the removal of aged RBCs relies mainly on the reduced deformability of the cells and macrophage recognition of immunoglobulin G and complement factor 3 on the surface of the senescent RBC. Externalization of PS was shown to be negligible in old RBCs (Franco et al., 2013). However, this RBC population is more susceptible to eryptosis induced by energy depletion (Ghashghaie et al., 2012). Thus, PS exposure seems to be more relevant for eryptosis rather than RBC senescence (Qadri et al., 2017).

Eryptosis is considered a useful mechanism to avoid a potentially fatal complication of hemolysis, by starting a cell death program with controlled removal before any damage can cause uncontrolled hemolysis (Föller et al., 2008). Since most of the iron content in the body is bound to hemoglobin, phagocytosis and the degradation of RBCs represent an important source of iron. The amount of recycled iron is sufficient to maintain the daily iron requirement for erythropoiesis (Ginzburg and Li, 2010). However, excessive eryptosis can compromise microcirculation through the adhesion of RBCs exposing PS to endothelial receptors of the vascular wall (Borst et al., 2012) and lead to anemia due to the exacerbated RBC

clearance by the immune system (Bonomini et al., 2001; Bonan et al., 2016). Enhanced eryptosis has been observed in some clinical conditions, such as diabetes, uremic hemolytic syndrome, sepsis, sickle cell anemia, and CKD, among others (Lang and Lang, 2015). PS exposure was observed to be significantly increased in RBCs from patients undergoing hemodialysis (HD) compared to RBCs from healthy individuals (Abed et al., 2014; Bissinger et al., 2016; Dias et al., 2018). Also, PS exposure was significantly higher in patients on peritoneal dialysis (PD) compared with HD patients (Bissinger et al., 2016). In PD patients, the residual glomerular filtration rate was inversely correlated with percentage of eryptosis. This correlation might be explained by a better clearance of retention solutes in patients with residual kidney function (Virzi et al., 2019). The question whether the HD therapy ameliorates or triggers eryptosis remains controversial. Results suggesting both an increase (Abed et al., 2014) and a reduction (Meyring-Wösten et al., 2017) of PS exposure post HD session were reported.

Eryptosis can be triggered by a range of both endogenous and exogenous insults, including toxins, drugs, and acute and chronic diseases (Lang and Lang, 2015). Among the uremic solutes that accumulate in CKD, acrolein (Ahmed et al., 2013b), methylglyoxal (Nicolay et al., 2006), and indoxyl sulfate (IS) (Ahmed et al., 2013a; Dias et al., 2018; Tozoni et al., 2019) were shown to increase eryptosis. Moreover, stressors including osmotic shifts, oxidative stress, and energy depletion may also contribute to a shortened RBC survival (Lang et al., 2006).

A reversion of PS exposure was shown by the addition of the antioxidant *N*-acetyl-L-cysteine to senescent RBCs (Ghashghaie et al., 2012) and incubation of uremic RBCs in healthy plasma (Bonomini et al., 1999). Also, the PS exposure induced by IS in healthy RBCs was attenuated by diphenyleneiodonium chloride (an NADPH oxidase inhibitor) and by ketoprofen (an organic anion transporter 2 inhibitor) (Dias et al., 2018).

RBC MICROVESICLES RELEASE

Microvesicle (MV) release is part of the physiological RBC aging process *in vivo*, which indicates a disruption of the network between the lipid bilayer and the cytoskeleton. Moreover, the presence of PS on the surface of MV allow for their recognition by the immune system (Burnier et al., 2009; Leal et al., 2018). The addition of Ca^{2+} to RBC media promotes MV release (Nguyen et al., 2016). This finding suggests the participation of MV in eryptosis when RBC Ca^{2+} is increased. However, the vesiculation process in eryptosis is still poorly understood.

The involvement of PS translocation in MV generation remains controversial. Some studies claim that MV release occurs independent of PS (Williamson et al., 1992; Bucki et al., 1998). Conversely, other authors reported that scramblase inhibition reduced MV release from Ca^{2+} -stimulated RBCs, suggesting the participation of PS translocation (Gonzalez et al., 2009). In contrast to cells undergoing apoptosis, RBC form MV from the plasma membrane with minute loss of the lipid order,

possibly due to the absence of intracellular organelle membranes (Pyrshv et al., 2018).

MV release was shown to be increased in RBCs from HD patients and attributed to an impacted membrane–cytoskeleton interaction, such as the proteolytic breakdown of band 3 (Antonelou et al., 2011). The uremic solutes IS and indol acetic acid (IAA) induced PS exposure and MV release from healthy RBCs (Gao et al., 2015). PS inhibition with lactadherin reduced MV release, reinforcing the participation of PS and micro-vesiculation in eryptosis. The authors also implicated MV release from RBC in thrombus formation, which may aggravate cardiovascular events in CKD (Gao et al., 2015).

THE ROLE OF IRON IN ANEMIA AND ERYPTOSIS

Another relevant aspect of renal anemia is the functional iron deficiency due to increased iron storage in the reticuloendothelial system. In addition, increased hepcidin levels are frequently observed in CKD patients, resulting in poor intestinal iron absorption. CKD patients are also prone to iron loss from (micro)bleeds and iatrogenic causes, such as frequent blood draws and blood loss in the extracorporeal system of dialysis machines. Poor iron availability contributes to impaired eryptosis in concert with the elevated levels of pro-inflammatory cytokines and hepcidin. Hence, ESA therapy is commonly accompanied by iron supplementation (Wish et al., 2018). RBCs from mice fed with an iron-deficient diet showed an increased Ca^{2+} uptake, RBC PS exposure, and eryptosis. Eryptotic RBCs were rapidly cleared from the circulation and thus may have amplified iron deficiency (Kempe et al., 2006). However, excessive iron administration may result in iron store pathologies driven by intracellular iron accumulation. As a consequence of inflammation and reticuloendothelial blockade of iron release, patients might still experience low erythropoiesis rate despite increased iron content (Wish, 2006). RBCs from patients with hemochromatosis showed increased PS exposure, mostly as a result of oxidative stress (Du Plooy et al., 2018).

THE ROLE OF REACTIVE OXYGEN SPECIES IN ERYPTOSIS

Patients with CKD, especially when on dialysis, are exposed to a variety of stimuli that change RBC number and phenotype. A critical contributor to eryptosis in CKD is the enhanced oxidative stress. The overproduction of pro-oxidant molecules in CKD is multifactorial and HD itself can activate inflammatory responses; in addition, essential antioxidants, such as vitamins, may be cleared by HD (Bissinger et al., 2018). Oxidative stress is classically defined as the imbalance between pro-oxidants and antioxidants in favor of the former. Oxidative stress exerts its detrimental effects through oxidation of macromolecules. However, it is now clear that oxidative stress is a compartmentalized event that occurs at different levels,

from cellular compartments to cells to the whole organism (Santolini et al., 2019). A more recent definition of oxidative stress indicates the importance of a disruption of redox signaling and control and/or molecular damage (Jones, 2006). This broader definition recognizes that damage to macromolecules is not the only pathway by which oxidative stress promotes disease. In fact, changes in cell signaling mediated by ROS can develop in a series of alterations and affect the body in a pathway- and organ-specific manner (Jones, 2006; Halliwell and Gutteridge, 2015).

Both enzymatic and non-enzymatic antioxidant systems are altered in CKD patients (Ling and Kuo, 2018). The thiol glutathione (GSH) is important for the maintenance of RBC redox homeostasis, where it is present at higher concentrations in the cytosol (Valko et al., 2007). This powerful redox buffer system provides an overall picture of the organism's redox state (Jones, 2006). In one study, the GSH concentration in RBCs from HD patients and healthy subjects was similar while the ratio of GSH and its oxidized form, glutathione disulfide (GSSG), was 40% lower (Khazim et al., 2013). We recently found that the GSH content in RBCs from HD patients is halved compared to RBCs from healthy subjects (Dias et al., 2018); however, the fact that the control subjects were significantly younger may have impacted the results since RBCs from elderly individuals tend to have lower GSH levels (Lupescu et al., 2015). Consistent with this finding, previous studies in uremic and HD patients reported low activity of γ -glutamylcysteine synthetase, a key enzyme in GSH biosynthesis (Alhamdani, 2005). Antioxidant enzymes, such as glutathione peroxidase, which detoxifies hydrogen peroxide (H_2O_2), also show a reduced activity in RBCs and plasma of uremic patients (Zachara et al., 2004). Although HD partially increased plasma antioxidant enzyme activities immediately after treatment, their function is not completely restored compared to healthy controls (El-Far et al., 2005).

Different from their non-uremic counterparts, uremic RBCs show activated non-selective Ca^{2+} transporters and subsequent increased Ca^{2+} influx, which triggers eryptosis (Abed et al., 2014). Oxidative stress participates in this process by maintaining Ca^{2+} levels high through the inhibition of the enzyme Ca-ATPase (Mohanty et al., 2014). Autoxidation of hemoglobin is the main pathway of free radical production in RBCs, leading to anion superoxide formation (Çimen, 2008). It was observed that RBCs can release H_2O_2 (Huertas et al., 2013; Rifkind et al., 2018). Under hypoxic conditions, RBCs increased superoxide formation and further dismutation to H_2O_2 . The latter was then diffused from the RBCs and promoted inflammation in the lung microvascular endothelium (Kieffmann et al., 2008). Given the high concentration of hemoglobin in the blood, it is conceivable that even a minor increase of hemoglobin autoxidation could trigger an imbalanced redox state, especially in a population with an already defective antioxidant system, such as CKD.

Moreover, iron facilitates redox reactions, and its accumulation leads to the generation of hydroxyl radical, a powerful ROS, via Fenton's reaction (Nakanishi et al., 2019). Ferritin levels not only reflect body iron stores but also serve as a biomarker of inflammation. Ferritin and oxidative stress

markers are correlated, possibly due to an increased dissociation of iron from ferritin. An increase in unbound iron catalyzes oxidative reactions and promotes cell damage (Kell, 2009; Kell and Pretorius, 2014). The addition of physiological iron levels results in slight RBC shape changes (Pretorius, 2013). Scanning electron microscopy showed that generation of hydroxyl radicals induced by iron overload triggers the aggregation of RBC with fibrin-like fibers, resulting in a pro-thrombotic state (Lipinski et al., 2012).

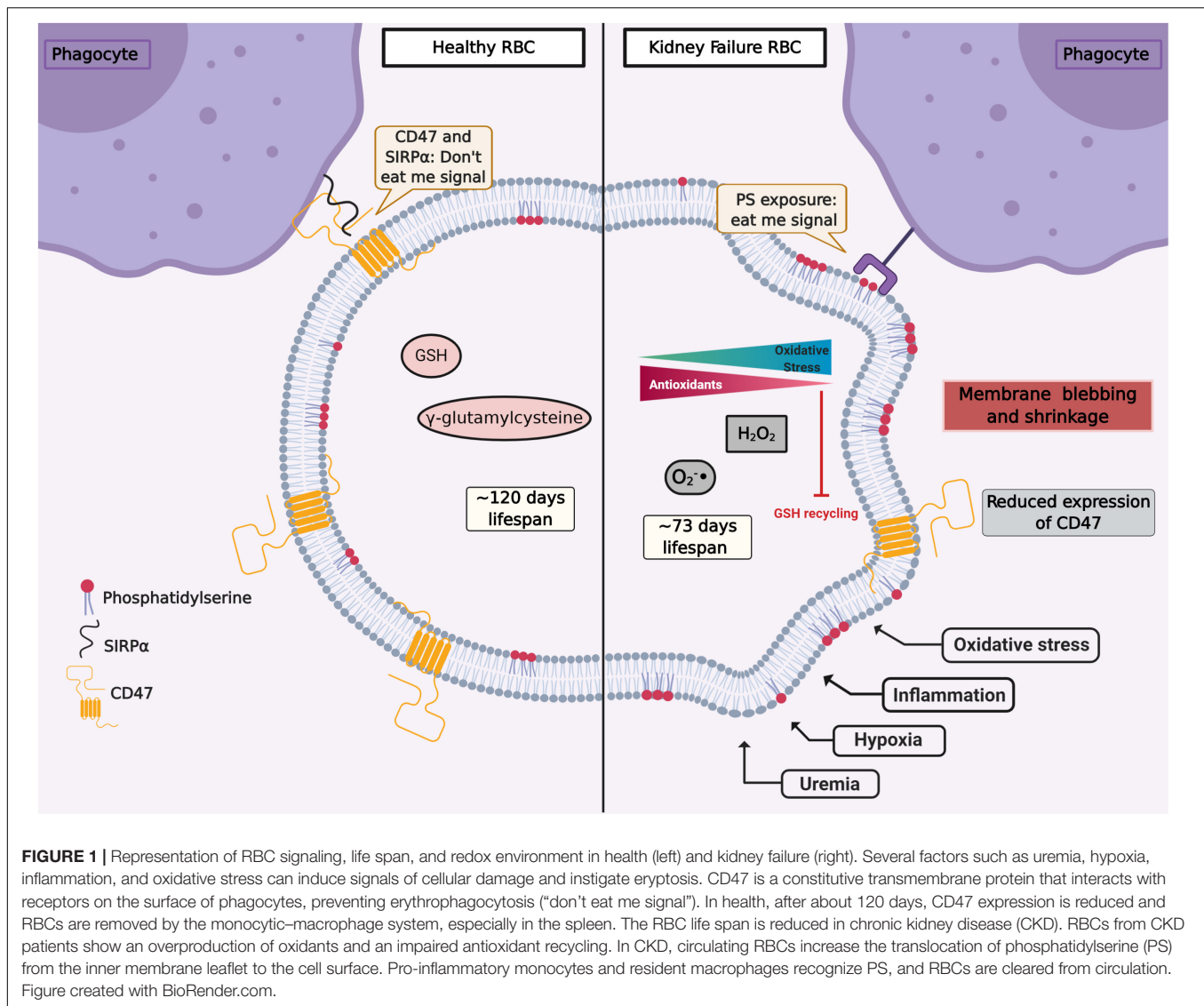
Despite substantial evidence regarding oxidative biomarkers in CKD, some findings remain controversial and their significance is unclear (Tucker et al., 2013). The high levels of pro-oxidants in tandem with the defective antioxidant machinery found in CKD may contribute to oxidative stress, an enhanced susceptibility of RBCs for eryptosis and worsening of renal anemia.

OXIDATIVE STRESS, INFLAMMATION, AND AGING

The triad of aging, inflammation, and oxidative stress reduces the quality of life of CKD patients. The emblematic term *inflammaging* has been introduced to highlight the role of these factors in the often rapid deterioration of the patient's health, longevity, and well-being (Ebert et al., 2020). Interestingly, inflammatory biomarkers such as interleukin 6 and C-reactive protein are not correlated with RBC life span in HD patients (Ma et al., 2017). Aging and oxidative stress are processes that can take place at the cellular level or the whole-body level and aging is associated with an imbalanced redox environment and rise in inflammatory biomarkers (Maurya et al., 2015).

The oxidative injury during the RBC life span may lead to dysfunction and cell death. Although oxidative stress is fundamental to RBC senescence, it is not the sole reason for its progression. CD47, a constitutive membrane receptor, acts as a protective ("do not eat me") signal against phagocytosis by interacting with the macrophage receptor SIRP α . Conversely, the expression of PS on RBC surface has the opposite effect and acts as an "eat me" signal to phagocytic cells (Lutz and Bogdanova, 2013; Arias and Arias, 2017; **Figure 1**). Moreover, Burger et al. found that aging promoted by oxidative stress induces a conformational change of CD47, which enables this molecule to bind to thrombospondin-1, converting CD47 into an "eat me" signal (Burger et al., 2012). The role of O_2 is highlighted by the observation that RBCs from male subjects performing hypoxic exercise training (15% O_2) showed less CD47 expression as well as a reduction of the cytoskeleton proteins actin and spectrin. RBC deformability, which is essential for their physiological function, was compromised in hypoxic conditions by the activation of Gardos channel (Mao et al., 2011). Moreover, in RBCs from CKD patients, a reduced expression of CD47 was observed (Antonelou et al., 2011). These different mechanisms underlying RBC senescence are still subject of ongoing research.

From an inflammation perspective, there are several molecules that play a role in renal anemia. The lipid peroxidation

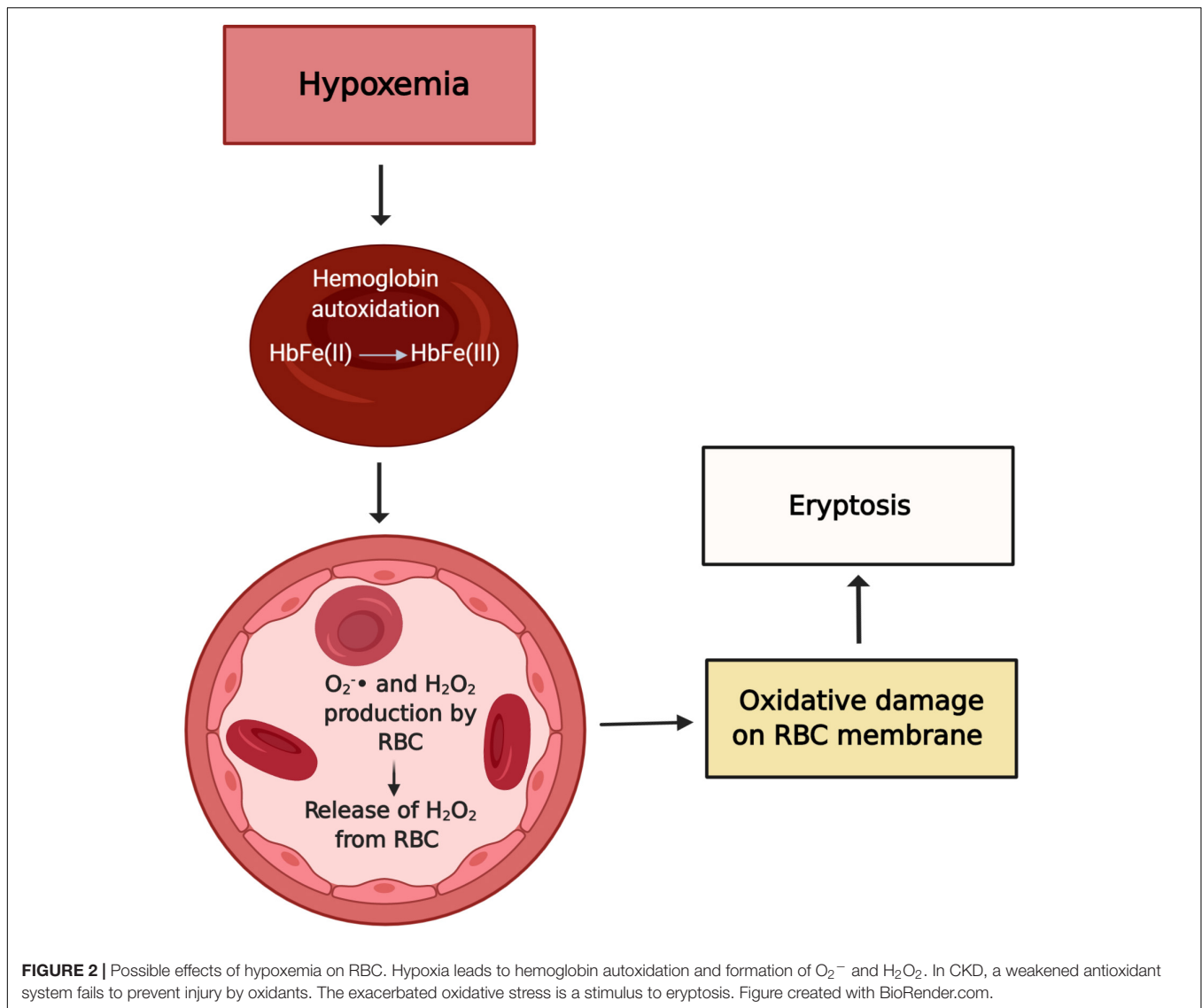


product 4-hydroxy-trans-2-nonenal (HNE) contributes to several inflammatory and degenerative processes. It is overexpressed in kidneys from aged rats and leads to NF- κ B activation (Jang et al., 2016). In RBCs, HNE exerts a pro-eryptotic effect, initiating the classical eryptotic markers as well as agglutination elements and adhesion molecules, resulting in binding of RBCs to endothelial cells, possibly promoting thrombosis (Allegra et al., 2020).

HYPOXIA IN DIALYSIS PATIENTS AND ITS ASSOCIATION WITH ERYPTOSIS

Hypoxia *per se* is well known to provoke oxidative stress. In the early 1990s, Rifkind et al. (1991) showed that the hypoxemic condition facilitates hemoglobin autooxidation and, as a result, the free radical anion superoxide is exacerbated despite the high levels of antioxidants normally present in RBC. Importantly, about 10% of patients undergoing HD experience

prolonged intradialytic hypoxemia (PIH), a clinical phenotype characterized by an arterial oxygen saturation below 90% for at least one third of the dialysis treatment time (Meyring-Wosten et al., 2016). Previously, we explored the effect of low oxygen partial pressure and the uremic toxin IS on eryptosis (Tozoni et al., 2019). Interestingly, we found that hypoxemia and IS independently increase eryptosis and ROS generation and decrease GSH levels, possibly contributing to the reduced RBC life span observed in CKD (Figures 1, 2). Of note, high altitude, another hypoxia model, had a different effect on RBC homeostasis. Epo produced in response to hypoxia inhibits Ca^{2+} channels and thus attenuated eryptosis (Myssina et al., 2003). In rats kept at high altitude (5,000 m) for 30 days, chronic hypoxia inhibited eryptosis, possibly by increasing CD47 expression and decreasing intracellular Ca^{2+} levels (Tang et al., 2018). This observation is possibly caused by the protective effect of Epo and production of new RBC with high CD47 expression.



Any harmful insult to RBC will generate membrane modifications and possibly signal an eryptotic event, reversible or not (Pretorius et al., 2016a). Raman spectroscopy reveals several changes in hemoglobin morphology and function of RBCs under hypoxia. According to Revin et al. (2017), not only the lipid composition of RBC is profoundly altered in hypoxia, but also the ability of hemoglobin to bind and select ligands is reduced, including its affinity for oxygen (Chowdhury and Dasgupta, 2017). Morphological modifications of RBCs in tandem with low hemoglobin concentration can result in poor O_2 -carrying capacity and compound tissue hypoxia.

ION CHANNEL MODIFICATIONS IN ERYPTOSIS

The disturbance of membrane asymmetry that favors PS exposure and subsequent eryptosis is caused by the increase of cytosolic

Ca^{2+} (Segawa and Nagata, 2015; Pretorius et al., 2016a). Ca^{2+} enters RBC through several ion channels, pumps, and exchangers that transport Ca^{2+} through the plasma membrane (Polak-Jonkisz et al., 2010b; Brini and Carafoli, 2011; Polak-Jonkisz and Purzyc, 2012). Several factors such as oxidative stress, energy depletion, or uremic toxins activate Ca^{2+} influx into the RBC (Lang and Lang, 2015). Ca^{2+} efflux occurs mainly by a high-affinity, low-capacity Ca^{2+} -ATPase, the plasma membrane Ca^{2+} pump (PMCA) (Brini and Carafoli, 2011).

The distribution of PS on the inner and outer membrane leaflet is determined by the activity of translocase proteins in the RBC membrane: flippase, floppase, and scramblase. Flippase is an ATP-dependent transporter that transfers phospholipids from the extracellular leaflet to the cytoplasm, while floppase is an ATP-binding cassette transporter that catalyzes the movement of phospholipids in the opposite direction (Hankins et al., 2015). To maintain an optimal distribution of lipid bilayer phospholipids, scramblases

regulate PS movement in both directions, independent of ATP. These enzymes are regulated by intracellular Ca^{2+} levels (Bitbol et al., 1987; Pretorius et al., 2016a; Föller and Lang, 2020). A high concentration of cytosolic Ca^{2+} inhibits flippase, which results in the activation of the scramblase, followed by the translocation of PS from the internal leaflet to the surface of the eryptotic RBC (Williamson et al., 1992; **Figures 3, 4**).

Intracellular Ca^{2+} regulation is mediated mainly by its low passive permeability and its active removal by the calcium ATPase pump dependent on Ca^{2+} - Mg^{2+} and by the $\text{Na}^{+}/\text{Ca}^{2+}$ exchanger (Carafoli, 1987; Blaustein, 1988; Reeves et al., 1994). The Ca^{2+} PMCA1 and PMCA4 regulate and maintain the internal concentration of Ca^{2+} . About 10% of the plasma RBC membrane proteins are PMCA (Rothstein et al., 1976). These enzymes are important regulators of Ca^{2+} homeostasis, being activated by a series of mechanisms, some of them though still unknown.

Ca^{2+} efflux from the cytosol is against a steep chemical gradient and hence PMCA requires ATP. RBCs from CKD patients have a decreased PMCA activity as well as reduced calmodulin concentration as renal failure progresses (Polak-Jonkisz et al., 2010a). Thus, elucidating the relationship between the systems that control both Ca^{2+} influx and efflux in eryptosis would be an important step in determining potential inhibitory targets for the accelerated RBC death in CKD.

Although RBC's PMCA has been well characterized, the knowledge of ion transport systems that mediate Ca^{2+} uptake in RBC is quite limited. The incubation of RBC with Ca^{2+} ionophore ionomycin causes exposure of PS in the outer membrane leaflet (Föller et al., 2009b). In addition to PS exposure, elevated levels of intracellular Ca^{2+} promote oxidative stress by directly activating NADPH oxidase and nitric oxide synthase in uncoupled mode (Özüyaman et al., 2008; George et al., 2013). Among the transport systems that contribute to the uptake of Ca^{2+} in human RBCs, there are several classes of cation channels (Kaestner, 2011). Some ionotropic receptors have been described in RBCs, like the GluA1, the AMP glutamate ionotropic receptor subunit (Makhro et al., 2016; Kaestner et al., 2020), as well as N-methyl-D-aspartate (NMDA) (Makhro et al., 2017), contributing to Ca^{2+} homeostasis in these cells. Moreover, after removal of Cl^{-} or extracellular glucose, alpha-amino-3-hydroxy-5-methyl-4-isoxazolepropionic acid (AMPA) antagonist receptors drive the increase in cytosolic Ca^{2+} and induce eryptosis by stimulating Ca^{2+} influx (Föller et al., 2009a).

Circulating RBCs are exposed to significant mechanical forces that influence their physiology and function in several ways, including deformability, the release of products such as ATP (Sprague et al., 2001), and the Ca^{2+} influx. Ca^{2+} influx also influences cell volume. Changes in RBC volume affect their ability

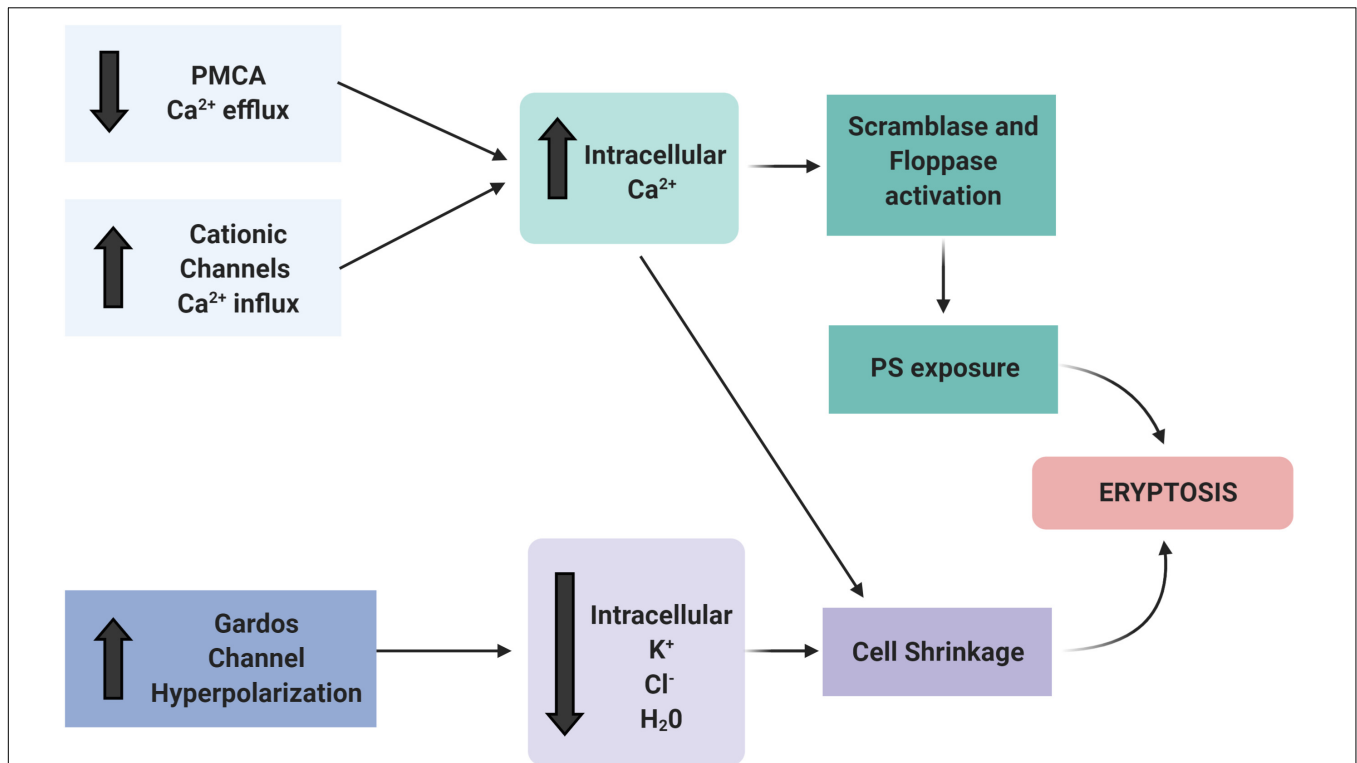
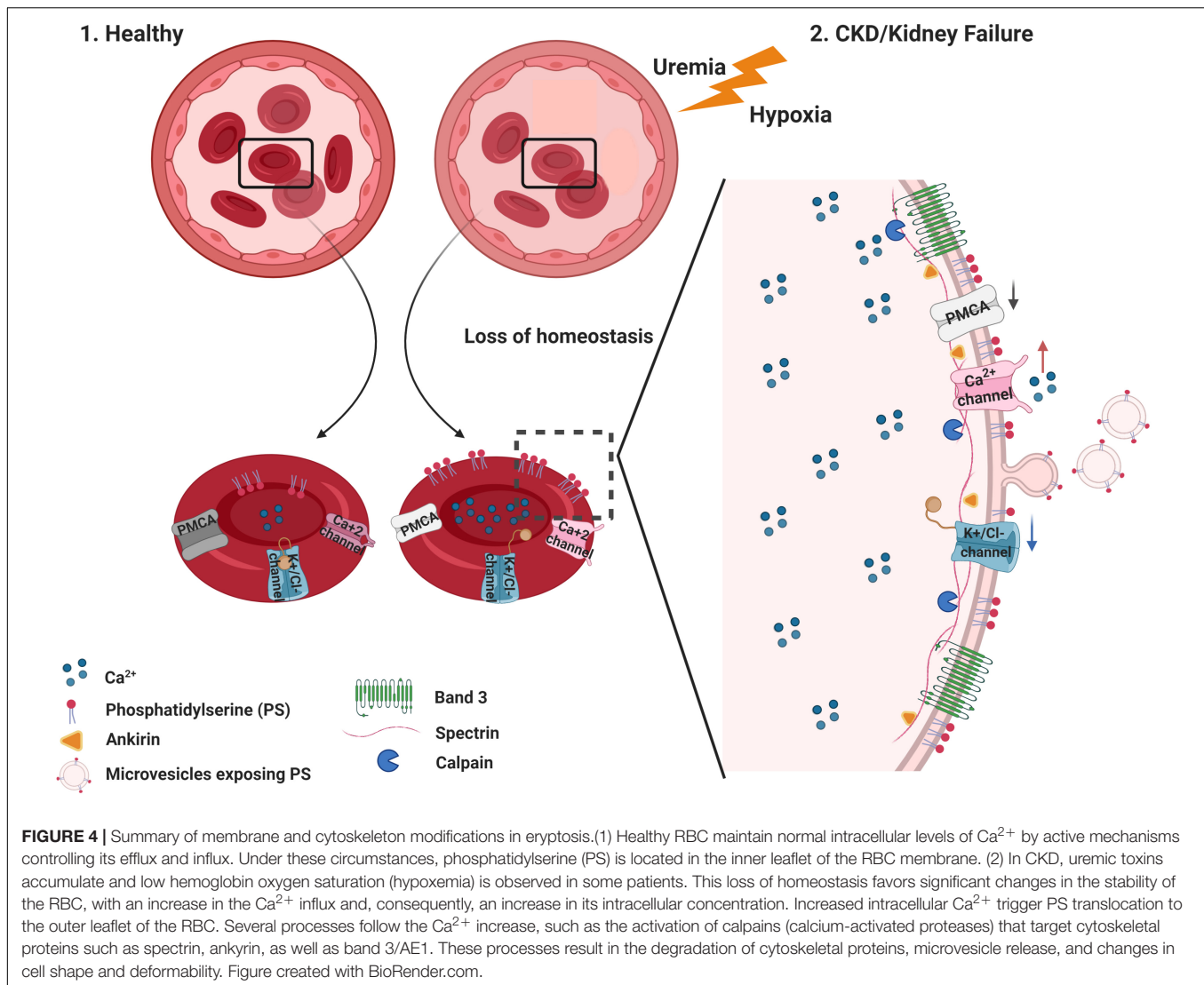


FIGURE 3 | Ion channels involved in eryptosis. The activation of Ca^{2+} channels (e.g., by uremic toxins, oxidative stress, hypoxia) is the main trigger to initiate the events that culminate in eryptosis. The increased intracellular Ca^{2+} activates scramblase and floppase proteins that promote PS exposure on the cell surface. Patients with CKD have PMCA inactivation and subsequent reduced Ca^{2+} efflux. In addition, other ion channels, such as the Gardos channel, are altered. The resulting efflux of K^{+} , Cl^{-} , and water result in RBC shrinkage and induce eryptosis. Figure created with BioRender.com.



to traverse capillaries. The molecular mechanisms involved in sensing mechanical forces and their effects on RBC volume are not fully understood. The mechanosensitive Ca²⁺ channel PIEZO1 is located on the RBC membrane. PIEZO1 is an important regulator of cell volume in response to mechanical stress (Cahalan et al., 2015). The connection between mechanical forces and RBC volume via Ca²⁺ influx through PIEZO1 is closely linked to the cells' ability to change shape and reduce cell volume and enable passage through small-diameter capillaries. Of note, the intensity of the mechanical force can induce the initial steps of eryptosis, since an increase of PIEZO1-dependent Ca²⁺ influx stimulates Gardos' channels and subsequent RBC shrinkage (Cahalan et al., 2015).

Increased Ca²⁺ influx due to Ca²⁺ channel activation combined with reduced Ca²⁺ efflux from the cytosol may affect the homeostasis of other ions, most prominently K⁺. Activation of the Gardos channel, a K⁺ efflux channel activated by intracellular Ca²⁺ increase, results in membrane hyperpolarization and increased Cl⁻ efflux. Finally, the loss of

water leads to cell shrinkage (Thomas et al., 2011; Boulet et al., 2018; **Figures 3, 4**). Even a local membrane deformation can trigger this process and induce cell dehydration, which may explain the higher density of senescent RBCs (Dyrda et al., 2010).

CYTOSKELETON MODIFICATIONS

The RBC cytoskeleton plays an important role in cell homeostasis. The spectrin-actin network interacts with ankyrin and controls RBC deformability (Pretorius et al., 2016b). This interaction of the cytoplasmic domain of membrane proteins with cytoskeleton proteins prevents membrane vesiculation and breakup (Mohandas and Gallagher, 2008). Besides the role of Ca²⁺ on the eryptotic process, the prolonged Ca²⁺ permeability activates μ calpain, which can degrade cytoskeleton components, such as the ankyrin R complex that forms bridges to connect membrane proteins to the spectrin-based skeleton, assuring membrane stability and assembly of signaling and

structural components on the inner membrane surface (Berg et al., 2001; **Figure 4**).

The band 3 protein, also called anion exchanger 1 (AE1), is one of the transport proteins that mediate the exchange of Cl^- and HCO_3^- . Through interaction with lipids and proteins, the multifunctional band 3 unites the multiprotein complex of the cytoskeleton and confers mechanical and elastic properties to RBC and thus blood viscosity (Burton and Bruce, 2011). Moreover, studies of RBC membrane proteins in CKD stage 5 patients showed lower levels of ankyrin and spectrin, as well as altered ankyrin/band 3 ratio. In addition to these alterations, the same study showed that patients in CKD stage 5 who do not respond to ESA have a lower spectrin/ankyrin ratio (Costa et al., 2008).

RBC LIFE SPAN IN HEALTH AND CKD

Aging RBCs lose the flexibility needed to traverse the network of tight capillaries. Senescent RBCs are removed from circulation by splenic red pulp macrophages. While the key role of Epo deficiency in renal anemia is undisputed, the impact of RBC life span has received only little attention (Dou et al., 2012). One reason is that RBC life span measurements are impractical in the clinical environment. Studies show that the life span of RBC from HD patients is dramatically reduced. Several groups have measured RBC life span in HD patients and arrived, for example, at values of 73 ± 18 days (Ma et al., 2017) and 89 ± 28 days (Sato et al., 2012). While there are rare obvious reasons for hemolysis in dialysis patients (e.g., contaminations with chloramine or nitrate; overheated dialysate) (Saha and Allon, 2017), the pathogenesis of the reduced RBC life span is ill-defined. The shortened RBC life span in CKD has been attributed to the uremic environment rather than mechanical stress induced by HD (Vos et al., 2011). As the RBC life span declines, higher doses of ESAs are needed to attain hemoglobin target levels in HD patients (Sato et al., 2012). Interestingly, ESA administration was positively correlated with PS exposure on RBC from HD and PD patients (Bissinger et al., 2016). On the other hand, eryptosis in healthy RBCs induced by osmotic shock showed the opposite effect, where PS exposure was ameliorated in the presence of Epo (Myssina et al., 2003). These contradictory findings demonstrate that the response of the RBCs to Epo may be dependent on the nature of the eryptotic trigger and the prevailing milieu interieur. Although the administration of ESAs is crucial for the correction of renal anemia, it may promote the clearance of young RBCs, a process called neocytolysis (Alfrey and Fishbane, 2007).

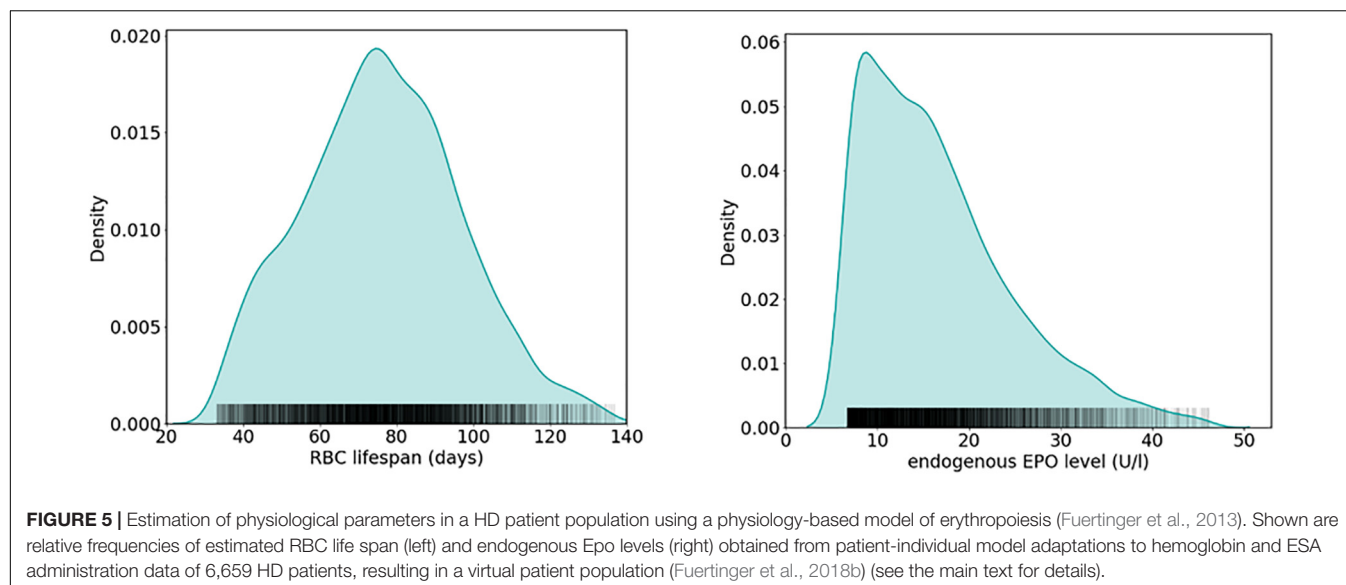
Of note, serum Epo levels do not differ substantially across CKD stages. Interestingly, reticulocyte count was reduced only in CKD stage 5 when compared with stage 1 (Li et al., 2019). Such findings suggest that other factors besides Epo deficiency, such as RBC life span, compound renal anemia. Indeed, the decline of kidney function is correlated with a progressive shortening of RBC life span (122 ± 50 , 112 ± 26 , 90 ± 32 , 88 ± 28 , and 60 ± 24 days, from CKD stages 1–5, respectively) (Li et al., 2019), and the

prevalence of anemia also increases with the progression of the disease (KDIGO, 2012).

RELATION BETWEEN RBC LIFE SPAN AND EPO REQUIREMENT: INSIGHTS FROM BIOMATHEMATICAL MODELING

The higher ESA requirement in patients with a lower RBC life span can also be elucidated using computational models of erythropoiesis. Such models encapsulate key features of human erythropoietic physiology and, through simulations, enable one to study how physiological factors such as RBC life span determine a patient's response to ESA administrations. Furthermore, they provide a tool to augment the design and interpretation of clinical and laboratory studies and aid the development of treatment algorithms. Phenomenological approaches have focused on an abstract description of the hematocrit as the only model variable, in which ESA administrations lead to an effective increase in hematocrit, without resolving the underlying physiological mechanisms (Uehlinger et al., 1992; Kalicki and Uehlinger, 2008). In this scheme, the duration and progression of the ESA-induced hematocrit increase is determined by RBC life span and its variability, whereas the speed of the increase is determined by effective parameters accounting for ESA efficacy and the concentration threshold for ESA response. Using model simulations, it has been illustrated that a lower RBC life span results in lower hematocrit levels for the same ESA dose (Kalicki and Uehlinger, 2008), consistent with higher ESA doses being required to achieve a desired hematocrit target for lower RBC life span.

How does RBC life span affect Epo requirements within an entire patient population, taking into account inter-patient variability in other physiological parameters related to RBC fate as well? Modeling approaches based on “virtual patient populations” can provide insights into this question, as can be illustrated considering an established physiological model of erythropoiesis (Fuertinger et al., 2013, 2018a). This model explicitly represents the proliferative hierarchy of erythroid progenitor populations in the bone marrow including the dynamics of cell birth, maturation, differentiation, and apoptosis; in this modeling scheme, Epo acts as a regulator of apoptosis of the colony-forming unit-erythroid (CFU-E) and erythrocyte populations. Previously, this model has been adapted on a patient-individual level to a large population of HD patients treated with methoxy polyethylene glycol-epoetin beta (6,659 patients randomly sampled from a U.S. HD population comprising over 37,000 patients) (Fuertinger et al., 2018b). These model adaptations were carried out such that previously recorded hemoglobin responses to ESA therapy for the specific patient were described by the model within a predefined accuracy. Individual patients were represented by a patient-specific parameter set (RBC life span, ESA half-life, endogenous Epo levels, and effective parameters accounting for the ESA's effect on erythroid progenitor apoptosis and maturation velocity) capturing their erythropoiesis-related physiology (Fuertinger

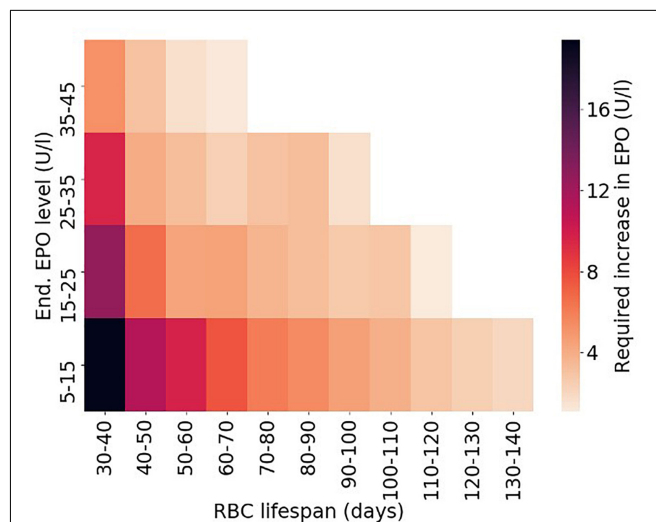
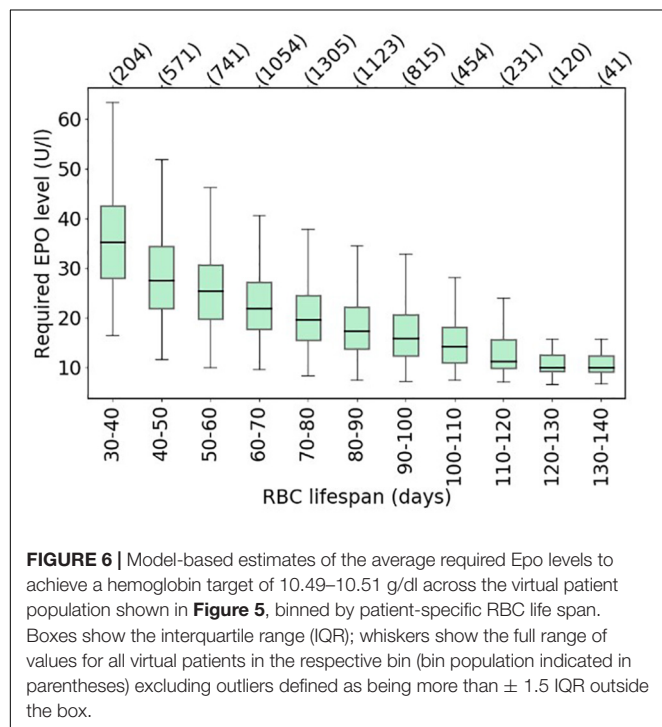


et al., 2018b). Although iron availability is not an explicit part of the model, its effects are implicitly present in the effective bone marrow-related parameters. These patient representations through patient-specific parameter sets within the model paradigm are termed “anemia avatars” or “virtual patients.” Estimated mean RBC life span across all virtual patients was 76 ± 21 days (mean \pm SD; range: 33–137 days), close to reported values in urban HD centers (see, e.g., Ma et al., 2017; mean \pm SD: 73 ± 18 days; range: 38–116 days); the median estimated endogenous Epo level is 15 U/L (25th, 75th percentiles:

10.2 U/L, 21.1 U/L). The relative frequencies of estimated RBC life spans and endogenous Epo levels among the population of virtual patients reported in Fuerterer et al. (2018b) are shown in **Figure 5**.

Making use of this established set of virtual patients, it is straightforward to illustrate how RBC life span affects the amount of Epo required for simulated patients to meet a specific hemoglobin level (10.49–10.51 g/dl). To this end, for each virtual patient, required total Epo levels¹ are determined. **Figure 6** shows

¹Total Epo levels instead of ESA utilization are chosen to eliminate the effects of ESA half-life, which has a high inter-patient variability that would confound the relation between RBC life span and Epo requirement.



the distribution of required Epo serum concentrations to achieve the hemoglobin target, with virtual patients being grouped into RBC life span bins of 10 days. The model analysis suggests a systematic increase in Epo requirement with decreasing RBC life span, a marked trend despite the variability of the virtual patient population in other physiological parameters affecting RBC generation and fate. This inter-patient variability is responsible for the partially large spread of required Epo levels within each binned group, an effect that becomes more prominent for small RBC life spans. Dissecting the virtual patient population by RBC life span and endogenous Epo levels, the mean required increase in Epo concentration to achieve the hemoglobin target is shown in **Figure 7**: Within the same Epo range, the shorter the RBC life span, the higher the required increase in Epo level, as is most clearly visible for the smallest Epo level range (5–15 U/L). Notwithstanding the effects of ESA half-life, these insights obtained from modeling approaches involving “virtual patient populations” illustrate that (i) a reduced RBC life span may necessitate frequent and high-dose ESA administrations and may present a cause of Epo hypo-responsiveness; (ii) within some (virtual) patients, the effects of a reduced RBC life span on Epo requirements are partially compensated by other physiological factors affecting RBC generation and fate such as endogenous Epo levels.

CONCLUSION

Among the many causes that contribute to anemia in kidney failure, eryptosis is a key process whose significance has not been fully acknowledged so far. Although improving hemoglobin levels, ESA and iron administration alone are only one strategy to correct renal anemia that can be limited by a decreased RBC life span. Oxidative stress, inflammation, hypoxemia, and

accumulation of uremic solutes promote an imbalance of RBC homeostasis and need to be considered. Even in a scenario where ESA administration increases erythropoiesis rate, the newly formed RBCs can undergo eryptosis within a few days in circulation, resulting in ESA hypo-responsiveness and thus preventing attainment of desired hemoglobin targets. These mechanisms center around (i) increased Ca^{2+} influx and reduced activity of enzymes mediating Ca^{2+} efflux (PMCA), (ii) Gardos channels activation and RBC volume loss, (iii) PS exposure on cell surface and subsequent RBC clearance from circulation. More research in this field is needed to further elucidate these processes and develop potential therapeutic interventions. Extending RBC life span in uremia may evolve as a novel therapeutic strategy for renal anemia.

AUTHOR CONTRIBUTIONS

GD and AM-A wrote, reviewed and edited, contributed to the discussion, and created figures. NG wrote, reviewed and edited, and contributed to the discussion. SR wrote, reviewed and edited, contributed to the discussion and carried out the mathematical analysis. DJ and RP-F reviewed, edited, and contributed to the discussion. PK conceptualized, wrote, reviewed and edited, and contributed to the discussion. All authors contributed to the article and approved the submitted version.

FUNDING

This work was supported by the Renal Research Institute, New York, United States. GD was a recipient of research fellowship from the Coordenacao de Aperfeicoamento de Pessoal de Nivel Superior—Brasil (CAPES).

REFERENCES

- Abed, M., Artunc, F., Alzoubi, K., Honisch, S., Baumann, D., Föller, M., et al. (2014). Suicidal erythrocyte death in end-stage renal disease. *J. Mol. Med.* 92, 871–879. doi: 10.1007/s00109-014-1151-4
- Ahmed, M. S. E., Abed, M., Voelkl, J., and Lang, F. (2013a). Triggering of suicidal erythrocyte death by uremic toxin indoxyl sulfate. *BMC Nephrol.* 14:244. doi: 10.1186/1471-2369-14-244
- Ahmed, M. S. E., Langer, H., Abed, M., Voelkl, J., and Lang, F. (2013b). The uremic toxin acrolein promotes suicidal erythrocyte death. *Kidney Blood Press. Res.* 37, 158–167. doi: 10.1159/000350141
- Alfrey, C. P., and Fishbane, S. (2007). Implications of neocytolysis for optimal management of anaemia in chronic kidney disease. *Nephron - Clin. Pract.* 106, 149–156. doi: 10.1159/000104425
- Alhamedani, M. S. S. (2005). Impairment of glutathione biosynthetic pathway in uraemia and dialysis. *Nephrol. Dial. Trans.* 20, 124–128. doi: 10.1093/ndt/gfh569
- Allegria, M., Restivo, I., Fucarino, A., Pitruzzella, A., Vasto, S., Livrea, M. A., et al. (2020). Proeryptotic activity of 4-hydroxynonenal: a new potential physiopathological role for lipid peroxidation products. *Biomolecules* 10:770. doi: 10.3390/biom10050770
- Antonellou, M. H., Kriebardis, A. G., Velentzas, A. D., Kokkalis, A. C., Georgakopoulou, S.-C., and Papassideri, I. S. (2011). Oxidative stress-associated shape transformation and membrane proteome remodeling in erythrocytes of end stage renal disease patients on hemodialysis. *J. Proteom.* 74, 2441–2452. doi: 10.1016/j.jprot.2011.04.009
- Arias, C. F., and Arias, C. F. (2017). How do red blood cells know when to die? *R. Soc. Open Sci.* 4:160850. doi: 10.1098/rsos.160850
- Berg, C. P., Engels, I. H., Rothbart, A., Lauber, K., Renz, A., Schlosser, S. F., et al. (2001). Human mature red blood cells express caspase-3 and caspase-8, but are devoid of mitochondrial regulators of apoptosis. *Cell Death Diff.* 8, 1197–1206. doi: 10.1038/sj.cdd.4400905
- Bissinger, R., Artunc, F., Qadri, S. M., and Lang, F. (2016). Reduced erythrocyte survival in uremic patients under hemodialysis or peritoneal dialysis. *Kidney Blood Press. Res.* 41, 966–977. doi: 10.1159/000452600
- Bissinger, R., Bhuyan, A. A. M., Qadri, S. M., and Lang, F. (2018). Oxidative stress, eryptosis and anemia: a pivotal mechanistic nexus in systemic diseases. *FEBS J.* 286, 826–854. doi: 10.1111/febs.14606
- Bitbol, M., Fellmann, P., Zachowski, A., and Devaux, P. F. (1987). Ion regulation of phosphatidylserine and phosphatidylethanolamine outside-inside translocation in human erythrocytes. *Biochim. et Biophys. Acta* 904, 268–282. doi: 10.1016/0005-2736(87)90376-2
- Blaustein, M. P. (1988). Calcium transport and buffering in neurons. *Trends Neurosci.* 11, 438–443. doi: 10.1016/0166-2236(88)90195-6
- Bonan, N. B., Steiner, T. M., Kuntsevich, V., Virzi, G. M., Azevedo, M., Nakao, L. S., et al. (2016). Uremic toxicity-induced eryptosis and monocyte modulation: the erythrophagocytosis as a novel pathway to renal anemia. *Blood Purif.* 41, 317–323. doi: 10.1159/000443784

- Bonomini, M., Sirolli, V., Reale, M., and Arduini, A. (2001). Involvement of phosphatidylserine exposure in the recognition and phagocytosis of uremic erythrocytes. *Am. J. Kidney Dis.* 37, 807–814. doi: 10.1016/S0272-6386(01)80130-X
- Bonomini, M., Sirolli, V., Settefrati, N., Dottori, S., Di Liberato, L., and Arduini, A. (1999). Increased erythrocyte phosphatidylserine exposure in chronic renal failure. *J. Am. Soc. Nephrol.* 10, 1982–1990. <http://www.ncbi.nlm.nih.gov/pubmed/10477151>
- Borst, O., Abed, M., Alesutan, I., Towhid, S. T., Qadri, S. M., Foller, M., et al. (2012). Dynamic adhesion of eryptotic erythrocytes to endothelial cells via CXCL16/SR-PSOX. *Am. J. Physiol. Cell Physiol.* 302, 644–651. doi: 10.1152/ajpcell.00340.2011
- Boulet, C., Doerig, C. D., and Carvalho, T. G. (2018). Manipulating eryptosis of human red blood cells: a novel antimalarial strategy? *Front. Cell. Infect. Microbiol.* 8:419. doi: 10.3389/fcimb.2018.00419
- Brini, M., and Carafoli, E. (2011). The plasma membrane Ca²⁺ ATPase and the plasma membrane sodium calcium exchanger cooperate in the regulation of cell calcium. *Cold Spring Harbor Perspect. Biol.* 3:a004168. doi: 10.1101/cshperspect.a004168
- Bucki, R., Bachelot-Loza, C., Zachowski, A., Giraud, F., and Sulpice, J. C. (1998). Calcium induces phospholipid redistribution and microvesicle release in human erythrocyte membranes by independent pathways. *Biochemistry* 37, 15383–15391. doi: 10.1021/bi9805238
- Bunn, H. F. (2013). Erythropoietin. *Franklin Bunn. Cold Spring Harbor Perspect. Med.* 3, 1–20. doi: 10.1101/cshperspect.a011619
- Burger, P., Hilarius-Stokman, P., De Korte, D., Van Den Berg, T. K., and Van Bruggen, R. (2012). CD47 functions as a molecular switch for erythrocyte phagocytosis. *Blood* 119, 5512–5521. doi: 10.1182/blood-2011-10-386805
- Burnier, L., Fontana, P., Kwak, B. R., and Anne, A. S. (2009). Cell-derived microparticles in haemostasis and vascular medicine. *Thrombosis Haemostasis* 101, 439–451. doi: 10.1160/TH08-08-0521
- Burton, N. M., and Bruce, L. J. (2011). Modelling the structure of the red cell membrane. *Biochem. Cell Biol.* 89, 200–215. doi: 10.1139/O10-154
- Cahalan, S. M., Lukacs, V., Ranade, S. S., Chien, S., Bandell, M., and Patapoutian, A. (2015). Piezo1 links mechanical forces to red blood cell volume. *Elife* 4:e07370. doi: 10.7554/eLife.07370
- Carafoli, E. (1987). Intracellular Calcium Homeostasis. *Ann. Rev. Biochem.* 56, 395–433. doi: 10.1002/9781118675410
- Chowdhury, A., and Dasgupta, R. (2017). Effects of acute hypoxic exposure on oxygen affinity of human red blood cells. *Appl. Opt.* 56, 439–445. doi: 10.1364/AO.56.000439
- Çimen, M. Y. B. (2008). Free radical metabolism in human erythrocytes. *Clin. Chim. Acta* 390, 1–11. doi: 10.1016/j.cca.2007.12.025
- Costa, E., Rocha, S., Rocha-Pereira, P., Castro, E., Miranda, V., Do Sameiro, et al. (2008). Altered erythrocyte membrane protein composition in chronic kidney disease stage 5 patients under haemodialysis and recombinant human erythropoietin therapy. *Blood Purif.* 26, 267–273. doi: 10.1159/000126922
- Dias, G. F., Bonan, N. B., Steiner, T. M., Tozoni, S. S., Rodrigues, S., Nakao, L. S., et al. (2018). Indoxyl sulfate, a uremic toxin, stimulates reactive oxygen species production and erythrocyte cell death supposedly by an organic anion transporter 2 (OAT2) and NADPH oxidase activity-dependent pathways. *Toxins* 10:280. doi: 10.3390/toxins10070280
- Dou, Y., Kruse, A., Kotanko, P., Rosen, H., Levin, N. W., and Thijssen, S. (2012). Red blood cell life span and erythropoietin resistance. *Kidney Int.* 81, 1275–1276. doi: 10.1038/ki.2012.54
- Du Plooy, J. N., Bester, J., and Pretorius, E. (2018). Eryptosis in haemochromatosis: Implications for rheology. *Clin. Hemorheol. Microcirc.* 69, 457–469. doi: 10.3233/CH-170325
- Dyrda, A., Cytlak, U., Ciurazkiewicz, A., Lipinska, A., Cuffe, A., Bouyer, G., et al. (2010). Local membrane deformations activate Ca²⁺-dependent K⁺ and anionic currents in intact human red blood cells. *PLoS One* 5:e9447. doi: 10.1371/journal.pone.0009447
- Ebert, T., Pawelzik, S. C., Witasz, A., Arefin, S., Hobson, S., Kublickiene, K., et al. (2020). Inflammation and premature ageing in chronic kidney disease. *Toxins* 12:227. doi: 10.3390/toxins12040227
- El-Far, M. A., Bakr, M. A., Farahat, S. E., and Abd El-Fattah, E. A. (2005). Glutathione peroxidase activity in patients with renal disorders. *Clin. Exp. Nephrol.* 9, 127–131. doi: 10.1007/s10157-005-0343-1
- Eschbach, J. W., Egrie, J. C., Downing, M. R., Browne, J. K., and Adamson, J. W. (1987). Correction of the anemia of end-stage renal disease with recombinant human erythropoietin. *N. Eng. J. Med.* 316, 73–78. doi: 10.1056/NEJM198707233170416
- Föller, M., Huber, S. M., and Lang, F. (2008). Erythrocyte programmed cell death. *IUBMB Life* 60, 661–668. doi: 10.1002/iub.106
- Föller, M., and Lang, F. (2020). Ion transport in eryptosis, the suicidal death of erythrocytes. *Front. Cell Dev. Biol.* 8:597. doi: 10.3389/fcell.2020.00597
- Föller, M., Mahmud, H., Gu, S., Kucherenko, Y., Gehring, E. M., Shumilina, E., et al. (2009a). Modulation of suicidal erythrocyte cation channels by an AMPA antagonist. *J. Cell. Mol. Med.* 13, 3680–3686. doi: 10.1111/j.1582-4934.2009.00745.x
- Föller, M., Sopjani, M., Koka, S., Gu, S., Mahmud, H., Wang, K., et al. (2009b). Regulation of erythrocyte survival by AMP-activated protein kinase. *FASEB J.* 23, 1072–1080. doi: 10.1096/fj.08-121772
- Franco, R. S., Puchulu-campanella, M. E., Barber, L. A., Mary, B., Joiner, C. H., Low, P. S., et al. (2013). Changes in the properties of normal human red blood cells during in vivo aging. *NIH Public Access* 88, 44–51. doi: 10.1002/ajh.23344
- Changes
- Fuertinger, D. H., Kappel, F., Thijssen, S., Levin, N. W., and Kotanko, P. (2013). A model of erythropoiesis in adults with sufficient iron availability. *J. Mathemat. Biol.* 66, 1209–1240. doi: 10.1007/s00285-012-0530-0
- Fuertinger, D. H., Kappel, F., Zhang, H., Thijssen, S., and Kotanko, P. (2018a). Prediction of hemoglobin levels in individual hemodialysis patients by means of a mathematical model of erythropoiesis. *PLoS One* 13:e0195918. doi: 10.1371/journal.pone.0195918
- Fuertinger, D. H., Topping, A., Kappel, F., Thijssen, S., and Kotanko, P. (2018b). The virtual anemia trial: an assessment of model-based in silico clinical trials of anemia treatment algorithms in patients with hemodialysis. *CPT: Pharmacomet. Systems Pharmacol.* 7, 219–227. doi: 10.1002/psp4.12276
- Gallagher, P. G. (2013). Disorders of red cell volume regulation. *Curr. Opin. Hematol.* 20, 201–207. doi: 10.1097/MOH.0b013e32835f6870
- Gao, C., Ji, S., Dong, W., Qi, Y., Song, W., Cui, D., et al. (2015). Indolic uremic solutes enhance procoagulant activity of red blood cells through phosphatidylserine exposure and microparticle release. *Toxins* 7, 4390–4403. doi: 10.3390/toxins7114390
- George, A., Pushkaran, S., Konstantinidis, D. G., Koochaki, S., Malik, P., Mohandas, N., et al. (2013). Erythrocyte NADPH oxidase activity modulated by Rac GTPases. PKC, and plasma cytokines contributes to oxidative stress in sickle cell disease. *Blood* 121, 2099–2107. doi: 10.1182/blood-2012-07-441188
- Ghashghaieina, M., Cluitmans, J. C. A., Akel, A., Dreischer, P., Toulany, M., Köberle, M., et al. (2012). The impact of erythrocyte age on eryptosis. *Br. J. Haematol.* 157, 606–614. doi: 10.1111/j.1365-2141.2012.09100.x
- Ginzburg, Y. Z., and Li, H. (2010). Crosstalk between iron metabolism and erythropoiesis. *Adv. Hematol.* 2010:605435. doi: 10.1155/2010/605435
- Glogowska, E., and Gallagher, P. G. (2015). Disorders of erythrocyte volume homeostasis. *Int. J. Lab. Hematol.* 37, 85–91. doi: 10.1016/j.physbeh.2017.03.040
- Gonzalez, L. J., Gibbons, E., Bailey, R. W., Fairbourn, J., Nguyen, T., Smith, S. K., et al. (2009). The influence of membrane physical properties on microvesicle release in human erythrocytes. *PMC Biophys.* 2:7. doi: 10.1186/1757-5036-2-7
- Guedes, M., Robinson, B. M., Obrador, G., Tong, A., Pisoni, R. L., and Pecoits-Filho, R. (2020). Management of anemia in non-dialysis chronic kidney disease: current recommendations, real-world practice, and patient perspectives. *Kidney* 360 1, 855–862. doi: 10.34067/KID.0001442020
- Halliwell, B., and Gutteridge, J. M. C. (2015). *Free Radicals in Biology and Medicine*. Oxford: Oxford University Press, 906.
- Hankins, H. M., Baldridge, R. D., Xu, P., and Graham, T. R. (2015). Role of flippases, scramblases and transfer proteins in phosphatidylserine subcellular distribution. *Traffic* 16, 35–47. doi: 10.1111/tra.12233
- Huertas, A., Das, S. R., Emin, M., Sun, L., Rifkind, J. M., Bhattacharya, J., et al. (2013). Erythrocytes induce proinflammatory endothelial activation in hypoxia. *Am. J. Respiratory Cell Mol. Biol.* 48, 78–86. doi: 10.1165/rcmb.2011-0402OC
- Iseki, K., and Kohagura, K. (2007). Anemia as a risk factor for chronic kidney disease. *Kidney Int.* 72, S4–S9. doi: 10.1038/sj.ki.5002481
- Jang, E. J., Kim, D. H., Lee, B., Lee, E. K., Chung, K. W., Moon, K. M., et al. (2016). Activation of proinflammatory signaling by 4-hydroxynonenal- Src adducts in aged kidneys. *Oncotarget* 7, 50864–50874. doi: 10.18632/oncotarget.10854

- Jones, D. P. (2006). Redefining Oxidative Stress. *Antioxidants Redox Signal.* 8, 1865–1879. doi: 10.1089/ars.2006.8.1865
- Kaestner, L. (2011). Cation channels in erythrocytes - historical and future perspective. *Open Biol.* 1, 27–34. doi: 10.1098/rsos.1104010027
- Kaestner, L., Bogdanova, A., and Egee, S. (2020). An update to calcium binding proteins. *Adv. Exp. Med. Biol.* 1131, 183–213. doi: 10.1007/978-3-030-12457-1_8
- Kalicki, R. M., and Uehlinger, D. E. (2008). Red cell survival in relation to changes in the hematocrit: more important than you think. *Blood Purif.* 26, 355–360. doi: 10.1159/000133838
- KDIGO (2012). KDIGO clinical practice guideline for anemia in chronic kidney disease. *Kidney Int.* 2, 279–335. doi: 10.1038/kisup.2012.40
- Kell, D. B. (2009). Iron behaving badly: inappropriate iron chelation as a major contributor to the aetiology of vascular and other progressive inflammatory and degenerative diseases. *BMC Med. Genom.* 2:2. doi: 10.1186/1755-8794-2-2
- Kell, D. B., and Pretorius, E. (2014). Serum ferritin is an important inflammatory disease marker, as it is mainly a leakage product from damaged cells. *Metallomics* 6, 748–773. doi: 10.1039/c3mt00347g
- Kempe, D. S., Lang, P. A., Duranton, C., Akel, A., Lang, K. S., Huber, S. M., et al. (2006). Enhanced programmed cell death of iron-deficient erythrocytes. *FASEB J.* 20, 368–370. doi: 10.1096/fj.05-4872fje
- Khazim, K., Giustarini, D., Rossi, R., Verkaik, D., Cornell, J. E., Cunningham, S. E. D., et al. (2013). Glutathione redox potential is low and glutathionylated and cysteinylated hemoglobin levels are elevated in maintenance hemodialysis patients. *Transl. Res.* 162, 16–25. doi: 10.1016/j.pestbp.2011.02.012
- Kieffmann, R., Rifkind, J. M., Nagababu, E., and Bhattacharya, J. (2008). Red blood cells induce hypoxic lung inflammation. *Blood* 111, 5205–5214. doi: 10.1182/blood-2007-09-113902
- Lang, E., and Lang, F. (2015). Triggers, inhibitors, mechanisms, and significance of eryptosis: the suicidal erythrocyte death. *BioMed. Res. Int.* 2015:513518. doi: 10.1155/2015/513518
- Lang, F., Bissinger, R., Abed, M., and Artunc, F. (2017). Eryptosis - the neglected cause of anemia in end stage renal disease. *Kidney Blood Press. Res.* 42, 749–760. doi: 10.1159/000484215
- Lang, F., Gulbins, E., Lang, P., Zappulla, D., and Foller, M. (2010). Ceramide in suicidal death of erythrocytes. *Cell. Physiol. Biochem.* 26, 21–28. doi: 10.1159/000315102
- Lang, F., Huber, S. M., Szabo, I., and Gulbins, E. (2007). Plasma membrane ion channels in suicidal cell death. *Arch. Biochem. Biophys.* 462, 189–194. doi: 10.1016/j.abb.2006.12.028
- Lang, F., Lang, E., and Filler, M. (2012). Physiology and pathophysiology of eryptosis. *Trans. Med. Hemotherapy* 39, 308–314. doi: 10.1159/000342534
- Lang, F., Lang, K. S., Lang, P. A., Huber, S. M., and Wieder, T. (2006). Osmotic shock-induced suicidal death of erythrocytes. *Acta Physiol.* 187, 191–198. doi: 10.1111/j.1748-1716.2006.01564.x
- Lang, F., and Qadri, S. M. (2012). Mechanisms and significance of eryptosis, the suicidal death of erythrocytes. *Blood Purif.* 33, 125–130. doi: 10.1159/000334163
- Leal, J. K. F., Adjubo-Hermans, M. J. W., and Bosman, G. J. C. G. M. (2018). Red blood cell homeostasis: mechanisms and effects of microvesicle generation in health and disease. *Front. Physiol.* 9:703. doi: 10.3389/fphys.2018.00703
- Li, J. H., Luo, J. F., Jiang, Y., Ma, Y. J., Ji, Y. Q., Zhu, G. L., et al. (2019). Red blood cell lifespan shortening in patients with early-stage chronic kidney disease. *Kidney Blood Press. Res.* 44, 1158–1165. doi: 10.1159/000502525
- Ling, X. C., and Kuo, K. L. (2018). Oxidative stress in chronic kidney disease. *Renal Replacement Therapy* 4:53. doi: 10.1186/s41100-018-0195-2
- Lipinski, B., Pretorius, E., Oberholzer, H. M., and Van Der Spuy, W. J. (2012). Interaction of fibrin with red blood cells: the role of iron. *Ultrastruct. Pathol.* 36, 79–84. doi: 10.3109/01913123.2011.627491
- Lupescu, A., Bissinger, R., Goebel, T., Salker, M. S., Alzoubi, K., Liu, G., et al. (2015). Enhanced suicidal erythrocyte death contributing to anemia in the elderly. *Cell. Physiol. Biochem.* 36, 773–783. doi: 10.1159/000430137
- Lutz, H. U., and Bogdanova, A. (2013). Mechanisms tagging senescent red blood cells for clearance in healthy humans. *Front. Physiol.* 4:387. doi: 10.3389/fphys.2013.00387
- Ma, J., Dou, Y., Zhang, H., Thijssen, S., Williams, S., Kuntsevich, V., et al. (2017). Correlation between inflammatory biomarkers and red blood cell life span in chronic hemodialysis patients. *Blood Purif.* 43, 200–205. doi: 10.1159/000452728
- Makhro, A., Huisjes, R., Verhagen, L. P., Mañú-Pereira, M., del, M., Llaudet-Planas, E., et al. (2016). Red cell properties after different modes of blood transportation. *Front. Physiol.* 7:288. doi: 10.3389/fphys.2016.00288
- Makhro, A., Kaestner, L., and Bogdanova, A. (2017). NMDA receptor activity in circulating red blood cells: methods of detection. *Methods Mol. Biol.* 1677, 265–282. doi: 10.1007/978-1-4939-7321-7
- Mao, T.-Y., Fu, L.-L., and Wang, J.-S. (2011). Hypoxic exercise training causes erythrocyte senescence and rheological dysfunction by depressed Gardos channel activity. *J. Appl. Physiol.* 111, 382–391. doi: 10.1152/japplphysiol.00096.2011
- Maurya, P. K., Kumar, P., and Chandra, P. (2015). Biomarkers of oxidative stress in erythrocytes as a function of human age. *World J. Methodol.* 5:216. doi: 10.5662/wjm.v5.i4.216
- Meyring-Wösten, A., Kuntsevich, V., Campos, I., Williams, S., Ma, J., Patel, S., et al. (2017). Erythrocyte sodium sensitivity and eryptosis in chronic hemodialysis patients. *Kidney Blood Press. Res.* 42, 314–326. doi: 10.1159/000477608
- Meyring-Wösten, A., Zhang, H., Ye, X., Fuertinger, D. H., Chan, L., Kappel, F., et al. (2016). Intradialytic hypoxemia and clinical outcomes in patients on hemodialysis. *Clin. J. Am. Soc. Nephrol.* 11, 616–625. doi: 10.2215/CJN.08510815
- Mohandas, N., and Gallagher, P. G. (2008). Red cell membrane: past, present, and future. *Blood* 112, 3939–3948. doi: 10.1182/blood-2008-07-161166
- Mohanty, J. G., Nagababu, E., and Rifkind, J. M. (2014). Red blood cell oxidative stress impairs oxygen delivery and induces red blood cell aging. *Front. Physiol.* 5:84. doi: 10.3389/fphys.2014.00084
- Myssina, S., Huber, S. M., Birka, C., Lang, P. A., Lang, K. S., Friedrich, B., et al. (2003). Inhibition of erythrocyte cation channels by erythropoietin. *J. Am. Soc. Nephrol.* 14, 2750–2757. doi: 10.1097/01.ASN.0000093253.42641.C1
- Nakanishi, T., Kuragano, T., Nanami, M., Nagasawa, Y., and Hasuike, Y. (2019). Misdistribution of iron and oxidative stress in chronic kidney disease. *Free Radical Biol. Med.* 133, 248–253. doi: 10.1016/j.freeradbiomed.2018.06.025
- Narla, J., and Mohandas, N. (2017). Red cell membrane disorders. *Int. J. Lab. Hematol.* 39, 47–52. doi: 10.1111/ijlh.12657
- Nemkov, T., Reisz, J. A., Xia, Y., Zimring, J. C., and D'Alessandro, A. (2018). Red blood cells as an organ? how deep omics characterization of the most abundant cell in the human body highlights other systemic metabolic functions beyond oxygen transport. *Exp. Rev. Proteom.* 15, 855–864. doi: 10.1080/14789450.2018.1531710
- Nguyen, D. B., Thuy, Ly, T. B., Wesseling, M. C., Hittinger, M., Torge, A., et al. (2016). Characterization of microvesicles released from human red blood cells. *Cell. Physiol. Biochem.* 38, 1085–1099. doi: 10.1159/000443059
- Nicolay, J. P., Schneider, J., Niemoeller, O. M., Artunc, F., Portero-Otin, M., Haik, G., et al. (2006). Stimulation of suicidal erythrocyte death by methylglyoxal. *Cell. Physiol. Biochem.* 18, 223–232. doi: 10.1159/000097669
- Ogawa, T., and Nitta, K. (2015). Erythropoiesis-stimulating agent hyporesponsiveness in end-stage renal disease patients. *Contrib. Nephrol.* 185, 76–86. doi: 10.1159/000380972
- Özüyan, B., Grau, M., Kelm, M., Merx, M. W., and Kleinbongard, P. (2008). RBC NOS: regulatory mechanisms and therapeutic aspects. *Trends Mol. Med.* 14, 314–322. doi: 10.1016/j.molmed.2008.05.002
- Polak-Jonkisz, D., and Purzyc, L. (2012). Ca influx versus efflux during eryptosis in uremic erythrocytes. *Blood Purif.* 34, 209–210. doi: 10.1159/000341627
- Polak-Jonkisz, D., Purzyc, L., Laszki-Szczchor, K., Musiał, K., and Zwolińska, D. (2010a). The endogenous modulators of Ca²⁺-Mg²⁺-dependent ATPase in children with chronic kidney disease (CKD). *Nephrol. Dial. Trans.* 25, 438–444. doi: 10.1093/ndt/gfp436
- Polak-Jonkisz, D., Purzyc, L., and Zwolińska, D. (2010b). Ca²⁺-Mg²⁺-dependent ATPase activity in hemodialyzed children. *Effect Hemodial. Sess. Pediatric Nephrol.* 25, 2501–2507. doi: 10.1007/s00467-010-1634-7
- Pretorius, E. (2013). The adaptability of red blood cells. *Cardiovas. Diabetol.* 12:63doi: 10.1186/1475-2840-12-63
- Pretorius, E., Du Plooy, J. N., and Bester, J. (2016a). A comprehensive review on eryptosis. *Cell. Physiol. Biochem.* 39, 1977–2000. doi: 10.1159/000447895

- Pretorius, E., Olumuyiwa-Akeredolu, O. O., Mbotwe, S., and Bester, J. (2016b). Erythrocytes and their role as health indicator: using structure in a patient-orientated precision medicine approach. *Blood Rev.* 30, 263–274. doi: 10.1016/j.blre.2016.01.001
- Pyrshv, K. A., Klymchenko, A. S., Csúcs, G., and Demchenko, A. P. (2018). Apoptosis and eryptosis: striking differences on biomembrane level. *Biochim. et Biophys. Acta - Biomembranes* 1860, 1362–1371. doi: 10.1016/j.bbmem.2018.03.019
- Qadri, S. M., Bissinger, R., Solh, Z., and Oldenborg, P. A. (2017). Eryptosis in health and disease: a paradigm shift towards understanding the (patho)physiological implications of programmed cell death of erythrocytes. *Blood Rev.* 31, 349–361. doi: 10.1016/j.blre.2017.06.001
- Reeves, J. P., Condrescu, M., Chernaya, G., and Gardner, J. P. (1994). Na⁺/Ca²⁺ antiport in the mammalian heart. *J. Exp. Biol.* 196, 375–388.
- Revin, V., Gruntyushkin, I., Gromova, N., Revina, E., Abdulwahid, A. S. A., Solomadin, I., et al. (2017). Effect of hypoxia on the composition and state of lipids and oxygen-transport properties of erythrocyte haemoglobin. *Biotechnol. Biotechnol. Equipment* 31, 128–137. doi: 10.1080/13102818.2016.1261637
- Rifkind, J. M., Mohanty, J. G., Nagababu, E., Salgado, M. T., and Cao, Z. (2018). Potential modulation of vascular function by nitric oxide and reactive oxygen species released from erythrocytes. *Front. Physiol.* 9:690. doi: 10.3389/fphys.2018.00690
- Rifkind, J. M., Zhang, L., Levy, A., and Manoharan, P. T. (1991). The hypoxic stress on erythrocytes associated with superoxide formation. *Free Radical Res.* 13, 645–652. doi: 10.3109/10715769109145842
- Rothstein, A., Cabantchik, Z. I., and Knauf, P. (1976). Mechanism of anion transport in red blood cells: role of membrane proteins. *Fed. Proc.* 35, 3–10.
- Saha, M., and Allon, M. (2017). Diagnosis, treatment, and prevention of hemodialysis emergencies. *Clin. J. Am. Soc. Nephrol.* 12, 357–369. doi: 10.2215/CJN.05260516
- Santolini, J., Wootton, S. A., Jackson, A. A., and Feelisch, M. (2019). The Redox architecture of physiological function. *Curr. Opin. Physiol.* 9, 34–47. doi: 10.1016/j.cophys.2019.04.009
- Sato, Y., Mizuguchi, T., Shigenaga, S., Yoshikawa, E., Chujo, K., Minakuchi, J., et al. (2012). Shortened red blood cell lifespan is related to the dose of erythropoiesis-stimulating agents requirement in patients on hemodialysis. *Therapeutic Apheresis Dial.* 16, 522–528. doi: 10.1111/j.1744-9987.2012.01089.x
- Segawa, K., and Nagata, S. (2015). An apoptotic “Eat Me” signal: phosphatidylserine exposure. *Trends Cell Biol.* 25, 639–650. doi: 10.1016/j.tcb.2015.08.003
- Sprague, R. S., Ellsworth, M. L., Stephenson, A. H., and Lonigro, A. J. (2001). Participation of cAMP in a signal-transduction pathway relating erythrocyte deformation to ATP release. *Am. J. Physiol. Cell Physiol.* 281, 1158–1164. doi: 10.1152/ajpcell.2001.281.4.c1158
- Tang, F., Feng, L., Li, R., Wang, W., Liu, H., Yang, Q., et al. (2018). Inhibition of suicidal erythrocyte death by chronic hypoxia. *High Altitude Med. Biol.* 20, 112–119. doi: 10.1089/ham.2017.0159
- Thomas, S. L. Y., Bouyer, G., Cuff, A., Egée, S., Glogowska, E., and Ollivaux, C. (2011). Ion channels in human red blood cell membrane: actors or relics? *Blood Cells Mol. Dis.* 46, 261–265. doi: 10.1016/j.bcmd.2011.02.007
- Tozoni, S. S., Dias, G. F., Bohnen, G., Grobe, N., Pecoits-Filho, R., Kotanko, P., et al. (2019). Uremia and hypoxia independently induce eryptosis and erythrocyte redox imbalance. *Cell. Physiol. Biochem.* 53, 794–804. doi: 10.33594/000000173
- Tucker, P. S., Dalbo, V. J., Han, T., and Kingsley, M. I. (2013). Clinical and research markers of oxidative stress in chronic kidney disease. *Biomarkers* 18, 103–115. doi: 10.3109/1354750X.2012.749302
- Uehlinger, D. E., Gotch, F. A., and Sheiner, L. B. (1992). A pharmacodynamic erythropoietin therapy for uremic anemia. *Clin. Pharmacol. Therapeutics* 51, 76–89. doi: 10.1038/clpt.1992.10
- Valko, M., Leibfritz, D., Moncol, J., Cronin, M. T. D., Mazur, M., and Telser, J. (2007). Free radicals and antioxidants in normal physiological functions and human disease. *Int. J. Biochem. Cell Biol.* 39, 44–84. doi: 10.1016/j.biocel.2006.07.001
- Virzi, G. M., Milan Manani, S., Clementi, A., Castegnaro, S., Brocca, A., Riello, C., et al. (2019). Eryptosis is altered in peritoneal dialysis patients. *Blood Purif.* 48, 351–357. doi: 10.1159/000501541
- Vos, F. E., Schollum, J. B., Coulter, C. V., Doyle, T. C. A., Duffull, S. B., and Walker, R. J. (2011). Red blood cell survival in long-term dialysis patients. *Am. J. Kidney Dis.* 58, 591–598. doi: 10.1053/j.ajkd.2011.03.031
- Williamson, P., Kulick, A., Zachowski, A., Schlegel, R. A., and Devaux, P. F. (1992). Ca²⁺ Induces transbilayer redistribution of all major phospholipids in human erythrocytes. *Biochemistry* 31, 6355–6360. doi: 10.1021/bi00142a027
- Wish, J. B. (2006). Assessing iron status: beyond serum ferritin and transferrin saturation. *Clin. J. Am. Soc. Nephrol.: CJASN* 1(Suppl. 1), 4–8. doi: 10.2215/CJN.01490506
- Wish, J. B., Aronoff, G. R., Bacon, B. R., Brugnara, C., Eckardt, K. U., Ganz, T., et al. (2018). Positive iron balance in chronic kidney disease: how much is too much and how to tell? *Am. J. Nephrol.* 47, 72–83. doi: 10.1159/000486968
- Zachara, B., Salak, A., Koterska, D., Manitus, J., and Wasowicz, W. (2004). Selenium and glutathione peroxidases in blood of patients with different stages of chronic renal failure. *Trace Elem. Med. Biol.* 17, 291–299. doi: 10.1016/s0946-672x(04)80031-2

Conflict of Interest: PK holds stock in Fresenius Medical Care. The Renal Research Institute is a wholly owned subsidiary of Fresenius Medical Care.

The remaining authors declare that the research was conducted in the absence of any commercial or financial relationships that could be construed as a potential conflict of interest.

Copyright © 2020 Dias, Grobe, Rogg, Jörg, Pecoits-Filho, Moreno-Amaral and Kotanko. This is an open-access article distributed under the terms of the Creative Commons Attribution License (CC BY). The use, distribution or reproduction in other forums is permitted, provided the original author(s) and the copyright owner(s) are credited and that the original publication in this journal is cited, in accordance with accepted academic practice. No use, distribution or reproduction is permitted which does not comply with these terms.



Voltage-Gated Potassium Channels as Regulators of Cell Death

Magdalena Bachmann^{1,2}, Weiwei Li², Michael J. Edwards², Syed A. Ahmad², Sameer Patel², Ildiko Szabo^{1,3*†} and Erich Gulbins^{2,4*†}

¹ Department of Biology, University of Padova, Padua, Italy, ² Department of Surgery, Medical School, University of Cincinnati, Cincinnati, OH, United States, ³ Consiglio Nazionale delle Ricerche Institute of Neuroscience, Padua, Italy, ⁴ Department of Molecular Biology, University of Duisburg-Essen, Essen, Germany

OPEN ACCESS

Edited by:

Markus Ritter,
Paracelsus Medical University, Austria

Reviewed by:

Silvia Dossena,
Paracelsus Medical University, Austria
M. Teresa Perez-Garcia,
University of Valladolid, Spain
Marjan Slak Rupnik,
Medical University of Vienna, Austria

*Correspondence:

Ildiko Szabo
ildiko.szabo@unipd.it;
ildi@mail.bio.unipd.it
Erich Gulbins
erich.gulbins@uni-due.de

[†]These authors share last authorship

Specialty section:

This article was submitted to
Cell Death and Survival,
a section of the journal
Frontiers in Cell and Developmental
Biology

Received: 29 September 2020

Accepted: 23 November 2020

Published: 14 December 2020

Citation:

Bachmann M, Li W, Edwards MJ,
Ahmad SA, Patel S, Szabo I and
Gulbins E (2020) Voltage-Gated
Potassium Channels as Regulators
of Cell Death.
Front. Cell Dev. Biol. 8:611853.
doi: 10.3389/fcell.2020.611853

Ion channels allow the flux of specific ions across biological membranes, thereby determining ion homeostasis within the cells. Voltage-gated potassium-selective ion channels crucially contribute to the setting of the plasma membrane potential, to volume regulation and to the physiologically relevant modulation of intracellular potassium concentration. In turn, these factors affect cell cycle progression, proliferation and apoptosis. The present review summarizes our current knowledge about the involvement of various voltage-gated channels of the Kv family in the above processes and discusses the possibility of their pharmacological targeting in the context of cancer with special emphasis on Kv1.1, Kv1.3, Kv1.5, Kv2.1, Kv10.1, and Kv11.1.

Keywords: Kv-channels, cancer, cell proliferation, mitochondria, cell death

INTRODUCTION

Potassium channels allow the flux of K⁺ down the electrochemical gradient across the plasma membrane as well as across membranes of intracellular organelles. Among the different types of K⁺ channels encoded by more than 80 genes, the voltage-gated potassium channels represent the largest and most complex family with numerous members, classified into Kv1-Kv12 subfamilies (Alexander et al., 2017). Most subfamilies have distinct channels (e.g., Kv1.1-Kv1.8, Kv2.1-Kv2.2, Kv3.1-Kv3.4, etc.) based on their different biophysical properties and pharmacological profile (Gutman et al., 2005; González et al., 2012). Kv5.1, Kv6s, Kv8s, and Kv9s encode subunits that have a regulatory role and are unable to form homotetramers on their own. Functional channel-forming alpha subunits harboring six transmembrane segments have been associated with different functions, ranging from ensuring cell excitability to the regulation of cell cycle. These proteins, expressed in different tissues, belong to six subfamilies named Kv1 (Shaker), Kv2 (Shab), Kv3 (Shaw), Kv4 (Shal), Kv7 (of which Kv7.1 is named KvLQT), and ether a go-go (EAG; Kv10, Kv11, Kv12). In some cases, members of a given subfamily can heteromultimerize to give a functional channel composed of four alpha subunits. Frequent alternate splicing and association with regulatory beta subunits further contributes to the enormous diversity of potassium channel functions. The crucial role of Kv channels in cellular and organ physiology is illustrated by the vast number of pathologies linked to their mutation [e.g., the long QT syndrome for Kv11.1 and Kv7.1 (Brewer et al., 2020), non-syndromic sensorineural deafness type 2 for Kv7.4 (Xia et al., 2020), etc.].

In addition to the Kv subfamilies whose members mediate efflux of potassium from the cell at depolarizing potentials (outward rectifiers), the so-called inward rectifiers (Kir) contribute to cells physiology by allowing greater influx than efflux of potassium ions at a comparable driving force. While Kv voltage-dependent potassium channels display an intrinsic gating thanks to the positively

charged S4 transmembrane segment, inward rectification is caused by voltage-dependent block of the channel pore by cytoplasmic ions, including Mg^{2+} and polyamines. In addition, some of the calcium-dependent potassium channel family members (e.g., Big-conductance Ca^{2+} -dependent K^+ channel BKCa) are also activated by changes in membrane potential in addition of changes in intracellular $[Ca^{2+}]$ (González et al., 2012). Some members of the two-pore K^+ channel family (e.g., some members of the TASK family) also show a slight voltage-dependence of their probability of being open (Enyedi and Czirjak, 2010).

In this review we will focus our attention on the members of the classical voltage-gated Kv channel family, who were among the first channels to be linked to the regulation of cell cycle (DeCoursey et al., 1984; McKinnon and Ceredig, 1986; Arcangeli et al., 1993; Pardo et al., 1998) and cell death (Szabo et al., 1996; Gómez-Angelats et al., 2000), both processes instrumental to cancer progression (for recent reviews see e.g., Pardo and Stuhmer, 2014; Serrano-Novillo et al., 2019; Capatina et al., 2020). Indeed, dysregulated cell cycle leading to unlimited proliferation as well as apoptosis resistance are two hallmarks of cancer cells (Hanahan and Weinberg, 2000). While the notion that intracellular voltage-gated K^+ channels are also linked to cancer is emerging (e.g., Bachmann et al., 2019; Peruzzo and Szabo, 2019; Teisseyre et al., 2019), the present review focuses on the Kv channels located in the plasma membrane. **Table 1** summarizes the major findings discussed throughout this review about the role of different Kv channels in cell proliferation, apoptosis induction and tumor growth. Furthermore, voltage-gated potassium channels as possible targets for pharmacological cancer therapy are discussed.

VOLTAGE-GATED POTASSIUM CHANNELS AND THE REGULATION OF CELL CYCLE AND PROLIFERATION

Cell proliferation plays a fundamental role during embryogenesis, tissue renewal and remodeling as well as wound healing. The process is tightly regulated, and aberrant cell cycle progression leads to pathological conditions such as cancer. Voltage-gated potassium channels are important contributors to the mechanisms that control cell division. Because the topic has been extensively reviewed in the last years, we will only briefly summarize by which means Kv channels control cell cycle progression and show some recent advances in the field. The interested reader is referred to some excellent reviews [for general coverage of the topic, for instance (Blackiston et al., 2009; Urrego et al., 2014; Liu and Wang, 2019); regarding cancer (Leanza et al., 2016; Rao et al., 2015; Serrano-Novillo et al., 2019)]. Among the various voltage-gated channels, the most abundant information regarding their role in cell cycle regulation/proliferation is available about Kv1.1, Kv1.3 (for recent reviews see Pérez-García et al., 2018; Teisseyre et al., 2019), Kv1.5, Kv10.1 (Urrego et al., 2017), and Kv11.1 (He S. et al., 2020).

Voltage-gated potassium channels regulate the progression through cell cycle checkpoints based on both their

ion-conducting properties and their interaction with other proteins belonging to signaling complexes at the plasma membrane (**Figure 1**). The membrane potential is not constant during the cell cycle. At the transition between the G1 and S phase, the plasma membrane hyperpolarizes, while a depolarization is necessary for cells to proceed from G2 to M (Blackiston et al., 2009). Cells with a high proliferation rate tend to be less polarized at each step of the cell cycle. Consequently, cancer cells generally exhibit a depolarized phenotype (Pardo and Stuhmer, 2014; Serrano-Novillo et al., 2019). Potassium channels, as important contributors to setting the membrane potential, regulate cell cycle progression. Their role in mitogenesis was first proposed in 1984, when Cahalan and his team found that potassium channel blockers inhibited the proliferation of T lymphocytes (DeCoursey et al., 1984).

Kv channels influence cell cycle progression not only by setting the membrane potential, but also, as a consequence, by contributing to ensuring the driving force for calcium entry (for reviews see e.g., Cahalan and Chandy, 2009; Urrego et al., 2014) and the exit of chloride ions (and the resulting cell shrinkage). Accordingly, Kv channel expression changes during the progression through the different phases of the cell cycle, as first revealed more than 30 years ago in T lymphocyte development (McKinnon and Ceredig, 1986). Changes in the subcellular localization of different Kv channels also seem to play a relevant role (Serrano-Novillo et al., 2019). Independently from their ion-conducting properties, also the interaction of specific Kv channels with proteins mediating intracellular signaling cascades regulates cell cycle progression (Urrego et al., 2014; He S. et al., 2020).

Kv1 Channels

As important regulators of cell proliferation, numerous reports have correlated the activity and expression of various potassium channels to the growth and progression of multiple kinds of cancers (recently reviewed in Serrano-Novillo et al., 2019). Kv1.1, along with Kv1.3, has been identified as a critical player to thymocyte pre-clonal expansion (Freedman et al., 1995). Later on, Kv1.1 was shown to be expressed in the breast cancer cell line MCF-7 and its blocker Dendrotoxin (DTX) (10 nM) reduced proliferation by 30% (Ouadid-Ahidouch et al., 2000). Likewise, DTX suppressed lung adenocarcinoma growth *in vivo* (Jang et al., 2011b) and at 100 nM concentration, it reduced proliferation of chemoresistant non-small cell lung cancer (NSCLC) cells both *in vitro* and *in vivo* (Jeon et al., 2012). Inhibition of Kv1.1 by KAaH2 toxin targeting specifically Kv1.1 was shown to inhibit proliferation of glioblastoma via the Epidermal Growth Factor Receptor (EGFR) signaling pathway (Aissaoui et al., 2018). In addition, Kv1.1's high expression was observed to correlate with poor prognosis of cervical cancer patients and silencing of the channel blunted proliferation of HeLa cells (Liu et al., 2019).

Inhibition of other Kv channels by specific toxins was also shown to reduce cancer cell proliferation and tumor size. In general, many studies addressed the relevance of Kv1.3 for proliferation in different cancer lines (e.g., Abdul et al., 2003; Preussat et al., 2003; Wu J. et al., 2013) or in primary cells (e.g.,

TABLE 1 | Targeting of Kv channels and its effects on cell death and proliferation.

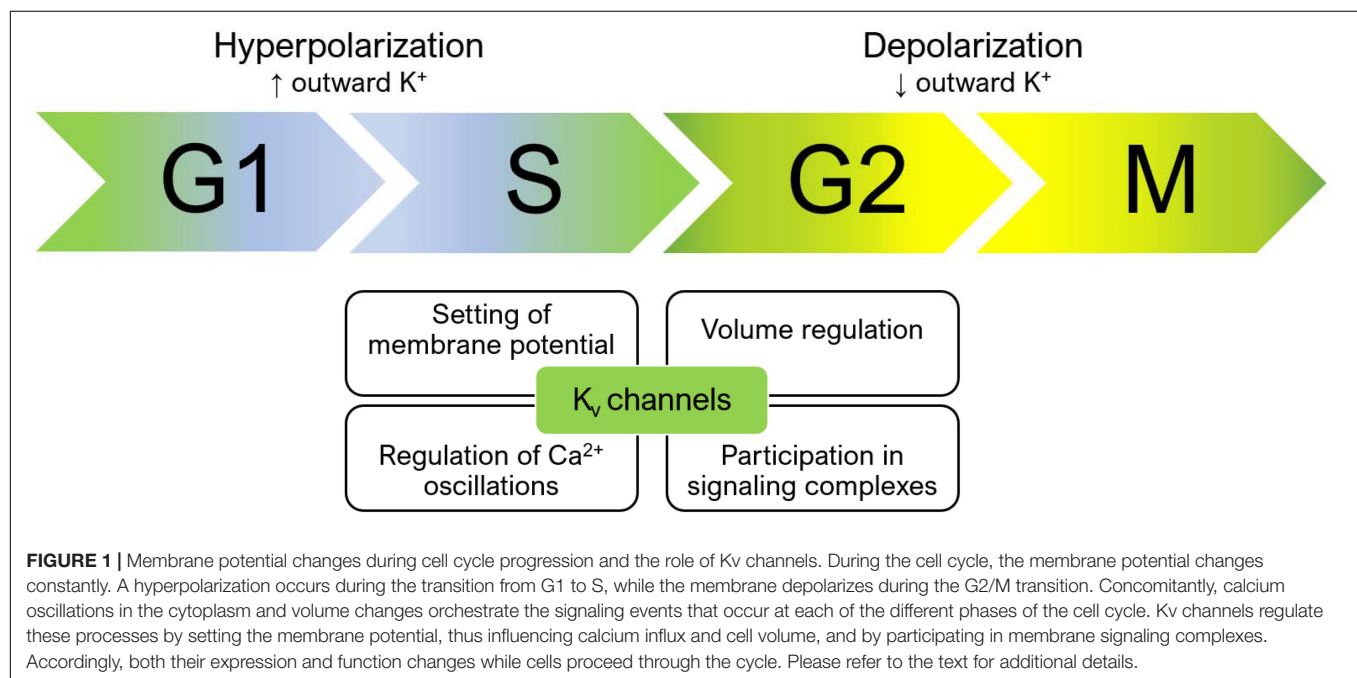
Kv1.1	<ul style="list-style-type: none"> – Inhibition with 200 nM Dendrotoxin decreases preclonal expansion of thymocytes – Inhibition with 1–10 nM Dendrotoxin reduces proliferation of MCF-7 breast cancer cells – Inhibition with 100 nM Dendrotoxin arrests gefitinib-resistant H-460 NSCLC cells at G1/S and reduces tumor growth – Enhanced expression protects neurons from cell death stimuli – Downregulation or inhibition with 50 μM Agitoxin-2 in retinal ganglion cells rescues neurodegeneration – Inhibition with 50 μg/ml KAaH2 reduces proliferation of U-87 glioblastoma cells – Kv1.1 silencing decreased proliferation of HeLa cells 	<ul style="list-style-type: none"> – Freedman et al., 1995 – Quadid-Ahidouch et al., 2000 – Jeon et al., 2012 – Lee et al., 2003; Shen et al., 2009 – Koeberle et al., 2010 – Aissaoui et al., 2018 – Liu et al., 2019
Kv1.3	<ul style="list-style-type: none"> – Inhibition with 200 nM Charybdotoxin decreases preclonal expansion of thymocytes – Knockdown or inhibition with 1 nM Margatoxin arrests A-549 lung adenocarcinoma cells at G1/S and reduces tumor growth – Expression of Kv1.3 increases cell proliferation independently from ion conductance – Inhibition with 0.1–5 μM PAP-1 reduces proliferation of smooth muscle cells – Activation with 0.1–1 μM LJ101019C increases NK cell proliferation and progression through G1/S – Downregulation or inhibition with 50 μM Margatoxin in retinal ganglion cells rescues neurodegeneration – Downregulation of both Kv1.3 and Kv1.5 protects macrophages from staurosporine-induced cell death 	<ul style="list-style-type: none"> – Freedman et al., 1995 – Jang et al., 2011a – Ciudad et al., 2012; Jimenez-Perez et al., 2016 – Lasch et al., 2020 – Geng et al., 2020 – Koeberle et al., 2010 – Leanza et al., 2012b
Kv1.5	<ul style="list-style-type: none"> – Knockdown reduces proliferation, induces an arrest at G0/G1 and increases apoptosis of MG-63 osteosarcoma cells – Downregulation of both Kv1.5 and Kv1.3 protects macrophages from staurosporine-induced cell death – Knockdown protects endothelial cells from palmitate-induced apoptosis – Inhibition with 1 μM DPO-1 rescues the suppression of proliferation and induction of apoptosis mediated by apogonin in pulmonary artery smooth muscle cells – Inhibition with 0.3–3 mg/kg DPO-1 rescues H₂O₂-induced endothelial cell apoptosis 	<ul style="list-style-type: none"> – Wu et al., 2015 – Leanza et al., 2012b – Du et al., 2017 – He Y. et al., 2020 – Chen et al., 2012
Kv2.1	<ul style="list-style-type: none"> – Inhibition with 0.2–1 μM Hanatoxin reduces proliferation of uterine cancer cells – Dominant-negative isoforms protect against DTDP-induced apoptosis of cortical neurons, while overexpression increases susceptibility – Inhibition with 3 μM 48F10 confers resistance to DTDP-induced cell death in cortical neurons – Inhibition with 1–20 μM 48F10 confers resistance to DTDP-induced cell death in enterocytes – Inhibition with 10 mM TEA or 30 μM Donezepil reduces oxygen-glucose deprivation-induced apoptosis of HEK293 cells – Inhibition with 1 μM Ts15 reduces proliferation of T cells (Ts15 also inhibits Kv1.3 and Kv1.2) – Interfering with Kv2.1 membrane insertion by a syntaxin-1A-mimicking peptide ameliorates cell death in an ischemic stroke model – Inhibition with 20 mg/kg vindoline, 1–10 μM or 50 mg/kg SP6616 or 10 μM or 20 mg/kg ETA improves β-cell dysfunction and ameliorates hyperglycemia in diabetes models – Silencing of Kv2.1 partner Kv9.3 arrested cell cycle in A549 lung carcinoma 	<ul style="list-style-type: none"> – Suzuki and Takimoto, 2004 – Pal et al., 2003 – Zaks-Makhina et al., 2004 – Grishin et al., 2005 – Yuan et al., 2011 – Pucca et al., 2016 – Yeh et al., 2017 – Yao et al., 2013; Zhou et al., 2016, 2018 – Lee et al., 2015
Kv3.1	<ul style="list-style-type: none"> – Inhibition with anti-Kv3.1 antibodies or downregulation reduces proliferation of oligodendrocyte progenitor cells 	<ul style="list-style-type: none"> – Tiwari-Woodruff et al., 2006
Kv3.4	<ul style="list-style-type: none"> – Increased expression under hypoxia increases proliferation of oral squamous cell carcinoma cells – Increased activity after radiotherapy arrests myeloid leukemia cells at G2/M due to hyperpolarization of the membrane 	<ul style="list-style-type: none"> – Qian et al., 2019 – Palme et al., 2013
Kv7.4	<ul style="list-style-type: none"> – Inhibition with 10 μM Linopirdine increases cell death of spiral ganglion neurons 	<ul style="list-style-type: none"> – Lv et al., 2010
Kv10.1	<ul style="list-style-type: none"> – Blockage with a monoclonal antibody decreases proliferation of different cancer cell lines and inhibits breast and pancreatic tumor growth – Inhibition with 10 μM Astemizole reduces cell proliferation and viability in a cervical cancer model – Inhibition with 1–3 μM Astemizole synergistically enhances the anti-proliferative effects of calcitriol on breast cancer cells – Simultaneous knockdown of Kv10.1 and overexpression of TRAIL induces apoptosis of MG-63 osteosarcoma cells and reduces tumor growth – Inhibition with 5 μM Astemizole reduces HepG2 and HuH-7 hepatocellular carcinoma cell viability and proliferation and tumor growth – TRAIL-ligated antibodies sensitize chemoresistant MDA-MB-435S breast cancer cells to chemotherapeutics and reduce tumor growth – Knockdown or inhibition with 5 μM Astemizole increases U-87MG glioblastoma sensitivity to Temozolomide – Knockdown or inhibition with 2.5–7.5 μM Astemizole increases the sensitivity of SH-SY5Y to rotenone-induced apoptosis – Inhibition with 7.5–9 μM Astemizole acts synergistically with Gefitinib to reduce proliferation and increase apoptosis of lung cancer cell lines – TRAIL-ligated nanobodies induce apoptosis in prostate and pancreatic cancer cells – Inhibition with 1–100 μM or 15 mg/kg Procyanidin B1 inhibits proliferation and migration of liver cancer cells and hepatoma growth 	<ul style="list-style-type: none"> – Gomez-Varela et al., 2007 – Diaz et al., 2009 – García-Quiroz et al., 2012, 2014 – He et al., 2013 – de Guadalupe Chávez-López et al., 2015 – Hartung and Pardo, 2016 – Sales et al., 2016 – Horst et al., 2017 – de Guadalupe Chávez-López et al., 2017 – Hartung et al., 2020 – Na et al., 2020

(Continued)

TABLE 1 | Continued

Kv11.1 – Inhibition with 1 μ M E-4031 reduces proliferation of uterine cancer cells and arrests cells at G0/G1	– Suzuki and Takimoto, 2004
– Inhibition with 25–50 μ M erythromycin increases the sensitivity of HT-29 colon carcinoma cells to chemotherapeutics and vincristine-induced G2/M arrest	– Chen et al., 2005
– Inhibition with 100 nM Cisapride arrests the cell cycle at G1/S and increases apoptosis of gastric cancer cells	– Shao et al., 2005
– Inhibition with 5–20 μM E-4031, 20 μM WAY, 1 μM Sertindole, 100 μM erythromycin or 20 μM R-Roscovotine increases susceptibility of acute lymphoblastic leukemia cells to chemotherapeutics and 20 mg/kg E-4031 reduces leukemia burden <i>in vivo</i>	– Pillozzi et al., 2011
– Knockdown or inhibition with 20–40 μ M Doxazosin arrests the cell cycle at G0/G1 and induces apoptosis in glioblastoma cells	– Bishopric et al., 2014
– Inhibition with < 10 μM CD-160130 leads to growth arrest and apoptosis of leukemic cells and reduces tumor growth	– Gasparoli et al., 2015
– Antibodies fused to Doxorubicin-loaded nanoparticles increase PANC-01 pancreatic cancer cell death and growth arrest at G2/M	– Spadavecchia et al., 2016
– Inhibition with 7 μM E-4031 concomitantly with KCa3.1 activation increases cisplatin-induced cell death and G2/M arrest in colorectal carcinoma cells and reduces tumor growth	– Pillozzi et al., 2018
– Kv11.1 activity stimulates proliferation of esophageal squamous cell carcinoma cells, knockdown reduces tumor growth	– Wang et al., 2019
– Decreased expression after application of a miR-96 inhibitor arrests bladder cancer cells at G1	– Xu et al., 2018
– Activation with 50 μM or 6 mg/kg NS-1643 arrests proliferation of MDA-MB-231 breast cancer cells and reduces tumor growth and metastatic spread	– Fukushima-Lopes et al., 2017; Breuer et al., 2019
– Knockdown or inhibition with 10–20 μ M E-4031 reduces proliferation and increases apoptosis of MG-63 osteosarcoma cells, while activation with 5–10 μ M PD 118057 increases proliferation	– Zeng et al., 2016
– Inhibition with 40–160 μM Clarithromycin induces a G2/M arrest and apoptosis of HCT-116 colorectal cancer cells and potentiates the effect of 5-FU <i>in vivo</i>	– Petroni et al., 2020

Studies listed in the text in which direct modulation of channel expression or function (or both) was used to study their involvement in cell cycle progression and apoptosis induction are summarized. Papers in which an *in vivo* approach was also used are highlighted in bold.



Smith et al., 2002; Grossinger et al., 2014; Petho et al., 2016). The proposed mechanism linking Kv1.3 function and its ability to set membrane potential to proliferation is summarized in **Figure 2** for the case of lymphocytes. The same proliferation-promoting mechanism may apply for pathological lymphocytes, where upregulation of Kv1.3 ensures a continuous driving force for calcium entry into the cells. Margatoxin (MgTx), an inhibitor of Kv1.3 (but also of Kv1.1 and Kv1.2; Bartok

et al., 2014), when injected directly into the xenograft nude mice model of A549 human lung adenocarcinoma at 1 nM concentration, significantly inhibited tumor growth. This was proposed to be ascribable to the effect of MgTx on cell cycle progression (Jang et al., 2011a). In addition to cancer, Kv1.3 activity has been correlated to the proliferation of many other types of cells, including vascular smooth muscle cells (Cidad et al., 2010; Cheong et al., 2011). Kv1.3 blockade with PAP-1

decreased the proliferation rate of these cells by downregulating receptor tyrosine kinases and the cell cycle regulator Early Growth Response-1 (EGR1) (Lasch et al., 2020). Further, a recent report highlighted that the cajanine derivative LJ101019C (1 μ M), able to enhance Kv1.3 activity and expression, leads to natural killer (NK) cell proliferation and activation *via* AKT/mammalian Target Of Rapamycin (mTOR) signaling (Geng et al., 2020), representing thus a promising candidate for NK-based immunotherapy against cancer.

As to Kv1.5, this channel has been shown to be upregulated in many types of tumors and metastatic tissues and promotes proliferation. However, expression of Kv1.5 shows an inversed correlation with malignancy in some gliomas and non-Hodgkin's lymphomas (Comes et al., 2013, 2015), while its high expression, along with that of Kv1.3, correlates with leiomyosarcoma proliferation and aggressiveness (Bielanska et al., 2012). In accordance, silencing Kv1.5 expression in osteosarcoma significantly inhibited proliferation and induced a cell cycle arrest at G0/G1 phase (Wu et al., 2015) and channel expression has been linked to proliferation in several works (see e.g., Vallejo-Gracia et al., 2013; Chow et al., 2018).

Altogether, a conclusive general picture regarding the involvement of Kv1.1, Kv1.3, and Kv1.5 in promoting cancer cell proliferation in different types of cancers where these channels are expressed is still lacking, such as the exact mechanism(s) involved in channel-mediated signaling leading to proliferation. These proteins can apparently promote proliferation also independently of their ion-conducting properties, but in function of the presence of two phosphorylation sites at the C-terminus of the channels (Figure 3; see e.g., Ciudad et al., 2012; Jimenez-Perez et al., 2016). Only sporadic studies addressed the role of other Kv1. channels in proliferation (see e.g., Vautier et al., 2004).

Kv2 Channels

Among channels of the Kv2. family, Kv2.1 (in heteromers with the silent subunit Kv9.3) seems to be the major component of Kv channels in cervical adenocarcinoma cells. Silencing of the Kv2.1 partner Kv9.3 using small interfering RNA caused G0/G1 cell cycle arrest in colon and lung carcinoma cell lines (Lee et al., 2015). The specific blocker of Kv2.1 Hanatoxin-1 significantly reduced proliferation of different cell lines by up to 40% (Suzuki and Takimoto, 2004). Another study showed that Ts15, a toxin from *Tityus serrulatus*, inhibited proliferation of central memory T cells, where Kv2.1 is highly expressed (Pucca et al., 2016), similarly to the hippocampus. In contrast, downregulation of Kv2.1 expression in HEK293 cells by Tacrine, a cholinesterase inhibitor, was able to boost proliferation (Hu X.M. et al., 2020). To our knowledge, Ts15 and Hanatoxin-1 have not been explored in the context of cancer in other studies.

Kv3 Channels

It has been reported that block of Kv3.1-specific currents or genetic ablation of the channel inhibits proliferation and migration of oligodendrocyte progenitor cells (Tiwari-Woodruff et al., 2006), while block of Kv3.4 resulted in a reduced proliferation rate of vascular smooth muscle cells (Miguel-Velado et al., 2005, 2010). Kv3.1 and Kv3.4 both contribute

to lung adenocarcinoma and breast cancer cell migration and tumor invasiveness, although their inhibition did not affect cell proliferation (Song et al., 2018). On the other hand, a recent report elucidated the mechanism by which Kv3.4 channel is involved in oral squamous cell carcinoma growth (Qian et al., 2019). In this study, hypoxia was found to induce the Hypoxia-Inducible Factor (HIF-1 α), which mediates increased Kv3.4 expression, proliferation, migration and invasion of oral squamous cell carcinoma cells. Kv3.4 also plays a role in mediating radio-resistance of myeloid leukemia cells by increasing its activity after application of ionizing radiation and inducing a G2/M arrest due to hyperpolarization of the membrane, calcium influx, Calcium/calmodulin-dependent protein Kinase (CamKII) activation and following inactivation of the phosphatase cdc25B and the cyclin-dependent kinase cdc2, both important for the G2/M transition (Palme et al., 2013).

Kv4 Channels

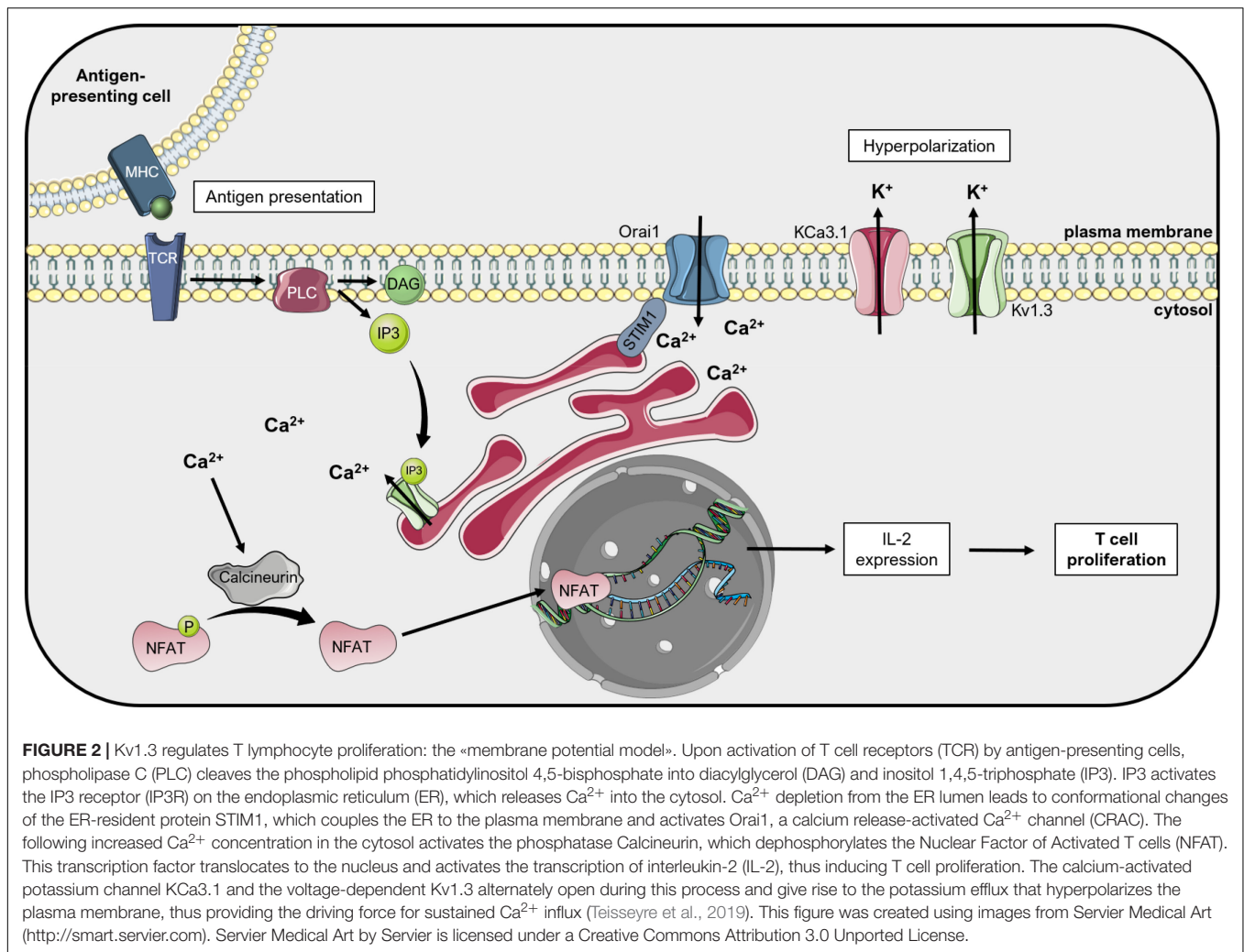
Kv4 channels have been characterized mainly in the context of neuronal function, but a recent work identified peptidyl-prolyl cis-trans isomerase NIMA-interacting 1 (Pin1), a prolyl isomerase that promotes cancer cell proliferation, as an interactor of Kv4.2 (Hu J.H. et al., 2020). The importance of this interaction was underlined in the context of cognitive flexibility, but not of cancer so far.

Kv7 Channels

The Kv7 channels are encoded by *KCNQ* genes and are expressed in cardiac myocytes, smooth muscle cells, neurons, and epithelial cells, where they play a role in various physiological processes (González et al., 2012), including that of regulating proliferation (Roura-Ferrer et al., 2008). A recent work highlighted Kv7.5 as promising therapeutic target for vascular tumors, as its expression clearly correlated with neoplastic malignancy (Serrano-Novillo et al., 2020). Interestingly, Tamoxifen, often used against breast cancer, inhibits Kv7.2 and Kv7.3 that are the main ion channels contributing to the so-called M-current, which regulates neuronal excitability (Ferrer et al., 2013). However, the role of this effect in the context of breast or other cancers has not been explored.

Kv10 and Kv11 Channels

In addition to the above-mentioned channels, work from different labs on Kv10.1 and Kv11.1 indicated their important role in cancer development and progression. The Kv10.1 channel was the first with proven oncogenic potential (Pardo et al., 1999) and is overexpressed in about 70% of human tumor biopsies (Urrego et al., 2014). Kv10.1 was proposed to be crucially involved in the resorption of the primary cilium during the G2/M phase of the cell cycle, thus favoring cell cycle progression (Urrego et al., 2017). As to Kv11.1, this channel has been associated to different tumoral processes such as cell cycle progression, angiogenesis, invasiveness and metastasis formation and the channel is also overexpressed in a variety of cancer cells with respect to corresponding non-cancer tissues (He S. et al., 2020). Indeed, implications of Kv11.1 on cell



cycle and proliferation in gastric, pancreatic and breast cancer have already been established, and the channel was shown to influence tumor progression of esophageal squamous cell carcinoma, bladder cancer and osteosarcoma as well (Zeng et al., 2016; Xu et al., 2018; Wang et al., 2019). Recent results revealed that in esophageal squamous cell carcinoma, Kv11.1 stimulates Phosphatidylinositol 3-Kinase (PI3K)/Akt, which leads to upregulation of thioredoxin domain-containing protein 5 (TXNDC5), thus increasing proliferation, inhibiting apoptosis and favoring epithelial-to-mesenchymal transition. Kv11.1 knockdown accordingly reduced tumor growth and metastasis formation *in vivo* (Wang et al., 2019). In bladder cancer, miR-96 was found to regulate Kv11.1 expression. Using a miR-96 inhibitor, Kv11.1 expression decreased, and cells were arrested at the G1 phase. miR-96 inhibition further increased apoptosis and decreased migration of bladder cancer cells (Xu et al., 2018). Similar effects on proliferation, migration and apoptosis were obtained in osteosarcoma cells by inhibition of Kv11.1, which reduced Nuclear Factor kappa-light-chain-enhancer of activated B cells (NF- κ B) activity through decreased PI3/Akt signaling (Zeng et al., 2016).

VOLTAGE-GATED POTASSIUM CHANNELS AND REGULATION OF PROGRAMMED CELL DEATH

Strikingly, most of the above-mentioned channels are intimately linked not only to proliferation, but also to the regulation of apoptosis (Szabo et al., 2010). Here, we discuss the role of Kv channels in cell death.

Kv1 Channels

Kv1.3 was one of the first ion channels whose function was shown to be modulated under various phases of apoptosis. In particular, the channel was shown to be inhibited within a few minutes following apoptosis induction by CD95 (Szabo et al., 1996) or by ceramide (Gulbins et al., 1997), due to tyrosine phosphorylation of the channel. This post-translational modification was shown to inhibit Kv1.3 activity also in other contexts (Holmes et al., 1996; Cayabyab et al., 2000). On the other hand, in a still early phase of apoptosis, the channel was shown to be activated by apoptotic stimuli and to contribute to the so-called apoptotic volume

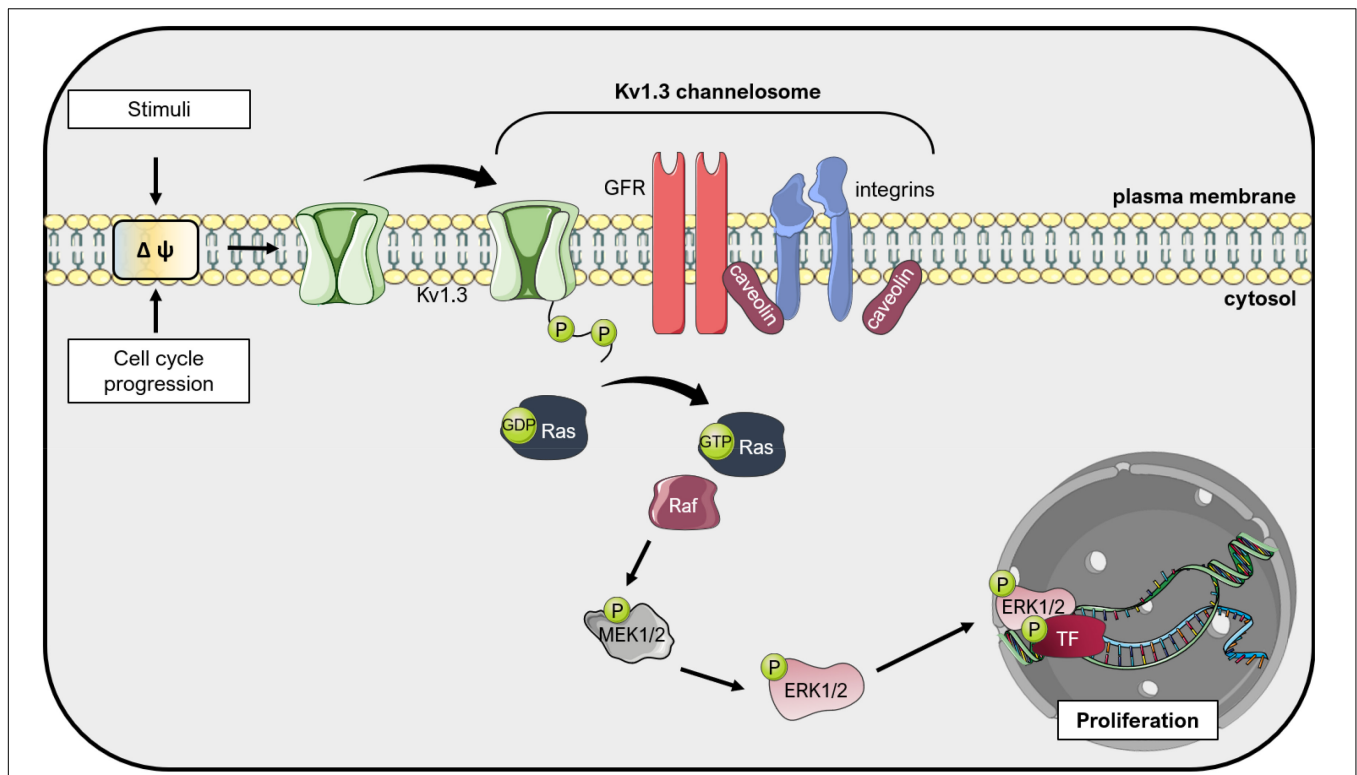


FIGURE 3 | Kv1.3 regulates cell proliferation independently from ion conductance: the «voltage sensor model». Changes in the plasma membrane potential, that occur during cell cycle progression or upon application of external stimuli, induce a conformational change in Kv1.3 due to its voltage-sensor domain. Because Kv1.3 interacts with other proteins in large complexes (the so-called Kv1.3 channelosome), these conformational changes translate into phosphorylation of the C-terminus of Kv1.3 and activation of pro-proliferative signal transduction cascades, including integrin and growth factor receptor (GFR) signaling. These events result in activation of Ras, which activates the Raf/Mitogen-activated protein kinase (MEK)/Extracellular signal-Regulated Kinase (ERK) pathway, finally leading to proliferation mediated by different downstream transcription factors (TF) such as c-Myc (Pérez-García et al., 2018). This figure was created using images from Servier Medical Art (<http://smart.servier.com>). Servier Medical Art by Servier is licensed under a Creative Commons Attribution 3.0 Unported License.

decrease in lymphocytes (Storey et al., 2003) that is associated with the activation of the apoptotic machinery (Bortner and Cidlowski, 2004, 2014). Further work is required to understand the importance of these findings, since Margatoxin, an inhibitor of Kv1.3, neither induced nor inhibited apoptosis in these studies. Nonetheless, using genetic models or silencing of Kv1.3, it was clearly shown that Kv1.3 expression is required for apoptosis (Bock et al., 2002), even in primary cells (Szabo et al., 2008), since in the absence of the channel the cells turned apoptosis-resistant. This finding might explain why the channel is found less expressed in several types of cancer tissue samples at advanced stage with respect to healthy tissues (Serrano-Novillo et al., 2019). Similar findings were reported for Kv1.1 in the same study. As a follow up of these findings, Kv1.3 was identified as functional channel in mitochondria (Szabo et al., 2005) and later studies identified the mitochondrial counterpart of the channel as a crucial player for intrinsic apoptosis (Szabo et al., 2011; Leanza et al., 2012a, 2017).

In addition to Kv1.3, other Kv1 channels have been linked to the apoptotic cascade (Szabo et al., 2010; Shah and Aizenman, 2014). For example, enhanced Kv1.1 expression protected hippocampal neurons against staurosporine- or glutamate-induced apoptosis (Lee et al., 2003; Shen et al., 2009). In contrast,

downregulation of specifically Kv1.1 and of Kv1.3 expression in retinal ganglion cells (but not of Kv1.2 and Kv1.5) rescued neurodegeneration of these cells. In agreement, Margatoxin reduced cell death in this system, where Kv1.1 depletion was shown to increase the expression of the antiapoptotic Bcl-X_L, while depletion of Kv1.3 reduced the pro-apoptotic caspase-3, caspase-9 and Bad (Koeberle et al., 2010). Thus, also in the case of Kv1.1, further work is required to understand the different contribution of this channel to degenerative death in distinct cell types.

Since Kv1.5 is overexpressed in many types of cancer cells (Comes et al., 2013), it represents a good target in this context. Indeed, the role of Kv1.5 in apoptosis has been extensively studied. Bonnet and colleagues correlated low Kv1.5 expression in cancer cells to apoptosis resistance (Bonnet et al., 2007). In particular, these authors observed that metabolic shift toward oxidative phosphorylation and the consequent reactive oxygen species release from mitochondria activates plasma membrane Kv1.5 with a resulting reduction of proliferation and induction of apoptosis. On the other hand, a more recent work showed that silencing Kv1.5 expression in osteosarcoma cells not only reduces proliferation by blocking the cell cycle at G0/G1 phase, as expected, but also enhances apoptosis through upregulation

of Bax and caspase-3 and downregulation of anti-apoptotic Bcl-2 and Bik (Wu et al., 2015). Pharmacological inhibition of Kv1.5 by diphenyl phosphine oxide-1 (DPO-1) contributed to apoptosis induction in macrophages (Leanza et al., 2012b). In another study however, silencing of Kv1.5 with siRNA reduced palmitate-induced endothelial apoptosis (Du et al., 2017). In a recent investigation, inhibition of Kv1.5 by DPO-1 prevented the mitochondria-dependent apoptosis-triggering effect of Apigenin, a dietary flavonoid, in pulmonary artery smooth muscle cells (He Y. et al., 2020). Similarly, DPO-1 reduced hydrogen peroxide-evoked endothelial cell apoptosis (Chen et al., 2012).

In summary, while considerable experimental work links plasma membrane Kv channels to apoptosis, contrasting findings about their expression level in cancer cells as well as their involvement in the regulation of the apoptotic pathway deserves attention. While expression levels might change depending on the cancer stage (with downregulation of the channels associated with apoptosis-resistance in advanced stage and/or metastatic cells), the different outcome on apoptosis might be tentatively explained by modulation of channel activity by yet-undefined factors such as protein interaction partners, whose nature might change depending on the type/stage of cancer.

Kv2 Channels

The Kv2.1 channel has been extensively studied in the context of neuronal apoptosis (Figure 4). An involvement of Kv2.1 in the initiation of programmed cell death has already been proposed in 2001, when Ekhterae and colleagues found that an overexpression of Bcl-2 in rat pulmonary artery smooth muscle cells inhibited staurosporin-induced apoptosis by downregulating Kv1.1, Kv1.5, and Kv2.1 expression and reducing the potassium efflux that initiates the apoptotic volume decrease (Ekhterae et al., 2001). The importance of Kv2.1 for programmed cell death of cortical neurons was first shown by Pal and co-workers. They demonstrated that the expression of dominant-negative Kv2.1 in cortical neurons abolished the potassium efflux that characterizes the onset of apoptosis and increased the resistance to apoptotic stimuli induced by the oxidant 2,2'-dithiodipyridine (DTDP) or staurosporine. Accordingly, the transient expression of functional Kv2.1 in Chinese hamster ovary (CHO) cells increased the susceptibility to DTDP treatment and caspase-dependent cell death (Pal et al., 2003). The same group identified compound 48F10 that inhibits Kv2.1 in the low micromolar range and confers resistance to DTDP treatment in cortical neurons and enterocytes (Zaks-Makhina et al., 2004; Grishin et al., 2005). Upon application of apoptotic stimuli, an increased trafficking of Kv2.1 to the plasma membrane is responsible for the augmented outgoing current. The *de novo* insertion of Kv2.1 channels in the cell membrane depends on syntaxin and synaptosomal-associated protein (SNAP-25), proteins belonging to the SNAP receptor (t-SNARE) complex, normally responsible for exocytotic neurotransmitter release (Pal et al., 2006; Yao et al., 2009; McCord et al., 2014). The interaction of Kv2.1 with syntaxin and its insertion in the plasma membrane upon oxidative stress signals also requires the action of CamKII. Calcium thus emerges as a regulator of the potassium current surge at the onset of neuronal apoptosis (McCord and Aizenman, 2013). Interestingly, targeting

the Kv2.1-syntaxin interaction with a peptide mimicking the syntaxin-1A binding domain of Kv2.1 ameliorated cell death in an *in vivo* model of ischemic stroke (Yeh et al., 2017).

Membrane trafficking of Kv2.1 is regulated by multiple phosphorylation events (Figure 4). For example, activation of the mitogen-activated protein (MAP) kinase p38 is necessary for the induction of neuronal apoptosis after oxidative injury. By phosphorylating a serine residue at the C-terminal of the channel protein (S800), active p38 leads to membrane insertion of Kv2.1 and the potassium current surge that initiates cell death, possibly by changing the association of Kv2.1 with other proteins (such as syntaxin) (Redman et al., 2007). p38 activation, in turn, depends on an intracellular zinc increase caused by oxidants such as peroxynitrite (Zhang et al., 2004). Intracellular zinc leads, in addition to p38 activation, also to inhibition of the phosphatase Cyt-PTP ϵ that in standard conditions dephosphorylates Kv2.1 at a tyrosine residue at the N-terminal (Y124). Src kinase is responsible for phosphorylation of the channel at Y124, enhancing the Kv2.1-mediated current at the onset of apoptosis (Redman et al., 2009). Phosphorylation at S800 and Y124 mutually co-regulate each other, with P-Y124 facilitating the action of p38 on S800 and *vice versa* (He et al., 2015). Additionally, serum deprivation, which induces apoptosis of cortical neurons in a model of excitotoxicity, leads to N-Methyl-D-aspartate (NMDA) receptor activation and enhanced plasma membrane expression of Kv2.1 due to dephosphorylation of the channel protein by the Protein Phosphatase 1 (PP1) and/or 2A (PP2A) (Yao et al., 2009). It was further shown that activation of Protein Kinase A (PKA) following an increase in cyclic AMP protects cerebellar granular neurons from cell death induced by potassium-low and serum-free medium (Jiao et al., 2007). In this study, PKA activation decreased the Kv2.1-dependent outgoing potassium current upon application of the pro-apoptotic stimulus, likely by reducing Kv2.1 expression. Cleavage of Kv2.1 can also affect cell death induction. Liu et al. recently showed that beta-secretase 2 (BACE2), a protease that frequently shows increased expression in Alzheimer's disease, cleaves Kv2.1 at three different sites, reducing the current surge at the onset of apoptosis and protecting neurons from cell death (Liu et al., 2018).

The complex interplay between Kv2.1 and cell death plays an important role in different diseases. In many central nervous system (CNS) disorders, microglia are involved in promoting neurodegeneration. The mechanisms described above partly account for the neurodegenerative effect of microglia: Knoch et al. (2008) showed that activated microglia release reactive oxygen and nitrogen species, which increase the intracellular zinc concentration in co-cultured neurons, finally leading to p38 activation, a surge in Kv2.1-mediated potassium currents and induction of cell death. In addition to neurodegeneration, p38 activation and apoptosis induction play a relevant role also in hepatitis virus C (HVC) infections. The viral protein NS5A blocks oxidative stress-mediated p38 activation by directly binding and blocking the upstream MAPK kinase MLK3, thus effectively inhibiting apoptosis initiation via Kv2.1 and favoring the survival of HCV-infected hepatoma cells even in the presence of pro-apoptotic stimuli (Mankouri et al.,

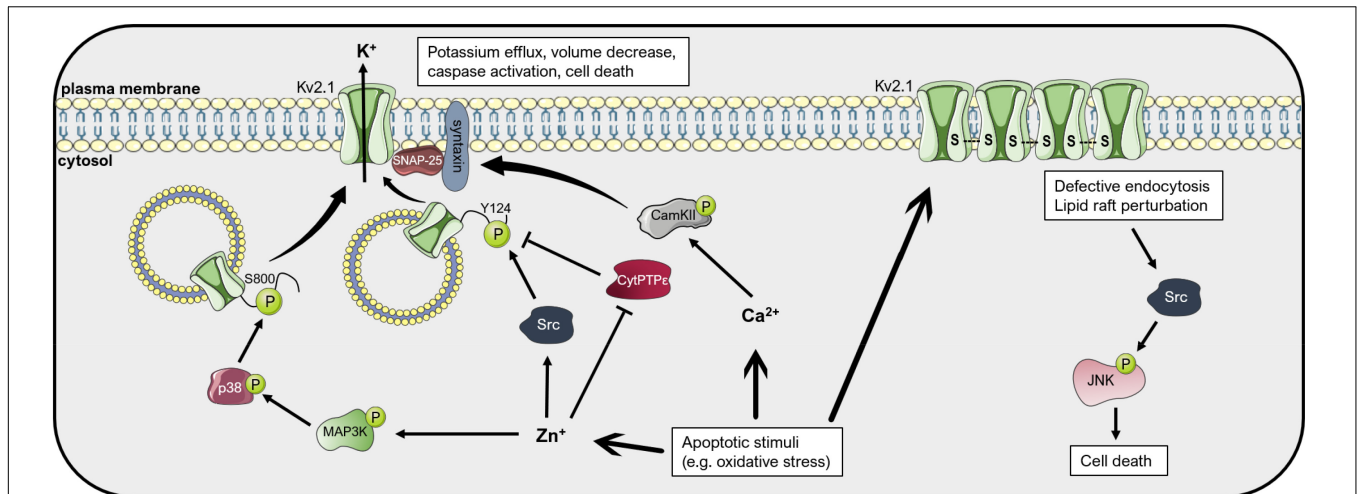


FIGURE 4 | Mechanisms of Kv2.1-mediated cell death. Apoptotic stimuli such as oxidative stress lead to an increase in cytosolic free Zn^{2+} and Ca^{2+} concentrations. Zn^{2+} induces the activation of the kinases p38 and Src, which phosphorylate the intracellular pool of Kv2.1 at the residues Ser800 and Tyr124, respectively. These phosphorylations lead to insertion of Kv2.1 in the plasma membrane, an increase in the outgoing K^+ current, apoptotic volume decrease and cell death. Plasma membrane insertion of the channel depends on interaction with the t-SNARE proteins SNAP-25 and syntaxin. The latter interacts with CamKII, activated upon an increase in Ca^{2+} , favoring Kv2.1 localization to the membrane. Kv2.1 can induce apoptosis also in an ion-conducting-independent manner. Oxidative stress favors oligomerization of the protein by formation of disulfide bridges, which leads to defective endocytosis and lipid raft perturbation, resulting in activation of the Src-JNK signaling axis, finally inducing apoptosis. Please refer to the text for references and additional details. This figure was created using images from Servier Medical Art (<http://smart.servier.com>). Servier Medical Art by Servier is licensed under a Creative Commons Attribution 3.0 Unported License.

2009; Amako et al., 2013). Interestingly, also expression of NS5A1b in neurons is protective as it inhibits Kv2.1-mediated apoptosis, although in a Src-dependent manner (Norris et al., 2012). Human immunodeficiency virus 1 (HIV-1) is involved in neuronal apoptosis as well. Its envelope glycoprotein gp120 has been associated to the pathogenesis of HIV-1-associated neurodegenerative disorders by acting on Kv2.1. In hippocampal neurons, gp120 was shown to increase Kv2.1 expression and current density in a p38- and caspase-3-dependent manner, thus enhancing apoptosis (Shepherd et al., 2012, 2013; Liu et al., 2013; Zhu et al., 2015). p38 plays a role also in methamphetamine-induced neuronal damage. This addictive drug exhibits strong neurotoxicity, inducing apoptosis *via* activation of p38, upregulation of Kv2.1 and cleavage of caspase-3 (Zhu et al., 2018).

Oxidative stress has been associated to different conditions that involve neuronal damage, including Alzheimer's (AD) and Parkinson's disease (PD), aging, amyotrophic lateral sclerosis and stroke (Radi et al., 2014). It has been shown that carbon monoxide (CO) protects neurons from oxidant-induced apoptosis by inhibition of Kv2.1, and that this inhibition is in part exerted by mitochondrial reactive oxygen species (ROS) (Dallas et al., 2011). Kv2.1 inhibition exerted by CO may also play a relevant role in the resistance mechanism against oxidative stress of medulloblastoma cells. In fact, the hypoxic environment of tumors favors the constitutive expression of heme oxygenase 1 (HO-1), which catalyzes heme and releases CO as a byproduct, finally leading to Kv2.1 inhibition and apoptosis resistance (Al-Owais et al., 2012). Interestingly, Donepezil, an acetylcholinesterase inhibitor used in AD, was shown to inhibit Kv2.1 with an IC_{50} value of 7.6 μM and may thus add

protection against neuronal cell death (Yuan et al., 2011). Direct oxidation of Kv2.1 has also been proposed as a mechanism of neurotoxicity (Figure 4). Cotella et al. (2012) found in both *in vitro* and *in vivo* settings that an oxidative environment leads to channel oligomerization at the plasma membrane due to the formation of disulfide bridges between channel subunits. These oligomers, although exhibiting decreased open probability, triggered apoptotic cell death. Kv2.1 oligomerization was greatly increased in the brain of a mouse model of AD. In addition, application of amyloid- β to cultured cells induced the formation of oligomers and cell death (Cotella et al., 2012). Kv2.1 oligomerization resulted in defective endocytosis, lipid raft perturbation and stress-activated c-Src/c-Jun N-terminal kinase (JNK) signaling which finally initiated apoptosis. Cholesterol, by stabilizing lipid rafts, could revert the onset of apoptosis (Wu X. et al., 2013). Accordingly, transgenic mice harboring a non-oxidizable Kv2.1 mutant showed decreased inflammation, neurodegeneration and cell death after traumatic brain injury and exhibited improved outcomes in cognitive and motor behavioral assays with respect to control mice (Yu et al., 2016). Importantly, the results from these experiments were mimicked by treatment of control mice with Dasatinib, a Src kinase inhibitor. The findings of these studies suggest that under oxidizing conditions, such as during aging or neurodegenerative diseases, Kv2.1 channels play a critical role in the regulation of cell death in a manner that may be independent from their ion-conducting properties.

In addition to its well-established role in neuronal apoptosis, Kv2.1 is involved in the cell death regulation of the neuroendocrine pancreatic β -cells. In these cells, Kv2.1 channel controls glucose-stimulated insulin secretion and death

induction. The incretin hormones Gastric Inhibitory Peptide (GIP) and Glucagon-like peptide-1 (GLP-1) have been found to profoundly alter Kv2.1 posttranslational modifications, promoting the channel's internalization and promoting cell survival in stress conditions (Kim et al., 2012). Additionally, the small-molecule inhibitors of Kv2.1 vindoline, SP6616 and ETA were shown to improve β -cell dysfunction and survival and ameliorate hyperglycemia *in vivo*, suggesting that Kv2.1 inhibition may be exploited in anti-diabetic therapies (Yao et al., 2013; Zhou et al., 2016, 2018).

Kv3 and Kv4 Channels

Similarly to Kv2.1, some reports assign a role in the regulation of neuronal apoptosis to Kv3.4. For example, amyloid- β has been found to increase both Kv3.4 expression and activity in hippocampal neurons through NF- κ B and to induce cell death, an effect that could be reverted by a pan-Kv3 inhibitor (Pannaccione et al., 2007). Similarly, Kv3.4 downregulation exerted by HIF-1 α under oxidative stress reduced the potassium current and exhibited a neuroprotective effect in the neuroblastoma cell line SH-SY5Y (Song et al., 2017). Interestingly, the authors of this study suggest an involvement of mitochondrial Kv3.4 in the regulation of oxidative stress-induced neuronal damage. Amyloid- β peptides were also found to increase the expression of Kv4.2 and Kv4.3 channels, leading to increased potassium currents and apoptosis of cerebellar granule cells (Pieri et al., 2010).

Kv7 Channels

Regarding Kv7 channels, their inhibition was demonstrated to trigger spiral ganglion neuron death, possibly underlying the autosomal dominant version of progressive hearing loss associated with Kv7.4 mutations (Lv et al., 2010). On the other hand, activation of Kv7.2 and Kv7.3 in hippocampal neurons induced Extracellular signal-Regulated Kinase (ERK) 1/2 activation and caspase-3 cleavage, an effect that could be prevented by the pan-Kv7 blocker XE991 (Zhou et al., 2010). Interestingly, blockade of Kv7 channels by amyloid precursor proteins may regulate neuronal excitation and possibly cell death (Lee et al., 2020).

Kv10 and Kv11 Channels

Voltage-gated potassium channels belonging to the ether-à-go-go (EAG) family are also involved in the regulation of cell death. This family comprises three subgroups, namely EAG (aka Kv10), EAG-Related Gene (ERG, aka Kv11), and EAG-Like (ELK, aka Kv12). While Kv10 and Kv12 channels are expressed primarily in the central nervous system, Kv11 is present also in the heart, where it regulates the termination of the cardiac action potential, and in smooth muscle tissues (Barros et al., 2020). Ion channels belonging to the EAG family have been intensively studied in the context of cancer. Their expression is frequently high in a wide range of tumor types, while lacking in the corresponding non-tumoral tissues (He S. et al., 2020). Although, to our knowledge, in-depth mechanistic studies regarding the involvement of EAG channels in the regulation of apoptosis are missing, different studies suggest that channel activity may either promote or block

the induction of cell death depending on the cell type and the environment. Studies in which targeting Kv10 or Kv11 channels was exploited to induce tumor cell death will be analyzed more in detail below.

TARGETING VOLTAGE-GATED POTASSIUM CHANNELS IN CANCER

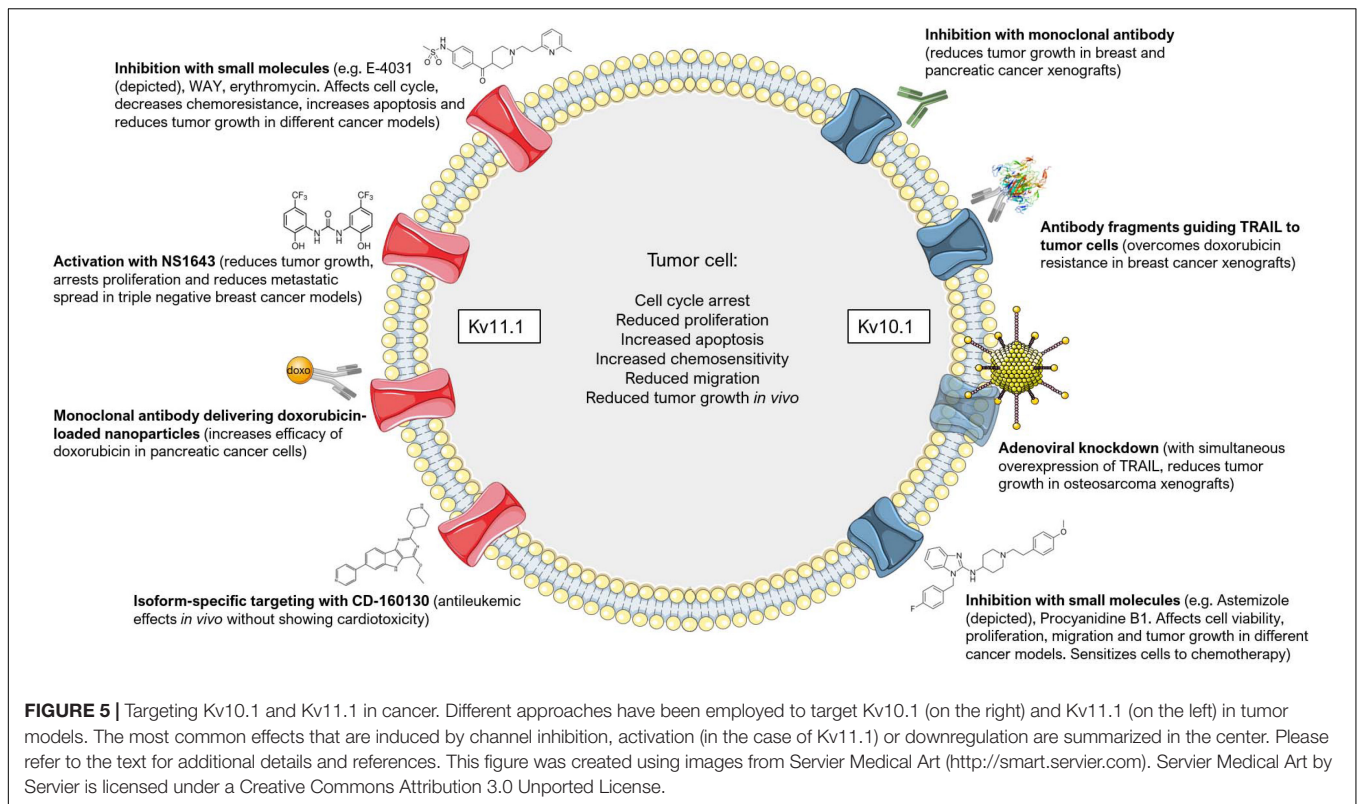
Although several types of Kv channels are linked to either altered proliferation, or to apoptosis induction, concrete steps toward cancer treatment have been obtained only in few cases. This situation is most probably due to our limitation of having promiscuous pharmacological inhibitors as tools to modulate the function of these channels. Nonetheless, the use of toxins, small molecules and specific antibodies is emerging as promising strategy (for recent review see e.g., Wulff et al., 2019; Díaz-García and Varela, 2020).

Kv1 Channels

Intratumoral injection of Margatoxin, a Kv1.3 inhibitor acting on the plasma membrane Kv1.3, reduced lung cancer volume *in vivo* (Jang et al., 2011a), while intraperitoneal injection of PAP-1, the small molecule inhibitor of this channel, did not reduce tumor volume in an orthotopic melanoma model (Leanza et al., 2017; Peruzzo et al., 2020). Two toxins, acting on Kv1.1 (KAaH2) and Kv1.3 (KAaH1 that acts on Kv1.1 as well) derived from the *Androctonus australis* Hector venom, were shown to inhibit glioma proliferation and migration, at least *in vitro* (Aissaoui et al., 2018). A disadvantage of these toxins, however, is their inability to cross the blood brain barrier and to act on intracellular potassium channels. Instead, recent evidence indicates that mitochondrial ion channels can be of importance in fighting cancer. For example, pharmacological inhibition of the mitochondria-located counterpart of Kv1.3 channel by specific mitochondria-targeted drugs was shown to trigger apoptotic death selectively in cancer cells *in vivo*, without inducing alterations to healthy cells and tissues (Leanza et al., 2017).

Kv10.1

Different strategies have been exploited to specifically target Kv10.1 and Kv11.1 channels in order to either block proliferation of cancer cells or to induce their apoptosis, as summarized in **Figure 5**. Given the structural similarity between the potassium channel superfamily, specific blockers are difficult to obtain, therefore some of the research has focused on antibody-based or genetic strategies. For example, a monoclonal antibody raised against Kv10.1 dose-dependently inhibited Kv10.1 currents in neuroblastoma cells, decreased the proliferation of different human cancer cell lines and reduced tumor growth in xenograft models of breast and pancreatic cancer, notably, without acting on Kv10.2 or Kv11.1 (Gomez-Varela et al., 2007). Additionally, specific small antibody fragments targeting the extracellular pore domain of Kv10.1 were exploited to selectively guide the Tumor necrosis factor-Related Apoptosis-Inducing Ligand (TRAIL) to tumor cells. These constructs sensitized breast cancer cells to chemotherapeutics they were



otherwise resistant to Hartung and Pardo (2016), or directly induced cell death in prostate and pancreatic cancer cells when fused to a TRAIL variant with enhanced pro-apoptotic activity (Hartung et al., 2020). This antibody-based strategy was proven efficacious also *in vivo* (Hartung and Pardo, 2016). The specificity of this treatment relies on the enhanced expression of Kv10.1 in many cancer types (Pardo et al., 1999; Pardo and Stuhmer, 2014) and the tumor selectivity of TRAIL. Similarly, treating the human osteosarcoma cell line MG-63 or mice bearing an osteosarcoma xenograft with adenoviral vectors that simultaneously knockdown Kv10.1 and overexpress TRAIL led to tumor regression and apoptosis of cancer cells (He et al., 2013).

Another strategy for the treatment of cancer that has gained increased interest in recent years is drug repositioning using clinically safe drugs already exploited for some other disease. Regarding Kv10.1, the anti-histaminic drug Astemizole was found to inhibit this channel with an IC_{50} value of only 200 nM (García-Ferreiro et al., 2004). This compound was associated with a reduced cancer mortality by sensitizing cells to chemotherapy (Ellegaard et al., 2016). It reduced, for instance, proliferation and viability of keratinocytes expressing the human papilloma virus (HPV) oncogenes E6/E7, that mimic cervical cancer cells and express Kv10.1 (Díaz et al., 2009). The same drug was used to target proliferation and viability of hepatocellular carcinoma cells *in vitro* and in an *in vivo* mouse model, where it decreased Kv10.1 expression (de Guadalupe Chávez-López et al., 2015). Furthermore, Astemizole increased the anti-proliferative effects of calcitriol on breast cancer both *in vitro* and *in vivo* by acting also on Kv10.1 (García-Quiroz et al., 2012, 2014) and

increased the sensitivity of lung cancer cell lines to the EGFR inhibitor Gefitinib possibly by acting on both Kv10.1 subcellular localization and expression (de Guadalupe Chávez-López et al., 2017). Knockdown of Kv10.1 or its inhibition by Astemizole sensitized glioblastoma cells to Temozolomide treatment, and SH-SY5Y cells to rotenone-induced apoptosis (Sales et al., 2016; Horst et al., 2017). Astemizole thus represents a valid candidate for drug repositioning (Figure 5).

Natural compounds are also promising tools. Very recently, the natural compound Procyanidin B1 was identified as a rather specific inhibitor of Kv10.1. It reduced the potassium current with an IC_{50} value of 10 μ M, suppressed proliferation and migration of hepatoma cells and inhibited tumor growth *in vivo* in a xenograft model of liver cancer (Na et al., 2020). In addition, the only Kv10.1-specific toxin, k-Hefutoxin 1 from *Heterometrus fulvipes* scorpion venom (Moreels et al., 2017), might be useful in the context of cancer therapy, but to our knowledge no attempts have been made so far to test its *in vitro* and *in vivo* effects (Díaz-García and Varela, 2020).

Kv11.1

Although representing an interesting target for cancer therapy, Kv11.1 inhibitors have limited use in the clinic because they are potentially cardio-toxic. Kv11.1 is expressed in the heart, where it regulates the cardiac action potential, and the use of channel blockers has been associated with cardiac arrhythmia (extensively reviewed in Arcangeli and Becchetti, 2010). Nonetheless, some studies achieved promising results with channel activators or blockers (Figure 5). For example, the incidental administration

of FDA-approved drugs with proven inhibitory activity on Kv11.1 increased the survival of glioblastoma patients that showed a high expression of Kv11.1 (Pointer et al., 2017). These drugs did not have any adverse side-effect on cardiac activity and include Phenytoin, Haloperidol, Fluoxetine, Tamoxifen, Amitriptyline, and Ketoconazole (Pointer et al., 2017). In acute lymphoblastic leukemia (ALL) cells, the Kv11.1 inhibitors E-4031, WAY123,398 and erythromycin (which, importantly, shows no cardiotoxicity) decreased the chemoresistance of these cells and increased the pro-apoptotic effect of the chemotherapeutics Doxorubicin, Prednisone and Methotrexate. E-4031 significantly reduced tumor progression and improved survival also *in vivo* (Pillozzi et al., 2011). Simultaneous activation of the calcium- and voltage-dependent potassium channel KCa3.1 with SKA-31 and inhibition of Kv11.1 with E-4031 further sensitized colorectal cancer cells to cisplatin treatment both *in vitro* and *in vivo* (Pillozzi et al., 2018). Erythromycin was also shown to increase the cytotoxic effect of paclitaxel, vincristine and hydroxycamptothecin on different cancer cell lines that express Kv11.1 and induce an arrest in the G2/M phase (Chen et al., 2005). Similarly, the gastroprokinetic drug cisapride was shown to inhibit Kv11.1 at low nanomolar concentrations and, accordingly, arrested cell growth and increased apoptosis in Kv11.1-expressing gastric cancer cell lines (Shao et al., 2005). Further, inhibition of Kv11.1 by doxazosin led to apoptosis and cell cycle arrest in the G0/G1 phase of glioblastoma cells. The effect of doxazosin was mimicked by siRNA-mediated knockdown of the channel (Bishopric et al., 2014).

Interestingly, two main isoforms are known for Kv11.1, namely Kv11.1A and Kv11.1B. While Kv11.1A is expressed predominantly in the heart, Kv11.1B is the prevalent isoform in leukemia. This peculiarity has been exploited by Gasparoli et al. (2015), that characterized compound CD-160130, a small-molecule inhibitor of Kv11.1 that does not cause cardiac arrhythmia, possibly by blocking isoform B with a higher efficiency than isoform A (Figure 5). CD-160130 caused apoptosis and growth arrest of leukemic cells *in vitro* and showed strong antileukemic effects *in vivo* (Gasparoli et al., 2015). The higher expression of Kv11.1 in cancer cells with respect to healthy tissues (Pardo and Stuhmer, 2014) was also exploited by Spadavecchia and colleagues. They engineered polyethylene-glycol gold nanoparticles fused to an anti-Kv11.1 antibody to selectively deliver doxorubicin to pancreatic cancer cells (Spadavecchia et al., 2016). In addition, the antibiotic clarithromycin, whose mammalian targets include Kv11.1, was shown to induce apoptotic cell death and increase the cytotoxic effects of 5-fluorouracil both *in vitro* and *in vivo* in colorectal cancer models (Petroni et al., 2020). Finally, to avoid cardiac side-effects, Gentile and co-workers proposed an opposite approach to Kv11.1 channel blockers. They used a small-molecule activator of the channel, NS1643, to achieve *in vivo* inhibition of tumor growth of triple-negative breast cancer (Fukushiro-Lopes et al., 2017; Figure 5). In their model, prolonged activation of the channel leads to hyperpolarization, increase in ROS production, DNA damage, activation of a senescence program and arrest of proliferation. Importantly, NS1643 did not cause cardiac arrhythmias. In a subsequent study, they showed NS1643 to

reduce the metastatic spread *in vivo* in breast cancer models and to reprogram epithelial-to-mesenchymal transition and cancer stemness of MDA-MD-231 cells by reducing Wnt/ β -catenin signaling (Breuer et al., 2019). However, possible side effects of NS1643, other than cardiotoxicity, have not been investigated in a systematic way *in vivo*.

In addition, toxins might offer a way of intervention: CsEKerg1 toxin, from the *Centruroides sculpturatus* scorpion, inhibits Kv11.1 currents in neuroblastoma cells, although with relatively low affinity (Nastainczyk et al., 2002). Unfortunately, this toxin has not been tested on brain-derived tumor cell proliferation (Díaz-García and Varela, 2020).

CONCLUSION AND FUTURE OUTLOOK

Collectively, these studies demonstrate that several ion channels are attractive targets for cancer therapy and regulation of the immune response. As outlined in the present review, many channels share at least some functional aspects with other channels and it might be necessary to define combinations of drugs acting on ion channels for successful tumor treatment. In addition, many channels are expressed in several cell types and it remains to be defined whether channels can be selectively targeted in tumor cells. Altogether, taking into account the information reported here, Kv10 and Kv11 family members seem to represent the most promising target among the plasma-membrane located voltage-gated potassium channels, although the issues of specificity and possible cardiotoxicity warrants caution for Kv10- and Kv11-targeting drugs, respectively. Finally, most channels that were studied so far localize to the plasma membrane or mitochondria, but it is certainly possible that ion channels in other organelles, for instance lysosomes, also play an important role in tumor cell growth or can be exploited as novel targets for tumor therapy in the future.

AUTHOR CONTRIBUTIONS

MB, IS, and EG: writing of the manuscript. WL, ME, SAA, and SP: commenting and editing. All authors contributed to the article and approved the submitted version.

FUNDING

The research in the authors laboratories were funded by Italian Association for Cancer Research (IG2017 20286 to IS) and Italian Ministry of University and Education (PRIN 20174TB8KW_004 to IS) and DFG GU 335/29-2 and Sander Stiftung grant 2019.115.1 to EG.

ACKNOWLEDGMENTS

We are grateful to respective laboratory members for useful discussion.

REFERENCES

- Abdul, M., Santo, A., and Hoosein, N. (2003). Activity of potassium channel-blockers in breast cancer. *Anticancer Res.* 23, 3347–3351.
- Aissouli, D., Mlayah-Bellalouna, S., Jebali, J., Abdelkafi-Koubaa, Z., Souid, S., Moslah, W., et al. (2018). Functional role of Kv1.1 and Kv1.3 channels in the neoplastic progression steps of three cancer cell lines, elucidated by scorpion peptides. *Int. J. Biol. Macromol.* 111, 1146–1155. doi: 10.1016/j.ijbiomac.2018.01.144
- Alexander, S. P., Striessnig, J., Kelly, E., Marrión, N. V., Peters, J. A., Faccenda, E., et al. (2017). THE CONCISE GUIDE TO PHARMACOLOGY 2017/18: voltage-gated ion channels. *Br. J. Pharmacol.* 174(Suppl. 1), S160–S194. doi: 10.1111/bph.13884
- Al-Owais, M. M., Scragg, J. L., Dallas, M. L., Boycott, H. E., Warburton, P., Chakrabarty, A., et al. (2012). Carbon monoxide mediates the anti-apoptotic effects of heme oxygenase-1 in medulloblastoma DAOY cells via K⁺ channel inhibition. *J. Biol. Chem.* 287, 24754–24764. doi: 10.1074/jbc.M112.357012
- Amako, Y., Igloi, Z., Mankouri, J., Kazlauskas, A., Saksela, K., Dallas, M., et al. (2013). Hepatitis C virus NS5A inhibits mixed lineage kinase 3 to block apoptosis. *J. Biol. Chem.* 288, 24753–24763. doi: 10.1074/jbc.M113.491985
- Arcangeli, A., and Becchetti, A. (2010). New trends in cancer therapy: targeting ion channels and transporters. *Pharmaceuticals* 3:1202–1224. doi: 10.3390/ph3041202
- Arcangeli, A., Becchetti, A., Mannini, A., Mugnai, G., De Filippi, P., Tarone, G., et al. (1993). Integrin-mediated neurite outgrowth in neuroblastoma cells depends on the activation of potassium channels. *J. Cell Biol.* 122, 1131–1143.
- Bachmann, M., Pontarin, G., and Szabo, I. (2019). The contribution of mitochondrial ion channels to cancer development and progression. *Cell. Physiol. Biochem.* 53, 63–78. doi: 10.33594/000000198
- Barros, F., de la Peña, P., Domínguez, P., Sierra, L. M., and Pardo, L. A. (2020). The EAG voltage-dependent K⁺ channel subfamily: similarities and differences in structural organization and gating. *Front. Pharmacol.* 11:411. doi: 10.3389/fphar.2020.00411
- Bartok, A., Toth, A., Somodi, S., Szanto, T. G., Hajdu, P., Panyi, G., et al. (2014). Margatoxin is a non-selective inhibitor of human Kv1.3 K⁺ channels. *Toxicon* 87, 6–16. doi: 10.1016/j.toxicon.2014.05.002
- Bielanska, J., Hernández-Losa, J., Moline, T., Somoza, R., Ramón, Y. C. S., Condom, E., et al. (2012). Increased voltage-dependent K⁺ channel Kv1.3 and Kv1.5 expression correlates with leiomyosarcoma aggressiveness. *Oncol. Lett.* 4, 227–230. doi: 10.3892/ol.2012.718
- Bishopric, N. H., Staudacher, I., Jehle, J., Staudacher, K., Pledl, H.-W., Lemke, D., et al. (2014). Herg K⁺ channel-dependent apoptosis and cell cycle arrest in human glioblastoma cells. *PLoS One* 9:e0088164. doi: 10.1371/journal.pone.0088164
- Blackiston, D. J., McLaughlin, K. A., and Levin, M. (2009). Bioelectric controls of cell proliferation: ion channels, membrane voltage and the cell cycle. *Cell Cycle* 8, 3519–3528.
- Bock, J., Szabó, I., Jekle, A., and Gulbins, E. (2002). Actinomycin D-induced apoptosis involves the potassium channel Kv1.3. *Biochem. Biophys. Res. Commun.* 295, 526–531. doi: 10.1016/s0006-291x(02)00695-2
- Bonnet, S., Archer, S. L., Allalunis-Turner, J., Haromy, A., Beaulieu, C., Thompson, R., et al. (2007). A mitochondria-K⁺ channel axis is suppressed in cancer and its normalization promotes apoptosis and inhibits cancer growth. *Cancer Cell* 11, 37–51. doi: 10.1016/j.ccr.2006.10.020
- Bortner, C. D., and Cidlowski, J. A. (2004). The role of apoptotic volume decrease and ionic homeostasis in the activation and repression of apoptosis. *Pflugers Arch.* 448, 313–318. doi: 10.1007/s00424-004-1266-5
- Bortner, C. D., and Cidlowski, J. A. (2014). Ion channels and apoptosis in cancer. *Philos. Trans. R. Soc. Lond. B Biol. Sci.* 369:20130104. doi: 10.1098/rstb.2013.0104
- Breuer, E. K., Fukushima-Lopes, D., Dalheim, A., Burnette, M., Zartman, J., Kaja, S., et al. (2019). Potassium channel activity controls breast cancer metastasis by affecting β -catenin signaling. *Cell Death Dis.* 10:180.
- Brewer, K. R., Kuenze, G., Vanoye, C. G., George, A. L. Jr., Meiler, J., and Sanders, C. R. (2020). Structures illuminate cardiac ion channel functions in health and in long QT syndrome. *Front. Pharmacol.* 11:550. doi: 10.3389/fphar.2020.00550
- Cahalan, M. D., and Chandy, K. G. (2009). The functional network of ion channels in T lymphocytes. *Immunol. Rev.* 231, 59–87. doi: 10.1111/j.1600-065X.2009.00816.x
- Capatina, A. L., Lagos, D., and Brackenbury, W. J. (2020). Targeting ion channels for cancer treatment: current progress and future challenges. *Rev. Physiol. Biochem. Pharmacol.* doi: 10.1007/112_2020_46. [Epub ahead of print].
- Cayabyab, F. S., Khanna, R., Jones, O. T., and Schlichter, L. C. (2000). Suppression of the rat microglia Kv1.3 current by src-family tyrosine kinases and oxygen/glucose deprivation. *Eur. J. Neurosci.* 12, 1949–1960. doi: 10.1046/j.1460-9568.2000.00083.x
- Chen, S. Z., Jiang, M., and Zhen, Y. S. (2005). HERG K⁺ channel expression-related chemosensitivity in cancer cells and its modulation by erythromycin. *Cancer Chemother. Pharmacol.* 56, 212–220. doi: 10.1007/s00280-004-0960-5
- Chen, W. L., Huang, X. Q., Zhao, L. Y., Li, J., Chen, J. W., Xiao, Y., et al. (2012). Involvement of Kv1.5 protein in oxidative vascular endothelial cell injury. *PLoS One* 7:e49758. doi: 10.1371/journal.pone.0049758
- Cheong, A., Li, J., Sukumar, P., Kumar, B., Zeng, F., Riches, K., et al. (2011). Potent suppression of vascular smooth muscle cell migration and human neointimal hyperplasia by KV1.3 channel blockers. *Cardiovasc. Res.* 89, 282–289. doi: 10.1093/cvr/cvq305
- Chow, L. W., Cheng, K. S., Wong, K. L., and Leung, Y. M. (2018). Voltage-gated K⁺ channels promote BT-474 breast cancer cell migration. *Chin. J. Cancer Res.* 30, 613–622. doi: 10.21147/j.issn.1000-9604.2018.06.06
- Cidad, P., Jiménez-Pérez, L., García-Arribas, D., Miguel-Velado, E., Tajada, S., Ruiz-McDavitt, C., et al. (2012). Kv1.3 channels can modulate cell proliferation during phenotypic switch by an ion-flux independent mechanism. *Arterioscler. Thromb. Vasc. Biol.* 32, 1299–1307. doi: 10.1161/atvbaha.111.242727
- Cidad, P., Moreno-Domínguez, A., Novensá, L., Roqué, M., Barquin, L., Heras, M., et al. (2010). Characterization of ion channels involved in the proliferative response of femoral artery smooth muscle cells. *Arterioscler. Thromb. Vasc. Biol.* 30, 1203–1211. doi: 10.1161/atvbaha.110.205187
- Comes, N., Bielanska, J., Vallejo-Gracia, A., Serrano-Albarras, A., Marruecos, L., Gomez, D., et al. (2013). The voltage-dependent K⁺ channels Kv1.3 and Kv1.5 in human cancer. *Front. Physiol.* 4:283. doi: 10.3389/fphys.2013.00283
- Comes, N., Serrano-Albarras, A., Capera, J., Serrano-Novillo, C., Condom, E., Ramon, Y. C. S., et al. (2015). Involvement of potassium channels in the progression of cancer to a more malignant phenotype. *Biochim. Biophys. Acta* 1848(10 Pt B), 2477–2492. doi: 10.1016/j.bbame.2014.12.008
- Cotella, D., Hernandez-Enriquez, B., Wu, X., Li, R., Pan, Z., Leveille, J., et al. (2012). Toxic role of K⁺ channel oxidation in mammalian brain. *J. Neurosci.* 32, 4133–4144. doi: 10.1523/JNEUROSCI.6153-11.2012
- Dallas, M. L., Boyle, J. P., Milligan, C. J., Sayer, R., Kerrigan, T. L., McKinsty, C., et al. (2011). Carbon monoxide protects against oxidant-induced apoptosis via inhibition of Kv2.1. *FASEB J.* 25, 1519–1530. doi: 10.1096/fj.10-173450
- de Guadalupe Chávez-López, M., Pérez-Carreón, J., Zúñiga-García, V., Díaz-Chávez, J., Herrera, L. A., Caro-Sánchez, C. H., et al. (2015). Astemizole-based anticancer therapy for hepatocellular carcinoma (HCC), and Eag1 channels as potential early-stage markers of HCC. *Tumor Biol.* 36, 6149–6158. doi: 10.1007/s13277-015-3299-0
- de Guadalupe Chávez-López, M., Zúñiga-García, V., Hernández-Gallegos, E., Vera, E., Chasiquiza-Anchutua, C. A., Viteri-Yáñez, M., et al. (2017). The combination astemizole/gefitinib as a potential therapy for human lung cancer. *Oncotargets Ther.* 10, 5795–5803. doi: 10.2147/ott.S144506
- DeCoursey, T. E., Chandy, K. G., Gupta, S., and Cahalan, M. D. (1984). Voltage-gated K⁺ channels in human T lymphocytes: A role in mitogenesis? *Nature* 307, 465–468.
- Diaz, L., Ceja-Ochoa, I., Restrepo-Angulo, I., Larrea, F., Avila-Chavez, E., Garcia-Becerra, R., et al. (2009). Estrogens and human papilloma virus oncogenes regulate human ether-a-go-go-1 potassium channel expression. *Cancer Res.* 69, 3300–3307. doi: 10.1158/0008-5472.Can-08-2036
- Díaz-García, A., and Varela, D. (2020). Voltage-Gated K⁺/Na⁺ channels and scorpion venom toxins in cancer. *Front. Pharmacol.* 11:913. doi: 10.3389/fphar.2020.00913
- Du, J. Y., Yuan, F., Zhao, L. Y., Zhu, J., Huang, Y. Y., Zhang, G. S., et al. (2017). Suppression of Kv1.5 protects against endothelial apoptosis induced by palmitate and in type 2 diabetes mice. *Life Sci.* 168, 28–37. doi: 10.1016/j.lfs.2015.12.054

- Ekhterae, D., Platoshyn, O., Krick, S., Yu, Y., McDaniel, S. S., and Yuan, J. X. (2001). Bcl-2 decreases voltage-gated K⁺ channel activity and enhances survival in vascular smooth muscle cells. *Am. J. Physiol. Cell Physiol.* 281, C157–C165. doi: 10.1152/ajpcell.2001.281.1.C157
- Ellegaard, A. M., Dehlendorf, C., Vind, A. C., Anand, A., Cederkvist, L., Petersen, N. H. T., et al. (2016). Repurposing cationic amphiphilic antihistamines for cancer treatment. *EBioMedicine* 9, 130–139.
- Enyedi, P., and Czirjak, G. (2010). Molecular background of leak K⁺ currents: two-pore domain potassium channels. *Physiol. Rev.* 90, 559–605. doi: 10.1152/physrev.00029.2009
- Ferrer, T., Aréchiga-Figueroa, I. A., Shapiro, M. S., Tristani-Firouzi, M., and Sanchez-Chapula, J. A. (2013). Tamoxifen inhibition of kv7.2/kv7.3 channels. *PLoS One* 8:e76085. doi: 10.1371/journal.pone.0076085
- Freedman, B. D., Fleischmann, B. K., Punt, J. A., Gaulton, G., Hashimoto, Y., and Kotlikoff, M. I. (1995). Identification of Kv1.1 expression by murine CD4-CD8-thymocytes. A role for voltage-dependent K⁺ channels in murine thymocyte development. *J. Biol. Chem.* 270, 22406–22411. doi: 10.1074/jbc.270.38.22406
- Fukushiro-Lopes, D. F., Hegel, A. D., Rao, V., Wyatt, D., Baker, A., Breuer, E. K., et al. (2017). Preclinical study of a Kv11.1 potassium channel activator as antineoplastic approach for breast cancer. *Oncotarget* 9, 3321–3337.
- García-Ferreiro, R. E., Kerschenshtainer, D., Major, F., Monje, F., Stühmer, W., and Pardo, L. A. (2004). Mechanism of block of hEag1 K⁺ channels by imipramine and astemizole. *J. Gen. Physiol.* 124, 301–317.
- García-Quiroz, J., García-Becerra, R., Barrera, D., Santos, N., Avila, E., Ordaz-Rosado, D., et al. (2012). Astemizole synergizes calcitriol antiproliferative activity by inhibiting CYP24A1 and upregulating VDR: a novel approach for breast cancer therapy. *PLoS One* 7:e45063. doi: 10.1371/journal.pone.0045063
- García-Quiroz, J., García-Becerra, R., Santos-Martínez, N., Barrera, D., Ordaz-Rosado, D., Avila, E., et al. (2014). *In vivo* dual targeting of the oncogenic Ether-à-go-go-1 potassium channel by calcitriol and astemizole results in enhanced antineoplastic effects in breast tumors. *BMC Cancer* 14:745. doi: 10.1186/1471-2407-14-745
- Gasparoli, L., D'Amico, M., Masselli, M., Pillozzi, S., Caves, R., Khuwailah, R., et al. (2015). New Pyrimido-Indole Compound CD-160130 Preferentially Inhibits the KV11.1B Isoform and Produces Antileukemic Effects without Cardiotoxicity. *Mol. Pharmacol.* 87, 183–196. doi: 10.1124/mol.114.094920
- Geng, J., Wang, Y., Zhang, L., Wang, R., Li, C., Sheng, W., et al. (2020). The cajanine derivative LJ101019C regulates the proliferation and enhances the activity of NK cells via Kv1.3 channel-driven activation of the AKT/mTOR pathway. *Phytomedicine* 66:153113. doi: 10.1016/j.phymed.2019.153113
- Gómez-Angelats, M., Bortner, C. D., and Cidlowski, J. A. (2000). Cell volume regulation in immune cell apoptosis. *Cell Tissue Res.* 301, 33–42. doi: 10.1007/s004410000216
- Gomez-Varela, D., Zwick-Wallasch, E., Knotgen, H., Sanchez, A., Hettmann, T., Ossipov, D., et al. (2007). Monoclonal antibody blockade of the human Eag1 potassium channel function exerts antitumor activity. *Cancer Res.* 67, 7343–7349. doi: 10.1158/0008-5472.CAN-07-0107
- González, C., Baez-Nieto, D., Valencia, I., Oyarzún, I., Rojas, P., Naranjo, D., et al. (2012). K(+) channels: function-structural overview. *Compr. Physiol.* 2, 2087–2149. doi: 10.1002/cphy.c110047
- Grishin, A., Ford, H., Wang, J., Li, H., Salvador-Recatala, V., Levitan, E. S., et al. (2005). Attenuation of apoptosis in enterocytes by blockade of potassium channels. *Am. J. Physiol. Gastrointest. Liver Physiol.* 289, G815–G821.
- Grossinger, E. M., Weiss, L., Zierler, S., Rebhandl, S., Krenn, P. W., Hinterseer, E., et al. (2014). Targeting proliferation of chronic lymphocytic leukemia (CLL) cells through KCa3.1 blockade. *Leukemia* 28, 954–958. doi: 10.1038/leu.2014.37
- Gulbins, E., Szabo, I., Baltzer, K., and Lang, F. (1997). Ceramide-induced inhibition of T lymphocyte voltage-gated potassium channel is mediated by tyrosine kinases. *Proc. Natl. Acad. Sci. U.S.A.* 94, 7661–7666.
- Gutman, G. A., Chandy, K. G., Grissmer, S., Lazdunski, M., McKinnon, D., Pardo, L. A., et al. (2005). International Union of Pharmacology. LIII. Nomenclature and molecular relationships of voltage-gated potassium channels. *Pharmacol. Rev.* 57, 473–508. doi: 10.1124/pr.57.4.10
- Hanahan, D., and Weinberg, R. A. (2000). The hallmarks of cancer. *Cell* 100, 57–70. doi: 10.1016/s0092-8674(00)81683-9
- Hartung, F., Krüwel, T., Shi, X., Pfizenmaier, K., Kontermann, R., Chames, P., et al. (2020). A Novel Anti-Kv10.1 nanobody fused to single-chain trail enhances apoptosis induction in cancer cells. *Front. Pharmacol.* 11:686. doi: 10.3389/fphar.2020.00686
- Hartung, F., and Pardo, L. A. (2016). Guiding TRAIL to cancer cells through Kv10.1 potassium channel overcomes resistance to doxorubicin. *Eur. Biophys. J.* 45, 709–719. doi: 10.1007/s00249-016-1149-7
- He, K., McCord, M. C., Hartnett, K. A., and Aizenman, E. (2015). Regulation of pro-apoptotic phosphorylation of Kv2.1 K⁺ Channels. *PLoS One* 10:e0129498. doi: 10.1371/journal.pone.0129498
- He, L., Wang, F., Dai, W. Q., Wu, D., Lin, C. L., Wu, S. M., et al. (2013). Mechanism of action of salinomycin on growth and migration in pancreatic cancer cell lines. *Pancreatol.* 13, 72–78. doi: 10.1016/j.pan.2012.11.314
- He, S., Moutaoufik, M. T., Islam, S., Persad, A., Wu, A., Aly, K. A., et al. (2020). HERG channel and cancer: a mechanistic review of carcinogenic processes and therapeutic potential. *Biochim. Biophys. Acta* 1873:188355.
- He, Y., Fang, X., Shi, J., Li, X., Xie, M., and Liu, X. (2020). Apigenin attenuates pulmonary hypertension by inducing mitochondria-dependent apoptosis of PASMCs via inhibiting the hypoxia inducible factor 1α-KV1.5 channel pathway. *Chem. Biol. Interact.* 317:108942. doi: 10.1016/j.cbi.2020.108942
- Holmes, T. C., Fadool, D. A., and Levitan, I. B. (1996). Tyrosine phosphorylation of the Kv1.3 potassium channel. *J. Neurosci.* 16, 1581–1590. doi: 10.1523/jneurosci.16-05-01581.1996
- Horst, C. H., Titze-De-Almeida, R., and Titze-De-Almeida, S. S. (2017). The involvement of Eag1 potassium channels and miR-34a in rotenone-induced death of dopaminergic SH-SY5Y cells. *Mol. Med. Rep.* 15, 1479–1488. doi: 10.3892/mmr.2017.6191
- Hu, J. H., Malloy, C., Tabor, G. T., Gutzmann, J. J., Liu, Y., Abebe, D., et al. (2020). Activity-dependent isomerization of Kv4.2 by Pin1 regulates cognitive flexibility. *Nat. Commun.* 11:1567. doi: 10.1038/s41467-020-15390-x
- Hu, X. M., Ren, S., Li, K., and Li, X. T. (2020). Tacrine modulates Kv2.1 channel gene expression and cell proliferation. *Int. J. Neurosci.* 130, 781–787. doi: 10.1080/00207454.2019.1705811
- Jang, S. H., Choi, S. Y., Ryu, P. D., and Lee, S. Y. (2011a). Anti-proliferative effect of Kv1.3 blockers in A549 human lung adenocarcinoma *in vitro* and *in vivo*. *Eur. J. Pharmacol.* 651, 26–32. doi: 10.1016/j.ejphar.2010.10.066
- Jang, S. H., Ryu, P. D., and Lee, S. Y. (2011b). Dendrotoxin-κ suppresses tumor growth induced by human lung adenocarcinoma A549 cells in nude mice. *J. Vet. Sci.* 12, 35–40. doi: 10.4142/jvs.2011.12.1.35
- Jeon, W. I., Ryu, P. D., and Lee, S. Y. (2012). Effects of voltage-gated K⁺ channel blockers in gefitinib-resistant H460 non-small cell lung cancer cells. *Anticancer Res.* 32, 5279–5284.
- Jiao, S., Liu, Z., Ren, W. H., Ding, Y., Zhang, Y. Q., Zhang, Z. H., et al. (2007). cAMP/protein kinase A signalling pathway protects against neuronal apoptosis and is associated with modulation of Kv2.1 in cerebellar granule cells. *J. Neurochem.* 100, 979–991. doi: 10.1111/j.1471-4159.2006.04261.x
- Jimenez-Perez, L., Ciudad, P., Alvarez-Miguel, I., Santos-Hipolito, A., Torres-Merino, R., Alonso, E., et al. (2016). Molecular determinants of kv1.3 potassium channels-induced proliferation. *J. Biol. Chem.* 291, 3569–3580. doi: 10.1074/jbc.M115.678995
- Kim, S. J., Widenmaier, S. B., Choi, W. S., Nian, C., Ao, Z., Warnock, G., et al. (2012). Pancreatic beta-cell prosurvival effects of the incretin hormones involve post-translational modification of Kv2.1 delayed rectifier channels. *Cell Death Differ.* 19, 333–344. doi: 10.1038/cdd.2011.102
- Knoch, M. E., Hartnett, K. A., Hara, H., Kandler, K., and Aizenman, E. (2008). Microglia induce neurotoxicity via intraneuronal Zn(2+) release and a K(+) current surge. *Glia* 56, 89–96. doi: 10.1002/glia.20592
- Koerberle, P. D., Wang, Y., and Schlichter, L. C. (2010). Kv1.1 and Kv1.3 channels contribute to the degeneration of retinal ganglion cells after optic nerve transection *in vivo*. *Cell Death Differ.* 17, 134–144. doi: 10.1038/cdd.2009.113
- Lasch, M., Caballero Martinez, A., Kumaraswami, K., Ishikawa-Ankerhold, H., Meister, S., and Deindl, E. (2020). Contribution of the potassium channels KV1.3 and KCa3.1 to smooth muscle cell proliferation in growing collateral arteries. *Cells* 9:913. doi: 10.3390/cells9040913
- Leanza, L., Henry, B., Sassi, N., Zoratti, M., Chandy, K. G., Gulbins, E., et al. (2012a). Inhibitors of mitochondrial Kv1.3 channels induce Bax/Bak-independent death of cancer cells. *EMBO Mol. Med.* 4, 577–593. doi: 10.1002/emmm.201200235
- Leanza, L., Manago, A., Zoratti, M., Gulbins, E., and Szabo, I. (2016). Pharmacological targeting of ion channels for cancer therapy: *in vivo* evidences.

- Biochim. Biophys. Acta* 1863(6 Pt B), 1385–1397. doi: 10.1016/j.bbamcr.2015.11.032
- Leanza, L., Romio, M., Becker, K. A., Azzolini, M., Trentin, L., Manago, A., et al. (2017). Direct pharmacological targeting of a mitochondrial ion channel selectively kills tumor cells *in vivo*. *Cancer Cell* 31, 516–531.e10. doi: 10.1016/j.ccell.2017.03.003
- Leanza, L., Zoratti, M., Gulbins, E., and Szabo, I. (2012b). Induction of apoptosis in macrophages via Kv1.3 and Kv1.5 potassium channels. *Curr. Med. Chem.* 19, 5394–5404.
- Lee, A. L., Dumas, T. C., Tarapore, P. E., Webster, B. R., Ho, D. Y., Kaufer, D., et al. (2003). Potassium channel gene therapy can prevent neuron death resulting from necrotic and apoptotic insults. *J. Neurochem.* 86, 1079–1088. doi: 10.1046/j.1471-4159.2003.01880.x
- Lee, J. H., Park, J. W., Byun, J. K., Kim, H. K., Ryu, P. D., Lee, S. Y., et al. (2015). Silencing of voltage-gated potassium channel KV9.3 inhibits proliferation in human colon and lung carcinoma cells. *Oncotarget* 6, 8132–8143. doi: 10.18632/oncotarget.3517
- Lee, S. H., Kang, J., Ho, A., Watanabe, H., Bolshakov, V. Y., and Shen, J. (2020). APP family regulates neuronal excitability and synaptic plasticity but not neuronal survival. *Neuron*. doi: 10.1016/j.neuron.2020.08.011 [Epub ahead of print].
- Liu, F., Zhang, Y., Liang, Z., Sun, Q., Liu, H., Zhao, J., et al. (2018). Cleavage of potassium channel Kv2.1 by BACE2 reduces neuronal apoptosis. *Mol. Psychiatry* 23, 1542–1554. doi: 10.1038/s41380-018-0060-2
- Liu, H., Liu, J., Liang, S., and Xiong, H. (2013). Plasma gelsolin protects HIV-1 gp120-induced neuronal injury via voltage-gated K⁺ channel Kv2.1. *Mol. Cell. Neurosci.* 57, 73–82.
- Liu, L., Chen, Y., Zhang, Q., and Li, C. (2019). Silencing of KCNA1 suppresses the cervical cancer development via mitochondria damage. *Channels* 13, 321–330. doi: 10.1080/19336950.2019.1648627
- Liu, Y., and Wang, K. (2019). Exploiting the diversity of ion channels: modulation of ion channels for therapeutic indications. *Handb. Exp. Pharmacol.* 260, 187–205. doi: 10.1007/164_2019_333
- Lv, P., Wei, D., and Yamoah, E. N. (2010). Kv7-type channel currents in spiral ganglion neurons: involvement in sensorineural hearing loss. *J. Biol. Chem.* 285, 34699–34707. doi: 10.1074/jbc.M110.136192
- Mankouri, J., Dallas, M. L., Hughes, M. E., Griffin, S. D., Macdonald, A., Peers, C., et al. (2009). Suppression of a pro-apoptotic K⁺ channel as a mechanism for hepatitis C virus persistence. *Proc. Natl. Acad. Sci. U.S.A.* 106, 15903–15908. doi: 10.1073/pnas.0906798106
- McCord, M. C., and Aizenman, E. (2013). Convergent Ca²⁺ and Zn²⁺ signaling regulates apoptotic Kv2.1 K⁺ currents. *Proc. Natl. Acad. Sci. U.S.A.* 110, 13988–13993. doi: 10.1073/pnas.1306238110
- McCord, M. C., Kullmann, P. H., He, K., Hartnett, K. A., Horn, J. P., Lotan, I., et al. (2014). Syntaxin-binding domain of Kv2.1 is essential for the expression of apoptotic K⁺ currents. *J. Physiol.* 592, 3511–3521. doi: 10.1113/jphysiol.2014.276964
- McKinnon, D., and Ceredig, R. (1986). Changes in the expression of potassium channels during mouse T cell development. *J. Exp. Med.* 164, 1846–1861. doi: 10.1084/jem.164.6.1846
- Miguel-Velado, E., Moreno-Domínguez, A., Colinas, O., Ciudad, P., Heras, M., Pérez-García, M. T., et al. (2005). Contribution of Kv channels to phenotypic remodeling of human uterine artery smooth muscle cells. *Circ. Res.* 97, 1280–1287. doi: 10.1161/01.res.0000194322.91255.13
- Miguel-Velado, E., Pérez-Carretero, F. D., Colinas, O., Ciudad, P., Heras, M., López-López, J. R., et al. (2010). Cell cycle-dependent expression of Kv3.4 channels modulates proliferation of human uterine artery smooth muscle cells. *Cardiovasc. Res.* 86, 383–391. doi: 10.1093/cvr/cvq011
- Moreels, L., Peigneur, S., Yamaguchi, Y., Vriens, K., Waelkens, E., Zhu, S., et al. (2017). Expanding the pharmacological profile of κ -hefutoxin 1 and analogues: a focus on the inhibitory effect on the oncogenic channel K(v)10.1. *Peptides* 98, 43–50. doi: 10.1016/j.peptides.2016.08.008
- Na, W., Ma, B., Shi, S., Chen, Y., Zhang, H., Zhan, Y., et al. (2020). Procyanidin B1, a novel and specific inhibitor of Kv10.1 channel, suppresses the evolution of hepatoma. *Biochem. Pharmacol.* 178, 114089. doi: 10.1016/j.bcp.2020.114089
- Nastainczyk, W., Meves, H., and Watt, D. D. (2002). A short-chain peptide toxin isolated from *Centruroides sculpturatus* scorpion venom inhibits ether-à-go-go-related gene K(+) channels. *Toxicon* 40, 1053–1058. doi: 10.1016/s0041-0101(02)00100-9
- Norris, C. A., He, K., Springer, M. G., Hartnett, K. A., Horn, J. P., and Aizenman, E. (2012). Regulation of neuronal proapoptotic potassium currents by the hepatitis C virus nonstructural protein 5A. *J. Neurosci.* 32, 8865–8870. doi: 10.1523/JNEUROSCI.0937-12.2012
- Ouadid-Ahidouch, H., Chaussade, F., Roudbaraki, M., Slomianny, C., Dewailly, E., Delcourt, P., et al. (2000). KV1.1 K(+) channels identification in human breast carcinoma cells: involvement in cell proliferation. *Biochem. Biophys. Res. Commun.* 278, 272–277. doi: 10.1006/bbrc.2000.3790
- Pal, S., Hartnett, K. A., Nerbonne, J. M., Levitan, E. S., and Aizenman, E. (2003). Mediation of neuronal apoptosis by Kv2.1-encoded potassium channels. *J. Neurosci.* 23, 4798–4802. doi: 10.1523/jneurosci.23-12-04798.2003
- Pal, S. K., Takimoto, K., Aizenman, E., and Levitan, E. S. (2006). Apoptotic surface delivery of K⁺ channels. *Cell Death Differ.* 13, 661–667. doi: 10.1038/sj.cdd.4401792
- Palme, D., Misovic, M., Schmid, E., Klumpp, D., Salih, H. R., Rudner, J., et al. (2013). Kv3.4 potassium channel-mediated electrosignaling controls cell cycle and survival of irradiated leukemia cells. *Pflugers Arch.* 465, 1209–1221. doi: 10.1007/s00424-013-1249-5
- Pannaccione, A., Boscia, F., Scorziello, A., Adornetto, A., Castaldo, P., Sirabella, R., et al. (2007). Up-regulation and increased activity of KV3.4 channels and their accessory subunit MinK-related peptide 2 induced by amyloid peptide are involved in apoptotic neuronal death. *Mol. Pharmacol.* 72, 665–673. doi: 10.1124/mol.107.034868
- Pardo, L. A., Bruggemann, A., Camacho, J., and Stuhmer, W. (1998). Cell cycle-related changes in the conducting properties of r-eag K⁺ channels. *J. Cell Biol.* 143, 767–775.
- Pardo, L. A., del Camino, D., Sánchez, A., Alves, F., Bruggemann, A., Beckh, S., et al. (1999). Oncogenic potential of EAG K(+) channels. *EMBO J.* 18, 5540–5547.
- Pardo, L. A., and Stuhmer, W. (2014). The roles of K(+) channels in cancer. *Nat. Rev. Cancer* 14, 39–48. doi: 10.1038/nrc3635
- Pérez-García, M. T., Ciudad, P., and López-López, J. R. (2018). The secret life of ion channels: Kv1.3 potassium channels and proliferation. *Am. J. Physiol. Cell Physiol.* 314, C27–C42. doi: 10.1152/ajpcell.00136.2017
- Peruzzo, R., Mattarei, A., Azzolini, M., Becker-Flegler, K. A., Romio, M., Rigoni, G., et al. (2020). Insight into the mechanism of cytotoxicity of membrane-permeant psoralenic Kv1.3 channel inhibitors by chemical dissection of a novel member of the family. *Redox Biol.* 37, 101705. doi: 10.1016/j.redox.2020.101705
- Peruzzo, R., and Szabo, I. (2019). Contribution of mitochondrial ion channels to chemo-resistance in cancer cells. *Cancers* 11:761. doi: 10.3390/cancers11060761
- Petho, Z., Balajthy, A., Bartok, A., Bene, K., Somodi, S., Szilagyi, O., et al. (2016). The anti-proliferative effect of cation channel blockers in T lymphocytes depends on the strength of mitogenic stimulation. *Immunol. Lett.* 171, 60–69. doi: 10.1016/j.imlet.2016.02.003
- Petroni, G., Bagni, G., Iorio, J., Duranti, C., Lottini, T., Stefanini, M., et al. (2020). Clarithromycin inhibits autophagy in colorectal cancer by regulating the hERG1 potassium channel interaction with PI3K. *Cell Death Dis.* 11:161. doi: 10.1038/s41419-020-2349-8
- Pieri, M., Amadoro, G., Carunchio, I., Ciotti, M. T., Quaresima, S., Florenzano, F., et al. (2010). SP protects cerebellar granule cells against β -amyloid-induced apoptosis by down-regulation and reduced activity of Kv4 potassium channels. *Neuropharmacology* 58, 268–276. doi: 10.1016/j.neuropharm.2009.06.029
- Pillozzi, S., D'Amico, M., Bartoli, G., Gasparoli, L., Petroni, G., Crociani, O., et al. (2018). The combined activation of KCa3.1 and inhibition of Kv11.1/hERG1 currents contribute to overcome Cisplatin resistance in colorectal cancer cells. *Br. J. Cancer* 118, 200–212. doi: 10.1038/bjc.2017.392
- Pillozzi, S., Masselli, M., De Lorenzo, E., Accordi, B., Cilia, E., Crociani, O., et al. (2011). Chemotherapy resistance in acute lymphoblastic leukemia requires hERG1 channels and is overcome by hERG1 blockers. *Blood* 117, 902–914. doi: 10.1182/blood-2010-01-262691
- Pointer, K. B., Clark, P. A., Eliceiri, K. W., Salamat, M. S., Robertson, G. A., and Kuo, J. S. (2017). Administration of non-torsadogenic human ether-a-go-go-related gene inhibitors is associated with better survival for high hERG-expressing glioblastoma patients. *Clin. Cancer Res.* 23, 73–80. doi: 10.1158/1078-0432.CCR-15-3169
- Preussat, K., Beetz, C., Schrey, M., Kraft, R., Wölfl, S., Kalff, R., et al. (2003). Expression of voltage-gated potassium channels Kv1.3 and Kv1.5 in human gliomas. *Neurosci. Lett.* 346, 33–36. doi: 10.1016/s0304-3940(03)00562-7

- Pucca, M. B., Bertolini, T. B., Cerni, F. A., Bordon, K. C., Peigneur, S., Tytgat, J., et al. (2016). Immunosuppressive evidence of *Tityus serrulatus* toxins Ts6 and Ts15: insights of a novel K(+) channel pattern in T cells. *Immunology* 147, 240–250. doi: 10.1111/imm.12559
- Qian, C., Dai, Y., Xu, X., and Jiang, Y. (2019). HIF-1 α regulates proliferation and invasion of oral cancer cells through Kv3.4 channel. *Ann. Clin. Lab. Sci.* 49, 457–467.
- Radi, E., Formichi, P., Battisti, C., and Federico, A. (2014). Apoptosis and oxidative stress in neurodegenerative diseases. *J. Alzheimers Dis.* 42(Suppl 3), S125–S152.
- Rao, V. R., Perez-Neut, M., Kaja, S., and Gentile, S. (2015). Voltage-gated ion channels in cancer cell proliferation. *Cancers* 7, 849–875. doi: 10.3390/cancers7020813
- Redman, P. T., Hartnett, K. A., Aras, M. A., Levitan, E. S., and Aizenman, E. (2009). Regulation of apoptotic potassium currents by coordinated zinc-dependent signalling. *J. Physiol.* 587(Pt 18), 4393–4404. doi: 10.1113/jphysiol.2009.176321
- Redman, P. T., He, K., Hartnett, K. A., Jefferson, B. S., Hu, L., Rosenberg, P. A., et al. (2007). Apoptotic surge of potassium currents is mediated by p38 phosphorylation of Kv2.1. *Proc. Natl. Acad. Sci. U.S.A.* 104, 3568–3573. doi: 10.1073/pnas.0610159104
- Roura-Ferrer, M., Solé, L., Martínez-Mármol, R., Villalonga, N., and Felipe, A. (2008). Skeletal muscle Kv7 (KCNQ) channels in myoblast differentiation and proliferation. *Biochem. Biophys. Res. Commun.* 369, 1094–1097. doi: 10.1016/j.bbrc.2008.02.152
- Sales, T. T., Resende, F. F. B., Chaves, N. L., Titze-De-Almeida, S. S., Bão, S. N., Brettas, M. L., et al. (2016). Suppression of the Eag1 potassium channel sensitizes glioblastoma cells to injury caused by temozolomide. *Oncol. Lett.* 12, 2581–2589. doi: 10.3892/ol.2016.4992
- Serrano-Novillo, C., Capera, J., Colomer-Molera, M., Condom, E., Ferreres, J. C., and Felipe, A. (2019). Implication of voltage-gated potassium channels in neoplastic cell proliferation. *Cancers* 11:287. doi: 10.3390/cancers11030287
- Serrano-Novillo, C., Oliveras, A., Ferreres, J. C., Condom, E., and Felipe, A. (2020). Remodeling of Kv7.1 and Kv7.5 expression in vascular tumors. *Int. J. Mol. Sci.* 21:6019. doi: 10.3390/ijms21176019
- Shah, N. H., and Aizenman, E. (2014). Voltage-gated potassium channels at the crossroads of neuronal function, ischemic tolerance, and neurodegeneration. *Transl. Stroke Res.* 5, 38–58. doi: 10.1007/s12975-013-0297-7
- Shao, X. D., Wu, K. C., Hao, Z. M., Hong, L., Zhang, J., and Fan, D. M. (2005). The potent inhibitory effects of cisapride, a specific blocker for human ether-a-gogo-related gene (HERG) channel, on gastric cancer cells. *Cancer Biol. Ther.* 4, 295–301. doi: 10.4161/cbt.4.3.1500
- Shen, Q. J., Zhao, Y. M., Cao, D. X., and Wang, X. L. (2009). Contribution of Kv channel subunits to glutamate-induced apoptosis in cultured rat hippocampal neurons. *J. Neurosci. Res.* 87, 3153–3160. doi: 10.1002/jnr.22136
- Shepherd, A. J., Loo, L., Gupte, R. P., Mickle, A. D., and Mohapatra, D. P. (2012). Distinct modifications in Kv2.1 channel via chemokine receptor CXCR4 regulate neuronal survival-death dynamics. *J. Neurosci.* 32, 17725–17739. doi: 10.1523/JNEUROSCI.3029-12.2012
- Shepherd, A. J., Loo, L., and Mohapatra, D. P. (2013). Chemokine co-receptor CCR5/CXCR4-dependent modulation of Kv2.1 channel confers acute neuroprotection to HIV-1 glycoprotein gp120 exposure. *PLoS One* 8:e76698. doi: 10.1371/journal.pone.0076698
- Smith, G. A., Tsui, H. W., Newell, E. W., Jiang, X., Zhu, X. P., Tsui, F. W., et al. (2002). Functional up-regulation of HERG K+ channels in neoplastic hematopoietic cells. *J. Biol. Chem.* 277, 18528–18534. doi: 10.1074/jbc.M200592200
- Song, M. S., Park, S. M., Park, J. S., Byun, J. H., Jin, H. J., Seo, S. H., et al. (2018). Kv3.1 and Kv3.4, are involved in cancer cell migration and invasion. *Int. J. Mol. Sci.* 19:1061. doi: 10.3390/ijms19041061
- Song, M. S., Ryu, P. D., and Lee, S. Y. (2017). Kv3.4 is modulated by HIF-1 α to protect SH-SY5Y cells against oxidative stress-induced neural cell death. *Sci. Rep.* 7:2075. doi: 10.1038/s41598-017-02129-w
- Spadavecchia, J., Movia, D., Moore, C., Maguire, C. M., Moustou, H., Casale, S., et al. (2016). Targeted polyethylene glycol gold nanoparticles for the treatment of pancreatic cancer: from synthesis to proof-of-concept in vitro studies. *Int. J. Nanomed.* 11, 791–822. doi: 10.2147/IJN.S97476
- Storey, N. M., Gómez-Angelats, M., Bortner, C. D., Armstrong, D. L., and Cidlowski, J. A. (2003). Stimulation of Kv1.3 potassium channels by death receptors during apoptosis in Jurkat T lymphocytes. *J. Biol. Chem.* 278, 33319–33326. doi: 10.1074/jbc.M300443200
- Suzuki, T., and Takimoto, K. (2004). Selective expression of HERG and Kv2 channels influences proliferation of uterine cancer cells. *Int. J. Oncol.* 25, 153–159.
- Szabo, I., Bock, J., Grassme, H., Soddemann, M., Wilker, B., Lang, F., et al. (2008). Mitochondrial potassium channel Kv1.3 mediates Bax-induced apoptosis in lymphocytes. *Proc. Natl. Acad. Sci. U.S.A.* 105, 14861–14866. doi: 10.1073/pnas.0804236105
- Szabo, I., Bock, J., Jekle, A., Soddemann, M., Adams, C., Lang, F., et al. (2005). A novel potassium channel in lymphocyte mitochondria. *J. Biol. Chem.* 280, 12790–12798. doi: 10.1074/jbc.M413548200
- Szabo, I., Gulbins, E., Apfel, H., Zhang, X., Barth, P., Busch, A. E., et al. (1996). Tyrosine phosphorylation-dependent suppression of a voltage-gated K+ channel in T lymphocytes upon Fas stimulation. *J. Biol. Chem.* 271, 20465–20469.
- Szabo, I., Soddemann, M., Leanza, L., Zoratti, M., and Gulbins, E. (2011). Single-point mutations of a lysine residue change function of Bax and Bcl-xL expressed in Bax- and Bak-less mouse embryonic fibroblasts: novel insights into the molecular mechanisms of Bax-induced apoptosis. *Cell Death Differ.* 18, 427–438. doi: 10.1038/cdd.2010.112
- Szabo, I., Zoratti, M., and Gulbins, E. (2010). Contribution of voltage-gated potassium channels to the regulation of apoptosis. *FEBS Lett.* 584, 2049–2056. doi: 10.1016/j.febslet.2010.01.038
- Teisseyre, A., Palko-Labuz, A., Sroda-Pomianek, K., and Michalak, K. (2019). Voltage-gated potassium channel Kv1.3 as a target in therapy of cancer. *Front. Oncol.* 9:933. doi: 10.3389/fonc.2019.00933
- Tiwari-Woodruff, S., Beltran-Parrazal, L., Charles, A., Keck, T., Vu, T., and Bronstein, J. (2006). K+ channel KV3.1 associates with OSP/claudin-11 and regulates oligodendrocyte development. *Am. J. Physiol. Cell Physiol.* 291, C687–C698. doi: 10.1152/ajpcell.00510.2005
- Urrego, D., Sanchez, A., Tomczak, A. P., and Pardo, L. A. (2017). The electric fence to cell-cycle progression: Do local changes in membrane potential facilitate disassembly of the primary cilium?: Timely and localized expression of a potassium channel may set the conditions that allow retraction of the primary cilium. *Bioessays* 39:1600190. doi: 10.1002/bies.201600190
- Urrego, D., Tomczak, A. P., Zahed, F., Stühmer, W., and Pardo, L. A. (2014). Potassium channels in cell cycle and cell proliferation. *Philos. Trans. R Soc. Lond. Ser. B Biol. Sci.* 369:20130094. doi: 10.1098/rstb.2013.0094
- Vallejo-Gracia, A., Bielanska, J., Hernández-Losa, J., Castellví, J., Ruiz-Marcellan, M. C., Ramón y Cajal, S., et al. (2013). Emerging role for the voltage-dependent K+ channel Kv1.5 in B-lymphocyte physiology: expression associated with human lymphoma malignancy. *J. Leukoc. Biol.* 94, 779–789. doi: 10.1189/jlb.0213094
- Vautier, F., Belachew, S., Chittajallu, R., and Gallo, V. (2004). Shaker-type potassium channel subunits differentially control oligodendrocyte progenitor proliferation. *Glia* 48, 337–345. doi: 10.1002/glia.20088
- Wang, H., Yang, X., Guo, Y., Shui, L., Li, S., Bai, Y., et al. (2019). HERG1 promotes esophageal squamous cell carcinoma growth and metastasis through TXNDC5 by activating the PI3K/AKT pathway. *J. Exp. Clin. Cancer Res.* 38:324. doi: 10.1186/s13046-019-1284-y
- Wu, J., Chen, Z., Liu, Q., Zeng, W., Wu, X., and Lin, B. (2015). Silencing of Kv1.5 Gene inhibits proliferation and induces apoptosis of osteosarcoma cells. *Int. J. Mol. Sci.* 16, 26914–26926. doi: 10.3390/ijms161126002
- Wu, J., Zhong, D., Wu, X., Sha, M., Kang, L., and Ding, Z. (2013). Voltage-gated potassium channel Kv1.3 is highly expressed in human osteosarcoma and promotes osteosarcoma growth. *Int. J. Mol. Sci.* 14, 19245–19256. doi: 10.3390/ijms140919245
- Wu, X., Hernandez-Enriquez, B., Banas, M., Xu, R., and Sesti, F. (2013). Molecular mechanisms underlying the apoptotic effect of KCNB1 K+ channel oxidation. *J. Biol. Chem.* 288, 4128–4134. doi: 10.1074/jbc.M112.440933
- Wulff, H., Christophersen, P., Colussi, P., Chandy, K. G., and Yarov-Yarovoy, V. (2019). Antibodies and venom peptides: new modalities for ion channels. *Nat. Rev. Drug Discov.* 18, 339–357. doi: 10.1038/s41573-019-0013-8
- Xia, X., Zhang, Q., Jia, Y., Shu, Y., Yang, J., Yang, H., et al. (2020). Molecular basis and restoration of function deficiencies of Kv7.4 variants associated with inherited hearing loss. *Hear. Res.* 388:107884. doi: 10.1016/j.heares.2020.107884

- Xu, T., Du, X. W., Hu, J. B., Zhu, Y. F., Wu, H. L., Dai, G. P., et al. (2018). Anticancer effect of miR-96 inhibitor in bladder cancer cell lines. *Oncol. Lett.* 15, 3814–3819. doi: 10.3892/ol.2018.7745
- Yao, H., Zhou, K., Yan, D., Li, M., and Wang, Y. (2009). The Kv2.1 channels mediate neuronal apoptosis induced by excitotoxicity. *J. Neurochem.* 108, 909–919. doi: 10.1111/j.1471-4159.2008.05834.x
- Yao, X. G., Chen, F., Li, P., Quan, L., Chen, J., Yu, L., et al. (2013). Natural product vindoline stimulates insulin secretion and efficiently ameliorates glucose homeostasis in diabetic murine models. *J. Ethnopharmacol.* 150, 285–297. doi: 10.1016/j.jep.2013.08.043
- Yeh, C. Y., Bulas, A. M., Moutal, A., Saloman, J. L., Hartnett, K. A., Anderson, C. T., et al. (2017). Targeting a potassium channel/syntaxin interaction ameliorates cell death in ischemic stroke. *J. Neurosci.* 37, 5648–5658. doi: 10.1523/JNEUROSCI.3811-16.2017
- Yu, W., Parakramaweera, R., Teng, S., Gowda, M., Sharad, Y., Thakker-Varia, S., et al. (2016). Oxidation of KCNB1 potassium channels causes neurotoxicity and cognitive impairment in a mouse model of traumatic brain injury. *J. Neurosci.* 36, 11084–11096. doi: 10.1523/JNEUROSCI.2273-16.2016
- Yuan, H., Wang, W. P., Feng, N., Wang, L., and Wang, X. L. (2011). Donepezil attenuated oxygen-glucose deprivation insult by blocking Kv2.1 potassium channels. *Eur. J. Pharmacol.* 657, 76–83. doi: 10.1016/j.ejphar.2011.01.054
- Zaks-Makhina, E., Kim, Y., Aizenman, E., and Levitan, E. S. (2004). Novel neuroprotective K⁺ channel inhibitor identified by high-throughput screening in yeast. *Mol. Pharmacol.* 65, 214–219. doi: 10.1124/mol.65.1.214
- Zeng, W., Liu, Q., Chen, Z., Wu, X., Zhong, Y., and Wu, J. (2016). Silencing of hERG1 gene inhibits proliferation and invasion, and induces apoptosis in human osteosarcoma cells by targeting the NF-kappaB pathway. *J. Cancer* 7, 746–757. doi: 10.7150/jca.13289
- Zhang, Y., Wang, H., Li, J., Jimenez, D. A., Levitan, E. S., Aizenman, E., et al. (2004). Peroxynitrite-induced neuronal apoptosis is mediated by intracellular zinc release and 12-lipoxygenase activation. *J. Neurosci.* 24, 10616–10627.
- Zhou, T., Du, M., Zhao, T., Quan, L., Zhu, Z., and Chen, J. (2018). ETA as a novel Kv2.1 inhibitor ameliorates beta-cell dysfunction and hyperglycaemia. *Clin. Exp. Pharmacol. Physiol.* 45, 1257–1264. doi: 10.1111/1440-1681.13011
- Zhou, T. T., Quan, L. L., Chen, L. P., Du, T., Sun, K. X., Zhang, J. C., et al. (2016). SP6616 as a new Kv2.1 channel inhibitor efficiently promotes beta-cell survival involving both PKC/Erk1/2 and CaM/PI3K/Akt signaling pathways. *Cell Death Dis.* 7:e2216. doi: 10.1038/cddis.2016.119
- Zhou, X., Wei, J., Song, M., Francis, K., and Yu, S. P. (2010). Novel role of KCNQ2/3 channels in regulating neuronal cell viability. *Cell Death Differ.* 18, 493–505. doi: 10.1038/cdd.2010.120
- Zhu, J., Zang, S., Chen, X., Jiang, L., Gu, A., Cheng, J., et al. (2018). Involvement of the delayed rectifier outward potassium channel Kv2.1 in methamphetamine-induced neuronal apoptosis via the p38 mitogen-activated protein kinase signaling pathway. *J. Appl. Toxicol.* 38, 696–704. doi: 10.1002/jat.3576
- Zhu, Q., Song, X., Zhou, J., Wang, Y., Xia, J., Qian, W., et al. (2015). Target of HIV-1 envelope glycoprotein gp120-induced hippocampal neuron damage: role of voltage-gated K⁺ Channel Kv2.1. *Viral Immunol.* 28, 495–503. doi: 10.1089/vim.2015.0020

Conflict of Interest: The authors declare that the research was conducted in the absence of any commercial or financial relationships that could be construed as a potential conflict of interest.

Copyright © 2020 Bachmann, Li, Edwards, Ahmad, Patel, Szabo and Gulbins. This is an open-access article distributed under the terms of the Creative Commons Attribution License (CC BY). The use, distribution or reproduction in other forums is permitted, provided the original author(s) and the copyright owner(s) are credited and that the original publication in this journal is cited, in accordance with accepted academic practice. No use, distribution or reproduction is permitted which does not comply with these terms.



Mitochondrial Ion Channels of the Inner Membrane and Their Regulation in Cell Death Signaling

Andrea Urbani^{1,2*}, Elena Prosdocimi², Andrea Carrer^{1,2}, Vanessa Checchetto^{2*} and Ildikò Szabò²

¹ Department of Biomedical Sciences, University of Padova, Padua, Italy, ² Department of Biology, University of Padova, Padua, Italy

OPEN ACCESS

Edited by:

Alexander A. Mongin,
Albany Medical College, United States

Reviewed by:

Nickolay Brustovetsky,
Indiana University Bloomington,
United States
Geeta Upadhyay,
Uniformed Services University of the
Health Sciences, United States
Evgeny V. Pavlov,
New York University, United States

*Correspondence:

Andrea Urbani
andrea.urbani@unipd.it
Vanessa Checchetto
vanessa.checchetto@unipd.it

Specialty section:

This article was submitted to
Cell Death and Survival,
a section of the journal
Frontiers in Cell and Developmental
Biology

Received: 21 October 2020

Accepted: 07 December 2020

Published: 05 January 2021

Citation:

Urbani A, Prosdocimi E, Carrer A,
Checchetto V and Szabò I (2021)
Mitochondrial Ion Channels of the
Inner Membrane and Their Regulation
in Cell Death Signaling.
Front. Cell Dev. Biol. 8:620081.
doi: 10.3389/fcell.2020.620081

Mitochondria are bioenergetic organelles with a plethora of fundamental functions ranging from metabolism and ATP production to modulation of signaling events leading to cell survival or cell death. Ion channels located in the outer and inner mitochondrial membranes critically control mitochondrial function and, as a consequence, also cell fate. Opening or closure of mitochondrial ion channels allow the fine-tuning of mitochondrial membrane potential, ROS production, and function of the respiratory chain complexes. In this review, we critically discuss the intracellular regulatory factors that affect channel activity in the inner membrane of mitochondria and, indirectly, contribute to cell death. These factors include various ligands, kinases, second messengers, and lipids. Comprehension of mitochondrial ion channels regulation in cell death pathways might reveal new therapeutic targets in mitochondria-linked pathologies like cancer, ischemia, reperfusion injury, and neurological disorders.

Keywords: mitochondria, ion channel, cell death, cell signaling, apoptosis

INTRODUCTION

Mitochondria are dynamic organelles that are primarily recognized as the “powerhouse” of the cell, where the energy stored in nutrients is converted to ATP molecules through the oxidative phosphorylation (OXPHOS). Besides the production of ATP, mitochondria also play fundamental roles in other cellular functions, including metabolism of fatty/amino acids (Spinelli and Haigis, 2018), Ca^{2+} homeostasis (De Stefani et al., 2016), thermogenesis (Chouchani et al., 2019), redox signaling (Zorov et al., 2014), and cell death (Galluzzi et al., 2016).

Regulated cell death is critical to development, tissue homeostasis, and removal of cells with abnormal behavior. Some key cell death controlling proteins include caspases, Bcl-2 family proteins, death receptors, RIP kinases, inhibitor of apoptosis proteins (IAPs), Endonuclease G, Apoptosis Inducing Factor (AIF), Caspase-Activated DNAase, Apaf-1, SMAC/DIABLO, and HtrA2/OMI. In several studies, various ion channels emerge as crucial regulators of various forms of cell death [for reviews see e.g., (Bortner and Cidlowski, 2014; Kondratskyi et al., 2015; Leanza et al., 2015; Fricker et al., 2018; Bachmann et al., 2019)].

The role of mitochondria in cell death is linked to apoptosis, where mitochondrial outer membrane permeabilization (MOMP) originates a signaling cascade leading to cell death (Bock and Tait, 2020). MOMP is initiated by the formation of macropores in the outer mitochondrial membrane (OMM) (Szabo and Zoratti, 2014), allowing the release of soluble proteins from the

mitochondrial intermembrane space (IMS) in a process regulated by the B cell lymphoma 2 (BCL-2) protein family. The proteins comprised in this family can be subdivided into three types: anti-apoptotic proteins (BCL-2, BCL-W, BCL-X_L, A1, and MCL1), pro-apoptotic proteins (BAK, BAX, and BOK), and pro-apoptotic BH3-only proteins (BID, BIM, BAD, BIK, BMF, HRK, NOXA, and PUMA) (Bock and Tait, 2020). In the presence of pro-apoptotic stimuli, activation of BH3-only proteins leads to activation of BAK, BAX, and BOK (Correia et al., 2015). These active pro-apoptotic proteins undergo hetero-homo oligomerization forming dynamic macropores in the OMM through which IMS proteins are released into the cytosol (McArthur et al., 2018) (**Figure 1**). Among IMS proteins, cytochrome *c* (an essential component of the electron transport chain), when released into the cytosol, contributes to the formation of apoptosomes, which initiate the caspase cascade. Also, MOMP causes the release of other pro-apoptotic proteins, including SMAC/DIABLO and HtrA2/OMI [for a recent review see Bock and Tait (2020)].

In addition to the aforementioned factors, in several studies, ion channels, including potassium, calcium, sodium, and chloride channels, have been pointed out as crucial regulators of apoptotic cell death (Razik and Cidrowski, 2002; Lang et al., 2005; Leanza et al., 2013). Ion channels are integral membrane proteins mediating ionic fluxes, driven by electrochemical gradient, through biological membranes. Ion channels allow ion compartmentalization and regulation of membrane potential and cell volume. Their opening and closing are often regulated by many factors, including chemical signals and mechanical stimulation (O'Rourke, 2007). In mitochondria, ion channels, present both in the OMM and in the inner mitochondrial membrane (IMM), are actively involved in the regulation of several mitochondrial processes such as regulation of membrane potential and ROS release as well as, volume regulation (O'Rourke, 2007; Szabo and Zoratti, 2014).

Many recent reviews describe the role of mitochondrial ion channels in cell death, especially in apoptosis and necrosis (Biasutto et al., 2016; Krabbendam et al., 2018; Magri et al., 2018; Szewczyk et al., 2018; Peruzzo and Szabo, 2019). In this minireview, we provide an updated overview specifically on the link between the complex regulation of the IMM channels and death induction, with special attention given to the permeability transition pore (PTP) and the mitochondrial calcium uniporter, two master regulators of cell fate.

THE PERMEABILITY TRANSITION PORE

Permeability Transition: A Mitochondrial Catastrophe Regulated by a Mitochondrial Megachannel Whose Molecular Identity Is Still Debated

Even when signaling pathways responsible for MOMP initiation are not fully activated, cytochrome *c* and other IMS proteins can be released in the cytosol via the rupture of the OMM due to mitochondrial swelling initiated by a process called

“permeability transition” (PT) (Petronilli et al., 2001). PT is defined as a sudden increase in IMM permeability to ions and other solutes up to 1.5 kDa, leading to mitochondrial depolarization, cessation of ATP synthesis, and eventually to cell death. This process occurs during profound stress that are often linked to pathological conditions. PT is a regulated and reversible process, requiring matrix Ca²⁺ accumulation and is caused by the opening of a channel called PTP. PTP opening is a highly regulated event, being facilitated by binding of cyclophilin D (CyPD), free fatty acids, Pi (in mammalian mitochondria), accumulation of matrix calcium, of reactive oxygen species (ROS), or by low transmembrane potential. PTP is inhibited by adenine nucleotides and Mg²⁺, detachment of CyPD by cyclosporin A (CsA), and mildly acidic matrix pH [for review see e.g., (Bernardi et al., 2015)].

The idea that PT could be due to a regulated pore (Hunter and Haworth, 1979) was corroborated by the discovery of a Ca²⁺-activated, unselective, high-conductance channel in the IMM with the same characteristics of PTP (Szabo and Zoratti, 1992). This channel, named mitochondrial megachannel (MMC) or multi-conductance channel (MCC), has been deeply characterized using patch clamp on mitoplasts: typically, MMC opens at potential (V) values near to 0 and displays a very high maximal conductance (1.3–1.5 nS) with a large number of lower conductance substates (Kinnally et al., 1989; Petronilli et al., 1989). Ca²⁺ drives MMC activation in the sub-mM range on the matrix side while inhibition takes place at mildly acidic matrix pH, and in the presence of divalent cations other than Ca²⁺ as well as of CSA.

The molecular identity of PTP has long been elusive; here, we briefly mention the potential consensus candidates for pore formation: the adenine nucleotide translocator (ANT) and F_oF₁-ATP synthase. ANT is a family of IMM transmembrane proteins whose physiological role is to exchange matrix ATP for cytosolic ADP. ANT was the first molecular candidate to be proposed for PTP formation (**Figure 2**) on the basis of pharmacological (Hunter and Haworth, 1979) and electrophysiological (Brustovetsky and Klingenberg, 1996) considerations. On the other hand, mitochondria from ANT1/2-null mice underwent Ca²⁺-dependent PTP opening, although with higher Ca²⁺ level required for PT initiation, compared to wild-type (WT) (Kokoszka et al., 2004). Likewise, mitochondria from *Ant1*^{-/-}, *Ant2*^{-/-}, and *Ant4*^{-/-} triple KO mice required a higher matrix Ca²⁺ load for PTP opening, that still occurred and was inhibited by both CsA and by ablation of CyPD (Karch et al., 2019). These findings indicate that PT can take place in the absence of any ANT isoforms, although they suggest that ANT can team up with the pore to ensure higher order regulation.

The other, best-accredited candidate is the mitochondrial F_oF₁-ATP synthase (or F-ATP synthase), a key actor of OXPHOS that converts transmembrane proton motive force into chemical energy via mechanical rotation, leading to the synthesis of ATP molecules (Carraro et al., 2020). The F-ATP synthase hypothesis of pore formation may appear quite unlikely, given the lack of obvious structural evidence of an ion permeation pathway other than H⁺ and the chemiosmotic principle

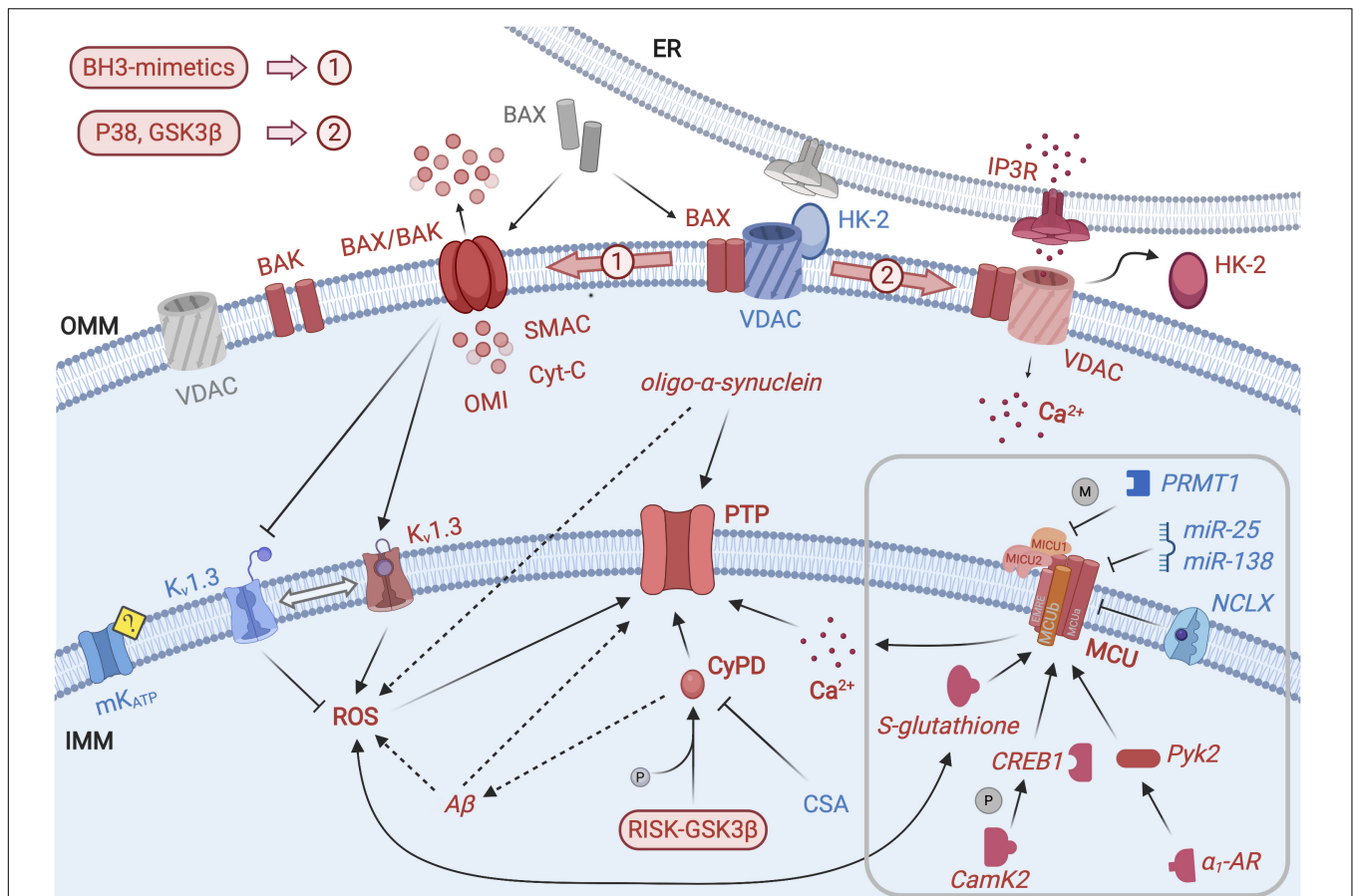


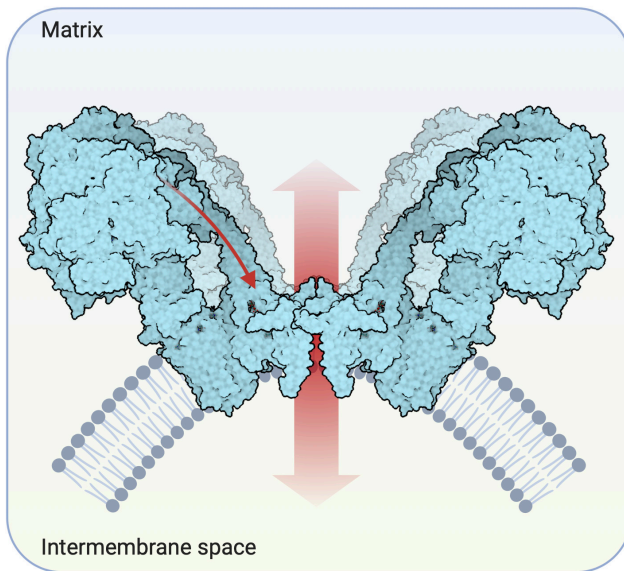
FIGURE 1 | Permeability transition, MCU modulation and mitochondrial regulation of apoptosis. Scheme representing the main ion channels and molecular actors responsible for mitochondrial regulation of apoptosis. Promoters of PT and cell death are depicted as red elements, while blue elements represent inhibitors of PT/cell death or pro-survival factors; molecular actors in a neutral/inactive state are represented as gray elements. PTP is located at the IMM and is the center of converging signaling pathways regulating PT. PTP opening is triggered by Ca^{2+} and facilitated by mitochondrial ROS and by the binding of CyPD. The latter is favored by CyPD phosphorylation by GSK3 β and by RISK kinases; conversely CsA-driven detachment of CyPD has an inhibitory effect on PTP. IMM-localized MCU allows Ca^{2+} internalization in the mitochondrial matrix and, in turn, PTP opening. Kv1.3 indirectly regulates ROS formation, since mitochondrial accumulation of the latter is promoted when the former is inhibited. Channel activity of ATP-dependent K^+ channel (mKATP) has recently been shown to exert a pro-survival and anti-apoptotic action, although through unclear mechanisms. $\text{A}\beta$ and oligomers of α -synuclein probably exert both a direct and ROS-mediated action on the PTP, promoting its opening, but the molecular mechanism is still lacking. The main actors of MOMP, located in the OMM, are in an active equilibrium between inactive and pro-apoptotic state. In particular, in the presence of pro-apoptotic stimuli, BAX localizes in the OMM and forms BAX/BAK complexes, allowing the release in the cytosol of pro-apoptotic factors, initiating the caspase cascade. BAX/BAK activation is promoted by BH3-mimetics. Moreover, the interaction between OMM-localized BAX and Kv1.3 in the IMM causes the inhibition of the latter, with a PT-promoting effect. VDAC and HK-2 are associated at the interface with the ER but the activation of p38 and GSK3 β stimulates the detachment of HK-2, leading to cell death via Ca^{2+} release through IP3R. The MCU located in the IMM is responsible for Ca^{2+} uptake. In the gray square, modulation of the MCU activity is depicted in detail. The expression of the MCU subunits is post-transcriptionally down-regulated by miR-25 and miR-138. ROS regulate MCU activity; especially, Cys-97 in the MCU sequence has been identified as a target of mROS and undergoes S-glutathionylation. Moreover, MCU is positively regulated by CamK2: activated CamK2 promotes CREB phosphorylation and enhances its gene transcriptional function. Furthermore, MCU opening is modulated by Pyk2: α_1 -AR signaling leads to translocation of activated Pyk2 from the cytosol to the mitochondrial matrix; this event accelerates mitochondrial Ca^{2+} uptake increasing mitochondrial ROS production and promoting PTP opening and apoptotic signaling. MCU is controlled by PRMT1 that asymmetrically methylates MICU1 subunit, resulting in decreased Ca^{2+} sensitivity. Finally, NCLX activates mitochondrial Ca^{2+} extrusion via a protein kinase A-mediated phosphorylation-dependent manner.

for which a tightly coupled F-ATP synthase is essential to power ATP generation. Despite this, evidence, mainly based on a combination of pharmacology, molecular biology, and electrophysiology were obtained, pointing to a crucial role of this enzyme in PTP formation (Giorgio et al., 2013; Antonietti et al., 2018; Carraro et al., 2018). However, Walker's group provided opposing evidence: PTP formation was assessed in HAP1 haploid human cells devoid of individual subunits of the

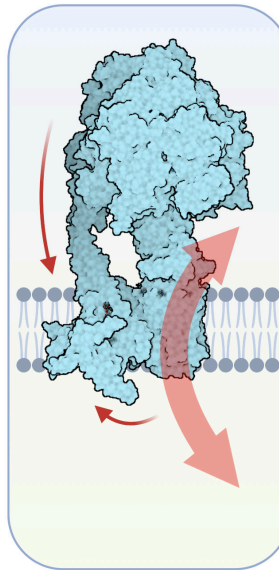
peripheral stalk of F-ATP synthase and, as a consequence, lacking a fully functional enzyme; those cells underwent Ca^{2+} -dependent swelling, although with a slower kinetics compared to WT, and showed CsA-sensitive Ca^{2+} -induced Ca^{2+} release (He et al., 2017; Carroll et al., 2019). Overall, these results were interpreted contrasting with the idea that PTP originates from F-ATP synthase (Walker et al., 2020) and alternative hypotheses have been raised (Carraro and Bernardi, 2020; Carraro et al., 2020).

Main PTP opening models

F_0F_1 -ATP synthase: dimers/tetramers



F_0F_1 -ATP synthase: c-ring/"death finger"



Adenine nucleotide translocator (ANT)

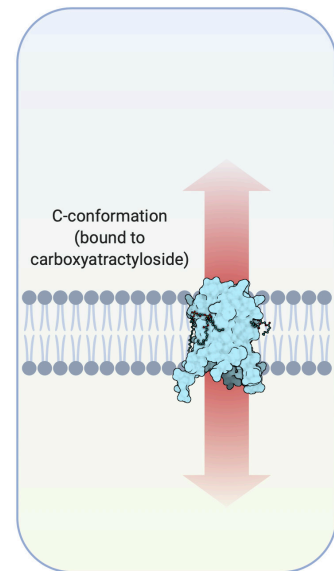


FIGURE 2 | Main PTP opening models. Here the most recent and supported models for PTP opening are depicted. On the left: the F_0F_1 -ATP synthase dimer/tetramer hypothesis postulates that the pore forms within the membrane-embedded domain, comprising the e and g subunits at the dimer/tetramer interface; a conformational change is induced by Ca^{2+} binding to the F_1 portion of the enzyme and is transmitted (arrow) via the peripheral stalk (Giorgio et al., 2018). The diagram was drawn on the basis of a recent crystal structure (Spikes et al., 2020) of dimeric bovine F-ATP synthase. In the middle: the c-ring hypothesis proposes that the pore opens within the c-ring after the Ca^{2+} -dependent dissociation of the F_1 domain from F_0 (Alavian et al., 2014). The "death finger" hypothesis (Gerle, 2016, 2020) posits that Ca^{2+} binding in the F_1 domain determines a conformational change in the region that is transmitted along the peripheral stalk (upper arrow), leading to the displacement of subunits e and g subunits at the dimer/tetramer interface; this, in turn, allows the removal of the lipid plug from the c-ring leading to PTP opening. The diagram was drawn on the basis of the same crystal structure referred above (Spikes et al., 2020). On the right: the ANT hypothesis [extensively reviewed in Broun et al. (2020)] proposes that a Ca^{2+} -dependent conformational change of the ANT leads to PTP opening. The ANT c-state diagram was adapted from a crystal structure (Nury et al., 2005) of ANT in association with its selective inhibitor, carboxyatractyloside, that has been recognized as a PTP-inducer.

Importantly, recent data showed that highly purified F-ATP synthase can give rise to MMC-like activity upon reconstitution into artificial membranes (Mnatsakanyan et al., 2019; Urbani et al., 2019). In support of the crucial role of subunit e for PTP opening, emerging from recent studies (Carraro et al., 2018), and of the death finger model (Gerle, 2016, 2020), new Cryo-EM data of the enzyme exposed to calcium revealed that retraction of subunit e led to a gradually disassembled c-ring, suggesting pore formation by spaced out c subunits (Pinke et al., 2020; Figure 2).

PTP in Physiopathology

Prolonged PTP opening has long been known to be relevant in a high number of pathological conditions - heart injury was the first to be recognized, based on the protective effect of CsA against ischemia-reperfusion injury (Duchen et al., 1993; Griffiths and Halestrap, 1993). Apart from heart injury, several neurodegenerative diseases share calcium mishandling and increased ROS production in neurons, linked to persistent PTP opening (Mattson et al., 2008). Those diseases include

excitotoxicity (Pivovarova and Andrews, 2010), Huntington's disease (Quintanilla et al., 2017) [however, several works from Brustovetsky's group indicates that Ca^{2+} mishandling and mitochondrial function are not impaired in this pathology (Pellman et al., 2015; Hamilton et al., 2016, 2017, 2019)], Alzheimer's disease (Du et al., 2011), and Parkinson's disease (Martin et al., 2014). Furthermore, strong evidence supports a role for CyPD and PTP in the pathology of the Bethlem or Ullrich type muscular dystrophies, consequences of deficiency of collagen VI, delta-sarcoglycan, or laminin-2 (Millay et al., 2008; Palma et al., 2009). Recent studies point to PTP implication in bone loss associated with osteoporosis (Shum et al., 2016) and suggest that pore inhibition could improve bone fracture repair (Shares et al., 2020).

Despite the defined role of prolonged pore openings in pathologies, transient PTP openings have early been hypothesized not to be detrimental (Gunter and Pfeiffer, 1990; Zoratti and Szabo, 1995), and later they were shown to be relevant in the physiological Ca^{2+} homeostasis in several experimental settings (Hüser and Blatter, 1999;

Petronilli et al., 1999; Hausenloy et al., 2004; Agarwal et al., 2017; Ying et al., 2018).

PTP Opening Modulation by Intracellular Factors in the Context of Cell Death

Given the fundamental role of PTP in cell death and, consequently, in various pathologies, understanding its regulation under physiopathological conditions is of utmost importance. PTP can be regulated by ions, small molecule drugs [for a recent review see e.g., (Leanza et al., 2018)], lipids (Brini et al., 2017) as well as proteins (see below). Besides requiring Ca^{2+} , PTP opening is induced by ROS, by-products of OXPHOS. Indeed, accumulation of mitochondrial ROS during reperfusion after ischemia in cardiomyocytes induces PTP openings that can be suppressed by antioxidants administration (Assaly et al., 2012). Modulation of PTP by ROS seems to play a role also in Parkinson's disease: redox-active α -synuclein oligomers, able to impair mitochondrial function and cause PTP opening, have been shown to trigger ROS generation and to directly oxidize a PTP candidate, F-ATP synthase (Ludtmann et al., 2018).

Although its physiological role remains elusive, CyPD, a highly conserved mitochondrial peptidyl-prolyl cis-trans isomerase, has long been known to be a sensitizer of the PTP to Ca^{2+} and ROS and the mediator of the action of the typical PTP inhibitor, CsA (Giorgio et al., 2010). Several CyPD post-translational modifications (PTMs) correlating with pore regulation have been identified by recent studies (Amanakis and Murphy, 2020). One of the most relevant PTMs pathway is the RISK-GSK3 β -CyPD axis: a set of kinases known as RISK (reperfusion injury salvage kinases, including AKT, cdk5, ERK, PKA, PKC, and PKG, – constitutively active Ser/Thr protein kinase that phosphorylates, among other substrates, CyPD, favoring its interaction with PTP (Rasola et al., 2010; **Figure 1**). p38, as well as GSK3 β , contribute to the regulation of PTP also by another mechanism: they control the mitochondrial localization of Isoform 2 of the glycolytic enzyme hexokinase (HK2) in a still unclarified way (Bikkavilli et al., 2008). Activation of p38 or GSK3 β initiates mitochondrial dissociation of HK2, which, in turn, promotes cell death (Tanaka et al., 2018; Ciscato et al., 2020), presumably due to a burst of Ca^{2+} released from the endoplasmic reticulum (ER) via IP3R, leading to a massive Ca^{2+} uptake into the mitochondrial matrix that in turn opens the PTP (Ciscato et al., 2020). In cancer cells, elevated levels of OMM-bound HK2 results in evasion of PTP-dependent apoptosis (Marchi et al., 2019).

CyPD can also interact with amyloid- β protein (A β), resulting in enhanced ROS levels that ultimately triggers PTP opening (Du et al., 2008). Indeed, CyPD deficiency alleviates mitochondrial stress and neuronal damage (Du et al., 2011). A β *per se* may act directly on PTP, since it can interact with the oligomycin sensitivity conferring protein (OSCP) subunit of F_0F_1 -ATP synthase, inducing the formation of an A β -OSCP complex; OSCP sequestration, in turn, disrupts F_0F_1 -ATP synthase, leading to dampened ATP production, increased oxidative stress, and PTP activation (Beck et al., 2016).

Interestingly, PTP regulation by CyPD/CsA has also been linked to viral infection. Apoptosis represents an important

defense mechanism for host cells in the case of many viruses (SADS-COV, hepatitis B/C virus, PDCoV, SARS-COV, and MERS) (Zhang et al., 2020). Virus infections promote BAX translocation and, in turn, MOMP and PTP activation, eventually leading to cytochrome *c* release (Lee and Lee, 2018); CsA treatment efficiently inhibited both virus replication/infection and host cell death. Despite this, it is still unclear if CsA treatment prevents apoptosis by sequestering CyPD (with direct implication in PTP opening) or CyPA (affecting virus replication and BAX translocation) (Glowacka et al., 2020; Molyvdas and Matalon, 2020).

Permeability transition pore opening is facilitated in the presence of variants of Apolipoprotein L1 (APOL1) associated with kidney disease and linked to mitochondrial dysfunction. Whereas APOL1 is mostly monomeric, APOL1 risk-variants display self-aggregation in higher-order oligomers that can physically interact with putative PTP components (F-ATP synthase and ANT2), triggering PTP opening and cell death (Shah et al., 2019).

Finally, it has to be mentioned that the F-ATP synthase can be physiologically regulated also by the ATPase Inhibitory Factor 1 that mediates cell survival by promoting mild ROS release resulting from metabolic shift due to inhibition of F-ATP synthase (Martínez-Reyes and Cuezva, 2014).

THE MITOCHONDRIAL CALCIUM FLUXES AND THEIR REGULATION IN CELL DEATH

Mitochondrial Calcium Uniporter Complex

Mitochondrial Ca^{2+} channels participate in many intracellular signaling pathways both in physiological and in pathological conditions and crucially balance cell life versus death (Giacomello et al., 2007; Duchen et al., 2008). Indeed, as mentioned above, calcium overload in the mitochondria matrix leads to persistent PTP opening and eventually to cell death. Therefore, matrix calcium level has to be highly regulated by modulating the activity of IMM calcium-permeable ion channels and transporters (Rizzuto et al., 2012; Zavodnik, 2016).

Mitochondria can rapidly achieve a high $[\text{Ca}^{2+}]_{\text{matrix}}$ thanks to the presence of a huge driving force generated by a $\Delta\Psi_{\text{m}}$ of -180 mV under physiological conditions, and to the tight contact between the ER and mitochondria that allows direct channeling for Ca^{2+} (Rizzuto et al., 1998; Naon and Scorrano, 2014; Giorgi et al., 2015) (see **Figure 1**).

Calcium entry is primarily mediated by the mitochondrial calcium uniport (MCU) complex (Baughman et al., 2011; De Stefani et al., 2011), which is able to sense the Ca^{2+} signals originating from the ER, while release takes place through the $\text{Na}^+/\text{Ca}^{2+}$ exchanger NCLX (Palty et al., 2010). At the current stage, the mammalian MCUC appears to consist of at least of the pore-forming protein MCU, a dominant-negative MCU paralog (MCUb), the essential MCU regulator (EMRE), the regulatory MICU proteins (MICU1-3), and possibly, the mitochondrial

calcium uniport regulator 1 (MCUR1) (for reviews see e.g., (Marchi and Pinton, 2014; De Stefani et al., 2015; Wagner et al., 2016; Cui et al., 2019). Interestingly, MCU also conducts Mn^{2+} , depending on the presence of MICU1 (Kamer et al., 2018).

Regulation of MCU and of NCLX Affecting Cell Death

Mitochondrial calcium uniport has a documented, crucial role in both proliferation and apoptosis [for reviews see e.g., (De Stefani et al., 2015; Bustos et al., 2017; Cui et al., 2017; Bachmann et al., 2019)]. The expression of the MCU subunit can be post-transcriptionally down-regulated by several small non-coding regulatory RNAs (miR), miR-25, and miR-138 (Marchi et al., 2013; Hong et al., 2017; Jaquenod De Giusti et al., 2018; **Figure 1**). The miRs drastically decrease MCU protein levels, blocking thus mitochondrial Ca^{2+} uptake without affecting $[Ca^{2+}]_C$ and $[Ca^{2+}]_{ER}$, causing reduced apoptosis in cancer cells. These miRs also affect the expression of proapoptotic proteins, like Bim (Zhang et al., 2012), TRAIL (Razumilava et al., 2012), and PTEN (Poliseno et al., 2010).

Similarly to PTP, MCU activity can be regulated by ROS: a highly conserved Cys-97 at the matrix side of MCU was observed to be S-glutathionylated under oxidative stress, leading to enhanced MCU tetramerization and channel activity that, in turn, exacerbates mitochondrial Ca^{2+} overload and triggers cell death (Dong et al., 2017).

Other types of PTMs can also regulate MCU. One of the first reported cases envisioned Ca^{2+} /calmodulin-dependent protein kinase 2 (CaMK2) as a regulator of MCU, however, this finding has been challenged (Joiner et al., 2012, 2014; Fieni et al., 2014). Moreover, MCU is regulated by the proline-rich tyrosine kinase 2 (Pyk2), accelerating mitochondrial Ca^{2+} uptake via Pyk2-dependent MCU phosphorylation and tetrametric MCU channel pore formation under α_1 -adrenoceptor (α_1 -AR) signaling.

Furthermore, mitochondrial Ca^{2+} uptake is controlled by the modification of MCU regulators. For example, the protein arginine methyltransferase 1 (PRMT1) methylates MICU1 subunit, decreasing its Ca^{2+} sensitivity, thus resulting in reduced calcium uptake into the matrix (Madreiter-Sokolowski et al., 2016). Interestingly, it has been observed that the uncoupling proteins 2/3, previously shown to affect mitochondrial calcium handling, were able to ensure the sensitivity of MICU1 to calcium even upon increased methylation activity (Madreiter-Sokolowski et al., 2016). However, this finding does not explain how upregulation of UCP2 expression can protect mitochondria against calcium overload and cells from apoptosis (Pan et al., 2018). Independently of this, a similar interplay between ANT and F-ATP synthase may exist since the mitochondrial lysine (K)-specific methyltransferase (KMT) FAM173B targets the c-subunit of mitochondrial ATP synthase while FAM173A methylates ANT2 and 3 (Małecki et al., 2019).

As to NCLX, a recent study illustrates the physiological relevance of its post-translational regulation: adrenergic stimulation of brown adipose tissue was shown to activate mitochondrial Ca^{2+} extrusion via the mitochondrial NCLX in a protein kinase A-mediated phosphorylation-dependent manner, in order to prevent cell death despite the sharp increase

of $[Ca^{2+}]_{matrix}$ during thermogenesis (Assali et al., 2020). Inhibition of NCLX by the microtubule-associated tau protein implicated in the tauopathies was instead linked to increased death in neurons (Britti et al., 2020). Recent pieces of evidence from NCLX KO mice suggest an anti-apoptotic role exerted by NCLX by preventing mitochondrial Ca^{2+} overload (Luongo et al., 2017; Assali et al., 2020).

MODULATION OF OTHER IMM ION CHANNELS AFFECTS CELL SURVIVAL

Many other ion channels in the IMM have been linked to cell survival/cell death, including the mitochondrial counterparts of potassium channels TASK-3 (Nagy et al., 2014), calcium-activated potassium channels (Dolga et al., 2013; Krabbendam et al., 2018), the recently identified ATP-dependent K^+ channel (Laskowski et al., 2019; Paggio et al., 2019) and voltage-gated K^+ channels (Szabo et al., 2005; Testai et al., 2015) and the uncoupling proteins (Adams et al., 2010; Pitt, 2015). Unfortunately, only limited information is available about the intracellular regulation of these channels, apart the classical ligands known to modulate these channels such as ATP, protons, fatty acids and calcium. One exception is the voltage-gated Kv1.3, shown to interact with OMM-inserted BAX (Szabo et al., 2008) via critical lysine residues during apoptosis (Szabo et al., 2011; **Figure 1**). The channel becomes inhibited, and via interaction with complex I, Kv1.3 inhibitors trigger ROS release (Peruzzo et al., 2020), leading to PTP opening. This observation inspired the design of a mitochondriotropic inhibitor of the channel that triggered apoptosis and drastically reduced tumor volume of both melanoma and pancreatic ductal adenocarcinoma *in vivo*. Hopefully future research will identify ways to target other channels that are differentially expressed in various tissues and cancer types.

CONCLUSION AND FUTURE OUTLOOK

In conclusion, advances in the genetic identification of IMM channel components, along with the availability of Mitocarta (Pagliarini et al., 2008) and novel tools to identify interaction partners in intact cells (Branon et al., 2018), will certainly revolutionize the field of mitochondrial ion channels. As illustrated above, considerable new information allowed to link pathways/proteins that regulate IMM channels to cell death/survival signaling during the last decade. Since factors that regulate mitochondrial calcium accumulation play a crucial role in this context, understanding of the relation between channel modulation and localized $[Ca^{2+}]$ changes, thanks to novel, sub-mitochondrial targeted Ca^{2+} sensors (Waldeck-Weiermair et al., 2019), may further widen our view. Similarly, measurement of simultaneous, real-time dynamics of ATP and ROS in mitochondria *in vivo* (van Hameren et al., 2019) may provide important insights to integrate IMM (and OMM) channels into death signaling pathways. As a challenging future outlook, we may envision constructing artificial, light-gated ion channels (Cosentino et al., 2015) targeted to mitochondria.

AUTHOR CONTRIBUTIONS

All authors contributed to the writing of the manuscript.

FUNDING

The work in the laboratory of the authors is financed by the Italian association for cancer research (AIRC) grant (IG 2017

20286 to IS), by the Italian Association for Multiple Sclerosis (Grant 2018/R/20), by Telethon (GGP19118) and the Italian Ministry of University and Education (PRIN 2015795S5W to IS).

ACKNOWLEDGMENTS

The authors thank all members of the laboratory for useful discussion. Figures were created with BioRender.com.

REFERENCES

- Adams, A. E., Kelly, O. M., and Porter, R. K. (2010). Absence of mitochondrial uncoupling protein 1 affects apoptosis in thymocytes, thymocyte/T-cell profile and peripheral T-cell number. *Biochim. Biophys. Acta* 1797, 807–816. doi: 10.1016/j.bbabi.2010.04.016
- Agarwal, A., Wu, P. H., Hughes, E. G., Fukaya, M., Tischfield, M. A., Langseth, A. J., et al. (2017). Transient opening of the mitochondrial permeability transition pore induces microdomain calcium transients in astrocyte processes. *Neuron* 93, 587.e–605.e.
- Alavian, K. N., Beutner, G., Lazrove, E., Sacchetti, S., Park, H. A., Licznarski, P., et al. (2014). An uncoupling channel within the c-subunit ring of the F1FO ATP synthase is the mitochondrial permeability transition pore. *Proc. Natl. Acad. Sci. U.S.A.* 111, 10580–10585. doi: 10.1073/pnas.1401591111
- Amanakis, G., and Murphy, E. (2020). Cyclophilin D: an integrator of mitochondrial function. *Front. Physiol.* 11:595. doi: 10.3389/fphys.2020.00595
- Antoniell, M., Jones, K., Antonucci, S., Spolaore, B., Fogolari, F., Petronilli, V., et al. (2018). The unique histidine in OSCP subunit of F-ATP synthase mediates inhibition of the permeability transition pore by acidic pH. *EMBO Rep.* 19, 257–268. doi: 10.15252/embr.201744705
- Assali, E. A., Jones, A. E., Veliova, M., Acín-Pérez, R., Taha, M., Miller, N., et al. (2020). NCLX prevents cell death during adrenergic activation of the brown adipose tissue. *Nat. Commun.* 11:3347.
- Assaly, R., de Tassigny, A., Paradis, S., Jacquin, S., Berdeaux, A., and Morin, D. (2012). Oxidative stress, mitochondrial permeability transition pore opening and cell death during hypoxia-reoxygenation in adult cardiomyocytes. *Eur. J. Pharmacol.* 675, 6–14. doi: 10.1016/j.ejphar.2011.11.036
- Bachmann, M., Pontarin, G., and Szabo, I. (2019). The contribution of mitochondrial ion channels to cancer development and progression. *Cell. Physiol. Biochem.* 53, 63–78. doi: 10.33594/000000198
- Baughman, J. M., Perocchi, F., Girgis, H. S., Plovanich, M., Belcher-Timme, C. A., Sancak, Y., et al. (2011). Integrative genomics identifies MCU as an essential component of the mitochondrial calcium uniporter. *Nature* 476, 341–345. doi: 10.1038/nature10234
- Beck, S. J., Guo, L., Phensy, A., Tian, J., Wang, L., Tandon, N., et al. (2016). Deregulation of mitochondrial F1FO-ATP synthase via OSCP in Alzheimer's disease. *Nat. Commun.* 7:11483.
- Bernardi, P., Rasola, A., Forte, M., and Lippe, G. (2015). The Mitochondrial Permeability Transition Pore: Channel Formation by F-ATP Synthase, Integration in Signal Transduction, and Role in Pathophysiology. *Physiol. Rev.* 95, 1111–1155. doi: 10.1152/physrev.00001.2015
- Biasutto, L., Azzolini, M., Szabo, I., and Zoratti, M. (2016). The mitochondrial permeability transition pore in AD 2016: An update. *Biochim. Biophys. Acta* 1863, 2515–2530. doi: 10.1016/j.bbamcr.2016.02.012
- Bikkavilli, R. K., Feigin, M. E., and Malbon, C. C. (2008). p38 mitogen-activated protein kinase regulates canonical Wnt-beta-catenin signaling by inactivation of GSK3beta. *J. Cell Sci.* 121(Pt. 21), 3598–3607. doi: 10.1242/jcs.032854
- Bock, F. J., and Tait, S. W. G. (2020). Mitochondria as multifaceted regulators of cell death. *Nat. Rev. Mol. Cell Biol.* 21, 85–100. doi: 10.1038/s41580-019-0173-8
- Bortner, C. D., and Cidlowski, J. A. (2014). Ion channels and apoptosis in cancer. *Philos. Trans. Royal Soc. Lond. Ser. B Biol. Sci.* 369:20130104. doi: 10.1098/rstb.2013.0104
- Branon, T. C., Bosch, J. A., Sanchez, A. D., Udeshi, N. D., Svinkina, T., Carr, S. A., et al. (2018). Efficient proximity labeling in living cells and organisms with TurboID. *Nat. Biotechnol.* 36, 880–887. doi: 10.1038/nbt.4201
- Brini, M., Leanza, L., and Szabo, I. (2017). Lipid-mediated modulation of intracellular ion channels and redox state: physiopathological implications. *Antioxidants Redox Signal.* 28, 949–972. doi: 10.1089/ars.2017.7215
- Britti, E., Ros, J., Esteras, N., and Abramov, A. Y. (2020). Tau inhibits mitochondrial calcium efflux and makes neurons vulnerable to calcium-induced cell death. *Cell Calcium* 86:102150. doi: 10.1016/j.ceca.2019.102150
- Bround, M. J., Bers, D. M., and Molkentin, J. D. (2020). A 20/20 view of ANT function in mitochondrial biology and necrotic cell death. *J. Mol. Cell. Cardiol.* 144, A3–A13.
- Brustovetsky, N., and Klingenberg, M. (1996). Mitochondrial ADP/ATP carrier can be reversibly converted into a large channel by Ca²⁺. *Biochemistry* 35, 8483–8488. doi: 10.1021/bi960833v
- Bustos, G., Cruz, P., Lovy, A., and Cardenas, C. (2017). Endoplasmic reticulum-mitochondria calcium communication and the regulation of mitochondrial metabolism in cancer: a novel potential target. *Front. Oncol.* 7:199. doi: 10.3389/fonc.2017.00199
- Carraro, M., and Bernardi, P. (2020). Measurement of membrane permeability and the mitochondrial permeability transition. *Methods Cell Biol.* 155, 369–379. doi: 10.1016/bs.mcb.2019.10.004
- Carraro, M., Carrer, A., Urbani, A., and Bernardi, P. (2020). Molecular nature and regulation of the mitochondrial permeability transition pore(s), drug target(s) in cardioprotection. *J. Mol. Cell. Cardiol.* 144, 76–86. doi: 10.1016/j.yjmcc.2020.05.014
- Carraro, M., Checchetto, V., Sartori, G., Kucharczyk, R., di Rago, J. P., Minervini, G., et al. (2018). High-conductance channel formation in yeast mitochondria is mediated by F-ATP Synthase e and g Subunits. *Cell. Physiol. Biochem.* 50, 1840–1855. doi: 10.1159/000494864
- Carroll, J., He, J., Ding, S., Fearnley, I. M., and Walker, J. E. (2019). Persistence of the permeability transition pore in human mitochondria devoid of an assembled ATP synthase. *Proc. Natl. Acad. Sci. U.S.A.* 116, 12816–12821. doi: 10.1073/pnas.1904005116
- Chouchani, E. T., Kazak, L., and Spiegelman, B. M. (2019). New advances in adaptive thermogenesis: UCP1 and beyond. *Cell Metab.* 29, 27–37. doi: 10.1016/j.cmet.2018.11.002
- Ciscato, F., Filadi, R., Masgras, I., Pizzi, M., Marin, O., Damiano, N., et al. (2020). Hexokinase 2 displacement from mitochondria-associated membranes prompts Ca(2+) -dependent death of cancer cells. *EMBO Rep.* 21:e49117.
- Correia, C., Lee, S. H., Meng, X. W., Vincelette, N. D., Knorr, K. L., Ding, H., et al. (2015). Emerging understanding of Bcl-2 biology: Implications for neoplastic progression and treatment. *Biochim. Biophys. Acta* 1853, 1658–1671. doi: 10.1016/j.bbamcr.2015.03.012
- Cosentino, C., Alberio, L., Gazzarrini, S., Aquila, M., Romano, E., Cermenati, S., et al. (2015). Optogenetics. *Engineering of a light-gated potassium channel. Science* 348, 707–710.
- Cui, C., Merritt, R., Fu, L., and Pan, Z. (2017). Targeting calcium signaling in cancer therapy. *Acta Pharm. Sin. B* 7, 3–17. doi: 10.1016/j.apsb.2016.11.001
- Cui, C., Yang, J., Fu, L., Wang, M., and Wang, X. (2019). Progress in understanding mitochondrial calcium uniporter complex-mediated calcium signalling: a potential target for cancer treatment. *Br. J. Pharmacol.* 176, 1190–1205. doi: 10.1111/bph.14632

- De Stefani, D., Patron, M., and Rizzuto, R. (2015). Structure and function of the mitochondrial calcium uniporter complex. *Biochim. Biophys. Acta* 1853, 2006–2011. doi: 10.1016/j.bbamcr.2015.04.008
- De Stefani, D., Raffaello, A., Teardo, E., Szabo, I., and Rizzuto, R. (2011). A forty-kilodalton protein of the inner membrane is the mitochondrial calcium uniporter. *Nature* 476, 336–340. doi: 10.1038/nature10230
- De Stefani, D., Rizzuto, R., and Pozzan, T. (2016). Enjoy the trip: calcium in mitochondria back and forth. *Annu. Rev. Biochem.* 85, 161–192. doi: 10.1146/annurev-biochem-060614-034216
- Dolga, A. M., Netter, M. F., Perocchi, F., Doti, N., Meissner, L., Tobaben, S., et al. (2013). Mitochondrial small conductance SK2 channels prevent glutamate-induced oxytosis and mitochondrial dysfunction. *J. Biol. Chem.* 288, 10792–10804. doi: 10.1074/jbc.m113.453522
- Dong, Z., Shanmughapriya, S., Tomar, D., Siddiqui, N., Lynch, S., Nemani, N., et al. (2017). Mitochondrial Ca(2+) uniporter is a mitochondrial luminal redox sensor that augments MCU channel activity. *Mol. Cell* 65, 1014.e–1028.e.
- Du, H., Guo, L., Fang, F., Chen, D., Sosunov, A. A., McKhann, G. M., et al. (2008). Cyclophilin D deficiency attenuates mitochondrial and neuronal perturbation and ameliorates learning and memory in Alzheimer's disease. *Nat. Med.* 14, 1097–1105. doi: 10.1038/nm.1868
- Du, H., Guo, L., Zhang, W., Rydzewska, M., and Yan, S. (2011). Cyclophilin D deficiency improves mitochondrial function and learning/memory in aging Alzheimer disease mouse model. *Neurobiol. Aging* 32, 398–406. doi: 10.1016/j.neurobiolaging.2009.03.003
- Duchen, M. R., McGuinness, O., Brown, L. A., and Crompton, M. (1993). On the involvement of a cyclosporin A sensitive mitochondrial pore in myocardial reperfusion injury. *Cardiovascu. Res.* 27, 1790–1794. doi: 10.1093/cvr/27.10.1790
- Duchen, M. R., Verkhratsky, A., and Muallem, S. (2008). Mitochondria and calcium in health and disease. *Cell Calcium* 44, 1–5. doi: 10.1016/j.ceca.2008.02.001
- Fieni, F., Johnson, D. E., Hudmon, A., and Kirichok, Y. (2014). Mitochondrial Ca2+ uniporter and CaMKII in heart. *Nature* 513, E1–E2.
- Fricker, M., Tolkovsky, A. M., Borutaite, V., Coleman, M., and Brown, G. C. (2018). Neuronal cell death. *Physiol. Rev.* 98, 813–880.
- Galluzzi, L., Kepp, O., and Kroemer, G. (2016). Mitochondrial regulation of cell death: a phylogenetically conserved control. *Microb. Cell* 3, 101–108. doi: 10.15698/mic2016.03.483
- Gerle, C. (2016). On the structural possibility of pore-forming mitochondrial FoF1 ATP synthase. *Biochim. Biophys. Acta* 1857, 1191–1196. doi: 10.1016/j.bbatio.2016.03.008
- Gerle, C. (2020). Mitochondrial F-ATP synthase as the permeability transition pore. *Pharmacol. Res.* 160:105081. doi: 10.1016/j.phrs.2020.105081
- Giacomello, M., Drago, I., Pizzo, P., and Pozzan, T. (2007). Mitochondrial Ca2+ as a key regulator of cell life and death. *Cell Death Differ.* 14, 1267–1274. doi: 10.1038/sj.cdd.4402147
- Giorgi, C., Missiroli, S., Patergnani, S., Duszyński, J., Wieckowski, M. R., and Pinton, P. (2015). Mitochondria-associated membranes: composition, molecular mechanisms, and physiopathological implications. *Antioxid Redox Signal* 22, 995–1019. doi: 10.1089/ars.2014.6223
- Giorgio, V., Guo, L., Bassot, C., Petronilli, V., and Bernardi, P. (2018). Calcium and regulation of the mitochondrial permeability transition. *Cell Calcium* 70, 56–63. doi: 10.1016/j.ceca.2017.05.004
- Giorgio, V., Soriano, M. E., Basso, E., Bisetto, E., Lippe, G., Forte, M. A., et al. (2010). Cyclophilin D in mitochondrial pathophysiology. *Biochim. Biophys. Acta* 1797, 1113–1118.
- Giorgio, V., von Stockum, S., Antoniel, M., Fabbro, A., Fogolari, F., Forte, M., et al. (2013). Dimers of mitochondrial ATP synthase form the permeability transition pore. *Proc. Natl. Acad. Sci. U.S.A.* 110, 5887–5892. doi: 10.1073/pnas.1217823110
- Glowacka, P., Rudnicka, L., Warsawik-Hendzel, O., Sikora, M., Goldust, M., Hajda, P., et al. (2020). The antiviral properties of cyclosporine. focus on coronavirus, hepatitis c virus, influenza virus, and human immunodeficiency virus infections. *Biology* 9:192. doi: 10.3390/biology9080192
- Griffiths, E. J., and Halestrap, A. P. (1993). Protection by Cyclosporin A of ischemia/reperfusion-induced damage in isolated rat hearts. *J. Mol. Cell. Cardiol.* 25, 1461–1469. doi: 10.1006/jmcc.1993.1162
- Gunter, T. E., and Pfeiffer, D. R. (1990). Mechanisms by which mitochondria transport calcium. *Am. J. Physiol.* 258(5 Pt. 1), C755–C786.
- Hamilton, J., Brustovetsky, T., and Brustovetsky, N. (2017). Oxidative metabolism and Ca(2+) handling in striatal mitochondria from YAC128 mice, a model of Huntington's disease. *Neurochem. Int.* 109, 24–33. doi: 10.1016/j.neuint.2017.01.001
- Hamilton, J., Brustovetsky, T., and Brustovetsky, N. (2019). Mutant huntingtin fails to directly impair brain mitochondria. *J. Neurochem.* 151, 716–731. doi: 10.1111/jnc.14852
- Hamilton, J., Pellman, J. J., Brustovetsky, T., Harris, R. A., and Brustovetsky, N. (2016). Oxidative metabolism and Ca2+ handling in isolated brain mitochondria and striatal neurons from R6/2 mice, a model of Huntington's disease. *Hum. Mol. Genet.* 25, 2762–2775.
- Hausenloy, D., Wynne, A., Duchon, M., and Yellon, D. (2004). Transient mitochondrial permeability transition pore opening mediates preconditioning-induced protection. *Circulation* 109, 1714–1717. doi: 10.1161/01.cir.0000126294.81407.7d
- He, J., Ford, H. C., Carroll, J., Ding, S., Fearnley, I. M., and Walker, J. E. (2017). Persistence of the mitochondrial permeability transition in the absence of subunit c of human ATP synthase. *Proc. Natl. Acad. Sci. U.S.A.* 114, 3409–3414. doi: 10.1073/pnas.1702357114
- Hong, Z., Chen, K. H., DasGupta, A., Potus, F., Dunham-Snary, K., Bonnet, S., et al. (2017). MicroRNA-138 and MicroRNA-25 down-regulate mitochondrial calcium uniporter, causing the pulmonary arterial hypertension cancer phenotype. *Am. J. Respirat. Crit. Care Med.* 195, 515–529. doi: 10.1164/rccm.201604-0814oc
- Hunter, D. R., and Haworth, R. A. (1979). The Ca2+-induced membrane transition in mitochondria. I. The protective mechanisms. *Arch. Biochem. Biophys.* 195, 453–459. doi: 10.1016/0003-9861(79)90371-0
- Hüser, J., and Blatter, L. A. (1999). Fluctuations in mitochondrial membrane potential caused by repetitive gating of the permeability transition pore. *Biochem. J.* 343 (Pt. 2), 311–317. doi: 10.1042/bj3430311
- Jaquenod De Giusti, C., Roman, B., and Das, S. (2018). The Influence of MicroRNAs on Mitochondrial Calcium. *Front. Physiol.* 9:1291. doi: 10.3389/fphys.2018.01291
- Joiner, M. L., Koval, O. M., Li, J., He, B. J., Allamargot, C., Gao, Z., et al. (2012). CaMKII determines mitochondrial stress responses in heart. *Nature* 491, 269–273. doi: 10.1038/nature11444
- Joiner, M. L., Koval, O. M., Li, J., He, B. J., Allamargot, C., Gao, Z., et al. (2014). Joiner et al. reply. *Nature* 513:E3.
- Kamer, K. J., Sancak, Y., Fomina, Y., Meisel, J. D., Chaudhuri, D., Grabarek, Z., et al. (2018). MICU1 imparts the mitochondrial uniporter with the ability to discriminate between Ca(2+) and Mn(2+). *Proc. Natl. Acad. Sci. U.S.A.* 115, E7960–E7969.
- Karch, J., Broun, M. J., Khalil, H., Sargent, M. A., Latchman, N., Terada, N., et al. (2019). Inhibition of mitochondrial permeability transition by deletion of the ANT family and CypD. *Sci. Adv.* 5:eaaw4597. doi: 10.1126/sciadv.aaw4597
- Kinnally, K. W., Campo, M. L., and Tedeschi, H. (1989). Mitochondrial channel activity studied by patch-clamping mitoplasts. *J. Bioenerget. Biomemb.* 21, 497–506. doi: 10.1007/bf00762521
- Kokoszka, J. E., Waymire, K. G., Levy, S. E., Sligh, J. E., Cai, J., Jones, D. P., et al. (2004). The ADP/ATP translocator is not essential for the mitochondrial permeability transition pore. *Nature* 427, 461–465. doi: 10.1038/nature02229
- Kondratsky, A., Kondratska, K., Skryma, R., and Prevarskaya, N. (2015). Ion channels in the regulation of apoptosis. *Biochim. Biophys. Acta* 1848(10 Pt. B), 2532–2546.
- Krabbendam, I. E., Honrath, B., Culmsee, C., and Dolga, A. M. (2018). Mitochondrial Ca(2+)-activated K(+) channels and their role in cell life and death pathways. *Cell Calcium* 69, 101–111. doi: 10.1016/j.ceca.2017.07.005
- Lang, F., Föller, M., Lang, K. S., Lang, P. A., Ritter, M., Gulbins, E., et al. (2005). Ion channels in cell proliferation and apoptotic cell death. *J. Membr. Biol.* 205, 147–157. doi: 10.1007/s00232-005-0780-5
- Laskowski, M., Augustynek, B., Bednarczyk, P., Żochowska, M., Kalisz, J., O'Rourke, B., et al. (2019). Single-Channel Properties of the ROMK-pore-forming subunit of the mitochondrial ATP-sensitive potassium channel. *Int. J. Mol. Sci.* 20:5323. doi: 10.3390/ijms20215323

- Leanza, L., Biasutto, L., Manago, A., Gulbins, E., Zoratti, M., and Szabo, I. (2013). Intracellular ion channels and cancer. *Front. Physiol.* 4:227. doi: 10.3389/fphys.2013.00227
- Leanza, L., Checchetto, V., Biasutto, L., Rossa, A., Costa, R., Bachmann, M., et al. (2018). Pharmacological modulation of mitochondrial ion channels. *Br. J. Pharmacol.* 176, 4258–4283.
- Leanza, L., Manago, A., Zoratti, M., Gulbins, E., and Szabo, I. (2015). Pharmacological targeting of ion channels for cancer therapy: in vivo evidences. *Biochim. Biophys. Acta* 1863(6 Pt B), 1385–1397. doi: 10.1016/j.bbamcr.2015.11.032
- Lee, Y. J., and Lee, C. (2018). Porcine deltacoronavirus induces caspase-dependent apoptosis through activation of the cytochrome c-mediated intrinsic mitochondrial pathway. *Virus Res.* 253, 112–123. doi: 10.1016/j.virusres.2018.06.008
- Ludtmann, M. H. R., Angelova, P. R., Horrocks, M. H., Choi, M. L., Rodrigues, M., Baev, A. Y., et al. (2018). α -synuclein oligomers interact with ATP synthase and open the permeability transition pore in Parkinson's disease. *Nat. Commun.* 9:2293.
- Luongo, T. S., Lambert, J. P., Gross, P., Nwokedi, M., Lombardi, A. A., Shanmughapriya, S., et al. (2017). The mitochondrial Na. *Nature* 545, 93–97.
- Madreiter-Sokolowski, C. T., Klec, C., Parichatikanond, W., Stryeck, S., Gottschalk, B., Pulido, S., et al. (2016). PRMT1-mediated methylation of MICU1 determines the UCP2/3 dependency of mitochondrial Ca(2+) uptake in immortalized cells. *Nat. Commun.* 7:12897.
- Magri, A., Reina, S., and De Pinto, V. (2018). VDAC1 as pharmacological target in cancer and neurodegeneration: focus on its role in apoptosis. *Front. Chem.* 6:108. doi: 10.1016/j.neuron.2014.06.020
- Małeck, J. M., Willemsen, H., Pinto, R., Ho, A. Y. Y., Moen, A., Eijkelkamp, N., et al. (2019). Human FAM173A is a mitochondrial lysine-specific methyltransferase that targets adenine nucleotide translocase and affects mitochondrial respiration. *J. Biol. Chem.* 294, 11654–11664. doi: 10.1074/jbc.ra119.009045
- Marchi, S., Lupini, L., Patergnani, S., Rimessi, A., Missiroli, S., Bonora, M., et al. (2013). Downregulation of the mitochondrial calcium uniporter by cancer-related miR-25. *Curr. Biol.* 23, 58–63. doi: 10.1016/j.cub.2012.11.026
- Marchi, S., and Pinton, P. (2014). The mitochondrial calcium uniporter complex: molecular components, structure and physiopathological implications. *J. Physiol.* 592(Pt. 5), 829–839. doi: 10.1113/jphysiol.2013.268235
- Marchi, S., Vitto, V. A. M., Patergnani, S., and Pinton, P. (2019). High mitochondrial Ca(2+) content increases cancer cell proliferation upon inhibition of mitochondrial permeability transition pore (mPTP). *Cell Cycle* 18, 914–916. doi: 10.1080/15384101.2019.1598729
- Martin, L. J., Semenkow, S., Hanaford, A., and Wong, M. (2014). Mitochondrial permeability transition pore regulates Parkinson's disease development in mutant alpha-synuclein transgenic mice. *Neurobiol. Aging* 35, 1132–1152. doi: 10.1016/j.neurobiolaging.2013.11.008
- Martínez-Reyes, I., and Cuezva, J. M. (2014). The H(+)-ATP synthase: a gate to ROS-mediated cell death or cell survival. *Biochim. Biophys. Acta* 1837, 1099–1112. doi: 10.1016/j.bbabi.2014.03.010
- Mattson, M. P., Gleichmann, M., and Cheng, A. (2008). Mitochondria in neuroplasticity and neurological disorders. *Neuron* 60, 748–766. doi: 10.1016/j.neuron.2008.10.010
- McArthur, K., Whitehead, L. W., Heddlestone, J. M., Li, L., Padman, B. S., Oorschot, V., et al. (2018). BAK/BAX macropores facilitate mitochondrial herniation and mtDNA efflux during apoptosis. *Science* 359:6378.
- Millay, D. P., Sargent, M. A., Osinska, H., Baines, C. P., Barton, E. R., Vuagniaux, G., et al. (2019). Genetic and pharmacologic inhibition of mitochondrial-dependent necrosis attenuates muscular dystrophy. *Nat. Med.* 14, 442–447. doi: 10.1038/nm1736
- Mnatsakanyan, N., Park, H.-A., Jing, W., Llaguno, M. C., Murtishi, B., Latta, M., et al. (2019). Mitochondrial Megachannel Resides in Monomeric ATP Synthase. *Biophysical Journal* 116, 156a. doi: 10.1016/j.bpj.2018.11.863
- Molyvdas, A., and Matalon, S. (2020). Cyclosporine: an old weapon in the fight against Coronaviruses. *Eur. Respirat. J.* 56:2002484. doi: 10.1183/13993003.02484-2020
- Nagy, D., Gonczi, M., Dienes, B., Szoor, A., Fodor, J., Nagy, Z., et al. (2014). Silencing the KCNK9 potassium channel (TASK-3) gene disturbs mitochondrial function, causes mitochondrial depolarization, and induces apoptosis of human melanoma cells. *Arch. Dermatol. Res.* 306, 885–902. doi: 10.1007/s00403-014-1511-5
- Naon, D., and Scorrano, L. (2014). At the right distance: ER-mitochondria juxtaposition in cell life and death. *Biochim. Biophys. Acta* 1843, 2184–2194. doi: 10.1016/j.bbamcr.2014.05.011
- Nury, H., Dahout-Gonzalez, C., Trézéguet, V., Lauquin, G., Brandolin, G., and Pebay-Peyroula, E. (2005). Structural basis for lipid-mediated interactions between mitochondrial ADP/ATP carrier monomers. *FEBS Lett.* 579, 6031–6036. doi: 10.1016/j.febslet.2005.09.061
- O'Rourke, B. (2007). Mitochondrial ion channels. *Annu. Rev. Physiol.* 69, 19–49.
- Paggio, A., Checchetto, V., Campo, A., Menabo, R., Di Marco, G., Di Lisa, F., et al. (2019). Identification of an ATP-sensitive potassium channel in mitochondria. *Nature* 572, 609–613.
- Pagliarini, D. J., Calvo, S. E., Chang, B., Sheth, S. A., Vafai, S. B., Ong, S.-E., et al. (2008). A mitochondrial protein compendium elucidates complex I disease biology. *Cell* 134, 112–123. doi: 10.1016/j.cell.2008.06.016
- Palma, E., Tiepolo, T., Angelin, A., Sabatelli, P., Maraldi, N. M., Basso, E., et al. (2009). Genetic ablation of cyclophilin D rescues mitochondrial defects and prevents muscle apoptosis in collagen VI myopathic mice. *Hum. Mol. Genet.* 18, 2024–2031. doi: 10.1093/hmg/ddp126
- Palty, R., Silverman, W. F., Hershfinkel, M., Caporale, T., Sensi, S. L., Parnis, J., et al. (2010). NCLX is an essential component of mitochondrial Na+/Ca2+ exchange. *Proc. Natl. Acad. Sci. U.S.A.* 107, 436–441. doi: 10.1073/pnas.0908099107
- Pan, P., Zhang, H., Su, L., Wang, X., and Liu, D. (2018). Melatonin Balance the Autophagy and Apoptosis by Regulating UCP2 in the LPS-Induced Cardiomyopathy. *Molecules* 23:675. doi: 10.3390/molecules23030675
- Pellman, J. J., Hamilton, J., Brustovetsky, T., and Brustovetsky, N. (2015). Ca(2+) handling in isolated brain mitochondria and cultured neurons derived from the YAC128 mouse model of Huntington's disease. *J. Neurochem.* 134, 652–667. doi: 10.1111/jnc.13165
- Peruzzo, R., Mattarei, A., Azzolini, M., Becker-Flegler, K. A., Romio, M., Rigoni, G., et al. (2020). Insight into the mechanism of cytotoxicity of membrane-permeant psoralenic Kv1.3 channel inhibitors by chemical dissection of a novel member of the family. *Redox Biol.* 37:101705. doi: 10.1016/j.redox.2020.101705
- Peruzzo, R., and Szabo, I. (2019). Contribution of mitochondrial ion channels to chemo-resistance in cancer cells. *Cancers* 11:761. doi: 10.3390/cancers11060761
- Petronilli, V., Miotto, G., Canton, M., Brini, M., Colonna, R., Bernardi, P., et al. (1999). Transient and long-lasting openings of the mitochondrial permeability transition pore can be monitored directly in intact cells by changes in mitochondrial calcein fluorescence. *Biophys. J.* 76, 725–734. doi: 10.1016/s0006-3495(99)77239-5
- Petronilli, V., Penzo, D., Scorrano, L., Bernardi, P., and Di Lisa, F. (2001). The mitochondrial permeability transition, release of cytochrome c and cell death. Correlation with the duration of pore openings in situ. *J. Biol. Chem.* 276, 12030–12034. doi: 10.1074/jbc.m010604200
- Petronilli, V., Szabò, I., and Zoratti, M. (1989). The inner mitochondrial membrane contains ion-conducting channels similar to those found in bacteria. *FEBS Lett.* 259, 137–143. doi: 10.1016/0014-5793(89)81513-3
- Pinke, G., Zhou, L., and Sazanov, L. A. (2020). Cryo-EM structure of the entire mammalian F-type ATP synthase. *Nat. Struct. Mol. Biol.* 27, 1077–1085. doi: 10.1038/s41594-020-0503-8
- Pitt, M. A. (2015). Overexpression of uncoupling protein-2 in cancer: metabolic and heat changes, inhibition and effects on drug resistance. *Inflammopharmacology* 23, 365–369. doi: 10.1007/s10787-015-0250-3
- Pivovarova, N. B., and Andrews, S. B. (2010). Calcium-dependent mitochondrial function and dysfunction in neurons. *FEBS J.* 277, 3622–3636. doi: 10.1111/j.1742-4658.2010.07754.x
- Poliseno, L., Salmena, L., Riccardi, L., Fornari, A., Song, M. S., Hobbs, R. M., et al. (2010). Identification of the miR-106b/25 microRNA cluster as a proto-oncogenic PTEN-targeting intron that cooperates with its host gene MCM7 in transformation. *Sci. Signal* 3:ra29. doi: 10.1126/scisignal.2000594
- Quintanilla, R. A., Tapia, C., and Pérez, M. J. (2017). Possible role of mitochondrial permeability transition pore in the pathogenesis of Huntington disease. *Biochem. Biophys. Res. Commun.* 483, 1078–1083. doi: 10.1016/j.bbrc.2016.09.054

- Rasola, A., Sciacovelli, M., Pantic, B., and Bernardi, P. (2010). Signal transduction to the permeability transition pore. *FEBS Lett.* 584, 1989–1996. doi: 10.1016/j.febslet.2010.02.022
- Razik, M. A., and Cidlowski, J. A. (2002). Molecular interplay between ion channels and the regulation of apoptosis. *Biol. Res.* 35, 203–207.
- Razumilava, N., Bronk, S. F., Smoot, R. L., Fingas, C. D., Werneburg, N. W., Roberts, L. R., et al. (2012). miR-25 targets TNF-related apoptosis inducing ligand (TRAIL) death receptor-4 and promotes apoptosis resistance in cholangiocarcinoma. *Hepatology* 55, 465–475. doi: 10.1002/hep.24698
- Rizzuto, R., De Stefani, D., Raffaello, A., and Mammucari, C. (2012). Mitochondria as sensors and regulators of calcium signalling. *Nat. Rev. Mol. Cell Biol.* 13, 566–578. doi: 10.1038/nrm3412
- Rizzuto, R., Pinton, P., Carrington, W., Fay, F. S., Fogarty, K. E., Lifshitz, L. M., et al. (1998). Close contacts with the endoplasmic reticulum as determinants of mitochondrial Ca²⁺ responses. *Science* 280, 1763–1766. doi: 10.1126/science.280.5370.1763
- Shah, S. S., Lannon, H., Dias, L., Zhang, J. Y., Alper, S. L., Pollak, M. R., et al. (2019). APOL1 kidney risk variants induce cell death via mitochondrial translocation and opening of the mitochondrial permeability transition pore. *J. Am. Soc. Nephrol.* 30, 2355–2368. doi: 10.1681/asn.2019020114
- Shares, B. H., Smith, C. O., Sheu, T. J., Sautchuk, R. Jr., Schilling, K., Shum, L. C., et al. (2020). Inhibition of the mitochondrial permeability transition improves bone fracture repair. *Bone* 137:115391. doi: 10.1016/j.bone.2020.115391
- Shum, L. C., White, N. S., Nadtochiy, S. M., Bentley, K. L., Brookes, P. S., Jonason, J. H., et al. (2016). Cyclophilin D knock-out mice show enhanced resistance to osteoporosis and to metabolic changes observed in aging bone. *PLoS One* 11:e0155709. doi: 10.1371/journal.pone.0155709
- Spikes, T. E., Montgomery, M. G., and Walker, J. E. (2020). Structure of the dimeric ATP synthase from bovine mitochondria. *Proc. Natl. Acad. Sci. U.S.A.* 117, 23519–23526. doi: 10.1073/pnas.2013998117
- Spinelli, J. B., and Haigis, M. C. (2018). The multifaceted contributions of mitochondria to cellular metabolism. *Nat. Cell Biol.* 20, 745–754. doi: 10.1038/s41556-018-0124-1
- Szabo, I., Bock, J., Grassme, H., Soddemann, M., Wilker, B., Lang, F., et al. (2008). Mitochondrial potassium channel Kv1.3 mediates Bax-induced apoptosis in lymphocytes. *Proc. Natl. Acad. Sci. U.S.A.* 105, 14861–14866. doi: 10.1073/pnas.0804236105
- Szabo, I., Bock, J., Jekle, A., Soddemann, M., Adams, C., Lang, F., et al. (2005). A novel potassium channel in lymphocyte mitochondria. *J. Biol. Chem.* 280, 12790–12798. doi: 10.1074/jbc.m413548200
- Szabo, I., Soddemann, M., Leanza, L., Zoratti, M., and Gulbins, E. (2011). Single-point mutations of a lysine residue change function of Bax and Bcl-xL expressed in Bax- and Bak-less mouse embryonic fibroblasts: novel insights into the molecular mechanisms of Bax-induced apoptosis. *Cell Death Differ.* 18, 427–438. doi: 10.1038/cdd.2010.112
- Szabo, I., and Zoratti, M. (1992). The mitochondrial megachannel is the permeability transition pore. *J. Bioenerget. Biomemb.* 24, 111–117. doi: 10.1007/bf00769537
- Szabo, I., and Zoratti, M. (2014). Mitochondrial channels: ion fluxes and more. *Physiol. Rev.* 94, 519–608. doi: 10.1152/physrev.00021.2013
- Szewczyk, A., Bednarczyk, P., Jedraszko, J., Kampa, R. P., Koprowski, P., Krajewska, M., et al. (2018). Mitochondrial potassium channels - an overview. *Postepy Biochem.* 64, 196–212.
- Tanaka, T., Saotome, M., Katoh, H., Satoh, T., Hasan, P., Ohtani, H., et al. (2018). Glycogen synthase kinase-3 β opens mitochondrial permeability transition pore through mitochondrial hexokinase II dissociation. *J. Physiol. Sci.* 68, 865–871. doi: 10.1007/s12576-018-0611-y
- Testai, L., Barrese, V., Soldovieri, M. V., Ambrosino, P., Martelli, A., Vinciguerra, I., et al. (2015). Expression and function of Kv7.4 channels in Rat cardiac mitochondria: possible targets for cardioprotection. *Cardiovascu. Res.* 20:5323.
- Urbani, A., Giorgio, V., Carrer, A., Franchin, C., Arrigoni, G., Jiko, C., et al. (2019). Purified F-ATP synthase forms a Ca(2+)-dependent high-conductance channel matching the mitochondrial permeability transition pore. *Nat. Commun.* 10:4341.
- van Hameren, G., Campbell, G., Deck, M., Berthelot, J., Gautier, B., Quintana, P., et al. (2019). In vivo real-time dynamics of ATP and ROS production in axonal mitochondria show decoupling in mouse models of peripheral neuropathies. *Acta Neuropathol. Commun.* 7:86.
- Wagner, S., De Bortoli, S., Schwarzlander, M., and Szabo, I. (2016). Regulation of mitochondrial calcium in plants versus animals. *J. Exp. Bot.* 67, 3809–3829. doi: 10.1093/jxb/erw100
- Waldeck-Weiermair, M., Gottschalk, B., Madreiter-Sokolowski, C. T., Ramadani-Muja, J., Ziomek, G., Klec, C., et al. (2019). Development and Application of Sub-Mitochondrial Targeted Ca(2+) Biosensors. *Front. Cell. Neurosci.* 13:449. doi: 10.3389/fncel.2019.00449
- Walker, J. E., Carroll, J., and He, J. (2020). Reply to Bernardi: The mitochondrial permeability transition pore and the ATP synthase. *Proc. Natl. Acad. Sci. U.S.A.* 117, 2745–2746. doi: 10.1073/pnas.1921409117
- Ying, Z., Xiang, G., Zheng, L., Tang, H., Duan, L., Lin, X., et al. (2018). Short-Term Mitochondrial Permeability Transition Pore Opening Modulates Histone Lysine Methylation at the Early Phase of Somatic Cell Reprogramming. *Cell Metab.* 28, 935.e5–945.e5.
- Zavodnik, I. B. (2016). [Mitochondria, calcium homeostasis and calcium signaling]. *Biomed. Khim.* 62, 311–317. doi: 10.18097/pbmc20166203311
- Zhang, H., Zuo, Z., Lu, X., Wang, L., Wang, H., and Zhu, Z. (2012). MiR-25 regulates apoptosis by targeting Bim in human ovarian cancer. *Oncol. Rep.* 27, 594–598.
- Zhang, J., Han, Y., Shi, H., Chen, J., Zhang, X., Wang, X., et al. (2020). Swine acute diarrhea syndrome coronavirus-induced apoptosis is caspase- and cyclophilin D- dependent. *Emerg. Microb. Infect.* 9, 439–456. doi: 10.1080/22221751.2020.1722758
- Zoratti, M., and Szabo, I. (1995). The mitochondrial permeability transition. *Biochim. Biophys. Acta* 1241, 139–176.
- Zorov, D. B., Juhaszova, M., and Sollott, S. J. (2014). Mitochondrial reactive oxygen species (ROS) and ROS-induced ROS release. *Physiol. Rev.* 94, 909–950. doi: 10.1152/physrev.00026.2013

Conflict of Interest: The authors declare that the research was conducted in the absence of any commercial or financial relationships that could be construed as a potential conflict of interest.

Copyright © 2021 Urbani, Prosdocimi, Carrer, Checchetto and Szabò. This is an open-access article distributed under the terms of the Creative Commons Attribution License (CC BY). The use, distribution or reproduction in other forums is permitted, provided the original author(s) and the copyright owner(s) are credited and that the original publication in this journal is cited, in accordance with accepted academic practice. No use, distribution or reproduction is permitted which does not comply with these terms.



Cell Death Induction and Protection by Activation of Ubiquitously Expressed Anion/Cation Channels. Part 1: Roles of VSOR/VRAC in Cell Volume Regulation, Release of Double-Edged Signals and Apoptotic/Necrotic Cell Death

OPEN ACCESS

Edited by:

Nu Zhang,
The University of Texas Health
Science Center at San Antonio,
United States

Reviewed by:

Min Zhou,
The Ohio State University,
United States
Guo Li,
Central South University, China

*Correspondence:

Yasunobu Okada
okada@nips.ac.jp

Specialty section:

This article was submitted to
Cell Death and Survival,
a section of the journal
*Frontiers in Cell and Developmental
Biology*

Received: 05 October 2020

Accepted: 15 December 2020

Published: 12 January 2021

Citation:

Okada Y, Sabirov RZ,
Sato-Numata K and Numata T (2021)
Cell Death Induction and Protection
by Activation of Ubiquitously
Expressed Anion/Cation Channels.
Part 1: Roles of VSOR/VRAC in Cell
Volume Regulation, Release
of Double-Edged Signals
and Apoptotic/Necrotic Cell Death.
Front. Cell Dev. Biol. 8:614040.
doi: 10.3389/fcell.2020.614040

Yasunobu Okada^{1,2,3*}, Ravshan Z. Sabirov⁴, Kaori Sato-Numata^{5,6} and
Tomohiro Numata⁶

¹ National Institute for Physiological Sciences, Okazaki, Japan, ² Department of Physiology, School of Medicine, Aichi Medical University, Nagakute, Japan, ³ Department of Physiology, Kyoto Prefectural University of Medicine, Kyoto, Japan,

⁴ Laboratory of Molecular Physiology, Institute of Biophysics and Biochemistry, National University of Uzbekistan, Tashkent, Uzbekistan, ⁵ Japan Society for the Promotion of Science, Tokyo, Japan, ⁶ Department of Physiology, School of Medicine, Fukuoka University, Fukuoka, Japan

Cell volume regulation (CVR) is essential for survival and functions of animal cells. Actually, normotonic cell shrinkage and swelling are coupled to apoptotic and necrotic cell death and thus called the apoptotic volume decrease (AVD) and the necrotic volume increase (NVI), respectively. A number of ubiquitously expressed anion and cation channels are involved not only in CVD but also in cell death induction. This series of review articles address the question how cell death is induced or protected with using ubiquitously expressed ion channels such as swelling-activated anion channels, acid-activated anion channels and several types of TRP cation channels including TRPM2 and TRPM7. The Part 1 focuses on the roles of the volume-sensitive outwardly rectifying anion channels (VSOR), also called the volume-regulated anion channel (VRAC), which is activated by cell swelling or reactive oxygen species (ROS) in a manner dependent on intracellular ATP. First we describe phenotypical properties, the molecular identity, and physical pore dimensions of VSOR/VRAC. Second, we highlight the roles of VSOR/VRAC in the release of organic signaling molecules, such as glutamate, glutathione, ATP and cGAMP, that play roles as double-edged swords in cell survival. Third, we discuss how VSOR/VRAC is involved in CVR and cell volume dysregulation as well as in the induction of or protection from apoptosis, necrosis and regulated necrosis under pathophysiological conditions.

Keywords: cell volume regulation, apoptotic cell death, necrotic cell death, VSOR/VRAC, glutamate release, GSH release, cisplatin resistance, programmed necrosis

INTRODUCTION

For the survival of animal cells, control of their cell volume is essential, since the water permeability of cell membranes is high enough to allow passive water fluxes in response to changes in the extracellular and/or intracellular osmolarity under both physiological and pathological situations (see Books: Okada, 1998; Lang, 2006). Animal cells cope with osmotic cell swelling by the regulatory volume decrease (RVD) and with osmotic cell shrinkage by the regulatory volume increase (RVI) attained by losing KCl and gaining NaCl from intracellular and extracellular solutions, respectively (Lang et al., 1998; Okada, 2004; Hoffmann et al., 2009). Among a large variety of ion channels and transporters, most ubiquitously expressed anion and cation channels ought to predominantly participate in the mechanisms of cell volume regulation (CVR), because this fundamental function is conserved throughout evolution in animal cells irrespective of cell types for cell survival. These ubiquitous volume-regulatory ion channels include swelling-activated anion channels and stretch-activated TRP cation channels as well as cell shrinkage-activated cation channels, that is called the hypertonicity-induced cation channel (HICC) (Wehner et al., 2003b). These volume-regulatory ion channels also play protective roles against cell injury and death caused by osmotic stress. The most ubiquitous swelling-activated, volume-regulatory anion channel is called the volume-sensitive outwardly rectifying anion channel (VSOR) (Okada, 1997), the volume-regulated anion channel (VRAC) (Nilius et al., 1997) or the volume-sensitive organic osmolyte/anion channel (VSOAC) (Strange et al., 1996). Here, we call VSOR/VRAC or simply VSOR.

Dysfunction of CVR leads to cell death. Actually, persistent cell shrinkage and swelling are major hallmarks of apoptotic and necrotic cell death, and called the apoptotic volume decrease (AVD) (Maeno et al., 2000) and the necrotic volume increase (NVI) (Okada et al., 2001), respectively. AVD and NVI are brought about by water fluxes driven by net loss of cellular KCl and net gain of ambient NaCl, respectively. Thus, cell death is initiated by dysfunction or impairments of CVR mechanisms. Common pathological situations are injuries caused by hypoxia or ischemia and that followed by re-oxygenation or reperfusion, and they cause a variety of tissue stress including not only osmotic perturbation but also production of reactive oxygen species (ROS) and acidic overload. ROS are known to activate VSOR, TRPM7 and TRPM2. Extracellular acidification is known to directly activate one type of anion channel which is called the acid-sensitive outwardly rectifying anion channels (ASOR) (Wang et al., 2007) or the proton-activated chloride channel (PAC) (Yang et al., 2019a). Acidity also rapidly augments TRPM7 cation channel activity (Jiang et al., 2005; Numata et al., 2019). Thus, altered activities of VSOR/VRAC and ASOR/PAC anion channels as well as of TRPM2 and TRPM7 cation channels are involved in dysfunction of CVR that eventually leads to cell death. In the present article, we review the roles of VSOR activity (in Part 1), as well as of ASOR/PAC, TRPM2, and TRPM7 activities (in Part 2) in cell death induction and protection.

PHENOTYPIC PORE PROPERTIES AND MOLECULAR IDENTITY OF VSOR/VRAC

Phenotypical Properties of VSOR/VRAC Currents

Among a number of types of mammalian anion channels, VSOR and the maxi-anion channel (Maxi-Cl) are activated by cell swelling and thereafter involved in RVD, thus both being called volume-regulatory anion channels (Okada et al., 2018). The functional expression of VSOR was first discovered in 1988 independently by two groups (Cahalan and Lewis, 1988; Hazama and Okada, 1988). Its phenotypical properties were fully clarified by a large number of groups (Strange et al., 1996; Nilius et al., 1997; Okada, 1997), and can be summarized as volume-sensitive, mildly outward-rectifying, non-hydrolytically ATP-dependent anion channels with exhibiting an intermediate single-channel conductance, low electric-field anion selectivity (of Eisenman's sequence I), sensitivity to intracellular free Mg^{2+} , and inactivation kinetics at large positive potentials (Okada et al., 2019b). VSOR was found to be activated not only by cell swelling but also by ROS independently by three groups (Browe and Baumgarten, 2004; Shimizu et al., 2004; Varela et al., 2004) and by a rise of nano-domain intracellular free Ca^{2+} induced by G protein-coupled receptor (GPCR) stimulation (Akita and Okada, 2011; Akita et al., 2011).

Molecular Identities of VSOR/VRAC Core Components

Since the discovery of VSOR activity in 1988, its molecular entity had not been uncovered for a quarter of a century, despite much efforts of proposing and disproving a number of false-positive candidates including *P*-glycoprotein, p1cln, ClC-3, Best1 and some TMEM16 (ANO) members especially TMEM16F (ANO6), as summarized in recent review articles (Pedersen et al., 2016; Okada et al., 2018, 2019b). At last, through unbiased genome-wide approaches, LRRC8A was recently identified as the core component of human VSOR independently by two groups (Qiu et al., 2014; Voss et al., 2014). This fact was subsequently confirmed to hold for VSOR endogenously expressing in zebrafish (Yamada et al., 2016), mouse (Okada et al., 2017), rat (Elorza-Vidal et al., 2018), and insect (Kern et al., 2019). Furthermore, Jentsch's group elucidated that functional VSOR activity requires LRRC8A together with LRRC8C, LRRC8D and/or LRRC8E (Voss et al., 2014). Sequential co-immunoprecipitation studies evidenced physical interactions between LRRC8A, LRRC8C and LRRC8E (Lutter et al., 2017). In fact, a recent cryo-electron microscope (cryo-EM) study demonstrated the hexameric structure of LRRC8A together with LRRC8C (Deneka et al., 2018). However, it must be noted that there may be some missing component or subcomponent other than LRRC8 members, in light of the following facts. (1) Double overexpression of LRRC8A and LRRC8C/8D/8E never increased VSOR currents over the endogenous level in HEK293 and HCT116 cells (Voss et al., 2014) and HeLa cells (Okada et al., 2017). (2) Overexpression of LRRC8A *plus* LRRC8D/8E in cisplatin-resistant KCP-4 cells, that are largely deficient in

VSOR activity, failed to restore VSOR currents up to the level in its parental cisplatin-sensitive KB cells (Okada et al., 2017). (3) Different cell types with similar LRRC8 expression levels showed differences in VSOR activities (Okada et al., 2017). (4) The activity of channels reconstituted with LRRC8A *plus* LRRC8D/8E was found to be independent of intracellular ATP (Syeda et al., 2016), the fact being at variance with native VSOR activity that is requisitely dependent on intracellular ATP (Jackson et al., 1994; Oiki et al., 1994). (5) Furthermore, the channel reconstituted with purified LRRC8A *plus* LRRC8D/8E was not activated by inflation-induced membrane expansion (Syeda et al., 2016), the fact being contradictory to a known fact that VSOR can be activated by pressure-induced cell inflation (Hagiwara et al., 1992; Doroshenko, 1998; Best and Brown, 2009). In place of LRRC8 members, more recently, TTYH homologs (TTYH1, TTYH2, and TTYH3) were proposed as the VSOR core molecules in mouse astrocytes by Han et al. (2019). Subsequently, TTYH1 and TTYH2 were reported to serve as VSOR, in a manner independent of LRRC8A, in human cancer cells including gastric SNU-601, hepatic HepG2 and colonic LoVo cells by Bae et al. (2019). Our data also showed that hypotonicity-induced VSOR currents were significantly suppressed by siRNA-mediated triple knockdown of TTYH1, TTYH2 and TTYH3 in human cervical HeLa cells (Okada et al., 2020), suggesting an involvement of TTYHs in the regulation or formation of VSOR. However, it must be pointed out that studies with making gene knockout and channel reconstitution of TTYH1, TTYH2, and TTYH3 are still missing to firmly support the essential roles of TTYHs in the VSOR/VRAC channel formation. At moment, we need to know as to whether TTYHs can physically interact with LRRC8s and whether the VSOR activity can be restored by overexpression of TTYHs into cells in which all LRRC8s are knocked out. Also, it must be stressed that it is still not definitely determined whether LRRC8 and/or TTYH form the VSOR pore *per se*, as summarized elsewhere (Okada et al., 2018; Okada, 2019), because drastic alterations in the anion selectivity Eisenman's sequence and/or in the anion/cation permeability ratio have not as yet been shown to be elicited by any charge-modifying, especially charge-reversing, mutations at their putative pore-forming regions.

Physical Dimensions of the VSOR/VRAC Pore

The pore size of native VSOR channel was evaluated by three different methods. First, the cut-off size of the organic anions with limited permeability yielded the radius (R) of 0.37 nm; when the same data were approximated using the excluded area theory with taking frictional forces into account, the value of 0.58 nm was obtained (Nilius et al., 1999; Nilius and Droogmans, 2003). Second, the cross-sectional radius of the VSOR pore was estimated from the experiments with calixarenes, basket-shaped compounds, acting as permeant blockers, and was found to be 0.57–0.71 nm (Droogmans et al., 1998, 1999). Third, a value of 0.63 nm was obtained by the non-electrolyte partitioning method using

non-charged polyethylene glycols (Ternovsky et al., 2004). Thus, based on three different and unrelated methods, it is concluded that the native VSOR pore has a functional radius of 0.6–0.7 nm at the narrowest portion of the ion-conducting pathway.

Cryo-EM studies of the recombinant LRRC8 paralogs combined with single particle analysis generated a series of spectacular 3D-structures of the VSOR channel (Deneka et al., 2018; Kasuya et al., 2018; Kefauver et al., 2018; Kern et al., 2019; Nakamura et al., 2020), which produced pore dimensions along the central axis of the channel, as depicted together with the above functional radii in **Figure 1** (left panel). According to the structure of the mouse LRRC8A homohexamer reported by Deneka et al. (2018), the pore is ~10 nm long but not uniform: it begins with a wide extracellular vestibule with a radius of ~0.8 nm followed by a constriction with $R \sim 0.29$ nm located at about 1.5 nm from the entrance; then the pore widens up to $R \sim 1.6$ nm around the TM region and ends with an intracellular vestibule with a radius of ~0.7 nm. The structure of human homohexameric LRRC8A was found to have a similar extracellular vestibule of ~0.74 nm, but the constriction, the transmembrane (TM) region and the intracellular vestibule were wider with radii of ~0.38, 2.54, and 1.13 nm, respectively (Kasuya et al., 2018). It is plausible that the narrowest constriction part of the pore serves as the selectivity filter, which restricts the passage of ions and osmolytes. The radius of constriction was smallest ($R \sim 0.1$ nm) in the structure reported by Kefauver et al. (2018). It should be noted that the ionic strength conditions and lipid environments significantly affect the packaging of the channel protein generating tighter structures with a narrower pore or more relaxed structures with a wider pore (Deneka et al., 2018; Kasuya et al., 2018; Kefauver et al., 2018; Kern et al., 2019). The largest radius of the constriction part ($R \sim 0.57$ nm), which is close to the functional radius of the native VSOR pore, was reported for the homohexameric channel formed by human LRRC8D (Nakamura et al., 2020). This paralog is known to play an important role in the permeability for charged and non-charged organic osmolytes (Lutter et al., 2017) including Pt-based anti-cancer drugs (Planells-Cases et al., 2015) and antibiotic blasticidin S (Lee et al., 2014). As seen in **Figure 1** (left panel), the radii structurally evaluated by cryo-EM observations are smaller than those functionally estimated by electrophysiological recordings. In this regard, it must be pointed out that the cryo-EM structural radii correspond to homohexamer of LRRC8A or LRRC8D but not the native VSOR-forming heterohexamer of LRRC8A+LRRC8C/D/E. Also, one cannot rule out a possibility that the cryo-EM structure may represent the closed state, but not the open state, of the channel.

Taken together, it appears that the native heterohexameric channel composed of various combinations of LRRC8 paralogs in native lipid environments should have an effective radius of 0.6–0.7 nm in the open state. As depicted in **Figure 1** (right panel), this size would thus allow passage of not only chloride ($R \sim 0.18$ nm) but also of taurine ($R \sim 0.31$ nm), excitatory amino acids such as aspartate ($R \sim 0.34$ nm) and glutamate ($R \sim 0.35$ nm) very freely, and also ATP, ADP and UTP

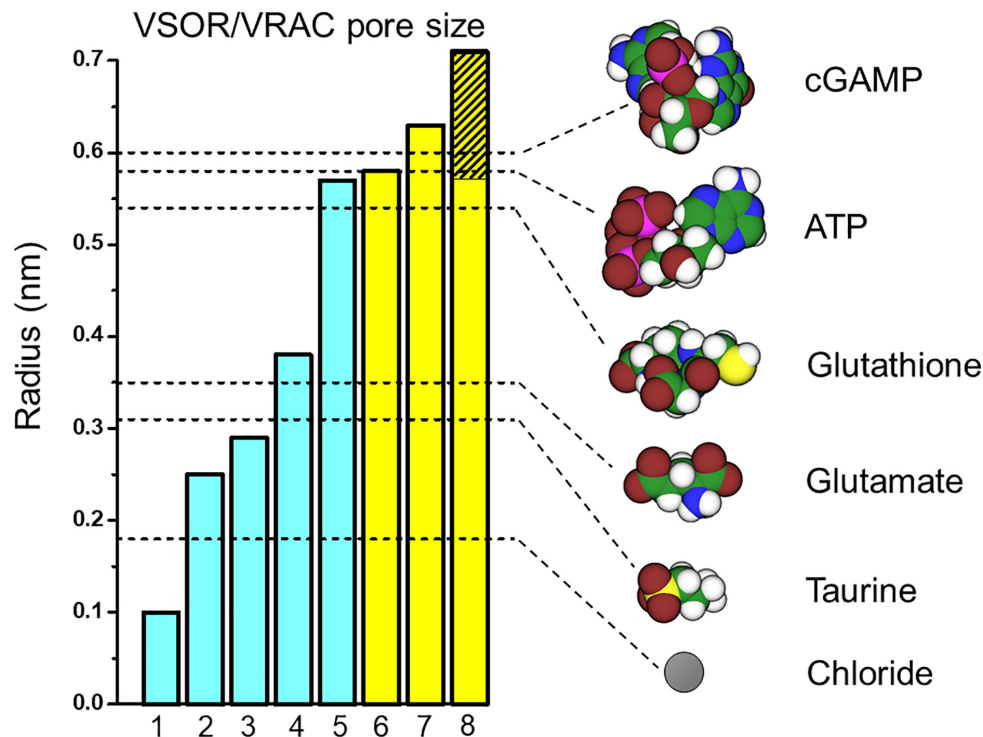


FIGURE 1 | VSOR/VRAC pore size and dimensions of the signaling molecules released via VSOR/VRAC. The pore radii depicted as the bar graphs were taken from: 1 – Kefauver et al., 2018; 2 – Kern et al., 2019; 3 – Deneka et al., 2018; 4 – Kasuya et al., 2018; 5 – Nakamura et al., 2020; 6 – Nilius et al., 1999; Nilius and Droogmans, 2003; 7 – Ternovsky et al., 2004; 8 – Droogmans et al., 1998, 1999. The values for bars #1 and #2 were deduced from the graphs of the pore radius plotted against the distance along the pore axis by the cited authors. Other values are as given by the cited authors. The hatched part of bar #8 indicates lower and upper limits given by the authors. Blue and yellow bars represent the radii structurally evaluated by cryo-EM studies for LRRC8A/D homohexamers and those functionally estimated for the native VSOR channel by electrophysiological studies, respectively. The unhydrated radii of the organic anions (shown as dashed lines) were calculated as a geometric mean of molecular dimensions produced using Molecular Modeling Pro computer software (Norgwyn Montgomery Software Inc., North Wales, PA, United States). Values for ATP and glutamate were reported previously (Sabirov and Okada, 2005). Color coding: C, green; H, white; O, red; N, blue; P, purple; S, yellow; Cl, gray.

($R \sim 0.53\text{--}0.61$ nm) in a very limited manner (for more osmolytes see Table 2 in Sabirov and Okada, 2005).

ROLES OF VSOR/VRAC IN RELEASE OF ORGANIC SIGNALS FOR CELL DEATH INDUCTION/PROTECTION

Role of VSOR/VRAC in Release of Excitotoxic Glutamate

Glutamate is the principal and most important excitatory neurotransmitter in the vertebrate nervous system under physiological conditions (Meldrum, 2000). Glutamate is released from neurons by the vesicular exocytosis mechanism into the synaptic cleft, and then is cleared by a Na^+ -dependent reuptake mechanism, which keeps the extracellular glutamate at concentrations below the activation threshold for glutamate receptors. The extracellular space normally occupies about one quarter of the total brain volume, but it decreases down to 12–17% during over-excitation by repetitive stimulation or even down to $\sim 5\%$ upon ischemia by redistribution of water

between the extracellular and intracellular space leading to swelling of neurons and astrocytes (Nicholson, 2005; Syková, 2004). Brain edema also occurs as a result of stroke, trauma, brain tumors, systemic viral and bacterial infections (Kimelberg, 2004, 2005; Kimelberg et al., 2004). Swollen neurons and astroglia massively release glutamate, which in turn induces excitotoxicity – neuronal death caused by overexcitation of glutamatergic receptors (Kimelberg et al., 1990; Strange et al., 1996; Liu et al., 2006, 2009; Akita and Okada, 2014; Hyzinski-García et al., 2014; Planells-Cases et al., 2015; Lutter et al., 2017; Schober et al., 2017; Okada et al., 2019a). Thus, glutamate exhibits double-edged functions in the brain.

The putative pathways for glutamate release from swollen cells include: (i) Ca^{2+} -dependent vesicular exocytosis, (ii) Na^+ -dependent glutamate transporters functioning in a reverse mode, and (iii) ion channel-mediated conductive release through gap junction hemichannels and/or chloride channels including VSOR and the maxi-anion channel (Phillis and O'Regan, 2003; Evanko et al., 2004; Parpura et al., 2004; Mongin, 2007, 2016; Sabirov et al., 2016; Osei-Owusu et al., 2018; Wilson and Mongin, 2018; Chen et al., 2019; König and Stauber, 2019; Okada et al., 2019a,b; Strange et al., 2019).

First evidence for conductance of VSOR to amino acids such as glutamate was provided by Banderali and Roy (1992). The effective radius of the native VSOR is sufficient to pass glutamate and aspartate (Sabirov and Okada, 2005) (**Figure 1**). Indeed, the astrocytic channel was permeable to glutamate (Glu) with $P_{Glu}/P_{Cl} = 0.15$ (Liu et al., 2006), close to $P_{Glu}/P_{Cl} = 0.14$ found in C6 glioma cells (Jackson et al., 1994). These values are within the range of $P_{Glu}/P_{Cl} \sim 0.06$ – 0.2 reported for many other cells (Banderali and Roy, 1992; Chan et al., 1994; Roy and Banderali, 1994; Roy, 1995; Arreola et al., 1996; Basavappa et al., 1996; Boese et al., 1996; Levitan and Garber, 1998; Schmid et al., 1998; Carpaneto et al., 1999; Sakai et al., 1999; Schlichter et al., 2011). A somewhat higher glutamate permeability was recently reported for cultured primary astrocytes (~ 0.3) (Yang et al., 2019b).

Pharmacological studies using VSOR blockers indicated that osmotic swelling or oxygen-glucose deprivation induces massive VSOR-mediated release of glutamate (Liu et al., 2006, 2009; Rudkouskaya et al., 2008; Hyzinski-García et al., 2011; Bowens et al., 2013) and aspartate (Kimelberg et al., 1990; Mongin et al., 1999; Mongin and Kimelberg, 2002; Haskew-Layton et al., 2005, 2008; Mongin and Kimelberg, 2005; Abdullaev et al., 2006; Bowens et al., 2013; Hyzinski-García et al., 2014) from primary cultured astrocytes *in vitro*. Stimulation with hypotonic solution or zymosan was found to induce release of excitatory amino acids from rat microglia in a manner sensitive to VSOR blockers including the most selective blocker DCPIB (Harrigan et al., 2008). An inflammatory initiator bradykinin, which is also released upon brain ischemia, triggers ROS production and thus induces VSOR activation in astrocytes, thereby releasing glutamate therefrom (Haskew-Layton et al., 2005; Liu et al., 2009). Osmotic cell swelling and cell swelling associated with spreading depression also caused massive release of excitatory amino acids from brain slices in a manner sensitive to VSOR blockers (Basarsky et al., 1999; Bothwell et al., 2001). Release of excitatory amino acids, which is inhibited by VSOR blockers, was observed *in vivo* in animal models of global and focal ischemia (Phillis et al., 1997, 1998; Seki et al., 1999; Kimelberg et al., 2000, 2003; Feustel et al., 2004; Zhou J.J. et al., 2020). VSOR blockers protected neurons from delayed neuronal death after transient forebrain ischemia (Abdullaev et al., 2006; Inoue et al., 2007).

After a hetero-multimer of LRRC8 family proteins was identified as the core component of VSOR, a causative relationship between VSOR and swelling-induced release of excitatory amino acids was verified by siRNA-mediated LRRC8A knockdown (Hyzinski-García et al., 2014; Sørensen et al., 2014) and by LRRC8A knockout (Lutter et al., 2017; Yang et al., 2019b) and also by LRRC8D knockout (Lutter et al., 2017) and its knockdown (Schober et al., 2017).

It should be noted that VSOR is not the only anion channel contributing to the glutamate release. Involvements of at least two different pathways in osmolyte release were suggested based on their time courses, Ca^{2+} dependence, and pharmacological profiles (Mongin et al., 1999; Franco et al., 2001; Mongin and Kimelberg, 2002; Pasantes-Morales et al., 2002; Netti et al., 2018). Astrocytes express high levels of the glutamate-permeable ($P_{Glu}/P_{Cl} = 0.21$) maxi-anion channel which accounts for about half of the hypotonicity-induced and one third of

the ischemia-induced glutamate release (Liu et al., 2006). Note that this channel does not contribute to the bradykinin-induced glutamate release, which is solely mediated by VSOR activated by ROS and a Ca^{2+} nanodomain-related mechanism in astrocytes (Liu et al., 2009; Akita and Okada, 2011, 2014).

Role of VSOR/VRAC in Release of Natural Antioxidant Glutathione

The tripeptide glutathione (γ -L-glutamyl-L-cysteinylglycine: GSH) is the most prevalent and ubiquitous constituent of cytosol and is involved in many cellular processes such as antioxidant defense, drug detoxification, cell signaling, cell metabolism and proliferation (Meister, 1995; Hammond et al., 2001; Wu et al., 2004). Over 98% of GSH inside the cells exists in its reduced monomeric form at the concentrations of 1–10 mM depending on cell types (Meister and Anderson, 1983; Meister, 1995). GSH is synthesized inside the cells and degraded exclusively outside in the process termed γ -glutamyl cycle. Extracellularly, GSH exists at micromolar levels and protects tissues and cells from oxidative stress: the lung epithelium upon intensive breathing, heart and brain cells during ischemia-reperfusion. Transmembrane delivery of GSH is an important step in the γ -glutamyl cycle; it is performed through the activity of transporters, such as ABCC/MRP (Minich et al., 2006; Ballatori et al., 2009), SLCO/OATP family (Briz et al., 2006; Franco and Cidrowski, 2006), and SLC22A/OAT group transporters (Garcia et al., 2011). Since the GSH molecule bears one net negative charge, its release is caused by activation of conductive pathways, such as CFTR (Linsdell and Hanrahan, 1998; l'Hoste et al., 2010) with a functional pore radius of ~ 0.7 nm (Krasilnikov et al., 2011) and gap junction hemichannel (Tong et al., 2015). GSH efflux is known to be a prerequisite to apoptosis induction (Ghibelli et al., 1998; Franco and Cidrowski, 2006; Circu et al., 2009). Thus, GSH release exhibits double-edged actions by playing an anti-oxidant cell-protective role on the extracellular side but a cell death-inducing role on the intracellular side.

The radius of GSH molecule (0.52–0.56 nm) (Sabirov et al., 2013) is slightly less than the effective VSOR pore size (**Figure 1**, right panel), and, therefore, it is expected that this channel could serve as a pathway for GSH release. Immature thymic lymphocytes exhibit robust RVD ability upon hypotonic stimulation and express high levels of VSOR activity (Kurbannazarova et al., 2003, 2011). As expected, VSOR in rat thymocytes was permeable to this anionic tripeptide with the permeability ratio P_{GSH}/P_{Cl} of ~ 0.1 for outward (efflux) and 0.32 for inward (influx) directions, and this permeability was sufficient to provide the observed GSH release rate of ~ 6 attomol/cell/min, which occurred predominantly by a diffusion mechanism and in a DCPIB-sensitive manner (Sabirov et al., 2013). Kidney epithelial cells, HEK293 and HK-2, were shown to express GSH-conductive VSOR with $P_{GSH}/P_{Cl} \sim 0.1$ (efflux) and exhibited massive swelling-induced GSH release, which was inhibited by DCPIB and not observed LRRC8A-knockout HEK293 cells (Friard et al., 2019). The VSOR activation and associated GSH release were observed in HK-2 cells under isotonic conditions upon exposure to the pleiotropic growth

factor TGF β 1 and was essential for the epithelial-to-mesenchymal transition (Friard et al., 2019).

Role of VSOR/VRAC in ATP Release

Release of adenosine triphosphate (ATP) is a key event in powerful purinergic signaling in most animal tissues (Burnstock, 2012). Released ATP facilitates RVD via stimulation of P2Y receptors (Dezaki et al., 2000; Braunstein et al., 2001; Varela et al., 2010; Islam et al., 2012; Espelt et al., 2013). ATP and glutamate are two major gliotransmitters, which not only modulate synaptic transmission but also protect and repair neuronal tissues after damage. In the heart, extracellular ATP is protective in ischemia-reperfusion damage (Ninomiya et al., 2002; Wee et al., 2007; Burnstock and Pelleg, 2015). It is also known to be degraded by ecto-ATPases to adenosine, which is, in turn, a well-established cardio-protector (Burnstock and Pelleg, 2015). Released ATP produces not only beneficial effects but also detrimental effects depending on cell types and situations. For example, ATP is known to act as a danger signal in a variety of neurological diseases (Franke et al., 2012), brain trauma, hypoxia/ischemia and epilepsy-associated seizures (Rodrigues et al., 2015), and inflammation responses activating apoptosis and autophagy in oxidative conditions (Linden et al., 2019).

ATP is an anion bearing 2–4 negative charges depending on binding to Mg²⁺ and protonation (see Table 1 in Sabirov and Okada, 2005). Its calculated effective radius (0.56–0.61 nm; see Table 2 in Sabirov and Okada, 2005) is compatible with the possible conductive transport via VSOR (Figure 1). Consistent with this possibility, a voltage-dependent open-channel blockage of VSOR by ATP added from the extracellular side (Jackson and Strange, 1995; Tsumura et al., 1996) was found to be relieved at large positive voltages due to translocation of the blocker to the opposite side of the membrane by Hisadome et al. (2002) in accord with the permeating blocker mechanism (Droogmans et al., 1998, 1999). VSOR inhibitors glibenclamide, verapamil, tamoxifen, and fluoxetine suppressed the hypotonicity-induced ATP release in these cells, suggesting that this pathway is used by the nucleotide to exit the cells. More recently, hypotonicity-induced ATP release from HEK293 cells and primary cerebellar granule neurons was observed to be sensitive to treatment with DCPIB and shRNA for LRRC8A, suggesting an involvement of VSOR in the ATP release pathway (Dunn et al., 2020).

Cultured neonatal cardiac myocytes (Dutta et al., 2004) and myocytes isolated from mature left ventricles (Dutta et al., 2008) responded with ATP release to osmotic stress and chemical ischemia. However, this process had a pharmacological profile inconsistent with the role of VSOR but closer to the profile of the maxi-anion channel (Sabirov et al., 2016; Okada et al., 2019a,b). A similar conclusion was made for the ATP release from primary cultured astrocytes (Liu et al., 2008a,b) and from mammary C127 cells (Sabirov et al., 2001). There remains a possibility, thus, that contribution of the channel to the net ATP release is different in different cell types depending on the paralog combinations, since conductive properties of VSOR depends on subunit composition of the LRRC8 hexamers (Syeda et al., 2016). Also, it is feasible that LRRC8 may somehow be involved in regulation of other ATP-releasing pathways, because LRRC8A is

known to interact with other plasmalemmal proteins (Benedetto et al., 2016; Choi et al., 2016; Fujii et al., 2018) often via their LRR motifs (Kobe and Kajava, 2001).

Roles of VSOR/VRAC in Release of Other Signaling Molecules

Taurine (2-aminoethanesulfonic acid) is one of the most abundant intracellular osmolytes. The cytosolic concentration of taurine in the brain neurons and astrocytes is usually 10–20 mM (Walz and Allen, 1987) and may reach as high as 50 mM (Voaden et al., 1977; Huxtable, 1982), and its release has long been considered as one of the key molecular events in volume regulation (Oja and Saransaari, 2017). Taurine with its radius of ~ 0.31 nm is well-suited for transport via VSOR (Figure 1), and the process of osmosensitive taurine release is one of the well-documented functions of the LRRC8/VSOR (Jentsch et al., 2016; König and Stauber, 2019; Okada et al., 2019b). Both LRRC8A and LRRC8D are known to be required for hypotonicity-induced taurine release (Planells-Cases et al., 2015; Lutter et al., 2017). Once released, taurine acts on glycine and GABA receptors as a co-agonist, resulting in reduction of neuronal firing and protection from over-excitation (Ye et al., 2013; Oja and Saransaari, 2017).

GABA (gamma-aminobutyric acid) is also released from HEK293 cells via VSOR in an LRRC8D- and LRRC8E-dependent manner (Lutter et al., 2017). LRRC8A deletion and silencing abolished GABA release from mouse and human pancreatic β cells (Menegaz et al., 2019). Since GABA has strong protective and regenerative effects on β cells (Fiorina, 2013), it is likely that an impairment of VSOR-mediated GABA release may participate in etiology of diabetes mellitus. Actually, Type-1 and -2 diabetic islets of human patients were shown to exhibit disrupted secretion of GABA (Menegaz et al., 2019).

Cyclic guanosine monophosphate-adenosine monophosphate (2'3'cGMP-AMP or cGAMP) is synthesized by an enzyme cyclic cGAMP synthase, which senses double-stranded DNA in infected and malignant cells; it is then transferred to the neighboring cells either by gap junctions or by a release-uptake mechanism to trigger interferon production as the cell/host defense against DNA viral infection and other malignancies. It was recently demonstrated that the cGAMP release occurs via LRRC8A/LRRC8E-containing VSOR (Zhou C. et al., 2020). The calculated size of cGAMP ($R \sim 0.6$ nm) is compatible with the size of VSOR pore (Figure 1). Thus, it is likely that VSOR is involved in the cell/host defense against DNA virus by releasing cGAMP.

ROLES OF VSOR/VRAC IN CELL VOLUME REGULATION AND CELL DEATH INDUCTION/PROTECTION

Cell Volume Regulation in Mammalian Cells

Cell volume regulation is physiologically essential for the cell survival with exhibiting normal functions, and an optimal cell

size is likely to be prerequisite to a particular cell's function. CVR dysfunction is also pathophysiologically important, because sizable changes in the plasma osmolarity are known to often be coupled to a variety of diseases and iatrogenic outcomes (see Table 1 in Okada et al., 2019a). Even under physiological normotonic conditions, the volume of cells is subjected to alterations because of steady-state physicochemical osmotic load and of non-steady state physiological cell activity-dependent fluctuations in intracellular osmolarity (Okada, 2004). The former physicochemical load is caused by the intracellular presence of large numbers of polyvalently anionic macromolecules (X^{n-}) which are membrane-impermeable (Figure 2A). Such fixed negative charges attract membrane-permeable inorganic cations (C^+) to the cytosol, and then the cation entry should drive the entry of membrane-permeable inorganic anions (A^-) due to the electroneutral restraint. However, the inorganic anion entry should be resisted by fixed macromolecular anions by electrostatic repulsion. The resultant equilibrium, called the Gibbs-Donnan equilibrium, brings about increased intracellular osmolarity under normotonic extracellular conditions. This situation can be mathematically expressed as follows, on the basis of Gibbs-Donnan equation: $(RT/F) \ln ([C^+]_i/[C^+]_o) = (RT/F) \ln ([A^-]_o/[A^-]_i)$ where i and o stand for the intracellular and extracellular side, respectively. This equation can be transformed to $[C^+]_i \times [A^-]_i = [A^-]_o^2$ because of $[A^-]_o = [C^+]_o$. Thus, $[C^+]_i + [A^-]_i > [C^+]_o + [A^-]_o$, because $a + b > 2c$ when $a \times b = c^2$ in general. Coping with such oncotic osmotic pressure, steady-state volume regulation is attained by the pump-leak balance (P-LB) mechanism (Tosteson and Hoffman, 1960), in which net Na^+ extrusion is persistently produced by active operation of Na^+ - K^+ pump with simultaneous operation of K^+ channels for recycling of K^+ . Electrogenic operation of Na^+ - K^+ pump and electrogenic K^+ channel opening produce a negative membrane potential, thereby driving the passive extrusion of intracellular Cl^- through some anion channels (Figure 2A, left panel). The resultant reduction of intracellular Cl^- concentration compensates for the existence of polyvalently anionic macromolecules. In addition to the steady-state oncotic load, cell activities themselves produce non-steady state osmotic load as above stated. Cell volume changes are thus induced by fluctuations of the cellular osmolarity caused by fundamental physiological cell activities such as transport and metabolism of biological substances (see Table 1 in Okada, 2004). Thus, cells need to quickly readjust their volume, in a non-stationary manner, through volume-regulatory transports of osmolyte and water. Under such anisotonic conditions, animal cells cope with osmotic cell swelling and shrinkage by RVD and RVI mechanisms, respectively. The RVD and RVI events are attained by water efflux and influx driven by the exit of KCl and entry of $NaCl$, respectively. A variety of volume-regulatory KCl and $NaCl$ transport pathways including ion channels and transporters for both symport and antiport have been listed to be involved in CVR mechanisms in the early 1980s (Grinstein et al., 1984; Hoffmann et al., 1984; Sarkadi et al., 1984a; Lauf, 1985).

Role of VSOR/VRAC in RVD

Conductive K^+ and Cl^- pathways have been suggested to play predominant roles in RVD mechanisms in animal cells by measuring cell volume changes and ionic fluxes in the 1980s (Grinstein et al., 1982, 1983; Sarkadi et al., 1984b, 1985; Hoffmann et al., 1986; Abdullaev et al., 2006). Direct electrophysiological evidence for parallel activation of K^+ and Cl^- channels was first provided in 1988 in human epithelial cells by applying two-microelectrode voltage/current-clamp techniques (Hazama and Okada, 1988). A large variety of K^+ channels preinstalled in the plasma membrane are known to serve as volume-regulatory K^+ channels in most mammalian cells (Wehner et al., 2003a; Hoffmann et al., 2009). The volume-regulatory Cl^- channel activated by osmotic cell swelling was thereafter well characterized by applying patch-clamp techniques and is called VSOR or VRAC (Nilius et al., 1997; Okada, 1997). The fact that VSOR is prerequisite involved in RVD was shown by observations of RVD inhibition by VSOR blockers in a wide variety of cell types (Hazama and Okada, 1988; Kubo and Okada, 1992; Chan et al., 1994; Fatherazi et al., 1994; Robson and Hunter, 1994; Gschwentner et al., 1995a,b; Nilius et al., 1995; Best et al., 1996; Gosling et al., 1996; Shen et al., 1996; Zhang and Jacob, 1996; Leaney et al., 1997; Pasantes-Morales et al., 1997; Bond et al., 1998; Patel et al., 1998; Walker et al., 1999; Mitchell et al., 2002; Al-Nakkash et al., 2004; Parkerson and Sontheimer, 2004; Inoue et al., 2005; Ducharme et al., 2007; Okumura et al., 2009; Chen et al., 2010; Inoue et al., 2010; Cao et al., 2011; Sato et al., 2011; Ponce et al., 2012; Hernández-Benítez et al., 2014; Friard et al., 2017; Trothe et al., 2018). Molecular evidence for the involvement of VSOR in RVD was recently provided by observing inhibition of RVD by LRRC8A knockdown in human HeLa cells (Qiu et al., 2014) and rat astrocytes (Formaggio et al., 2019) as well as by LRRC8A knockout in human HEK293 cells (Voss et al., 2014) and keratinocytes (Trothe et al., 2018). Thus, it is now established that VSOR activity is essentially involved in RVD by cooperating with the activity of K^+ channels (Figure 2B, left panel).

Roles of VSOR/VRAC in Apoptosis Induction and Protection

Apoptosis is a physiological type of cell death, by which unnecessary or damaged cells are eliminated, and is classified into two types. One is the intrinsic apoptosis, which is mediated by mitochondria and induced by growth factor withdrawal, oxidative stress, ER stress or DNA damage, and another is the extrinsic apoptosis, which is mediated by stimulation of death receptors such as Fas, TNFR1 and TRAILR1~4 (Sauler et al., 2019). Normotonic cell shrinkage is a major hallmark of apoptotic cell death (Wyllie et al., 1980) and was termed AVD (Maeno et al., 2000). The AVD induction preceded cytochrome *c* release, caspase-3 activation, DNA laddering and cell death, and all these apoptotic events were prevented by blocking K^+ and Cl^- channels (Maeno et al., 2000). These findings were also reproduced in the process of Fas-induced apoptosis not only in HeLa cells but also lymphoblastoid SKW6.4

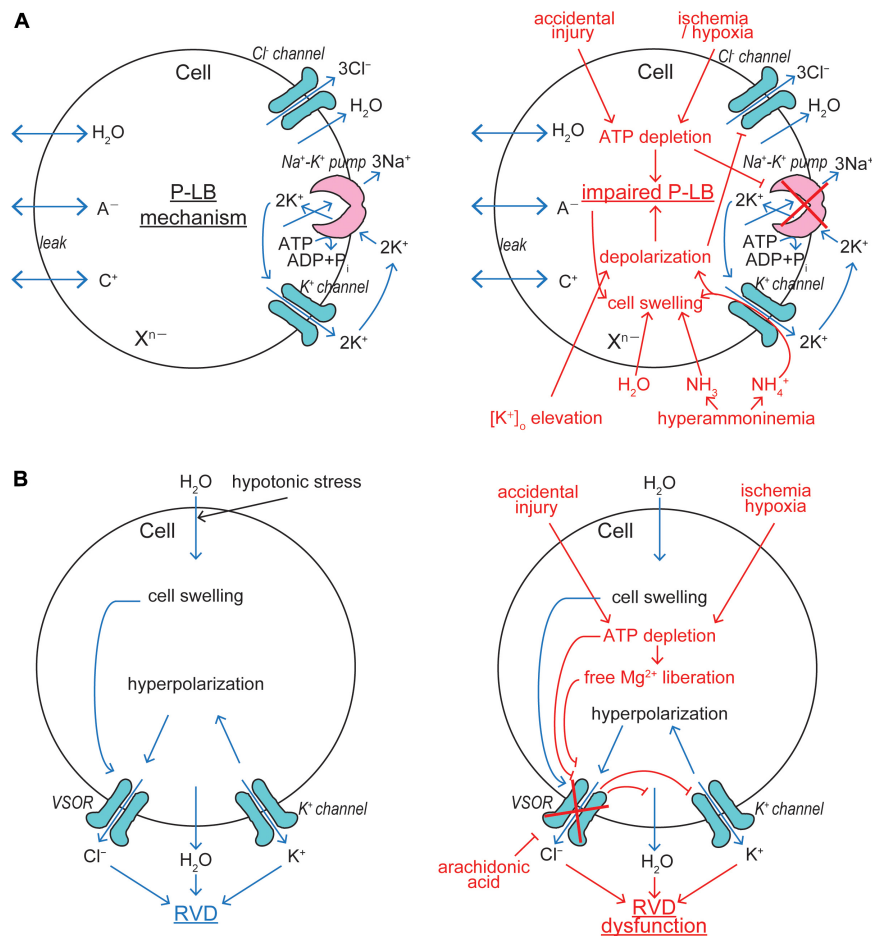


FIGURE 2 | VSOR/VRAC involvements in cell volume regulation/dysregulation. **(A)** The pump-leak balance (P-LB) mechanism coping with steady-state oncotic cell swelling (left panel) and its dysfunction leading to NVI (right panel). The Cl^- channel involved in this mechanism is not identified as yet. **(B)** The RVD mechanism coping with non-steady state osmotic cell swelling (left panel) and its dysfunction leading to necrosis (right panel). VSOR plays a key role in this mechanism by sensing cell swelling (See the text for details).

cells (Maeno et al., 2012). Since SKW6.4 cells undergo Fas-induced apoptosis without involving mitochondria (Eguchi et al., 1999), we concluded that the AVD induction is an early event independent of the mitochondrial apoptotic signaling pathway (Maeno et al., 2012). In addition, the AVD induction in HeLa cells treated with an intrinsic apoptosis inducer, staurosporine (STS), was found to precede activation of caspase-8 and caspase-9, and overexpression of Bcl-2 failed to inhibit the STS-induced AVD in mouse B lymphoma WEHI-231 cells (Maeno et al., 2012). Also, the AVD induction occurred earlier than apoptotic activation of MAP kinase (Hasegawa et al., 2012). These facts indicate that the AVD induction is an early event independent of activation of initiator caspases and MAP kinases. However, the AVD event further proceeds after activation of caspase-3, as clearly demonstrated by parallel observations of the time courses of AVD and caspase-3 activation (Maeno et al., 2012) (also see Figure 4 in Okada et al., 2019a). Thus, the AVD process is divided by the early phase cell shrinkage independent of caspase activation but dependent on K^+ and Cl^- channels and the late-phase shrinkage

dependent on caspase activation. We also demonstrated that apoptotic cells failed to exhibit RVI, and therefore persistence of apoptotic cell shrinkage requires not only AVD induction but also RVI dysfunction (Maeno et al., 2006b). Furthermore, it must be noted that persistent osmotic cell shrinkage experimentally induced *per se* causes induction of apoptotic cell death (Maeno et al., 2006a; Nukui et al., 2006). Taken together, it appears that AVD is the early prerequisite event, which triggers the following executive biochemical processes, for apoptotic cell death.

Multiple types of K^+ channels serve as the AVD-inducing K^+ release pathway depending on cell types (Burg et al., 2006). On the other hand, we identified, for the first time, that VSOR is responsible for the AVD-inducing Cl^- channel in HeLa cells under apoptotic stimulation with STS, Fas ligand (FasL), $\text{TNF}\alpha$ +CHX, and ROS directly by patch-clamping (Shimizu et al., 2004). It is noted that increased expression of LRRC8A was recently found to be coupled to FasL-induced apoptosis in smooth muscle cells (Kenagy et al., 2011). Also, caspase activation induced by exposure to STS was found to be strongly

reduced in HCT116 cells in which LRRC8A or all LRRC8 genes were disrupted (Planells-Cases et al., 2015). Opening of VSOR channels leads to Cl^- efflux driven by hyperpolarization induced by K^+ channel activation (Figure 3A). Furthermore, we showed the involvement of VSOR in induction of AVD and apoptosis in cardiac myocytes stimulated with STS (Takahashi et al., 2005; Tanabe et al., 2005; Okada et al., 2006) and ROS (Wang et al., 2005). Also, evidence for the involvement of VSOR in ischemia-reperfusion-induced apoptosis was provided in cardiac myocytes (Wang et al., 2005) and for that in delayed neuronal death (DND) of CA1 pyramidal neurons in the hippocampus *in vivo* (Inoue et al., 2007), which is largely due to apoptosis with exhibiting AVD (Okada et al., 2019a) and occurs several days after starting reperfusion following transient forebrain ischemia. Neuronal LRRC8A was judged to contribute to ischemia-induced brain injury, because middle cerebral artery occlusion induced upregulation of LRRC8A expression and augmentation of VSOR currents in hippocampal CA1 neurons derived from control mice but never in those from LRRC8A-knockout mice (Zhou J.J. et al., 2020). Actually, VSOR was found to be involved in induction of AVD and apoptosis in many other cell types by other laboratories (Souktani et al., 2000; Porcelli et al., 2003; d'Anglemont de Tassigny et al., 2004; Liu et al., 2008a, 2013; He et al., 2010; l'Hoste et al., 2010; Shen et al., 2014a,b; Shimizu et al., 2015; Yang et al., 2015; Kumagai et al., 2016; Wang et al., 2017). Thus, it is concluded that VSOR represents the AVD-inducing Cl^- channel independent of cell types and apoptotic stimuli.

Cellular GSH depletion or decreased GSH/GSSH (glutathione-disulfide) ratio is known to be a common early event in apoptotic cell death induced by death receptor activation, mitochondrial apoptotic signaling and oxidative stress (Circu and Aw, 2008). For example, GSH depletion sensitizes to $\text{TNF}\alpha$ -induced apoptosis in hepatocytes (Matsumaru et al., 2003). GSH depletion and post-translational modifications of proteins through glutathionylation (protein-SSG formation) are critical regulators of apoptosis (Franco and Cidlowski, 2009). Actually, GSH efflux leading to its depletion was shown to be a prerequisite to apoptosis induction (Ghibelli et al., 1998; Franco and Cidlowski, 2006; Circu et al., 2009). The candidates for GSH efflux pathways so far reported were the multidrug resistant protein (MRP), the organic anion transporting polypeptide (OATP), and CFTR (Circu and Aw, 2012). Our study, as noted above, demonstrated that VSOR can serve as a pathway for GSH release (Sabirov et al., 2013). Thus, VSOR activity is likely to be doubly involved in apoptosis induction first by inducing AVD and second by releasing antioxidant GSH (Figure 3A).

The platinum-based drug cisplatin (CDDP) is a widely used anti-cancer drug, which induces apoptotic death in cancer cells after invading the cells. We demonstrated that VSOR activity is involved in induction of AVD and apoptosis in human cancer KB cells stimulated with cisplatin (Ise et al., 2005). In agreement with this observation, LRRC8A expression was found to be increased in human cancer A549 cells exposed to cisplatin (Thorsteinsdottir et al., 2016). Overexpression of LRRC8A was also observed to augment apoptosis induced by another anti-cancer drug, temozolomide, in glioma cells (Yang et al., 2019). Furthermore, cisplatin-induced apoptosis in human HCT116

cells was prevented by gene knockout of LRRC8A, LRRC8D and all members of LRRC8 (Planells-Cases et al., 2015). CDDP is not much lipid-soluble but largely water-soluble (see Figure 5 in Okada et al., 2019a), and therefore its entry needs to be mediated by some channels or transporters. Recently, the cisplatin entry pathway was demonstrated to be provided by the VSOR channel composed of both LRRC8A and LRRC8D (Planells-Cases et al., 2015). In fact, the VSOR pore size was found to be large enough to be permeated by CDDP (see Figure 5 in Okada et al., 2019a).

The acquisition of resistance to cisplatin by cancer cells is the major limitation for cancer chemotherapy with cisplatin. Our study (Lee et al., 2007) demonstrated, for the first time, that protection from cisplatin-induced apoptosis, called cisplatin resistance, is coupled to downregulation of VSOR channel activity in a cisplatin-resistant cancer cell line, KCP-4, which is derived from cisplatin-sensitive parental KB cells (Fujii et al., 1994), suggesting VSOR is an essential factor in cisplatin sensitivity and resistance of the cancer cells. This inference was proven by the observations that cisplatin sensitivity of KCP-4 cells was restored when the VSOR activity was restored by treatment of two different histone deacetylase (HDAC) inhibitors (Lee et al., 2007; Shimizu et al., 2008). An essential role of VSOR in anti-cancer drug resistance was thereafter shown in numbers of other cell types (Poulsen et al., 2010; Min et al., 2011; Yang et al., 2015). This conclusion was molecularly confirmed by recent observations that cisplatin resistance is correlated with reduced expression of LRRC8A in human cancer cells (Planells-Cases et al., 2015; Sørensen et al., 2016a,b; Thorsteinsdottir et al., 2016). Also, temozolomide resistance was found to be associated with downregulation of LRRC8A in glioma cells (Yang et al., 2019). In contrast, cisplatin resistance in KCP-4 cells was recently found to be coupled to VSOR dysfunction due to disruption of actin filaments but not due to decreased expression of LRRC8A (Shimizu et al., 2020). Taken together, it is clear that VSOR is involved in AVD induction and CDDP uptake and that downregulation of VSOR activity causes cisplatin resistance in cancer cells by reducing both AVD-inducing and cisplatin-permeating activities of VSOR (Figure 3A).

Roles of VSOR/VRAC in Necrosis Induction and Protection

Necrosis is induced by a variety of insults and starts with normotonic cell swelling, called NVI (Okada et al., 2001). Persistence of necrotic cell swelling requires not only NVI induction but also RVD dysfunction (Okada et al., 2004). Necrosis is classified into accidental necrosis, which is induced by injury, ischemia/hypoxia, DNA strand break, hyperammonemia, acidosis, lactic acidosis and excitotoxicity, and programmed or regulated necrosis, including necroptosis, pyroptosis and ferroptosis, which is induced by lipopolysaccharide, viral infection, Toll-like receptor activation, and TNF receptor activation in the absence of caspase-8 activity.

Intracellular ATP depletion by $\geq 80\%$ is a characteristic of necrosis (Simard et al., 2012). This is in contrast to the fact that apoptosis requires ATP generation and is associated with a rise of the intracellular ATP level (Zamaraeva et al., 2005, 2007).

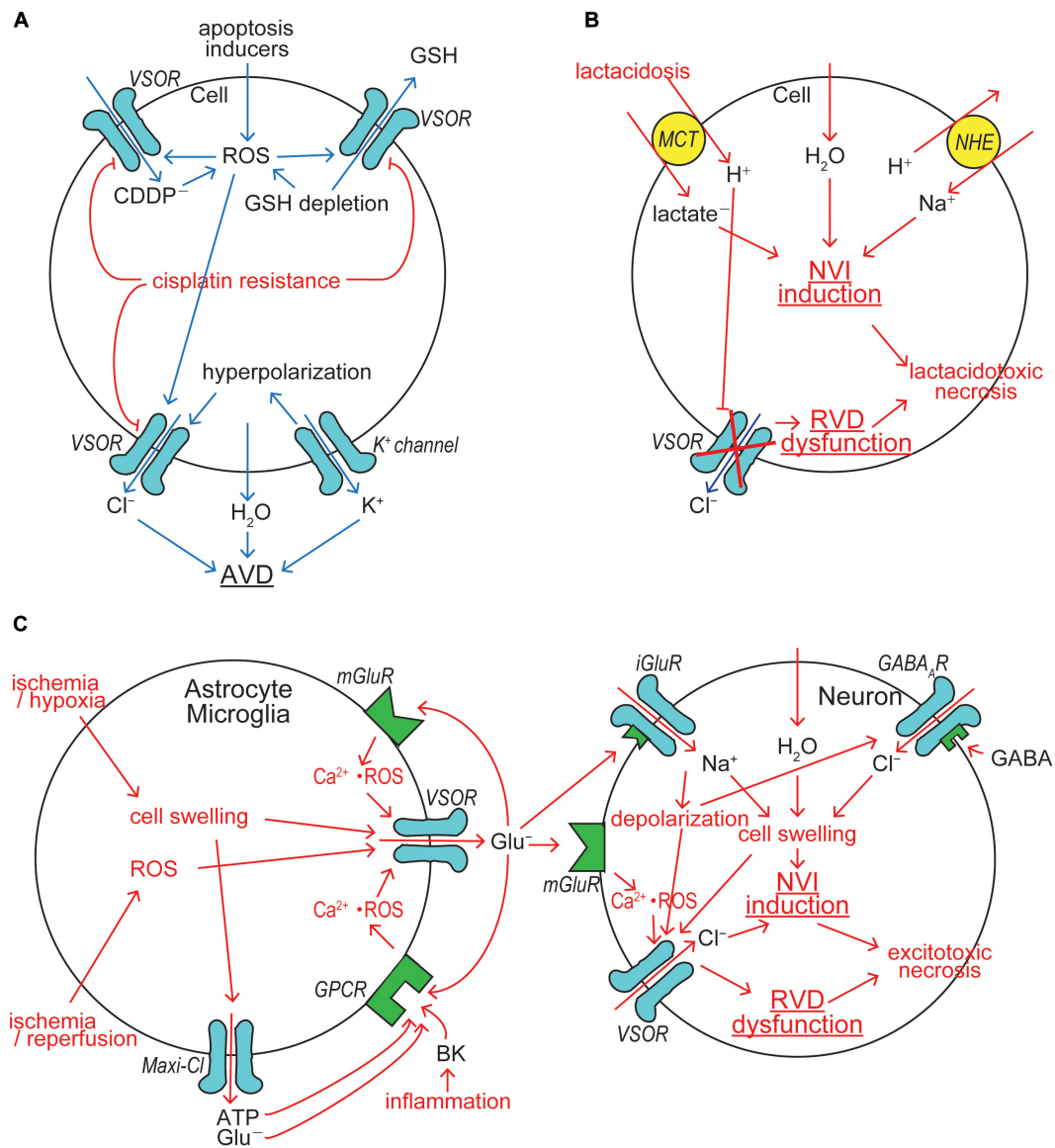


FIGURE 3 | VSOR/VRAC involvements in cell death induction/protection. **(A)** The mechanisms for AVD induction and cisplatin resistance acquisition. VSOR contributes to AVD induction by mediating Cl^- efflux, GSH release and cisplatin (CDDP^-) uptake, whereas VSOR downregulation contributes to cisplatin resistance acquisition. **(B)** The mechanism for lactacidosis-induced NVI in neuronal and glial cells in which VSOR activity is abolished. **(C)** The mechanism for excitotoxicity-induced NVI in neuronal cells in which VSOR rather mediates Cl^- influx under depolarization induced by activation of ionotropic glutamate receptor (iGluR) by glutamate released via VSOR from nearby glial cells (See the text for details).

Thus, depletion of cellular ATP even switches the form of cell death from apoptosis to necrosis (Eguchi et al., 1997; Leist et al., 1997). Ischemia/hypoxia insults and accidental injury cause NVI induction due to ATP depletion, because resultant inhibition of Na^+ - K^+ pump impairs the P-LB mechanism which contributes to steady-state CVR (Figure 2A, right panel). In addition, ATP depletion directly and indirectly, via a rise of intracellular free Mg^{2+} liberated from Mg-ATP, inhibits VSOR activity (Oiki et al., 1994; Okada et al., 2019b), thereby causing RVD dysfunction (Figure 2B, right panel). Arachidonic acid, which is produced in the ischemic/hypoxic tissues, was shown to be a very

potent blocker for VSOR and thereby abolish RVD (Kubo and Okada, 1992). In the ischemic/hypoxic brain, the extracellular K^+ concentration is known to largely elevate (Hansen, 1985). Also, extracellular K^+ accumulation is induced by excessive neuronal activity during epileptic episodes (Heinemann et al., 1986; Walz, 2000; Carmignoto and Haydon, 2012). Elevation of the extracellular K^+ level results in membrane depolarization which drives Cl^- inflow, but not outflow, thereby disrupting the P-LB mechanism and then leading to NVI (Figure 2A, right panel). Hyperammonemia, which is caused by liver diseases, also brings about NVI by impairing the P-LB mechanism, as

summarized by Wilson and Mongin (2018), because the K^+ channel-mediated NH_4^+ conductance impairs the K^+ channel role in this steady-state CVR mechanism not only by provoking depolarization and thus reducing Cl^- efflux but also by shunting K^+ recycling and thus retarding the Na^+-K^+ pump operation (Figure 2A, right panel).

Cerebral ischemia/hypoxia, trauma, seizure and spreading depression often result in not only acidosis due to proton liberation from hydrolysis of ATP greater than its synthesis but also lactate accumulation due to enhanced anaerobic glycolysis-fermentation reactions (Siesjö, 1988; Marmarou, 1992). Acidosis coupled to lactate accumulation, that is lactic acidosis, causes glial and neuronal cell swelling, cytotoxic brain edema and necrotic death of these brain cells (Kraig et al., 1987; Siesjö, 1988; Staub et al., 1990, 1993). Anionic lactate is taken up with H^+ by the monocarboxylate transporter (MCT), thereby causing intracellular accumulation of lactate and proton which stimulates the Na^+/H^+ antiporter (NHE) and leads to Na^+ accumulation, thereby causing NVI induction. Accumulated protons, on the other hand, inhibit VSOR activity (Gérard et al., 1998; Sabirov et al., 2000; Kittl et al., 2019), thereby resulting in RVD dysfunction. Lactic acidosis-induced NVI induction and RVD dysfunction were actually observed in both neuronal cells (Mori et al., 2002) and glial cells (Nabekura et al., 2003). Persistent cell swelling caused by the NVI induction and RVD dysfunction should finally lead to necrotic cell death, here called lactic acidotoxic necrosis, in neuronal and glial cells (Okada et al., 2019a), as depicted in Figure 3B.

Cerebral ischemia, ischemia-reperfusion, stroke, brain trauma, brain inflammation and a number of neurodegenerative disorders or neurogenic diseases often cause massive release of glutamate (Glu^-) from astrocytes (Olney et al., 1971), and neuronal and glial cell swelling and death, coined excitotoxicity (Olney, 1969), are produced due to exposure to excessive glutamate (Hasbani et al., 1998). Glial glutamate release is mediated by VSOR, as depicted in Figure 3C (left panel). Hypoxia/ischemia-induced swelling in astrocytes releases glutamate largely via VSOR (Abdullaev et al., 2006; Liu et al., 2006; Zhang et al., 2008; Bowens et al., 2013) and also glutamate and ATP via Maxi-Cl channels (Liu et al., 2006). Anoxia-induced glutamate release was inhibited by gene silencing of LRRC8A in astrocytes (Wilson et al., 2019). Astroglial LRRC8A is also required for stroke-induced brain damage, because conditional knockout of LRRC8A protected from ischemic stroke (Yang et al., 2019b). Ischemia causes release of bradykinin (BK), an initial mediator of brain inflammation (Gröger et al., 2005). BK was shown to activate VSOR via stimulation of BK type 2 receptor (BK2) in mouse astrocytes, thereby releasing glutamate (Liu et al., 2009). Since astrocytic VSOR is activated by ATP (Akita et al., 2011) and glutamate (Akita and Okada, 2014) through stimulation of their GPCRs via a signal here called Ca^{2+} -ROS which represents ROS production mediated by Ca^{2+} nanodomains, glutamate release may also be induced from astrocytes exposed to extracellular ATP and glutamate. Glial glutamate release was also shown to be induced by ROS by activating VSOR in rat astrocytes

(Haskew-Layton et al., 2005) and microglia (Harrigan et al., 2008). These activation mechanisms of glutamate-releasing VSOR channels are also summarized in Figure 3C (left panel).

Chronic excitotoxicity may play a role in pathogenesis of a variety of neurodegenerative diseases including amyotrophic lateral sclerosis, Alzheimer's disease, and Huntington's disease (Lewerenz and Maher, 2015). Excessive glutamate release from glial cells causes neuronal cell swelling (NVI) and necrotic death by the excitotoxic mechanism. Such acute excitotoxicity is known to be dependent on the entry of Na^+ and Cl^- rather than Ca^{2+} entry into neurons (Rothman, 1985; Olney et al., 1986; Chen et al., 1998; Inglefield and Schwartz-Bloom, 1998). Glutamate-induced stimulation of ionotropic glutamate receptor (iGluR) cation channels causes Na^+ influx and depolarization in neuronal cells. Ischemia induces release of gamma-aminobutyric acid (GABA) from neurons and astrocytes (Inglefield and Schwartz-Bloom, 1998). Glutamate also induces GABA release from GABAergic neurons (Weiss, 1988; Harris and Miller, 1989; Pin and Bockaert, 1989). Released GABA stimulates GABA_A receptor (GABA_AR) anion channels leading to Cl^- inflow driven by iGluR-induced depolarization. Resultant NaCl inflow brings about neuronal swelling (Inoue et al., 2007; Tymianski, 2011) and activation of VSOR (Inoue et al., 2007). Glutamate released from astrocytes activates neuronal metabotropic glutamate receptor (mGluR) and then neuronal VSOR by Ca^{2+} nanodomain-mediated ROS production (Akita and Okada, 2014) (also see Figure 4 in Okada et al., 2019b). VSOR channels thus activated under excitotoxic conditions serve as a swelling-exaggerating, instead of volume-regulatory, Cl^- inflow pathway, because of depolarization induced by activation of iGluR, thereby causing NVI induction and RVD dysfunction, and then eventually leading to necrotic cell death (Inoue et al., 2007), as summarized in Figure 3C (right panel). Thus, VSOR doubly contributes to excitotoxic neuronal NVI and necrosis by mediating glutamate release from astrocytes and by enhancing Cl^- inflow into neurons (Figure 3C).

Regulated or programmed necrosis, which occurs in genetically controlled, but not accidental, manner, includes necroptosis, pyroptosis, and ferroptosis. Necroptosis is dependent on receptor-interacting protein kinase 3 (RIPK3), triggered by activation of death receptors or Toll-like-receptor (TLR) in the presence of caspase-8 inhibition (Green, 2019; Sauler et al., 2019), and regulated by activation of RIPK3 (Kaiser et al., 2013) which induces phosphorylation of mixed lineage kinase domain-like protein (MLKL). Phosphorylated MLKL oligomerizes and translocates to the plasma membrane to form a pore of ~4 nm diameter (Ros et al., 2017) leading to rapid rupture of the plasma membrane. Necroptosis exhibits marked cell swelling (Chen et al., 2016), but the ionic mechanism of this NVI event remains unexplored. Necroptosis is known to be characterized by intracellular ATP depletion (Henriquez et al., 2008; Vandenabeele et al., 2010) which is possibly induced by ATP consuming process of activation of poly(ADP-ribose)polymerase 1 (PARP1) (Jouan-Lanhuet et al., 2012). Thus, it is likely that ATP depletion is responsible for induction of NVI associated with necroptosis (see Figures 2A,B, right panels).

On the other hand, pyroptosis is inflammatory caspase-dependent programmed necrosis. Pyroptosis is triggered by exposure of cells to bacteria, virus and toxins, called pathogen-associated or danger-associated molecular patterns (PAMPs or DAMPs), which induce formation of multiprotein complexes called inflammasomes in inflammatory cells (Broz and Dixit, 2016). Pyroptosis is regulated by inflammatory caspases (caspase-1, -4, -5, and -11) which mediate cleavage of gasdermin D (GSDMD) into the NH₂-terminal of GSDMD (GSDMD-N), the oligomer of which forms the non-selective membrane pore (Ding et al., 2016; Sborgi et al., 2016; Ruan et al., 2018). Pyroptosis exhibits discernible, though less markedly compared to necroptosis, cell swelling (NVI) (Fink and Cookson, 2006; Chen et al., 2016). Since pyroptotic inflammasome activation involves K⁺ efflux, TRPM2/V2-mediated Ca²⁺ influx and Cl⁻ channel activation (Tang et al., 2017; Green et al., 2018), it is possible that ionic fluxes are also implicated in the pyroptotic NVI induction. Especially, it is noted that the Cl⁻ channel was shown to be sensitive to VSOR blockers including DCPiB and NPPB (Green et al., 2018) and that flufenamic acid (FFA), which is a known inhibitor of cyclooxygenase (COX), was shown to inhibit inflammasome via blocking VSOR but not via COX-1/COX-2 inhibition (Daniels et al., 2016).

The third type of programmed necrosis is ferroptosis dependent on lipid peroxide. Ferroptosis is triggered by GSH depletion induced by small molecule ferroptosis inducers such as erastin, sorafenib, sulfasalazine bothonine sulfoximine (BSO) and RSL3 (Cao and Dixon, 2016; Sun et al., 2018). This process is regulated by inhibition of GSH-dependent antioxidant enzyme, glutathione peroxidase 4 (GPX4) (Cao and Dixon, 2016; Lei et al., 2019). Ferroptotic cell death is caused by iron-dependent accumulation of lipid peroxides (L-ROS) which give rise to oxidative damage to the cell membrane (Del Re et al., 2019; Lei et al., 2019). No study has been reported as to whether ferroptosis also exhibits cell swelling. It is also warranted to examine whether VSOR is involved in ferroptosis-associated GSH depletion.

CONCLUSION AND PERSPECTIVE

In conclusion, VSOR/VRAC activity is essentially involved not only in CVR and protection from cell injury/death but also in induction of apoptotic/necrotic cell death by inducing Cl⁻ outflow or inflow and releasing organic signal

molecules. However, their detailed molecular mechanisms remain unexplored.

Urgent issues to be clarified are to provide firm evidence for pore formation by the LRRC8 heteromer, information about the 3-D structure of LRRC8 heterohexamer by cryo-EM studies, and actual roles of VSOR/VRAC in programmed necrosis such as necroptosis, pyroptosis, and ferroptosis. Also, a question to be soon unraveled is what are missing molecular components actually involved in activation and regulation of VSOR/VRAC.

Recently, an essential involvement of VSOR/VRAC in stroke-induced brain damage was clearly demonstrated by *in vivo* studies using conditional LRRC8A-knockout mice (Yang et al., 2019b). In this context, it is noted that accumulating evidence has been provided for neuroprotective effects of VSOR/VRAC blockers on ischemic neuronal damage/death in the brain by *ex vivo* slice experiments (Zhang et al., 2011) and by *in vivo* experiments (Phillis et al., 1997, 1998; Seki et al., 1999; Kimelberg et al., 2000; Feustel et al., 2004; Kimelberg, 2005; Inoue et al., 2007; Zhang et al., 2008; Alibrahim et al., 2013). Thus, more specific, less toxic, and blood-brain barrier-permeable VSOR/VRAC blocking agents are awaited to be developed for clinical use hopefully within the next decade.

AUTHOR CONTRIBUTIONS

YO conceived of the project. YO and RS wrote the manuscript (Part 1) with input from KS-N and TN. TN and RS prepared figures. KS-N prepared references. All authors contributed to the article and approved the submitted version.

FUNDING

This work was supported by Grants-in-Aid for Scientific Research from JSPS of Japan to YO (#17K19517), KS-N (#18J90103), and TN (#18K06864) and from the Ministry of Innovative Development of Uzbekistan to RS (#FA-F5-014 and #PZ-2017-0920-49).

ACKNOWLEDGMENTS

The authors thank Dr. Petr G. Merzlyak for help in manuscript preparation and critical reading.

REFERENCES

- Abdullaev, I. F., Rudkouskaya, A., Schools, G. P., Kimelberg, H. K., and Mongin, A. A. (2006). Pharmacological comparison of swelling-activated excitatory amino acid release and Cl⁻ currents in cultured rat astrocytes. *J. Physiol.* 572(Pt 3), 677–689. doi: 10.1113/jphysiol.2005.103820
- Akita, T., Fedorovich, S. V., and Okada, Y. (2011). Ca²⁺ nanodomain-mediated component of swelling-induced volume-sensitive outwardly rectifying anion current triggered by autocrine action of ATP in mouse astrocytes. *Cell. Physiol. Biochem.* 28, 1181–1190. doi: 10.1159/000335867
- Akita, T., and Okada, Y. (2011). Regulation of bradykinin-induced activation of volume-sensitive outwardly rectifying anion channels by Ca²⁺ nanodomains in mouse astrocytes. *J. Physiol.* 589(Pt 16), 3909–3927. doi: 10.1113/jphysiol.2011.208173
- Akita, T., and Okada, Y. (2014). Characteristics and roles of the volume-sensitive outwardly rectifying (VSOR) anion channel in the central nervous system. *Neuroscience* 275, 211–231. doi: 10.1016/j.neuroscience.2014.06.015
- Alibrahim, A., Zhao, L. Y., Bae, C. Y., Barszcyk, A., Sun, C. L., Wang, G. L., et al. (2013). Neuroprotective effects of volume-regulated anion channel blocker DCPiB on neonatal hypoxic-ischemic injury. *Acta Pharmacol. Sin.* 34, 113–118. doi: 10.1038/aps.2012.148

- Al-Nakkash, L., Iserovich, P., Coca-Prados, M., Yang, H., and Reinach, P. S. (2004). Functional and molecular characterization of a volume-activated chloride channel in rabbit corneal epithelial cells. *J. Membr. Biol.* 201, 41–49. doi: 10.1007/s00232-004-0706-5
- Arreola, J., Park, K., Melvin, J. E., and Begenisich, T. (1996). Three distinct chloride channels control anion movements in rat parotid acinar cells. *J. Physiol.* 490(Pt 2), 351–362. doi: 10.1113/jphysiol.1996.sp021149
- Bae, Y., Kim, A., Cho, C. H., Kim, D., Jung, H. G., Kim, S. S., et al. (2019). TTYH1 and TTYH2 serve as LRRC8A-independent volume-regulated anion channels in cancer cells. *Cells* 8:562. doi: 10.3390/cells8060562
- Ballatori, N., Krance, S. M., Marchan, R., and Hammond, C. L. (2009). Plasma membrane glutathione transporters and their roles in cell physiology and pathophysiology. *Mol. Aspects Med.* 30, 13–28. doi: 10.1016/j.mam.2008.08.004
- Banderali, U., and Roy, G. (1992). Anion channels for amino acids in MDCK cells. *Am. J. Physiol.* 263(6 Pt 1), C1200–C1207. doi: 10.1152/ajpcell.1992.263.6.C1200
- Basarsky, T. A., Feighan, D., and MacVicar, B. A. (1999). Glutamate release through volume-activated channels during spreading depression. *J. Neurosci.* 19, 6439–6445. doi: 10.1523/jneurosci.19-15-06439.1999
- Basavappa, S., Huang, C. C., Mangel, A. W., Lebedev, D. V., Knauf, P. A., and Ellory, J. C. (1996). Swelling-activated amino acid efflux in the human neuroblastoma cell line CHP-100. *J. Neurophysiol.* 76, 764–769. doi: 10.1152/jn.1996.76.2.764
- Benedetto, R., Sirianant, L., Pankonien, I., Wanitchakool, P., Ousingsawat, J., Cabrita, I., et al. (2016). Relationship between TMEM16A/anoctamin 1 and LRRC8A. *Pflugers Arch.* 468, 1751–1763. doi: 10.1007/s00424-016-1862-1
- Best, L., and Brown, P. D. (2009). Studies of the mechanism of activation of the volume-regulated anion channel in rat pancreatic beta-cells. *J. Membr. Biol.* 230, 83–91. doi: 10.1007/s00232-009-9189-x
- Best, L., Shader, E. A., and Brown, P. D. (1996). A volume-activated anion conductance in insulin-secreting cells. *Pflugers Arch.* 431, 363–370. doi: 10.1007/bf02207273
- Boese, S. H., Wehner, F., and Kinne, R. K. (1996). Taurine permeation through swelling-activated anion conductance in rat IMCD cells in primary culture. *Am. J. Physiol.* 271(3 Pt 2), F498–F507. doi: 10.1152/ajprenal.1996.271.3.F498
- Bond, T. D., Ambikapathy, S., Mohammad, S., and Valverde, M. A. (1998). Osmosensitive Cl[−] currents and their relevance to regulatory volume decrease in human intestinal T84 cells: outwardly vs. inwardly rectifying currents. *J. Physiol.* 511(Pt 1), 45–54. doi: 10.1111/j.1469-7793.1998.045bi.x
- Bothwell, J. H., Rae, C., Dixon, R. M., Styles, P., and Bhakoo, K. K. (2001). Hypo-osmotic swelling-activated release of organic osmolytes in brain slices: implications for brain oedema *in vivo*. *J. Neurochem.* 77, 1632–1640. doi: 10.1046/j.1471-4159.2001.00403.x
- Bowens, N. H., Dohare, P., Kuo, Y. H., and Mongin, A. A. (2013). DCPIB, the proposed selective blocker of volume-regulated anion channels, inhibits several glutamate transport pathways in glial cells. *Mol. Pharmacol.* 83, 22–32. doi: 10.1124/mol.112.080457
- Braunstein, G. M., Roman, R. M., Clancy, J. P., Kudlow, B. A., Taylor, A. L., Shylonsky, V. G., et al. (2001). Cystic fibrosis transmembrane conductance regulator facilitates ATP release by stimulating a separate ATP release channel for autocrine control of cell volume regulation. *J. Biol. Chem.* 276, 6621–6630. doi: 10.1074/jbc.M005893200
- Briz, O., Romero, M. R., Martinez-Becerra, P., Macias, R. I., Perez, M. J., Jimenez, F., et al. (2006). OATP8/1B3-mediated cotransport of bile acids and glutathione: An export pathway for organic anions from hepatocytes? *J. Biol. Chem.* 281, 30326–30335. doi: 10.1074/jbc.M602048200
- Browe, D. M., and Baumgarten, C. M. (2004). Angiotensin II (AT1) receptors and NADPH oxidase regulate Cl[−] current elicited by beta1 integrin stretch in rabbit ventricular myocytes. *J. Gen. Physiol.* 124, 273–287. doi: 10.1085/jgp.200409040
- Broz, P., and Dixit, V. M. (2016). Inflammasomes: mechanism of assembly, regulation and signalling. *Nat. Rev. Immunol.* 16, 407–420. doi: 10.1038/nri.2016.58
- Burg, E. D., Remillard, C. V., and Yuan, J. X. (2006). K⁺ channels in apoptosis. *J. Membr. Biol.* 209, 3–20. doi: 10.1007/s00232-005-0838-4
- Burnstock, G. (2012). Purinergic signalling: its unpopular beginning, its acceptance and its exciting future. *Bioessays* 34, 218–225. doi: 10.1002/bies.201100130
- Burnstock, G., and Pelleg, A. (2015). Cardiac purinergic signalling in health and disease. *Purinergic Signal.* 11, 1–46. doi: 10.1007/s11302-014-9436-1
- Cahalan, M. D., and Lewis, R. S. (1988). Role of potassium and chloride channels in volume regulation by T lymphocytes. *Soc. Gen. Physiol. Ser.* 43, 281–301.
- Cao, G., Zuo, W., Fan, A., Zhang, H., Yang, L., Zhu, L., et al. (2011). Volume-sensitive chloride channels are involved in maintenance of basal cell volume in human acute lymphoblastic leukemia cells. *J. Membr. Biol.* 240, 111–119. doi: 10.1007/s00232-011-9349-7
- Cao, J. Y., and Dixon, S. J. (2016). Mechanisms of ferroptosis. *Cell. Mol. Life Sci.* 73, 2195–2209. doi: 10.1007/s00018-016-2194-1
- Carmignoto, G., and Haydon, P. G. (2012). Astrocyte calcium signaling and epilepsy. *Glia* 60, 1227–1233. doi: 10.1002/glia.22318
- Carpaneto, A., Accardi, A., Pisciotto, M., and Gambale, F. (1999). Chloride channels activated by hypotonicity in N2A neuroblastoma cell line. *Exp. Brain Res.* 124, 193–199. doi: 10.1007/s002210050614
- Chan, H. C., Fu, W. O., Chung, Y. W., Huang, S. J., Chan, P. S., and Wong, P. Y. (1994). Swelling-induced anion and cation conductances in human epididymal cells. *J. Physiol.* 478(Pt 3), 449–460. doi: 10.1113/jphysiol.1994.sp020264
- Chen, B., Jefferson, D. M., and Cho, W. K. (2010). Characterization of volume-activated chloride currents in regulatory volume decrease of human cholangiocyte. *J. Membr. Biol.* 235, 17–26. doi: 10.1007/s00232-010-9252-7
- Chen, L., König, B., Liu, T., Pervaiz, S., Razaque, Y. S., and Stauber, T. (2019). More than just a pressure relief valve: physiological roles of volume-regulated LRRC8 anion channels. *Biol. Chem.* 400, 1481–1496. doi: 10.1515/hsz-2019-0189
- Chen, Q., Olney, J. W., Lukaszewicz, P. D., Alml, T., and Romano, C. (1998). Ca²⁺-independent excitotoxic neurodegeneration in isolated retina, an intact neural net: a role for Cl[−] and inhibitory transmitters. *Mol. Pharmacol.* 53, 564–572. doi: 10.1124/mol.53.3.564
- Chen, X., He, W. T., Hu, L., Li, J., Fang, Y., Wang, X., et al. (2016). Pyroptosis is driven by non-selective gasdermin-D pore and its morphology is different from MLKL channel-mediated necroptosis. *Cell Res.* 26, 1007–1020. doi: 10.1038/cr.2016.100
- Choi, H., Ettinger, N., Rohrbough, J., Dikalova, A., Nguyen, H. N., and Lamb, F. S. (2016). LRRC8A channels support TNF α -induced superoxide production by Nox1 which is required for receptor endocytosis. *Free Radic. Biol. Med.* 101, 413–423. doi: 10.1016/j.freeradbiomed.2016.11.003
- Circu, M. L., and Aw, T. Y. (2008). Glutathione and apoptosis. *Free Radic. Res.* 42, 689–706. doi: 10.1080/10715760802317663
- Circu, M. L., and Aw, T. Y. (2012). Glutathione and modulation of cell apoptosis. *Biochim. Biophys. Acta* 1823, 1767–1777. doi: 10.1016/j.bbamcr.2012.06.019
- Circu, M. L., Stringer, S., Rhoads, C. A., Moyer, M. P., and Aw, T. Y. (2009). The role of GSH efflux in staurosporine-induced apoptosis in colonic epithelial cells. *Biochem. Pharmacol.* 77, 76–85. doi: 10.1016/j.bcp.2008.09.011
- d'Anglemont de Tassigny, A., Souktani, R., Henry, P., Ghaleh, B., and Berdeaux, A. (2004). Volume-sensitive chloride channels (ICl_{vol}) mediate doxorubicin-induced apoptosis through apoptotic volume decrease in cardiomyocytes. *Fundam. Clin. Pharmacol.* 18, 531–538. doi: 10.1111/j.1472-8206.2004.00273.x
- Daniels, M. J., Rivers-Auty, J., Schilling, T., Spencer, N. G., Watremez, W., Fasolino, V., et al. (2016). Fenamate NSAIDs inhibit the NLRP3 inflammasome and protect against Alzheimer's disease in rodent models. *Nat. Commun.* 7:12504. doi: 10.1038/ncomms12504
- Del Re, D. P., Amgalan, D., Linkermann, A., Liu, Q., and Kitsis, R. N. (2019). Fundamental mechanisms of regulated cell death and implications for heart disease. *Physiol. Rev.* 99, 1765–1817. doi: 10.1152/physrev.00022.2018
- Deneka, D., Sawicka, M., Lam, A. K. M., Paulino, C., and Dutzler, R. (2018). Structure of a volume-regulated anion channel of the LRRC8 family. *Nature* 558, 254–259. doi: 10.1038/s41586-018-0134-y
- Dezaki, K., Tsumura, T., Maeno, E., and Okada, Y. (2000). Receptor-mediated facilitation of cell volume regulation by swelling-induced ATP release in human epithelial cells. *Jpn. J. Physiol.* 50, 235–241. doi: 10.2170/jjphysiol.50.235
- Ding, J., Wang, K., Liu, W., She, Y., Sun, Q., Shi, J., et al. (2016). Pore-forming activity and structural autoinhibition of the gasdermin family. *Nature* 535, 111–116. doi: 10.1038/nature18590
- Doroshenko, P. (1998). Pervanadate inhibits volume-sensitive chloride current in bovine chromaffin cells. *Pflugers Arch.* 435, 303–309. doi: 10.1007/s004240050516
- Droogmans, G., Maertens, C., Prenen, J., and Nilius, B. (1999). Sulphonic acid derivatives as probes of pore properties of volume-regulated anion channels in endothelial cells. *Br. J. Pharmacol.* 128, 35–40. doi: 10.1038/sj.bjp.0702770

- Droogmans, G., Prenen, J., Eggermont, J., Voets, T., and Nilius, B. (1998). Voltage-dependent block of endothelial volume-regulated anion channels by calix[4]arenes. *Am. J. Physiol.* 275, C646–C652. doi: 10.1152/ajpcell.1998.275.3.C646
- Ducharme, G., Newell, E. W., Pinto, C., and Schlichter, L. C. (2007). Small-conductance Cl^- channels contribute to volume regulation and phagocytosis in microglia. *Eur. J. Neurosci.* 26, 2119–2130. doi: 10.1111/j.1460-9568.2007.05802.x
- Dunn, P. J., Salm, E. J., and Tomita, S. (2020). ABC transporters control ATP release through cholesterol-dependent volume-regulated anion channel activity. *J. Biol. Chem.* 295, 5192–5203. doi: 10.1074/jbc.RA119.010699
- Dutta, A. K., Korchev, Y. E., Shevchuk, A. I., Hayashi, S., Okada, Y., and Sabirov, R. Z. (2008). Spatial distribution of maxi-anion channel on cardiomyocytes detected by smart-patch technique. *Biophys. J.* 94, 1646–1655. doi: 10.1529/biophysj.107.117820
- Dutta, A. K., Sabirov, R. Z., Uramoto, H., and Okada, Y. (2004). Role of ATP-conductive anion channel in ATP release from neonatal rat cardiomyocytes in ischaemic or hypoxic conditions. *J. Physiol.* 559(Pt 3), 799–812. doi: 10.1113/jphysiol.2004.069245
- Eguchi, Y., Shimizu, S., and Tsujimoto, Y. (1997). Intracellular ATP levels determine cell death fate by apoptosis or necrosis. *Cancer Res.* 57, 1835–1840.
- Eguchi, Y., Srinivasan, A., Tomaselli, K. J., Shimizu, S., and Tsujimoto, Y. (1999). ATP-dependent steps in apoptotic signal transduction. *Cancer Res.* 59, 2174–2181.
- Elorza-Vidal, X., Sirisi, S., Gaitán-Peñas, H., Pérez-Rius, C., Alonso-Gardón, M., Armand-Ugón, M., et al. (2018). GlialCAM/MLC1 modulates LRRC8/VRAC currents in an indirect manner: implications for megalencephalic leukoencephalopathy. *Neurobiol. Dis.* 119, 88–99. doi: 10.1016/j.nbd.2018.07.031
- Espelt, M. V., de Tezanos Pinto, F., Alvarez, C. L., Alberti, G. S., Incicco, J., Leal Denis, M. F., et al. (2013). On the role of ATP release, ectoATPase activity, and extracellular ADP in the regulatory volume decrease of Huh-7 human hepatoma cells. *Am. J. Physiol. Cell Physiol.* 304, C1013–C1026. doi: 10.1152/ajpcell.00254.2012
- Evanko, D. S., Zhang, Q., Zorec, R., and Haydon, P. G. (2004). Defining pathways of loss and secretion of chemical messengers from astrocytes. *Glia* 47, 233–240. doi: 10.1002/glia.20050
- Fatherazi, S., Izutsu, K. T., Wellner, R. B., and Belton, C. M. (1994). Hypotonically activated chloride current in HSG cells. *J. Membr. Biol.* 142, 181–193. doi: 10.1007/bf00234940
- Feustel, P. J., Jin, Y., and Kimelberg, H. K. (2004). Volume-regulated anion channels are the predominant contributors to release of excitatory amino acids in the ischemic cortical penumbra. *Stroke* 35, 1164–1168. doi: 10.1161/01.STR.0000124127.57946.a1
- Fink, S. L., and Cookson, B. T. (2006). Caspase-1-dependent pore formation during pyroptosis leads to osmotic lysis of infected host macrophages. *Cell. Microbiol.* 8, 1812–1825. doi: 10.1111/j.1462-5822.2006.00751.x
- Fiorina, P. (2013). GABAergic system in β -cells: from autoimmunity target to regeneration tool. *Diabetes* 62, 3674–3676. doi: 10.2337/db13-1243
- Formaggio, F., Saracino, E., Mola, M. G., Rao, S. B., Amiry-Moghaddam, M., Muccini, M., et al. (2019). LRRC8A is essential for swelling-activated chloride current and for regulatory volume decrease in astrocytes. *FASEB J.* 33, 101–113. doi: 10.1096/fj.201701397RR
- Franco, R., and Cidlowski, J. A. (2006). SLCO/OATP-like transport of glutathione in FasL-induced apoptosis: glutathione efflux is coupled to an organic anion exchange and is necessary for the progression of the execution phase of apoptosis. *J. Biol. Chem.* 281, 29542–29557. doi: 10.1074/jbc.M602500200
- Franco, R., and Cidlowski, J. A. (2009). Apoptosis and glutathione: beyond an antioxidant. *Cell Death Differ.* 16, 1303–1314. doi: 10.1038/cdd.2009.107
- Franco, R., Torres-Márquez, M. E., and Pasantes-Morales, H. (2001). Evidence for two mechanisms of amino acid osmolyte release from hippocampal slices. *Pflügers Arch.* 442, 791–800. doi: 10.1007/s004240100604
- Franke, H., Verkhratsky, A., Burnstock, G., and Illes, P. (2012). Pathophysiology of astroglial purinergic signalling. *Purinergic Signal.* 8, 629–657. doi: 10.1007/s11302-012-9300-0
- Friard, J., Corinus, A., Coughnon, M., Tauc, M., Pisani, D. F., Duranton, C., et al. (2019). LRRC8/VRAC channels exhibit a noncanonical permeability to glutathione, which modulates epithelial-to-mesenchymal transition (EMT). *Cell Death Dis.* 10:925. doi: 10.1038/s41419-019-2167-z
- Friard, J., Tauc, M., Coughnon, M., Compan, V., Duranton, C., and Rubera, I. (2017). Comparative effects of chloride channel inhibitors on LRRC8/VRAC-mediated chloride conductance. *Front. Pharmacol.* 8:328. doi: 10.3389/fphar.2017.00328
- Fujii, R., Mutoh, M., Niwa, K., Yamada, K., Aikou, T., Nakagawa, M., et al. (1994). Active efflux system for cisplatin in cisplatin-resistant human KB cells. *Jpn. J. Cancer Res.* 85, 426–433. doi: 10.1111/j.1349-7006.1994.tb02376.x
- Fujii, T., Shimizu, T., Yamamoto, S., Funayama, K., Fujita, K., Tabuchi, Y., et al. (2018). Crosstalk between Na^+ , K^+ -ATPase and a volume-regulated anion channel in membrane microdomains of human cancer cells. *Biochim. Biophys. Acta Mol. Basis Dis.* 1864, 3792–3804. doi: 10.1016/j.bbadis.2018.09.014
- Garcia, T. B., Oliveira, K. R., do Nascimento, J. L., Crespo-López, M. E., Picanço-Diniz, D. L., Mota, T. C., et al. (2011). Glutamate induces glutathione efflux mediated by glutamate/aspartate transporter in retinal cell cultures. *Neurochem. Res.* 36, 412–418. doi: 10.1007/s11064-010-0356-3
- Gérard, V., Rouzaire-Dubois, B., Dilda, P., and Dubois, J. M. (1998). Alterations of ionic membrane permeabilities in multidrug-resistant neuroblastoma x glioma hybrid cells. *J. Exp. Biol.* 201(Pt 1), 21–31.
- Ghibelli, L., Fanelli, C., Rotilio, G., Lafavia, E., Coppola, S., Colussi, C., et al. (1998). Rescue of cells from apoptosis by inhibition of active GSH extrusion. *FASEB J.* 12, 479–486. doi: 10.1096/fasebj.12.6.479
- Gosling, M., Poyner, D. R., and Smith, J. W. (1996). Effects of arachidonic acid upon the volume-sensitive chloride current in rat osteoblast-like (ROS 17/2.8) cells. *J. Physiol.* 493(Pt 3), 613–623. doi: 10.1113/jphysiol.1996.sp021408
- Green, D. R. (2019). The coming decade of cell death research: five riddles. *Cell* 177, 1094–1107. doi: 10.1016/j.cell.2019.04.024
- Green, J. P., Yu, S., Martín-Sánchez, F., Pelegrin, P., Lopez-Castejon, G., Lawrence, C. B., et al. (2018). Chloride regulates dynamic NLRP3-dependent ASC oligomerization and inflammasome priming. *Proc. Natl. Acad. Sci. U.S.A.* 115, E9371–E9380. doi: 10.1073/pnas.1812744115
- Grinstein, S., Clarke, C. A., Dupre, A., and Rothstein, A. (1982). Volume-induced increase of anion permeability in human lymphocytes. *J. Gen. Physiol.* 80, 801–823. doi: 10.1085/jgp.80.6.801
- Grinstein, S., Clarke, C. A., Rothstein, A., and Gelfand, E. W. (1983). Volume-induced anion conductance in human B lymphocytes is cation independent. *Am. J. Physiol.* 245, C160–C163. doi: 10.1152/ajpcell.1983.245.1.C160
- Grinstein, S., Rothstein, A., Sarkadi, B., and Gelfand, E. W. (1984). Responses of lymphocytes to anisotonic media: volume-regulating behavior. *Am. J. Physiol.* 246(3 Pt 1), C204–C215. doi: 10.1152/ajpcell.1984.246.3.C204
- Gröger, M., Lebesgue, D., Pruneau, D., Relton, J., Kim, S. W., Nussberger, J., et al. (2005). Release of bradykinin and expression of kinin B2 receptors in the brain: role for cell death and brain edema formation after focal cerebral ischemia in mice. *J. Cereb. Blood Flow Metab.* 25, 978–989. doi: 10.1038/sj.jcbfm.9600096
- Gschwentner, M., Nagl, U. O., Wöll, E., Schmarda, A., Ritter, M., and Paulmichl, M. (1995a). Antisense oligonucleotides suppress cell-volume-induced activation of chloride channels. *Pflügers Arch.* 430, 464–470. doi: 10.1007/bf00373882
- Gschwentner, M., Susanna, A., Wöll, E., Ritter, M., Nagl, U. O., Schmarda, A., et al. (1995b). Antiviral drugs from the nucleoside analog family block volume-activated chloride channels. *Mol. Med.* 1, 407–417.
- Hagiwara, N., Masuda, H., Shoda, M., and Irisawa, H. (1992). Stretch-activated anion currents of rabbit cardiac myocytes. *J. Physiol.* 456, 285–302. doi: 10.1113/jphysiol.1992.sp019337
- Hammond, C. L., Lee, T. K., and Ballatori, N. (2001). Novel roles for glutathione in gene expression, cell death, and membrane transport of organic solutes. *J. Hepatol.* 34, 946–954. doi: 10.1016/s0168-8278(01)00037-x
- Han, Y. E., Kwon, J., Won, J., An, H., Jang, M. W., Woo, J., et al. (2019). Tweety-homolog (Ttyh) family encodes the pore-forming subunits of the swelling-dependent volume-regulated anion channel (VRAC(swell)) in the brain. *Exp. Neurobiol.* 28, 183–215. doi: 10.5607/en.2019.28.2.183
- Hansen, A. J. (1985). Effect of anoxia on ion distribution in the brain. *Physiol. Rev.* 65, 101–148. doi: 10.1152/physrev.1985.65.1.101
- Harrigan, T. J., Abdullaev, I. F., Jourdeuil, D., and Mongin, A. A. (2008). Activation of microglia with zymosan promotes excitatory amino acid release via volume-regulated anion channels: the role of NADPH oxidases. *J. Neurochem.* 106, 2449–2462. doi: 10.1111/j.1471-4159.2008.05553.x

- Harris, K. M., and Miller, R. J. (1989). Excitatory amino acid-evoked release of [3H]GABA from hippocampal neurons in primary culture. *Brain Res.* 482, 23–33. doi: 10.1016/0006-8993(89)90538-6
- Hasbani, M. J., Hyrc, K. L., Faddis, B. T., Romano, C., and Goldberg, M. P. (1998). Distinct roles for sodium, chloride, and calcium in excitotoxic dendritic injury and recovery. *Exp. Neurobiol.* 154, 241–258. doi: 10.1006/exnr.1998.6929
- Hasegawa, Y., Shimizu, T., Takahashi, N., and Okada, Y. (2012). The apoptotic volume decrease is an upstream event of MAP kinase activation during Staurosporine-induced apoptosis in HeLa cells. *Int. J. Mol. Sci.* 13, 9363–9379. doi: 10.3390/ijms13079363
- Haskew-Layton, R. E., Mongin, A. A., and Kimelberg, H. K. (2005). Hydrogen peroxide potentiates volume-sensitive excitatory amino acid release via a mechanism involving Ca^{2+} /calmodulin-dependent protein kinase II. *J. Biol. Chem.* 280, 3548–3554. doi: 10.1074/jbc.M409803200
- Haskew-Layton, R. E., Rudkouskaya, A., Jin, Y., Feustel, P. J., Kimelberg, H. K., and Mongin, A. A. (2008). Two distinct modes of hypoosmotic medium-induced release of excitatory amino acids and taurine in the rat brain *in vivo*. *PLoS One* 3:e3543. doi: 10.1371/journal.pone.0003543
- Hazama, A., and Okada, Y. (1988). Ca^{2+} sensitivity of volume-regulatory K^{+} and Cl^{-} channels in cultured human epithelial cells. *J. Physiol.* 402, 687–702. doi: 10.1113/jphysiol.1988.sp017229
- He, W., Li, H., Min, X., Liu, J., Hu, B., Hou, S., et al. (2010). Activation of volume-sensitive Cl^{-} channel is involved in carboplatin-induced apoptosis in human lung adenocarcinoma cells. *Cancer Biol. Ther.* 9, 885–891. doi: 10.4161/cbt.9.11.11666
- Heinemann, U., Konnerth, A., Pumain, R., and Wadman, W. J. (1986). Extracellular calcium and potassium concentration changes in chronic epileptic brain tissue. *Adv. Neurol.* 44, 641–661.
- Henriquez, M., Armisen, R., Stutzin, A., and Quest, A. F. (2008). Cell death by necrosis, a regulated way to go. *Curr. Mol. Med.* 8, 187–206. doi: 10.2174/156652408784221289
- Hernández-Benítez, R., Sedeño-Cortés, A., Ramos-Mandujano, G., and Pasantes-Morales, H. (2014). Regulatory volume decrease in neural precursor cells: taurine efflux and gene microarray analysis. *Cell. Physiol. Biochem.* 34, 2038–2048. doi: 10.1159/000366399
- Hisadome, K., Koyama, T., Kimura, C., Droogmans, G., Ito, Y., and Oike, M. (2002). Volume-regulated anion channels serve as an auto/paracrine nucleotide release pathway in aortic endothelial cells. *J. Gen. Physiol.* 119, 511–520. doi: 10.1085/jgp.20028540
- Hoffmann, E. K., Lambert, I. H., and Pedersen, S. F. (2009). Physiology of cell volume regulation in vertebrates. *Physiol. Rev.* 89, 193–277. doi: 10.1152/physrev.00037.2007
- Hoffmann, E. K., Lambert, I. H., and Simonsen, L. O. (1986). Separate, Ca^{2+} -activated K^{+} and Cl^{-} transport pathways in Ehrlich ascites tumor cells. *J. Membr. Biol.* 91, 227–244. doi: 10.1007/bf01868816
- Hoffmann, E. K., Simonsen, L. O., and Lambert, I. H. (1984). Volume-induced increase of K^{+} and Cl^{-} permeabilities in Ehrlich ascites tumor cells. Role of internal Ca^{2+} . *J. Membr. Biol.* 78, 211–222. doi: 10.1007/bf01925969
- Huxtable, R. J. (1982). Guanidinoethane sulfonate and the disposition of dietary taurine in the rat. *J. Nutr.* 112, 2293–2300. doi: 10.1093/jn/112.12.2293
- Hyzinski-García, M. C., Rudkouskaya, A., and Mongin, A. A. (2014). LRRC8A protein is indispensable for swelling-activated and ATP-induced release of excitatory amino acids in rat astrocytes. *J. Physiol.* 592, 4855–4862. doi: 10.1113/jphysiol.2014.278887
- Hyzinski-García, M. C., Vincent, M. Y., Haskew-Layton, R. E., Dohare, P., Keller, R. W. Jr., and Mongin, A. A. (2011). Hypo-osmotic swelling modifies glutamate-glutamine cycle in the cerebral cortex and in astrocyte cultures. *J. Neurochem.* 118, 140–152. doi: 10.1111/j.1471-4159.2011.07289.x
- Inglefield, J. R., and Schwartz-Bloom, R. D. (1998). Activation of excitatory amino acid receptors in the rat hippocampal slice increases intracellular Cl^{-} and cell volume. *J. Neurochem.* 71, 1396–1404. doi: 10.1046/j.1471-4159.1998.7104.1396.x
- Inoue, H., Mori, S., Morishima, S., and Okada, Y. (2005). Volume-sensitive chloride channels in mouse cortical neurons: characterization and role in volume regulation. *Eur. J. Neurosci.* 21, 1648–1658. doi: 10.1111/j.1460-9568.2005.04006.x
- Inoue, H., Ohtaki, H., Nakamachi, T., Shioda, S., and Okada, Y. (2007). Anion channel blockers attenuate delayed neuronal cell death induced by transient forebrain ischemia. *J. Neurosci. Res.* 85, 1427–1435. doi: 10.1002/jnr.21279
- Inoue, H., Takahashi, N., Okada, Y., and Konishi, M. (2010). Volume-sensitive outwardly rectifying chloride channel in white adipocytes from normal and diabetic mice. *Am. J. Physiol. Cell Physiol.* 298, C900–C909. doi: 10.1152/ajpcell.00450.2009
- Ise, T., Shimizu, T., Lee, E. L., Inoue, H., Kohno, K., and Okada, Y. (2005). Roles of volume-sensitive Cl^{-} channel in cisplatin-induced apoptosis in human epidermoid cancer cells. *J. Membr. Biol.* 205, 139–145. doi: 10.1007/s00232-005-0779-y
- Islam, M. R., Uramoto, H., Okada, T., Sabirov, R. Z., and Okada, Y. (2012). Maxi-anion channel and pannexin 1 hemichannel constitute separate pathways for swelling-induced ATP release in murine L929 fibrosarcoma cells. *Am. J. Physiol. Cell Physiol.* 303, C924–C935. doi: 10.1152/ajpcell.00459.2011
- Jackson, P. S., Morrison, R., and Strange, K. (1994). The volume-sensitive organic osmolyte-anion channel VSOAC is regulated by nonhydrolytic ATP binding. *Am. J. Physiol.* 267(5 Pt 1), C1203–C1209. doi: 10.1152/ajpcell.1994.267.5.C1203
- Jackson, P. S., and Strange, K. (1995). Characterization of the voltage-dependent properties of a volume-sensitive anion conductance. *J. Gen. Physiol.* 105, 661–676. doi: 10.1085/jgp.105.5.661
- Jentsch, T. J., Lutter, D., Planells-Cases, R., Ullrich, F., and Voss, F. K. (2016). VRAC: molecular identification as LRRC8 heteromers with differential functions. *Pflugers Arch.* 468, 385–393. doi: 10.1007/s00424-015-1766-5
- Jiang, J., Li, M., and Yue, L. (2005). Potentiation of TRPM7 inward currents by protons. *J. Gen. Physiol.* 126, 137–150. doi: 10.1085/jgp.200409185
- Jouan-Lanhouet, S., Arshad, M. I., Piquet-Pellorce, C., Martin-Chouly, C., Le Moigne-Muller, G., Van Herreweghe, F., et al. (2012). TRAIL induces necroptosis involving RIPK1/RIPK3-dependent PARP-1 activation. *Cell Death Differ.* 19, 2003–2014. doi: 10.1038/cdd.2012.90
- Kaiser, W. J., Upton, J. W., and Mocarski, E. S. (2013). Viral modulation of programmed necrosis. *Curr. Opin. Virol.* 3, 296–306. doi: 10.1016/j.coviro.2013.05.019
- Kasuya, G., Nakane, T., Yokoyama, T., Jia, Y., Inoue, M., Watanabe, K., et al. (2018). Cryo-EM structures of the human volume-regulated anion channel LRRC8. *Nat. Struct. Mol. Biol.* 25, 797–804. doi: 10.1038/s41594-018-0109-6
- Kefauver, J. M., Saotome, K., Dubin, A. E., Pallesen, J., Cottrell, C. A., Cahalan, S. M., et al. (2018). Structure of the human volume regulated anion channel. *eLife* 7:e38461. doi: 10.7554/eLife.38461
- Kenagy, R. D., Min, S. K., Mulvihill, E., and Clowes, A. W. (2011). A link between smooth muscle cell death and extracellular matrix degradation during vascular atrophy. *J. Vasc. Surg.* 54, 182–191.e24. doi: 10.1016/j.jvs.2010.12.070
- Kern, D. M., Oh, S., Hite, R. K., and Brohawn, S. G. (2019). Cryo-EM structures of the DCPIB-inhibited volume-regulated anion channel LRRC8A in lipid nanodiscs. *eLife* 8:e42636. doi: 10.7554/eLife.42636
- Kimelberg, H. K. (2004). Water homeostasis in the brain: basic concepts. *Neuroscience* 129, 851–860. doi: 10.1016/j.neuroscience.2004.07.033
- Kimelberg, H. K. (2005). Astrocytic swelling in cerebral ischemia as a possible cause of injury and target for therapy. *Glia* 50, 389–397. doi: 10.1002/glia.20174
- Kimelberg, H. K., Feustel, P. J., Jin, Y., Paquette, J., Boulos, A., Keller, R. W., et al. (2000). Acute treatment with tamoxifen reduces ischemic damage following middle cerebral artery occlusion. *Neuroreport* 11, 2675–2679. doi: 10.1097/00001756-200008210-00014
- Kimelberg, H. K., Goderie, S. K., Higman, S., Pang, S., and Wanievski, R. A. (1990). Swelling-induced release of glutamate, aspartate, and taurine from astrocyte cultures. *J. Neurosci.* 10, 1583–1591. doi: 10.1523/jneurosci.10-05-01583.1990
- Kimelberg, H. K., Jin, Y., Charniga, C., and Feustel, P. J. (2003). Neuroprotective activity of tamoxifen in permanent focal ischemia. *J. Neurosurg.* 99, 138–142. doi: 10.3171/jns.2003.99.1.0138
- Kimelberg, H. K., Nestor, N. B., and Feustel, P. J. (2004). Inhibition of release of taurine and excitatory amino acids in ischemia and neuroprotection. *Neurochem. Res.* 29, 267–274. doi: 10.1023/b:nere.0000010455.78121.53
- Kittl, M., Helm, K., Beyreis, M., Mayr, C., Gaisberger, M., Winklmayr, M., et al. (2019). Acid- and volume-sensitive chloride currents in microglial cells. *Int. J. Mol. Sci.* 20:3475. doi: 10.3390/ijms20143475

- Kobe, B., and Kajava, A. V. (2001). The leucine-rich repeat as a protein recognition motif. *Curr. Opin. Struct. Biol.* 11, 725–732. doi: 10.1016/s0959-440x(01)00266-4
- König, B., and Stauber, T. (2019). Biophysics and structure-function relationships of LRRC8-formed volume-regulated anion channels. *Biophys. J.* 116, 1185–1193. doi: 10.1016/j.bpj.2019.02.014
- Kraig, R. P., Petito, C. K., Plum, F., and Pulsinelli, W. A. (1987). Hydrogen ions kill brain at concentrations reached in ischemia. *J. Cereb. Blood Flow Metab.* 7, 379–386. doi: 10.1038/jcbfm.1987.80
- Krasilnikov, O. V., Sabirov, R. Z., and Okada, Y. (2011). ATP hydrolysis-dependent asymmetry of the conformation of CFTR channel pore. *J. Physiol. Sci.* 61, 267–278. doi: 10.1007/s12576-011-0144-0
- Kubo, M., and Okada, Y. (1992). Volume-regulatory Cl^- channel currents in cultured human epithelial cells. *J. Physiol.* 456, 351–371. doi: 10.1113/jphysiol.1992.sp019340
- Kumagai, K., Toyoda, F., Staunton, C. A., Maeda, T., Okumura, N., Matsuura, H., et al. (2016). Activation of a chondrocyte volume-sensitive Cl^- conductance prior to macroscopic cartilage lesion formation in the rabbit knee anterior cruciate ligament transection osteoarthritis model. *Osteoarthritis Cartilage* 24, 1786–1794. doi: 10.1016/j.joca.2016.05.019
- Kurbannazarova, R. S., Bessonova, S. V., Okada, Y., and Sabirov, R. Z. (2011). Swelling-activated anion channels are essential for volume regulation of mouse thymocytes. *Int. J. Mol. Sci.* 12, 9125–9137. doi: 10.3390/ijms12129125
- Kurbannazarova, R. S., Tashmukhamedov, B. A., and Sabirov, R. Z. (2003). Osmotic water permeability and regulatory volume decrease of rat thymocytes. *Gen. Physiol. Biophys.* 22, 221–232.
- Lang, F. (2006). *Mechanisms and Significance of Cell Volume Regulation*. Basel: Karger.
- Lang, F., Busch, G. L., Ritter, M., Völkl, H., Waldegger, S., Gulbins, E., et al. (1998). Functional significance of cell volume regulatory mechanisms. *Physiol. Rev.* 78, 247–306. doi: 10.1152/physrev.1998.78.1.247
- Lauf, P. K. (1985). $\text{K}^+:\text{Cl}^-$ cotransport: sulfhydryls, divalent cations, and the mechanism of volume activation in a red cell. *J. Membr. Biol.* 88, 1–13. doi: 10.1007/bf01871208
- Leaney, J. L., Marsh, S. J., and Brown, D. A. (1997). A swelling-activated chloride current in rat sympathetic neurones. *J. Physiol.* 501(Pt 3), 555–564. doi: 10.1111/j.1469-7793.1997.555bm.x
- Lee, C. C., Freinkman, E., Sabatini, D. M., and Ploegh, H. L. (2014). The protein synthesis inhibitor blasticidin S enters mammalian cells via leucine-rich repeat-containing protein 8D. *J. Biol. Chem.* 289, 17124–17131. doi: 10.1074/jbc.M114.571257
- Lee, E. L., Shimizu, T., Ise, T., Numata, T., Kohno, K., and Okada, Y. (2007). Impaired activity of volume-sensitive Cl^- channel is involved in cisplatin resistance of cancer cells. *J. Cell. Physiol.* 211, 513–521. doi: 10.1002/jcp.20961
- Lei, P., Bai, T., and Sun, Y. (2019). Mechanisms of ferroptosis and relations with regulated cell death: a review. *Front. Physiol.* 10:139. doi: 10.3389/fphys.2019.00139
- Leist, M., Single, B., Castoldi, A. F., Kühnle, S., and Nicotera, P. (1997). Intracellular adenosine triphosphate (ATP) concentration: a switch in the decision between apoptosis and necrosis. *J. Exp. Med.* 185, 1481–1486. doi: 10.1084/jem.185.8.1481
- Levitan, I., and Garber, S. S. (1998). Anion competition for a volume-regulated current. *Biophys. J.* 75, 226–235. doi: 10.1016/s0006-3495(98)77509-5
- Lewerenz, J., and Maher, P. (2015). Chronic glutamate toxicity in neurodegenerative diseases—What is the evidence? *Front. Neurosci.* 9:469. doi: 10.3389/fnins.2015.00469
- l'Hoste, S., Chargui, A., Belfodil, R., Corcelle, E., Duranton, C., Rubera, I., et al. (2010). CFTR mediates apoptotic volume decrease and cell death by controlling glutathione efflux and ROS production in cultured mice proximal tubules. *Am. J. Physiol. Renal Physiol.* 298, F435–F453. doi: 10.1152/ajprenal.00286.2009
- Linden, J., Koch-Nolte, F., and Dahl, G. (2019). Purine release, metabolism, and signaling in the inflammatory response. *Annu. Rev. Immunol.* 37, 325–347. doi: 10.1146/annurev-immunol-051116-052406
- Linsdell, P., and Hanrahan, J. W. (1998). Adenosine triphosphate-dependent asymmetry of anion permeation in the cystic fibrosis transmembrane conductance regulator chloride channel. *J. Gen. Physiol.* 111, 601–614. doi: 10.1085/jgp.111.4.601
- Liu, H. T., Akita, T., Shimizu, T., Sabirov, R. Z., and Okada, Y. (2009). Bradykinin-induced astrocyte-neuron signalling: glutamate release is mediated by ROS-activated volume-sensitive outwardly rectifying anion channels. *J. Physiol.* 587(Pt 10), 2197–2209. doi: 10.1113/jphysiol.2008.165084
- Liu, H. T., Sabirov, R. Z., and Okada, Y. (2008a). Oxygen-glucose deprivation induces ATP release via maxi-anion channels in astrocytes. *Purinergic Signal.* 4, 147–154. doi: 10.1007/s11302-007-9077-8
- Liu, H. T., Tashmukhamedov, B. A., Inoue, H., Okada, Y., and Sabirov, R. Z. (2006). Roles of two types of anion channels in glutamate release from mouse astrocytes under ischemic or osmotic stress. *Glia* 54, 343–357. doi: 10.1002/glia.20400
- Liu, H. T., Toychiev, A. H., Takahashi, N., Sabirov, R. Z., and Okada, Y. (2008b). Maxi-anion channel as a candidate pathway for osmosensitive ATP release from mouse astrocytes in primary culture. *Cell Res.* 18, 558–565. doi: 10.1038/cr.2008.49
- Liu, Y., Wang, B., Zhang, W. W., Liu, J. N., Shen, M. Z., Ding, M. G., et al. (2013). Modulation of staurosporine-activated volume-sensitive outwardly rectifying Cl^- channel by PI3K/Akt in cardiomyocytes. *Curr. Pharm. Des.* 19, 4859–4864. doi: 10.2174/1381612811319270008
- Lutter, D., Ullrich, F., Lueck, J. C., Kempa, S., and Jentsch, T. J. (2017). Selective transport of neurotransmitters and modulators by distinct volume-regulated LRRC8 anion channels. *J. Cell Sci.* 130, 1122–1133. doi: 10.1242/jcs.196253
- Maeno, E., Ishizaki, Y., Kanaseki, T., Hazama, A., and Okada, Y. (2000). Normotonic cell shrinkage because of disordered volume regulation is an early prerequisite to apoptosis. *Proc. Natl. Acad. Sci. U.S.A.* 97, 9487–9492. doi: 10.1073/pnas.140216197
- Maeno, E., Shimizu, T., and Okada, Y. (2006a). Normotonic cell shrinkage induces apoptosis under extracellular low Cl^- conditions in human lymphoid and epithelial cells. *Acta Physiol.* 187, 217–222. doi: 10.1111/j.1748-1716.2006.01554.x
- Maeno, E., Takahashi, N., and Okada, Y. (2006b). Dysfunction of regulatory volume increase is a key component of apoptosis. *FEBS Lett.* 580, 6513–6517. doi: 10.1016/j.febslet.2006.10.074
- Maeno, E., Tsubata, T., and Okada, Y. (2012). Apoptotic volume decrease (AVD) is independent of mitochondrial dysfunction and initiator caspase activation. *Cells* 1, 1156–1167. doi: 10.3390/cells1041156
- Marmarou, A. (1992). Intracellular acidosis in human and experimental brain injury. *J. Neurotrauma* 9(Suppl. 2), S551–S562.
- Matsumaru, K., Ji, C., and Kaplowitz, N. (2003). Mechanisms for sensitization to TNF-induced apoptosis by acute glutathione depletion in murine hepatocytes. *Hepatology* 37, 1425–1434. doi: 10.1053/jhep.2003.50230
- Meister, A. (1995). Glutathione metabolism. *Methods Enzymol.* 251, 3–7. doi: 10.1016/0076-6879(95)51106-7
- Meister, A., and Anderson, M. E. (1983). Glutathione. *Annu. Rev. Biochem.* 52, 711–760. doi: 10.1146/annurev.bi.52.070183.003431
- Meldrum, B. S. (2000). Glutamate as a neurotransmitter in the brain: review of physiology and pathology. *J. Nutr.* 130(4S Suppl.), 1007s–1015s. doi: 10.1093/jn/130.4.1007S
- Menegaz, D., Hagan, D. W., Almacá, J., Cianciaruso, C., Rodriguez-Diaz, R., Molina, J., et al. (2019). Mechanism and effects of pulsatile GABA secretion from cytosolic pools in the human beta cell. *Nat. Metab.* 1, 1110–1126. doi: 10.1038/s42255-019-0135-7
- Min, X. J., Li, H., Hou, S. C., He, W., Liu, J., Hu, B., et al. (2011). Dysfunction of volume-sensitive chloride channels contributes to cisplatin resistance in human lung adenocarcinoma cells. *Exp. Biol. Med.* 236, 483–491. doi: 10.1258/ebm.2011.010297
- Minich, T., Riemer, J., Schulz, J. B., Wieling, P., Wijnholds, J., and Dringen, R. (2006). The multidrug resistance protein 1 (Mrp1), but not Mrp5, mediates export of glutathione and glutathione disulfide from brain astrocytes. *J. Neurochem.* 97, 373–384. doi: 10.1111/j.1471-4159.2006.03737.x
- Mitchell, C. H., Fleischhauer, J. C., Stamer, W. D., Peterson-Yantorno, K., and Civan, M. M. (2002). Human trabecular meshwork cell volume regulation. *Am. J. Physiol. Cell Physiol.* 283, C315–C326. doi: 10.1152/ajpcell.00544.2001
- Mongin, A. A. (2007). Disruption of ionic and cell volume homeostasis in cerebral ischemia: the perfect storm. *Pathophysiology* 14, 183–193. doi: 10.1016/j.pathophys.2007.09.009
- Mongin, A. A. (2016). Volume-regulated anion channel—a frenemy within the brain. *Pflugers Arch.* 468, 421–441. doi: 10.1007/s00424-015-1765-6

- Mongin, A. A., and Kimelberg, H. K. (2002). ATP potently modulates anion channel-mediated excitatory amino acid release from cultured astrocytes. *Am. J. Physiol. Cell Physiol.* 283, C569–C578. doi: 10.1152/ajpcell.00438.2001
- Mongin, A. A., and Kimelberg, H. K. (2005). ATP regulates anion channel-mediated organic osmolyte release from cultured rat astrocytes via multiple Ca^{2+} -sensitive mechanisms. *Am. J. Physiol. Cell Physiol.* 288, C204–C213. doi: 10.1152/ajpcell.00330.2004
- Mongin, A. A., Reddi, J. M., Charniga, C., and Kimelberg, H. K. (1999). [3H]taurine and D-[3H]aspartate release from astrocyte cultures are differently regulated by tyrosine kinases. *Am. J. Physiol.* 276, C1226–C1230. doi: 10.1152/ajpcell.1999.276.5.C1226
- Mori, S., Morishima, S., Takasaki, M., and Okada, Y. (2002). Impaired activity of volume-sensitive anion channel during lacticidosis-induced swelling in neurally differentiated NG108-15 cells. *Brain Res.* 957, 1–11. doi: 10.1016/s0006-8993(02)03574-6
- Nabekura, T., Morishima, S., Cover, T. L., Mori, S., Kannan, H., Komune, S., et al. (2003). Recovery from lacticidosis-induced glial cell swelling with the aid of exogenous anion channels. *Glia* 41, 247–259. doi: 10.1002/glia.10190
- Nakamura, R., Numata, T., Kasuya, G., Yokoyama, T., Nishizawa, T., Kusakizako, T., et al. (2020). Cryo-EM structure of the volume-regulated anion channel LRRC8D isoform identifies features important for substrate permeation. *Commun. Biol.* 3:240. doi: 10.1038/s42003-020-0951-z
- Netti, V., Pizzoni, A., Pérez-Domínguez, M., Ford, P., Pasantes-Morales, H., Ramos-Mandujano, G., et al. (2018). Release of taurine and glutamate contributes to cell volume regulation in human retinal Müller cells: differences in modulation by calcium. *J. Neurophysiol.* 120, 973–984. doi: 10.1152/jn.00725.2017
- Nicholson, C. (2005). Factors governing diffusing molecular signals in brain extracellular space. *J. Neural Transm.* 112, 29–44. doi: 10.1007/s00702-004-0204-1
- Nilius, B., and Droogmans, G. (2003). Amazing chloride channels: an overview. *Acta Physiol. Scand.* 177, 119–147. doi: 10.1046/j.1365-201X.2003.01060.x
- Nilius, B., Eggermont, J., Voets, T., Buyse, G., Manolopoulos, V., and Droogmans, G. (1997). Properties of volume-regulated anion channels in mammalian cells. *Prog. Biophys. Mol. Biol.* 68, 69–119. doi: 10.1016/s0079-6107(97)00021-7
- Nilius, B., Sehr, J., De Smet, P., Van Driessche, W., and Droogmans, G. (1995). Volume regulation in a toad epithelial cell line: role of coactivation of K^+ and Cl^- channels. *J. Physiol.* 487(Pt 2), 367–378. doi: 10.1113/jphysiol.1995.sp020886
- Nilius, B., Voets, T., Eggermont, J., and Droogmans, G. (1999). “VRAC: a multifunctional volume regulated anion channel,” in *The Chloride Channels*, ed. R. Kozłowski (Oxford: Isis Medical Media Limited), 47–63.
- Ninomiya, H., Otani, H., Lu, K., Uchiyama, T., Kido, M., and Imamura, H. (2002). Complementary role of extracellular ATP and adenosine in ischemic preconditioning in the rat heart. *Am. J. Physiol. Heart Circ. Physiol.* 282, H1810–H1820. doi: 10.1152/ajpheart.00760.2001
- Nukui, M., Shimizu, T., and Okada, Y. (2006). Normotonic cell shrinkage induced by Na^+ deprivation results in apoptotic cell death in human epithelial HeLa cells. *J. Physiol. Sci.* 56, 335–339. doi: 10.2170/physiolsci.RP009606
- Numata, T., Sato-Numata, K., and Okada, Y. (2019). TRPM7 is involved in acid-induced necrotic cell death in a manner sensitive to progesterone in human cervical cancer cells. *Physiol. Rep.* 7:e14157. doi: 10.14814/phy2.14157
- Oiki, S., Kubo, M., and Okada, Y. (1994). Mg^{2+} and ATP-dependence of volume-sensitive Cl^- channels in human epithelial cells. *Jpn. J. Physiol.* 44(Suppl. 2), S77–S79.
- Oja, S. S., and Saransaari, P. (2017). Significance of taurine in the brain. *Adv. Exp. Med. Biol.* 975(Pt 1), 89–94. doi: 10.1007/978-94-024-1079-2_8
- Okada, T., Islam, M. R., Tsiferova, N. A., Okada, Y., and Sabirov, R. Z. (2017). Specific and essential but not sufficient roles of LRRC8A in the activity of volume-sensitive outwardly rectifying anion channel (VSOR). *Channels* 11, 109–120. doi: 10.1080/19336950.2016.1247133
- Okada, Y. (1997). Volume expansion-sensing outward-rectifier Cl^- channel: fresh start to the molecular identity and volume sensor. *Am. J. Physiol.* 273(3 Pt 1), C755–C789. doi: 10.1152/ajpcell.1997.273.3.C755
- Okada, Y. (1998). *Cell Volume Regulation: The Molecular Mechanism and Volume Sensing Machinery*. Amsterdam: Elsevier.
- Okada, Y. (2004). Ion channels and transporters involved in cell volume regulation and sensor mechanisms. *Cell Biochem. Biophys.* 41, 233–258.
- Okada, Y. (2019). Tweety homologs (TTYH) freshly join the journey of molecular identification of the VRAC/VSOR channel pore. *Exp. Neurobiol.* 28, 131–133. doi: 10.5607/en.2019.28.2.131
- Okada, Y., Maeno, E., Shimizu, T., Dezaki, K., Wang, J., and Morishima, S. (2001). Receptor-mediated control of regulatory volume decrease (RVD) and apoptotic volume decrease (AVD). *J. Physiol.* 532(Pt 1), 3–16. doi: 10.1111/j.1469-7793.2001.0003g.x
- Okada, Y., Maeno, E., Shimizu, T., Manabe, K., Mori, S., and Nabekura, T. (2004). Dual roles of plasmalemmal chloride channels in induction of cell death. *Pflügers Arch.* 448, 287–295. doi: 10.1007/s00424-004-1276-3
- Okada, Y., Numata, T., Sato-Numata, K., Sabirov, R. Z., Liu, H., Mori, S. I., et al. (2019a). Roles of volume-regulatory anion channels, VSOR and Maxi-Cl, in apoptosis, cisplatin resistance, necrosis, ischemic cell death, stroke and myocardial infarction. *Curr. Top. Membr.* 83, 205–283. doi: 10.1016/bs.ctm.2019.03.001
- Okada, Y., Okada, T., Islam, M. R., and Sabirov, R. Z. (2018). Molecular identities and ATP release activities of two types of volume-regulatory anion channels, VSOR and Maxi-Cl. *Curr. Top. Membr.* 81, 125–176. doi: 10.1016/bs.ctm.2018.07.004
- Okada, Y., Okada, T., Sato-Numata, K., Islam, M. R., Ando-Akatsuka, Y., Numata, T., et al. (2019b). Cell volume-activated and volume-correlated anion channels in mammalian cells: their biophysical, molecular, and pharmacological properties. *Pharmacol. Rev.* 71, 49–88. doi: 10.1124/pr.118.015917
- Okada, Y., Okada, T., Sato-Numata, K., and Numata, T. (2020). Reexamination of the roles of LRRC8 and TTYH in the molecular identity of volume-sensitive outwardly rectifying anion channel VSOR. *J. Physiol. Sci.* 70(Suppl. 1):S150.
- Okada, Y., Shimizu, T., Maeno, E., Tanabe, S., Wang, X., and Takahashi, N. (2006). Volume-sensitive chloride channels involved in apoptotic volume decrease and cell death. *J. Membr. Biol.* 209, 21–29. doi: 10.1007/s00232-005-0836-6
- Okumura, N., Imai, S., Toyoda, F., Isoya, E., Kumagai, K., Matsuura, H., et al. (2009). Regulatory role of tyrosine phosphorylation in the swelling-activated chloride current in isolated rabbit articular chondrocytes. *J. Physiol.* 587(Pt 15), 3761–3776. doi: 10.1113/jphysiol.2009.174177
- Olney, J. W. (1969). Brain lesions, obesity, and other disturbances in mice treated with monosodium glutamate. *Science* 164, 719–721. doi: 10.1126/science.164.3880.719
- Olney, J. W., Adamo, N. J., and Ratner, A. (1971). Monosodium glutamate effects. *Science* 172:294. doi: 10.1126/science.172.3980.294
- Olney, J. W., Price, M. T., Samson, L., and Labruyere, J. (1986). The role of specific ions in glutamate neurotoxicity. *Neurosci. Lett.* 65, 65–71. doi: 10.1016/0304-3940(86)90121-7
- Osei-Owusu, J., Yang, J., Vitery, M. D. C., and Qiu, Z. (2018). Molecular Biology and Physiology of Volume-Regulated Anion Channel (VRAC). *Curr. Top. Membr.* 81, 177–203. doi: 10.1016/bs.ctm.2018.07.005
- Parkerson, K. A., and Sontheimer, H. (2004). Biophysical and pharmacological characterization of hypotonically activated chloride currents in cortical astrocytes. *Glia* 46, 419–436. doi: 10.1002/glia.10361
- Parpura, V., Scemes, E., and Spray, D. C. (2004). Mechanisms of glutamate release from astrocytes: gap junction “hemichannels”, purinergic receptors and exocytotic release. *Neurochem. Int.* 45, 259–264. doi: 10.1016/j.neuint.2003.12.011
- Pasantes-Morales, H., Franco, R., Ochoa, L., and Ordaz, B. (2002). Osmosensitive release of neurotransmitter amino acids: relevance and mechanisms. *Neurochem. Res.* 27, 59–65. doi: 10.1023/a:1014850505400
- Pasantes-Morales, H., Sánchez Olea, R., Miranda, D., and Morán, J. (1997). Volume regulation in NIH/3T3 cells not expressing P-glycoprotein. I. Regulatory volume decrease. *Am. J. Physiol.* 272(6 Pt 1), C1798–C1803. doi: 10.1152/ajpcell.1997.272.6.C1798
- Patel, A. J., Lauritzen, I., Lazdunski, M., and Honoré, E. (1998). Disruption of mitochondrial respiration inhibits volume-regulated anion channels and provokes neuronal cell swelling. *J. Neurosci.* 18, 3117–3123. doi: 10.1523/jneurosci.18-09-03117.1998
- Pedersen, S. F., Okada, Y., and Nilius, B. (2016). Biophysics and Physiology of the Volume-Regulated Anion Channel (VRAC)/Volume-Sensitive Outwardly Rectifying Anion Channel (VSOR). *Pflügers Arch.* 468, 371–383. doi: 10.1007/s00424-015-1781-6

- Phillis, J. W., and O'Regan, M. H. (2003). Characterization of modes of release of amino acids in the ischemic/reperfused rat cerebral cortex. *Neurochem. Int.* 43, 461–467. doi: 10.1016/s0197-0186(03)00035-4
- Phillis, J. W., Song, D., and O'Regan, M. H. (1997). Inhibition by anion channel blockers of ischemia-evoked release of excitotoxic and other amino acids from rat cerebral cortex. *Brain Res.* 758, 9–16. doi: 10.1016/s0006-8993(97)00155-8
- Phillis, J. W., Song, D., and O'Regan, M. H. (1998). Tamoxifen, a chloride channel blocker, reduces glutamate and aspartate release from the ischemic cerebral cortex. *Brain Res.* 780, 352–355. doi: 10.1016/s0006-8993(97)01352-8
- Pin, J. P., and Bockaert, J. (1989). Two distinct mechanisms, differentially affected by excitatory amino acids, trigger GABA release from fetal mouse striatal neurons in primary culture. *J. Neurosci.* 9, 648–656. doi: 10.1523/jneurosci.09-02-00648.1989
- Planells-Cases, R., Lutter, D., Guyader, C., Gerhards, N. M., Ullrich, F., Elger, D. A., et al. (2015). Subunit composition of VRAC channels determines substrate specificity and cellular resistance to Pt-based anti-cancer drugs. *EMBO J.* 34, 2993–3008. doi: 10.15252/embj.201592409
- Ponce, A., Jimenez-Peña, L., and Tejeda-Guzman, C. (2012). The role of swelling-activated chloride currents (ICL_{swell}) in the regulatory volume decrease response of freshly dissociated rat articular chondrocytes. *Cell. Physiol. Biochem.* 30, 1254–1270. doi: 10.1159/000343316
- Porcelli, A. M., Ghelli, A., Zanna, C., Valente, P., Ferroni, S., and Rugolo, M. (2003). Staurosporine induces apoptotic volume decrease (AVD) in ECV304 cells. *Ann. N.Y. Acad. Sci.* 1010, 342–346. doi: 10.1196/annals.1299.062
- Poulsen, K. A., Andersen, E. C., Hansen, C. F., Klausen, T. K., Hougaard, C., Lambert, I. H., et al. (2010). Deregulation of apoptotic volume decrease and ionic movements in multidrug-resistant tumor cells: role of chloride channels. *Am. J. Physiol. Cell Physiol.* 298, C14–C25. doi: 10.1152/ajpcell.00654.2008
- Qiu, Z., Dubin, A. E., Mathur, J., Tu, B., Reddy, K., Miraglia, L. J., et al. (2014). SWELL1, a plasma membrane protein, is an essential component of volume-regulated anion channel. *Cell* 157, 447–458. doi: 10.1016/j.cell.2014.03.024
- Robson, L., and Hunter, M. (1994). Volume regulatory responses in frog isolated proximal cells. *Pflügers Arch.* 428, 60–68. doi: 10.1007/bf00374752
- Rodrigues, G. R., Kandraticius, L., Peixoto-Santos, J. E., Monteiro, M. R., Gargaro, A. C., Geraldi Cde, V., et al. (2015). Increased frequency of hippocampal sclerosis ILAE type 2 in patients with mesial temporal lobe epilepsy with normal episodic memory. *Brain* 138(Pt 6), e359. doi: 10.1093/brain/awu340
- Ros, U., Peña-Blanco, A., Hänggi, K., Kunzendorf, U., Krautwald, S., Wong, W. W., et al. (2017). Necroptosis execution is mediated by plasma membrane nanopores independent of calcium. *Cell Rep.* 19, 175–187. doi: 10.1016/j.celrep.2017.03.024
- Rothman, S. M. (1985). The neurotoxicity of excitatory amino acids is produced by passive chloride influx. *J. Neurosci.* 5, 1483–1489. doi: 10.1523/jneurosci.05-06-01483.1985
- Roy, G. (1995). Amino acid current through anion channels in cultured human glial cells. *J. Membr. Biol.* 147, 35–44. doi: 10.1007/bf00235396
- Roy, G., and Banderali, U. (1994). Channels for ions and amino acids in kidney cultured cells (MDCK) during volume regulation. *J. Exp. Zool.* 268, 121–126. doi: 10.1002/jez.1402680208
- Ruan, J., Xia, S., Liu, X., Lieberman, J., and Wu, H. (2018). Cryo-EM structure of the gasdermin A3 membrane pore. *Nature* 557, 62–67. doi: 10.1038/s41586-018-0058-6
- Rudkouskaya, A., Chernoguz, A., Haskew-Layton, R. E., and Mongin, A. A. (2008). Two conventional protein kinase C isoforms, alpha and beta I, are involved in the ATP-induced activation of volume-regulated anion channel and glutamate release in cultured astrocytes. *J. Neurochem.* 105, 2260–2270. doi: 10.1111/j.1471-4159.2008.05312.x
- Sabirov, R. Z., Dutta, A. K., and Okada, Y. (2001). Volume-dependent ATP-conductive large-conductance anion channel as a pathway for swelling-induced ATP release. *J. Gen. Physiol.* 118, 251–266. doi: 10.1085/jgp.118.3.251
- Sabirov, R. Z., Kurbannazarova, R. S., Melanova, N. R., and Okada, Y. (2013). Volume-sensitive anion channels mediate osmosensitive glutathione release from rat thymocytes. *PLoS One* 8:e55646. doi: 10.1371/journal.pone.0055646
- Sabirov, R. Z., Merzlyak, P. G., Islam, M. R., Okada, T., and Okada, Y. (2016). The properties, functions, and pathophysiology of maxi-anion channels. *Pflügers Arch.* 468, 405–420. doi: 10.1007/s00424-015-1774-5
- Sabirov, R. Z., and Okada, Y. (2005). ATP release via anion channels. *Purinergic Signal.* 1, 311–328. doi: 10.1007/s11302-005-1557-0
- Sabirov, R. Z., Prenen, J., Droogmans, G., and Nilius, B. (2000). Extra- and intracellular proton-binding sites of volume-regulated anion channels. *J. Membr. Biol.* 177, 13–22. doi: 10.1007/s002320001090
- Sakai, H., Nakamura, F., and Kuno, M. (1999). Synergetic activation of outwardly rectifying Cl⁻ currents by hypotonic stress and external Ca²⁺ in murine osteoclasts. *J. Physiol.* 515(Pt 1), 157–168. doi: 10.1111/j.1469-7793.1999.157ad.x
- Sarkadi, B., Attisano, L., Grinstein, S., Buchwald, M., and Rothstein, A. (1984a). Volume regulation of Chinese hamster ovary cells in anisoosmotic media. *Biochim. Biophys. Acta* 774, 159–168. doi: 10.1016/0005-2736(84)90287-6
- Sarkadi, B., Cheung, R., Mack, E., Grinstein, S., Gelfand, E. W., and Rothstein, A. (1985). Cation and anion transport pathways in volume regulatory response of human lymphocytes to hyposmotic media. *Am. J. Physiol.* 248(5 Pt 1), C480–C487. doi: 10.1152/ajpcell.1985.248.5.C480
- Sarkadi, B., Mack, E., and Rothstein, A. (1984b). Ionic events during the volume response of human peripheral blood lymphocytes to hypotonic media. II. Volume- and time-dependent activation and inactivation of ion transport pathways. *J. Gen. Physiol.* 83, 513–527. doi: 10.1085/jgp.83.4.513
- Sato, K., Numata, T., Saito, T., Ueta, Y., and Okada, Y. (2011). V2 receptor-mediated autocrine role of somatodendritic release of AVP in rat vasopressin neurons under hypo-osmotic conditions. *Sci. Signal.* 4:ra5. doi: 10.1126/scisignal.2001279
- Sauler, M., Bazan, I. S., and Lee, P. J. (2019). Cell death in the lung: the apoptosis-necroptosis axis. *Annu. Rev. Physiol.* 81, 375–402. doi: 10.1146/annurev-physiol-020518-114320
- Sborgi, L., Rühl, S., Mulvihill, E., Pipercevic, J., Heilig, R., Stahlberg, H., et al. (2016). GSDMD membrane pore formation constitutes the mechanism of pyroptotic cell death. *EMBO J.* 35, 1766–1778. doi: 10.15252/embj.201694696
- Schlichter, L. C., Mertens, T., and Liu, B. (2011). Swelling activated Cl⁻ channels in microglia: biophysics, pharmacology and role in glutamate release. *Channels* 5, 128–137. doi: 10.4161/chan.5.2.14310
- Schmid, A., Blum, R., and Krause, E. (1998). Characterization of cell volume-sensitive chloride currents in freshly prepared and cultured pancreatic acinar cells from early postnatal rats. *J. Physiol.* 513(Pt 2), 453–465. doi: 10.1111/j.1469-7793.1998.453bb.x
- Schober, A. L., Wilson, C. S., and Mongin, A. A. (2017). Molecular composition and heterogeneity of the LRRC8-containing swelling-activated osmolyte channels in primary rat astrocytes. *J. Physiol.* 595, 6939–6951. doi: 10.1113/jp275053
- Seki, Y., Feustel, P. J., Keller, R. W. Jr., Tranmer, B. I., and Kimelberg, H. K. (1999). Inhibition of ischemia-induced glutamate release in rat striatum by dihydrokinate and an anion channel blocker. *Stroke* 30, 433–440. doi: 10.1161/01.str.30.2.433
- Shen, M., Wang, L., Wang, B., Wang, T., Yang, G., Shen, L., et al. (2014a). Activation of volume-sensitive outwardly rectifying chloride channel by ROS contributes to ER stress and cardiac contractile dysfunction: involvement of CHOP through Wnt. *Cell Death Dis.* 5:e1528. doi: 10.1038/cddis.2014.479
- Shen, M., Wang, L., Yang, G., Gao, L., Wang, B., Guo, X., et al. (2014b). Baicalin protects the cardiomyocytes from ER stress-induced apoptosis: inhibition of CHOP through induction of endothelial nitric oxide synthase. *PLoS One* 9:e88389. doi: 10.1371/journal.pone.0088389
- Shen, M. R., Wu, S. N., and Chou, C. Y. (1996). Volume-sensitive chloride channels in the primary culture cells of human cervical carcinoma. *Biochim. Biophys. Acta* 1315, 138–144. doi: 10.1016/0925-4439(95)00115-8
- Shimizu, T., Fujii, T., Ohtake, H., Tomii, T., Takahashi, R., Kawashima, K., et al. (2020). Impaired actin filaments decrease cisplatin sensitivity via dysfunction of volume-sensitive Cl⁻ channels in human epidermoid carcinoma cells. *J. Cell. Physiol.* 235, 9589–9600. doi: 10.1002/jcp.29767
- Shimizu, T., Lee, E. L., Ise, T., and Okada, Y. (2008). Volume-sensitive Cl⁻ channel as a regulator of acquired cisplatin resistance. *Anticancer Res.* 28, 75–83.
- Shimizu, T., Numata, T., and Okada, Y. (2004). A role of reactive oxygen species in apoptotic activation of volume-sensitive Cl⁻ channel. *Proc. Natl. Acad. Sci. U.S.A.* 101, 6770–6773. doi: 10.1073/pnas.0401604101
- Shimizu, T., Ohtake, H., Fujii, T., Tabuchi, Y., and Sakai, H. (2015). Volume-sensitive outwardly rectifying Cl⁻ channels contribute to butyrate-triggered apoptosis of murine colonic epithelial MCE301 cells. *J. Physiol. Sci.* 65, 151–157. doi: 10.1007/s12576-014-0352-5

- Siesjö, B. K. (1988). Acidosis and ischemic brain damage. *Neurochem. Pathol.* 9, 31–88. doi: 10.1007/bf03160355
- Simard, J. M., Woo, S. K., and Gerzanich, V. (2012). Transient receptor potential melastatin 4 and cell death. *Pflugers Arch.* 464, 573–582. doi: 10.1007/s00424-012-1166-z
- Sørensen, B. H., Dam, C. S., Stürup, S., and Lambert, I. H. (2016a). Dual role of LRRC8A-containing transporters on cisplatin resistance in human ovarian cancer cells. *J. Inorg. Biochem.* 160, 287–295. doi: 10.1016/j.jinorgbio.2016.04.004
- Sørensen, B. H., Nielsen, D., Thorsteinsdottir, U. A., Hoffmann, E. K., and Lambert, I. H. (2016b). Downregulation of LRRC8A protects human ovarian and alveolar carcinoma cells against Cisplatin-induced expression of p53, MDM2, p21Waf1/Cip1, and Caspase-9/-3 activation. *Am. J. Physiol. Cell Physiol.* 310, C857–C873. doi: 10.1152/ajpcell.00256.2015
- Sørensen, B. H., Thorsteinsdottir, U. A., and Lambert, I. H. (2014). Acquired cisplatin resistance in human ovarian A2780 cancer cells correlates with shift in taurine homeostasis and ability to volume regulate. *Am. J. Physiol. Cell Physiol.* 307, C1071–C1080. doi: 10.1152/ajpcell.00274.2014
- Soukani, R., Berdeaux, A., Ghaleh, B., Giudicelli, J. F., Guize, L., Le Heuzey, J. Y., et al. (2000). Induction of apoptosis using sphingolipids activates a chloride current in *Xenopus laevis* oocytes. *Am. J. Physiol. Cell Physiol.* 279, C158–C165. doi: 10.1152/ajpcell.2000.279.1.C158
- Staub, F., Baethmann, A., Peters, J., Weigt, H., and Kempfski, O. (1990). Effects of lactacidosis on glial cell volume and viability. *J. Cereb. Blood Flow Metab.* 10, 866–876. doi: 10.1038/jcbfm.1990.143
- Staub, F., Mackert, B., Kempfski, O., Peters, J., and Baethmann, A. (1993). Swelling and death of neuronal cells by lactic acid. *J. Neurol. Sci.* 119, 79–84. doi: 10.1016/0022-510x(93)90194-4
- Strange, K., Emma, F., and Jackson, P. S. (1996). Cellular and molecular physiology of volume-sensitive anion channels. *Am. J. Physiol.* 270(3 Pt 1), C711–C730. doi: 10.1152/ajpcell.1996.270.3.C711
- Strange, K., Yamada, T., and Denton, J. S. (2019). A 30-year journey from volume-regulated anion currents to molecular structure of the LRRC8 channel. *J. Gen. Physiol.* 151, 100–117. doi: 10.1085/jgp.201812138
- Sun, Y., Zheng, Y., Wang, C., and Liu, Y. (2018). Glutathione depletion induces ferroptosis, autophagy, and premature cell senescence in retinal pigment epithelial cells. *Cell Death Dis.* 9:753. doi: 10.1038/s41419-018-0794-4
- Syeda, R., Qiu, Z., Dubin, A. E., Murthy, S. E., Florendo, M. N., Mason, D. E., et al. (2016). LRRC8 proteins form volume-regulated anion channels that sense ionic strength. *Cell* 164, 499–511. doi: 10.1016/j.cell.2015.12.031
- Syková, E. (2004). Diffusion properties of the brain in health and disease. *Neurochem. Int.* 45, 453–466. doi: 10.1016/j.neuint.2003.11.009
- Takahashi, N., Wang, X., Tanabe, S., Uramoto, H., Jishage, K., Uchida, S., et al. (2005). ClC-3-independent sensitivity of apoptosis to Cl⁻ channel blockers in mouse cardiomyocytes. *Cell. Physiol. Biochem.* 15, 263–270. doi: 10.1159/000087236
- Tanabe, S., Wang, X., Takahashi, N., Uramoto, H., and Okada, Y. (2005). HCO₃⁻-independent rescue from apoptosis by stilbene derivatives in rat cardiomyocytes. *FEBS Lett.* 579, 517–522. doi: 10.1016/j.febslet.2004.12.020
- Tang, T., Lang, X., Xu, C., Wang, X., Gong, T., Yang, Y., et al. (2017). CLICs-dependent chloride efflux is an essential and proximal upstream event for NLRP3 inflammasome activation. *Nat. Commun.* 8:202. doi: 10.1038/s41467-017-00227-x
- Ternovsky, V. I., Okada, Y., and Sabirov, R. Z. (2004). Sizing the pore of the volume-sensitive anion channel by differential polymer partitioning. *FEBS Lett.* 576, 433–436. doi: 10.1016/j.febslet.2004.09.051
- Thorsteinsdottir, U. A., Thorsteinsdottir, M., and Lambert, I. H. (2016). Protolichsterinic acid, isolated from the lichen cetraria islandica, reduces LRRC8A expression and volume-sensitive release of organic osmolytes in human lung epithelial cancer cells. *Phytother. Res.* 30, 97–104. doi: 10.1002/ptr.5507
- Tong, X., Lopez, W., Ramachandran, J., Ayad, W. A., Liu, Y., Lopez-Rodriguez, A., et al. (2015). Glutathione release through connexin hemichannels: implications for chemical modification of pores permeable to large molecules. *J. Gen. Physiol.* 146, 245–254. doi: 10.1085/jgp.201511375
- Tosteson, D. C., and Hoffman, J. F. (1960). Regulation of cell volume by active cation transport in high and low potassium sheep red cells. *J. Gen. Physiol.* 44, 169–194. doi: 10.1085/jgp.44.1.169
- Trothe, J., Ritzmann, D., Lang, V., Scholz, P., Pul, Ü., Kaufmann, R., et al. (2018). Hypotonic stress response of human keratinocytes involves LRRC8A as component of volume-regulated anion channels. *Exp. Dermatol.* 27, 1352–1360. doi: 10.1111/exd.13789
- Tsumura, T., Oiki, S., Ueda, S., Okuma, M., and Okada, Y. (1996). Sensitivity of volume-sensitive Cl⁻ conductance in human epithelial cells to extracellular nucleotides. *Am. J. Physiol.* 271(6 Pt 1), C1872–C1878. doi: 10.1152/ajpcell.1996.271.6.C1872
- Tymianski, M. (2011). Emerging mechanisms of disrupted cellular signaling in brain ischemia. *Nat. Neurosci.* 14, 1369–1373. doi: 10.1038/nn.2951
- Vandenabeele, P., Galluzzi, L., Vanden Berghe, T., and Kroemer, G. (2010). Molecular mechanisms of necroptosis: an ordered cellular explosion. *Nat. Rev. Mol. Cell Biol.* 11, 700–714. doi: 10.1038/nrm2970
- Varela, D., Penna, A., Simon, F., Eguiguren, A. L., Leiva-Salcedo, E., Cerda, O., et al. (2010). P2X4 activation modulates volume-sensitive outwardly rectifying chloride channels in rat hepatoma cells. *J. Biol. Chem.* 285, 7566–7574. doi: 10.1074/jbc.M109.063693
- Varela, D., Simon, F., Riveros, A., Jørgensen, F., and Stutzin, A. (2004). NAD(P)H oxidase-derived H₂O₂ signals chloride channel activation in cell volume regulation and cell proliferation. *J. Biol. Chem.* 279, 13301–13304. doi: 10.1074/jbc.C400020200
- Voaden, M. J., Lake, N., Marshall, J., and Morjaria, B. (1977). Studies on the distribution of taurine and other neuroactive amino acids in the retina. *Exp. Eye Res.* 25, 249–257. doi: 10.1016/0014-4835(77)90091-4
- Voss, F. K., Ullrich, F., Münch, J., Lazarow, K., Lutter, D., Mah, N., et al. (2014). Identification of LRRC8 heteromers as an essential component of the volume-regulated anion channel VRAC. *Science* 344, 634–638. doi: 10.1126/science.1252826
- Walker, V. E., Stelling, J. W., Miley, H. E., and Jacob, T. J. (1999). Effect of coupling on volume-regulatory response of ciliary epithelial cells suggests mechanism for secretion. *Am. J. Physiol.* 276, C1432–C1438. doi: 10.1152/ajpcell.1999.276.6.C1432
- Walz, W. (2000). Role of astrocytes in the clearance of excess extracellular potassium. *Neurochem. Int.* 36, 291–300. doi: 10.1016/s0197-0186(99)00137-0
- Walz, W., and Allen, A. F. (1987). Evaluation of the osmoregulatory function of taurine in brain cells. *Exp. Brain Res.* 68, 290–298. doi: 10.1007/bf00248794
- Wang, H. Y., Shimizu, T., Numata, T., and Okada, Y. (2007). Role of acid-sensitive outwardly rectifying anion channels in acidosis-induced cell death in human epithelial cells. *Pflugers Arch.* 454, 223–233. doi: 10.1007/s00424-006-0193-z
- Wang, L., Shen, M., Guo, X., Wang, B., Xia, Y., Wang, N., et al. (2017). Volume-sensitive outwardly rectifying chloride channel blockers protect against high glucose-induced apoptosis of cardiomyocytes via autophagy activation. *Sci. Rep.* 7:44265. doi: 10.1038/srep44265
- Wang, X., Takahashi, N., Uramoto, H., and Okada, Y. (2005). Chloride channel inhibition prevents ROS-dependent apoptosis induced by ischemia-reperfusion in mouse cardiomyocytes. *Cell. Physiol. Biochem.* 16, 147–154. doi: 10.1159/000089840
- Wee, S., Peart, J. N., and Headrick, J. P. (2007). P2 purinoceptor-mediated cardioprotection in ischemic-reperfused mouse heart. *J. Pharmacol. Exp. Ther.* 323, 861–867. doi: 10.1124/jpet.107.125815
- Wehner, F., Olsen, H., Tinel, H., Kinne-Saffran, E., and Kinne, R. K. (2003a). Cell volume regulation: osmolytes, osmolyte transport, and signal transduction. *Rev. Physiol. Biochem. Pharmacol.* 148, 1–80. doi: 10.1007/s10254-003-0009-x
- Wehner, F., Shimizu, T., Sabirov, R., and Okada, Y. (2003b). Hypertonic activation of a non-selective cation conductance in HeLa cells and its contribution to cell volume regulation. *FEBS Lett.* 551, 20–24. doi: 10.1016/s0014-5793(03)00868-8
- Weiss, S. (1988). Excitatory amino acid-evoked release of gamma-[3H]aminobutyric acid from striatal neurons in primary culture. *J. Neurochem.* 51, 435–441. doi: 10.1111/j.1471-4159.1988.tb01057.x
- Wilson, C. S., Bach, M. D., Ashkavand, Z., Norman, K. R., Martino, N., Adam, A. P., et al. (2019). Metabolic constraints of swelling-activated glutamate release in astrocytes and their implication for ischemic tissue damage. *J. Neurochem.* 151, 255–272. doi: 10.1111/jnc.14711

- Wilson, C. S., and Mongin, A. A. (2018). Cell volume control in healthy brain and neuropathologies. *Curr. Top. Membr.* 81, 385–455. doi: 10.1016/bs.ctm.2018.07.006
- Wu, G., Fang, Y. Z., Yang, S., Lupton, J. R., and Turner, N. D. (2004). Glutathione metabolism and its implications for health. *J. Nutr.* 134, 489–492. doi: 10.1093/jn/134.3.489
- Wyllie, A. H., Kerr, J. F., and Currie, A. R. (1980). Cell death: the significance of apoptosis. *Int. Rev. Cytol.* 68, 251–306. doi: 10.1016/s0074-7696(08)62312-8
- Yamada, T., Wondergem, R., Morrison, R., Yin, V. P., and Strange, K. (2016). Leucine-rich repeat containing protein LRRC8A is essential for swelling-activated Cl^- currents and embryonic development in zebrafish. *Physiol. Rep.* 4:e12940. doi: 10.14814/phy2.12940
- Yang, C., He, L., Chen, G., Ning, Z., and Xia, Z. (2019). LRRC8A potentiates temozolomide sensitivity in glioma cells via activating mitochondria-dependent apoptotic pathway. *Hum. Cell* 32, 41–50. doi: 10.1007/s13577-018-0221-2
- Yang, J., Chen, J., del Carmen Vitery, M., Osei-Owusu, J., Chu, J., Yu, H., et al. (2019a). PAC, an evolutionarily conserved membrane protein, is a proton-activated chloride channel. *Science* 364, 395–399. doi: 10.1126/science.aav9739
- Yang, J., Vitery, M. D. C., Chen, J., Osei-Owusu, J., Chu, J., and Qiu, Z. (2019b). Glutamate-releasing SWELL1 channel in astrocytes modulates synaptic transmission and promotes brain damage in stroke. *Neuron* 102, 813–827.e6. doi: 10.1016/j.neuron.2019.03.029
- Yang, X., Zhu, L., Lin, J., Liu, S., Luo, H., Mao, J., et al. (2015). Cisplatin activates volume-sensitive like chloride channels via purinergic receptor pathways in nasopharyngeal carcinoma cells. *J. Membr. Biol.* 248, 19–29. doi: 10.1007/s00232-014-9724-2
- Ye, H. B., Shi, H. B., and Yin, S. K. (2013). Mechanisms underlying taurine protection against glutamate-induced neurotoxicity. *Can. J. Neurol. Sci.* 40, 628–634. doi: 10.1017/s0317167100014840
- Zamaraeva, M. V., Sabirov, R. Z., Maeno, E., Ando-Akatsuka, Y., Bessonova, S. V., and Okada, Y. (2005). Cells die with increased cytosolic ATP during apoptosis: a bioluminescence study with intracellular luciferase. *Cell Death Differ.* 12, 1390–1397. doi: 10.1038/sj.cdd.4401661
- Zamaraeva, M. V., Sabirov, R. Z., Manabe, K., and Okada, Y. (2007). Ca^{2+} -dependent glycolysis activation mediates apoptotic ATP elevation in HeLa cells. *Biochem. Biophys. Res. Commun.* 363, 687–693. doi: 10.1016/j.bbrc.2007.09.019
- Zhang, H., Cao, H. J., Kimelberg, H. K., and Zhou, M. (2011). Volume regulated anion channel currents of rat hippocampal neurons and their contribution to oxygen-and-glucose deprivation induced neuronal death. *PLoS One* 6:e16803. doi: 10.1371/journal.pone.0016803
- Zhang, J. J., and Jacob, T. J. (1996). Volume regulation in the bovine lens and cataract. The involvement of chloride channels. *J. Clin. Invest.* 97, 971–978. doi: 10.1172/jci118521
- Zhang, Y., Zhang, H., Feustel, P. J., and Kimelberg, H. K. (2008). DCPIB, a specific inhibitor of volume regulated anion channels (VRACs), reduces infarct size in MCAo and the release of glutamate in the ischemic cortical penumbra. *Exp. Neurol.* 210, 514–520. doi: 10.1016/j.expneurol.2007.11.027
- Zhou, C., Chen, X., Planells-Cases, R., Chu, J., Wang, L., Cao, L., et al. (2020). Transfer of cGAMP into bystander cells via LRRC8 volume-regulated anion channels augments STING-mediated interferon responses and anti-viral immunity. *Immunity* 52:767–781.e6. doi: 10.1016/j.immuni.2020.03.016
- Zhou, J. J., Luo, Y., Chen, S. R., Shao, J. Y., Sah, R., and Pan, H. L. (2020). LRRC8A-dependent volume-regulated anion channels contribute to ischemia-induced brain injury and glutamatergic input to hippocampal neurons. *Exp. Neurol.* 332:113391. doi: 10.1016/j.expneurol.2020.113391

Conflict of Interest: The authors declare that the research was conducted in the absence of any commercial or financial relationships that could be construed as a potential conflict of interest.

Copyright © 2021 Okada, Sabirov, Sato-Numata and Numata. This is an open-access article distributed under the terms of the Creative Commons Attribution License (CC BY). The use, distribution or reproduction in other forums is permitted, provided the original author(s) and the copyright owner(s) are credited and that the original publication in this journal is cited, in accordance with accepted academic practice. No use, distribution or reproduction is permitted which does not comply with these terms.



Intracellular Ca^{2+} Imbalance Critically Contributes to Paraptosis

Eunhee Kim¹, Dong Min Lee², Min Ji Seo², Hong Jae Lee² and Kyeong Sook Choi^{2*}

¹ Department of Biological Sciences, Ulsan National Institute Science and Technology, Ulsan, South Korea, ² Department of Biochemistry, Ajou University School of Medicine, Suwon, South Korea

OPEN ACCESS

Edited by:

Markus Ritter,
Paracelsus Medical University, Austria

Reviewed by:

Ildikó Szabó,
University of Padua, Italy
Hubert Hannes Kerschbaum,
University of Salzburg, Austria

*Correspondence:

Kyeong Sook Choi
kschoi@ajou.ac.kr

Specialty section:

This article was submitted to
Cell Death and Survival,
a section of the journal
Frontiers in Cell and Developmental
Biology

Received: 18 September 2020

Accepted: 07 December 2020

Published: 12 January 2021

Citation:

Kim E, Lee DM, Seo MJ, Lee HJ
and Choi KS (2021) Intracellular Ca^{2+}
Imbalance Critically Contributes
to Paraptosis.
Front. Cell Dev. Biol. 8:607844.
doi: 10.3389/fcell.2020.607844

Paraptosis is a type of programmed cell death that is characterized by dilation of the endoplasmic reticulum (ER) and/or mitochondria. Since paraptosis is morphologically and biochemically different from apoptosis, understanding its regulatory mechanisms may provide a novel therapeutic strategy in malignant cancer cells that have proven resistant to conventional pro-apoptotic treatments. Relatively little is known about the molecular basis of paraptosis, but perturbations of cellular proteostasis and ion homeostasis appear to critically contribute to the process. Ca^{2+} transport has been shown to be important in the paraptosis induced by several natural products, metal complexes, and co-treatment with proteasome inhibitors and certain Ca^{2+} -modulating agents. In particular, the Ca^{2+} -mediated communication between the ER and mitochondria plays a crucial role in paraptosis. Mitochondrial Ca^{2+} overload from the intracellular Ca^{2+} -flux system located at the ER-mitochondrial axis can induce mitochondrial dilation during paraptosis, while the accumulation of misfolded proteins within the ER lumen is believed to exert an osmotic force and draw water from the cytoplasm to distend the ER lumen. In this process, Ca^{2+} release from the ER also critically contributes to aggravating ER stress and ER dilation. This review focuses on the role of Ca^{2+} transport in paraptosis by summarizing the recent findings related to the actions of Ca^{2+} -modulating paraptosis-inducing agents and discussing the potential cancer therapeutic strategies that may effectively induce paraptosis via Ca^{2+} signaling.

Keywords: paraptosis, Ca^{2+} , endoplasmic reticulum, mitochondria, cancer

INTRODUCTION

The term “paraptosis” was first introduced to describe a form of programmed cell death displaying cytoplasmic vacuolation consisting in mitochondrial and/or endoplasmic reticulum (ER) dilation (Sperandio et al., 2000). Paraptosis was initially observed in 293T cells and mouse embryonic fibroblasts overexpressing insulin-like growth factor 1 receptor (IGF-1R) (Sperandio et al., 2000) and was subsequently shown to be induced by different natural compounds *in vitro* and *in vivo* in tumor cells (Lee et al., 2016; Fontana et al., 2020b). In addition, paraptosis appears to be implicated in neurodegeneration (Wei et al., 2015). Paraptosis lacks apoptotic features (e.g., DNA condensation and fragmentation, membrane blebbing, and apoptotic bodies), and unlike necrosis, no loss of membrane integrity is seen in paraptosis (Sperandio et al., 2000, 2004). As the underlying mechanisms of paraptosis, impaired proteostasis (due to proteasomal inhibition or disrupted protein thiol homeostasis), and/or imbalanced homeostasis of ions (e.g., Ca^{2+} and K^{+}) have been

proposed to trigger stress to the ER and mitochondria (Lee et al., 2016; Fontana et al., 2020b). Paraptosis is successfully inhibited by the translation inhibitor, cycloheximide (CHX) (Sperandio et al., 2000), suggesting that inhibition of protein synthesis may prevent this cell death by reducing the potential burden of misfolded proteins and proteotoxicity (Lee et al., 2016). The activation of mitogen-activated protein (MAP) kinases, such as c-Jun N-terminal protein kinases (JNKs), MAP kinase kinase 2 (MEK-2), and p38, has been found to be positively involved in the paraptosis induced by many natural products or chemicals (Zhang et al., 2009, 2010; Yoon et al., 2010, 2012, 2014; Wang et al., 2012; Yumnam et al., 2014; Hager et al., 2018; Han et al., 2018; Fontana et al., 2019; Yokoi et al., 2020), whereas AIP-1/Alix appears to be negatively involved in some cases of paraptosis (Sperandio et al., 2004; Valamanesh et al., 2007; Yoon et al., 2010, 2014; Han et al., 2018; Xue et al., 2018). The term “paraptosis-like cell death” has been used to describe the types of cell death accompanied by the dilation of either the mitochondria or the ER alone or those that do not share multiple biochemical features of paraptosis, including the activation of MAP kinases, the downregulation of AIP-1/Alix, and the inhibition of vacuolation and cell death by cycloheximide, etc. (Zhang et al., 2010; Xue et al., 2018; Kim et al., 2019). Recently, Ca^{2+} depletion in the ER and the subsequent mitochondrial Ca^{2+} overload have been shown to play a critical role in the paraptosis induced by various natural products and chemicals (Yoon et al., 2012, 2014; Yumnam et al., 2016; Kim et al., 2019). Here we review the recent understanding of paraptosis, focusing on the involvement of intracellular Ca^{2+} transport in paraptosis, provide mechanistic insight into the Ca^{2+} -mediated regulatory pathways of paraptosis, and finally discuss the cancer therapeutic strategy of inducing paraptosis by manipulating intracellular Ca^{2+} homeostasis.

THE MACHINERY INVOLVED IN THE ER-MITOCHONDRIA Ca^{2+} TRANSPORT

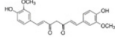
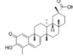
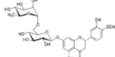
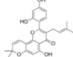
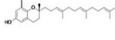
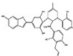
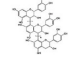
The ER and mitochondria both participate in regulating intracellular Ca^{2+} homeostasis due to their ability to store Ca^{2+} and respond to cytosolic Ca^{2+} signals. Under normal physiological conditions, the concentrations of both cytosolic Ca^{2+} and Ca^{2+} stored within the ER lumen are strictly regulated. The cytosolic Ca^{2+} concentration $[(\text{Ca}^{2+})_c]$ is approximately 0.1 μM , compared to an extracellular (Ca^{2+}) of ~ 1 mM and an ER Ca^{2+} concentration $[(\text{Ca}^{2+})_{er}]$ of ~ 0.5 mM (Bianchi et al., 2004). The import of Ca^{2+} into the ER is governed by sarcoplasmic/ER Ca^{2+} ATPase (SERCA) pumps (Vandecaetsbeek et al., 2011). In response to cellular stress requiring Ca^{2+} -signal, Ca^{2+} is released from ER stores *via* ryanodine receptors (RyRs) and (especially) inositol 1,4,5-triphosphate receptors (IP₃Rs) (Marks, 1997); the latter are primarily clustered in the mitochondria-associated membrane (MAM), an ER structure that is located near the mitochondria (Rizzuto et al., 1998; Csordás et al., 1999; Bartok et al., 2019). The mitochondria serve as important regulators of cellular Ca^{2+} by sequestering and releasing Ca^{2+} . The Ca^{2+} concentration (Ca^{2+}) inside

the mitochondria has similar values measured in the bulk cytoplasm (0.1–0.2 μM) under resting conditions; however, mitochondrial Ca^{2+} concentration increased 10–20-fold more than the cytosolic compartment during stimulation with (Ca^{2+})-increasing agents (Giorgi et al., 2018). In particular, Ca^{2+} ions released from the ER by IP₃Rs or RyRs flux across the outer mitochondrial membrane (OMM) mainly through the voltage-dependent anion channel (VDAC) (Gincel et al., 2001; Rapizzi et al., 2002). After reaching the intermembrane space, Ca^{2+} ions pass through the inner mitochondrial membrane (IMM) mainly through the mitochondrial Ca^{2+} uniporter (MCU) complex (Baughman et al., 2011; De Stefani et al., 2011). This MCU complex consists of two pore-forming proteins; mitochondrial calcium uptake protein (MCU)1–3 (Baughman et al., 2011; De Stefani et al., 2011) and essential MCU regulator (Sancak et al., 2013); the dominant-negative pore-forming subunit, MCUb (Raffaello et al., 2013), and the scaffolding factor, mitochondrial calcium uniporter regulator 1 (MCUR1) (Mallilankaraman et al., 2012; Tomar et al., 2016). The activity of the MCU complex is regulated by mitochondrial calcium uptake 1 (MICU1) (Perocchi et al., 2010) and its paralog MICU2 (Plovanich et al., 2013); they together comprise the MCU complex, which allows for mitochondrial Ca^{2+} uptake exclusively at high Ca^{2+} concentrations (Patron et al., 2014). Therefore, the MCU complex has been proposed to be the key player responsible for the rate-limiting step of mitochondrial Ca^{2+} accumulation, and it may be pivotal to Ca^{2+} -overload-induced cell death. The Ca^{2+} taken up by the mitochondria is rapidly extruded into the cytosol *via* a complex antiporter system to restore the basal state. The mitochondrial $\text{Na}^+/\text{Ca}^{2+}$ exchanger (mNCX) and the mitochondrial $\text{H}^+/\text{Ca}^{2+}$ exchanger (mHCX) play major roles in mitochondrial Ca^{2+} efflux mechanisms. The stoichiometry of mNCX-driven transport is electrogenic, with three (or four) Na^+ for one Ca^{2+} (Jung et al., 1995; Dash and Beard, 2008), whereas the exchange ratio of mHCX is electroneutral (two H^+ for one Ca^{2+}) (Gunter et al., 1991). The mitochondrial permeability transition pore (mPTP) has been also proposed to be involved as an alternative Ca^{2+} efflux pathway under certain conditions when the mPTP is transiently opened (Elrod et al., 2010; Lu et al., 2016).

PARAPTOSIS-INDUCING AGENTS ASSOCIATED WITH Ca^{2+} IMBALANCE

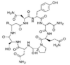
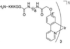
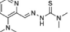
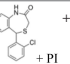
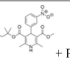
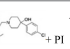
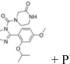
The natural products and chemicals that are listed in **Table 1** induce paraptosis. During this process, they disrupt Ca^{2+} homeostasis at the ER by altering Ca^{2+} store content and Ca^{2+} dynamics (including the uptake, release, and leakage of Ca^{2+}) and/or at the mitochondria by affecting the activities of MCU complex components to regulate the mitochondrial Ca^{2+} levels. In addition, recent studies have shown that treatment of cancer cells with drugs that perturb Ca^{2+} homeostasis [CGP-37157 (Yoon et al., 2012), lercanidipine (Lee et al., 2019), and loperamide (Kim et al., 2019)] or Nutlin-3, which is a chemical that triggers the mitochondrial unfolded protein response (mtUPR) (Lee et al., 2017), induces paraptosis when

TABLE 1 | Paraptotic inducers and their pro-paraptotic mechanisms of action.

Paraptotic inducers			Cell death mode	Dilated organelles	Method(s)		Ca ²⁺ -related mechanism				Other mechanisms	Tested cells		References
Class	Name	Structure			ER	Mitochondria	(Ca ²⁺) _{cyto}	Source of increased Ca ²⁺	(Ca ²⁺) _{mito}	Mediator for (Ca ²⁺) _{mito} ↑		Cancer cell lines	Safety in normal cell lines	
Natural compounds	Curcumin (40 μM)		Paraptosis	ER/ mitochondria	TEM YFP-ER	TEM YFP-Mito, probe	↑	RyR-mediated ER Ca ²⁺ release	↑	MCU	Proteasomal activity↓, poly-Ub↑, ER stress↑, requirement of protein synthesis, Alix/ AIP↓, ROS↑, p-JNK↑, p-ERK1/ 2↑	Breast	MCF-10A, HMEC	Yoon et al., 2010
	Celastrol (1.2–2 μM)		Paraptosis	ER/ mitochondria	TEM YFP-ER, probe, ICC	TEM YFP-Mito, ICC	↑	IP ₃ R-mediated ER Ca ²⁺ release	↑	MCU	Proteasomal activity↓, poly-Ub↑, ER stress↑, requirement of protein synthesis, p-JNK↑, p-ERK1/ 2↑, p-p38↑	Breast, colon, cervix, lung, prostate	NT	Wang et al., 2012; Yoon et al., 2014
	Hesperidin (1 mM)		Paraptosis	ER/ mitochondria	TEM	TEM probe	↑	RyR/ IP ₃ R-mediated ER Ca ²⁺ release	↑	MCU	ROS↑, mitochondrial superoxide↑, MMP↓, p-ERK1/ 2↑	Liver	Thle-2	Yumnam et al., 2014, 2016
	Morusin (30 μM)		Paraptosis-like cell death	ER/ mitochondria	TEM probe LM	TEM probe	↑		↑	VDAC	ER stress↑, Alix/ AIP↓, ROS↑, MMP↓	Ovary	NT	Xue et al., 2018
	δ-Tocotrienol (15 μg/ ml)		Paraptosis autophagy apoptosis	Cytoplasmic vacuoles	TEM LM	TEM	↑		↑	VDAC	ER stress↑, requirement of protein synthesis, ROS↑, p-JNK↑, p-p38↑, Akt/ mTOR↓	Prostate	RWPE-1	Fontana et al., 2019, 2020a
	Chalcomoracin (4–6 μM)		Paraptosis mitophagy	ER	ICC LM		↑				Poly-Ub↑, ER stress↑, requirement of protein synthesis, Alix/ AIP1↓, ROS↑, MMP↓, p-ERK1/ 2↑	Prostate, breast, lung	MCF-10A	Han et al., 2018
	Procyanidins (30 μg/ ml)		Paraptosis-like cell death	Cytoplasmic vacuoles	LM	LM	↑	Influx of extracellular Ca ²⁺			Requirement of protein synthesis, MMP↓, p-ERK1/ 2↑, p-p38↑	Brain, liver, leukemia	NT	Zhang et al., 2009, 2010

(Continued)

TABLE 1 | Continued

Paraptotic inducers			Cell death mode	Dilated organelles	Method(s)		Ca^{2+} -related mechanism				Other mechanisms	Tested cells		References
Class	Name	Structure			ER	Mitochondria	$(\text{Ca}^{2+})_{\text{cyto}}$	Source of increased Ca^{2+}	$(\text{Ca}^{2+})_{\text{mito}}$	Mediator for $(\text{Ca}^{2+})_{\text{mito}} \uparrow$		Cancer cell lines	Safety in normal cell lines	
	Iturin A-like lipopeptides (30.89 μM)		Paraptosis apoptosis	ER/ mitochondria	TEM	TEM	\uparrow				ROS \uparrow , MMP \downarrow	Colon	NT	Zhao et al., 2019
Metal compounds	IPH 4 (25 μM)		Paraptosis	Cytoplasmic vacuoles	TEM LM	TEM LM	\uparrow	Inhibition of CaM- Ca^{2+} binding	\uparrow	MMP-dependent	CHOP \uparrow , MMP \downarrow , p-JNK \uparrow , p-ERK1/2 \uparrow	Leukemia	NT	Yokoi et al., 2020
	Me_2NNMe_2 (1, 10 μM)		Paraptosis	ER/ mitochondria	YFP-ER LM	Probe			\uparrow		Thiol homeostasis \downarrow , CHOP \uparrow , MMP \downarrow , p-ERK1/2 \uparrow , p-MEK1/2 \uparrow	Colon	NT	Hager et al., 2018
Combined regimen	CGP-37157 + PI (50 μM + 15 nM)	 + PI	Paraptosis	ER/ mitochondria	YFP-ER	YFP-Mito			\uparrow	MCU, inhibition of mNCX	Proteasomal activity \downarrow , poly-Ub \uparrow , CHOP \uparrow , requirement of protein synthesis, Alix/ AIP \downarrow , p-JNK \uparrow , p-ERK1/2 \uparrow	Breast	NT	Yoon et al., 2012
	Lercanidipine + PI (5~15 μM + 4 nM)	 + PI	Paraptosis	ER/ mitochondria	YFP-ER LM	YFP-Mito, probe LM	\uparrow	RyR-mediated ER Ca^{2+} release	\uparrow	MCU	Poly-Ub \uparrow , ER stress \uparrow , requirement of protein synthesis	Breast, liver, gastric, lung, pancreas, lymphocyte	MCF-10A, Chang liver	Lee et al., 2019
	Loperamide + PI (20 μM + 40 nM)	 + PI	Paraptosis-like cell death	ER	TEM YFP-ER, ICC LM	TEM probe LM	\uparrow	Influx of extracellular Ca^{2+}	\uparrow		Poly-Ub \uparrow , CHOP \uparrow , requirement of protein synthesis	Colon, cervix, renal, breast, liver, brain	CCD-112CoN	Kim et al., 2019
	Nutlin-3 + PI (30 μM + 5 nM)	 + PI	Paraptosis	ER/ mitochondria	TEM YFP-ER, ICC LM	TEM YFP-Mito, probe, ICC LM	\uparrow	Influx of extracellular Ca^{2+}	\uparrow	MCU	Proteostasis \downarrow , poly-Ub \uparrow , CHOP \uparrow , requirement of protein synthesis	Breast, brain, colon, cervix	MCF-10A, CCD-841CoN	Lee et al., 2017

Normal cell line: MCF-10A, human mammary epithelial cell line; HMEC, primary mammary epithelial cells; Thle-2, primary normal liver cells by infection with SV40 large T antigen; RWPE-1, human prostatic epithelial cells; IMR90, human lung fibroblast cells; Chang Liver, normal liver cell line; CCD-112CoN, human colon fibroblast cells; CCD-841CoN: human colon epithelial cells. TEM, transmission electron microscopy; LM, light microscopy; ICC, immunocytochemistry; \uparrow , upregulation; \downarrow , downregulation; $(\text{Ca}^{2+})_{\text{cyto}}$, concentration of cytosolic Ca^{2+} ; $(\text{Ca}^{2+})_{\text{mito}}$, concentration of mitochondrial Ca^{2+} .

combined with proteasome inhibitors (PIs). The proposed targets through which these paraptosis-inducing agents disrupt Ca^{2+} homeostasis are summarized in **Figure 1**. In this section, we will summarize and discuss their Ca^{2+} -associated regulatory effects in paraptosis.

Curcumin

Curcumin, the main natural polyphenol extracted from the rhizomes of *Curcuma longa*, demonstrates chemopreventive (Park et al., 2013), chemosensitizing, and radiosensitizing activity in cancer cells (Goel and Aggarwal, 2010). Yoon et al. (2010) showed that curcumin can induce paraptosis by promoting vacuolization *via* the swelling and fusion of the mitochondria and the ER in various breast cancer cell lines, but not in normal breast cells. The curcumin-induced vacuolation and cell death were effectively abrogated by the protein synthesis blocker, cycloheximide. The authors found that impairment of proteasome activity by curcumin is the main cause of paraptosis-related ER stress and ER dilation and that mitochondrial Ca^{2+} overload is needed for mitochondrial dilation seen during curcumin-induced paraptosis. More specifically, curcumin-induced activation of RyRs mediates the release of Ca^{2+} from the ER. Subsequently, MCU-mediated mitochondrial Ca^{2+} uptake causes Ca^{2+} overload, contributing to the dilations of the mitochondria and the ER, and cell death (Yoon et al., 2010). These results suggest that mitochondrial Ca^{2+} overload is an initial and important signal for curcumin-induced paraptosis. The activations of ERK2 or JNKs were also found to critically contribute to curcumin-induced paraptosis. Furthermore, the protein levels of AIP-1/Alix were decreased by curcumin, and AIP-1/Alix overexpression attenuated curcumin-induced paraptosis (Yoon et al., 2010).

Celastrol

Celastrol, a quinone methide triterpene derived from Thunder God Vine, exhibits antioxidant, antidiabetic, antiobesity, and anti-tumor activity (Cascão et al., 2017). Celastrol has been found to trigger paraptosis in various cancer cells (Yoon et al., 2014). In HeLa cells, celastrol-induced paraptosis was found to be accompanied by apoptosis and autophagy, suggesting that different cellular fates could be induced by celastrol depending on the cell type and/or cellular context (Wang et al., 2012). Celastrol treatment of MDA-MB-435S cells was shown to induce mitochondrial Ca^{2+} overload and ER stress. IP_3R -mediated Ca^{2+} release from the ER and its subsequent MCU-mediated mitochondrial Ca^{2+} influx appear to be critically implicated in celastrol-induced paraptosis. Mitochondrial Ca^{2+} overload results in its functional defect and the generation of reactive oxygen species (ROS), which further impair proteasome activity. This proteasome-inhibiting activity of celastrol may stabilize IP_3R and MCU to reinforce the Ca^{2+} -mediated effects of celastrol, leading to ER stress, ER vacuolation, and subsequent cell death (Yoon et al., 2014).

Hesperidin

Hesperidin, a flavanone glycoside present in citrus fruits, was shown to kill HepG2 cells through the induction of paraptosis

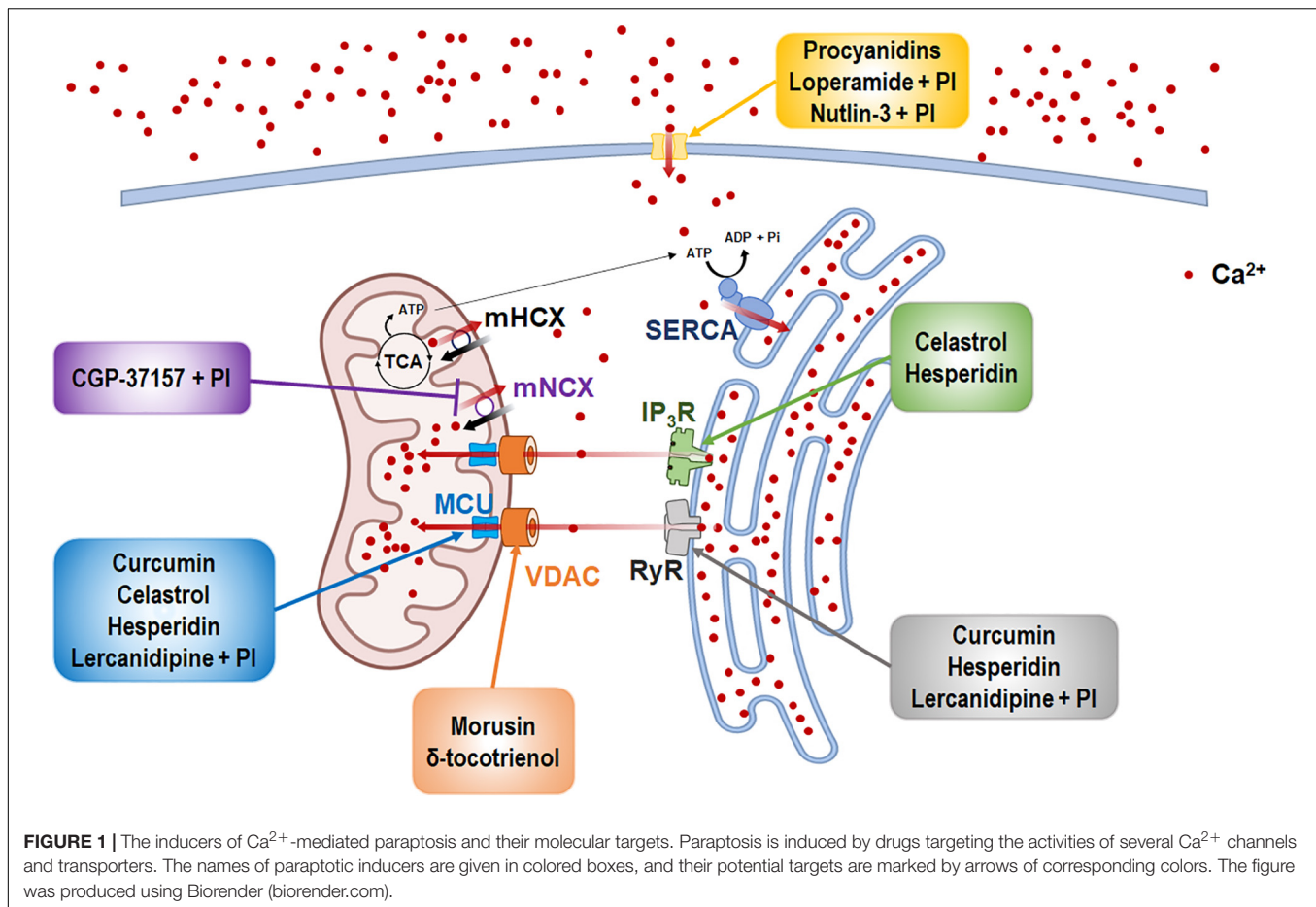
accompanied by mitochondrial and ER swelling without apoptotic features (Yumnam et al., 2014, 2016). Treatment with hesperidin was found to increase the mitochondrial Ca^{2+} levels in these cells, and MCU-mediated mitochondrial Ca^{2+} overload was revealed to play an important role in hesperidin-induced paraptosis. Ca^{2+} -mediated increase in ROS generation was shown to induce the hesperidin-induced loss of mitochondrial membrane potential, and ERK1/2 activation was found to positively influence hesperidin-induced vacuolation (Yumnam et al., 2014, 2016). Both IP_3R and RyR mediate the release of Ca^{2+} from the ER and subsequent MCU-mediated Ca^{2+} influx into the mitochondria, thereby contributing to the paraptosis induced by hesperidin in HepG2 cells (Yumnam et al., 2016).

Morusin

Morusin, a prenylated flavonoid isolated from the root bark of *Morus australis*, exhibits anti-oxidant, anti-bacterial, and anti-tumor properties (Zoofishan et al., 2018). Treatment of epithelial ovarian cancer (EOC) cells with morusin triggers paraptosis-like cell death accompanied by extensive cytoplasmic vacuolation due to the dilation and fusion of the ER and the mitochondria (Xue et al., 2018). Morusin induced mitochondrial Ca^{2+} overload, accumulation of ER stress marker proteins, ROS generation, and loss of the mitochondrial membrane potential (MMP, $\Delta\Psi\text{m}$) in these cells. These morusin-induced mitochondrial Ca^{2+} influx, ROS generation, MMP depletion, cytoplasmic vacuolization, and cell death were suppressed by a pretreatment with 4,4'-diisothiocyanostilbene-2,2'-disulfonic acid (DIDS), an inhibitor of anion channels, including VDAC (Jessen et al., 1986; Ben-Hail and Shoshan-Barmatz, 2016). In addition, DIDS inhibited the morusin-induced antiproliferative effects, which were associated with ER stress, both *in vitro* and *in vivo* in ovarian cancer xenograft models. In conclusion, morusin may have antitumor potential against EOC by inducing paraptosis *via* VDAC-mediated mitochondrial Ca^{2+} overload (Xue et al., 2018).

δ -Tocotrienol

δ -Tocotrienol (d-TT) induces paraptosis together with autophagy and apoptosis in castration resistance prostate cancer (CRPC) cells. d-TT-induced paraptosis was demonstrated by the reported dilation of ER cisternae and swollen and damaged mitochondria with disintegrated cristae (Fontana et al., 2019). δ -TT-induced vacuolation was prevented by salubrinal (the ER stress inhibitor) and cycloheximide (the protein synthesis inhibitor). δ -TT was found to trigger significant impairments of mitochondrial metabolic functions and structural dynamics (Fontana et al., 2020a). In addition, δ -TT significantly increases the levels of cytoplasmic Ca^{2+} , mitochondrial Ca^{2+} , and ROS, which contribute to the pro-death activities (paraptosis, apoptosis, and autophagy) of this agent in these cells. Pretreatment with the VDAC inhibitor, DIDS, significantly attenuated the effects of δ -TT on cell viability (paraptosis and apoptosis), suggesting that mitochondrial Ca^{2+} overload is critical for the anticancer activity of δ -TT in CRPC cells (Fontana et al., 2020a).



Chalcomoracin

Treatment with chalcomoracin (CMR), one of the major secondary metabolites found in fungus-infected mulberry leaves, induces mitophagy and a paraptosis that is accompanied by extensive cytoplasmic vacuolation originated from the ER in PC-3 and MDA-MB-231 cells (Han et al., 2018). In this process, CMR treatment upregulated PTEN-induced kinase 1, a key marker of mitophagy, and downregulated the protein levels of AIP-1/Alix, an inhibitory protein of paraptosis. CMR-induced ROS generation and MMP loss were effectively inhibited by a pretreatment with the antioxidant, N-acetylcysteine (NAC). Moreover, increases in the level of Ca^{2+} and the activation of the Ca^{2+} -activated protease, calpain, preceded CMR-induced cytoplasmic vacuolation, and a pretreatment with the intracellular Ca^{2+} chelator, BAPTA-AM, blocked CMR-induced cytoplasmic vacuolation. These findings together suggest that ROS-mediated impairment of MMP and Ca^{2+} homeostasis may contribute to CMR-induced paraptotic cell death (Han et al., 2018).

Procyanidins

Oligomeric procyanidins (F2), which are abundant in grape seeds, can induce paraptosis in U-87 cells (Zhang et al., 2009). Apoptotic features were not observed in cells treated with F2.

However, a further study indicated that activation of the ERK1/2 and p38 pathways, as well as Ca^{2+} mobilization, was involved in the F2-mediated cell death of U-87 cell (Zhang et al., 2010).

Iturin A-Like Lipopeptides

Iturin A-like lipopeptides produced by *Bacillus subtilis* were reported to simultaneously induce paraptosis, apoptosis, and autophagy in heterogeneous human epithelial colorectal adenocarcinoma (Caco-2) cells (Zhao et al., 2019). Induction of paraptosis in Caco-2 cells was shown by cytoplasmic vacuolization accompanied by ER dilation and swelling as well as mitochondrial dysfunction. The antitumor effect of the iturin A-like lipopeptides on Caco-2 cells was decreased by more than 50% in the presence of an apoptosis inhibitor, suggesting that paraptosis may play a crucial role in its anticancer activity. A significant increase in Ca^{2+} and ROS levels was also observed with ER stress in cells (Zhao et al., 2019).

Triscyclometalated Iridium(III) Complex-Peptide Hybrids 4

Yokoi et al. (2020) demonstrated that the amphiphilic iridium complex-peptide hybrid (IPH) 4, which contains a glycolic acid moiety between the iridium core and the peptide part, induces paraptosis-like cell death in Jurkat cells (Yokoi et al., 2020).

The authors found that IPH4 increased the influx of Ca^{2+} from the ER to the mitochondria and induced the subsequent loss of MMP ($\Delta\Psi\text{m}$), resulting in vacuolization of the cytoplasm and intracellular organelles (Yokoi et al., 2020).

Me_2NNMe_2

Me_2NNMe_2 , which is a new derivative of α -N-heterocyclic thiosemicarbazones, induces major hallmarks of paraptotic cell death, including ER-derived vacuolation, mitochondrial swelling, activation of MEK/ERK signaling pathway, and caspase-independent cell death (Hager et al., 2018). In this process, the copper complex of Me_2NNMe_2 accumulates in the ER to inhibit the reductive potential of protein disulfide isomerase (PDI). The resultant disruption of thiol redox homeostasis in the ER, in turn, activates protein kinase R (PKR)-like endoplasmic reticulum kinase signaling and the release of Ca^{2+} ions from the ER. This prolonged Ca^{2+} imbalance triggers the swelling of the ER and the mitochondria as well as mitochondrial membrane depolarization, leading to cell death (Hager et al., 2018).

CGP-37157 + Proteasome Inhibitor

Yoon et al. (2012) showed that proteasome inhibition alone is not effective to kill breast cancer cells. However, the CGP-37157-mediated inhibition of mNCX could sensitize breast cancer cells (but not normal cells) to a PI by inducing paraptosis accompanied by dilation of both the mitochondria and the ER (Yoon et al., 2012). In addition, co-treatment of CGP-37157 enhanced bortezomib (Btz)-mediated ER stress, ERK activation, JNK activation, and AIP-1/Alix downregulation. While the mitochondrial Ca^{2+} levels were transiently increased by CGP-37157 alone, CGP-37157/Btz induced a sustained mitochondrial Ca^{2+} overload. A pretreatment with ruthenium red significantly inhibited the cell death induced by CGP-37157/Btz, possibly by inhibiting the influx of Ca^{2+} into the mitochondria. These findings together indicate that the simultaneous inhibition of the proteasome and mNCX effectively induces paraptosis *via* mitochondrial Ca^{2+} overload and that dilations of the ER and the mitochondria seem to be interdependent during paraptosis (Yoon et al., 2012).

Lercanidipine + Proteasome Inhibitor

A recent study showed that lercanidipine (Ler), a third-generation 1,4-dihydropyridine (DHP) used to treat high blood pressure, potentiates the antitumor effects of various PIs (e.g., Btz, carfilzomib, and ixazomib) in many solid cancer cell lines by inducing paraptosis, a cell death mode accompanied by extensive vacuolation derived from the ER and the mitochondria (Lee et al., 2019). Ler enhances Btz-mediated ER stress and ER dilation in MDA-MB 435S cells. Mitochondrial Ca^{2+} overload was followed by the increase in cytosolic Ca^{2+} levels in cancer cells treated with Ler and Btz. Mechanistic studies employing various Ca^{2+} antagonists revealed that an MCU-mediated mitochondrial Ca^{2+} overload may be critical for Ler/Btz-induced mitochondrial dilation, subsequent ER dilation, and cell death. In contrast, an increase in cytosolic Ca^{2+} contributes solely to ER dilation at the later phase of Ler/Btz treatment. As the possible underlying mechanism, the authors proposed that the Ler/Btz-mediated

stabilization of DHP receptor and RyR may result in the release of Ca^{2+} from the ER and the subsequent MCU-mediated mitochondrial Ca^{2+} uptake. This sustained mitochondrial Ca^{2+} overload may cause mitochondrial dilation and prompt opening of mPTP, leading to the leakage of Ca^{2+} into the cytosol (Lee et al., 2019).

Loperamide + Proteasome Inhibitor

Kim et al. (2019) showed that the widely used anti-diarrheal drug, loperamide (Lop), effectively enhances the cytotoxicity of PIs in various colon cancer cells, but not in normal colon epithelial cells (Kim et al., 2019). The combination of sublethal concentrations of Btz and Lop (Lop/Btz) effectively triggered paraptosis-like cell death accompanied by severe vacuolation derived from the ER in various colon cancer cells, whereas either agent alone failed to induce notable vacuolation or cell death. In Lop/Btz-treated cancer cells, mitochondrial fragmentation was observed. Lop enhances Btz-mediated ER stress and ER dilation due to misfolded protein accumulation, leading to the upregulation of C/EBP homologous protein (CHOP) and subsequent paraptosis-like cell death. In addition, Btz/Lop increased both cytosolic and mitochondrial Ca^{2+} levels. An increase in Ca^{2+} (possibly by an influx of extracellular Ca^{2+}) appears to play a critical role in the anticancer effects of Lop/Btz by affecting ER-derived vacuolation. Mitochondrial Ca^{2+} overload also contributes to Lop/Btz-mediated cytotoxicity, although it does not affect the dilations of the ER and the mitochondria (Kim et al., 2019).

Nutlin-3 + Proteasome Inhibitor

The small molecule mouse double minute 2 homolog antagonist, Nutlin-3, exhibits promising therapeutic anti-cancer activity (Vassilev et al., 2004; Vassilev, 2007). Lee et al. (2017) showed that the combined treatment with Nutlin-3 and Btz triggered the formation of megamitochondria and progressive fusion of swollen ER, leading to paraptotic cell death in various p53-defective Btz-resistant solid tumor cells (Lee et al., 2017). Neither Nutlin-3 alone nor Btz alone did significantly affect the cellular morphology and viability, although Nutlin-3 alone induced a transient mitochondrial dilation. Mechanistically, proteasomal-impairment-induced ER stress (particularly CHOP upregulation) critically contributes to Nutlin-3/Btz-induced ER dilation and subsequent cell death induced by Nutlin-3/Btz. In addition, Nutlin-3/Btz, but not either agent alone, increased both cytosolic and mitochondrial Ca^{2+} levels. An increase in cytosolic Ca^{2+} , possibly by an influx of extracellular Ca^{2+} , plays an important role in Nutlin-3/Btz-induced ER dilation and subsequent cell death. For Nutlin-3/Btz-induced mitochondrial dilation, Nutlin-3-mediated mitochondrial stress due to the accumulation of misfolded proteins within the mitochondria may be more important than mitochondrial Ca^{2+} overload (Lee et al., 2017).

INVOLVEMENT OF Ca^{2+} IN PARAPTOSIS

Role of Ca^{2+} in Mitochondrial Dilation

Mitochondrial dilation is a key morphological feature of paraptosis, together with ER dilation (Sperandio et al., 2000).

Mitochondrial dilation generally includes both mitochondrial swelling and their fusion to form megamitochondria (giant mitochondria) in paraptosis (Yoon et al., 2010, 2012, 2014; Yumnam et al., 2014; Lee et al., 2017; Fontana et al., 2019; Zhao et al., 2019). Mitochondrial swelling is defined as an increase in mitochondrial volume due to an influx of fluid and is known to occur first by expansion of the intracristal space and later by swelling of the matrix compartment (Trump and Ginn, 1968). Some degree of mitochondrial swelling may occur as a reversible, pre-lethal form of cellular damage (Halestrap, 1989; Lim et al., 2002). The mitochondria become enlarged at most three times, by simple swelling, compared to their original size (typically 0.5–1 μm in length). The size of the dilated mitochondria, including megamitochondria (with width and length > 1 μm) (Lee et al., 2017; Wieczorek et al., 2017; Palma et al., 2019), in paraptosis often exceed those of swollen mitochondria observed during apoptosis or necrosis. Swollen mitochondria can be distinguished from megamitochondria by other morphological features, in addition to the degree of enlargement. Swollen mitochondria are seen to be round with pale matrix and cristae are observed only on the periphery, whereas the shape of megamitochondria in early stages are often irregular and the density of their matrix appears well maintained (Teranishi et al., 1999). When megamitochondria are further swollen, they are seen with a pale matrix and their cristae are detected only on the periphery. Previously, a treatment with Ca-SANDOZ reportedly induce the formation of megamitochondria in brown adipocyte of Wistar rats (Golic et al., 2014), but the exact role and the regulatory mechanism of megamitochondria formation in paraptosis remain to be clarified. In the paraptosis induced by hesperidin (Yumnam et al., 2016), δ -TT (Fontana et al., 2020a), IPH4 (Yokoi et al., 2020), and iturin A-like lipopeptides (Zhao et al., 2019), the mitochondria undergo swelling and show cristae disintegration and loss. On the other hand, megamitochondria formation due to the fusion of mitochondria is observed in the paraptosis induced by curcumin (Yoon et al., 2010), celastrol (Yoon et al., 2014), CGP-37157/Btz (Yoon et al., 2012), and Nutlin-3/Btz (Lee et al., 2017).

Ca^{2+} and K^{+} play important roles in the physiological and pathological swelling of the mitochondria. Imbalances of these ions between the cytosol and matrix increase the osmotic pressure and enhance the water influx, leading to matrix swelling (Kaasik et al., 2007; Javadov et al., 2018). The transport of Ca^{2+} and K^{+} across the IMM is associated with influx/efflux mechanisms for other ions, such as Na^{+} , Cl^{-} , and H^{+} (Halestrap et al., 1986; Halestrap, 1994; Kaasik et al., 2007; Javadov et al., 2018). This complex interplay between mitochondrial swelling and ion homeostasis maintains the mitochondrial function and metabolism under physiological conditions. Mild Ca^{2+} -mediated increases in matrix volume over the physiological range can promote oxidative phosphorylation and electron transfer chain and thus help satisfy the metabolic requirements of the cell (Halestrap, 1987, 1989; Lim et al., 2002). In addition, changes in IMM fluidity due to the altered mitochondrial shape and membrane tension may affect the activity of ion channels and other transporters, including the mechanosensitive

mitochondrial large-conductance Ca^{2+} -activated K^{+} channel (Walewska et al., 2018). Therefore, a slight increase of the matrix volume can regulate mitochondrial function and metabolism, possibly representing an adaptive response to protect the mitochondria against severe oxidative stress and delaying the onset of cell death. On the other hand, massive Ca^{2+} release from the ER causes the prolonged mitochondrial Ca^{2+} overload and excessive mitochondrial swelling (Rovere et al., 2016; Marchi et al., 2018). Mitochondrial Ca^{2+} overload has been commonly reported in paraptosis-associated cell death by curcumin (Yoon et al., 2012), celastrol (Yoon et al., 2014), hesperidin (Yumnam et al., 2016), morusin (Xue et al., 2018), δ -TT (Fontana et al., 2020a), IPH4 (Yokoi et al., 2020), Me_2NNMe_2 (Hager et al., 2018), CGP-37157/PI (Yoon et al., 2012), Ler/PI (Lee et al., 2019), Lop/PI (Kim et al., 2019), and Nutlin-3/PI (Lee et al., 2017). Among them, the functional significance of MCU-mediated mitochondrial Ca^{2+} overload as an early signal for paraptosis was confirmed by the reports that pharmacological and/or genetic inhibition of MCU attenuates the mitochondrial dilation and subsequent paraptotic cascades (i.e., ER stress, ER dilation, and subsequent cell death) induced by curcumin (Yoon et al., 2012), celastrol (Yoon et al., 2014), hesperidin (Yumnam et al., 2016), CGP-37157/PI (Yoon et al., 2012), and Ler/PI (Lee et al., 2019). VDAC-mediated mitochondria Ca^{2+} uptake was shown to be involved in morusin- or δ -TT-induced paraptotic cell death (Xue et al., 2018; Fontana et al., 2020a). The source of overloaded Ca^{2+} in the mitochondria was the ER (Yoon et al., 2012, 2014; Lee et al., 2019); RyR is reportedly involved in the release of Ca^{2+} from the ER in curcumin- or Ler/PI-induced paraptosis (Yoon et al., 2012; Lee et al., 2019), whereas IP₃R was involved in that process during celastrol-induced cell death (Yoon et al., 2014). In addition, both RyR and IP₃R were reported to mediate the release of Ca^{2+} from the ER during hesperidin-induced paraptosis (Yumnam et al., 2016). Furthermore, inhibition of the mNCC-mediated Ca^{2+} efflux from the mitochondria can contribute to mitochondrial Ca^{2+} accumulation and subsequent paraptotic events (Yoon et al., 2012). The combination of PI and the mNCC inhibitor, CGP-37157, induces paraptosis accompanied by sustained mitochondrial Ca^{2+} overload, mitochondrial dilation, ER stress, and ER dilation (Yoon et al., 2012). Collectively, these results suggest that an excessive Ca^{2+} overload in the mitochondria not only triggers mitochondrial dilation but also contributes to subsequent paraptotic events including ER dilation.

Role of Ca^{2+} in ER Dilation

Appropriate maintenance of the intraluminal homeostasis in the ER is needed to keep the cellular viability, and ER dilation is the most common morphological feature of paraptosis (Yoon et al., 2010, 2012, 2014; Yumnam et al., 2014; Lee et al., 2017, 2019; Hager et al., 2018; Xue et al., 2018; Fontana et al., 2019; Kim et al., 2019). Regarding the involvement of Ca^{2+} in paraptosis, Ca^{2+} depletion within the ER can contribute to ER dilation during paraptosis. Maintenance of sufficient Ca^{2+} levels within the ER is crucial for the function of components

of the protein folding machinery, such as chaperones and folding enzymes; this is because the chaperone activities of the molecular chaperones, Ig binding protein (Bip)/glucose-regulated protein 78 (GRP78), PDI, GRP94, and ERp57/PDIA3, are regulated by the binding of Ca^{2+} (Prins and Michalak, 2011; Carreras-Sureda et al., 2018). Therefore, alteration of the Ca^{2+} concentration within the ER by activation of IP₃R or RyR can contribute to ER stress and ER dilation by causing incorrect protein folding and an accumulation of misfolded proteins. Mimnaugh et al. (2006) showed that geldanamycin/Btz induces ER-derived vacuolation and proposed that this effect was due to a massive accumulation of misfolded proteins within the ER lumen. The authors believed that this would exert an osmotic force, resulting in the induction of an influx of water from the cytoplasm and the distension of the ER into vacuoles. The increased ER volume provided by ER-derived vacuolation may reduce the amount of misfolded proteins in the ER and facilitate their utilization, providing cells with an adaptive cellular response under mild stress (Mimnaugh et al., 2006). However, long-term unresolved ER stress may trigger extensive fusion among the swollen ER membranes and subsequently irreversible ER-derived vacuolation, resulting in an ER-associated degradation-compromised condition and cell death (Shubin et al., 2016). Recent studies have shown that impairment of protein thiol homeostasis also plays a critical role in plumbagin-induced paraptosis-associated cell death (Binoy et al., 2019), likewise with gambogic acid (Seo et al., 2019), ophiobolin A (Kim et al., 2017), and PDTC/doxorubicin (Park et al., 2018). These paraptosis-inducing agents commonly harbor highly electrophilic features that are used to covalently modify free sulfhydryl or hydroxyl groups on proteins, causing protein misfolding, misfolded protein accumulation in the ER lumen, ER stress, and ER dilation (Kim et al., 2017; Park et al., 2018; Seo et al., 2019). The thiol-reactivity of these agents may be responsible for their inhibitory effects on proteasomal activity; in fact, most paraptosis-inducing agents demonstrate proteasome inhibitory activity (Yoon et al., 2010, 2014; Wang et al., 2012). In addition, the copper complex of Me₂NNM₂-mediated PDI inhibition was shown to be responsible for the induction of paraptosis by the disruption of the ER protein thiol homeostasis (Hager et al., 2018). The authors proposed that disruption of the ER thiol redox homeostasis by PDI inhibition contributes to Ca^{2+} release from the ER, organelle swelling, mitochondrial membrane depolarization, and subsequent cell death. Collectively, these findings suggest that the cross-modulation between imbalanced Ca^{2+} in the ER and impaired proteostasis may be part of the progression of paraptosis.

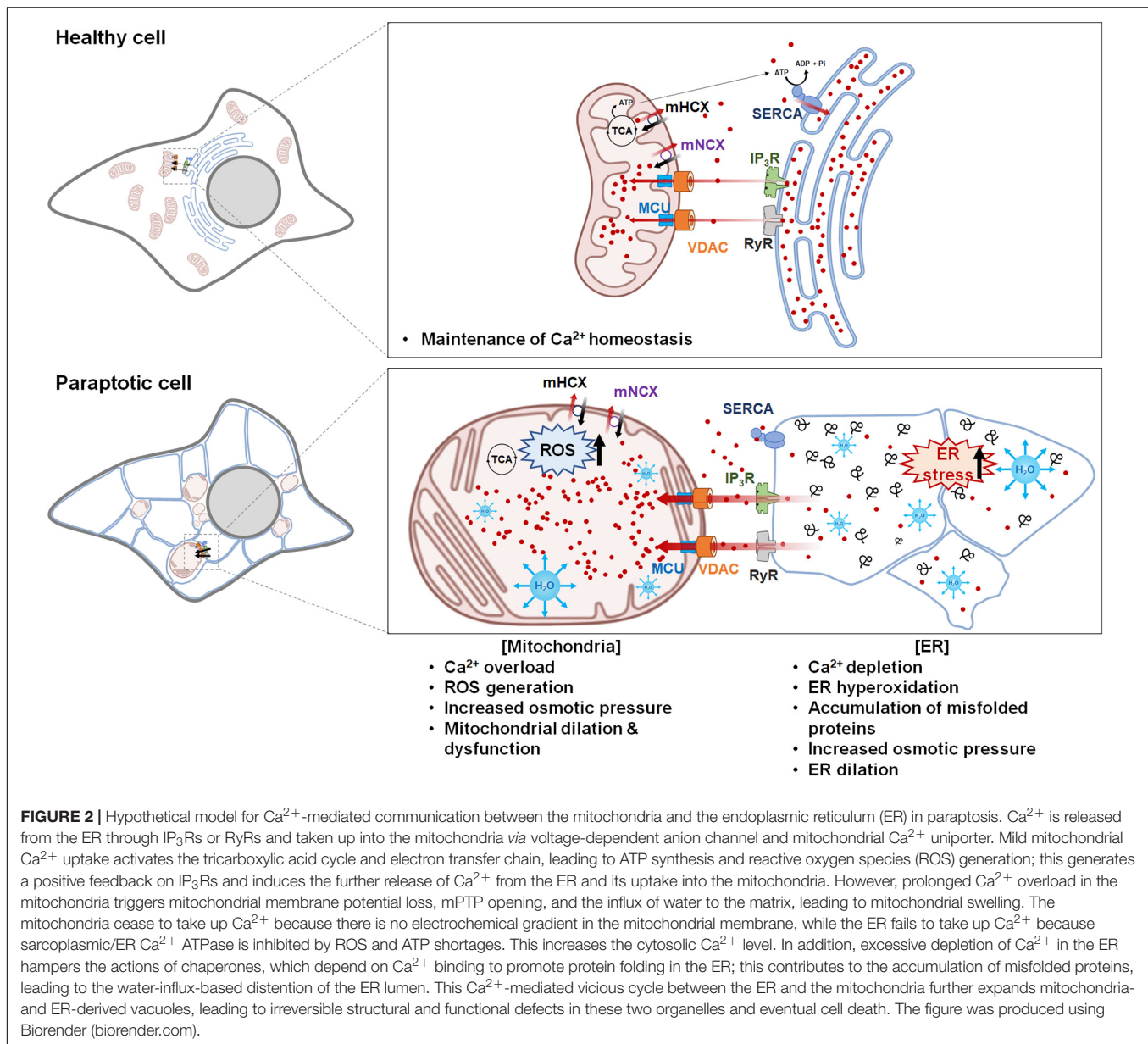
Ca^{2+} -Mediated Communication Between the ER and the Mitochondria in Paraptosis

During the progression of paraptosis, the dilation of the mitochondria and the ER appears to be interdependently controlled, although mitochondrial dilation generally precedes ER dilation. Based on reports indicating that intracellular Ca^{2+} transport is involved in the paraptosis induced by

various triggers, the following hypothetical model of the mechanisms underlying Ca^{2+} -mediated paraptosis can be proposed (Figure 2).

The regulation of Ca^{2+} signaling by the ER depends on SERCA-mediated Ca^{2+} uptake activity (Vandecaetsbeek et al., 2011), the expression of luminal Ca^{2+} binding proteins, and the activity of Ca^{2+} release channels, including IP₃R and RyR (Marks, 1997; Rovere et al., 2016). As an initial step of Ca^{2+} -mediated paraptosis, Ca^{2+} is released from the ER to the MAM through IP₃Rs or RyRs. The subsequent uptake of Ca^{2+} by the mitochondria is driven by the difference of membrane potential generated by the respiratory chain, which provides the electrochemical force needed for positively charged ions, such as Ca^{2+} , to enter the mitochondrial matrix (Giorgi et al., 2018). VDAC at the OMM (Gincel et al., 2001; Rapizzi et al., 2002) and MCU at the IMM mediate the uptake of Ca^{2+} into the mitochondria (Baughman et al., 2011; De Stefani et al., 2011). Mild mitochondrial Ca^{2+} uptake can activate the tricarboxylic acid cycle and electron transport chain, triggering mitochondrial ROS generation and the release of H₂O₂ at the MAM (Feissner et al., 2009; Rizzuto et al., 2012). This may provide positive feedback to IP₃Rs, enhancing their ability to sustain the release of Ca^{2+} from the ER and promote mitochondrial Ca^{2+} uptake. Furthermore, ER hyperoxidation due to thiol-oxidizing compounds also can promote Ca^{2+} release by opening of Ca^{2+} channels in the ER and inhibiting SERCA, thereby indirectly contributing to ER stress (Lizák et al., 2020). Interestingly, ROS generation was often associated with the paraptosis induced by Ca^{2+} homeostasis-perturbing drugs, including curcumin (Yoon et al., 2010), hesperidin (Yumnam et al., 2016), morusin (Xue et al., 2018), 8-TT (Fontana et al., 2020a), and chalcomoracin (Han et al., 2018), as shown in Table 1. However, the paraptosis induced by various drugs with thiol reactivity due to their high electrophilic nature, including Me₂NNM₂ (Hager et al., 2018), plumbagin (Binoy et al., 2019), gambogic acid (Seo et al., 2019), and ophiobolin A (Kim et al., 2017), was not correlated with ROS generation despite the fact that their vacuolation and cell death were successfully inhibited by the thiol-containing antioxidants. These results suggest that a thiol-dependent mechanism, rather than ROS, is critical for the anti-cancer activities of these drugs.

When considering the role of Ca^{2+} in mitochondrial dilation, it is notable that, at the early phase of paraptosis, Ca^{2+} -mediated mitochondrial dilation may represent an adaptive response aimed at facilitating the removal of Ca^{2+} released from the ER and regulating the mitochondrial matrix volume by relieving stress to support the functional and morphological integrity of the mitochondria and delay the onset of cell death. The phenomenon of the formation of megamitochondria at the initial phase of paraptosis could be also considered as an adaptive process at the organelle level to unfavorable conditions, although further studies are definitely needed to prove this hypothesis. However, prolonged Ca^{2+} influx from the ER may exceed the loading capacity of the mitochondria; this could cause mitochondrial depolarization and compromise mitochondrial function, ultimately resulting in irreversible cell death. In support of this hypothesis, several studies have shown that mitochondrial Ca^{2+} overload triggers the production of ROS, which can further



promote opening of mPTP (Hajnóczky et al., 2006; Görlach et al., 2015). This results in mitochondrial swelling because it allows water, ions, and other solutes to enter the matrix and equilibrate the solutes on both sides of the IMM (Kaasik et al., 2007; Javadov et al., 2018). Subsequent dissipation of the MMP results in uncoupling of oxidative phosphorylation and metabolic collapse. At the same time, loss of MMP might reduce the mitochondrial capacity to retain Ca^{2+} , resulting in increased cytosolic Ca^{2+} levels. In addition, cytosolic Ca^{2+} cannot be taken up into the ER due to the shortage of ATP, which is required for the ability of SERCA to pump Ca^{2+} into the ER. As a result, Ca^{2+} is severely depleted in the ER; this leads to the accumulation of misfolded proteins in the ER lumen, contributing to further ER dilation. Expansion of the luminal space of the ER and the subsequent fusion of swollen ER progress to the point that most

of the cellular space is occupied by large ER-derived vacuoles. Thus, sequential and multifactorial cross-modulation among mitochondrial Ca^{2+} , ROS, and $\Delta\Delta(\Psi_m)$ may contribute to the sequential and cooperative dilation of the mitochondria and the ER in paraptosis.

INVOLVEMENT OF OTHER IONS IN PARAPTOSIS

In addition to the disruption of Ca^{2+} homeostasis, imbalances of other ions, including K^+ and Cl^- , are reportedly involved in paraptosis. Previously, Hoa et al. (2007) reported that human monocytes/macrophages induce paraptotic cell death in human glioma cells expressing macrophage colony-stimulating factor;

this occurs *via* activation of BKCa channels, which are found at the ER and the mitochondria. The authors hypothesized that, when BKCa channels open, K^+ is expelled in exchange for the entry of Na^+ to maintain the electroneutrality of the cell. The entry of Na^+ results in the uptake of water, generating the observed cellular swelling and vacuolation (Hoa et al., 2007). Conversely, however, ophiobolin A was shown to induce paraptosis-like cell death in human glioblastoma cells by inhibiting BKCa channel activity (Bury et al., 2013). These authors proposed that BKCa inactivation would presumably induce the accumulation of K^+ in the ER and the mitochondria, leading to the increased osmotic pressure responsible for vacuolation. Subsequently, opening of Ca^{2+} channels present in the membrane or the ER may also contribute to the paraptotic cascade. Future work will be needed to investigate how both the activation of BKCa and its inhibition can induce paraptosis. Furthermore, an increase in intracellular Cl^- concentration by the activation of chloride intracellular channel-1 (CLIC1) was shown to be involved in the paraptosis induced by a purified resin glycoside fraction (RFP) of *Pharbitidis Semen* (Zhu et al., 2019). Blockade of CLIC1 by DIDS (an inhibitor of anion channels) attenuated ER stress, cytoplasmic vacuolization, and cell death, suggesting that CLIC1 may act as a critical and early signal in RFP-induced paraptosis. Taken together, these results indicate that the movements of both cations and anions can contribute to the induction of paraptosis.

DISCUSSION

The inherent or acquired resistance of tumor cells to apoptosis is a major hurdle limiting successful anticancer therapy and the cause of many cancer-related deaths (Holohan et al., 2013). Therefore, targeting cancer cells by the induction of an alternative caspase-independent cell death pathway (Mathiasen and Jäättelä, 2002), such as paraptosis, offers the opportunity to overcome apoptosis resistance in cancer cells. Rapidly proliferating and aneuploid cancer cells demand a much higher level of protein-folding activity in the ER, compared to normal cells (Deshaies, 2014). Additionally, cancer cells exhibit greater oxidative stress than normal cells due (at least partially) to oncogenic activation and altered mitochondrial activity (Gupta et al., 2011). Since paraptosis-inducing agents simultaneously target both the mitochondria and the ER, which are already under stress in cancer cells, therapeutic strategies aimed at inducing paraptosis may offer a two-pronged attack strategy to selectively kill cancer cells.

Although various models have been proposed to classify programmed cell death, exclusive definitions are difficult to conceptualize and probably factitious, given the crosstalk between cell death signaling pathway (Bröker et al., 2005). In addition, some morphological and biochemical features are shared in different cell death modes. Excessive swelling due to prolonged mitochondrial Ca^{2+} overload was reported to be able to induce apoptosis or necrosis, depending on the availability of ATP (Rovere et al., 2016; Marchi et al., 2018). In apoptosis, mitochondrial outer membrane permeabilization is critical for

the release of cytochrome c and other molecules, leading to the activation of caspases (Green and Kroemer, 1998). Although mitochondrial swelling is also an important morphological feature of paraptosis, no release of mitochondrial cytochrome c (Valamanesh et al., 2007; Gandin et al., 2012; Yoon et al., 2014) and/or AIF (Valamanesh et al., 2007) into the cytosol was shown in several models of paraptosis. In addition, no requirement of caspases has been reported in many studies on paraptosis (Lee et al., 2016; Fontana et al., 2020b). Mitochondrial swelling is also a key feature of oncosis, the cell death mode accompanied by cellular swelling, organelle swelling, blebbing, and increased membrane permeability, resulting in bursting of the plasma membrane (Majno and Joris, 1995; Weerasinghe and Buja, 2012). However, paraptosis is not associated with cell swelling. Furthermore, obvious damage to the OMM has not been shown in transmission electron microscopy pictures of cells undergoing paraptosis (Yoon et al., 2010, 2014; He et al., 2018; Xue et al., 2018; Yokoi et al., 2020). MMP was fairly maintained in the progression of paraptosis, but its loss was detected at the excessively expanded megamitochondria at the late stage of paraptosis (Lee et al., 2019; Seo et al., 2019). Reduced ATP synthesis is also observed following the extensive vacuolation derived from the mitochondria and/or the ER in paraptosis (He et al., 2018; Binoy et al., 2019; Nedungadi et al., 2019). Therefore, we presume that swelling and fusion of the mitochondria at the pre-lethal phase may provide an adaptive response that helps maintain mitochondrial membrane integrity and function before leading to irreversible paraptotic cell death. Further studies on the detailed changes in the structure/function of the mitochondria as well as the relationship between Ca^{2+} imbalance and the integrity of mitochondrial membrane during the progression of paraptosis will be helpful to clearly understand paraptosis and clarify the differences among various cell death modes accompanied by mitochondrial Ca^{2+} overload and swelling.

While curcumin (Yoon et al., 2010), celastrol (Yoon et al., 2014), hesperidin (Yumnam et al., 2014), IPH4 (Yokoi et al., 2020), and Me_2NNMe_2 (Hager et al., 2018) induce paraptosis independently of apoptosis and/or autophagy in the tested cancer cells, several agents, including δ -tocotrienol (Fontana et al., 2019, 2020a), chalcemorain (Han et al., 2018), and iturin A-like lipopeptides (Zhao et al., 2019), induce not only paraptosis but also simultaneous apoptosis and/or autophagy, as shown in **Table 1**. It is intriguing to speculate why the same agent can induce different cellular fates in some types of cells. The cellular response to a cytotoxic drug can be affected by various factors, including the type and dose of the drug, the extent of cytotoxic stress exerted to the cells, and the cellular context. It has been shown that more than one kind of cell death program can be activated at the same time (Unal-Cevik et al., 2004). The dominant cell death phenotype may be determined by the relative speed and effectiveness of the available death programs: In response to cellular damage, the characteristics of several death pathways can be exhibited, but in general, only the most effective and the fastest pathway is evident (Bröker et al., 2005). Furthermore, cellular heterogeneity (even within the same cell line) can contribute to the ability of a given drug to induce different cell death modes (Inde and Dixon, 2018). We now

know that many cancer cells are not homogeneous in nature but rather contain a variety of cells with different characteristics (Meacham and Morrison, 2013; Dagogo-Jack and Shaw, 2018). Thus, the presence of heterogeneous populations of cancer cells may yield different drug sensitivities, treatment resistances, and the induction of different or mixed types of cell death modes.

Although the molecular basis of paraptosis needs further investigation, many reports have indicated that impaired proteostasis is critical for the induction of paraptosis, as evidenced by the accumulation of poly-ubiquitinated proteins and ER stress marker proteins as well as the ability of the protein synthesis blocker to effectively inhibit vacuolation and cell death (Lee et al., 2016; Fontana et al., 2020b). As shown in **Table 1**, various chemicals have been shown to induce Ca^{2+} imbalance-mediated paraptosis. Interestingly, these Ca^{2+} homeostasis-disrupting drugs also induced proteostatic impairment, leading to the accumulation of poly-ubiquitinated proteins and ER stress marker proteins. Genetic or pharmacological inhibition of Ca^{2+} imbalance effectively blocked this proteostatic impairment and subsequent paraptosis (Yoon et al., 2010, 2014). These results suggest that disruption of Ca^{2+} homeostasis may negatively affect cellular proteostasis and enhance proteotoxicity, contributing to paraptosis. Pretreatment with CHX almost completely inhibited Ca^{2+} release from the ER, mitochondrial Ca^{2+} overload, disruption of proteostasis, and subsequent paraptotic events (Yoon et al., 2010, 2012; Yumnam et al., 2014; Lee et al., 2019). Taken together, these results suggest that Ca^{2+} imbalance and proteostatic disruption are interdependently regulated during the progression of paraptosis. In addition, simultaneous disruption of Ca^{2+} homeostasis and proteostasis, rather than induction of Ca^{2+} imbalance or proteostatic disruption alone, may be an effective means to kill cancer cells by inducing paraptosis (Yoon et al., 2012; Kim et al., 2019; Lee et al., 2019).

Btz, the first PI approved by FDA for clinical application, has shown efficacy in both front-line and relapsed/refractory settings, but its use can be limited by the development of resistance and/or side effects. The principal dose-limiting toxic effects of Btz are peripheral neuropathy, thrombocytopenia, neutropenia, fatigue, and diarrhea (Dou and Zonder, 2014). In addition, the PIs have shown limited clinical efficacy as monotherapies for solid tumors (Huang et al., 2014). However, Ca^{2+} homeostasis-perturbing drugs, such as lercanidipine, loperamide, and CGP-37157, act together with PIs to induce paraptosis (Yoon et al., 2012; Kim et al., 2019; Lee et al., 2019). Treatment with these Ca^{2+} homeostasis-perturbing drugs alone slightly and transiently induced mitochondrial dilation without dilation of the ER, whereas treatment with the PIs

alone was not enough to induce paraptosis in these studies. It is possible that either Ca^{2+} imbalance or proteasome inhibition may trigger cellular adaptive responses, including the autophagy, UPR, and reactivation of the ubiquitin-proteasome system, contributing to the restoration of cellular homeostasis and viability (Cooper et al., 1997; Brostrom and Brostrom, 2003; Ding et al., 2007). Additionally, the proteasome is involved in the degradation of both IP₃R (Oberdorf et al., 1999) and RyR (Pedrozo et al., 2010); thus, the PI-mediated stabilization of these Ca^{2+} channels may induce the enhanced and sustained release of Ca^{2+} from the ER in cells treated with these Ca^{2+} homeostasis-perturbing drugs, contributing to the effective induction of paraptosis. A combination of Ca^{2+} homeostasis-perturbing drugs and PIs may therefore effectively induce paraptosis by triggering a vicious cycle of ER-mitochondria Ca^{2+} signaling. Furthermore, the combined regimen of a PI plus Ca^{2+} -modulating clinical drugs may provide us many advantages, including enhanced therapeutic effectiveness, better safety due to the reduced side effects of a PI by the use of its lower dose, and the potential to expand the applicability of PIs to solid tumors (Kim et al., 2019; Lee et al., 2019). Therefore, induction of paraptosis through modulation of Ca^{2+} signaling may provide a novel therapeutic strategy to overcome the resistance of solid tumors against PIs in the future. It will be intriguing to explore the processes/regulatory pathways underlying the differences between ER and mitochondrial Ca^{2+} transfer in cancer cells vs. normal cells under paraptosis-inducing conditions. Further investigation of the regulatory mechanisms of Ca^{2+} in paraptosis may provide new insights into paraptosis and potential therapeutic strategies for the treatment of resistant cancer.

AUTHOR CONTRIBUTIONS

EK and KSC wrote the manuscript. KSC supervised the preparation of the manuscript. DML created the figures. MJS and HJL created the table. All the authors contributed to the article and approved the submitted version.

FUNDING

This work was supported by the National Research Foundation of Korea (NRF) grants funded by the Korea Government: Mid-career Research Program, NRF-2020R1A2C1013562 (KSC), and Basic Science Research Program, NRF-2018R1A6A1A03025810 (EK).

REFERENCES

- Bartok, A., Weaver, D., Golenar, T., Nichtova, Z., Katona, M., Bansaghi, S., et al. (2019). IP₃ receptor isoforms differently regulate ER-mitochondrial contacts and local calcium transfer. *Nat. Commun.* 10:3726. doi: 10.1038/s41467-019-11646-3
- Baughman, J. M., Perocchi, F., Girgis, H. S., Plovanich, M., Belcher-Timme, C. A., Sancak, Y., et al. (2011). Integrative genomics identifies MCU as an essential component of the mitochondrial calcium uniporter. *Nature* 476, 341–345. doi: 10.1038/nature10234
- Ben-Hail, D., and Shoshan-Barmatz, V. (2016). VDAC1-interacting anion transport inhibitors inhibit VDAC1 oligomerization and apoptosis. *Biochim. Biophys. Acta Mol. Cell Res.* 1863(7 Pt A), 1612–1623. doi: 10.1016/j.bbamer.2016.04.002
- Bianchi, K., Rimessi, A., Prandini, A., Szabadkai, G., and Rizzuto, R. (2004). Calcium and mitochondria: mechanisms and functions of a troubled

- relationship. *Biochim. Biophys. Acta Mol. Cell Res.* 1742, 119–131. doi: 10.1016/j.bbamcr.2004.09.015
- Binoi, A., Nedungadi, D., Katiyar, N., Bose, C., Shankarappa, S. A., Nair, B. G., et al. (2019). Plumbagin induces paraptosis in cancer cells by disrupting the sulphydryl homeostasis and proteasomal function. *Chem. Biol. Interact.* 310:108733. doi: 10.1016/j.cbi.2019.108733
- Bröker, L. E., Kruyt, F. A., and Giaccone, G. (2005). Cell death independent of caspases: a review. *Clin. Cancer Res.* 11, 3155–3162. doi: 10.1158/1078-0432.Ccr-04-2223
- Brostrom, M. A., and Brostrom, C. O. (2003). Calcium dynamics and endoplasmic reticular function in the regulation of protein synthesis: implications for cell growth and adaptability. *Cell Calcium* 34, 345–363. doi: 10.1016/s0143-4160(03)00127-1
- Bury, M., Girault, A., Mégallizi, V., Spiegl-Kreinecker, S., Mathieu, V., Berger, W., et al. (2013). Ophiobolin A induces paraptosis-like cell death in human glioblastoma cells by decreasing BKCa channel activity. *Cell Death Dis.* 4:e561. doi: 10.1038/cddis.2013.85
- Carreras-Sureda, A., Pihán, P., and Hetz, C. (2018). Calcium signaling at the endoplasmic reticulum: fine-tuning stress responses. *Cell Calcium* 70, 24–31. doi: 10.1016/j.ceca.2017.08.004
- Cascão, R., Fonseca, J. E., and Moita, L. F. (2017). Celastrol: a spectrum of treatment opportunities in chronic diseases. *Front. Med.* 4:69. doi: 10.3389/fmed.2017.00069
- Cooper, G. R., Brostrom, C. O., and Brostrom, M. A. (1997). Analysis of the endoplasmic reticular Ca^{2+} requirement for alpha1-antitrypsin processing and transport competence. *Biochem. J.* 325(Pt 3), 601–608. doi: 10.1042/bj3250601
- Csordás, G., Thomas, A. P., and Hajnóczky, G. (1999). Quasi-synaptic calcium signal transmission between endoplasmic reticulum and mitochondria. *EMBO J.* 18, 96–108. doi: 10.1093/emboj/18.1.96
- Dagogo-Jack, I., and Shaw, A. T. (2018). Tumour heterogeneity and resistance to cancer therapies. *Nat. Rev. Clin. Oncol.* 15, 81–94. doi: 10.1038/nrclinonc.2017.166
- Dash, R. K., and Beard, D. A. (2008). Analysis of cardiac mitochondrial Na^{+} - Ca^{2+} exchanger kinetics with a biophysical model of mitochondrial Ca^{2+} handling suggests a 3:1 stoichiometry. *J. Physiol.* 586, 3267–3285. doi: 10.1113/jphysiol.2008.151977
- De Stefani, D., Raffaello, A., Teardo, E., Szabò, I., and Rizzuto, R. (2011). A forty-kilodalton protein of the inner membrane is the mitochondrial calcium uniporter. *Nature* 476, 336–340. doi: 10.1038/nature10230
- Deshaies, R. J. (2014). Proteotoxic crisis, the ubiquitin-proteasome system, and cancer therapy. *BMC Biol.* 12:94. doi: 10.1186/s12915-014-0094-0
- Ding, W.-X., Ni, H.-M., Gao, W., Yoshimori, T., Stolz, D. B., Ron, D., et al. (2007). Linking of autophagy to ubiquitin-proteasome system is important for the regulation of endoplasmic reticulum stress and cell viability. *Am. J. Pathol.* 171, 513–524. doi: 10.2353/ajpath.2007.070188
- Dou, Q. P., and Zonder, J. A. (2014). Overview of proteasome inhibitor-based anti-cancer therapies: perspective on bortezomib and second generation proteasome inhibitors versus future generation inhibitors of ubiquitin-proteasome system. *Curr. Cancer Drug Targets* 14, 517–536. doi: 10.2174/1568009614666140804154511
- Elrod, J. W., Wong, R., Mishra, S., Vagnozzi, R. J., Sakthivel, B., Goonasekera, S. A., et al. (2010). Cyclophilin D controls mitochondrial pore-dependent Ca^{2+} exchange, metabolic flexibility, and propensity for heart failure in mice. *J. Clin. Invest.* 120, 3680–3687. doi: 10.1172/jci43171
- Feissner, R. F., Skalska, J., Gaum, W. E., and Sheu, S.-S. (2009). Crosstalk signaling between mitochondrial Ca^{2+} and ROS. *Front. Biosci.* 14:1197–1218. doi: 10.2741/3303
- Fontana, F., Moretti, R. M., Raimondi, M., Marzagalli, M., Beretta, G., Procacci, P., et al. (2019). 8-Tocotrienol induces apoptosis, involving endoplasmic reticulum stress and autophagy, and paraptosis in prostate cancer cells. *Cell Prolif.* 52:e12576. doi: 10.1111/cpr.12576
- Fontana, F., Raimondi, M., Marzagalli, M., Audano, M., Beretta, G., Procacci, P., et al. (2020a). Mitochondrial functional and structural impairment is involved in the antitumor activity of 8-tocotrienol in prostate cancer cells. *Free Radic. Biol. Med.* 160, 376–390. doi: 10.1016/j.freeradbiomed.2020.07.009
- Fontana, F., Raimondi, M., Marzagalli, M., Domizio, A. D., and Limonta, P. (2020b). The emerging role of paraptosis in tumor cell biology: perspectives for cancer prevention and therapy with natural compounds. *Biochim. Biophys. Acta Rev. Cancer* 1873:188338. doi: 10.1016/j.bbcan.2020.188338
- Gandin, V., Pellei, M., Tisato, F., Porchia, M., Santini, C., and Marzano, C. (2012). A novel copper complex induces paraptosis in colon cancer cells via the activation of ER stress signalling. *J. Cell Mol. Med.* 16, 142–151. doi: 10.1111/j.1582-4934.2011.01292.x
- Gincel, D., Zaid, H., and Shoshan-Barmatz, V. (2001). Calcium binding and translocation by the voltage-dependent anion channel: a possible regulatory mechanism in mitochondrial function. *Biochem. J.* 358, 147–155. doi: 10.1042/bj3580147
- Giorgi, C., Marchi, S., and Pinton, P. (2018). The machineries, regulation and cellular functions of mitochondrial calcium. *Nat. Rev. Mol. Cell Biol.* 19, 713–730. doi: 10.1038/s41580-018-0052-8
- Goel, A., and Aggarwal, B. B. (2010). Curcumin, the golden spice from Indian saffron, is a chemosensitizer and radiosensitizer for tumors and chemoprotector and radioprotector for normal organs. *Nut. r Cancer* 62, 919–930. doi: 10.1080/01635581.2010.509835
- Golic, I., Velickovic, K., Markelic, M., Stancic, A., Jankovic, A., Vucetic, M., et al. (2014). Calcium-induced alteration of mitochondrial morphology and mitochondrial-endoplasmic reticulum contacts in rat brown adipocytes. *Eur. J. Histochem.* 58:2377. doi: 10.4081/ejh.2014.2377
- Görlach, A., Bertram, K., Hudecova, S., and Krizanová, O. (2015). Calcium and ROS: a mutual interplay. *Redox Biol.* 6, 260–271. doi: 10.1016/j.redox.2015.08.010
- Green, D., and Kroemer, G. (1998). The central executioners of apoptosis: caspases or mitochondria? *Trends Cell Biol.* 8, 267–271. doi: 10.1016/s0962-8924(98)01273-2
- Gunter, K. K., Zuscik, M. J., and Gunter, T. E. (1991). The Na^{+} -independent Ca^{2+} efflux mechanism of liver mitochondria is not a passive $\text{Ca}^{2+}/2\text{H}^{+}$ exchanger. *J. Biol. Chem.* 266, 21640–21648.
- Gupta, S. C., Hevia, D., Patchva, S., Park, B., Koh, W., and Aggarwal, B. B. (2011). Upsides and downsides of reactive Oxygen species for cancer: the roles of reactive Oxygen Species in tumorigenesis, prevention, and therapy. *Antioxidants Redox Signal.* 16, 1295–1322. doi: 10.1089/ars.2011.4414
- Hager, S., Korbula, K., Bielec, B., Grusch, M., Pirker, C., Schosserer, M., et al. (2018). The thiosemicarbazone Me(2)NNMe(2) induces paraptosis by disrupting the ER thiol redox homeostasis based on protein disulfide isomerase inhibition. *Cell Death Dis.* 9:1052. doi: 10.1038/s41419-018-1102-z
- Hajnóczky, G., Csordás, G., Das, S., Garcia-Perez, C., Saotome, M., Sinha Roy, S., et al. (2006). Mitochondrial calcium signalling and cell death: approaches for assessing the role of mitochondrial Ca^{2+} uptake in apoptosis. *Cell Calcium* 40, 553–560. doi: 10.1016/j.ceca.2006.08.016
- Halestrap, A. P. (1987). The regulation of the oxidation of fatty acids and other substrates in rat heart mitochondria by changes in the matrix volume induced by osmotic strength, valinomycin and Ca^{2+} . *Biochem. J.* 244, 159–164. doi: 10.1042/bj2440159
- Halestrap, A. P. (1989). The regulation of the matrix volume of mammalian mitochondria in vivo and in vitro and its role in the control of mitochondrial metabolism. *Biochim. Biophys. Acta - Bioenerg.* 973, 355–382. doi: 10.1016/S0005-2728(89)80378-0
- Halestrap, A. P. (1994). Regulation of mitochondrial metabolism through changes in matrix volume. *Biochem. Soc. Trans.* 22, 522–529. doi: 10.1042/bst0220522
- Halestrap, A. P., Quinlan, P. T., Whipps, D. E., and Armston, A. E. (1986). Regulation of the mitochondrial matrix volume in vivo and in vitro. The role of calcium. *Biochem. J.* 236, 779–787. doi: 10.1042/bj2360779
- Han, H., Chou, C. C., Li, R., Liu, J., Zhang, L., Zhu, W., et al. (2018). Chalconoracin is a potent anticancer agent acting through triggering Oxidative stress via a mitophagy- and paraptosis-dependent mechanism. *Sci. Rep.* 8:9566. doi: 10.1038/s41598-018-27724-3
- He, L., Wang, K. N., Zheng, Y., Cao, J. J., Zhang, M. F., Tan, C. P., et al. (2018). Cyclometalated iridium(III) complexes induce mitochondria-derived paraptotic cell death and inhibit tumor growth in vivo. *Dalton. Trans.* 47, 6942–6953. doi: 10.1039/c8dt00783g
- Hoa, N. T., Zhang, J. G., Delgado, C. L., Myers, M. P., Callahan, L. L., Vandeusen, G., et al. (2007). Human monocytes kill M-CSF-expressing glioma cells by BK channel activation. *Lab. Invest.* 87, 115–129. doi: 10.1038/labinvest.3700506

- Holohan, C., Van Schaeybroeck, S., Longley, D. B., and Johnston, P. G. (2013). Cancer drug resistance: an evolving paradigm. *Nat. Rev. Cancer* 13, 714–726. doi: 10.1038/nrc3599
- Huang, Z., Wu, Y., Zhou, X., Xu, J., Zhu, W., Shu, Y., et al. (2014). Efficacy of therapy with bortezomib in solid tumors: a review based on 32 clinical trials. *Future Oncol.* 10, 1795–1807. doi: 10.2217/fon.14.30
- Inde, Z., and Dixon, S. J. (2018). The impact of non-genetic heterogeneity on cancer cell death. *Crit. Rev. Biochem. Mol. Biol.* 53, 99–114. doi: 10.1080/10409238.2017.1412395
- Javadov, S., Chapa-Dubocq, X., and Makarov, V. (2018). Different approaches to modeling analysis of mitochondrial swelling. *Mitochondrion* 38, 58–70. doi: 10.1016/j.mito.2017.08.004
- Jessen, F., Sjöholm, C., and Hoffmann, E. K. (1986). Identification of the anion exchange protein of Ehrlich cells: a kinetic analysis of the inhibitory effects of 4,4'-diisothiocyanato-2,2'-stilbene-disulfonic acid (DIDS) and labeling of membrane proteins with 3H-DIDS. *J. Membr. Biol.* 92, 195–205. doi: 10.1007/bf01869388
- Jung, D. W., Baysal, K., and Brierley, G. P. (1995). The sodium-calcium antiporter of heart mitochondria is not electroneutral. *J. Biol. Chem.* 270, 672–678. doi: 10.1074/jbc.270.2.672
- Kaasik, A., Safulina, D., Zharkovsky, A., and Veksler, V. (2007). Regulation of mitochondrial matrix volume. *Am. J. Physiol. Cell Physiol.* 292, C157–C163. doi: 10.1152/ajpcell.00272.2006
- Kim, I. Y., Kwon, M., Choi, M. K., Lee, D., Lee, D. M., Seo, M. J., et al. (2017). Ophiobolin A kills human glioblastoma cells by inducing endoplasmic reticulum stress via disruption of thiol proteostasis. *Oncotarget* 8, 106740–106752. doi: 10.18632/oncotarget.22537
- Kim, I. Y., Shim, M. J., Lee, D. M., Lee, A. R., Kim, M. A., Yoon, M. J., et al. (2019). Loperamide overcomes the resistance of colon cancer cells to bortezomib by inducing CHOP-mediated paraptosis-like cell death. *Biochem. Pharmacol.* 162, 41–54. doi: 10.1016/j.bcp.2018.12.006
- Lee, A. R., Seo, M. J., Kim, J., Lee, D. M., Kim, I. Y., Yoon, M. J., et al. (2019). Lercanidipine synergistically enhances bortezomib cytotoxicity in cancer cells via enhanced endoplasmic reticulum stress and mitochondrial Ca^{2+} overload. *Int. J. Mol. Sci.* 20:6112. doi: 10.3390/ijms20246112
- Lee, D., Kim, I., Saha, S., and Choi, K. (2016). Paraptosis in the anti-cancer arsenal of natural products. *Pharmacol. Ther.* 162, 120–133. doi: 10.1016/j.pharmthera.2016.01.003
- Lee, D. M., Kim, I. Y., Seo, M. J., Kwon, M. R., and Choi, K. S. (2017). Nutlin-3 enhances the bortezomib sensitivity of p53-defective cancer cells by inducing paraptosis. *Exp. Mol. Med.* 49:e365. doi: 10.1038/emmm.2017.112
- Lim, K. H. H., Javadov, S. A., Das, M., Clarke, S. J., Suleiman, M. S., and Halestrap, A. P. (2002). The effects of ischaemic preconditioning, diazoxide and 5-hydroxydecanoate on rat heart mitochondrial volume and respiration. *J. Physiol.* 545, 961–974. doi: 10.1111/jphysiol.2002.031484
- Lizák, B., Birk, J., Zana, M., Kosztyi, G., Kratschmar, D. V., Odermatt, A., et al. (2020). Ca^{2+} mobilization-dependent reduction of the endoplasmic reticulum lumen is due to influx of cytosolic glutathione. *BMC Biol.* 18:19. doi: 10.1186/s12915-020-0749-y
- Lu, X., Kwong, J. Q., Molkentin, J. D., and Bers, D. M. (2016). Individual cardiac mitochondria undergo rare transient permeability transition pore openings. *Circ Res* 118, 834–841. doi: 10.1161/circresaha.115.308093
- Majno, G., and Joris, I. (1995). Apoptosis, oncosis, and necrosis. An overview of cell death. *Am. J. Pathol.* 146, 3–15.
- Mallilankaraman, K., Cárdenas, C., Doonan, P. J., Chandramoorthy, H. C., Irrinki, K. M., Golenár, T., et al. (2012). MCUR1 is an essential component of mitochondrial Ca^{2+} uptake that regulates cellular metabolism. *Nat. Cell Biol.* 14, 1336–1343. doi: 10.1038/ncb2622
- Marchi, S., Patergnani, S., Missiroli, S., Morciano, G., Rimessi, A., Wieckowski, M. R., et al. (2018). Mitochondrial and endoplasmic reticulum calcium homeostasis and cell death. *Cell Calcium* 69, 62–72. doi: 10.1016/j.ceca.2017.05.003
- Marks, A. R. (1997). Intracellular calcium-release channels: regulators of cell life and death. *Am. J. Physiol. Heart Circ. Physiol.* 272, H597–H605. doi: 10.1152/ajpheart.1997.272.2.H597
- Mathiasen, I. S., and Jäättelä, M. (2002). Triggering caspase-independent cell death to combat cancer. *Trends Mol. Med.* 8, 212–220. doi: 10.1016/S1471-4914(02)02328-6
- Meacham, C. E., and Morrison, S. J. (2013). Tumour heterogeneity and cancer cell plasticity. *Nature* 501, 328–337. doi: 10.1038/nature12624
- Mimnaugh, E. G., Xu, W., Vos, M., Yuan, X., and Neckers, L. (2006). Endoplasmic reticulum vacuolization and valosin-containing protein relocation result from simultaneous Hsp90 inhibition by geldanamycin and proteasome inhibition by velcade. *Mol. Cancer Res.* 4, 667–681. doi: 10.1158/1541-7786.Mcr-06-0019
- Nedungadi, D., Binoy, A., Vinod, V., Vanuopadath, M., Nair, S. S., Nair, B. G., et al. (2019). Ginger extract activates caspase independent paraptosis in cancer cells via ER stress, mitochondrial dysfunction, AIF translocation and DNA damage. *Nutr. Cancer* 1–13. doi: 10.1080/01635581.2019.1685113 [Epub ahead of print].
- Oberdorf, J., Webster, J. M., Zhu, C. C., Luo, S. G., and Wojcikiewicz, R. J. (1999). Down-regulation of types I, II and III inositol 1,4,5-trisphosphate receptors is mediated by the ubiquitin/proteasome pathway. *Biochem. J.* 339(Pt 2), 453–461.
- Palma, E., Ma, X., Riva, A., Iansante, V., Dhawan, A., Wang, S., et al. (2019). Dynamin-1-Like protein inhibition drives megamitochondria formation as an adaptive response in alcohol-induced hepatotoxicity. *Am. J. Pathol.* 189, 580–589. doi: 10.1016/j.ajpath.2018.11.008
- Park, S. S., Lee, D. M., Lim, J. H., Lee, D., Park, S. J., Kim, H. M., et al. (2018). Pyrrolidine dithiocarbamate reverses Bcl-xL-mediated apoptotic resistance to doxorubicin by inducing paraptosis. *Carcinogenesis* 39, 458–470. doi: 10.1093/carcin/bgy003
- Park, W., Amin, A. R., Chen, Z. G., and Shin, D. M. (2013). New perspectives of curcumin in cancer prevention. *Cancer Prev. Res.* 6, 387–400. doi: 10.1158/1940-6207.Capr-12-0410
- Patron, M., Checchetto, V., Raffaello, A., Teardo, E., Vecellio Reane, D., Mantoan, M., et al. (2014). MICU1 and MICU2 finely tune the mitochondrial Ca^{2+} uniporter by exerting opposite effects on MCU activity. *Mol. Cell* 53, 726–737. doi: 10.1016/j.molcel.2014.01.013
- Pedrozo, Z., Sánchez, G., Torrealba, N., Valenzuela, R., Fernández, C., Hidalgo, C., et al. (2010). Calpains and proteasomes mediate degradation of ryanodine receptors in a model of cardiac ischemic reperfusion. *Biochim. Biophys. Acta* 1802, 356–362. doi: 10.1016/j.bbdis.2009.12.005
- Perocchi, F., Gohil, V. M., Girgis, H. S., Bao, X. R., McCombs, J. E., Palmer, A. E., et al. (2010). MICU1 encodes a mitochondrial EF hand protein required for Ca^{2+} uptake. *Nature* 467, 291–296. doi: 10.1038/nature09358
- Plovanič, M., Bogorad, R. L., Sancak, Y., Kamer, K. J., Strittmatter, L., Li, A. A., et al. (2013). MICU2, a paralog of MICU1, resides within the mitochondrial uniporter complex to regulate calcium handling. *PLoS One* 8:e55785. doi: 10.1371/journal.pone.0055785
- Prins, D., and Michalak, M. (2011). Organellar calcium buffers. *Cold Spring Harbor Perspect. Biol.* 3:a004069. doi: 10.1101/cshperspect.a004069
- Raffaello, A., De Stefani, D., Sabbadin, D., Teardo, E., Merli, G., Picard, A., et al. (2013). The mitochondrial calcium uniporter is a multimer that can include a dominant-negative pore-forming subunit. *EMBO J.* 32, 2362–2376. doi: 10.1038/emboj.2013.157
- Rapizzi, E., Pinton, P., Szabadkai, G., Wieckowski, M. R., Vandecasteele, G., Baird, G., et al. (2002). Recombinant expression of the voltage-dependent anion channel enhances the transfer of Ca^{2+} microdomains to mitochondria. *J. Cell Biol.* 159, 613–624. doi: 10.1083/jcb.200205091
- Rizzuto, R., De Stefani, D., Raffaello, A., and Mammucari, C. (2012). Mitochondria as sensors and regulators of calcium signalling. *Nat. Rev. Mol. Cell Biol.* 13, 566–578. doi: 10.1038/nrm3412
- Rizzuto, R., Pinton, P., Carrington, W., Fay, F. S., Fogarty, K. E., Lifshitz, L. M., et al. (1998). Close contacts with the endoplasmic reticulum as determinants of mitochondrial Ca^{2+} responses. *Science* 280, 1763–1766. doi: 10.1126/science.280.5370.1763
- Rovere, R. M. L. L., Roest, G., Bultynck, G., and Parys, J. B. (2016). Intracellular Ca^{2+} signaling and Ca^{2+} microdomains in the control of cell survival, apoptosis and autophagy. *Cell Calcium* 60, 74–87. doi: 10.1016/j.ceca.2016.04.005
- Sancak, Y., Markhard, A. L., Kitami, T., Kovács-Bogdán, E., Kamer, K. J., Udeshi, N. D., et al. (2013). EMRE is an essential component of the mitochondrial calcium uniporter complex. *Science* 342, 1379–1382. doi: 10.1126/science.1242993
- Seo, M. J., Lee, D. M., Kim, I. Y., Lee, D., Choi, M. K., Lee, J. Y., et al. (2019). Gambogic acid triggers vacuolization-associated cell death in cancer cells via

- disruption of thiol proteostasis. *Cell Death Dis.* 10:187. doi: 10.1038/s41419-019-1360-4
- Shubin, A. V., Demidyuk, I. V., Komissarov, A. A., Rafeeva, L. M., and Kostrov, S. V. (2016). Cytoplasmic vacuolization in cell death and survival. *Oncotarget* 7, 55863–55889. doi: 10.18632/oncotarget.10150
- Sperandio, S., de Belle, I., and Bredesen, D. E. (2000). An alternative, nonapoptotic form of programmed cell death. *Proc. Natl. Acad. Sci. U.S.A.* 97, 14376–14381. doi: 10.1073/pnas.97.26.14376
- Sperandio, S., Poksay, K., de Belle, I., Lafuente, M. J., Liu, B., Nasir, J., et al. (2004). Paraptosis: mediation by MAP kinases and inhibition by AIP-1/Alix. *Cell Death Differ.* 11, 1066–1075. doi: 10.1038/sj.cdd.4401465
- Teranishi, M., Karbowski, M., Kurono, C., Soji, T., and Wakabayashi, T. (1999). Two types of the enlargement of mitochondria related to apoptosis: simple swelling and the formation of megamitochondria. *J. Electron. Microsc.* 48, 637–651. doi: 10.1093/oxfordjournals/jmicro.a023730
- Tomar, D., Dong, Z., Shanmughapriya, S., Koch, D. A., Thomas, T., Hoffman, N. E., et al. (2016). MCU1 Is a Scaffold Factor for the MCU Complex Function and Promotes Mitochondrial Bioenergetics. *Cell Rep.* 15, 1673–1685. doi: 10.1016/j.celrep.2016.04.050
- Trump, B. F., and Ginn, F. L. (1968). Studies of cellular injury in isolated flounder tubules. II. Cellular swelling in high potassium media. *Lab. Invest.* 18, 341–351.
- Unal-Cevik, I., Kiling, M., Can, A., Gürsoy-Ozdemir, Y., and Dalkara, T. (2004). Apoptotic and necrotic death mechanisms are concomitantly activated in the same cell after cerebral ischemia. *Stroke* 35, 2189–2194. doi: 10.1161/01.STR.0000136149.81831.c5
- Valamanesh, F., Torriglia, A., Savoldelli, M., Gandolphe, C., Jeanny, J. C., BenEzra, D., et al. (2007). Glucocorticoids induce retinal toxicity through mechanisms mainly associated with paraptosis. *Mol. Vis.* 13, 1746–1757.
- Vandecaetsbeek, I., Vangheluwe, P., Raeymaekers, L., Wuytack, F., and Vanoevelen, J. (2011). The Ca^{2+} pumps of the endoplasmic reticulum and golgi apparatus. *Cold Spring Harbor Perspect. Biol.* 3:a004184. doi: 10.1101/cshperspect.a004184
- Vassilev, L. T. (2007). MDM2 inhibitors for cancer therapy. *Trends Mol. Med.* 13, 23–31. doi: 10.1016/j.molmed.2006.11.002
- Vassilev, L. T., Vu, B. T., Graves, B., Carvajal, D., Podlaski, F., Filipovic, Z., et al. (2004). In vivo activation of the p53 pathway by small-molecule antagonists of MDM2. *Science* 303, 844–848. doi: 10.1126/science.1092472
- Walewska, A., Kulawiak, B., Szewczyk, A., and Koprowski, P. (2018). Mechanosensitivity of mitochondrial large-conductance calcium-activated potassium channels. *Biochim. Biophys. Acta Bioenerg.* 1859, 797–805. doi: 10.1016/j.bbmbio.2018.05.006
- Wang, W. B., Feng, L. X., Yue, Q. X., Wu, W. Y., Guan, S. H., Jiang, B. H., et al. (2012). Paraptosis accompanied by autophagy and apoptosis was induced by celastrol, a natural compound with influence on proteasome, ER stress and Hsp90. *J. Cell Physiol.* 227, 2196–2206. doi: 10.1002/jcp.22956
- Weerasinghe, P., and Buja, L. M. (2012). Oncosis: an important non-apoptotic mode of cell death. *Exp. Mol. Pathol.* 93, 302–308. doi: 10.1016/j.yexmp.2012.09.018
- Wei, T., Kang, Q., Ma, B., Gao, S., Li, X., and Liu, Y. (2015). Activation of autophagy and paraptosis in retinal ganglion cells after retinal ischemia and reperfusion injury in rats. *Exp. Ther. Med.* 9, 476–482. doi: 10.3892/etm.2014.2084
- Wieczorek, A., Stępień, P. M., Zarębska-Michaluk, D., Kryczka, W., Pabjan, P., and Król, T. (2017). Megamitochondria formation in hepatocytes of patient with chronic hepatitis C - a case report. *Clin. Exp. Hepatol.* 3, 169–175. doi: 10.5114/ceh.2017.68287
- Xue, J., Li, R., Zhao, X., Ma, C., Lv, X., Liu, L., et al. (2018). Morusin induces paraptosis-like cell death through mitochondrial calcium overload and dysfunction in epithelial ovarian cancer. *Chem. Biol. Interact.* 283, 59–74. doi: 10.1016/j.cbi.2018.02.003
- Yokoi, K., Balachandran, C., Umezawa, M., Tsuchiya, K., Mitriae, A., and Aoki, S. (2020). Amphiphilic Cationic Triscyclometalated Iridium(III) complex-peptide hybrids induce paraptosis-like cell death of cancer cells via an intracellular Ca^{2+} -Dependent pathway. *ACS Omega* 5, 6983–7001. doi: 10.1021/acsomega.0c00337
- Yoon, M. J., Kim, E. H., Kwon, T. K., Park, S. A., and Choi, K. S. (2012). Simultaneous mitochondrial Ca^{2+} overload and proteasomal inhibition are responsible for the induction of paraptosis in malignant breast cancer cells. *Cancer Lett.* 324, 197–209. doi: 10.1016/j.canlet.2012.05.018
- Yoon, M. J., Kim, E. H., Lim, J. H., Kwon, T. K., and Choi, K. S. (2010). Superoxide anion and proteasomal dysfunction contribute to curcumin-induced paraptosis of malignant breast cancer cells. *Free Radic. Biol. Med.* 48, 713–726. doi: 10.1016/j.freeradbiomed.2009.12.016
- Yoon, M. J., Lee, A. R., Jeong, S. A., Kim, Y. S., Kim, J. Y., Kwon, Y. J., et al. (2014). Release of Ca^{2+} from the endoplasmic reticulum and its subsequent influx into mitochondria trigger celastrol-induced paraptosis in cancer cells. *Oncotarget* 5, 6816–6831. doi: 10.18632/oncotarget.2256
- Yumnam, S., Hong, G. E., Raha, S., Saralamma, V. V., Lee, H. J., Lee, W. S., et al. (2016). Mitochondrial dysfunction and Ca^{2+} overload contributes to hesperidin induced paraptosis in hepatoblastoma cells. *HepG2. J. Cell Physiol.* 231, 1261–1268. doi: 10.1002/jcp.25222
- Yumnam, S., Park, H. S., Kim, M. K., Nagappan, A., Hong, G. E., Lee, H. J., et al. (2014). hesperidin induces paraptosis like cell death in hepatoblastoma, HepG2 cells: involvement of ERK1/2 MAPK [corrected]. *PLoS One* 9:e101321. doi: 10.1371/journal.pone.0101321
- Zhang, F. J., Yang, J. Y., Mou, Y. H., Sun, B. S., Ping, Y. F., Wang, J. M., et al. (2009). Inhibition of U-87 human glioblastoma cell proliferation and formyl peptide receptor function by oligomer procyanidins (F2) isolated from grape seeds. *Chem. Biol. Interact.* 179, 419–429. doi: 10.1016/j.cbi.2008.12.017
- Zhang, F. J., Yang, J. Y., Mou, Y. H., Sun, B. S., Wang, J. M., and Wu, C. F. (2010). Oligomer procyanidins from grape seeds induce a paraptosis-like programmed cell death in human glioblastoma U-87 cells. *Pharm. Biol.* 48, 883–890. doi: 10.3109/13880200903311102
- Zhao, H., Xu, X., Lei, S., Shao, D., Jiang, C., Shi, J., et al. (2019). Iturin A-like lipopeptides from *Bacillus subtilis* trigger apoptosis, paraptosis, and autophagy in Caco-2 cells. *J. Cell Physiol.* 234, 6414–6427. doi: 10.1002/jcp.27377
- Zhu, D., Chen, C., Xia, Y., Kong, L. Y., and Luo, J. (2019). A purified resin glycoside fraction from pharbitidis semen induces paraptosis by activating chloride intracellular Channel-1 in Human colon cancer cells. *Integr. Cancer Ther.* 18:1534735418822120. doi: 10.1177/1534735418822120
- Zoofishan, Z., Hohmann, J., and Hunyadi, A. (2018). Phenolic antioxidants of Morus nigra roots, and antitumor potential of morusin. *Phytochem. Rev.* 17, 1031–1045. doi: 10.1007/s11101-018-9565-1

Conflict of Interest: The authors declare that the research was conducted in the absence of any commercial or financial relationships that could be construed as a potential conflict of interest.

Copyright © 2021 Kim, Lee, Seo, Lee and Choi. This is an open-access article distributed under the terms of the Creative Commons Attribution License (CC BY). The use, distribution or reproduction in other forums is permitted, provided the original author(s) and the copyright owner(s) are credited and that the original publication in this journal is cited, in accordance with accepted academic practice. No use, distribution or reproduction is permitted which does not comply with these terms.



Positive Inotropic Effects of ATP Released *via* the Maxi-Anion Channel in Langendorff-Perfused Mouse Hearts Subjected to Ischemia-Reperfusion

Hiroshi Matsuura^{1*}, Akiko Kojima², Yutaka Fukushima², Yu Xie¹, Xinya Mi¹, Ravshan Z. Sabirov³ and Yasunobu Okada^{4,5,6}

¹ Department of Physiology, Shiga University of Medical Science, Otsu, Japan, ² Department of Anesthesiology, Shiga University of Medical Science, Otsu, Japan, ³ Institute of Biophysics and Biochemistry, National University of Uzbekistan, Tashkent, Uzbekistan, ⁴ National Institute for Physiological Sciences (NIPS), Okazaki, Japan, ⁵ Department of Physiology, School of Medicine, Aichi Medical University, Nagakute, Japan, ⁶ Department of Physiology, Kyoto Prefectural University of Medicine, Kyoto, Japan

OPEN ACCESS

Edited by:

Bin Li,

Shanghai Jiao Tong University School of Medicine, China

Reviewed by:

Yayi Gao,

National Cancer Institute (NCI),

United States

Rudolf Gesztelyi,

University of Debrecen, Hungary

Vladimir Lj Jakovljevic,

University of Kragujevac, Serbia

*Correspondence:

Hiroshi Matsuura

matuurah@belle.shiga-med.ac.jp

Specialty section:

This article was submitted to

Cell Death and Survival,

a section of the journal

Frontiers in Cell and Developmental

Biology

Received: 23 August 2020

Accepted: 04 January 2021

Published: 21 January 2021

Citation:

Matsuura H, Kojima A, Fukushima Y, Xie Y, Mi X, Sabirov RZ and Okada Y (2021) Positive Inotropic Effects of ATP Released *via* the Maxi-Anion Channel in Langendorff-Perfused Mouse Hearts Subjected to Ischemia-Reperfusion. *Front. Cell Dev. Biol.* 9:597997. doi: 10.3389/fcell.2021.597997

The organic anion transporter SLCO2A1 constitutes an essential core component of the ATP-conductive large-conductance anion (Maxi-Cl) channel. Our previous experiments using Langendorff-perfused mouse hearts showed that the Maxi-Cl channel contributes largely to the release of ATP into the coronary effluent observed during 10-min reperfusion following a short period (6 min) of oxygen-glucose deprivation. The present study examined the effect of endogenous ATP released *via* Maxi-Cl channels on the left ventricular contractile function of Langendorff-perfused mouse hearts, using a fluid-filled balloon connected to a pressure transducer. After the initial 30-min stabilization period, the heart was then perfused with oxygen-glucose-deprived Tyrode solution for 6 min, which was followed by a 10-min perfusion with oxygenated normal Tyrode solution in the absence and presence of an ATP-hydrolyzing enzyme, apyrase, and/or an adenosine A1 receptor antagonist, 8-cyclopentyl-1,3-dipropylxanthine (DPCPX). In the absence of apyrase and DPCPX, the left ventricular developed pressure (LVDP) decreased from a baseline value of 72.3 ± 7.1 to 57.5 ± 5.5 mmHg ($n = 4$) at the end of 6-min perfusion with oxygen-glucose-deprived Tyrode solution, which was followed by a transient increase to 108.5 ± 16.5 mmHg during subsequent perfusion with oxygenated normal Tyrode solution. However, in the presence of apyrase and DPCPX, the LVDP decreased to the same degree during 6-min perfusion with oxygen-glucose-deprived Tyrode solution, but failed to exhibit a transient increase during a subsequent perfusion with oxygenated normal Tyrode solution. These results strongly suggest that endogenous ATP released through Maxi-Cl channels contributes to the development of transient positive inotropy observed during reperfusion after short-period hypoxia/ischemia in the heart.

Keywords: ATP release, endogenous ATP, ischemia-reperfusion, left ventricular contractile function, maxi-anion channel, Langendorff perfusion, mouse heart

INTRODUCTION

During hypoxia or ischemia, ATP is known to be released from the heart (Paddle and Burnstock, 1974; Forrester and Williams, 1977; Clemens and Forrester, 1981; Williams and Forrester, 1983; Vial et al., 1987; Borst and Schrader, 1991) and cardiomyocytes (Borst and Schrader, 1991; Kuzmin et al., 1998, 2000; Dutta et al., 2004; Kunugi et al., 2011). In neonatal rat cardiomyocytes, it was demonstrated that ATP is released predominantly through the maxi-anion channel in response to hypoxia or ischemia (Dutta et al., 2004; Kunugi et al., 2011). By applying unbiased genome-wide approaches and by using targeted siRNA screening and CRISPR/Cas9-mediated knockout, we recently demonstrated that the organic anion transporter *SLCO2A1* constitutes the core component of the maxi-anion channel (Sabirov et al., 2017). In addition, our experiments using the Langendorff-perfused mouse heart model showed (i) that the release of ATP into the coronary effluent is markedly enhanced during 10-min reperfusion after a short period (6 min) of the oxygen-glucose deprivation, and (ii) that treatment of the mouse with *Slco2a1*-targeting siRNA significantly reduces the release of ATP (Sabirov et al., 2017). These observations support the view that ATP is released through the ATP-conductive large-conductance anion (Maxi-Cl) channel during reperfusion following a short period of hypoxia in the Langendorff-perfused mouse heart model. The present study was designed to investigate the effect of endogenous ATP released during hypoxia/reperfusion on the left ventricular contractile function of Langendorff-perfused mouse heart model.

Previous studies showed that extracellular application of ATP, but not ADP, AMP or adenosine, increases the contractility of rat ventricular myocytes (Danziger et al., 1988) and that when adenosine receptors were blocked, this exogenously applied ATP produces a positive inotropic effect in isolated left atria from guinea-pig (Mantelli et al., 1993). In the present study, we aimed to examine whether endogenous ATP, but not its hydrolyzed products, released from the mouse heart during hypoxia/reperfusion exerts a positive inotropic action.

MATERIALS AND METHODS

Langendorff Perfusion of Mouse Heart

All animal care and experimental procedures were performed in accordance with the Guide for the Care and Use of Laboratory Animals published by the US National Institutes of Health (NIH Publication No. 85-23, revised 1996) and were approved by the Shiga University of Medical Science Institutional Animal Care and Use Committee [approval numbers 2015-3-4H, 2016-7-21(H1), and 2018-11-2]. Female C57BL/6J mice of 8 to 10 weeks (body weight, 16–20 g) were used in the present study, in the same manner as was reported in our previous study (Sabirov et al., 2017). The mice were deeply anesthetized with an overdose of sodium pentobarbital (300 mg/kg, intraperitoneal injection) with heparin (8,000 U/kg), and the heart was excised and transferred rapidly to a Langendorff perfusion apparatus (ADInstruments, Castle Hill, NSW, Australia). Hearts were perfused with oxygenated (bubbled with 100% O₂) normal

Tyrode solution at 37°C at a constant hydrostatic pressure of 80 mmHg. The normal Tyrode solution contained (in mM) 140 NaCl, 5.4 KCl, 1.8 CaCl₂, 0.5 MgCl₂, 0.33 NaH₂PO₄, 5.5 glucose and 5 HEPES (pH adjusted to 7.4 with NaOH). A fluid-filled balloon (made of plastic film) connected to a pressure transducer (ADInstruments) was introduced into the left ventricular cavity through an opening of the left atrial appendage and inflated to achieve a left ventricular end-diastolic pressure (LVEDP) of approximately 5–10 mmHg (Kojima et al., 2018). The pressure was continuously measured and recorded with PowerLab 8/30 and LabChart Pro-7.0 software programs (ADInstruments). Hearts were immersed in warmed perfusate in a water-jacketed organ chamber (approximately 100 ml in volume) maintained at 37°C (Reichelt et al., 2009).

Experimental Protocols

The Langendorff perfusion protocol was essentially the same as that used in our previous study for the measurement of ATP released into the coronary effluent in the mouse heart (Sabirov et al., 2017). After the initial 30 min of stabilization with oxygenated normal Tyrode solution, the experiments were started with following protocols: 6 min of oxygen-glucose deprivation (OGD) followed by 10 min of reperfusion with oxygenated normal (glucose-containing) Tyrode solution (OGD/reperfusion). The OGD treatment was conducted by perfusing the heart with 100% N₂-bubbled Tyrode solution in which glucose was replaced with an equimolar concentration of 2-deoxyglucose (Sigma Chemical Company, St. Louis, MO, United States). In the next set of experiments, we added 1 U/ml of an ATP-hydrolyzing enzyme, apyrase (Sigma), to the perfusion medium to degrade (remove) ATP, together with a selective adenosine A1 receptor antagonist, 8-cyclopentyl-1,3-dipropylxanthine (DPCPX, Sigma), at 10 μM. Apyrase sequentially catalyzes the breakdown of ATP to AMP, which is then degraded to adenosine by the action of the endothelial ecto-5'-nucleotidase (Gündüz et al., 2006). Possible stimulation of the adenosine A1 receptor is, however, prevented by the presence of DPCPX under this condition. Apyrase and DPCPX were added to the perfusion medium 10 min prior to imposition of OGD and were present throughout the experiment. During the same time period, apyrase (1 U/ml) or DPCPX (10 μM) was separately added to the perfusion medium to investigate the functional basis of ATP action. These perfusion protocols are summarized in **Figure 1**. The effect of OGD/reperfusion on the cardiac function was evaluated by measuring the following parameters: left ventricular developed pressure (LVDP), calculated by subtracting left ventricular end-diastolic pressure (LVEDP) from left ventricular (LV) systolic pressure, and the peak positive and negative differentials of pressure change with time (+dP/dt and -dP/dt, respectively). These parameters were evaluated before and at the end of 6-min OGD, and at 2–5 min and 10 min after reperfusion.

Statistical Analysis

All of the average data are presented as the mean ± SD, and the number of experiments is indicated by *n*. Statistical comparisons were evaluated using ANOVA with Tukey's *post hoc* test (Prism

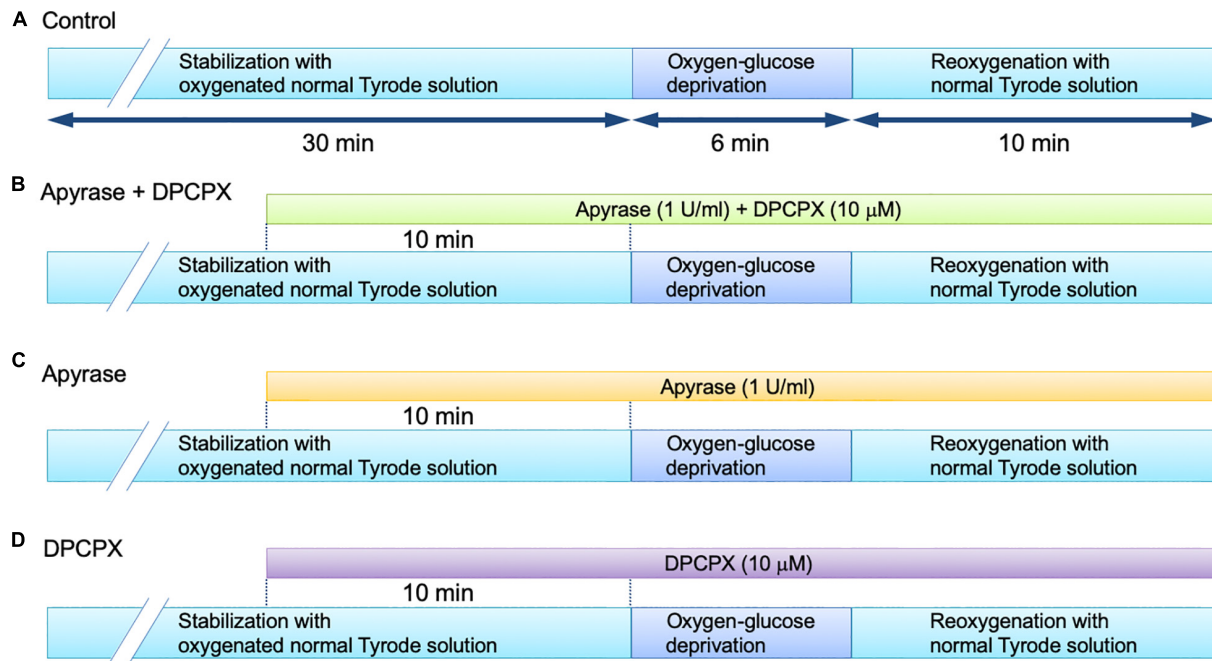


FIGURE 1 | Langendorff-perfusion protocol for isolated mouse hearts in the absence (A) and presence of apyrase + DPCPX (B), apyrase alone (C) and DPCPX alone (D).

Version 5.0; GraphPad Software, La Jolla, CA, United States). We used two-tailed hypothesis testing for all tests. Differences were considered to be statistically significant at $P < 0.05$.

RESULTS

In the present study, we examined the functional effect of endogenous ATP released upon OGD/reperfusion on the left ventricular contractile activity, using exactly the same perfusion protocol as that used by Sabirov et al. (2017). The LV pressure was measured using an intraventricular balloon as an index of the left ventricular contractile function. **Figure 2A** shows continuous recordings of LV pressure, measured before, during and after the 6-min OGD. The LV pressure gradually decreased during 6 min of OGD, which was followed by a transient increase over baseline levels during reperfusion with glucose-containing oxygenated medium.

We then conducted the same experiments in the concomitant presence of the ATP-hydrolyzing enzyme apyrase (1 U/ml) and the selective adenosine A1 receptor antagonist DPCPX (10 μ M). Under these conditions, the released ATP is expected to be degraded to adenosine (Gündüz et al., 2006), which, however, cannot stimulate the adenosine A1 receptor. **Figure 2B** demonstrates a representative experiment examining the effect of OGD/reperfusion on LV pressure during the continuous presence of apyrase and DPCPX. The LV pressure gradually decreased during OGD, similarly to the decrease observed in the experiment performed without apyrase and DPCPX (**Figure 2A**). However, a transient increase in LV pressure was

largely abolished during reperfusion in the presence of apyrase and DPCPX. Thus, concomitant addition of apyrase and DPCPX appears to scarcely affect the gradual decline in LV pressure observed during OGD but to significantly prevent a transient increase in LV pressure detected during reperfusion. We also examined the effect of apyrase and DPCPX added separately to the perfusion medium during the same time period, and found that a transient increase in LV pressure upon reperfusion following OGD appeared in the presence of DPCPX alone but was abolished in the presence of apyrase alone (data not shown, $n = 4$; see **Figures 3C, 4C**).

We next compared LVDP, measured at various time points during Langendorff perfusion conducted in the absence and presence of apyrase and DPCPX (**Figure 3**). Apyrase and DPCPX, added together or separately to the perfusion medium, did not significantly affect LVDP measured before OGD (**Figure 3A**). LVDP similarly decreased during 6-min OGD, irrespective of the presence of apyrase and/or DPCPX (**Figure 3B**). However, in the presence of apyrase + DPCPX or apyrase alone, LVDP measured at 2–5 min after reperfusion was significantly smaller than that measured without apyrase and DPCPX (Control) (**Figure 3C**). On the other hand, LVDP measured at 2–5 min after reperfusion did not significantly differ between control and DPCPX groups. There was no significant difference in LVDP measured at 10 min after reperfusion, irrespective of the presence of apyrase and/or DPCPX (**Figure 3D**). These experimental results indicate that the transient increase in LVDP observed during 10-min reperfusion after 6-min OGD is ascribable to ATP itself but not to its hydrolyzed product, adenosine, which stimulates the adenosine A1 receptors.

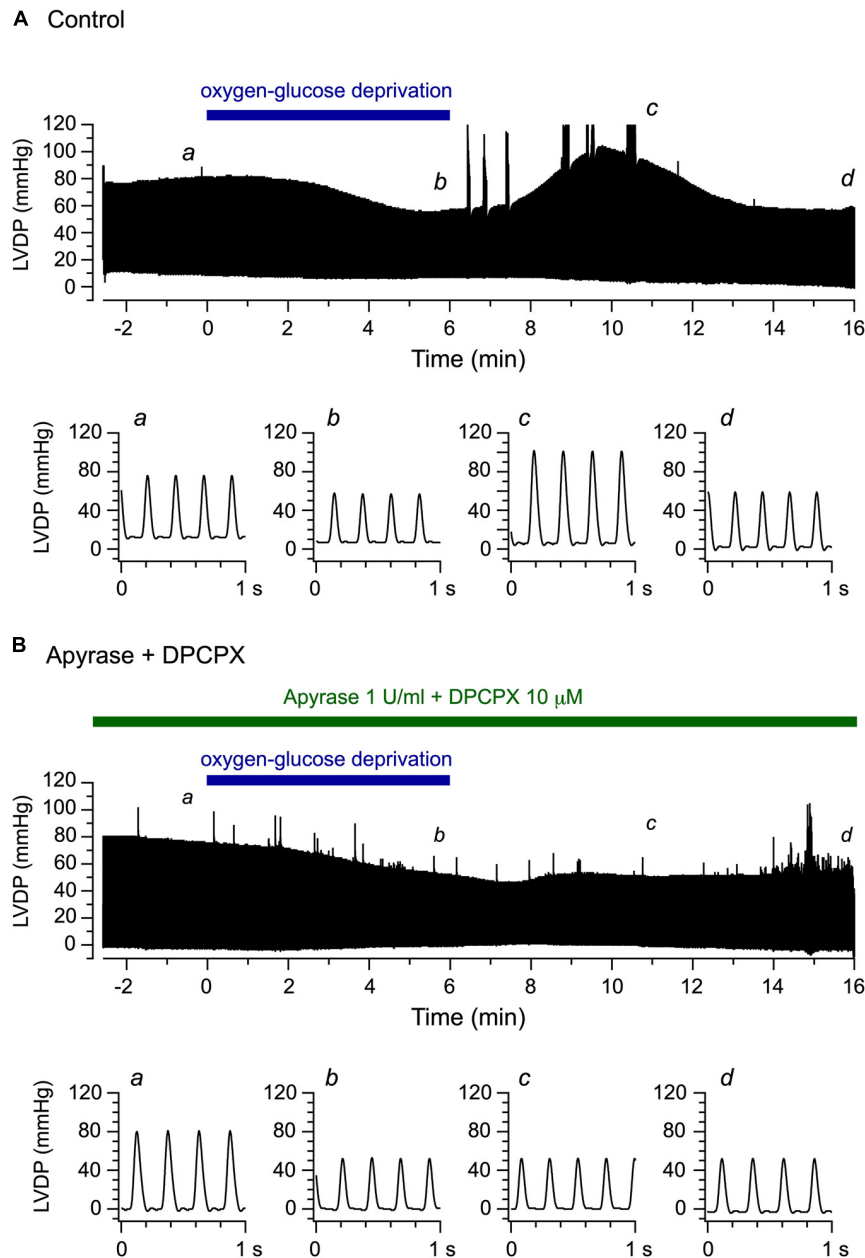


FIGURE 2 | Effects of oxygen-glucose deprivation (OGD) and reperfusion with an oxygenated, glucose-containing solution on the left ventricular function of the Langendorff-perfused mouse heart model. **(A,B)** Continuous traces of left ventricular pressure recorded before, during and after 6-min OGD in the absence **(A)** and presence **(B)** of 1 U/ml apyrase and 10 μ M DPCPX (upper panels). Lower panels illustrate original traces of left ventricular pressure, recorded at a, b, c, and d in upper panels, on expanded time scale.

We also evaluated the possible changes in the rate of contraction and relaxation (as assessed by $+dP/dt$ and $-dP/dt$, respectively) at various time points during Langendorff perfusion in the absence and presence of apyrase and/or DPCPX. As shown in **Figure 4**, both $+dP/dt$ and $-dP/dt$ measured at 2–5 min after reperfusion were significantly smaller in hearts perfused with apyrase + DPCPX or apyrase alone, in comparison to those perfused without apyrase and DPCPX (Control). It should also be noted that addition of DPCPX alone

did not produce any significant effect on $+dP/dt$ and $-dP/dt$ values measured at 2–5 min after reperfusion. There were no significant differences in $+dP/dt$ and $-dP/dt$ values measured at other time points. This observation suggests that endogenous ATP released during reperfusion following OGD causes a transient inotropic effect on Langendorff-perfused mouse hearts (**Figures 2, 3C**), which was associated with a considerable increase in the maximum rate of contraction ($+dP/dt$) and relaxation ($-dP/dt$) (**Figure 4C**).

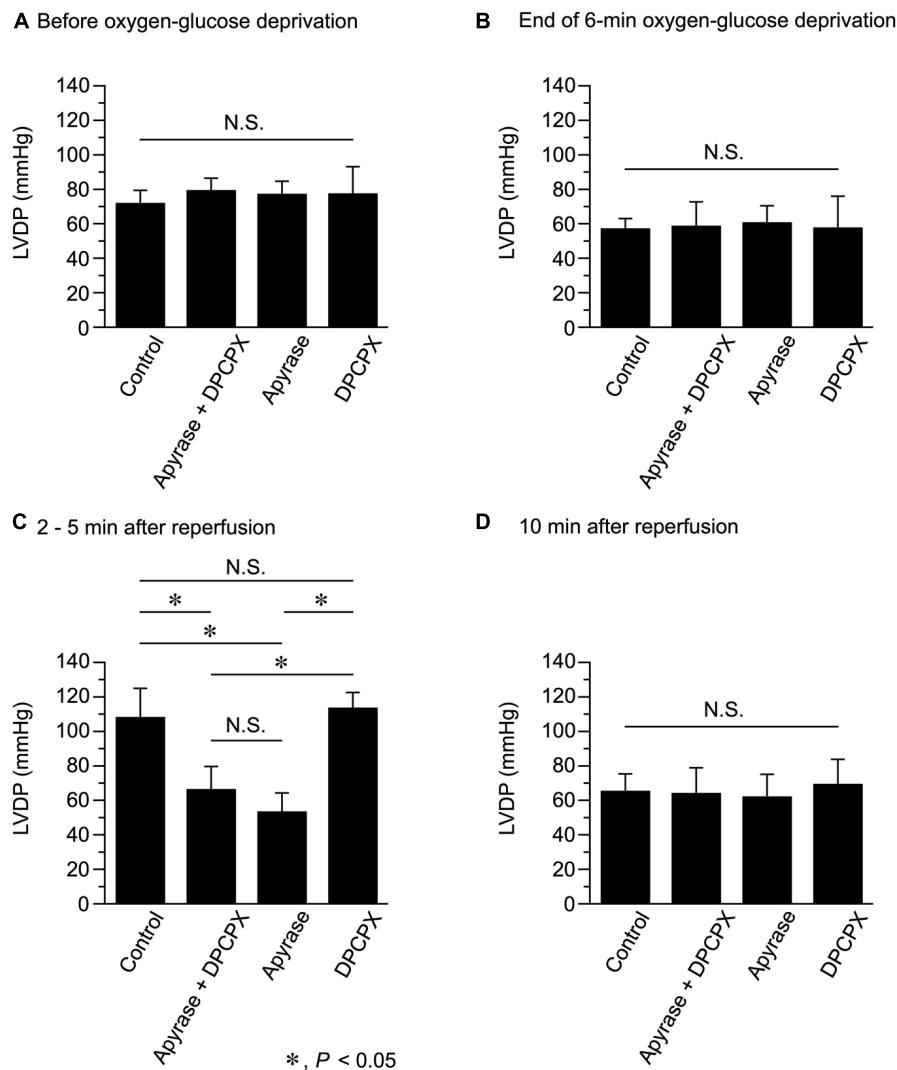


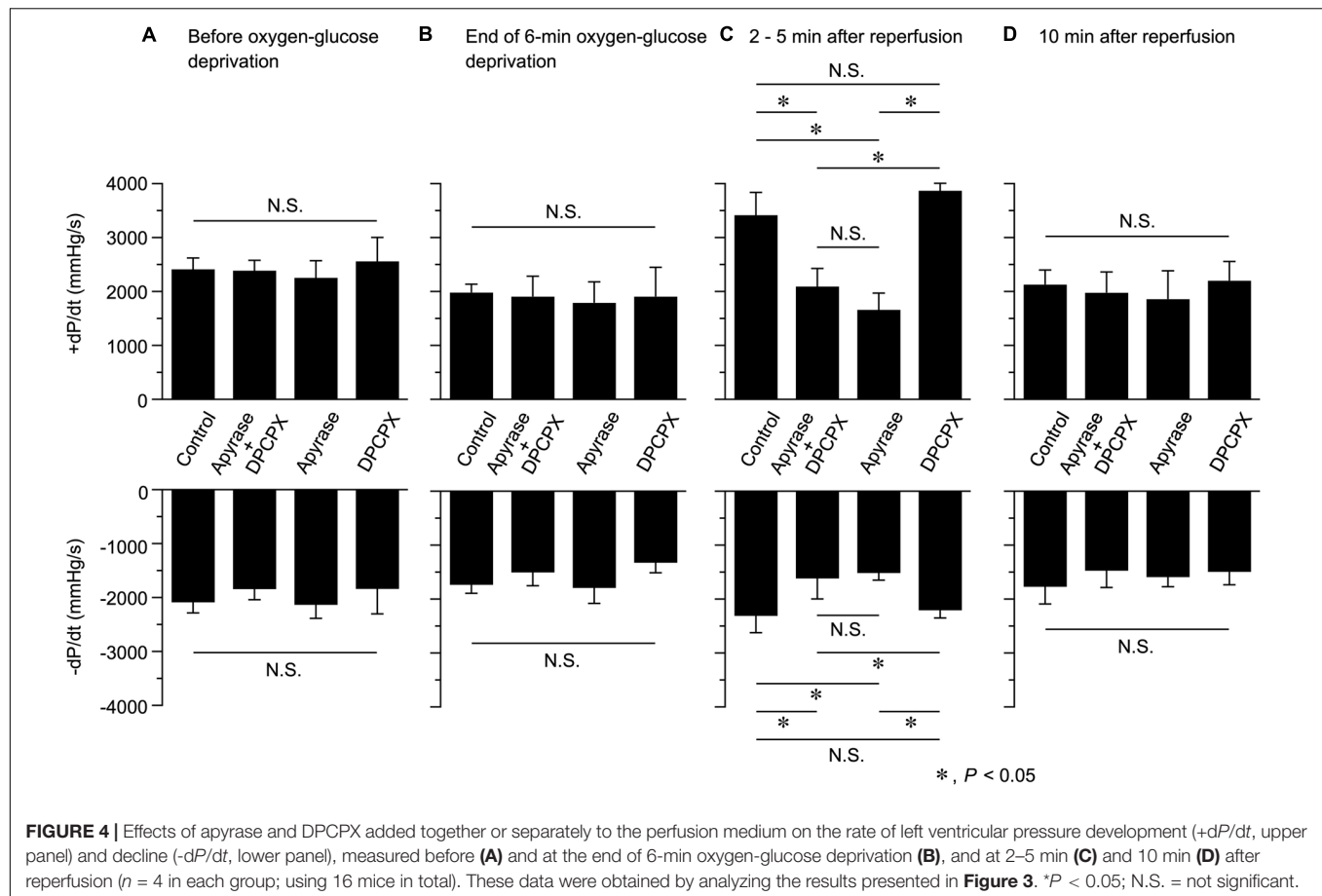
FIGURE 3 | Effects of apyrase and DPCPX added together or separately to the perfusion medium on left ventricular developed pressure (LVDP), measured before (A) and at the end of 6-min oxygen-glucose deprivation (B), and at 2–5 min (C) and 10 min (D) after reperfusion ($n = 4$ for each group; using 16 mice in total).

* $P < 0.05$; N.S. = not significant.

DISCUSSION

We previously showed that the amount of ATP release, which is largely mediated by the Maxi-Cl channel, is markedly enhanced during 10-min reperfusion following a short period (6 min) of perfusion with OGD (hypoxia) in the Langendorff-perfused mouse heart model (Sabirov et al., 2017). The present study investigated the functional effect of endogenous ATP on left ventricular contractility by directly measuring the developed pressure using exactly the same perfusion protocol in the mouse heart. The LVDP gradually decreased during 6-min OGD, which was followed by a transient increase in LVDP during 10-min reperfusion with oxygenated medium (Figure 2A). These results are in accordance with a previous study showing that LVDP is transiently increased over baseline levels during reperfusion following a short period (90 s) of global ischemia

in Langendorff-perfused mouse hearts (Bratkovsky et al., 2004). This transient inotropy was largely abolished under conditions in which ATP degradation was facilitated by the extracellular presence of apyrase and the adenosine A1 receptor was blocked by DPCPX (Figure 2B). Furthermore, this transient inotropy was similarly abolished by the presence of apyrase alone (Figure 3C), indicating that this inotropic response was caused by extracellular ATP. In contrast, the inotropic response was scarcely affected by the presence of DPCPX alone (Figure 3C). These results strongly suggest that a positive inotropy upon reperfusion after a short-period of OGD is evoked by ATP itself and is not due to the stimulation of adenosine A1 receptor by adenosine produced by degradation of ATP. It should be noted that the increase in ATP release during reperfusion is transient, peaking at approximately 4 min after reperfusion [see Figure 8C in Sabirov et al. (2017)]. Thus, the time course of



this transient increase in LVDP during reperfusion (Figure 2A) is qualitatively similar to the time course of the transient increase of ATP release, which largely occurs through the Maxi-Cl channel (Sabirov et al., 2017). Taken together, it is highly likely that the Maxi-Cl channel-mediated ATP release contributes to the development of transient positive inotropy during reperfusion following a short period of hypoxia in the mouse heart.

Extracellular ATP has been recognized as a local regulator of physiological functions in the cardiovascular system (Vassort, 2001; Burnstock and Pelleg, 2015). Extracellular ATP elicits various cellular responses by binding to specific cell membrane receptors, which can be divided into two major subfamilies, namely P2X receptors, which constitute ligand-gated channels and P2Y receptors, which are coupled to G-proteins and downstream signaling molecules (Burnstock and Pelleg, 2015). Several mechanisms have been proposed to explain the positive inotropic action of ATP in the heart (Vassort, 2001). For example, extracellular ATP enhances the L-type Ca^{2+} current (Scamps et al., 1990), produces inositol-1,4,5-trisphosphate (IP_3) (Legssyer et al., 1988) and cyclic AMP (Balogh et al., 2005), thereby activating the cardiac CFTR anion channels (Matsuura and Ehara, 1992; Kaneda et al., 1994; Levesque and Hume, 1995), or depolarizes the cell membrane through activation of non-selective cation channels (Christie et al.,

1992). All these cellular processes can lead to elevation of the intracellular free Ca^{2+} concentration $[(\text{Ca}^{2+})_i]$ and a subsequent positive inotropic action of ATP in the heart (Vassort, 2001).

The adenine nucleotides, ATP and ADP, are released from various types of cells in the heart, including sympathetic nerves, smooth muscles cells, blood cells and cardiac myocytes (Clemens and Forrester, 1981; Gordon, 1986; Vassort, 2001; Burnstock and Pelleg, 2015). Hypoxic conditions are regarded as prominent activators of the ATP release in the heart (Vassort, 2001). Evidence has been presented to support P2 purinoceptor-mediated cardioprotection during ischemia and reperfusion. For example, the stimulation of P2Y2 receptors with low concentrations of uridine triphosphate (UTP) improves the recovery of the contractile function and reduces the release of lactate dehydrogenase (LDH) during 45 min of reperfusion after 20 min of global ischemia in the Langendorff-perfused mouse heart model (Wee et al., 2007). It is also interesting to note that UTP and uridine diphosphate (UDP) produce positive inotropic effects on adult mouse cardiomyocytes by activating P2Y2 and P2Y6 receptors, as evaluated by stimulation-induced cell shortening (Wihlborg et al., 2006). It thus seems probable that endogenous ATP released through the Maxi-Cl channel contributes to a rapid recovery of left ventricular contractile function (Figures 2–4) and thereby

produces some protective effects on ischemia-reperfused hearts. Furthermore, our findings that endogenous ATP produces moderate positive inotropy may provide a clue for development of new type of inotropic agents for clinical settings. The present investigation represents an ischemia insult simulated by perfusing the mouse heart with oxygen-glucose-deprived Tyrode solution *in situ*. However, future studies should examine the functional role of ATP release using ischemic conditions that can occur in clinical conditions, such as occlusion of the coronary artery *in vivo*.

In conclusion, our results provide the experimental evidence supporting a possible role for endogenous ATP released through the Maxi-Cl channel during reperfusion as a positive inotropic factor for the heart.

DATA AVAILABILITY STATEMENT

The raw data supporting the conclusions of this article will be made available by the authors, without undue reservation.

REFERENCES

- Balogh, J., Wihlborg, A. K., Isackson, H., Joshi, B. V., Jacobson, K. A., Arner, A., et al. (2005). Phospholipase C and cAMP-dependent positive inotropic effects of ATP in mouse cardiomyocytes via P2Y₁₁-like receptors. *J. Mol. Cell. Cardiol.* 39, 223–230. doi: 10.1016/j.yjmcc.2005.03.007
- Borst, M. M., and Schrader, J. (1991). Adenine nucleotide release from isolated perfused guinea pig hearts and extracellular formation of adenosine. *Circ. Res.* 68, 797–806. doi: 10.1161/01.res.68.3.797
- Bratkovsky, S., Aasum, E., Birkeland, C. H., Riemersma, R. A., Myhre, E. S., and Larsen, T. S. (2004). Measurement of coronary flow reserve in isolated hearts from mice. *Acta. Physiol. Scand.* 181, 167–172. doi: 10.1111/j.1365-201X.2004.01280.x
- Burnstock, G., and Pelleg, A. (2015). Cardiac purinergic signalling in health and disease. *Purinergic Signal.* 11, 1–46. doi: 10.1007/s11302-014-9436-1
- Christie, A., Sharma, V. K., and Sheu, S. S. (1992). Mechanism of extracellular ATP-induced increase of cytosolic Ca²⁺ concentration in isolated rat ventricular myocytes. *J. Physiol.* 445, 369–388. doi: 10.1113/jphysiol.1992.sp018929
- Clemens, M. G., and Forrester, T. (1981). Appearance of adenosine triphosphate in the coronary sinus effluent from isolated working rat heart in response to hypoxia. *J. Physiol.* 312, 143–158. doi: 10.1113/jphysiol.1981.sp013621
- Danziger, R. S., Raffaeli, S., Moreno-Sanchez, R., Sakai, M., Capogrossi, M. C., Spurgeon, H. A., et al. (1988). Extracellular ATP has a potent effect to enhance cytosolic calcium and contractility in single ventricular myocytes. *Cell Calcium.* 9, 193–199. doi: 10.1016/0143-4160(88)90023-1
- Dutta, A. K., Sabirov, R. Z., Uramoto, H., and Okada, Y. (2004). Role of ATP-conductive anion channel in ATP release from neonatal rat cardiomyocytes in ischaemic or hypoxic conditions. *J. Physiol.* 559, 799–812. doi: 10.1113/jphysiol.2004.069245
- Forrester, T., and Williams, C. A. (1977). Release of adenosine triphosphate from isolated adult heart cells in response to hypoxia. *J. Physiol.* 268, 371–390. doi: 10.1113/jphysiol.1977.sp011862
- Gordon, J. L. (1986). Extracellular ATP: effects, sources and fate. *Biochem. J.* 233, 309–319. doi: 10.1042/bj2330309
- Gündüz, D., Kasseckert, S. A., Härtel, F. V., Aslam, M., Abdallah, Y., Schäfer, M., et al. (2006). Accumulation of extracellular ATP protects against acute reperfusion injury in rat heart endothelial cells. *Cardiovasc. Res.* 71, 764–773. doi: 10.1016/j.cardiores.2006.06.011
- Kaneda, M., Fukui, K., and Doi, K. (1994). Activation of chloride current by P2-purinoceptors in rat ventricular myocytes. *Br. J. Pharmacol.* 111, 1355–1360. doi: 10.1111/j.1476-5381.1994.tb14894.x

ETHICS STATEMENT

The animal study was reviewed and approved by The Shiga University of Medical Science Institutional Animal Care and Use Committee [approval numbers 2015-3-4H, 2016-7-21(H1), and 2018-11-2].

AUTHOR CONTRIBUTIONS

HM, RZS, and YO conceived and designed the study and drafted the manuscript. HM performed the experiments. HM, AK, YF, YX, and XM analyzed the data. All authors contributed to the article and approved the submitted version.

FUNDING

This study was supported by JSPS (The Japan Society for the Promotion of Science, Tokyo, Japan) KAKENHI Grant Numbers 17K08536 (to HM), 17K11050 (to AK), and 26293045 (to YO).

- Kojima, A., Fukushima, Y., Ito, Y., Ding, W. G., Kitagawa, H., and Matsuura, H. (2018). Transient receptor potential canonical channel blockers improve ventricular contractile functions after ischemia/reperfusion in a Langendorff-perfused mouse heart model. *J. Cardiovasc. Pharmacol.* 71, 248–255. doi: 10.1097/FJC.0000000000000566
- Kunugi, S., Iwabuchi, S., Matsuyama, D., Okajima, T., and Kawahara, K. (2011). Negative-feedback regulation of ATP release: ATP release from cardiomyocytes is strictly regulated during ischemia. *Biochem. Biophys. Res. Commun.* 416, 409–415. doi: 10.1016/j.bbrc.2011.11.068
- Kuzmin, A. I., Gourine, A. V., Molosh, A. I., Lakomkin, V. L., and Vassort, G. (2000). Effects of preconditioning on myocardial interstitial levels of ATP and its catabolites during regional ischemia and reperfusion in the rat. *Basic Res. Cardiol.* 95, 127–136. doi: 10.1007/s003950050174
- Kuzmin, A. I., Lakomkin, V. L., Kapelko, V. I., and Vassort, G. (1998). Interstitial ATP level and degradation in control and postmyocardial infarcted rats. *Am. J. Physiol.* 275, C766–C771. doi: 10.1152/ajpcell.1998.275.3.C766
- Legssyer, A., Poggioli, J., Renard, D., and Vassort, G. (1988). ATP and other adenine compounds increase mechanical activity and inositol triphosphate production in rat heart. *J. Physiol.* 401, 185–199. doi: 10.1113/jphysiol.1988.sp017157
- Levesque, P. C., and Hume, J. R. (1995). ATPo but not cAMPi activates a chloride conductance in mouse ventricular myocytes. *Cardiovasc. Res.* 29, 336–343. doi: 10.1016/0008-6363(96)88590-7
- Mantelli, L., Amerini, S., Filippi, S., and Ledda, F. (1993). Blockade of adenosine receptors unmasks a stimulatory effect of ATP on cardiac contractility. *Br. J. Pharmacol.* 109, 1268–1271. doi: 10.1111/j.1476-5381.1993.tb13759.x
- Matsuura, H., and Ehara, T. (1992). Activation of chloride current by purinergic stimulation in guinea pig heart cells. *Circ. Res.* 70, 851–855. doi: 10.1161/01.res.70.4.851
- Paddle, B. M., and Burnstock, G. (1974). Release of ATP from perfused heart during coronary vasodilatation. *Blood Vessels* 11, 110–119. doi: 10.1159/000158005
- Reichelt, M. E., Willems, L., Hack, B. A., Peart, J. N., and Headrick, J. P. (2009). Cardiac and coronary function in the Langendorff-perfused mouse heart model. *Exp. Physiol.* 94, 54–70. doi: 10.1113/expphysiol
- Sabirov, R. Z., Merzlyak, P. G., Okada, T., Islam, M. R., Uramoto, H., Mori, T., et al. (2017). The organic anion transporter SLCO2A1 constitutes the core component of the Maxi-Cl channel. *EMBO J.* 36, 3309–3324. doi: 10.15252/emboj.201796685
- Scamps, F., Legssyer, A., Mayoux, E., and Vassort, G. (1990). The mechanism of positive inotropy induced by adenosine triphosphate in rat heart. *Circ. Res.* 67, 1007–1016. doi: 10.1161/01.res.67.4.1007

- Vassort, G. (2001). Adenosine 5'-triphosphate: a P₂-purinergic agonist in the myocardium. *Physiol. Rev.* 81, 767–806. doi: 10.1152/physrev.2001.81.2.767
- Vial, C., Owen, P., Opie, L. H., and Posel, D. (1987). Significance of release of adenosine triphosphate and adenosine induced by hypoxia or adrenaline in perfused rat heart. *J. Mol. Cell. Cardiol.* 19, 187–197. doi: 10.1016/s0022-2828(87)80561-8
- Wee, S., Peart, J. N., and Headrick, J. P. (2007). P₂ purinoceptor-mediated cardioprotection in ischemic-reperfused mouse heart. *J. Pharmacol. Exp. Ther.* 323, 861–867. doi: 10.1124/jpet.107.125815
- Wihlborg, A. K., Balogh, J., Wang, L., Borna, C., Dou, Y., Joshi, B. V., et al. (2006). Positive inotropic effects by uridine triphosphate (UTP) and uridine diphosphate (UDP) via P₂Y₂ and P₂Y₆ receptors on cardiomyocytes and release of UTP in man during myocardial infarction. *Circ. Res.* 98, 970–976. doi: 10.1161/01.RES.0000217402.73402.cd
- Williams, C. A., and Forrester, T. (1983). Possible source of adenosine triphosphate released from rat myocytes in response to hypoxia and acidosis. *Cardiovasc. Res.* 17, 301–312. doi: 10.1093/cvr/17.5.301
- Conflict of Interest:** The authors declare that the research was conducted in the absence of any commercial or financial relationships that could be construed as a potential conflict of interest.

Copyright © 2021 Matsuura, Kojima, Fukushima, Xie, Mi, Sabirov and Okada. This is an open-access article distributed under the terms of the Creative Commons Attribution License (CC BY). The use, distribution or reproduction in other forums is permitted, provided the original author(s) and the copyright owner(s) are credited and that the original publication in this journal is cited, in accordance with accepted academic practice. No use, distribution or reproduction is permitted which does not comply with these terms.



The Role of pH_i in Intestinal Epithelial Proliferation–Transport Mechanisms, Regulatory Pathways, and Consequences

Mahdi Amiri, Ursula E. Seidler and Katerina Nikolovska*

Department of Gastroenterology, Hannover Medical School, Hannover, Germany

OPEN ACCESS

Edited by:

Markus Ritter,
Paracelsus Medical University, Austria

Reviewed by:

John Geibel,
School of Medicine Yale University,
United States
Laurent Counillon,
University of Nice Sophia Antipolis,
France

*Correspondence:

Katerina Nikolovska
Nikolovska.Katerina@mh-hannover.de

Specialty section:

This article was submitted to
Cell Death and Survival,
a section of the journal
Frontiers in Cell and Developmental
Biology

Received: 16 October 2020

Accepted: 04 January 2021

Published: 22 January 2021

Citation:

Amiri M, Seidler UE and
Nikolovska K (2021) The Role of pH_i
in Intestinal Epithelial
Proliferation–Transport Mechanisms,
Regulatory Pathways,
and Consequences.
Front. Cell Dev. Biol. 9:618135.
doi: 10.3389/fcell.2021.618135

During the maturation of intestinal epithelial cells along the crypt/surface axis, a multitude of acid/base transporters are differentially expressed in their apical and basolateral membranes, enabling processes of electrolyte, macromolecule, nutrient, acid/base and fluid secretion, and absorption. An intracellular pH (pH_i)-gradient is generated along the epithelial crypt/surface axis, either as a consequence of the sum of the ion transport activities or as a distinctly regulated entity. While the role of pH_i on proliferation, migration, and tumorigenesis has been explored in cancer cells for some time, emerging evidence suggests an important role of the pH_i in the intestinal stem cells (ISCs) proliferative rate under physiological conditions. The present review highlights the current state of knowledge about the potential regulatory role of pH_i on intestinal proliferation and differentiation.

Keywords: intracellular pH, epithelial ion transport, proliferation, signaling pathways, intestinal epithelial cells

INTRODUCTION

Mechanisms of acid/base control in the gastrointestinal tract came into focus a century ago, because during the decades of very high gastric ulcer prevalence, a relationship between peptic ulcers and gastric acidity had been recognized (Banic et al., 2011). The ability to assess pH_i in mammalian gastrointestinal cells with the use of fluorescent dyes (Thomas, 1986) made the study of pH_i -recovery after an acidic or alkaline insult possible, as well as the delineation of the involved ion transporters (Flemstrom and Isenberg, 2001; Kaunitz and Akiba, 2006; Seidler, 2013). pH_i measurements have also been utilized to outline the transport proteins involved in intestinal absorptive and secretory processes (Zachos et al., 2005; Hug et al., 2011; Seidler and Nikolovska, 2019).

In the apical membranes, the anion channel cystic fibrosis transmembrane conductance regulator (CFTR) and the $\text{Cl}^-/\text{HCO}_3^-$ exchanger SLC26A3 (and possibly SLC26A6) export HCO_3^- into the lumen and are therefore “acid loaders.” Likewise, proton-coupled nutrient transporters load the enterocytes with acid moieties during digestion. The activity of acid loaders

Abbreviations: ISCs, intestinal stem cells; CFTR, cystic fibrosis transmembrane conductance regulator; SLC26A3, Solute Carrier Family 26 Member 3 ($\text{Cl}^-/\text{HCO}_3^-$ exchangers); NHE1/2/3/8 (SLC9A), sodium/hydrogen exchangers 1/2/3/8; AE2 (SLC4A2), Anion exchange protein 2; NBCn1 (SLC4A7), Electroneutral sodium/bicarbonate-dependent cotransporter; NBCn1 (SLC4A4), Electrogenic sodium/bicarbonate cotransporter; GI, gastrointestinal; WT, wild type; KO, knock out; CF, cystic fibrosis; EGF, epidermal growth factor; BMP, bone morphogenetic protein; Dvl, Dishevelled; Fz, Frizzled receptor; Hh, Hedgehog signaling.

is counteracted by the apical acid extruders, the Na⁺/H⁺ exchangers NHE2, NHE3, and NHE8 (SLC9A2/3/8); a process that results in salt and water absorption. Apical proton ATPases are also expressed in various cell types along the GI tract. The basolateral membranes also express both acid loaders, such as the Cl⁻/HCO₃⁻ exchanger AE2 (SLC4A2), and acid extruders, such as the NHE1 and the Na⁺/HCO₃⁻ cotransporters NBCn1 (SLC4A7) and NBCe1 (SLC4A4). Immunostaining and *in situ* hybridization techniques localized these transporters in the respective membranes, often with an expression gradient along cryptal or crypt/villus axis, and along the proximal to distal gut axis (Strong et al., 1994; Ameen et al., 1995; Ameen N. et al., 2000; Ameen N.A. et al., 2000; Alper et al., 1999; Chu et al., 2002; Jacob et al., 2002; Wang et al., 2002; Boedtkjer et al., 2008; Jakab et al., 2011; Singh et al., 2013b). **Figure 1** depicts a colonic crypt, with experimentally determined pH_i-gradient along its axis, and the relevant acid/base transporters on the apical and basolateral membranes.

The role of the steady-state pH_i in the cellular physiology of the intestinal epithelium has not been addressed experimentally, partially because of experimental uncertainties in the calibration process that allows conversion of the fluorometric intensity into an actual pH_i value (O'Connor and Silver, 2013), and because of the short lifetime of isolated intestinal mucosal preparations. Recent progress toward preservation of functional intestinal stem cells and therefore cultivation of native intestinal epithelium in so-called “organoid cultures” has enabled scientists to observe cellular functions, including the pH_i, of the intestinal epithelium in “steady-state.” This minireview highlights recent novel findings regarding the role of pH_i in intestinal proliferation and discusses the potential role of pH_i in the signaling pathways that regulate the constant renewal of the intestinal mucosa.

pH_i-Regulatory Studies in the Intestinal Epithelium

Temporal changes in the pH_i of epithelial cells in the GI tract are imposed physiologically due to changes in luminal pH. For example, the consequences of short-term exposure of the mouse gastric and duodenal epithelium to acidic luminal perfusate (mimicking the stage of gastric emptying), or of the colonic epithelium by short chain fatty acids (mimicking bacterial metabolism), have been studied in detail. The epithelium counteracts this intracellular acidification by activation and/or rapid trafficking of a variety of ion transporters to the brush border and basolateral membrane, facilitating proton extrusion, and HCO₃⁻ import to re-establish the resting pH_i (Chu and Montrose, 1995; Akiba et al., 2001; Singh et al., 2013a). These processes are coordinated by a large array of neural, paracrine, and direct epithelial regulatory mechanisms (Smith et al., 2006; Singh et al., 2012; Takeuchi et al., 2012; Akiba and Kaunitz, 2014).

In contrast to transient pH_i alterations, the consequences of sustained deviations from the resting pH_i as a result of impaired ion transport have hardly been studied in the native intestinal epithelium. For decades, the role of steady-state pH_i alterations has been addressed primarily in tumor cells. In cancer cells numerous H⁺ extrusion and base loading

mechanisms are upregulated, which generally leads to an inverted transmembrane pH gradient, characterized by alkalization of intracellular pH and extracellular acidosis, which is considered a hallmark of cancer metabolism (Webb et al., 2011; Swietach et al., 2014; Pedersen et al., 2017; Flinck et al., 2018; Becker and Deitmer, 2020; Liu et al., 2020). In this scenario, both the high intracellular and the low extracellular pH contribute to the malignant behavior (Pillai et al., 2019; Boedtkjer and Pedersen, 2020). Early studies supporting a role of mitogenic activation of Na⁺/H⁺ exchange and intracellular alkalization in proliferation of non-transformed cells, such as fibroblasts (Grinstein et al., 1989) has been met with criticism because a concomitant activation of acid loaders abolished the rise in pH_i in fibroblasts in the presence of CO₂/HCO₃⁻ in the medium (Gillies and Martinezaguilan, 1991). Recent technological advances and an expanded knowledge about the molecular nature of acid/base transporters as well as the mechanisms of epithelial growth and differentiation allow addressing the question about the influence of pH_i in epithelial homeostasis.

Alkaline Steady-State pH_i Caused by Loss of the CFTR Channel in Intestinal Stem Cells (ISCs) Is a Causative Factor in ISC Hyperproliferation

Simpson et al. (2005) had identified an alkaline pH_i in the intact epithelium of *Cftr*^{-/-} compared to identically treated wild type (*wt*) mouse duodenal mucosa. When techniques became available for intestinal stem cell maintenance and thus long term culture of native intestinal organoids, the same group used the technique to demonstrate a sustained alkalized resting pH_i in the epithelial cells of small intestinal organoids grown from *Cftr*^{-/-} crypts (Walker et al., 2016). Interestingly, the group demonstrated that the alkaline pH_i was not primarily due to the defective HCO₃⁻ conductance via CFTR, but to its defective Cl⁻ conductance, resulting in intracellular Cl⁻ retention and an inability of the basolateral acid loader AE2 to export HCO₃⁻_i in exchange for Cl⁻_o. Accordingly, pH_i could be normalized by normalizing [Cl⁻]_i in *Cftr*^{-/-} enterocytes (Walker et al., 2016). Employing an array of sophisticated methods, the group demonstrated an expression and functional activity of CFTR in murine ISCs, an alkaline intracellular pH_i in *Cftr*^{-/-} ISCs, accompanied by hyperproliferation in *Cftr*^{-/-} organoids. These findings suggest that the *Cftr*^{-/-}-associated crypt and villus elongations, which are also observed in the absence of inflammatory markers (Tan et al., 2020) and the hyperproliferation described in murine *Cftr*^{-/-} intestinal epithelium (Gallagher and Gottlieb, 2001) may be partially a consequence of the lack of CFTR in ISCs. Crossbreeding of *Cftr*^{-/-} and *wt* mice with transgenic mice which express a fluorophore (EGFP)-labeled WNT transducer Dishevelled (Dsv) and the cell membrane-targeted, two-color fluorescent Cre-reporter Rosa^{TmT/mG} enabled the group to study the proximity of Dsv to the membrane receptor Frizzled 7, which has been recognized as a key event in WNT signaling (Axelrod, 2001) in *Cftr*^{-/-} and *wt* ISCs with live cell imaging. Subjecting the organoids to manipulations that reduced inner membrane negative charge, [Cl⁻]_i or pH_i, the authors established

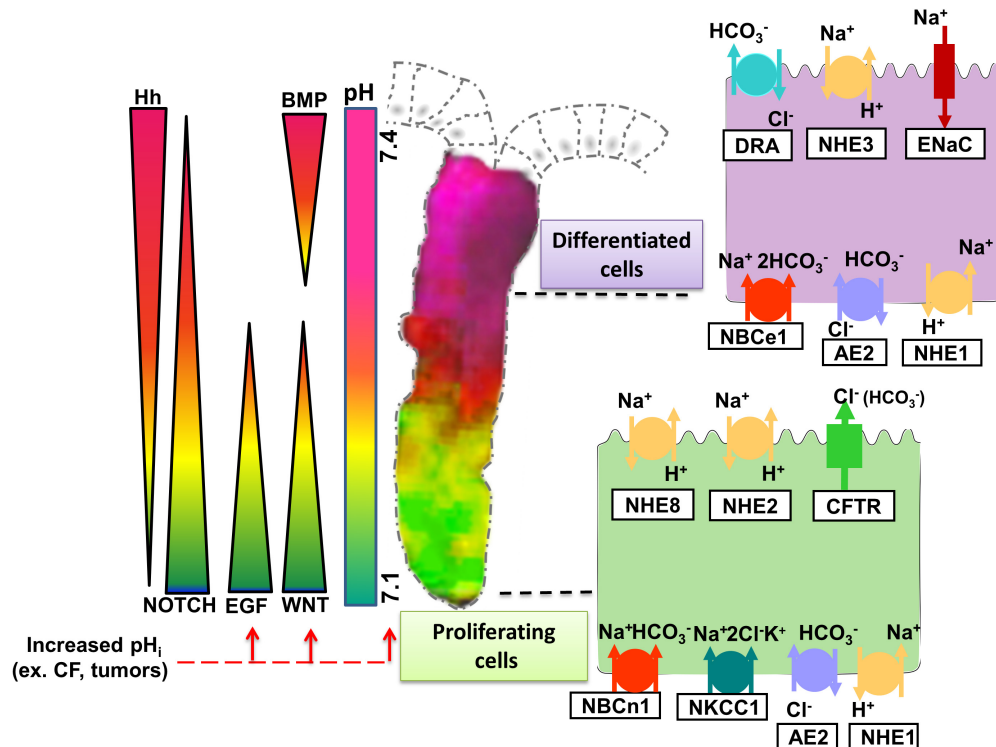


FIGURE 1 | Representation of experimentally determined pH_i gradient and the major signaling cascades in the colonic crypt that together control intestinal homeostasis. Wnt and EGF are essential for proliferation and maintenance of ISCs. Notch signaling targets the proliferating cells directing them to secretory or absorptive lineage differentiation. Hedgehog (Hh), expressed by epithelial cells in the upper part of the crypt maintains the myofibroblasts and prompts BMP ligand expression, which then promotes differentiation while restraining cell proliferation of the epithelial cells. Since they are involved in different steps of intestinal homeostasis, the signaling pathways form an opposing gradient along the crypt axis. The activity of the signaling pathways is influenced by a pH_i gradient spread along the crypt, with more acidic pH_i values present at the bottom and more alkaline values toward the cryptal surface. The pH_i gradient is generated by the activity of the different ion transporters expressed on the intestinal epithelial cells. Proliferating cells are characterized by high activity/expression of CFTR, NHE2, and NHE8 on their apical membrane, and NBCn1, NKCC1, AE2, and NHE1 on the basolateral membrane. As the cells transition from proliferating to differentiated state, the expression of NHE3, DRA (Slc26a3), and ENaC becomes more dominant at the apical membrane and NBCe1, NHE1, and AE2 on the basolateral membrane. Tightly regulated expression and activity of the ion transporters at different segments of the crypt allows maintenance of distinct pH_i values that in turn control the activity of the signaling pathways essential for synchronized proliferation and differentiation to retain intestinal homeostasis. Increase of pH_i caused by alterations in ion transporter expression/activity (e.g., Cystic Fibrosis-CF) or tumors leads to activation of certain signaling pathways and hyperproliferation.

the causative role of pH_i alkalinity for increased WNT signaling in *Cftr*^{-/-} ISCs.

Loss of CFTR function in CF patients is associated with a significantly increased risk of developing digestive tract cancers, but not of lung cancers (Neglia et al., 1995; Maisonneuve et al., 2003, 2013; Scott et al., 2020). CFTR is expressed in ISCs, but not detectable in the progenitor basal cells of the respiratory mucosa (Plasschaert et al., 2018). Since both organs are subjected to the typical CF epithelial manifestations of dysbiosis, inflammation, and remodeling, the findings by Strubberg et al. (2018) may have identified an intrinsic factor favoring malignant growth in the CF intestinal epithelium.

Associations Between pH_i and/or Acid/Base Transporters and Epithelial Morphogenesis in Native Intestinal Epithelium

From the existing literature pool, only the study done by Strubberg et al. (2018) provides a molecular mechanism linking

steady-state pH_i and proliferation in native epithelium. In a number of cellular systems, however, it is found that slightly alkaline pH (~0.3 pH units above the steady-state pH_i) is important for initiating DNA synthesis and proliferation [reviewed in Flinck et al. (2018)]. Here we report studies in native intestinal epithelium in which pH_i and/or proliferation was measured, but the molecular mechanism linking the two has yet to be explored.

SLC4A4 (NBCe1) is expressed predominantly in small intestinal villous (Jakab et al., 2011) and colonic surface cells and NBCe1 KO proximal surface colonocytes have significantly reduced steady-state pH_i compared to WT (Yu et al., 2016). Due to the short life span and the tiny intestine of these mice, the proliferation rate in the colon was not addressed, but a study with LS174 cells (human colonic adenocarcinoma cells) showed that SLC4A4 knockdown impaired cell proliferation (Parks and Pouyssegur, 2015). The Cl⁻/HCO₃⁻ exchanger Slc26a3, which mutation is the molecular cause of congenital chloride diarrhea, is mainly expressed in the colonic absorptive epithelial cells lining the luminal surface, not in the ISCs (Hoglund et al., 1996;

Xiao et al., 2012). Loss of Slc26a3 function, in the colon leads to increased steady state pH_i in the surface epithelium (Xiao et al., 2014). Colonic epithelial hyperplasia has been described in the original publication of the *Slc26a3*^{-/-} mouse (Schweinfest et al., 2006). Possibly the alkaline pH interferes with intracellular acidification required to trigger programmed cell death at the colonic surface epithelium (Park et al., 1999; Kniep et al., 2006). Increased crypt length, seen in *Cftr*^{-/-} epithelium, is not a feature of *Slc26a3*^{-/-} colonic epithelium (Kini et al., 2020).

What about the effect of an acidic pH_i on proliferation and differentiation? While many cell lines are viable in acidic medium, the pharmacological or genetic inhibition of acid extruders or base loaders generally curbs proliferation and has been repeatedly suggested as an antiproliferative treatment in tumors (Chambard and Pouyssegur, 1986). It was recently reported that a genetic deletion of an acid extruder, namely NHE8, in colonic ISC displays hyperproliferative phenotype, but the pH_i in the affected cells was not measured (Xu et al., 2019).

Cellular Signaling Pathways That May Link pH_i to Proliferation and Differentiation

Regeneration, expansion and lineage differentiation of the intestinal epithelium is modulated by various signaling pathways, namely Wnt/β-catenin, EGF (epidermal growth factor), BMP (bone morphogenetic protein), Notch, Hedgehog, and Eph-eprhrin which mainly occur in gradients along the crypt/villus axis as depicted in **Figure 1** (Spit et al., 2018). These signaling cascades are derived from the epithelial or the mesenchymal niche (Spit et al., 2018). A potential cross-interaction between the gradients of signaling pathways and the intracellular pH gradient along the crypt/villus axis might exist, but is understudied. In this paragraph we point out important signaling pathways for proliferation and differentiation in which a relationship to pH_i has been delineated in other cellular system, and which are worth studying in the native intestinal epithelium.

Wnt signaling is the main driving force of ISC proliferation. Increased Wnt/β-catenin signaling leads to hyperproliferation observed in *Cftr*^{-/-} ISCs as described above. The molecular mechanism behind the increased Wnt activity involves the alkaline pH_i-facilitated association of the Wnt transducer Dishevelled (Dvl) to the plasma membrane and binding to the Frizzled-7 receptor (Fz) (Walker et al., 2016; Strubberg et al., 2018). Similarly, a study in *Drosophila melanogaster* cells shows that the activity of dNhe2 (a *Drosophila* analog of the mammalian NHE1), which allows maintenance of alkaline pH_i, is necessary for the binding and surface recruitment of Dvl by Fz (Simons et al., 2009). Another component of the Wnt signaling pathway, β-catenin is also influenced by the pH_i. Increasing the pH_i by glycolysis stimulates β-catenin acetylation leading to Wnt signaling activation in embryos and human tail bud-like cells differentiated *in vitro* from iPS cells (Oginuma et al., 2020). Intracellular acidification induces the transcriptional repressor DDIT3 that suppresses the activity of Wnt, as shown *in vitro* and in a mouse xenograft tumor model (Melnik et al., 2018). However, another group has shown that cell

alkalization with NH₄Cl in MDCK epithelial cells and *Drosophila melanogaster* led to decreased β-catenin abundance at cell-cell junctions and in the nucleus (White et al., 2018), while lower pH_i in NHE1-deficient PS120 fibroblasts significantly increased β-catenin at membrane protrusions (White et al., 2018). Recently the involvement of potassium channels, namely KCNQ1, in the Wnt/β-catenin signaling pathway has been shown. A colocalization of KCNQ1 and β-catenin at the adherence junctions was detected in rat colonic crypts and HT29 cells (Rapetti-Mauss et al., 2017) and KCNQ1 inhibition leads to re-localization of β-catenin in the cytosol, Wnt/β-catenin signaling pathway stimulation with increased expression of Cyclin D1 and C-Jun as Wnt target genes (Rapetti-Mauss et al., 2017, 2020). Although, pH_i is not directly implied, K⁺ channels allow hyperpolarization of the membrane voltage, thus contributing indirectly to pH regulation (Spitzner et al., 2007).

EGF signaling is another important modulator of ISC proliferation. EGF is produced by the adjacent fibroblasts and Paneth cells (Sato et al., 2011; Farin et al., 2014), and activates the signaling cascade by binding to the EGF receptor (EGFR) on ISCs. Extracellular pH influences the binding of EGF to its receptor, with maximized binding at pH8 and reduced interaction at pH6.5 (Nunez et al., 1993). Early research showed that EGF can increase pH_i in A431 human epidermoid carcinoma cell line (Rothenberg et al., 1983). Later investigation in chicken granulosa cells (Li et al., 1991), Hep G2 hepatoma cells (Strazzabosco et al., 1995), and in primary cultured rabbit surface epithelial cells (Nylander-Koski et al., 2006) showed that EGF induced intracellular alkalization occurs via activation of NHE1. These data point that an alkaline pH_i shift, caused by activation of NHE1 on the basolateral membrane, is an important event in EGF signaling pathway that stimulates cell proliferation. Indeed, EGFR forms a complex with NHE1 via NHERF1 (Cardone et al., 2015). Apical EGF can also activate EGFR signaling and promote proliferation similarly to basolaterally induced EGFR activation (Kuwada et al., 1998). EGF impacts the apical NHEs, it stimulates NHE2 mRNA expression and activity in rat intestinal epithelial (RIE) cell (Xu et al., 2001), but it has a negative effect on NHE8 expression (Xu et al., 2010). The interplay between apical or basolateral EGFR activation, different NHEs, and the pH_i is not completely understood. It seems plausible that a constant slightly acidic pH_i in the ISC zone may prevent hyperactivation of the signaling pathways that could result in hyperproliferation and possible tumor formation (Liu et al., 2020).

BMP, Notch, Hh, and Eph are more dominant in the upper sections of the crypt and involved in cell fate decision and terminal differentiation. Knowledge about the impact of the pH_i on the later signaling cascades is scarce. The activation of the Notch signaling involves binding of the ligands to the receptor, and subsequent activation of the endocytosis machinery and this later step is influenced by the vacuolar (H⁺)-ATPase (V-ATPase), a proton transporter involved in the acidification of endosomal compartments (Yan et al., 2009). Notch signaling plays an important role in the determination of cell fate by regulating the balance between cell proliferation and differentiation (Baron, 2003), thus impacting the transit amplifying cells. Therefore, there is a high possibility that the Notch signaling can be affected

by the activity of ion transporters present in the transit amplifying cells, such as NHE2 (Guan et al., 2006) via fine-tuning the pH_i value. A shift in the pH_i toward more alkaline values (from 7.4 to a 7.65) has been observed in mouse embryonic stem cells during their differentiation *in vitro* (Ulmschneider et al., 2016). Hh signaling, important for the follicle stem cells differentiation in *Drosophila*, is also strongly influenced by pH_i alterations.

The reported studies are only examples, which, taken together, suggest that the pH_i may trigger stimulation or inhibition of different signaling pathways active in proliferation and differentiation of the intestinal epithelium. However, the exact molecular mechanism correlating the pH_i and signaling pathways gradient in the intestinal epithelium is yet to be determined.

CONCLUSION AND OUTLOOK

Addressing the role of the steady-state pH_i in intestinal epithelial homeostasis has been hampered by the absence of models that accurately assess the pH_i in different epithelial compartments along the crypt-villus axis, and to induce long-term and selective pH_i-alterations. The ability to generate intestinal organoids and monitor their growth over days in culture has enabled scientists to intensely study the process of intestinal cell renewal and differentiation. Some of the molecular events that link the elevated pH_i secondary to loss of functional CFTR to intestinal epithelial hyperproliferation were elegantly explored

by generating intestinal organoids from *Cftr*^{-/-} and *wt* mice crossed onto a variety of transgenic reporter mouse lines (Strubberg et al., 2018). These seminal studies may provide clarification of the increased incidence of colorectal cancer in CF patients and contribute toward their prevention. Recent progress in the drug development for CFTR corrector and modifiers with the potential to rescue CFTR function in CF patients may correct the pH_i-regulatory dysfunction and reduce cancer risk (Phuan et al., 2019; Egan, 2020). The potential to combine direct pH_i assessment with genetic, molecular biological and pharmacological tools, as already established for tumor cells (Liu et al., 2020; Stock, 2020), in intestinal organoids may provide insight into protonation/deprotonation events of key regulatory proteins in enterocyte proliferation and differentiation.

AUTHOR CONTRIBUTIONS

MA, US, and KN designed and wrote the review. All the authors contributed to the article and approved the submitted version.

FUNDING

The work on this review was supported by the grant DFG Se460/21-1 and FOR5046/P7 to US.

REFERENCES

- Akiba, Y., Furukawa, O., Guth, P. H., Engel, E., Nastaskin, I., Sassani, P., et al. (2001). Cellular bicarbonate protects rat duodenal mucosa from acid-induced injury. *J. Clin. Invest.* 108, 1807–1816. doi: 10.1172/jci200112218
- Akiba, Y., and Kaunitz, J. D. (2014). Prostaglandin pathways in duodenal chemosensing. *J. Gastroenterol. Hepatol.* 29, 93–98. doi: 10.1111/jgh.12731
- Alper, S. L., Rossmann, H., Wilhelm, S., Stuart-Tilley, A. K., Shmukler, B. E., and Seidler, U. (1999). Expression of AE2 anion exchanger in mouse intestine. *Am. J. Physiol.* 277, G321–G332.
- Ameen, N., Alexis, J., and Salas, P. (2000). Cellular localization of the cystic fibrosis transmembrane conductance regulator in mouse intestinal tract. *Histochem. Cell Biol.* 114, 69–75. doi: 10.1007/s004180000164
- Ameen, N. A., van Donselaar, E., Posthuma, G., de Jonge, H., McLaughlin, G., Geuze, H. J., et al. (2000). Subcellular distribution of CFTR in rat intestine supports a physiologic role for CFTR regulation by vesicle traffic. *Histochem. Cell Biol.* 114, 219–228. doi: 10.1007/s004180000167
- Ameen, N. A., Ardito, T., Kashgarian, M., and Marino, C. R. (1995). A unique subset of rat and human intestinal villus cells express the cystic fibrosis transmembrane conductance regulator. *Gastroenterology* 108, 1016–1023. doi: 10.1016/0016-5085(95)90198-1
- Axelrod, J. D. (2001). Unipolar membrane association of dishevelled mediates frizzled planar cell polarity signaling. *Genes Dev.* 15, 1182–1187.
- Banic, M., Malfertheiner, P., Babic, Z., Ostojic, R., Kujundzic, M., Fatovic-Ferencic, S., et al. (2011). Historical impact to drive research in peptic ulcer disease. *Dig. Dis.* 29, 444–453. doi: 10.1159/000331512
- Baron, M. (2003). An overview of the Notch signalling pathway. *Semin Cell Dev. Biol.* 14, 113–119. doi: 10.1016/s1084-9521(02)00179-9
- Becker, H. M., and Deitmer, J. W. (2020). Transport metabolons and acid/base balance in tumor cells. *Cancers* 12:899. doi: 10.3390/cancers12040899
- Boedtker, E., and Pedersen, S. F. (2020). The acidic tumor microenvironment as a driver of cancer. in: annual review of physiology. *Palo Alto Annu. Rev.* 82, 103–126. doi: 10.1146/annurev-physiol-021119-034627
- Boedtker, E., Praetorius, J., Fuchtbauer, E. M., and Aalkjaer, C. (2008). Antibody-independent localization of the electroneutral Na⁺-HCO₃⁻ cotransporter NBCn1 (slc4a7) in mice. *Am. J. Physiol. Cell Physiol.* 294, C591–C603.
- Cardone, R. A., Greco, M. R., Zeeberg, K., Zaccagnino, A., Saccomano, M., Bellizzi, A., et al. (2015). A novel NHE1-Centered signaling cassette drives epidermal growth factor receptor-dependent pancreatic tumor metastasis and is a target for combination therapy. *Neoplasia* 17, 155–166. doi: 10.1016/j.neo.2014.12.003
- Chambard, J. C., and Pouyssegur, J. (1986). Intracellular pH controls growth factor-induced ribosomal-protein S6-phosphorylation and protein-synthesis in the GO- G1-transition of fibroblasts. *Exp. Cell Res.* 164, 282–294. doi: 10.1016/0014-4827(86)90029-7
- Chu, J. S., Chu, S. Y., and Montrose, M. H. (2002). Apical Na⁺/H⁺ exchange near the base of mouse colonic crypts. *Am. J. Physiol. Cell Physiol.* 283, C358–C372.
- Chu, S. C., and Montrose, M. H. (1995). An Na⁺-independent short-chain fatty-acid transporter contributes to intracellular pH regulation in murine colonocytes. *J. Gen. Physiol.* 105, 589–615. doi: 10.1085/jgp.105.5.589
- Egan, M. E. (2020). Cystic fibrosis transmembrane conductance receptor modulator therapy in cystic fibrosis, an update. *Curr. Opin. Pediatr.* 32, 384–388. doi: 10.1097/mop.0000000000000892
- Farin, H. F., Karthaus, W. R., Kujala, P., Rakhshandehroo, M., Schwank, G., Vries, R. G. J., et al. (2014). Paneth cell extrusion and release of antimicrobial products is directly controlled by immune cell-derived IFN-γ. *J. Exp. Med.* 211, 1393–1405. doi: 10.1084/jem.20130753
- Flemstrom, G., and Isenberg, J. I. (2001). Gastrointestinal mucosal alkaline secretion and mucosal protection. *News Physiol. Sci.* 16, 23–28. doi: 10.1152/physiologyonline.2001.16.1.23
- Flinck, M., Kramer, S. H., and Pedersen, S. F. (2018). Roles of pH in control of cell proliferation. *Acta Physiol.* 223:e13068. doi: 10.1111/apha.13068
- Gallagher, A. M., and Gottlieb, R. A. (2001). Proliferation, not apoptosis, alters epithelial cell migration in small intestine of CFTR null mice. *Am. J. Physiol. Gastrointest. Liver Physiol.* 281, G681–G687.
- Gillies, R. J., and Martinezaguilan, R. (1991). Regulation of intracellular pH in BALB/C 3T3 cells - bicarbonate raises pH via NAHCO₃/HCL exchange and

- attenuates the activation of Na^+/H^+ exchange by serum. *J. Biol. Chem.* 266, 1551–1556. doi: 10.1016/s0021-9258(18)52329-2
- Grinstein, S., Rotin, D., and Mason, M. J. (1989). Na^+/H^+ exchange and growth factor-induced cytosolic pH changes - role in cellular proliferation. *Biochim. Biophys. Acta* 988, 73–97. doi: 10.1016/0304-4157(89)90004-x
- Guan, Y., Dong, J., Tackett, L., Meyer, J. W., Shull, G. E., and Montrose, M. H. (2006). NHE2 is the main apical NHE in mouse colonic crypts but an alternative Na^+ -dependent acid extrusion mechanism is upregulated in NHE2-null mice. *Am. J. Physiol. Gastrointest. Liver Physiol.* 291, G689–G699.
- Hoglund, P., Haila, S., Socha, J., Tomaszewski, L., Saarialho-Kere, U., Karjalainen-Lindsberg, M. L., et al. (1996). Mutations of the Down-regulated in adenoma (DRA) gene cause congenital chloride diarrhoea. *Nat. Genet.* 14, 316–319. doi: 10.1038/ng1196-316
- Hug, M. J., Clarke, L. L., and Gray, M. A. (2011). How to measure CFTR-dependent bicarbonate transport: from single channels to the intact epithelium. *Methods Mol. Biol.* 741, 489–509. doi: 10.1007/978-1-61779-117-8_30
- Jacob, P., Rossmann, H., Lamprecht, G., Kretz, A., Neff, C., Lin-Wu, E., et al. (2002). Down-regulated in adenoma mediates apical $\text{Cl}^-/\text{HCO}_3^-$ exchange in rabbit, rat, and human duodenum. *Gastroenterology* 122, 709–724. doi: 10.1053/gast.2002.31875
- Jakab, R. L., Collaco, A. M., and Ameen, N. A. (2011). Physiological relevance of cell-specific distribution patterns of CFTR, NKCC1, NBCe1, and NHE3 along the crypt-villus axis in the intestine. *Am. J. Physiol. Gastroint. Liver Physiol.* 300, G82–G98.
- Kaunitz, J. D., and Akiba, Y. (2006). Review article: duodenal bicarbonate - mucosal protection, luminal chemosensing and acid-base balance. *Alimen. Pharmacol. Ther.* 24, 169–176. doi: 10.1111/j.1365-2036.2006.00041.x
- Kini, A., Singh, A. K., Riederer, B., Yang, I., Tan, X. J., di Stefano, G., et al. (2020). Slc26a3 deletion alters pH-microclimate, mucin biosynthesis, microbiome composition and increases the TNF α expression in murine colon. *Acta Physiol.* 230:e13498. doi: 10.1111/apha.13498
- Kniep, E. M., Roehlecke, C., Ozkucur, N., Steinberg, A., Reber, F., Knels, L., et al. (2006). Inhibition of apoptosis and reduction of intracellular pH decrease in retinal neural cell cultures by a blocker of carbonic anhydrase. *Invest. Ophthalmol. Vis. Sci.* 47, 1185–1192. doi: 10.1167/iovs.05-0555
- Kuwada, S. K., Lund, K. A., Li, X. F., Clifton, P., Amsler, K., Opreko, L. K., et al. (1998). Differential signaling and regulation of apical vs. basolateral EGFR in polarized epithelial cells. *Am. J. Physiol. Cell Physiol.* 275, C1419–C1428.
- Li, M., Morley, P., Asem, E. K., and Tsang, B. K. (1991). Epidermal growth factor elevates intracellular pH in chicken granulosa cells. *Endocrinology* 129, 656–662. doi: 10.1210/endo-129-2-656
- Liu, Y., White, K. A., and Barber, D. L. (2020). Intracellular pH regulates cancer and stem cell behaviors: a protein dynamics perspective. *Front. Oncol.* 10:401. doi: 10.3389/fonc.2020.01401
- Maisonneuve, P., FitzSimmons, S. C., Neglia, J. P., Campbell, P. W., and Lowenfels, A. B. (2003). Cancer risk in nontransplanted and transplanted cystic fibrosis patients: a 10-year study. *JNCI Natl. Cancer Inst.* 95, 381–387. doi: 10.1093/jnci/95.5.381
- Maisonneuve, P., Marshall, B. C., Knapp, E. A., and Lowenfels, A. B. (2013). Cancer risk in cystic fibrosis: a 20-year nationwide study from the United States. *JNCI Natl. Cancer Inst.* 105, 122–129. doi: 10.1093/jnci/djs481
- Melnik, S., Dvornikov, D., Muller-Decker, K., Depner, S., Stannek, P., Meister, M., et al. (2018). Cancer cell specific inhibition of Wnt/ β -catenin signaling by forced intracellular acidification. *Cell Discov.* 4:37.
- Neglia, J. P., Fitzsimmons, S. C., Maisonneuve, P., Schoni, M. H., Schoniaffolter, F., Corey, M., et al. (1995). The risk of cancer among patients with cystic-fibrosis. *N. Engl. J. Med.* 332, 494–499.
- Nunez, M., Mayo, K. H., Starbuck, C., and Lauffenburger, D. (1993). pH sensitivity of epidermal growth factor receptor complexes. *J. Cell Biochem.* 51, 312–321. doi: 10.1002/jcb.240510310
- Nylander-Koski, O., Mustonen, H., Puolakkainen, P., Kiviluoto, T., and Kivilaakso, E. (2006). Epidermal growth factor enhances intracellular pH regulation via calcium signaling in acid-exposed primary cultured rabbit gastric epithelial cells. *Digest. Dis. Sci.* 51, 1322–1330. doi: 10.1007/s10620-006-9075-7
- O'Connor, N., and Silver, R. B. (2013). *Ratio Imaging: Practical Considerations for Measuring Intracellular Ca^{2+} and pH in Living Cells*. In: *Digital Microscopy*, 4th Edn. San Diego, CA: Elsevier Academic Press Inc, 387–406.
- Oginuma, M., Harima, Y., Tarazona, O. A., Diaz-Cuadros, M., Michaut, A., Ishitani, T., et al. (2020). Intracellular pH controls WNT downstream of glycolysis in amniote embryos. *Nature* 584, 98–101. doi: 10.1038/s41586-020-2428-0
- Park, H. J., Lyons, J. C., Ohtsubo, T., and Song, C. W. (1999). Acidic environment causes apoptosis by increasing caspase activity. *Br. J. Cancer* 80, 1892–1897. doi: 10.1038/sj.bjc.6690617
- Parks, S. K., and Pouyssegur, J. (2015). The $\text{Na}^+/\text{HCO}_3^-$ Co-Transporter SLC4A4 plays a role in growth and migration of colon and breast cancer cells. *J. Cell. Physiol.* 230, 1954–1963. doi: 10.1002/jcp.24930
- Pedersen, S. F., Novak, I., Alves, F., Schwab, A., and Pardo, L. A. (2017). Alternating pH landscapes shape epithelial cancer initiation and progression: focus on pancreatic cancer. *Bioessays* 39:1600253. doi: 10.1002/bies.201600253
- Phuan, P. W., Tan, J. A., Rivera, A. A., Zlock, L., Nielson, D. W., Finkbeiner, W. E., et al. (2019). Nanomolar-potency 'co-potentiator' therapy for cystic fibrosis caused by a defined subset of minimal function CFTR mutants. *Sci. Rep.* 9:17640.
- Pillai, S. R., Damaghi, M., Marunaka, Y., Spugnini, E. P., Fais, S., and Gillies, R. J. (2019). Causes, consequences, and therapy of tumors acidosis. *Cancer Metastasis Rev.* 38, 205–222. doi: 10.1007/s10555-019-09792-7
- Plasschaert, L. W., Zilionis, R., Choo-Wing, R., Savova, V., Knehr, J., Roma, G., et al. (2018). A single-cell atlas of the airway epithelium reveals the CFTR-rich pulmonary ionocyte. *Nature* 560, 377–381. doi: 10.1038/s41586-018-0394-6
- Rapetti-Mauss, R., Berenguier, C., Allegrini, B., and Soriani, O. (2020). Interplay between ion channels and the wnt/ β -catenin signaling pathway in cancers. *Front. Pharmacol.* 11:525020. doi: 10.3389/fphar.2020.525020
- Rapetti-Mauss, R., Bustos, V., Thomas, W., McBryan, J., Harvey, H., Lajczak, N., et al. (2017). Bidirectional KCNQ1: β -catenin interaction drives colorectal cancer cell differentiation. *Proc. Natl. Acad. Sci. U.S.A.* 114, 4159–4164. doi: 10.1073/pnas.1702913114
- Rothenberg, P., Glaser, L., Schlesinger, P., and Cassel, D. (1983). Activation of Na^+/H^+ exchange by epidermal growth factor elevates intracellular pH in A431 cells. *J. Biol. Chem.* 258, 12644–12653. doi: 10.1016/s0021-9258(17)44225-6
- Sato, T., van Es, J. H., Snippert, H. J., Stange, D. E., Vries, R. G., van den Born, M., et al. (2011). Paneth cells constitute the niche for Lgr5 stem cells in intestinal crypts. *Nature* 469, 415–418. doi: 10.1038/nature09637
- Schweinfest, C. W., Spyropoulos, D. D., Henderson, K. W., Kim, J. H., Chapman, J. M., Barone, S., et al. (2006). slc26a3 (dra)-deficient mice display chloride-losing diarrhea, enhanced colonic proliferation, and distinct up-regulation of ion transporters in the colon. *J. Biol. Chem.* 281, 37962–37971. doi: 10.1074/jbc.m607527200
- Scott, P., Anderson, K., Singhania, M., and Cormier, R. (2020). Cystic Fibrosis. CFTR, and colorectal cancer. *Int. J. Mol. Sci.* 21:2891. doi: 10.3390/ijms21082891
- Seidler, U., and Nikolovska, K. (2019). Slc26 family of anion transporters in the gastrointestinal tract: expression, function, regulation, and role in disease. *Compr. Physiol.* 9, 839–872. doi: 10.1002/cphy.c180027
- Seidler, U. E. (2013). Gastrointestinal HCO_3^- transport and epithelial protection in the gut: new techniques, transport pathways and regulatory pathways. *Curr. Opin. Pharmacol.* 13, 900–908. doi: 10.1016/j.coph.2013.10.001
- Simons, M., Gault, W. J., Gotthardt, D., Rohatgi, R., Klein, T. J., Shao, Y. M., et al. (2009). Electrochemical cues regulate assembly of the Frizzled/Dishevelled complex at the plasma membrane during planar epithelial polarization. *Nat. Cell Biol.* 11, 286–U142.
- Simpson, J. E., Gawenis, L. R., Walker, N. M., Boyle, K. T., and Clarke, L. L. (2005). Chloride conductance of CFTR facilitates basal $\text{Cl}^-/\text{HCO}_3^-$ exchange in the villous epithelium of intact murine duodenum. *Am. J. Physiol. Gastroint. Liver Physiol.* 288, G1241–G1251.
- Singh, A. K., Liu, Y. J., Riederer, B., Engelhardt, R., Thakur, B. K., Soleimani, M., et al. (2013a). Molecular transport machinery involved in orchestrating luminal acid-induced duodenal bicarbonate secretion in vivo. *J. Physiol. Lond.* 591, 5377–5391. doi: 10.1113/jphysiol.2013.254854
- Singh, A. K., Xia, W. L., Riederer, B., Juric, M., Li, J. H., Zheng, W., et al. (2013b). Essential role of the electroneutral $\text{Na}^+/\text{HCO}_3^-$ cotransporter NBCn1 in murine duodenal acid-base balance and colonic mucus layer build-up in vivo. *J. Physiol. Lond.* 591, 2189–2204. doi: 10.1113/jphysiol.2012.247874
- Singh, A. K., Spiessberger, B., Zheng, W., Xiao, F., Lukowski, R., Wegener, J. W., et al. (2012). Neuronal cGMP kinase I is essential for stimulation of duodenal

- bicarbonate secretion by luminal acid. *FASEB J.* 26, 1745–1754. doi: 10.1096/fj.11-200394
- Smith, A. J., Chappell, A. E., Buret, A. G., Barrett, K. E., and Dong, H. (2006). 5-hydroxytryptamine contributes significantly to a reflex pathway by which the duodenal mucosa protects itself from gastric acid injury. *FASEB J.* 20, 2486–2495. doi: 10.1096/fj.06-6391com
- Spit, M., Koo, B.-K., and Maurice, M. M. (2018). Tales from the crypt: intestinal niche signals in tissue renewal, plasticity and cancer. *Open Biol.* 8:180120. doi: 10.1098/rsob.180120
- Spitzner, M., Ousingsawat, J., Scheidt, K., Kunzelmann, K., and Schreiber, R. (2007). Voltage-gated K⁺ channels support proliferation of colonic carcinoma cells. *FASEB J.* 21, 35–44. doi: 10.1096/fj.06-6200com
- Stock, C. (2020). How dysregulated ion channels and transporters take a hand in esophageal, liver, and colorectal cancer. *Rev. Physiol. Biochem. Pharmacol.* [Epub ahead of print].
- Strazzabosco, M., Poci, C., Spirli, C., Zsembery, A., Granato, A., Massimino, M. L., et al. (1995). Intracellular pH regulation in Hep G2 cells: effects of epidermal growth factor, transforming growth factor- α , and insulinlike growth factor-II on Na⁺/H⁺ exchange activity. *Hepatology* 22, 588–597. doi: 10.1016/0270-9139(95)90584-7
- Strong, T. V., Boehm, K., and Collins, F. S. (1994). Localization of cystic fibrosis transmembrane conductance regulator mRNA in the human gastrointestinal tract by in situ hybridization. *J. Clin. Invest.* 93, 347–354. doi: 10.1172/jci116966
- Strubberg, A. M., Liu, J. H., Walker, N. M., Stefanski, C. D., MacLeod, R. J., Magness, S. T., et al. (2018). Cfr Modulates Wnt/ β -catenin signaling and stem cell proliferation in murine intestine. *Cell. Mol. Gastroenterol. Hepatol.* 5, 253–271. doi: 10.1016/j.jcmgh.2017.11.013
- Swietach, P., Vaughan-Jones, R. D., Harris, A. L., and Hulikova, A. (2014). The chemistry, physiology and pathology of pH in cancer. *Philos. Trans. R. Soc. B Biol. Sci.* 369:20130099. doi: 10.1098/rstb.2013.0099
- Takeuchi, K., Aihara, E., Kimura, M., Dogishi, K., Hara, T., and Hayashi, S. (2012). Gas mediators involved in modulating duodenal HCO₃⁻ secretion. *Curr. Med. Chem.* 19, 43–54.
- Tan, Q., di Stefano, G., Tan, X., Renjie, X., Römermann, D., Talbot, S. R., et al. (2020). Linacotide, lubiprostone and tenapanor improve gut fluidity and alkalinity in CFTR-deficient and F508del mutant mice via NHE3 inhibition. *Br. J. Pharmacol.* [Epub ahead of print].
- Thomas, J. A. (1986). Intracellularly trapped pH indicators. *Soc. Gen. Physiol. Ser.* 40, 311–325.
- Ulmschneider, B., Grillo-Hill, B. K., Benitez, M., Azimova, D. R., Barber, D. L., and Nystul, T. G. (2016). Increased intracellular pH is necessary for adult epithelial and embryonic stem cell differentiation. *J. Cell Biol.* 215, 345–355. doi: 10.1083/jcb.201606042
- Walker, N. M., Liu, J. H., Stein, S. R., Stefanski, C. D., Strubberg, A. M., and Clarke, L. L. (2016). Cellular chloride and bicarbonate retention alters intracellular pH regulation in Cfr KO crypt epithelium. *Am. J. Physiol. Gastroint. Liver Physiol.* 310, G70–G80.
- Wang, Z. H., Petrovic, S., Mann, E., and Soleimani, M. (2002). Identification of an apical Cl⁻/HCO₃⁻ exchanger in the small intestine. *Am. J. Physiol. Gastroint. Liver Physiol.* 282, G573–G579.
- Webb, B. A., Chimenti, M., Jacobson, M. P., and Barber, D. L. (2011). Dysregulated pH: a perfect storm for cancer progression. *Nat. Rev. Cancer* 11, 671–677. doi: 10.1038/nrc3110
- White, K. A., Grillo-Hill, B. K., Esquivel, M., Peralta, J., Bui, V. N., Chire, I., et al. (2018). β -Catenin is a pH sensor with decreased stability at higher intracellular pH. *J. Cell Biol.* 217, 3965–3976. doi: 10.1083/jcb.201712041
- Xiao, F., Juric, M., Li, J. H., Riederer, B., Yeruva, S., Singh, A. K., et al. (2012). Loss of downregulated in adenoma (DRA) impairs mucosal HCO₃⁻ secretion in murine ileocolonic inflammation. *Inflammatory Bowel Dis.* 18, 101–111. doi: 10.1002/ibd.21744
- Xiao, F., Yu, Q., Li, J., Johansson, M. E. V., Singh, A. K., Xia, W., et al. (2014). Slc26a3 deficiency is associated with loss of colonic HCO₃⁻ secretion, absence of a firm mucus layer and barrier impairment in mice. *Acta Physiol.* 211, 161–175. doi: 10.1111/apha.12220
- Xu, H., Collins, J. F., Bai, L. Q., Kiela, P. R., Lynch, R. M., and Ghishan, F. K. (2001). Epidermal growth factor regulation of rat NHE2 gene expression. *Am. J. Physiol. Cell Physiol.* 281, C504–C513.
- Xu, H., Li, J., Chen, H., and Ghishan, F. K. (2019). NHE8 deficiency promotes colitis-associated cancer in mice via expansion of Lgr5-Expressing cells. *Cell. Mol. Gastroenterol. Hepatol.* 7, 19–31. doi: 10.1016/j.jcmgh.2018.08.005
- Xu, H., Zhang, B., Li, J., Chen, H. C., Tooley, J., and Ghishan, F. K. (2010). Epidermal growth factor inhibits intestinal NHE8 expression via reducing its basal transcription. *Am. J. Physiol. -Cell Physiol.* 299, C51–C57.
- Yan, Y., Denef, N., and Schupbach, T. (2009). The vacuolar proton pump, V-ATPase, is required for notch signaling and endosomal trafficking in *Drosophila*. *Dev. Cell.* 17, 387–402. doi: 10.1016/j.devcel.2009.07.001
- Yu, Q., Liu, X. M., Liu, Y. J., Riederer, B., Li, T. L., Tian, D. A., et al. (2016). Defective small intestinal anion secretion, dipeptide absorption, and intestinal failure in suckling NBCe1-deficient mice. *Pflugers Arch. Eur. J. Physiol.* 468, 1419–1432. doi: 10.1007/s00424-016-1836-3
- Zachos, N. C., Tse, M., and Donowitz, M. (2005). Molecular physiology of intestinal Na⁺/H⁺ exchange. *Annu. Rev. Physiol.* 67, 411–443. doi: 10.1146/annurev.physiol.67.031103.153004

Conflict of Interest: The authors declare that the research was conducted in the absence of any commercial or financial relationships that could be construed as a potential conflict of interest.

Copyright © 2021 Amiri, Seidler and Nikolovska. This is an open-access article distributed under the terms of the Creative Commons Attribution License (CC BY). The use, distribution or reproduction in other forums is permitted, provided the original author(s) and the copyright owner(s) are credited and that the original publication in this journal is cited, in accordance with accepted academic practice. No use, distribution or reproduction is permitted which does not comply with these terms.



Neurodegeneration Upon Dysfunction of Endosomal/Lysosomal CLC Chloride Transporters

Shroddha Bose^{1†}, Hailan He^{1,2†} and Tobias Stauber^{1,3*}

¹ Institute for Chemistry and Biochemistry, Freie Universität Berlin, Berlin, Germany, ² Department of Pediatrics, Xiangya Hospital, Central South University, Changsha, China, ³ Department of Human Medicine and Institute for Molecular Medicine, MSH Medical School Hamburg, Hamburg, Germany

OPEN ACCESS

Edited by:

Markus Ritter,
Paracelsus Medical University, Austria

Reviewed by:

Raúl Estévez,
University of Barcelona, Spain
Alexi K. Alekov,
Hannover Medical School, Germany

*Correspondence:

Tobias Stauber
tobias.stauber@
medicalschooll-hamburg.de

[†]These authors have contributed
equally to this work

Specialty section:

This article was submitted to
Cell Death and Survival,
a section of the journal
Frontiers in Cell and Developmental
Biology

Received: 08 December 2020

Accepted: 03 February 2021

Published: 23 February 2021

Citation:

Bose S, He H and Stauber T (2021)
Neurodegeneration Upon Dysfunction
of Endosomal/Lysosomal CLC
Chloride Transporters.
Front. Cell Dev. Biol. 9:639231.
doi: 10.3389/fcell.2021.639231

The regulation of luminal ion concentrations is critical for the function of, and transport between intracellular organelles. The importance of the acidic pH in the compartments of the endosomal-lysosomal pathway has been well-known for decades. Besides the V-ATPase, which pumps protons into their lumen, a variety of ion transporters and channels is involved in the regulation of the organelles' complex ion homeostasis. Amongst these are the intracellular members of the CLC family, CIC-3 through CIC-7. They localize to distinct but overlapping compartments of the endosomal-lysosomal pathway, partially with tissue-specific expression. Functioning as $2\text{Cl}^-/\text{H}^+$ exchangers, they can support the vesicular acidification and accumulate luminal Cl^- . Mutations in the encoding genes in patients and mouse models underlie severe phenotypes including kidney stones with *CLCN5* and osteopetrosis or hypopigmentation with *CLCN7*. Dysfunction of those intracellular CLCs that are expressed in neurons lead to neuronal defects. Loss of endosomal CIC-3, which heteromerizes with CIC-4, results in neurodegeneration. Mutations in CIC-4 are associated with epileptic encephalopathy and intellectual disability. Mice lacking the late endosomal CIC-6 develop a lysosomal storage disease with reduced pain sensitivity. Human gene variants have been associated with epilepsy, and a gain-of-function mutation causes early-onset neurodegeneration. Dysfunction of the lysosomal CIC-7 leads to a lysosomal storage disease and neurodegeneration in mice and humans. Reduced luminal chloride, as well as altered calcium regulation, has been associated with lysosomal storage diseases in general. This review discusses the properties of endosomal and lysosomal Cl^-/H^+ exchange by CLCs and how various alterations of ion transport by CLCs impact organellar ion homeostasis and function in neurodegenerative disorders.

Keywords: autophagy, chloride transport, endosome, ion homeostasis, lysosome, neurodegeneration

INTRODUCTION

A plethora of ion channels and transporters are responsible for the establishment and maintenance of particular ion concentrations within cells and their membrane-bounded organelles. This ion homeostasis is essential for cellular physiology and its perturbation may lead to dysfunction and eventually to cell death. As long-living post-mitotic cells, neurons are particularly reliant on a

functioning endosomal-lysosomal system because of its function in cellular clearance and stress sensing (Boland et al., 2018; Mallucci et al., 2020; Nixon, 2020). Numerous pumps, transporters and channels also mediate the transport of ions required for the physiological functions of these compartments in the endosomal-lysosomal pathway and their dysfunction often underlies inherited disorders of various kinds (Xu and Ren, 2015; Xu et al., 2015; Astaburuaga et al., 2019; Huizing and Gahl, 2020). A key player in the ion homeostasis of endosomes and lysosomes, as well as synaptic vesicles, is the V-ATPase. This multi-subunit enzyme pumps protons into the vesicular lumen and generates the acidic internal pH that regulates enzyme activities, secondary active transport, and membrane trafficking (Mellman et al., 1986; Marshansky and Futai, 2008; Mindell, 2012). Besides the pH, calcium ions (Ca^{2+}) have been shown to be of pivotal importance to fusion and fission processes and signaling from endosomes and lysosomes (Luzio et al., 2007; Morgan et al., 2011; Lakpa et al., 2020). For the other major inorganic ions, sodium (Na^+), potassium (K^+) and chloride (Cl^-) it has become clearer during the last years that they may play roles beyond merely provide for electrical and osmotic balance of the organelles. Data from patients, mouse models and cell biophysical measurements highlight an important role for Cl^- which is accumulated in a secondary active transport by CLC Cl^-/H^+ exchangers (Jentsch, 2007; Stauber and Jentsch, 2013; Schwappach, 2020). Loss, dysfunction or mutations altering biophysical properties of these CLCs lead to severe phenotypes, including neurological defects and neurodegeneration for those CLCs expressed in neurons (Stauber et al., 2012; Jentsch and Pusch, 2018).

In this review we will discuss the physiological roles of the CLC Cl^-/H^+ exchangers in the endosomal-lysosomal pathway and their involvement in neuropathologies including neurodegeneration.

THE CLC FAMILY OF Cl^- CHANNELS AND Cl^-/H^+ EXCHANGERS

The most abundant physiological anion is chloride. Like for other ions, there are various chloride channels and transporters that conduct chloride, either alone or in symport with, or exchange for other ions. Among these are the members of the CLC family, which notably comprises both chloride channels and chloride/proton exchangers (Stauber et al., 2012; Jentsch and Pusch, 2018). In mammals, there are nine CLC family members that can be divided in three groups by their sequence homology. The first branch contains CLC-1, CLC-2, CLC-Ka, and CLC-Kb, all chloride channels localized to the plasma membrane. By contrast, CLC-3, CLC-4, and CLC-5 of the second group and lastly CLC-6 and CLC-7 function as chloride/proton exchangers on intracellular compartments, mainly in the endosomal/lysosomal pathway.

CLCs function as dimers—mostly homomeric, but some CLCs can heteromerize within the same homology branch—with two independent translocation pathways (Jentsch and Pusch, 2018). Each subunit is composed of a transmembrane domain with

a complex structure of multiple alpha helices spanning or penetrating the membrane (Dutzler et al., 2002), and a globular cytosolic domain containing two cystathionine- β -synthase (CBS) domains (**Figure 1**). The CBS domains of some CLCs can bind adenine nucleotides and may be involved in the regulation and common gating of the transporter or channel (Meyer et al., 2007; Ludwig et al., 2013; Jentsch and Pusch, 2018; Grieschat et al., 2020; Schrecker et al., 2020). Some CLCs additionally bind accessory proteins. Barttin serves as a β -subunit for CLC-Ka and -Kb (Estévez et al., 2001) and more recently, an interaction with CLC-5 has been reported (Wojciechowski et al., 2018). CLC-2 and CLC-7 bind to GlialCAM and Ostm1, respectively, that contribute to the subcellular localization, protein stability or ion transport activity of the CLCs (Lange et al., 2006; Leisle et al., 2011; Jeworutzki et al., 2012). A conserved glutamate residue in the ion translocation pathway is critically involved in the gating of the plasma membrane CLC channels and hence referred to as a “gating glutamate” (Jentsch and Pusch, 2018). In the intracellular CLC exchangers, this glutamate is crucial for the strong outward rectification and for the coupling of Cl^- transport to H^+ countertransport. CLC exchangers typically (there are some exceptions in other species) possess a further glutamate, referred to as “proton glutamate,” whose mutation abolishes or strongly diminishes the transport of both protons and chloride (Jentsch and Pusch, 2018; Pusch and Zifarelli, 2021).

Among the CLC channels of the plasma membrane, CLC-1 is expressed in skeletal muscle where it mediates the major resting conductance and hence is involved in the control of muscular excitability (Steinmeyer et al., 1991; Stauber et al., 2012; Jentsch and Pusch, 2018). The homologous CLC-K isoforms are, together with their β -subunit barttin, involved in transepithelial transport in the nephron, inner ear and salivary glands (Jentsch and Pusch, 2018). The broadly expressed CLC-2 plays diverse physiological roles by regulating transepithelial transport, extracellular ion homeostasis and cellular excitability (Stauber et al., 2012; Jentsch and Pusch, 2018). The physiological importance of these plasma membrane chloride channels is evident from patients with mutations of the coding genes and from the phenotypes of engineered mouse models. In case of the CLC-2 knock-out mouse, the phenotype includes a degeneration of the testes and retina leading to male infertility and blindness, and leukodystrophy (Bösl et al., 2001; Nehrke et al., 2002; Blanz et al., 2007; Cortez et al., 2010). Loss-of-function mutations of CLC-2 have been described for some leukodystrophy patients (Depienne et al., 2013; Guo et al., 2019). The two proteins GlialCAM and MLC1, whose mutations can underlie the leukodystrophy megalencephalic leukoencephalopathy with subcortical cysts (MLC) (Leegwater et al., 2001; Lopez-Hernandez et al., 2011), interact with CLC-2 in glia cells and affect the localization and biophysical properties of the chloride channel (Jeworutzki et al., 2012; Hoegg-Beiler et al., 2014). The molecular mechanism leading to leukodystrophy remains to be elucidated, but changes in CLC-2 gating (Jeworutzki et al., 2014) do not seem to be involved (Göppner et al., 2020).

CLC-3 through CLC-7 reside on intracellular organelles, predominantly of the endosomal-lysosomal pathway, with a differential distribution between the compartments (**Figure 2**)

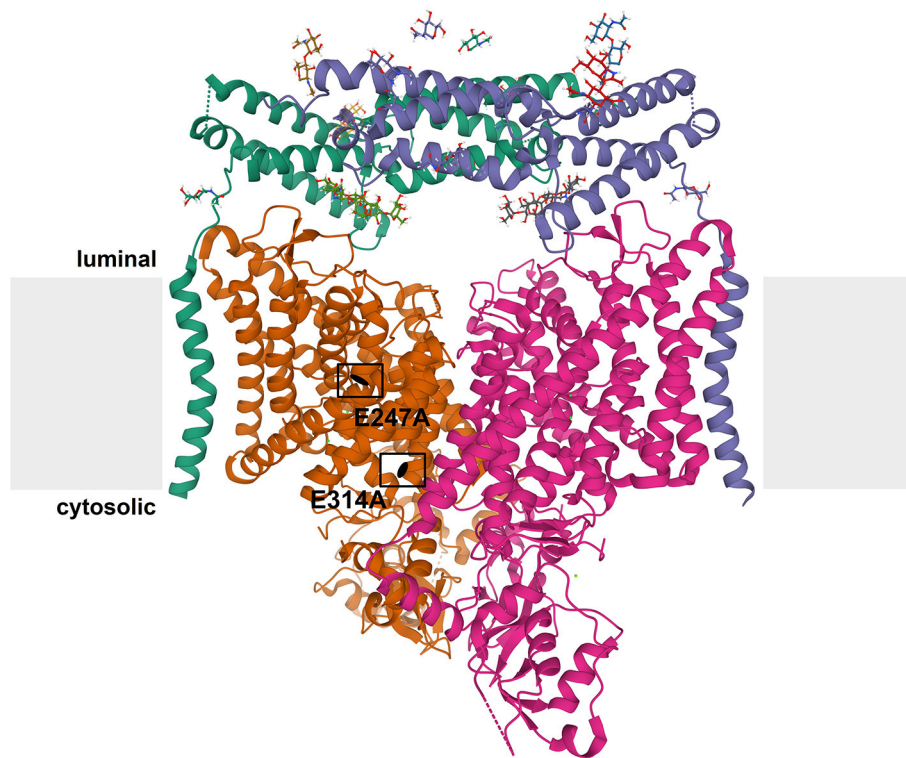
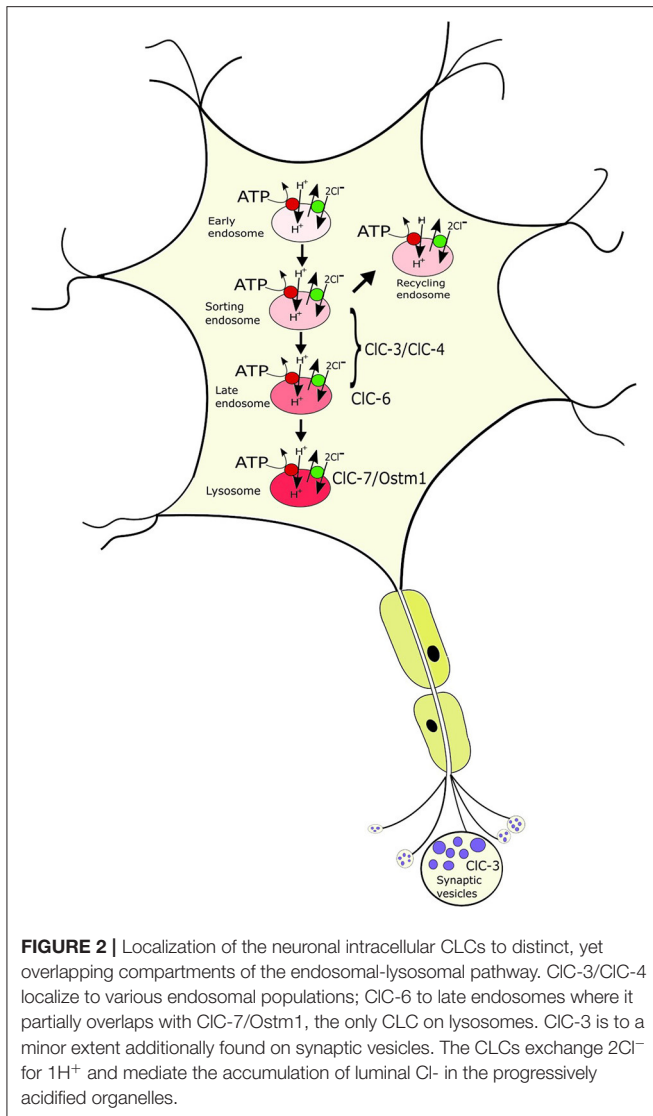


FIGURE 1 | Structure of CLC exchangers. The structure of human CLC-7 in complex with Ostm1 [Protein Data Bank [PDB]: 7JM7 (Schrecker et al., 2020)] viewed parallel to the membrane (depicted in gray) is shown as an example for the structure of CLC proteins. The subunits of the CLC homodimer are represented in orange and magenta. The globular CBS-containing domain of each subunit protrudes into the cytoplasm. Each CLC subunit provides an independent ion transport pathway. For one subunit, the positions of two key amino acids, the “gating glutamate” (E247 in CLC-7) and the “proton glutamate” (E314 in CLC-7), are indicated. The CLC-7 dimer binds two copies of its β -subunit, Ostm1, presented in green and blue. The heavily glycosylated Ostm1 is thought to shield CLC-7 from acidic proteases in the lysosomal lumen.

(Suzuki et al., 2006; Wartosch et al., 2009; Stauber et al., 2012; Stauber and Jentsch, 2013; Jentsch and Pusch, 2018): CLC-5, which is mainly expressed in the kidney, localizes to early endosomes where it is involved in endocytic uptake in the proximal tubule; the ubiquitously expressed CLC-3 and CLC-4 localize to various endosome populations; CLC-6, which at protein level is almost exclusively expressed in neurons, resides on late endosomes; CLC-7 localizes together with its β -subunit Ostm1 to lysosomes in all cells and additionally to the ruffled border of bone-resorbing osteoclasts. The physiological importance of the intracellular CLCs is evident from the broad spectrum of disorders resulting from their dysfunction in patients and mouse models (Stauber et al., 2012; Jentsch and Pusch, 2018; Schwappach, 2020). Neuronal phenotypes, including intellectual disability, epilepsy, lysosomal storage and neurodegeneration with CLC-3/-4/-6 and -7, respectively (Stobrawa et al., 2001; Kasper et al., 2005; Poët et al., 2006; Veeramah et al., 2013; Hu et al., 2016; Palmer et al., 2018; Nicoli et al., 2019; Polovitskaya et al., 2020), will be discussed in more detail below. In addition, mutations in CLC-5 lead to impaired endocytosis in the renal proximal tubule and kidney stones (Lloyd et al., 1996; Piwon et al., 2000). Mutations in CLC-7 and the associated Ostm1 underlie osteopetrosis due to its role in osteoclast bone resorption

(Kornak et al., 2001; Chalhoub et al., 2003) and to impaired skin pigmentation (Nicoli et al., 2019).

CLC-3 though CLC-7 were at first thought to be chloride channels like their plasma membrane-localized homologs that mediate the import of negative charge to counterbalance the electrogenic acidification of the respective organelles (Günther et al., 1998; Piwon et al., 2000; Kornak et al., 2001). However, after the discovery that the bacterial EcCLC-1 actually mediates $2\text{Cl}^-/\text{H}^+$ exchange (Accardi and Miller, 2004), this transport mode has been shown for the five vesicular CLCs as well (Picollo and Pusch, 2005; Scheel et al., 2005; Graves et al., 2008; Matsuda et al., 2008; Neagoe et al., 2010; Leisle et al., 2011; Guzman et al., 2013). It was proposed that instead of merely allowing Cl^- influx to allow for acidification by the V-ATPase, CLC-5 and CLC-3 actively acidified early endosomal compartments by exchanging the initially high luminal chloride for protons (Smith and Lippiat, 2010; Rohrbough et al., 2018). This transport direction would be easier to reconcile with the strong outward rectification, which is observed for all vesicular CLCs upon heterologous expression at the plasma membrane (Friedrich et al., 1999; Li et al., 2000; Neagoe et al., 2010; Leisle et al., 2011) because this would favor Cl^- efflux from the lumen through the CLC when localized intracellular vesicles. However, it is questionable



whether such a mechanism would effectively acidify the lumen with the typical buffering capacity and it would quickly build up an inside positive potential that would prevent further Cl^- efflux through the CLC (Stauber et al., 2012). For CIC-3, it has been shown that low extracytosolic pH partially uncouples Cl^- transport from H^+ exchange (Rohrbough et al., 2018). The authors proposed that at the luminal low pH, CIC-3 would then function as a Cl^- conductance that provided the countercharge for further acidification by the V-ATPase. However, more recently, the proton-activated chloride channel PAC has been shown to mediate Cl^- efflux from acidified endosomes (Osei-Owusu et al., 2021). The increase in endosomal $[\text{Cl}^-]$ and reduced pH upon its depletion (Osei-Owusu et al., 2021) are compatible with the parallel presence of a CLC exchanger that mediates pH gradient-driven Cl^- influx (Jentsch, 2007; Stauber and Jentsch, 2013). For lysosomes, Cl^- accumulation by the CIC-7 Cl^-/H^+ exchanger has indeed been shown (Weinert et al.,

2010). The electrogenic $2\text{Cl}^-/\text{H}^+$ exchange can of course still support luminal acidification, and this seems to be an important role for CIC-5 on early endosomes (Novarino et al., 2010). By contrast, the acidification of lysosomes does not necessarily depend on parallel Cl^- influx as it can be supported by cation efflux (Steinberg et al., 2010; Weinert et al., 2010). In addition to the acidification of early endosomes, a pivotal role of the vesicular CLCs is the pH gradient-dependent secondary active accumulation of luminal Cl^- , as highlighted in engineered mouse models in which individual CLC exchangers were mutated to pure chloride conductors (Novarino et al., 2010; Weinert et al., 2010, 2020). The importance of lysosomal Cl^- is still elusive, but it may affect further parameters of the vesicular ion homeostasis including Ca^{2+} (Stauber and Jentsch, 2013; Chakraborty et al., 2017; Astaburuaga et al., 2019).

NEUROPATHIES WITH CLC-3 AND CLC-4

CIC-3/CIC-4 Mediate Endosomal Cl^-/H^+ Exchange in Neurons

Within their branch of CLCs, CIC-3, CIC-4 and CIC-5 share sequence identity of approximately 80%. Whilst CIC-5 is mainly expressed in the kidney (Steinmeyer et al., 1995), CIC-3 is widely expressed and has been detected in virtually all mammalian tissues, including brain, retina, adrenal gland, heart, liver, kidney, pancreas, intestines, epididymis and skeletal muscle (Kawasaki et al., 1994; Borsani et al., 1995; Stobrawa et al., 2001; Maritzen et al., 2008). Within the brain, CIC-3 is predominantly expressed in neuronal cells of the hippocampus and Purkinje cells in the cerebellum (Kawasaki et al., 1994). CIC-3 predominantly localizes on endosomes (Stobrawa et al., 2001; Hara-Chikuma et al., 2005; Shibata et al., 2006). Additionally, it is found on synaptic vesicles (SVs) (Stobrawa et al., 2001; Salazar et al., 2004; Weinert et al., 2020) and synaptic-like micro vesicles (Salazar et al., 2004; Maritzen et al., 2008). CIC-4 displays similarly broad tissue expression as CIC-3, but its relative abundance is lower in tissues other than brain and muscle (Van Slegtenhorst et al., 1994; Mohammad-Panah et al., 2002, 2003; Weinert et al., 2020).

Alternative splice variants of CIC-3 have been reported. The isoforms (CIC-3A, CIC-3B, and CIC-3C) display similar transport properties but differential subcellular localization (Guzman et al., 2015). CIC-3A resides on late endosomes/lysosomes (Li et al., 2002; Gentzsch et al., 2003), CIC-3B might localize to the Golgi (Ogura et al., 2002; Gentzsch et al., 2003), and CIC-3C is targeted to recycling endosomes via an amino-terminal sorting motif (Guzman et al., 2015). Upon heterologous expression, CIC-3 through-5 can form heteromers amongst each other, but not with CIC-6 or CIC-7 (Suzuki et al., 2006). In heterologous expression, CIC-4 is predominantly retained in the endoplasmic reticulum (ER), with a minor portion on the plasma membrane (Okkenhaug et al., 2006; Guzman et al., 2017; Weinert et al., 2020). Co-expression with distinct CIC-3 splice variants targets CIC-4 to late endosome/lysosomes (CIC-3A and CIC-3B) or recycling endosomes (CIC-3C) (Guzman et al., 2017). Also endogenous CIC-3 and CIC-4 interact *in vivo*, and CIC-4 requires CIC-3

for ER export and protein stability (Weinert et al., 2020). This, together with the relative expression levels, suggests that in brain, CIC-3/CIC-4 function as heterodimers, whereas in other tissues there may be a more prominent role for CIC-3 homomers. CIC-4, on the other hand, seems to rely on heteromerization with CIC-3, which may explain the apparent lack of endosomal sorting signals in CIC-4 (Stauber and Jentsch, 2010).

There are numerous conflicting studies concerning the transport properties and cellular functions of CIC-3 (Jentsch and Pusch, 2018). For example, previously CIC-3 was reported to function as a plasma membrane chloride channel regulated by the protein kinase C or the calcium/calmodulin-dependent protein kinase II (Kawasaki et al., 1994; Huang et al., 2001). Another function that had been ascribed to CIC-3 was that of the volume-regulated anion channel (VRAC) (Duan et al., 1997). However, like many other candidates, CIC-3 was excluded as VRAC and the typical VRAC currents were unchanged in the various tested cell types from independent CIC-3 knock-out mouse models (Stauber, 2015; Jentsch and Pusch, 2018); VRAC has more recently been shown to be formed by LRRC8 proteins (Qiu et al., 2014; Voss et al., 2014; König and Stauber, 2019). Instead, CIC-3 is an outwardly rectifying, vesicular $2\text{Cl}^-/\text{H}^+$ exchanger like the other intracellular CLCs (Stobrawa et al., 2001; Matsuda et al., 2008; Guzman et al., 2013, 2015; Rohrbough et al., 2018). CIC-3 was reported to provide an electrical shunt for the efficient proton pumping of the electrogenic H^+ -ATPase into the lumen, thereby facilitating the acidification of SVs (Stobrawa et al., 2001; Riazanski et al., 2011; Guzman et al., 2013) and compartments in the endosomal/lysosomal pathway (Stobrawa et al., 2001; Hara-Chikuma et al., 2005; Weylandt et al., 2007). Indeed, endosomal acidification and chloride accumulation were significantly enhanced in CIC-3A-transfected Chinese hamster ovary cells and impaired in hepatocytes from CIC-3-deficient mice (Hara-Chikuma et al., 2005). The acidification of SVs derived from CIC-3-deficient *Clcn3*^{-/-} mice was impaired (Stobrawa et al., 2001; Riazanski et al., 2011). However, the impaired acidification of SVs can be attributed to a secondary decrease in the vesicular glutamate transporter VGLUT1, which itself represents a major Cl^- permeation pathway in synaptic vesicles (Schenck et al., 2009; Preobraschenski et al., 2014; Eriksen et al., 2016; Martineau et al., 2017). In young *Clcn3*^{-/-} mice, before the onset of neurodegeneration (see below) and the loss of VGLUT1, SV acidification was not impaired (Weinert et al., 2020). The partial plasma membrane localization of CIC-4 allowed its electrophysiological characterization as a strongly voltage-dependent intracellular $2\text{Cl}^-/\text{H}^+$ exchanger (Picollo and Pusch, 2005; Scheel et al., 2005). Also for CIC-4, a role in endosomal acidification was reported, with a more alkaline endosomal pH and resultant defects in recycling of the transferrin receptor in fibroblasts derived from CIC-4-deficient mice (Mohammad-Panah et al., 2003, 2009).

CIC-3/CIC-4 in Neurodegeneration and Other Neurological Disorders

Three independently generated CIC-3 knock-out mouse models displayed similar phenotypes of severe postnatal degeneration of the retina and brain, that led to an almost total loss of the hippocampus after 3 months (Stobrawa et al., 2001; Dickerson

et al., 2002; Yoshikawa et al., 2002) (**Table 1**). Neurodegeneration in these *Clcn3*^{-/-} mice is not associated with obvious deposits of lysosomal storage material found in *Clcn6*^{-/-} or *Clcn7*^{-/-} mice (Kasper et al., 2005; Poët et al., 2006) (see below). However, one *Clcn3*^{-/-} mouse model displayed deposits of the mitochondrial ATP synthase subunit c, typically found in the lysosomal storage disease neuronal ceroid lipofuscinosis (NCL) (Yoshikawa et al., 2002). The neurodegeneration was accompanied by an activation of microglia and astrogliosis (Stobrawa et al., 2001; Dickerson et al., 2002). Despite their severe neurodegeneration, CIC-3 knock-out mice are viable and have a normal life span.

It is tempting to speculate that the severe neurodegeneration in *Clcn3*^{-/-} mice is caused by impaired synaptic function. The frequency and amplitude of miniature excitatory postsynaptic currents (mEPSCs) in primary neurons from CIC-3-deficient mice was reported to be reduced, suggesting that glutamate toxicity due to excessive glutamate release contributes to the neurodegeneration (Guzman et al., 2014). However, a recent study found virtually unaltered mEPSCs (Weinert et al., 2020). Another study reported reduced miniature inhibitory postsynaptic currents (mIPSCs) in *Clcn3*^{-/-} mice (Riazanski et al., 2011), in agreement with the reduced glutamate uptake in SVs of CIC-3-deficient mice, but in contrast to mIPSC measurements in a previous study (Stobrawa et al., 2001). Both the impaired acidification and the glutamate loading of SVs can be explained by the concomitant reduction of VGLUT1 in *Clcn3*^{-/-} mice (Stobrawa et al., 2001; Schenck et al., 2009; Weinert et al., 2020), which is a likely consequence—and hence not cause—of the neurodegeneration.

A recent study described knock-in mice in which the “gating glutamate” in CIC-3 is replaced by alanine to form the “CIC-3^{unc}” mutant, in which Cl^- transport is *uncoupled* from H^+ countertransport (Weinert et al., 2020). These mice, referred to as *Clcn3*^{unc/unc}, presented no obvious phenotype (**Table 1**). This is in stark contrast to previous observations from equivalent mouse models expressing CIC-5^{unc} and CIC-7^{unc} that display similar phenotypes as the respective knock-out mouse models (Novarino et al., 2010; Weinert et al., 2010). The explanation lies in the heteromerization of CIC-3 with CIC-4 (Weinert et al., 2020). Although mRNA levels of CIC-4 were not significantly altered in the brain of *Clcn3*^{-/-} mice, CIC-4 protein levels were decreased to ~30%. In contrast, no reduction in CIC-4 levels was observed in *Clcn3*^{unc/unc} mice. CIC-3^{unc} stabilizes and promotes the transport of CIC-4 from the ER to endosomal compartments like wild-type CIC-3. Therefore, CIC-4 may compensate for a loss of CIC-3 function in *Clcn3*^{unc/unc}, but not in *Clcn3*^{-/-} mice, and the partial loss of CIC-4 may contribute to the severe neurodegeneration of *Clcn3*^{-/-} mice (Weinert et al., 2020). Mice deficient in CIC-4, as well as *Clcn3*^{unc/unc} mice displayed no obvious phenotypes (Rickheit et al., 2010; Hu et al., 2016; Weinert et al., 2020). However, the combination of these genotypes in *Clcn3*^{unc/unc};*Clcn4*^{-/-} mice results in an even more severe neurodegeneration than observed in *Clcn3*^{-/-} mice (Weinert et al., 2020) (**Table 1**). Yet, the milder phenotype of *Clcn3*^{unc/unc};*Clcn4*^{-/-} mice compared to *Clcn3*^{-/-};*Clcn4*^{-/-} mice suggests that the pure Cl^- conductance of the uncoupled CIC-3^{unc} can also partially substitute for

TABLE 1 | Mouse models with *Clcn3*, *Clcn4* or *Clcn5* mutations.

	<i>Clcn3</i> ^{-/-} (3 independent lines)	<i>Clcn3</i> ^{unc/unc}	<i>Clcn4</i> ^{-/-}	<i>Clcn3</i> ^{unc/unc} ; <i>Clcn4</i> ^{-/-}	<i>Clcn3</i> ^{-/-} ; <i>Clcn4</i> ^{-/-}	<i>Clcn5</i> ^{y/-}	<i>Clcn5</i> ^{y/unc}
Ion transport by respective CLC	No current	No proton transport	No current	No proton transport/no current	No current	No current	No proton transport
Age at death	>1 year	Normal	Normal	5–10 weeks	Shortly after birth	Normal	Normal
Weight	↓	Normal	Normal	↓		Normal	Normal
Neuro-degeneration	Yes	No	No	Yes (severe)	Yes (very severe)		
Retina degeneration	Yes	No	No	Yes			
CLC-3 protein levels	No	Normal	Normal	Normal	No	Normal	Normal
CLC-4 protein levels	↓	Normal	No	No	No	Normal	Normal
PH of synaptic vesicles	Normal in young mice; ↑ in old mice	Normal	Normal	↑			
Endosomal pH	↑ in hepatocytes; normal in neurons					↑	Normal
Endosomal chloride	↓ in hepatocytes; not tested in neurons						
Others						Impaired renal endocytosis	Impaired renal endocytosis

See main text for references.

functions of the wild-type CLC-3 Cl^-/H^+ exchanger in the absence of compensating CLC-4 (Weinert et al., 2020). The absence of neurodegeneration in *Clcn4*^{-/-} mice can be explained by the remaining, unaltered levels of CLC-3 which may be sufficient, as CLC-3 can form homodimers and does not require CLC-4 for its endosomal localization. For the properties of CLC-3, only subtle consequences of the heteromerization with CLC-4 are expected.

Like in *Clcn3*^{-/-} mice, the acidification of SVs and hippocampal miniature postsynaptic currents were unaltered in *Clcn3*^{unc/unc} mice before major neuronal loss, suggesting that the severe neurodegeneration does probably not result from SV dysfunction (Weinert et al., 2020). Only a minor fraction of CLC-3 is found on SVs, while also in neurons the majority is present on endosomes. Endosomal acidification and concomitant Cl^- accumulation was found significantly impaired in hepatocytes from CLC-3-deficient mice (Hara-Chikuma et al., 2005). However, pH measurements of transferrin-positive endosomes in cultured neurons from *Clcn3*^{-/-} mice revealed normal acidification (Weinert et al., 2020), resembling findings with lysosomes from mice lacking CLC-7 or Ostml (Kasper et al., 2005; Lange et al., 2006) (see below). Mouse models expressing CLC-5^{unc} or CLC-7^{unc} suggested an important role for pH gradient-driven vesicular Cl^- accumulation in early endosomes and lysosomes, respectively (Novarino et al., 2010; Weinert et al., 2010). So the severe neurodegeneration observed in *Clcn3*^{-/-} mice or *Clcn3*^{unc/unc}/*Clcn4*^{-/-} mice may be ascribed to an impairment of endosomal chloride accumulation rather than to defective endosomal acidification (Weinert et al., 2020).

So far, no convincing disease-causing mutations have been identified in the human *CLCN3* gene. However, a variety of

inherited and *de novo* mutations in *CLCN4*, which in humans is located X-chromosomal in contrast to the autosomal positioning of the *Clcn4* gene in the laboratory mouse *Mus musculus* (Palmer et al., 1995; Rugarli et al., 1995), have recently been identified in patients with intellectual disability, epilepsy and behavior disorders, but lacking neurodegeneration (Veeramah et al., 2013; Hu et al., 2016; Palmer et al., 2018; Zhou et al., 2018). The identified *CLCN4* mutations included frameshifts, missense, intragenic copy number deletion and splice site alterations. *In vitro* electrophysiological studies showed that the majority of the disease-associated missense mutations cause a loss of function as they diminished or abolished the outwardly rectifying CLC-4 currents upon heterologous expression. Although no neurological phenotype and no morphological changes in the brain were detected in *Clcn4*^{-/-} mice (Rickheit et al., 2010; Palmer et al., 2018), the number of dendritic branches and dendritic length were reduced in primary neurons derived from *Clcn4*^{-/-} mice and in knock-down of the *Clcn4* gene cultures neurons (Hur et al., 2013; Hu et al., 2016). This suggests an involvement of CLC-4 in neuronal differentiation, which may contribute to the neurological disorders in patients with *CLCN4* mutations.

THE LATE ENDOSOMAL CLC-6

CLC-6 and CLC-7, which share ~45% sequence identity, constitute the third branch of mammalian CLCs (Brandt and Jentsch, 1995). Despite the ubiquitous expression of *CLCN6* mRNA (Brandt and Jentsch, 1995; Kida et al., 2001), the protein is almost exclusively found in neurons (Poët et al., 2006). Whilst upon heterologous expression in cell culture

CLC-6 is mainly targeted to recycling endosomes (Ignoul et al., 2007; Stauber and Jentsch, 2010), endogenous CLC-6 resides predominantly on Lamp1-positive late endosomes (Poët et al., 2006), partially overlapping with endosomal CLC-3 and late endosomal/lysosomal CLC-7 (Stauber et al., 2012; Jentsch and Pusch, 2018). The partial plasma membrane localization of CLC-6 with green-fluorescent protein (GFP) fused to its amino-terminus allowed for its biophysical characterization as a Cl^-/H^+ exchanger (Neagoe et al., 2010). CLC-6 shares typical properties with the other intracellular CLCs, such as the outward rectification and the uncoupling of Cl^- transport from H^+ countertransport by mutation of the “gating glutamate.”

CLC-6-deficient *Clcn6*^{-/-} mice are fertile and display a normal life span without any immediately apparent phenotype (Poët et al., 2006) (Table 2). However, their neurons accumulate lysosomal storage material, also containing the mitochondrial ATP synthase subunit c, specifically in the initial axon segments that become swollen (Poët et al., 2006). Detailed analysis of brains from *Clcn6*^{-/-} mice revealed a late-onset—much milder than for CLC-3 or CLC-7 deficiency—neurodegeneration (Pressey et al., 2010). CLC-6 knock-out mice also exhibited minor cognitive defects and reduced pain sensitivity, which may arise from the accumulation of storage material in neurons of the dorsal root ganglia (Poët et al., 2006). While two out of 75 tested patients with Kuf's disease, which features phenotypes in common with those found in CLC-6 knock-out mice (Berkovic et al., 1988), were heterozygous for *CLCN6* missense variants, no further evidence for CLC-6 dysfunction underlying this disease was found (Poët et al., 2006).

Variations in *CLCN6* were identified in patients with epilepsy (Yamamoto et al., 2015; Wang et al., 2017; Peng et al., 2018;

He et al., 2021). Interestingly, these include a mutation of the “gating glutamate” at position E200 in the commonly used *CLCN6* transcript variant 1 (He et al., 2021), while the mutation was referred to as E178A in earlier studies (Wang et al., 2017; Peng et al., 2018). This amino acid substitution converts CLC-6 into a pure Cl^- conductor (Neagoe et al., 2010). Interestingly, a recent study shows that this CLC-6^{unc} mutant, identified in a patient with the early infantile epileptic encephalopathy West syndrome, impairs the autophagic-lysosomal pathway upon heterologous expression (He et al., 2021). Very recently, a heterozygous *de novo* *CLCN6* missense mutation was identified in three independent patients with variable early-onset neurodegeneration with brainstem lesions and cortical or cerebral atrophy, respectively (Polovitskaya et al., 2020). The affected children displayed global developmental delay with regression and further neurological disorders such as peripheral sensory neuropathy to varying degrees, but lacked seizures. The identified mutation, p.Tyr553Cys, affects a tyrosine that is conserved between the mammalian CLC exchangers. The electrophysiological characterization of the CLC-6^{Y553C} mutant revealed that at cytosolic-positive membrane potentials, it mediated larger currents than wild-type CLC-6, which were not affected by an extra-cytosolic pH of 5.5 similar to that in late endosomes. Voltage-dependent activation of the mutant was slowed down in comparison to wild-type, but the instantaneous currents were already of the amplitude of maximal wild-type currents. So this mutation resulted in a gain of function (Polovitskaya et al., 2020). Upon heterologous expression in cultured cells it colocalized with the marker protein Lamp1 to drastically enlarged late endosomal structures (Polovitskaya et al., 2020), resembling those observed with gain-of-function

TABLE 2 | Mouse models with *Clcn6* or *Clcn7* mutations.

	<i>Clcn6</i> ^{-/-}	<i>Clcn7</i> ^{-/-}	<i>Clcn7</i> ^{unc/unc}	<i>Clcn7</i> ^{td/td}	<i>Clcn7</i> ^{G213R/G213R}	<i>Clcn7</i> ^{F316L/F316L}	<i>Clcn7</i> ^{+/Y713A}
Transporter properties	No CLC-6 protein	No CLC-7 protein	No proton transport, no rectification, instantaneous currents	Only residual currents	Mis-localization	Reduced current	More currents at cytosolic-positive potential
Age at death	Normal	4-6 weeks	Up to 5 weeks	Up to 6 weeks	Up to 30 days	Up to 30 days	18 weeks (heterozygous)
Fur color	Normal	Gray	Normal	Normal			Albinism
Bone mineralization		↑	↑	↑	↑	↑	Normal
Storage material	Yes	Yes	Yes	Yes	Yes		Yes
Neuro-degeneration	No	Yes	Yes	Yes	Yes		Yes
Retina degeneration		↑	↑	No			
Autophagic accumulation		↑	↑	No	↑		
Lysosomal pH	Normal	Normal	Normal	Normal	↑		↓
Lysosomal chloride		↓	↓	↓			
Others	Reduced pain sensitivity, moderate behavioral abnormalities	Splenomegaly			Fibrosis in lung, kidney, muscle		Intracellular vacuoles

See main text for references.

CLC-7 mutant (Nicoli et al., 2019) (see below). The lumen of these vacuoles was poorly acidified (Polovitskaya et al., 2020), which may cause alterations of membrane fusion and fission with or from these structures. The consequent impairment of the endosomal-lysosomal pathway is likely to underlie the neuropathy of the patients.

The two disease-causing mutations have differential effects on the ion transport properties of CLC-6. However, the fact that loss of CLC-6 in *Clcn6*^{-/-} mice leads to only mild phenotypes (Poët et al., 2006), suggests that the heterozygous CLC-6^{E200A}, just like CLC-6^{Y553C} (Polovitskaya et al., 2020), presents a gain-of-function mutation. The uncoupling of chloride transport from proton countertransport by the E200A mutation may be considered a loss of function. Indeed, mouse models expressing the equivalent mutation in CLC-5 or CLC-7 display similar disorders as the respective knock-out models (Novarino et al., 2010; Weinert et al., 2010). However, these uncoupling mutations additionally abolish the outward rectification of the CLC and hence would increase currents at luminal positive potentials, which may well be of patho-physiological relevance. Nonetheless, the two CLC-6 mutations also affect the morphology of endosomal compartments differentially –with only mildly or drastically enlarged compartments for CLC-6^{E200A} and CLC-6^{Y553C}, respectively (Polovitskaya et al., 2020)– and eventually lead to different neurological disorders, infantile epilepsy or early-onset neurodegeneration.

NEURODEGENERATION UPON DYSFUNCTION OF CLC-7/OSTM1

CLC-7/Ostm1 –a Lysosomal Cl^-/H^+ Exchanger

The ubiquitously expressed CLC-7 is the only member of the CLC protein family that primarily localizes to lysosomes (Brandt and Jentsch, 1995; Kornak et al., 2001). In bone-resorbing osteoclasts, it additionally resides in the ruffled border, a specialized membrane domain built up by the fusion of lysosomes with the plasma membrane (Teitelbaum, 2000; Kornak et al., 2001). It forms a stable complex with the single-pass type I membrane protein Ostm1 (for osteopetrosis-associated membrane protein 1) (Lange et al., 2006; Schrecker et al., 2020; Zhang et al., 2020) (Figure 1). This interaction is required for stability for protein stability of CLC-7, likely due to the heavily N-glycosylated Ostm1, of which two subunits bind to the CLC-7 dimer, shielding the unglycosylated CLC-7 from lysosomal proteases (Lange et al., 2006; Schrecker et al., 2020; Zhang et al., 2020), and for ion transport by the CLC-7/Ostm1 complex (Leisle et al., 2011). On the other hand, Ostm1 is reliant on CLC-7 for exit from the ER and lysosomal targeting (Lange et al., 2006; Leisle et al., 2011). Hence, a drastic reduction in protein levels can be observed for Ostm1 in tissues of CLC-7-deficient *Clcn7*^{-/-} mice and for CLC-7 in spontaneous Ostm1-deficient *grey-lethal* mouse line (Lange et al., 2006). Ostm1 is a 70 kDa protein which is proteolytically processed upon arrival in lysosomes (Lange et al., 2006). Recently

solved cryo-EM structures of CLC-7/Ostm1 revealed that the luminal domain of Ostm1 has a tightly packed core of helical bundles linked with several disulfide bonds (Schrecker et al., 2020; Zhang et al., 2020).

In osteoclasts, expression of CLC-7 and Ostm1 are coregulated by the transcription factor microphthalmia (Meadows et al., 2007). In addition, CLC-7 expression has been shown to be upregulated, like that of many lysosomal proteins, by the transcription factor TFEB (Sardiello et al., 2009). The subcellular localization of CLC-7/Ostm1 on late endosomes/lysosomes has been shown by various means for all tested tissues and cell types, including neurons, fibroblasts, renal proximal tubule cells, liver, macrophages, activated microglia and HeLa cells (Kornak et al., 2001; Kasper et al., 2005; Graves et al., 2008; Wartosch et al., 2009; Steinberg et al., 2010; Majumdar et al., 2011; Hennings et al., 2012). Lysosomal localization increases reportedly during microglia activation (Majumdar et al., 2011). Recently, an influence of protein kinase A (PKA) signaling on lysosomal delivery of CLC-7/Ostm1 and an impairment thereof in presenilin-1 knock-out has been proposed (Lee et al., 2020). In neurons, the CLC-7 may partially overlap with CLC-6 in their localization to late endosomes, but CLC-7 is exclusively found on lysosomes to which CLC-6 is only shifted in brain of CLC-7-deficient mice (Poët et al., 2006).

Like for CLC-6, the exclusive intracellular localization of CLC-7 hampered a biophysical characterization of the protein for several years. The presence of a conserved “proton glutamate” (E312 or E314 in mouse and human CLC-7, respectively) pointed to the activity of CLC-7 as a Cl^-/H^+ antiporter. This was confirmed by flux measurements on isolated lysosomes (Graves et al., 2008) and with lysosomes in living cells, including CLC-7 knock-out cells as control (Weinert et al., 2010). Subsequently, the identification of endosomal sorting motifs in the amino-terminal domain of CLC-7 enabled partial cell surface localization of CLC-7/Ostm1 (Stauber and Jentsch, 2010). The plasma membrane-targeted CLC-7 mutant depleted of the sorting motifs, referred to as CLC-7^{PM}, mediates strongly outward-rectifying voltage-activated currents by exchanging 2 Cl^- for 1 H^+ (Leisle et al., 2011). Both Cl^- and H^+ transport could also be visualized in an optical activity assay for CLC-7/Ostm1 (Zanardi et al., 2013). The electrophysiological analysis revealed that CLC-7/Ostm1 shares many properties with the other intracellular CLCs, including the uncoupling of Cl^- transport from proton countertransport and the drastic reduction in transport upon mutation of the “gating” and “proton” glutamates, respectively (Leisle et al., 2011). CLC-7^{PM} required co-expression of Ostm1 for ion transport activity (Leisle et al., 2011), which may be due to minor effects of Ostm1 on the ion translocation pathway in the CLC-7 subunit (Schrecker et al., 2020). A striking difference to the currents mediated by the endosomal CLCs was the slow activation and relaxation kinetics of CLC-7/Ostm1 (Leisle et al., 2011). This slow “gating” involves the common gating of the subunits (Ludwig et al., 2013) and depends on the interaction of the CLC-7 transmembrane domain interface with the amino-terminus and the CBS domains of the C-terminal region (Leisle et al., 2011; Schrecker et al., 2020; Zhang et al., 2020).

Neurodegeneration in Mouse Models With Dysfunction of CLC-7/Ostm1

The physiological importance of CLC-7/Ostm1 was first revealed by the analysis of engineered *Clcn7*^{-/-} mice (Kornak et al., 2001) and the *grey-lethal* mouse line, which was found to harbor a mutation leading to Ostm1 deficiency (Chalhoub et al., 2003). Homozygous mice of both lines develop a severe osteopetrosis, i.e., hypermineralization of bones and obliteration of bone marrow cavities, accompanied by secondary effects such as a lack of tooth eruption. The osteopetrosis is owed to an impairment in the build-up and in the acidification of the osteoclast ruffled border (Kornak et al., 2001; Rajapurohitam et al., 2001; Stauber et al., 2012; Jentsch and Pusch, 2018). The mice display a shortened life span of only few weeks. In an *agouti* background, when wild-type mice have brown fur, CLC-7- and Ostm1-deficient mice have a gray coat color, suggesting a role for CLC-7/Ostm1 in hair pigmentation (Kornak et al., 2001; Chalhoub et al., 2003).

Besides the immediately obvious osteopetrotic phenotype, *Clcn7*^{-/-} and *grey-lethal* mice develop a progressive neurodegeneration in the brain and retina (Kasper et al., 2005; Lange et al., 2006; Pressey et al., 2010). Neurons of various brain regions accumulated electron-dense deposits in lysosomes scattered throughout the cell bodies (Kasper et al., 2005). With the autofluorescence of the lysosomal storage material and the accumulation of the subunit c of the mitochondrial ATP synthase, the phenotype resembled a neuronal ceroid lipofuscinosis (NCL). Neuronal cell loss, prominent in the hippocampal CA3 region, in the thalamocortical system and of Purkinje cells in the cerebellum, was accompanied by inflammatory responses such as microglia activation and astrogliosis, another hallmark of NCL and other neurodegenerative pathologies, in *Clcn7*^{-/-} mice (Kasper et al., 2005; Pressey et al., 2010). The generation of tissue-specific CLC-7 knock-out mice enabled the analysis of neurodegeneration in mice with a normal life span (Wartosch et al., 2009). Brains of adult mice with a forebrain-specific CLC-7 knock-out (*Clcn7*^{lox/lox}; *EMX1-cre*), displayed conspicuous loss of hippocampal and cortical neurons. Starting in the CA3 region of hippocampus neuronal loss progressed into the dentate gyrus and by the age of 1.5 years no hippocampal structures in *Clcn7*^{lox/lox}; *EMX1cre* mice could be detected (Wartosch et al., 2009). *In vivo* protein degradation experiments using kidney-specific CLC-7 knock-out mice (*Clcn7*^{lox/lox}; *ApoE-cre*) revealed slowed lysosomal degradation of endocytosed protein (Wartosch et al., 2009). Consistent with an impairment of lysosomal function, *grey-lethal* mice accumulated sphingolipids in the brain (Prinetti et al., 2009) and an increase in the autophagic marker LC3-II was observed in brain and kidney of *Clcn7*^{-/-} and in *grey-lethal* mice (Wartosch et al., 2009; Heraud et al., 2014), but it is not clear whether this is due to reduced autophagosome clearance or an induction of autophagy (Wartosch and Stauber, 2010).

Lysosomes in neurons and other cells from CLC-7- or Ostm1-deficient mice were found to be normally acidified (Kasper et al., 2005; Lange et al., 2006; Steinberg et al., 2010), contradicting the previous assumption that CLC-7 mediated the required

counterion transport for the lysosomal acidification. Instead, the counterion conductance can be provided by cation efflux from lysosomes (Steinberg et al., 2010; Weinert et al., 2010). *Clcn7*^{unc/unc} mice, in which CLC-7 functions as a pure Cl^- conductor due to the E245A mutation of its “gating glutamate” did not display a fur color phenotype and they presented an osteopetrosis that was milder than in *Clcn7*^{-/-} mice (Weinert et al., 2010). However, they developed the same lysosomal storage disease and neurodegeneration as CLC-7 knock-out mice (Table 2). As in *Clcn7*^{-/-} cells, lysosomes were acidified to the normally low pH. As predictable from model calculations (Weinert et al., 2010; Ishida et al., 2013; Astaburuaga et al., 2019), the lysosomal Cl^- concentration was reduced in both *Clcn7*^{-/-} and *Clcn7*^{unc/unc} mice compared to wild-type (Weinert et al., 2010). Similar results, reduced $[\text{Cl}^-]$ but normally acidic pH, were obtained with nematode models with reduced CLC-7 or Ostm1 orthologs (Chakraborty et al., 2017). Together with the equivalent CLC-3^{unc} and CLC-5^{unc} knock-in mouse models, this suggests an important, acidification-independent role for Cl^- accumulation in the endo-lysosomal pathway, while in early endosomes Cl^- additionally supports luminal acidification (Novarino et al., 2010; Weinert et al., 2010, 2020; Scott and Gruenberg, 2011; Stauber and Jentsch, 2013; Schwappach, 2020).

Another knock-in mouse model expressed CLC-7 with a E312A mutation of the “proton glutamate,” dubbed CLC-7^{td} because of the supposed transport deficiency of the mutant (Weinert et al., 2014) (Table 2). Like *Clcn7*^{unc/unc} mice, these *Clcn7*^{td/td} mice lacked a coat color phenotype. However, in contrast to *Clcn7*^{unc/unc} mice, the osteopetrosis of *Clcn7*^{td/td} mice was as pronounced as in *Clcn7*^{-/-} mice, but intriguingly their neuropathy with lysosomal storage and neurodegeneration was less severe and no accumulation of autophagic material was detected (Weinert et al., 2014). An explanation for the differential effects in the mouse models may be that the Cl^- conductance of CLC-7^{unc} could partially compensate for CLC-7 loss in its osteoclast function in bone resorption, while it is deleterious for neuronal lysosomes. On the other hand, the presence of the CLC-7^{td} protein—and with that of Ostm1 which is normally transported to lysosomes in *Clcn7*^{td/td} mice (Weinert et al., 2014)—can sustain lysosomal function in neurons, possibly by protein-protein interactions as proposed for Ostm1 (Pandruvada et al., 2016). An alternative explanation for the milder neuropathy of *Clcn7*^{td/td} mice compared to *Clcn7*^{-/-} mice was recently provided by the unexpected finding that the mutation of the “proton glutamate” to alanine does not completely abolish currents by CLC-7^{td} (Pusch and Zifarelli, 2021). With its residual ion transport activity, CLC-7^{td} may partially exert its function in the neuronal endo-lysosomal pathway. Nonetheless, while lysosomes of *Clcn7*^{td/td} mice were normally acidified, the lysosomal Cl^- concentration was reduced (Weinert et al., 2014).

Patient CLCN7 Mutations Causing Neuropathies

Mutations in *CLCN7* and *OSTM1* also underlie severe, autosomal recessive osteopetrosis (ARO) in humans (Kornak et al., 2001;

Chalhoub et al., 2003). In addition, intermediate autosomal osteopetrosis (IAO) and the milder, autosomal dominant osteopetrosis type 2 (ADO2, or Albers-Schönberg disease) are caused by *CLCN7* mutations (Cleiren et al., 2001; Frattini et al., 2003; Sobacchi et al., 2013). The most severe forms of *CLCN7*-related ARO in about 50% of the cases, as well as *OSTM1*-related ARO, are also neuropathic with primary neurodegeneration manifesting in developmental delay, hypotonia, retinal atrophy and seizures (Steward, 2003; Pangrazio et al., 2006; Sobacchi et al., 2013), which is critical for therapy (Teti and Econs, 2017). Dominant *CLCN7* mutations, which may lead to subcellular mislocalization of the CLC-7/Ostm1 complex or the impingement of the dysfunctional subunit on the ion transport properties of the unaffected subunit (Schulz et al., 2010; Ludwig et al., 2013), do not lead to neuropathy in mild ADO2. A mouse model recapitulating the most common CLC-7 mutation in ADO2, G215R (G213R in mouse), which was reported to impinge on subcellular trafficking (Schulz et al., 2010), developed a late-onset osteopetrosis as expected for heterozygous animals while homozygous mice displayed a phenotype similar to that of *Clcn7*^{-/-} mice with death after only a few weeks and neurodegeneration (Alam et al., 2014) (Table 2). Similar findings were made with another ADO2 mouse model with the F318L (F316L in mouse) mutation (Caetano-Lopes et al., 2017), which strongly diminishes currents mediated by CLC-7^{PM}/Ostm1 (Leisle et al., 2011). However, heterozygous *Clcn7*^{+/G213R} ADO2 mice also presented fibrosis in non-skeletal tissues such as lung and muscle; their brains exhibited perivascular fibrosis, β -amyloid accumulation and astrogliosis, and the animals showed behavioral abnormalities (Maurizi et al., 2019).

During the first electrophysiological analysis of osteopetrosis-causing CLC-7 missense mutations, it was surprisingly found that, besides loss-of-function mutations due to impaired ER exit or reduced ion transport, several pathogenic CLC-7 mutations accelerated the voltage-dependent activation of CLC-7^{PM}/Ostm1 (Leisle et al., 2011). Most of the amino acids changed by these mutations are involved in the interaction between the transmembrane domain and the cytoplasmic CBS domains of CLC-7, which highlights the role of the domain interface in the common gating that is responsible for the slow activation kinetics (Leisle et al., 2011; Ludwig et al., 2013; Schrecker et al., 2020; Zhang et al., 2020). Such apparent gain-of-function by fast exchanger activation was subsequently shown for further mutants (Barvencik et al., 2014; Sartelet et al., 2014; Di Zanni et al., 2020). There seems to be no strict correlation between the effect a given mutation exerts on the current properties—whether it diminishes currents or accelerates the voltage-dependent activation—and the neuropathy of osteopetrosis. Instead, it was recently proposed that the mere presence of CLC-7/Ostm1 may determine the severity of the disease (Di Zanni et al., 2020), but the genotype-phenotype correlation is far from clarified.

Recently, a heterozygous *de novo* mutation of CLC-7 was identified in two children with hypopigmentation and delayed development (Nicoli et al., 2019). The patients exhibited organomegaly and their brains displayed delayed myelination, a thin posterior corpus callosum, hyperintensity of the subthalamic nuclei, and cerebellar atrophy in MRI. Remarkably, they had no

signs of osteopetrosis. Huge intracellular vacuoles and storage material was found in various tested tissues. The phenotype of knock-in mice heterozygous for the identified Y715C (Y713C in mouse) mutation recapitulated the disease (Nicoli et al., 2019) (Table 2). Electrophysiological characterization of the mutant revealed a tremendous increase in current amplitude. Heterologous expression of CLC-7^{Y715C} led to a drastic enlargement of late endosomal/lysosomal compartments (Nicoli et al., 2019), similar to those with the gain-of-function CLC-6^{Y553C} mutant (Polovitskaya et al., 2020). In the case of CLC-7^{Y715C}, the enlarged compartments were reported not to be acidified in contrast to surrounding smaller, hyperacidified lysosomes, which was attributed to the hyperactivity of the CLC-7 mutant (Nicoli et al., 2019). The mechanism of the endosomal/lysosomal enlargement remains elusive. This mutant corroborates the notion that osteopetrosis and neuropathy with CLC-7 mutations may develop with independent pathomechanisms as CLC-7 may exert cell type-specific functions.

CONCLUSIONS

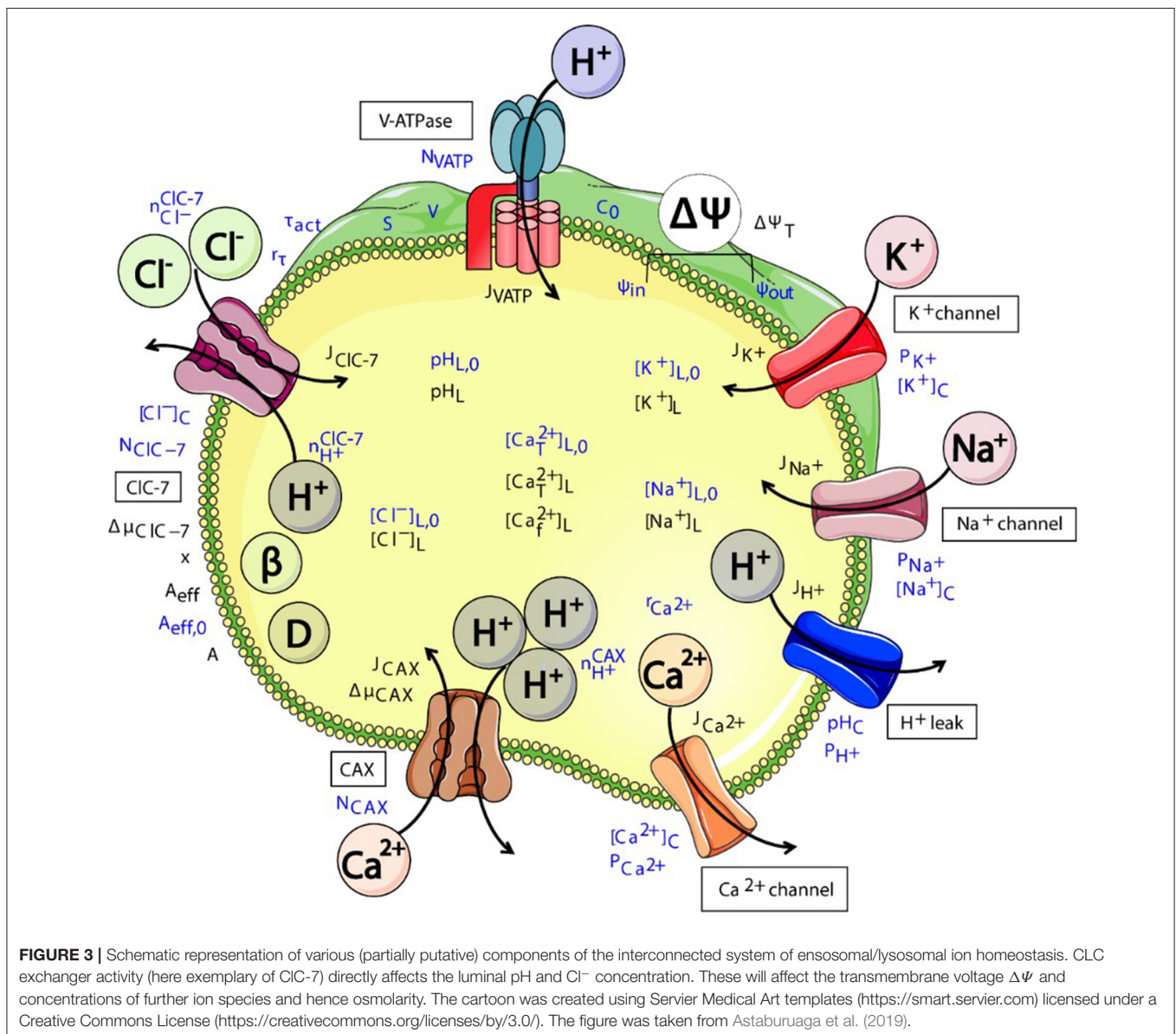
Loss-of-function and in some cases also gain-of-function of the intracellular CLCs, CLC-3/CLC-4, CLC-6 and CLC-7/Ostm1, lead to neuropathies, often neurodegeneration. They all function as Cl^-/H^+ exchangers on distinct, but overlapping organelles of the endosomal-lysosomal pathway (Stauber et al., 2012; Jentsch and Pusch, 2018). Trafficking and function of these compartments is detrimental for cellular physiology and dysfunction of the degradative pathway, lysosomal clearance by exocytosis or autophagic delivery to this pathway are associated with neurodegenerative disorders (Hara et al., 2006; Komatsu et al., 2006; LaPlante et al., 2006; Nixon, 2013; Wang et al., 2013; Menzies et al., 2017; Ballabio and Bonifacino, 2020; Mallucci et al., 2020).

In some cases, it has been proposed that the CLC serves as a structural protein that functions to recruit other proteins such as components of the transport machinery by direct protein-protein interaction. Amongst others, the existence of different missense mutations which unlikely all prevent the same interactions argues against this. Although a role a role for protein-protein interactions of intracellular CLCs in vesicular trafficking cannot be excluded, the most straight-forward explanation for the importance of CLCs is their role in the regulation of the vesicular ion homeostasis. In this respect, the pronounced outward rectification of the vesicular CLCs remains enigmatic, because it would strongly favor Cl^- export from endosomes/lysosomes. At membrane voltages in the range of those measured for endosomal/lysosomal compartments, which can be up to inside-positive 100 mV (Koivusalo et al., 2011; Saminathan et al., 2021), the CLC exchangers are virtually inactive in heterologous expression systems (Friedrich et al., 1999; Li et al., 2000; Neagoe et al., 2010; Leisle et al., 2011). Nonetheless, the effects of CLC depletion or various mutations—both loss and gain of function—demonstrate Cl^- accumulation by CLCs and the necessity of their ion transport. Mutation of the “gating glutamate” does not

only convert the exchanger into a pure Cl^- conductor, but also abolishes its voltage dependence. Therefore, such a mutation may indeed represent a gain of function in respect to Cl^- transport. Interestingly, while the uncoupling mutation of CLC-5 or CLC-7 leads to effects that are similar to the respective knock-out in mouse models, the heterozygous mutant of CLC-6 results in a much more severe disorder in patients than in the murine gene knock-out model (Poët et al., 2006; He et al., 2021).

The luminal pH is of undisputed importance for endosomes and lysosomes and impaired acidification is linked to neurodegeneration (Mellman et al., 1986; Mindell, 2012; Song et al., 2020). However, while the early endosomal CLC-5 critically supports acidification by providing the counterion (Günther et al., 1998; Piwon et al., 2000), this does not seem to be the case for CLC-3/-4, CLC-6 or CLC-7 on later endosomes

and lysosomes (Kasper et al., 2005; Poët et al., 2006; Weinert et al., 2020) where the larger cation conductance can support acidification (Van Dyke, 1993; Steinberg et al., 2010). Instead, analyses of various mouse models have shown that the secondary active, pH-gradient driven accumulation of Cl^- by their Cl^-/H^+ exchange mechanism is pivotal –also for CLC-5, in addition to the acidification- (Novarino et al., 2010; Weinert et al., 2010, 2020). Along the endosomal-lysosomal pathway, the luminal Cl^- concentration rises to $> 100 \text{ mM}$ in the lysosome (Saha et al., 2015). Reduced lysosomal Cl^- concentrations, but a normally low pH, have been found in nematode models of various neurodegenerative lysosomal storage diseases including Gaucher and Nieman-Pick A and B (Chakraborty et al., 2017). The Cl^- concentration has been shown to influence the enzymatic activity of the lysosomal protease cathepsin C (Cigić and Pain, 1999), but



the general mechanism by which luminal Cl^- affects vesicular function is elusive (Stauber and Jentsch, 2013).

The presence of a Cl^-/H^+ exchanger does not only – if at all – affect the luminal Cl^- concentration and pH, but ion homeostasis in general, including the transmembrane voltage and concentrations of other ion species (Ishida et al., 2013; Stauber and Jentsch, 2013; Astaburuaga et al., 2019) (Figure 3). One particularly important ion species that may be affected is Ca^{2+} (Chakraborty et al., 2017; Astaburuaga et al., 2019), as it is crucially involved in signaling and trafficking in the endosomal-lysosomal pathway (Luzio et al., 2007; Morgan et al., 2011; Ureshino et al., 2019; Lakpa et al., 2020). In addition, the exchange activity of CLCs has osmotic effects on the respective organelles. The enlargement of late endosomal/lysosomal compartments upon overexpression of CLC-3 (Li et al., 2002) or with gain-of-function mutants of CLC-6 or CLC-7 (Nicoli et al., 2019; Polovitskaya et al., 2020), may be partially due to osmotic swelling. Furthermore, osmotic volume changes promote membrane trafficking events (Freeman and Grinstein, 2018; Freeman et al., 2020; Saric and Freeman, 2020) and the number of known osmo-sensitive cation channels of endosomes and lysosomes is growing (Chen et al., 2020a,b). Recently, the LRRC8-formed volume-regulated anion channel (VRAC) has been reported to localize to lysosomes where it contributed to cellular osmoregulation (Li et al., 2020). This plasma membrane channel, which is involved in multiple physiological processes, does not only mediate cell volume regulatory ion transport (Chen et al., 2019). By releasing

glutamate from swollen cells under ischemic conditions, it contributes to excitotoxicity and neuronal cell death after stroke (Mongin, 2016; Yang et al., 2019).

In summary, dysfunction of the intracellular CLC Cl^-/H^+ exchangers impinges on the trafficking, function and possibly signaling of endosomal and lysosomal organelles and interconnected pathways such as autophagy, which in turn leads to cell death of vulnerable neurons. Future work is required to uncover in detail the molecular mechanism by which these CLCs contribute to the functioning of the endosomal-lysosomal pathway.

AUTHOR CONTRIBUTIONS

SB, HH, and TS wrote the manuscript. All authors contributed to the article and approved the submitted version.

FUNDING

This work was supported by grants from the German Federal Ministry of Education and Research (BMBF, Grant No. 031A314) and the German Research Foundation (DFG, FOR 2625) to TS, and by a fellowship from the China Scholarship Council to HH.

ACKNOWLEDGMENTS

We acknowledge support by the Open Access Publication Initiative of Freie Universität Berlin.

REFERENCES

- Accardi, A., and Miller, C. (2004). Secondary active transport mediated by a prokaryotic homologue of CLC Cl^- channels. *Nature* 427, 803–807. doi: 10.1038/nature02314
- Alam, I., Gray, A. K., Chu, K., Ichikawa, S., Mohammad, K. S., Capannolo, M., et al. (2014). Generation of the first autosomal dominant osteopetrosis type II (ADO2) disease models. *Bone* 59, 66–75. doi: 10.1016/j.bone.2013.10.021
- Astaburuaga, R., Quintanar Haro, O. D., Stauber, T., and Relógio, A. (2019). A mathematical model of lysosomal ion homeostasis points to differential effects of Cl^- transport in Ca^{2+} dynamics. *Cells* 8:1263. doi: 10.3390/cells8101263
- Ballabio, A., and Bonifacino, J. S. (2020). Lysosomes as dynamic regulators of cell and organismal homeostasis. *Nat. Rev.* 21, 101–118. doi: 10.1038/s41580-019-0185-4
- Barvencik, F., Kurth, I., Koehne, T., Stauber, T., Zustin, J., Tsiakas, K., et al. (2014). CLCN7 and TCIRG1 mutations differentially affect bone matrix mineralization in osteopetrotic individuals. *J. Bone Miner. Res.* 29, 982–991. doi: 10.1002/jbmr.2100
- Berkovic, S. F., Carpenter, S., Andermann, F., Andermann, E., and Wolfe, L. S. (1988). Kufs' disease: a critical reappraisal. *Brain* 111, 27–62. doi: 10.1093/brain/111.1.27
- Blanz, J., Schweizer, M., Auberson, M., Maier, H., Muenscher, A., Hübner, C. A., et al. (2007). Leukoencephalopathy upon disruption of the chloride channel CLC-2. *J. Neurosci.* 27, 6581–6589. doi: 10.1523/JNEUROSCI.0338-07.2007
- Boland, B., Yu, W. H., Corti, O., Mollereau, B., Henriques, A., Bezard, E., et al. (2018). Promoting the clearance of neurotoxic proteins in neurodegenerative disorders of ageing. *Nat. Rev. Drug Discovery* 17, 660–688. doi: 10.1038/nrd.2018.109
- Borsani, G., Rugari, E. I., Tagliatela, M., Wong, C., and Ballabio, A. (1995). Characterization of a human and murine gene (CLCN3) sharing similarities to voltage-gated chloride channels and to a yeast integral membrane protein. *Genomics* 27, 131–141. doi: 10.1006/geno.1995.1015
- Bösl, M. R., Stein, V., Hübner, C., Zdebik, A. A., Jordt, S. E., Mukhopadhyay, A. K., et al. (2001). Male germ cells and photoreceptors, both depending on close cell-cell interactions, degenerate upon CLC-2 Cl^- -channel disruption. *EMBO J.* 20, 1289–1299. doi: 10.1093/emboj/20.6.1289
- Brandt, S., and Jentsch, T. J. (1995). CLC-6 and CLC-7 are two novel broadly expressed members of the CLC chloride channel family. *FEBS Lett.* 377, 15–20. doi: 10.1016/0014-5793(95)01298-2
- Caetano-Lopes, J., Lessard, S. G., Hann, S., Espinoza, K., Kang, K. S., Lim, K. E., et al. (2017). *Clcn7*^{F318L/+} as a new mouse model of Albers-Schönberg disease. *Bone* 105, 253–261. doi: 10.1016/j.bone.2017.09.007
- Chakraborty, K., Leung, K., and Krishnan, Y. (2017). High luminal chloride in the lysosome is critical for lysosome function. *Elife* 6:e28862. doi: 10.7554/eLife.28862.026
- Chalhoub, N., Benachenhou, N., Rajapurohitam, V., Pata, M., Ferron, M., Frattini, A., et al. (2003). Grey-lethal mutation induces severe malignant autosomal recessive osteopetrosis in mouse and human. *Nat. Med.* 9, 399–406. doi: 10.1038/nm842
- Chen, C. C., Krogsaeter, E., Butz, E. S., Li, Y., Puertollano, R., Wahl-Schott, C., et al. (2020a). TRPML2 is an osmo/mechanosensitive cation channel in endolysosomal organelles. *Sci. Adv.* 6:eabb5064. doi: 10.1126/sciadv.abb5064
- Chen, L., König, B., Liu, T., Pervaiz, S., Razzaque, Y. S., and Stauber, T. (2019). More than just a pressure relief valve: physiological roles of volume-regulated LRRC8 anion channels. *Biol. Chem.* 400, 1481–1496. doi: 10.1515/hsz-2019-0189
- Chen, C. C., Krogsaeter, E., and Grimm, C. (2020b). Two-pore and TRP cation channels in endolysosomal osmo/mechanosensation and volume regulation. *Biochim. Biophys. Acta Mol. Cell Res.* 1868:118921. doi: 10.1016/j.bbamcr.2020.118921
- Cigić, B., and Pain, R. H. (1999). Location of the binding site for chloride ion activation of cathepsin C. *Eur. J. Biochem.* 264, 944–951. doi: 10.1046/j.1432-1327.1999.00697.x

- Cleiren, E., Benichou, O., Van Hul, E., Gram, J., Bollerslev, J., Singer, F. R., et al. (2001). Albers-Schönberg disease (autosomal dominant osteopetrosis, type II) results from mutations in the *CLCN7* chloride channel gene. *Hum. Mol. Genet.* 10, 2861–2867. doi: 10.1093/hmg/10.25.2861
- Cortez, M. A., Li, C., Whitehead, S. N., Dhani, S. U., D'Antonio, C., Huan, L. J., et al. (2010). Disruption of CLC-2 expression is associated with progressive neurodegeneration in aging mice. *Neuroscience* 167, 154–162. doi: 10.1016/j.neuroscience.2010.01.042
- Depienne, C., Bugiani, M., Dupuits, C., Galanaud, D., Touitou, V., Postma, N., et al. (2013). Brain white matter oedema due to CLC-2 chloride channel deficiency: an observational analytical study. *Lancet Neurol.* 12, 659–668. doi: 10.1016/S1474-4422(13)70053-X
- Di Zanni, E., Palagano, E., Lagostena, L., Strina, D., Rehman, A., Abinun, M., et al. (2020). Pathobiologic mechanisms of neurodegeneration in osteopetrosis derived from structural and functional analysis of 14 CLC-7 mutants. *J. Bone Miner. Res.* 29, 2520–2526. doi: 10.1002/jbmr.4200
- Dickerson, L. W., Bonthuis, D. J., Schutte, B. C., Yang, B., Barna, T. J., Bailey, M. C., et al. (2002). Altered GABAergic function accompanies hippocampal degeneration in mice lacking CLC-3 voltage-gated chloride channels. *Brain Res.* 958, 227–250. doi: 10.1016/S0006-8993(02)03519-9
- Duan, D., Winter, C., Cowley, S., Hume, J. R., and Horowitz, B. (1997). Molecular identification of a volume-regulated chloride channel. *Nature* 390, 417–421. doi: 10.1038/37151
- Dutzler, R., Campbell, E. B., Cadene, M., Chait, B. T., and MacKinnon, R. (2002). X-ray structure of a CLC chloride channel at 3.0 Å reveals the molecular basis of anion selectivity. *Nature* 415, 287–294. doi: 10.1038/415287a
- Eriksen, J., Chang, R., McGregor, M., Silm, K., Suzuki, T., and Edwards, R. H. (2016). Protons regulate vesicular glutamate transporters through an allosteric mechanism. *Neuron* 90, 768–780. doi: 10.1016/j.neuron.2016.03.026
- Estévez, R., Boettger, T., Stein, V., Birkenhäger, R., Otto, M., Hildebrandt, F., et al. (2001). Barttin is a Cl^- -channel β -subunit crucial for renal Cl^- -reabsorption and inner ear K^+ -secretion. *Nature* 414, 558–561. doi: 10.1038/35107099
- Fratini, A., Pangrazio, A., Susani, L., Sobacchi, C., Mirolo, M., Abinun, M., et al. (2003). Chloride channel *CLCN7* mutations are responsible for severe recessive, dominant, and intermediate osteopetrosis. *J. Bone Miner. Res.* 18, 1740–1747. doi: 10.1359/jbmr.2003.18.10.1740
- Freeman, S. A., and Grinstein, S. (2018). Resolution of macropinosomes, phagosomes and autolysosomes: osmotically driven shrinkage enables tubulation and vesiculation. *Traffic* 19, 965–974. doi: 10.1111/tra.12614
- Freeman, S. A., Uderhardt, S., Saric, A., Collins, R. F., Buckley, C. M., Mylvaganam, S., et al. (2020). Lipid-gated monovalent ion fluxes regulate endocytic traffic and support immune surveillance. *Science* 367, 301–305. doi: 10.1126/science.aaw9544
- Friedrich, T., Breiderhoff, T., and Jentsch, T. J. (1999). Mutational analysis demonstrates that CLC-4 and CLC-5 directly mediate plasma membrane currents. *J. Biol. Chem.* 274, 896–902. doi: 10.1074/jbc.274.2.896
- Gentzsch, M., Cui, L., Mengos, A., Chang, X. B., Chen, J. H., and Riordan, J. R. (2003). The PDZ-binding chloride channel CLC-3B localizes to the Golgi and associates with CFTR-interacting PDZ proteins. *J. Biol. Chem.* 278, 6440–6449. doi: 10.1074/jbc.M211050200
- Göppner, C., Soria, A. H., Hoegg-Beiler, M. B., and Jentsch, T. J. (2020). Cellular basis of CLC-2 Cl^- channel-related brain and testis pathologies. *J. Biol. Chem.* 296:100074. doi: 10.1074/jbc.RA120.016031
- Graves, A. R., Curran, P. K., Smith, C. L., and Mindell, J. A. (2008). The Cl^-/H^+ antiporter CLC-7 is the primary chloride permeation pathway in lysosomes. *Nature* 453, 788–792. doi: 10.1038/nature06907
- Grieschat, M., Guzman, R. E., Langschwager, K., Fahlke, C., and Alekov, A. K. (2020). Metabolic energy sensing by mammalian CLC anion/proton exchangers. *EMBO Rep.* 21:e47872. doi: 10.15252/embr.201947872
- Günther, W., Lüchow, A., Cluzeaud, F., Vandewalle, A., and Jentsch, T. J. (1998). CLC-5, the chloride channel mutated in Dent's disease, colocalizes with the proton pump in endocytically active kidney cells. *Proc. Natl. Acad. Sci. U.S.A.* 95, 8075–8080. doi: 10.1073/pnas.95.14.8075
- Guo, Z., Lu, T., Peng, L., Cheng, H., Peng, F., Li, J., et al. (2019). CLCN2-related leukoencephalopathy: a case report and review of the literature. *BMC Neurol.* 19:156. doi: 10.1186/s12883-019-1390-7
- Guzman, R. E., Alekov, A. K., Filippov, M., Hegermann, J., and Fahlke, C. (2014). Involvement of CLC-3 chloride/proton exchangers in controlling glutamatergic synaptic strength in cultured hippocampal neurons. *Front. Cell. Neurosci.* 8:143. doi: 10.3389/fncel.2014.00143
- Guzman, R. E., Bungert-Plumke, S., Franzen, A., and Fahlke, C. (2017). Preferential association with CLC-3 permits sorting of CLC-4 into endosomal compartments. *J. Biol. Chem.* 292, 19055–19065. doi: 10.1074/jbc.M117.801951
- Guzman, R. E., Grieschat, M., Fahlke, C., and Alekov, A. K. (2013). CLC-3 is an intracellular chloride/proton exchanger with large voltage-dependent nonlinear capacitance. *ACS Chem. Neurosci.* 4, 994–1003. doi: 10.1021/cn400032z
- Guzman, R. E., Miranda-Laferte, E., Franzen, A., and Fahlke, C. (2015). Neuronal CLC-3 splice variants differ in subcellular localizations, but mediate identical transport functions. *J. Biol. Chem.* 290, 25851–25862. doi: 10.1074/jbc.M115.668186
- Hara, T., Nakamura, K., Matsui, M., Yamamoto, A., Nakahara, Y., Suzuki-Migishima, R., et al. (2006). Suppression of basal autophagy in neural cells causes neurodegenerative disease in mice. *Nature* 441, 885–889. doi: 10.1038/nature04724
- Hara-Chikuma, M., Yang, B., Sonawane, N. D., Sasaki, S., Uchida, S., and Verkman, A. S. (2005). CLC-3 chloride channels facilitate endosomal acidification and chloride accumulation. *J. Biol. Chem.* 280, 1241–1247. doi: 10.1074/jbc.M407030200
- He, H., Cao, X., Yin, F., Wu, T., Stauber, T., and Peng, J. (2021). West syndrome caused by a chloride/proton exchange-uncoupling CLCN6 mutation related to autophagic-lysosomal dysfunction. *Mol. Neurobiol.* doi: 10.1007/s12035-021-02291-3. [Epub ahead of print].
- Hennings, J. C., Picard, N., Huebner, A. K., Stauber, T., Maier, H., Brown, D., et al. (2012). A mouse model for distal renal tubular acidosis reveals a previously unrecognized role of the V-ATPase a4 subunit in the proximal tubule. *EMBO Mol. Med.* 4, 1057–1071. doi: 10.1002/emmm.201201527
- Heraud, C., Griffiths, A., Pandravad, S. N., Kilimann, M. W., Pata, M., and Vacher, J. (2014). Severe neurodegeneration with impaired autophagy mechanism triggered by ostm1 deficiency. *J. Biol. Chem.* 289, 13912–13925. doi: 10.1074/jbc.M113.537233
- Hoegg-Beiler, M. B., Sirisi, S., Orozco, I. J., Ferrer, I., Hohensee, S., Auberson, M., et al. (2014). Disrupting MLC1 and GlialCAM and CLC-2 interactions in leukodystrophy entails glial chloride channel dysfunction. *Nat. Commun.* 5:3475. doi: 10.1038/ncomms4475
- Hu, H., Haas, S. A., Chelly, J., Van Esch, H., Raynaud, M., de Brouwer, A. P. M., et al. (2016). X-exome sequencing of 405 unresolved families identifies seven novel intellectual disability genes. *Mol. Psychiatr.* 21, 133–148. doi: 10.1038/mp.2014.193
- Huang, P., Liu, J., Robinson, N. C., Musch, M. W., Kaetzel, M. A., and Nelson, D. J. (2001). Regulation of human CLC-3 channels by multifunctional Ca^{2+} /calmodulin dependent protein kinase. *J. Biol. Chem.* 276, 20093–20100. doi: 10.1074/jbc.M009376200
- Huizing, M., and Gahl, W. A. (2020). Inherited disorders of lysosomal membrane transporters. *Biochim. Biophys. Acta Biomembr.* 1862:183336. doi: 10.1016/j.bbmem.2020.183336
- Hur, J., Jeong, H. J., Park, J., and Jeon, S. (2013). Chloride channel 4 is required for nerve growth factor-induced trkA signaling and neurite outgrowth in Pcl2 cells and cortical neurons. *Neuroscience* 253, 389–397. doi: 10.1016/j.neuroscience.2013.09.003
- Ignoul, S., Simaels, J., Hermans, D., Annaert, W., and Eggermont, J. (2007). Human CLC-6 is a late endosomal glycoprotein that associates with detergent-resistant lipid domains. *PLoS ONE* 2:e474. doi: 10.1371/journal.pone.000474
- Ishida, Y., Nayak, S., Mindell, J. A., and Grabe, M. (2013). A model of lysosomal pH regulation. *J. Gen. Physiol.* 141, 705–720. doi: 10.1085/jgp.201210930
- Jentsch, T. J. (2007). Chloride and the endosomal-lysosomal pathway: emerging roles of CLC chloride transporters. *J. Physiol.* 578, 633–640. doi: 10.1113/jphysiol.2006.124719
- Jentsch, T. J., and Pusch, M. (2018). CLC chloride channels and transporters: structure, function, physiology, and disease. *Physiol. Rev.* 98, 1493–1590. doi: 10.1152/physrev.00047.2017
- Jeworutzki, E., Lagostena, L., Elorza-Vidal, X., Lopez-Hernandez, T., Estevez, R., and Pusch, M. (2014). GlialCAM, a CLC-2 Cl^- channel subunit, activates the slow gate of CLC chloride channels. *Biophys. J.* 107, 1105–1116. doi: 10.1016/j.bpj.2014.07.040

- Jeworutzki, E., López-Hernández, T., Capdevila-Nortes, X., Sirisi, S., Bengtsson, L., Montolio, M., et al. (2012). GlialCAM, a protein defective in a leukodystrophy, serves as a ClC-2 Cl^- channel auxiliary subunit. *Neuron* 73, 951–961. doi: 10.1016/j.neuron.2011.12.039
- Kasper, D., Planells-Cases, R., Fuhrmann, J. C., Scheel, O., Zeitz, O., Ruether, K., et al. (2005). Loss of the chloride channel ClC-7 leads to lysosomal storage disease and neurodegeneration. *EMBO J.* 24, 1079–1091. doi: 10.1038/sj.emboj.7600576
- Kawasaki, M., Uchida, S., Monkawa, T., Miyawaki, A., Mikoshiba, K., Marumo, F., et al. (1994). Cloning and expression of a protein kinase C-regulated chloride channel abundantly expressed in rat brain neuronal cells. *Neuron* 12, 597–604. doi: 10.1016/0896-6273(94)90215-1
- Kida, Y., Uchida, S., Miyazaki, H., Sasaki, S., and Marumo, F. (2001). Localization of mouse ClC-6 and ClC-7 mRNA and their functional complementation of yeast CLC gene mutant. *Histochem. Cell Biol.* 115, 189–194. doi: 10.1007/s004180000245
- Koivusalo, M., Steinberg, B. E., Mason, D., and Grinstein, S. (2011). *In situ* measurement of the electrical potential across the lysosomal membrane using FRET. *Traffic* 12, 972–982. doi: 10.1111/j.1600-0854.2011.01215.x
- Komatsu, M., Waguri, S., Chiba, T., Murata, S., Iwata, J., Tanida, I., et al. (2006). Loss of autophagy in the central nervous system causes neurodegeneration in mice. *Nature* 441, 880–884. doi: 10.1038/nature04723
- König, B., and Stauber, T. (2019). Biophysics and structure-function relationships of LRRC8-formed volume-regulated anion channels. *Biophys. J.* 116, 1185–1193. doi: 10.1016/j.bpj.2019.02.014
- Kornak, U., Kasper, D., Bösl, M. R., Kaiser, E., Schweizer, M., Schulz, A., et al. (2001). Loss of the ClC-7 chloride channel leads to osteopetrosis in mice and man. *Cell* 104, 205–215. doi: 10.1016/S0092-8674(01)00206-9
- Lakpa, K. L., Halcrow, P. W., Chen, X., and Geiger, J. D. (2020). Readily releasable stores of calcium in neuronal endolysosomes: physiological and pathophysiological relevance. *Adv. Exp. Med. Biol.* 1131, 681–697. doi: 10.1007/978-3-030-12457-1_27
- Lange, P. F., Wartosch, L., Jentsch, T. J., and Fuhrmann, J. C. (2006). ClC-7 requires Ostm1 as a β -subunit to support bone resorption and lysosomal function. *Nature* 440, 220–223. doi: 10.1038/nature04535
- LaPlante, J. M., Sun, M., Falardeau, J., Dai, D., Brown, E. M., Slaugenaupt, S. A., et al. (2006). Lysosomal exocytosis is impaired in mucopolidiosis type IV. *Mol. Genet. Metab.* 89, 339–348. doi: 10.1016/j.ymgme.2006.05.016
- Lee, J. H., Wolfe, D. M., Darji, S., McBrayer, M. K., Colacurcio, D. J., Kumar, A., et al. (2020). β 2-adrenergic agonists rescue lysosome acidification and function in PSEN1 deficiency by reversing defective ER-to-lysosome delivery of ClC-7 . *J. Mol. Biol.* 432, 2633–2650. doi: 10.1016/j.jmb.2020.02.021
- Leegwater, P. A., Yuan, B. Q., van der Steen, J., Mulders, J., Konst, A. A., Boor, P. K., et al. (2001). Mutations of MLC1 (KIAA0027) , encoding a putative membrane protein, cause megalencephalic leukoencephalopathy with subcortical cysts. *Am. J. Hum. Genet.* 68, 831–838. doi: 10.1086/319519
- Leisle, L., Ludwig, C. F., Wagner, F. A., Jentsch, T. J., and Stauber, T. (2011). ClC-7 is a slowly voltage-gated $2\text{Cl}^-/\text{H}^+$ -exchanger and requires Ostm1 for transport activity. *EMBO J.* 30, 2140–2152. doi: 10.1038/emboj.2011.137
- Li, P., Hu, M., Wang, C., Feng, X., Zhao, Z., Yang, Y., et al. (2020). LRRC8 family proteins within lysosomes regulate cellular osmoregulation and enhance cell survival to multiple physiological stresses. *Proc. Natl. Acad. Sci. U.S.A.* 117, 29155–29165. doi: 10.1073/pnas.2016539117
- Li, X., Shimada, K., Showalter, L. A., and Weinman, S. A. (2000). Biophysical properties of ClC-3 differentiate it from swelling-activated chloride channels in chinese hamster ovary-K1 cells. *J. Biol. Chem.* 275, 35994–35998. doi: 10.1074/jbc.M002712200
- Li, X., Wang, T., Zhao, Z., and Weinman, S. A. (2002). The ClC-3 chloride channel promotes acidification of lysosomes in CHO-K1 and Huh-7 cells. *Am. J. Physiol.* 282, C1483–C1491. doi: 10.1152/ajpcell.00504.2001
- Lloyd, S. E., Pearce, S. H., Fisher, S. E., Steinmeyer, K., Schwappach, B., Scheinman, S. J., et al. (1996). A common molecular basis for three inherited kidney stone diseases. *Nature* 379, 445–449. doi: 10.1038/379445a0
- Lopez-Hernandez, T., Ridder, M. C., Montolio, M., Capdevila-Nortes, X., Polder, E., Sirisi, S., et al. (2011). Mutant GlialCAM causes megalencephalic leukoencephalopathy with subcortical cysts, benign familial macrocephaly, and macrocephaly with retardation and autism. *Am. J. Hum. Genet.* 88, 422–432. doi: 10.1016/j.ajhg.2011.02.009
- Ludwig, C. F., Ullrich, F., Leisle, L., Stauber, T., and Jentsch, T. J. (2013). Common gating of both CLC transporter subunits underlies voltage-dependent activation of the $2\text{Cl}^-/\text{H}^+$ exchanger ClC-7/Ostm1 . *J. Biol. Chem.* 288, 28611–28619. doi: 10.1074/jbc.M113.509364
- Luzio, J. P., Bright, N. A., and Pryor, P. R. (2007). The role of calcium and other ions in sorting and delivery in the late endocytic pathway. *Biochem. Soc. Trans.* 35, 1088–1091. doi: 10.1042/BST0351088
- Majumdar, A., Capetillo-Zarate, E., Cruz, D., Gouras, G. K., and Maxfield, F. R. (2011). Degradation of Alzheimer's amyloid fibrils by microglia requires delivery of ClC-7 to lysosomes. *Mol. Biol. Cell* 22, 1664–1676. doi: 10.1091/mbc.e10-09-0745
- Mallucci, G. R., Klennerman, D., and Rubinsztein, D. C. (2020). Developing therapies for neurodegenerative disorders: insights from protein aggregation and cellular stress responses. *Annu. Rev. Cell Dev. Biol.* 36, 165–189. doi: 10.1146/annurev-cellbio-040320-120625
- Maritzen, T., Keating, D. J., Neagoe, I., Zdebek, A. A., and Jentsch, T. J. (2008). Role of the vesicular chloride transporter ClC-3 in neuroendocrine tissue. *J. Neurosci.* 28, 10587–10598. doi: 10.1523/JNEUROSCI.3750-08.2008
- Marshansky, V., and Futai, M. (2008). The V-type H^+ -ATPase in vesicular trafficking: targeting, regulation and function. *Curr. Opin. Cell Biol.* 20, 415–426. doi: 10.1016/j.ccb.2008.03.015
- Martineau, M., Guzman, R. E., Fahlke, C., and Klingauf, J. (2017). VGLUT1 functions as a glutamate/proton exchanger with chloride channel activity in hippocampal glutamatergic synapses. *Nat. Commun.* 8:2279. doi: 10.1038/s41467-017-02367-6
- Matsuda, J. J., Filali, M. S., Volk, K. A., Collins, M. M., Moreland, J. G., and Lamb, F. S. (2008). Overexpression of ClC-3 in HEK293T cells yields novel currents that are pH-dependent. *Am. J. Physiol.* 294, C251–C262. doi: 10.1152/ajpcell.00338.2007
- Maurizi, A., Capulli, M., Curle, A., Patel, R., Ucci, A., Cortes, J. A., et al. (2019). Extra-skeletal manifestations in mice affected by Clcn7 -dependent autosomal dominant osteopetrosis type 2 clinical and therapeutic implications. *Bone Res.* 7:17. doi: 10.1038/s41413-019-0055-x
- Meadows, N. A., Sharma, S. M., Faulkner, G. J., Ostrowski, M. C., Hume, D. A., and Cassady, A. I. (2007). The expression of Clcn7 and Ostm1 in osteoclasts is coregulated by microphthalmia transcription factor. *J. Biol. Chem.* 282, 1891–1904. doi: 10.1074/jbc.M608572200
- Mellman, I., Fuchs, R., and Helenius, A. (1986). Acidification of the endocytic and exocytic pathways. *Annu. Rev. Biochem.* 55, 663–700. doi: 10.1146/annurev.bi.55.070186.003311
- Menzies, F. M., Fleming, A., Caricasole, A., Bento, C. F., Andrews, S. P., Ashkenazi, A., et al. (2017). Autophagy and neurodegeneration: pathogenic mechanisms and therapeutic opportunities. *Neuron* 93, 1015–1034. doi: 10.1016/j.neuron.2017.01.022
- Meyer, S., Savaresi, S., Forster, I. C., and Dutzler, R. (2007). Nucleotide recognition by the cytoplasmic domain of the human chloride transporter ClC-5 . *Nat. Struct. Mol. Biol.* 14, 60–67. doi: 10.1038/nsmb1188
- Mindell, J. A. (2012). Lysosomal acidification mechanisms. *Annu. Rev. Physiol.* 74, 69–86. doi: 10.1146/annurev-physiol-012110-142317
- Mohammad-Panah, R., Ackerley, C., Rommens, J., Choudhury, M., Wang, Y., and Bear, C. E. (2002). The chloride channel ClC-4 co-localizes with cystic fibrosis transmembrane conductance regulator and may mediate chloride flux across the apical membrane of intestinal epithelia. *J. Biol. Chem.* 277, 566–574. doi: 10.1074/jbc.M106968200
- Mohammad-Panah, R., Harrison, R., Dhani, S., Ackerley, C., Huan, L. J., Wang, Y., et al. (2003). The chloride channel ClC-4 contributes to endosomal acidification and trafficking. *J. Biol. Chem.* 278, 29267–29277. doi: 10.1074/jbc.M304357200
- Mohammad-Panah, R., Wellhauser, L., Steinberg, B. E., Wang, Y., Huan, L. J., Liu, X. D., et al. (2009). An essential role for ClC-4 in transferrin receptor function revealed in studies of fibroblasts derived from Clcn4 -null mice. *J. Cell Sci.* 122, 1229–1237. doi: 10.1242/jcs.037317
- Mongin, A. A. (2016). Volume-regulated anion channel—a frenemy within the brain. *Pflügers Arch.* 468, 421–441. doi: 10.1007/s00424-015-1765-6
- Morgan, A. J., Platt, F. M., Lloyd-Evans, E., and Galione, A. (2011). Molecular mechanisms of endolysosomal Ca^{2+} signalling in health and disease. *Biochem. J.* 439, 349–374. doi: 10.1042/BJ20110949
- Neagoe, I., Stauber, T., Fidzinski, P., Bergsdorf, E. Y., and Jentsch, T. J. (2010). The late endosomal ClC-6 mediates proton/chloride countertransport in

- heterologous plasma membrane expression. *J. Biol. Chem.* 285, 21689–21697. doi: 10.1074/jbc.M110.125971
- Nehrke, K., Arreola, J., Nguyen, H. V., Pilato, J., Richardson, L., Okunade, G., et al. (2002). Loss of hyperpolarization-activated Cl^- current in salivary acinar cells from *Clcn2* knockout mice. *J. Biol. Chem.* 276, 23604–23611. doi: 10.1074/jbc.M202900200
- Nicoli, E. R., Weston, M. R., Hackbarth, M., Becerril, A., Larson, A., Zein, W. M., et al. (2019). Lysosomal storage and albinism due to effects of a *de novo* CLCN7 variant on lysosomal acidification. *Am. J. Hum. Genet.* 104, 1127–1138. doi: 10.1016/j.ajhg.2019.04.008
- Nixon, R. A. (2013). The role of autophagy in neurodegenerative disease. *Nat. Med.* 19, 983–997. doi: 10.1038/nm.3232
- Nixon, R. A. (2020). The aging lysosome: an essential catalyst for late-onset neurodegenerative diseases. *Biochim. Biophys. Acta Proteins Proteom.* 1868, 140443. doi: 10.1016/j.bbapap.2020.140443
- Novarino, G., Weinert, S., Rickheit, G., and Jentsch, T. J. (2010). Endosomal chloride-proton exchange rather than chloride conductance is crucial for renal endocytosis. *Science* 328, 1398–1401. doi: 10.1126/science.1188070
- Ogura, T., Furukawa, T., Toyozaki, T., Yamada, K., Zheng, Y. J., Katayama, Y., et al. (2002). CLC-3B, a novel CLC-3 splicing variant that interacts with EBP50 and facilitates expression of CFTR-regulated ORCC. *FASEB J.* 16, S63–S65. doi: 10.1096/fj.01-0845fj
- Okkenhaug, H., Weylandt, K. H., Carmena, D., Wells, D. J., Higgins, C. F., and Sardini, A. (2006). The human CLC-4 protein, a member of the CLC chloride channel/transporter family, is localized to the endoplasmic reticulum by its N-terminus. *FASEB J.* 20, 2390–2392. doi: 10.1096/fj.05-5588fj
- Osei-Owusu, J., Yang, J., Leung, K. H., Ruan, Z., Lu, W., Krishnan, Y., et al. (2021). Proton-activated chloride channel PAC regulates endosomal acidification and transferrin receptor-mediated endocytosis. *Cell Rep.* 34, 108683. doi: 10.1016/j.celrep.2020.108683
- Palmer, E. E., Stuhlmann, T., Weinert, S., Haan, E., Van Esch, H., Holvoet, M., et al. (2018). *De novo* and inherited mutations in the X-linked gene CLCN4 are associated with syndromic intellectual disability and behavior and seizure disorders in males and females. *Mol. Psychiatry* 23, 222–230. doi: 10.1038/mp.2016.135
- Palmer, S., Perry, J., and Ashworth, A. (1995). A contravention of Ohno's law in mice. *Nat. Genet.* 10, 472–476. doi: 10.1038/ng0895-472
- Pandruvada, S. N., Beaugregard, J., Benjannet, S., Pata, M., Lazure, C., Seidah, N. G., et al. (2016). Role of Ostm1 cytosolic complex with kinesin 5B in intracellular dispersion and trafficking. *Mol. Cell. Biol.* 36, 507–521. doi: 10.1128/MCB.00656-15
- Pangrazio, A., Poliani, P. L., Megarbane, A., Lefranc, G., Lanino, E., Di Rocco, M., et al. (2006). Mutations in *OSTM1* (grey lethal) define a particularly severe form of autosomal recessive osteopetrosis with neural involvement. *J. Bone Miner. Res.* 21, 1098–1105. doi: 10.1359/jbmr.060403
- Peng, J., Wang, Y., He, F., Chen, C., Wu, L. W., Yang, L. F., et al. (2018). Novel West syndrome candidate genes in a Chinese cohort. *CNS Neurosci. Ther.* 24, 1196–1206. doi: 10.1111/cns.12860
- Piccolo, A., and Pusch, M. (2005). Chloride / proton antiporter activity of mammalian CLC proteins CLC-4 and CLC-5. *Nature* 436, 420–423. doi: 10.1038/nature03720
- Piwon, N., Günther, W., Schwake, M., Bösl, M. R., and Jentsch, T. J. (2000). CLC-5 Cl^- -channel disruption impairs endocytosis in a mouse model for Dent's disease. *Nature* 408, 369–373. doi: 10.1038/35042597
- Poët, M., Kornak, U., Schweizer, M., Zdebik, A. A., Scheel, O., Hoelter, S., et al. (2006). Lysosomal storage disease upon disruption of the neuronal chloride transport protein CLC-6. *Proc. Natl. Acad. Sci. U.S.A.* 103, 13854–13859. doi: 10.1073/pnas.0606137103
- Polovitskaya, M. M., Barbini, C., Martinelli, D., Harms, F. L., Cole, F. S., Calligari, P., et al. (2020). A recurrent gain-of-function mutation in CLCN6, encoding the CLC-6 Cl^-/H^+ -exchanger, causes early-onset neurodegeneration. *Am. J. Hum. Genet.* 107, 1062–1077. doi: 10.1016/j.ajhg.2020.11.004
- Preobraschenski, J., Zander, J. F., Suzuki, T., Ahnert-Hilger, G., and Jahn, R. (2014). Vesicular glutamate transporters use flexible anion and cation binding sites for efficient accumulation of neurotransmitter. *Neuron* 84, 1287–1301. doi: 10.1016/j.neuron.2014.11.008
- Pressey, S. N., O'Donnell, K. J., Stauber, T., Fuhrmann, J. C., Tyynela, J., Jentsch, T. J., et al. (2010). Distinct neuropathologic phenotypes after disrupting the chloride transport proteins CLC-6 or CLC-7/Ostm1. *J. Neuropathol. Exp. Neurol.* 69, 1228–1246. doi: 10.1097/NEN.0b013e3181ffe742
- Prinetti, A., Rocchetta, F., Costantino, E., Frattini, A., Caldana, E., Rucci, F., et al. (2009). Brain lipid composition in grey-lethal mutant mouse characterized by severe malignant osteopetrosis. *Glycoconj. J.* 26, 623–633. doi: 10.1007/s10719-008-9179-8
- Pusch, M., and Zifarelli, G. (2021). Large transient capacitive currents in wild-type lysosomal Cl^-/H^+ antiporter CLC-7 and residual transport activity in the proton glutamate mutant E312A. *J. Gen. Physiol.* 153:e202012583. doi: 10.1085/jgp.202012583
- Qiu, Z., Dubin, A. E., Mathur, J., Tu, B., Reddy, K., Miraglia, L. J., et al. (2014). SWELL1, a plasma membrane protein, is an essential component of volume-regulated anion channel. *Cell* 157, 447–458. doi: 10.1016/j.cell.2014.03.024
- Rajapurohitam, V., Chalhoub, N., Benachenhon, N., Neff, L., Baron, R., and Vacher, J. (2001). The mouse osteopetrotic grey-lethal mutation induces a defect in osteoclast maturation/function. *Bone* 28, 513–523. doi: 10.1016/S8756-3282(01)00416-1
- Riazanski, V., Deriy, L. V., Shevchenko, P. D., Le, B., Gomez, E. A., and Nelson, D. J. (2011). Presynaptic CLC-3 determines quantal size of inhibitory transmission in the hippocampus. *Nat. Neurosci.* 14, 487–494. doi: 10.1038/nn.2775
- Rickheit, G., Wartosch, L., Schaffer, S., Stobrawa, S. M., Novarino, G., Weinert, S., et al. (2010). Role of CLC-5 in renal endocytosis is unique among CLC exchangers and does not require PY-motif-dependent ubiquitylation. *J. Biol. Chem.* 285, 17595–17603. doi: 10.1074/jbc.M110.115600
- Rohrbough, J., Nguyen, H. N., and Lamb, F. S. (2018). Modulation of CLC-3 gating and proton/anion exchange by internal and external protons and the anion selectivity filter. *J. Physiol. London* 596, 4091–4119. doi: 10.1113/JP276332
- Rugarli, E. I., Adler, D. A., Borsani, G., Tsuchiya, K., Franco, B., Hauge, X., et al. (1995). Different chromosomal localization of the *Clcn4* gene in Mus spretus and C57BL/6J mice. *Nat. Genet.* 10, 466–471. doi: 10.1038/ng0895-466
- Saha, S., Prakash, V., Halder, S., Chakraborty, K., and Krishnan, Y. (2015). A pH-independent DNA nanodevice for quantifying chloride transport in organelles of living cells. *Nat. Nanotechnol.* 10, 645–651. doi: 10.1038/nnano.2015.130
- Salazar, G., Love, R., Styers, M. L., Werner, E., Peden, A., Rodriguez, S., et al. (2004). AP-3-dependent mechanisms control the targeting of a chloride channel (CLC-3) in neuronal and non-neuronal cells. *J. Biol. Chem.* 279, 25430–25439. doi: 10.1074/jbc.M402331200
- Saminathan, A., Devany, J., Veetil, A. T., Suresh, B., Pillai, K. S., Schwake, M., et al. (2021). A DNA-based voltmeter for organelles. *Nat. Nanotechnol.* 16, 96–103. doi: 10.1038/s41565-020-00784-1
- Sardiello, M., Palmieri, M., di Ronza, A., Medina, D. L., Valenza, M., Gennarino, V. A., et al. (2009). A gene network regulating lysosomal biogenesis and function. *Science* 325, 473–477. doi: 10.1126/science.1174447
- Saric, A., and Freeman, S. A. (2020). Endomembrane Tension and Trafficking. *Front. Cell Dev. Biol.* 8:611326. doi: 10.3389/fcell.2020.611326
- Sartelet, A., Stauber, T., Coppieters, W., Ludwig, C. F., Fasquelle, C., Druet, T., et al. (2014). A missense mutation accelerating the gating of the lysosomal Cl^-/H^+ -exchanger CLC-7/Ostm1 causes osteopetrosis with gingival hamartomas in cattle. *Dis. Model. Mech.* 7, 119–128. doi: 10.1242/dmm.012500
- Scheel, O., Zdebik, A., Lourdel, S., and Jentsch, T. J. (2005). Voltage-dependent electrogenic chloride proton exchange by endosomal CLC proteins. *Nature* 436, 424–427. doi: 10.1038/nature03860
- Schenck, S., Wojcik, S. M., Brose, N., and Takamori, S. (2009). A chloride conductance in VGLUT1 underlies maximal glutamate loading into synaptic vesicles. *Nat. Neurosci.* 12, 156–162. doi: 10.1038/nn.2248
- Schrecker, M., Korobenko, J., and Hite, R. K. (2020). Cryo-EM structure of the lysosomal chloride-proton exchanger CLC-7 in complex with OSTM1. *Elife* 9:e59555. doi: 10.7554/eLife.59555.sa2
- Schulz, P., Werner, J., Stauber, T., Henriksen, K., and Fendler, K. (2010). The G215R mutation in the Cl^-/H^+ -antiporter CLC-7 found in ADO II osteopetrosis does not abolish function but causes a severe trafficking defect. *PLoS ONE* 5:e12585. doi: 10.1371/journal.pone.0012585
- Schwappach, B. (2020). Chloride accumulation in endosomes and lysosomes: facts checked in mice. *EMBO J.* 39:e104812. doi: 10.15252/embj.2020104812
- Scott, C. C., and Gruenberg, J. (2011). Ion flux and the function of endosomes and lysosomes: pH is just the start: the flux of ions across endosomal membranes influences endosome function not only through regulation of the luminal pH. *Bioessays* 33, 103–110. doi: 10.1002/bies.201000108

- Shibata, T., Hibino, H., Doi, K., Suzuki, T., Hisa, Y., and Kurachi, Y. (2006). Gastric type H^+/K^+ -ATPase in the cochlear lateral wall is critically involved in formation of the endocochlear potential. *Am. J. Physiol.* 291, C1038–C1048. doi: 10.1152/ajpcell.00266.2006
- Smith, A. J., and Lippiat, J. D. (2010). Direct endosomal acidification by the outwardly rectifying CLC-5 Cl^-/H^+ exchanger. *J. Physiol.* 588, 2033–2045. doi: 10.1113/jphysiol.2010.188540
- Sobacchi, C., Schulz, A., Coxon, F. P., Villa, A., and Helfrich, M. H. (2013). Osteopetrosis: genetics, treatment and new insights into osteoclast function. *Nat. Rev. Endocrinol.* 9, 522–536. doi: 10.1038/nrendo.2013.137
- Song, Q., Meng, B., Xu, H., and Mao, Z. (2020). The emerging roles of vacuolar-type ATPase-dependent Lysosomal acidification in neurodegenerative diseases. *Transl. Neurodegener.* 9:17. doi: 10.1186/s40035-020-00196-0
- Stauber, T. (2015). The volume-regulated anion channel is formed by LRRC8 heteromers - molecular identification and roles in membrane transport and physiology. *Biol. Chem.* 396, 975–990. doi: 10.1515/hsz-2015-0127
- Stauber, T., and Jentsch, T. J. (2010). Sorting motifs of the endosomal/lysosomal CLC chloride transporters. *J. Biol. Chem.* 285, 34537–34548. doi: 10.1074/jbc.M110.162545
- Stauber, T., and Jentsch, T. J. (2013). Chloride in vesicular trafficking and function. *Annu. Rev. Physiol.* 75, 453–477. doi: 10.1146/annurev-physiol-030212-183702
- Stauber, T., Weinert, S., and Jentsch, T. J. (2012). Cell biology and physiology of CLC chloride channels and transporters. *Compr. Physiol.* 2, 1701–1744. doi: 10.1002/cphy.c110038
- Steinberg, B. E., Huynh, K. K., Brodovitch, A., Jabs, S., Stauber, T., Jentsch, T. J., et al. (2010). A cation counterflux supports lysosomal acidification. *J. Cell Biol.* 189, 1171–1186. doi: 10.1083/jcb.200911083
- Steinmeyer, K., Klocke, R., Ortland, C., Gronemeier, M., Jockusch, H., Gründer, S., et al. (1991). Inactivation of muscle chloride channel by transposon insertion in myotonic mice. *Nature* 354, 304–308. doi: 10.1038/354304a0
- Steinmeyer, K., Schwappach, B., Bens, M., Vandewalle, A., and Jentsch, T. J. (1995). Cloning and functional expression of rat CLC-5, a chloride channel related to kidney disease. *J. Biol. Chem.* 270, 31172–31177. doi: 10.1074/jbc.270.52.31172
- Steward, C. G. (2003). Neurological aspects of osteopetrosis. *Neuropathol. Appl. Neurobiol.* 29, 87–97. doi: 10.1046/j.1365-2990.2003.00474.x
- Stobrawa, S. M., Breiderhoff, T., Takamori, S., Engel, D., Schweizer, M., Zdebik, A. A., et al. (2001). Disruption of CLC-3, a chloride channel expressed on synaptic vesicles, leads to a loss of the hippocampus. *Neuron* 29, 185–196. doi: 10.1016/S0896-6273(01)00189-1
- Suzuki, T., Rai, T., Hayama, A., Sahara, E., Suda, S., Itoh, T., et al. (2006). Intracellular localization of CLC chloride channels and their ability to form hetero-oligomers. *J. Cell. Physiol.* 206, 792–798. doi: 10.1002/jcp.20516
- Teitelbaum, S. L. (2000). Bone resorption by osteoclasts. *Science* 289, 1504–1508. doi: 10.1126/science.289.5484.1504
- Teti, A., and Econs, M. J. (2017). Osteopetroses, emphasizing potential approaches to treatment. *Bone* 102, 50–59. doi: 10.1016/j.bone.2017.02.002
- Ureshino, R. P., Erustes, A. G., Bassani, T. B., Wachilewski, P., Guarache, G. C., Nascimento, A. C., et al. (2019). The interplay between Ca^{2+} signaling pathways and neurodegeneration. *Int. J. Mol. Sci.* 20:6004. doi: 10.3390/ijms20236004
- Van Dyke, R. W. (1993). Acidification of rat liver lysosomes: quantitation and comparison with endosomes. *Am. J. Physiol.* 265, C901–C917. doi: 10.1152/ajpcell.1993.265.4.C901
- Van Slegtenhorst, M. A., Bassi, M. T., Borsani, G., Wapenaar, M. C., Ferrero, G. B., de Conclis, L., et al. (1994). A gene from the Xp22.3 region shares homology with voltage-gated chloride channels. *Hum. Mol. Genet.* 3, 547–552. doi: 10.1093/hmg/3.4.547
- Veeramah, K. R., Johnstone, L., Karafet, T. M., Wolf, D., Sprissler, R., Salogiannis, J., et al. (2013). Exome sequencing reveals new causal mutations in children with epileptic encephalopathies. *Epilepsia* 54, 1270–1281. doi: 10.1111/epi.12201
- Voss, F. K., Ullrich, F., Münch, J., Lazarow, K., Lutter, D., Mah, N., et al. (2014). Identification of LRRC8 heteromers as an essential component of the volume-regulated anion channel VRAC. *Science* 344, 634–638. doi: 10.1126/science.1252826
- Wang, D., Chan, C. C., Cherry, S., and Hiesinger, P. R. (2013). Membrane trafficking in neuronal maintenance and degeneration. *Cell. Mol. Life Sci.* 70, 2919–2934. doi: 10.1007/s00018-012-1201-4
- Wang, Y., Du, X., Bin, R., Yu, S., Xia, Z., Zheng, G., et al. (2017). Genetic variants identified from epilepsy of unknown etiology in chinese children by targeted exome sequencing. *Sci. Rep.* 7:40319. doi: 10.1038/srep46520
- Wartosch, L., Fuhrmann, J. C., Schweizer, M., Stauber, T., and Jentsch, T. J. (2009). Lysosomal degradation of endocytosed proteins depends on the chloride transport protein CLC-7. *FASEB J.* 23, 4056–4068. doi: 10.1096/fj.09-130880
- Wartosch, L., and Stauber, T. (2010). A role for chloride transport in lysosomal protein degradation. *Autophagy* 6, 158–159. doi: 10.4161/auto.6.1.10590
- Weinert, S., Gimber, N., Deuschel, D., Stuhlmann, T., Puchkov, D., Farsi, Z., et al. (2020). Uncoupling endosomal CLC chloride/proton exchange causes severe neurodegeneration. *EMBO J.* 39:e103358. doi: 10.15252/embj.2019103358
- Weinert, S., Jabs, S., Hohensee, S., Chan, W. L., Kornak, U., and Jentsch, T. J. (2014). Transport activity and presence of CLC-7/Ostm1 complex account for different cellular functions. *EMBO Rep.* 15, 784–791. doi: 10.15252/embr.201438553
- Weinert, S., Jabs, S., Supanchart, C., Schweizer, M., Gimber, N., Richter, M., et al. (2010). Lysosomal pathology and osteopetrosis upon loss of H^+ -driven lysosomal Cl^- accumulation. *Science* 328, 1401–1403. doi: 10.1126/science.1188072
- Weylandt, K. H., Nebrig, M., Jansen-Rosseck, N., Amey, J. S., Carmena, D., Wiedenmann, B., et al. (2007). CLC-3 expression enhances etoposide resistance by increasing acidification of the late endocytic compartment. *Mol. Cancer Ther.* 6, 979–986. doi: 10.1158/1535-7163.MCT-06-0475
- Wojciechowski, D., Kovalchuk, E., Yu, L., Tan, H., Fahlke, C., Stoltz, G., et al. (2018). Barttin regulates the subcellular localization and posttranslational modification of human Cl^-/H^+ antiporter CLC-5. *Front. Physiol.* 9:1490. doi: 10.3389/fphys.2018.01490
- Xu, H., Martinoia, E., and Szabo, I. (2015). Organellar channels and transporters. *Cell Calcium* 58, 1–10. doi: 10.1016/j.ceca.2015.02.006
- Xu, H., and Ren, D. (2015). Lysosomal physiology. *Annu. Rev. Physiol.* 77, 57–80. doi: 10.1146/annurev-physiol-021014-071649
- Yamamoto, T., Shimojima, K., Sangu, N., Komoike, Y., Ishii, A., Abe, S., et al. (2015). Single nucleotide variations in CLCN6 identified in patients with benign partial epilepsies in infancy and/or febrile seizures. *PLoS ONE* 10:e0118946. doi: 10.1371/journal.pone.0118946
- Yang, J., Vitery, M. D. C., Chen, J., Osei-Owusu, J., Chu, J., and Qiu, Z. (2019). Glutamate-releasing SWELL1 channel in astrocytes modulates synaptic transmission and promotes brain damage in stroke. *Neuron* 102, 813–827.e6. doi: 10.1016/j.neuron.2019.03.029
- Yoshikawa, M., Uchida, S., Ezaki, J., Rai, T., Hayama, A., Kobayashi, K., et al. (2002). CLC-3 deficiency leads to phenotypes similar to human neuronal ceroid lipofuscinosis. *Genes Cells* 7, 597–605. doi: 10.1046/j.1365-2443.2002.00539.x
- Zanardi, I., Zifarelli, G., and Pusch, M. (2013). An optical assay of the transport activity of CLC-7. *Sci. Rep.* 3:1231. doi: 10.1038/srep01231
- Zhang, S., Liu, Y., Zhang, B., Zhou, J., Li, T., Liu, Z., et al. (2020). Molecular insights into the human CLC-7/Ostm1 transporter. *Sci. Adv.* 6: eabb4747. doi: 10.1126/sciadv.abb4747
- Zhou, P., He, N., Zhang, J. W., Lin, Z. J., Wang, J., Yan, L. M., et al. (2018). Novel mutations and phenotypes of epilepsy-associated genes in epileptic encephalopathies. *Genes Brain Behav.* 17(Suppl. 2):e12456. doi: 10.1111/gbb.12456

Conflict of Interest: The authors declare that the research was conducted in the absence of any commercial or financial relationships that could be construed as a potential conflict of interest.

Copyright © 2021 Bose, He and Stauber. This is an open-access article distributed under the terms of the Creative Commons Attribution License (CC BY). The use, distribution or reproduction in other forums is permitted, provided the original author(s) and the copyright owner(s) are credited and that the original publication in this journal is cited, in accordance with accepted academic practice. No use, distribution or reproduction is permitted which does not comply with these terms.



Roles of Ion and Water Channels in the Cell Death and Survival of Upper Gastrointestinal Tract Cancers

Atsushi Shiozaki^{1*}, Yoshinori Marunaka^{2,3,4} and Eigo Otsuji¹

¹ Division of Digestive Surgery, Department of Surgery, Kyoto Prefectural University of Medicine, Kyoto, Japan, ² Department of Molecular Cell Physiology, Graduate School of Medical Science, Kyoto Prefectural University of Medicine, Kyoto, Japan, ³ Research Institute for Clinical Physiology, Kyoto Industrial Health Association, Kyoto, Japan, ⁴ Research Center for Drug Discovery and Pharmaceutical Development Science, Research Organization of Science and Technology, Ritsumeikan University, Kusatsu, Japan

OPEN ACCESS

Edited by:

Giovanna Valenti,
University of Bari Aldo Moro, Italy

Reviewed by:

Darren Finlay,
Sanford Burnham Institute for Medical
Research, United States
Shutao Zheng,
Xinjiang Medical University, China
Giorgio Santoni,
University of Camerino, Italy

*Correspondence:

Atsushi Shiozaki
shiozaki@koto.kpu-m.ac.jp

Specialty section:

This article was submitted to
Cell Death and Survival,
a section of the journal
Frontiers in Cell and Developmental
Biology

Received: 13 October 2020

Accepted: 22 February 2021

Published: 11 March 2021

Citation:

Shiozaki A, Marunaka Y and
Otsuji E (2021) Roles of Ion and Water
Channels in the Cell Death
and Survival of Upper Gastrointestinal
Tract Cancers.
Front. Cell Dev. Biol. 9:616933.
doi: 10.3389/fcell.2021.616933

Ion and water channels were recently shown to be involved in cancer cell functions, and various transporter types have been detected in upper gastrointestinal tract (UGI) cancers. Current information on the expression and roles of these channels and transporters in the death and survival of UGI cancer cells was reviewed herein, and the potential of their regulation for cancer management was investigated. Esophageal cancer (EC) and gastric cancer (GC) cells and tissues express many different types of ion channels, including voltage-gated K⁺, Cl⁻, and Ca²⁺, and transient receptor potential (TRP) channels, which regulate the progression of cancer. Aquaporin (AQP) 1, 3, and 5 are water channels that contribute to the progression of esophageal squamous cell carcinoma (ESCC) and GC. Intracellular pH regulators, including the anion exchanger (AE), sodium hydrogen exchanger (NHE), and vacuolar H⁺-ATPases (V-ATPase), also play roles in the functions of UGI cancer cells. We have previously conducted gene expression profiling and revealed that the regulatory mechanisms underlying apoptosis in ESCC cells involved various types of Cl⁻ channels, Ca²⁺ channels, water channels, and pH regulators (Shimizu et al., 2014; Ariyoshi et al., 2017; Shiozaki et al., 2017, 2018a; Kobayashi et al., 2018; Yamazato et al., 2018; Konishi et al., 2019; Kudou et al., 2019; Katsurahara et al., 2020, 2021; Matsumoto et al., 2021; Mitsuda et al., 2021). We have also previously demonstrated the clinicopathological and prognostic significance of their expression in ESCC patients, and shown that their pharmacological blockage and gene silencing had an impact on carcinogenesis, indicating their potential as targets for the treatment of UGI cancers. A more detailed understanding of the molecular regulatory mechanisms underlying cell death and survival of UGI cancers may result in the application of cellular physiological methods as novel therapeutic approaches.

Keywords: esophageal cancer, gastric cancer, ion channels, water channels, intracellular pH

INTRODUCTION

Upper gastrointestinal tract (UGI) cancers, such as esophageal cancer (EC) and gastric cancer (GC), have high recurrence rates and are one of the leading causes of cancer-related death globally (Kamangar et al., 2006; Brenner et al., 2009; Hartgrink et al., 2009). EC is the ninth most common cancer and the sixth most common cause of cancer deaths worldwide, and GC is the sixth

most common cancer and the third most common cause of cancer deaths (Bray et al., 2018). The vast majority of ECs are either esophageal squamous cell carcinoma (ESCC) or esophageal adenocarcinomas (EAC). Although the prognosis of patients with UGI cancers has recently been improved by advances in surgical techniques, chemotherapy, radiotherapy, immunotherapy, and molecular targeted therapy (Jemal et al., 2011; Udagawa et al., 2012; Nashimoto et al., 2013; Tachimori et al., 2019), they remain poor, particularly for patients with advanced disease. Limited information is currently available on the efficacy of potential drug combinations against EC and GC because of the ability of these cells to evade apoptosis. Therefore, further studies on the molecular mechanisms regulating the cell death and survival of UGI cancers are needed for the development of more effective treatments.

Ion and water channels/transporters have important roles in cellular functions. Their physiological contribution to cell death and survival is crucial because cell volume changes, which require the movement of ions and water molecules across cell membranes, are critical for apoptosis (Okada et al., 2001, 2006). The involvement of ion and water channels in cancer cell functions was recently demonstrated, and thus, their regulation has potential as a novel strategy in cancer therapies (Pedersen and Stock, 2013; Pardo and Stuhmer, 2014; Shiozaki et al., 2014; Lastraioli et al., 2015; Nagaraju et al., 2016; Xia et al., 2017; Anderson et al., 2019).

Current information on the functions of ion and water channels in the cell death and survival of UGI cancers was systematically reviewed herein. The main aim of this review was to investigate the potential of cellular physiological strategies, such as the regulation of ion channels, water channels, and pH regulators, in the clinical management of EC and GC.

Potassium (K⁺) Channels

Several subtypes of K⁺ channels were recently shown to be expressed in human EC and GC cells and play important roles in cell death and survival (Table 1). The expression of several voltage-gated K⁺ channels (Kv) is modified in UGI cancers. Han et al. (2007) reported that the up-regulated expression of potassium voltage-gated channel, shaker-related subfamily, member 5 (KCNA5), also known as Kv1.5, increased K⁺ current density as well as GC cell sensitivity to multiple chemotherapeutic drugs by regulating drug-induced apoptosis. Furthermore, a component of the delayed rectifier K⁺ current was found to be encoded by the human ether-a-go-go-related gene (HERG). The expression of HERG channels was shown to be limited in GC, and the HERG channel blocker, cisapride, and genetic knockdown by small interfering RNA (siRNA) technology induced apoptosis (Shao et al., 2005, 2008). Zhang et al. (2012) demonstrated that the expression of HERG was crucial for the cisplatin-mediated induction of apoptosis in human GC. However, in these studies, molecular mechanisms of the regulation of apoptosis via HERG had not been shown in detail. Instead, HERG1 expression was found to regulate apoptosis in ESCC through thioredoxin domain-containing protein 5 (TXNDC5) by activating the phosphatidylinositol-3 kinase (PI3K)/Akt pathway (Wang et al., 2019). Yu et al. (2020) reported that the

overexpression of the long non-coding RNA (lncRNA), heart and neural crest derivatives expressed 2 antisense RNA 1 (HAND2-AS1) promoted apoptosis in GC cells, and showed that it bound with miR-590-3p to alter the expression of potassium sodium-activated channel subfamily T member 2 (KCNT2). Potassium channel subfamily K member 9 (TASK-3) (KCNK9 or K2P9.1) is a K⁺ channel from the K_{2P} family that forms functional homo- or heterodimers (Enyedi and Czirjak, 2010). Cikutović-Molina et al. (2019) recently showed that the knockdown of the TASK-3 gene promoted apoptosis in KATO III and MKN-45 human GC cell lines. The protein encoded by *potassium calcium-activated channel Subfamily M Alpha 1* (KCNMA1) is a voltage- and Ca²⁺-activated K⁺ channel. Ma et al. (2017) found that KCNMA1 significantly inhibited the biological malignant behavior of GC cells *in vitro* by inducing apoptosis, and suppressed xenograft tumor growth in subcutaneous mouse models. The importance of this study was to reveal that the anti-tumor effect of KCNMA1 was mediated through suppressing the expression of the key apoptosis gene *protein tyrosine kinase 2* (PTK2).

Collectively, these findings clearly demonstrate the involvement of K⁺ channels in the apoptosis of ESCC and GC cells, and thus, further studies on their clinical potential are warranted.

Chloride (Cl⁻) Channels

Cl⁻ channels play a role in the cell death and survival of UGI cancers (Table 2). Ma et al. (2012) reported that the strong expression of chloride intracellular channel 1 (CLIC1) suppressed the proliferation of GC cells and promoted their apoptosis, migration, and invasion. Li et al. (2018) also demonstrated that the genetic knockdown of CLIC1 by siRNA technology strongly induced apoptosis in GC cells by regulating the mitogen-activated protein kinase (MAPK)/protein kinase B

TABLE 1 | Overview of potassium channels with roles in the cell death and survival of upper gastrointestinal tract cancers.

Channels	Organ	Mechanism/ pathway	Induction	References
KCNA5	GC		Aminopyridine, tetraethylammonium	Han et al., 2007
HERG	GC		Cisapride	Shao et al., 2005
	GC		siRNA technology	Shao et al., 2008
	GC		siRNA technology	Zhang et al., 2012
HERG1	ESCC	TXNDC5, PI3K/AKT pathway	shRNA technology	Wang et al., 2019
KCNT2	GC	HAND2-AS1, miR-590-3p	overexpression vector	Yu et al., 2020
KCNK9	GC		siRNA technology	Cikutović-Molina et al., 2019
KCNMA1	GC	PTK2	Overexpression plasmid	Ma et al., 2017

ESCC, esophageal squamous cell carcinoma; GC, gastric cancer.

TABLE 2 | Overview of chloride channels with roles in the cell death and survival of upper gastrointestinal tract cancers.

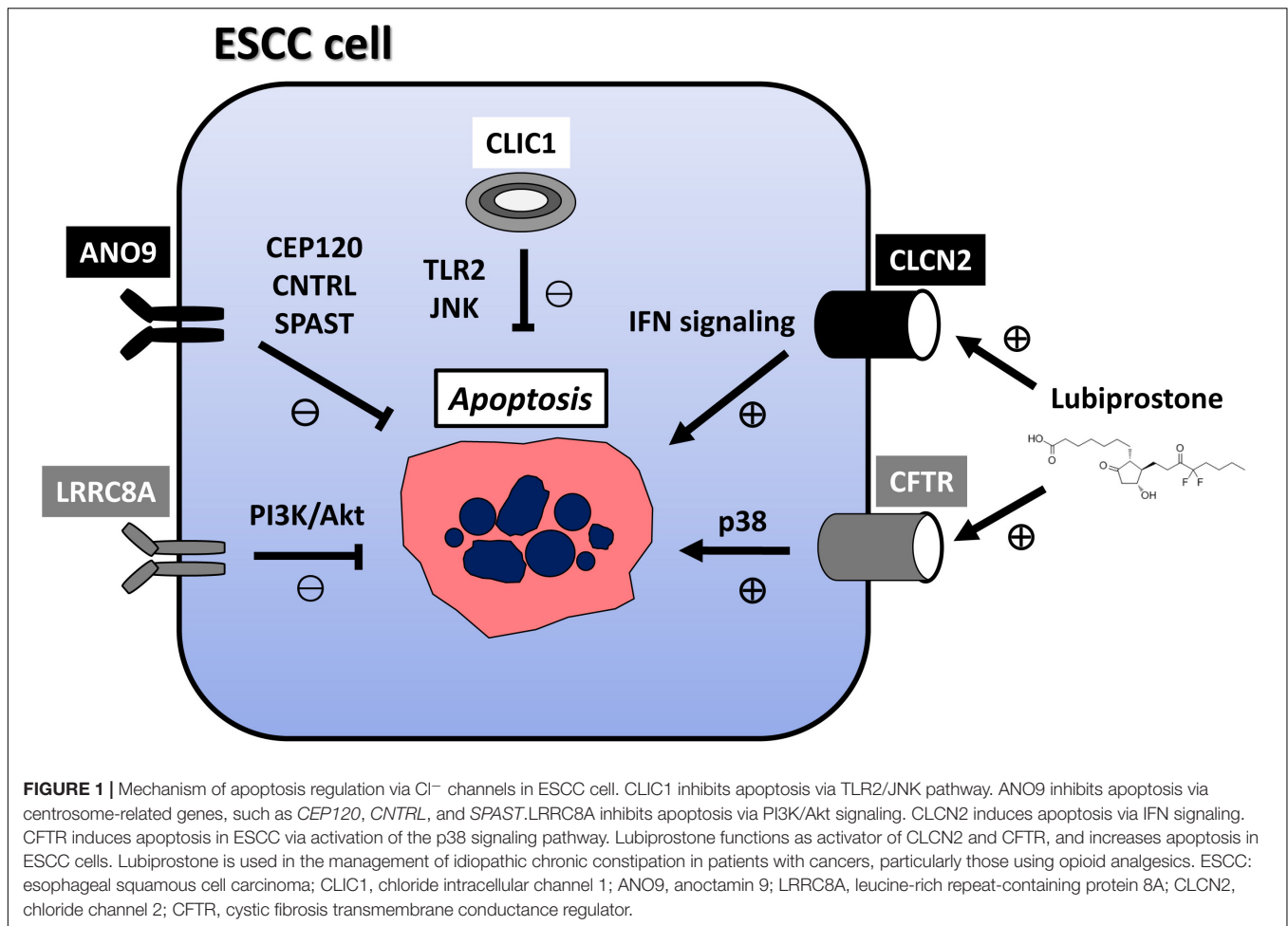
Channels	Organ	Mechanism/ pathway	Induction	References
CLIC1	ESCC	TLR2/JNK pathway	siRNA technology	Kobayashi et al., 2018
	GC		siRNA technology	Ma et al., 2012
	GC	PI3K/AKT, MAPK/ERK, and MAPK/p38 pathways	siRNA technology	Li et al., 2018
	GC	Exosome-mediated transfer	siRNA technology	Zhao et al., 2019
ANO1	GC		3n, Ani-FCC	Seo et al., 2020
	GC	LncRNA OIP5-AS1, miR-422a	RNA interference	Xie et al., 2020
ANO9	ESCC	Centrosome-related genes	siRNA technology	Katsurahara et al., 2020
	GC	IFN signaling, PD-L2	siRNA technology	Katsurahara et al., 2021
CLCN2	ESCC	IFN signaling	Lubiprostone, overexpression plasmid	Mitsuda et al., 2021
CFTR	ESCC	p38 signaling pathway	Overexpression plasmid	Matsumoto et al., 2021
LRRC8A	ESCC	Phosphatidylinositol 3-kinase/AKT signaling	siRNA technology	Konishi et al., 2019

ESCC, esophageal squamous cell carcinoma; GC, gastric cancer.

(Akt) pathways. Zhao et al. (2019) described a role for exosome-mediated transfer of CLIC1 in vincristine resistance via the regulation of P-gp and B-cell lymphoma 2 (Bcl-2) in GC cells. We previously reported the induction of apoptosis in ESCC via the Toll-like receptor 2 (TLR2)/c-Jun N-terminal kinase (JNK) pathway by the genetic knockdown of CLIC1 with siRNA technology (Kobayashi et al., 2018). The anoctamin family consists of transmembrane proteins in 10 isoforms, and the best-known anoctamin gene is *anoctamin 1* (ANO1), a Cl⁻ channel activated by Ca²⁺ (Schreiber et al., 2010). Seo et al. (2020) showed that 3n, Ani-FCC, a novel, potent, and selective ANO1 inhibitor, significantly enhanced apoptosis by activating caspase 3 and cleaving poly (ADP-ribose) polymerase (PARP) in GC cells. Xie et al. (2020) reported that long non-coding RNA (lncRNA) OPA-interacting protein 5 antisense transcript 1 (OIP5-AS1) regulated apoptosis in GC by targeting the microRNA (miR)-422a/ANO1 axis. We recently demonstrated that the genetic knockdown of ANO9 by siRNA technology increased apoptosis in ESCC cells (Katsurahara et al., 2020). Moreover, the findings of our microarray analysis indicated that the expression of a number of centrosome-related genes, such as centrosomal protein 120 (*CEP120*), *CNTRL*, and *SPAST*, was up- or down-regulated in ANO9-depleted KYSE150 cells, while immunohistochemistry (IHC) showed that the strong expression of ANO9 was associated with a poor prognosis in ESCC patients (Katsurahara et al., 2020). Over the past decade, one of the most important breakthroughs in cancer

treatment has been immune checkpoint blockage (ICB) of programmed cell death-1 (PD-1). In GC, we have observed tumor suppressive effects following the genetic knockdown of ANO9 with siRNA technology, such as decreased proliferation, and increased apoptosis (Katsurahara et al., 2021). The results of microarray and IHC indicated that ANO9 regulates programmed cell death 1 ligand 2 (PD-L2) and binding ability to PD-1 via interferon (IFN)-related genes, suggesting that ANO9 has potential as a biomarker and target of ICB for GC. Leucine-rich repeat-containing protein 8A (LRRC8A) is a ubiquitous and integral component of the volume-regulated anion channel, which is required for the regulation of cell volume (Qiu et al., 2014). We reported that the depletion of LRRC8A promoted apoptosis in ESCC cells, microarray data revealed the altered regulation of phosphatidylinositol-3 kinase (PI3K)/Akt signaling in LRRC8A-depleted cells, and IHC showed that the strong LRRC8A expression correlated with a poorer prognosis in ESCC patients (Konishi et al., 2019). Chloride channel 2 (CLCN2) is a member of the CLC family, which is an inwardly rectifying chloride channel. We also demonstrated that downregulated expression of CLCN2 decreased apoptosis, whereas its upregulation increased it in ESCC cells (Mitsuda et al., 2021). The effects of lubiprostone, a CLCN2 activator, were also investigated, and apoptosis was increased in lubiprostone-treated ESCC cells. The results of microarray and IHC indicated that tumor progression is regulated by CLCN2 through its effects on IFN signaling, and that weak CLCN2 expression was associated with poorer outcomes in ESCC patients. Lubiprostone is used in the management of idiopathic chronic constipation in patients with various cancers, particularly those using opioid analgesics. Lubiprostone functioned as a pharmacological activator of CLCN2, and enhanced the inhibitory effects of cisplatin (CDDP) in ESCC cells (Mitsuda et al., 2021), suggesting the potential of its clinical application for ESCC. The cystic fibrosis transmembrane conductance regulator (CFTR) is a cyclic AMP-dependent chloride anion conducting channel, and inactivating germline mutations in CFTR cause the cystic-fibrosis (CF), which is the most common autosomal recessive hereditary disease among Caucasians. We have recently demonstrated that the overexpression of CFTR induced apoptosis in ESCC via activation of the p38 signaling pathway and was associated with a good patient prognosis (Matsumoto et al., 2021). The relationship between the incidence of cancer and genetic variations in the CFTR gene has been attracting increasing attention because CF patients are at a significantly higher risk of developing various cancers. Our results may explain the molecular mechanism of this clinical features and indicate the potential of CFTR as a mediator of and/or a biomarker for ESCC. Further, lubiprostone is also known as the CFTR activator, suggesting the future prospects of therapeutic strategies targeting CFTR against ESCC patients. Mechanism of apoptosis regulation via these Cl⁻ channels in ESCC cell were summarized in Figure 1.

Collectively, these findings indicate the important roles of Cl⁻ channels in the apoptosis of UGI cancer cells and the potential of CLIC1, ANO1, ANO9, and LRRC8A as therapeutic targets against ESCC and GC.



Calcium (Ca²⁺) Channels

Ca²⁺ channels participate in regulation of intracellular Ca²⁺ concentrations ([Ca²⁺]_i), and play important roles in the cell death and survival of UGI cancers (Table 3). The transient receptor potential (TRP) superfamily comprises a very diverse group of ion channels, most of which exhibit permeability to monovalent and divalent cations. TRP family members are divided into seven subfamilies, such as classical (TRPC), vanilloid receptor-related (TRPV), and melastatin-related (TRPM) channels. Ding et al. (2018) previously demonstrated that pyrazolo[1,5-a]pyrimidine TRPC6 antagonists suppressed the proliferation of GC cells, and this anti-tumor effect on GC was confirmed in xenograft models using nude mice. We also recently reported that the genetic knockdown of TRPV2 by siRNA technology induced apoptosis in ESCC. A pathway analysis of microarray data showed that the depletion of TRPV2 down-regulated WNT/β-catenin signaling-related genes, and an IHC analysis revealed a correlation between strong TRPV2 expression and a poor prognosis in ESCC patients (Kudou et al., 2019). We also demonstrated the overexpression of TRPV2 in cancer stem cells (CSCs) derived from ESCC, and suggested the potential of tranilast, a TRPV2-specific inhibitor, as a therapeutic agent against CSCs (Shiozaki et al., 2018b).

Tranilast has been used to treat patients with inflammatory diseases, such as asthma, dermatitis, allergic conjunctivitis, keloids, and hypertrophic scars, and its safety for clinical use has already been demonstrated. Preoperative adjuvant chemotherapy with CDDP and 5-fluorouracil (5FU) is currently used with beneficial effects to treat localized advanced ESCC in Japan (Ando et al., 2012). To confirm the clinical safety and efficacy of the additional use of tranilast with neoadjuvant 5-FU/CDDP, and to develop a novel therapeutic strategy for patients with advanced ESCC, we designed phase I/II study, and it is ongoing (Shiozaki et al., 2020). Chow et al. (2007) showed that TRPV6 mediated capsaicin-induced apoptosis in GC cells and also that capsaicin induced apoptosis by stabilizing p53 through the activation of JNK. Almasi et al. (2018) reported that the TRPM2 channel-mediated regulation of autophagy maintained mitochondrial function and promoted GC cell survival via the JNK signaling pathway. Quercetin induced apoptosis in GC cells by inhibiting MAPKs and TRPM7 channels (Kim et al., 2014). Calcium channel, voltage-dependent, alpha 2/delta subunit 3 (CACNA2D3) is an auxiliary member of the alpha-2/delta subunit family of the voltage-dependent Ca²⁺ channel complex. Li et al. (2013) reported the down-regulation of CACNA2D3 in 56.7% of ESCC, which correlated with lymph node metastasis,

TABLE 3 | Overview of calcium channels with roles in the cell death and survival of upper gastrointestinal tract cancers.

Channels	Organ	Mechanism/ pathway	Induction	References
TRPC6	GC		Pyrazolo[1,5- <i>a</i>]pyrimidine	Ding et al., 2018
TRPV2	ESCC	WNT/ β -catenin signaling, Cancer stem cells	Tranilast, siRNA technology	Kudou et al., 2019
TRPV6	GC	Bax, p53, JNK	Capsaicin, overexpression plasmid	Chow et al., 2007
TRPM2	GC	JNK signaling pathway	shRNA technology	Almasi et al., 2018
TRPM7	GC	MAPK	Quercetin	Kim et al., 2014
CACNA2D1	GC	Cancer stem cells	Amlodipine	Shiozaki et al., 2021
CACNA2D3	ESCC	Up-regulate intracellular free cytosolic Ca^{2+}	Overexpression vector	Li et al., 2013
	ESCC	Ca^{2+} -mediated apoptosis, PI3K/Akt pathways	Cisplatin, overexpression plasmid	Nie et al., 2019
CACNB4	GC	Cancer stem cells	Verapamil	Shiozaki et al., 2021

ESCC, esophageal squamous cell carcinoma; GC, gastric cancer.

TNM staging, and the poor outcomes of ESCC patients, and suggested that CACNA2D3 up-regulates intracellular cytosolic Ca^{2+} , thereby inducing apoptosis. Nie et al. (2019) demonstrated that CACNA2D3 enhanced the chemosensitivity of ESCC to cisplatin by inducing Ca^{2+} -mediated apoptosis and suppressing the PI3K/Akt pathways. Recently, we have demonstrated that voltage-gated Ca^{2+} channels (VGCCs), including calcium voltage-gated channel auxiliary subunit $\alpha_2\delta_1$ (CACNA2D1) and calcium voltage-gated channel auxiliary subunit β_4 (CACNB4), were strongly expressed in gastric CSCs (Shiozaki et al., 2021). The cytotoxicities of the CACNA2D1 inhibitor amlodipine and the CACNB4 inhibitor verapamil were greater at lower concentrations in CSCs than in non-CSCs. Amlodipine, a specific inhibitor of CACNA2D1, has been widely used in the treatment of hypertension and cardiac angina. Verapamil, a specific inhibitor of CACNB4, has been widely used in the treatment of arrhythmia. These results indicate that VGCCs play a role in maintaining CSCs, and demonstrated the potential of their specific inhibitors as targeted therapeutic agents against GC.

These findings clearly demonstrate that Ca^{2+} channels contribute to UGI cancer cell death, and thus, future studies are needed on their clinical potential.

Water Channels

Under physiological and pathophysiological conditions, the volume of cells is regulated and the electrolyte balance is maintained by aquaporins (AQPs), which are transmembrane proteins that facilitate water transport. Thirteen AQP subtypes have so far been identified in humans and their functions

have been elucidated. AQPs have also been shown to play important roles in the cell death and survival of UGI cancers (Table 4). We recently demonstrated the induction of apoptosis in ESCC cells by the genetic knockdown of AQP1 with siRNA technology, alterations in Death receptor signaling pathway-related genes in AQP1-depleted TE5 cells by a microarray analysis, and a correlation between the cytoplasmic dominant expression of AQP1 and a poor prognosis in patients with ESCC by IHC (Yamazato et al., 2018). Sun et al. (2016) reported that AQP1 expression in GC was associated with apoptosis and the survival of patients, however, molecular mechanisms of the regulation of apoptosis via AQP1 had not been shown in detail. Kusayama et al. (2011) attributed cell death in ESCC due to the genetic knockdown of AQP3 by siRNA technology to the direct interference of cell adhesion involving the intracellular focal adhesion kinase (FAK)-MAPK signaling pathways. Several studies demonstrating the regulatory mechanisms via miR were valuable. Jiang et al. (2014) demonstrated that the down-regulation of Bcl-2 and up-regulation of caspase-3 activity and Bcl-2-associated X protein (Bax) were involved in the induction of cell apoptosis in GC cells by miR-874 through the targeting of AQP3. Furthermore, Zhu et al. (2020) showed that the up-regulated expression of miR-877 promoted apoptosis in GC cells, and luciferase reporter assays revealed that AQP3 was a direct downstream target of miR-877. We also demonstrated that the genetic knockdown of AQP5 by siRNA technology induced apoptosis in ESCC cells, while a microarray analysis identified tumor protein p53-induced nuclear protein 1 (TP53INP1) as one of the top ranking up-regulated genes widely known as the gene related to cell apoptosis in AQP5-depleted ESCC cells (Shimizu et al., 2014). IHC staining of samples collected from ESCC patients revealed relationships between the expression of AQP5 and tumor size, histological type, and tumor recurrence (Shimizu et al., 2014).

Therefore, AQPs appear to be crucially involved in the cell death and survival of ESCC and GC, and these findings indicate the potential of AQP1, 3, and 5 as therapeutic targets in UGI cancers.

TABLE 4 | Overview of water channels with roles in the cell death and survival of upper gastrointestinal tract cancers.

Channels	Organ	Mechanism/ pathway	Induction	References
AQP1	ESCC	Death receptor signaling pathway	siRNA technology	Yamazato et al., 2018
	GC	Apoptosis		Sun et al., 2016
AQP3	ESCC	FAK-MAPK signaling pathways	pan-AQP inhibitor, siRNA technology	Kusayama et al., 2011
	GC	miR-874	Overexpression vector	Jiang et al., 2014
	GC	miR-877	miRNA mimics	Zhu et al., 2020
AQP5	ESCC	p53	siRNA technology	Shimizu et al., 2014

ESCC, esophageal squamous cell carcinoma; GC, gastric cancer.

pH Regulators

The regulation of cytoplasmic pH by ion transporters was recently shown to be important for tumor cell functions. pH regulators, including the anion exchanger (AE), Na^+/H^+ exchanger (NHE), and vacuolar H^+ -ATPase (V-ATPase), directly contribute to maintaining the tumor microenvironment, and play critical roles in the cell death and survival of UGI cancers (Table 5). The electroneutral exchange of Cl^- for HCO_3^- across the plasma membrane of mammalian cells is facilitated by AE proteins and maintains intracellular pH. Three AE isoforms have been identified: AE1, AE2, and AE3. Shen et al. (2007) showed that the genetic knockdown of AE1 by siRNA technology in GC cells induced the release of p16 from the cytoplasm to the nucleus, leading to the death of tumor cells. Importantly, the transfection with miR-24 induced the return of p16 to the nucleus, confirming the miR-24-controlled AE1 down-regulation in GC (Wu et al., 2010). We performed IHC on primary tumor samples obtained from ESCC patients and found that significantly fewer samples exhibited diffuse AE1 expression than focal expression (Shiozaki et al., 2017). In addition, the genetic knockdown of AE1 by siRNA technology induced apoptosis, and a microarray analysis of AE1-depleted ESCC cells showed the down-regulated expression of MAPK and Hedgehog signaling pathway-related genes (Shiozaki et al., 2017). However, we subsequently demonstrated that the depletion of AE2 in ESCC cells enhanced cell migration and suppressed the induction of apoptosis (Shiozaki et al., 2018a). The microarray analysis of AE2-depleted ESCC cells also showed the changes expression of various matrix metalloproteinase (MMP) signaling pathway-related genes. The expression levels of MMP1 and MMP12 mRNA were higher, and mRNA of tissue inhibitor of metalloproteinase 4 (TIMP4), metalloproteinase inhibitor, was lower in AE2-depleted ESCC cells, suggesting that MMP regulation is a key mechanism by which AE2 controls the movement of ESCC cells. Further, IHC staining revealed a relationship between the weak expression of AE2 at the invasive front and shorter postoperative survival in ESCC patients (Shiozaki et al., 2018a).

NHE plays a role in the regulation of intracellular pH by mediating the coupled counter-transport of one H^+ for one Na^+ . Goldman et al. (2011) demonstrated that NHE controlled deoxycholic acid-induced apoptosis in EAC cells via a H^+ -activated, Na^+ -dependent ionic shift. Guan et al. (2014) reported the strong expression of NHE1 in EAC tissues, and showed that the knockdown of NHE1 in EC cells reduced their viability and induced apoptosis. We also demonstrated the inhibition of apoptosis and activation of PI3K/Akt signaling in ESCC cells following the knockdown of NHE1 (Ariyoshi et al., 2017) in ESCC. These findings indicated that the Notch signaling pathway was inhibited by the knockdown of NHE1, while IHC of primary ESCC samples showed a lower survival rate in the NHE1 low group than in the NHE1 high group (Ariyoshi et al., 2017). Liu et al. (2008) reported the significant suppression of the malignant behavior of human GC cells, the inhibition of cell growth, the induction of cell apoptosis, and the partial reversal of the malignant phenotypes of SGC-7901 following NHE1 antisense gene transfection.

TABLE 5 | Overview of pH regulators with roles in the cell death and survival of upper gastrointestinal tract cancers.

Channels	Organ	Mechanism/ pathway	Induction	References
AE1	ESCC	MAPK and Hedgehog signaling pathways	siRNA technology	Shiozaki et al., 2017
	GC	p16	siRNA technology	Shen et al., 2007
AE2	ESCC		siRNA technology	Shiozaki et al., 2018a
NHE1	EAC		Deoxycholic acid	Goldman et al., 2011
	EAC		Amiloride, Guggulsterone	Guan et al., 2014
	ESCC	PI3K-AKT signaling, Notch signaling	siRNA technology	Ariyoshi et al., 2017
	GC		Antisense gene	Liu et al., 2008
V-ATPase	GC		Proton pump inhibitors	Chen et al., 2009
	GC	Phosphorylation of LRP6, Wnt/ β -catenin signaling	Diphyllin	Shen et al., 2011
	GC		Pantoprazole	Shen et al., 2013

ESCC, esophageal squamous cell carcinoma; EAC, esophageal adenocarcinoma; GC, gastric cancer.

V-ATPase is a proton pump in cells that is important for the maintenance of intracellular pH. Chen et al. (2009) showed that proton pump inhibitors (PPIs) reduced intracellular pH in SGC7901, human GC cell line, by suppressing V-ATPase and also promoted the apoptotic effects of antitumor drug, adriamycin. They showed that administration of adriamycin after PPI pretreatment produced the most cytotoxic effects on SGC7901 cells and increased the early and total apoptosis rates. PPI also significantly reduced the adriamycin-releasing index and increased the intracellular adriamycin concentration. Shen et al. (2011) demonstrated that diphyllin, a new V-ATPase inhibitor, decreased intracellular pH and induced apoptosis by inhibiting the phosphorylation of low-density lipoprotein receptor-related protein 6 (LRP6) in Wnt/ β -catenin signaling. They subsequently reported that pantoprazole induced the apoptosis of GC cells, and indicated the potential of pantoprazole as a V-ATPase inhibitor for the treatment of GC through the suppressed phosphorylation of LRP6 in Wnt/ β -catenin signaling (Shen et al., 2013).

Collectively, these findings indicate the potential of pH regulators, including AEs, NHEs, and V-ATPases, as key therapeutic targets, and the silencing of their expression may represent a novel therapeutic strategy against UGI cancers.

CONCLUSION

There is recent considerable emphasis on determining better treatment strategies for advanced cancers with poor prognosis.

UGI cancers are aggressive, rapidly metastasize and still have low survival rate, especially for ESCC. Further, disseminated metastasis is one of the most common forms of recurrence of disease and is associated with a poor prognosis in GC patients. Therefore, detecting effective targets for UGI cancers is crucial for improving treatment options. Current information on advances in cellular physiological research on the roles of ion and water channels/transporters in the cell death and survival of UGI cancers was systematically reviewed herein. Human EC and GC express many different ion channels, AQP, and pH regulators, the pharmacological manipulation and gene silencing of which affected apoptosis, and may be involved in tumorigenesis and progression. The findings of previous studies indicate the roles of ion transporter, water channels, and pH regulators as functional biomarkers and therapeutic targets in EC and GC. One of the powerful charms of the research in this field is that anti-cancer effect has been newly identified in several inhibitors or stimulators of ion channels, such as lubiprostone, tranilast, amlodipine, verapamil, and PPI, which

have been used to treat patients with other disorders, and their safeties for clinical use has already been demonstrated. In addition, the targeting of ion and water channels specifically activated in CSCs may become an important strategy for cancer therapy. On the other hand, there are inborn limitations of the review, such as the lack of a critical view of these channels in the current clinical oncology field. A more detailed understanding of the molecular mechanisms regulating cell death and survival may result in the application of cellular physiological strategies, such as the regulation of ion transporters, water channels, and intracellular pH, as novel therapeutic approaches for UGI cancers.

AUTHOR CONTRIBUTIONS

AS wrote the manuscript. YM and EO edited the manuscript. All authors contributed to the article and approved the submitted version.

REFERENCES

- Almasi, S., Kennedy, B. E., El-Aghil, M., Sterea, A. M., Gujar, S., Partida-Sanchez, S., et al. (2018). TRPM2 channel-mediated regulation of autophagy maintains mitochondrial function and promotes gastric cancer cell survival via the JNK-signaling pathway. *J. Biol. Chem.* 293, 3637–3650. doi: 10.1074/jbc.M117.817635
- Anderson, K. J., Cormier, R. T., and Scott, P. M. (2019). Role of ion channels in gastrointestinal cancer. *World J. Gastroenterol.* 25, 5732–5772. doi: 10.3748/wjg.v25.i38.5732
- Ando, N., Kato, H., Igaki, H., Shinoda, M., Ozawa, S., Shimizu, H., et al. (2012). A randomized trial comparing postoperative adjuvant chemotherapy with cisplatin and 5-fluorouracil versus preoperative chemotherapy for localized advanced squamous cell carcinoma of the thoracic esophagus (JCOG9907). *Ann. Surg. Oncol.* 19, 68–74. doi: 10.1245/s10434-011-2049-9
- Ariyoshi, Y., Shiozaki, A., Ichikawa, D., Shimizu, H., Kosuga, T., Konishi, H., et al. (2017). Na⁺/H⁺ exchanger 1 has tumor suppressive activity and prognostic value in esophageal squamous cell carcinoma. *Oncotarget* 8, 2209–2223. doi: 10.18632/oncotarget.13645
- Bray, F., Ferlay, J., Soerjomataram, I., Siegel, R. L., Torre, L. A., and Jemal, A. (2018). Global cancer statistics 2018: GLOBOCAN estimates of incidence and mortality worldwide for 36 cancers in 185 countries. *CA. Cancer J. Clin.* 68, 394–424. doi: 10.3322/caac.21492
- Brenner, H., Rothenbacher, D., and Arndt, V. (2009). Epidemiology of stomach cancer. *Methods Mol. Biol.* 472, 467–477. doi: 10.1007/978-1-60327-492-0_23
- Chen, M., Zou, X., Luo, H., Cao, J., Zhang, X., Zhang, B., et al. (2009). Effects and mechanisms of proton pump inhibitors as a novel chemosensitizer on human gastric adenocarcinoma (SGC7901) cells. *Cell. Biol. Int.* 33, 1008–1019. doi: 10.1016/j.cellbi.2009.05.004
- Chow, J., Norng, M., Zhang, J., and Chai, J. (2007). TRPV6 mediates capsaicin-induced apoptosis in gastric cancer cells—mechanisms behind a possible new “hot” cancer treatment. *Biochim. Biophys. Acta.* 1773, 565–576. doi: 10.1016/j.bbamcr.2007.01.001
- Cikutović-Molina, R., Herrada, A. A., Gonzalez, W., Brown, N., and Zuniga, L. (2019). TASK-3 gene knockdown dampens invasion and migration and promotes apoptosis in KATO III and MKN-45 human gastric adenocarcinoma cell lines. *Int. J. Mol. Sci.* 20:6077. doi: 10.3390/ijms20236077
- Ding, M., Wang, H., Qu, C., Xu, F., Zhu, Y., Lv, G., et al. (2018). Pyrazolo[1,5-a]pyrimidine TRPC6 antagonists for the treatment of gastric cancer. *Cancer Lett.* 432, 47–55. doi: 10.1016/j.canlet.2018.05.041
- Enyedi, P., and Czirjak, G. (2010). Molecular background of leak K⁺ currents: Two-pore domain potassium channels. *Physiol. Rev.* 90, 559–605. doi: 10.1152/physrev.00029.2009
- Goldman, A., Chen, H., Khan, M. R., Roesly, H., Hill, K. A., Shahidullah, M., et al. (2011). The Na⁺/H⁺ exchanger controls deoxycholic acid-induced apoptosis by a H⁺-activated, Na⁺-dependent ionic shift in esophageal cells. *PLoS One* 6:e23835. doi: 10.1371/journal.pone.0023835
- Guan, B., Hoque, A., and Xu, X. (2014). Amiloride and guggulsterone suppression of esophageal cancer cell growth *in vitro* and in nude mouse xenografts. *Front. Biol. (Beijing)* 9, 75–81. doi: 10.1007/s11515-014-1289-z
- Han, Y., Shi, Y., Han, Z., Sun, L., and Fan, D. (2007). Detection of potassium currents and regulation of multidrug resistance by potassium channels in human gastric cancer cells. *Cell. Biol. Int.* 31, 741–747. doi: 10.1016/j.cellbi.2007.01.008
- Hartgrink, H. H., Jansen, E. P., van Grieken, N. C., and van de Velde, C. (2009). J. Gastric. Cancer. *Lancet.* 37, 477–490. doi: 10.1016/S0140-6736(09)60617-6
- Jemal, A., Bray, F., Center, M. M., Ferlay, J., Ward, E., and Forman, D. (2011). Global cancer statistics. *CA. Cancer J. Clin.* 61, 69–90. doi: 10.3322/caac.20107
- Jiang, B., Li, Z., Zhang, W., Wang, H., Zhi, X., Feng, J., et al. (2014). miR-874 Inhibits cell proliferation, migration and invasion through targeting aquaporin-3 in gastric cancer. *J. Gastroenterol.* 49, 1011–1025. doi: 10.1007/s00535-013-0851-9
- Kamangar, F., Dores, G. M., and Anderson, W. F. (2006). Patterns of cancer incidence, mortality, and prevalence across five continents: Defining priorities to reduce cancer disparities in different geographic regions of the world. *J. Clin. Oncol.* 24, 2137–2150. doi: 10.1200/JCO.2005.05.2308
- Katsurahara, K., Shiozaki, A., Kosuga, T., Kudou, M., Shoda, K., Arita, T., et al. (2020). ANO9 regulated cell cycle in human esophageal squamous cell carcinoma. *Ann. Surg. Oncol.* 27, 3218–3230. doi: 10.1245/s10434-020-08368-y
- Katsurahara, K., Shiozaki, A., Kosuga, T., Shimizu, H., Kudou, M., Arita, T., et al. (2021). ANO9 regulates PD-L2 expression and binding ability to PD-1 in gastric cancer. *Cancer Sci.* doi: 10.1111/cas.14796 [Epub ahead of print].
- Kim, M. C., Lee, H. J., Lim, B., Ha, K. T., Kim, S. Y., So, I., et al. (2014). Quercetin induces apoptosis by inhibiting MAPKs and TRPM7 channels in AGS cells. *Int. J. Mol. Med.* 33, 1657–1663. doi: 10.3892/ijmm.2014.1704
- Kobayashi, T., Shiozaki, A., Nako, Y., Ichikawa, D., Kosuga, T., Shoda, K., et al. (2018). Chloride intracellular channel 1 as a switch among tumor behaviors in human esophageal squamous cell carcinoma. *Oncotarget* 9, 23237–23252. doi: 10.18632/oncotarget.25296

- Konishi, T., Shiozaki, A., Kosuga, T., Kudou, M., Shoda, K., Arita, T., et al. (2019). LRRC8A expression influences growth of esophageal squamous cell carcinoma. *Am. J. Pathol.* 189, 1973–1985. doi: 10.1016/j.ajpath.2019.06.006
- Kudou, M., Shiozaki, A., Yamazato, Y., Katsurahara, K., Kosuga, T., Shoda, K., et al. (2019). The expression and role of TRPV2 in esophageal squamous cell carcinoma. *Sci. Rep.* 9:16055. doi: 10.1038/s41598-019-52227-0
- Kusayama, M., Wada, K., Nagata, M., Ishimoto, S., Takahashi, H., Yoneda, M., et al. (2011). Critical role of aquaporin 3 on growth of human esophageal and oral squamous cell carcinoma. *Cancer Sci.* 102, 1128–1136. doi: 10.1111/j.1349-7006.2011.01927.x
- Lastraioli, E., Iorio, J., and Arcangeli, A. (2015). Ion channel expression as promising cancer biomarker. *Biochim. Biophys. Acta.* 1848, 2685–2702. doi: 10.1016/j.bbame.2014.12.016
- Li, B. P., Mao, Y. T., Wang, Z., Chen, Y. Y., Wang, Y., Zhai, C. Y., et al. (2018). CLIC1 promotes the progression of gastric cancer by regulating the MAPK/AKT pathways. *Cell. Physiol. Biochem.* 46, 907–924. doi: 10.1159/000488822
- Li, Y., Zhu, C. L., Nie, C. J., Li, J. C., Zeng, T. T., Zhou, J., et al. (2013). Investigation of tumor suppressing function of CACNA2D3 in esophageal squamous cell carcinoma. *PLoS One* 8:e60027. doi: 10.1371/journal.pone.0060027
- Liu, H. F., Teng, X. C., Zheng, J. C., Chen, G., and Wang, X. W. (2008). Effect of NHE1 antisense gene transfection on the biological behavior of SGC-7901 human gastric carcinoma cells. *World J. Gastroenterol.* 14, 2162–2167. doi: 10.3748/wjg.14.2162
- Ma, G., Liu, H., Hua, Q., Wang, M., Du, M., Lin, Y., et al. (2017). KCNA1 cooperating with PTK2 is a novel tumor suppressor in gastric cancer and is associated with disease outcome. *Mol. Cancer* 16:46. doi: 10.1186/s12943-017-0613-z
- Ma, P. F., Chen, J. Q., Wang, Z., Liu, J. L., and Li, B. P. (2012). Function of chloride intracellular channel 1 in gastric cancer cells. *World J. Gastroenterol.* 18, 3070–3080. doi: 10.3748/wjg.v18.i24.3070
- Matsumoto, Y., Shiozaki, A., Kosuga, T., Kudou, M., Shimizu, H., Arita, T., et al. (2021). Expression and role of CFTR in human esophageal squamous cell carcinoma. *Ann. Surg. Oncol.* (in press). doi: 10.1245/s10434-021-09752-y
- Mitsuda, M., Shiozaki, A., Kudou, M., Shimizu, H., Arita, T., Kosuga, T., et al. (2021). Functional analysis and clinical significance of chloride channel 2 expression in esophageal squamous cell carcinoma. *Ann. Surg. Oncol.* doi: 10.1245/s10434-021-09659-8 [Epub ahead of print].
- Nagaraju, G. P., Basha, R., Rajitha, B., Alese, O. B., Alam, A., Pattnaik, S., et al. (2016). Aquaporins: their role in gastrointestinal malignancies. *Cancer Lett.* 373, 12–18. doi: 10.1016/j.canlet.2016.01.003
- Nashimoto, A., Akazawa, K., Isobe, Y., Miyashiro, I., Katai, H., Kadera, Y., et al. (2013). Gastric cancer treated in 2002 in Japan: 2009 annual report of the JGCA nationwide registry. *Gastric. Cancer.* 16, 1–27. doi: 10.1007/s10120-012-0163-4
- Nie, C., Qin, X., Li, X., Tian, B., Zhao, Y., Jin, Y., et al. (2019). CACNA2D3 enhances the chemosensitivity of esophageal squamous cell carcinoma to cisplatin via inducing Ca(2+) -mediated apoptosis and suppressing PI3K/Akt Pathways. *Front. Oncol.* 9:185. doi: 10.3389/fonc.2019.00185
- Okada, Y., Maeno, E., Shimizu, T., Dezaki, K., Wang, J., and Morishima, S. (2001). Receptor-mediated control of regulatory volume decrease (RVD) and apoptotic volume decrease (AVD). *J. Physiol.* 532, 3–16. doi: 10.1111/j.1469-7793.2001.00033.x
- Okada, Y., Shimizu, T., Maeno, E., Tanabe, S., Wang, X., and Takahashi, N. (2006). Volume-sensitive chloride channels involved in apoptotic volume decrease and cell death. *J. Membr. Biol.* 209, 21–29. doi: 10.1007/s00232-005-0836-6
- Pardo, L. A., and Stuhmer, W. (2014). The roles of K(+) channels in cancer. *Nat. Rev. Cancer.* 14, 39–48. doi: 10.1038/nrc3635
- Pedersen, S. F., and Stock, C. (2013). Ion channels and transporters in cancer: pathophysiology, regulation, and clinical potential. *Cancer Res.* 73, 1658–1661. doi: 10.1158/0008-5472.CAN-12-4188
- Qiu, Z., Dubin, A. E., Mathur, J., Reddy, K., Miraglia, L. J., Reinhardt, J., et al. (2014). SWELL1, a plasma membrane protein, is an essential component of volume-regulated anion channel. *Cell* 157, 447–458. doi: 10.1016/j.cell.2014.03.024
- Schreiber, R., Uliyakina, I., Kongsuphol, P., Warth, R., Mirza, M., Martins, J. R., et al. (2010). Expression and function of epithelial anoctamins. *J. Biol. Chem.* 285, 7838–7845. doi: 10.1074/jbc.M109.065367
- Seo, Y., Choi, J., Lee, J. H., Kim, T. G., Park, S. H., Han, G., et al. (2020). Diversity-oriented generation and biological evaluation of new chemical scaffolds bearing a 2,2-dimethyl-2H-chromene unit: Discovery of novel potent ANO1 inhibitors. *Bioorg. Chem.* 101:104000. doi: 10.1016/j.bioorg.2020.104000
- Shao, X. D., Wu, K. C., Guo, X. Z., Xie, M. J., Zhang, J., and Fan, D. M. (2008). Expression and significance of HERG protein in gastric cancer. *Cancer Biol. Ther.* 7, 45–50. doi: 10.4161/cbt.7.1.5126
- Shao, X. D., Wu, K. C., Hao, Z. M., Hong, L., Zhang, J., and Fan, D. M. (2005). The potent inhibitory effects of cisapride, a specific blocker for human ether-a-go-go-related gene (HERG) channel, on gastric cancer cells. *Cancer Biol. Ther.* 4, 295–301. doi: 10.4161/cbt.4.3.1500
- Shen, W., Zou, X., Chen, M., Liu, P., Shen, Y., Huang, S., et al. (2011). Effects of diphyllin as a novel V-ATPase inhibitor on gastric adenocarcinoma. *Eur. J. Pharmacol.* 667, 330–338. doi: 10.1016/j.ejphar.2011.05.042
- Shen, W., Zou, X., Chen, M., Shen, Y., Huang, S., Guo, H., et al. (2013). Effect of pantoprazole on human gastric adenocarcinoma SGC7901 cells through regulation of phosphor-LRP6 expression in Wnt/ β -catenin signaling. *Oncol. Rep.* 30, 851–855. doi: 10.3892/or.2013.2524
- Shen, W. W., Wu, J., Cai, L., Liu, B. Y., Gao, Y., Chen, G. Q., et al. (2007). Expression of anion exchanger 1 sequesters p16 in the cytoplasm in gastric and colonic adenocarcinoma. *Neoplasia* 9, 812–819. doi: 10.1593/neo.07403
- Shimizu, H., Shiozaki, A., Ichikawa, D., Fujiwara, H., Konishi, H., Ishii, H., et al. (2014). The expression and role of aquaporin 5 in esophageal squamous cell carcinoma. *J. Gastroenterol.* 49, 655–666. doi: 10.1007/s00535-013-0827-9
- Shiozaki, A., Hikami, S., Ichikawa, D., Kosuga, T., Shimizu, H., Kudou, M., et al. (2018a). Anion exchanger 2 suppresses cellular movement and has prognostic significance in esophageal squamous cell carcinoma. *Oncotarget* 9, 25993–26006. doi: 10.18632/oncotarget.25417
- Shiozaki, A., Ichikawa, D., Otsuji, E., and Marunaka, Y. (2014). Cellular physiological approach for treatment of gastric cancer. *World J. Gastroenterol.* 20, 11560–11566. doi: 10.3748/wjg.v20.i33.11560
- Shiozaki, A., Katsurahara, K., Kudou, M., Shimizu, H., Kosuga, T., Ito, H., et al. (2021). Amlodipine and verapamil, voltage-gated Ca²⁺ channel inhibitors, suppressed the growth of gastric cancer stem cells. *Ann. Surg. Oncol.* doi: 10.1245/s10434-021-09645-0 [Epub ahead of print].
- Shiozaki, A., Kudou, M., Fujiwara, H., Konishi, H., Shimizu, H., Arita, T., et al. (2020). Clinical safety and efficacy of neoadjuvant combination chemotherapy of tranilast in advanced esophageal squamous cell carcinoma: Phase I/II study (TNAC). *Medicine (Baltimore)* 99:e23633. doi: 10.1097/MD.00000000000023633
- Shiozaki, A., Kudou, M., Ichikawa, D., Fujiwara, H., Shimizu, H., Ishimoto, T., et al. (2018b). Esophageal cancer stem cells are suppressed by tranilast, a TRPV2 channel inhibitor. *J. Gastroenterol.* 53, 197–207. doi: 10.1007/s00535-017-1338-x
- Shiozaki, A., Kudou, M., Ichikawa, D., Shimizu, H., Arita, T., Kosuga, T., et al. (2017). Expression and role of anion exchanger 1 in esophageal squamous cell carcinoma. *Oncotarget* 8, 17921–17935. doi: 10.18632/oncotarget.14900
- Sun, W. J., Hu, D. H., Wu, H., Xiao, H., Lu, M. D., Guo, W. J., et al. (2016). Expression of AQP1 was associated with apoptosis and survival of patients in gastric adenocarcinoma. *Dig. Surg.* 33, 190–196. doi: 10.1159/000443843
- Tachimori, Y., Ozawa, S., Numasaki, H., Ishihara, R., Matsubara, H., Muro, K., et al. (2019). Comprehensive registry of esophageal cancer in Japan, 2012. *Esophagus* 16, 221–245. doi: 10.1007/s10388-019-00674-z
- Udagawa, H., Ueno, M., Shinohara, H., Haruta, S., Kaida, S., Nakagawa, M., et al. (2012). The importance of grouping of lymph node stations and rationale of three-field lymphadenectomy for thoracic esophageal cancer. *J. Surg. Oncol.* 106, 742–747. doi: 10.1002/jso.23122
- Wang, H., Yang, X., Guo, Y., Shui, L., Li, S., Bai, Y., et al. (2019). HERG1 promotes esophageal squamous cell carcinoma growth and metastasis through TXNDC5 by activating the PI3K/AKT pathway. *J. Exp. Clin. Cancer Res.* 38:324. doi: 10.1186/s13046-019-1284-y
- Wu, J., Zhang, Y. C., Suo, W. H., Liu, X. B., Shen, W. W., Tian, H., et al. (2010). Induction of anion exchanger-1 translation and its opposite roles in the

- carcinogenesis of gastric cancer cells and differentiation of K562 cells. *Oncogene* 29, 1987–1996. doi: 10.1038/onc.2009.481
- Xia, J., Wang, H., Li, S., Wu, Q., Sun, L., Huang, H., et al. (2017). Ion channels or aquaporins as novel molecular targets in gastric cancer. *Mol. Cancer*. 1:54. doi: 10.1186/s12943-017-0622-y
- Xie, R., Liu, L., Lu, X., and Hu, Y. (2020). LncRNA OIP5-AS1 facilitates gastric cancer cell growth by targeting the miR-422a/ANO1 axis. *Acta Biochim. Biophys. Sin. (Shanghai)* 52, 430–438. doi: 10.1093/abbs/gmaa012
- Yamazato, Y., Shiozaki, A., Ichikawa, D., Kosuga, T., Shoda, K., Arita, T., et al. (2018). Aquaporin 1 suppresses apoptosis and affects prognosis in esophageal squamous cell carcinoma. *Oncotarget* 9, 29957–29974. doi: 10.18632/oncotarget.25722
- Yu, L., Li, H., Li, Z., Jia, J., Wu, Z., Wang, M., et al. (2020). Long non-coding RNA HAND2-AS1 inhibits growth and migration of gastric cancer cells through regulating the miR-590-3p/KCNT2 Axis. *Onco. Targets Ther.* 13, 3187–3196. doi: 10.2147/OTT.S233256
- Zhang, R., Tian, P., Chi, Q., Wang, J., Wang, Y., Sun, L., et al. (2012). Human ether-a-go-go-related gene expression is essential for cisplatin to induce apoptosis in human gastric cancer. *Oncol. Rep.* 27, 433–440. doi: 10.3892/or.2011.1515
- Zhao, K., Wang, Z., Li, X., Liu, J. L., Tian, L., and Chen, J. Q. (2019). Exosome-mediated transfer of CLIC1 contributes to the vincristine-resistance in gastric cancer. *Mol. Cell. Biochem.* 462, 97–105. doi: 10.1007/s11010-019-03613-9
- Zhu, H., Wu, Y., Kang, M., and Zhang, B. (2020). MiR-877 suppresses gastric cancer progression by downregulating AQP3. *J. Int. Med. Res.* 48:300060520903661. doi: 10.1177/0300060520903661

Conflict of Interest: The authors declare that the research was conducted in the absence of any commercial or financial relationships that could be construed as a potential conflict of interest.

Copyright © 2021 Shiozaki, Marunaka and Otsuji. This is an open-access article distributed under the terms of the Creative Commons Attribution License (CC BY). The use, distribution or reproduction in other forums is permitted, provided the original author(s) and the copyright owner(s) are credited and that the original publication in this journal is cited, in accordance with accepted academic practice. No use, distribution or reproduction is permitted which does not comply with these terms.



From Pinocytosis to Methuosis—Fluid Consumption as a Risk Factor for Cell Death

Markus Ritter^{1,2,3,4,5*}, Nikolaus Bresgen⁶ and Hubert H. Kerschbaum^{6*}

¹ Center for Physiology, Pathophysiology and Biophysics, Institute for Physiology and Pathophysiology, Paracelsus Medical University, Salzburg, Austria, ² Institute for Physiology and Pathophysiology, Paracelsus Medical University, Nuremberg, Germany, ³ Gastein Research Institute, Paracelsus Medical University, Salzburg, Austria, ⁴ Ludwig Boltzmann Institute for Arthritis und Rehabilitation, Salzburg, Austria, ⁵ Kathmandu University School of Medical Sciences, Dhulikhel, Nepal, ⁶ Department of Biosciences, University of Salzburg, Salzburg, Austria

OPEN ACCESS

Edited by:

Baojun Zhang,
Xi'an Jiaotong University, China

Reviewed by:

Yong Liu,
Xuzhou Medical University, China
Lianjun Zhang,
Suzhou Institute of Systems Medicine,
China

*Correspondence:

Markus Ritter
markus.ritter@pmu.ac.at
Hubert H. Kerschbaum
Hubert.Kerschbaum@sbg.ac.at

Specialty section:

This article was submitted to
Cell Death and Survival,
a section of the journal
Frontiers in Cell and Developmental
Biology

Received: 11 January 2021

Accepted: 29 April 2021

Published: 23 June 2021

Citation:

Ritter M, Bresgen N and
Kerschbaum HH (2021) From
Pinocytosis to Methuosis—Fluid
Consumption as a Risk Factor for Cell
Death.
Front. Cell Dev. Biol. 9:651982.
doi: 10.3389/fcell.2021.651982

The volumes of a cell [cell volume (CV)] and its organelles are adjusted by osmoregulatory processes. During pinocytosis, extracellular fluid volume equivalent to its CV is incorporated within an hour and membrane area equivalent to the cell's surface within 30 min. Since neither fluid uptake nor membrane consumption leads to swelling or shrinkage, cells must be equipped with potent volume regulatory mechanisms. Normally, cells respond to outwardly or inwardly directed osmotic gradients by a volume decrease and increase, respectively, i.e., they shrink or swell but then try to recover their CV. However, when a cell death (CD) pathway is triggered, CV persistently decreases in isotonic conditions in apoptosis and it increases in necrosis. One type of CD associated with cell swelling is due to a dysfunctional pinocytosis. Methuosis, a non-apoptotic CD phenotype, occurs when cells accumulate too much fluid by macropinocytosis. In contrast to functional pinocytosis, in methuosis, macropinosomes neither recycle nor fuse with lysosomes but with each other to form giant vacuoles, which finally cause rupture of the plasma membrane (PM). Understanding methuosis longs for the understanding of the ionic mechanisms of cell volume regulation (CVR) and vesicular volume regulation (VVR). In nascent macropinosomes, ion channels and transporters are derived from the PM. Along trafficking from the PM to the perinuclear area, the equipment of channels and transporters of the vesicle membrane changes by retrieval, addition, and recycling from and back to the PM, causing profound changes in vesicular ion concentrations, acidification, and—most importantly—shrinkage of the macropinosome, which is indispensable for its proper targeting and cargo processing. In this review, we discuss ion and water transport mechanisms with respect to CVR and VVR and with special emphasis on pinocytosis and methuosis. We describe various aspects of the complex mutual interplay between extracellular and intracellular ions and ion gradients, the PM and vesicular membrane, phosphoinositides, monomeric G proteins and their targets, as well as the submembranous cytoskeleton. Our aim is to highlight important cellular mechanisms, components, and processes that may lead to methuotic CD upon their derangement.

Keywords: pinocytosis, macropinocytosis, endocytosis, intracellular vesicle, ion transport, cell volume regulation, cell death, methuosis

INTRODUCTION







Individual cells have the same need entire organisms have: They have to drink. At the cellular level, water drinking is known as pinocytosis and the fluid-containing organelle is the pinosome. Fluid uptake, intracellular distribution, and processing require precise spatial and temporal coordination of membrane and cytoskeletal proteins. Macropinocytosis is an actin-driven process, where a cup-like structure emerges from the cell surface, which engulfs extracellular fluid and forms a vesicle (Swanson and Watts, 1995; Swanson, 2008; Kerr and Teasdale, 2009; Lim and Gleeson, 2011; Hinze and Boucrot, 2018; Doodnauth et al., 2019; King and Kay, 2019; Swanson and King, 2019). The vesicle membrane contains ion channels and transporters that are used for the flux of water, osmolytes, and nutrients, and it is decorated by distinct phospholipids and proteins that are required for intracellular sorting and transport of the organelle (Bohdanowicz and Grinstein, 2013; Levin et al., 2015; Freeman and Grinstein, 2018; Williamson and Donaldson, 2019; Stow et al., 2020) (Table 1). Macropinocytosis serves seemingly unrelated cellular functions, such as nutrition acquisition to satisfy cellular energy demands (Recouvreux and Commisso, 2017; Palm, 2019; Lin et al., 2020), immune surveillance leading to antigen presentation to lymphocytes (Lanzavecchia, 1996; Von Delwig et al., 2006; Liu and Roche, 2015; Canton, 2018), intracellular replication of pathogenic bacteria (Bloomfield and Kay, 2016; Di Russo Case et al., 2016), and CD by drinking too much fluid, i.e., methuosis (Maltese and Overmeyer, 2014, 2015). Careful examination of these functions showed similarities in the initial steps of fluid uptake and differences in the final processing steps, such as fusion or not fusion with lysosomes.

Abbreviations: AA, arachidonic acid; Akt1, AKT serine/threonine kinase 1; ALS2, amyotrophic lateral sclerosis 2; ANO, anoctamin; APPL1, adaptor protein, phosphotyrosine interacting with PH domain and leucine zipper 1; AQP, aquaporin; Arf6, ADP-ribosylation factor 6; ARNO, ARF nucleotide binding-site opener; Arp2/3, actin-related protein 2/3; ASIC, acid-sensing ion channel; ALS2, alsin Rho guanine nucleotide exchange factor; ASOR, acid-activated outwardly rectifying chloride channel; ATP, adenosine triphosphate; AVD, apoptotic volume decrease; AVP, arginine vasopressin; BK channel, big-conductance Ca^{2+} -activated K^{+} channel; CA, carbonic anhydrase; $\text{Ca}^{2+}_{\text{i}}$, intracellular Ca^{2+} concentration; CaMK, Ca^{2+} /calmodulin-dependent kinase; Ca_v , voltage-dependent calcium channel; Cav-1, caveolin-1; CD, cell death; CK, casein kinase; Cdc42, cell division control protein 42 homolog; CFTR, cystic fibrosis transmembrane conductance regulator; ClC, voltage-dependent chloride channel/exchanger; CLIC, chloride intracellular channel; 3Cpro, 3C protease of human hepatitis A virus; CV, cell volume; CVR, cell volume regulation; EFA6, ARF6 guanine nucleotide exchange factor; ECF, extracellular fluid; EDRF, endothelium-derived relaxing factor; EGF, epidermal growth factor; EGFR, epidermal growth factor receptor; EIPA, 5-(N-ethyl-N-isopropyl)-amiloride; ENaC, epithelial Na^{+} channel; EET, 5'-6'-epoxyeicosatrienoic acid; ERK, extracellular signal-regulated kinase; Fig4, factor-induced gene 4; FRET, Förster/fluorescence resonance energy transfer; GAP, GTPase activating protein; GB, glioblastoma; GBM, glioblastoma multiforme; GEF, guanine nucleotide exchange factor; GluCL, glutamate-gated chloride channel; GLUT, glucose transporter; GPCR, see GPR; GPHR, Golgi pH regulator; GPR, G protein-coupled receptor; Grb2, growth factor receptor-bound protein 2; HLEK, human limbal keratinocytes; HGF, hepatocyte growth factor; hTCEpi, human limbal-derived epithelial cell line; HUVEC, human umbilical vein endothelial cell; ICF, intracellular fluid; $\text{ICl}_{\text{swell}}$, swelling-activated Cl^{-} current; IGF-1, insulin like growth factor 1; IPMK, inositol polyphosphate multikinase; INO1, inositol-3-phosphate synthase; IMPase, inositol-1(or4)-monophosphatase; $\text{Ins}(1,4,5)\text{P}_3$ or IP_3 , inositol 1,4,5-trisphosphate; IP, inositolphosphate; IP_3K , inositol-trisphosphate 3-kinase; IP_3R , IP_3 receptor; IPP, inositol-1,4 biphosphate

The prototypic experiments examining pinocytosis were done on macrophages and malignant cells by Lewis in the 1930s (Lewis, 1936, 1937). Then, Lewis was among the few researchers using time-lapse microscopy to study the dynamics of living cells. Lewis introduced the term “*pinocytosis*” to describe the fact that ruffle formation is associated with vesicle formation and uptake of extracellular fluid (Lewis, 1936, 1937). In line with Lewis’s statement “*Pinocytosis is easily seen in motion pictures*” (Lewis, 1937), we use video microscopy to visualize the dynamics of pinocytosis (Figure 1 and Supplementary Videos 1, 2). In the words of Lewis, Supplementary Video 1 shows that vesicles “*taken in vary greatly in size,*” “*several fuse... to form larger ones,*” “*move centrally,*” and “*finally reach... the neighborhood of... the nucleus*” (Lewis, 1937). Lewis also

1-phosphatase; INF γ , interferon gamma; INPP5, inositol-polyphosphate 5-phosphatase; INPase, inositol-phosphate phosphatase; INPP, inositol-1,4-bisphosphate 1-phosphatase; INPP5, inositol polyphosphate 5 phosphatase; IPPK, inositol-pentakisphosphate 2-kinase; ITPK, inositol 1,3,4-trisphosphate 5/6 kinase, acts also as inositol polyphosphate phosphatase; K_v , voltage-gated potassium channel; LPS, lipopolysaccharide; LTD4, leukotriene D4; mAb, monoclonal antibody; MAPK, mitogen-activated protein kinase; M-CSF, macrophage colony-stimulating factor; MHC, major histocompatibility complex; MINPP, multiple inositol-polyphosphate phosphatase; MIPP, 3-(2-methyl-1H-indol-3-yl)-1-(4-pyridinyl)-2-propen-1-one; miR, microRNA; MKK4, mitogen-activated protein kinase kinase 4; MLC1, megalencephalic leukoencephalopathy with subcortical cysts 1; MOMIPP, 3-(5-methoxy, 2-methyl-1H-indol-3-yl)-1-(4-pyridinyl)-2-propen-1-one; MTM1, myotubularin 1; MTMR, myotubularin-related protein; MTMR6, myotubularin R6; mTOR, mammalian target of rapamycin; MVB, multi-vesicular body; NAADP, nicotinic acid adenine dinucleotide phosphate; NCX, $\text{Na}^{+}/\text{Ca}^{2+}$ -exchanger; NFAT5, nuclear factor of activated T cells 5; NGF, nerve growth factor; NOSTRIN, nitric oxide synthase trafficking inducer; NRF2, nuclear factor erythroid 2-related factor 2; NVI, necrotic volume increase; OCR, Lowe oculocerebrorenal syndrome protein; Orai, named after the keepers of the gates of heaven in Greek mythology, synonym: CRACM, calcium release-activated calcium channel protein; OMIM, Online Mendelian Inheritance in Man[®]; Ostm1, osteoclastogenesis-associated transmembrane protein; p53, tumor protein P53 or cellular tumor antigen p53; Pak, p21-activated kinase; Panx1, pannexin 1; PDGF, platelet-derived growth factor; PDK1, 3-phosphoinositide-dependent protein kinase 1; PEG, polyethyleneglycol; Pf, osmotic water permeability; PFKFB3, 6-phosphofructo-2-kinase/fructose-2,6 biphosphatase 3; PH, pleckstrin homology; pH_{i} , intracellular pH; PI, phosphoinositide or phosphatidylinositol; $\text{PI}(3)\text{P}$, phosphatidylinositol 3-phosphate; $\text{PI}(3,4,5)\text{P}_3$, phosphatidylinositol (3,4,5)-trisphosphate; $\text{PI}(4,5)\text{P}_2$, phosphatidylinositol 4,5-bisphosphate; $\text{PI}3\text{K}$, phosphatidylinositol 3 kinase; PIKfyve , phosphoinositide kinase FYVE-type zinc finger containing; PKB, protein kinase B; PLA2, phospholipase A2; PLC, phospholipase C; PM, plasma membrane; PS, phosphatidylserine; PRR, pattern recognition receptor; PTEN, phosphatase and tensin homolog; P2X-R , ATP-gated P2X receptor cation channel; RA, retinoic acid; Rab, Ras-related in brain; Rac, Ras-related C3 botulinum toxin substrate; RACK1, receptor for activated C kinase 1; Raf1, rapidly accelerated fibrosarcoma 1; Rap1, Ras-proximate-1/Ras-related protein 1; Ras, rat sarcoma; Rasal, Ras-GTPase-activating-like protein; RGBARG, RCC1-RhoGEF-BAR-and-RasGAP-containing protein; Rheb, Ras homolog enriched in brain; Rho, Ras homologous; RIN1, Ras and Rab interactor 1; RN-tre, Related to the N-terminus of tre; ROS, reactive oxygen species; RVD, regulatory volume decrease; RVI, regulatory volume increase; SGK, serum- and glucocorticoid-inducible protein kinase; SLC, solute carrier; SMIT, $\text{Na}^{+}/\text{myo-inositol}$ transporter; SOCE, store-operated calcium entry; STIM1, stromal interaction molecule 1; TFEB, transcription factor EB; TMEM, transmembrane protein; TonEBP, tonicity responsive enhancer (TonE) binding protein; TORC, target of rapamycin complex; TPC, two-pore channel; TRP, transient receptor potential; TRPML, TRP channel of mucolipin subfamily; TRPM7, Transient receptor potential cation channel subfamily M member 7; TSC, tuberous sclerosis complex; Ttyh, Tweety homolog; v-ATPase, vacuolar H^{+} -ATPase; Vps34, vacuolar protein sorting 34; VSOR, volume-sensitive outwardly rectifying Cl^{-} channel/current; VRAC, volume-regulated anion channel/current; VVR, vesicular volume regulation; WASP, Wiskott-Aldrich syndrome protein; WNK, with no lysine kinase

TABLE 1 | Some characteristics and ion concentrations of macropinocytosis and the endolysosomal pathway.

		Appearance	PIPs	Decoration	Ψ_m (mV)	pH	Na ⁺ (mM)	K ⁺ (mM)	Cl ⁻ (mM)	HCO ₃ ⁻ (mM)	Ca ²⁺ (mM)
ECF		Irregular	PI(4,5)P2	Rab5, Rab20	~-30 to -70	7.4	120–150	4–5	110–120	24–27	2
NP						6.9	12	140	20–80	8–15	0.1–2
ICF						6.0–6.2			20–30		0.003–2
EE		Spherical	PI3P, PI(3,4)P2	Rab4, Rab5, Rab20	10–20	5.0–5.5	20		40–70		2.5
LE		Tubulated	PI3P, PI(3,5)P2	Rab7, Rab9, Rab20		5.5			40		0.009
MVB		Intraluminal vesicles	PI3P + PI(3,5)P2	Rab7, Rab9, Rab20							
LE/LY Hybrid			PI3P	Rab7, LAMP1							
LY		Spherical	PI(3)P + PI(3,5)P2	LAMP1	~-40 to +20	4.3–5.5	20–145	2–60	>80		0.4–0.7

ECF, extracellular fluid; ICF, intracellular fluid; NP nascent pinosome; EE, early endosome; LE, late endosome; MVB, multivesicular body; LY, lysosome. For details, see text. References: (Sonawane and Verkman, 2003; Dong et al., 2010; Morgan et al., 2011; Scott and Gruenberg, 2011; Welliver and Swanson, 2012; Bohdanowicz and Grinstein, 2013; Ishida et al., 2013; Stauber and Jentsch, 2013; Chang et al., 2014; Egami et al., 2014; Levin et al., 2015; Saha et al., 2015; Xu and Ren, 2015; Xiong and Zhu, 2016; Chakraborty et al., 2017; Kim et al., 2018; Sterea et al., 2018; King and Kay, 2019; Li P. et al., 2019; Adjemian et al., 2020; Jin et al., 2020; Trivedi et al., 2020; Chadwick et al., 2021b; Riess et al., 2021; Zhang et al., 2021).

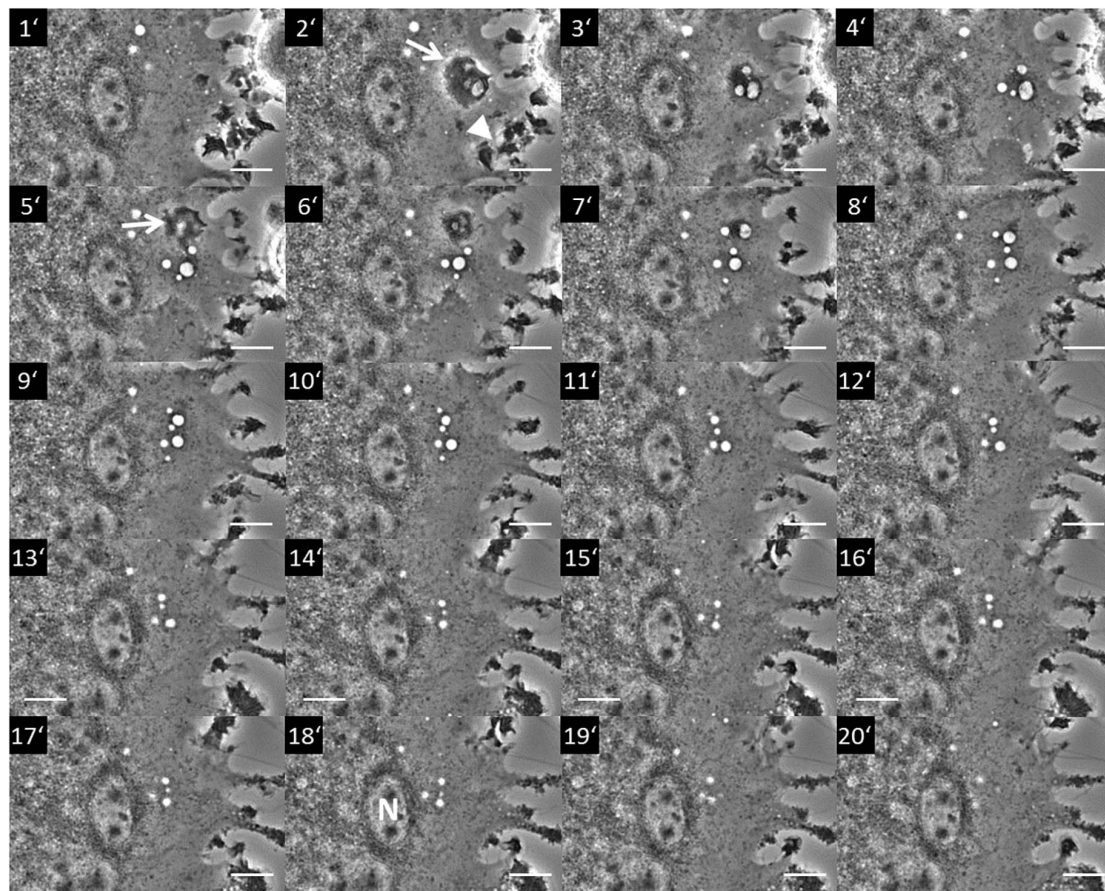


FIGURE 1 | Macropinocytosis occurring in a section of a multinucleated giant cell from a rat non-parenchymal hepatic cell line putatively representing immortalized monocytes (Kupffer cells). The image series shows a section of a giant cell where pinocytosis occurs. The process starts with the formation of a membrane ruffle at minute 2 (2'; arrow) from which an array of vesicles (pinosomes) originates (3'–4'). Further ruffling can be seen at the cell periphery (2'; arrowhead). A second ruffle is forming at minute 5 (5'; arrow) from which additional pinosomes derive (5'–7'). The whole pinosome array subsequently moves toward the center area of the giant cell (8'–18') locating to the vicinity of a nucleus (N in 18'). Terminally, the vesicles start to disappear in the perinuclear (pericentral) cytosol (20'). Scale bar = 10 μ m. The whole live cell imaging sequence can be seen in **Supplementary Video 1**.

suggested that proteins in the vesicles are “split by the digestive enzymes into simpler products which can be utilized or can diffuse out of the cell.” He also related the “disappearance” of the vesicles “with the completion of the digestion of their contents” as the vesicles “slowly shrink in size and disappear, leaving a small granule...” (Lewis, 1937). Lewis’s experiments also showed that the cells do not increase in volume, although “they may take in several times their volume of fluid” and he “assumed that the fluid diffuses out of the cells when the globules disappear” (Lewis, 1937). These experiments demonstrate that volume regulatory processes at the cellular and organelle levels are of paramount importance to maintain CV while cells incorporate large volumes of extracellular fluid and digest macromolecules present in the fluid. The fact that the fluid taken up by macropinocytosis outweighs its elimination by recycling vesicles (Swanson, 1989; Choy et al., 2018) highlights that VVR and CVR are inevitably linked to each other. This becomes evident from the massive cell swelling seen upon inhibition of water channels in pinocytosing cells (De Baey and Lanzavecchia, 2000). Furthermore, considering that the total volume of the endolysosomal compartment can make up a substantial part of the total CV (Choy et al., 2018) makes evident that the exchange of osmotically active solutes between the endolysosomal compartment and the cytosol will strictly affect the volumes of either part.

Given the importance of CVR, a central question is: What determines the size of a vesicle? That is, which transporters and ion channels in the PM and vesicle membrane are activated, incorporated, and terminated at which spatial and temporal check points? How does the macropinosomal solute composition and the vesicular membrane properties change after having gulped a lot of extracellular fluid during maturation along the endolysosomal pathway, and what are the determinants of this change? And finally: How are these cellular and subcellular volume regulatory mechanisms altered in methuosis?

To understand subcellular volume regulation, findings related to CVR provide clues to identify factors maintaining the set points of the vesicle.

As ion channels and transporters in the PM are central in CVR, they also contribute to VVR (Freeman and Grinstein, 2018; Freeman et al., 2020; Chadwick et al., 2021b). Thus, Lewis’s statement in the 1930s that “The factors involved in the diffusion of the fluid out of the cell are as mysterious as most of the other processes which take place” (Lewis, 1937) is now transforming to hypotheses trying to explain CVR and VVR in macropinocytosis at the molecular level and by facts generated by electrophysiological, molecular-biological, and imaging studies. Notably, Freeman and Grinstein (2018); Freeman et al. (2020), and Chadwick et al. (2021b) demonstrated that contributions from ion transporters are essential for normal shrinkage in macropinosome maturation.

This review focuses on the complex mutual interplay between extracellular and intracellular ions and ion gradients, the PM and vesicular membrane, phosphoinositides, monomeric G proteins and their targets, as well as the submembranous cytoskeleton in pinocytosis, with special emphasis on its connection to CVR and

VVR. It aims at highlighting important cellular mechanisms and components that govern these processes and that may lead to methuotic cell death upon their derangement.

Figure 2 schematically shows key steps of vesicle/vacuole formation and processing during normal macropinocytosis and in methuosis.

MACROPINOCYTOSIS

Macropinocytosis is a form of clathrin-independent endocytosis. Ruffling of cholesterol-rich membrane microdomains leads to the unselective incorporation of large volumes of extracellular fluid in macropinosomes with a diameter of 0.2 up to 5.0 μm (Levin et al., 2015; Donaldson, 2019). Macropinocytosis may occur constitutively or be induced by growth factors, chemokines, microbial products, viruses (Freeman et al., 2014; Marques et al., 2017; Canton, 2018; Doodnauth et al., 2019; Tejada-Munoz et al., 2019), crosslinking of cell surface molecules (Imamura et al., 2011), knockdown of genes (Choi et al., 2017; Fomin et al., 2018; Fomin, 2019; Su et al., 2021), and constitutive expression (Kasahara et al., 2007) or mutations of signal transduction molecules (Yoo et al., 2020). Some cells, like innate immune cells and Ras-transformed cancer cells, are able to perform both forms of macropinocytosis (Amyere et al., 2000; Stow et al., 2020). Importantly, this process ensures that cells incorporate everything animals ingest and digest, including nutrients as well as toxic substances and metabolites released by neighboring cells, exosomes, microparticles, and pathogens, such as bacteria and viruses (Suda et al., 2007; Mercer and Helenius, 2009, 2012; Mercer et al., 2010; Commisso et al., 2013; Bloomfield and Kay, 2016; Jiang et al., 2017; Commisso, 2019). Furthermore, macropinocytosis is involved in cell migration (Wen et al., 2016; Swanson and King, 2019).

Remarkably, within 1 h, a volume equivalent of the entire cytoplasm is incorporated by macropinocytosis, and within 30 min, macropinosome formation requires the entire cellular PM surface (Steinman et al., 1976; Cullen and Steinberg, 2018; Freeman and Grinstein, 2018). Against the compelling background of conserved CV and cell surface, sorting mechanisms distinguishing between recycling and digestion routes are of eminent importance. Membrane recycling is not only of importance for maintaining the cell surface but also for supplying the PM with receptors and transporters, such as neonatal Fc-receptor (Toh et al., 2019), bone morphogenetic protein receptor (Kim et al., 2019), PDGF β -receptor (Schmees et al., 2012), EGF receptor (Chiasson-Mackenzie et al., 2018; Freeman et al., 2020), and other plasmalemmal components such as integrins (Buckley et al., 2016; Freeman et al., 2020) as well as small GTPases, which fuel macropinocytosis (Cullen and Steinberg, 2018). Furthermore, as the intercellular volume is usually small, changes in extracellular ion composition may greatly affect ion gradients, which drive nutrient transporters, e.g., Na^+ -dependent glucose or amino acid uptake (Ganapathy et al., 2008; Wright et al., 2011; Broer, 2014). This exceptional well-balanced system is keeping CV and cell surface during macropinocytic flow reasonably constant, but puts the cell at

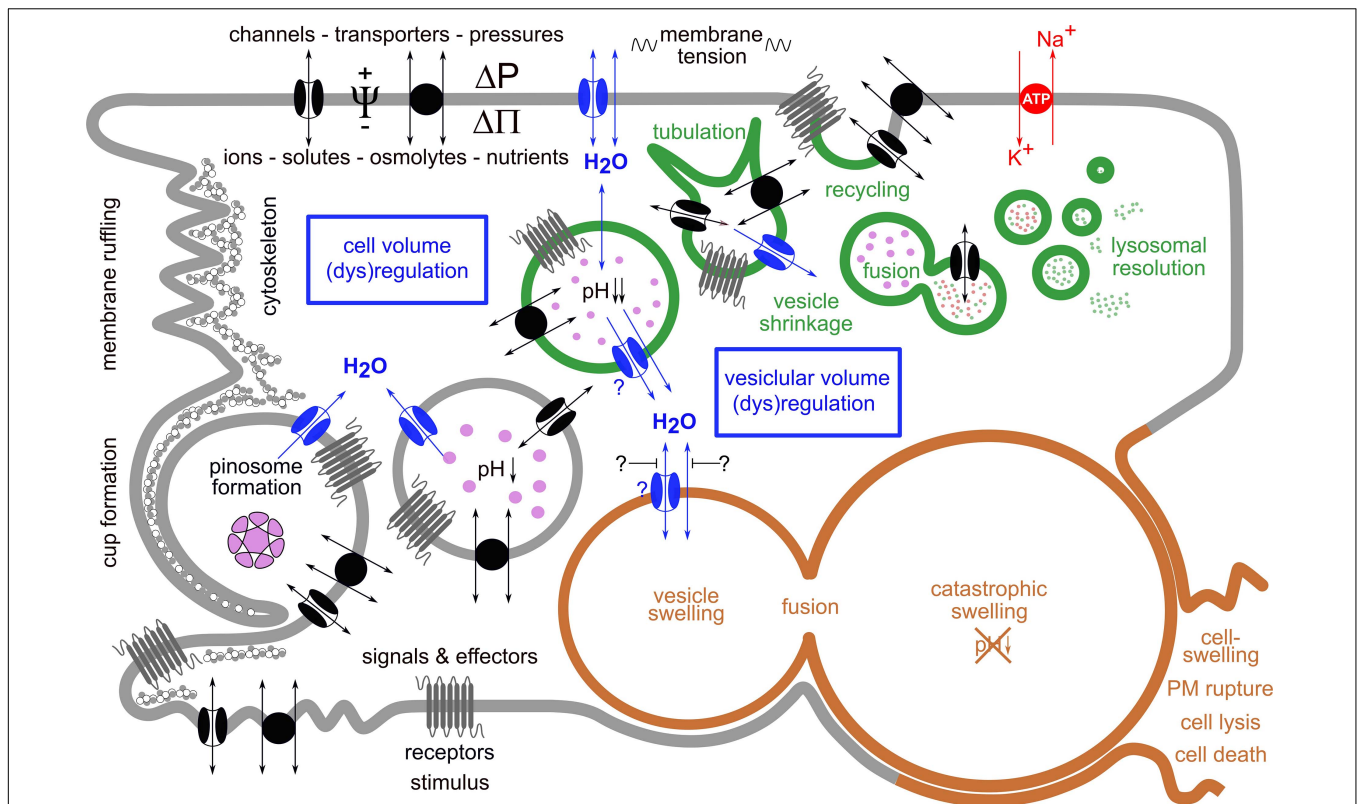


FIGURE 2 | Simplified scheme of key processes in vesicle/vacuole formation and processing during normal macropinocytosis and in methuosis. Macropinocytosis is an actin-driven process that is triggered by various stimuli. It starts with ruffling of the plasma membrane (PM) and formation of a pinocytotic cup, which engulfs extracellular fluid and forms a pinosome by membrane fusion at the tip of a lamellipodium-like structure. Its membrane contains ion channels and transporters, receptors, among other various PM constituents, e.g., phospholipids. The nascent pinosome unselectively engulfs extracellular fluid, along with its ions, nutrients, and metabolites and eventually also toxins or drugs. It may also enclose particulate matter-like exosomes, micro- or nanoparticles, or pathogens such as bacteria and viruses (pink enclosed structure). Under normal conditions (green vesicles), pinosomes move centripetally, become more and more acidic, shrink along their route, and become tubulated, a process necessary for proper sorting and recycling of the vesicles and their cargo. This requires also its decoration with distinct phospholipids and proteins (not shown). Reusable membrane proteins may become inserted again into the PM when vesicles fuse with it. This also recycles incorporated membrane back to the PM and relieves its tension. Vesicles designated for delivery of their contents to lysosomes—for further processing, digestion, or destruction—fuse with them and finally resolve. The resulting products may be further used, e.g., for the cell's nutrition. To ensure these processes, cell volume regulation and vesicular volume regulation must work hand in hand. This becomes evident from the fact that during pinocytosis, an extracellular fluid volume and membrane area equivalent to the cell's volume and to the cell's surface are incorporated within 1 h and 30 min, respectively. The volume regulatory mechanisms involve movement of ions and osmolytes across the PM by means of specific ion channels and transporters. The driving forces for these fluxes are determined by the electrochemical gradients. Water flux is driven mainly by the osmotic ($\Delta\Pi$) but eventually also by the hydrostatic (ΔP) pressure differences. The water permeability of the PM is greatly enhanced by water channels (aquaporins, blue). All of these movements are primarily driven by the activity of the Na^+/K^+ -ATPase (red transporter in the PM), an ion pump that moves Na^+ ions out of and K^+ ions into the cell, while hydrolyzing ATP as energy source. This process sets up the required ionic and osmotic gradients and determines the electrical potential difference Ψ across the PM. The mechanisms for vesicular volume regulation follow the same rules and are in principle identical to those in cell volume regulation, while utilizing their individual set of transporters and channels. In methuosis, a lethal process of aberrant pinocytosis where cells “drink themselves to death,” these processes are severely disturbed (brown vesicles). Fluid uptake by macropinocytosis is enhanced, and instead of shrinking, the vesicles swell, do not acidify, remain non-functional, and do not fuse with lysosomes, but instead they with each other. This leads to the formation of giant vacuoles, catastrophic cell swelling, and consequently to rupture of the PM, cell lysis, and death.

risk to damage either when CVR fails or when it accumulates metabolic waste products as seen in lysosomal storage diseases (Platt et al., 2012, 2018; Rappaport et al., 2016). Excessive fluid uptake in *in vitro* conditions leading to a distinct form of CD has been recently recognized and named methuosis (Maltese and Overmeyer, 2014, 2015).

Ruffle and Cup Formation

Ruffle and cup formation is an actin-driven process, which is closely related to the formation of phagocytic cups and

pseudopods (Lim and Gleeson, 2011; Freeman and Grinstein, 2014; Buckley and King, 2017; Williamson and Donaldson, 2019). Actin cytoskeleton rearrangement depends on phospholipids, lipid kinases and phosphatases, small GTPases, actin-modulating proteins, ion channels, and proton (H^+) pumps (Welliver and Swanson, 2012). Among the numerous small GTPases, the Ras and Rho family member, Rac1, is critical in the formation of ruffles and macropinocytic cups (Egami et al., 2014; Donaldson, 2019). For small GTPases, the switch from an inactive guanosine diphosphate (GDP)-bound form to an

active guanosine triphosphate (GTP)-bound form is facilitated by GEFs, which promote GDP dissociation. The inactivation of the small GTPases is mediated by GTPase-activating proteins (GAPs), which enhance GTP hydrolysis (Cherfils and Zeghouf, 2013). Critically, the activation of the GTPase cycle—activation, inactivation, removal from the membrane—is transient. Oscillations of Ca^{2+}_i may drive parallel oscillatory association and dissociation of the Ras-GAP, Rasal (Ras-GTPase-activating-like protein), to and from the PM. Only when bound to the PM, Rasal is active and can inactivate Ras. Thus, Ras is repetitively activated and inactivated (Walker et al., 2004). In macropinocytosis, Ras activity is terminated by RasGAP, which is recruited to the cup as it closes (Veltman et al., 2016; Buckley et al., 2020). When GTPases are persistently activated, e.g., when RasGAPs are inactive like in neurofibromatosis (Bloomfield et al., 2015; Ghoshal et al., 2019) or when Ras is constitutively active like in oncogenic H-Ras mutants, macropinosome formation and maturation deviate from the normal physiological pathway. The Ras-related G protein Rap1 is a negative regulator of Ras (Zwartkruis and Bos, 1999; Nussinov et al., 2020). Rap1 is found in early and late endocytic vesicles and lysosomes (Pizon et al., 1994), and its overexpression negatively regulates macropinocytosis (Seastone et al., 1999). In *Dictyostelium discoideum*, hyperosmotic stress activates Rap1 and decreases endocytic activity due to cellular acidification (Pintsch et al., 2001), and it promotes the formation of giant vacuoles of pinocytotic origin (Yuan and Chia, 2001).

Notably, in human intestinal cells, hypotonicity increases the activity of the H-Ras-Raf1-Erk signaling pathway (Van Der Wijk et al., 1998). The clustering of Ras proteins in distinct microdomains at the PM (lipid rafts) influences Ras structure, orientation, and Ras-isoform accessibility and thus the activation states of its effectors. Accordingly, GTP-bound H-Ras may remain in a locked state and as such not able to associate with its downstream effectors (Jang et al., 2016; Nussinov et al., 2018). Activation occurs once the lipid-anchored GTPases Ras1 and H-Ras are shifted out of the lipid rafts. This happens upon thinning of the PM in combination with changes of its curvature induced by cell swelling (Cohen, 2018).

Active Rac and Ras are located at the cup wall. Rac1 activation is associated with ruffle formation, and Rac1 inactivation precedes cup closure (Buckley and King, 2017). In *Dictyostelium discoideum*, the multidomain protein, RGBARG (RCC1, RhoGEF, BAR, and RasGAP-containing protein), orchestrates Ras and Rac activity in a small membrane patch, where RGBARG is localized at the protruding rim region (Buckley et al., 2020). Oncogenic H-Ras promotes the translocation of the vacuolar H^+ -ATPase (v-ATPase) from intracellular vesicles to the PM. The accumulation of v-ATPase is necessary for the cholesterol-dependent association of Rac1 with the PM, which is a prerequisite for the stimulation of membrane ruffling and macropinocytosis. Knockdown of the v-ATPase or its inhibition suppresses macropinocytosis, while addition of cholesterol to these cells restores both Rac1 membrane localization and macropinocytosis (Ramirez et al., 2019). In addition, Ras binds and activates phosphatidylinositol 3-kinases (PI3Ks), which have a Ras-binding domain (Gupta et al., 2007; Castellano

and Downward, 2011; Castellano et al., 2013). Activation of PI3Ks phosphorylates phosphatidylinositol 4,5-bisphosphate [PI(4,5)P₂] to phosphatidylinositol (3,4,5)-trisphosphate [PI(3,4,5)P₃] and promotes its enrichment in the PM (Rupper et al., 2001; Nussinov et al., 2020). In EGF-stimulated A431 cells, PI(4,5)P₂ increases in the ruffles-forming macropinocytic cups, reaches its maximum just before macropinosome closure, and then rapidly falls as the cup closes. In contrast, PI(3,4,5)P₃ increases locally at the site of macropinosome formation and peaks at the time of closure (Araki et al., 2007). The extension of PI(3,4,5)P₃ patches, which can reach a diameter of several micrometers, reflects the balanced activity of PI3Ks and the lipid phosphatase, phosphatase and tensin homolog (PTEN), which dephosphorylates PI(3,4,5)P₃ back to PI(4,5)P₂. The kinetics of PI(4,5)P₂ and PI(3,4,5)P₃ are mechanistically linked to actin-remodeling during macropinocytosis (Araki et al., 1996, 2007; Worby and Dixon, 2014; Swanson and Yoshida, 2019; Nussinov et al., 2020) and to the regulation of many ion channels and transporters relevant to pinocytosis as well as CVR (Araki et al., 1996; Lang et al., 1998; Ritter et al., 2001; Furst et al., 2002; Jakab et al., 2002; Okada, 2004; Lang, 2007; Suh and Hille, 2008; Hoffmann et al., 2009; Abu Jawdeh et al., 2011; Lang and Hoffmann, 2012; Balla, 2013; Hansen, 2015; Hille et al., 2015; Kunzelmann, 2015; Jentsch, 2016; Pasantés-Morales, 2016; De Los Heros et al., 2018; Delpire and Gagnon, 2018; König et al., 2019; Okada et al., 2019; Centeio et al., 2020; Larsen and Hoffmann, 2020; Model et al., 2020). For cup closure, the progressive dephosphorylation of PI(3,4,5)P₃ seems to be important. Among its dephosphorylation products, PI(3)P has been shown to directly activate the Ca^{2+} -activated K^+ -channel, KCa3.1, at ruffles, which is necessary for closure (Maekawa et al., 2014). The significance of Ras activation, which peaks shortly after cup closure (Welliver and Swanson, 2012; Egami et al., 2014), as well as of the antagonistic behavior of PI3Ks and PTEN in the initiation and termination of cup formation is nicely documented by the observations that injection of Ras in cells induces ruffle formation, that inhibitors of PI3K inhibit cup closure in macrophages, and that deletion of PTEN in prostate cancer cells enhances macropinocytosis (Bohdanowicz and Grinstein, 2013; Levin et al., 2015; Kim et al., 2018; King and Kay, 2019).

Phosphatidylinositol (3,4,5)-trisphosphate enrichment promotes the translocation of the serine/threonine protein kinase Akt/PKB via binding to the pleckstrin homology (PH) domain and kinase activation by target of rapamycin complex 2 (TORC2) and 3-phosphoinositide-dependent protein kinase-1 (PDK1) (Yoshida et al., 2018; Kay et al., 2019). Among the downstream targets of Akt is the tuberous sclerosis complex 2 (TSC2), which is—together with TSC1—located on the lysosomal membrane, from which it subsequently dissociates to act as a GAP for the Ras-related small GTPase, Rheb, which in turn activates mammalian target of rapamycin complex 1 (mTORC1). In *Dictyostelium discoideum* downstream of PI(3,4,5)P₃, the homologs of mammalian Akt, Pkba, and of the related glucocorticoid-regulated kinase (SGK), Pkbr1, as well as their activating protein kinases, TORC2 and PdkA, increase the size of the macropinocytic patch

and macropinosome (Kay et al., 2019; Williams et al., 2019). Combined inhibition of mTORC1/mTORC2 induces massive catastrophic macropinocytosis, i.e., methuosis, in cancer cells (Srivastava et al., 2019). Akt and TORC2 target SGK1, which regulates a plentitude of cell functions, including ion channels and transporters (Lang et al., 2018) and endomembrane trafficking (Zhu et al., 2015). SGK transcription is stimulated by cell shrinkage *via* p38-kinase and inhibited by cell swelling due to transcriptional stop (Waldegger et al., 1997, 2000; Lang et al., 2006, 2018). Furthermore, the isoform Akt3 controls actin-dependent macropinocytosis in macrophages by suppressing the expression of with no lysine kinase 2 (WNK2) and the activity of SGK1, while increased activity of SGK1 leads to stimulation of Cdc42-mediated macropinocytosis of lipoprotein (Ding et al., 2017). However, in macrophages stimulated by macrophage colony-stimulating factor (M-CSF), the Akt pathway is induced by this growth factor but not required for macropinosome formation (Yoshida et al., 2015).

In myoblasts, an acute decrease of PM tension leads to phospholipase D2 activation, production of phosphatidic acid, F-actin and development of PI(4,5)P2-enriched membrane ruffling, and macropinocytosis without an increase in PI(3,4,5)P3 (Loh et al., 2019).

In parallel to the lipid and protein phosphorylation cascades, the cortical actin filaments are reorganized. This is controlled by PI3K and PLC, Rac, Cdc42, Arf6, Rab5, and Pak (Swanson, 2008). In the cup region, polymerized actin is seen as a ring-like structure (Hinze and Boucrot, 2018). Active Ras and PIP(3,4,5)P3 coincidentally form patches in macropinosomes, which are surrounded by a ring of the Scar/WAVE complex, an activator of the Arp2/3 complex. Arp2/3 drives actin polymerization by filament branching, leading to the formation of dendritic F-actin, which populates the wall of the cup and forms rings of protrusive actin under the PM and the circular ruffles (Swanson, 2008; Saarikangas et al., 2010; Pollard, 2016; Buckley and King, 2017; Hinze and Boucrot, 2018; Kay et al., 2019; Williamson and Donaldson, 2019). PI(3,4,5)P3 also recruits myosin proteins to macropinocytic cups (Chen et al., 2012). The synthesis of PI(3,4,5)P3 from PI(4,5)P2 occurs simultaneously with the recruitment of Rab5 to the PM in COS-7 cells expressing oncogenic H-Ras^{G12V} (Porat-Shliom et al., 2008). Rab5 promotes macropinosome sealing and scission downstream of ruffling. To this end, Rab5-containing vesicles are recruited to circular ruffles of the PM, which requires soluble N-ethylmaleimide-sensitive-factor attachment receptor (SNARE)-dependent endomembrane fusion. This is paralleled by the disappearance of PI(4,5)P2 and accompanies macropinosome closure. The removal of PI(4,5)P2 is dependent on Rab5 through its recruitment of the inositol 5-phosphatase Inpp5b/OCRL and *via* APPL1, an adaptor protein that regulates vesicle trafficking and endosomal signaling (Maxson et al., 2021). Rab5 and RN-tre, which is a Rab5-specific GAP as well as a Rab5 effector, are also recruited to the PM. RN-tre interacts with actin as well as actinin-4, which contributes to actin bundling (Lanzetti et al., 2004). The Rab5 cycle is active on nascent macropinosomes and stabilizes the macropinosomes. Rab5 activity is increased on macropinosome tubules (Feliciano et al., 2011). In BHK-21

cells, H-Ras^{G12V} has been shown to separately activate Rab5 and Rac1 *via* distinct Ras signal transduction pathways. While Rab5 activation stimulates pinocytosis, Rac1 stimulation causes membrane ruffling but does not contribute to the stimulation of pinocytosis (Li et al., 1997).

Intracellular Trafficking of Macropinosomes

In *Dictyostelium*, the nascent vesicles lose their actin coat within 1 min after pinching off and internalization (Lee and Knecht, 2002). In rat basophilic leukemia (RBL) cells, “*pinosomes... ignite a burst of actin polymerization when they are pinched off from the plasma membrane*” and “*then move into the cytosol at the tips of short-lived actin ‘comet tails,’*” which fade within 2 min after their appearance. These brief bursts of actin polymerization are thought to help move the vesicles into the cytosol (Merrifield et al., 1999). They also require recruitment of annexin-2 to nascent macropinosome membranes as an essential prerequisite for actin polymerization-dependent vesicle locomotion (Merrifield et al., 2001).

Organelle shrinkage concentrates the to-be-digested material and recycles membrane back to the PM. Macropinosomes show two routes of structural adaptations to maximize the organelle surface area and to minimize its volume: tubulation and shrinkage (Freeman and Grinstein, 2018; King and Kay, 2019; Chadwick et al., 2021b). Macropinosomes retrieve v-ATPase from fusion with other vesicles and mature toward acidic organelles that contain hydrolytic enzymes, such as proteases, nucleases, and lipases, which are required for the degeneration of macromolecules, as well as transporters facilitating the efflux of cholesterol, cystine (the disulfide form of cysteine, which is generated during protein degradation), amino acids, cobalamin, and inorganic ions (Neuhaus et al., 2002; Buckley and King, 2017; Trivedi et al., 2020).

Mobilization and maturation of macropinosomes depend on the decoration of the vesicle membrane with distinct small GTPases (Egami et al., 2014; Egami, 2016). Transient activation of ADP-ribosylation factor 6 (Arf6), a member of the Ras superfamily, by the exchange factor, EFA6, promotes PM protrusion, formation of macropinosomes, and recycling of the vesicle membrane back to the PM (Brown et al., 2001). Arf6 colocalizes and activates phosphatidylinositol 4-phosphate 5-kinase (PIP 5-kinase), which phosphorylates phosphatidylinositol 4-phosphate PI(4)P to PI(4,5)P2 (Egami et al., 2014). Subsequently, PI(4,5)P2 and Cdc42-GTP coordinate the activation of Wiskott-Aldrich syndrome protein (WASP), which promotes the actin-nucleating and actin filament-branching activity of Arp2/3 (Higgs and Pollard, 2000). The recruitment of Arf6 and its exchange factor, ARF nucleotide binding-site opener (ARNO), from cytosol to endosomal membranes relies on v-ATPase-dependent intra-endosomal acidification, thus regulating the protein-degradative pathway (Hurtado-Lorenzo et al., 2006). Persistent activation of Arf6, as seen in the GTP hydrolysis-resistant mutant Arf6^{Q67L} or by overexpression of the PIP 5-kinase, results in the accumulation of macropinosomes. Interestingly,

PI(4,5)P₂-enriched macropinosomes in apposition to each other fuse with one another and give rise to large vacuoles. Furthermore, entrapped PM proteins in these vacuoles are not recycled (Brown et al., 2001). The GTPase septin is involved in endosome fusion. Whereas septin downregulation decreases macropinosome fusion events as well as lysosomal delivery, septin overexpression increases delivery to lysosomes (Dolat and Spiliotis, 2016).

Early macropinosomes harbor Rab5 (Feliciano et al., 2011; Maxson et al., 2021), which in turn recruits the class III PI3K Vps34, which catalyzes the reaction from PI to PI(3)P (Christoforidis et al., 1999; Kerr and Teasdale, 2009). In macropinosomes routed toward lysosomes, Rab5 is replaced by Rab7 (Racoosin and Swanson, 1993; Kerr et al., 2006; Langemeyer et al., 2018; Morishita et al., 2019). In an analogy to an electrical safety-breaker, Del Conte-Zerial et al. (2008) compare the replacement of Rab5 by Rab7 as a “cut-out switch.” This model predicts that Rab5 drives Rab7 activation above a distinct threshold. Above the threshold, Rab7 shows a self-sustained activity and suppresses Rab5 activity *via* a negative feedback. In this model, crossing the Rab7 activation threshold excludes reactivation of Rab5 and activation of a different trafficking pathway. Thus, the Rab5 to Rab7 switch ensures a unidirectional route of cargo-loaded macropinosomes toward lysosomes. Using Förster/fluorescence resonance energy transfer (FRET) imaging, Morishita et al. (2019) describe that active Rab5 facilitates Rab7 activation until Rab7 sustains its own activity and inactivates Rab5. Furthermore, recruitment of amyotrophic lateral sclerosis 2 (ALS2) to the macropinosome coincides with Rab5 activation, and ALS2 detachment is associated with Rab5 inactivation (Morishita et al., 2019). In earlier studies using Texas red-labeled dextran macropinosomes, Racoosin and Swanson showed that Rab7-positive macropinosomes fuse with tubular lysosomes (Racoosin and Swanson, 1993). The fate of waste-containing vesicles is not known.

Dysfunction or inhibition of Vps34 or PIKfyve, which phosphorylates PI(3)P to PI(3,5)P₂, leads to the formation of massive and progressively exacerbating cytoplasmic vacuolization due to loss of PI(3,5)P₂. This requires active v-ATPase activity and a functional Rab5a cycle. Interestingly, the formation of the enlarged vacuoles does not require their acidification (Compton et al., 2016; Saveanu and Lotersztajn, 2016), pointing to an osmotic function of the v-ATPase. In melanoma cells, oncogenic class I PI3K elicits a hyperactive influx of macropinosomes, which is counteracted by Rab7A (Alonso-Curbelo et al., 2015). Furthermore, by stimulating RIN1, which is a Rab5 GEF, activation of H-Ras or H-Ras^{G12V} also mediates homotypic fusion of early endosomes, thus leading to endosome enlargement (Roberts et al., 2000; Tall et al., 2001).

Microtubules are associated with peripheral actin/myosin-enriched lamellae, and they are the scaffold for the unidirectional transport of macropinosomes. Critically, inhibitors of microtubule assembly, and the dynein inhibitor ciliobrevin D, decrease fluid uptake, indicating that the microtubules are involved in an early step of macropinocytosis (Williamson and Donaldson, 2019).

CELL VOLUME REGULATION

In general, cells respond to alterations of the osmotic equilibrium with a change of their volume due to water movement into or out of the cell. While an increase in intracellular or a decrease in extracellular osmolarity leads to cell swelling, a decrease in intracellular or an increase in extracellular osmolarity leads to cell shrinkage. Physiologically, such changes arise when cells invade anisotonic extracellular environments, e.g., the renal medulla, or following changes in intracellular osmolyte concentrations, such as during uptake or release of ions or nutrients, but also from metabolic changes, such as formation or degradation of macromolecules, e.g., proteins or glycogen. Likewise, perturbations of the double Donnan equilibrium, established by the so-called pump-leak balance (Okada, 2004; Kay, 2017; Kay and Blaustein, 2019), such as changes in intracellular pH (pH_i) or inhibition of the Na⁺/K⁺-ATPase by cardiac glycosides or low temperature (Russo et al., 2015), will lead to alterations of CV (for review, see Lang et al., 1998; Ritter et al., 2001; Furst et al., 2002; Jakab et al., 2002; Okada, 2004, 2020; Lang, 2007; Hoffmann et al., 2009; Kunzelmann, 2015; Jentsch, 2016; Pasantes-Morales, 2016; De Los Heros et al., 2018; Delpire and Gagnon, 2018; Okada et al., 2019; Centeio et al., 2020; Larsen and Hoffmann, 2020; Model et al., 2020).

The kinetics and degree of the actual volume changes critically depend on the water permeability of the PM, which is intrinsically low but greatly enhanced by aquaporins (AQPs) (Day et al., 2014; Kitchen et al., 2015) and also by the efficiency as well as the time of onset of CVR mechanisms. If the regulatory mechanisms [i.e., regulatory volume decrease (RVD) and regulatory volume increase (RVI); see below] have high transport efficiency and/or will start to work quickly, the degree of swelling or shrinkage will deviate from a perfect osmometer-like behavior.

When the actual CV deviates from the given set point, regulatory mechanisms are spurred, aiming at readjusting the original volume. Thus, upon swelling, cells initiate a process termed RVD (cells shrink back toward their original volume), while cell shrinkage is counteracted by RVI (cells swell back toward their original volume). The mechanisms driving the regulatory water fluxes during RVD and RVI are complex and involve rapid release or uptake of ions, amino acids, sugars, or alcohols across the cell membrane but also metabolic changes such as the formation or degradation of macromolecules to pack or unpack abundant osmotically active solutes.

Acute CVR relies on distinct sets of ion channels and transporters. The Na⁺/K⁺-ATPase actively pumps K⁺ into and Na⁺ out of the cell. K⁺ permeating through K⁺ channels generates a negative PM potential Ψ_{PM} and thus creates the driving force for the cellular exit of anions such as Cl⁻ and HCO₃⁻. Canonically, during RVD, volume-sensitive K⁺ and anion channels, KCl cotransport, or parallel activation of K⁺/H⁺ exchange and Cl⁻/HCO₃⁻ exchange is activated, while during RVI, Na⁺/H⁺ exchangers (NHEs) and Na⁺/K⁺/2Cl⁻ cotransporters (NKCCs) in parallel to Cl⁻/HCO₃⁻ exchange or Na⁺ channels are activated to release or take up ions and osmotically obliged water through AQPs. Thus, RVD is mainly accomplished *via* cellular exit of K⁺, Cl⁻, and HCO₃⁻, whereas

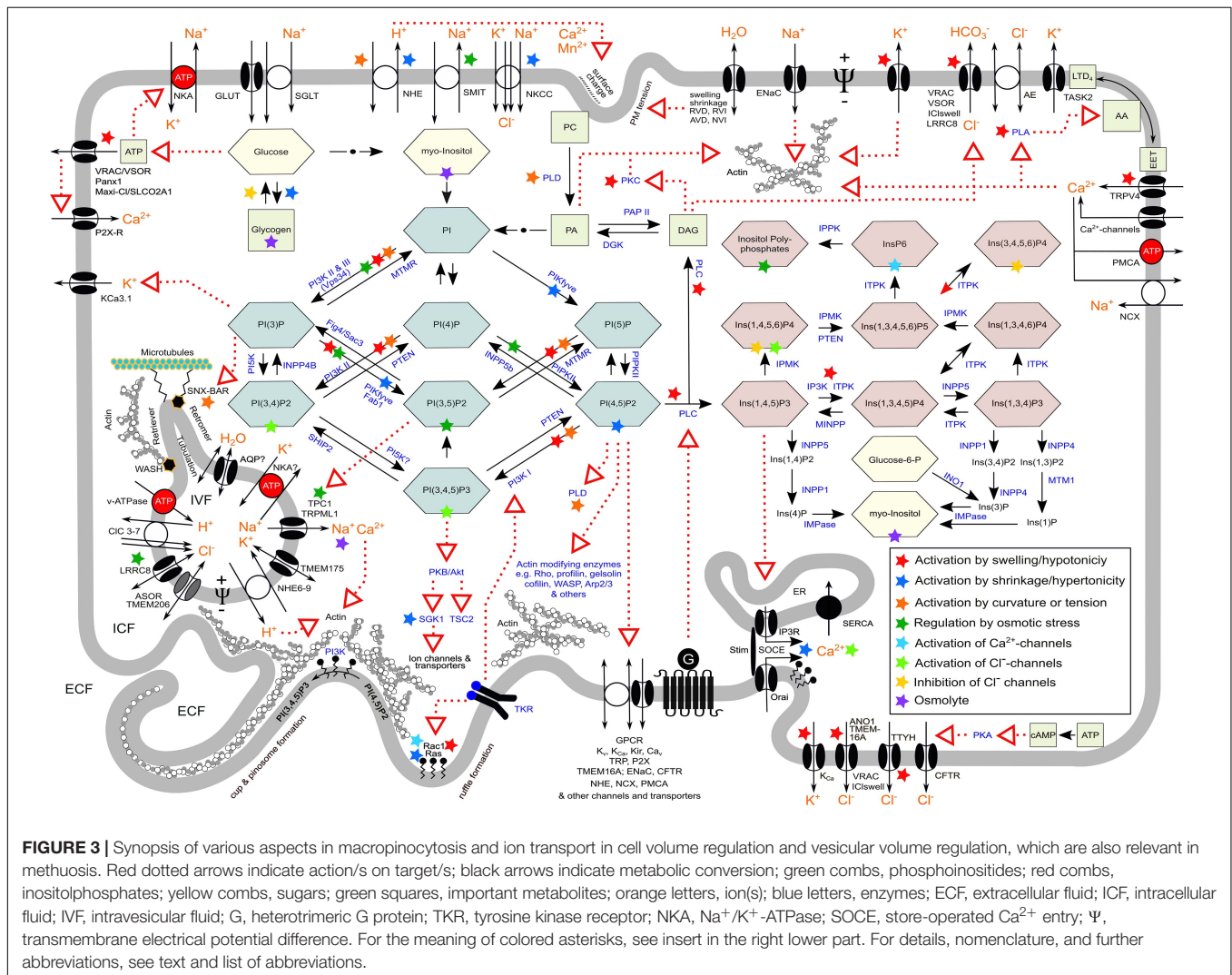
RVI is achieved by uptake of Na^+ and Cl^- . Frequently, RVD mechanisms are inhibited during RVI and *vice versa*.

Furthermore, shrunken cells can accumulate organic osmolytes such as amino acids, myoinositol, betaine, and taurine either by synthesis or by Na^+ -coupled uptake of sorbitol, glycerophosphorylcholine, and monomeric amino acids. These osmolytes are then released upon cell swelling. Though inhibition of the Na^+/K^+ -ATPase leads to cell swelling at least in some cells (Alvarez-Leefmans et al., 1992), interestingly, in certain cell types, CVR can also be performed by formation and exocytosis of vesicles even when the Na^+/K^+ -ATPase is inhibited (Russo et al., 2015).

Cell volume also greatly affects macromolecular crowding, i.e., the concentration of macromolecules (mainly proteins and nucleic acids) within the cell and hence their biological activities, which in turn has widespread consequences for cellular functions, including CVR itself (Model et al., 2020). Macromolecular crowding also induces liquid-liquid phase separation as part of the cellular osmosensing system (Ishihara et al., 2021; Watanabe et al., 2021).

As mentioned above, in myoblasts, an acute decrease of PM tension induces macropinocytosis. This was established by hypotonic swelling (stretching the PM and inducing RVD) of the cells followed by returning to isosmotic conditions (inducing cell shrinkage and PM relaxation) (Loh et al., 2019).

Both PIPs and IPs are involved in CVR. As shown in **Figure 3**, $\text{PI}(4,5)\text{P}_2$ is metabolized to $\text{Ins}(1,4,5)\text{P}_3$ and further to the various inositol (poly)phosphates (Hatch and York, 2010). Prominently, $\text{Ins}(1,4,5)\text{P}_3$ binds to its receptor on internal Ca^{2+} stores like the endoplasmic reticulum (ER) and triggers the release of Ca^{2+} into the cytosol (Berridge, 2009). Given the plentitude of cellular functions governed by Ca^{2+}_i and the numerous components of CVR dependent on it, $\text{Ins}(1,4,5)\text{P}_3$ is crucial to it. Notably, the levels of IPs are altered in Ras-transformed cells (Fleischman et al., 1986; Maly et al., 1995; Ritter et al., 1997a). Besides, other inositol (poly)phosphates are activated or inhibited by anisotonicity and/or changes in CV (Fleischman et al., 1986; Lang et al., 1998; Jakab et al., 2002; Pesesse et al., 2004; Hoffmann et al., 2009; Wundenberg and Mayr, 2012; Lee et al., 2020).



In programmed CD, cell shrinkage is characteristic (though not universal) of apoptosis and in its initial phase accomplished by RVD-like cellular exit of ions, termed apoptotic volume decrease (AVD). In contrast, cell swelling is characteristic of necrosis and ischemic cell death/onkosis (derived from the Greek word *ὄγκος*, i.e., tumor/swelling Von Recklinghausen, 1910; Majno and Joris, 1995; Weerasinghe and Buja, 2012), termed necrotic volume increase (NVI) (Okada et al., 2001; Orlov and Hamet, 2004; Lang and Hoffmann, 2012, 2013a,b; Orlov et al., 2013; Bortner and Cidlowski, 2014, 2020; Model, 2014; Okada, 2020), and related modes of CD such as secondary necrosis, pyroptosis, or ferroptosis (Zong and Thompson, 2006; D'Arcy, 2019; Nirmala and Lopus, 2020; Riegman et al., 2020). In methuosis, not only is cell shrinkage absent but cells actually are swollen (Overmeyer et al., 2008), such as seen in cells expressing an activated form of the H-Ras^{G12V} oncoprotein (see below) (Maltese and Overmeyer, 2014; Alonso-Curbelo et al., 2015). This may be related to altered ion transport in cells expressing the H-Ras oncogene.

The set point of a given cell for regulation of its volume is not a fixed constant but may change intrinsically to adjust the CV to altered functional needs. For instance, proliferating cells have to gain volume prior to mitosis, and hence, the set point for volume regulation varies in a cell cycle-dependent manner (Lang et al., 1992a, 2007; Doroshenko et al., 2001; Chen et al., 2002; Klausen et al., 2007; Pedersen et al., 2013). Expression of H-Ras^{G12V} in NIH 3T3 fibroblasts leads to an upshift of the set point for CVR, i.e., the cells swell (Lang et al., 1992a). This is related to alterations of cellular metabolism, ion transport, and structural remodeling. Such cells proliferate independently of growth factors and have altered PI metabolism (Fleischman et al., 1986; Maly et al., 1995), stimulated Ca^{2+} influx (Maly et al., 1995; Ritter et al., 1997b), and increased intracellular pH (pH_i) due to activation of NHE (Maly et al., 1989; Ritter et al., 1997b) and Na^+ , K^+ , 2Cl^- cotransport (NKCC1) (Lang et al., 1992a). Furthermore, mitogens, like serum or bradykinin, cause pulsatile release of Ca^{2+} from internal stores and activation of a store-operated calcium entry (SOCE), which leads to oscillations of Ψ_{PM} via Ca^{2+} -activated K^+ channels, NHE activation, and actin depolymerization (Lang et al., 1992b; Dartsch et al., 1994b, 1995; Ritter et al., 1997b). In NIH 3T3 fibroblasts that do not express the H-Ras oncogene, bradykinin causes a single transient hyperpolarization, is without effect on actin stress fibers, and leads to cell shrinkage, unless actin is depolymerized (Lang et al., 1992b) (for review, see Ritter and Woll, 1996). The H-Ras-induced Ψ_{PM} oscillations are stimulated by hypertonic cell shrinkage (Ritter et al., 1993) presumably via fostering physical apposition and hence interaction of STIM and Orai, which accomplish SOCE (Lang et al., 2018). In line with that, SOCE has been shown to be inhibited by cell swelling (Liu et al., 2010). Furthermore, SOCE is stimulated by hypertonicity via NFAT5 (TonEBP) (Sahu et al., 2017) and SGK1 (Lang et al., 2018). Oncogenic K-Ras^{G13D} has been shown to suppress SOCE by altered expression of STIM1 in colorectal cancer cells (Huang and Rane, 1993; Pierro et al., 2018). Interestingly, fibroblastic L cells also display spontaneous oscillations of the cell membrane

potential driven by oscillations of Ca^{2+}_i and concomitant K^+ channel activation. These oscillations are modulated by low- and high-density lipoproteins in parallel with Ca^{2+} -dependent stimulation of their pinocytosis (Tsuchiya et al., 1981; Rane, 1991; Huang and Rane, 1993). Oncogenic H-Ras also activates volume-regulated anion channels (VRACs) (Schneider et al., 2008). An inverse relationship between CV and cell number has been described for T24H-Ras (H-Ras^{G12V}) bearing Rat1 and M1 fibroblasts (Kunzschughart et al., 1995).

WATER, IONS, AND THEIR CHANNELS AND TRANSPORTERS IN PINOCYTOSIS

Extracellular Ionic Composition, Osmolarity, and Extracellular pH

The ionic composition of the extracellular fluid affects pinocytosis by modulating the surface charge of the cell membrane and the cell membrane potential. Electrostatic interactions with the [normally negative (Cevc, 1990)] outer surface charge of a cell and/or the presence of positive charges in macromolecules play an important role in the induction of pinocytosis. In *Amoeba proteus*, monovalent cations induce pinocytosis in the order $\text{Cs}^+ > \text{K}^+ > \text{Na}^+ > \text{Li}^+$, while divalent cations are less effective. Critically, Ca^{2+} and Mn^{2+} reduce the sensitivity of monovalent cations but are themselves without effects on pinocytosis (Stockem, 1966; Josefsson, 1968; Josefsson et al., 1975). Furthermore, the initial binding of pinocytosis inducers to the outer cell surface promotes displacement of surface-associated Ca^{2+} ions and induces changes in various membrane parameters, such as increased membrane conductance and decreased Ψ_{PM} along with an increase in plasmalemma hydration. Although pinocytosis in the amoeba can be induced by a great number of different solutes, all of them characteristically possess net positive charges that interact with negative surface charges. Hence, increasing extracellular Na^+ displaces most of the exchangeable surface-associated Ca^{2+} and, therefore, induces pinocytosis. In the yolk sac, cationic macromolecules lead to pinocytosis (Lloyd, 1990). In human corneal epithelial cells, fibroblasts, and human umbilical vein endothelial cells (HUVECs), the uptake of an antibody–drug conjugate by macropinocytosis is facilitated by the presence of positive charges or hydrophobic residues on the surface of the macromolecule (Zhao et al., 2018). In contrast, in mammalian macrophages, anionic molecules are better inducers of pinocytosis than neutral or cationic ones (Cohn and Parks, 1967). The uptake of positively charged nanoparticles in colon carcinoma Caco-2 cells is reduced by inhibition of macropinocytosis with 5-(*N*-ethyl-*N*-isopropyl)-amiloride (EIPA) and by cholesterol depletion of the PM, whereas these inhibitors have no effect on negatively charged systems (Bannunah et al., 2014). Modulation of the charge for intracellular delivery carriers aims at increasing the efficiency of macropinocytosis of cellular entry for therapeutic nucleic acids to tumor cells (Desai et al., 2019).

Anisotonicity modulates endocytosis in a diversity of cell types. In rat Kupffer cells, hypoosmotic and hyperosmotic conditions have been shown to stimulate and inhibit, respectively, phagocytosis (Warskulat et al., 1996), and in microglial BV-2 cells, preconditioning with hypotonic or hypertonic medium attenuates microsphere uptake (Harl et al., 2013). Hypertonic medium has been shown to disrupt the interaction of caveolae with endosomes. Increased phosphorylation due to phosphatase inhibition induces removal of caveolae from the PM. In the presence of hypertonic medium, this is followed by their redistribution to the center of the cell close to the microtubule-organizing center (Parton et al., 1994).

Only a few studies have addressed the action of anisotonicity on pinocytosis. In *Dictyostelium*, hyperosmotic conditions lead to a decrease in endocytic activity that can be attributed to cellular acidification (Pintsch et al., 2001), and it can foster the formation of giant vacuoles of pinocytotic origin, which appear to have a function in cellular osmoregulation (see above) (Yuan and Chia, 2001). In murine bone marrow-derived macrophages, hypotonic cell swelling stimulates phagocytosis and pinocytosis, both of which appear to require ClC-3 chloride channels. In this study, the ion channels have on the one hand been suggested to act as volume-activated anion channels in the PM and, on the other hand, shown to support acidification the endosomal compartment (Yan et al., 2014). Hypertonicity inhibits pinocytosis in rat hepatocytes (Synnes et al., 1999). In mouse L929 fibroblasts, cellular uptake of horseradish peroxidase is inhibited in hypertonic sucrose medium, which is reversed to stimulated uptake in the presence 10% PEG 1000 in the medium (Okada and Rechsteiner, 1982; Hughey et al., 2007). Similarly, in murine embryonic fibroblasts, cellular uptake of native proteins *via* macropinocytosis in hypertonic conditions is stimulated by alkali metal ions (Na^+ , Rb^+ , K^+ , Li^+) but not by hypertonicity created by addition of sugars or sugar alcohols. This finding points to the contribution of surface charge in macropinocytosis. Also, hypotonic stress has been demonstrated to greatly enhance receptor-independent retroviral transduction efficiency in NIH 3T3 fibroblasts *via* stimulated intensive endocytosis (Lee and Peng, 2009).

An interesting concept explaining how extracellular pH elicits such effects is that protonation of the cell surface produces local charge asymmetries across the cell membrane, which induce inward bendings of the lipid bilayer, thus favoring vesicle formation and uptake of macromolecules (Ben-Dov and Korenstein, 2012).

In dendritic cells and bone marrow-derived macrophages, extracellular acidosis improves uptake and presentation of antigens by stimulation of macropinocytosis (Vermeulen et al., 2004; Martínez et al., 2007). This effect is related to acid-sensing ion channels (ASICs) and can be inhibited by their blocker amiloride (Kong et al., 2013). As macropinocytosis depends on phospholipase C (Amyere et al., 2002; Yoshida et al., 2015), its activation by proton-sensing G protein-coupled receptors such as ovarian cancer G protein-coupled receptor 1 (OGR1/GPR68), G protein-coupled receptor 4 (GPR4), T-cell death-associated gene 8 (TDAG8/GPR65), and GPR132/G2A (Seuwen et al., 2006; Alexander et al., 2017; Insel et al., 2020) may also

explain the observed stimulatory effect of extracellular acidosis on pinocytosis. Notably, in HEK293 cells expressing mutated wild-type OGR1 or mutated OGR1^{L74P}, receptor internalization, Ca^{2+}_i mobilization, and morphological changes observed upon activation of OGR1 by H^+ or Ni^{2+} are severely compromised. This missense mutation of the H^+ ion-sensing receptor has been found to cause familial amelogenesis imperfecta (Sato et al., 2020). Experiments with HEK293 cells transfected with active OGR1 receptor or a mutant lacking five histidine residues (H5Phe-OGR1) unraveled that receptor activation by H^+ stimulates NHE- and v-ATPase activity only in OGR1- but not in H5Phe-OGR1-transfected cells. Furthermore, the known OGR1 inhibitors Zn^{2+} and Cu^{2+} reduce the stimulatory effect (Mohebbi et al., 2012). Given the importance of NHE1 and the v-ATPase for pinocytosis, it is tempting to speculate that OGR1 is a regulator thereof.

By contrast, in pancreatic acinar cells, low extracellular pH selectively impairs apical endocytosis. This is seen in mice lacking cystic fibrosis transmembrane conductance regulator (CFTR), which normally couples endocytosis at the apical PM to HCO_3^- secretion into the ductal lumen by normally rendering it alkaline. The acidic luminal fluid and impaired endocytosis due to lack of CFTR can be restored by alkalizing it *in vitro* (Freedman et al., 2001).

Ion Fluxes Drive Gel–Sol Transitions of the Cortical Actin Rim

Reorganization of the submembranous cytoskeleton is an essential step in pinocytosis. The cortical actin network is a major determinant of cell stiffness, and a correlation between stiffness of the actin network and the activity of endocytosis has been demonstrated (Planade et al., 2019). Extracellular K^+ and Na^+ antagonistically modulate the gel-to-sol transition of the cortical actin cytoskeleton beneath the PM (for review, see Oberleithner et al., 2009; Callies et al., 2011; Oberleithner and De Wardener, 2011; Warnock et al., 2014). Elevations of extracellular Na^+ and K^+ concentration stiffen and soften, respectively, the submembranous actin cytoskeleton of endothelial cells within minutes (Oberleithner et al., 2009). The Na^+ -dependent stiffening is mediated by an aldosterone-induced upregulation and activation of epithelial Na^+ channels (ENaCs) and, presumably, by downregulation of the endothelial nitric oxide synthase (eNOS) activity. Conversely, inhibition of ENaCs upregulates nitric oxide [NO; formerly termed endothelium-derived relaxing factor (EDRF)] production. Depolarizing Ψ_{PM} by increasing extracellular K^+ concentration, by blocking K^+ channels with Ba^{2+} , and by decreasing extracellular Cl^- concentration decreases the mechanical stiffness of endothelial cells (Callies et al., 2011). Thus, modulation of the sol–gel transition of the actin cytoskeleton is thought to be due to the G-actin-dependent activation of eNOS (Fels et al., 2010).

It has to be mentioned that hypotonic swelling of endothelial cells was shown to cause stiffening of the PM due to an increase in cellular hydrostatic pressure rather than to disruption of the submembranous actin network. In this study, a change in membrane tension was not observed upon osmotic swelling, and

depolymerization of F-actin did not abrogate swelling-induced stiffening of the PM (Ayee et al., 2018).

Cell Volume, Nitric Oxide, and the Cytoskeleton May Act Together in Regulating Endocytosis

In endothelial cells, a reciprocal regulatory relationship between eNOS and caveolin-1 (Cav-1) has been found, whereby Cav-1 and eNOS regulate the function of each other. On the one hand, Cav-1 stabilizes eNOS expression and regulates its activity, and eNOS-derived NO promotes caveolae-mediated endocytosis of albumin and insulin; on the other hand, a sustained NO production and persistent S-nitrosylation of Cav-1 lead to its ubiquitination and degradation (Chen et al., 2018).

Besides eNOS, also an association of inducible NO synthase (iNOS) with the submembranous actin cytoskeleton and intracytoplasmic vesicles in lipopolysaccharide (LPS)- and interferon gamma (INF γ)-stimulated macrophages and other cells was shown (Webb et al., 2001; Su et al., 2005).

Nitric oxide is a regulator of endocytosis, phagocytosis, and vesicle trafficking (Weinberg, 1998; Chen et al., 2018). For example, NO downregulates endocytosis in rat liver endothelial cells (Martinez et al., 1996) but promotes caveolae-mediated endocytosis as mentioned above (Chen et al., 2018). Macrophages stimulated by the thymic peptide thy1 display enhanced NO levels as well as increased pinocytosis (Shrivastava et al., 2004), as do amphotericin B-stimulated microglial cells (Kawabe et al., 2017). Conversely, mouse peritoneal macrophages stimulated with activin A display both reduced NO and pinocytosis (Zhou et al., 2009). Also, macropinocytosis of drugs may promote enhancement of iNOS expression, as exemplified for the chemotherapeutic nab-paclitaxel, which synergizes to this end with INF γ (Cullis et al., 2017).

Recently, it has been shown that NO regulates endocytic vesicle budding by S-nitrosylation of dynamin—a GTPase that regulates vesicle budding from the PM—and increases its enzymatic activity in response to NO (Wang et al., 2006). Dynamin is bound by NOS trafficking inducer (NOSTRIN), an eNOS-interacting adaptor protein, which forms a complex with Cav-1 and eNOS, and colocalizes with WASP and actin to promote its polymerization. It thus regulates caveolar endocytosis and eNOS internalization (Schilling et al., 2006; Su, 2014).

Nitric oxide/EDRF is also released in response to changes in extracellular osmolarity, which also greatly affect the cortical actin organization. This is also relevant in apoptosis, where NO metabolism, actin organization, and CV-regulatory ion transport are linked together (Bortner, 2005).

Nitric oxide release in response to hypertonicity occurs in vessels and endothelial cells (Steenbergen and Bohlen, 1993; Vacca et al., 1996; Zani and Bohlen, 2005). Hypertonicity downregulates eNOS in human aortic endothelial cells (HAECs), an effect that is mediated by activation of AQP1 and NHE-1, and which involves PKC β -mediated intracellular signaling (Madonna et al., 2010). In insulin-treated HAECs, hypertonicity, established by high glucose or mannitol, downregulates the PI3K/Akt/mTOR/eNOS pathway and impairs their ability to

respond to insulin. This may contribute to insulin resistance. The mechanism involves AQP1 and the transcription factor Ton/EBP (NFAT5) for osmosensing, and the effect can be reversed by silencing the transcription of these proteins (Madonna et al., 2020).

Hypotonic swelling has been shown to promote the release of NO and reactive nitrogen oxide species in various cells (Kimura et al., 2000; Haussinger and Schliess, 2005; Takeda-Nakazawa et al., 2007; Kruczek et al., 2009; Gonano et al., 2014) and to augment LPS-triggered iNOS expression in RAW 264.7 macrophages (Warskulat et al., 1998). Recently, it has been shown that in HUVECs, VRAC/SWELL1/LRRC8A mediates endothelial cell alignment *via* stretch-dependent Akt-eNOS signaling and formation of a signaling complex made up by Grb2, Cav-1, and eNOS (Alghanem et al., 2021).

While osmotic shrinkage in general is associated with an increase in actin polymerization, cell swelling leads to its depolymerization, though both with exceptions (Hoffmann et al., 2009).

Hypertonic shrinkage fosters the translocation of the actin-binding protein cortactin to the cortical actin net, where it interacts with the Arp2/3 complex, WASP, dynamin, and myosin light-chain kinase (for review, see Pedersen et al., 2001; Hoffmann et al., 2009). Cortactin stabilizes microfilament assembly at the cell periphery, is recruited to PM ruffles, and participates in macropinocytosis (Mettlen et al., 2006). In human-induced pluripotent stem cells, hyperosmolarity, created by high glucose or mannitol, upregulates AQP1 and induces cytoskeletal remodeling with increased ratios of F-actin to G-actin, effects that could be by reversed siRNA-mediated inhibition of AQP1 expression (Madonna et al., 2014).

Cell swelling can lead to reorganization of intermediate filaments (Dartsch et al., 1994a; Li J. et al., 2019). In Cos-7 fibroblast-like cells, hypotonicity causes a rapid calcium/calpain-dependent cleavage of the intermediate filament vimentin, whereby hypotonicity leads to the generation of IP $_3$ by hydrolysis of PI(4,5)P $_2$ and Ca $^{2+}$ release from the ER (Pan et al., 2019). Vimentin in turn is involved in the regulation of vesicular trafficking (Margiotta and Bucci, 2016) and was also shown to be modulated by NO (Sripathi et al., 2012).

Na $^+$ /H $^+$ Exchangers and Pinosome Formation

A distinctive hallmark to distinguish clathrin-dependent endocytosis from clathrin-independent macropinocytosis is the sensitivity of the latter to inhibitors of NHEs such as amiloride, EIPA, or HOE-694 (West et al., 1989; Koivusalo et al., 2010; Canton, 2018; Lin et al., 2020). Besides NHEs, amiloride also directly inhibits ion channels of the epithelial sodium channel/degenerin family, such as ENaC and ASIC1 (Kellenberger and Schild, 2002; Qadri et al., 2010) and growth factor receptor tyrosine kinase activity (Davis and Czech, 1985). Moreover, amiloride is a weak permeant base that can accumulate in acidic vesicles, thus, eventually dissipating the H $^+$ -gradient driving cation exchange, and thereby inhibiting pinocytosis (Dubinsky and Frizzell, 1983; Bakker-Grunwald et al., 1986).

Of note, EIPA does not inhibit a newly described form of CD, which is induced by fenretinide, which is similar to methuosis characterized by hyperstimulated macropinocytosis and massive vacuolization (Brack et al., 2020).

Na^+/H^+ exchangers, which are members of the solute carrier (SLC) 9 family, are electroneutral transporters that exchange Na^+ for H^+ across membranes (Pedersen and Counillon, 2019). The NHE1 isoform is expressed almost ubiquitously and regulates cellular and organelle pH, motility, phagocytosis, proliferation, as well as cell survival and CD (Orlowski and Grinstein, 2011; Pedersen and Counillon, 2019). Cell shrinkage is a strong stimulator of NHE1 activity and serves for RVI (see above) (Ritter et al., 2001; Baumgartner et al., 2004; Orlowski and Grinstein, 2011; Pedersen and Counillon, 2019). NHE1 is activated by a drop in pH_i , a broad diversity of PM receptors, such as tyrosine kinase receptors, G-protein-coupled receptors or integrin receptors, and it is regulated by second messengers, asymmetric membrane tensions, and phosphoinositides, such as $\text{PI}(4,5)\text{P}_2$ (Orlowski and Grinstein, 2011; Pang et al., 2012; Pedersen and Counillon, 2019). In proximal tubular cells, NHE1 is activated by $\text{PI}(4,5)\text{P}_2$ and inhibited by $\text{PI}(3,4,5)\text{P}_3$ (Abu Jawdeh et al., 2011; Pang et al., 2012). NHE1-borne changes in pH_i may also be confined to distinct subcellular domains or compartments. Such subcellular compartments are the lamellipodia formed during cell spreading and migration, pseudopodia in phagocytosis, ruffles and the cup wall formation in macropinocytosis. In all of these processes, NHE1 is also involved in cytoskeletal rearrangement (Schwab and Stock, 2014; Pedersen and Counillon, 2019). NHE1 is connected to actin via ezrin/radixin/moesin (ERM) family of actin-binding proteins. Migrating cells undergo cell polarity-dependent subcellular volume changes. Repetitive cycles of protrusion at the leading edge (lamellipodium) are followed by retraction of the cell's rear, i.e., the trailing edge. Waves of local water movement across the PM locally increase and decrease CV during the protrusion and retraction of the lamellipodium, respectively. Hence, cell migration requires an alternating cycle of subcellular RVI at the leading edge and RVD at the trailing edge of the cell. Most of the ion transporters known to participate in CVR are also involved in the regulation of cell migration. As part of the RVI transporters, NHE1 is confined to the lamellipodium, where it also serves for local extracellular acidification (Lang et al., 1998; Schneider et al., 2000; Loitto et al., 2002, 2009; Jakab and Ritter, 2006; Hoffmann et al., 2009; Schwab et al., 2012; Stock et al., 2013). This is also given in breast cancer cell invadopodia, where NHE1 is allosterically regulated by NaV1.5 Na^+ channels (Brisson et al., 2012, 2013). In T47D human breast cancer cells, NHE1 colocalizes with Akt and ERK in prolactin-induced ruffles (Pedraz-Cuesta et al., 2016).

Although inhibition of macropinocytosis by NHE inhibitors is a fingerprint feature of macropinocytosis, the molecular mechanisms how NHEs contribute to macropinocytosis are barely known. Interestingly, activation of the small GTPases, Rac1/Cdc42, and consequently actin polymerization and, thus, ruffle formation are sensitive to submembranous pH (pH_{sm}). Submembranous acidification due to inhibition of NHE1 by amiloride prevents Rac1/Cdc42 activation and suppresses actin

polymerization (Koivusalo et al., 2010). Moreover, NHE1 inhibition favors the accumulation of cytosolic H^+ , which neutralizes the negative charges on the inner leaflet of the PM. Thus the interaction of the negatively charged headgroups of phosphoinositides and the polybasic motifs in Rac and Cdc42 as well as the SCAR/WAVE complex and WASP is hampered. This also explains the inhibitory effect of NHE1 blockers on macropinocytosis (Marques et al., 2017). Therefore, amiloride might not directly inhibit macropinocytosis but cause submembranous accumulation of metabolically generated H^+ in thin lamellipodium-like membrane extensions by inhibition of H^+ efflux. Given the small volume of these structures, only a few H^+ will change pH_{sm} and, consequently, the state of actin polymerization. However, in HeLa cells, oncogenic Ras-induced macropinocytosis does not require a decrease in pH_{sm} (Ramirez et al., 2019).

Notably, in mice bearing xenograft tumors derived from oncogenic K-Ras bearing MIA PaCa-2 cells, intratumoral macropinocytosis and tumor growth are suppressed by treatment of the animals with EIPA, which is, however, effective only in tumors with high but not low macropinocytic activity (Commisso et al., 2013; Recouvreux and Commisso, 2017).

The ionophoric NHE monensin induces vesicular swelling and the formation of giant multivesicular bodies (MVBs) (Stein and Sussman, 1986; Savina et al., 2003) and release of exosomes, which can be inhibited by the NHE inhibitor dimethyl amiloride (DMA) (Chalmin et al., 2010; Pironti et al., 2015). Moreover, deletion of the *Saccharomyces cerevisiae* NHE, Nhx1, disrupts the fusogenicity of the MVB in a manner dependent on pH and monovalent cation gradients (Karim and Brett, 2018).

The Ion Composition in Macropinosomes and Endolysosomal Vesicles

After pinching off, the nascent macropinosome has entrapped extracellular fluid that equals the extracellular fluid in the intimate vicinity of its formation site. Traveling along the endolysosomal pathway, its ionic composition is modified to render the vesicular volume, shape, and fluid suitable for processing its cargo, as shown in Table 1 (Scott and Gruenberg, 2011; Freeman and Grinstein, 2018; Chadwick et al., 2021b).

Water Permeability, Aquaporins, and Osmolarity

The permeabilities of the PM and vesicular membranes for water play crucial roles in pinocytosis. The importance of PM AQP for macropinocytosis is seen in dendritic cells where they are needed as essential elements of a CV control mechanism necessary to concentrate the macrosolutes and present antigens (De Baey and Lanzavecchia, 2000; Hara-Chikuma et al., 2011; Kitchen et al., 2015).

Macropinosomes shrink along their cellular route by moving ions and osmotically obliged water out of its lumen into the cytosol (Freeman and Grinstein, 2018; Chadwick et al., 2021b). Despite the dramatic decrease in pinosome volume, the water permeation pathway is not characterized yet. Studies on osmotic water permeability (Pf) indicate that Pf values higher than

0.01 cm/s indicate water flux through channels (Verkman et al., 1996), Pf values in the range from 0.003 to 0.005 cm/s designate membranes lacking water channels, and Pf values between 0.0001 and 0.005 cm/s characterize pure phospholipid bilayers (Fettiplace and Haydon, 1980; Echevarria and Verkman, 1992; Olbrich et al., 2000). These values could be used to evaluate the presence or absence of water channels in endosomes.

Clathrin-coated vesicles from bovine brain that lack water channels have a low Pf of ~ 0.001 cm/s and retain this value after stripping off the coat. Vesicles prepared from bovine renal cortex and inner medulla revealed two populations: one containing water channels with high (0.02 cm/s) and one lacking them with low values compared to brain-derived vesicles (Verkman et al., 1989). Vasopressin-induced endosomes of rat kidney papilla and toad bladder endocytic vesicles have Pf values of 0.03 and >0.1 cm/s, respectively, whereas isolated toad bladder granules have a Pf value as low as 0.0005 cm/s (Verkman and Masur, 1988; Verkman et al., 1988; Shi and Verkman, 1989; Verkman, 1989).

Only a few studies have investigated Pf of pinosomes and lysosomes. In J774 macrophages, the Pf of the PM is in the range of ~ 0.004 – 0.009 cm/s (Fischbarg et al., 1989; Ye et al., 1989; Echevarria and Verkman, 1992). The water permeability of the macropinosome membrane of J774.A1 cells increases non-linearly from ~ 0.001 cm/s 3 min after formation to ~ 0.005 cm/s after 25 min of formation (Chaurra-Arboleda, 2009). The lysosomal Pf of CHO-K1 cells is in the same range (Chaurra et al., 2011). In J774.A1 cells, Pf shows pH dependency. It decreases from ~ 0.007 to 0.0009 cm/s following lysosomal alkalization with NH_4Cl (pH_{lys} 6.5–6.8) and to 0.0001 cm/s after inhibition of the v-ATPase (pH_{lys} ~ 7.0). These values are similar to those in early macropinosomes, which have a pH of ~ 6.7 (Chaurra-Arboleda, 2009). Taken together, the low Pf values of J774 macrophages indicate the absence of AQPs in the endolysosomal compartment.

Despite these specific observations, the role of AQPs in the endolysosomal compartment is poorly investigated, while their importance in volume regulation of secretory vesicles is well documented (Cho and Jena, 2006; Sugiya et al., 2008; Jena, 2020). In toad urinary bladder endosomes, AQP-TB has been shown to be present (Siner et al., 1996), and incorporation of PM-derived AQP2 into endosomes is well known for AVP-stimulated renal collecting duct principal cells (Shi and Verkman, 1989; Verkman, 2005). In astrocytes, AQP4-laden vesicles may fuse with the PM upon cell swelling (Potokar et al., 2013; Vardjan et al., 2015). AQP6 was shown to be present in intracellular vesicles of acid-secreting intercalated cells of the renal collecting duct where it colocalizes with the H^+ -ATPase and serves also as an anion channel (Yasui et al., 1999; King et al., 2004). Lack of AQP11 causes defective endosomal pH regulation, as seen in mice devoid of AQP11. This is accompanied by the appearance of huge vacuoles in the renal proximal tubules and polycystic kidneys (Ishibashi et al., 2009).

An example for the function of organellar AQPs in VVR and CVR is evident in *Trypanosoma cruzi*, as briefly described below.

Alternatively to AQPs, water permeation through transporters and ion channels has been described for glucose transporters (Loike et al., 1993; Fischbarg and Vera, 1995), NKCC1, KCC,

SGLT1, and CFTR (Hamann et al., 2010; Zeuthen, 2010; Zeuthen and Macaulay, 2012; Huang et al., 2017). Eventually, these transporters or ion channels could be used in pinosomes for water efflux as well.

By whatever way, as upon hypertonic cell shrinkage also vesicles rapidly shrink, it can be deduced that the intrinsic water permeability is sufficiently high to allow for timely vesicular volume changes during resolution of macropinosomes (Freeman and Grinstein, 2018). Using fluorescence enhancement of Lucifer yellow dextran by deuterated water, Li et al. (2020) have recently demonstrated that lysosomes rapidly swell in response to a hypoosmotic challenge, indicating that there is substantial water influx into the lumen of lysosomes soon after water penetration across the PM, again indicating that the intrinsic water permeability of these organelles is high.

Vesicular pH Regulation and Ions in Pinosome Maturation

The pH of the ingested fluid of nascent pinosomes resembles that of the extracellular fluid, which is under physiological conditions (7.4). During trafficking, vesicular pH (pH_{ves}) gradually decreases to the value prevailing in lysosomes, i.e., 4.5–5.0. pH_{ves} regulates enzyme activities and enables oxidation reactions, the release of internalized receptors from their ligands and their recycling back to the PM, movement and assembly of organellar surface coat proteins, vesicle maturation, as well as membrane fusion processes (Demaurex, 2002; Ohgaki et al., 2011).

Vacuolar ATPase

The acidification is primarily achieved by insertion of the v-ATPase. The v-ATPase is an evolutionarily highly conserved primary active H^+ transporter. As already outlined, it can be found both in the PM and in various intracellular organelles. Structurally, it comprises a multiprotein complex that forms two distinct domains, i.e., the pore-forming transmembrane V_0 domain and the cytosolic V_1 domain. The latter hydrolyzes ATP to drive H^+ movement. This creates the electrochemical H^+ gradient across the membrane, thereby driving secondary active transport processes, which act together for proper adjustment of pH_{ves} and vesicular ion and osmolyte composition. In particular, parallel to H^+ pumping, ion channels and transporters move Cl^- , H^+ , and other cations to establish an electrical shut aiming for electroneutrality of the net charge transfer. Otherwise, the acidification would be limited by the transmembrane potential Ψ_{ves} , which is set up by the v-ATPase itself (Demaurex, 2002; Steinberg et al., 2010; Koivusalo et al., 2011; Xiong and Zhu, 2016; Freeman and Grinstein, 2018; Jentsch and Pusch, 2018; Sterea et al., 2018; Li P. et al., 2019; Freeman et al., 2020; Chadwick et al., 2021a). pH_{ves} is stabilized by the buffering capacity of the vesicle content (~ 60 mM/pH at pH 4.5–5) (Weisz, 2003; Steinberg et al., 2010).

In addition, the v-ATPase also serves as a protein interaction hub. For the proper sorting and targeting of the vesicles, small GTPases are recruited to their membranes in an acidification-dependent manner. The v-ATPase itself is able to associate with some of them and with other regulatory proteins. Thus, the v-ATPase seems not only to serve for creating the acidic pH_{ves} but

also to sense it and to transmit this information to its cytoplasmic domain, thus enabling trafficking molecules to bind and perform their targeting functions. The v-ATPase is also involved in signaling pathways for the regulation of macropinocytosis, as outlined throughout this review. Its dysfunction may play critical roles in various diseases including diabetes, cancer, neurodegeneration, osteopetrosis, skin disorders, or renal tubular acidosis and other pathologies. Furthermore, it is also essential for viral entry into cells (for reviews on v-ATPase, see Nishi and Forgac, 2002; Platt et al., 2012; Maxson and Grinstein, 2014; Rappaport et al., 2016; Kissing et al., 2018; Futai et al., 2019; Collins and Forgac, 2020; Song Q. et al., 2020; Vasanthakumar and Rubinstein, 2020; Chadwick et al., 2021a,b; Eaton et al., 2021).

Cl⁻ Ions

Within 1 min after internalization, the luminal Cl⁻ concentration in endosomes/macropinosomes drops from ~120–150 mM to ~20 mM (Sonawane et al., 2002). This decrease is insensitive to Cl⁻ channel inhibition and can be attributed to Cl⁻ expulsion by an interior negative Donnan potential (Ohshima and Ohki, 1985; Sonawane and Verkman, 2003; Hryciw et al., 2012). During maturation, the vesicular Cl⁻ concentration increases again up to ~130 mM in lysosomes (Saha et al., 2015). The Cl⁻ accumulation of late endosomes can be suppressed by inhibition of the v-ATPase and restored by the K⁺ ionophore valinomycin. Also, replacement of Cl⁻ by gluconate and Cl⁻ channel inhibition slow endosomal acidification. Thus, Cl⁻ is an important counter ion accompanying endosomal acidification (Sonawane and Verkman, 2003) (for review, see Faundez and Hartzell, 2004; Stauber and Jentsch, 2013). The accumulation of lysosomal Cl⁻ appears to be important for the adjustment of the lysosomal volume and the activity of proteases. Reduced lysosomal Cl⁻ concentrations may lead to lysosomal storage diseases, e.g., Gaucher's disease (OMIM entries 230800, 230900, 231000) or Nieman–Pick's disease (OMIM entries 257200, 607616, 257220, 607625) (Cigić and Pain, 1999; Platt et al., 2012, 2018; Stauber and Jentsch, 2013; Rappaport et al., 2016; Chakraborty et al., 2017; Astaburuaga et al., 2019).

The Cl⁻ channels and transporters expressed in intracellular organelles include the ClC family members ClC-3 through 7, chloride intracellular channels (CLICs), CFTR, AQP6, transmembrane proteins (TMEM)16C–G/anoctamin (ANO) 3–7, bestrophin-1, Golgi pH regulator (GPHR) (reviewed in Stauber et al., 2012; Stauber and Jentsch, 2013), Tweety homolog 1 (Ttyh1) proteins (Wiernasz et al., 2014), LRRC8 (Li et al., 2020), and TMEM206 (Osei-Owusu et al., 2021).

The ClC-3 to 7 transporters are confined to distinct endolysosomal compartments with partially overlapping appearance (Jentsch and Pusch, 2018). They are electrogenic outwardly rectifying 2Cl⁻/H⁺ exchangers working in parallel with the v-ATPase. As per exchange cycle, two Cl⁻ enter and one H⁺ leaves the vesicle, three negative charges accumulate in the vesicle. To maintain electroneutrality, three H⁺ are pumped in, one of which leaves the vesicle again *via* the 2Cl⁻/H⁺ exchanger, thus leading to a net uptake of two H⁺ (Guzman et al., 2013;

Jentsch and Pusch, 2018). This proposed mechanism allows a more efficient H⁺ and Cl⁻ accumulation, as it generates a more inside-negative Ψ_{ves} than an ohmic Cl⁻ conductance could do. Yet, this mechanism may be restricted to ClC-5 (Zifarelli, 2015). However, Ψ_{ves} is generally thought to be negative (i.e., positive in the lumen) due to the rheogenic v-ATPase. The reason for this discrepancy is still elusive (Weinert et al., 2010) (reviewed in Jentsch, 2007; Stauber et al., 2012; Stauber and Jentsch, 2013; Jentsch and Pusch, 2018). Dysfunctional ClC exchangers may lead to a broad variety of symptoms and disorders including neurodegeneration and other neuropathies, proteinuria and kidney stones, osteopetrosis, albinism, and lysosomal storage diseases (Jentsch and Pusch, 2018; Nicoli et al., 2019; Schwappach, 2020; Bose et al., 2021). Overexpression of ClC-3 or gain-of-function mutations of ClC-6 or ClC-7/Ostm1 leads to swelling of late endosomes and lysosomes (Li et al., 2002; Nicoli et al., 2019; Polovitskaya et al., 2020). In B-cell non-Hodgkin lymphoma cells, the PIKfyf inhibitor apilimod leads to CD by formation of giant vacuoles and disruption of endolysosomal function, an effect that requires functional ClC-7/Ostm1 transporters (Gayle et al., 2017). In HeLa and NIH3T3 cells, a short natural ClC3 splice variant (Clc3s) has been shown to lead to the formation of large vacuoles (Wu et al., 2016), and in Chinese hamster ovary CHO-K1 or human hepatoma Huh-7 cells, the volume of such vesicles is governed by their Cl⁻ concentration (Li et al., 2002).

Endothelial cells lacking CLIC4 display defective endothelial cell tubulogenesis and impaired acidification of large intracellular vesicles, while lysosomes are unaffected (Ulmasov et al., 2009).

Previous work showed that cell swelling leads to alkalinization of acidic cellular vesicles, regardless whether the cells are swollen by hypotonicity, isoosmotically with high-K⁺ solutions, inhibition of K⁺ channels, or concentrative uptake of solutes such as amino acids. At least in liver cells, swelling-induced alkalinization occurs rather in the pre-lysosomal than lysosomal compartments. The increased pH_{ves} affects proteolysis, trafficking of cell membrane proteins, and antigen presentation (Busch et al., 1994, 1996, 1997; Völkl et al., 1994). The mechanisms leading to swelling-induced rise of pH_{ves} are still elusive. Interestingly, overexpression of a naturally occurring C-terminally truncated splice variant of mouse bestrophin-3, Best3V2, leads to, besides swelling, alkalinization of lysosomes (Wu et al., 2016). Manipulation of the intracellular Cl⁻ concentration leads to alterations of lysosomal volume due to the high ClC-3-endowed Cl⁻ permeability. Accordingly, a decrease in intracellular Cl⁻ concentration during RVD following cell swelling could alter pH_{ves}. In H-Ras oncogene-expressing fibroblasts, which have a higher CV (see above), the swelling-induced vesicular alkalinization is less pronounced compared to cells not expressing the oncogene. Hence, in H-Ras-expressing cells, any effect of the swelling-induced vesicle alkalinization on cell function may be altered (Busch et al., 1997). Notably, murine and human fibroblasts expressing oncogenic K-Ras also display significant alkalinization of lysosomes (Jiang et al., 1990).

In several cell types, the fusion of late endosomes to lysosomes is prevented by isotonic K⁺ buffers as a consequence of an increased permeability of cells to K⁺ and concomitant cell

swelling. This inhibition is selective for late endosomes, since other endosome fusion events, such as homotypic fusion of early or late endosomes or fusion of recycling endosomes with the PM, are not affected. Cell swelling is regarded to be causative for this effect (Ward et al., 1990). As cell swelling and lack of fusion of endosomes to lysosomes are also hallmarks of methuosis (see below and **Figure 2**), it is tempting to speculate that cell swelling in methuosis might not only be a passive consequence of swollen vacuoles but also be a cause of it.

A link between CVR and vacuolar pH regulation is also established by the proteins MLC1 and GlialCAM, which are defective in megalencephalic leukoencephalopathy with subcortical cysts. This rare congenital disease is characterized by macrocephaly, ataxia, seizures, degeneration of motor functions, and cognitive decline, morphologically by chronic white matter edema and subcortical cysts, and on the ultrastructural level by intra-myelinic vacuole formation and enlarged intracellular vacuoles (Van Der Knaap et al., 2012). The protein MLC1 is involved in astrocytic CVR. It may be a volume-sensitive ion channel itself, but it is also part of a macromolecular complex composed of the Na^+/K^+ -ATPase, Kir4.1 K^+ -channels, AQP4, syntrophin, and caveolin-1, as well as volume-sensitive TRPV4 cation channels, which mediate cellular Ca^{2+} influx upon cell swelling. In addition, MLC1 also influences CLC-2 chloride channels as well as the volume-sensitive anion channel(s)/current(s) (VRACs) and therefore also RVD. It has been shown that knockdown of LRRC8 annihilates the potentiating effect of MLC1 on VRAC currents *via* modulation of the phosphorylation state of the channel subunit LRRC8C (Elorza-Vidal et al., 2018). GlialCAM serves as an escort protein for MLC1 and CLC-2, and it is necessary for its proper activation by cell swelling. MLC1 is expressed in early and recycling endosomes, which they use to travel to the PM during hypotonic stress (Capdevila-Nortes et al., 2013). Importantly, MLC1 also interacts with the v-ATPase, and it is involved in regulating early endosomal pH (Lanciotti et al., 2012). Defective MLC1 may result in impaired recycling and retention of TRPV4 channels in the cytoplasmic perinuclear area and thus disturbed swelling-induced cellular Ca^{2+} influx (Lanciotti et al., 2012) such as seen in monocyte-derived macrophages from MLC patients (Ridder et al., 2011; Petrini et al., 2013; Brignone et al., 2014, 2015; Elorza-Vidal et al., 2018). Furthermore, CLC-2 knockout mice exhibit myelin vacuolization, which is thought to arise from dysregulation of extracellular ion concentrations (Stauber et al., 2012). Moreover, CLC-2 channels are functionally regulated by SGKs by inhibiting the ubiquitin ligase Nedd4-2, which in turn results in reduced clearance of CLC-2 protein from the PM (Palmada et al., 2004). As outlined above, SGK1 is involved in the regulation of macropinocytosis, and hence, both CLC-2 and SGKs may be tight together in the regulation of macropinocytosis.

The acid-activated outwardly rectifying chloride channel/current (ASOR; also termed proton-activated, outwardly rectifying anion current, PAC, PAORAC; or $I_{\text{Cl,H}}$) could be a candidate to serve as electrical shut for endolysosomal acidification. This anion channel or its core component is made up by TMEM206 proteins, which form a trimeric channel that is architecturally related to ENaCs/degenerin channels and

ASICs (Ullrich et al., 2019; Ruan et al., 2020; Deng et al., 2021). TMEM206 has been shown to interact with Akt (Zhao et al., 2019) and to contribute to acid-induced CD (Osei-Owusu et al., 2020). The ASOR current is characterized by activation at pH values < 5.0 , strong outward rectification, activation at positive transmembrane potentials, and sensitivity to typical Cl^- channel blockers (Sato-Numata et al., 2013, 2017; Kittl et al., 2019, 2020; Ullrich et al., 2019). In contrast to CLCs, which are inhibited by extracellular/luminal acidic pH (Scheel et al., 2005; Jentsch, 2007; Jentsch and Pusch, 2018), ASOR is activated by it. Accordingly, endosomal ASOR and CLCs could regulate Ψ_{ves} and vesicular ion concentrations. TMEM206 is mainly localized in the PM, but variable cytoplasmic labeling has been documented (Ullrich et al., 2019). Recently, it has been shown that TMEM206 indeed traffics from the PM to endosomes. Its deletion annihilates the endosomal Cl^- conductance, raises the luminal Cl^- concentration, lowers pH_{ves} , and increases transferrin receptor-mediated endocytosis. Moreover, its overexpression generates a large endosomal Cl^- current with properties resembling the endogenous conductance and reduces endosomal acidification as well as transferrin uptake. Thus, endosomal TMEM206 appears to function as a sensor for low pH and may prevent hyperacidification by releasing Cl^- from the lumen (Osei-Owusu et al., 2021). Clearly, the role of TMEM206/ASOR/PAORAC in the regulation for Ψ_{ves} and pH_{ves} warrants further investigations. Likewise, its role in VVR needs to be investigated.

LRRC8A-E/SWELL1 proteins are essential components of the volume-regulated outwardly rectifying Cl^- current (VRAC, VSOR, VSOAC, $\text{ICl}_{\text{swell}}$, ICl_{vol}) elicited in most cells during cell swelling (Qiu et al., 2014; Voss et al., 2014; Jentsch, 2016; Jentsch et al., 2016; Okada, 2020; Bertelli et al., 2021), and they are involved in a broad variety of cellular functions (Chen et al., 2019). LRRC8A-E/SWELL1 also regulate the PI3K-Akt, Erk1/2, mTOR signaling cascade (Kumar et al., 2020; Alghanem et al., 2021). Recently, Li et al. (2020) demonstrated the expression of LRRC8 family members on lysosomal membranes and their ability to build functional lysosomal VRACs (Lyso-VRACs). Patch clamp investigation of these vacuoles revealed that Lyso-VRACs are activated by ionic strength and permeable for anions, like Cl^- , NO_3^- , HCO_3^- , acetate, aspartate, or glutamate. They are inhibited by known VRAC blockers. Early endosome membranes lack Lyso-VRACs. Hypotonic swelling promotes the formation of large cytoplasmic vacuoles containing markers for late endosomes and lysosomes with a diameter of $>2 \mu\text{m}$, which require functional Lyso-VRACs. Loss of VRAC channels enhances necrotic CD triggered by sustained hypotonic, hypoxic, and hypothermic stress. Furthermore, the authors demonstrated that endolysosome-derived giant vacuoles are subject to exocytosis. This releases PM tension and simultaneously reduces CV. Thus, by acting as water store-and-release compartments, the swelling-induced giant vesicles have been compared to the “cell’s ‘bladder,’ sequestering intracellular excess water through vacuolation and then expelling the potentially toxic level of water through exocytosis, which also relieves the plasma membrane tension stress” (Li et al., 2020).

AQP6 is activated by low pH and acts as Cl^- channel in acid-secreting α -intercalated cells in renal collecting ducts. There

it is found in endosomes where it colocalizes along with ClC-5 and the v-ATPase. However, ClC-5 is inhibited at acidic pH, whereas the anion conductance of AQP6 is turned on. Hence, ClC-5 may rather operate when acidification of the vesicles starts, whereas AQP6 may take over this role as their pH drops. Furthermore, AQP6, though its water permeability is low, may mediate vesicle swelling and membrane fusion during exocytosis or other cellular processes (Yasui et al., 1999; Hazama et al., 2002; Kitchen et al., 2015).

HCO₃⁻ Ions

The role of HCO₃⁻ in pinocytosis has not met much attention yet. Carbonic anhydrase (CA) catalyzes the dissociation of HCO₃⁻ to generate H⁺ of CO₂. CA isoforms are present at the PM, in the cytosol, and in lysosomes (Rikihisa, 1985; Reibring et al., 2014). There they associate with numerous acid-base transporters such as anion exchangers 1-3 (AE1-3), sodium bicarbonate cotransporters NBCe1 and NBCn1, and NHE1 (Becker et al., 2014). Recently, Sedlyarov et al. (2018) found that electroneutral NBCn1 (NBC3, SLC4A7) is essential for phagosome acidification in macrophages. NBCn1 resides in the PM, and lack of it leads to cytoplasmic acidification, which in turn hampers phagosome maturation and impairs bacterial killing. If membrane-associated CA is internalized during the formation of the pinosomes, it will catalyze the dissociation of HCO₃⁻ to generate CO₂, which in turn will rapidly equilibrate across the vesicular membrane. Notably, in global CVR, VRAC may actually work more effectively in driving RVD by passing HCO₃⁻ than Cl⁻, as the former can be virtually unlimitedly replenished from CO₂ in the presence of CA, whereas Cl⁻ can only exit the cell as long as the Ψ_{PM} is more negative than the equilibrium potential for this ion (Völkl and Lang, 1988; Ritter et al., 1991). In line with these considerations, the VRAC channels made up of LRRC8A with B through E subunits are permeable to HCO₃⁻ (Gaitan-Penas et al., 2016). Hence, Lyso-VRAC may provide a vesicular HCO₃⁻-conductive pathway as well.

Na⁺ Ions

Among the internalized ion transporters, the Na⁺/K⁺-ATPase may limit endosomal acidification. Its rheogenic Na⁺ transport contributes to the $\Psi_{vesicle}$ of endosomes, thereby opposing H⁺ transport. This is, however, only evident in early but not in late endosomes (Fuchs et al., 1989). In line with this, it has been shown in Swiss 3T3 fibroblasts that inhibition of the Na⁺/K⁺-ATPase by ouabain strongly enhances the acidification of early but not late endosomes or lysosomes. Ouabain has also been shown to produce stronger endosomal acidification and parallel Cl⁻ accumulation in transferrin-labeled early and recycling endosomes of J774 cells (Sonawane and Verkman, 2003). Ouabain exerts its effect by acting on the interior side of the vesicles rather than on the PM (Zen et al., 1992). In contrast, in early rat liver endosomes, the Na⁺/K⁺-ATPase does not regulate acidification (Anbari et al., 1994).

Whether internalized PM retrieved NHE1 contributes to pinosomal acidification remains to be determined. According to the prevailing Na⁺ gradient between the lumen and the cytosol, NHEs should serve to acidify nascent macropinosomes.

NHE1 does, however, not play a direct role in phagosome acidification due to the rapidly dissipating Na⁺ gradient between the phagosome and the cytosol and the absence of the Na⁺/K⁺-ATPase to maintain such a gradient. Instead, phagosomal acidification is established by the v-ATPase (Hackam et al., 1997, 1999). By analogy, this also may hold true for macropinosomes.

The human orthologs of yeast NHX1 are the endosomal Na⁺(K⁺)/H⁺ exchangers NHE-6 and NHE-9. NHE-6 is present in early and NHE-9 in late recycling vesicles. NHE-6 is also inserted into the PM upon vesicular recycling. NHE-6 and NHE-9 bind to the adaptor protein for activated PKC, receptor for activated C kinase (RACK1), which interacts with metabolic enzymes, kinase receptors, and ion transporters and contributes to the maintenance of pH_{ves} by regulating the distribution of the transporters between endosomes and the PM. They are involved in clathrin-dependent endocytosis by alkalizing early endocytic vesicles. Endosomes of NHE-6-deficient neurons appear to be strongly acidic. Such a hyperacidification occurs upon hypoxia-induced mobilization of NHE-6 to the PM (Lucien et al., 2017). In mouse, loss of NHE-6 causes endolysosomal storage disease with accumulation of gangliosides and unesterified cholesterol in late endosomes and lysosomes of neurons of selective brain regions. In humans, mutations of NHE-6, NHE-7, and NHE-9 cause neurological syndromes (Ilie et al., 2014, 2016; Kondapalli et al., 2014; Schwede et al., 2014). NHE-5 may contribute to organellar pH regulation and regulate cell surface expression of the receptor tyrosine kinase MET and the EGF receptor (Fan et al., 2016). NHE-7 is found in the *trans*-Golgi network and in endosomes and also interacts with RACK1. Interestingly, NHE-7 mediates an acidification of intracellular vesicles that adds to that set up by the v-ATPase and that accelerates endocytosis (Milosavljevic et al., 2014). NHE-8 is found in the mid- to *trans*-Golgi compartment and MVBs. It regulates late endosomal morphology and function. In HeLa-M cells, NHE-8 silencing results in perturbation of MVB protein sorting, disrupted endosomal protein trafficking, and perinuclear clustering of endosomes and lysosomes (Lawrence et al., 2010). In the kidney, it also localizes to the apical PM and regions of coated pits. NHA-2 appears to localize to multiple compartments. It is expressed in endosomes of pancreatic β cells and synaptic-like microvesicles and participates in clathrin-dependent but not -independent endocytosis (Fuster and Alexander, 2014). In lysosomes, NHEs are absent (Nakamura et al., 2005) (for review, see Donowitz et al., 2013; Pedersen and Counillon, 2019).

Na⁺/H⁺ exchangers could fulfill a dual role in pH_{ves} regulation. In endosomes, NHEs face the acidic organellar interior and the high K⁺ concentration of the cytosol and act as H⁺/K⁺ exchangers to alkalize vesicles. Once recycled through the PM, they face the high Na⁺ concentration within the nascent vesicle. As Na⁺ is then following its gradient into the cytosol, H⁺ is transported into the vesicular lumen, thus acidifying it (Pedersen and Counillon, 2019).

K⁺ Ions

As mentioned above, extracellular and intracellular K⁺ greatly affects endocytosis and vesicle trafficking. After pinching off, the

pinosomes may retain the channel equipment of the PM, and they may contribute to the initial changes in the ionic composition of the intra-pinosomal fluid. Given the normally high K^+ conductance of the PM and the prevailing electrochemical driving force for K^+ , this is expected to be in favor of setting up a negative Ψ_{ves} in the nascent pinosome, which in turn would initially drive its early ionic movements.

Following endosome formation, the intraluminal K^+ concentration changes from ~ 5 mM to values in lysosomes ranging from 2 to 60 mM in a manner depending on $pH_{lysosome}$ (Steinberg et al., 2010; Sterea et al., 2018). In maturing endosomes, the accumulation of K^+ has been shown to be dependent on cholesterol, as its depletion impairs this process (Charlton et al., 2019).

The K^+ channel KCa3.1 is activated *via* PI(3)P and a putative regulatory subunit that is required for Ca^{2+} gating. In addition, KCa3.1 interacts with the phosphatase myotubularin R6 (MTMR6), which dephosphorylates PI(3)P, thereby inactivating the ion channel (Srivastava et al., 2005, 2006). Using coelomocytes of *Caenorhabditis elegans*, Maekawa et al. (2014) showed that the sequential dephosphorylation of phosphoinositides [in the order PI(3,4,5)P₃, PI(3,4)P₂, PI(3)P, PI] by phosphoinositide phosphatases, which are activated after ruffle formation, is related to the activation of KCa3.1. Before induction of macropinocytosis with EGF, KCa3.1 is enriched in “intracellular punctate structures” but not in the PM. Following EGF treatment, KCa3.1 is recruited to F-actin-positive membrane ruffles. Interestingly, exposure of coelomocytes to TRAM-34, a selective inhibitor of KCa3.1 (Panyi et al., 2006), or using a mutant KCa3.1, which is not activated by PI(3)P, impairs cellular dextran uptake. TRAM-34 treatment does not inhibit ruffle formation or actin polymerization. Interestingly, supplementation by sucrose to cells treated with TRAM-34 restores macropinocytosis, indicating that KCa3.1 contributes to macropinocytosis at least partially by regulating local osmolarity *via* a decrease of the intracellular K^+ concentration. The authors suggest that KCa3.1 is involved in the closure of ruffles and that amiloride and TRAM-34 might be used to dissect macropinosome formation pharmacologically—amiloride inhibits the formation and TRAM-34 the closure of the ruffle (Maekawa et al., 2014).

Endosomal and lysosomal K^+ concentration and $\Psi_{vesicle}$ are also regulated by the selective K^+ channel TMEM175, which in turn regulates organellar functions including fusions with each other. *Via* this channel, vesicular K^+ concentration and $\Psi_{vesicle}$ are hence also influenced by the cytosolic K^+ concentration. The “resting” $\Psi_{lysosome}$ is, however, also largely determined by the vesicular H^+ permeability. It is predicted to be in the range of -18 mV at pH 5.0 and $+12$ mV at pH 4.5 when assuming a cytosolic K^+ concentration of 140 mM (Cang et al., 2014, 2015).

Furthermore, large-conductance Ca^{2+} -activated K^+ channels (BK channels) are found in lysosomes. They are physically and functionally coupled to TRPML1 channels and facilitate release of Ca^{2+} ions, which activate further BK channels. This hyperpolarizes $\Psi_{lysosome}$ and thus further facilitates Ca^{2+} release. BK overexpression has been shown to rescue abnormal lysosomal

storage in cells from patients with the lysosomal storage disease Niemann–Pick’s disease (Cao et al., 2015).

Ca^{2+} Ions

Ca^{2+} ions are indispensable regulators of pinocytosis and endolysosomal functions. They induce macropinocytosis *via* F-actin depolymerization (Kabayama et al., 2009) and establish compensating exocytosis of large endosomes in parallel to ongoing macropinocytosis, thereby preventing cellular volume overload (Falcone et al., 2006). Furthermore, they regulate lysosomal fusion events and condensation of the luminal content (Xu and Ren, 2015).

Intravesicular H^+ and Ca^{2+} concentrations are interdependently tied together. In 3T3 Swiss fibroblasts, after uptake of 2 mM extracellular Ca^{2+} , the endosomal concentration rapidly drops to ~ 30 μ M within 3 min and further on to ~ 3 μ M after 20 min. This is proportionally paralleled by a drop of $pH_{vesicle}$ from 7.4 to 7.0 and 5.7 at the same time points. The loss of vesicular Ca^{2+} can be prevented if the acidification is inhibited by blocking the v-ATPase. By reducing the external Ca^{2+} to 200 μ M, the acidification is completely suppressed. Hence, the acidification can occur only when the initial Ca^{2+} concentration in the endosomes is high (Gerasimenko et al., 1998; Petersen et al., 2020).

Lysosomal Ca^{2+} homeostasis involves a putative Ca^{2+}/H^+ exchanger and Ca^{2+} pumps. The relationship between luminal Ca^{2+} and H^+ is suggested to be as follows: the lower the $pH_{lysosome}$, the higher the Ca^{2+} concentration (Morgan et al., 2011). In macrophages, the lysosomal Ca^{2+} concentration is ~ 500 μ M and dependent on extracellular and cytosolic Ca^{2+} concentration as well as on $pH_{lysosome}$. Alkalinizing pH_{lumen} reversibly decreases Ca^{2+} by shifting it into the cytosol. However, in contrast to fibroblasts, alterations of extracellular or lysosomal Ca^{2+} do not alter $pH_{lysosome}$ in macrophages (Christensen et al., 2002; Sterea et al., 2018). This model has been challenged by the finding that lysosomal stores are rather refilled pH-independently with Ca^{2+} *via* the ER in an Ins(1,4,5)P₃ receptor-dependent process and *via* involvement of an unknown Ca^{2+} transport mechanism to move Ca^{2+} into the lysosome (Garrity et al., 2016).

The Ca^{2+} permeability of the endolysosomal membranes is set up by several cation channels. Among them are the transient receptor potential channel family members TRPML1, 2, and 3 (mucolipins), two-pore channels TPC1, 2, and 3, and voltage-gated Ca^{2+} channels (Cheng et al., 2010; Abe and Puertollano, 2011; Grimm et al., 2012; Xiong and Zhu, 2016; Clement et al., 2020; Freeman et al., 2020; Jin et al., 2020).

TRP channel of mucolipin subfamilies mainly localize to lysosomes and endosomes but are also found in the PM. The channels are activated by PI(3,5)P₂. TRPML1 is inhibited by PI(4,5)P₂, which is abundantly present in the PM. Hence, if residing there, it is likely to be functionally suppressed (Sun et al., 2015; Venkatachalam et al., 2015).

TRPML1 is encoded by the Mcoln1 gene and expressed in late endosomes and lysosomes. It is responsible for the enlarged vacuole formation and the lysosomal storage disease mucopolipidosis IV if mutated to loss of function (OMIM entry

#252650) (Lloyd-Evans et al., 2008; Grimm et al., 2012). The channel is permeable to Ca^{2+} , Na^+ , K^+ , Fe^{2+} , and Mg^{2+} , and activated by PI(3,5)P₂, but inhibited by PI(4,5)P₂ and sphingomyelin. TRPML1 acts as a lysosomal pH regulator as it senses the $\text{pH}_{\text{lysosome}}$ and initiates the release of H^+ . Being activated at low pH, it allows for Ca^{2+} influx (Li et al., 2017). Accordingly, lysosomal acidification is hindered when PI(3,5)P₃ generation is suppressed by inhibition or lack of PIKfyve and rescued by overexpression of TRPML1 or raising lysosomal Ca^{2+} . However, the vacuole formation observed in PIKfyve-deficient cells is not rescued by Ca^{2+} or overexpressed TRPML1 (Cheng et al., 2010; Isobe et al., 2019).

PIKfyve converts PI(3)P into PI(3,5)P₂ in the endocytic pathway and the enzyme Fig4 dephosphorylates it back to educt. In yeast, hyperosmotic stress leads to the rapid transient synthesis of PI(3,5)P₂ *via* activation of PI(3)P kinase (Dove et al., 1997; Duex et al., 2006) and the TRPML1 ortholog Yvc1. Lack of PI(3,5)P₂ synthesis leads to severe swelling of the endolysosomal compartment due to concentrating K^+ up to ~85 mM. This effect is relieved by inactivating mutations of the vacuolar monovalent cation/ H^+ -antiporter Vnx1 or v-ATPase or by activating mutations of Yvc1. This identifies PI(3,5)P₃ and the ion transporters regulated by it as crucial osmoregulators (Dove et al., 1997; Wilson et al., 2018). In contrast to yeast, hyperosmotic stress decreases and hypoosmotic treatment enhances PI(3,5)P₂ production in monkey Cos-7 cells (Dove et al., 1997). PI(3,5)P₂ regulates vacuole size in part *via* TRPML1 channels (Krishna et al., 2016). Hypertonicity also activates PIKfyve and its upstream regulator hVac14 in differentiated 3T3-L1 adipocytes, but not in their undifferentiated precursor cells (Sbrissa and Shisheva, 2005). In dendritic cells, TRPML1 releases lysosomal Ca^{2+} upon bacterial sensing, which activates the actin-based motor protein myosin II for directional migration. In addition, it induces the activation of the transcription factor EB (TFEB), which translocates to the nucleus to maintain TRPML1 expression. This TRPML1–TFEB axis results from the downregulation of macropinocytosis after bacterial sensing (Bretou et al., 2017). Moreover, TRPML1 is a lysosomal sensor of reactive oxygen species (ROS) (Zhang et al., 2016), which are known, on the one hand, to be generated during cell swelling (Gorg et al., 2013) and, on the other hand, to activate VRACs (Lambert, 2003; Varela et al., 2004; Browe and Baumgarten, 2006; Lambert et al., 2015). Such a link between ROS, endosomal function, and CVR may be mediated by ClC-3-dependent endosomal ROS production and isosmotic activation of VRAC (Matsuda et al., 2010).

Activating H-Ras mutations—known to drive macropinocytosis—elevates TRPML1 expression. In H-Ras-driven cancer cells, the channel is needed to restore PM cholesterol, which gets internalized during endocytosis. Inhibition or lack of TRPML1 causes false localization of cholesterol from the PM to endolysosomes and loss of oncogenic H-Ras from the cell surface (Jung and Venkatachalam, 2019). Hence, cells expressing oncogenic H-Ras are vulnerable to inhibition of TRPML1 (Jung and Venkatachalam, 2019; Jung et al., 2019).

TRPML2 is an osmo/mechanosensitive endolysosomal channel conductive to Ca^{2+} , Na^+ , K^+ , and Fe^{2+} and also activated by PI(3,5)P₂. It is involved in Arf6-regulated recycling pathway and in endolysosomal membrane trafficking by means of its sensitivity to hypotonicity. In late endosomes, TRPML2 is activated by free cytosolic ADP-ribose and eventually by nicotinic acid adenine dinucleotide phosphate (NAADP) (Dong et al., 2010; Viet et al., 2019). Mutations in TRPML2 may induce CD due to Ca^{2+} overload (Sun et al., 2015; Sterea et al., 2018; Chen et al., 2020a).

TRPML3 localizes to both early endosomes and endolysosomes, is Ca^{2+} permeable, activated by PI(3,5)P₂, and inhibited by PI(4,5)P₂, Na^+ , as well as acidic pH (Dong et al., 2010).

The two-pore channels (TPCs) are voltage-gated cation channels that function as homodimers. TPC1 localizes predominantly to the proximal endosomal system, while TPC2 is found mainly on late endosomes and lysosomes, where they act as Na^+ and Ca^{2+} release channels. They are activated by PI(3,5)P₂ (rather than NAADP) (Wang et al., 2012; Cang et al., 2013; She et al., 2019; Jin et al., 2020) and play important roles for vesicular fusion and endosomal trafficking, autophagy, nutrient sensing, protein processing, and macropinocytic virus entry (Wang et al., 2012; Bellono and Oancea, 2014; Sakurai et al., 2015; Xiong and Zhu, 2016; Castonguay et al., 2017). Inhibition or loss of TPC channels critically reduces cellular entry of severe acute respiratory syndrome coronavirus 2 (SARS-CoV-2) (Ou et al., 2020) and Ebola virus (Sakurai et al., 2015; Petersen et al., 2020). TPC1 activity is high at alkaline $\text{pH}_{\text{vesicle}}$ and open over a wide voltage range but low at acidic $\text{pH}_{\text{vesicle}}$. Also, low intracellular ATP concentration increases TPC1 opening. This leads to Na^+ efflux and thus facilitates the v-ATPase and luminal acidification (Cang et al., 2014). TPC2 channels are important in organelle fusion and pH regulation. They mediate the rapid decrease of vesicular Ca^{2+} after uptake (Petersen et al., 2020). TPC2 inhibition or loss suppresses virus uptake (Sakurai et al., 2015; Petersen et al., 2020), increases the risk to develop non-alcoholic steatohepatitis (NASH) and fatty liver disease (NAFLD); Grimm et al., 2014, p. 707]. TPC2 is also involved in pigmentation (Bellono and Oancea, 2014; Lin et al., 2015).

Lysosomes seem also to possess voltage-gated calcium channel, which might serve to release Ca^{2+} upon depolarization of Ψ_{vesicle} and which are required for lysosomal fusion with endosomes and autophagosomes (Tian et al., 2015).

VESICULAR VOLUME REGULATION

Macropinosome shrinkage or swelling is accomplished by osmotically driven exchange of water between the vesicle lumen and the cytosol (VVR) (Freeman and Grinstein, 2018; Chen et al., 2020b; King and Smythe, 2020; Chadwick et al., 2021b), in adjunction with global CVR (see above). The direction of ion flux—efflux or influx—is determined by the transmembrane ion gradients, the levels of Ψ_{PM} and Ψ_{vesicle} , and the reversal potentials of the respective ions. The composition of the fluid in a nascent macropinosome initially equals the fluid in the intimate

extracellular vicinity of its emergence and may be identical to the extracellular fluid. This creates a transmembrane gradient across the membrane of the macropinosome and the cytosol similar to that across the PM. Macropinosome shrinkage is therefore largely mediated by Na^+ flux across the vesicle membrane. Recent studies demonstrated that Na^+ efflux down its gradient from the pinosome to the cytosol is controlled by the non-selective TRPML cation channels and TPC Na^+ channels (Laplanche et al., 2002; Freeman et al., 2020; Chadwick et al., 2021a,b; Saric and Freeman, 2021).

In addition to Na^+ , also Cl^- permeates through the macropinosomal membrane (Freeman and Grinstein, 2018). As described above, vesicular LRRC8 channels/LysoVRACs may play a role for the flux of anions across the vesicular membrane, and their importance in VVR has been recognized (Li et al., 2020; Osei-Owusu et al., 2021). A role for TMEM206/ASOR/PAORAC seems feasible, and an eventual functional coupling of vesicular VSOR and ASOR channels/currents, as described to occur in the PM (Nobles et al., 2004; Lambert and Oberwinkler, 2005; Kittl et al., 2019, 2020), awaits future investigation.

The efflux of Na^+ and Cl^- is coupled to cotransporters such as the electroneutral cation- Cl^- cotransporters (SLC12A family members; carrying K^+), NHEs (SLC9A family members; carrying H^+), and anion exchangers (AE; SLC4A family members; carrying HCO_3^-) (Freeman and Grinstein, 2018). Moreover, HCO_3^- forms water and CO_2 , which exits the macropinosome as described above. The net result of these ion fluxes leads to osmotically driven vesicular water exit and shrinkage in parallel to H^+ ion accumulation, thus generating small acidic late endosomes, in which the to-be-digested substances are highly concentrated (for review, see Freeman and Grinstein, 2018; Chadwick et al., 2021b).

Accordingly, macropinosome shrinkage is prevented if Na^+ or Cl^- is replaced by a non-permeant cation or anion. Importantly, the osmotically driven vesicle shrinkage is necessary for the vesiculation, tubulation, and scission processes, as it confers—by creating membrane wrinkles—the appropriate curvature necessary to recruit and stabilize the protein complexes required for proper sorting and recycling of the vesicles and their cargo, e.g., anchor sites for microtubule-associated motors, branched actin generation, or cargo recognition proteins. The latter are composed of the sorting nexins (SNXs), which contain a Bin-amphiphysin-Rvs (BAR) domain. BAR domains are able to electrostatically interact with phospholipids of appropriately bent concave membrane stretches. Also, proteins of the ESCRT complexes take advantage of the slack membrane to induce inwardly budding intraluminal vesicles (ILVs) and further on MVBs. Thus, the vesicular shrinkage creates organelles with high surface-to-volume ratios, relieves the hydrostatic tension of their membranes, and is hence critical for their resolution (for review, see Freeman and Grinstein, 2018; Chen et al., 2020b; Saric and Freeman, 2020, 2021; Chadwick et al., 2021a,b).

As pointed out above, the role of and function of AQPs in VVR is still elusive. A clue about their usage may come from observations in *T. cruzi* epimastigotes. They respond to cell swelling with trafficking and fusion of acidocalcisomes, which contain osmolytes and the AQP, TcAQP1, to the so-called

bladder of the contractile vacuole complex, thereby loading their content to it. This enables the bladder to take up and store excess cellular water, whereby it swells by the aid of TcAQP1. Subsequently, the water is expelled to the extracellular environment, thus driving RVD (reviewed in Docampo et al., 2011, 2013). The basic mechanistic principle of this mechanism—soak up, store, and release excess intracellular water to/from intracellular organelles—is somehow recapitulated in Cos1 cells in response to a hypotonicity as described above (Li et al., 2020). It will be interesting to find out whether this principle of linking CVR and VVR is a more general one and if it might function in other cells as well.

METHUOSIS

Regulated CD in response to perturbation of the extracellular or intracellular milieu is an essential hallmark of multicellular organisms and is mediated mainly by apoptotic and necrotic phenotypes (Galluzzi et al., 2018). Methuosis is a non-apoptotic CD phenotype characterized by large and lucent vacuoles, which are limited by a single membrane as well as by cell swelling and, finally, rupture of the PM (Maltese and Overmeyer, 2014). Currently, methuosis is seen as a dysfunctional pinocytosis. Although Lewis first described macropinocytosis already in 1937 (Lewis, 1937), the fatal consequences for the cell by “drinking too much” have been described by Overmeyer et al. (2008) several decades later. While macropinocytosis is associated with vesicle shrinkage during processing of the vesicle content, methuosis reflects the abnormal growth of pinosomes. Despite that cell vacuolization is a common feature in many diseases, such as the lysosomal storage disease Gaucher’s disease or in microglia in Alzheimer’s disease, it is still uncertain whether methuosis plays a critical role in the etiology of these diseases (Kruth et al., 2005; Rappaport et al., 2016). There is also evidence that methuosis may be an eventual CD modality outcome of cell senescence (Adjemian et al., 2020).

H-Ras is required for macropinocytosis, and oncogenic mutants of a Ras allele are associated with methuosis. Chi et al. (1999) tested the assumption that the persistent activation of an oncogenic mutant of a Ras allele induces CD on those malignant tumors, which in general do not show an expression of Ras alleles. They found that transfection of oncogenic H-Ras (Ras^{G12V}) in human malignant glioma cells and human gastric cancer cell lines causes CD associated with intense vacuolization (Chi et al., 1999). These authors concluded that H-Ras expression triggers a type-2 CD, meaning that, in this condition, autophagy leads to CD. Overmeyer et al. (2008) replicated, confirmed, and extended these findings, but they excluded a type-2 form of CD. As in the study of Chi et al. (1999), they used a human glioblastoma cell line and induced the expression of Ras. Within a few days, Ras-expressing cells revealed lucent cytoplasmic vacuoles in phase-contrast microscopy, which did contain neither cell organelles nor cytoplasmic components when analyzed using electron microscopy. Furthermore, electron microscopy revealed that the vacuoles are limited by a single and not by a double membrane, as would be distinctive for autophagy. Fluid-phase

traces, like Lucifer yellow or dextran-Alexa Fluor 488, accumulate in large vacuoles, whereas transferrin-Alexa Fluor 594 labels small endosomes, which contain—in contrast to pinosomes—transferrin receptors. Furthermore, the small endosomes are decorated with clathrin, whereas large vacuoles do not contain a clathrin coat. In contrast to functional pinocytosis, large vacuoles are not acidic. Finally, the cells detach from the surface and swell, and the PM ruptures. Because of the similarities with pinocytosis, but the fatal consequences of fluid uptake, the authors suggest that this is a dysfunctional pinocytosis, which leads to a distinct form of CD. Accordingly, Overmeyer et al. (2008) named this form of CD methuosis, derived from the Greek word *methuo*, meaning “to drink to intoxication.”

In normal macropinocytosis, nascent macropinosomes dynamically engage with cytoskeletal elements and either are tagged for recycling or finally fuse with lysosomes. With methuosis, however, vesicles fuse with each other to form large vacuoles, leading to the presumption that methuosis is a dysfunctional pinocytosis (Maltese and Overmeyer, 2014). In molecular–biological terms, methuosis shows its relationship to macropinocytosis by its dependence on H-Ras. Despite having the late endosome markers, LAMP1 and Rab7, vacuoles are not acidic, as demonstrated by their failure to accumulate acridine orange and LysoTracker. Interestingly, inhibition of v-ATPase by bafilomycin A1 also inhibits vacuolization (Maltese and Overmeyer, 2014). An important aspect in macropinocytosis is shrinkage of the vesicles *via* osmoregulatory processes (see above). Ras and phosphoinositides are required for the activation of a variety of ion channels, including those involved in vesicle shrinkage and CVR (see above) (Ritter and Woll, 1996). Assuming that formation of large vacuoles is not only due to fusion of pinosomes but also related to organelle swelling, an imbalance in the signaling cascade from Ras to ion channels could play a key role in methuosis. In line with the crucial role of NHE1 in macropinocytosis is the observation that methuosis induced by an ursolic acid-derived small molecule, compound 17, has been shown to be prevented by EIPA (Sun et al., 2017). As outlined above, H-Ras^{G12V}-expressing cells experience to shift of CVR toward higher volumes and also the intracellular vesicles have more alkaline pH. Inducers of methuosis and formation of extremely enlarged vacuoles are given in Table 2.

Figure 3 highlights major cellular aspects of the interrelation of (macro)pinocytosis, CVR, and VVR as discussed in this review.

PERSPECTIVES

Understanding the mechanisms of pinocytosis and how it exerts its cell protective effects is critical to appreciate its diversity of physiological functions. It is also necessary to understand its dysfunctions and how they might lead to disease as well as to unravel how influencing pinocytosis may translate to potential applications for medical and other use.

For instance, designing of compounds like proteolytically stable peptidomimetics that are taken up by macropinocytosis, but which are able to escape from endosomes, could be used for intracellular biomolecular targeting (Yoo et al., 2020).

Likewise, development of versatile drug carriers with a high loading capacity, such as nanoparticles, which are optimized for specific binding to cell surface receptors, and which are favoring both macropinocytic uptake and intracellular release by degradation of their shells, may open new ways for, e.g., cancer therapy. This principle was proven for hyaluronic acid-modified polymeric biodegradable mesoporous silica nanoparticles (Palanikumar et al., 2018).

Cancer cells frequently depend on autophagy to support their metabolic and energetic demands. However, inhibition of autophagy leads to compensatory stimulation of macropinocytosis to ensure cellular nutrient supply. This switch depends on the transcription factor NRF2, which is recruited to promoter regions of macropinocytosis-related genes. Recently, it has been shown that dual inhibition of autophagy and macropinocytosis is a successful strategy in treating mice with pancreatic ductal adenocarcinomas. Advancing this strategy to clinical applications may be promising for cancer therapy (Staff, 2021; Su et al., 2021).

Cell death by methuosis should meet special attention. The formation of huge cellular vacuoles, which eventually leads to cell death, is a frequently observed phenomenon in numerous pathologies and known for decades (Cameron, 1952; Henics and Wheatley, 1999). However, in many studies, the origin and mechanisms of the development of such cellular vacuoles were not or could not be determined. The term methuosis was coined in 2008 (Overmeyer et al., 2008). Hence, it will be necessary to carefully scrutinize the available body of literature for work describing methuosis-like phenomena and to eventually reevaluate it for better understanding the underlying mechanisms of deadly vacuolization and related types of cell death (Chi et al., 1999).

Recent studies indicate that volume regulation in cells and cell organelles is governed by the same biophysical principles and by the overlapping use of ion channels and transporters in distinct cellular compartments (Saric and Freeman, 2020, 2021; Chadwick et al., 2021a,b). That is, it starts with the asymmetric distribution of ions and materializes in the well-orchestrated uptake and processing of engulfed material in specialized vesicles (Chadwick et al., 2021a).

However, the contribution of inorganic ions may go beyond volume regulation. Inflammation and tissue injury are associated with a local extracellular increase in Ca^{2+} and enhancement of macropinocytosis in antigen-presenting cells (Canton, 2018). Presumably, the extracellular Ca^{2+} concentration is sensed by the calcium-sensing receptor (CaSR), which is expressed in myeloid cells (Canton, 2018). Accordingly, change in the extracellular ion composition may be critical in antigen processing and presentation *via* major histocompatibility complexes (MHCs) as well as recognition of non-self-antigens or modified endogenous substances by pattern recognition receptors (PRRs) (Canton, 2018). Consequently, failure in proper pinocytosis due to the formation of large vesicles could impair degradation of organic compounds or its delivery to PRRs or MHCs, which may have detrimental consequences in the immune response. The

TABLE 2 | Inducers of methuosis, cell death associated with aberrant vacuolization, and formation of strongly enlarged vacuoles.

Inducers of methuosis, methuosis-like vacuolization, formation of giant vacuoles	Cell type/organism	Mode of action	References
Activating H-Ras mutations	U251 and U343 human GB cells, MKN-1, TMK-1 gastric cancer cells	Activation of Rac1; inactivation of Arf6	Kaul et al., 2007; Overmeyer et al., 2008; Bhanot et al., 2010; Chi et al., 1999*
Activated Rac1	U251 human GB cells	Ras–Rac-dependent pathway	Overmeyer et al., 2008
Activating K-ras mutations	Human lung adenocarcinoma, HCK1 cervical keratinocytes; HeLa cervical cancer cells, A549 lung cancer cells	Rac1 activation	Unni et al., 2015; Dendo et al., 2018
Ionizing radiation	K-Ras ^{G13R} -bearing murine uterine cervix cancer (MUCC) cells	Iron-dependent CD assumed	Adjemian et al., 2020
Activating EGFR mutations	Human lung adenocarcinomas	MAPK signaling pathway	Unni et al., 2015
NGF	Daoy medulloblastoma cells	TrkA-dependent casein kinase 1 activation	Li et al., 2010
CD99 (mAB-triggered activation)	Ewing sarcoma cells	IGF-1R/Ras/Rac1 signaling	Manara et al., 2016
PFK158	Malignant pleural mesothelioma cells	Inhibition of PFKFB3	Sarkar Bhattacharya et al., 2019
OSI-027; PP242	RD, RH30 and RMS rhabdomyosarcoma cells; HeLa cervical cancer cells, MCF7 breast cancer cells; A549 lung cancer cells; A431 epidermoid cells; HaCaT and Ker-CT keratinocytes	mTORC1/mTORC2 inhibition	Srivastava et al., 2019
AS1411, G-rich quadruplex-forming oligodeoxynucleotide	DU145, MDA-MB-468, A549, LNCaP prostate cancer cells	AS1411 binding to nucleolin; activation of EGFR and Rac1	Reyes-Reyes et al., 2015
miR-199a-3p	K1 papillary thyroid carcinoma cells	Eventually involvement of HGF pathway(s)	Minna et al., 2014
Kalata B1 cyclotide	<i>Heterodera filipjevi</i> ; nematode, juveniles, pre-parasitic second stage	Eventually involvement of ROS	Labudda et al., 2020
Methamphetamine	RA-differentiated SH-SY5Y neuroblastoma cells	Involving Ras–Rac1	Nara et al., 2010
MIPP	U251 GB cells	Targets endosomal trafficking involving Rab5 and Rab7	Overmeyer et al., 2011
MOMIPP	U251 and U373 GB cells; MCF-7 breast cancer cells; HMEC mammary epithelial cells; skin fibroblasts; HCT116 cells	Interference with glucose uptake; induction of JNK-mediated phosphorylation of Bcl-2 family members	Robinson et al., 2012; Trabbic et al., 2014, 2016; Cho et al., 2018; Colin et al., 2019; Li Z. et al., 2019; Oppong et al., 2020
Compound 13	MDA-MB-231, A375, HCT116, MCF-7 cancer cells		Huang et al., 2018
Isobavachalcone	NB4, U937, primary leukemic blast cells	Eventually AKT signaling	Yang et al., 2019
Azaindole-based compounds	MDA-MB-231 cells and other cells		Huang et al., 2018
Vacquinol-1	U-87 and #12537-GB glioma cells; rat GB models, RG2 and NS1; U373 GB cells	Involving MKK4 signaling; involving TRPM7 channels	Sander et al., 2017; Ahlstedt et al., 2018; Colin et al., 2019
Ursolic acid-derived compound 17	HeLa cervical cancer cells		Sun et al., 2017
Tubeimoside-1	SW480 colon carcinoma cells		Gong et al., 2018
Jaspine B	HGC-27 gastric cancer cells		Cingolani et al., 2017
Indolyl-pyridinyl-propenones; compounds 1a, 2b, 2p, 2q	U251 GB cells		Trabbic et al., 2015, 2016
Maduramicin	Primary chicken myocardial cells	Involving K-Ras–Rac 1 signaling	Gao et al., 2020
5-Iodoindole	<i>M. incognita</i> ; <i>Bursaphelenchus xylophilus</i> ; nematodes	Involving ROS	Rajasekharan et al., 2017, 2019, 2020
7-Iodoindole	<i>Bursaphelenchus xylophilus</i>		Rajasekharan et al., 2017
Abamectin	<i>Bursaphelenchus xylophilus</i> , nematode	Interaction with GluCL, disruption of osmoregulation	Rajasekharan et al., 2017
Extract of <i>Platycarya strobilacea</i> Sieb. et Zucc.	CNE1, CNE2 nasopharyngeal carcinoma cells	Involvement of Ras–MAPK signaling and c-Fos signaling; Rac1 activation	Zhu et al., 2017; Liu J. et al., 2020
Bacoside A from <i>Bacopa monnieri</i>	LN229 GB cells	CaMK2A phosphorylation, Ca ²⁺ release from ER	John et al., 2017
Citreoviridin + Bortezomib	MCF7 human breast cancer cells	Inhibition of F1Fo ATP synthase (citreoviridin) + inhibition of 26S proteasome (bortezomib)	Chang et al., 2014
Abemaciclib	GBM neurospheres, glioma stem-like cells	Inhibition of CDK isoforms 4/6	Riess et al., 2021
Dinaciclib	GBM neurospheres, glioma stem-like cells	Inhibition of CDK isoforms 1/2/5/9	Riess et al., 2021

(Continued)

TABLE 2 | Continued

Inducers of methuosis, methuosis-like vacuolization, formation of giant vacuoles	Cell type/organism	Mode of action	References
s-Triazine compound V6	U87 GB cells	Binding to vimentin	Zhang et al., 2021
CX-4945 (Silitasertib)	SW-480, DLD-1, HT-29, HCT-116 colorectal cancer cells	Inhibition of CK2	Silva-Pavez et al., 2019
CX-4945 (Silitasertib)	KKU-M213 cholangiocarcinoma cell line; eventually also in a wide range of cancer and immortalized cell lines	Independent of protein kinase CK2	Lertsuwan et al., 2018
CX-5011	HepG2 human hepatoma cells, zebrafish	Independent of protein kinase CK2	D'Amore et al., 2020
Graphene oxide (GO) nanoparticles	LO2 normal human hepatocytes	Eventually involving ROS-mediated cell stress following GO adherence and aggregation to the PM	Zheng et al., 2018
YM201636; Apilimod (STA-5326); Vacuolin-1; dominant-negative PIKfyfe expression; wortmannin	COS7 African green monkey kidney cells, mouse embryonic fibroblasts; immortalized podocytes; B-cell non-Hodgkin lymphoma cells; C ₂ C ₁₂ myoblasts; HEK 293 Human embryonic kidney cells, COS7 cells; NIH3T3 fibroblasts; CHO-T cells, 3T3L1 fibroblasts; U251 GB cells; HeLa cells	PYKfyfe inhibition; lack of active PIKfyfe; lack of Vps34 activity; inhibition of PI3Ks; vacuolation requires v-ATPase activity	Jefferies et al., 2008; Sbrissa et al., 2012, 2018; Compton et al., 2016; Sano et al., 2016; Saveanu and Lotersztajn, 2016; Gayle et al., 2017; Ikononov et al., 2018; Li Z. et al., 2019
Rare earth oxide nanoparticles	HeLa cells	Leads to mTOR deactivation and nucleus translocation of TFEB	Lin et al., 2016
F14512	A549 non-small-cell lung cancer cells	Involves increased β -galactosidase activity	Brel et al., 2011
3Cpro	A549 and Calu-1 non-small-cell lung cancer cells	Dependent on v-ATPase, not dependent on Rac-1, Rab5, Rab7 or hyperstimulated macropinocytosis	Shubin et al., 2015
Antagomir knockdown of microRNA -103/107	HLEK cells, hTCEpi cells	Loss of microRNA-103/107; involvement of Src, Ras (no CD observed)	Park et al., 2016
Fenretinide	Rh4 and Rh30 alveolar rhabdomyosarcoma cells	EIPA-independent hyperstimulation of macropinocytosis; accumulation of early and late endosomal vacuoles; dependent on dynamin and ROS (new form of CD different from methuosis)	Brack et al., 2020
Epimedokoreanin C	NCI-H292 lung cancer cells	Involving Rac1 and Arf6	Liu X. et al., 2020
Hypertonicity	<i>Dictyostelium discoideum</i> , axenically grown strain AX2		Yuan and Chia, 2001
Knockdown of non-coding region of the C9orf72 gene		Altered of immune system genes expression; involving p53 activation, endothelin signaling; mitochondrial dysfunction; cellular glutamate accumulation; repression of mevalonate pathway; inhibition of isoprenylation; ROS formation	Fomin et al., 2018; Fomin, 2019

*Not yet termed methuosis; instead designated as "type 2 physiological cell death" (autophagic degeneration). For abbreviations and acronyms see list of abbreviations.

studies on CVR and VVR, pinocytotic activity, and delivery of compounds to MHCs or PRRs exemplify the power of ion gradients to understand physiology and pathophysiology of pinocytosis and methuosis, respectively. Despite Ca^{2+} , other inorganic ions may have comparable dual effects on volume regulation and delivering of ligands to MHCs or PRRs. Thus, identification of ion channels and transporters required for establishing ion gradients could lead to a more detailed understanding of the complex interaction between distinct inorganic ions and cellular responses to tissue injuries or inflammation.

Beyond that, targeting specific ion transport mechanisms or their regulators will help to combat cellular entry of pathogens such as viruses or bacteria. For example, inhibition

of PIKfyfe, TPCs, NHEs, or the v-ATPase could help prevent cellular infection by Ebola virus, SARS-CoV-2, and other viruses (Mercer and Helenius, 2009; Sakurai et al., 2015; Kang et al., 2020; Mercer et al., 2020; Petersen et al., 2020; Spix et al., 2020; Eaton et al., 2021).

The number of compounds and materials that can induce or inhibit methuosis in various cell types and organisms is growing, and the fields of their use are just emerging. It will be necessary to unravel not only their specific modes of actions but also their harmful effects, as they might be used for a broad variety of applications, e.g., for eco-friendly biological pest control in agriculture to overcome multidrug resistance of parasites (Bogner et al., 2017; Rajasekharan and Lee, 2020; Rajasekharan et al., 2020). Importantly, they may emerge as new treatment options

for various diseases, e.g., cancer (Song S. et al., 2020; Xiao et al., 2021), ALS, or dementia (Fomin et al., 2018; Fomin, 2019).

AUTHOR CONTRIBUTIONS

HK conceptualized the manuscript. HK, MR, and NB wrote and finalized the manuscript. NB captured and arranged the images displayed in **Figure 1** and the accompanying **Supplementary Video 1**. MR prepared **Tables 1, 2**, and **Figures 2, 3**. All authors contributed to the article and approved the submitted version.

REFERENCES

- Abe, K., and Puertollano, R. (2011). Role of TRP channels in the regulation of the endosomal pathway. *Physiology* 26, 14–22. doi: 10.1152/physiol.00048.2010
- Abu Jawdeh, B. G., Khan, S., Deschenes, I., Hoshi, M., Goel, M., Lock, J. T., et al. (2011). Phosphoinositide binding differentially regulates NHE1 Na⁺/H⁺ exchanger-dependent proximal tubule cell survival. *J. Biol. Chem.* 286, 42435–42445. doi: 10.1074/jbc.m110.212845
- Adjemian, S., Oltean, T., Martens, S., Wiernicki, B., Goossens, V., Vanden Berghe, T., et al. (2020). Ionizing radiation results in a mixture of cellular outcomes including mitotic catastrophe, senescence, methuosis, and iron-dependent cell death. *Cell Death Dis.* 11:1003.
- Ahlstedt, J., Förnvik, K., Zolfaghari, S., Kwak, D., Hammarström, L. G. J., Ernfors, P., et al. (2018). Evaluating vacuolin-1 in rats carrying glioblastoma models RG2 and NS1. *Oncotarget* 9, 8391–8399. doi: 10.18632/oncotarget.23842
- Alexander, S. P., Kelly, E., Marrion, N. V., Peters, J. A., Faccenda, E., Harding, S. D., et al. (2017). THE concise guide to pharmacology 2017/18: overview. *Br. J. Pharmacol.* 174(Suppl. 1), S1–S16.
- Alghanem, A. F., Abello, J., Maurer, J. M., Kumar, A., Ta, C. M., Gunasekar, S. K., et al. (2021). The SWELL1-LRRC8 complex regulates endothelial AKT-eNOS signaling and vascular function. *eLife* 10:e61313.
- Alonso-Curbelo, D., Osterloh, L., Canon, E., Calvo, T. G., Martinez-Herranz, R., Karras, P., et al. (2015). RAB7 counteracts PI3K-driven macropinocytosis activated at early stages of melanoma development. *Oncotarget* 6, 11848–11862. doi: 10.18632/oncotarget.4055
- Alvarez-Leefmans, F. J., Gamino, S. M., and Reuss, L. (1992). Cell volume changes upon sodium pump inhibition in *Helix aspersa* neurones. *J. Physiol.* 458, 603–619. doi: 10.1113/jphysiol.1992.sp019436
- Amyere, M., Mettlen, M., Van Der Smissen, P., Platek, A., Payrastra, B., Veithen, A., et al. (2002). Origin, originality, functions, subversions and molecular signalling of macropinocytosis. *Int. J. Med. Microbiol.* 291, 487–494. doi: 10.1078/1438-4221-00157
- Amyere, M., Payrastra, B., Krause, U., Van Der Smissen, P., Veithen, A., and Courttoy, P. J. (2000). Constitutive macropinocytosis in oncogene-transformed fibroblasts depends on sequential permanent activation of phosphoinositide 3-kinase and phospholipase C. *Mol. Biol. Cell.* 11, 3453–3467. doi: 10.1091/mbc.11.10.3453
- Anbari, M., Root, K. V., and Van Dyke, R. W. (1994). Role of Na,K-ATPase in regulating acidification of early rat liver endocytic vesicles. *Hepatology* 19, 1034–1043. doi: 10.1016/0270-9139(94)90306-9
- Araki, N., Egami, Y., Watanabe, Y., and Hatae, T. (2007). Phosphoinositide metabolism during membrane ruffling and macropinosome formation in EGF-stimulated A431 cells. *Exp. Cell. Res.* 313, 1496–1507. doi: 10.1016/j.yexcr.2007.02.012
- Araki, N., Johnson, M. T., and Swanson, J. A. (1996). A role for phosphoinositide 3-kinase in the completion of macropinocytosis and phagocytosis by macrophages. *J. Cell Biol.* 135, 1249–1260. doi: 10.1083/jcb.135.5.1249
- Astaburuaga, R., Quintanar Haro, O. D., Stauber, T., and Relogio, A. (2019). A mathematical model of lysosomal homeostasis points to differential effects of Cl⁻ transport in Ca²⁺ dynamics. *Cells* 8:1263. doi: 10.3390/cells8101263
- Ayee, M. A. A., Lemaster, E., Teng, T., Lee, J., and Levitan, I. (2018). Hypotonic challenge of endothelial cells increases membrane stiffness with no effect on tether force. *Biophys. J.* 114, 929–938. doi: 10.1016/j.bpj.2017.12.032

SUPPLEMENTARY MATERIAL

The Supplementary Material for this article can be found online at: <https://www.frontiersin.org/articles/10.3389/fcell.2021.651982/full#supplementary-material>

Supplementary Video 1 | Pinocytosis occurring in a multinucleated giant cell from a rat non-parenchymal hepatic cell line putatively representing immortalized monocytes (Kupffer cells). For explanations, see **Figure 1** and text.

Supplementary Video 2 | Close-up of **Supplementary Video 1**.

- Bakker-Grunwald, T., Keller, F., and Trissl, D. (1986). Effects of amiloride on Na⁺ content and pinocytosis in *Entamoeba histolytica*. *Biochim. Biophys. Acta Biomembr.* 854, 265–269. doi: 10.1016/0005-2736(86)90119-7
- Balla, T. (2013). Phosphoinositides: tiny lipids with giant impact on cell regulation. *Physiol. Rev.* 93, 1019–1137. doi: 10.1152/physrev.00028.2012
- Bannunah, A. M., Vllasaliu, D., Lord, J., and Stolnik, S. (2014). Mechanisms of nanoparticle internalization and transport across an intestinal epithelial cell model: effect of size and surface charge. *Molecular Pharmaceutics* 11, 4363–4373. doi: 10.1021/mp500439c
- Baumgartner, M., Patel, H., and Barber, D. L. (2004). Na⁺/H⁺ exchanger NHE1 as plasma membrane scaffold in the assembly of signaling complexes. *Am. J. Physiol. Cell Physiol.* 287, C844–C850.
- Becker, H. M., Klier, M., and Deitmer, J. W. (2014). “Carbonic anhydrases and their interplay with acid/base-coupled membrane transporters,” in *Carbonic Anhydrase: Mechanism, Regulation, Links to Disease, and Industrial Applications*, eds S. C. Frost and R. McKenna (Dordrecht: Springer), 105–134. doi: 10.1007/978-94-007-7359-2_7
- Bellono, N. W., and Oancea, E. V. (2014). Ion transport in pigmentation. *Arch. Biochem. Biophys.* 563, 35–41. doi: 10.1016/j.abb.2014.06.020
- Ben-Dov, N., and Korenstein, R. (2012). Enhancement of cell membrane invaginations, vesiculation and uptake of macromolecules by protonation of the cell surface. *PLoS One* 7:e35204. doi: 10.1371/journal.pone.0035204
- Berridge, M. J. (2009). Inositol trisphosphate and calcium signalling mechanisms. *Biochim. Biophys. Acta* 1793, 933–940. doi: 10.1016/j.bbamcr.2008.10.005
- Bertelli, S., Remigante, A., Zuccolini, P., Barbieri, R., Ferrera, L., Picco, C., et al. (2021). Mechanisms of activation of LRRC8 volume regulated anion channels. *Cell Physiol. Biochem.* 55, 41–56. doi: 10.33594/000000329
- Bhanot, H., Young, A. M., Overmeyer, J. H., and Maltese, W. A. (2010). Induction of nonapoptotic cell death by activated Ras requires inverse regulation of Rac1 and Arf6. *Mol. Cancer Res.* 8, 1358–1374. doi: 10.1158/1541-7786.mcr-10-0090
- Bloomfield, G., and Kay, R. R. (2016). Uses and abuses of macropinocytosis. *J. Cell Sci.* 129, 2697–2705.
- Bloomfield, G., Traynor, D., Sander, S. P., Veltman, D. M., Pachebat, J. A., and Kay, R. R. (2015). Neurofibromin controls macropinocytosis and phagocytosis in *Dictyostelium*. *eLife* 4:e04940.
- Bogner, C. W., Kamdem, R. S., Sichtermann, G., Matthaues, C., Holscher, D., Popp, J., et al. (2017). Bioactive secondary metabolites with multiple activities from a fungal endophyte. *Microb. Biotechnol.* 10, 175–188. doi: 10.1111/1751-7915.12467
- Bohdanowicz, M., and Grinstein, S. (2013). Role of phospholipids in endocytosis, phagocytosis, and macropinocytosis. *Physiol. Rev.* 93, 69–106. doi: 10.1152/physrev.00002.2012
- Bortner, C. D. (2005). Apoptotic volume decrease and nitric oxide. *Toxicology* 208, 213–221. doi: 10.1016/j.tox.2004.11.024
- Bortner, C. D., and Cidlowski, J. A. (2014). Ion channels and apoptosis in cancer. *Philos. Trans. R. Soc. Lond. B Biol. Sci.* 369:20130104. doi: 10.1098/rstb.2013.0104
- Bortner, C. D., and Cidlowski, J. A. (2020). Ions, the movement of water and the apoptotic volume decrease. *Front. Cell Dev. Biol.* 8:611211. doi: 10.3389/fcell.2020.611211
- Bose, S., He, H., and Stauber, T. (2021). Neurodegeneration upon dysfunction of endosomal/lysosomal CLC chloride transporters. *Front. Cell Dev. Biol.* 9:639231. doi: 10.3389/fcell.2021.639231

- Brack, E., Wachtel, M., Wolf, A., Kaech, A., Ziegler, U., and Schafer, B. W. (2020). Fenretinide induces a new form of dynamin-dependent cell death in pediatric sarcoma. *Cell Death Differ.* 27, 2500–2516. doi: 10.1038/s41418-020-0518-z
- Brel, V., Annereau, J. P., Vispe, S., Kruczyński, A., Bailly, C., and Guilbaud, N. (2011). Cytotoxicity and cell death mechanisms induced by the polyamine-vectorized anti-cancer drug F14512 targeting topoisomerase II. *Biochem. Pharmacol.* 82, 1843–1852. doi: 10.1016/j.bcp.2011.08.028
- Bretou, M., Saez, P. J., Sanseau, D., Maurin, M., Lankar, D., Chabaud, M., et al. (2017). Lysosome signaling controls the migration of dendritic cells. *Sci. Immunol.* 2:eak9573. doi: 10.1126/sciimmunol.aak9573
- Brignone, M. S., Lanciotti, A., Camerini, S., De Nuccio, C., Petrucci, T. C., Visentin, S., et al. (2015). MLC1 protein: a likely link between leukodystrophies and brain channelopathies. *Front. Cell. Neurosci.* 9:66. doi: 10.3389/fncel.2015.00106
- Brignone, M. S., Lanciotti, A., Visentin, S., De Nuccio, C., Molinari, P., Camerini, S., et al. (2014). Megalencephalic leukoencephalopathy with subcortical cysts protein-1 modulates endosomal pH and protein trafficking in astrocytes: relevance to MLC disease pathogenesis. *Neurobiol. Dis.* 66, 1–18. doi: 10.1016/j.nbd.2014.02.003
- Brisson, L., Driffort, V., Benoist, L., Poet, M., Counillon, L., Antelmi, E., et al. (2013). NaV1.5 Na(+) channels allosterically regulate the NHE-1 exchanger and promote the activity of breast cancer cell invadopodia. *J. Cell Sci.* 126, 4835–4842.
- Brisson, L., Reshkin, S. J., Gore, J., and Roger, S. (2012). pH regulators in invadosomal functioning: proton delivery for matrix tasting. *Eur. J. Cell Biol.* 91, 847–860. doi: 10.1016/j.ejcb.2012.04.004
- Broer, S. (2014). The SLC38 family of sodium-amino acid co-transporters. *Pflugers Arch.* 466, 155–172. doi: 10.1007/s00424-013-1393-y
- Browe, D. M., and Baumgarten, C. M. (2006). EGFR kinase regulates volume-sensitive chloride current elicited by integrin stretch via PI-3K and NADPH oxidase in ventricular myocytes. *J. Gen. Physiol.* 127, 237–251. doi: 10.1085/jgp.200509366
- Brown, F. D., Rozelle, A. L., Yin, H. L., Balla, T., and Donaldson, J. G. (2001). Phosphatidylinositol 4,5-bisphosphate and Arf6-regulated membrane traffic. *J. Cell Biol.* 154, 1007–1017. doi: 10.1083/jcb.200103107
- Buckley, C. M., Gopaldass, N., Bosmani, C., Johnston, S. A., Soldati, T., Insall, R. H., et al. (2016). WASH drives early recycling from macropinosomes and phagosomes to maintain surface phagocytic receptors. *Proc. Natl. Acad. Sci. U.S.A.* 113, E5906–E5915.
- Buckley, C. M., and King, J. S. (2017). Drinking problems: mechanisms of macropinosome formation and maturation. *FEBS J.* 284, 3778–3790. doi: 10.1111/febs.14115
- Buckley, C. M., Pots, H., Gueho, A., Vines, J. H., Munn, C. J., Phillips, B. A., et al. (2020). Coordinated Ras and Rac activity shapes macropinosome cups and enables phagocytosis of geometrically diverse bacteria. *Curr. Biol.* 30, 2912.e5–2926.e5.
- Busch, G., Völkl, H., Haller, T., Ritter, M., Siemen, D., Moest, J., et al. (1997). Vesicular pH is sensitive to changes in cell volume. *Cell. Physiol. Biochem.* 7, 25–34. doi: 10.1159/000154849
- Busch, G. L., Lang, H. J., and Lang, F. (1996). Studies on the mechanism of swelling-induced lysosomal alkalization in vascular smooth muscle cells. *Pflugers Arch.* 431, 690–696. doi: 10.1007/BF02253831
- Busch, G. L., Schreiber, R., Dartsch, P. C., Völkl, H., Vom Dahl, S., Häussinger, D., et al. (1994). Involvement of microtubules in the link between cell volume and pH of acidic cellular compartments in rat and human hepatocytes. *Proc. Natl. Acad. Sci. U.S.A.* 91, 9165–9169. doi: 10.1073/pnas.91.19.9165
- Callies, C., Fels, J., Liashkovich, I., Kliche, K., Jeggle, P., Kusche-Vihrog, K., et al. (2011). Membrane potential depolarization decreases the stiffness of vascular endothelial cells. *J. Cell. Sci.* 124, 1936–1942. doi: 10.1242/jcs.084657
- Cameron, G. R. (1952). *Pathology of the Cell*. Edinburgh: Oliver and Boyd.
- Cang, C., Aranda, K., Seo, Y. J., Gasnier, B., and Ren, D. (2015). TMEM175 is an organelle K(+) channel regulating lysosomal function. *Cell* 162, 1101–1112. doi: 10.1016/j.cell.2015.08.002
- Cang, C., Bekele, B., and Ren, D. (2014). The voltage-gated sodium channel TPC1 confers endolysosomal excitability. *Nat. Chem. Biol.* 10, 463–469. doi: 10.1038/nchembio.1522
- Cang, C., Zhou, Y., Navarro, B., Seo, Y. J., Aranda, K., Shi, L., et al. (2013). mTOR regulates lysosomal ATP-sensitive two-pore Na(+) channels to adapt to metabolic state. *Cell* 152, 778–790. doi: 10.1016/j.cell.2013.01.023
- Canton, J. (2018). Macropinocytosis: new insights into its underappreciated role in innate immune cell surveillance. *Front. Immunol.* 9:2286. doi: 10.3389/fimmu.2018.02286
- Cao, Q., Zhong, X. Z., Zou, Y., Zhang, Z., Toro, L., and Dong, X. P. (2015). BK channels alleviate lysosomal storage diseases by providing positive feedback regulation of lysosomal Ca²⁺ release. *Dev. Cell.* 33, 427–441. doi: 10.1016/j.devcel.2015.04.010
- Capdevila-Nortes, X., Lopez-Hernandez, T., Apaja, P. M., Lopez De Heredia, M., Sirisi, S., Callejo, G., et al. (2013). Insights into MLC pathogenesis: glialCAM is an MLC1 chaperone required for proper activation of volume-regulated anion currents. *Hum. Mol. Genet.* 22, 4405–4416. doi: 10.1093/hmg/ddt290
- Castellano, E., and Downward, J. (2011). “Role of RAS in the regulation of PI 3-kinase,” in *Phosphoinositide 3-kinase in Health and Disease*, eds C. Rommel, B. Vanhaesebroeck, and P. K. Vogt (Berlin: Springer), 143–169. doi: 10.1007/82_2010_56
- Castellano, E., Sheridan, C., Thin, M. Z., Nye, E., Spencer-Dene, B., Diefenbacher, M. E., et al. (2013). Requirement for interaction of PI3-kinase p110alpha with RAS in lung tumor maintenance. *Cancer Cell* 24, 617–630. doi: 10.1016/j.ccr.2013.09.012
- Castonguay, J., Orth, J. H. C., Muller, T., Sleman, F., Grimm, C., Wahl-Schott, C., et al. (2017). The two-pore channel TPC1 is required for efficient protein processing through early and recycling endosomes. *Sci. Rep.* 7:10038.
- Centeio, R., Ousingawat, J., Schreiber, R., and Kunzelmann, K. (2020). Ca²⁺ dependence of volume-regulated VRAC/LRRC8 and TMEM16A Cl[−] channels. *Front. Cell Dev. Biol.* 8:596879. doi: 10.3389/fcell.2020.596879
- Cevc, G. (1990). Membrane electrostatics. *Biochim. Biophys. Acta* 1031, 311–382.
- Chadwick, S. R., Grinstein, S., and Freeman, S. A. (2021a). From the inside out: ion fluxes at the centre of endocytic traffic. *Curr. Opin. Cell Biol.* 71, 77–86. doi: 10.1016/j.ccb.2021.02.006
- Chadwick, S. R., Wu, J., and Freeman, S. A. (2021b). Solute transport controls membrane tension and organelle volume. *Cell Physiol. Biochem.* 55, 1–24. doi: 10.33594/000000318
- Chakraborty, K., Leung, K., and Krishnan, Y. (2017). High luminal chloride in the lysosome is critical for lysosome function. *eLife* 6:e28862.
- Chalmin, F., Ladoire, S., Mignot, G., Vincent, J., Bruchard, M., Remy-Martin, J. P., et al. (2010). Membrane-associated Hsp72 from tumor-derived exosomes mediates STAT3-dependent immunosuppressive function of mouse and human myeloid-derived suppressor cells. *J. Clin. Invest.* 120, 457–471.
- Chang, H. Y., Huang, T. C., Chen, N. N., Huang, H. C., and Juan, H. F. (2014). Combination therapy targeting ectopic ATP synthase and 26S proteasome induces ER stress in breast cancer cells. *Cell Death Dis.* 5:e1540. doi: 10.1038/cddis.2014.504
- Charlton, F. W., Hover, S., Fuller, J., Hewson, R., Fontana, J., Barr, J. N., et al. (2019). Cellular cholesterol abundance regulates potassium accumulation within endosomes and is an important determinant in bunyavirus entry. *J. Biol. Chem.* 294, 7335–7347. doi: 10.1074/jbc.ra119.007618
- Chaurra, A., Gutzman, B. M., Taylor, E., Ackroyd, P. C., and Christensen, K. A. (2011). Lucifer Yellow as a live cell fluorescent probe for imaging water transport in subcellular organelles. *Appl. Spectrosc.* 65, 20–25. doi: 10.1366/10-06095
- Chaurra-Arboleda, A. M. C. (2009). *Development of A Fluorescent Probe for Determination of Water Transport in Subcellular Organelles*. Clemson: Clemson University.
- Chen, C. C., Krogsaeter, E., Butz, E. S., Li, Y., Puertollano, R., Wahl-Schott, C., et al. (2020a). TRPML2 is an osmo/mechanosensitive cation channel in endolysosomal organelles. *Sci. Adv.* 6:eabb5064. doi: 10.1126/sciadv.abb5064
- Chen, C. C., Krogsaeter, E., and Grimm, C. (2020b). Two-pore and TRP cation channels in endolysosomal osmo-/mechanosensation and volume regulation. *Biochim. Biophys. Acta Mol. Cell. Res.* 1868:118921. doi: 10.1016/j.bbamcr.2020.118921
- Chen, C. L., Wang, Y., Sesaki, H., and Iijima, M. (2012). Myosin I links PIP3 signaling to remodeling of the actin cytoskeleton in chemotaxis. *Sci. Signal.* 5:ra10. doi: 10.1126/scisignal.2002446
- Chen, L., König, B., Liu, T., Pervaiz, S., Razzaque, Y. S., and Stauber, T. (2019). More than just a pressure relief valve: physiological roles of volume-regulated

- LRRC8 anion channels. *Biol. Chem.* 400, 1481–1496. doi: 10.1515/hsz-2019-0189
- Chen, L., Wang, L., Zhu, L., Nie, S., Zhang, J., Zhong, P., et al. (2002). Cell cycle-dependent expression of volume-activated chloride currents in nasopharyngeal carcinoma cells. *Am. J. Physiol. Cell. Physiol.* 283, C1313–C1323.
- Chen, Z., Zimnicka, A. M., Jiang, Y., Sharma, T., Chen, S., Lazarov, O., et al. (2018). Reciprocal regulation of eNOS and caveolin-1 functions in endothelial cells. *Mol. Biol. Cell.* 29, 1190–1202. doi: 10.1091/mbc.e17-01-0049
- Cheng, X., Shen, D., Samie, M., and Xu, H. (2010). Mucolipins: intracellular TRPML1-3 channels. *FEBS Lett.* 584, 2013–2021. doi: 10.1016/j.febslet.2009.12.056
- Cherfils, J., and Zeghouf, M. (2013). Regulation of small GTPases by GEFs, GAPs, and GDIs. *Physiol. Rev.* 93, 269–309. doi: 10.1152/physrev.00003.2012
- Chi, S., Kitanaka, C., Noguchi, K., Mochizuki, T., Nagashima, Y., Shirouzu, M., et al. (1999). Oncogenic Ras triggers cell suicide through the activation of a caspase-independent cell death program in human cancer cells. *Oncogene* 18, 2281–2290. doi: 10.1038/sj.onc.1202538
- Chiasson-Mackenzie, C., Morris, Z. S., Liu, C. H., Bradford, W. B., Koorman, T., and McClatchey, A. I. (2018). Merlin/ERM proteins regulate growth factor-induced macropinocytosis and receptor recycling by organizing the plasma membrane:cytoskeleton interface. *Genes Dev.* 32, 1201–1214. doi: 10.1101/gad.317354.118
- Cho, H., Geno, E., Patoor, M., Reid, A., McDonald, R., Hild, M., et al. (2018). Indolyl-pyridinyl-propenone-induced methuosis through the inhibition of PIKFYVE. *ACS Omega* 3, 6097–6103. doi: 10.1021/acsomega.8b00202
- Cho, S.-J., and Jena, B. P. (2006). “Secretory vesicle swelling by atomic force microscopy,” in *Cell Imaging Techniques: Methods and Protocols*, eds D. J. Taatjes and B. T. Mossman (Totowa, NJ: Humana Press), 317–330. doi: 10.1007/978-1-59259-993-6_16
- Choi, J., Kim, H., Bae, Y. K., and Cheong, H. (2017). REP1 modulates autophagy and macropinocytosis to enhance cancer cell survival. *Int. J. Mol. Sci.* 18:1866. doi: 10.3390/ijms18091866
- Choy, C. H., Saffi, G., Gray, M. A., Wallace, C., Dayam, R. M., Ou, Z. A., et al. (2018). Lysosome enlargement during inhibition of the lipid kinase PIKFyve proceeds through lysosome coalescence. *J. Cell Sci.* 131:jcs213587.
- Christensen, K. A., Myers, J. T., and Swanson, J. A. (2002). pH-dependent regulation of lysosomal calcium in macrophages. *J. Cell Sci.* 115, 599–607. doi: 10.1242/jcs.115.3.599
- Christoforidis, S., Miaczynska, M., Ashman, K., Wilm, M., Zhao, L., Yip, S. C., et al. (1999). Phosphatidylinositol-3-OH kinases are Rab5 effectors. *Nat. Cell Biol.* 1, 249–252. doi: 10.1038/12075
- Cigic, B., and Pain, R. H. (1999). Location of the binding site for chloride ion activation of cathepsin C. *Eur. J. Biochem.* 264, 944–951. doi: 10.1046/j.1432-1327.1999.00697.x
- Cingolani, F., Simbari, F., Abad, J. L., Casasampere, M., Fabrias, G., Futerman, A. H., et al. (2017). Jaspine B induces nonapoptotic cell death in gastric cancer cells independently of its inhibition of ceramide synthase. *J. Lipid Res.* 58, 1500–1513. doi: 10.1194/jlr.m072611
- Clement, D., Goodridge, J. P., Grimm, C., Patel, S., and Malmberg, K. J. (2020). TRP channels as interior designers: remodeling the endolysosomal compartment in natural killer cells. *Front. Immunol.* 11:753. doi: 10.3389/fimmu.2020.00753
- Cohen, B. E. (2018). Membrane thickness as a key factor contributing to the activation of osmosensors and essential ras signaling pathways. *Front. Cell Dev. Biol.* 6:76. doi: 10.3389/fcell.2018.00076
- Cohn, Z. A., and Parks, E. (1967). The regulation of pinocytosis in mouse macrophages. II. Factors inducing vesicle formation. *J. Exp. Med.* 125, 213–232. doi: 10.1084/jem.125.2.213
- Colin, M., Delporte, C., Janky, R., Lechon, A. S., Renard, G., Van Antwerpen, P., et al. (2019). Dysregulation of macropinocytosis processes in glioblastomas may be exploited to increase intracellular anti-cancer drug levels: the example of temozolomide. *Cancers* 11:411. doi: 10.3390/cancers11030411
- Collins, M. P., and Forgac, M. (2020). Regulation and function of V-ATPases in physiology and disease. *Biochim. Biophys. Acta Biomembr.* 1862:183341. doi: 10.1016/j.bbamem.2020.183341
- Commisso, C. (2019). The pervasiveness of macropinocytosis in oncological malignancies. *Philos. Trans. R. Soc. Lond. B Biol. Sci.* 374:20180153. doi: 10.1098/rstb.2018.0153
- Commisso, C., Davidson, S. M., Soydaner-Azeloglu, R. G., Parker, S. J., Kamphorst, J. J., Hackett, S., et al. (2013). Macropinocytosis of protein is an amino acid supply route in Ras-transformed cells. *Nature* 497, 633–637. doi: 10.1038/nature12138
- Compton, L. M., Ikonov, O. C., Sbrissa, D., Garg, P., and Shisheva, A. (2016). Active vacuolar H⁺ ATPase and functional cycle of Rab5 are required for the vacuolation defect triggered by PtdIns(3,5)P₂ loss under PIKfyve or Vps34 deficiency. *Am. J. Physiol. Cell Physiol.* 311, C366–C377.
- Cullen, P. J., and Steinberg, F. (2018). To degrade or not to degrade: mechanisms and significance of endocytic recycling. *Nat. Rev. Mol. Cell Biol.* 19, 679–696. doi: 10.1038/s41580-018-0053-7
- Cullis, J., Siolas, D., Avanzi, A., Barui, S., Maitra, A., and Bar-Sagi, D. (2017). Macropinocytosis of Nab-paclitaxel drives macrophage activation in pancreatic cancer. *Cancer Immunol. Res.* 5, 182–190. doi: 10.1158/2326-6066.cir-16-0125
- D’Amore, C., Moro, E., Borgo, C., Itami, K., Hirota, T., Pinna, L. A., et al. (2020). “Janus” efficacy of CX-5011: CK2 inhibition and methuosis induction by independent mechanisms. *Biochim. Biophys. Acta Mol. Cell Res.* 1867:118807. doi: 10.1016/j.bbamcr.2020.118807
- D’Arcy, M. S. (2019). Cell death: a review of the major forms of apoptosis, necrosis and autophagy. *Cell Biol. Int.* 43, 582–592. doi: 10.1002/cbin.11137
- Dartsch, P. C., Kolb, H. A., Beckmann, M., and Lang, F. (1994a). Morphological alterations and cytoskeletal reorganization in opossum kidney (OK) cells during osmotic swelling and volume regulation. *Histochemistry* 102, 69–75. doi: 10.1007/bf00271051
- Dartsch, P. C., Ritter, M., Haussinger, D., and Lang, F. (1994b). Cytoskeletal reorganization in NIH 3T3 fibroblasts expressing the ras oncogene. *Eur. J. Cell Biol.* 63, 316–325.
- Dartsch, P. C., Ritter, M., Gschwentner, M., Lang, H. J., and Lang, F. (1995). Effects of calcium channel blockers on NIH 3T3 fibroblasts expressing the Ha-ras oncogene. *Eur. J. Cell Biol.* 67, 372–378.
- Davis, R. J., and Czech, M. P. (1985). Amiloride directly inhibits growth factor receptor tyrosine kinase activity. *J. Biol. Chem.* 260, 2543–2551. doi: 10.1016/s0021-9258(18)89586-2
- Day, R. E., Kitchen, P., Owen, D. S., Bland, C., Marshall, L., Conner, A. C., et al. (2014). Human aquaporins: regulators of transcellular water flow. *Biochim. Biophys. Acta* 1840, 1492–1506. doi: 10.1016/j.bbagen.2013.09.033
- De Baey, A., and Lanzavecchia, A. (2000). The role of aquaporins in dendritic cell macropinocytosis. *J. Exp. Med.* 191, 743–748. doi: 10.1084/jem.191.4.743
- De Los Heros, P., Pacheco-Alvarez, D., and Gamba, G. (2018). “Chapter seven - role of WNK kinases in the modulation of cell volume,” in *Current Topics in Membranes*, eds I. Levitan, E. Delpire, and H. Rasgado-Flores (London: Academic Press), 207–235. doi: 10.1016/bs.ctm.2018.08.002
- Del Conte-Zerial, P., Brusch, L., Rink, J. C., Collinet, C., Kalaidzidis, Y., Zerial, M., et al. (2008). Membrane identity and GTPase cascades regulated by toggle and cut-out switches. *Mol. Syst. Biol.* 4:206. doi: 10.1038/msb.2008.45
- Delpire, E., and Gagnon, K. B. (2018). Water homeostasis and cell volume maintenance and regulation. *Curr. Top. Membr.* 81, 3–52. doi: 10.1016/bs.ctm.2018.08.001
- Demaurex, N. (2002). pH Homeostasis of cellular organelles. *News Physiol. Sci.* 17, 1–5. doi: 10.1152/physiologyonline.2002.17.1.1
- Dendo, K., Yugawa, T., Nakahara, T., Ohno, S. I., Goshima, N., Arakawa, H., et al. (2018). Induction of non-apoptotic programmed cell death by oncogenic RAS in human epithelial cells and its suppression by MYC overexpression. *Carcinogenesis* 39, 202–213. doi: 10.1093/carcin/bgx124
- Deng, Z., Zhao, Y., Feng, J., Zhang, J., Zhao, H., Rau, M. J., et al. (2021). Cryo-EM structure of a proton-activated chloride channel TMEM206. *Sci. Adv.* 7:eabe5983. doi: 10.1126/sciadv.abe5983
- Desai, A. S., Hunter, M. R., and Kapustin, A. N. (2019). Using macropinocytosis for intracellular delivery of therapeutic nucleic acids to tumour cells. *Philos. Trans. R. Soc. Lond. B Biol. Sci.* 374:20180156. doi: 10.1098/rstb.2018.0156
- Di Russo Case, E. D., Smith, J. A., Ficht, T. A., Samuel, J. E., and De Figueiredo, P. (2016). Space: a final frontier for vacuolar pathogens. *Traffic* 17, 461–474. doi: 10.1111/tra.12382
- Ding, L., Zhang, L., Kim, M., Byzova, T., and Podrez, E. (2017). Akt3 kinase suppresses pinocytosis of low-density lipoprotein by macrophages via a novel WNK/SGK1/Cdc42 protein pathway. *J. Biol. Chem.* 292, 9283–9293. doi: 10.1074/jbc.m116.773739

- Docampo, R., Jimenez, V., King-Keller, S., Li, Z. H., and Moreno, S. N. (2011). The role of acidocalcisomes in the stress response of *Trypanosoma cruzi*. *Adv. Parasitol.* 75, 307–324. doi: 10.1016/b978-0-12-385863-4.00014-9
- Docampo, R., Jimenez, V., Lander, N., Li, Z. H., and Niyogi, S. (2013). New insights into roles of acidocalcisomes and contractile vacuole complex in osmoregulation in protists. *Int. Rev. Cell. Mol. Biol.* 305, 69–113. doi: 10.1016/b978-0-12-407695-2.00002-0
- Dolat, L., and Spiliotis, E. T. (2016). Septins promote macropinosome maturation and traffic to the lysosome by facilitating membrane fusion. *J. Cell. Biol.* 214, 517–527. doi: 10.1083/jcb.201603030
- Donaldson, J. G. (2019). Macropinosome formation, maturation and membrane recycling: lessons from clathrin-independent endosomal membrane systems. *Philos. Trans. R. Soc. Lond. B Biol. Sci.* 374:20180148. doi: 10.1098/rstb.2018.0148
- Dong, X. P., Wang, X., and Xu, H. (2010). TRP channels of intracellular membranes. *J. Neurochem.* 113, 313–328. doi: 10.1111/j.1471-4159.2010.06626.x
- Donowitz, M., Ming Tse, C., and Fuster, D. (2013). SLC9/NHE gene family, a plasma membrane and organellar family of Na(+)/H(+) exchangers. *Mol. Aspects Med.* 34, 236–251. doi: 10.1016/j.mam.2012.05.001
- Doodnauth, S. A., Grinstein, S., and Maxson, M. E. (2019). Constitutive and stimulated macropinocytosis in macrophages: roles in immunity and in the pathogenesis of atherosclerosis. *Philos. Trans. R. Soc. Lond. B Biol. Sci.* 374:20180147. doi: 10.1098/rstb.2018.0147
- Doroshenko, P., Sabanov, V., and Doroshenko, N. (2001). Cell cycle-related changes in regulatory volume decrease and volume-sensitive chloride conductance in mouse fibroblasts. *J. Cell Physiol.* 187, 65–72. doi: 10.1002/1097-4652(200104)187:1<65::aid-jcp1052>3.0.co;2-a
- Dove, S. K., Cooke, F. T., Douglas, M. R., Sayers, L. G., Parker, P. J., and Michell, R. H. (1997). Osmotic stress activates phosphatidylinositol-3,5-bisphosphate synthesis. *Nature* 390, 187–192. doi: 10.1038/36613
- Dubinsky, W. P. Jr., and Frizzell, R. A. (1983). A novel effect of amiloride on H⁺-dependent Na⁺ transport. *Am. J. Physiol.* 245, C157–C159.
- Duex, J. E., Nau, J. J., Kauffman, E. J., and Weisman, L. S. (2006). Phosphoinositide 5-phosphatase Fig 4p is required for both acute rise and subsequent fall in stress-induced phosphatidylinositol 3,5-bisphosphate levels. *Eukaryot Cell* 5, 723–731. doi: 10.1128/ec.5.4.723-731.2006
- Eaton, A. F., Merkulova, M., and Brown, D. (2021). The H(+)-ATPase (V-ATPase): from proton pump to signaling complex in health and disease. *Am. J. Physiol. Cell Physiol.* 320, C392–C414.
- Echevarria, M., and Verkman, A. S. (1992). Optical measurement of osmotic water transport in cultured cells. Role of glucose transporters. *J. Gen. Physiol.* 99, 573–589. doi: 10.1085/jgp.99.4.573
- Egami, Y. (2016). Molecular imaging analysis of Rab GTPases in the regulation of phagocytosis and macropinocytosis. *Anat. Sci. Int.* 91, 35–42. doi: 10.1007/s12565-015-0313-y
- Egami, Y., Taguchi, T., Maekawa, M., Arai, H., and Araki, N. (2014). Small GTPases and phosphoinositides in the regulatory mechanisms of macropinosome formation and maturation. *Front. Physiol.* 5:374. doi: 10.3389/fphys.2014.00374
- Elorza-Vidal, X., Sirisi, S., Gaitán-Peñas, H., Pérez-Rius, C., Alonso-Gardón, M., Armand-Ugón, M., et al. (2018). GlialCAM/MLC1 modulates LRRC8/VRAC currents in an indirect manner: implications for megalencephalic leukoencephalopathy. *Neurobiol. Dis.* 119, 88–99. doi: 10.1016/j.nbd.2018.07.031
- Falcone, S., Cocucci, E., Podini, P., Kirchhausen, T., Clementi, E., and Meldolesi, J. (2006). Macropinocytosis: regulated coordination of endocytic and exocytic membrane traffic events. *J. Cell Sci.* 119, 4758–4769. doi: 10.1242/jcs.03238
- Fan, S. H., Numata, Y., and Numata, M. (2016). Endosomal Na⁺/H⁺ exchanger NHE5 influences MET recycling and cell migration. *Mol. Biol. Cell.* 27, 702–715. doi: 10.1091/mbc.e15-04-0257
- Faundez, V., and Hartzell, H. C. (2004). Intracellular chloride channels: determinants of function in the endosomal pathway. *Sci. STKE* 2004:re8. doi: 10.1126/stke.2332004re8
- Feliciano, W. D., Yoshida, S., Straight, S. W., and Swanson, J. A. (2011). Coordination of the Rab5 cycle on macropinosomes. *Traffic* 12, 1911–1922. doi: 10.1111/j.1600-0854.2011.01280.x
- Fels, J., Callies, C., Kusche-Vihrog, K., and Oberleithner, H. (2010). Nitric oxide release follows endothelial nanomechanics and not vice versa. *Pflugers Arch.* 460, 915–923. doi: 10.1007/s00424-010-0871-8
- Fettiplace, R., and Haydon, D. A. (1980). Water permeability of lipid membranes. *Physiol. Rev.* 60, 510–550. doi: 10.1152/physrev.1980.60.2.510
- Fischbarg, J., Kuang, K. Y., Hirsch, J., Lecuona, S., Rogozinski, L., Silverstein, S. C., et al. (1989). Evidence that the glucose transporter serves as a water channel in J774 macrophages. *Proc. Natl. Acad. Sci. U.S.A.* 86, 8397–8401. doi: 10.1073/pnas.86.21.8397
- Fischbarg, J., and Vera, J. C. (1995). Multifunctional transporter models: lessons from the transport of water, sugars, and ring compounds by GLUTs. *Am. J. Physiol.* 268, C1077–C1089.
- Fleischman, L. F., Chahwala, S. B., and Cantley, L. (1986). ras-transformed cells: altered levels of phosphatidylinositol-4,5-bisphosphate and catabolites. *Science* 231, 407–410. doi: 10.1126/science.3001936
- Fomin, V. (2019). *Novel Functions of C9ORF72, A Gene Involved in ALS/FTD*. New York, NY: Columbia University.
- Fomin, V., Richard, P., Hoque, M., Li, C., Gu, Z., Fissore-O'leary, M., et al. (2018). The C9ORF72 gene, implicated in amyotrophic lateral sclerosis and frontotemporal dementia, encodes a protein that functions in control of endothelin and glutamate signaling. *Mol. Cell Biol.* 38:e00155-18.
- Freedman, S. D., Kern, H. F., and Scheele, G. A. (2001). Pancreatic acinar cell dysfunction in CFTR(-/-) mice is associated with impairments in luminal pH and endocytosis. *Gastroenterology* 121, 950–957. doi: 10.1053/gast.2001.27992
- Freeman, M. C., Peek, C. T., Becker, M. M., Smith, E. C., and Denison, M. R. (2014). Coronaviruses induce entry-independent, continuous macropinocytosis. *mBio* 5:e01340-14.
- Freeman, S. A., and Grinstein, S. (2014). Phagocytosis: receptors, signal integration, and the cytoskeleton. *Immunol. Rev.* 262, 193–215. doi: 10.1111/imr.12212
- Freeman, S. A., and Grinstein, S. (2018). Resolution of macropinosomes, phagosomes and autolysosomes: osmotically driven shrinkage enables tubulation and vesiculation. *Traffic* 19, 965–974. doi: 10.1111/tra.12614
- Freeman, S. A., Uderhardt, S., Saric, A., Collins, R. F., Buckley, C. M., Mylvaganam, S., et al. (2020). Lipid-gated monovalent ion fluxes regulate endocytic traffic and support immune surveillance. *Science* 367, 301–305. doi: 10.1126/science.aaw9544
- Fuchs, R., Schmid, S., and Mellman, I. (1989). A possible role for Na⁺,K⁺-ATPase in regulating ATP-dependent endosome acidification. *Proc. Natl. Acad. Sci. U.S.A.* 86, 539–543. doi: 10.1073/pnas.86.2.539
- Furst, J., Gschwentner, M., Ritter, M., Botta, G., Jakab, M., Mayer, M., et al. (2002). Molecular and functional aspects of anionic channels activated during regulatory volume decrease in mammalian cells. *Pflugers Arch.* 444, 1–25. doi: 10.1007/s00424-002-0805-1
- Fuster, D. G., and Alexander, R. T. (2014). Traditional and emerging roles for the SLC9 Na⁺/H⁺ exchangers. *Pflugers Arch.* 466, 61–76. doi: 10.1007/s00424-013-1408-8
- Futai, M., Sun-Wada, G. H., Wada, Y., Matsumoto, N., and Nakanishi-Matsui, M. (2019). Vacuolar-type ATPase: a proton pump to lysosomal trafficking. *Proc. Jpn. Acad. Ser. B Phys. Biol. Sci.* 95, 261–277. doi: 10.2183/pjab.95.018
- Gaitan-Peñas, H., Gradogna, A., Laparra-Cuervo, L., Solsona, C., Fernandez-Duenas, V., Barrallo-Gimeno, A., et al. (2016). Investigation of LRRC8-mediated volume-regulated anion currents in *Xenopus oocytes*. *Biophys. J.* 111, 1429–1443. doi: 10.1016/j.bpj.2016.08.030
- Galluzzi, L., Vitale, I., Aaronson, S. A., Abrams, J. M., Adam, D., Agostinis, P., et al. (2018). Molecular mechanisms of cell death: recommendations of the Nomenclature Committee on Cell Death 2018. *Cell Death Differ.* 25, 486–541.
- Ganapathy, V., Thangaraju, M., Gopal, E., Martin, P. M., Itagaki, S., Miyauchi, S., et al. (2008). Sodium-coupled monocarboxylate transporters in normal tissues and in cancer. *AAPS J.* 10, 193–199.
- Gao, X., Ruan, X., Ji, H., Peng, L., Qiu, Y., Yang, D., et al. (2020). Maduramicin triggers methuosis-like cell death in primary chicken myocardial cells. *Toxicol. Lett.* 333, 105–114. doi: 10.1016/j.toxlet.2020.07.025
- Garrity, A. G., Wang, W., Collier, C. M., Levey, S. A., Gao, Q., and Xu, H. (2016). The endoplasmic reticulum, not the pH gradient, drives calcium refilling of lysosomes. *eLife* 5:e15887.
- Gayle, S., Landrette, S., Beehar, N., Conrad, C., Hernandez, M., Beckett, P., et al. (2017). Identification of apilimod as a first-in-class PIKfyve kinase inhibitor

- for treatment of B-cell non-Hodgkin lymphoma. *Blood* 129, 1768–1778. doi: 10.1182/blood-2016-09-736892
- Gerasimenko, J. V., Tepikin, A. V., Petersen, O. H., and Gerasimenko, O. V. (1998). Calcium uptake via endocytosis with rapid release from acidifying endosomes. *Curr. Biol.* 8, 1335–1338. doi: 10.1016/s0960-9822(07)00565-9
- Ghoshal, P., Singla, B., Lin, H., Cherian-Shaw, M., Tritz, R., Padgett, C. A., et al. (2019). Loss of GTPase activating protein neurofibromin stimulates paracrine cell communication via macropinocytosis. *Redox Biol.* 27:101224. doi: 10.1016/j.redox.2019.101224
- Gonano, L. A., Morell, M., Burgos, J. I., Dulce, R. A., De Giusti, V. C., Aiello, E. A., et al. (2014). Hypotonic swelling promotes nitric oxide release in cardiac ventricular myocytes: impact on swelling-induced negative inotropic effect. *Cardiovasc. Res.* 104, 456–466. doi: 10.1093/cvr/cvu230
- Gong, X., Sun, R., Gao, Z., Han, W., Liu, Y., Zhao, L., et al. (2018). Tubeimoside 1 acts as a chemotherapeutic synergist via stimulating macropinocytosis. *Front. Pharmacol.* 9:1044. doi: 10.3389/fphar.2018.01044
- Gorg, B., Schliess, F., and Haussinger, D. (2013). Osmotic and oxidative/nitrosative stress in ammonia toxicity and hepatic encephalopathy. *Arch. Biochem. Biophys.* 536, 158–163. doi: 10.1016/j.abb.2013.03.010
- Grimm, C., Hassan, S., Wahl-Schott, C., and Biel, M. (2012). Role of TRPML and two-pore channels in endolysosomal cation homeostasis. *J. Pharmacol. Exp. Ther.* 342, 236–244. doi: 10.1124/jpet.112.192880
- Grimm, C., Holdt, L. M., Chen, C. C., Hassan, S., Muller, C., Jors, S., et al. (2014). High susceptibility to fatty liver disease in two-pore channel 2-deficient mice. *Nat. Commun.* 5, 4699. doi: 10.1038/ncomms5699
- Gupta, S., Ramjaun, A. R., Haiko, P., Wang, Y., Warne, P. H., Nicke, B., et al. (2007). Binding of ras to phosphoinositide 3-kinase p110alpha is required for ras-driven tumorigenesis in mice. *Cell* 129, 957–968. doi: 10.1016/j.cell.2007.03.051
- Guzman, R. E., Grieschat, M., Fahlke, C., and Alekov, A. K. (2013). ClC-3 is an intracellular chloride/proton exchanger with large voltage-dependent nonlinear capacitance. *ACS Chem. Neurosci.* 4, 994–1003. doi: 10.1021/cn400032z
- Hackam, D. J., Rotstein, O. D., and Grinstein, S. (1999). “Phagosomal acidification mechanisms and functional significance,” in *Phagocytosis: The Host*, ed. S. Gordon (Mumbai: JAI), 299–319. doi: 10.1016/s1874-5172(99)80037-6
- Hackam, D. J., Rotstein, O. D., Zhang, W. J., Demareux, N., Woodside, M., Tsai, O., et al. (1997). Regulation of phagosomal acidification. Differential targeting of Na⁺/H⁺ exchangers, Na⁺/K⁺-ATPases, and vacuolar-type H⁺-ATPases. *J. Biol. Chem.* 272, 29810–29820.
- Hamann, S., Herrera-Perez, J. J., Zeuthen, T., and Alvarez-Leefmans, F. J. (2010). Cotransport of water by the Na⁺-K⁺-2Cl⁻ cotransporter NKCC1 in mammalian epithelial cells. *J. Physiol.* 588, 4089–4101. doi: 10.1113/jphysiol.2010.194738
- Hansen, S. B. (2015). Lipid agonism: the PIP2 paradigm of ligand-gated ion channels. *Biochim. Biophys. Acta* 1851, 620–628. doi: 10.1016/j.bbali.2015.01.011
- Hara-Chikuma, M., Sugiyama, Y., Kabashima, K., Sohara, E., Uchida, S., Sasaki, S., et al. (2011). Involvement of aquaporin-7 in the cutaneous primary immune response through modulation of antigen uptake and migration in dendritic cells. *FASEB J.* 26, 211–218. doi: 10.1096/fj.11-186627
- Harl, B., Schmolzer, J., Jakab, M., Ritter, M., and Kerschbaum, H. H. (2013). Chloride channel blockers suppress formation of engulfment pseudopodia in microglial cells. *Cell Physiol. Biochem.* 31, 319–337. doi: 10.1159/000343370
- Hatch, A. J., and York, J. D. (2010). SnapShot: inositol phosphates. *Cell* 143, 1030.e1–1030.e1.
- Haussinger, D., and Schliess, F. (2005). Astrocyte swelling and protein tyrosine nitration in hepatic encephalopathy. *Neurochem. Int.* 47, 64–70. doi: 10.1016/j.neuint.2005.04.008
- Hazama, A., Kozono, D., Guggino, W. B., Agre, P., and Yasui, M. (2002). Ion permeation of AQP6 water channel protein. Single channel recordings after Hg2⁺ activation. *J. Biol. Chem.* 277, 29224–29230. doi: 10.1074/jbc.m204258200
- Henics, T., and Wheatley, D. N. (1999). Cytoplasmic vacuolation, adaptation and cell death: a view on new perspectives and features. *Biol. Cell* 91, 485–498. doi: 10.1016/s0248-4900(00)88205-2
- Higgs, H. N., and Pollard, T. D. (2000). Activation by Cdc42 and PIP(2) of Wiskott-Aldrich syndrome protein (WASP) stimulates actin nucleation by Arp2/3 complex. *J. Cell. Biol.* 150, 1311–1320. doi: 10.1083/jcb.150.6.1311
- Hille, B., Dickson, E. J., Kruse, M., Vivas, O., and Suh, B. C. (2015). Phosphoinositides regulate ion channels. *Biochim. Biophys. Acta* 1851, 844–856. doi: 10.1016/j.bbali.2014.09.010
- Hinze, C., and Boucrot, E. (2018). Local actin polymerization during endocytic carrier formation. *Biochem. Soc. Trans.* 46, 565–576. doi: 10.1042/bst20170355
- Hoffmann, E. K., Lambert, I. H., and Pedersen, S. F. (2009). Physiology of cell volume regulation in vertebrates. *Physiol. Rev.* 89, 193–277. doi: 10.1152/physrev.00037.2007
- Hryciw, D. H., Jenkin, K. A., Simcocks, A. C., Grinfeld, E., Mcainch, A. J., and Poronnik, P. (2012). The interaction between megalin and ClC-5 is scaffolded by the Na⁺-H⁺ exchanger regulatory factor 2 (NHERF2) in proximal tubule cells. *Int. J. Biochem. Cell Biol.* 44, 815–823. doi: 10.1016/j.biocel.2012.02.007
- Huang, B., Wang, H., and Yang, B. (2017). “Water transport mediated by other membrane proteins,” in *Aquaporins*, ed. B. Yang (Dordrecht: Springer), 251–261. doi: 10.1007/978-94-024-1057-0_17
- Huang, W., Sun, X., Li, Y., He, Z., Li, L., Deng, Z., et al. (2018). Discovery and identification of small molecules as methuosis inducers with in vivo antitumor activities. *J. Med. Chem.* 61, 5424–5434. doi: 10.1021/acs.jmedchem.8b00753
- Huang, Y., and Rane, S. G. (1993). Single channel study of a Ca(2+)-activated K⁺ current associated with ras-induced cell transformation. *J. Physiol.* 461, 601–618. doi: 10.1113/jphysiol.1993.sp019531
- Hughey, J. J., Wikswo, J. P., and Seale, K. T. (2007). “Intra-microfluidic pinocytic loading of human T cells,” in *Proceedings of the 2007 IEEE/Nih Life Science Systems and Applications Workshop* (Piscataway, NJ: IEEE), 132–135.
- Hurtado-Lorenzo, A., Skinner, M., El Annan, J., Futai, M., Sun-Wada, G. H., Bourgoin, S., et al. (2006). V-ATPase interacts with ARNO and Arf6 in early endosomes and regulates the protein degradative pathway. *Nat. Cell Biol.* 8, 124–136. doi: 10.1038/ncb1348
- Ikonov, O. C., Altankov, G., Sbrissa, D., and Shisheva, A. (2018). PIKfyve inhibitor cytotoxicity requires AKT suppression and excessive cytoplasmic vacuolation. *Toxicol. Appl. Pharmacol.* 356, 151–158. doi: 10.1016/j.taap.2018.08.001
- Ilie, A., Gao, A. Y., Reid, J., Boucher, A., Mcewan, C., Barriere, H., et al. (2016). A Christianson syndrome-linked deletion mutation ((287)ES(288)) in SLC9A6 disrupts recycling endosomal function and elicits neurodegeneration and cell death. *Mol. Neurodegener.* 11:63.
- Ilie, A., Weinstein, E., Boucher, A., McKinney, R. A., and Orlowski, J. (2014). Impaired posttranslational processing and trafficking of an endosomal Na⁺/H⁺ exchanger NHE6 mutant (Delta(370)WST(372)) associated with X-linked intellectual disability and autism. *Neurochem. Int.* 73, 192–203. doi: 10.1016/j.neuint.2013.09.020
- Imamura, J., Suzuki, Y., Gonda, K., Roy, C. N., Gatanaga, H., Ohuchi, N., et al. (2011). Single particle tracking confirms that multivalent Tat protein transduction domain-induced heparan sulfate proteoglycan cross-linkage activates Rac1 for internalization. *J. Biol. Chem.* 286, 10581–10592. doi: 10.1074/jbc.m110.187450
- Insel, P. A., Sriram, K., Salmeron, C., and Wiley, S. Z. (2020). Proton-sensing G protein-coupled receptors: detectors of tumor acidosis and candidate drug targets. *Future Med. Chem.* 12, 523–532. doi: 10.4155/fmc-2019-0357
- Ishibashi, K., Koike, S., Kondo, S., Hara, S., and Tanaka, Y. (2009). The role of a group III AQP, AQP11 in intracellular organelle homeostasis. *J. Med. Invest.* 56, 312–317. doi: 10.2152/jmi.56.312
- Ishida, Y., Nayak, S., Mindell, J. A., and Grabe, M. (2013). A model of lysosomal pH regulation. *J. Gen. Physiol.* 141, 705–720. doi: 10.1085/jgp.201210930
- Ishihara, S., Ichijo, H., and Watanabe, K. (2021). A novel lens for cell volume regulation: liquid-liquid phase separation. *Cell Physiol. Biochem.* 55, 135–160. doi: 10.33594/000000357
- Isobe, Y., Nigorikawa, K., Tsurumi, G., Takemasu, S., Takasuga, S., Kofuji, S., et al. (2019). PIKfyve accelerates phagosome acidification through activation of TRPML1 while arrests aberrant vacuolation independent of the Ca2⁺ channel. *J. Biochem.* 165, 75–84. doi: 10.1093/jb/mvy084
- Jakab, M., Furst, J., Gschwentner, M., Botta, G., Garavaglia, M. L., Bazzini, C., et al. (2002). Mechanisms sensing and modulating signals arising from cell swelling. *Cell Physiol. Biochem.* 12, 235–258. doi: 10.1159/000067895
- Jakab, M., and Ritter, M. (2006). Cell volume regulatory ion transport in the regulation of cell migration. *Contrib. Nephrol.* 152, 161–180. doi: 10.1159/000096322

- Jang, H., Banerjee, A., Chavan, T. S., Lu, S., Zhang, J., Gaponenko, V., et al. (2016). The higher level of complexity of K-Ras4B activation at the membrane. *FASEB J.* 30, 1643–1655. doi: 10.1096/fj.15-279091
- Jefferies, H. B., Cooke, F. T., Jat, P., Boucheron, C., Koizumi, T., Hayakawa, M., et al. (2008). A selective PIKfyve inhibitor blocks PtdIns(3,5)P(2) production and disrupts endomembrane transport and retroviral budding. *EMBO Rep.* 9, 164–170. doi: 10.1038/sj.embor.7401155
- Jena, B. P. (2020). “Aquaporin regulation: lessons from secretory vesicles,” in *Aquaporin Regulation*, ed. G. Litwack (New York, NY: Academic Press), 147–162. doi: 10.1016/bs.vh.2019.08.007
- Jentsch, T. J. (2007). Chloride and the endosomal-lysosomal pathway: emerging roles of CLC chloride transporters. *J. Physiol.* 578, 633–640. doi: 10.1113/jphysiol.2006.124719
- Jentsch, T. J. (2016). VRACs and other ion channels and transporters in the regulation of cell volume and beyond. *Nat. Rev. Mol. Cell Biol.* 17, 293–307. doi: 10.1038/nrm.2016.29
- Jentsch, T. J., Lutter, D., Planells-Cases, R., Ullrich, F., and Voss, F. K. (2016). VRAC: molecular identification as LRRC8 heteromers with differential functions. *Pflügers Arch. Eur. J. Physiol.* 468, 385–393. doi: 10.1007/s00424-015-1766-5
- Jentsch, T. J., and Pusch, M. (2018). CLC chloride channels and transporters: structure, function, physiology, and disease. *Physiol. Rev.* 98, 1493–1590. doi: 10.1152/physrev.00047.2017
- Jiang, J., Kao, C. Y., and Papoutsakis, E. T. (2017). How do megakaryocytic microparticles target and deliver cargo to alter the fate of hematopoietic stem cells? *J. Control. Release* 247, 1–18. doi: 10.1016/j.jconrel.2016.12.021
- Jiang, L. W., Maher, V. M., McCormick, J. J., and Schindler, M. (1990). Alkalinization of the lysosomes is correlated with ras transformation of murine and human fibroblasts. *J. Biol. Chem.* 265, 4775–4777. doi: 10.1016/s0021-9258(19)34037-2
- Jin, X., Zhang, Y., Alharbi, A., Hanbashi, A., Alhoshani, A., and Parrington, J. (2020). Targeting two-pore channels: current progress and future challenges. *Trends Pharmacol. Sci.* 41, 582–594. doi: 10.1016/j.tips.2020.06.002
- John, S., Sivakumar, K. C., and Mishra, R. (2017). Bacoside A induces tumor cell death in human glioblastoma cell lines through catastrophic macropinocytosis. *Front. Mol. Neurosci.* 10:171. doi: 10.3389/fnmol.2017.00171
- Josefsson, J. O. (1968). Induction and inhibition of pinocytosis in *Amoeba proteus*. *Acta Physiol. Scand.* 73, 481–490. doi: 10.1111/j.1365-201x.1968.tb10887.x
- Josefsson, J.-O., Holmer, N.-G., and Hansson, S. E. (1975). Membrane potential and conductance during pinocytosis induced in amoeba proteus with alkali metal ions. *Acta Physiol. Scand.* 94, 278–288. doi: 10.1111/j.1748-1716.1975.tb05887.x
- Jung, J., Cho, K. J., Naji, A. K., Clemons, K. N., Wong, C. O., Villanueva, M., et al. (2019). HRAS-driven cancer cells are vulnerable to TRPML1 inhibition. *EMBO Rep.* 20:e46685.
- Jung, J., and Venkatachalam, K. (2019). TRPML1 and RAS-driven cancers - exploring a link with great therapeutic potential. *Channels* 13, 374–381. doi: 10.1080/19336950.2019.1666457
- Kabayama, H., Nakamura, T., Takeuchi, M., Iwasaki, H., Taniguchi, M., Tokushige, N., et al. (2009). Ca²⁺ induces macropinocytosis via F-actin depolymerization during growth cone collapse. *Mol. Cell. Neurosci.* 40, 27–38. doi: 10.1016/j.mcn.2008.08.009
- Kang, Y. L., Chou, Y. Y., Rothlauf, P. W., Liu, Z., Soh, T. K., Cureton, D., et al. (2020). Inhibition of PIKfyve kinase prevents infection by Zaire ebolavirus and SARS-CoV-2. *Proc. Natl. Acad. Sci. U.S.A.* 117, 20803–20813. doi: 10.1073/pnas.2007837117
- Karim, M. A., and Brett, C. L. (2018). The Na⁺/(K⁺)/H⁺ exchanger Nhx1 controls multivesicular body-vacuolar lysosome fusion. *Mol. Biol. Cell* 29, 317–325. doi: 10.1091/mbc.e17-08-0496
- Kasahara, K., Nakayama, Y., Sato, I., Ikeda, K., Hoshino, M., Endo, T., et al. (2007). Role of Src-family kinases in formation and trafficking of macropinosomes. *J. Cell. Physiol.* 211, 220–232. doi: 10.1002/jcp.20931
- Kaul, A., Overmeyer, J. H., and Maltese, W. A. (2007). Activated Ras induces cytoplasmic vacuolation and non-apoptotic death in glioblastoma cells via novel effector pathways. *Cell Signal.* 19, 1034–1043. doi: 10.1016/j.cellsig.2006.11.010
- Kawabe, K., Takano, K., Moriyama, M., and Nakamura, Y. (2017). Amphotericin B Increases Transglutaminase 2 Expression Associated with Upregulation of Endocytotic Activity in Mouse Microglial Cell Line BV-2. *Neurochem. Res.* 42, 1488–1495. doi: 10.1007/s11064-017-2205-0
- Kay, A. R. (2017). How cells can control their size by pumping ions. *Front. Cell Dev. Biol.* 5:41. doi: 10.3389/fcell.2017.00041
- Kay, A. R., and Blaustein, M. P. (2019). Evolution of our understanding of cell volume regulation by the pump-leak mechanism. *J. Gen. Physiol.* 151, 407–416. doi: 10.1085/jgp.201812274
- Kay, R. R., Williams, T. D., Manton, J. D., Traynor, D., and Paschke, P. (2019). Living on soup: macropinocytic feeding in amoebae. *Int. J. Dev. Biol.* 63, 473–483. doi: 10.1387/ijdb.190220rk
- Kellenberger, S., and Schild, L. (2002). Epithelial sodium channel/degenerin family of ion channels: a variety of functions for a shared structure. *Physiol. Rev.* 82, 735–767. doi: 10.1152/physrev.00007.2002
- Kerr, M. C., Lindsay, M. R., Luetterforst, R., Hamilton, N., Simpson, F., Parton, R. G., et al. (2006). Visualisation of macropinosome maturation by the recruitment of sorting nexins. *J. Cell Sci.* 119, 3967–3980. doi: 10.1242/jcs.03167
- Kerr, M. C., and Teasdale, R. D. (2009). Defining macropinocytosis. *Traffic* 10, 364–371. doi: 10.1111/j.1600-0854.2009.00878.x
- Kim, N., Kim, S., Nahm, M., Kopke, D., Kim, J., Cho, E., et al. (2019). BMP-dependent synaptic development requires Abi-Abl-Rac signaling of BMP receptor macropinocytosis. *Nat. Commun.* 10:684.
- Kim, S. M., Nguyen, T. T., Ravi, A., Kubiniok, P., Finicle, B. T., Jayashankar, V., et al. (2018). PTEN deficiency and AMPK activation promote nutrient scavenging and anabolism in prostate cancer cells. *Cancer Discov.* 8, 866–883. doi: 10.1158/2159-8290.cd-17-1215
- Kimura, C., Koyama, T., Oike, M., and Ito, Y. (2000). Hypotonic stress-induced NO production in endothelium depends on endogenous ATP. *Biochem. Biophys. Res. Commun.* 274, 736–740. doi: 10.1006/bbrc.2000.3205
- King, J. S., and Kay, R. R. (2019). The origins and evolution of macropinocytosis. *Philos. Trans. R. Soc. Lond. B Biol. Sci.* 374:20180158. doi: 10.1098/rstb.2018.0158
- King, J. S., and Smythe, E. (2020). Water loss regulates cell and vesicle volume. *Science* 367, 246–247. doi: 10.1126/science.aba3623
- King, L. S., Kozono, D., and Agre, P. (2004). From structure to disease: the evolving tale of aquaporin biology. *Nat. Rev. Mol. Cell Biol.* 5, 687–698. doi: 10.1038/nrm1469
- Kissing, S., Saftig, P., and Haas, A. (2018). Vacuolar ATPase in phago(lyso)somes biology. *Int. J. Med. Microbiol.* 308, 58–67. doi: 10.1016/j.ijmm.2017.08.007
- Kitchen, P., Day, R. E., Salman, M. M., Conner, M. T., Bill, R. M., and Conner, A. C. (2015). Beyond water homeostasis: diverse functional roles of mammalian aquaporins. *Biochim. Biophys. Acta* 1850, 2410–2421. doi: 10.1016/j.bbagen.2015.08.023
- Kittl, M., Helm, K., Beyreis, M., Mayr, C., Gaisberger, M., Winklmayr, M., et al. (2019). Acid- and volume-sensitive chloride currents in microglial cells. *Int. J. Mol. Sci.* 20:3475. doi: 10.3390/ijms20143475
- Kittl, M., Winklmayr, M., Helm, K., Lettner, J., Gaisberger, M., Ritter, M., et al. (2020). Acid- and volume-sensitive chloride currents in human chondrocytes. *Front. Cell Dev. Biol.* 8:583131. doi: 10.3389/fcell.2020.583131
- Klausen, T. K., Bergdahl, A., Hougaard, C., Christophersen, P., Pedersen, S. F., and Hoffmann, E. K. (2007). Cell cycle-dependent activity of the volume- and Ca²⁺-activated anion currents in Ehrlich lettré ascites cells. *J. Cell Physiol.* 210, 831–842. doi: 10.1002/jcp.20918
- Koivusalo, M., Steinberg, B. E., Mason, D., and Grinstein, S. (2011). In situ measurement of the electrical potential across the lysosomal membrane using FRET. *Traffic* 12, 972–982. doi: 10.1111/j.1600-0854.2011.01215.x
- Koivusalo, M., Welch, C., Hayashi, H., Scott, C. C., Kim, M., Alexander, T., et al. (2010). Amiloride inhibits macropinocytosis by lowering submembranous pH and preventing Rac1 and Cdc42 signaling. *J. Cell Biol.* 188, 547–563. doi: 10.1083/jcb.200908086
- Kondapalli, K. C., Prasad, H., and Rao, R. (2014). An inside job: how endosomal Na⁺/(K⁺)/H⁺ exchangers link to autism and neurological disease. *Front. Cell Neurosci.* 8:172. doi: 10.3389/fncel.2014.00172
- Kong, X., Tang, X., Du, W., Tong, J., Yan, Y., Zheng, F., et al. (2013). Extracellular acidosis modulates the endocytosis and maturation of macrophages. *Cell Immunol.* 281, 44–50. doi: 10.1016/j.cellimm.2012.12.009
- König, B., Hao, Y., Schwartz, S., Plested, A. J., and Stauber, T. (2019). A FRET sensor of C-terminal movement reveals VRAC activation by plasma membrane DAG signaling rather than ionic strength. *eLife* 8:e45421.

- Krishna, S., Palm, W., Lee, Y., Yang, W., Bandyopadhyay, U., Xu, H., et al. (2016). PIKfyve regulates vacuole maturation and nutrient recovery following engulfment. *Dev. Cell* 38, 536–547. doi: 10.1016/j.devcel.2016.08.001
- Kruczek, C., Gorg, B., Keitel, V., Pirev, E., Kroncke, K. D., Schliess, F., et al. (2009). Hypoosmotic swelling affects zinc homeostasis in cultured rat astrocytes. *Glia* 57, 79–92. doi: 10.1002/glia.20737
- Kruth, H. S., Jones, N. L., Huang, W., Zhao, B., Ishii, I., Chang, J., et al. (2005). Macropinocytosis is the endocytic pathway that mediates macrophage foam cell formation with native low density lipoprotein. *J. Biol. Chem.* 280, 2352–2360. doi: 10.1074/jbc.m407167200
- Kumar, A., Xie, L., Ta, C. M., Hinton, A. O., Gunasekar, S. K., Minerath, R. A., et al. (2020). SWELL1 regulates skeletal muscle cell size, intracellular signaling, adiposity and glucose metabolism. *eLife* 9:e58941.
- Kunzelmann, K. (2015). TMEM16, LRRC8A, bestrophin: chloride channels controlled by Ca(2+) and cell volume. *Trends Biochem. Sci.* 40, 535–543. doi: 10.1016/j.tibs.2015.07.005
- Kunzschughart, L., Simm, A., and Muellerklieser, W. (1995). Oncogene-associated transformation of rodent fibroblasts is accompanied by large morphologic and metabolic alterations. *Oncol. Rep.* 2, 651–661. doi: 10.3892/or.2.4.651
- Labudda, M., Rozanska, E., Prabucka, B., Muszynska, E., Marecka, D., Kozak, M., et al. (2020). Activity profiling of barley vacuolar processing enzymes provides new insights into the plant and cyst nematode interaction. *Mol. Plant Pathol.* 21, 38–52. doi: 10.1111/mpp.12878
- Lambert, I. H. (2003). Reactive oxygen species regulate swelling-induced taurine efflux in NIH3T3 mouse fibroblasts. *J. Membr. Biol.* 192, 19–32. doi: 10.1007/s00232-002-1061-1
- Lambert, I. H., Kristensen, D., Holm, J. B., and Mortensen, O. H. (2015). Physiological role of taurine—from organism to organelle. *Acta Physiol.* 213, 191–212. doi: 10.1111/apha.12365
- Lambert, S., and Oberwinkler, J. (2005). Characterization of a proton-activated, outwardly rectifying anion channel. *J. Physiol.* 567, 191–213. doi: 10.1113/jphysiol.2005.089888
- Lancioti, A., Brignone, M. S., Molinari, P., Visentin, S., De Nuccio, C., Macchia, G., et al. (2012). Megalencephalic leukoencephalopathy with subcortical cysts protein 1 functionally cooperates with the TRPV4 cation channel to activate the response of astrocytes to osmotic stress: dysregulation by pathological mutations. *Hum. Mol. Genet.* 21, 2166–2180. doi: 10.1093/hmg/dds032
- Lang, F. (2007). Mechanisms and significance of cell volume regulation. *J. Am. Coll. Nutr.* 26, 613S–623S.
- Lang, F., Böhmer, C., Palmada, M., Seeböhm, G., Strutz-Seeböhm, N., and Vallon, V. (2006). (Patho)physiological significance of the serum- and glucocorticoid-inducible kinase isoforms. *Physiol. Rev.* 86, 1151–1178. doi: 10.1152/physrev.00050.2005
- Lang, F., Busch, G. L., Ritter, M., Volkl, H., Waldegger, S., Gulbins, E., et al. (1998). Functional significance of cell volume regulatory mechanisms. *Physiol. Rev.* 78, 247–306. doi: 10.1152/physrev.1998.78.1.247
- Lang, F., Föller, M., Lang, K., Lang, P., Ritter, M., Vereninov, A., et al. (2007). “Cell volume regulatory ion channels in cell proliferation and cell death,” in *Osmosensing and Osmosignaling*, eds D. Häussinger and H. Sies (London: Academic Press), 209–225. doi: 10.1016/s0076-6879(07)28011-5
- Lang, F., and Hoffmann, E. K. (2012). “Role of ion transport in control of apoptotic cell death,” in *Comprehensive Physiology*, ed. Y. S. Prakash (Hoboken, NJ: Wiley), 2037–2061.
- Lang, F., and Hoffmann, E. K. (2013a). CrossTalk proposal: cell volume changes are an essential step in the cell death machinery. *J. Physiol.* 591, 6119–6121. doi: 10.1113/jphysiol.2013.258632
- Lang, F., and Hoffmann, E. K. (2013b). Rebuttal from Florian Lang and Else K. Hoffmann. *J. Physiol.* 591:6127. doi: 10.1113/jphysiol.2013.265231
- Lang, F., Ritter, M., Woll, E., Weiss, H., Häussinger, D., Hoflacher, J., et al. (1992a). Altered cell volume regulation in ras oncogene expressing NIH fibroblasts. *Pflügers Arch.* 420, 424–427. doi: 10.1007/bf00374615
- Lang, F., Stournaras, C., Zacharopoulou, N., Voelkl, J., and Alesutan, I. (2018). Serum- and glucocorticoid-inducible kinase 1 and the response to cell stress. *Cell Stress* 3, 1–8. doi: 10.15698/cst2019.01.170
- Lang, F., Woll, E., Waldegger, S., Friedrich, F., Ritter, M., Pinggera, G., et al. (1992b). Cell membrane potential oscillations induced by kinins in fibroblasts expressing the Ha-ras oncogene. *Agents Actions Suppl.* 38(Pt 2), 73–80.
- Langemeyer, L., Fröhlich, F., and Ungermann, C. (2018). Rab GTPase function in endosome and lysosome biogenesis. *Trends Cell Biol.* 28, 957–970. doi: 10.1016/j.tcb.2018.06.007
- Lanzavecchia, A. (1996). Mechanisms of antigen uptake for presentation. *Curr. Opin. Immunol.* 8, 348–354. doi: 10.1016/s0952-7915(96)80124-5
- Lanzetti, L., Palamidessi, A., Arces, L., Scita, G., and Di Fiore, P. P. (2004). Rab5 is a signalling GTPase involved in actin remodelling by receptor tyrosine kinases. *Nature* 429, 309–314. doi: 10.1038/nature02542
- Laplanche, J. M., Falardeau, J., Sun, M., Kanazirska, M., Brown, E. M., Slaughter, S. A., et al. (2002). Identification and characterization of the single channel function of human mucolipin-1 implicated in mucopolidosis type IV, a disorder affecting the lysosomal pathway. *FEBS Lett.* 532, 183–187. doi: 10.1016/s0014-5793(02)03670-0
- Larsen, E. H., and Hoffmann, E. K. (2020). “Volume regulation in epithelia,” in *Basic Epithelial Ion Transport Principles and Function*, eds K. L. Hamilton and D. C. Devor (Cham: Springer), 395–460.
- Lawrence, S. P., Bright, N. A., Luzio, J. P., and Bowers, K. (2010). The sodium/proton exchanger NHE8 regulates late endosomal morphology and function. *Mol. Biol. Cell* 21, 3540–3551. doi: 10.1091/mbc.e09-12-1053
- Lee, E., and Knecht, D. A. (2002). Visualization of actin dynamics during macropinocytosis and exocytosis. *Traffic* 3, 186–192. doi: 10.1034/j.1600-0854.2002.030304.x
- Lee, S., Kim, M. G., Ahn, H., and Kim, S. (2020). Inositol pyrophosphates: signaling molecules with pleiotropic actions in mammals. *Molecules* 25:2208. doi: 10.3390/molecules25092208
- Lee, Y. H., and Peng, C. A. (2009). Effect of hypotonic stress on retroviral transduction. *Biochem. Biophys. Res. Commun.* 390, 1367–1371. doi: 10.1016/j.bbrc.2009.10.161
- Lertsuwan, J., Lertsuwan, K., Sawasichai, A., Tasnawijitwong, N., Lee, K. Y., Kitchen, P., et al. (2018). CX-4945 induces methuosis in cholangiocarcinoma cell lines by a CK2-independent mechanism. *Cancers* 10:283. doi: 10.3390/cancers10090283
- Levin, R., Grinstein, S., and Schlam, D. (2015). Phosphoinositides in phagocytosis and macropinocytosis. *Biochim. Biophys. Acta* 1851, 805–823. doi: 10.1016/j.bbalip.2014.09.005
- Lewis, W. H. (1936). *Pinocytosis: Drinking by Cells*. Baltimore, MD: The Johns Hopkins Medical Institutions.
- Lewis, W. H. (1937). Pinocytosis by malignant cells. *Am. J. Cancer* 29, 666–679.
- Li, C., Macdonald, J. I., Hryciw, T., and Meakin, S. O. (2010). Nerve growth factor activation of the TrkA receptor induces cell death, by macropinocytosis, in medulloblastoma Daoy cells. *J. Neurochem.* 112, 882–899. doi: 10.1111/j.1471-4159.2009.06507.x
- Li, G., D’Souza-Schorey, C., Barbieri, M. A., Cooper, J. A., and Stahl, P. D. (1997). Uncoupling of membrane ruffling and pinocytosis during Ras signal transduction. *J. Biol. Chem.* 272, 10337–10340. doi: 10.1074/jbc.272.16.10337
- Li, J., Gao, W., Zhang, Y., Cheng, F., Eriksson, J. E., Etienne-Manneville, S., et al. (2019). Engagement of vimentin intermediate filaments in hypotonic stress. *J. Cell Biochem.* 120, 13168–13176. doi: 10.1002/jcb.28591
- Li, M., Zhang, W. K., Benveniste, N. M., Zhou, X., Su, D., Li, H., et al. (2017). Structural basis of dual Ca(2+)/pH regulation of the endolysosomal TRPML1 channel. *Nat. Struct. Mol. Biol.* 24, 205–213. doi: 10.1038/nsmb.3362
- Li, P., Gu, M., and Xu, H. (2019). Lysosomal ion channels as decoders of cellular signals. *Trends Biochem. Sci.* 44, 110–124. doi: 10.1016/j.tibs.2018.10.006
- Li, P., Hu, M., Wang, C., Feng, X., Zhao, Z., Yang, Y., et al. (2020). LRRC8 family proteins within lysosomes regulate cellular osmoregulation and enhance cell survival to multiple physiological stresses. *Proc. Natl. Acad. Sci. U.S.A.* 117, 29155–29165. doi: 10.1073/pnas.2016539117
- Li, X., Wang, T., Zhao, Z., and Weinman, S. A. (2002). The ClC-3 chloride channel promotes acidification of lysosomes in CHO-K1 and Huh-7 cells. *Am. J. Physiol. Cell Physiol.* 282, C1483–C1491.
- Li, Z., Mbah, N. E., Overmeyer, J. H., Sarver, J. G., George, S., Trabbic, C. J., et al. (2019). The JNK signaling pathway plays a key role in methuosis (non-apoptotic cell death) induced by MOMIPP in glioblastoma. *BMC Cancer* 19:77. doi: 10.1186/s12885-019-5288-y
- Lim, J. P., and Gleeson, P. A. (2011). Macropinocytosis: an endocytic pathway for internalising large gulps. *Immunol. Cell Biol.* 89, 836–843. doi: 10.1038/icb.2011.20

- Lin, J., Shi, S. S., Zhang, J. Q., Zhang, Y. J., Zhang, L., Liu, Y., et al. (2016). Giant cellular vacuoles induced by rare earth oxide nanoparticles are abnormally enlarged Endo/lysosomes and promote mTOR-dependent TFEF nucleus translocation. *Small* 12, 5759–5768. doi: 10.1002/sml.201601903
- Lin, P. H., Duann, P., Komazaki, S., Park, K. H., Li, H., Sun, M., et al. (2015). Lysosomal two-pore channel subtype 2 (TPC2) regulates skeletal muscle autophagic signaling. *J. Biol. Chem.* 290, 3377–3389. doi: 10.1074/jbc.m114.608471
- Lin, X. P., Minter, J. D., and Gleeson, P. A. (2020). Macropinocytosis in different cell types: similarities and differences. *Membranes* 10:177. doi: 10.3390/membranes10080177
- Liu, J., Ying, M., Wu, B., and Fu, C. (2020). Ethanol extract of the infructescence of *Platycarya strobilacea* Sieb. et Zucc. Induces methuosis of human nasopharyngeal carcinoma cells. *Evid. Based Complement. Alternat. Med.* 2020:2760979.
- Liu, X., Ong, H. L., Pani, B., Johnson, K., Swaim, W. B., Singh, B., et al. (2010). Effect of cell swelling on ER/PM junctional interactions and channel assembly involved in SOCE. *Cell Calcium* 47, 491–499. doi: 10.1016/j.ceca.2010.04.002
- Liu, X., Wang, S., Zheng, H., Liu, Q., Shen, T., Wang, X., et al. (2020). Epimediokoreanin c, a prenylated flavonoid isolated from epimedium koreanum, induces non-apoptotic cell death with the characteristics of methuosis in lung cancer cells. *Res. Square* [Epub ahead of print].
- Liu, Z., and Roche, P. A. (2015). Macropinocytosis in phagocytes: regulation of MHC class-II-restricted antigen presentation in dendritic cells. *Front. Physiol.* 6:1. doi: 10.3389/fphys.2015.00001
- Lloyd, J. B. (1990). Cell physiology of the rat visceral yolk sac: a study of pinocytosis and lysosome function. *Teratology* 41, 383–393. doi: 10.1002/tera.1420410404
- Lloyd-Evans, E., Morgan, A. J., He, X., Smith, D. A., Elliot-Smith, E., Sillence, D. J., et al. (2008). Niemann-Pick disease type C1 is a sphingosine storage disease that causes deregulation of lysosomal calcium. *Nat. Med.* 14:1247. doi: 10.1038/nm.1876
- Loh, J., Chuang, M. C., Lin, S. S., Joseph, J., Su, Y. A., Hsieh, T. L., et al. (2019). An acute decrease in plasma membrane tension induces macropinocytosis via PLD2 activation. *J. Cell. Sci.* 132:jcs232579.
- Loike, J. D., Cao, L., Kuang, K., Vera, J. C., Silverstein, S. C., and Fischbarg, J. (1993). Role of facilitative glucose transporters in diffusional water permeability through J774 cells. *J. Gen. Physiol.* 102, 897–906. doi: 10.1085/jgp.102.5.897
- Loitto, V. M., Forslund, T., Sundqvist, T., Magnusson, K. E., and Gustafsson, M. (2002). Neutrophil leukocyte motility requires directed water influx. *J. Leukoc. Biol.* 71, 212–222.
- Loitto, V. M., Karlsson, T., and Magnusson, K. E. (2009). Water flux in cell motility: expanding the mechanisms of membrane protrusion. *Cell Motil. Cytoskeleton*. 66, 237–247. doi: 10.1002/cm.20357
- Lucien, F., Pelletier, P. P., Lavoie, R. R., Lacroix, J. M., Roy, S., Parent, J. L., et al. (2017). Hypoxia-induced mobilization of NHE6 to the plasma membrane triggers endosome hyperacidification and chemoresistance. *Nat. Commun.* 8:15884.
- Madonna, R., Geng, Y. J., Shelat, H., Ferdinandy, P., and De Caterina, R. (2014). High glucose-induced hyperosmolarity impacts proliferation, cytoskeleton remodeling and migration of human induced pluripotent stem cells via aquaporin-1. *Biochim. Biophys. Acta* 1842, 2266–2275. doi: 10.1016/j.bbdis.2014.07.030
- Madonna, R., Montebello, E., Lazzerini, G., Zurro, M., and De Caterina, R. (2010). NA⁺/H⁺ exchanger 1- and aquaporin-1-dependent hyperosmolarity changes decrease nitric oxide production and induce VCAM-1 expression in endothelial cells exposed to high glucose. *Int. J. Immunopathol. Pharmacol.* 23, 755–765. doi: 10.1177/039463201002300309
- Madonna, R., Pieragostino, D., Rossi, C., Confalone, P., Cicalini, I., Minnucci, I., et al. (2020). Simulated hyperglycemia impairs insulin signaling in endothelial cells through a hyperosmolar mechanism. *Vascul. Pharmacol.* 130:106678. doi: 10.1016/j.vph.2020.106678
- Maekawa, M., Terasaka, S., Mochizuki, Y., Kawai, K., Ikeda, Y., Araki, N., et al. (2014). Sequential breakdown of 3-phosphorylated phosphoinositides is essential for the completion of macropinocytosis. *Proc. Natl. Acad. Sci. U.S.A.* 111, E978–E987.
- Majno, G., and Joris, I. (1995). Apoptosis, oncosis, and necrosis. An overview of cell death. *Am. J. Pathol.* 146, 3–15.
- Maltese, W. A., and Overmeyer, J. H. (2014). Methuosis: nonapoptotic cell death associated with vacuolization of macropinosome and endosome compartments. *Am. J. Pathol.* 184, 1630–1642.
- Maltese, W. A., and Overmeyer, J. H. (2015). Non-apoptotic cell death associated with perturbations of macropinocytosis. *Front. Physiol.* 6:38. doi: 10.3389/fphys.2015.00038
- Maly, K., Kindler, E., Tinhofer, I., and Grunicke, H. H. (1995). Activation of Ca²⁺ influx by transforming Ha-ras. *Cell Calcium* 18, 120–134. doi: 10.1016/0143-4160(95)90003-9
- Maly, K., Ueberall, F., Loferer, H., Doppler, W., Oberhuber, H., Groner, B., et al. (1989). Ha-ras activates the Na⁺/H⁺ antiporter by a protein kinase C-independent mechanism. *J. Biol. Chem.* 264, 11839–11842. doi: 10.1016/s0021-9258(18)80142-9
- Manara, M. C., Terracciano, M., Mancarella, C., Sciandra, M., Guerzoni, C., Pasello, M., et al. (2016). CD99 triggering induces methuosis of Ewing sarcoma cells through IGF-1R/RAS/Rac1 signaling. *Oncotarget* 7, 79925–79942. doi: 10.18632/oncotarget.13160
- Margiotta, A., and Bucci, C. (2016). Role of intermediate filaments in vesicular traffic. *Cells* 5:20. doi: 10.3390/cells5020020
- Marques, P. E., Grinstein, S., and Freeman, S. A. (2017). SnapShot:macropinocytosis. *Cell* 169, 766.e1–766.e1.
- Martinez, D., Vermeulen, M., Von Euw, E., Sabatté, J., Maggini, J., Ceballos, A., et al. (2007). Extracellular acidosis triggers the maturation of human dendritic cells and the production of IL-12. *J. Immunol.* 179, 1950–1959. doi: 10.4049/jimmunol.179.3.1950
- Martinez, I., Sveinbjornsson, B., and Smedsrod, B. (1996). Nitric oxide down-regulates endocytosis in rat liver endothelial cells. *Biochem. Biophys. Res. Commun.* 222, 688–693. doi: 10.1006/bbrc.1996.0805
- Matsuda, J. J., Filali, M. S., Moreland, J. G., Miller, F. J., and Lamb, F. S. (2010). Activation of swelling-activated chloride current by tumor necrosis factor- α requires ClC-3-dependent endosomal reactive oxygen production. *J. Biol. Chem.* 285, 22864–22873. doi: 10.1074/jbc.m109.099838
- Maxson, M. E., and Grinstein, S. (2014). The vacuolar-type H⁺-ATPase at a glance - more than a proton pump. *J. Cell. Sci.* 127, 4987–4993. doi: 10.1242/jcs.158550
- Maxson, M. E., Sarantis, H., Volchuk, A., Brumell, J. H., and Grinstein, S. (2021). Rab5 regulates macropinocytosis by recruiting the inositol 5-phosphatases OCRL/Inpp5b that hydrolyze PtdIns(4,5)P₂. *J. Cell. Sci.* [Epub ahead of print].
- Mercer, J., and Helenius, A. (2009). Virus entry by macropinocytosis. *Nat. Cell Biol.* 11, 510–520. doi: 10.1038/ncb0509-510
- Mercer, J., and Helenius, A. (2012). Gulping rather than sipping: macropinocytosis as a way of virus entry. *Curr. Opin. Microbiol.* 15, 490–499. doi: 10.1016/j.mib.2012.05.016
- Mercer, J., Lee, J. E., Saphire, E. O., and Freeman, S. A. (2020). SnapShot: enveloped virus entry. *Cell* 182, 786.e1–786.e1.
- Mercer, J., Schelhaas, M., and Helenius, A. (2010). Virus entry by endocytosis. *Annu. Rev. Biochem.* 79, 803–833. doi: 10.1146/annurev-biochem-060208-104626
- Merrifield, C. J., Moss, S. E., Ballestrem, C., Imhof, B. A., Giese, G., Wunderlich, I., et al. (1999). Endocytic vesicles move at the tips of actin tails in cultured mast cells. *Nat. Cell Biol.* 1, 72–74. doi: 10.1038/9048
- Merrifield, C. J., Rescher, U., Almers, W., Proust, J., Gerke, V., Sechi, A. S., et al. (2001). Annexin 2 has an essential role in actin-based macropinocytic rocketing. *Curr. Biol.* 11, 1136–1141. doi: 10.1016/s0960-9822(01)00321-9
- Mettlen, M., Platek, A., Van Der Smissen, P., Carpentier, S., Amyere, M., Lanzetti, L., et al. (2006). Src triggers circular ruffling and macropinocytosis at the apical surface of polarized MDCK cells. *Traffic* 7, 589–603. doi: 10.1111/j.1600-0854.2006.00412.x
- Milosavljevic, N., Monet, M., Lena, I., Brau, F., Lacas-Gervais, S., Feliciangeli, S., et al. (2014). The intracellular Na⁺/H⁺ exchanger NHE7 effects a Na⁺-coupled, but not K⁺-coupled proton-loading mechanism in endocytosis. *Cell Rep.* 7, 689–696. doi: 10.1016/j.celrep.2014.03.054
- Minna, E., Romeo, P., De Cecco, L., Dugo, M., Cassinelli, G., Pilotti, S., et al. (2014). miR-199a-3p displays tumor suppressor functions in papillary thyroid carcinoma. *Oncotarget* 5, 2513–2528. doi: 10.18632/oncotarget.1830
- Model, M. A. (2014). Possible causes of apoptotic volume decrease: an attempt at quantitative review. *Am. J. Physiol. Cell Physiol.* 306, C417–C424.

- Model, M. A., Hollembeak, J. E., and Kurokawa, M. (2020). Macromolecular crowding: a hidden link between cell volume and everything else. *Cell Physiol. Biochem.* 55, 25–40. doi: 10.33594/000000319
- Mohebbi, N., Benabbas, C., Vidal, S., Daryadel, G., Bourgeois, S., Velic, A., et al. (2012). The proton-activated G protein coupled receptor OGR1 acutely regulates the activity of epithelial proton transport proteins. *Cell Physiol. Biochem.* 29, 313–324. doi: 10.1159/000338486
- Morgan, A. J., Platt, F. M., Lloyd-Evans, E., and Galione, A. (2011). Molecular mechanisms of endolysosomal Ca²⁺ signalling in health and disease. *Biochem. J.* 439, 349–374. doi: 10.1042/bj20110949
- Morishita, S., Wada, N., Fukuda, M., and Nakamura, T. (2019). Rab5 activation on macropinosomes requires ALS2, and subsequent Rab5 inactivation through ALS2 detachment requires active Rab7. *FEBS Lett.* 593, 230–241.
- Nakamura, N., Tanaka, S., Teko, Y., Mitsui, K., and Kanazawa, H. (2005). Four Na⁺/H⁺ exchanger isoforms are distributed to Golgi and post-Golgi compartments and are involved in organelle pH regulation. *J. Biol. Chem.* 280, 1561–1572. doi: 10.1074/jbc.M410041200
- Nara, A., Aki, T., Funakoshi, T., and Uemura, K. (2010). Methamphetamine induces macropinocytosis in differentiated SH-SY5Y human neuroblastoma cells. *Brain Res.* 1352, 1–10. doi: 10.1016/j.brainres.2010.07.043
- Neuhaus, E. M., Almers, W., and Soldati, T. (2002). Morphology and dynamics of the endocytic pathway in *Dictyostelium discoideum*. *Mol. Biol. Cell.* 13, 1390–1407. doi: 10.1091/mbc.01-08-0392
- Nicoli, E.-R., Weston, M. R., Hackbarth, M., Becerril, A., Larson, A., Zein, W. M., et al. (2019). Lysosomal storage and albinism due to effects of a de novo CLCN7 variant on lysosomal acidification. *Am. J. Hum. Genet.* 104, 1127–1138.
- Nirmala, J. G., and Lopus, M. (2020). Cell death mechanisms in eukaryotes. *Cell. Biol. Toxicol.* 36, 145–164. doi: 10.1007/s10565-019-09496-2
- Nishi, T., and Forgac, M. (2002). The vacuolar (H⁺)-ATPases—nature's most versatile proton pumps. *Nat. Rev. Mol. Cell Biol.* 3, 94–103. doi: 10.1038/nrm729
- Nobles, M., Higgins, C. F., and Sardini, A. (2004). Extracellular acidification elicits a chloride current that shares characteristics with ICl(swell). *Am. J. Physiol. Cell Physiol.* 287, C1426–C1435.
- Nussinov, R., Tsai, C.-J., and Jang, H. (2018). Oncogenic Ras isoforms signaling specificity at the membrane. *Cancer Res.* 78, 593–602. doi: 10.1158/0008-5472.can-17-2727
- Nussinov, R., Tsai, C. J., and Jang, H. (2020). Ras assemblies and signaling at the membrane. *Curr. Opin. Struct. Biol.* 62, 140–148. doi: 10.1016/j.sbi.2020.01.009
- Oberleithner, H., Callies, C., Kusche-Vihrog, K., Schillers, H., Shahin, V., Riethmüller, C., et al. (2009). Potassium softens vascular endothelium and increases nitric oxide release. *Proc. Natl. Acad. Sci. U.S.A.* 106, 2829–2834. doi: 10.1073/pnas.0813069106
- Oberleithner, H., and De Wardener, H. E. (2011). Sodium: a wolf in sheep's clothing. *Blood Purif.* 31, 82–85. doi: 10.1159/000321842
- Ohgaki, R., Van, I. S. C., Matsushita, M., Hoekstra, D., and Kanazawa, H. (2011). Organellar Na⁺/H⁺ exchangers: novel players in organelle pH regulation and their emerging functions. *Biochemistry* 50, 443–450. doi: 10.1021/bi101082e
- Ohshima, H., and Ohki, S. (1985). Donnan potential and surface potential of a charged membrane. *Biophys. J.* 47, 673–678. doi: 10.1016/s0006-3495(85)83963-1
- Okada, C. Y., and Rechsteiner, M. (1982). Introduction of macromolecules into cultured mammalian cells by osmotic lysis of pinocytic vesicles. *Cell* 29, 33–41. doi: 10.1016/0092-8674(82)90087-3
- Okada, Y. (2004). Ion channels and transporters involved in cell volume regulation and sensor mechanisms. *Cell Biochem. Biophys.* 41, 233–258. doi: 10.1385/cbb:41:2:233
- Okada, Y. (2020). Cell death induction and protection by activation of ubiquitously expressed anion/cation channels. Part 1: roles of VSOR/VRAC in cell volume regulation, release of double-edged signals and apoptotic/necrotic cell death. *Front. Cell Dev. Biol.* 8:614040. doi: 10.3389/fcell.2020.614040
- Okada, Y., Maeno, E., Shimizu, T., Dezaki, K., Wang, J., and Morishima, S. (2001). Receptor-mediated control of regulatory volume decrease (RVD) and apoptotic volume decrease (AVD). *J. Physiol.* 532, 3–16. doi: 10.1111/j.1469-7793.2001.0003g.x
- Okada, Y., Okada, T., Sato-Numata, K., Islam, M. R., Ando-Akatsuka, Y., Numata, T., et al. (2019). Cell volume-activated and volume-correlated anion channels in mammalian cells: their biophysical, molecular, and pharmacological properties. *Pharmacol. Rev.* 71, 49–88. doi: 10.1124/pr.118.015917
- Olbrich, K., Rawicz, W., Needham, D., and Evans, E. (2000). Water permeability and mechanical strength of polyunsaturated lipid bilayers. *Biophys. J.* 79, 321–327. doi: 10.1016/s0006-3495(00)76294-1
- Oppong, F., Li, Z., Fakhrabadi, E. A., Raorane, T., Giri, P. M., Liberatore, M. W., et al. (2020). Investigating the potential to deliver and maintain plasma and brain levels of a novel practically insoluble methuosis inducing anticancer agent 5-methoxy MOMIPP through an injectable in situ forming thermoresponsive hydrogel formulation. *J. Pharm. Sci.* 109, 2719–2728. doi: 10.1016/j.xphs.2020.05.014
- Orlov, S. N., and Hamet, P. (2004). Apoptosis vs. oncosis: role of cell volume and intracellular monovalent cations. *Adv. Exp. Med. Biol.* 559, 219–233. doi: 10.1007/0-387-23752-6_21
- Orlov, S. N., Model, M. A., and Grygorczyk, R. (2013). CrossTalk opposing view: the triggering and progression of the cell death machinery can occur without cell volume perturbations. *J. Physiol.* 591, 6123–6125. doi: 10.1113/jphysiol.2013.258624
- Orlowski, J., and Grinstein, S. (2011). “Na⁺/H⁺ exchangers,” in *Comprehensive Physiology*, ed. Y. S. Prakash (Hoboken, NJ: Wiley), 2083–2100.
- Osei-Owusu, J., Yang, J., Del Carmen Vitery, M., Tian, M., and Qiu, Z. (2020). PAC proton-activated chloride channel contributes to acid-induced cell death in primary rat cortical neurons. *Channels* 14, 53–58. doi: 10.1080/19336950.2020.1730019
- Osei-Owusu, J., Yang, J., Leung, K. H., Ruan, Z., Lu, W., Krishnan, Y., et al. (2021). Proton-activated chloride channel PAC regulates endosomal acidification and transferrin receptor-mediated endocytosis. *Cell. Rep.* 34:108683. doi: 10.1016/j.celrep.2020.108683
- Ou, X., Liu, Y., Lei, X., Li, P., Mi, D., Ren, L., et al. (2020). Characterization of spike glycoprotein of SARS-CoV-2 on virus entry and its immune cross-reactivity with SARS-CoV. *Nat. Commun.* 11:1620.
- Overmeyer, J. H., Kaul, A., Johnson, E. E., and Maltese, W. A. (2008). Active ras triggers death in glioblastoma cells through hyperstimulation of macropinocytosis. *Mol. Cancer Res.* 6, 965–977. doi: 10.1158/1541-7786.mcr-07-2036
- Overmeyer, J. H., Young, A. M., Bhanot, H., and Maltese, W. A. (2011). A chalcone-related small molecule that induces methuosis, a novel form of non-apoptotic cell death, in glioblastoma cells. *Mol. Cancer* 10:69. doi: 10.1186/1476-4598-10-69
- Palanikumar, L., Kim, J., Oh, J. Y., Choi, H., Park, M. H., Kim, C., et al. (2018). Hyaluronic acid-modified polymeric gatekeepers on biodegradable mesoporous silica nanoparticles for targeted cancer therapy. *ACS Biomater. Sci. Eng.* 4, 1716–1722. doi: 10.1021/acsbmaterials.8b00218
- Palm, W. (2019). Metabolic functions of macropinocytosis. *Philos. Trans. R. Soc. Lond. B Biol. Sci.* 374:20180285. doi: 10.1098/rstb.2018.0285
- Palmada, M., Dieter, M., Boehmer, C., Waldegger, S., and Lang, F. (2004). Serum and glucocorticoid inducible kinases functionally regulate ClC-2 channels. *Biochem. Biophys. Res. Commun.* 321, 1001–1006. doi: 10.1016/j.bbrc.2004.07.064
- Pan, L., Zhang, P., Hu, F., Yan, R., He, M., Li, W., et al. (2019). Hypotonic stress induces fast, reversible degradation of the vimentin cytoskeleton via intracellular calcium release. *Adv. Sci.* 6:1900865. doi: 10.1002/adv.20190865
- Pang, V., Counillon, L., Lagadic-Gossmann, D., Poet, M., Lacroix, J., Sergent, O., et al. (2012). On the role of the difference in surface tensions involved in the allosteric regulation of NHE-1 induced by low to mild osmotic pressure, membrane tension and lipid asymmetry. *Cell Biochem. Biophys.* 63, 47–57. doi: 10.1007/s12013-012-9340-7
- Panyi, G., Possani, L. D., Rodriguez De La Vega, R. C., Gaspar, R., and Varga, Z. (2006). K⁺ channel blockers: novel tools to inhibit T cell activation leading to specific immunosuppression. *Curr. Pharm. Des.* 12, 2199–2220. doi: 10.2174/13816120677585120
- Park, J. K., Peng, H., Katsnelson, J., Yang, W., Kaplan, N., Dong, Y., et al. (2016). MicroRNAs-103/107 coordinately regulate macropinocytosis and autophagy. *J. Cell Biol.* 215, 667–685. doi: 10.1083/jcb.201604032
- Parton, R. G., Joggerst, B., and Simons, K. (1994). Regulated internalization of caveolae. *J. Cell Biol.* 127, 1199–1215. doi: 10.1083/jcb.127.5.1199

- Pasantes-Morales, H. (2016). Channels and volume changes in the life and death of the cell. *Mol. Pharmacol.* 90, 358–370. doi: 10.1124/mol.116.104158
- Pedersen, S. F., and Counillon, L. (2019). The SLC9A-C mammalian Na(+)/H(+) exchanger family: molecules. *Mech. Physiol. Physiol. Rev.* 99, 2015–2113. doi: 10.1152/physrev.00028.2018
- Pedersen, S. F., Hoffmann, E. K., and Mills, J. W. (2001). The cytoskeleton and cell volume regulation. *Comp. Biochem. Physiol. A Mol. Integr. Physiol.* 130, 385–399.
- Pedersen, S. F., Hoffmann, E. K., and Novak, I. (2013). Cell volume regulation in epithelial physiology and cancer. *Front. Physiol.* 4:233. doi: 10.3389/fphys.2013.00233
- Pedraz-Cuesta, E., Fredsted, J., Jensen, H. H., Bornebusch, A., Nejsum, L. N., Kragelund, B. B., et al. (2016). Prolactin signaling stimulates invasion via Na(+)/H(+) exchanger NHE1 in T47D human breast cancer cells. *Mol. Endocrinol.* 30, 693–708. doi: 10.1210/me.2015-1299
- Pesesse, X., Choi, K., Zhang, T., and Shears, S. B. (2004). Signaling by higher inositol polyphosphates. Synthesis of bisdiphosphoinositol tetrakisphosphate ("InsP8") is selectively activated by hyperosmotic stress. *J. Biol. Chem.* 279, 43378–43381.
- Petersen, O. H., Gerasimenko, J. V., and Gerasimenko, O. V. (2020). Endocytic uptake of SARS-CoV-2: the critical roles of pH, Ca²⁺, and NAADP. *Function* 1:zqaa003.
- Petrini, S., Minnone, G., Coccetti, M., Frank, C., Aiello, C., Cutarelli, A., et al. (2013). Monocytes and macrophages as biomarkers for the diagnosis of megalencephalic leukoencephalopathy with subcortical cysts. *Mol. Cell Neurosci.* 56, 307–321. doi: 10.1016/j.mcn.2013.07.001
- Pierro, C., Zhang, X., Kankeu, C., Trebak, M., Bootman, M. D., and Roderick, H. L. (2018). Oncogenic KRAS suppresses store-operated Ca(2+) entry and ICRAC through ERK pathway-dependent remodelling of STIM expression in colorectal cancer cell lines. *Cell Calcium* 72, 70–80. doi: 10.1016/j.ceca.2018.03.002
- Pintsch, T., Satre, M., Klein, G., Martin, J. B., and Schuster, S. C. (2001). Cytosolic acidification as a signal mediating hyperosmotic stress responses in *Dictyostelium discoideum*. *BMC Cell Biol.* 2:9. doi: 10.1186/1471-2121-2-9
- Pironti, G., Strachan, R. T., Abraham, D., Mon-Wei Yu, S., Chen, M., Chen, W., et al. (2015). Circulating exosomes induced by cardiac pressure overload contain functional angiotensin II type 1 receptors. *Circulation* 131, 2120–2130. doi: 10.1161/circulationaha.115.015687
- Pizon, V., Desjardins, M., Bucci, C., Parton, R. G., and Zerial, M. (1994). Association of Rap1a and Rap1b proteins with late endocytic/phagocytic compartments and Rap2a with the Golgi complex. *J. Cell Sci.* 107(Pt 6), 1661–1670. doi: 10.1242/jcs.107.6.1661
- Planade, J., Belbahri, R., Boiero Sanders, M., Guillotin, A., Du Roure, O., Michelot, A., et al. (2019). Mechanical stiffness of reconstituted actin patches correlates tightly with endocytosis efficiency. *PLoS Biol.* 17:e3000500. doi: 10.1371/journal.pbio.3000500
- Platt, F. M., Boland, B., and Van Der Spoel, A. C. (2012). The cell biology of disease: lysosomal storage disorders: the cellular impact of lysosomal dysfunction. *J. Cell Biol.* 199, 723–734. doi: 10.1083/jcb.201208152
- Platt, F. M., D'azzo, A., Davidson, B. L., Neufeld, E. F., and Tiff, C. J. (2018). Lysosomal storage diseases. *Nat. Rev. Dis Primers* 4:27.
- Pollard, T. D. (2016). Actin and actin-binding proteins. *Cold Spring Harb. Perspect. Biol.* 8:a018226.
- Polovitskaya, M. M., Barbini, C., Martinelli, D., Harms, F. L., Cole, F. S., Calligari, P., et al. (2020). A recurrent gain-of-function mutation in CLCN6, encoding the CLC-6 Cl(-)/H(+)-exchanger, causes early-onset neurodegeneration. *Am. J. Hum. Genet.* 107, 1062–1077. doi: 10.1016/j.ajhg.2020.11.004
- Porat-Shliom, N., Kloog, Y., and Donaldson, J. G. (2008). A unique platform for H-Ras signaling involving clathrin-independent endocytosis. *Mol. Biol. Cell.* 19, 765–775. doi: 10.1091/mbc.e07-08-0841
- Potokar, M., Stenovec, M., Jorgacevski, J., Holen, T., Kreft, M., Ottersen, O. P., et al. (2013). Regulation of AQP4 surface expression via vesicle mobility in astrocytes. *Glia* 61, 917–928. doi: 10.1002/glia.22485
- Qadri, Y. J., Song, Y., Fuller, C. M., and Benos, D. J. (2010). Amiloride docking to acid-sensing ion channel-1. *J. Biol. Chem.* 285, 9627–9635. doi: 10.1074/jbc.m109.082735
- Qiu, Z., Dubin, A. E., Mathur, J., Tu, B., Reddy, K., Miraglia, L. J., et al. (2014). SWELL1, a plasma membrane protein, is an essential component of volume-regulated anion channel. *Cell* 157, 447–458. doi: 10.1016/j.cell.2014.03.024
- Racoosin, E. L., and Swanson, J. A. (1993). Macropinosome maturation and fusion with tubular lysosomes in macrophages. *J. Cell Biol.* 121, 1011–1020. doi: 10.1083/jcb.121.5.1011
- Rajasekharan, S. K., Kim, S., Kim, J. C., and Lee, J. (2020). Nematicidal activity of 5-iodoindole against root-knot nematodes. *Pestic Biochem. Physiol.* 163, 76–83. doi: 10.1016/j.pestbp.2019.10.012
- Rajasekharan, S. K., and Lee, J. (2020). Hydrotic anthelmintics against parasitic nematodes. *PLoS Pathog.* 16:e1008202. doi: 10.1371/journal.ppat.1008202
- Rajasekharan, S. K., Lee, J., Ravichandran, V., Kim, J., Park, J. G., and Lee, J. (2019). Nematicidal and insecticidal activities of halogenated indoles. *Sci. Rep.* 9:2010. doi: 10.1038/s41598-019-38561-3
- Rajasekharan, S. K., Lee, J. H., Ravichandran, V., and Lee, J. (2017). Assessments of iodoindoles and abamectin as inducers of methuosis in pinewood nematode, *Bursaphelenchus xylophilus*. *Sci. Rep.* 7:6803.
- Ramirez, C., Hauser, A. D., Vucic, E. A., and Bar-Sagi, D. (2019). Plasma membrane V-ATPase controls oncogenic RAS-induced macropinocytosis. *Nature* 576, 477–481. doi: 10.1038/s41586-019-1831-x
- Rane, S. G. (1991). A Ca²⁺-activated K⁺ current in ras-transformed fibroblasts is absent from nontransformed cells. *Am. J. Physiol.* 260, C104–C112.
- Rappaport, J., Manthe, R. L., Solomon, M., Garnacho, C., and Muro, S. (2016). A comparative study on the alterations of endocytic pathways in multiple lysosomal storage disorders. *Mol. Pharm.* 13, 357–368. doi: 10.1021/acs.molpharmaceut.5b00542
- Recouvreux, M. V., and Commisso, C. (2017). Macropinocytosis: a metabolic adaptation to nutrient stress in cancer. *Front. Endocrinol.* 8:261. doi: 10.3389/fendo.2017.00261
- Reibring, C. G., El Shahawy, M., Hallberg, K., Kannius-Janson, M., Nilsson, J., Parkkila, S., et al. (2014). Expression patterns and subcellular localization of carbonic anhydrases are developmentally regulated during tooth formation. *PLoS One* 9:e96007. doi: 10.1371/journal.pone.0096007
- Reyes-Reyes, E. M., Salipur, F. R., Shams, M., Forsthoefel, M. K., and Bates, P. J. (2015). Mechanistic studies of anticancer aptamer AS1411 reveal a novel role for nucleolin in regulating Rac1 activation. *Mol. Oncol.* 9, 1392–1405. doi: 10.1016/j.molonc.2015.03.012
- Ridder, M. C., Boor, I., Lodder, J. C., Postma, N. L., Capdevila-Nortes, X., Duarri, A., et al. (2011). Megalencephalic leukoencephalopathy with cysts: defect in chloride currents and cell volume regulation. *Brain* 134, 3342–3354. doi: 10.1093/brain/awr255
- Riegman, M., Sagie, L., Galed, C., Levin, T., Steinberg, N., Dixon, S. J., et al. (2020). Ferroptosis occurs through an osmotic mechanism and propagates independently of cell rupture. *Nat. Cell Biol.* 22, 1042–1048. doi: 10.1038/s41556-020-0565-1
- Riess, C., Koczan, D., Schneider, B., Linke, C., Del Moral, K., Classen, C. F., et al. (2021). Cyclin-dependent kinase inhibitors exert distinct effects on patient-derived 2D and 3D glioblastoma cell culture models. *Cell Death Discov.* 7:54.
- Rikhiya, Y. (1985). Ultrastructural localization of carbonic anhydrase in lysosomes. *Anat. Rec.* 211, 1–8. doi: 10.1002/ar.1092110102
- Ritter, M., Dartsch, P., Waldegger, S., Haller, T., Zwierzina, H., Lang, H. J., et al. (1997a). Effects of bradykinin on NIH 3T3 fibroblasts pretreated with lithium. Mimicking events of Ha-ras oncogene expression. *Biochim. Biophys. Acta* 1358, 23–30. doi: 10.1016/s0167-4889(97)00046-3
- Ritter, M., Fuerst, J., Woll, E., Chwatal, S., Gschwentner, M., Lang, F., et al. (2001). Na(+)/H(+)exchangers: linking osmotic disequilibrium to modified cell function. *Cell Physiol. Biochem.* 11, 1–18. doi: 10.1159/000047787
- Ritter, M., Woll, E., Haller, T., Dartsch, P. C., Zwierzina, H., and Lang, F. (1997b). Activation of Na(+)/H(+)exchanger by transforming Ha-ras requires stimulated cellular calcium influx and is associated with rearrangement of the actin cytoskeleton. *Eur. J. Cell Biol.* 72, 222–228.
- Ritter, M., Paulmichl, M., and Lang, F. (1991). Further characterization of volume regulatory decrease in cultured renal epitheloid (MDCK) cells. *Pflügers Arch.* 418, 35–39. doi: 10.1007/bf00370449
- Ritter, M., and Woll, E. (1996). Modification of cellular ion transport by the ha-ras oncogene: steps towards malignant transformation. *Cell Physiol. Biochem.* 6, 245–270. doi: 10.1159/000154827
- Ritter, M., Woll, E., Waldegger, S., Haussinger, D., Lang, H. J., Scholz, W., et al. (1993). Cell shrinkage stimulates bradykinin-induced cell membrane potential oscillations in NIH 3T3 fibroblasts expressing the ras-oncogene. *Pflügers Arch.* 423, 221–224. doi: 10.1007/bf00374398

- Roberts, R. L., Barbieri, M. A., Ullrich, J., and Stahl, P. D. (2000). Dynamics of rab5 activation in endocytosis and phagocytosis. *J. Leukoc. Biol.* 68, 627–632.
- Robinson, M. W., Overmeyer, J. H., Young, A. M., Erhardt, P. W., and Maltese, W. A. (2012). Synthesis and evaluation of indole-based chalcones as inducers of methuosis, a novel type of nonapoptotic cell death. *J. Med. Chem.* 55, 1940–1956. doi: 10.1021/jm201006x
- Ruan, Z., Osei-Owusu, J., Du, J., Qiu, Z., and Lu, W. (2020). Structures and pH-sensing mechanism of the proton-activated chloride channel. *Nature* 588, 350–354. doi: 10.1038/s41586-020-2875-7
- Rupper, A., Lee, K., Knecht, D., and Cardelli, J. (2001). Sequential activities of phosphoinositide 3-kinase, PKB/Akt, and Rab7 during macropinosome formation in Dictyostelium. *Mol. Biol. Cell.* 12, 2813–2824. doi: 10.1091/mbc.12.9.2813
- Russo, M. A., Morgante, E., Russo, A., Van Rossum, G. D., and Tafani, M. (2015). Ouabain-induced cytoplasmic vesicles and their role in cell volume maintenance. *Biomed. Res. Int.* 2015:487256.
- Saarikangas, J., Zhao, H., and Lappalainen, P. (2010). Regulation of the actin cytoskeleton-plasma membrane interplay by phosphoinositides. *Physiol. Rev.* 90, 259–289. doi: 10.1152/physrev.00036.2009
- Saha, S., Prakash, V., Halder, S., Chakraborty, K., and Krishnan, Y. (2015). A pH-independent DNA nanodevice for quantifying chloride transport in organelles of living cells. *Nat. Nanotechnol.* 10, 645–651. doi: 10.1038/nnano.2015.130
- Sahu, I., Pelzl, L., Sukkar, B., Fakhri, H., Al-Maghout, T., Cao, H., et al. (2017). NFAT5-sensitive Orai1 expression and store-operated Ca(2+) entry in megakaryocytes. *FASEB J.* 31, 3439–3448. doi: 10.1096/fj.201601211r
- Sakurai, Y., Kolokoltsov, A. A., Chen, C. C., Tidwell, M. W., Bauta, W. E., Klugbauer, N., et al. (2015). Two-pore channels control Ebola virus host cell entry and are drug targets for disease treatment. *Science* 347, 995–998. doi: 10.1126/science.1258758
- Sander, P., Mostafa, H., Soboh, A., Schneider, J. M., Pala, A., Baron, A. K., et al. (2017). Vacuolin-1 inducible cell death in glioblastoma multiforme is counter regulated by TRPM7 activity induced by exogenous ATP. *Oncotarget* 8, 35124–35137. doi: 10.18632/oncotarget.16703
- Sano, O., Kazetani, K., Funata, M., Fukuda, Y., Matsui, J., and Iwata, H. (2016). Vacuolin-1 inhibits autophagy by impairing lysosomal maturation via PIKfyve inhibition. *FEBS Lett.* 590, 1576–1585. doi: 10.1002/1873-3468.12195
- Saric, A., and Freeman, S. A. (2020). Endomembrane tension and trafficking. *Front. Cell Dev. Biol.* 8:611326. doi: 10.3389/fcell.2020.611326
- Saric, A., and Freeman, S. A. (2021). Solutes as controllers of endomembrane dynamics. *Nat. Rev. Mol. Cell Biol.* 22, 237–238. doi: 10.1038/s41580-021-00334-0
- Sarkar Bhattacharya, S., Thirusangu, P., Jin, L., Roy, D., Jung, D., Xiao, Y., et al. (2019). PFKFB3 inhibition reprograms malignant pleural mesothelioma to nutrient stress-induced macropinocytosis and ER stress as independent binary adaptive responses. *Cell Death Dis.* 10:725.
- Sato, K., Mogi, C., Mighell, A. J., and Okajima, F. (2020). A missense mutation of Leu74Pro of OGR1 found in familial amelogenesis imperfecta actually causes the loss of the pH-sensing mechanism. *Biochem. Biophys. Res. Commun.* 526, 920–926. doi: 10.1016/j.bbrc.2020.04.005
- Sato-Numata, K., Numata, T., Inoue, R., Sabirov, R. Z., and Okada, Y. (2017). Distinct contributions of LRRC8A and its paralogs to the VSOR anion channel from those of the ASOR anion channel. *Channels* 11, 167–172. doi: 10.1080/19336950.2016.1230574
- Sato-Numata, K., Numata, T., Okada, T., and Okada, Y. (2013). Acid-sensitive outwardly rectifying (ASOR) anion channels in human epithelial cells are highly sensitive to temperature and independent of ClC-3. *Pflugers Arch.* 465, 1535–1543. doi: 10.1007/s00424-013-1296-y
- Saveanu, L., and Lotersztajn, S. (2016). New pieces in the complex puzzle of aberrant vacuolation. Focus on “Active vacuolar H+ ATPase and functional cycle of Rab5 are required for the vacuolation defect triggered by PtdIns(3,5)P2 loss under PIKfyve or Vps34 deficiency”. *Am. J. Physiol. Cell Physiol.* 311, C363–C365.
- Savina, A., Furlán, M., Vidal, M., and Colombo, M. I. (2003). Exosome release is regulated by a calcium-dependent mechanism in K562 cells. *J. Biol. Chem.* 278, 20083–20090. doi: 10.1074/jbc.m301642200
- Sbrissa, D., Ikononov, O. C., Filios, C., Delvecchio, K., and Shisheva, A. (2012). Functional dissociation between PIKfyve-synthesized PtdIns5P and PtdIns(3,5)P2 by means of the PIKfyve inhibitor YM201636. *Am. J. Physiol. Cell Physiol.* 303, C436–C446.
- Sbrissa, D., Naisan, G., Ikononov, O. C., and Shisheva, A. (2018). Apilimod, a candidate anticancer therapeutic, arrests not only PtdIns(3,5)P2 but also PtdIns5P synthesis by PIKfyve and induces bafilomycin A1-reversible aberrant endomembrane dilation. *PLoS One* 13:e0204532. doi: 10.1371/journal.pone.0204532
- Sbrissa, D., and Shisheva, A. (2005). Acquisition of unprecedented phosphatidylinositol 3,5-bisphosphate rise in hyperosmotically stressed 3T3-L1 adipocytes, mediated by ArPIKfyve-PIKfyve pathway. *J. Biol. Chem.* 280, 7883–7889. doi: 10.1074/jbc.m412729200
- Scheel, O., Zdebik, A. A., Lourdel, S., and Jentsch, T. J. (2005). Voltage-dependent electrogenic chloride/proton exchange by endosomal CLC proteins. *Nature* 436, 424–427. doi: 10.1038/nature03860
- Schilling, K., Opitz, N., Wiesenthal, A., Oess, S., Tikkanen, R., Muller-Esterl, W., et al. (2006). Translocation of endothelial nitric-oxide synthase involves a ternary complex with caveolin-1 and NOSTRIN. *Mol. Biol. Cell* 17, 3870–3880. doi: 10.1091/mbc.e05-08-0709
- Schmees, C., Villaseñor, R., Zheng, W., Ma, H., Zerial, M., Heldin, C. H., et al. (2012). Macropinocytosis of the PDGF beta-receptor promotes fibroblast transformation by H-RasG12V. *Mol. Biol. Cell* 23, 2571–2582. doi: 10.1091/mbc.e11-04-0317
- Schneider, L., Klausen, T. K., Stock, C., Mally, S., Christensen, S. T., Pedersen, S. F., et al. (2008). H-ras transformation sensitizes volume-activated anion channels and increases migratory activity of NIH3T3 fibroblasts. *Pflugers Arch.* 455, 1055–1062. doi: 10.1007/s00424-007-0367-3
- Schneider, S. W., Pagel, P., Rotsch, C., Danker, T., Oberleithner, H., Radmacher, M., et al. (2000). Volume dynamics in migrating epithelial cells measured with atomic force microscopy. *Pflugers Arch.* 439, 297–303. doi: 10.1007/s004249900176
- Schwab, A., Fabian, A., Hanley, P. J., and Stock, C. (2012). Role of ion channels and transporters in cell migration. *Physiol. Rev.* 92, 1865–1913. doi: 10.1152/physrev.00018.2011
- Schwab, A., and Stock, C. (2014). Ion channels and transporters in tumour cell migration and invasion. *Philos. Trans. R. Soc. Lond. B Biol. Sci.* 369:20130102. doi: 10.1098/rstb.2013.0102
- Schwappach, B. (2020). Chloride accumulation in endosomes and lysosomes: facts checked in mice. *EMBO J.* 39:e104812.
- Schwede, M., Garbett, K., Mirnics, K., Geschwind, D. H., and Morrow, E. M. (2014). Genes for endosomal NHE6 and NHE9 are misregulated in autism brains. *Mol. Psychiatry* 19, 277–279. doi: 10.1038/mp.2013.28
- Scott, C. C., and Gruenberg, J. (2011). Ion flux and the function of endosomes and lysosomes: pH is just the start: the flux of ions across endosomal membranes influences endosome function not only through regulation of the luminal pH. *Bioessays* 33, 103–110. doi: 10.1002/bies.201000108
- Seastone, D. J., Zhang, L., Buczynski, G., Rebstein, P., Weeks, G., Spiegelman, G., et al. (1999). The small Mr Ras-like GTPase Rap1 and the phospholipase C pathway act to regulate phagocytosis in Dictyostelium discoideum. *Mol. Biol. Cell.* 10, 393–406. doi: 10.1091/mbc.10.2.393
- Sedlyarov, V., Eichner, R., Girardi, E., Essletzbichler, P., Goldmann, U., Nunes-Hasler, P., et al. (2018). The bicarbonate transporter SLC4A7 plays a key role in macrophage phagosome acidification. *Cell Host Microbe* 23, 766.e5–774.e5.
- Seuwen, K., Ludwig, M. G., and Wolf, R. M. (2006). Receptors for protons or lipid messengers or both? *J. Recept. Signal. Transduct. Res.* 26, 599–610. doi: 10.1080/10799890600932220
- She, J., Zeng, W., Guo, J., Chen, Q., Bai, X. C., Jiang, Y. (2019). Structural mechanisms of phospholipid activation of the human TPC2 channel. *eLife* 8:e45222.
- Shi, L. B., and Verkman, A. S. (1989). Very high water permeability in vasopressin-induced endocytic vesicles from toad urinary bladder. *J. Gen. Physiol.* 94, 1101–1115. doi: 10.1085/jgp.94.6.1101
- Shrivastava, P., Singh, S. M., and Singh, N. (2004). Activation of tumor-associated macrophages by thymosin alpha 1. *Int. J. Immunopathol. Pharmacol.* 17, 39–47. doi: 10.1177/039463200401700106
- Shubin, A. V., Demidyuk, I. V., Lunina, N. A., Komissarov, A. A., Roschina, M. P., Leonova, O. G., et al. (2015). Protease 3C of hepatitis A virus induces vacuolization of lysosomal/endosomal organelles and caspase-independent cell death. *BMC Cell. Biol.* 16:4. doi: 10.1186/s12860-015-0050-z

- Silva-Pavez, E., Villar, P., Trigo, C., Caamano, E., Niechi, I., Perez, P., et al. (2019). CK2 inhibition with silmitasertib promotes methuosis-like cell death associated to catastrophic massive vacuolization of colorectal cancer cells. *Cell Death Dis.* 10:73.
- Siner, J., Paredes, A., Hosselet, C., Hammond, T., Strange, K., and Harris, H. W. (1996). Cloning of an aquaporin homologue present in water channel containing endosomes of toad urinary bladder. *Am. J. Physiol.* 270, C372–C381.
- Sonawane, N., Thiagarajah, J. R., and Verkman, A. (2002). Chloride concentration in endosomes measured using a ratioable fluorescent Cl⁻ indicator evidence for chloride accumulation during acidification. *J. Biol. Chem.* 277, 5506–5513. doi: 10.1074/jbc.m110818200
- Sonawane, N. D., and Verkman, A. S. (2003). Determinants of [Cl⁻] in recycling and late endosomes and Golgi complex measured using fluorescent ligands. *J. Cell Biol.* 160, 1129–1138. doi: 10.1083/jcb.200211098
- Song, Q., Meng, B., Xu, H., and Mao, Z. (2020). The emerging roles of vacuolar-type ATPase-dependent Lysosomal acidification in neurodegenerative diseases. *Transl. Neurodegener.* 9:17.
- Song, S., Zhang, Y., Ding, T., Ji, N., and Zhao, H. (2020). The dual role of macropinocytosis in cancers: promoting growth and inducing methuosis to participate in anticancer therapies as targets. *Front. Oncol.* 10:570108. doi: 10.3389/fonc.2020.570108
- Spix, B., Chao, Y. K., Abrahamian, C., Chen, C. C., and Grimm, C. (2020). TRPML cation channels in inflammation and immunity. *Front. Immunol.* 11:225. doi: 10.3389/fimmu.2020.00225
- Sripathi, S. R., He, W., Um, J. Y., Moser, T., Dehnbostel, S., Kindt, K., et al. (2012). Nitric oxide leads to cytoskeletal reorganization in the retinal pigment epithelium under oxidative stress. *Adv. Biosci. Biotechnol.* 3, 1167–1178. doi: 10.4236/abb.2012.38143
- Srivastava, R. K., Li, C., Khan, J., Banerjee, N. S., Chow, L. T., and Athar, M. (2019). Combined mTORC1/mTORC2 inhibition blocks growth and induces catastrophic macropinocytosis in cancer cells. *Proc. Natl. Acad. Sci. U.S.A.* 116, 24583–24592. doi: 10.1073/pnas.1911393116
- Srivastava, S., Choudhury, P., Li, Z., Liu, G., Nadkarni, V., Ko, K., et al. (2006). Phosphatidylinositol 3-phosphate indirectly activates KCa3.1 via 14 amino acids in the carboxy terminus of KCa3.1. *Mol. Biol. Cell.* 17, 146–154. doi: 10.1091/mbc.e05-08-0763
- Srivastava, S., Li, Z., Lin, L., Liu, G., Ko, K., Coetzee, W. A., et al. (2005). The phosphatidylinositol 3-phosphate phosphatase myotubularin-related protein 6 (MTMR6) is a negative regulator of the Ca²⁺-activated K⁺ channel KCa3.1. *Mol. Cell. Biol.* 25, 3630–3638. doi: 10.1128/mcb.25.9.3630-3638.2005
- Staff, C. D. E. (2021). Autophagy-deficient pancreatic cancer cells depend on macropinocytosis. *Cancer Discov.* [Epub ahead of print].
- Stauber, T., and Jentsch, T. J. (2013). Chloride in vesicular trafficking and function. *Annu. Rev. Physiol.* 75, 453–477. doi: 10.1146/annurev-physiol-030212-183702
- Stauber, T., Weinert, S., and Jentsch, T. J. (2012). Cell biology and physiology of CLC chloride channels and transporters. *Compr. Physiol.* 2, 1701–1744.
- Steenbergen, J. M., and Bohlen, H. G. (1993). Sodium hyperosmolarity of intestinal lymph causes arteriolar vasodilation in part mediated by EDRF. *Am. J. Physiol.* 265, H323–H328.
- Stein, B. S., and Sussman, H. H. (1986). Demonstration of two distinct transferrin receptor recycling pathways and transferrin-independent receptor internalization in K562 cells. *J. Biol. Chem.* 261, 10319–10331. doi: 10.1016/s0021-9258(18)67527-1
- Steinberg, B. E., Huynh, K. K., Brodovitch, A., Jabs, S., Stauber, T., Jentsch, T. J., et al. (2010). A cation counterflux supports lysosomal acidification. *J. Cell. Biol.* 189, 1171–1186. doi: 10.1083/jcb.200911083
- Steinman, R. M., Brodie, S. E., and Cohn, Z. A. (1976). Membrane flow during pinocytosis. A stereologic analysis. *J. Cell Biol.* 68, 665–687. doi: 10.1083/jcb.68.3.665
- Sterea, A. M., Almasi, S., and El Hiani, Y. (2018). The hidden potential of lysosomal ion channels: a new era of oncogenes. *Cell Calcium* 72, 91–103. doi: 10.1016/j.ceca.2018.02.006
- Stock, C., Ludwig, F. T., Hanley, P. J., and Schwab, A. (2013). Roles of ion transport in control of cell motility. *Compr. Physiol.* 5, 59–119.
- Stockem, W. (1966). Pinocytose und bewegung von amöben. *Z. Zellforschung Mikroskopische Anatomie* 74, 372–400. doi: 10.1007/bf00401263
- Stow, J. L., Hung, Y., and Wall, A. A. (2020). Macropinocytosis: insights from immunology and cancer. *Curr. Opin. Cell Biol.* 65, 131–140. doi: 10.1016/j.ccb.2020.06.005
- Su, H., Yang, F., Fu, R., Li, X., French, R., Mose, E., et al. (2021). Cancer cells escape autophagy inhibition via NRE2-induced macropinocytosis. *Cancer Cell.* 39, 678.e11–693.e11.
- Su, Y. (2014). Regulation of endothelial nitric oxide synthase activity by protein-protein interaction. *Curr. Pharm. Des.* 20, 3514–3520. doi: 10.2174/13816128113196660752
- Su, Y., Kondrikov, D., and Block, E. R. (2005). Cytoskeletal regulation of nitric oxide synthase. *Cell Biochem. Biophys.* 43, 439–449. doi: 10.1385/cbb.43.3.439
- Suda, T., Gao, X., Stolz, D. B., and Liu, D. (2007). Structural impact of hydrodynamic injection on mouse liver. *Gene Ther.* 14, 129–137. doi: 10.1038/sj.gt.3302865
- Sugiya, H., Matsuki-Fukushima, M., and Hashimoto, S. (2008). Role of aquaporins and regulation of secretory vesicle volume in cell secretion. *J. Cell Mol. Med.* 12, 1486–1494. doi: 10.1111/j.1582-4934.2008.00239.x
- Suh, B. C., and Hille, B. (2008). PIP2 is a necessary cofactor for ion channel function: how and why? *Annu. Rev. Biophys.* 37, 175–195. doi: 10.1146/annurev.biophys.37.032807.125859
- Sun, L., Hua, Y., Vergarauregui, S., Diab, H. I., and Puertollano, R. (2015). Novel role of TRPML2 in the regulation of the innate immune response. *J. Immunol.* 195, 4922–4932. doi: 10.4049/jimmunol.1500163
- Sun, L., Li, B., Su, X., Chen, G., Li, Y., Yu, L., et al. (2017). An ursolic acid derived small molecule triggers cancer cell death through hyperstimulation of macropinocytosis. *J. Med. Chem.* 60, 6638–6648. doi: 10.1021/acs.jmedchem.7b00592
- Swanson, J. A. (1989). Phorbol esters stimulate macropinocytosis and solute flow through macrophages. *J. Cell Sci.* 94, 135–142. doi: 10.1242/jcs.94.1.135
- Swanson, J. A. (2008). Shaping cups into phagosomes and macropinosomes. *Nat. Rev. Mol. Cell Biol.* 9, 639–649. doi: 10.1038/nrm2447
- Swanson, J. A., and King, J. S. (2019). The breadth of macropinocytosis research. *Philos. Trans. R. Soc. Lond. B Biol. Sci.* 374:20180146. doi: 10.1098/rstb.2018.0146
- Swanson, J. A., and Watts, C. (1995). Macropinocytosis. *Trends Cell Biol.* 5, 424–428.
- Swanson, J. A., and Yoshida, S. (2019). Macropinosomes as units of signal transduction. *Philos. Trans. R. Soc. Lond. B Biol. Sci.* 374:20180157. doi: 10.1098/rstb.2018.0157
- Synnes, M., Prydz, K., Lovdal, T., Brech, A., and Berg, T. (1999). Fluid phase endocytosis and galactosyl receptor-mediated endocytosis employ different early endosomes. *Biochim. Biophys. Acta* 1421, 317–328. doi: 10.1016/s0005-2736(99)00134-0
- Takeda-Nakazawa, H., Harada, N., Shen, J., Kubo, N., Zenner, H. P., and Yamashita, T. (2007). Hyposmotic stimulation-induced nitric oxide production in outer hair cells of the guinea pig cochlea. *Hear. Res.* 227, 59–70. doi: 10.1016/j.heares.2006.09.007
- Tall, G. G., Barbieri, M. A., Stahl, P. D., and Horazdovsky, B. F. (2001). Ras-activated endocytosis is mediated by the Rab5 guanine nucleotide exchange activity of RIN1. *Dev. Cell* 1, 73–82. doi: 10.1016/s1534-5807(01)00008-9
- Tejeda-Munoz, N., Albrecht, L. V., Bui, M. H., and De Robertis, E. M. (2019). Wnt canonical pathway activates macropinocytosis and lysosomal degradation of extracellular proteins. *Proc. Natl. Acad. Sci. U.S.A.* 116, 10402–10411. doi: 10.1073/pnas.1903506116
- Tian, X., Gala, U., Zhang, Y., Shang, W., Nagarkar Jaiswal, S., Di Ronza, A., et al. (2015). A voltage-gated calcium channel regulates lysosomal fusion with endosomes and autophagosomes and is required for neuronal homeostasis. *PLoS Biol.* 13:e1002103. doi: 10.1371/journal.pbio.1002103
- Toh, W. H., Louber, J., Mahmoud, I. S., Chia, J., Bass, G. T., Dower, S. K., et al. (2019). FcRn mediates fast recycling of endocytosed albumin and IgG from early macropinosomes in primary macrophages. *J. Cell. Sci.* 133:jcs235416.
- Trabbic, C. J., Dietsch, H. M., Alexander, E. M., Nagy, P. I., Robinson, M. W., Overmeyer, J. H., et al. (2014). Differential induction of cytoplasmic vacuolization and methuosis by novel 2-indolyl-substituted pyridinylpropenones. *ACS Med. Chem. Lett.* 5, 73–77. doi: 10.1021/ml4003925
- Trabbic, C. J., George, S. M., Alexander, E. M., Du, S., Offenbacher, J. M., Crissman, E. J., et al. (2016). Synthesis and biological evaluation of isomeric methoxy

- substitutions on anti-cancer indolyl-pyridinyl-propenones: effects on potency and mode of activity. *Eur. J. Med. Chem.* 122, 79–91. doi: 10.1016/j.ejmech.2016.06.016
- Trabbic, C. J., Overmeyer, J. H., Alexander, E. M., Crissman, E. J., Kvale, H. M., Smith, M. A., et al. (2015). Synthesis and biological evaluation of indolyl-pyridinyl-propenones having either methuosis or microtubule disruption activity. *J. Med. Chem.* 58, 2489–2512. doi: 10.1021/jm501997q
- Trivedi, P. C., Bartlett, J. J., and Pulinilkunnil, T. (2020). Lysosomal biology and function: modern view of cellular debris bin. *Cells* 9:1131. doi: 10.3390/cells9051131
- Tsuchiya, W., Okada, Y., Yano, J., Murai, A., Miyahara, T., and Tanaka, T. (1981). Membrane potential changes associated with pinocytosis of serum lipoproteins in L cells. *Exp. Cell Res.* 136, 271–278. doi: 10.1016/0014-4827(81)90005-7
- Ullrich, F., Blin, S., Lazarow, K., Daubitz, T., Von Kries, J. P., and Jentsch, T. J. (2019). Identification of TMEM206 proteins as pore of PAORAC/ASOR acid-sensitive chloride channels. *eLife* 8:e49187.
- Ulmasov, B., Bruno, J., Gordon, N., Hartnett, M. E., and Edwards, J. C. (2009). Chloride intracellular channel protein-4 functions in angiogenesis by supporting acidification of vacuoles along the intracellular tubulogenic pathway. *Am. J. Pathol.* 174, 1084–1096. doi: 10.2353/ajpath.2009.080625
- Unni, A. M., Lockwood, W. W., Zejnullahu, K., Lee-Lin, S. Q., and Varmus, H. (2015). Evidence that synthetic lethality underlies the mutual exclusivity of oncogenic KRAS and EGFR mutations in lung adenocarcinoma. *eLife* 4: e06907.
- Vacca, G., Papillo, B., Battaglia, A., Grossini, E., Mary, D. A., and Pelosi, G. (1996). The effects of hypertonic saline solution on coronary blood flow in anesthetized pigs. *J. Physiol.* 491(Pt 3), 843–851. doi: 10.1113/jphysiol.1996.sp021261
- Van Der Knaap, M. S., Boor, I., and Estévez, R. (2012). Megalencephalic leukoencephalopathy with subcortical cysts: chronic white matter oedema due to a defect in brain ion and water homeostasis. *Lancet Neurol.* 11, 973–985. doi: 10.1016/s1474-4422(12)70192-8
- Van Der Wijk, T., Dorrestijn, J., Narumiya, S., Maassen, J. A., De Jonge, H. R., and Tilly, B. C. (1998). Osmotic swelling-induced activation of the extracellular-signal-regulated protein kinases Erk-1 and Erk-2 in intestine 407 cells involves the Ras/Raf-signalling pathway. *Biochem. J.* 331(Pt 3), 863–869. doi: 10.1042/bj3310863
- Vardjan, N., Verkhatsky, A., and Zorec, R. (2015). Pathologic potential of astrocytic vesicle traffic: new targets to treat neurologic diseases? *Cell Transplant* 24, 599–612. doi: 10.3727/096368915x687750
- Varela, D., Simon, F., Riveros, A., Jørgensen, F., and Stutzin, A. (2004). NAD (P) H oxidase-derived H₂O₂ signals chloride channel activation in cell volume regulation and cell proliferation. *J. Biol. Chem.* 279, 13301–13304. doi: 10.1074/jbc.c400020200
- Vasanthakumar, T., and Rubinstein, J. L. (2020). Structure and Roles of V-type ATPases. *Trends Biochem. Sci.* 45, 295–307. doi: 10.1016/j.tibs.2019.12.007
- Veltman, D. M., Williams, T. D., Bloomfield, G., Chen, B. C., Betzig, E., Insall, R. H., et al. (2016). A plasma membrane template for macropinocytic cups. *eLife* 5:e20085.
- Venkatachalam, K., Wong, C. O., and Zhu, M. X. (2015). The role of TRPMLs in endolysosomal trafficking and function. *Cell Calcium* 58, 48–56. doi: 10.1016/j.ceca.2014.10.008
- Verkman, A., Weyer, P., Brown, D., and Ausiello, D. (1989). Functional water channels are present in clathrin-coated vesicles from bovine kidney but not from brain. *J. Biol. Chem.* 264, 20608–20613. doi: 10.1016/s0021-9258(19)47106-8
- Verkman, A. S. (1989). Mechanisms and regulation of water permeability in renal epithelia. *Am. J. Physiol.* 257, C837–C850.
- Verkman, A. S. (2005). More than just water channels: unexpected cellular roles of aquaporins. *J. Cell Sci.* 118, 3225–3232. doi: 10.1242/jcs.02519
- Verkman, A. S., Lencer, W. I., Brown, D., and Ausiello, D. A. (1988). Endosomes from kidney collecting tubule cells contain the vasopressin-sensitive water channel. *Nature* 333, 268–269. doi: 10.1038/333268a0
- Verkman, A. S., and Masur, S. K. (1988). Very low osmotic water permeability and membrane fluidity in isolated toad bladder granules. *J. Membr. Biol.* 104, 241–251. doi: 10.1007/bf01872326
- Verkman, A. S., Van Hoek, A. N., Ma, T., Frigeri, A., Skach, W. R., Mitra, A., et al. (1996). Water transport across mammalian cell membranes. *Am. J. Physiol.* 270, C12–C30.
- Vermeulen, M., Giordano, M., Trevani, A. S., Sedlik, C., Gamberale, R., Fernández-Calotti, P., et al. (2004). Acidosis improves uptake of antigens and MHC class I-restricted presentation by dendritic cells. *J. Immunol.* 172, 3196–3204. doi: 10.4049/jimmunol.172.5.3196
- Viet, K. K., Wagner, A., Schwickert, K., Hellwig, N., Brennich, M., Bader, N., et al. (2019). Structure of the human TRPML2 ion channel extracytosolic/lumenal domain. *Structure* 27, 1246.e5–1257.e5.
- Völkl, H., Busch, G. L., Häussinger, D., and Lang, F. (1994). Alkalinization of acidic cellular compartments following cell swelling. *FEBS Lett.* 338, 27–30. doi: 10.1016/0014-5793(94)80110-x
- Völkl, H., and Lang, F. (1988). Ionic requirement for regulatory cell volume decrease in renal straight proximal tubules. *Pflügers Arch.* 412, 1–6. doi: 10.1007/bf00583723
- Von Delwig, A., Hilken, C. M., Altmann, D. M., Holmdahl, R., Isaacs, J. D., Harding, C. V., et al. (2006). Inhibition of macropinocytosis blocks antigen presentation of type II collagen in vitro and in vivo in HLA-DR1 transgenic mice. *Arthritis Res. Ther.* 8:R93.
- Von Recklinghausen, F. (1910). *Untersuchungen Über Rachitis und Osteomalacie*. Jena: G. Fischer.
- Voss, F. K., Ullrich, F., Munch, J., Lazarow, K., Lutter, D., Mah, N., et al. (2014). Identification of LRRC8 heteromers as an essential component of the volume-regulated anion channel VRAC. *Science* 344, 634–638. doi: 10.1126/science.1252826
- Waldegger, S., Barth, P., Raber, G., and Lang, F. (1997). Cloning and characterization of a putative human serine/threonine protein kinase transcriptionally modified during anisotonic and isotonic alterations of cell volume. *Proc. Natl. Acad. Sci. U.S.A.* 94, 4440–4445. doi: 10.1073/pnas.94.9.4440
- Waldegger, S., Gabrysch, S., Barth, P., Fillon, S., and Lang, F. (2000). h-sgk serine-threonine protein kinase as transcriptional target of p38/MAP kinase pathway in HepG2 human hepatoma cells. *Cell Physiol. Biochem.* 10, 203–208. doi: 10.1159/000016351
- Walker, S. A., Kupzig, S., Bouyoucef, D., Davies, L. C., Tsuboi, T., Bivona, T. G., et al. (2004). Identification of a Ras GTPase-activating protein regulated by receptor-mediated Ca²⁺ oscillations. *EMBO J.* 23, 1749–1760. doi: 10.1038/sj.emboj.7600197
- Wang, G., Moniri, N. H., Ozawa, K., Stamler, J. S., and Daaka, Y. (2006). Nitric oxide regulates endocytosis by S-nitrosylation of dynamin. *Proc. Natl. Acad. Sci. U.S.A.* 103, 1295–1300. doi: 10.1073/pnas.0508354103
- Wang, X., Zhang, X., Dong, X. P., Samie, M., Li, X., Cheng, X., et al. (2012). TPC proteins are phosphoinositide-activated sodium-selective ion channels in endosomes and lysosomes. *Cell* 151, 372–383. doi: 10.1016/j.cell.2012.08.036
- Ward, D. M., Hackenjos, D. P., Davis-Kaplan, S., and Kaplan, J. (1990). Inhibition of late endosome-lysosome fusion: studies on the mechanism by which isotonic-K⁺ buffers alter intracellular ligand movement. *J. Cell Physiol.* 145, 522–530. doi: 10.1002/jcp.1041450319
- Warnock, D. G., Kusche-Vihrog, K., Tarjus, A., Sheng, S., Oberleithner, H., Kleyman, T. R., et al. (2014). Blood pressure and amiloride-sensitive sodium channels in vascular and renal cells. *Nat. Rev. Nephrol.* 10, 146–157. doi: 10.1038/nrneph.2013.275
- Warskulat, U., Schliess, F., and Haussinger, D. (1998). Compatible organic osmolytes and osmotic modulation of inducible nitric oxide synthetase in RAW 264.7 mouse macrophages. *Biol. Chem.* 379, 867–874. doi: 10.1515/bchm.1998.379.7.867
- Warskulat, U., Zhang, F., and Haussinger, D. (1996). Modulation of phagocytosis by anisoosmolarity and betaine in rat liver macrophages (Kupffer cells) and RAW 264.7 mouse macrophages. *FEBS Lett.* 391, 287–292. doi: 10.1016/0014-5793(96)00753-3
- Watanabe, K., Morishita, K., Zhou, X., Shiizaki, S., Uchiyama, Y., Koike, M., et al. (2021). Cells recognize osmotic stress through liquid-liquid phase separation lubricated with poly(ADP-ribose). *Nat. Commun.* 12:1353.
- Webb, J. L., Harvey, M. W., Holden, D. W., and Evans, T. J. (2001). Macrophage nitric oxide synthase associates with cortical actin but is not recruited to phagosomes. *Infect. Immun.* 69, 6391–6400. doi: 10.1128/iai.69.10.6391-6400.2001

- Weerasinghe, P., and Buja, L. M. (2012). Oncosis: an important non-apoptotic mode of cell death. *Exp. Mol. Pathol.* 93, 302–308. doi: 10.1016/j.yexmp.2012.09.018
- Weinberg, J. B. (1998). Nitric oxide production and nitric oxide synthase type 2 expression by human mononuclear phagocytes: a review. *Mol. Med.* 4, 557–591. doi: 10.1007/bf03401758
- Weinert, S., Jabs, S., Supanchart, C., Schweizer, M., Gimber, N., Richter, M., et al. (2010). Lysosomal pathology and osteopetrosis upon loss of H⁺-driven lysosomal Cl⁻ accumulation. *Science* 328, 1401–1403. doi: 10.1126/science.1188072
- Weisz, O. A. (2003). Acidification and protein traffic. *Int. Rev. Cytol.* 226, 259–319. doi: 10.1016/s0074-7696(03)01005-2
- Welliver, T. P., and Swanson, J. A. (2012). A growth factor signaling cascade confined to circular ruffles in macrophages. *Biol. Open* 1, 754–760. doi: 10.1242/bio.20121784
- Wen, M. H., Wang, J. Y., Chiu, Y. T., Wang, M. P., Lee, S. P., and Tai, C. Y. (2016). N-cadherin regulates cell migration through a Rab5-dependent temporal control of macropinocytosis. *Traffic* 17, 769–785. doi: 10.1111/tra.12402
- West, M. A., Bretscher, M. S., and Watts, C. (1989). Distinct endocytotic pathways in epidermal growth factor-stimulated human carcinoma A431 cells. *J. Cell Biol.* 109, 2731–2739. doi: 10.1083/jcb.109.6.2731
- Wiernasz, E., Kaliszewska, A., Brulkowski, W., Bednarczyk, J., Gorniak, M., Kaza, B., et al. (2014). Ttyh1 protein is expressed in glia in vitro and shows elevated expression in activated astrocytes following status epilepticus. *Neurochem. Res.* 39, 2516–2526. doi: 10.1007/s11064-014-1455-3
- Williams, T. D., Peak-Chew, S. Y., Paschke, P., and Kay, R. R. (2019). Akt and SGK protein kinases are required for efficient feeding by macropinocytosis. *J. Cell Sci.* 132:jcs224998.
- Williamson, C. D., and Donaldson, J. G. (2019). Arf6, JIP3, and dynein shape and mediate macropinocytosis. *Mol. Biol. Cell* 30, 1477–1489. doi: 10.1091/mbc.e19-01-0022
- Wilson, Z. N., Scott, A. L., Dowell, R. D., and Odorizzi, G. (2018). PI(3,5)P₂ controls vacuole potassium transport to support cellular osmoregulation. *Mol. Biol. Cell* 29, 1718–1731. doi: 10.1091/mbc.e18-01-0015
- Worby, C. A., and Dixon, J. E. (2014). Pten. *Annu. Rev. Biochem.* 83, 641–669.
- Wright, E. M., Loo, D. D., and Hirayama, B. A. (2011). Biology of human sodium glucose transporters. *Physiol. Rev.* 91, 733–794. doi: 10.1152/physrev.00055.2009
- Wu, L., Sun, Y., Ma, L., Zhu, J., Zhang, B., Pan, Q., et al. (2016). A C-terminally truncated mouse Best3 splice variant targets and alters the ion balance in lysosome-endosome hybrids and the endoplasmic reticulum. *Sci. Rep.* 6:27332.
- Wunderberg, T., and Mayr, G. W. (2012). Synthesis and biological actions of diphosphoinositol phosphates (inositol pyrophosphates), regulators of cell homeostasis. *Biol. Chem.* 393, 979–998. doi: 10.1515/hsz-2012-0133
- Xiao, F., Li, J., Huang, K., Li, X., Xiong, Y., Wu, M., et al. (2021). Macropinocytosis: mechanism and targeted therapy in cancers. *Am. J. Cancer Res.* 11, 14–30.
- Xiong, J., and Zhu, M. X. (2016). Regulation of lysosomal ion homeostasis by channels and transporters. *Sci. China Life Sci.* 59, 777–791. doi: 10.1007/s11427-016-5090-x
- Xu, H., and Ren, D. (2015). Lysosomal physiology. *Annu. Rev. Physiol.* 77, 57–80. doi: 10.1146/annurev-physiol-021014-071649
- Yan, Y., Ding, Y., Ming, B., Du, W., Kong, X., Tian, L., et al. (2014). Increase in hypotonic stress-induced endocytic activity in macrophages via CIC-3. *Mol. Cells* 37, 418–425. doi: 10.14348/molcells.2014.0031
- Yang, L., Song, L., Zhao, S., Ma, C., Wu, D., and Wu, Y. L. (2019). Isobavachalcone reveals novel characteristics of methuosis-like cell death in leukemia cells. *Chem. Biol. Interact.* 304, 131–138. doi: 10.1016/j.cbi.2019.03.011
- Yasui, M., Hazama, A., Kwon, T. H., Nielsen, S., Guggino, W. B., and Agre, P. (1999). Rapid gating and anion permeability of an intracellular aquaporin. *Nature* 402, 184–187. doi: 10.1038/46045
- Ye, R. G., Shi, L. B., Lencer, W. I., and Verkman, A. S. (1989). Functional colocalization of water channels and proton pumps in endosomes from kidney proximal tubule. *J. Gen. Physiol.* 93, 885–902. doi: 10.1085/jgp.93.5.885
- Yoo, D. Y., Barros, S. A., Brown, G. C., Rabot, C., Bar-Sagi, D., and Arora, P. S. (2020). Macropinocytosis as a key determinant of peptidomimetic uptake in cancer cells. *J. Am. Chem. Soc.* 142, 14461–14471. doi: 10.1021/jacs.0c02109
- Yoshida, S., Gaeta, I., Pacitto, R., Krienke, L., Alge, O., Gregorka, B., et al. (2015). Differential signaling during macropinocytosis in response to M-CSF and PMA in macrophages. *Front. Physiol.* 6:8. doi: 10.3389/fphys.2015.00008
- Yoshida, S., Pacitto, R., Sesi, C., Kotula, L., and Swanson, J. A. (2018). Dorsal ruffles enhance activation of Akt by growth factors. *J. Cell Sci.* 131:jcs220517.
- Yuan, A., and Chia, C. P. (2001). Giant vacuoles observed in *Dictyostelium discoideum*. *Cell Biol. Int.* 25, 147–155. doi: 10.1006/cbir.2000.0577
- Zani, B. G., and Bohlen, H. G. (2005). Sodium channels are required during in vivo sodium chloride hyperosmolarity to stimulate increase in intestinal endothelial nitric oxide production. *Am. J. Physiol. Heart Circ. Physiol.* 288, H89–H95.
- Zen, K., Biwersi, J., Periasamy, N., and Verkman, A. S. (1992). Second messengers regulate endosomal acidification in Swiss 3T3 fibroblasts. *J. Cell Biol.* 119, 99–110. doi: 10.1083/jcb.119.1.99
- Zeuthen, T. (2010). Water-transporting proteins. *J. Membr. Biol.* 234, 57–73. doi: 10.1007/s00232-009-9216-y
- Zeuthen, T., and Macaulay, N. (2012). Cotransport of water by Na(+)-K(+)-2Cl(-) cotransporters expressed in *Xenopus oocytes*: NKCC1 versus NKCC2. *J. Physiol.* 590, 1139–1154. doi: 10.1113/jphysiol.2011.226316
- Zhang, L., Qu, Z., Wu, J., Yao, S., Zhang, Q., Zhang, T., et al. (2021). SARs of a novel series of s-triazine compounds targeting vimentin to induce methuotic phenotype. *Eur. J. Med. Chem.* 214:113188. doi: 10.1016/j.ejmech.2021.113188
- Zhang, X., Cheng, X., Yu, L., Yang, J., Calvo, R., Patnaik, S., et al. (2016). MCOLN1 is a ROS sensor in lysosomes that regulates autophagy. *Nat. Commun.* 7: 12109.
- Zhao, H., Atkinson, J., Gulesserian, S., Zeng, Z., Nater, J., Ou, J., et al. (2018). Modulation of macropinocytosis-mediated internalization decreases ocular toxicity of antibody-drug conjugates. *Cancer Res.* 78, 2115–2126. doi: 10.1158/0008-5472.can-17-3202
- Zhao, J., Zhu, D., Zhang, X., Zhang, Y., Zhou, J., and Dong, M. (2019). TMEM206 promotes the malignancy of colorectal cancer cells by interacting with AKT and extracellular signal-regulated kinase signaling pathways. *J. Cell Physiol.* 234, 10888–10898. doi: 10.1002/jcp.27751
- Zheng, T., Gao, Y., Deng, X., Liu, H., Liu, J., Liu, R., et al. (2018). Comparisons between graphene oxide and graphdiyne oxide in physicochemistry biology and cytotoxicity. *ACS Appl. Mater. Interfaces* 10, 32946–32954. doi: 10.1021/acsami.8b06804
- Zhou, J., Tai, G., Liu, H., Ge, J., Feng, Y., Chen, F., et al. (2009). Activin A down-regulates the phagocytosis of lipopolysaccharide-activated mouse peritoneal macrophages in vitro and in vivo. *Cell Immunol.* 255, 69–75. doi: 10.1016/j.cellimm.2008.11.001
- Zhu, J. Y., Tu, W., Zeng, C., Mao, H. X., Du, Q. F., and Cai, H. B. (2017). [Mechanism of *Platycarya strobilacea* Sieb. et Zucc extract-induced methuosis in human nasopharyngeal carcinoma CNE1 and CNE2 cells]. *Nan Fang Yi Ke Da Xue Xue Bao* 37, 827–832.
- Zhu, M., Wu, G., Li, Y. X., Stevens, J. K., Fan, C. X., Spang, A., et al. (2015). Serum- and glucocorticoid-inducible kinase-1 (SGK-1) plays a role in membrane trafficking in *Caenorhabditis elegans*. *PLoS One* 10:e0130778. doi: 10.1371/journal.pone.0130778
- Zifarelli, G. (2015). A tale of two CLCs: biophysical insights toward understanding CIC-5 and CIC-7 function in endosomes and lysosomes. *J. Physiol.* 593, 4139–4150. doi: 10.1113/jp270604
- Zong, W. X., and Thompson, C. B. (2006). Necrotic death as a cell fate. *Genes Dev.* 20, 1–15. doi: 10.1101/gad.1376506
- Zwartkruis, F. J., and Bos, J. L. (1999). Ras and Rap1: two highly related small GTPases with distinct function. *Exp. Cell Res.* 253, 157–165. doi: 10.1006/excr.1999.4695

Conflict of Interest: The authors declare that the research was conducted in the absence of any commercial or financial relationships that could be construed as a potential conflict of interest.

Copyright © 2021 Ritter, Bresgen and Kerschbaum. This is an open-access article distributed under the terms of the Creative Commons Attribution License (CC BY). The use, distribution or reproduction in other forums is permitted, provided the original author(s) and the copyright owner(s) are credited and that the original publication in this journal is cited, in accordance with accepted academic practice. No use, distribution or reproduction is permitted which does not comply with these terms.



Transient Receptor Potential (TRP) Ion Channels Involved in Malignant Glioma Cell Death and Therapeutic Perspectives

Florence Lefranc*

Department of Neurosurgery, Hôpital Erasme, Université Libre de Bruxelles, Brussels, Belgium

OPEN ACCESS

Edited by:

Giovanna Valenti,
University of Bari Aldo Moro, Italy

Reviewed by:

Ella L. Kim,
Johannes Gutenberg University
Mainz, Germany
Federica Barbieri,
University of Genoa, Italy
Maria Beatrice Morelli,
University of Camerino, Italy

*Correspondence:

Florence Lefranc
Florence.lefranc@erasme.ulb.ac.be

Specialty section:

This article was submitted to
Cell Death and Survival,
a section of the journal
Frontiers in Cell and Developmental
Biology

Received: 19 October 2020

Accepted: 29 April 2021

Published: 12 August 2021

Citation:

Lefranc F (2021) Transient
Receptor Potential (TRP) Ion
Channels Involved in Malignant
Glioma Cell Death and Therapeutic
Perspectives.
Front. Cell Dev. Biol. 9:618961.
doi: 10.3389/fcell.2021.618961

Among the most biologically, thus clinically, aggressive primary brain tumors are found malignant gliomas. Despite recent advances in adjuvant therapies, which include targeted and immunotherapies, after surgery and radio/chemotherapy, the tumor is recurrent and always lethal. Malignant gliomas also contain a pool of initiating stem cells that are highly invasive and resistant to conventional treatment. Ion channels and transporters are markedly involved in cancer cell biology, including glioma cell biology. Transient receptor potential (TRP) ion channels are calcium-permeable channels implicated in Ca^{2+} changes in multiple cellular compartments by modulating the driving force for Ca^{2+} entry. Recent scientific reports have shown that these channels contribute to the increase in glioblastoma aggressiveness, with glioblastoma representing the ultimate level of glioma malignancy. The current review focuses on each type of TRP ion channel potentially involved in malignant glioma cell death, with the ultimate goal of identifying new therapeutic targets to clinically combat malignant gliomas. It thus appears that cannabidiol targeting the TRPV2 type could be such a potential target.

Keywords: malignant glioma, cell death, TRP ion channels, treatment, cannabidiol

INTRODUCTION

Malignant Glioma Generality

Among the most common malignant primary tumors are encountered malignant gliomas, which are associated with dismal prognosis. Precise statistics from the United States report for example 17,000 new diagnoses in 2017 (Ostrom et al., 2017). These tumors are characterized by extensive proliferation, invasion, migration, angiogenesis, immunosuppression, and resistance to conventional treatment (Lefranc et al., 2018; Locarno et al., 2020). Malignant gliomas include grade II (gliomas), III (anaplastic gliomas), and IV (glioblastoma) tumors. The median survival of glioblastoma is only 16 months because of the high rate of tumor recurrence (>95%) (Lefranc et al., 2018), even under aggressive treatment, including large surgical resection followed by combined radio- and temozolomide chemotherapy and adjuvant chemotherapy with the same compound (Stupp et al., 2009). This high rate of tumor recurrence is linked to the dramatic infiltrative properties of glioma cells into the brain parenchyma, rendering therefore elusive curative surgical resection as well as conventional treatments using genotoxic

radiotherapy and cytotoxic chemotherapy, and even antiangiogenic therapies (Wick et al., 2017). Targeted therapies and immunotherapies also failed in efficaciously combating malignant gliomas (McGranahan et al., 2019).

Heterogeneous populations of tumor-differentiated cells coexisting with subpopulations displaying stem cell properties are present in glioblastomas. The marked biological, thus clinical, aggressiveness of glioblastoma stem cells (GSCs) relates among others to their dramatic invasive nature into the brain parenchyma, high level of mobility into the brain parenchyma, and high resistance to both radio- and chemotherapy. GSCs have also the capacity to self-renew and are now known to be directly responsible for the recurrence and clinical relapse of glioblastomas (Colwell et al., 2017; Matarredona and Pastor, 2019).

All grade II gliomas have the tendency to transform into more aggressive grade III (anaplastic) or even grade IV gliomas (secondary glioblastoma); likewise, grade III gliomas can similarly transform into grade IV (secondary glioblastoma).

A glioblastoma is a mosaic of various cell populations associated with distinct dynamic cell states as recently revealed by genome-wide sequencing, and this dramatic cell heterogeneity within a given glioblastoma renders any type of treatment very difficult (Sottoriva et al., 2013; Patel et al., 2014; Bernstock et al., 2019).

Ion Channels Involved in Malignant Glioma Progression

Ion channels are classified by ion selectivity (sodium channels, potassium channels, chloride channels, proton channels, unselective channels, etc.), gating mechanism (voltage-gated, ligand-gated, cyclic nucleotide-gated, light-gated, and mechanosensitive), or localization (plasma membrane or intracellular) (Alexander et al., 2019). These channels display marked roles in a plethora of cellular processes and in cancer progression (Becchetti et al., 2013; Litan and Langhans, 2015; Prevarskaya et al., 2018).

Several ion channels are implicated in malignant glioma proliferation, migration, invasion, and cell death. For example, genome-wide analyses of glioblastoma revealed that, of 555 genes involved in potassium, sodium, chloride, calcium channels, and other ion transport, 55 mutations were detected, affecting 90% of the glioblastoma samples studied (Parsons et al., 2008).

It has been experimentally demonstrated already two decades ago that glioma cells invading the brain parenchyma must modify their shape and/or volume to perform their invasive journey (Soroceanu et al., 1999). Shape-volume changes in glioma cells are mediated, at least partly, by chloride currents, which, while affecting net salt fluxes across glioma cell membranes, induce water efflux, resulting in turn in glioma cell shrinkage facilitating their migration through minute extracellular spaces of the brain (Ransom et al., 2001; Habela et al., 2009).

In gliomas, cell condensation is a hallmark of intrinsic and extrinsic apoptosis and requires the concerted activation of chloride- and calcium-activated potassium channels, leading to

the loss of water (Ernst et al., 2008). We previously reviewed the implications of the roles of potassium channels in glioma progression and migration, e.g., Kv1.3 and Kv1.5, Kv10.1, Kv11.1, KCa1.1, and KCa3.1 (Lefranc et al., 2012, 2018).

Morrone et al. (2016) reviewed the role of calcium channels in malignant brain tumor therapy.

The present review focuses on transient receptor potential (TRP) calcium channels, which modulate the driving force for Ca^{2+} entry from extra- into intracellular compartments (**Figure 1**). For each type of TRP ion channel described below, we focused our attention in identifying specific TRP channels involved in glioma cell death, rendering them as potential new therapeutic targets to combat general malignant gliomas, with a particular focus on glioblastoma (**Table 1**).

Malignant Glioma Cell Death

Glioma, melanoma, non-small cell lung cancer, and esophageal cancer, among others, are resistant to proapoptotic stimuli and are typically associated with dismal prognoses (Hanahan and Weinberg, 2011; Kornienko et al., 2013) and display therefore resistance to conventional cytotoxic pro-apoptotic drugs. Cytotoxic compounds that induce non-apoptotic cellular mechanisms, such as necrosis, senescence, autophagy, and mitotic catastrophe, are of great hopes to combat these cancer types displaying various levels of resistance to pro-apoptotic stimuli (Tang et al., 2019). The readers interested by precise definitions about the various cell death types should refer to the nomenclature established by Kroemer and colleagues (Galluzzi et al., 2012). The authors distinguished 13 distinct cell death types (Galluzzi et al., 2012), to which we have added methuosis, paraptosis, oncosis, and lysosomal membrane permeabilization (LMP) cell death types (Kornienko et al., 2013).

In the current review, the subchapter entitled therapeutic perspective aims to analyze the types of TRP-targeting drugs that could be of help in overcoming the resistance of glioma cancer cells and glioma stem cells to conventional therapies (**Figure 2** and **Table 1**).

MODULATING TRANSIENT RECEPTOR POTENTIAL CHANNELS FOR INDUCING CELL DEATH IN MALIGNANT GLIOMA

Transient Receptor Potential Ion Channels

The mammalian TRP channel superfamily encompasses 28 identified members of Ca^{2+} -permeable channels, with diverse physiological functions and cellular distributions (Ramsey et al., 2006; Venkatachalam and Montell, 2007; Nilius and Owsianik, 2011). TRP channels can be localized on the plasma membrane or in intracellular membranes and are involved in numerous fundamental cell functions (Nilius and Owsianik, 2011). Based on their structural homology and function, TRP channels are grouped into seven subfamilies in mammals: TRPC (canonical), TRPM (melastatin), TRPV (vanilloid), TRPP (polycystin), TRPA (ankyrin-like), TRPML (mucolipin), and TRPN (*Drosophila*

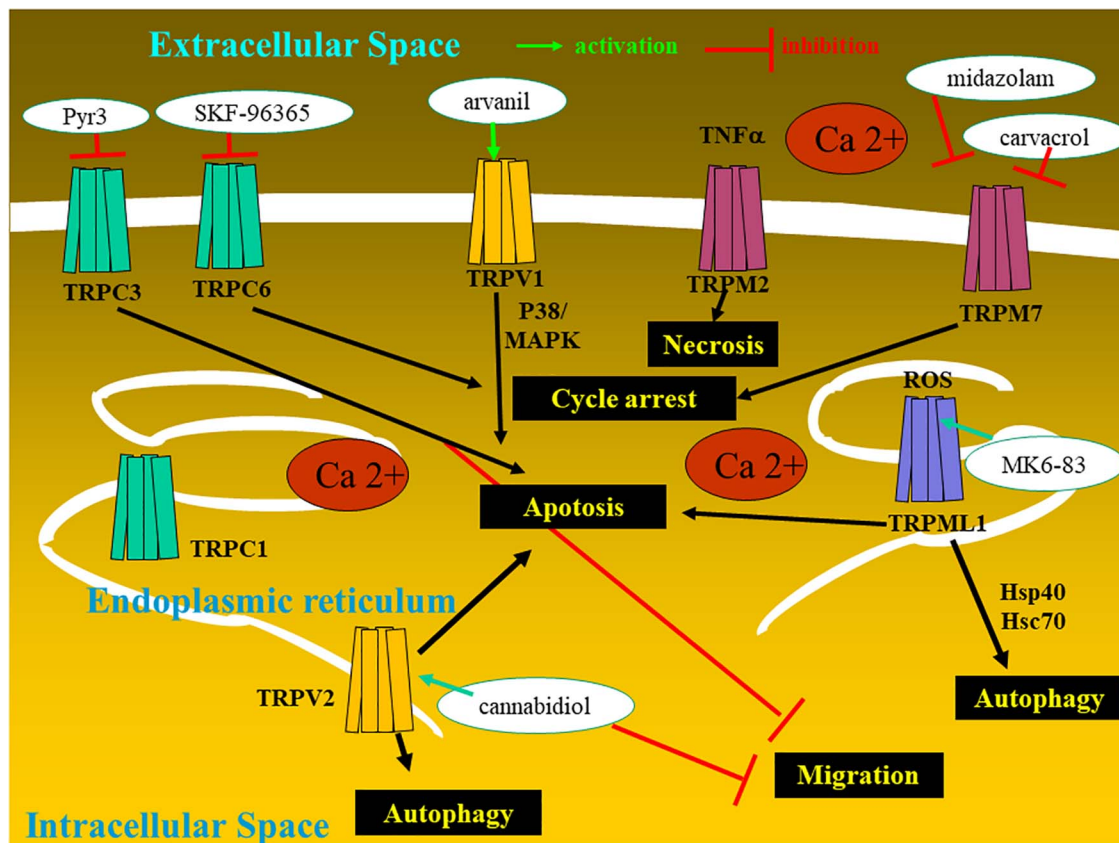


FIGURE 1 | Glioma cell with the expression of transient receptor potential (TRP) ion channels and the therapeutic potentialities.

NOMPC) (Montell et al., 2002; Li, 2017; **Table 1**). All TRP channels contain six transmembrane segments and a pore-forming loop between the 5th and 6th segments (Nilius and Owsianik, 2011). As TRPs are non-selective cation channels, their effects can be attributed to K⁺ and Na⁺ flux, but the role of Ca²⁺ is the most studied. TRP channels are non-selective Ca²⁺-permeable cation channels, with the exception of TRPM4 and TRPM5, which are Ca²⁺-impermeable. Some hallmarks of cancer pathophysiology are associated with the dysregulation of multiple downstream Ca²⁺-homeostasis-related effectors, a fact that explains why TRP channels are actually involved in the regulation versus dysregulation of growth, proliferation, migration, and invasion of cancer cells, including melanoma; prostate, breast, kidney, and bladder carcinomas; and gliomas (Bodding, 2007; Prevarskaya et al., 2007; Gkika and Prevarskaya, 2009; Chen et al., 2014; Bernardini et al., 2015; Santoni et al., 2020a,b; Yang and Kim, 2020).

Transient Receptor Potential Ion Channels in Malignant Glioma Cell Death

Among the TRP channels already identified in glioma cells with demonstrated regulatory effects on migration, proliferation, and apoptosis, let us cite TRPC1, TRPC3, TRPC6, TRPV1, TRPV2, TRPM1 and 2, TRPM2, TRPM7, and TRPM8

(Alptekin et al., 2015; Morelli et al., 2016, 2019; Chang et al., 2018; **Figure 1** and **Table 1**).

TRPC Channels

TRPCs relate to the canonical family, which includes seven members that assemble as homo- or heterotetramers (Putney, 2005; Schaefer, 2005). TRPC channels may be activated directly by diacylglycerol (Kress et al., 2008) or indirectly through calcium release from the endoplasmic reticulum following stimulation of the inositol triphosphate receptor (Sours-Brothers et al., 2009). We report below only those TRPC channels for which roles have been evidenced in glioma cell biology.

TRPC1

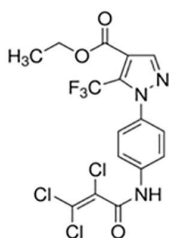
TRPC1 (subfamily C member 1) appears to be important for cytokinesis in cell proliferation and migration (Nesin and Tsiokas, 2014) and angiogenesis. TRPC1-lipid raft complexes are essential for certain stimulus-induced chemotaxis as it is for example the case with epidermal growth factors (Bomben et al., 2011).

Human malignant gliomas contain Ca²⁺-permeable TRPC1 channels as evidenced biophysically by Bomben and Sontheimer (2008), who also showed that multinucleated glioma cells resulting from incomplete cell division during their extensive proliferation result in the functional loss

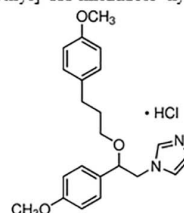
TABLE 1 | TRP ion channels involved in malignant glioma cell death and therapeutic perspectives.

TRP channels		Prognostic marker	Glioma cells <i>in vitro</i>				Experimental glioma <i>in vivo</i>		Potential therapeutic compounds (figure 2)	Clinical data	References
			Proliferation	Cell death	Migration/invasion	Chemo-sensitivity	Growth	Survival			
TRPC	C1	Yes	Decreased (shRNA)	–	–	–	Decreased (shRNA)	–	–	–	Bomben and Sontheimer, 2010
	C3	Yes	Decreased	Apoptosis	Decreased	–	Decreased	–	Pyr3 (antagonist)	–	Chang et al., 2018
	C5	–	–	–	–	–	–	–	Riluzole (agonist) Prednisolone (agonist)	–	Richter et al., 2014; Beckmann et al., 2017
	C6	Yes	–	Cell cycle arrest G2/M	–	–	Decreased	Increased	SKF-96365 (antagonist)	–	Ding et al., 2010; Song et al., 2014
TRPV	V1	Yes	–	Apoptosis endoplasmic reticulum stress	–	–	–	–	Arvanil (agonist)	–	Amantini et al., 2007; Stock et al., 2012
	V2	Yes	Decreased in hGBM cells and in GSCs	Apoptosis autophagy	Decreased	Increased	Decreased	Increased	Cannabidiol (agonist) delta9-THC (agonist)	Phase I (Dall'Stella et al., 2019 and Likar et al., 2019) Phase II trial (mixture of cannabidiol and delta9-THC) (Schultz and Beyer, 2017) Phase I trial (Guzmán et al., 2006; Velasco et al., 2007)	Marcu et al., 2010; Nabissi et al., 2010, 2013, 2015; Torres et al., 2011; Morelli et al., 2012; Ladin et al., 2016; López-Valero et al., 2018; Santoni et al., 2020a,b
TRPML	ML1	Yes	–	Autophagy apoptosis	–	–	–	–	MK6-83 (agonist)	–	Morelli et al., 2019
	ML2	Yes	Decreased (siRNA)	Apoptosis	–	–	–	–	–	–	Morelli et al., 2016
TRPM	M2	Yes	Decreased	Increased (TRPM2 transfection)	Decreased	–	–	–	–	–	Ishii et al., 2007; Bao et al., 2020
	M7	Yes	Decreased (siRNA and antagonist)	–	Decreased (antagonist)	–	–	–	Carvacrol (antagonist) Midazolam (antagonist)	–	Chen et al., 2015, 2016; Leng et al., 2015
	M8	Yes	–	Apoptosis repressed	Stimulated	Radio resistance	–	–	Antibodies	–	Klumpp et al., 2017

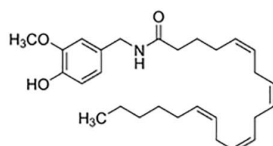
Ethyl-1-(4-2,3,3-trichloroacrylamide)phenyl)-5-(trifluoromethyl)-1H-pyrazole-4-carboxylate, Pyr3



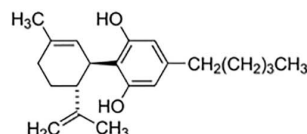
1-[2-(4-Methoxyphenyl)propoxy]ethylimidazole, 1-[β-(3-(4-Methoxyphenyl)propoxy)-4-methoxyphenethyl]-1H-imidazole hydrochloride, SKF-96365



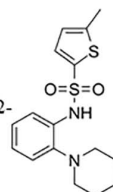
(5Z,8Z,11Z,14Z)-N-[(4-Hydroxy-3-methoxyphenyl)methyl]-5,8,11,14-Eicosatetraenamide, N-Vanillylarachidonamide, Arvanil



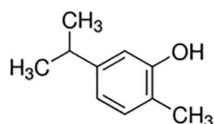
Cannabidiol



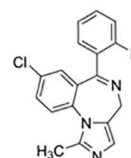
5-Methyl-N-[2-(1-piperidinyl)phenyl]-2-thiophenesulfonamide, MK6-83



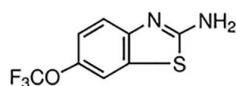
5-Isopropyl-2-methylphenol, Carvacrol



8-Chloro-6-(2-fluorophenyl)-1-methyl-4H-imidazo[1,5-a][1,4]benzodiazepine, Midazolam



2-Amino-6-(trifluoromethoxy)benzothiazole, Riluzole



1,4-Pregnadiene-11β,17α,21-triol-3,20-dione, 1-Dehydrocortisol, 1-Dehydrohydrocortisone, 11β,17α,21-Trihydroxy-1,4-pregnadiene-3,20-dione, Prednisolone

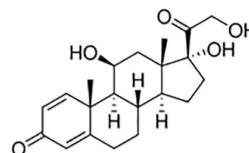


FIGURE 2 | Chemical structures.

of TRPC1 channels regulating calcium signaling during cytokinesis (Bomben and Sontheimer, 2010). These authors also provided *in vivo* evidence that loss of TRPC1 function impairs tumor growth in immunocompromised mice, suggesting that pharmacological inhibition of these channels may slow tumor growth (Bomben and Sontheimer, 2010).

TRPC3

TRPC3 levels are associated with both diagnostic and prognostic values: high-grade gliomas have higher TRPC3 expression levels than normal brain tissues, and glioma patients with high TRPC3

expression have a shorter survival time than patients with a lower TRPC3 expression (Chang et al., 2018). Reduced proliferation was demonstrated *in vitro* in U87MG glioma cells with a reduced expression of TRPC3 (Chang et al., 2018). Chang et al. (2018) showed, accordingly, that glioblastoma cell proliferation was decreased by ethyl-1-(4-2,3,3-trichloroacrylamide)phenyl)-5-(trifluoromethyl)-1H-pyrazole-4-carboxylate (Pyr3), a selective TRPC3 channel blocker (Figure 2). This compound induced caspase-dependent apoptosis and mitochondrial membrane potential imbalance in two glioblastoma cell lines as well as inhibition of migration and invasion *in vitro*; in a

xenograft animal model *in vivo*, this compound in combination with temozolomide inhibited glioblastoma tumor growth (Chang et al., 2018).

TRPC6

Not only is the TRPC6 channel overexpressed in human glioma cells at both the protein and mRNA levels, as compared to normal glial cells (Chigurupati et al., 2010), but also TRPC6 expression relates to the grade of glioma (Ding et al., 2010). Hypoxia increases Notch 1 activation, which in turn induces the expression of TRPC6 in primary samples and cell lines derived from glioblastoma (Chigurupati et al., 2010). Under hypoxia, TRPC6 channels also control *in vitro* hydroxylation and stability of hypoxia inducible factor-1 alpha in human glioma cells (Li et al., 2015). Impairing TRPC6 activity *in vitro* in human glioma cells induced cell cycle arrest at the G2/M phase and, *in vivo*, reduced human xenograft growth in immunocompromised mice, while increasing the survival of the xenografted mice (Ding et al., 2010).

TRPV Channels

TRPV1 is the prototype of the TRPV channel family, which includes six members; it is activated by heat and synthetic or endogenous vanilloids (Caterina et al., 1997). TRPV2 shares approximately 50% sequence identity with TRPV1, while showing distinct cellular functions from those mediated by TRPV1 (Cohen et al., 2015). TRPV1 expression is mainly localized to the plasma membrane, while TRPV2 is localized to the intracellular membranes under unstimulated conditions (Cohen et al., 2013). TRPV2 is not stimulated by heat or by vanilloid exposure (Cohen et al., 2013 and 2015). TRPV2 activity is induced by 2-aminoethoxydiphenyl borate, probenecid, and cannabidiol and inhibited by ruthenium red, gadolinium, and tranilast (Caterina et al., 1997; Bang et al., 2007; Perálvarez-Marín et al., 2013; Nabissi et al., 2015). The translocation of TRPV2 from the endosome to the plasma membrane, a feature that influences both cell proliferation and cell death, is stimulated for example by growth factors, cytokines, hormones, and endocannabinoids (Liberati et al., 2014a,b). Uncontrolled cell proliferation and apoptotic resistance occur with loss or changes in TRPV2-mediated signals, whereas TRPV2 activation stimulates both the migration and the invasiveness of cancer cells (Liberati et al., 2014a,b).

The scientific literature reports the implications of TRPV1 and TRPV2 in glioma cell biology, as described below.

TRPV1

TRPV1 is mainly expressed by primary sensory neurons involved in nociception and neurogenic inflammation (Caterina et al., 2000).

TRPV1 gene and protein expressions are progressively lost, while the level of malignancy increases in gliomas, with a marked loss of TRPV1 expression in almost all (93%) of the glioblastomas analyzed by Amantini et al. (2007). Moreover, TRPV1 mRNA expression was correlated with patients' overall survival (OS). TRPV1 variant 3 mRNA expression reached significance ($p = 0.0009$) for survival with short OS glioblastoma patients, showing a lower TRPV1 variant 3 mRNA expression

compared with long OS patients (Nabissi et al., 2016). TRPV1 is implicated in the capsaicin-induced p38 mitogen-activated protein kinase-dependent apoptosis of glioma cells *in vitro* (Amantini et al., 2007). TRPV1 stimulation also triggers tumor cell death via the activating transcription factor-3 (ATF3)-controlled branch of the endoplasmic reticulum stress pathway.

Somatic mutant neural stem and precursor cells (NPCs) are thought to be the source of high-grade astrocytomas which are much more frequent in adults than in children. Stock et al. (2012) have shown that high-grade astrocytoma-associated NPCs induce tumor cell death via the release of endovanilloids, which induce Ca^{2+} responses. Endovanilloids directly stimulate the vanilloid receptor TRPV1 (Toth et al., 2009). However, the anti-tumorigenic response of NPCs is lost with age. Stock et al. (2012) report that NPC-mediated tumor suppression can be mimicked in the adult brain by systemic administration of the synthetic brain barrier-permeable vanilloid Arvanil (Figure 2), suggesting that TRPV1 agonists hold potential as new high-grade glioma therapeutics.

TRPV2

TRPV2 expression decreases during glioma progression to higher clinical stages; TRPV2 negatively controls glioma cell survival and proliferation and protects cells from Fas-induced apoptosis in an ERK-dependent manner (Nabissi et al., 2010). This receptor also negatively controls resistance to carmustine (BCNU)-induced apoptosis (Nabissi et al., 2010). High glioblastoma resistance to standard chemotherapy is one of the major hallmarks of glioblastoma biological aggressiveness. The TRPV2 agonist cannabidiol, by increasing TRPV2 expression and activity by triggering TRPV2-dependent Ca^{2+} influx, increases chemotherapeutic drug uptake and synergizes with cytotoxic agents (doxorubicin, temozolomide, and BCNU) to induce *in vitro* apoptosis in glioma cells but not in normal human astrocytes (Nabissi et al., 2013). TRPV2 activation promotes differentiation and inhibits the proliferation of glioblastoma stem cells (GSCs) *in vitro* and *in vivo* (Morelli et al., 2012). Redifferentiating cancer stem cell subpopulations could be achieved while using drug-induced differentiation, knowing that cancer stem cells are radio- and chemoresistant. Stimulating TRPV2 cannabidiol triggers GSC differentiation by inducing autophagy and inhibiting GSC proliferation and clonogenicity. Moreover, the cannabidiol and BCNU combination overcame GCS resistance to BCNU treatment by inducing apoptosis (Nabissi et al., 2015). In glioblastoma, TRPV2 is part of an interactome-based signature complex (Doñate-Macián et al., 2018), which is negatively associated with patient survival, and it is expressed in high risk of recurrence and temozolomide-resistant patients (Santoni et al., 2020a).

TRPML Channels

Endosome/lysosome Ca^{2+} channel proteins are characteristic of the TRPML channel family. In mammals, there are three TRPML proteins (TRPML-1, TRPML-2, and TRPML-3). A link between TRPML channel physiology and tumor biology has been suggested, and we focus here on glioma biology.

TRPML1

TRPML1, which is primarily localized in the late endosome/lysosome, is ubiquitously expressed in mammalian cells. It plays roles in the control of cell viability and in chaperone-mediated autophagy (Venkatachalam et al., 2006). A mutated TRPML1 gene in humans causes a neurodegenerative disease in children, i.e., mucopolipidosis type IV (Bargal et al., 2000). TRPML1 is a proton-impermeable, cation-selective channel with permeability to both Ca^{2+} and Fe^{2+} . Chaperone-mediated autophagy-related proteins [for example the heat shock cognate protein Hsc70 and the 40-kDa heat shock protein (Hsp40)] interact with the large TRPML1 intraluminal loop (Venkatachalam et al., 2006).

Morelli et al. (2019) showed that the loss/reduction of TRPML1 mRNA expression strongly correlates with short survival in glioblastoma patients. This feature could be explained, at least partly, by the fact that TRPML1 targets the apoptosis-like gene 2 (ALG-2) gene whose protein promotes caspase-3-independent cell death associated with glioblastoma progression and poor prognosis (Vergarajauregui et al., 2009; Zhang et al., 2017). Morelli et al. (2019) have also conducted elegant experiments with various glioma cell types to demonstrate that TRPML1 is an oxidative stress sensor that activates irreversible autophagy leading to cell death.

TRPML2

While TRPML2 is found in normal astrocytes and neural stem/progenitor cells, its expression at both mRNA and protein levels dramatically augment (Morelli et al., 2016) in high-grade glioblastoma cell lines of astrocytic origin and glioblastoma tissues (Morelli et al., 2016). Morelli et al. (2016) experimentally demonstrated that cell viability and proliferation are inhibited in TRPML2 knockdown glioblastoma cells, while caspase-3-dependent apoptosis is increased.

TRPM Channels

The TRPM subfamily is composed of eight members consisting of four six-transmembrane domain subunits, resulting in homomeric or heteromeric channels. TRPM subfamily members have been involved in several physiological functions and pathophysiological human processes.

TRPM2

Oxidative stress and tumor necrosis factor alpha are two extracellular signals known to activate TRPM2 channels, with consequently the activation of necrotic cell death (Zhang et al., 2006). Ishii et al. (2007) showed that the insertion of TRPM2 channels by means of transfection into the malignant glioma cell line A172 enhanced cell death induced by H_2O_2 . In a recent study, Bao et al. (2020) observed a significant increase in TRPM2-AS, a long non-coding RNA with a length greater than 200 base pairs, which is transcribed from the antisense chain of TRPM2, in 111 glioma patients with glioma as compared to the normal control group. Overexpressing TRPM2-AS in human glioblastoma cells increases their proliferation, migration, and invasion, while downregulation of TRPM2-AS inhibits these three processes (Bao et al., 2020). TRPM2-AS signaling in glioma

cells involves c-Jun N-terminal kinase (JNK), c-Jun protein, and regulator of G-protein signaling 4 (RGS4) (Bao et al., 2020).

TRPM7

A large number of breast, lung, pancreatic, prostate, gastric, and head and neck cancers and malignant gliomas express high TRPM7 levels (Jiang et al., 2007; Kim et al., 2008; Guilbert et al., 2009; Rybarczyk et al., 2012; Sun et al., 2014; Alptekin et al., 2015; Chen et al., 2016). For example, malignant glioma tissues express higher TRPM7 mRNA than normal brain tissues (Chen et al., 2016; Wan et al., 2020). TRPM7 silencing reduced glioma cell growth by inhibiting cell entry into S and G2/M phases and promoting cell apoptosis (Wan et al., 2020). TRPM7 expression in glioblastoma cells was found to be positively correlated with Notch1 signaling activity and CD133 and ALDH1 expression; briefly, downregulation of TRPM7 by siTRPM7 decreased Notch1 signaling whereas upregulation of TRPM7 increased Notch1 signaling (Wan et al., 2020).

Carvacrol (Figure 2) is one of the several inhibitors of TRPM7 already identified (Parnas et al., 2009). This compound is a secondary metabolite (a monoterpenoid phenol) found in oregano essential oils from numerous genera (Baser, 2008). Suppression of TRPM7 activity through the use of carvacrol and the use of TRPM7-siRNA dramatically reduced the proliferation, migration, and invasion levels of the U87MG malignant glioma cell line, which expresses higher levels of TRPM7 mRNA and protein than normal human astrocytes (Chen et al., 2015; Leng et al., 2015). MGR2 glioma cells also express TRPM7 and display TRPM7 currents (Chen et al., 2016). Chen et al. (2016) identified a widely used anesthetic compound in clinics since the 1970s, i.e., midazolam (Figure 2), as a TRPM7 inhibitor. The use of midazolam for *in vitro* treatment periods as short as seconds on glioma cells suppressed TRPM7 currents and calcium influx, while treatment for 48 h vanished TRPM7 expression (Chen et al., 2016). The inhibitory effect of midazolam on TRPM7 currents results in a decrease in proliferation and G0/G1 phase cell cycle arrest in two human glioblastoma cell lines (Chen et al., 2016). Of note, midazolam is a short-acting benzodiazepine that crosses the blood-brain barrier with a favorable pharmacological profile, and it could be used at first glance to treat patients with malignant glioma if one considers TRPM7 as a valuable target. However, the concentration (100 μM) of midazolam used *in vitro* in the study reported by Chen et al. (2016) is much higher than the clinical concentration ranges reported for this compound. It must indeed be emphasized that midazolam used at high doses induces sedative and hypnotic effects and therefore precludes its use as a chronic treatment for malignant glioma patients (Olkola and Ahonen, 2008). Novel derivatives of midazolam or medical devices for its local delivery should be developed if it is to be used for glioma chemotherapy.

TRPM8

TRPM8 was first identified in prostate carcinoma (Tsavaler et al., 2001) and then in a number of other cancer types (Liu et al., 2014; Yee et al., 2014; Yu et al., 2014); it has been more recently shown to be upregulated in glioblastoma compared to normal brain tissue (Alptekin et al., 2015; Zeng et al., 2019),

while TRPM8 expression is highly heterogeneous in human glioblastoma specimens as well as in established cell lines (Klumpp et al., 2017). Zeng et al. (2019) showed that high expression of TRPM8 mRNA was associated with a shorter OS time in patients with glioblastoma. TRPM8 channels facilitate Ca^{2+} entry in glioblastoma cells, and their activation has been shown to stimulate large-conductance K^{+} channel activity and, consequently, glioblastoma cell migration (Wondergem et al., 2008; Wondergem and Bartley, 2009; Klumpp et al., 2017). *In vitro*, using the U251 human glioblastoma cell line, Zeng et al. (2019) showed that TRPM8 enhances the sensitivity of glioblastoma cells to apoptosis and regulates the proliferation and invasion abilities. Klumpp et al. (2017) showed *in vitro* using human glioblastoma cells that (i) TRPM8 signaling is involved in cell cycle regulation and represses apoptotic cell death; (ii) clinically compatible ionizing radiation doses for treating glioblastoma patients induce upregulation of TRPM8 function; and (iii) elevated TRPM8 function, in turn, confers radioresistance (Klumpp et al., 2017). A combination of TRPM8 targeting and radiotherapy could be an interesting approach for future glioblastoma therapy. As developed in the next section, some strategies to target TRPM8 have already been developed and/or are ongoing.

THERAPEUTIC PERSPECTIVES

As summarized above, TRP channels exert various roles in cancer cell biology, including glioma ones (Gaunt et al., 2016; He and Ma, 2016; Jardin and Rosado, 2016; Li and Ding, 2017; Zhan and Shi, 2017). A number of more or less specific compounds from synthetic versus natural origin that selectively target different subtypes of TRP channels have been discovered, including some preclinical candidates (Wang et al., 2020). We recall these promising compounds below.

Some reasonably specific pharmacological TRPM8 inhibitors are already available (Ohmi et al., 2014; Lehto et al., 2015), including antibodies binding the extracellular TRPM8 protein and inhibiting TRPM8 function (Miller et al., 2014). However, the available studies have been performed *in vitro* only, and preclinical studies in orthotopic glioblastoma animal models are still missing. There is still a long road ahead until these types of compounds will enter clinics for treating malignant glioma patients.

Riluzole (Figure 2) is a TRPC5 agonist; however, it can also act on other ion channels so this limits its use. Riluzole is an approved drug for the treatment of amyotrophic lateral sclerosis, and it entered clinical trials for melanoma therapy. The precise mechanism(s) of action of riluzole is not yet fully deciphered. The riluzole-induced activation of TRPC5 channels, while expressed heterologously (as in HEK293 Human Embryonic Kidney cells) or endogenously (as in U87MG glioblastoma cells), seems to be independent of various cytosolic components, such as phospholipase C activity or intracellular calcium stores, suggesting therefore that riluzole could have a rather direct effect on TRPC5 (Richter et al., 2014). Furthermore, prednisolone (Figure 2), largely used in the context of glioma treatment

to decrease glioblastoma-associated edema, also acts as a weak activator of TRPC5 (Beckmann et al., 2017). As emphasized above for TRPM8, there is still a long road before these types of compounds targeting TRPC5 will enter clinics to treat malignant glioma patients.

SKF-96365 (Figure 2), a non-specific TRPC6 and TRPC7 antagonist, displays cytotoxic effects in several cancer cell types (Song et al., 2014). In glioblastoma cells, SKF-96365 exerts anti-growth effects through the promotion of the reverse mode of $\text{Na}^{+}/\text{Ca}^{2+}$ exchangers, thereby increasing Ca^{2+} (Song et al., 2014). This compound does not seem very appropriate, at least in our current knowledge of its mode of action, to be an actual candidate to combat glioblastoma in clinical situations.

Cannabinoids: New Application for Old Agents

In contrast to the compounds we refer to above, certain cannabinoids could be of major importance to combat glioblastoma in clinical situations and a TRP context as explained hereafter. The term cannabinoids originally described bioactive constituents of the plant *Cannabis sativa*, used traditionally for their medicinal purpose as well as their recreational properties. Cannabinoids can reduce glioma growth both *in vitro* and *in vivo* (Velasco et al., 2007; Sarfaraz et al., 2008). Among the cannabinoid compounds, we emphasize the potential of cannabidiol (Figure 2) to combat glioblastoma in clinical situations for the reasons we explained here below. Cannabidiol is a cannabinoid that lacks unwanted psychotropic liability and has no significant agonist activity on cannabinoid receptors (Howlett et al., 2002; Pertwee et al., 2005). Cannabidiol has been investigated as an antitumoral agent in a number of studies (Dumitru et al., 2018 for review).

In vitro, cannabidiol inhibits migration (Vaccani et al., 2005) and induces apoptosis in human glioma cells (Massi et al., 2004, 2006; Solinas et al., 2013), while it increases chemotherapeutic drug uptake and parallelly potentiates the cytotoxic activity of chemotherapeutic agents in a TRPV2-dependent manner in human glioma cells (Nabissi et al., 2013). *In vitro*, cannabidiol enhances the inhibitory effects of cannabinoid 1 and cannabinoid 2 receptor agonist delta(9)-tetrahydrocannabinol (Δ^9 -THC) on human glioblastoma cell survival and proliferation (Marcu et al., 2010). The combination of cannabidiol with Δ^9 -THC and temozolomide reduces the growth of U87MG glioma xenografts (Torres et al., 2011). Cannabidiol may also be effective at reducing the proliferation of GSC chemoresistant subpopulations present in glioblastomas (Singh et al., 2004). In glioma xenografts, including those derived from glioma stem cells, López-Valero et al. (2018) showed that a combined therapy of oral cannabinoids and temozolomide synergistically reduced the growth and enhanced the survival of xenografted animals. Cannabidiol, by activating TRPV2, (i) triggers GSC differentiation, (ii) activates their autophagic processes, (iii) inhibits glioma stem cell proliferation, (iv) inhibits their clonogenic capability, and (v) abrogates their resistance to carmustine (BCNU) (Nabissi et al., 2015).

A pilot phase I clinical trial for the treatment of glioblastoma patients indicated a good safety profile for Δ^9 -THC, which is a psychoactive cannabinoid (Velasco et al., 2007). The intratumoral administration of this compound was first tested in a small series of nine patients (Guzmán et al., 2006). Preclinical studies have also investigated the antitumor effects of the cannabinoid combination (Δ^9 -THC and cannabidiol) and found an enhanced antineoplastic effect (Ladin et al., 2016) in combination with temozolomide or radiotherapy (Torres et al., 2011; Scott et al., 2014; Ladin et al., 2016).

A placebo-controlled phase II clinical trial investigated a tetrahydrocannabinol–cannabidiol mixture in combination with dose-intensive temozolomide in glioblastoma (NCT01812603) (Schultz and Beyer, 2017). This study included 21 adult glioblastoma patients receiving a maximum of 12 sprays orally per day, delivering 100 μ l of a solution containing 27 mg/ml Δ^9 -THC and 25 mg/ml cannabidiol. The control group received temozolomide and only reached a 44% 1-year survival rate. In sharp contrast, the tetrahydrocannabinol–cannabidiol mixture plus temozolomide group showed an 83% 1-year survival rate, with a median survival of over 662 days compared with 369 days in the control group (Schultz and Beyer, 2017; Schultz, 2018). In another study, nine consecutive patients with brain tumors received cannabidiol at a daily dose of 400 mg concomitantly to the standard therapeutic procedure of maximal resection followed by combined radio- and chemotherapy and adjuvant chemotherapy (Likar et al., 2019). The authors reported that, by the time of the submission of their article, all but one patient were still alive, with a mean survival time of 22.3 months

(range from 7 to 47). Importantly, the well-acknowledged median survival for glioblastoma patients is 16 months, as reported in the reference study by Stupp et al. (2009). A recent case report study demonstrated satisfactory clinical and imaging responses for two patients with a confirmed diagnosis of high-grade glioma (grades III or IV), benefiting after surgery from chemoradiation followed by the combination of procarbazine, lomustine, and vincristine associated with cannabidiol (Dall’Stella et al., 2019).

CONCLUSION

Multiple ion channels rely on intracellular Ca^{2+} , and it makes sense to target a common Ca^{2+} source, such as specific TRP channels, which are heavily involved in glioma cell biology.

We are only at the beginning of our understanding of the precise roles of various TRP channels in glioma cell biology, and further studies are required to truly understand the physiopathological roles of TRP channels in glioma progression. However, some promising data from the literature, even if still scarce, already point to the very high promise of targeting TRPV2 by means of cannabidiol, a cannabinoid that lacks unwanted psychotropic liability.

AUTHOR CONTRIBUTIONS

The author confirms being the sole contributor of this work and has approved it for publication.

REFERENCES

- Alexander, S. P. H., Mathie, A., Peters, J. A., Veale, E. L., Striessnig, J., Kelly, E., et al. (2019). The concise guide to pharmacology 2019/20: ion channels. *Br. J. Pharmacol.* 176(Suppl. 1), S142–S228. doi: 10.1111/bph.14749
- Alptekin, M., Eroglu, S., Tutar, E., Sencan, S., Geyik, M. A., Ulasli, M., et al. (2015). Gene expressions of TRP channels in glioblastoma multiforme and relation with survival. *Tumour. Biol.* 36, 9209–9213. doi: 10.1007/s13277-015-3577-x
- Amantini, C., Mosca, M., Nabissi, M., Lucciarini, R., Caprodossi, S., Arcella, A., et al. (2007). Capsaicin-induced apoptosis of glioma cells is mediated by TRPV1 vanilloid receptor and requires p38 MAPK activation. *J. Neurochem.* 102, 977–990. doi: 10.1111/j.1471-4159.2007.04582.x
- Bang, S., Kim, K. Y., Yoo, S., Lee, S. H., and Hwang, S. W. (2007). Transient receptor potential V2 expressed in sensory neurons is activated by probenecid. *Neurosci. Lett.* 425, 120–125. doi: 10.1016/j.neulet.2007.08.035
- Bao, M. H., Lv, Q. L., Szeto, V., Wong, R., Zhu, S. Z., Zhang, Y. Y., et al. (2020). TRPM2-AS inhibits the growth, migration, and invasion of gliomas through JNK, c-Jun, and RGS4. *J. Cell Physiol.* 235, 4594–4604. doi: 10.1002/jcp.29336
- Bargal, R., Avidan, N., Ben-Asher, E., Olender, Z., Zeigler, M., Frumkin, A., et al. (2000). Identification of the gene causing mucopolidosis type IV. *Nat. Genet.* 26, 118–123. doi: 10.1038/79095
- Baser, K. H. (2008). Biological and pharmacological activities of carvacrol and carvacrol bearing essential oils. *Curr. Pharm. Des.* 14, 3106–3119. doi: 10.2174/138161208786404227
- Becchetti, A., Munaron, L., and Arcangeli, A. (2013). The role of ion channels and transporters in cell proliferation and cancer. *Front. Physiol.* 4:312. doi: 10.3389/fphys.2013.00312
- Beckmann, H., Richter, J., Hill, K., Urban, N., Lemoine, H., and Schaefer, M. (2017). A benzothiadiazine derivative and methylprednisolone are novel and selective activators of transient receptor potential canonical 5 (TRPC5) channels. *Cell Calcium* 66, 10–18. doi: 10.1016/j.ceca.2017.05.012
- Bernardini, M., Fiorio Pla, A., Prevorskaya, N., and Gkika, D. (2015). Human transient receptor potential (TRP) channel expression profiling in carcinogenesis. *Int. J. Dev. Biol.* 59, 399–406. doi: 10.1387/ijdb.150232dg
- Bernstock, J. D., Mooney, J. H., Ilyas, A., Chagoya, G., Estevez-Ordóñez, D., Ibrahim, A., et al. (2019). Molecular and cellular intratumoral heterogeneity in primary glioblastoma: clinical and translational implications. *J. Neurosurg.* 23, 1–9. doi: 10.3171/2019.5.JNS19364
- Bodding, M. (2007). TRP proteins and cancer. *Cell Signal* 19, 617–624. doi: 10.1016/j.cellsig.2006.08.012
- Bomben, V. C., and Sontheimer, H. (2010). Disruption of transient receptor potential canonical channel 1 causes incomplete cytokinesis and slows the growth of human malignant gliomas. *Glia* 58, 1145–1156. doi: 10.1002/glia.20994
- Bomben, V. C., and Sontheimer, H. W. (2008). Inhibition of transient receptor potential canonical channels impairs cytokinesis in human malignant gliomas. *Cell Prolif.* 41, 98–121. doi: 10.1111/j.1365-2184.2007.00504.x
- Bomben, V. C., Turner, K. L., Barclay, T. T. C., and Sontheimer, H. (2011). Transient receptor potential canonical channels are essential for chemotactic migration of human malignant gliomas. *J. Cell Physiol.* 226, 1879–1888. doi: 10.1002/jcp.22518
- Caterina, M. J., Leffler, A., Malmberg, A. B., Martin, W. J., Trafton, J., Petersen-Zeit, K. R., et al. (2000). Impaired nociception and pain sensation in mice lacking the capsaicin receptor. *Science* 288, 306–313. doi: 10.1126/science.288.5464.306
- Caterina, M. J., Schumacher, M. A., Tominaga, M., Rosen, T. A., Levine, J. D., and Julius, D. (1997). The capsaicin receptor: a heat-activated ion channel in the pain pathway. *Nature* 389, 816–824. doi: 10.1038/39807

- Chang, H. H., Cheng, Y. C., Tsai, W. C., Tsai, M. J., and Chen, Y. (2018). Pyr3 induces apoptosis and inhibits migration in human glioblastoma cells. *Cell Physiol. Biochem.* 48, 1694–1702. doi: 10.1159/000492293
- Chen, J., Dou, Y., Zheng, X., Leng, T., Lu, X., Ouyang, Y., et al. (2016). TRPM7 channel inhibition mediates midazolam-induced proliferation loss in human malignant glioma. *Tumour. Biol.* 37, 14721–14731. doi: 10.1007/s13277-016-5317-2
- Chen, J., Luan, Y., Yu, R., Zhang, Z., Zhang, J., and Wang, W. (2014). Transient receptor potential (TRP) channels, promising potential diagnostic and therapeutic tools for cancer. *Biosci. Trends* 8, 1–10. doi: 10.5582/bst.8.1
- Chen, W. L., Barszczyk, A., Turlova, E., Deurloo, M., Liu, B., Yang, B. B., et al. (2015). Inhibition of TRPM7 by carvacrol suppresses glioblastoma cell proliferation, migration and invasion. *Oncotarget* 6, 16321–16340. doi: 10.18632/oncotarget.3872
- Chigurupati, S., Venkataraman, R., Barrera, D., Naganathan, A., Madan, M., Paul, L., et al. (2010). Receptor channel TRPC6 is a key mediator of Notch-driven glioblastoma growth and invasiveness. *Cancer Res.* 70, 418–427. doi: 10.1158/0008-5472.CAN-09-2654
- Cohen, M. R., Huynh, K. W., Cawley, D., and Moiseenkova-Bell, V. Y. (2013). Understanding the cellular function of TRPV2 channel through generation of specific monoclonal antibodies. *PLoS One* 8:e85392. doi: 10.1371/journal.pone.0085392
- Cohen, M. R., Johnson, W. M., Pilat, J. M., Kiselar, J., DeFrancesco-Lisowitz, A., Zigmund, R. E., et al. (2015). Nerve Growth factor regulates transient receptor potential vanilloid 2 via extracellular signal-regulated kinase signaling to enhance neurite outgrowth in developing neurons. *Mol. Cell Biol.* 35, 4238–4252. doi: 10.1128/MCB.00549-15
- Colwell, N., Larion, M., Giles, A. J., Seldomridge, A. N., Sizdahkhani, S., Gilbert, M. R., et al. (2017). Hypoxia in the glioblastoma microenvironment: shaping the phenotype of cancer stem-like cells. *Neuro. Oncol.* 19, 887–896. doi: 10.1093/neuonc/now258
- Dall' Stella, P. B., Docema, M. F. L., Maldaun, M. V. C., Feher, O., and Lancellotti, C. L. P. (2019). Case report: clinical outcome and image response of two patients with secondary high-grade glioma treated with chemoradiation, PCV, and cannabidiol. *Front. Oncol.* 8:643. doi: 10.3389/fonc.2018.00643
- Ding, X., He, Z., Zhou, K., Cheng, J., Yao, H., Lu, D., et al. (2010). Essential role of trpc6 channels in G2/M phase transition and development of human glioma. *J. Natl. Cancer Inst.* 102, 1052–1068. doi: 10.1093/jnci/djq217
- Doñate-Macián, P., Gómez, A., Dégano, I. R., and Perálvarez-Marín, A. A. (2018). TRPV2 interactome-based signature for prognosis in glioblastoma patients. *Oncotarget* 9, 18400–18409. doi: 10.18632/oncotarget.24843
- Dumitru, C. A., Sandalcioğlu, I. E., and Karsak, M. (2018). Cannabinoids in glioblastoma therapy: new applications for old drugs. *Front. Mol. Neurosci.* 11:159. doi: 10.3389/fnmol.2018.00159
- Ernst, N. J., Habela, C. W., and Sontheimer, H. (2008). Cytoplasmic condensation is both necessary and sufficient to induce apoptotic cell death. *J. Cell Sci.* 121(Pt 3), 290–297. doi: 10.1242/jcs.017343
- Galluzzi, L., Vitale, I., Abrams, J. M., Alnemri, E. S., Baehrecke, E. H., Blagosklonny, M. V., et al. (2012). Molecular definitions of cell death subroutines: recommendations of the Nomenclature Committee on Cell Death 2012. *Cell Death Differ.* 19, 107–120. doi: 10.1038/cdd.2011.96
- Gaunt, H. J., Vasudev, N. S., and Beech, D. J. (2016). Transient receptor potential canonical 4 and 5 proteins as targets in cancer therapeutics. *Eur. Biophys. J.* 45, 611–620. doi: 10.1007/s00249-016-1142-1
- Gkika, D., and Prevarskaya, N. (2009). Molecular mechanisms of TRP regulation in tumor growth and metastasis. *Biochim. Biophys. Acta* 1793, 953–958. doi: 10.1016/j.bbamcr.2008.11.010
- Guilbert, A., Gautier, M., Dhennin-Duthille, I., Haren, N., Sevestre, H., and Ouaïd-Ahidouch, H. (2009). Evidence that TRPM7 is required for breast cancer cell proliferation. *Am. J. Physiol. Cell Physiol.* 297, C493–C502. doi: 10.1152/ajpcell.00624.2008
- Guzmán, M., Duarte, M. J., Blázquez, C., Ravina, J., Rosa, M. C., Galve-Roperh, I., et al. (2006). A pilot clinical study of Delta9-tetrahydrocannabinol in patients with recurrent glioblastoma multiforme. *Br. J. Cancer* 95, 197–203. doi: 10.1038/sj.bjc.6603236
- Habela, C. W., Ernest, N. J., Swindall, A. F., and Sontheimer, H. (2009). Chloride accumulation drives volume dynamics underlying cell proliferation and migration. *J. Neurophysiol.* 101, 750–757. doi: 10.1152/jn.90840
- Hanahan, D., and Weinberg, R. A. (2011). Hallmarks of cancer: the next generation. *Cell* 144, 646–674. doi: 10.1016/j.cell.2011.02.013
- He, D. X., and Ma, X. (2016). Transient receptor potential channel C5 in cancer chemoresistance. *Acta Pharmacol. Sin.* 37, 19–24. doi: 10.1038/aps.2015.109
- Howlett, A. C., Barth, F., Bonner, T. I., Cabral, G., Casellas, P., Devane, W. A., et al. (2002). International union of pharmacology. XXVII. Classification of cannabinoid receptors. *Pharmacol. Rev.* 54, 161–202. doi: 10.1124/pr.54.2.161
- Ishii, M., Oyama, A., Hagiwara, T., Miyazaki, A., Mori, Y., Kiuchi, Y., et al. (2007). Facilitation of H₂O₂-induced A172 human glioblastoma cell death by insertion of oxidative stress-sensitive TRPM2 channels. *Anticancer Res.* 27, 3987–3992.
- Jardin, I., and Rosado, J. A. (2016). STIM and calcium channel complexes in cancer. *Biochim. Biophys. Acta* 1863(6 Pt B), 1418–1426. doi: 10.1016/j.bbamcr.2015.10.003
- Jiang, J., Li, M. H., Inoue, K., Chu, X. P., Seeds, J., and Xiong, Z. G. (2007). Transient receptor potential melastatin 7-like current in human head and neck carcinoma cells: role in cell proliferation. *Cancer Res.* 67, 10929–10938. doi: 10.1158/0008-5472.CAN-07-1121
- Kim, B. J., Park, E. J., Lee, J. H., Jeon, J.-H., Kim, S. J., and So, I. (2008). Suppression of transient receptor potential melastatin 7 channel induces cell death in gastric cancer. *Cancer Sci.* 99, 2502–2509. doi: 10.1111/j.1349-7006.2008.00982.x
- Klumpp, D., Frank, S. C., Klumpp, L., Sezgin, E. C., Eckert, M., Edalat, L., et al. (2017). TRPM8 is required for survival and radioresistance of glioblastoma cells. *Oncotarget* 8, 95896–95913. doi: 10.18632/oncotarget.21436
- Kornienko, A., Mathieu, V., Rastogi, S. K., Lefranc, F., and Kiss, R. (2013). Therapeutic agents triggering nonapoptotic cancer cell death. *J. Med. Chem.* 56, 4823–4839. doi: 10.1021/jm400136m
- Kress, M., Karasek, J., Ferrer-Montiel, A. V., Scherbakov, N., and Haberberger, R. V. (2008). TRPC channels and diacylglycerol dependent calcium signaling in rat sensory neurons. *Histochem. Cell Biol.* 130, 655–667. doi: 10.1007/s00418-008-0477-9
- Ladin, D. A., Soliman, E., Griffin, L., and Van Dross, R. (2016). Preclinical and clinical assessment of cannabinoids as anti-cancer agents. *Front. Pharmacol.* 7:361. doi: 10.3389/fphar.2016.00361
- Lefranc, F., Le Rhun, E., Kiss, R., and Weller, M. (2018). Glioblastoma quo vadis: will migration and invasiveness reemerge as therapeutic targets? *Cancer Treat. Rev.* 68, 145–154. doi: 10.1016/j.ctrv.2018.06.017
- Lefranc, F., Pouleau, H. B., Rynkowski, M., and De Witte, O. (2012). Voltage-dependent K⁺ channels as oncotargets in malignant gliomas. *Oncotarget* 3, 516–517. doi: 10.18632/oncotarget.514
- Lehto, S. G., Weyer, A. D., Zhang, M., Youngblood, B. D., Wang, J., Wang, W., et al. (2015). AMG2850, a potent and selective TRPM8 antagonist, is not effective in rat models of inflammatory mechanical hypersensitivity and neuropathic tactile allodynia. *Naunyn. Schmiedeb. Arch. Pharmacol.* 388, 465–476. doi: 10.1007/s00210-015-1090-9
- Leng, T. D., Li, M. H., Shen, J. F., Liu, M. L., Li, X. B., Sun, H. W., et al. (2015). Suppression of TRPM7 inhibits proliferation, migration, and invasion of malignant human glioma cells. *CNS Neurosci. Ther.* 21, 252–261. doi: 10.1111/cns.12354
- Li, H. (2017). TRP channel classification. *Adv. Exp. Med. Biol.* 976, 1–8. doi: 10.1007/978-94-024-1088-4_1
- Li, S., and Ding, X. (2017). TRPC channels and glioma. *Adv. Exp. Med. Biol.* 976, 157–165. doi: 10.1007/978-94-024-1088-4_14
- Li, S., Wang, J., Wei, Y., Liu, Y., Ding, X., Dong, B., et al. (2015). Crucial role of TRPC6 in maintaining the stability of HIF-1α in glioma cells under hypoxia. *J. Cell Sci.* 128, 3317–3329. doi: 10.1242/jcs.173161
- Liberati, S., Morelli, M. B., Amantini, C., Farfariello, V., Santoni, M., Conti, A., et al. (2014a). Loss of TRPV2 homeostatic control of cell proliferation drives tumor progression. *Cells* 3, 112–128. doi: 10.3390/cells3010112
- Liberati, S., Morelli, M. B., Amantini, C., Santoni, M., Nabissi, M., Cardinali, C., et al. (2014b). Advances in transient receptor potential vanilloid-2 channel expression and function in tumor growth and progression. *Curr. Protein Pept. Sci.* 15, 732–737. doi: 10.2174/138920371566614070415913
- Likar, R., Koestenberger, M., Stultschnig, M., and Nahler, G. (2019). Concomitant treatment of malignant brain tumors with CBD – A case series and review of the literature. *Anticancer Res.* 39, 5797–5801. doi: 10.21873/anticancer.13783
- Litan, A., and Langhans, S. A. (2015). Cancer as a channelopathy: ion channels and pumps in tumor development and progression. *Front. Cell Neurosci.* 9:86. doi: 10.3389/fncel.2015.00086

- Liu, J., Chen, Y., Shuai, S., Ding, D., Li, R., and Luo, R. (2014). TRPM8 promotes aggressiveness of breast cancer cells by regulating EMT via activating AKT/GSK-3 β pathway. *Tumour. Biol.* 35, 8969–8977. doi: 10.1007/s13277-014-2077-8
- Locarno, C. V., Simonelli, M., Carenza, C., Capucetti, A., Stanzani, E., Lorenzi, E., et al. (2020). Role of myeloid cells in the immunosuppressive microenvironment in gliomas. *Immunobiology* 225:151853. doi: 10.1016/j.imbio.2019.10.002
- López-Valero, I., Saiz-Ladera, C., Torres, S., Hernández-Tiedra, S., García-Taboada, E., Rodríguez-Fornés, F., et al. (2018). Targeting glioma initiating cells with a combined therapy of cannabinoids and temozolomide. *Biochem. Pharmacol.* 157, 266–274. doi: 10.1016/j.bcp.2018.09.007
- Marcu, J. P., Christian, R. T., Lau, D., Zielinski, A. J., Horowitz, M. P., Lee, J., et al. (2010). Cannabidiol enhances the inhibitory effects of delta9-tetrahydrocannabinol on human glioblastoma cell proliferation and survival. *Mol. Cancer Ther.* 9, 180–189. doi: 10.1158/1535-7163.MCT-09-0407
- Massi, P., Vaccani, A., Bianchessi, S., Costa, B., Macchi, P., and Parolaro, D. (2006). The non-psychoactive cannabidiol triggers caspase activation and oxidative stress in human glioma cells. *Cell Mol. Life Sci.* 63, 2057–2066. doi: 10.1007/s00018-006-6156-x
- Massi, P., Vaccani, A., Ceruti, S., Colombo, A., Abbracchio, M. P., and Parolaro, D. (2004). Antitumor effects of cannabidiol, a nonpsychoactive cannabinoid, on human glioma cell lines. *J. Pharmacol. Exp. Ther.* 308, 838–845. doi: 10.1124/jpet.103.061002
- Matarredona, E. R., and Pastor, A. M. (2019). Neural stem cells of the subventricular zone as the origin of human glioblastoma stem cells, therapeutic implications. *Front. Oncol.* 9:779. doi: 10.3389/fonc.2019.00779
- McGranahan, T., Therkelsen, K. E., Ahmad, S., and Nagpal, S. (2019). Current state of immunotherapy for treatment of glioblastoma. *Curr. Treat. Options Oncol.* 20:24. doi: 10.1007/s11864-019-0619-4
- Miller, S., Rao, S., Wang, W., Liu, H., Wang, J., and Gavva, N. R. (2014). Antibodies to the extracellular pore loop of TRPM8 act as antagonists of channel activation. *PLoS One* 9:e107151. doi: 10.1371/journal.pone.0107151
- Montell, C., Birnbaumer, L., and Flockerzi, V. (2002). The TRP channels, a remarkably functional family. *Cell* 108, 595–598. doi: 10.1016/s0092-8674(02)00670-0
- Morelli, M. B., Amantini, C., Tomassoni, D., Nabissi, M., Arcella, A., and Santoni, G. (2019). Transient receptor potential mucolipin-1 channels in glioblastoma: role in patient's survival. *Cancers (Basel)* 11:525. doi: 10.3390/cancers11040525
- Morelli, M. B., Nabissi, M., Amantini, C., Farfariello, V., Ricci-Vitiani, L., di Martino, S., et al. (2012). The transient receptor potential vanilloid-2 cation channel impairs glioblastoma stem-like cell proliferation and promotes differentiation. *Int. J. Cancer* 131, E1067–E1077. doi: 10.1002/ijc.27588
- Morelli, M. B., Nabissi, M., Amantini, C., Tomassoni, D., Rossi, F., Cardinali, C., et al. (2016). Overexpression of transient receptor potential mucolipin-2 ion channels in gliomas: role in tumor growth and progression. *Oncotarget* 7, 43654–43668. doi: 10.18632/oncotarget.9661
- Morrone, F. B., Gehring, M. P., and Nicoletti, N. F. (2016). Calcium channels and associated receptors in malignant brain tumor therapy. *Mol. Pharmacol.* 90, 403–409. doi: 10.1124/mol.116.103770
- Nabissi, M., Morelli, M. B., Amantini, C., Farfariello, V., Ricci-Vitiani, L., Caprodossi, S., et al. (2010). TRPV2 channel negatively controls glioma cell proliferation and resistance to Fas-induced apoptosis in ERK-dependent manner. *Carcinogenesis* 31, 794–803. doi: 10.1093/carcin/bgq019
- Nabissi, M., Morelli, M. B., Amantini, C., Liberati, S., Santoni, M., Ricci-Vitiani, L., et al. (2015). Cannabidiol stimulates Aml-1a-dependent glial differentiation and inhibits glioma stem-like cells proliferation by inducing autophagy in a TRPV2-dependent manner. *Int. J. Cancer* 137, 1855–1869. doi: 10.1002/ijc.29573
- Nabissi, M., Morelli, M. B., Arcella, A., Cardinali, C., Santoni, M., Bernardini, G., et al. (2016). Post-transcriptional regulation of 5'-untranslated regions of human transient receptor potential vanilloid type-1 (TRPV-1) channels: role in the survival of glioma patients. *Oncotarget* 7, 81541–81554. doi: 10.18632/oncotarget.13132
- Nabissi, M., Morelli, M. B., Santoni, M., and Santoni, G. (2013). Triggering of the TRPV2 channel by cannabidiol sensitizes glioblastoma cells to cytotoxic chemotherapeutic agents. *Carcinogenesis* 34, 48–57. doi: 10.1093/carcin/bgs328
- Nesin, V., and Tsiokas, L. (2014). TRPC1. *Handb. Exp. Pharmacol.* 222, 15–51. doi: 10.1007/978-3-642-54215-2_2
- Nilius, B., and Owsianik, G. (2011). The transient receptor potential family of ion channels. *Genome Biol.* 12:218. doi: 10.1186/gb-2011-12-3-218
- Ohmi, M., Shishido, Y., Inoue, T., Ando, K., Fujiuchi, A., Yamada, A., et al. (2014). Identification of a novel 2-pyridyl-benzensulfonamide derivative, RQ-00203078, as a selective and orally active TRPM8 antagonist. *Bioorg. Med. Chem. Lett.* 24, 5364–5368. doi: 10.1016/j.bmcl.2014.10.074
- Olkkola, K. T., and Ahonen, J. (2008). Midazolam and other benzodiazepines. *Handb. Exp. Pharmacol.* 182, 335–360. doi: 10.1007/978-3-540-74806-9_16
- Ostrom, Q. T., Gittleman, H., Liao, P., Vecchione-Koval, T., Wolinsky, Y., Kruchko, C., et al. (2017). CBTRUS Statistical Report: Primary brain and other central nervous system tumors diagnosed in the United States in 2010–2014. *Neuro Oncol.* 19(Suppl. 5), v1–v88. doi: 10.1093/neuonc/nox158
- Parnas, M., Peters, M., Dadon, D., Lev, S., Vertkin, I., Slutsky, I., et al. (2009). Carvacrol is a novel inhibitor of Drosophila TRPL and mammalian TRPM7 channels. *Cell Calcium* 45, 300–309. doi: 10.1016/j.ceca.2008.11.009
- Parsons, D. W., Jones, S., Zhang, X., Lin, J. C., Leary, R. J., Angenendt, P., et al. (2008). An integrated genomic analysis of human glioblastoma multiforme. *Science* 321, 1807–1812. doi: 10.1126/science.1164382
- Patel, A. P., Tirosh, I., Trombetta, J. J., Shalek, A. K., Gillespie, S. M., Wakimoto, H., et al. (2014). Single-cell RNA-seq highlights intratumoral heterogeneity in primary glioblastoma. *Science* 344, 1396–1401. doi: 10.1126/science.1254257
- Perálvarez-Marín, A., Doñate-Macian, P., and Gaudet, R. (2013). What do we know about the transient receptor potential vanilloid 2 (TRPV2) ion channel? *FEBS J.* 280, 5471–5487. doi: 10.1111/febs.12302
- Pertwee, R. G., Thomas, A., Stevenson, L. A., Maor, Y., and Mechoulam, R. (2005). Evidence that (-)-7-hydroxy-4'-dimethylheptyl-cannabidiol activates a non-CB(1), non-CB(2), non-TRPV1 target in the mouse vas deferens. *Neuropharmacology* 48, 1139–1146. doi: 10.1016/j.neuropharm.2005.01.010
- Prevarskaya, N., Skryma, R., and Shuba, Y. (2018). Ion channels in cancer: are cancer hallmarks oncochannelopathies? *Physiol. Rev.* 98, 559–621. doi: 10.1152/physrev.00044.2016
- Prevarskaya, N., Zhang, L., and Barritt, G. (2007). TRP channels in cancer. *Biochim. Biophys. Acta* 1772, 937–946. doi: 10.1016/j.bbadis.2007.05.006
- Putney, J. W. (2005). Physiological mechanisms of TRPC activation. *Pflugers Arch.* 451, 29–34. doi: 10.1007/s00424-005-1416-4
- Ramsey, I. S., Delling, M., and Clapham, D. E. (2006). An introduction to TRP channels. *Annu. Rev. Physiol.* 68, 619–647. doi: 10.1146/annurev.physiol.68.040204.100431
- Ransom, C. B., O'Neal, J. T., and Sontheimer, H. (2001). Volume-activated chloride currents contribute to the resting conductance and invasive migration of human glioma cells. *J. Neurosci.* 21, 7674–7683. doi: 10.1523/JNEUROSCI.21-19-07674
- Richter, J. M., Schaefer, M., and Hill, K. (2014). Riluzole activates TRPC5 channels independently of PLC activity. *Br. J. Pharmacol.* 171, 158–170. doi: 10.1111/bph.12436
- Rybarczyk, P., Gautier, M., Hague, F., Dhennin-Duthille, I., Chatelain, D., Kerr-Conte, J., et al. (2012). Transient receptor potential melastatin-related 7 channel is overexpressed in human pancreatic ductal adenocarcinomas and regulates human pancreatic cancer cell migration. *Int. J. Cancer* 131, E851–E861. doi: 10.1002/ijc.27487
- Santoni, G., Amantini, C., Maggi, F., Marinelli, O., Santoni, M., Nabissi, M., et al. (2020a). The TRPV2 cation channels: from urothelial cancer invasiveness to glioblastoma multiforme interactome signature. *Lab. Invest.* 100, 186–198. doi: 10.1038/s41374-019-0333-7
- Santoni, G., Morelli, M. B., Santoni, M., Nabissi, M., Marinelli, O., and Amantini, C. (2020b). Targeting transient receptor potential channels by MicroRNAs drives tumor development and progression. *Adv. Exp. Med. Biol.* 1131, 605–623. doi: 10.1007/978-3-030-12457-1_24
- Sarfaraz, S., Adhami, V. M., Syed, D. N., Afaq, F., and Mukhtar, H. (2008). Cannabinoids for cancer treatment: progress and promise. *Cancer Res.* 68, 339–342. doi: 10.1158/0008-5472.CAN-07-2785
- Schaefer, M. (2005). Homo- and heteromeric assembly of TRP channel subunits. *Pflugers Arch.* 451, 35–42. doi: 10.1007/s00424-005-1467-6

- Schultz, S. (2018). *GW Pharmaceuticals Plc Investor Presentation—February 2018*. Available online at: <http://ir.gwpharm.com/static-files/e7afb8d8-ab2c4c8a-8e21-b9d3a7d36c70> (accessed May, 2018).
- Schultz, S., and Beyer, M. (2017). *GW Pharmaceuticals Achieves Positive Results in Phase 2 Proof of Concept Study in Glioma*. Available online at: <http://ir.gwpharm.com/static-files/cde942fe-555c-4b2f-9cc9-f34d24c7ad27> (accessed May, 2018).
- Scott, K. A., Dalglish, A. G., and Liu, W. M. (2014). The combination of cannabidiol and Δ^9 -tetrahydrocannabinol enhances the anticancer effects of radiation in an orthotopic murine glioma model. *Mol. Cancer Ther.* 13, 2955–2967. doi: 10.1158/1535-7163.MCT-14-0402
- Singh, S. K., Hawkins, C., Clarke, I. D., Squire, J. A., Bayani, J., Hide, T., et al. (2004). Identification of human brain tumour initiating cells. *Nature* 432, 396–401. doi: 10.1038/nature03128
- Solinas, M., Massi, P., Cinquina, V., Valenti, M., Bolognini, D., Gariboldi, M., et al. (2013). Cannabidiol, a non-psychoactive cannabinoid compound, inhibits proliferation and invasion in U87-MG and T98G glioma cells through a multitarget effect. *PLoS One* 8:e76918. doi: 10.1371/journal.pone.0076918
- Song, M., Chen, D., and Yu, S. P. (2014). The TRPC channel blocker SKF 96365 inhibits glioblastoma cell growth by enhancing reverse mode of the Na(+)/Ca(2+) exchanger and increasing intracellular Ca(2+). *Br. J. Pharmacol.* 171, 3432–3447. doi: 10.1111/bph.12691
- Soroceanu, L., Manning, T. J. Jr., and Sontheimer, H. (1999). Modulation of glioma cell migration and invasion using Cl(-) and K(+) ion channel blockers. *J. Neurosci.* 19, 5942–5954. doi: 10.1523/JNEUROSCI.19-14-05942
- Sottoriva, A., Spiteri, I., Piccirillo, S. G., Touloumis, A., Collins, V. P., Marioni, J. C., et al. (2013). Intratumor heterogeneity in human glioblastoma reflects cancer evolutionary dynamics. *Proc. Natl. Acad. Sci. U.S.A.* 110, 4009–4014. doi: 10.1073/pnas.1219747110
- Sours-Brothers, S., Ding, M., Graham, S., and Ma, R. (2009). Interaction between TRPC1/TRPC4 assembly and STIM1 contributes to store-operated Ca²⁺ entry in mesangial cells. *Exp. Biol. Med. (Maywood)* 234, 673–682. doi: 10.3181/0809-RM-279
- Stock, K., Kumar, J., Synowitz, M., Petrosino, S., Imperatore, R., Smith, E. S., et al. (2012). Neural precursor cells induce cell death of high-grade astrocytomas through stimulation of TRPV1. *Nat. Med.* 18, 1232–1238. doi: 10.1038/nm.2827
- Stupp, R., Hegi, M. E., Mason, W. P., van den Bent, M. J., Taphoorn, M. J., Janzer, R. C., et al. (2009). European organisation for research and treatment of cancer brain tumour and radiation oncology groups; national cancer institute of Canada clinical trials group. Effects of radiotherapy with concomitant and adjuvant temozolomide versus radiotherapy alone on survival in glioblastoma in a randomised phase III study: 5-year analysis of the EORTC-NCIC trial. *Lancet Oncol.* 10, 459–466. doi: 10.1016/S1470-2045(09)70025-7
- Sun, Y., Sukumaran, P., Varma, A., Derry, S., Sahmoun, A. E., and Singh, B. B. (2014). Cholesterol-induced activation of TRPM7 regulates cell proliferation, migration, and viability of human prostate cells. *Biochim. Biophys. Acta* 1843, 1839–1850. doi: 10.1016/j.bbamer.2014.04.019
- Tang, D., Kang, R., Bergh, T. V., Vandenabeele, P., and Kroemer, G. (2019). The molecular machinery of regulated cell death. *Cell Res.* 29, 347–364. doi: 10.1038/s41422-019-0164-5
- Torres, S., Lorente, M., Rodríguez-Fornés, F., Hernández-Tiedra, S., Salazar, M., García-Taboada, E., et al. (2011). A combined preclinical therapy of cannabinoids and temozolomide against glioma. *Mol. Cancer Ther.* 10, 90–103. doi: 10.1158/1535-7163.MCT-10-0688
- Toth, A., Blumberg, P. M., and Boczan, J. (2009). Anandamide and the vanilloid receptor (TRPV1). *Vitam. Horm.* 81, 389–419. doi: 10.1016/S0083-6729(09)81015-7
- Tsavalier, L., Shaper, M. H., Morkowski, S., and Laus, R. (2001). Trp-p8, a novel prostate-specific gene, is up-regulated in prostate cancer and other malignancies and shares high homology with transient receptor potential calcium channel proteins. *Cancer Res.* 61, 3760–3769.
- Vaccani, A., Massi, P., Colombo, A., Rubino, T., and Parolaro, D. (2005). Cannabidiol inhibits human glioma cell migration through a cannabinoid receptor-independent mechanism. *Br. J. Pharmacol.* 144, 1032–1036. doi: 10.1038/sj.bjp.0706134
- Velasco, G., Carracedo, A., Blázquez, C., Lorente, M., Aguado, T., Haro, A., et al. (2007). Cannabinoids and gliomas. *Mol. Neurobiol.* 36, 60–67. doi: 10.1007/s12035-007-0002-5
- Venkatachalam, K., and Montell, C. (2007). TRP channels. *Annu. Rev. Biochem.* 76, 387–417. doi: 10.1146/annurev.biochem.75.103004.142819
- Venkatachalam, K., Hofmann, T., and Montell, C. (2006). Lysosomal localization of TRPML3 depends on TRPML2 and the mucopolidosis-associated protein TRPML1. *J. Biol. Chem.* 281, 17517–17527. doi: 10.1074/jbc.M600807200
- Vergara-Jauregui, S., Martina, J. A., and Puertollano, R. (2009). Identification of the penta-EF-hand protein ALG-2 as a Ca²⁺-dependent interactor of mucolipin-1. *J. Biol. Chem.* 284, 36357–36366. doi: 10.1074/jbc.M109.047241
- Wan, J., Guo, A. A., King, P., Guo, S., Saafir, T., Jiang, Y., et al. (2020). TRPM7 induces tumorigenesis and stemness through notch activation in glioma. *Front. Pharmacol.* 11:590723. doi: 10.3389/fphar.2020.590723
- Wang, H., Cheng, X., Tian, J., Xiao, Y., Tian, T., Xu, F., et al. (2020). TRPC channels: Structure, function, regulation and recent advances in small molecular probes. *Pharmacol. Ther.* 209:107497. doi: 10.1016/j.pharmthera.2020.107497
- Wick, W., Gorlia, T., Bendszus, M., Taphoorn, M., Sahm, F., Harting, I., et al. (2017). Lomustine and bevacizumab in progressive glioblastoma. *N. Engl. J. Med.* 377, 1954–1963. doi: 10.1056/NEJMoa1707358
- Wondergem, R., and Bartley, J. (2009). Menthol increases human glioblastoma intracellular Ca²⁺, BK channel activity and cell migration. *J. Biomed. Sci.* 16:90. doi: 10.1186/1423-0127-16-90
- Wondergem, R., Ecay, T. W., Mahieu, F., Owsianik, G., and Nilius, B. H. G. F. (2008). /SF and menthol increase human glioblastoma cell calcium and migration. *Biochem. Biophys. Res. Commun.* 372, 210–215. doi: 10.1016/j.bbrc.2008.05.032
- Yang, D., and Kim, J. (2020). Emerging role of transient receptor potential (TRP) channels in cancer progression. *BMB Rep.* 53, 125–132. doi: 10.5483/BMBRep.2020.53.3.016
- Yee, N. S., Li, Q., Kazi, A. A., Yang, Z., Berg, A., and Yee, R. K. (2014). Aberrantly over-expressed TRPM8 channels in pancreatic adenocarcinoma: correlation with tumor size/stage and requirement for cancer cells invasion. *Cells* 3, 500–516. doi: 10.3390/cells3020500
- Yu, S., Xu, Z., Zou, C., Wu, D., Wang, Y., Yao, X., et al. (2014). Ion channel TRPM8 promotes hypoxic growth of prostate cancer cells via an O₂-independent and RACK1-mediated mechanism of HIF-1 α stabilization. *J. Pathol.* 234, 514–525. doi: 10.1002/path.4413
- Zeng, J., Wu, Y., Zhuang, S., Qin, L., Hua, S., Mungur, R., et al. (2019). Identification of the role of TRPM8 in glioblastoma and its effect on proliferation, apoptosis and invasion of the U251 human glioblastoma cell line. *Oncol. Rep.* 42, 1517–1526. doi: 10.3892/or.2019.7260
- Zhan, C., and Shi, Y. (2017). TRPC channels and cell proliferation. *Adv. Exp. Med. Biol.* 976, 149–155. doi: 10.1007/978-94-024-1088-4_13
- Zhang, D., Wang, F., Pang, Y., Zhao, E., Zhu, S., Chen, F., et al. (2017). ALG2 regulates glioblastoma cell proliferation, migration and tumorigenicity. *Biochem. Biophys. Res. Commun.* 486, 300–306. doi: 10.1016/j.bbrc.2017.03.032
- Zhang, W., Hirschler-Laszkiewicz, I., Tong, Q., Conrad, K., Sun, S. C., Penn, L., et al. (2006). TRPM2 is an ion channel that modulates hematopoietic cell death through activation of caspases and PARP cleavage. *Am. J. Physiol. Cell Physiol.* 290, C1146–C1159. doi: 10.1152/ajpcell.00205.2005

Conflict of Interest: The author declares that the research was conducted in the absence of any commercial or financial relationships that could be construed as a potential conflict of interest.

Publisher's Note: All claims expressed in this article are solely those of the authors and do not necessarily represent those of their affiliated organizations, or those of the publisher, the editors and the reviewers. Any product that may be evaluated in this article, or claim that may be made by its manufacturer, is not guaranteed or endorsed by the publisher.

Copyright © 2021 Lefranc. This is an open-access article distributed under the terms of the Creative Commons Attribution License (CC BY). The use, distribution or reproduction in other forums is permitted, provided the original author(s) and the copyright owner(s) are credited and that the original publication in this journal is cited, in accordance with accepted academic practice. No use, distribution or reproduction is permitted which does not comply with these terms.

Advantages of publishing in Frontiers



OPEN ACCESS

Articles are free to read
for greatest visibility
and readership



FAST PUBLICATION

Around 90 days
from submission
to decision



HIGH QUALITY PEER-REVIEW

Rigorous, collaborative,
and constructive
peer-review



TRANSPARENT PEER-REVIEW

Editors and reviewers
acknowledged by name
on published articles

Frontiers

Avenue du Tribunal-Fédéral 34
1005 Lausanne | Switzerland

Visit us: www.frontiersin.org

Contact us: frontiersin.org/about/contact



REPRODUCIBILITY OF RESEARCH

Support open data
and methods to enhance
research reproducibility



DIGITAL PUBLISHING

Articles designed
for optimal readership
across devices



FOLLOW US

@frontiersin



IMPACT METRICS

Advanced article metrics
track visibility across
digital media



EXTENSIVE PROMOTION

Marketing
and promotion
of impactful research



LOOP RESEARCH NETWORK

Our network
increases your
article's readership